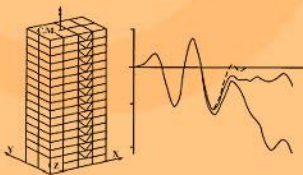

Matrix Analysis of Structural Dynamics

Applications and Earthquake Engineering



Franklin Y. Cheng

Matrix Analysis of Structural Dynamics

Matrix Analysis of Structural Dynamics

Applications and Earthquake Engineering

Franklin Y. Cheng

*University of Missouri, Rolla
Rolla, Missouri*



MARCEL DEKKER, INC.

NEW YORK • BASEL

Library of Congress Cataloging-in-Publication Data

Cheng, Franklin Y.

Matrix analysis of structural dynamics: applications and earthquake engineering/
Franklin Y. Cheng.

p. cm. – (Civil and environmental engineering ; 4)

Includes index.

ISBN 0-8427-0387-1 (alk. paper)

1. Structural dynamics. 2. Earthquake engineering. 3. Matrices. I. Title. II. Series

TA654.C515 2000

624.1'7–dc21

00-031595

This book printed on acid-free paper.

Headquarters

Marcel Dekker, Inc.

270 Madison Avenue, New York, NY 10016

tel: 212-696-9000; fax: 212-685-4540

Eastern Hemisphere Distribution

Marcel Dekker AG

Hutgasse 4, Postfach 812, CH-4001 Basel, Switzerland

tel: 41-61-261-8482; fax: 41-61-261-8896

World Wide Web

<http://www.dekker.com>

The publisher offers discounts on this book when ordered in bulk quantities. For more information,
write to Special Sales/Professional Marketing at the headquarters address above.

Copyright © 2001 by Marcel Dekker, Inc. All Rights Reserved.

Neither this book nor any part may be reproduced or transmitted in any form or by any means,
electronic or mechanical, including photocopying, microfilming, and recording, or by any information
storage and retrieval system, without permission in writing from the publisher.

Current printing (last digit):

10 9 8 7 6 5 4 3 2 1

PRINTED IN THE UNITED STATES OF AMERICA

Civil and Environmental Engineering
A Series of Reference Books and Textbooks

Editor

Michael D. Meyer

Department of Civil and Environmental Engineering
Georgia Institute of Technology
Atlanta, Georgia

1. Preliminary Design of Bridges for Architects and Engineers
Michele Melaragno
2. Concrete Formwork Systems
Awad S. Hanna
3. Multilayered Aquifer Systems: Fundamentals and Applications
Alexander H.-D. Cheng
4. Matrix Analysis of Structural Dynamics: Applications and Earthquake Engineering
Franklin Y. Cheng
5. Hazardous Gases Underground: Applications to Tunnel Engineering
Barry R. Doyle
6. Cold-Formed Steel Structures to the AISI Specification
Gregory J. Hancock, Thomas M. Murray, Duane S. Ellifritt
7. Fundamentals of Infrastructure Engineering: Civil Engineering Systems: Second Edition, Revised and Expanded
Patrick H. McDonald
8. Handbook of Pollution Control and Waste Minimization
Abbas Ghassemi
9. Introduction to Approximate Solution Techniques, Numerical Modeling, and Finite Element Methods
Victor N. Kaliakin
10. Geotechnical Engineering: Principles and Practices of Soil Mechanics and Foundation Engineering
V. N. S. Murthy

Additional Volumes in Production

Chemical Grouting and Soil Stabilization: Third Edition, Revised and Expanded
Reuben H. Karol
Estimating Building Costs
Calin M. Popescu, Kan Phaobunjong, Nuntapong Ovararin

PREFACE

OBJECTIVES AND ORGANIZATION

This book covers several related topics: the displacement method with matrix formulation, theory and analysis of structural dynamics as well as application to earthquake engineering, and seismic building codes. As computer technology rapidly advances and buildings become taller and more slender, dynamic behavior of such structures must be studied using state-of-the-art methodology with matrix formulation. Analytical accuracy and computational efficiency of dynamic structural problems depends on several key features: structural modeling, material property idealization, loading assumptions, and numerical techniques.

The features of this book can be summarized as follows. Three structural models are studied: lumped mass, consistent mass, and distributed mass. Material properties are presented in two categories: damping and hysteretic behavior. Damping is formulated in two types: proportional and nonproportional. Hysteretic behavior is studied with eight models suited to different construction materials such as steel and reinforced concrete. Loading comprises a range of time-dependent excitations, for example, steady-state vibration, impact loading, free and transient vibration, and earthquake ground motion. Numerical techniques emphasize two areas: eigensolution and numerical integration. The former covers fundamental as well as advanced techniques for five predominant methods; the latter covers five well-known integration techniques. Structural dynamics theory is used to substantiate seismic building-code provisions. Representative codes are discussed to illustrate their similarities and differences.

This book is intended for graduate students as well as advanced senior undergraduates in civil, mechanical, and aeronautical engineering. It is also intended as a reference tool for practitioners. In the preparation of this text, six organizing principles served as guidelines.

1. The book functions as a self-study unit. Its technical detail requires the reader to be knowledgeable only in strength of materials, fundamental static structural analysis, calculus, and linear algebra. Essential information on algebraic matrix formulation, ordi-

- nary and partial differential equations, vector analysis, and complex variables is reviewed where necessary.
2. Step-by-step numerical examples are provided. This serves to illustrate mathematical formulations and to interpret physical representations, enabling the reader to understand the formulae vis-à-vis their associated engineering applications.
 3. Each chapter discusses a specific topic. There is a progression in every chapter from fundamental to more advanced levels; for instance, eigensolution methods are grouped accordingly in Chapter 2, numerical integration techniques in Chapter 7, and hysteresis models in Chapter 9. This approach may help the reader to follow the subject matter and the instructor to select material for classroom presentation.
 4. Topic areas are covered comprehensively. For example, three structural models are studied for uncoupling and coupling vibrations with longitudinal, flexural, and torsional motions. Flexural vibration extends from bending deformation to bending and shear deformation, rotatory inertia, P-Δ effect, and elastic media support. The reader can attain greater understanding from this integrative approach.
 5. 3-D building structures are treated in one chapter. Comprehensive formulations are developed for member, joint, and global coordinate transformation for general 3-D structures. Building systems in particular are extensively analyzed with consideration of floor diaphragms, bracings, beams, columns, shear walls, and the rigid zone at connecting joints. These elements are not collectively covered in a structural dynamics text or a static structural analysis text; this book can supplement the latter.
 6. Examples are designed to help the reader grasp the concepts presented. Contained in the book are 114 examples and a set of problems with solutions for each chapter. A detailed solutions manual is available. Computer programs are included that further clarify the numerical procedures presented in the text.

SCOPE OF TEXT AND TEACHING SUGGESTIONS

The text can be used for two semesters of coursework, and the sequence of 10 chapters is organized accordingly. Chapters 1–6 compose the first semester, and Chapters 7–10 the second. Fundamental and advanced topics within chapters are marked as Part A and Part B, respectively. If the book is used for one semester, Part B can be omitted at the instructor's discretion.

The scope of the text is summarized as follows. Chapter 1 presents single degree-of-freedom (d.o.f.) systems. Various response behaviors are shown for different types of time-dependent excitations. Well-known solution techniques are elaborated.

Chapter 2 is devoted to response behavior of multiple d.o.f. systems without damping. The significance of individual modes contributing to this behavior is the focus, and comprehensive understanding of modal matrix is the goal of this chapter. As a function of computational accuracy and efficiency, eigensolution methods are examined. These methods include determinant, iteration, Jacobian, Choleski decomposition, and Sturm sequence. Response analysis extends from general problems with symmetric matrix and distinct frequencies to unsymmetric matrix as well as zero and repeated eigenvalues for various fields of engineering.

Chapter 3 examines the characteristics of proportional and nonproportional damping. Numerical methods for eigenvalues and for response considering both types of damping are included, and solutions are compared.

Chapter 4 presents the fundamentals of distributed mass systems. Emphasis is placed on dynamic stiffness formulation, steady-state vibration for undamped harmonic excitation, and transient vibration for general forcing function including earthquake excitation with and without damping.

Chapter 5 continues the topic of distributed mass systems to include longitudinal, flexural, and torsional coupling vibration. Also included are bending and shear deformation, rotatory inertia, and P-Δ effect with and without elastic media support. Vibrations of trusses, elastic frames, and plane grid systems are discussed.

Chapter 6 introduces consistent mass model for finite elements. Frameworks and plates are studied with emphasis on isoparametric finite element formulation. Advanced topics include tapered members with Timoshenko theory and P- Δ effect. Note that the structural model of a distributed mass system in Chapter 4 yields the lower bound of an eigensolution while the model in Chapter 6 yields a solution between a lumped mass and a distributed mass model. Solutions are thus compared.

Chapter 7 covers structural analysis and aseismic design as well as earthquake characteristics and ground rotational movement. Well-known numerical integration methods such as Newmark's, Wilson- θ , and Runge-Kutta fourth-order are presented with solution criteria for error and stability behavior. Procedures for constructing elastic and inelastic response spectra are established, followed by design spectra. This chapter introduces six components of ground motion: three translational and three rotational. Response spectra are then established to reveal the effect of those components on structural response. Modal combination techniques such as CQC (Complete Quadratic Combination) are presented in detail. Computer program listings are appended for the numerical integration and modal combination methods so that they can be used without sophisticated testing for possible bugs.

Chapter 8 focuses on 3-D build structural systems composed of various steel and reinforced concrete (RC) members. The formulations and numerical procedures outlined here are essential for tall building analysis with P- Δ effect, static load, seismic excitation, or dynamic force.

Chapter 9 presents inelastic response analysis and hysteresis models such as elasto-plastic, bilinear, curvilinear, and Ramberg-Osgood. Additional models for steel bracings, RC beams and columns, coupling bending shear and axial deformations of low-rise shear walls, and axial hysteresis of walls are provided with computer program listings to show calculation procedures in detail. These programs have been thoroughly tested and can be easily implemented for structural analysis. Also included are nonlinear geometric analysis and large deformation formulae.

Chapter 10 examines three seismic building codes: the Uniform Building Codes of 1994 and 1997 and the International Building Code of 2000. IBC-2000 creates uniformity among the US seismic building codes, and replaces them. This chapter relates code provisions to the analytical derivations of previous chapters. It explains individual specifications and compares them across the codes. Since the IBC departed from the UBC format in organization of sections, figures, tables and equations, the chapter concludes with summary comparisons of the codes. Numerical examples in parallel form delineate the similarities and differences.

ACKNOWLEDGMENTS

This book consolidates results from my years as a teacher and researcher. Teaching consists of classes at University of Missouri-Rolla (UMR) and the UMR Engineering Education Center in St. Louis, lectures for receiving honorary professorships in China at Harbin University of Architecture and Engineering, Xian University of Architecture and Technology, Taiyuan University of Technology, and Yunnan Polytechnic University as well as UMR Continuing Education short courses.

Distinguished guest speakers at the short courses—the late Professor Nathan M. Newmark, Professor N. Khachaturian, and Dr. V. B. Venkayya—have my wholehearted appreciation for their contribution. UMR has my continued thanks for bestowing on me the distinguished Curators' professorship to enhance my research and teaching. My deep gratitude goes to the National Science Foundation, particularly Dr. S. C. Liu, for sustained guidance and support of my research. I am grateful to my former graduate students, especially Drs. J. F. Ger, K. Z. Truman, G. E. Mertz, D. S. Juang, D. Li, K. Y. Lou, H. P. Jiang, and Z. Q. Wang as well as Misses. Y. Wang and C. Y. Luo, for their endeavors to improve the manuscript and solutions manual. Also my thanks go to Dr O. R. Mitchell, Dean of School of Engineering, for his enthusiasm in my career development, and to departmental staff members C. Ousley and E. Farrell who gracefully rendered their valuable assistance over a long period of time. I extend special appreciation to Brian Black, Technical Coordinator of book editorial, and B. J. Clark, executive acquisitions editor with Marcel Dekker Inc. Mr. Clarks' vision of engineering education and pub-

lication motivated accomplishment of this project. My mentors, Professors C. K. Wang and T. C. Huang, have my continued appreciation for their early influence and inspiration. Everlasting thanks go to my family, including my wife, brothers Jeffrey and Ji-Yu, son George, daughter Deborah, daughter-in-law Annie, and grandson Alex Haur-Yih. I dedicate this book to my wife Beatrice (Pi-Yu) for her care and encouragement throughout my academic career.

Franklin Y. Cheng

CONTENTS

Preface iii

1 Characteristics of Free and Forced Vibrations of Elementary Systems	1
1.1 Introduction	1
1.2 Free Undamped Vibration	1
1.2.1 Motion Equation and Solution	1
1.2.2 Initial Conditions, Phase Angle and Natural Frequency	3
1.2.3 Periodic and Harmonic Motion	6
1.3 Free Damped Vibration	7
1.3.1 Motion Equation and Viscous Damping	7
1.3.2 Critical Damping, Overdamping and Underdamping	9
1.3.3 Logarithmic Decrement and Evaluation of Viscous Damping Coefficient	11
1.4 Forced Undamped Vibration	14
1.4.1 Harmonic Forces	14
1.4.2 Steady-State Vibration and Resonance	15
1.4.3 Impulses and Shock Spectra	19
1.4.4 General Loading—Step Forcing Function Method vs. Duhamel's Integral	24
1.5 Forced Damped Vibration	29
1.5.1 Harmonic Forces	29
1.5.2 Steady-State Vibration for Damped Vibration, Resonant and Peak Amplitude	30
1.5.3 General Loading—Step-Forcing Function Method vs. Duhamel's Integral	32
1.5.4 Transmissibility and Response to Foundation Motion	36

1.6	Evaluation of Damping	42
1.6.1	Equivalent Damping Coefficient Method	42
1.6.2	Amplitude Method and Bandwidth Method	43
1.7	Overview	45
	Bibliography	45

2 Eigensolution Techniques and Undamped Response Analysis of Multiple-Degree-of-Freedom Systems 47

PART A FUNDAMENTALS 47

2.1	Introduction	47
2.1.1	Characteristics of the Spring–Mass Model	47
2.1.2	Advantages of the Lumped Mass Model	48
2.2	Characteristics of Free Vibration of Two-Degree-of-Freedom Systems	49
2.2.1	Motion Equations, Natural and Normal Modes	49
2.2.2	Harmonic and Periodic Motion	52
2.3	Dynamic Matrix Equation	54
2.4	Orthogonality of Normal Modes	55
2.5	Modal Matrix for Undamped Vibration	56
2.5.1	Modal Matrices and Characteristics	56
2.5.2	Response to Initial Disturbances, Dynamic Forces and Seismic Excitation	58
2.5.3	Effect of Individual Modes on Response	64
2.5.4	Response to Foundation Movement	67
2.6	Eigensolution for Symmetric Matrix	72
2.6.1	Iteration Method for Fundamental and Higher Modes	72
2.6.2	Proof of Iterative Solution	77
2.6.3	Extraction Technique for Natural Frequencies	80
2.6.4	Choleski's Decomposition Method	81
2.6.5	Generalized Jacobi Method	87
2.6.6	Sturm Sequence Method	95

PART B ADVANCED TOPICS 98

2.7	Eigensolution Technique for Unsymmetric Matrix	98
2.7.1	Classification of Cases	99
2.7.2	Iteration Method	100
2.8	Response Analysis for Zero and Repeating Eigenvalues	105
2.8.1	Zero and Repeating Eigenvalue Cases	105
2.8.2	Orthogonality Properties	105
2.8.3	Response Analysis	109
	Bibliography	114

3 Eigensolution Methods and Response Analysis for Proportional and Nonproportional Damping 117

PART A FUNDAMENTALS 117

3.1	Introduction	117
3.2	Response Analysis for Proportional Damping	117
3.2.1	Based on a Modal Matrix	117
3.2.2	Proportional Damping	120
3.3	Evaluation of Damping Coefficients and Factors	121
3.3.1	Two Modes Required	121
3.3.2	All Modes Required	125
3.3.3	Damping Factors from Damping Coefficients	125
3.4	Determination of Proportional and Nonproportional Damping	126

CONTENTS**ix**

PART B ADVANCED TOPICS	128
3.5	Characteristics of Complex Eigenvalues for Nonproportional Damping 128
3.6	Iteration Method for Fundamental and Higher Modes of Complex Eigenvalues 137
3.6.1	Fundamental Mode 137
3.6.2	Orthogonality Condition and Iteration for Higher Modes 139
3.6.3	Step-by-Step Procedures 139
3.7	Response Analysis with Complex Eigenvalues 149
3.8	Relationship Between Undamped, Proportional Damping, and Nonproportional Damping 156
Bibliography	159
4. Dynamic Stiffness and Energy Methods for Distributed Mass Systems	161
4.1	Introduction 161
4.2	Derivation of Bernoulli-Euler Equation 161
4.3	Derivation of Dynamic Stiffness Coefficients 166
4.4	Characteristics of Dynamic Stiffness Coefficients 168
4.4.1	Numerals and Curves for Coefficients 168
4.4.2	Rayleigh's Dynamic Reciprocal Principle 171
4.4.3	Müller-Breslau's Principle 173
4.5	Dynamic Stiffness, Load, and Mass Matrices 175
4.5.1	Degree-of-Freedom of Plane Structural Systems 175
4.5.2	Equilibrium Matrices 176
4.5.3	Compatibility Matrices 177
4.5.4	Dynamic Stiffness Matrix 178
4.5.5	Dynamic Load Matrix 179
4.5.6	System Matrix Equation 180
4.6	Derivation of Dynamic Fixed-end Moments and Fixed-end Shears 180
4.6.1	Differential Equations 181
4.6.2	Uniform Load 182
4.6.3	Triangular Load 183
4.6.4	Concentrated Load between Nodes 185
4.6.5	Foundation Movement 186
4.7	Numerical Technique for Eigensolutions 186
4.8	Steady-State Response Analysis 198
4.9	Response for General Forcing Functions with and without Damping 203
4.9.1	Kinetic and Strain Energy 203
4.9.2	Orthogonality Condition 204
4.9.3	Dissipated Energy and Work 205
4.9.4	Response Equations 206
Bibliography	212
5 Dynamic Stiffness Method for Coupling Vibration, Elastic Media and P-Δ Effect	213
PART A FUNDAMENTALS	213
5.1	Introduction 213
5.2	Longitudinal Vibration and Stiffness Coefficients 213
5.3	Longitudinal Vibration and Stiffness Coefficients with Elastic Media 214
5.4	Dynamic Analysis of Trusses and Elastic Frames 216
5.4.1	Dynamic Stiffness Coefficients of Pin-connected Member 216
5.4.2	Dynamic Stiffness Matrix of Trusses 218
5.4.3	Dynamic Stiffness Matrix of Elastic Frames 221
5.4.4	Coupling of Longitudinal and Flexural Vibration 224
5.5	Torsional Vibration and Stiffness Coefficients 229

5.6	Dynamic Stiffness Matrix of Grid Systems	230
5.7	Coupling of Torsional and Flexural Vibration	233
PART B ADVANCED TOPICS 237		
5.8	Bernoulli-Euler Equation with Elastic Media	237
5.9	Bernoulli-Euler Equation with Elastic Media and P-Δ Effect	238
5.10	Timoshenko Equation (Bending and Shear Deformation and Rotatory Inertia)	240
5.10.1	Differential Equations	240
5.10.2	Stiffness Coefficients	243
5.10.3	Fixed-end Forces for Steady-State Vibration	246
5.10.4	Response Analysis for General Forcing Functions	247
5.10.5	Effect of Various Parameters on Frequencies	252
5.11	Timoshenko Equation with Elastic Media and P-Δ Effect	252
5.11.1	Differential Equations	253
5.11.2	Stiffness Coefficients	255
5.11.3	Fixed-end Forces	256
5.11.4	Case Studies of the Effect of Various Parameters on Frequencies	257
Bibliography		258
6 Consistent Mass Method for Frames and Finite Elements 261		
PART A FUNDAMENTALS 261		
6.1	Introduction	261
6.2	Energy Method for Motion Equation	262
6.2.1	Rigid Frames	263
6.2.2	Elastic Frames	265
6.3	Stiffness, Mass and Generalized Force Matrices for Frame Members	265
6.3.1	Two-Force Member	265
6.3.2	Torsional Member	268
6.3.3	Flexural Member	270
6.4	Eigenvalue Comparisons Among Lumped Mass, Dynamic Stiffness and Consistent Mass Methods	283
PART B ADVANCED TOPICS 285		
6.5	Stiffness, Mass and Generalized Force Matrices for Finite Elements	285
6.5.1	Finite Element Formulation—Generalized Coordinates	286
6.5.2	Finite Element Formulation—Natural Coordinates	291
6.6	Motion Equation with P-Δ Effect	303
6.6.1	Potential Energy and Motion Equation	303
6.6.2	Geometric Matrix with Rotation and Deflection	305
6.6.3	Geometric Matrix (String Stiffness) with Deflection	305
6.7	Timoshenko Prismatic Member with P-Δ Effect	306
6.7.1	Displacement and Shape Functions	306
6.7.2	Stiffness Matrix	308
6.7.3	Mass Matrix	309
6.7.4	Generalized Force Matrix	312
6.7.5	Geometric Matrix	312
6.8	Timoshenko Tapered Member with P-Δ Effect	314
6.8.1	Stiffness Matrix	314
6.8.2	Mass Matrix	315
6.8.3	Generalized Force Matrix	317
6.8.4	Geometric Matrix	317
6.9	Comments on Lumped Mass, Consistent Mass, and Dynamic Stiffness Models	318
Bibliography		319

7 Numerical Integration Methods and Seismic Response Spectra for Single- and Multi-Component Seismic Input 321

PART A FUNDAMENTALS 321

7.1	Introduction	321
7.2	Earthquakes and Their Effects on Structures	321
7.2.1	Earthquake Characteristics	321
7.2.2	Intensity, Magnitude, and Acceleration of Earthquakes	322
7.2.3	Relationship Between Seismic Zone, Acceleration, Magnitude, and Intensity	326
7.2.4	Earthquake Principal Components	327
7.3	Numerical Integration and Stability	329
7.3.1	Newmark Integration Method	329
7.3.2	Wilson- θ Method	332
7.3.3	General Numerical Integration Related to Newmark and Wilson- θ Methods	334
7.3.4	Runge-Kutta Fourth-Order Method	338
7.3.5	Numerical Stability and Error of Newmark and Wilson- θ Methods	350
7.3.6	Numerical Stability of Runge-Kutta Fourth-Order Method	358
7.4	Seismic Response Spectra for Analysis and Design	361
7.4.1	Response Spectra, Pseudo-Spectra and Principal-Component Spectra	362
7.4.2	Housner's Average Design Spectra	369
7.4.3	Newmark Elastic Design Spectra	371
7.4.4	Newmark Inelastic Design Spectra	372
7.4.5	Site-Dependent Spectra and UBC-94 Design Spectra	378
7.4.6	Various Definitions of Ductility	380

PART B ADVANCED TOPICS 383

7.5	Torsional Response Spectra	383
7.5.1	Ground Rotational Records Generation	383
7.5.2	Construction of Torsional Response Spectra	389
7.6	Response Spectra Analysis of a Multiple d.o.f. Systems	390
7.6.1	SRSS Modal Combination Method	393
7.6.2	CQC Modal Combination Method	394
7.6.3	Structural Response Due to Multiple-Component Seismic Input	397
7.7	Maximum (Worst-Case) Response Analysis for Six Seismic Components	399
7.7.1	Based on SRSS Method	400
7.7.2	Based on CQC Method	404
7.8	Composite Translational Spectrum and Torsional Spectrum	410
7.8.1	Construction of the Composite Response Spectrum	411
7.8.2	Composite Spectral Modal Analysis	412
7.9	Overview	414
	Bibliography	414

8 Formulation and Response Analysis of Three-Dimensional Building Systems with Walls and Bracings 417

PART A FUNDAMENTALS 417

8.1	Introduction	417
8.2	Joints, Members, Coordinate Systems, and Degree of Freedom (d.o.f.)	417
8.3	Coordinate Transformation Between JCS and GCS: Methods 1 and 2	418
8.4	Force Transformation Between Slave Joint and Master Joint	424
8.5	System d.o.f. as Related to Coordinate and Force Transformation	426
8.6	Beam-Columns	429
8.6.1	Coordinate Transformation Between ECS and JCS or GCS: Methods 1 and 2	429

8.6.2	Beam–Column Stiffness in the ECS	431
8.6.3	Beam–Column Stiffness in the JCS or GCS Based on Method 1	434
8.6.4	Beam–Column Geometric Matrix (String Stiffness) in ECS and JCS or GCS Based on Method 1	438
8.7	Shear Walls	439
8.7.1	Shear-Wall ECS and GCS Relationship Based on Method 1	439
8.7.2	Shear-Wall Stiffness in the ECS	441
8.7.3	Shear-Wall Stiffness in the JCS or GCS Based on Method 1	447
8.7.4	Shear-Wall Geometric Matrix (String Stiffness) in the JCS or GCS Based on Method 1	455
8.8	Bracing Elements	455
8.8.1	Bracing-Element ECS and GCS Relationship Based on Method 1	455
8.8.2	Bracing-Element Stiffness in ECS	457
8.8.3	Bracing-Element Stiffness in the JCS or GCS Based on Method 1	457
8.9	Structural Characteristics of 3-D Building Systems	462
8.10	Rigid Zone Between Member End and Joint Center	462
8.11	Building-Structure-Element Stiffness with Rigid Zone	464
8.11.1	Beam–Column Stiffness in ECS Based on Method 2	464
8.11.2	Beam–Column Stiffness in GCS Based on Method 2	466
8.11.3	Beam–Column Geometric Matrix (String Stiffness) in JCS or GCS Based on Method 2	473
8.11.4	Beam Stiffness in the GCS Based on Method 2	475
8.11.5	Bracing-Element Stiffness in the JCS or GCS Based on Method 2	479
8.11.6	Shear-Wall Stiffness in the JCS or GCS Based on Method 2	482
8.11.7	Shear-Wall Geometric Matrix (String Stiffness) in the JCS or GCS Based on Method 2	487

PART B ADVANCED TOPICS 490

8.12	Assembly of Structural Global Stiffness Matrix	490
8.12.1	General System Assembly (GSA)	490
8.12.2	Floor-by-Floor Assembly (FFA)	498
8.13	Mass Matrix Assembly	504
8.14	Loading Matrix Assembly	508
8.14.1	Vertical Static or Harmonic Forces	509
8.14.2	Lateral Wind Forces	511
8.14.3	Lateral Dynamic Loads	513
8.14.4	Seismic Excitations	514
8.15	Analysis and Response Behavior of Sample Structural Systems	516
8.16	Overview	523
	Bibliography	525

9 Various Hysteresis Models and Nonlinear Response Analysis 527**PART A FUNDAMENTALS 527**

9.1	Introduction	527
9.1.1	Material Nonlinearity and Stress–Strain Models	528
9.1.2	Bauschinger Effect on Moment–Curvature Relationship	528
9.2	Elasto-Plastic Hysteresis Model	529
9.2.1	Stiffness Matrix Formulation	532
9.3	Bilinear Hysteresis Model	534
9.3.1	Stiffness Matrix Formulation	535
9.4	Convergence Techniques at Overshooting Regions	538
9.4.1	State of Yield and Time-Increment Technique	538
9.4.2	Unbalanced Force Technique	539
9.4.3	Equilibrium and Compatibility Checks for Numerical Solutions	552
9.5	Curvilinear Hysteresis Model	555

CONTENTS**xiii**

9.5.1	Stiffness Matrix Formulation	556
9.5.2	Stiffness Comparison Between Bilinear and Curvilinear Models	560
9.6	Ramberg-Osgood Hysteresis Model	562
9.6.1	Parameter Evaluations of Ramberg-Osgood Stress-Strain Curve	562
9.6.2	Ramberg-Osgood Moment-Curvature Curves	563
9.6.3	Stiffness Matrix Formulation for Skeleton Curve	565
9.6.4	Stiffness Matrix Formulation for Branch Curve	570
PART B ADVANCED TOPICS		579
9.7	Geometric Nonlinearity	579
9.8	Interaction Effect on Beam Columns	589
9.9	Elasto-Plastic Analysis of Consistent Mass Systems	591
9.9.1	Stiffness Matrix Formulation	591
9.9.2	Moments, Shears and Plastic Hinge Rotations	595
9.10	Hysteresis Models of Steel Bracing, RC Beams, Columns and Shear Walls	604
9.11	Overview	604
	Bibliography	605
10 Static and Dynamic Lateral-Force Procedures and Related Effects in Building Codes of UBC-94, UBC-97 and IBC-2000 607		
PART A FUNDAMENTALS		607
10.1	Introduction	607
10.2	Background of Lateral Force Procedures in Building Codes	608
10.2.1	Effective Earthquake Force and Effective Mass	608
10.2.2	Base Shear and Overturning Moment	610
10.3	UBC-94 and Design Parameters	612
10.3.1	Criteria for Appropriate Lateral-Force Procedure	612
10.3.2	Base Shear of Static Lateral-Force Procedure and Related Parameters	612
10.3.3	Vertical Distribution of Lateral Force	620
10.3.4	Story Shear and Overturning Moment	620
10.3.5	Torsion and P-Δ Effect	621
10.3.6	Story Drift Limitations	623
10.3.7	$3R_w/8$ Factor	623
10.4	UBC-97 and Design Parameters	624
10.4.1	Criteria for Appropriate Lateral-Force Procedure	624
10.4.2	Base Shear of Static Lateral-Force Procedure and Related Parameters	624
10.4.3	R_w and R Relationship vs Load Combination	626
10.4.4	Load Combination for Strength Design and Allowable Stress Design	627
10.4.5	Story Shear, Overturning Moment and Restoring Moment	631
10.4.6	Story Drift, P-Δ Effect and Torsion	632
10.4.7	Relationships Among $3R_w/8$, Ω_0 and $0.7R\Delta_s$	632
10.5	IBC-2000 and Design Parameters	633
10.5.1	Criteria for Appropriate Lateral-Force Procedure	633
10.5.2	Base Shear of Equivalent Lateral-Force Procedure and Related Parameters	633
10.5.3	Vertical Distribution of Lateral Force	638
10.5.4	Horizontal Shear Distribution and Overturning Moment	639
10.5.5	Deflection and Story Drift	639
10.5.6	P-Δ Effect	640
10.6	Summary Comparison of UBC-94, UBC-97 and IBC-2000 Lateral-Force Procedures	641

10.7	Numerical Illustrations of Lateral-Force Procedure for UBC-94, UBC-97 and IBC-2000	648
10.8	Techniques for Calculating Rigidity Center	672
	10.8.1 Method A—Using Individual Member Stiffness for Rigid-floor Shear Buildings	672
	10.8.2 Method B—Using Relative Rigidity of Individual Bays for General Buildings	673

PART B ADVANCED TOPICS 675

10.9	Dynamic Analysis Procedures of UBC-94, UBC-97 and IBC-2000	675
	10.9.1 UBC-94 Dynamic Analysis Procedure	675
	10.9.2 UBC-97 Dynamic Analysis Procedure	676
	10.9.3 IBC-2000 Dynamic Analysis Procedure	678
	10.9.4 Regionalized Seismic Zone Maps and Design Response Spectra in UBC-97 and IBC-2000	682
10.10	Summary Comparison of UBC-94, UBC-97 and IBC-2000 Dynamic Analysis Procedures	684
10.11	Numerical Illustrations of Dynamic Analysis Procedures for UBC-94, UBC-97 and IBC-2000	688
10.12	Overview	705
	Bibliography	705

Chapter 1	<i>Problems</i>	707
Chapter 2	<i>Problems</i>	715
Chapter 3	<i>Problems</i>	721
Chapter 4	<i>Problems</i>	723
Chapter 5	<i>Problems</i>	727
Chapter 6	<i>Problems</i>	733
Chapter 7	<i>Problems</i>	741
Chapter 8	<i>Problems</i>	745
Chapter 9	<i>Problems</i>	753
Chapter 10	<i>Problems</i>	757

Chapter 1	<i>Solutions</i>	763
Chapter 2	<i>Solutions</i>	767
Chapter 3	<i>Solutions</i>	773
Chapter 4	<i>Solutions</i>	777
Chapter 5	<i>Solutions</i>	783
Chapter 6	<i>Solutions</i>	791
Chapter 7	<i>Solutions</i>	797
Chapter 8	<i>Solutions</i>	799
Chapter 9	<i>Solutions</i>	807
Chapter 10	<i>Solutions</i>	811

Appendix A	Lagrange's Equation	817
Appendix B	Derivation of Ground Rotational Records	823
Appendix C	Vector Analysis Fundamentals	827
Appendix D	Transformation Matrix Between JCS and GCS	831
Appendix E	Transformation Matrix Between ECS and GCS for Beam Column	843
Appendix F	Transformation Matrix [A^i] and Stiffness Matrix [K_{eg}^i] of Beam Column with Rigid Zone	851
Appendix G	Computer Program for Newmark Method	855
Appendix H	Computer Program for Wilson-θ Method	863

CONTENTS**xv**

<i>Appendix I</i>	Computer Program for CQC Method	865
<i>Appendix J</i>	Jain-Goel-Hanson Steel-Bracing Hysteresis Model and Computer Program	875
<i>Appendix K</i>	Takeda Model for RC Columns and Beams and Computer Program	895
<i>Appendix L</i>	Cheng-Mertz Model for Bending Coupling with Shear and Axial Deformations of Low-Rise Shear Walls and Computer Program	913
	BENDING: Low-Rise Shear Wall Cheng-Mertz Hysteresis Model	913
	SHEAR: Low-Rise Shear Wall Cheng-Mertz Hysteresis Model	932
	AXIAL: Low-Rise Shear Wall Cheng-Mertz Hysteresis Model	952
<i>Appendix M</i>	Cheng-Lou Axial Hysteresis Model for RC Columns and Walls and Computer Program	967
<i>Notation</i>		979
<i>Index</i>		989

1

Characteristics of Free and Forced Vibrations of Elementary Systems

1.1. INTRODUCTION

A study of the dynamic analysis of structures may begin logically with an investigation of elementary systems. It is quite often that a complex structure is treated as if it were a simple spring-mass model for which various available mathematical solutions of dynamic response can be found in textbooks that deal with vibrations. An understanding of the dynamic behavior of elementary systems is essential for the practising engineer as well as for the student who, with the aid of high-capacity computer programs, intends to use matrix methods for the solution of structural dynamics problems.

1.2. FREE UNDAMPED VIBRATION

1.2.1. Motion Equation and Solution

Consider the spring mass model shown in Fig. 1.1a. This model, which consists of a mass of weight, W , suspended by means of a spring with stiffness, K , is idealized from the accompanying simple beam. The spring stiffness, K , is defined as the force necessary to stretch or compress the spring one unit of length; therefore, the force caused by a unit deflection at the center of the simple beam is $48EI/L^3$, where E is the modulus of elasticity, I is the moment of inertia of the cross-section, and L is the span length. Similarly, the spring-mass model shown in Fig. 1.1b is idealized from the accompanying rigid frame for which the spring stiffness should be $24EI/L^3$. In Fig. 1.1a, the mass is in equilibrium under the action of two equal and opposite forces: the weight, W , acts downward and the spring force, Kx_{st} , upward. The term x_{st} denotes *static deflection*, which is the amount of movement from the undeformed position to the *equilibrium position* where the displacement of the mass is usually measured.

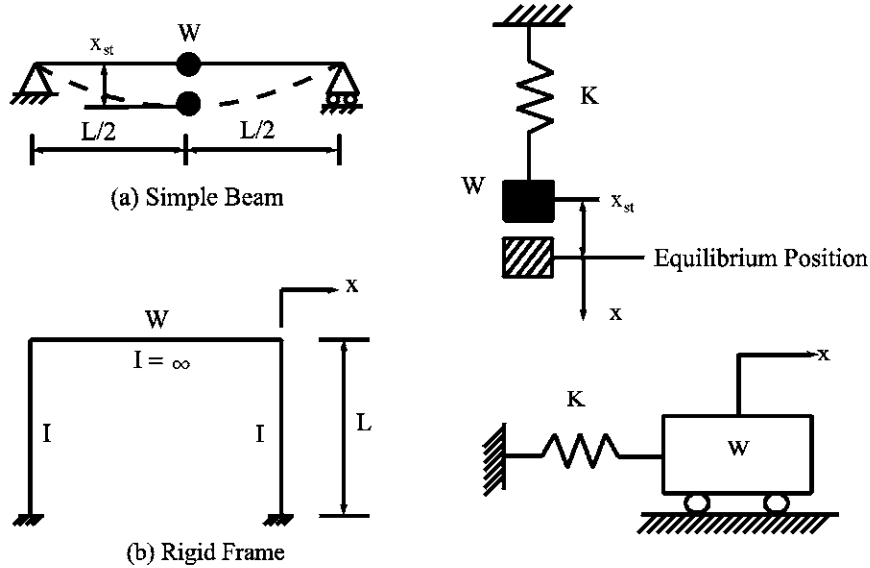


FIG. 1.1 Structures and spring-mass models.

Suppose now that the mass is forced downward a distance, x , from its equilibrium position and then suddenly released. The mass moves upward with a certain velocity, and when it reaches the equilibrium position it continues to move because of its momentum. Beyond this point, the spring force is greater than the upward force, and the mass moves with decreasing velocity until the velocity becomes zero. Now the mass reaches its extreme upper position. In a similar manner, the mass moves downward until it reaches its extreme lower position. At this point, the mass completes one cycle and begins another. Because the motion is performed under the action of the restoring force, starting from the initial displacement of x_0 at $t = 0$, without any external forces, the motion is called *free vibration*.

The equilibrium of a mass in motion is described by Newton's second law as

$$\Sigma F = M\ddot{x} \quad (1.1)$$

in which ΣF is the sum of the forces acting on a mass, M , and \ddot{x} is the acceleration of the mass. For the present case, we have

$$M \frac{d^2x}{dt^2} = -Kx \quad (1.2)$$

where x is positive downward. Because the downward force is positive, the upward force exerted on the mass by the spring is negative. Thus Eq. (1.2) can be rewritten as

$$M\ddot{x} + Kx = 0 \quad (1.3)$$

Now introduce the quantity

$$p = \sqrt{\frac{K}{M}} \quad (1.4)$$

and write Eq. (1.3) in the following form:

$$\ddot{x} + p^2x = 0 \quad (1.5)$$

The solution of the homogeneous second-order differential equation can be written as

$$x = Ce^{\alpha t} \quad (1.6)$$

Substituting Eq. (1.6) for the corresponding term in Eq. (1.5) yields

$$\alpha = \pm\sqrt{-1} p \quad (1.7)$$

Let $i = \sqrt{(-1)}$. Eq. (1.6) then becomes

$$x = C_1 e^{ipt} + C_2 e^{-ipt} \quad (1.8)$$

The above exponential form can be expressed as the trigonometric functions

$$e^{ipt} = \cos pt + i \sin pt \quad (1.9)$$

$$e^{-ipt} = \cos pt - i \sin pt \quad (1.10)$$

Substituting Eqs. (1.9) and (1.10) for the corresponding terms in Eq. (1.8) yields

$$x = A \sin pt + B \cos pt \quad (1.11)$$

in which $A = i(C_1 - C_2)$, $B = C_1 + C_2$, p is a constant called *angular frequency*, and pt is an angle measured in radians.

1.2.2. Initial Conditions, Phase Angle and Natural Frequency

Let T be the *period* in units of time per cycle; then $pT = 2\pi$. The integration constants A and B should be determined by using the information of motion as the known displacement, x , and velocity, \dot{x} , at any time, t . The displacement and velocity may be given at the same time, say x_{t0} and \dot{x}_{t0} , or at a different time, x_{t0} at t_0 and \dot{x}_{t1} at t_1 . To illustrate the procedure of evaluating initial conditions, let us assume that x and \dot{x} are given as x_{t0} and \dot{x}_{t0} at t_0 . From Eq. 1.11, we have

$$x_{t0} = A \sin pt_0 + B \cos pt_0 \quad (1.12)$$

$$\dot{x}_{t0} = pA \cos pt_0 - pB \sin pt_0 \quad (1.13)$$

Solving for A and B and then substituting the answers for the corresponding terms in Eq. 1.11 gives the motion equation

$$x = \left(x_{t0} \sin pt_0 + \frac{\dot{x}_{t0}}{p} \cos pt_0 \right) \sin pt + \left(x_{t0} \cos pt_0 - \frac{\dot{x}_{t0}}{p} \sin pt_0 \right) \cos pt \quad (1.14)$$

which can be expressed in a condensed form

$$x = x_{t0} \cos p(t - t_0) + \frac{\dot{x}_{t0}}{p} \sin p(t - t_0) \quad (1.15)$$

If x and \dot{x} are given as x_0 and \dot{x}_0 and at $t = 0$, Eq. (1.15) becomes

$$x = x_0 \cos pt + \frac{\dot{x}_0}{p} \sin pt \quad (1.16)$$

When the original time is measured from the instant that the mass is in one of the extreme positions, $x_0 = X$ (X denotes *amplitude*) and the initial velocity is zero (as the physical condition should be), the displacement, x , velocity, \dot{x} , and acceleration, \ddot{x} , can be expressed directly from Eq. (1.16). These are plotted in Fig. (1.2a).

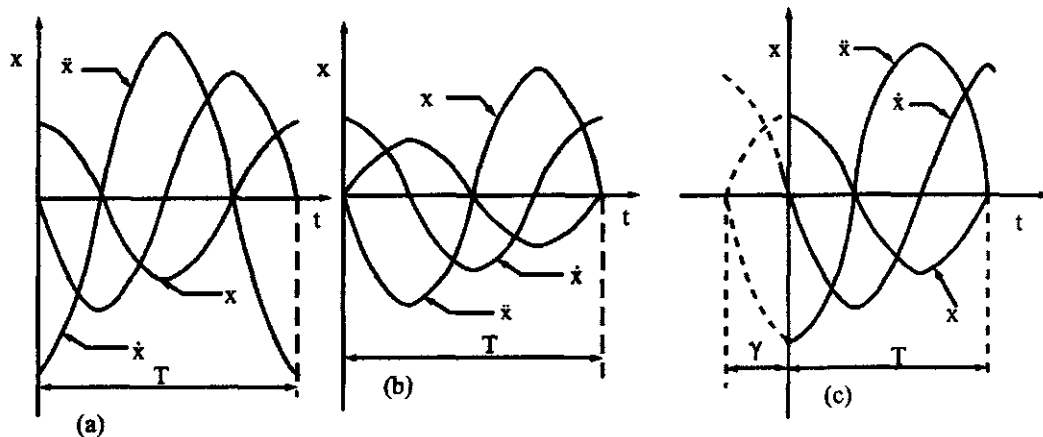


FIG. 1.2 Relationships between x , \dot{x} and \ddot{x} .

When time is measured from the instant that the mass is in the *neutral position*, the initial conditions are $x = 0$ and $\dot{x} = \dot{x}_0$. The relationships between x , \dot{x} , and \ddot{x} are shown in Fig. (1.2b) according to Eq. (1.16). In Fig. (1.2c), the origin is located at t_0 units of time after the mass passes the neutral position with the initial conditions of $x = x_{t_0}$. The equations for x , \dot{x} , and \ddot{x} are also obtained from Eq. (1.16). The general expression of x is given as

$$x = x_{t_0} \cos(pt - \gamma) + \frac{\dot{x}_{t_0}}{p} \sin(pt - \gamma) \quad (1.17)$$

or

$$x = \sqrt{x_{t_0}^2 + \left(\frac{\dot{x}_{t_0}}{p}\right)^2} \cos(pt - \gamma - \alpha) \quad (1.18)$$

in which

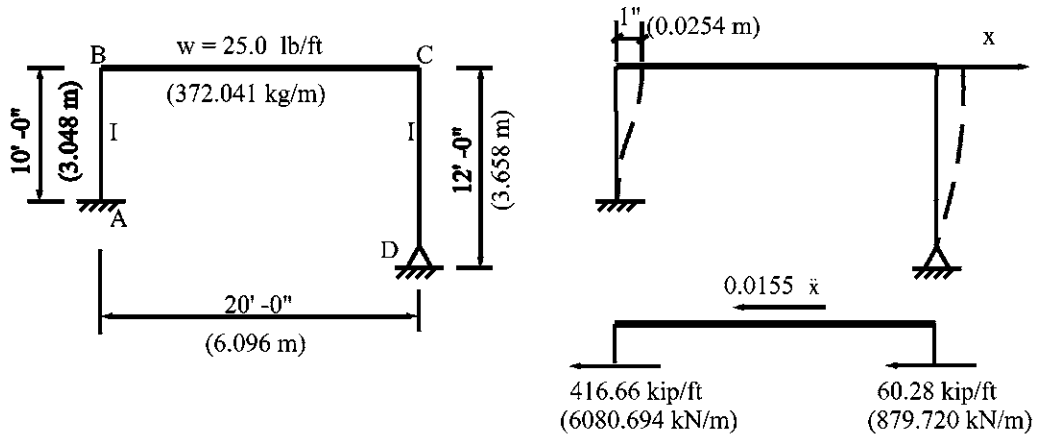
$$\alpha = \tan^{-1} \frac{\dot{x}_{t_0}/p}{x_{t_0}}, \quad \text{and} \quad \gamma = pt_0$$

Fig. 1.2 indicates that the amplitude of a motion depends on the given initial conditions and that all the motions are in the same manner except they are displaced relative to each other along the t axis. The relative magnitude in radians along the t axis between x , \dot{x} , and \ddot{x} is called the *phase angle*. For instance, in Fig. 1.2a, the velocity has a phase angle of 90° ahead of the displacement. This is because

$$\dot{x} = -x_0 p \sin pt = x_0 p \cos\left(pt + \frac{\pi}{2}\right) \quad (1.19)$$

where the displacement, $x = X \cos pt$, is used as the reference curve. Similarly, the displacement in Fig. 1.2b may be said to have a phase angle of 90° behind the displacement in Fig. 1.2a. This is because

$$x = \frac{\dot{x}_0}{p} \sin pt = \frac{\dot{x}_0}{p} \cos\left(pt - \frac{\pi}{2}\right) \quad (1.20)$$

**FIG. 1.3** Example 1.2.1.

The *natural period*, T , in Fig. 1.2 is related to the *natural frequency* f and the *angular frequency* p , as

$$p = \frac{2\pi}{T} = 2\pi f \quad (1.21)$$

$$f = \frac{1}{T} = \frac{p}{2\pi} \quad (1.22)$$

$$T = \frac{1}{f} = \frac{2\pi}{p} \quad (1.23)$$

EXAMPLE 1.2.1 Consider the rigid frame shown in Fig. 1.3 with its infinitely rigid girder, which is disturbed horizontally by the initial conditions of $x_0 = 0$ and $\dot{x}_0 = 10$ ft/sec (3.048 m/sec) at $t = 0$. Find (a) the natural frequency and period and (b) the displacement and velocity at $t = 2$ sec. Let $g = 32.2$ ft/sec 2 (9.815 m/sec 2), $I = 166.67$ in 4 (6,937.329 cm 4), and $E = 30,000$ ksi (20,684.271 kN/cm 2).

Solution: (a) The spring stiffness, K , is the amount of force needed to cause a unit displacement of the girder, BC. This force is equal to the total shear at the top of the columns

$$\frac{12EI}{L_{AB}^3} \quad \text{and} \quad \frac{3EI}{L_{CD}^3} \quad (a)$$

From the accompanying diagram, the equilibrium equation of the spring force and mass inertia is

$$\frac{20w}{g} \ddot{x} + \left(\frac{12EI}{L_{AB}^3} + \frac{3EI}{L_{CD}^3} \right) x = 0 \quad (b)$$

Substituting the given structural properties for the corresponding terms in the above equation yields

$$\frac{20(0.025)}{32.2} \ddot{x} + \frac{30,000(166.67)}{144} \left[\frac{12}{(10)^3} + \frac{3}{(12)^3} \right] x = 0 \quad (c)$$

The final differential equation becomes

$$0.0155 \ddot{x} + 476.9 x = 0 \quad (d)$$

The angular frequency is

$$\rho = \sqrt{\frac{K}{M}} = \sqrt{\frac{476.9}{0.0155}} = 175.4 \text{ rad/sec} \quad (\text{e})$$

from which the natural frequency and period are calculated by using

$$\begin{aligned} f &= \frac{\rho}{2\pi} = \frac{175.4}{2\pi} \\ &= 27.92 \text{ cycles/sec} \end{aligned} \quad (\text{f})$$

$$T = \frac{2\pi}{\rho} = 0.0358 \text{ sec/cycle} \quad (\text{g})$$

(b) Substituting the given initial conditions of $x_0 = 0$ and $\dot{x}_0 = 10 \text{ ft/sec}$ (3.048 m/sec) for the corresponding terms in Eq. (1.16) yields the motion equation

$$\begin{aligned} x &= \frac{\dot{x}_0}{\rho} \sin pt \\ &= \frac{10(12)}{175.4} \sin(175.4t) \end{aligned} \quad (\text{h})$$

and the velocity

$$\begin{aligned} \dot{x} &= \dot{x}_0 \cos pt \\ &= 10(12) \cos(175.4t) \end{aligned} \quad (\text{i})$$

At $t = 2 \text{ sec}$

$$x = -0.5962 \text{ in} \quad (-1.514 \text{ cm}) \quad (\text{j})$$

$$\dot{x} = -58.83 \text{ in/sec} \quad (-149.43 \text{ cm/sec}) \quad (\text{k})$$

By knowing the displacement and velocity at any time, the shears and moments of the constituent members can be calculated.

1.2.3. Periodic and Harmonic Motion

Note that the motion of the structure discussed above is *periodic* as well as *harmonic*; in general, vibrations are periodic but not necessarily harmonic. A typical periodic motion can be illustrated by adding two harmonic motions, each of which has a different frequency

$$x_1 = X_1 \sin p_1 t$$

$$x_2 = X_2 \sin p_2 t$$

If $p_1 = p$ and $p_2 = 2p$, the resultant motion becomes

$$x = X_1 \sin pt + X_2 \sin 2pt \quad (1.24)$$

In Fig. 1.4 the resultant motion represents an irregular periodic motion. The resultant motion can be harmonic if and only if p_1 and p_2 are the same. In other words, *the sum of harmonic motions with the same frequency is itself a harmonic*.

EXAMPLE 1.2.2 Add the harmonic motions of $x_1 = 4 \cos(pt + 32^\circ)$ and $x_2 = 6.5 \sin(pt + 40^\circ)$ for a resultant motion expressed in a sine function.

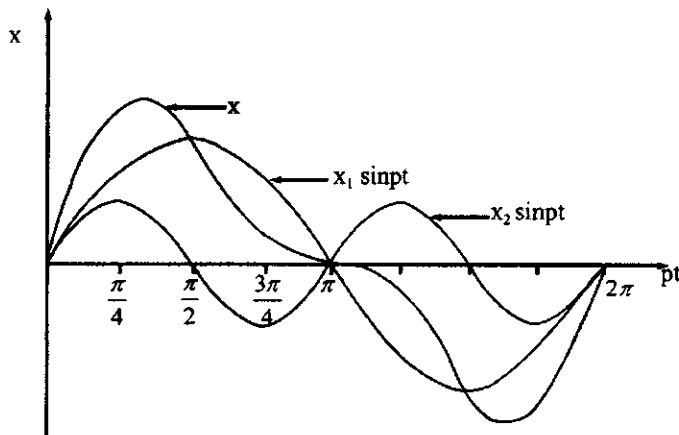


FIG. 1.4 Periodic motion.

Solution: The combined motion is the vector sum of x_1 and x_2 because

$$x = x_1 + x_2 = 4 \cos(pt + 32^\circ) + 6.5 \sin(pt + 40^\circ) \quad (a)$$

By trigonometric transformation, Eq. (a) becomes

$$x = \sin(pt(6.5 \cos 40^\circ - 4 \sin 32^\circ) + \cos(pt(4 \cos 32^\circ + 6.5 \sin 40^\circ)) \quad (b)$$

It is desired to express the resultant motion in a sine function as

$$\begin{aligned} x &= X \sin(pt + \alpha) \\ &= X \cos \alpha \sin pt + X \sin \alpha \cos pt \end{aligned} \quad (c)$$

A comparison of the terms involving $\sin pt$ and $\cos pt$ in Eq. (b) with the identical ones in Eq. (c) gives $X \cos \alpha$ and $X \sin \alpha$. X and α can be obtained through a simple trigonometric operation. The combined motion then becomes

$$x = 8.09 \sin(pt + 69^\circ - 19') \quad (d)$$

Equations (a) and (d) are graphically represented by Fig. 1.5.

1.3. FREE DAMPED VIBRATION

1.3.1. Motion Equation and Viscous Damping

In the previous discussion, we assumed an ideal vibrating system free from internal and external damping. *Damping* may be defined as a force that resists motion at all times. Therefore, a free undamped vibration continues in motion indefinitely without its amplitude diminishing or its frequency changing. Real systems, however, do not possess perfectly elastic springs nor are they surrounded by a frictionless medium. Various damping agents—such as the frictional forces of structural joints and bearing supports, the resistance of surrounding air, and the internal friction between molecules of the structural materials—always exist.

It is difficult if not impossible to derive a mathematical formula for damping resistance that represents the actual behavior of a physical system. A simple yet realistic damping model for mathematical analysis is that the damping force is proportional to velocity. This model can represent structural damping of which the force is produced by the viscous friction of a fluid

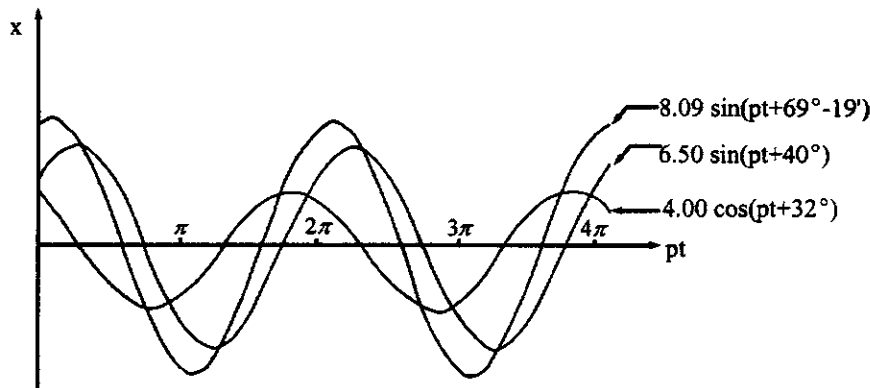


FIG. 1.5 Harmonic motion.

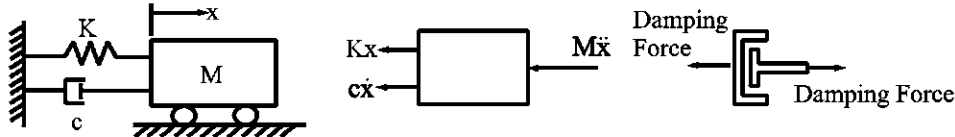


FIG. 1.6 Spring-mass and viscous damping model.

and is therefore called *viscous damping*. Fig. 1.6 shows a vibration model consisting of an ideal spring and *dashpot* in parallel. The dashpot exerts a damping force, $c\dot{x}$, proportional to the relative velocity, in which c is a proportionality and is called the *coefficient of viscous damping*. How to evaluate damping is further discussed in Section 1.3.3 and later in Section 1.6.

The governing differential equation for free vibrations accompanied by damping is

$$M\ddot{x} + c\dot{x} + Kx = 0 \quad (1.25)$$

of which the standard solution is

$$x = C_1 e^{\alpha_1 t} + C_2 e^{\alpha_2 t} \quad (1.26)$$

where C_1 and C_2 are integration constants, and α_1 and α_2 are two roots of the auxiliary equation which can be obtained by using $x = D e^{\alpha t}$. Substituting x , \dot{x} , and \ddot{x} into Eq. (1.25) yields

$$M\alpha^2 + c\alpha + K = 0 \quad (1.27)$$

which gives

$$\alpha_1 = -\frac{c}{2M} + \sqrt{\frac{c^2}{4M^2} - \frac{K}{M}} \quad (1.28)$$

$$\alpha_2 = -\frac{c}{2M} - \sqrt{\frac{c^2}{4M^2} - \frac{K}{M}} \quad (1.29)$$

After substituting Eqs. (1.28) and (1.29) for the corresponding terms in Eq. (1.26), three possible solutions can be obtained for the cases of $c^2/4M^2 = K/M$, $c^2/4M^2 > K/M$, and $c^2/4M^2 < K/M$. Each of these three cases is now discussed in detail.

1.3.2. Critical Damping, Overdamping and Underdamping

1.3.2.1. Critical Damping

When $c^2/4M^2 = K/M$, the value of c is called *critical damping* and takes the form

$$c_{cr} = 2\sqrt{KM} = 2Mp = \frac{2K}{p} \quad (1.30)$$

The ratio of c/c_{cr} is called *viscous damping factor* or simply *damping factor*, ρ , and may be expressed as

$$\rho = \frac{c}{c_{cr}} = \frac{c}{2Mp} = \frac{c}{2\sqrt{(KM)}} = \frac{cp}{2K} \quad (1.31)$$

When $\rho = 1$, Eqs. (1.28) and (1.29) become

$$\alpha_1 = \alpha_2 = -\rho p = -p \quad (1.32)$$

Substituting Eq. (1.32) for the corresponding element in Eq. (1.26) with consideration of repeating coefficients α_1 and α_2 yields

$$x = (C_1 + C_2 t)e^{-pt} \quad (1.33)$$

in which the arbitrary constants C_1 and C_2 should be determined by using the initial conditions of a motion. If $x_0 = 0$ and $\dot{x}_0 = p$ at $t = 0$ are inserted into Eq. (1.33), then

$$x = pte^{-pt} \quad (1.34)$$

This is plotted (x vs. pt) in Fig. (1.7) for $\rho = 1$. It can be seen that the critical damping produces a sluggish motion, and the mass moves very slowly back to the neutral position.

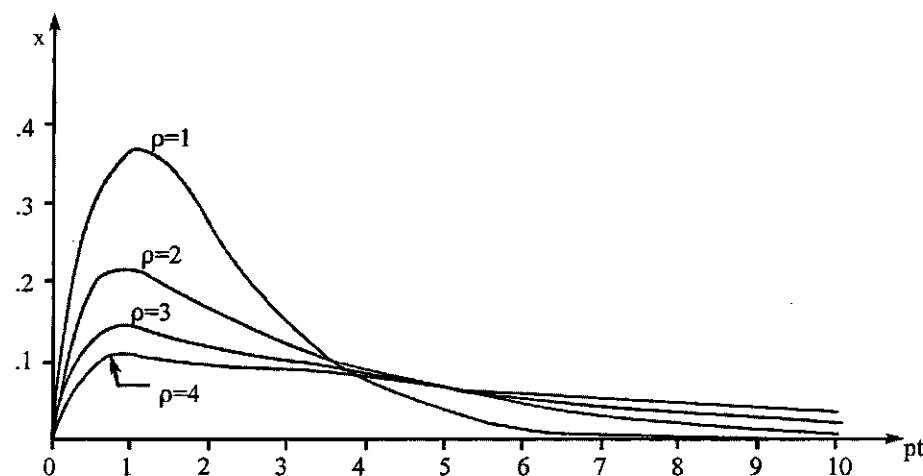


FIG. 1.7 Motion with overdamping.

1.3.2.2. Overdamping

When $c^2/4M^2 > K/M$ or $\rho > 1$, the damping is called *supercritical*. A structure with such a damping coefficient is said to be *overdamped*. For this case, Eqs. (1.28) and (1.29) become

$$\alpha_1 = -\rho p + p\sqrt{\rho^2 - 1} \quad (1.35)$$

$$\alpha_2 = -\rho p - p\sqrt{\rho^2 - 1} \quad (1.36)$$

Substituting α_1 and α_2 for the corresponding terms in Eq. (1.26) yields

$$x = e^{-\rho pt} \left(C_1 e^{(p\sqrt{(\rho^2-1)})t} + C_2 e^{(-p\sqrt{(\rho^2-1)})t} \right) \quad (1.37)$$

If the initial displacement and velocity are given as $x_0 = 0$ and $\dot{x}_0 = p$ at $t = 0$, Eq. (1.37) becomes

$$x = \frac{1}{2\sqrt{\rho^2 - 1}} \left(e^{(p\sqrt{(\rho^2-1)})t} - e^{(-p\sqrt{(\rho^2-1)})t} \right) e^{-\rho pt} \quad (1.38)$$

The effect of overdamping on a motion is shown in Fig. 1.7 for $\rho = 2, 3$, and 4 . When the damping factor is large, the mass moves more slowly back to the neutral position and the system exhibits larger displacement after a certain length of motion.

1.3.2.3. Underdamping

When $c^2/4M^2 < K/M$ or $\rho < 1$, the damping is called *subcritical* or *underdamping*. In most structural and mechanical systems, the assumption of underdamping is justified. For this case, Eqs. (1.28) and (1.29) become

$$\alpha_1 = -\rho p + ip\sqrt{1 - \rho^2} \quad (1.39)$$

$$\alpha_2 = -\rho p - ip\sqrt{1 - \rho^2} \quad (1.40)$$

Substitute the above for the corresponding terms in Eq. (1.26), which is then transformed into a trigonometric function as

$$x = e^{-\rho pt} \left(A \cos \sqrt{1 - \rho^2} pt + B \sin \sqrt{1 - \rho^2} pt \right) \quad (1.41)$$

where $A = C_1 + C_2$ and $B = i(C_1 - C_2)$. A compact form of Eq. (1.41) is

$$x = Ce^{-\rho pt} \cos \left(\sqrt{1 - \rho^2} pt - \alpha \right) \quad (1.42)$$

The relationship between C , α and A , B is

$$C^2 = A^2 + B^2$$

$$\alpha = \tan^{-1} \frac{B}{A}$$

Then the given initial conditions of x and \dot{x} can be used to determine either A and B from Eq. (1.41) or C and α from Eq. (1.42).

The oscillatory motion of Eq. (1.42) has the period which may be called *damped period* in order to differentiate from *undamped period*, T , as

$$T^* = \frac{2\pi}{p\sqrt{(1 - \rho^2)}} = \frac{T}{\sqrt{(1 - \rho^2)}} \quad (1.43)$$

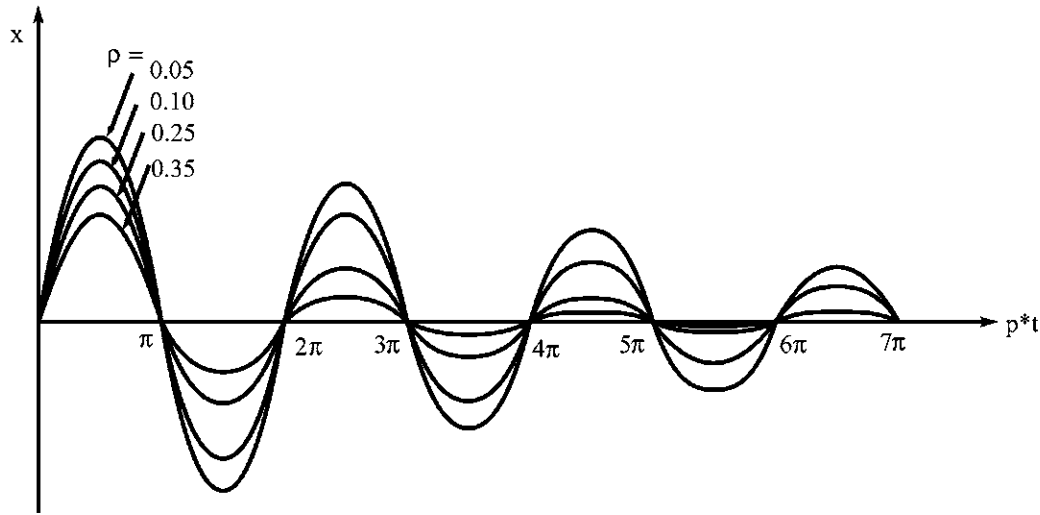


FIG. 1.8 Motion with underdamping.

of which the associated frequency, called *damped frequency*, is

$$p^* = p\sqrt{1 - \rho^2} \quad (1.44)$$

Observe that the difference between p^* , T^* and p , T is slight. The terms p and T may be used instead of p^* and T^* in damped vibrations without introducing a serious error.

If the given initial conditions of $x_0 = 0$ and $\dot{x}_0 = p$ at $t = 0$ are inserted into Eq. (1.42), we obtain

$$x = \frac{1}{\sqrt{1 - \rho^2}} e^{-\rho p t} \cos\left(\sqrt{1 - \rho^2} p t - \frac{\pi}{2}\right) \quad (1.45)$$

which is plotted in Fig. 1.8 for various damping factors of 0.05, 0.10, 0.25, and 0.35. It can be seen that the amplitudes of successive cycles are different and the periods of successive cycles are the same; strictly speaking, the motion is not regarded as being periodic but as *time-periodic*. In most engineering structures, ρ may vary from 0.02 to 0.08. Of course, the damping factor for some buildings may be as high as 0.15, depending on the nature of the material used in their construction and the degree of looseness in their connections.

1.3.3. Logarithmic Decrement and Evaluation of Viscous Damping Coefficient

Let

$$\rho^* = \frac{\rho}{\sqrt{1 - \rho^2}} \quad (1.46)$$

Then Eq. (1.42) can be rewritten as

$$x = C e^{-\rho^* p^* t} \cos(p^* t - \alpha) \quad (1.47)$$

which is plotted for x vs. p^*t in Fig. 1.9, showing that the displacements x_n and x_{n+1} at p^*t_n and

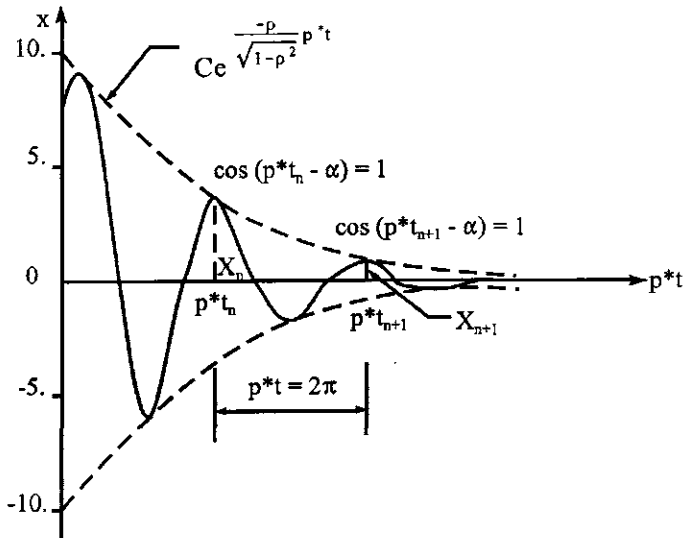


FIG. 1.9 Logarithmic decrement.

$p^* t_{n+1}$ are maximum because

$$\cos(p^* t_n - \alpha) = 1 = \cos(p^* t_{n+1} - \alpha)$$

and the period between these two displacements is

$$p^*(t_{n+1} - t_n) = 2\pi$$

for which the corresponding amplitudes are

$$X_n = C e^{-\rho^* p^* t_n} \quad (1.48)$$

$$X_{n+1} = C e^{-\rho^* (p^* t_n + 2\pi)} \quad (1.49)$$

Therefore, the ratio between any two consecutive amplitudes can be expressed by

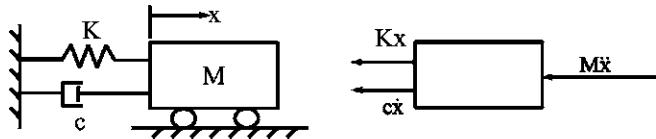
$$\frac{X_n}{X_{n+1}} = \frac{C e^{-\rho^* p^* t_n}}{C e^{-\rho^* (p^* t_n + 2\pi)}} = e^{\rho^* 2\pi} = e^\beta \quad (1.50)$$

From Eqs. (1.46) and (1.50)

$$\beta = \frac{\rho}{\sqrt{1 - \rho^2}} 2\pi = \ln \left(\frac{X_n}{X_{n+1}} \right) \quad (1.51)$$

β is called the *logarithmic decrement*, a measurement of the damping capacity of a structure, and is particularly useful in experiments designed for measuring the coefficient of viscous damping. As noted, other methods of evaluating damping coefficients are presented in Section 1.6.

EXAMPLE 1.3.1 The displacement-time record of a structure subjected to free vibrations has an exponentially decaying cosine curve for which the measurement indicates that the amplitudes decrease 90% after 10 cycles. Find the logarithmic decrement and the viscous damping factor.

**FIG. 1.10** Example 1.3.2.

Solution: Assume that the 10 consecutive cycles start at any cycle n ; then, by using Eq. (1.50), the result is

$$(e^{\beta})^{10} = \frac{X_n}{X_{n+1}} \cdot \frac{X_{n+1}}{X_{n+2}} \cdots \frac{X_{n+8}}{X_{n+9}} \cdot \frac{X_{n+9}}{X_{n+10}} \quad (a)$$

Inserting the 10% of amplitude decrease into the above equation gives

$$e^{10\beta} = \frac{X_n}{X_{n+10}} = \frac{X_n}{0.1X_n} = 10 \quad (b)$$

then

$$10\beta \ln(e) = \ln(10) \quad (c)$$

Therefore, the logarithmic decrement is

$$\beta = \frac{2.3026}{10} = 0.23026 \quad (d)$$

and the viscous damping factor is

$$\rho = \frac{\beta}{\sqrt{4\pi^2 + \beta^2}} = \frac{0.23026}{\sqrt{39.48 + 0.053}} = 0.0366 \quad (e)$$

EXAMPLE 1.3.2 Find the motion equation for the vibrating model shown in Fig. 1.10. The model consists of a mass, $M = 0.1 \text{ lb sec}^2/\text{in}$ ($1.240 \text{ kg sec}^2/\text{cm}$), a spring stiffness, $K = 100 \text{ lb/in}$ ($1.751 \times 10^4 \text{ N/m}$), and a coefficient of viscous damping, $c = 2 \text{ lb sec/in}$ (350.254 N sec/cm). Initial displacement and velocity are $x_0 = 1 \text{ in}$ (2.540 cm) and $\dot{x}_0 = 0$ at $t = 0$.

Solution: The critical damping coefficient and the damping factor are

$$c_{cr} = 2\sqrt{KM} = 2\sqrt{100(0.1)} \\ = 6.32 \text{ lb sec/in} (1,106.801 \text{ N sec/m}) \quad (a)$$

$$\rho = \frac{2}{6.32} = 0.316 \quad (b)$$

The angular frequencies with and without consideration of damping are

$$\rho = \sqrt{\frac{100}{0.1}} = 31.6 \text{ rad/sec} \quad (c)$$

$$\rho^* = \sqrt{1 - (0.316)^2} (31.6) = 30 \text{ rad/sec} \quad (d)$$

Displacement of the free underdamped vibration is given by Eq. (1.47) for which a general expression of the displacement motion can be found for the arbitrary initial conditions of x

$= x_0$ at $\dot{x} = \dot{x}_0$ at $t = 0$. Thus the phase angle and the amplitude are

$$\alpha = \tan^{-1} \frac{x_0 \rho^* p^* + \dot{x}_0}{x_0 p^*} \quad (e)$$

$$C = \frac{1}{p^*} \left(\dot{x}_0^2 + 2x_0 \dot{x}_0 \rho^* p + \frac{x_0^2 p^{*2}}{1 - \rho^2} \right)^{1/2} \quad (f)$$

For the given $x_0 = 1$ and $\dot{x}_0 = 0$, from Eq. (e), the phase angle becomes

$$\alpha = \tan^{-1} \frac{(1)(30)(0.3339) + 0}{(1)(30)} = 0.322 \text{ rad} \quad (g)$$

The amplitude can be calculated from Eq. (f) as

$$C = \frac{1}{30} \sqrt{\frac{(1)^2 (30)^2}{1 - (0.316)^2}} = \frac{31.6}{30} = 1.053 \text{ in (2.675 cm)} \quad (h)$$

Inserting the values for α and C into Eq. (1.47) gives the motion equation

$$x = 1.053 e^{-10t} \cos(30t - 0.322) \quad (i)$$

1.4. FORCED UNDAMPED VIBRATION

From the previous discussion, a system in time-dependent motion is due to an initial disturbance of either displacement or velocity, or a combination of both. This motion, due solely to the action of the restoring force and free from external forces, is called *free vibration*. Now the topic is *forced vibration*, which results from the action of various types of time-dependent excitation that may be sinusoidal forces, foundation movements, or impulsive loads. The response of a system may or may not involve the effect of free vibration resulting from an initial disturbance.

1.4.1. Harmonic Forces

Consider the spring-mass model shown in Fig. 1.11 where the mass is subjected to a harmonic force $F \sin \omega t$ with *forced frequency* ω . Let $F \sin \omega t$ be considered positive to the right of the equilibrium position from which displacement, x , is measured. The differential equation of motion is

$$M\ddot{x} + Kx = F \sin \omega t \quad (1.52)$$

for which the homogeneous solution is $x_h = A \sin pt + B \cos pt$; the term, $p = \sqrt{(K/M)}$, is independent of the forced frequency, ω . The particular solution may be obtained by trying the following

$$x_p = C_1 \sin \omega t + C_2 \cos \omega t \quad (1.53)$$

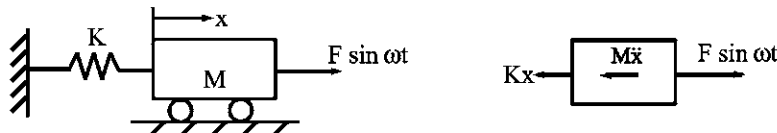


FIG. 1.11 Spring-mass model with harmonic force.

Substituting x_p and \ddot{x}_p for the corresponding terms in Eq. (1.52), and then collecting the terms, yields

$$[(-M\omega^2 + K)C_1 - F] \sin \omega t + (K - M\omega^2)C_2 \cos \omega t = 0 \quad (1.54)$$

Since it is unnecessary for $\sin \omega t$ and $\cos \omega t$ to be zero for any time, t , Eq. (1.54) can be satisfied only if the terms associated with $\sin \omega t$ and $\cos \omega t$ are each equal to zero. Consequently, the constants C_1 and C_2 are

$$C_1 = \frac{F}{K - M\omega^2} \quad (1.55)$$

$$C_2 = 0 \quad (1.56)$$

The complete solution of Eq. (1.52) finally becomes

$$\begin{aligned} x &= x_h + x_p \\ &= A \sin pt + B \cos pt + \frac{F}{K - M\omega^2} \sin \omega t \end{aligned} \quad (1.57)$$

in which A and B should be determined by using the initial conditions of free vibration. When the force $F \sin \omega t$ is applied from a position of rest, ignore x_h (free vibration due to x_0 and \dot{x}_0). The response of forced vibration corresponding to the third term of Eq. (1.57) is

$$x = \frac{F/K}{1 - (\omega^2/p^2)} \sin \omega t = H \sin \omega t \quad (1.58)$$

which indicates that the motion is periodic with the same frequency as that of the force and may endure as long as the force remains on the mass; this is called *steady-state vibration*.

In general, the application of a disturbing force can produce an additional motion superimposed on steady-state motion. This additional motion is from the homogeneous solution of the free vibration. Consider the initial conditions of $x_0 = 0$ and $\dot{x}_0 = 0$ at $t = 0$ in Eq. (1.57). The result is

$$A = -\frac{F\omega}{p(K - M\omega^2)}, \quad B = 0$$

and

$$x = \frac{F}{(K - M\omega^2)} \left(\sin \omega t - \frac{\omega}{p} \sin pt \right) \quad (1.59)$$

Comparing Eq. (1.59) with Eq. (1.58) reveals that there is another term associated with $\sin pt$. This is due to the fact that the application of a disturbing force produces some free vibrations of the system as represented by the integration constant A shown above. Thus the actual motion is a superposition of two harmonic motions with different frequencies, amplitudes, and phase angles. In practical engineering, there is always some damping. So free vibration is eventually damped out, and only forced vibration remains. The early part of a motion consisting of a forced vibration and a few cycles of free vibration is called *transient vibration*, which can be important in aircraft design for landing and for gust loading [1,2].

1.4.2. Steady-State Vibration and Resonance

Now examine the behavior of the steady-state vibration of Eq. (1.58). The plot of the absolute value of amplitude, H , as $|H|$ vs ω in Fig. 1.12 shows that when $\omega = 0$, the amplitude is equal to static deflection, F/K , and when $\omega \rightarrow \infty$, the amplitude is equal to zero. In the neighborhood of p , the amplitude approaches infinity.

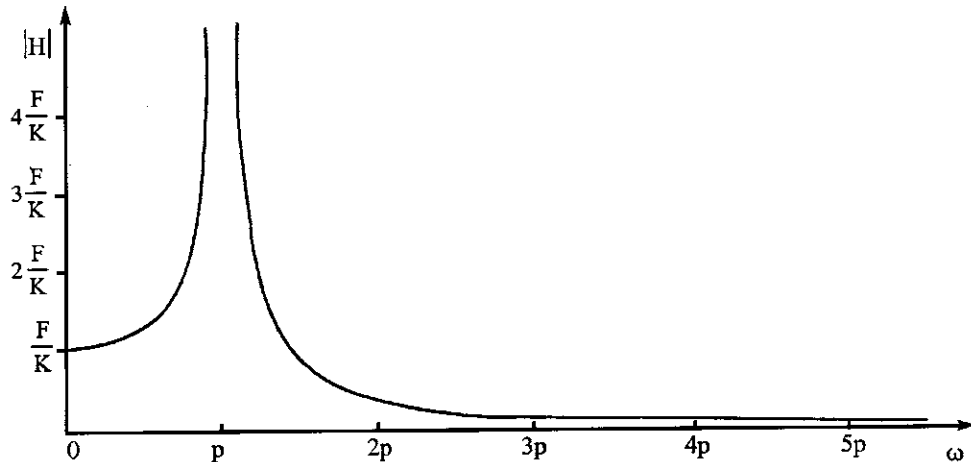


FIG. 1.12 Resonance.

When the forced frequency is equal to the natural frequency, as $\omega = p$, the vibratory displacement becomes infinitely large; this phenomenon is called *resonance*. The infinite amplitude, however, cannot build up in a finite length of time. To see how the amplitude behaves in resonance, we may find that Eq. (1.55) does not work for $\omega = p$ because using the trial solution shown in Eq. (1.53) yields Eq. (1.55) which becomes infinitive when $\omega = p$. Thus, Eq. (1.53) should be rewritten as

$$x_p = C_1 t \cos pt \quad (1.60)$$

Substituting x_p and \ddot{x}_p for the corresponding terms in Eq. (1.52) yields

$$C_1 = -\frac{F}{2Mp} \quad (1.61)$$

The complete solution of Eq. (1.52) is

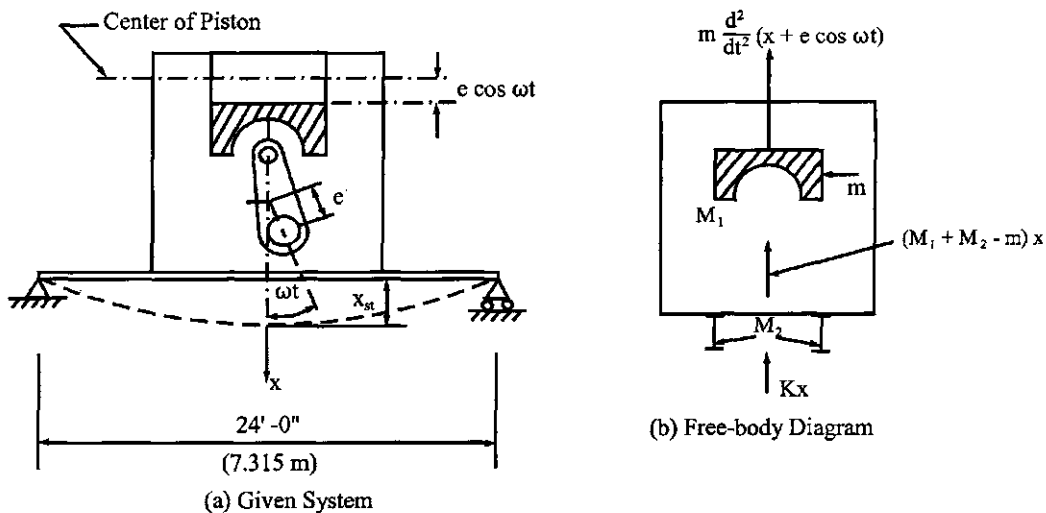
$$x = A \sin pt + B \cos pt - \frac{F}{2Mp} t \cos pt \quad (1.62)$$

For the initial conditions of $x = x_0$ and $\dot{x} = \dot{x}_0$ at $t = 0$, we have

$$x = x_0 \cos pt + \frac{\dot{x}_0}{p} \sin pt - \frac{F}{2Mp} \left(t \cos pt - \frac{\sin pt}{p} \right) \quad (1.63)$$

which shows that an infinitely large displacement of x can be obtained only when the force is applied for an infinitely long period of t . Practically, structural engineers are not interested in resonance but in a natural frequency in the neighborhood of forced frequency that may cause objectionable deflections and stresses.

EXAMPLE 1.4.1 A machine of mass, M_1 , weighs 5000 lb (2267.962 kg) and is supported by two beams as shown in Fig. 1.13. Each beam has $I = 2094.6 \text{ in}^4$ ($87,184 \text{ cm}^4$) and $S = 175.4 \text{ in}^3$ (2874 cm^3), and weight of 76 lb/ft (113.1 kg/m). This machine has a vertically reciprocating piston of mass, m , weighing 15 lb (6.804 kg) that is driven by an eccentric with 6 in (15.24 cm) eccentricity. Motion of the piston may be written as $e \cos \omega t$, where ω is the angular velocity of the eccentric, and e is the eccentricity. The motion of the system is denoted by x measured downward from the equilibrium position, and total motion of the piston is $x + e \cos \omega t$. Assume that the beam

**FIG. 1.13** Example 1.4.1.

mass, M_2 , is half the beam weight and is concentrated at the beam center, the allowable bending stress, F_b , equals 20 ksi (13.789 kN/cm^2), and the modulus of elasticity, E , is 30,000 ksi ($20,684.271 \text{ kN/cm}^2$). Find the desirable forced frequency.

Solution: From the free-body diagram shown in Fig. 1.13b, the differential equation of motion is

$$(M_1 + M_2 - m)\ddot{x} + m \frac{d^2}{dt^2}(x + e \cos \omega t) + Kx = 0 \quad (\text{a})$$

Let $M = M_1 + M_2$; then Eq. (a) becomes

$$M\ddot{x} + Kx = m\omega^2 \cos \omega t \quad (\text{b})$$

which is identical to Eq. (1.52). Thus the steady-state vibration is

$$x = \frac{m\omega^2}{K - M\omega^2} \cos \omega t \quad (\text{c})$$

When $\cos \omega t = \pm 1$, Eq. (c) yields

$$\frac{XK}{m\omega^2} = \pm \frac{1}{1 - (\omega/p)^2} \quad (\text{d})$$

Let $m\omega^2$ be interpreted as a static force; then $XK/m\omega^2$ represents the ratio of the dynamic force, XK , to the static force, $m\omega^2$, or the ratio of the amplitude, X , to the static deflection, $m\omega^2/K$. This ratio relationship is called *amplification factor*.

The spring stiffness, K , is the inverse of the deflection, $\delta = (1)L^3/48EI$, which is obtained by applying a unit load at the center of the simple beam (at the mass). Thus,

$$\begin{aligned} K &= \frac{48EI}{L^3} = \frac{48(30,000,000)(2094.6)2}{1728(24)^3} \\ &= 252,532 \text{ lb/in (3685.427 kN/m)} \end{aligned} \quad (\text{e})$$

Therefore the angular frequency is calculated as

$$\begin{aligned} M &= M_1 + M_2 = \frac{1}{32.2(12)} \left[\frac{24}{2} (76)(2) + 5000 \right] \\ &= 17.7 \text{ lb sec}^2/\text{in} (2.195 \text{ kg sec}^2/\text{m}) \end{aligned} \quad (\text{f})$$

$$\begin{aligned} p &= \sqrt{\frac{K}{M}} = \sqrt{\frac{252,532}{17.7}} \\ &= 119.5 \text{ rad/sec} \end{aligned} \quad (\text{g})$$

Because the displacement, x , is measured from the equilibrium position, the bending moment of the beam at any time during the motion should be the result of the effect of the deflection caused by the combined weight of beams and machine and that of the dynamic displacement. Let XK be an equivalent force called P_{equ} ; then the total force causing the bending moment is $P = P_{equ} + \text{half the weight of the beams} + \text{machine weight}$, for which the bending stress is

$$f = \frac{\text{moment}}{S} = \frac{PL}{4S} \quad (\text{h})$$

where S is the section modulus. Solving for P yields

$$\begin{aligned} P &= \frac{4Sf}{L} = \frac{4(175.4)(2)(20,000)}{24(12)} \\ &= 97,500 \text{ lb} (433.701 \text{ kN}) \end{aligned} \quad (\text{i})$$

Therefore, the equivalent force becomes

$$\begin{aligned} P_{equ} &= 97,500 - 1824 - 5000 \\ &= 90,676 \text{ lb} (403.347 \text{ kN}) \end{aligned} \quad (\text{j})$$

From Eq. (d), we have

$$XK \left[1 - \left(\frac{\omega}{p} \right)^2 \right] = \pm mew^2 \quad (\text{k})$$

in which

$$mew^2 = \frac{15}{32.2(12)} (6)\omega^2 = 0.233\omega^2 \quad (\text{l})$$

Thus,

$$90,676 - \frac{90,676}{(119.5)^2} \omega^2 \pm 0.233\omega^2 = 0 \quad (\text{m})$$

of which the solutions are

$$\omega_1^2 = 13,775 \quad \text{or} \quad \omega_1 = 117.4 \text{ rad/sec} \quad (\text{n})$$

$$\omega_2^2 = 14,823 \quad \text{or} \quad \omega_2 = 121.7 \text{ rad/sec} \quad (\text{o})$$

The frequencies between ω_1 and ω_2 , being close to $p = 119.5$ rad/sec, produce bending stress greater than allowable.

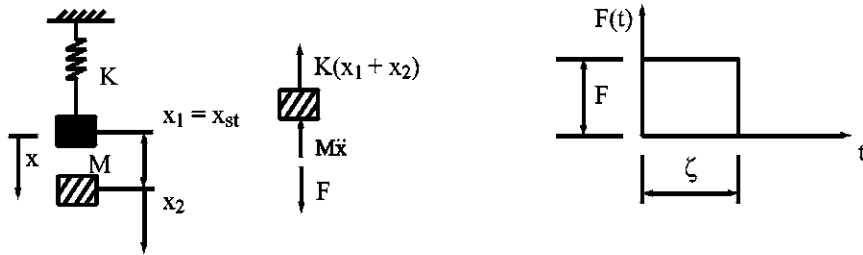


FIG. 1.14 Spring-mass model with rectangular impulse.

1.4.3. Impulses and Shock Spectra

1.4.3.1. Rectangular Force

When a mass is subjected to a suddenly applied force, the amplitude of the motion may be of considerable magnitude. Maximum amplitude may occur during or after the application of the *impulsive load*, and its amount depends on the ratio of natural period of the structure to the period of the force. Consider that the spring-mass system shown in Fig. 1.14 is subjected to a constant impulsive load as *rectangular force* F with a period of ζ . The differential equation of motion is

$$M\ddot{x} + Kx = F \quad (1.64)$$

of which the homogeneous solution is

$$x_h = A \sin pt + B \cos pt$$

For the second-order differential equation, the particular solution can be obtained by using the polynomial equation with three constants as

$$x_p = C_1 + C_2t + C_3t^2 \quad (1.65)$$

Substituting x_p and \dot{x}_p for the corresponding terms in Eq. (1.64) yields

$$C_1 = \frac{F}{K}, C_2 = C_3 = 0$$

The complete solution of Eq. (1.64) is

$$\begin{aligned} x &= x_h + x_p \\ &= A \sin pt + B \cos pt + \frac{F}{K} \end{aligned} \quad (1.66)$$

When initial conditions are given as $x = x_0$ and $\dot{x} = \dot{x}_0$ at $t = 0$, Eq. (1.66) takes the form

$$x = x_0 \cos pt + \frac{\dot{x}_0}{p} \sin pt + \frac{F}{K} (1 - \cos pt) \quad (1.67)$$

If the mass is at rest until the force is suddenly applied, the motion including the initial condition

due to the application of the force becomes

$$\begin{aligned} x &= \frac{F}{K} (1 - \cos pt) \\ &= x_{st} (1 - \cos pt) \end{aligned} \quad (1.68)$$

It is important to find the vibration's maximum amplitude because it may occur during or after the pulse. Take the first case of maximum displacement that occurs during the pulse for which the velocity is

$$\dot{x} = x_{st}p \sin pt = 0 \quad (1.69)$$

where $x_{st} \neq 0$ and $p \neq 0$. Then $\sin pt = 0$ or $pt = n\pi, n = 1, 2, \dots, \infty$. If $n = 1$, substituting π for pt in Eq. (1.68) and solving for the amplification factor yields

$$\begin{aligned} A_m &= \frac{X}{x_{st}} = 1 - \cos \pi \\ &= 2 \end{aligned} \quad (1.70)$$

Because $t = \pi/p$ and $p = 2\pi/T$, we obtain

$$t = \frac{T}{2} \text{ for } t \leq \zeta \text{ or } \frac{\zeta}{T} \geq 1/2 \quad (1.71)$$

It may be concluded that *if the natural period is less than or equal to twice the forcing period, then the maximum amplitude occurs during the pulse, and the amplification factor is 2.*

When the maximum displacement occurs after the pulse, the relationship between T and ζ is

$$\frac{\zeta}{T} < 1/2 \quad (1.72)$$

for which the motion equation is

$$x = A \sin pt_1 + B \cos pt_1 \quad (1.73)$$

where t_1 originates at $t = \zeta$ (see Fig. 1.14). Initial conditions of the free vibration in Eq. (1.73) are $x = x_0$ and $\dot{x} = \dot{x}_0$ at $t_1 = 0$, and should be the displacement and velocity obtained from Eq. (1.68) at $t = \zeta$ as

$$x_0 = x_{st}(1 - \cos p\zeta) \quad (1.74)$$

$$\dot{x}_0 = x_{st}p \sin p\zeta \quad (1.75)$$

Inserting Eqs. (1.74) and (1.75) into Eq. (1.73) gives

$$x = x_{st} \sin p\zeta \sin pt_1 + x_{st} (1 - \cos p\zeta) \cos pt_1 \quad (1.76)$$

of which the amplitude may be obtained by using $x = X \cos(pt_1 + \alpha)$ as

$$X = x_{st} \sqrt{2(1 - \cos p\zeta)} \quad (1.77)$$

Thus the amplification factor is

$$A_m = \sqrt{2 \left(1 - \cos \frac{2\pi\zeta}{T} \right)} \quad (1.78)$$

Note that the *amplification factor varies from zero to two and depends solely on the magnitudes of ζ and T .*

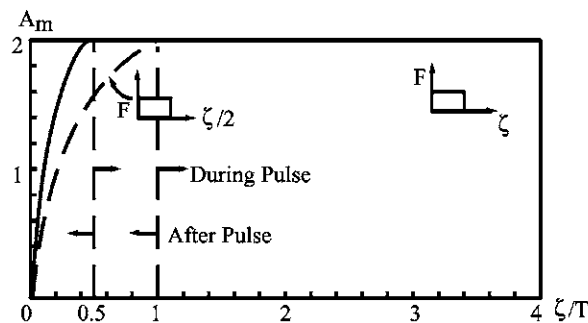


FIG. 1.15 Shock spectra for rectangular impulses.

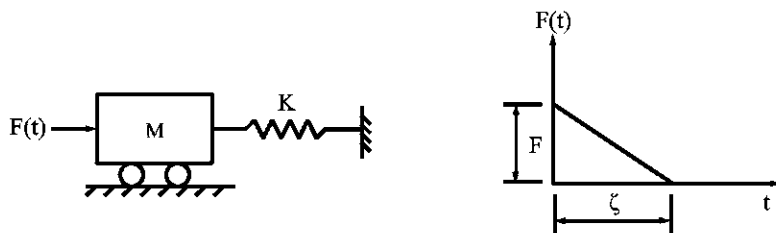


FIG. 1.16 Spring-mass model with triangular impulse.

EXAMPLE 1.4.2 Find the amplification factors corresponding to various ratios of ζ/T and plot a curve for A_m vs ζ/T .

Solution: From Eq. (1.71), it is known that when $\zeta/T \geq \frac{1}{2}$ the amplification is always 2. When $\zeta/T < \frac{1}{2}$, the amplification factors are calculated from Eq. (1.78) as follows

	ζ/T					
A_m Eq. (1.78)	0	$\frac{1}{8}$	$\frac{1}{6}$	$\frac{1}{4}$	$\frac{1}{3}$	$\frac{1}{2}$
	0	0.765	1	1.414	1.73	2

The plot of maximum values of amplitude X (or X/x_{st}) vs structural period T (or ζ/T) for a given disturbance is called the *response spectrum*. If the disturbance is an impulsive type, the plot of the response is usually referred to as a *shock spectrum*. Fig. 1.15 shows the *shock spectra* for two rectangular impulses.

1.4.3.2. Triangular Force

Consider Fig. 1.16, in which the mass is subjected to a *triangular impulse*. The force varies linearly from a maximum value of F at $t = 0$ to a minimum value of zero at $t = \zeta$; the forcing function is described by

$$F(t) = F \left(1 - \frac{t}{\zeta}\right) \quad (1.79)$$

Complete solution of the vibrating system is

$$x = A \sin pt + B \cos pt + \frac{F}{K} \left(1 - \frac{t}{\zeta} \right) \quad (1.80)$$

For $x_0 = 0$ and $\dot{x}_0 = 0$ at $t = 0$, the motion equation is

$$x = x_{st} \left[1 - \cos pt + \frac{1}{\zeta} \left(\frac{\sin pt}{p} - t \right) \right] \quad (1.81)$$

in which $x_{st} = F/K$. Suppose that the maximum displacement occurs during the pulse; then the time, t , corresponding to the maximum displacement can be determined from Eq. (1.81) for zero velocity. Thus, from Eq. (1.81)

$$\frac{1}{\zeta} (1 - \cos pt) = p \sin pt \quad (1.82)$$

After a simple trigonometric manipulation, substituting $p = 2\pi/T$ yields

$$\cos pt = \cos 2\pi \frac{t}{T} = \frac{1 - (2\pi(\zeta/T))^2}{1 + (2\pi(\zeta/T))^2} \quad (1.83a)$$

$$\sin pt = \frac{4\pi(\zeta/T)}{1 + (2\pi(\zeta/T))^2} \quad (1.83b)$$

Let t_m be the time when the maximum response occurs; the time can be obtained from

$$2\pi \frac{t_m}{T} = \cos^{-1} \frac{1 - (2\pi(\zeta/T))^2}{1 + (2\pi(\zeta/T))^2} \quad (1.84)$$

(t_m/T) vs (ζ/T) is plotted in Fig. 1.17b. By inserting Eq. (1.83a or b) into Eq. (1.81), the amplification factor is

$$A_m = \frac{X}{x_{st}} = 2 - \frac{t}{\zeta} \quad (1.85a)$$

Note that t must satisfy Eq. (1.83a,b) and that the amplification factor varies from 1 to 2. The

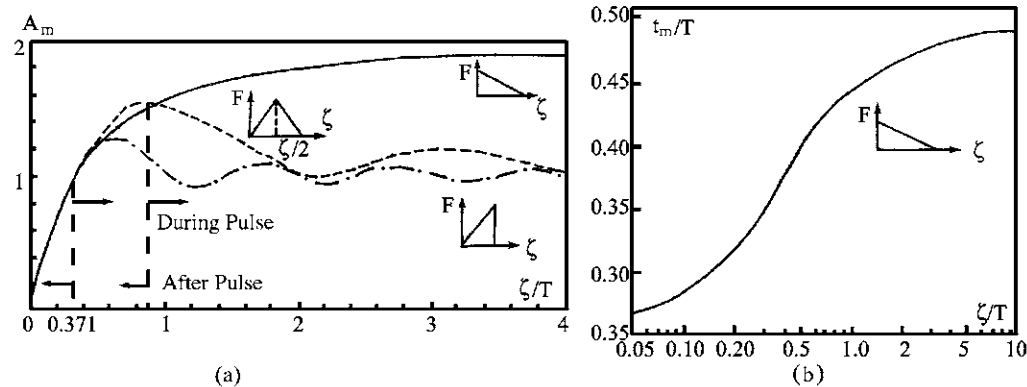


FIG. 1.17 Shock spectra for triangular impulses.

general expression of the amplification factor should be based on Eq. (1.81) as

$$A_m = 1 - \cos pt + \frac{\sin pt}{p\zeta} - \frac{t}{\zeta} \quad (1.85b)$$

EXAMPLE 1.4.3 Find the relationship between the natural period, T , and the forced period, ζ , of the impulsive load shown in Fig. 1.16 for the condition that the maximum displacement occurs during the pulse.

Solution: Since the amplification factor in Eq. (1.85a,b) is derived for the maximum displacement occurring at $t < \zeta$, $t = \zeta$ and $p = 2\pi/T$ can be substituted for the corresponding terms in Eq. (1.83) for the relationship of ζ/T . Solving by trial and error yields an equality condition that when $\zeta/T = 0.371$

$$\begin{aligned} -0.6905 &= \frac{1 - (2\pi)^2(0.371)^2}{1 + (2\pi)^2(0.371)^2} \\ &= -0.691 \end{aligned}$$

Thus, it is concluded that *when $\zeta/T \geq 0.371$, the maximum displacement occurs during the pulse*.

For the case when maximum displacement occurs after the pulse, the motion equation is

$$x = A \sin pt_1 + B \cos pt_1 \quad (a)$$

in which t_1 originates at the end of the pulse, i.e. $t = \zeta$, $t_1 = 0$. The terms A and B can be determined by using the displacement and velocity from either Eq. (1.80) or (1.81), whichever is appropriate, at $t = \zeta$. If Eq. (1.81) is used, the result is

$$x = x_{st} \left(\sin p\zeta + \frac{\cos p\zeta}{p\zeta} - \frac{1}{p\zeta} \right) \sin pt_1 + x_{st} \left(\frac{\sin p\zeta}{p\zeta} - \cos p\zeta \right) \cos pt_1 \quad (b)$$

or

$$x = \frac{x_{st}}{p\zeta} [\sin p(t_1 + \zeta) - \sin pt_1] - x_{st} \cos p(t_1 + \zeta) \quad (c)$$

First find the amplitude from Eq. (b) and then the amplification shown below

$$A_m = \frac{X}{x_{st}} = \sqrt{1 - \frac{\frac{2 \sin \left(\frac{2\pi\zeta}{T} \right)}{\frac{2\pi\zeta}{T}} + \frac{2}{\left(\frac{2\pi\zeta}{T} \right)^2} \left(1 - \cos \frac{2\pi\zeta}{T} \right)}{\left(\frac{2\pi\zeta}{T} \right)^2}} \quad (d)$$

which is valid for $\zeta/T \leq 0.371$. From Eq. (c), the amplification factor can also be

$$A_m = \frac{1}{p\zeta} [\sin p(t_1 + \zeta) - \sin pt_1] - \cos p(t_1 + \zeta) \quad (e)$$

EXAMPLE 1.4.4 Find the amplification factors for $\zeta/T = 0, 0.25, 0.371, 1, 2, 3$, and 4 , and then plot a curve for A_m vs ζ/T .

Solution: When $\zeta/T = 0$, the forcing function in Eq. (1.79) does not exist; consequently, there is no motion, and $A_m = 0$. The amplification factor for $\zeta/T = 0.25$ may be obtained from Eq. (d) of Example 1.4.3

$$A_m = \sqrt{1 - \frac{2 \sin(\pi/2)}{\pi/2} + \frac{2}{(\pi/2)^2} (1 - \cos \pi/2)} = 0.737 \quad (a)$$

When $\zeta/T = 0.371$, either Eq. (1.54) or Eq. (d) of Example 1.4.3 yields $A_m = 1$. When $\zeta/T = 1$, obtain t from Eq. (1.83a)

$$\begin{aligned}\cos pt &= \frac{1 - (2\pi)^2}{1 + (2\pi)^2} \\ &= -0.95\end{aligned}\tag{b}$$

or

$$pt = 2.8, \quad t = \frac{T}{2\pi}(2.8) = 0.446T\tag{c}$$

which is corresponding to $t_m = 0.446T$ in Fig. 1.17b. Inserting t into Eq. (1.85a) gives

$$\begin{aligned}A_m &= 2 - \frac{2.8}{2\pi} \\ &= 1.548\end{aligned}\tag{d}$$

Similarly, A_m may be obtained from Eq. (1.85a or b) as 1.76, 1.84 and 1.88 for $\zeta/T = 2, 3$, and 4, respectively. The curve for A_m vs ζ/T is shown in Fig. 1.17a, where two other spectra are also shown.

1.4.4. General Loading—Step Forcing Function Method vs Duhamel's Integral

1.4.4.1. Step Forcing Function Method

As discussed above, the behavior of dynamic response is derived from the differential equation of motion for the purpose of observing the relationship between the amplification factor and the ratio of the forced period to the natural period. Now a general method of superposition of integrals is presented for the purpose of describing the action of dynamic response to various regular and irregular forcing functions.

Let $F(t)$ be a step function of amplitude F as shown in Fig. 1.18; the motion equation is given by Eq. (1.67). If initial displacement and velocity are both equal to zero, and $F = 1$, then

$$x = A(t) = \frac{1}{Mp^2}(1 - \cos pt)\tag{1.86}$$

This represents the displacement response of a single-degree-of-freedom system subjected to a force described by the *unit step function*.

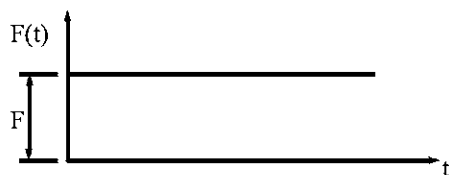


FIG. 1.18 Unit-step forcing function.

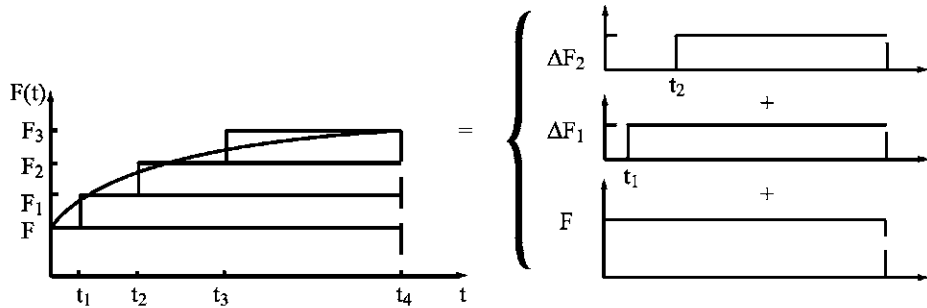


FIG. 1.19 Series of forcing functions.

Suppose that the arbitrary forcing function shown in Fig. 1.19 consists of a series of step increases, ΔF 's. Response to the total force can be evaluated as the cumulative action of the individual increases. Thus, a force consisting of n step increases is formulated as

$$\begin{aligned} x &= FA(t) + \sum_{i=1}^n \Delta F_i A(t - t_i) \\ &= FA(t) + \sum_{i=1}^n \frac{\Delta F_i}{\Delta t_i} A(t - t_i) \Delta t_i \end{aligned} \quad (1.87)$$

Hence, in the limit, replacing t_i by Δ as a dummy variable leads to

$$x = FA(t) + \int_{t_1}^t F'(\Delta) A(t - \Delta) d\Delta \quad (1.88)$$

When initial displacement and velocity are not zero, the motion equation becomes

$$x = x_0 \cos pt + \frac{\dot{x}_0}{p} \sin pt + \frac{F}{Mp^2} (1 - \cos pt) + \frac{1}{Mp^2} \int_{t_1}^t F'(\Delta) [1 - \cos p(t - \Delta)] d\Delta \quad (1.89)$$

When initial displacement and velocity are zero, the motion equation becomes

$$x = \frac{F}{Mp^2} (1 - \cos pt) + \frac{1}{Mp^2} \int_{t_1}^t F'(\Delta) [1 - \cos p(t - \Delta)] d\Delta \quad (1.90)$$

As discussed in Section 1.4.1, the application of a disturbing force can induce free vibration. Eq. (1.90) includes the free vibration resulting from the impulse. When the disturbing force cannot be represented by an analytical expression, use the approximate method of integration directly from Eq. (1.87). Let two step forces, F_1 and F_2 , be applied at t_1 and t_2 , respectively, with initial conditions of x_0 and \dot{x}_0 ; then the displacement at any time, t , can be obtained as

$$x = x_0 \cos pt + \frac{\dot{x}_0}{p} \sin pt + \frac{F_1}{K} [1 - \cos p(t - t_1)] + \frac{F_2}{K} [1 - \cos p(t - t_2)] \quad (1.91)$$

EXAMPLE 1.4.5 Find the motion equations for the step forcing function shown in Fig. 1.20 for $t < \zeta$ and $t > \zeta$. Assume that the initial conditions are x_0 and \dot{x}_0 at $t = 0$.

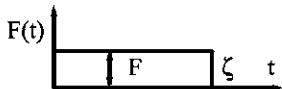


FIG. 1.20 Finite step forcing function.

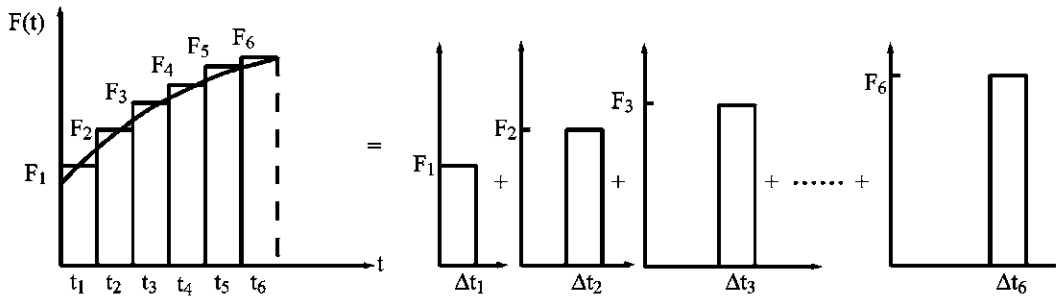


FIG. 1.21 Force consisting of series of impulses.

Solution: For $t < \zeta$, using Eq. (1.89) leads to

$$x = x_0 \cos pt + \frac{\dot{x}_0}{p} \sin pt + \frac{F}{Mp^2} (1 - \cos pt) \quad (a)$$

When $t > \zeta$, the displacement response in Eq. (a) for the force F beyond ζ should be eliminated by a superposition technique as

$$x = x_0 \cos pt + \frac{\dot{x}}{p} \sin pt + \frac{F}{Mp^2} (1 - \cos pt) - \frac{F}{Mp^2} [1 - \cos p(t - \zeta)] \quad (b)$$

1.4.4.2. Duhamel's Integral

Assume that the forcing function $F(t)$ in Fig. 1.19 consists of a series of impulses as shown in Fig. 1.21. When a single impulse, F , is applied to a one-degree-of-freedom system, Newton's second law gives

$$F\Delta t = M\Delta\dot{x} \quad (1.92)$$

If $F\Delta t$ is numerically equal to 1, then $M\Delta\dot{x} = 1$. For the mass that is at rest with $x = 0$ and $\dot{x} = 0$, when a unit impulse is applied, there will be an instantaneous change in the velocity in the amount of $\Delta\dot{x}$ without an instantaneous change in displacement as

$$\Delta\dot{x} = \frac{1}{M} \quad (1.93)$$

After this short interval Δt , no further external force is applied to the mass, and free vibration results. For $x = A \cos pt + B \sin pt$ with initial conditions of $\dot{x} = 1/M$ and $x = 0$ at $t = 0$, displacement becomes

$$x = h(t) = \frac{1}{Mp} \sin pt \quad (1.94)$$

Displacement resulting from the effect of the total force divided into n impulses can be expressed by

$$x = F_1 h(t - t_1) \Delta t_1 + F_2 h(t - t_2) \Delta t_2 + \cdots + F_n h(t - t_n) \Delta t_n = \sum_{i=1}^n F_i \Delta t_i h(t - t_i) \quad (1.95)$$

In the limit with Δ being used as a dummy variable, Eq. (1.95) yields

$$x = \frac{1}{Mp} \int_0^t F(\Delta) \sin p(t - \Delta) d\Delta \quad (1.96a)$$

or

$$x = \frac{p}{K} \int_0^t F(\Delta) \sin p(t - \Delta) d\Delta \quad (1.96b)$$

The complete solution of x is

$$x = x_0 \cos pt + \frac{\dot{x}_0}{p} \sin pt + \frac{1}{Mp} \int_0^t F(\Delta) \sin p(t - \Delta) d\Delta \quad (1.97)$$

The integral in Eqs. (1.96a,b) and (1.97) is called *Duhamel's integral* or *impulse integrals*. It can be directly derived from Eq. (1.88) using integration by parts, which will be shown in Section 1.5.3. Thus, both the step function method and Duhamel's integral possess similar mathematical characteristics.

EXAMPLE 1.4.6 Find the motion equations for $t < \zeta$ and $t > \zeta$ by using Duhamel's integral for the forcing function shown in Fig. 1.20. Initial conditions are $x = x_0$ and $\dot{x} = \dot{x}_0$ at $t = 0$.

Solution: The displacement for $t < \zeta$ is

$$\begin{aligned} x &= x_0 \cos pt + \frac{\dot{x}_0}{p} \sin pt + \frac{1}{Mp} \int_0^t F \sin p(t - \Delta) d\Delta \\ &= x_0 \cos pt + \frac{\dot{x}_0}{p} \sin pt + \frac{F}{Mp^2} (1 - \cos pt) \end{aligned} \quad (a)$$

For $t > \zeta$, the displacement becomes

$$\begin{aligned} x &= x_0 \cos pt + \frac{\dot{x}_0}{p} \sin pt + \frac{1}{Mp} \int_0^\zeta F \sin p(t - \Delta) d\Delta + \frac{1}{Mp} \int_\zeta^t (o) \sin p(t - \Delta) d\Delta \\ &= x_0 \cos pt + \frac{\dot{x}_0}{p} \sin pt + \frac{F}{Mp^2} [\cos p(t - \zeta) - \cos pt] \end{aligned} \quad (b)$$

Eqs. (a) and (b) are identical to Eqs. (a) and (b) of Example 1.4.5, respectively.

EXAMPLE 1.4.7 Find the displacements at $t = \zeta$ and $t = \zeta_1$ for the triangular impulse shown in Fig. 1.22 by using both the step function integrals and the impulse integrals with the initial conditions of $x_0 = 0$ and $\dot{x}_0 = 0$ at $t = 0$.

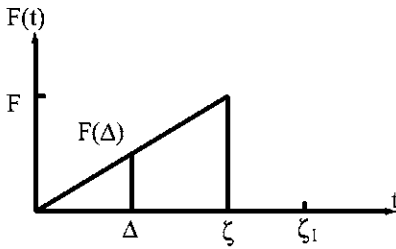


FIG. 1.22 Triangular impulse.

Solution: The forcing function can be expressed as $F(\Delta) = F\Delta/\zeta$ for the following step function integrals:

$$x = \frac{1}{K} \int_0^t F'(\Delta) [1 - \cos p(1 - \Delta)] d\Delta$$

Integrating the above equation for $t < \zeta$ gives

$$\begin{aligned} x &= \frac{F}{K\zeta} \int_0^t [1 - \cos p(t - \Delta)] d\Delta \\ &= \frac{F}{K\zeta} \left[t - \frac{1}{p} \sin p t \right] \end{aligned}$$

Displacement at $t = \zeta$ is

$$x = \frac{F}{K\zeta} \left[\zeta - \frac{1}{p} \sin p \zeta \right] \quad (\text{a})$$

When $t > \zeta$, a superposition technique should be employed for subtracting the force between t and ζ encountered in the integration

$$\begin{aligned} x &= \frac{1}{K} \int_0^\zeta F'(\Delta) [1 - \cos p(t - \Delta)] d\Delta - \frac{F}{K} [1 - \cos p(t - \zeta)] \\ &= \frac{F}{K\zeta} \left[\zeta + \frac{1}{p} \sin p(t - \zeta) - \frac{1}{p} \sin pt \right] - \frac{F}{K} [1 - \cos p(t - \zeta)] \end{aligned}$$

When $t = \zeta_1$, the motion becomes

$$x = \frac{F}{K\zeta p} [\sin p(\zeta_1 - \zeta) - \sin p \zeta_1 + \zeta p \cos p(\zeta_1 - \zeta)] \quad (\text{b})$$

For the impulse integrals, we have

$$x = \frac{1}{Mp} \int_0^t F(\Delta) \sin p(t - \Delta) d\Delta$$

Inserting $F(\Delta) = F\Delta/\zeta$ into the above equation and performing integration gives the displacement

for $t < \zeta$

$$\begin{aligned} x &= \frac{1}{Mp} \int_0^t \frac{F\Delta}{\zeta} \sin p(t - \Delta) d\Delta \\ &= \frac{F}{Mp\zeta} \left[\frac{t}{p} - \frac{1}{p^2} \sin pt \right] \end{aligned}$$

Displacement at $t = \zeta$ is

$$x = \frac{F}{K\zeta} \left(\zeta - \frac{1}{p} \sin p\zeta \right) \quad (\text{c})$$

Displacement for $t > \zeta$ may be obtained through the following integration:

$$\begin{aligned} x &= \frac{1}{Mp} \int_0^\zeta F(\Delta) \sin p(t - \Delta) d\Delta + \frac{1}{Mp} \int_\zeta^t (o) \sin p(t - \Delta) d\Delta \\ &= \frac{F}{Mp\zeta} \left[\frac{\zeta}{p} \cos p(t - \zeta) + \frac{1}{p^2} \sin p(t - \zeta) - \frac{1}{p^2} \sin pt \right] \end{aligned}$$

which gives the motion equation at $t = \zeta_1$

$$x = \frac{F}{K\zeta} \left[\zeta \cos p(\zeta_1 - \zeta) + \frac{1}{p} \sin p(\zeta_1 - \zeta) - \frac{1}{p} \sin p\zeta_1 \right] \quad (\text{d})$$

1.5. FORCED DAMPED VIBRATION

1.5.1. Harmonic Forces

Consider the spring-mass model shown in Fig. 1.23. It is subjected to a harmonic force, $F \sin \omega t$, with a frequency of ω . Displacement, x , from the equilibrium position is considered positive to right, as is the velocity and the acceleration \ddot{x} . Based on equilibrium conditions, the differential equation can be expressed as

$$M\ddot{x} + c\dot{x} + Kx = F \sin \omega t \quad (1.98)$$

By using the notations $\rho = c/c_{cr}$ and $x_{st} = F/K$, Eq. (1.98) can be rewritten as

$$\ddot{x} + 2\rho p\dot{x} + p^2 x = p^2 x_{st} \sin \omega t \quad (1.99)$$

For the general case of underdamping, the homogeneous solution of Eq. (1.99) is the same as Eq.

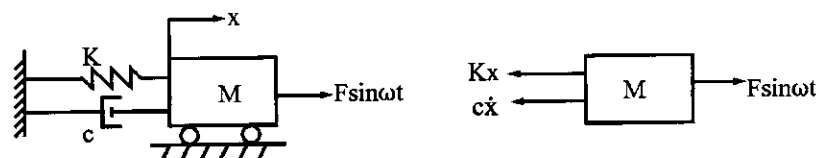


FIG. 1.23 Damped force vibration with harmonic force.

(1.41). The particular solution of Eq. (1.99) can be obtained by using

$$x_p = C_1 \sin \omega t + C_2 \cos \omega t \quad (1.100)$$

Inserting \ddot{x}_p , \dot{x}_p , and x_p into Eq. (1.99) and collecting the terms yield

$$C_1 = \frac{(p^2 - \omega^2)p^2 x_{st}}{(p^2 - \omega^2)^2 + (2\rho p\omega)^2} \quad (1.101)$$

$$C_2 = \frac{-2\rho\omega p^3 x_{st}}{(p^2 - \omega^2)^2 + (2\rho p\omega)^2} \quad (1.102)$$

After putting C_1 and C_2 into Eq. (1.100), the complete solution of Eq. (1.99) is

$$\begin{aligned} x &= x_h + x_p \\ &= e^{-\rho p t} (A \cos p^* t + B \sin p^* t) + \frac{p^2 x_{st}}{(p^2 - \omega^2)^2 + (2\rho p\omega)^2} [(p^2 - \omega^2) \sin \omega t - 2\rho p\omega \cos \omega t] \end{aligned} \quad (1.103)$$

For the *transient vibration*, A and B should be determined from the initial conditions due to the application of $F \sin \omega t$ when the system is at rest. When initial conditions are disregarded, the motion is called *steady-state forced damped vibration*.

1.5.2. Steady-State Vibration for Damped Vibration, Resonant and Peak Amplitude

As noted in Section 1.3, the effect of free vibration on displacement is of short duration and is damped out in a finite number of cycles. The resultant motion is a steady-state vibration with a forced frequency, ω . Thus, for most engineering problems, the particular solution in Eq. (1.103) suffices. Let x_p in Eq. (1.103) be expressed in a compact form as

$$\begin{aligned} x &= X \cos(\omega t - \alpha) = X (\cos \omega t \cos \alpha + \sin \omega t \sin \alpha) \\ &= \frac{p^2 x_{st}}{(p^2 - \omega^2)^2 + (2\rho p\omega)^2} [(p^2 - \omega^2) \sin \omega t - 2\rho p\omega \cos \omega t] \end{aligned} \quad (1.104)$$

Collecting the terms associated with $\sin \omega t$ and $\cos \omega t$ leads to the amplitude

$$X = \frac{x_{st}}{\sqrt{[1 - (\omega/p)^2]^2 + (2\rho\omega/p)^2}} \quad (1.105)$$

and the phase angle

$$\alpha = \tan^{-1} \left[\frac{1 - (\omega/p)^2}{-2\rho(\omega/p)} \right] \quad (1.106)$$

The amplification factor can be obtained from Eq. (1.105):

$$A_m = \frac{X}{x_{st}} = \frac{1}{\sqrt{[1 - (\omega/p)^2]^2 + (2\rho\omega/p)^2}} \quad (1.107)$$

Equation (1.107) is plotted in Fig. 1.24, A_m vs ω/p , for various values of ρ . It is seen that the *peak amplitude*, defined as the amplitude at $d(A_m)/d(\omega/p) = 0$, is greater than the *resonant amplitude*, defined as the amplitude at $\omega/p = 1$. Because they occur practically at the same frequency and it is easy to find the resonant frequency, engineers usually overlook peak amplitude.

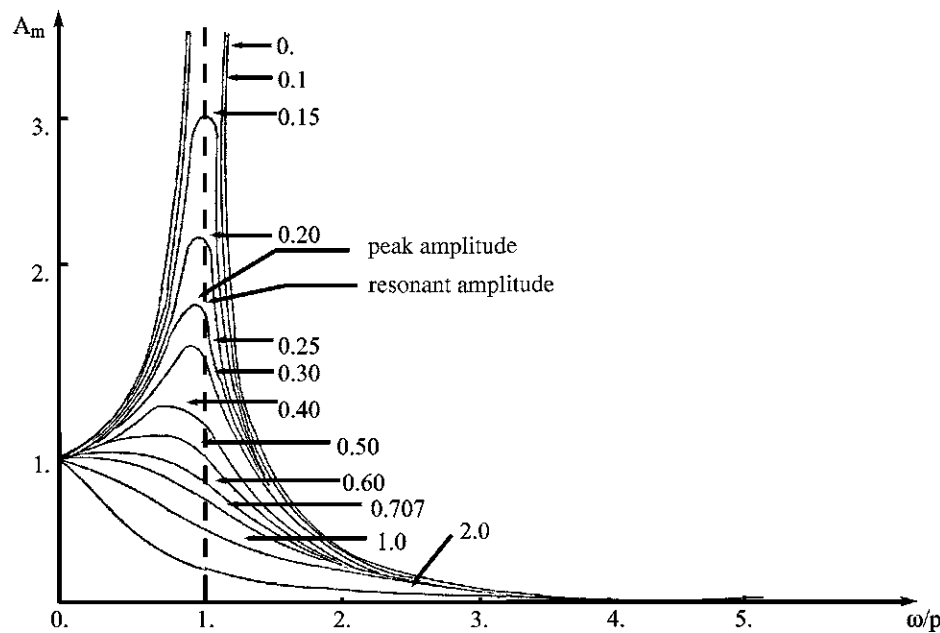


FIG. 1.24 A_m vs ω/p for various values of p .

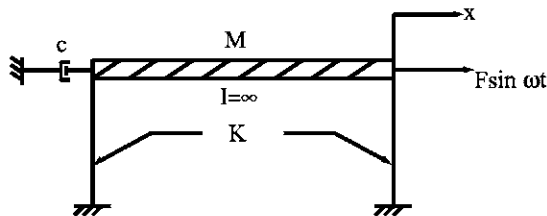


FIG. 1.25 Example 1.5.1.

EXAMPLE 1.5.1 A rigid frame shown in Fig. 1.25, subjected to a harmonic force, $F \sin \omega t$, is analyzed for displacement response for which the initial conditions are $x_0 = 0$ and $\dot{x}_0 = 0$ at $t = 0$. Plot the curve, x/x_{st} vs ωt , for $\rho = 0.1$ when $\omega/p = 0.5$ and $\omega/p = 1$, respectively.

Solution: Substituting Eq. (1.104) for Eq. (1.103) yields

$$x = e^{-\rho p^* t} (A \cos p^* t + B \sin p^* t) + X \cos(\omega t - \alpha) \quad (a)$$

The given initial conditions lead to

$$A = -X \cos \alpha$$

$$B = -X/p^* (\rho p \cos \alpha + \omega \sin \alpha)$$

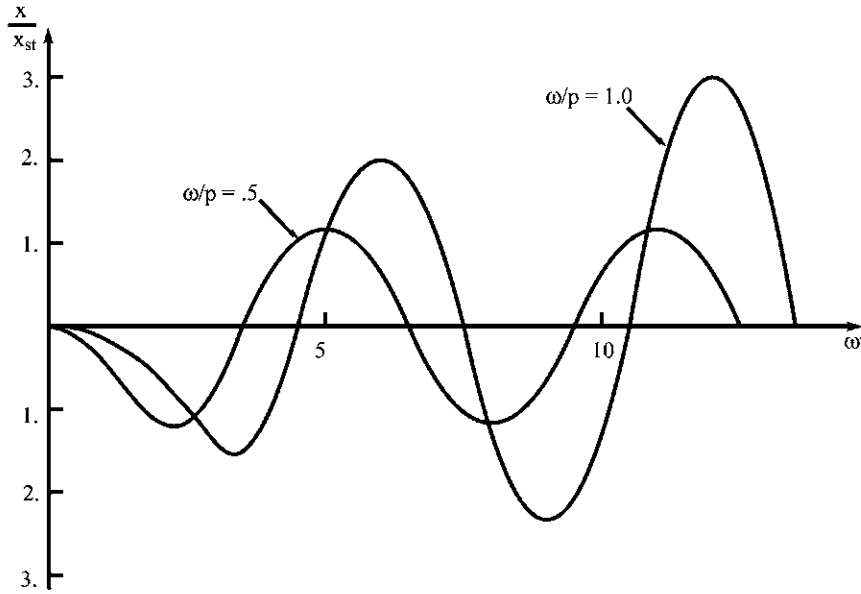


FIG. 1.26 Example 1.5.1.

After inserting the constants A and B into Eq. (a), the equation of displacement response becomes

$$x = X \left[\cos(\omega t - \alpha) + \frac{(\omega/p) e^{-\rho p t}}{\sqrt{1 - \rho^2}} \cos(p^* t - \alpha_0) \right] \quad (b)$$

in which X and α are as shown in Eqs. (1.105) and (1.106), respectively, and

$$\alpha_0 = \tan^{-1} \frac{2\rho^2 + (\omega/p)^2 - 1}{2\rho\sqrt{1 - \rho^2}} \quad (c)$$

Comparing Eq. (1.103) with Eq. (b) reveals that the second term in Eq. (b) is associated with free vibration resulting from the application of the disturbing force. Based on Eq. (b), the curves, x/x_{st} vs ωt , are plotted in Fig. 1.26 for $\rho = 0.1$ when $\omega/p = 0.5$ and 1, respectively.

Note that the amplitude corresponding to $\omega/p = 0.5$ is decreasing; the decrease is mainly due to *amplitude decay* of the free vibration part. The response becomes stable as a steady-state vibration after the free vibration is damped out in a few cycles. The amplitude corresponding to $\omega/p = 1$, however, is increasing. The increase will gradually build up because of the resonance.

1.5.3. General Loading—Step-Forcing Function Method vs Duhamel's Integral

1.5.3.1. Step-Forcing Function Method

Damped forced vibration for a nonperiodic forcing function can be studied by using either the unit step increases or the impulse integrals as presented in Section 1.4. Consider that the rigid frame sketched in Fig. 1.27 is subjected to a suddenly applied force, F , at $t = 0$, for which the initial conditions are $x_0 = 0$ and $\dot{x} = 0$ at $t = 0$ and the damping coefficient, c , is less than the critical damping, c_{cr} . The differential equation is

$$M\ddot{x} + c\dot{x} + Kx = F \quad (1.108)$$

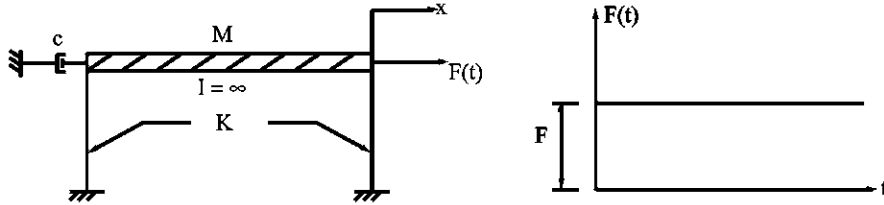


FIG. 1.27 Damped force vibration with impulsive load.

Using $x_{st} = F/K$ and $x_1 = x - x_{st}$ in Eq. (1.108) leads to

$$M\ddot{x}_1 + c\dot{x}_1 + Kx_1 = 0 \quad (1.109)$$

which is a differential equation for free vibration. Initial conditions are $x_{1(0)} = -x_{st}$ and $\dot{x}_{1(0)} = 0$ at $t = 0$. Taking the initial conditions in Eqs. (a) and (b) of Example 1.3 for α and C , and inserting into Eq. (1.42), gives the motion equation

$$x_1 = \frac{x_{st}\rho^*}{\rho} e^{-\rho\rho t} \cos(\rho^*t - \pi - R) \quad (1.110)$$

where

$$\rho^* = \frac{\rho}{\sqrt{1 - \rho^2}} \quad \text{and} \quad R = \tan^{-1} \rho^*$$

Expressing the displacement in x leads to

$$\begin{aligned} x &= x_1 + x_{st} \\ &= \frac{F}{K} \left[1 - \frac{\rho^*}{\rho} e^{-\rho\rho t} \cos(\rho^*t - R) \right] \end{aligned} \quad (1.111)$$

When $F = 1$, Eq. (1.111) becomes the displacement response for a *unit step* increase

$$x = A(t) = \frac{1}{K} \left[1 - \frac{\rho^*}{\rho} e^{-\rho\rho t} \cos(\rho^*t - R) \right] \quad (1.112)$$

For the forcing function shown in Fig. 1.19, the unit step increase can be used through a superposition technique similar to Eqs. (1.87) and (1.88) to find the total displacement

$$x = FA(t) + \int_0^t \frac{dF(\Delta)}{d\Delta} A(t - \Delta) d\Delta \quad (1.113)$$

Substituting $F'(\Delta) = dF(\Delta)/d\Delta$ and Eq. (1.112) for the corresponding terms in Eq. (1.113) yields

$$\begin{aligned} x &= \frac{F}{K} \left[1 - \frac{\rho^*}{\rho} e^{-\rho\rho t} \cos(\rho^*t - R) \right] \\ &\quad + \frac{1}{K} \int_0^t F'(\Delta) \left[1 - \frac{\rho^*}{\rho} e^{-\rho\rho(t-\Delta)} \cos(\rho^*(t-\Delta) - R) \right] d\Delta \end{aligned} \quad (1.114)$$

When the initial conditions x_0 and \dot{x}_0 are not zero, the displacement of free vibration shown in Eq. (1.42) should be added to Eq. (1.114).

1.5.3.2. Duhamel's Integral

An equivalent expression can be obtained from Eq. (1.113) by using integration by parts

$$\begin{aligned} x &= FA(t) + [F(\Delta)A(t - \Delta)]_{\Delta=0}^{\Delta=t} + \int_0^t F(\Delta)A'(t - \Delta) d\Delta \\ &= FA(t) + F(t)A(0) - F(0)A(t) + \int_0^t F(\Delta)A'(t - \Delta) d\Delta \end{aligned} \quad (1.115)$$

From Fig. 1.19, it follows that $F(0) = F$ and $A(0)$ can be obtained from Eq. (1.112) as

$$A(0) = \frac{1}{K} \left[1 - \frac{\rho^*}{\rho} \cos(-R) \right]$$

Therefore, Eq. (1.115) becomes

$$x = \int_0^t F(\Delta)A'(t - \Delta) d\Delta \quad (1.116)$$

Using Eq. (1.112), leads to

$$\begin{aligned} A'(t - \Delta) &= -\frac{d}{d\Delta} \left(\frac{1}{K} \right) \left[1 - \frac{\rho^*}{\rho} e^{-\rho^* p^*(t-\Delta)} \cos(p^*(t - \Delta) - R) \right] \\ &= \frac{\rho^* p^*}{K\rho} e^{-\rho^* p^*(t-\Delta)} [\rho^* \cos(p^*(t - \Delta) - R) \\ &\quad + \sin(p^*(t - \Delta) - R)] \end{aligned} \quad (1.117)$$

The terms in the brackets of Eq. (1.117) can be simplified as

$$\begin{aligned} \frac{\rho^*}{\rho} \left[\rho \cos(p^*(t - \Delta) - R) + \sqrt{1 - \rho^2} \sin p^*((t - \Delta) - R) \right] \\ = X \sin(p^*(t - \Delta) - R + \alpha_1) \end{aligned} \quad (1.118)$$

in which

$$X = \frac{1}{\sqrt{1 - \rho^2}} \quad (1.119a)$$

$$\alpha_1 = \tan^{-1} \left(\frac{\rho}{\sqrt{1 - \rho^2}} \right) \quad (1.119b)$$

Thus, Eq. (1.117) becomes

$$A'(t - \Delta) = \frac{p}{K\sqrt{1 - \rho^2}} e^{-\rho^* p^*(t-\Delta)} \sin p^*(t - \Delta) \quad (1.120)$$

The insertion of Eq. (1.120) into Eq. (1.116) gives the Duhamel's integral

$$x = \frac{p}{K\sqrt{1 - \rho^2}} \int_0^t e^{-\rho^* p^*(t-\Delta)} F(\Delta) \sin p^*(t - \Delta) d\Delta \quad (1.121a)$$

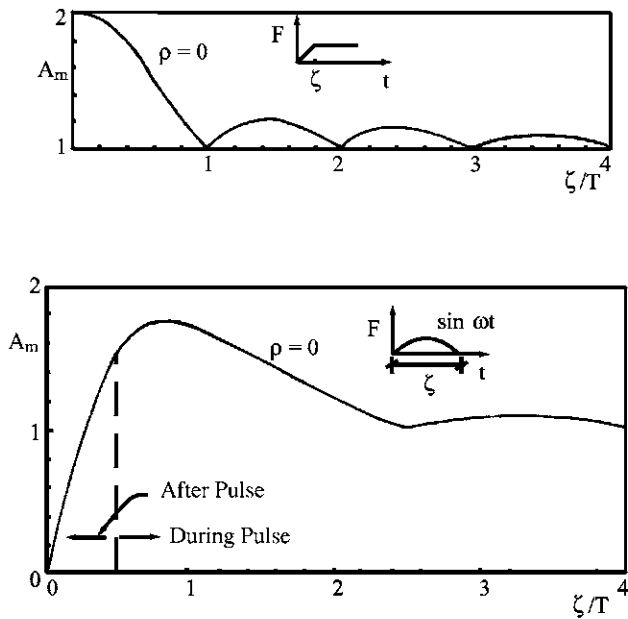


FIG. 1.28 Shock spectra.

For practical structural engineering problems, the damping factors are usually small ($\rho < 15\%$). p^* and ρ^* may be replaced by p and ρ , respectively. Thus, Eq. (1.121a) becomes

$$x = \frac{p}{K} \int_0^t e^{-\rho p(t-\Delta)} F(\Delta) \sin p(t-\Delta) d\Delta \quad (1.121b)$$

Free vibration resulting from the application of a disturbing force is included in Eq. (1.121a,b). It is apparent that Eq. (1.121) can be derived independently from the impulse integrals.

When $\rho = 0$, as in the case of undamped forced vibration, Eq. (1.121a,b) becomes Eq. (1.95a or b). Equations (1.95) and (1.121) are in function of forcing frequency, natural frequency, magnitude of the applied force, and damping ratio, if any. Force magnitude and stiffness can be combined as a static displacement, $x_{st} = F/K$. The Duhamel's integral can be used to find the maximum response for a given forcing function, natural period, and damping ratio during and after the force applied. Maximum responses may be plotted in a shock spectrum as discussed in Section 1.4.3. The spectra of two typical forces are shown in Fig. 1.28. For the force rising from zero to F at ζ , if ζ is less than one-quarter of T , then the effect is essentially the same as for a suddenly applied force. In practical design, the rise can be ignored if it is small. When ζ is a whole multiple of T , the response is the same as though F had been applied statically.

For the structure subjected to earthquake excitation, the motion equation of a single-mass system shown in Fig. 1.29 is

$$M\ddot{x} + c\dot{x} + Kx = -M\ddot{x}_g \quad (1.122)$$

in which \ddot{x}_g is the earthquake record expressed in terms of gravity, g . Fig. 1.29 shows the ground acceleration in N-S direction of the El Centro earthquake, 18 May, 1940. Numerical procedure of the Duhamel's integral can be used to generate an earthquake response spectrum (numerical integration methods are given in Chapter 7). In using Eq. (1.121), the forcing function should be expressed as $F(\Delta) = -M\ddot{x}_g$. In view of the nature of ground motion, the negative sign

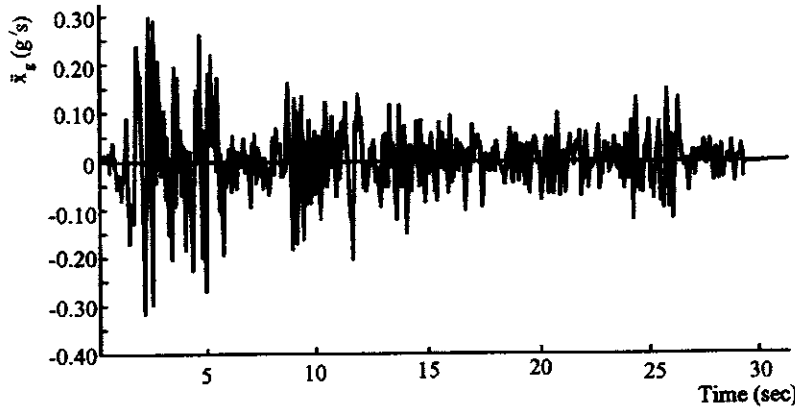


FIG. 1.29 N-S component of El Centro earthquake, 18 May, 1940.

has no real significance and can be ignored. Thus one may find the velocity response with or without considering damping [Eqs. (1.96a,b) or (1.121a,b)]. Using Eq. (1.121b) leads to the displacement response spectrum as

$$S_d = \frac{Mp}{K} \left| \int_0^t \ddot{x}_g e^{-\rho p(t-\Delta)} \sin p(t-\Delta) d\Delta \right|_{\max} = \frac{1}{p} \left| \int_0^t \ddot{x}_g e^{-\rho p(t-\Delta)} \sin p(t-\Delta) d\Delta \right|_{\max} \quad (1.123a)$$

Spectra for velocities, S_v , and accelerations, S_a , are

$$S_v = p S_d \quad (1.123b)$$

$$S_a = p S_v = p^2 S_d \quad (1.123c)$$

Maximum spring force may be obtained as

$$F_{\max} = K S_d = M S_a \quad (1.124)$$

Response spectra computed for the earthquake shown in Fig. 1.29 are given in a tripartite logarithmic plot as shown in Fig. 1.30. Note that, when the frequency is large, the relative displacement is small and the acceleration is large, but when the frequency is small, the displacement is large and the acceleration is relatively small; the velocity is always large around the region of intermediate frequencies [3,4]. Also note that the response given by Eq. (1.123a,b,c) does not reflect real time-history response but a maximum value; thus the response is called *pseudo-response*, such as *pseudo-displacement*, *pseudo-velocity*, and *pseudo-acceleration*. More detailed work on spectrum construction is given in Chapter 7.

1.5.4. Transmissibility and Response to Foundation Motion

Consider the structure shown in Fig. 1.31 with a harmonic force $F \cos \omega t$ acting on the mass. The motion equation is

$$M\ddot{x} + c\dot{x} + Kx = F \cos \omega t \quad (1.125)$$

As shown in Eqs. (1.99)–(1.105), the steady-state vibration is

$$x = X \cos(\omega t - \alpha) \quad (1.126)$$

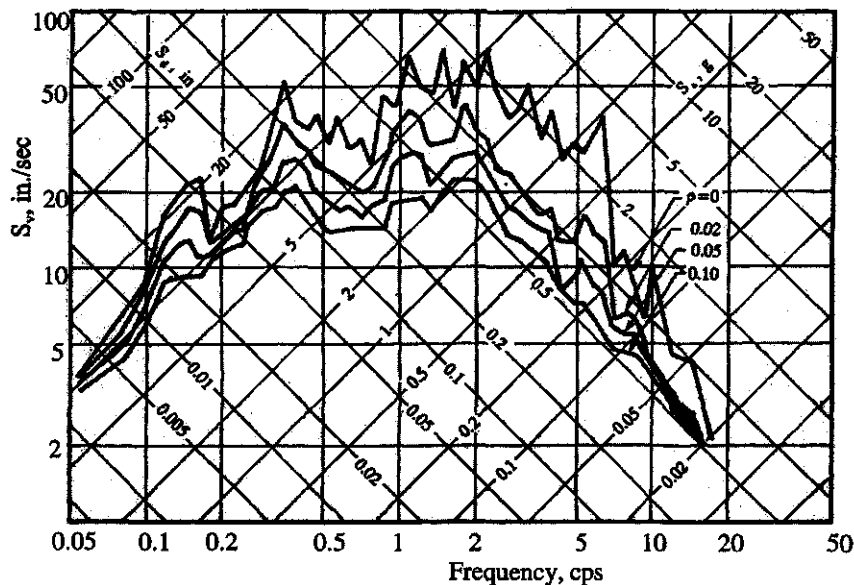


FIG. 1.30 Response spectra for N-S component of El Centro earthquake 18 May, 1940.

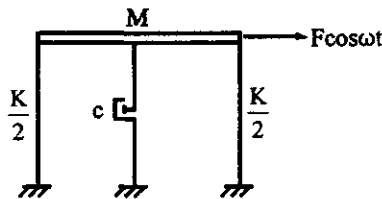


FIG. 1.31 Transmissibility.

in which the amplitude and the phase angle are

$$X = \frac{F}{K\sqrt{[1 - (\omega/p)^2]^2 + (2\rho(\omega/p))^2}} \quad (1.127a)$$

$$\alpha = \tan^{-1} \frac{2\rho\omega/p}{1 - (\omega/p)^2} \quad \left(\text{Note : } \sin \alpha = \frac{2\rho\omega/p}{\sqrt{(1 - (\omega/p)^2)^2 + (2\rho(\omega/p))^2}} \right) \quad (1.127b)$$

The force transmitted to the foundation through the spring and dashpot is

$$F_f = Kx + c\dot{x} \quad (1.128)$$

Substituting Eqs. (1.126) and (1.127a,b) into Eq. (1.128) yields the desired equation

$$F_f = X[K \cos(\omega t - \alpha) - c\omega \sin(\omega t - \alpha)] = X\sqrt{K^2 + c^2\omega^2} \cos(\omega t - \beta) \quad (1.129)$$

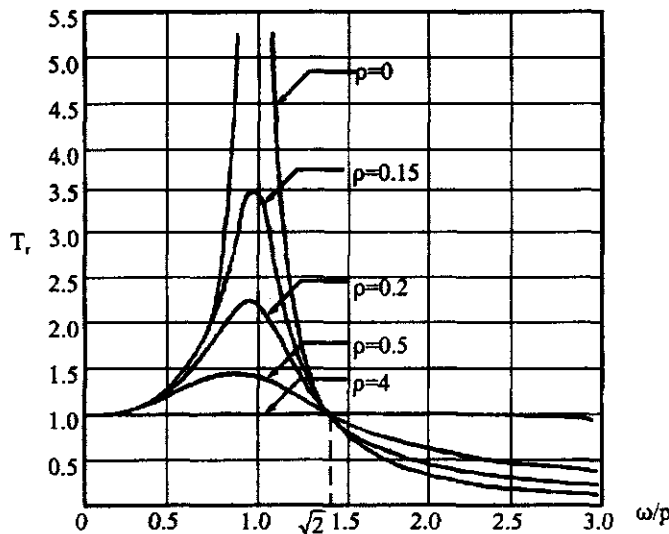


FIG. 1.32 T_r vs ω/p for transmissibility.

Amplitude and phase angle of the transmitting force are

$$A_f = X\sqrt{K^2 + c^2\omega^2} = F\sqrt{\frac{1 + (2\rho\omega/p)^2}{(1 - (\omega/p)^2)^2 + (2\rho\omega/p)^2}} \quad (1.130)$$

$$\beta = \tan^{-1}\left(\frac{2\rho(\omega/p)^3}{1 - (\omega/p)^2 + (2\rho\omega/p)^2}\right) \quad (1.131)$$

From Eq. (1.132), the *transmissibility*, which is defined as *the ratio between the amplitude of the force transmitted to the foundation and the amplitude of the driving force*, can be found as

$$T_r = \frac{A_f}{F} = \sqrt{\frac{1 + (2\omega\rho/p)^2}{[1 - (\omega/p)^2]^2 + (2\omega\rho/p)^2}} \quad (1.132)$$

Transmissibility for $\rho = 0$ to $\rho = 1$ is depicted in Fig. 1.32.

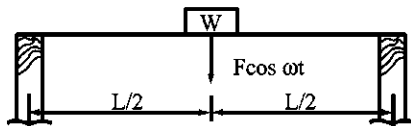
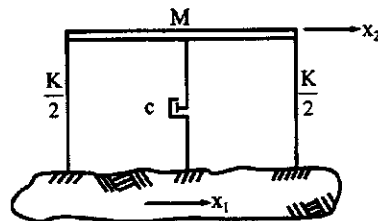
A few interesting features of vibration isolation can be observed from the figure: T_r is always less than 1 when ω/p is greater than $\sqrt{2}$ regardless of the damping ratio; when ω/p is less than $\sqrt{2}$, T_r , depending on the damping ratio, is always equal to or greater than 1; and T_r is equal to 1 when ω/p equals $\sqrt{2}$ regardless of the amount of damping.

EXAMPLE 1.5.2 Find A_f , β , and T_r for the simply supported beam shown in Fig. 1.33 subjected to a harmonic force at the mass. Let $F = 22.24$ kN (5k), $\omega = 45$ rad/sec, $W = 44.8$ kN (10k), $I = 1.7478 \times 10^{-3}$ m⁴(4199 in⁴), $E = 1.9994 \times 10^{11}$ N/m²(2.9×10^7 lb/in²), $\rho = 0.05$, and $L = 14.63$ m (48 ft).

Solution: For this structure, the stiffness, mass, and angular frequency are

$$K = \frac{48EI}{L^3} = 5.3568 \times 10^6 \text{ N/m}, \quad M = 4534.1 \text{ N sec}^2/\text{m}, \quad \text{and} \quad p = \sqrt{\frac{K}{M}} = 34.372 \text{ rad/sec} \quad (a)$$

Frequency ratio is $\omega/p = 45/34.372 = 1.309$; amplitude of the transmitting force can now be

**FIG. 1.33** Example 1.5.2.**FIG. 1.34** Structure subjected to ground motion.

obtained from Eq. (1.130) as

$$\begin{aligned} A_f &= 22.24 \sqrt{\frac{1 + [2(0.05)(1.309)]^2}{(1 - (1.309)^2)^2 + [2(0.05)(1.309)]^2}} \\ &= 22.24(1.933) \\ &= 42.991 \text{ kN} \end{aligned} \quad (\text{b})$$

The phase angle is calculated from Eq. (1.131) as

$$\begin{aligned} \beta &= \tan^{-1} \left(\frac{2(0.05)(1.309)^3}{1 - (1.309)^2 + [2(0.05)(1.309)]^2} \right) \\ &= 162.146^\circ \end{aligned} \quad (\text{c})$$

and the transmissibility, from Eq. (1.132), is

$$T_r = 1.933 \quad (\text{d})$$

If $\omega = 90$ rad/sec, then $\omega/p = 2.618$, and the solutions become

$$A_f = 3.923 \text{ kN}, \beta = 162.146^\circ, \text{ and } T_r = 0.1764 \quad (\text{e})$$

which reflects that the effect of the frequency ratio on the transmissibility is obviously significant as shown in Fig. 1.32.

Another important vibration isolation is the relative transmission from support motion to superstructure at which some mechanical equipment might be placed. The superstructure and the machinery, if any, must be protected from the harmful motion of the support.

Let the frame shown in Fig. 1.34 be subjected to a prescribed ground motion as

$$x_1 = X_1 \cos \omega t \quad (1.133)$$

Relative displacement between the mass and the foundation may be expressed as $x = x_2 - x_1$. The

motion equation of the mass becomes

$$M\ddot{x}_2 + c\dot{x}_2 + Kx_2 = 0 \quad (1.334)$$

Expressing the motion equation in terms of the relative displacement leads to

$$M\ddot{x} + c\dot{x} + Kx = M\omega^2 X_1 \cos \omega t \quad (1.135)$$

of which the steady-state vibration is

$$x = \frac{(\omega/p)^2 X_1 \cos(\omega t - \theta)}{\sqrt{[1 - (\omega/p)^2]^2 + [2\rho(\omega/p)]^2}} \quad (1.136)$$

If the motion equation is expressed in terms of x_2 of the mass displacement, then

$$M\ddot{x}_2 + c(\dot{x}_2 - \dot{x}_1) + K(x_2 - x_1) = 0 \quad (1.137)$$

Substituting Eq. (1.133) in the above yields

$$M\ddot{x}_2 + c\dot{x}_2 + Kx_2 = KX_1 \cos \omega t - cX_1 \omega \sin \omega t \quad (1.138)$$

For simplicity, the force on the right side of Eq. (1.138) is condensed as

$$KX_1 \cos \omega t - cX_1 \omega \sin \omega t = F \cos(\omega t - \alpha)$$

in which

$$F = X_1 \sqrt{K^2 + (c\omega)^2} = X_1 K \sqrt{1 + (2\rho\omega/p)^2} \quad (1.139)$$

$$\alpha = \tan^{-1}\left(\frac{-c\omega}{K}\right) = \tan^{-1}(-2\rho\omega/p) \quad (1.140)$$

Thus the solution of Eq. (1.138) is

$$x_2 = \frac{X_1 \sqrt{1 + (2\rho\omega/p)^2}}{\sqrt{[1 - (\omega/p)^2]^2 + (2\rho\omega/p)^2}} \cos(\omega t - \alpha - \beta) \quad (1.141a)$$

where

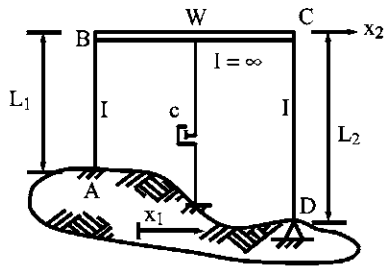
$$\beta = \tan^{-1} \frac{2\rho\omega/p}{1 - (\omega/p)^2} \quad (1.141b)$$

When $\cos(\omega t - \alpha - \beta) = 1$, the amplitude of x_2 is signified by X_2 . *Transmissibility* is defined as the ratio of the amplitude of the mass motion, X_2 , to the amplitude of the support motion, X_1 , as

$$T_r = \frac{X_2}{X_1} = \sqrt{\frac{1 + (2\rho\omega/p)^2}{[1 - (\omega/p)^2]^2 + (2\rho\omega/p)^2}} \quad (1.142)$$

Note that Eqs. (1.132) and (1.142) are identical.

EXAMPLE 1.5.3 The frame shown in Fig. 1.35 is subjected to a ground displacement $x_1 = 0.01016 \cos(170t)$ m (0.4 cos(170t) in). Let $I = 6.9374 \times 10^{-5}$ m⁴ (166.67 in⁴), $E = 2.0684 \times 10^8$ kN/m² (30,000 ksi), $W = 22.24$ kN (5k), $\rho = 0.05$, $L_1 = 3.048$ m (10 ft), and $L_2 = 3.6576$ m (12 ft). Find (1) maximum displacement of the girder, (2) maximum relative displacement between the girder and the foundation, and (3) shear transmitted to the foundation.

**FIG. 1.35** Example 1.5.3.

Solution: From the given data, we can calculate

$$K = K_{AB} + K_{CD} = \frac{12EI}{L_1^3} + \frac{3EI}{L_2^3} \\ = 6080.9 + 880.2 = 6961.1 \text{ kN/m} \quad (\text{a})$$

$$M = \frac{W}{g} = 22.24 \text{ kN sec}^2/\text{m} \quad (\text{b})$$

$$p = \sqrt{\frac{K}{M}} = 55.42 \text{ rad/sec} \quad (\text{c})$$

$$\frac{\omega}{p} = 3.067 \quad (\text{d})$$

The solutions are

(1) From Eq. (1.141a) for $X_1 = 1.016 \text{ cm}$, when $\cos(\omega t - \alpha - \beta) = 1$

$$X_2 = \frac{1.016 \sqrt{1 + [2(0.05)(3.067)]^2}}{\sqrt{[1 - (3.067)^2]^2 + [2(0.05)(3.067)]^2}} \\ = 1.016(0.12431) = 0.1263 \text{ cm} \quad (\text{e})$$

(2) From Eq. (1.135), when $\cos(\omega t - \theta) = 1$.

$$X = \frac{1.016 \sqrt{(3.067)^2}}{\sqrt{[1 - (3.067)^2]^2 + [2(0.05)(3.067)]^2}} \\ = 1.016(1.118) = 1.136 \text{ cm} \quad (\text{f})$$

(3) Shear transmitted from the columns to the foundation is

$$V = V_{AB} + V_{CD} = (K_{AB} + K_{CD})X \\ = (6080.9 + 880.2) \frac{1.136}{100} = 79.08 \text{ kN} \quad (\text{g})$$

Note that if the frequency ratio, ω/p , approaches 1, then X increases and a large shear results.

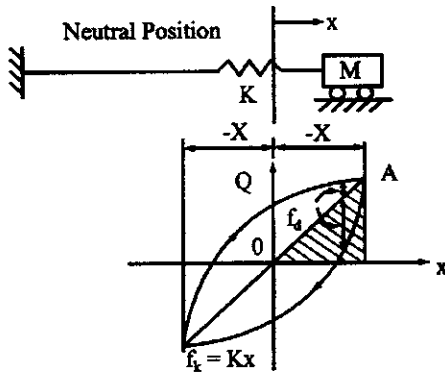


FIG. 1.36 Resisting force vs displacement.

1.6. EVALUATION OF DAMPING

1.6.1. Equivalent Damping Coefficient Method

In Section 1.3, a technique called logarithmic decrement was introduced to evaluate the viscous damping coefficient. As noted, the viscous damping is of a linear type, namely a force proportional to velocity, which is a mathematical model for simple dynamic analysis. In reality, the mechanism causing damping in a system could be many sources such as solid friction, joint friction, air or fluid resistance. Solid friction is one of the most important mechanisms; it occurs in all vibrating systems with elastic restoring forces. It is a function of amplitude only and is due to stress reversal behavior. When stresses are repeated indefinitely between two limits, the stress has a slightly higher value for the strain increasing than that corresponding to the strain decreasing. The increasing and decreasing strains are of the same magnitude and the maximum stress is below the elastic limit [5]. The *equivalent damping coefficient method* is to determine the viscous damping coefficient on the basis of the relationship between the energy dissipated by the viscous damping and the energy dissipated by the nonviscous damping. The nonviscous damping could be due to various mechanisms regardless of the characteristics of linearity and nonlinearity.

Consider a vibrating system with elastic restoring force, KX , shown in Fig. 1.36; the force and displacement relationship is shown in the accompanying figure. Resisting force, Q , consists of restoring force, f_k and damping force, f_d . The shaded area is the energy due to the elastic force; the elliptical area is the energy dissipated by damping, also a typical representation of solid friction. When the mass moves to the right (from 0 to A), $\dot{x} > 0$, the resisting force is $Q = f_k + f_d$ and when the mass moves to the left (from A to 0), $\dot{x} < 0$, the resisting force is $Q = f_k - f_d$. This means that, besides the restoring force, f_k , there is always a resisting force, f_d , opposite to the motion. To find the equivalent viscous damping, c_{eq} , first calculate the energy dissipated by viscous damping, E_v , during one cycle of steady state vibration, $x = X \cos(\omega t - \alpha)$, as

$$E_v = \int f_d dx = \int c\dot{x} dx = \int_0^{2\pi} \omega c X^2 \sin^2(\omega t - \alpha) d(\omega t) = \pi c \omega X^2 \quad (1.143)$$

Knowing the energy dissipated by nonviscous damping, E_{nv} , based on the experimental results, let

$$E_v = E_{nv} \quad (1.144)$$

Then the equivalent viscous damping is obtained as

$$c_{\text{eq}} = \frac{E_{\text{nv}}}{\pi \omega X^2} \quad (1.145)$$

The evaluation of E_{nv} is illustrated by the following example for a nonlinear damping force.

EXAMPLE 1.6.1 For a damping force proportional to the square of the velocity, $f_d = q\dot{x}^2$, find (a) the energy E_{nv} , dissipated by the force, (b) the equivalent viscous damping c_{eq} , and (c) the equivalent damping ρ_{eq} .

Solution: (a) The dissipated energy for one cycle is

$$E_{\text{nv}} = 2 \int_{-X}^{X} q\dot{x}^2 dx = \int_{-\pi}^{2\pi} \frac{1}{\omega} q\dot{x}^3 d(\omega t) = -2q\omega^2 X^3 \int_{-\pi}^{2\pi} \sin^3 \omega t d(\omega t) = \frac{8}{3} q\omega^2 X^3 \quad (\text{a})$$

(b) From Eq. (1.145)

$$c_{\text{eq}} = \frac{(8/3) q \omega^2 X^3}{\pi \omega X^2} = \frac{8}{3\pi} q \omega X \quad (\text{b})$$

(c) Using $\rho = c/c_r$, $c_r = 2 K/p$, let

$$\pi c \omega X^2 = \pi \omega X^2 \rho_{\text{eq}} (2 K/p) \quad (\text{c})$$

and

$$\pi \omega X^2 \rho_{\text{eq}} (2 K/p) = \frac{8}{3} q \omega^2 X^3 \quad (\text{d})$$

Then

$$\rho_{\text{eq}} = \frac{4}{3\pi K} q p \omega X \quad (\text{e})$$

1.6.2. Amplitude Method and Bandwidth Method

The *amplitude method* and the *bandwidth method* are based on the resonance behavior of a vibrating system with moderate damping. If a structure is applied with steady-state vibration with the forcing frequencies closely spaced, then a resonance curve may be shown in Fig. 1.38. When $\omega/p = 1$ at resonance, the amplitude may be found from Eq. (1.107) as

$$A_m = \frac{1}{2\rho} \quad (1.146)$$

and, in turn, the damping ratio

$$\rho = \frac{x_{\text{st}}}{2X} \quad (1.147)$$

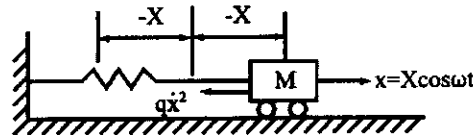


FIG. 1.37 Example 1.6.1.

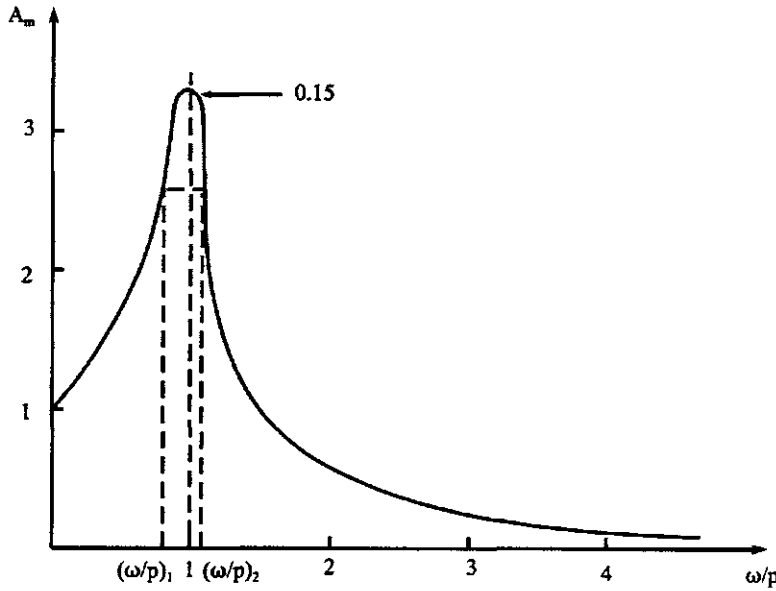


FIG. 1.38 Resonance curve.

Using Eq. (1.147) to determine ρ requires knowing the dynamic amplitude X and the static displacement x_{st} . Thus the *amplitude method* is named. The dynamic amplitude can be easily obtained by applying a vibrating equipment to excite with different frequencies. The static displacement, however, must be carefully obtained because static experiments are relatively difficult.

The bandwidth method is also based on the resonance curve and can be derived from Fig. 1.38. Let X at $\omega/p = 1$ be divided by $\sqrt{2}$; then $X_1 = X_2 = X/\sqrt{2}$ and the corresponding frequency ratios are $(\omega/p)_1$ and $(\omega/p)_2$. The *bandwidth is the difference between two frequencies corresponding to the same response amplitude*. From Eqs. (1.105) and (1.147), we have

$$\frac{x_{st}}{\sqrt{[1 - (\omega/p)^2]^2 + (2\rho\omega/p)^2}} = \frac{1}{\sqrt{2}} \frac{x_{st}}{2\rho} \quad (1.148)$$

from which

$$(\omega/p)_{1,2}^2 = 1 - 2\rho^2 \pm 2\rho\sqrt{\rho^2 + 1} \quad (1.149)$$

Since ρ is very small, the higher order term, ρ^2 , can be neglected; then

$$(\omega/p)_{1,2} = (1 \pm 2\rho)^{1/2} \quad (1.150)$$

using binomial expansion leads to

$$(\omega/p)_{1,2} = 1 \pm \frac{1}{2}(2\rho) + \dots \quad (1.151)$$

Thus,

$$(\omega/p)_1 = 1 - \rho, \quad \text{and} \quad (\omega/p)_2 = 1 + \rho \quad (1.152)$$

The damping ratio can now obtained as

$$\rho = \frac{(\omega/p)_2 - (\omega/p)_1}{2} \quad (1.153)$$

EXAMPLE 1.6.2 From Fig. 1.38, let $(\omega/p)_1 = 0.8$ and $(\omega/p)_2 = 1.1$ corresponding to $X/\sqrt{2}$, where $X = 3.28 x_{st}$. Find the damping ratio based on (a) the amplitude method and (b) the bandwidth method.

Solution: (a) From Eq. (1.147)

$$\rho = \frac{x_{st}}{2(3.28x_{st})} = 0.15$$

(b) From Eq. (1.153)

$$\rho = \frac{1.1 - 0.8}{2} = 0.15$$

1.7. OVERVIEW

This chapter is designed to emphasize the fundamental behavior of free and forced vibrations of a single-degree-of-freedom system. Several integration techniques such as unit step function and Duhamel's integral are discussed, and the effects of damping and various forcing functions on dynamic response are observed. The motion equation is derived on the basis of Newton's second law for which the solution is based on the integration of differential equations.

Note that the motion equation can be established by using different methods such as *d'Alembert's principle*, *Hamilton's principle*, and the principle of *virtual displacement*. Also the solution for motion can be obtained by employing *Laplace transforms*. Readers may refer to the texts of fundamental vibration and dynamics for such mathematical formulations in references [2] and [6].

BIBLIOGRAPHY

1. RED Bishop, AG Parkinson, JW Pendered. J Sound Vibr 9(2):313–337 (1969).
2. SP Timoshenko, DH Young, W Weaver Jr. Vibration Problems in Engineering (4th ed.). New York, John Wiley, 1974.
3. NM Newmark, E Rosenblueth. Fundamentals of Earthquake Engineering. Englewood Cliffs, NJ: Prentice-Hall, 1971.
4. NM Newmark, WJ Hall. Earthquake Spectra and Design. Oakland, CA: Earthquake Engineering Research Institute (EERI), 1982.
5. U.S. Army Corps of Engineers. Design of Structures to Resist the Effects of Atomic Weapons. Manuals 415–421.
6. JJ Tuma, FY Cheng. Dynamic Structural Analysis. New York: McGraw-Hill, 1983.
7. CW Bert. J Sound Vib 29:129–153, 1973.
8. RR Craig. Structural Dynamics. New York: John Wiley, 1981.
9. M Paz. Structural Dynamics (2nd ed.). New York: Van Nostrand, 1985.
10. RW Clough, J Penzien. Dynamics of Structures. McGraw-Hill, 1993.
11. AK Chopra. Dynamics of Structures. Oakland, CA: Earthquake Engineering Research Institute (EERI), 1981.
12. GW Housner. J Engng Mech Div, ASCE, 85(4):109–129, 1959.
13. AK Chopra. Dynamics of Structures. Englewood Cliffs, NJ: Prentice-Hall, 1995.

2

Eigensolution Techniques and Undamped Response Analysis of Multiple-Degree-of-Freedom Systems

PART A FUNDAMENTALS

2.1. INTRODUCTION

In order to comprehend response behavior and solution procedures for structural dynamics, this chapter was developed to introduce the modal matrix method for free and forced vibrations of *lumped mass* (*discrete parameter*) systems without damping. Several well-known eigensolution techniques of *iteration method*, *Choleski's decomposition*, *Jacobi method*, *Sturm sequence method*, and *extraction technique* are presented in detail. The characteristics of the eigensolutions are discussed for symmetric and nonsymmetric matrices and for repeating roots. Response analysis deals with rigid-body and elastic motion as well as repeating roots. All mathematical formulations are accompanied by numerical examples to illustrate detailed procedures and to examine response behavior.

2.1.1. Characteristics of the Spring–Mass Model

To understand the following discussion, a structure—which is assumed to be a discrete parameter (*lumped mass*) system—must be conceived of as a model consisting of a finite number of masses connected by massless springs. The *spring–mass model*, depending on the characteristics of the structure, can be established in different ways. An example is shown in Fig. 2.1, where M_1 and M_2 are masses lumped from girders and columns, and k_1 and k_2 represent column stiffness. When the girder is infinitely rigid, the structure has no joint rotations; this spring–mass model is shown in Fig. 2.1b. When the girders are flexible and structural joint rotations exist, the spring–mass model differs, as shown in Fig. 2.1c. Note the reason for the difference: if x_2 is dis-

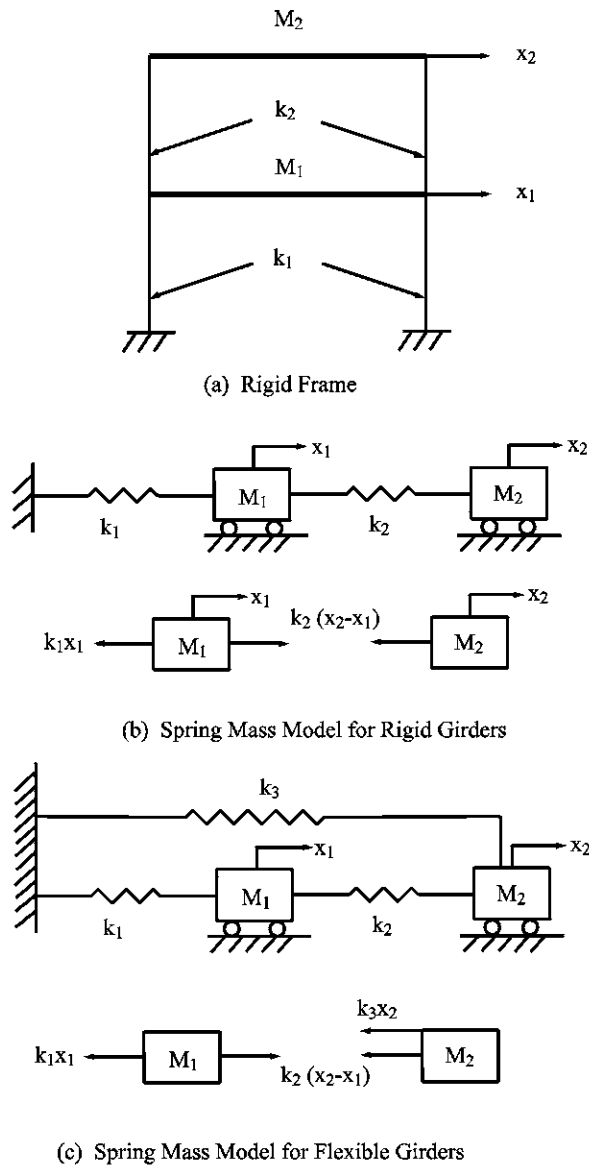


FIG. 2.1 Spring–mass models for rigid frame.

placed and the girders are rigid, no force is transmitted to the support. However, with flexible girders, the joints at the first floor rotate, the column below is distorted, and force is transmitted to the support.

2.1.2. Advantages of the Lumped Mass Model

The method is approximate because it is assumed that the masses of the floors and the columns are lumped at the floor levels, and that the columns are massless springs. In practical engineering, these assumptions are acceptable because they offer the following advantages to structural analysis:

1. Tall buildings have masses that are concentrated on the floors, and the columns can be practically considered as massless springs. This simplification makes it possible to replace a continuum system with a discrete system that has few degrees of freedom.
2. Most structural members do not have constant cross sections; if they do, they may also have other attached construction material which essentially causes the members to be nonuniform. The lumped parameter method can be used to solve this type of problem.
3. The numerical technique generally used to analyze a lumped parameter system with finite degrees of freedom can be used to surmount the mathematical obstacle in solving continuum problems that comprise infinite degrees of freedom.

2.2. CHARACTERISTICS OF FREE VIBRATION OF TWO-DEGREE-OF-FREEDOM SYSTEMS

2.2.1. Motion Equations, Natural and Normal Modes

Differential equations of motion for the structure shown in Fig. 2.1b can be established from the accompanying free-body diagram in which x_1 and x_2 represent both static and dynamic *degrees of freedom* (*d.o.f.*). Because the dynamic displacement, x , is a combination of time function, $g(t)$, and shape function, $X(x)$, that is, $x = g(t)X(x)$; x_1 and x_2 are actually the coordinates of the shape function. According to Newton's second law, the motion equation is expressed as

$$M_1\ddot{x}_1 + k_1x_1 - k_2(x_2 - x_1) = 0 \quad (2.1a)$$

$$M_2\ddot{x}_2 + k_2(x_2 - x_1) = 0 \quad (2.1b)$$

Similarly, the differential equations associated with the free-body diagrams of Fig. 2.1c are

$$M_1\ddot{x}_1 + k_1x_1 - k_2(x_2 - x_1) = 0 \quad (2.2a)$$

$$M_2\ddot{x}_2 + k_2(x_2 - x_1) + k_3x_2 = 0 \quad (2.2b)$$

Note that, due to joint rotations, k_1 and k_2 in Eq. (2.1a,b) are numerically different from those values in Eq. (2.2a,b), although member sizes are the same for both structures.

As discussed in Chapter 1, the general solution of a second-order equation, $M\ddot{x} + Kx = 0$, of a lumped mass is

$$x = A \cos pt + B \sin pt \quad (2.3a)$$

A convenient, alternate method of expressing Eq. (2.3a) is

$$x = g(t)X(x) = X \cos(pt - \alpha) \quad (2.3b)$$

The relationship between X , α and A , B can be expressed as

$$X^2 = A^2 + B^2 \quad \text{and} \quad \tan \alpha = B/A \quad (2.3c)$$

The physical aspect of X is an arbitrary amplitude of the mass from its equilibrium position, and the constant, α , is the arbitrary phase angle between the motion and the reference motion, $\cos pt$.

Let the time dependent displacements of the masses be expressed as

$$x_1 = X_1 \cos(pt - \alpha) \quad \text{and} \quad x_2 = x_2 \cos(pt - \alpha) \quad (2.3d)$$

Substituting x_1 and x_2 for the corresponding terms in Eqs. (2.1a) and (2.1b), and cancelling the common factor, $\cos(pt - \alpha)$, yield

$$p^2 M_1 X_1 + k_1 X_1 - k_2(X_1 - X_2) = 0 \quad (2.3e)$$

$$p^2 M_2 X_2 - k_2(X_2 - X_1) = 0 \quad (2.3f)$$

Assume that $k_1 = k_2 = k$ and $M_1 = M_2 = M$; then Eqs. (2.3c) and (2.3d) become

$$\left(p^2 - \frac{2k}{M}\right)X_1 + \frac{k}{M}X_2 = 0 \quad (2.4a)$$

$$\frac{k}{M}X_1 + \left(p^2 - \frac{k}{M}\right)X_2 = 0 \quad (2.4b)$$

The above homogeneous equations have variables, X_1 and X_2 , for which nontrivial solutions exist if and only if the *determinant* of X 's vanishes. This is stated as

$$\Delta = \begin{vmatrix} p^2 - \frac{2k}{M} & \frac{k}{M} \\ \frac{k}{M} & p^2 - \frac{k}{M} \end{vmatrix} = 0$$

which leads to the following *frequency equation*

$$p^4 - 3p^2 \frac{k}{M} + \frac{k^2}{M^2} = 0 \quad (2.5)$$

The two roots, p_1^2 and p_2^2 , in Eq. (2.5) are

$$p_1^2 = 0.382 \frac{k}{M} \quad \text{or} \quad p_1 = 0.618 \sqrt{\frac{k}{M}} \quad (2.6a)$$

$$p_2^2 = 2.618 \frac{k}{M} \quad \text{or} \quad p_2 = 1.618 \sqrt{\frac{k}{M}} \quad (2.6b)$$

The lower of the two natural frequencies is called a *fundamental frequency*. Substituting p_1^2 and p_2^2 in Eq. (2.4a) or (2.4b) yields two relationships for X_1 and X_2 , which are called *natural modes* of vibrations. The first natural mode corresponding to p_1^2 is denoted by $X_1^{(1)}$ and $X_2^{(1)}$ as

$$X_1^{(1)} = 0.618 X_2^{(1)} \quad (2.7a)$$

The second natural mode is

$$X_2^{(2)} = -0.618 X_1^{(2)} \quad (2.7b)$$

Mode shapes of Eqs. (2.7a) and (2.7b) are shown in Fig. 2.2a and b, respectively. Depending on the form of the initial disturbance, the system can vibrate in either of the two modes or in a periodic motion resulting from a combination of the two modes. For instance, if the initial displacements are applied according to Eq. (2.7a), then the structure vibrates in the mode shape shown in Fig. 2.2a; however, if an arbitrary initial disturbance is applied to the structure, then the motion can be considered as being composed of appropriate amounts of the natural modes (modes 1 and 2) as shown in Fig. 2.2c.

A determination of the system's motion at any time after the initial disturbance is presented as follows. Let $X^{(1)}$ be the amplitude of the first natural mode; we can then write

$$X_1^{(1)} = X^{(1)} a_1^{(1)} = X^{(1)} \quad (2.8)$$

$$X_2^{(1)} = X^{(1)} a_2^{(1)} \quad (2.9)$$

where $a_1^{(1)}$ and $a_2^{(1)}$ are coordinates of the first *normal mode*. A normal mode results from *normalization* of the natural mode in which the largest component of that mode becomes unity and the rest of the components are proportional to the unit. The method of obtaining a normal mode is demonstrated later in this chapter for various eigensolution techniques. Since $a_1^{(1)} = 1$, the coordinates become relative amplitudes, and $a_2^{(1)} = X_2^{(1)}/X_1^{(1)}$. Similarly, let $X^{(2)}$

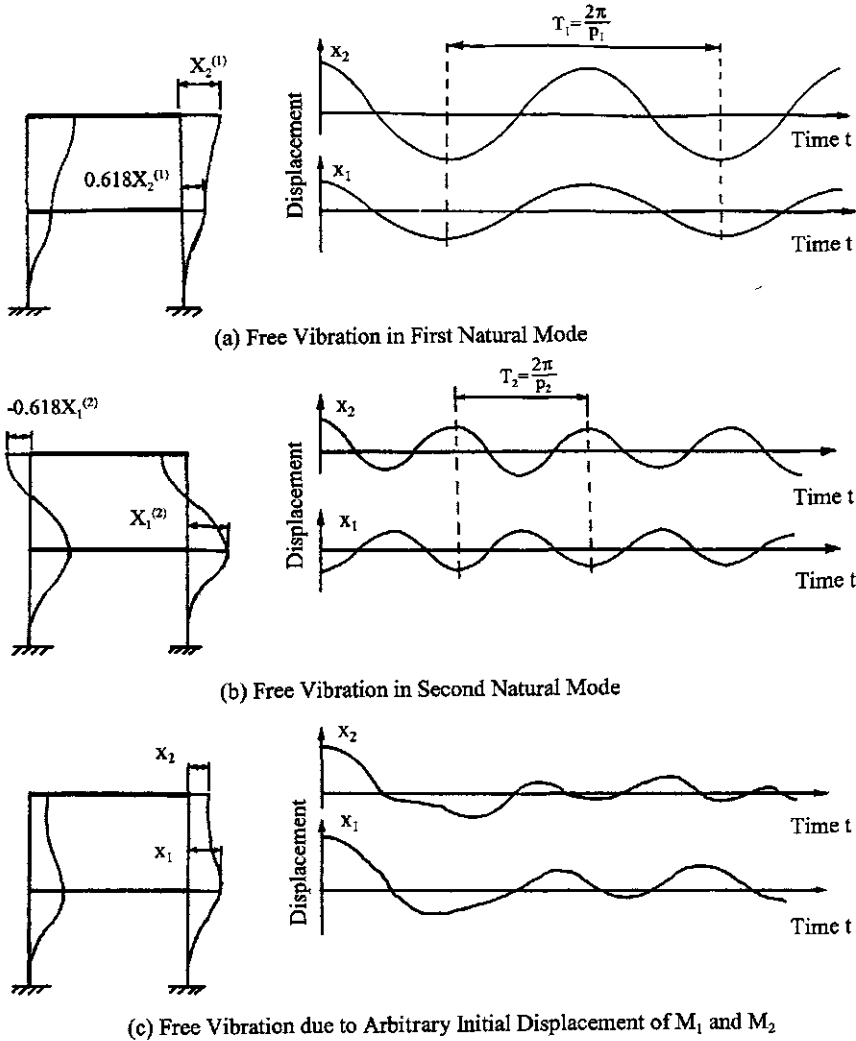


FIG. 2.2 Mode shapes.

be an arbitrary amplitude of the second natural mode; we can then write

$$X_1^{(2)} = X^{(2)} a_1^{(2)} = X^{(2)} \quad (2.10)$$

$$X_2^{(2)} = X^{(2)} a_2^{(2)} \quad (2.11)$$

where $a_1^{(2)}$ and $a_2^{(2)}$ are coordinates of the second normal mode. In the present example, $a_2^{(1)} = 1.618$ and $a_2^{(2)} = -0.618$. These results are obtained from Eqs. (2.7a) and (2.7b).

The complete solution for the system of equations in Eqs. (2.1a) and (2.1b) should be the resultant of X_1 and X_2 , and can be written in the form

$$x_1 = X^{(1)} a_1^{(1)} \cos(p_1 t - \alpha^{(1)}) + X^{(2)} a_1^{(2)} \cos(p_2 t - \alpha^{(2)}) \quad (2.12)$$

$$x_2 = X^{(1)} a_2^{(1)} \cos(p_1 t - \alpha^{(1)}) + X^{(2)} a_2^{(2)} \cos(p_2 t - \alpha^{(2)}) \quad (2.13)$$

where $a_1^{(1)}$, $a_1^{(2)}$, $a_2^{(1)}$, and $a_2^{(2)}$ are known coordinates of the normal modes, and $X^{(1)}$, $X^{(2)}$, $\alpha^{(1)}$, and

$\alpha^{(2)}$ are four arbitrary constants that should be determined using the initial conditions of displacement, x_1 , x_2 , and velocities, \dot{x}_1 (same as dx_1/dt), \dot{x}_2 at time, $t = t_0$, when the disturbance is applied. From Eqs. (2.12) and (2.13), it may be noted that the general solution is a sum of two harmonic motions with associated frequencies p_1 and p_2 .

2.2.2. Harmonic and Periodic Motion

The resultant motion of Eqs. (2.12) and (2.13) can be harmonic or periodic, depending on the given initial conditions. Generally the result is not harmonic, but periodic because motions of different frequencies, as discussed in Section 1.2.3, are added. The following examples serve to illustrate.

EXAMPLE 2.2.1 (a) *Harmonic motion in natural mode*—knowing the coordinates of the normal modes from Eqs. (2.7a) and (2.7b) as $a_1^{(1)} = 1$, $a_2^{(1)} = 1.618$, $a_1^{(2)} = 1.0$, and $a_2^{(2)} = -0.618$, the displacement solutions in Eqs. (2.12) and (2.13) are formulated as

$$x_1 = X^{(1)} \cos(p_1 t - \alpha^{(1)}) + X^{(2)} \cos(p_2 t - \alpha^{(2)}) \quad (a)$$

$$x_2 = 1.618X^{(1)} \cos(p_1 t - \alpha^{(1)}) - 0.618X^{(2)} \cos(p_2 t - \alpha^{(2)}) \quad (b)$$

from which the velocities can be expressed as

$$\dot{x}_1 = -p_1 X^{(1)} \sin(p_1 t - \alpha^{(1)}) - p_2 X^{(2)} \sin(p_2 t - \alpha^{(2)}) \quad (c)$$

$$\dot{x}_2 = -1.618p_1 X^{(1)} \sin(p_1 t - \alpha^{(1)}) + 0.618p_2 X^{(2)} \sin(p_2 t - \alpha^{(2)}) \quad (d)$$

Substituting initial conditions $x_{1(0)} = 0.618$ ft (0.188 m), $x_{2(0)} = 1.0$ ft (0.305 m), $\dot{x}_{1(0)} = 0$, and $\dot{x}_{2(0)} = 0$ at $t = 0$ for the corresponding terms in Eqs. (a)–(d) yields

$$0.618 = X^{(1)} \cos(-\alpha^{(1)}) + X^{(2)} \cos(-\alpha^{(2)}) \quad (e)$$

$$1.0 = 1.618X^{(1)} \cos(-\alpha^{(1)}) - 0.618X^{(2)} \cos(-\alpha^{(2)}) \quad (f)$$

$$0 = -p_1 X^{(1)} \sin(-\alpha^{(1)}) - p_2 X^{(2)} \sin(-\alpha^{(2)}) \quad (g)$$

$$0 = -1.618p_1 X^{(1)} \sin(-\alpha^{(1)}) + 0.618p_2 X^{(2)} \sin(-\alpha^{(2)}) \quad (h)$$

A comparison of Eq. (g) with Eq. (h) leads to

$$2.236p_2 X^{(2)} \sin(-\alpha^{(2)}) = 0 \quad \text{or} \quad 2.236p_1 X^{(1)} \sin(-\alpha^{(1)}) = 0 \quad (i)$$

p_1 , p_2 , $X^{(1)}$, and $X^{(2)}$ cannot be zero; therefore

$$\alpha^{(1)} = \alpha^{(2)} = n\pi, \quad n = 1, 2, \dots, \infty \quad (j)$$

Inserting $n\pi$ into Eqs. (e) and (f) gives

$$X^{(1)} = -0.618 \text{ ft (0.188 m)} \quad \text{and} \quad X^{(2)} = 0 \quad (k)$$

Thus the displacements in Eqs. (a) and (b) become

$$x_1 = 0.618 \cos p_1 t \quad (l)$$

$$x_2 = \cos p_1 t \quad (m)$$

Eqs. (l) and (m) are plotted in Fig. 2.3, showing that, because of the given initial conditions, the displacement response is the first natural mode of the vibration. This behavior has been demonstrated in Fig. 2.2.

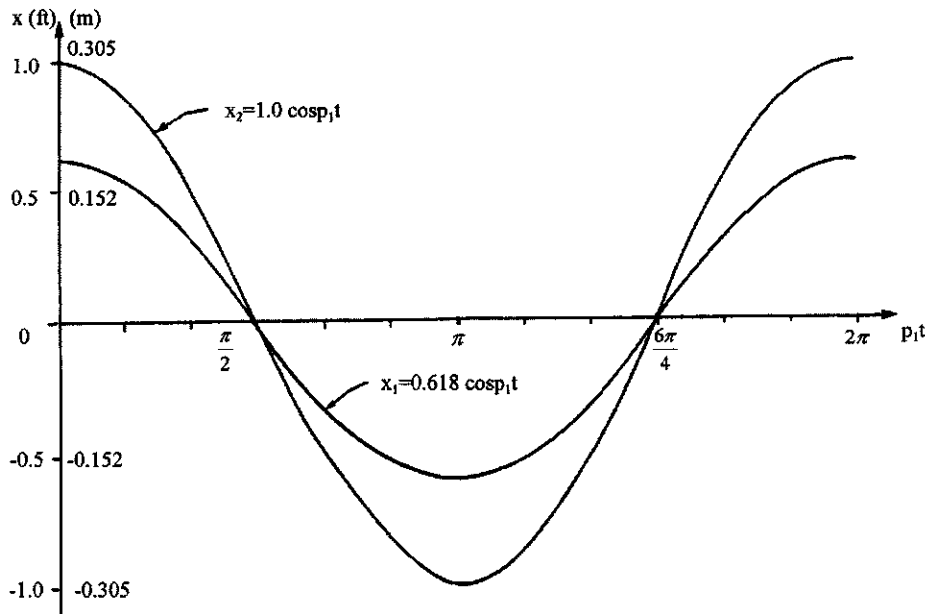


FIG. 2.3 Harmonic motion.

(b) *Periodic motion*—substituting the arbitrary initial conditions of $x_{1(0)} = 1$ ft (0.305 m), $x_{2(0)} = 0$, $\dot{x}_{1(0)} = 0$, and $\dot{x}_{2(0)} = 0$ at $t = 0$ for the corresponding terms in Eqs. (a)–(d), and then solving the constants, yields

$$\alpha^{(1)} = \alpha^{(2)} n\pi, \quad n = 1, 2, \dots, \infty \quad (\text{n})$$

$$X^{(1)} = -0.276 \text{ ft} (0.084 \text{ m}) \quad \text{and} \quad X^{(2)} = -0.724 \text{ ft} (-0.221 \text{ m}) \quad (\text{o})$$

The displacement solutions become

$$x_1 = 0.276 \cos p_1 t + 0.724 \cos p_2 t \quad (\text{p})$$

$$x_2 = 0.447 \cos p_1 t - 0.447 \cos p_2 t \quad (\text{q})$$

Eqs. (p) and (q) are plotted in Fig. 2.4.

(c) *Periodic motion*—for initial conditions $x_{1(0)} = 0$, $\dot{x}_{1(0)} = 1$ ft/sec (0.305 m/sec), $x_{2(0)} = 0$, and $\dot{x}_{2(0)} = 0$ at $t = 0$, the displacement response can be similarly expressed as

$$x_1 = \frac{0.276}{p_1} \sin p_1 t + \frac{0.724}{p_2} \sin p_2 t \quad (\text{r})$$

$$x_2 = \frac{0.447}{p_1} \sin p_1 t - \frac{0.447}{p_2} \sin p_2 t \quad (\text{s})$$

Numerical results of Eqs. (r) and (s) are shown in Fig. 2.5.

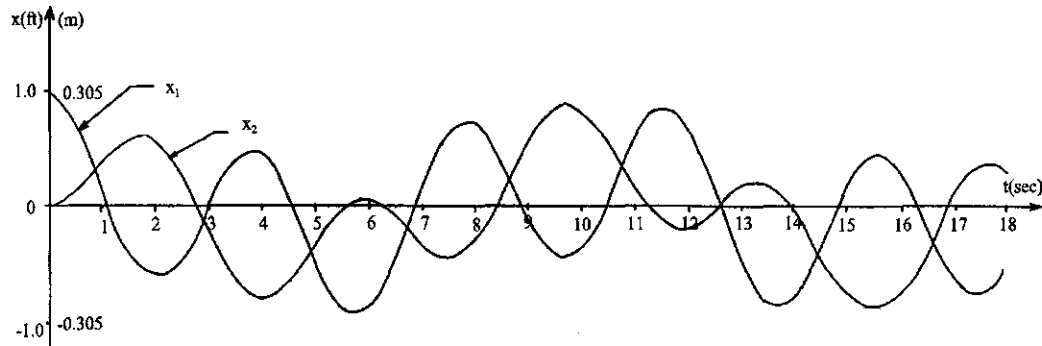


FIG. 2.4 Periodic motion of case (b).

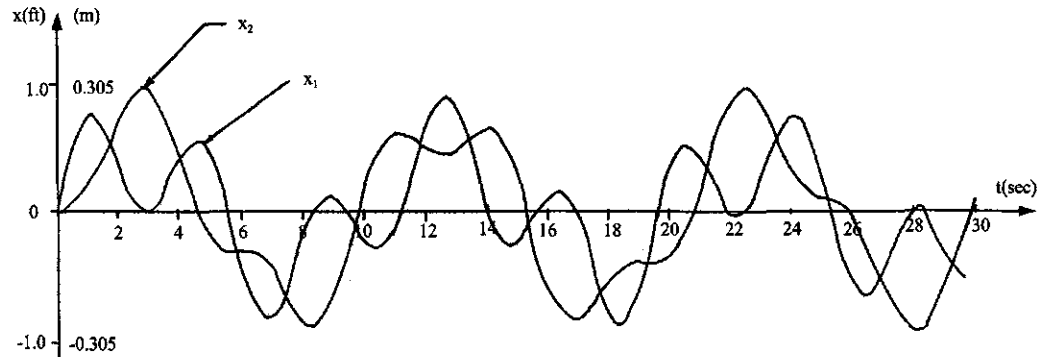


FIG. 2.5 Periodic motion of case (c).

2.3. DYNAMIC MATRIX EQUATION

The linear equations in Eqs. (2.1a) and (2.1b) can be expressed in a matrix notation:

$$\begin{bmatrix} M_1 & 0 \\ 0 & M_2 \end{bmatrix} \begin{Bmatrix} \ddot{x}_1 \\ \ddot{x}_2 \end{Bmatrix} + \begin{bmatrix} k_1 + k_2 & -k_2 \\ -k_2 & k_2 \end{bmatrix} \begin{Bmatrix} x_1 \\ x_2 \end{Bmatrix} = \{0\} \quad (2.14)$$

or symbolically

$$[M]\{\ddot{x}\} + [K]\{x\} = 0 \quad (2.15)$$

where \$[M]\$ and \$[K]\$ are called the *mass matrix* and *structural stiffness matrix*, respectively. To find the natural frequencies of the system, imagine that the masses are displaced by the amount of \$x_1\$ and \$x_2\$ signified by \$\{x_0\}\$ and suddenly released at time \$t = 0\$. As a result, the instantaneous velocities of the two masses, \$\dot{x}_1\$ and \$\dot{x}_2\$, are zero, or \$\{\dot{x}_0\} = 0\$; this value and \$\{x_0\}\$ represent the initial conditions of the equations of motion for which the solution can be simplified to \$x = X \cos pt\$, while the arbitrary constant \$B\$ in Eq. (2.3a) or \$\alpha\$ in Eq. (2.3b) vanishes as a result of one zero initial condition.

Let the displacement vector be expressed as

$$\{x\} = (\cos pt) \{X\} \quad (2.16)$$

of which the accelerations are

$$\{\ddot{x}\} = (-p^2 \cos pt) \{X\} \quad (2.17)$$

The term in parentheses is a scalar multiplier. By inserting Eqs. (2.16) and (2.17) into Eq. (2.15), we have either

$$-p^2 [M] \{X\} + [K] \{X\} = 0 \quad (2.18)$$

or

$$\left(\begin{bmatrix} -1 \\ p^2 \end{bmatrix} - [\delta] [M] \right) \{X\} = 0 \quad (2.19)$$

where $\begin{bmatrix} -1 \\ p^2 \end{bmatrix}$ denotes a diagonal matrix. Equations (2.18) and (2.19) are called *dynamic matrix equations* where $[\delta]$ is the *flexibility matrix*, an inversion of the *structural stiffness matrix* $[K]$. Equation (2.18) can be obtained directly from the matrix formulation, discussed in later chapters for various structural systems.

2.4. ORTHOGONALITY OF NORMAL MODES

Let $\{X\}_u$ and $\{X\}_v$ be the normal modes corresponding to the two different natural frequencies p_u and p_v ; then, from Eq. (2.18)

$$p_u^2 [M] \{X\}_u = [K] \{X\}_u \quad (2.20)$$

and

$$p_v^2 [M] \{X\}_v = [K] \{X\}_v \quad (2.21)$$

Postmultiplying the *transpose* of Eq. (2.20) by $\{X\}_v$ yields

$$(p_u^2 [M] \{X\}_u)^T \{X\}_v = ([K] \{X\}_u)^T \{X\}_v \quad (2.22)$$

or

$$p_u^2 \{X\}_u^T [M]^T \{X\}_v = \{X\}_u^T [K]^T \{X\}_v \quad (2.23)$$

Premultiply Eq. (2.21) by $\{X\}_u^T$; then obtain

$$p_v^2 \{X\}_u^T [M] \{X\}_v = \{X\}_u^T [K] \{X\}_v \quad (2.24)$$

Let $[M]$ and $[K]$ be symmetric; then $[M]^T = [M]$ and $[K]^T = [K]$; subtracting Eq. (2.24) from Eq. (2.23) gives

$$(p_u^2 - p_v^2) \{X\}_u^T [M] \{X\}_v = 0 \quad (2.25)$$

Since $u \neq v$, Eq. (2.25) is satisfied only if

$$\{X\}_u^T [M] \{X\}_v = 0 \quad \text{for } u \neq v \quad (2.26)$$

which is the *orthogonality condition for the u th and v th eigenvectors with respect to mass matrix*

$[M]$. Thus Eq. (2.24) becomes

$$\{X\}_u^T [K] \{X\}_v = 0 \quad \text{for} \quad u \neq v \quad (2.27)$$

which is the *orthogonality condition with respect to stiffness matrix* $[K]$.

For a system having an unsymmetric matrix or repeating natural frequencies, orthogonality is discussed in Sections 2.7 and 2.8, respectively.

EXAMPLE 2.4.1 Formulate the matrix product Eqs. (2.26) and (2.27) by using the mode shapes obtained in Section 2.2, where the frequencies and normal modes are

$$p_1 = 0.618\sqrt{\frac{k}{M}} \quad p_2 = 1.618\sqrt{\frac{k}{M}}$$

$$\{X\}_1 = \begin{Bmatrix} 0.618 \\ 1.000 \end{Bmatrix} \quad \{X\}_2 = \begin{Bmatrix} 1.000 \\ -0.618 \end{Bmatrix}$$

Solution: By substituting the above information into Eqs. (2.26) and (2.27), the orthogonality conditions become

$$\{X\}_1^T [M] \{X\}_2 = [0.618 \quad 1.0] \begin{bmatrix} M & 0 \\ 0 & M \end{bmatrix} \begin{Bmatrix} 1.000 \\ -0.618 \end{Bmatrix} = 0 \quad (a)$$

and

$$\{X\}_1^T [K] \{X\}_2 = [0.618 \quad 1.0] \begin{bmatrix} 2k & -k \\ -k & k \end{bmatrix} \begin{Bmatrix} 1.000 \\ -0.618 \end{Bmatrix} = 0 \quad (b)$$

2.5. MODAL MATRIX FOR UNDAMPED VIBRATION

2.5.1. Modal Matrices and Characteristics

Let $\{\Phi\}_u$ and $\{\Phi\}_v$ be *modal displacements* corresponding to u th and v th mode, respectively, such that

$$\{\Phi\}_u^T [M] \{\Phi\}_u = 1 \quad (2.28)$$

Modal displacements, $\{\Phi\}_u$, are evaluated to satisfy Eq. (2.28) and at the same time to keep the elements in the same proportion as those in $\{X\}_u$. The characteristic vector is then said to be *normalized*. Note that Eq. (2.25) has not been violated: if $u = v$, then $p_u^2 - p_u^2 = 0$; the remaining terms may be given any desired value. Let

$$\{X\}_u^T [M] \{X\}_u = L_u^2 \quad (2.29)$$

where L_u is called *length vector* at the u th mode. If the right and left sides are divided by L_u^2 , then

$$1 = \frac{\{X\}_u^T [M]}{L_u^2} \frac{\{X\}_u}{L_u} \quad (2.30)$$

Comparing Eq. (2.28) with Eq. (2.30) yields

$$\{\Phi\}_u = \frac{\{X\}_u}{L_u} \quad (2.31)$$

When the modal vectors are collected in a single square matrix of order n , corresponding to n

modes, the resulting matrix is called *modal matrix*, $[\Phi]$. Hence

$$[\Phi] = [\Phi_1, \Phi_2, \dots, \Phi_n] \quad (2.32)$$

From Eqs. (2.26) and (2.31), the orthogonality condition is expressed as

$$\{\Phi\}_u^T [M] \{\Phi\}_v = 0 \quad \text{for} \quad u \neq v \quad (2.33)$$

By using the definition in Eq. (2.28) and the orthogonality condition in Eq. (2.33), properties of the modal matrix, $[\Phi]$, are derived as

$$[\Phi]^T [M] [\Phi] = \begin{bmatrix} \{\Phi\}_1^T [M] \{\Phi\}_1 & \{\Phi\}_1^T [M] \{\Phi\}_2 & \dots & \{\Phi\}_1^T [M] \{\Phi\}_n \\ \{\Phi\}_2^T [M] \{\Phi\}_1 & \{\Phi\}_2^T [M] \{\Phi\}_2 & \dots & \{\Phi\}_2^T [M] \{\Phi\}_n \\ \vdots & \vdots & & \vdots \\ \{\Phi\}_n^T [M] \{\Phi\}_1 & \{\Phi\}_n^T [M] \{\Phi\}_2 & \dots & \{\Phi\}_n^T [M] \{\Phi\}_n \end{bmatrix} = [I] \quad (2.34)$$

Another relationship involving stiffness matrix, $[K]$, can be obtained by inserting Eq. (2.31) into Eq. (2.20)

$$[K]\{\Phi\}_u = p_u^2 [M] \{\Phi\}_u \quad (2.35)$$

Premultiply both sides of the above equation by $\{\Phi\}_v^T$, then on account of Eq. (2.33) we have

$$\{\Phi\}_v^T [K] \{\Phi\}_u = p_u^2 \{\Phi\}_v^T [M] \{\Phi\}_u = 0 \quad (2.36)$$

and

$$\{\Phi\}_v^T [K] \{\Phi\}_u = p_u^2 \quad \text{for} \quad u \neq v \quad (2.37)$$

Therefore

$$[\Phi]^T [K] [\Phi] = \begin{bmatrix} \{\Phi\}_1^T [K] \{\Phi\}_1 & \{\Phi\}_1^T [K] \{\Phi\}_2 & \dots & \{\Phi\}_1^T [K] \{\Phi\}_n \\ \{\Phi\}_2^T [K] \{\Phi\}_1 & \{\Phi\}_2^T [K] \{\Phi\}_2 & \dots & \{\Phi\}_2^T [K] \{\Phi\}_n \\ \vdots & \vdots & & \vdots \\ \{\Phi\}_n^T [K] \{\Phi\}_1 & \{\Phi\}_n^T [K] \{\Phi\}_2 & \dots & \{\Phi\}_n^T [K] \{\Phi\}_n \end{bmatrix} = [p_u^2] \quad (2.38)$$

EXAMPLE 2.5.1 Refer to Eqs. (2.34) and (2.38) and find the characteristics of the modal matrix for the example shown in Section 2.2 and Example 2.4.1.

Solution: From Eq. (2.29) the length vector can be calculated as

$$L_1^2 = \{X\}_1^T [M] \{X\}_1 = \begin{Bmatrix} 0.618 \\ 1.000 \end{Bmatrix}^T \begin{bmatrix} M & 0 \\ 0 & M \end{bmatrix} \begin{Bmatrix} 0.618 \\ 1.000 \end{Bmatrix} = 1.3819 M$$

or

$$L_1 = 1.1755 \sqrt{M} \quad (a)$$

The modal vector can be obtained from Eq. (2.31)

$$\{\Phi\}_1 = \frac{\{X\}_1}{L_1} = \frac{1}{\sqrt{M}} \begin{Bmatrix} 0.5257 \\ 0.8506 \end{Bmatrix} \quad (b)$$

Similarly, L_2 and $\{\Phi\}_2$ can be found as

$$L_2^2 = \{X\}_2^T [M] \{X\}_2 = \begin{Bmatrix} 1.000 \\ -0.618 \end{Bmatrix}^T \begin{bmatrix} M & 0 \\ 0 & M \end{bmatrix} \begin{Bmatrix} 1.000 \\ -0.618 \end{Bmatrix} = 1.3819 M$$

or

$$L_2 = 1.1755\sqrt{M} \quad (c)$$

Thus

$$\{\Phi\}_2 = \frac{\{X\}_2}{L_2} = \frac{1}{\sqrt{M}} \begin{Bmatrix} 0.8506 \\ -0.5257 \end{Bmatrix} \quad (d)$$

Using Eq. (2.32), the modal matrix is constructed as follows

$$[\Phi] = \frac{1}{\sqrt{M}} \begin{bmatrix} 0.5257 & 0.8506 \\ 0.8506 & -0.5257 \end{bmatrix} \quad (e)$$

The relationship involving the mass matrix and modal matrix is

$$\begin{aligned} [\Phi]^T [M] [\Phi] &= \frac{1}{\sqrt{M}} \begin{bmatrix} 0.5257 & 0.8506 \\ 0.8506 & -0.5257 \end{bmatrix} \begin{bmatrix} M & 0 \\ 0 & M \end{bmatrix} \frac{1}{\sqrt{M}} \begin{bmatrix} 0.5257 & 0.8506 \\ 0.8506 & -0.5257 \end{bmatrix} \\ &= \begin{bmatrix} 1.0 & 0 \\ 0 & 1.0 \end{bmatrix} \end{aligned} \quad (f)$$

while that involving the stiffness matrix and modal matrix is

$$\begin{aligned} [\Phi]^T [K] [\Phi] &= \frac{1}{\sqrt{M}} \begin{bmatrix} 0.5257 & 0.8506 \\ 0.8506 & -0.5257 \end{bmatrix} \begin{bmatrix} 2k & -k \\ -k & k \end{bmatrix} \begin{bmatrix} 0.5257 & 0.8506 \\ 0.8506 & -0.5257 \end{bmatrix} \\ &= \frac{k}{M} \begin{bmatrix} 0.3819 & 0 \\ 0 & 2.6177 \end{bmatrix} \end{aligned} \quad (g)$$

The resulting elements in Eq. (g) correspond to p_1^2 and p_2^2 .

2.5.2. Response to Initial Disturbances, Dynamic Forces and Seismic Excitation

The modal matrix method is presented here for structural response to initial velocities and displacements, dynamic loads, or seismic excitation resulting from free and forced vibrations. The applicability of the method is limited to elastic systems. Let a rigid frame be subjected to dynamic loads

$$\{F(t)\} = \{F\} f(t) \quad (2.39)$$

where $\{F(t)\}$ represents various forces, $\{F\}$, with time function, $f(t)$. The differential equations of motion in the matrix notation are

$$\{M\} \{\ddot{x}\} + [K] \{x\} = \{F(t)\} \quad (2.40)$$

We can convert the above equation into a set of *uncoupled equations* by letting structural response vector $\{x\}$ be expressed in terms of *generalized response vector* $\{x'\}$ [further discussed in Section 4.9.1 and 4.9.4; see Eqs. (4.114) and (4.139a)]

$$\{x\} = [\Phi] \{x'\} \quad (2.41)$$

whose accelerations are

$$\{\ddot{x}\} = [\Phi] \{\ddot{x}'\} \quad (2.42)$$

Substituting Eqs. (2.41) and (2.42) into Eq. (2.40) yields

$$[M][\Phi]\{\ddot{x}'\} + [K][\Phi]\{x'\} = \{F(t)\} \quad (2.43)$$

Premultiplying the above by $[\Phi]^T$ gives

$$[\Phi]^T[M][\Phi]\{\ddot{x}'\} + [\Phi]^T[K][\Phi]\{x'\} = [\Phi]^T\{F(t)\} \quad (2.44)$$

Using the orthogonality condition shown in Eqs. (2.34) and (2.38) leads to the following uncoupled equation

$$\{\ddot{x}'\} + \left[\begin{smallmatrix} \downarrow p_i^2 \\ \end{smallmatrix} \right] \{x'\} = [\Phi]^T\{F(t)\} \quad (2.45)$$

where a typical equation in row i is

$$\ddot{x}'_i + p_i^2 x'_i = [\Phi]_i^T\{F(t)\} \quad (2.46)$$

This is similar to the differential equation of motion for a system with a single d.o.f. Based on Duhamel's integral in Eq. (1.97), the solution of Eq. (2.46) becomes

$$\begin{aligned} x'_i &= x'_{i,t_0} \cos p_i(t - t_0) + \frac{\dot{x}'_{i,t_0}}{p_i} \sin p_i(t - t_0) \\ &\quad + \int_{t_0}^t \frac{1}{p_i} [\Phi]_i^T\{F(\Delta)\} \sin p_i(t - \Delta) d\Delta \end{aligned} \quad (2.47)$$

where x'_{i,t_0} and \dot{x}'_{i,t_0} should be expressed in terms of x_{i,t_0} and \dot{x}_{i,t_0} which are the initial conditions actually given. Premultiply Eq. (2.41) by $[\Phi]^T[M]$; we then have

$$[\Phi]^T[M]\{x_0\} = [\Phi]^T[M][\Phi]\{x'_0\} = \{x'_0\} \quad (2.48a)$$

Similarly, \dot{x}'_0 can be expressed as

$$[\Phi]^T[M]\{\dot{x}_0\} = [\Phi]^T[M][\Phi]\{\dot{x}'_0\} = \{\dot{x}'_0\} \quad (2.48b)$$

Expressing Eq. (2.47) in matrix form, and using the initial conditions shown above, leads to

$$\begin{aligned} \{x'\} &= \left[\begin{smallmatrix} \downarrow \cos p_i t \\ \downarrow \sin p_i t \end{smallmatrix} \right] [\Phi]^T[M]\{x_0\} + \left[\begin{smallmatrix} \downarrow \sin p_i t \\ \downarrow \cos p_i t \end{smallmatrix} \right] \left[\begin{smallmatrix} \downarrow p_i \\ \end{smallmatrix} \right]^{-1} [\Phi]^T[M]\{\dot{x}_0\} \\ &\quad + \int_0^t \left[\begin{smallmatrix} \downarrow \sin p_i(t - \Delta) \\ \downarrow \cos p_i(t - \Delta) \end{smallmatrix} \right] \left[\begin{smallmatrix} \downarrow p_i \\ \end{smallmatrix} \right]^{-1} [\Phi]^T\{F(\Delta)\} d\Delta \end{aligned} \quad (2.49)$$

where $t_0 = 0$. Use Eqs. (2.39), (2.41) and (2.45) to obtain the dynamic displacements and accelerations at any time, Δ ,

$$\{x\} = [\Phi]\{x'\} \quad (2.50)$$

$$\begin{aligned} \{\ddot{x}\} &= [\Phi]\{\ddot{x}'\} \\ &= [\Phi][\Phi]^T\{F(\Delta)\} - [\Phi] \left[\begin{smallmatrix} \downarrow p_i^2 \\ \end{smallmatrix} \right] [\Phi]^T[M]\{x\} \end{aligned} \quad (2.51)$$

In the forced vibration part of Eq. (2.49), the uncoupling displacement x'_i corresponding to i th mode is associated with normal mode $\{\Phi\}_i$, and the force $\{F(\Delta)\}$ applied at the dynamic d.o.f. as $\{\Phi\}_i^T \{F(\Delta)\}$, which represents a vector of applied forces in normal coordinates. Consider a force, $F_\ell(\Delta)$, acting at ℓ th dynamic d.o.f. only. Then the uncoupling displacement corresponding to the i th mode is

$$x'_i = \frac{\Phi_{\ell i}}{p_i} \int_0^t F_\ell(\Delta) \sin p_i(t - \Delta) d\Delta \quad (2.52)$$

and the displacement at m th dynamic d.o.f. in the original coordinates is

$$x_{m,\ell} = \sum_{i=1}^n \frac{\Phi_{mi}\Phi_{\ell i}}{p_i} \int_0^t F_\ell(\Delta) \sin p_i(t - \Delta) d\Delta \quad (2.53)$$

Now consider a force, $F_m(\Delta)$, acting at m th dynamic d.o.f.; the uncoupling displacement corresponding to the i th mode is

$$x'_i = \frac{\Phi_{mi}}{p_i} \int_0^t F_m(\Delta) \sin p_i(t - \Delta) d\Delta \quad (2.54)$$

and the displacement in the original coordinates at the ℓ th dynamic d.o.f. is

$$x_{\ell,m} = \sum_{i=1}^n \frac{\Phi_{\ell i}\Phi_{mi}}{p_i} \int_0^t F_m(\Delta) \sin p_i(t - \Delta) d\Delta \quad (2.55)$$

If $F_\ell(\Delta) = F_m(\Delta)$, then

$$x_{\ell,m} = x_{m,\ell} \quad (2.56)$$

which states that the *displacement response at the ℓ th dynamic d.o.f. due to the time-dependent force applied at the m th dynamic d.o.f. is equal to the displacement response at the m th dynamic d.o.f. due to the same force applied at ℓ th dynamic d.o.f.* This is *reciprocal theorem for dynamic loads* which is similar to Maxwell's reciprocal theorem for static loads.

EXAMPLE 2.5.2 Formulate displacement expressions for Example 2.5.1 for the following initial conditions at t_0 : $\{x_0\} = [2 \quad 1]^T y_0$, $\{\dot{x}_0\} = [1 \quad -1]^T \dot{y}_0$.

Solution: from Example 2.5.1

$$[\Phi]^T [M] \{x_0\} = \frac{1}{\sqrt{M}} \begin{bmatrix} 0.5257 & 0.8506 \\ 0.8506 & -0.5257 \end{bmatrix} \begin{bmatrix} M & 0 \\ 0 & M \end{bmatrix} \begin{Bmatrix} 2 \\ -1 \end{Bmatrix} y_0 = \sqrt{M} y_0 \begin{Bmatrix} 1.9020 \\ 1.1755 \end{Bmatrix} \quad (a)$$

$$[\Phi]^T [M] \{\dot{x}_0\} = \frac{1}{\sqrt{M}} \begin{bmatrix} 0.5257 & 0.8506 \\ 0.8506 & -0.5257 \end{bmatrix} \begin{bmatrix} M & 0 \\ 0 & M \end{bmatrix} \begin{Bmatrix} 1 \\ -1 \end{Bmatrix} \dot{y}_0 = \sqrt{M} \dot{y}_0 \begin{Bmatrix} -0.3249 \\ 1.3763 \end{Bmatrix} \quad (b)$$

The equation of motion may be obtained from Eqs. (2.49) and (2.50) as

$$\begin{aligned}
 \{x\} &= [\Phi] \left(\begin{bmatrix} \sin p(t-t_0) \\ \cos p(t-t_0) \end{bmatrix} [\Phi]^T [M] \{\dot{x}_0\} + \begin{bmatrix} \cos p(t-t_0) \\ -\sin p(t-t_0) \end{bmatrix} [\Phi]^T [M] \{x_0\} \right) \\
 &= \frac{1}{\sqrt{M}} \begin{bmatrix} 0.5257 & 0.8506 \\ 0.8506 & -0.5257 \end{bmatrix} \left(\begin{bmatrix} sn1 & 0 \\ 0 & sn2 \end{bmatrix} \sqrt{\frac{M}{k}} \begin{bmatrix} 1.618 & 0 \\ 0 & 0.618 \end{bmatrix} \sqrt{M} j_0 \begin{bmatrix} -0.3249 \\ 1.3763 \end{bmatrix} \right. \\
 &\quad \left. + \begin{bmatrix} cs1 & 0 \\ 0 & cs2 \end{bmatrix} \sqrt{M} y_0 \begin{bmatrix} 1.9020 \\ 1.1755 \end{bmatrix} \right) \\
 &= \begin{bmatrix} -0.2761sn1 + 0.7235sn2 \\ -0.4472sn1 - 0.4472sn2 \end{bmatrix} j_0 \sqrt{\frac{M}{k}} + \begin{bmatrix} cs1 + 0.9969cs2 \\ 1.6178cs1 - 0.618cs2 \end{bmatrix} y_0
 \end{aligned} \tag{c}$$

where $sn1 = \sin 0.618 \sqrt{k/M} (t-t_0)$, $sn2 = \sin 1.618 \sqrt{k/M} (t-t_0)$, $cs1 = \cos 0.618 \sqrt{k/M} (t-t_0)$, and $cs2 = \cos 1.618 \sqrt{k/M} (t-t_0)$.

EXAMPLE 2.5.3 Formulate the displacement response of the structure given in Example 2.5.2 at $\Delta = 1$ sec and $\Delta = 2$ sec. Initial conditions are $\{x_0\} = 0$ and $\{\dot{x}_0\} = 0$, and applied forces are $\{F(t)\} = [10 \ 20]^T$ kips, lasting for 1.5 sec.

Solution: From Eqs. (2.49) and (2.50), the displacement equations are expressed as

$$\begin{aligned}
 \{x\} &= [\Phi] \int_0^{1.5} \left[\begin{bmatrix} \sin p(t-\Delta) \\ \cos p(t-\Delta) \end{bmatrix} [\Phi]^T \{F(\Delta)\} d\Delta \right. \\
 &\quad \left. + [\Phi] \int_{1.5}^2 \left[\begin{bmatrix} \sin p(t-\Delta) \\ \cos p(t-\Delta) \end{bmatrix} [\Phi]^T \{0\} d\Delta \right] \right]
 \end{aligned} \tag{a}$$

Substituting the dynamic characteristics obtained in Example 2.5.2 into the above yields the following expression of the displacement response at $\Delta = 1$ sec

$$\{x\} = \frac{1}{k} \begin{bmatrix} 30.640(1 - cs1) - 0.662(1 - cs2) \\ 49.577(1 - cs1) + 0.409(1 - cs2) \end{bmatrix} \tag{b}$$

where $cs1 = \cos 0.618 \sqrt{k/M}$ and $cs2 = \cos 1.618 \sqrt{k/M}$. The second term in Eq. (a) must be zero because $\{F(\Delta)\}$ for $\Delta > 1.5$ sec. Therefore, the displacement response at $\Delta = 2$ sec becomes

$$\{x\} = \frac{1}{k} \begin{bmatrix} 30.640(cs1' - cs1'') - 0.662(cs2' - cs2'') \\ 49.577(cs1' - cs2'') + 0.409(cs2' - cs2'') \end{bmatrix} \tag{c}$$

where $cs1' = \cos[0.618 \sqrt{k/M} (t-1.5)]$, $cs1'' = \cos(0.618 \sqrt{k/M} t)$, $cs2' = \cos[1.618 \sqrt{k/M} (t-1.5)]$, and $cs2'' = \cos(1.618 \sqrt{k/M} t)$.

EXAMPLE 2.5.4 For the structure shown in Fig. 2.6, we have $p_1 = 2.218$ rad/sec, $p_2 = 10.781$ rad/sec, $\{X\}_1 = [1.0 \ 0.863]^T$, and $\{X\}_2 = [-0.863 \ 1.0]^T$. Applied forces are $F_1(t) = F_1 f(t) = F_2 f(t)$, where $F_1 = 20k$, $F_2 = 30k$, and $f(t) = 1 - (t/\zeta)$ as shown in the accompanying figure. Find the displacement contributed from each individual mode and the total response. Assume initial conditions are zero. Modal matrix $[\Phi]$ is also given.

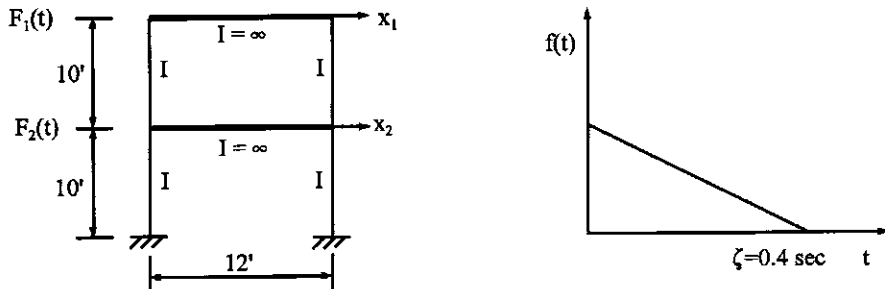


FIG. 2.6 Example 2.5.4.

Solution: From the given information, the frequencies, normal modes and modal matrices are

$$p_1 = 2.218 \text{ rad/sec}, \quad p_2 = 10.781 \text{ rad/sec} \quad (\text{a})$$

$$[X] = \begin{bmatrix} 1.000 & -0.863 \\ 0.863 & 1.000 \end{bmatrix}, \quad [\Phi] = \begin{bmatrix} 0.340 & -0.293 \\ 0.293 & 0.340 \end{bmatrix} \quad (\text{b})$$

Based on Eqs. (2.49) and (2.50), the displacement response is

$$\begin{aligned} \{x\} &= [\Phi] \int_0^t [\sin p(t-\Delta)] [\Phi^{-1}] [\Phi^T \{F(\Delta)\}] d\Delta \\ &= \begin{bmatrix} \Phi_{11}x'_1 + \Phi_{12}x'_2 \\ \Phi_{21}x'_1 + \Phi_{22}x'_2 \end{bmatrix} \\ &= \begin{bmatrix} x_1 & (\text{due to 1st mode}) + x_1 & (\text{due to 2nd mode}) \\ x_2 & (\text{due to 1st mode}) + x_2 & (\text{due to 2nd mode}) \end{bmatrix} \end{aligned} \quad (\text{c})$$

Numerical solutions of Eq. (c) can be obtained as previously shown, and the results are illustrated in Figs. 2.7 and 2.8.

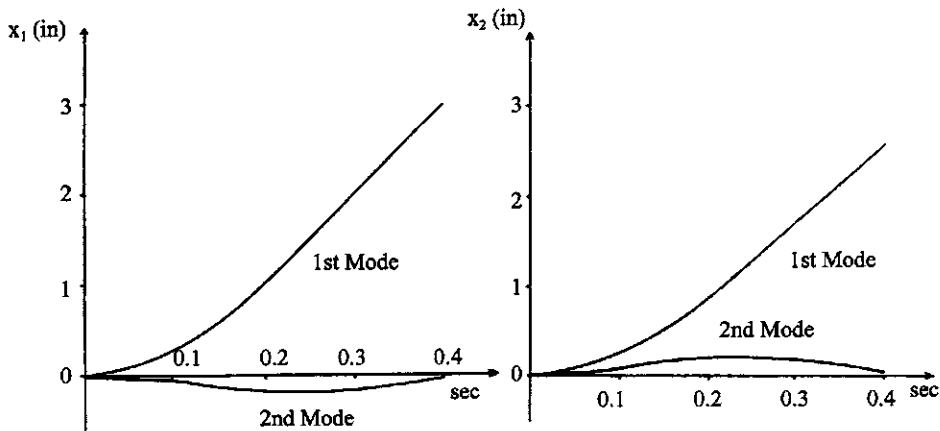


FIG. 2.7 x_1 and x_2 influenced by individual modes.

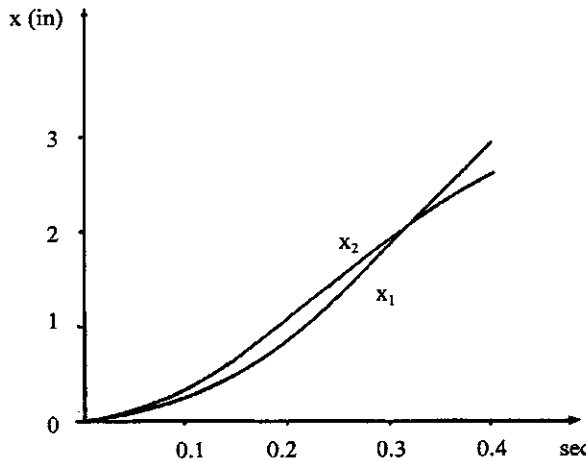


FIG. 2.8 Displacements x_1 and x_2 .

When the frame is subjected to ground excitation, \ddot{x}_g , then Eq. (2.40) becomes

$$[M]\{\ddot{x}\} + [K]\{x\} = -\{M\}\ddot{x}_g \quad (2.57)$$

where the negative sign may be dropped as discussed in Eq. (1.122). Following the aforementioned procedures, Eq. (2.57) may be decoupled as

$$\{\ddot{x}'\} + \left[\frac{1}{p_i^2}\right]\{x'\} = [\Phi]^T\{M\}\ddot{x}_g \quad (2.58)$$

Note that Eq. (2.58) is identical to Eq. (2.45) with $\{F(t)\} = \{M\}\ddot{x}_g$. Consequently, the solution of x'_i above is the same as Eq. (2.47), except for the last term, which should be (for simplicity, let $t_0 = 0$)

$$x'_i = \int_0^t \frac{1}{p_i} [\Phi]_i^T \{M\} \sin p_i(t - \Delta) \ddot{x}_g d\Delta \quad (2.59a)$$

or

$$x'_i = [\Phi]_i^T \{M\} \int_0^t \frac{1}{p_i} \ddot{x}_g \sin p_i(t - \Delta) d\Delta \quad (2.59b)$$

Comparison of (Eq. 2.47) with Eq. (1.97) reveals that the solution of free vibration for the single mass system is the same as that of the uncoupled equation except the term associated with forced vibration. The solution of the forced vibration in Eq. (1.97) is

$$x = \frac{1}{Mp} \int_0^t F(\Delta) \sin p(t - \Delta) d\Delta \quad (2.60)$$

Using $x_{st} = F/K$ and $F(\Delta) = Ff(t)$ in the above gives

$$x = x_{st} p \int_0^t f(t) \sin p_i(t - \Delta) d\Delta = x_{st} A_m \quad (2.61)$$

From Eq. (2.47), the forced vibration solution is

$$\begin{aligned} x'_i &= \int_0^t \frac{1}{p_i} [\Phi]_i^T \{F(\Delta)\} \sin p_i(t - \Delta) d\Delta \\ &= \sum_{r=1}^n \frac{\Phi_{ri} F_r}{p_i^2} \int_0^t p_i f(t) \sin p_i(t - \Delta) d\Delta = x'_{sti} A_{mi} \end{aligned} \quad (2.62)$$

where x'_{sti} is *pseudo-static displacement* and A_{mi} is the *amplification factor* corresponding to the i th mode. Similarly, Eq. (2.59b) can be expressed as

$$x'_i = \sum_{r=1}^n \frac{\Phi_{ri} M_r}{p_i^2} \int_0^t p_i \ddot{x}_g \sin p_i(t - \Delta) d\Delta = x'_{sti} p_i S_{vi} \quad (2.63)$$

where S_{vi} may be obtained from the *velocity response spectrum* as discussed in Section 1.5.3.

Note that the modal matrix formulation shown in Eqs. (2.49) and (2.62) is based on the assumption that $f(t)$ is the same for all forces acting on the structure. When $f(t)$ differs among individual forces, the modal matrix equation can be solved by using numerical integration.

2.5.3. Effect of Individual Modes on Response

Note that the decoupling procedures presented previously can be manipulated by using eigenvectors directly and are not necessarily dependent on the modal matrix, as already shown. Recall that the displacement was expressed in the modal matrix as $\{x\} = [\Phi]\{x'\}$, where $[\Phi] = [X]/L$. The orthogonality conditions are $[\Phi]^T [M] [\Phi] = [I]$ and $[\Phi]^T [K] [\Phi] = [p^2]$. If $[X]$ is not normalized and is directly used to uncouple the equation, then $[X]^T [M] [X] = [L^2]$ and $[X]^T [K] [X] = [L^2] [p^2]$. For simple notation, let $[L^2] = [\bar{M}]$; the orthogonality conditions can be rewritten as

$$[X]^T [M] [X] = [\bar{M}] \quad (2.64)$$

$$[X]^T [M] [X] = [\bar{M}] \left[p^2 \right] \quad (2.65)$$

Thus the uncoupled equations shown in Eq. (2.46) and (2.47) become

$$[\bar{M}] [\dot{x}']_i + [\bar{M}] \left[p^2 \right] \{x'\}_i = [X]_i^T \{F\} f(t) \quad (2.66)$$

$$\begin{aligned} x'_i &= x'_{it_0} \cos p_i(t - t_0) + \frac{\dot{x}_{it_0}}{p_i} \sin p_i(t - t_0) \\ &\quad + \frac{\{X\}_i^T \{F\}}{\bar{M}_i p_i} \int_0^t f(\Delta) \sin p_i(t - \Delta) d\Delta \end{aligned} \quad (2.67)$$

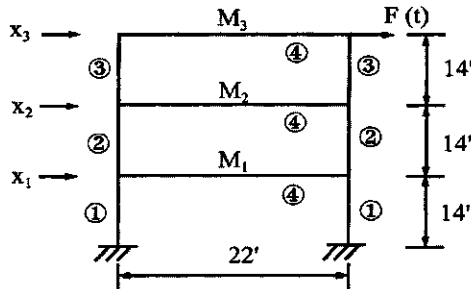


FIG. 2.9 Example 2.5.5.

and the displacements in Eqs. (2.62) and (2.63) are now expressed, respectively, in Eqs. (2.68) and (2.69) as

$$x'_i = \sum_{r=1}^n \frac{X_{ri} F_r}{\bar{M}_i p_i^2} A_{mi} = x'_{sti} A_{mi} \quad (2.68)$$

$$x'_i = \sum_{r=1}^n \frac{X_{ri} M_r}{\bar{M}_i p_i^2} p_i S_{vi} = x'_{sti} p_i S_{vi} \quad (2.69)$$

Observation of Eqs. (2.62) and (2.63) or (2.68) and (2.69) reveals that a displacement response can be obtained by using spectra and that a force, which excites a particular mode, can significantly dominate the total response. In Eqs. (2.62), (2.63), (2.68), and (2.69), $\Phi_{ri} F_r$, $\Phi_{ri} M_r$, $X_{ri} F_r$, and $X_{ri} M_r$, are called *participation factor(s)*, measuring how much the r th mode participates in synthesizing the structure's total load.

EXAMPLE 2.5.5 The structure shown in Fig. 2.9 is subjected to a harmonic force at the top floor without initial conditions. The stiffnesses, (EI/L), of members 1,2,3 and 4 are 7084.82 k ft, 5220.24 k ft, 3547.62 k ft, and 3212.12 k ft, respectively. The lumped masses are $M_1 = 0.88716 \text{ k sec}^2/\text{ft}$, $M_2 = 0.87697 \text{ k sec}^2/\text{ft}$, and $M_3 = 0.85738 \text{ k sec}^2/\text{ft}$. The natural frequencies and normal modes of the structure are given as:

	p (rad sec)		
Normal mode	$p_1 = 7.3068$	$p_2 = 23.6255$	$p_3 = 44.4920$
X_1	0.25710	0.94263	1.00000
X_2	0.67747	1.00000	-0.73140
X_3	1.00000	-0.94372	0.24080

If applied force is $F(t) = 10 \sin \omega t$ kips and the forcing frequency, ω , is assumed to be $0.8p_1$ and $1.2p_3$, find the displacement response induced by individual modes.

Solution: For the given harmonic forcing function, steady-state vibration is given in Eq. (1.58). Thus, using Eq. (2.68) yields the following displacement response in the i th degree of freedom:

$$\begin{aligned} \{x\} &= [X] [\mathbf{A}_{mi}] \frac{([X]^T \{F\})}{[\bar{M}_i] [p_i^2]} \\ &= \sum_{i=1}^3 \{X\}_i \frac{\{X\}_i^T \{F\}}{\bar{M}_i p_i^2} A_{mi} \end{aligned} \quad (a)$$

where i signifies the contribution of that mode; the amplification factor of the i th mode is

$$A_{mi} = \frac{1}{1 - (\omega/p_i)^2} \quad (b)$$

Substituting the given numerical values, we have

$$[\bar{M}] = \begin{bmatrix} 1.3185 & & \\ & 2.4255 & \\ & & 1.4060 \end{bmatrix} \quad \text{and} \quad [X]^T \{F\} = \begin{Bmatrix} 10.0000 \\ -9.4372 \\ 2.4080 \end{Bmatrix} \quad (c)$$

When $\omega = 0.8p_1$,

$$A_{mi} = \frac{1}{1 - \left(\frac{0.89_1}{p_i}\right)^2} = 2.778, 1.065, 1.018 \quad \text{for } i = 1, 2, 3 \quad (d)$$

When $\omega = 1.2p_3$,

$$A_{mi} = \frac{1}{1 - ((1.2p_3)/p_i)^2} = 0.0191, 0.7424, 1.2727 \quad \text{for } i = 1, 2, 3 \quad (e)$$

Substituting Eqs. (c) and (d) into Eq. (a) yields

$$\{x\}_1 = \begin{Bmatrix} 0.25710 \\ 0.67747 \\ 1.00000 \end{Bmatrix} \frac{10}{1.3185(7.3068)^2}(2.778) = \begin{Bmatrix} 0.1014 \\ 0.2673 \\ 0.3945 \end{Bmatrix} \quad (f)$$

Similarly

$$\{x\}_2 = \begin{Bmatrix} -6.990 \\ -7.415 \\ 6.998 \end{Bmatrix} \times 10^{-3}; \quad \{x\}_3 = \begin{Bmatrix} 8.804 \\ -6.439 \\ 2.120 \end{Bmatrix} \times 10^{-4}$$

For $\omega = 1.2p_3$, the identical procedure can be used to find the following displacements:

$$\{x\}_1 = \begin{Bmatrix} -0.6970 \\ -1.8365 \\ -2.7108 \end{Bmatrix} \times 10^{-3}; \quad \{x\}_2 = \begin{Bmatrix} 1.5977 \\ 1.6947 \\ -1.5996 \end{Bmatrix} \times 10^{-3}; \quad \{x\}_3 = \begin{Bmatrix} -1.9643 \\ 1.4381 \\ -0.4735 \end{Bmatrix} \times 10^{-3} \quad (g)$$

The superposition of displacement response resulting from individual modes may be summarized as:

Displacements (ft)	ω	1st mode	1st + 2nd mode	1st + 2nd + 3rd mode
x_1	$0.8p_1$	0.1014	9.441×10^{-2}	9.529×10^{-2}
	$1.2p_3$	-6.970×10^{-4}	9.007×10^{-4}	-1.0656×10^{-3}
x_2	$0.8p_1$	0.2673	0.2599	0.2592
	$1.2p_3$	-1.837×10^{-3}	-1.416×10^{-4}	1.2965×10^{-3}
x_3	$0.8p_1$	0.3945	0.4015	0.4017
	$1.2p_3$	-2.7108×10^{-3}	-4.3104×10^{-3}	-4.7839×10^{-3}

From the results we may conclude that the fundamental mode can always significantly influence the total response; the higher modes, however, may also remarkably affect the response behavior when a structure is excited in the neighborhood of that natural mode.

If A_{mi} in Eq. (a) is determined from the shock spectra of Fig. 1.28, then for $\omega = 0.8p_1$, and $\zeta = \pi/\omega = 0.5314$ sec, we have

$$A_{m1} = 1.69; \quad \text{for} \quad \zeta/T_1 = 0.6251 \quad (\text{i})$$

$$A_{m2} = 1.24, \quad \text{for} \quad \zeta/T_2 = 2.021 \quad (\text{j})$$

$$A_{m3} = 1.18, \quad \text{for} \quad \zeta/T_3 = 3.807 \quad (\text{k})$$

For $\omega = 1.2p_3$ and $\zeta = \pi/\omega = 0.05884$ sec

$$A_{m1} = 0.2, \quad \text{for} \quad \zeta/T_1 = 0.0684 \quad (\text{l})$$

$$A_{m2} = 0.9, \quad \text{for} \quad \zeta/T_2 = 0.2213 \quad (\text{m})$$

$$A_{m3} = 1.45, \quad \text{for} \quad \zeta/T_3 = 0.4167 \quad (\text{n})$$

Comparing Eq. (d) with Eqs. (i), (j) and (k) and Eq. (e) with Eqs. (l), (m) and (n) shows some significant differences. This is because Eqs. (d) and (e) are based on the mathematical resonance formulation, while Eqs. (i)–(n) are based on the shock spectrum of half-cycle loading with consideration of maximum response during and after pulse.

Note that solutions obtained from Eq. (a) are always the maximum for each mode during the vibration. The displacements are apparently overestimated and conservative. One technique to level off the overestimated response is called *root-mean-square method* or *square-root-of-the-sum-of-the-squares* (SSRS). Let displacement x_i result from vibrations of n modes; the method is then expressed as

$$x_i = \sqrt{(x_i)_1^2 + (x_i)_2^2 + \dots + (x_i)_n^2} \quad (\text{o})$$

The example of x_3 associated with $\omega = 0.8p_1$ becomes

$$\begin{aligned} x_3 &= \sqrt{(0.3945)^2 + (0.007)^2 + (0.0002)^2} \\ &= 0.39456 \end{aligned} \quad (\text{p})$$

which is less than 0.4017 as given in Eq. (h). Another technique of the *CQC modal combination* method, along with the SSRS method, is discussed in Sections 7.6.1 and 7.6.2.

2.5.4. Response to Foundation Movement

Time-dependent foundation movement may be due to displacements, accelerations or a combination of both at some or all of the supports of a system. The support movement may induce inertia forces from the super structural mass, M_s , and from the foundation mass, M_f .

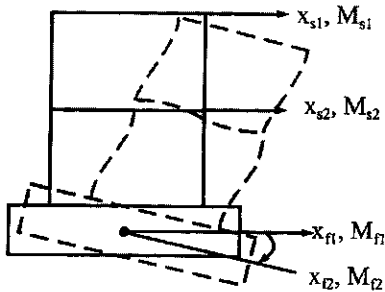


FIG. 2.10 Foundation movement.

In general, for a given set of foundation accelerations, $\{\ddot{x}_f\}$, foundation displacements, $\{x_f\}$, and externally applied loads, $\{P_s(t)\}$, as shown in Fig. 2.10, the motion equation may be

$$\begin{bmatrix} M_{ss} & | & M_{sf} \\ \hline M_{fs} & | & M_{ff} \end{bmatrix} \begin{Bmatrix} \ddot{x}_s \\ \hline \ddot{x}_f \end{Bmatrix} + \begin{bmatrix} K_{ss} & | & K_{sf} \\ \hline K_{fs} & | & K_{ff} \end{bmatrix} \begin{Bmatrix} x_s \\ \hline x_f \end{Bmatrix} = \begin{Bmatrix} P_s(t) \\ \hline P_f(t) \end{Bmatrix} \quad (2.70)$$

in which the subscripts, sf , signify the forces as s d.o.f. of the super structure resulting from the actions at f d.o.f. of the foundation, similarly for the subscripts, fs ; and $\{P_f(t)\}$ represents the reaction at the foundation. Using the matrix partition in Eq. (2.70) gives

$$[M_{ss}] \{\ddot{x}_s\} + [M_{sf}] \{\ddot{x}_f\} + [K_{ss}] \{x_s\} + [K_{sf}] \{x_f\} = \{P_s(t)\} \quad (2.71)$$

or

$$\begin{aligned} [M_{ss}] \{\ddot{x}_s\} + [K_{ss}] \{x_s\} &= \{P_s(t)\} - ([M_{sf}] \{\ddot{x}_f\} + [K_{sf}] \{x_f\}) \\ &= F(\Delta) \end{aligned} \quad (2.72)$$

and

$$[M_{fs}] \{\ddot{x}_s\} + [M_{ff}] \{\ddot{x}_f\} + [K_{fs}] \{x_s\} + [K_{ff}] \{x_f\} = \{P_f(t)\} \quad (2.73)$$

Since $\{P_s(t)\}$, $\{\ddot{x}_f\}$, and $\{x_f\}$ are given, the super structure displacements can be obtained by using the usual modal matrix technique from Eq. (2.72). The reactions can then be directly obtained from Eq. (2.73).

When the inertial force of the foundation mass is not considered, $[M_{ff}] \{\ddot{x}_f\}$ should be dropped; but $[M_{sf}] \{\ddot{x}_f\}$ can be dropped only for the lumped mass model, but should be included for consistent mass and distributed mass models. Distributed mass and consistent mass formulations are presented in Chapters 4 and 5, respectively.

EXAMPLE 2.5.6 Determine the displacements and accelerations of the shear building shown in Fig. 2.11 subjected to foundation movement of $x_f = -0.1 \sin 2t$ ft. Also find the reaction and make equilibrium checks at $t = \pi/4$. Let $M = 60 \text{ k sec}^2/\text{ft}$, $EI = 50,000 \text{ k ft}^2$, $k = 24 EI/(10)^3 = 1200 \text{ k}/\text{ft}$.

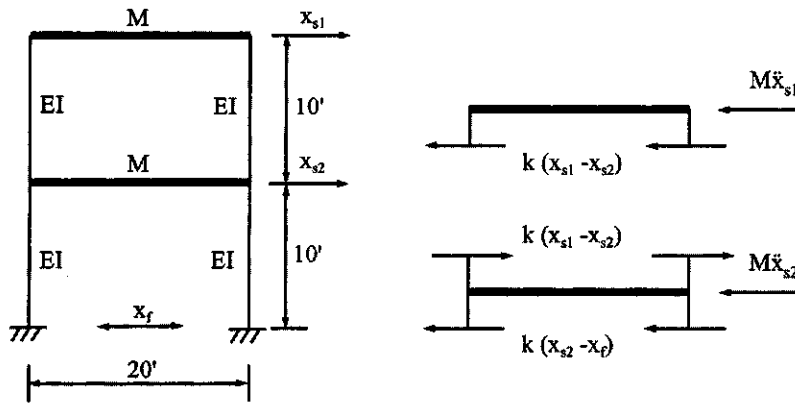


FIG. 2.11 Example 2.5.6.

Solution: For the lumped mass model, $[M_{sf}]$ and $[M_{fs}]$ are zero; Eq. (2.72) becomes

$$\begin{bmatrix} M & 0 \\ 0 & M \end{bmatrix} \begin{Bmatrix} \ddot{x}_{s1} \\ \ddot{x}_{s2} \end{Bmatrix} + \begin{bmatrix} k & -k \\ -k & 2k \end{bmatrix} \begin{Bmatrix} x_{s1} \\ x_{s2} \end{Bmatrix} = \begin{Bmatrix} 0 \\ -kx_f \end{Bmatrix} \quad (a)$$

or

$$[M]\{\ddot{x}_s\} + [K]\{x_s\} = \begin{Bmatrix} 0 \\ F(t) \end{Bmatrix} \quad (b)$$

For the given structural parameters, we obtain

$$[\Phi] = \begin{bmatrix} 0.10982 & -0.06787 \\ 0.06787 & 0.10982 \end{bmatrix} \quad (c)$$

$$[P] = \begin{bmatrix} 2.764 & 0 \\ 0 & 7.236 \end{bmatrix} \quad (d)$$

$$[P]^{-1}[\Phi]^T\{F(t)\} = \begin{Bmatrix} -2.946 \sin 2t \\ -1.821 \sin 2t \end{Bmatrix} \quad (e)$$

and then formulate the response as

$$\begin{aligned} \{x_s\} &= [\Phi] \int [\sin p(t - \Delta)] [P]^{-1} [\Phi]^T \{F(\Delta)\} d\Delta \\ &= [\Phi] \begin{bmatrix} -0.809415(2.764 \sin 2t - 2 \sin 2.764t) \\ -0.037655(7.236 \sin 2t - 2 \sin 7.236t) \end{bmatrix} \end{aligned} \quad (f)$$

Substituting $t = \pi/4$ into Eq. (f) yields

$$\{x_s\} = \begin{Bmatrix} -0.07761 \\ -0.09578 \end{Bmatrix} \text{ ft} \quad (g)$$

From Eq. (2.51), the accelerations at $t = \pi/4$ are

$$\begin{aligned}\{\ddot{x}_s\} &= [\Phi][\Phi]^T\{F(\Delta)\} - [\Phi]\left[\begin{smallmatrix} P \\ P^2 \end{smallmatrix}\right][\Phi]^T[M]\{x\} \\ &= \begin{Bmatrix} -0.3635 \\ 0.2790 \end{Bmatrix} \text{ ft/sec}^2\end{aligned}\quad (\text{h})$$

Using Eq. (2.73) gives the following reaction at the foundation

$$\begin{aligned}\{P_f(t)\} &= [K_{fs}]\{x_s\} + [K_{ff}]\{x_f\} \\ &= 1200[-0.09578] - (-0.1) = 5.064 \text{ k}\end{aligned}\quad (\text{i})$$

The equilibrium checks may be obtained from the free-body diagrams of Fig. 2.11 for the top girder

$$60(-0.3635) + 1200(-0.07761) - 1200(-0.09578) = 0 \quad (\text{j})$$

and for the lower girder

$$60(0.279) - 1200(-0.07761) + 2(1200)(-0.09572) - 1200(-0.1) = 0 \quad (\text{k})$$

EXAMPLE 2.5.7 Analyze the structure shown in Fig. 2.12 for (a) consistent mass model and (b) lumped mass model. Let the mass of the super-structure be $M_s = 1 \text{ k sec}^2/\text{ft}$ and the mass of the foundation be $M_f = 4 \text{ k sec}^2/\text{ft}$. The mass of the supporting member is $m = 0.015 \text{ k sec}^2/\text{ft}^2$ and the flexural rigidity is $EI = 360,000 \text{ k ft}^2$. The excitations are the ground acceleration, $\ddot{x}_f = 0.4 \sin 2t \text{ ft/sec}^2$, and the ground displacement, $x_f = -0.1 \sin 2t \text{ ft}$. Assume that no excitation is applied to the super-structure mass and that the mass has translational motion only.

Solution: (a) Based on the consistent mass model (see Chapter 5 for details), the elements of the mass matrix in the general motion equation given in Eq. (2.70) are

$$M_{ss} = M_s + \frac{13}{35}mL = 1 + \frac{13}{35}(0.015)(10) = 1.056 \text{ k sec}^2/\text{ft} \quad (\text{a})$$

$$M_{sf} = M_{fs} = \frac{9}{70}mL = \frac{9}{70}(0.015)(10) = 0.019 \text{ k sec}^2/\text{ft} \quad (\text{b})$$

$$M_{ff} = M_f + \frac{13}{35}mL = 4 + \frac{13}{35}(0.015)(10) = 4.056 \text{ k sec}^2/\text{ft} \quad (\text{c})$$

Since the supporting member does not rotate at the top because of the restraint imposed from the

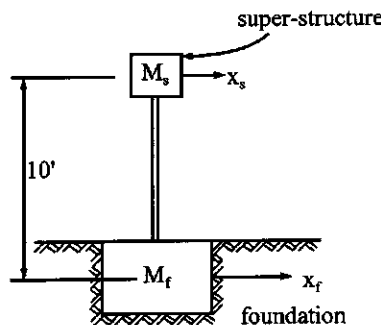


FIG. 2.12 Example 2.5.7.

super structure, the stiffness elements are

$$K_{sf} = K_{fs} = \frac{-12EI}{L^3} = \frac{-12(360,000)}{10^3} = -4320 \text{ k/ft} \quad (\text{d})$$

$$K_{ss} = K_{ff} = \frac{12EI}{L^3} = 4320 \text{ k/ft} \quad (\text{e})$$

Note that the stiffness at the foundation includes the member stiffness only. It could include soil stiffness, which supports the foundation and is neglected here. Substituting the mass and stiffness coefficients into Eq. (2.70) yields

$$\begin{bmatrix} 1.056 & 0.019 \\ 0.019 & 4.056 \end{bmatrix} \begin{Bmatrix} \ddot{x}_s \\ \ddot{x}_f \end{Bmatrix} + \begin{bmatrix} 4320 & -4320 \\ -4320 & 4320 \end{bmatrix} \begin{Bmatrix} x_s \\ x_f \end{Bmatrix} = \begin{Bmatrix} 0 \\ P_f(t) \end{Bmatrix} \quad (\text{f})$$

From the first row of Eq. (f) with \ddot{x}_s and x_f as given, the motion equation of the superstructure is

$$1.056\ddot{x}_s + 4320x_s = -432.0076 \sin 2t \quad (\text{g})$$

which is identical to Eq. (1.52) whose solution shown in Eq. (1.59) can be used here as

$$x_s = \frac{-432.0076}{4320 - 1.056(2)^2} \left(\sin 2t - \frac{2}{63.96} \sin 63.96t \right) \quad (\text{h})$$

where $p = \sqrt{4320/1.056} = 63.96$. At $t = \pi/4$, the responses are

$$x_s = -0.1001 \text{ ft}, \quad \ddot{x}_s = 0.8011 \text{ ft/sec}^2 \quad (\text{i})$$

From the second row of Eq. (f), the reaction at the foundation is

$$P_f(t) = 0.019 \ddot{x}_s + 4.056 \ddot{x}_f - 4320x_s + 4320x_f \quad (\text{j})$$

Based on x_s and \ddot{x}_s found in Eq. (i) and \ddot{x}_f and x_f as given, the reaction at $t = \pi/4$ is

$$P_f = 2.0696 \text{ kips} \quad (\text{k})$$

Applying the equilibrium check to the free-body diagram shown in Fig. 2.12 yields:

At the mass [first row of Eq. (f)]

$$1.056(0.8011) + 0.019(0.4) + 4320(-0.1001) - 4320(-0.1) = 0 \quad (\text{l})$$

At the foundation [second row of Eq. (f)] and from Eq. (j), the equilibrium condition is

$$0.019(0.8011) + 4.056(0.4) - 4320(-0.1001) + 4320(-0.1) - 2.0696 = 0 \quad (\text{m})$$

(b) For the lumped mass model, Eq. (2.65) becomes

$$\begin{bmatrix} M_{ss} & 0 \\ 0 & M_{ff} \end{bmatrix} \begin{Bmatrix} \ddot{x}_s \\ \ddot{x}_f \end{Bmatrix} + \begin{bmatrix} K_{ss} & K_{sf} \\ K_{fs} & K_{ff} \end{bmatrix} \begin{Bmatrix} x_s \\ x_f \end{Bmatrix} = \begin{Bmatrix} 0 \\ P_f(t) \end{Bmatrix} \quad (\text{n})$$

where the masses are $M_{ss} = 1 \text{ k sec}^2/\text{ft}$ and $M_{ff} = 4 \text{ k sec}^2/\text{ft}$. The solution may be obtained as shown in Eq. (h)

$$x_s(t) = \frac{-432.0}{4320 - 1(2)^2} \left(\sin 2t - \frac{2}{65.726} \sin 65.726t \right) \quad (\text{o})$$

where $p = \sqrt{(4320/1)} = 65.726 \text{ rad/sec}$. At $t = \pi/4$

$$x_s = -0.0971 \text{ ft} \quad \text{and} \quad \ddot{x}_s = -12.4524 \text{ ft/sec}^2 \quad (\text{p})$$

The reaction at the foundation is obtained from the second row of Eq. (n) as

$$P_f = 4 \ddot{x}_f - 4320 x_s + 4320 x_f = -10.9282 k \quad (q)$$

Note that the significant difference between P_f in Eqs. (p) and (q) is influenced by the sensitive $\sin p t$ values.

2.6. EIGEN SOLUTION FOR SYMMETRIC MATRIX

2.6.1. Iteration Method for Fundamental and Higher Modes

In Section 2.2, the natural frequencies were obtained by a classical method of solving the frequency equation. The polynomial frequency equation can be of very high order for a structure with a large number of d.o.f.; then the process of solving the natural frequencies and normal modes can be extremely difficult. In this section, several general numerical methods suitable for matrix formulation are discussed. First is the *iteration method*, which can be applied to both symmetric and unsymmetric matrices of mass and stiffness. This section deals with the symmetric case and the unsymmetric case is discussed in the next section. Numerical procedures of the method are: (a) iterate the dynamic equilibrium matrix for eigenvalues and eigenvectors of the fundamental mode; (b) modify the original dynamic equilibrium matrix to a new matrix called the *reduced dynamic matrix*, for which the iteration procedures are repeated for the second mode; and (c) modify the reduced dynamic matrix in (b) and then iterate the modified matrix for the third mode. As a result, the reduced dynamic matrix for the highest mode is the one modified from the previous mode. Proof of convergence for the numerical procedure is given in Section 2.6.2.

2.6.1.1. Fundamental mode

To simplify the expression shown in Eq. (2.18), let

$$[D] = [K]^{-1} [M], \quad \lambda = 1/p^2$$

Then the original and simplified equations become

$$\frac{1}{p^2} \{X\} = [\delta][M]\{X\}; \quad \lambda\{X\} = [D]\{X\} \quad (2.74a, b)$$

The iteration procedures can be applied to either of the above equations and are presented as follows. A first approximation of the column vector, $\{X\}$, can be chosen with some numerical values that may be close to the mode shape. Normally $\{X\}$ is assumed as a unit vector, say $^1\{X\}$, where the superscript at the upper left corner signifies the number of iterations. Then eigenvector is computed with a common factor R or λ as

$$R^2\{X\} = p^2[\delta][M]^1\{X\} \quad \text{or} \quad \lambda^2\{X\} = [D]^1\{X\} \quad (2.75a, b)$$

The absolute maximum vector component, X_i , of $^2\{X\}$ is taken as unity, and the numerical values of the rest of the components are less than 1. A column vector, $^2\{X\}$, will be used for the approximation for the new eigenvector as

$$R^3\{X\} = p^2[\delta][M]^2\{X\} \quad \text{or} \quad \lambda^3\{X\} = [D]^2\{X\} \quad (2.76a, b)$$

The iteration procedures are repeated for the succeeding approximation until the difference between $^{r-1}\{X\}$ and $^r\{X\}$ at the r th iteration is within a required tolerance. Then fundamental frequency, p , can finally be obtained in the form of

$$p^2 = \frac{^{r-1}(X)_i}{([{\delta}][M]^r\{X\})_i} \quad \text{or} \quad \lambda = \frac{([D]^r\{X\})_i}{^{r-1}(X)_i} \quad (2.77a, b)$$

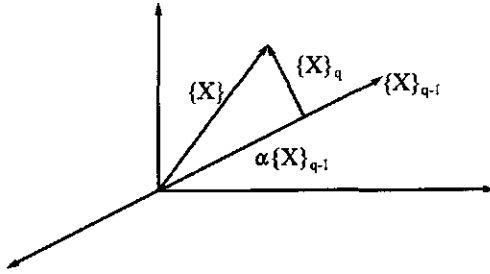


FIG. 2.13 Trial vector $\{X\}$.

In Eq. (2.77a), the unit component ${}^{r-1}(X)_i$ = the element in the i th row of ${}^{r-1}\{X\}$ at $(r - 1)$ th iteration, and $([\delta][M])^r \{X\}_i$ = the product of the elements in i th row of the matrix at the r th iteration. A similar procedure may be applied to Eq. (2.77b).

Since $'\{X\}$ is not necessarily equal to ${}^{r-1}\{X\}$, p^2 or λ can be somewhat different if different rows are used in Eq. (2.77a,b). Therefore, another approximation can be used as shown below

$$p^2 = \frac{\text{sum of elements of } {}^{r-1}\{X\}}{\text{sum of elements } ([\delta][M])^r \{X\}} \quad \text{or} \quad p^2 = \frac{\text{sum of elements } ([D])^r \{X\})}{\text{sum of elements of } {}^{r-1}\{X\}} \quad (2.78a, b)$$

Note that the convergence of eigenvectors is much slower than the convergence of eigenvalues. If $[K]^{-1}$ is used in the iteration, then the first solution yields the fundamental mode. If $[K]$ is used in the iteration, then the first solution is the highest mode. Proof of this is given in the next section.

2.6.1.2. Higher modes

The matrix equation in Eq. (2.74b) at the q th mode may be expressed as

$$[D]_{q-1}\{X\}_q = \lambda_q\{X\}_q \quad (2.79)$$

in which the matrix $[D]_{q-1}$ is unknown but is related to the eigensolution of the $(q - 1)$ th mode. The discussion below shows how to find $[D]_{q-1}$ and the $[D]_q$ and $[D]_{q-1}$ relationship. Since $\{X\}_q$ must be orthogonal to $\{X\}_{q-1}$, let

$$\{X\}_q = \{X\} - \alpha\{X\}_{q-1} \quad (2.80)$$

where $\{X\}$ is a trial vector and α is a scalar, which is chosen so that $\{X\}_q$ is orthogonal to $\{X\}_{q-1}$. The above equation may be expressed in Fig. 2.13.

Premultiply Eq. (2.80) by $\{X\}_{q-1}^T [M]$

$$\{X\}_{q-1}^T [M] \{X\}_q = \{X\}_{q-1}^T [M] \{X\} - \alpha \{X\}_{q-1}^T [M] \{X\}_{q-1} \quad (2.81)$$

which yields

$$\alpha = \frac{\{X\}_{q-1}^T [M] \{X\}}{\{X\}_{q-1}^T [M] \{X\}_{q-1}} \quad (2.82)$$

Substitute α into Eq. (2.80)

$$\{X\}_q = \left([I] - \left[\frac{\{X\}_{q-1}^T [M] \{X\}}{\{X\}_{q-1}^T [M] \{X\}_{q-1}} \right] \right) \{X\} \quad (2.83)$$

which can be symbolically written as

$$\{X\}_q = [a]\{X\} \quad (2.84)$$

Substitute the above into Eq. (2.79)

$$[D]_{q-1}[a]\{X\} = \lambda_q\{X\}_q \quad (2.85)$$

Let

$$[D]_q = [D]_{q-1}[a] \quad (2.86)$$

Then

$$[D]_q = [D]_{q-1} - \frac{[D]_{q-1}\{X\}_{q-1}\{X\}_{q-1}^T[M]}{\{X\}_{q-1}^T[M]\{X\}_{q-1}} \quad (2.87)$$

Since $[D]_{q-1}\{X\}_{q-1} = \lambda_{q-1}\{X\}_{q-1}$

$$[D]_q = [D]_{q-1} - \frac{\lambda_{q-1}\{X\}_{q-1}\{X\}_{q-1}^T[M]}{\{X\}_{q-1}^T[M]\{X\}_{q-1}} \quad (2.88)$$

where $[D]_q$ is called the *reduced dynamic matrix* for the q th mode. When $q = 2$, $[D]_{q-1}$ is the original matrix of $[K]^{-1}[M]$. Postmultiplying Eq. (2.87) by $\{X\}_q$ and recognizing that $\{X\}_{q-1}^T[M]\{X\}_q = 0$ yield

$$[D]_q\{X\}_q = [D]_{q-1}\{X\}_q \quad (2.89)$$

Relate Eq. (2.79) to the above; the dynamic matrix equation for the q th mode becomes

$$[D]_q\{X\}_q = \lambda_q\{X\}_q \quad (2.90)$$

Thus the $[D]_q$ and $[D]_{q-1}$ relationship is shown in Eq. (2.88), and $[D]_q$ can be calculated using the previous eigensolution. The aforementioned iteration procedure is similar to the *sweeping matrix* (see Example 2.7.1) and can be applied here to obtain the q th mode. Continuing the process, we may obtain all possible n modes. When searching for $(n + 1)$ th mode, $[D]_{n+1}$ will become zero because it does not exist. Note that $[D]_{n+1} = [0]$ can be further explained by analogy of solving n homogeneous equations as follows. Applying an orthogonal condition to two homogeneous equations results in one equation; three equations become two which then become one after application of orthogonality once more. Consequently, n equations can have $n - 1$ successive applications of orthogonal conditions for n eigensolutions. Thus, *in matrix form*, $[D]_{n+1}$ implies n orthogonality applications that simply do not exist mathematically for n d.o.f.

EXAMPLE 2.6.1. To illustrate the method described above, the example in Section 2.2.1 is again used to solve for natural frequencies and normal modes. Let Eqs. (2.4a) and (2.4b) be written as follows:

$$\begin{Bmatrix} X_1 \\ X_2 \end{Bmatrix} = p^2 \begin{bmatrix} M & M \\ k & k \\ \hline M & 2M \\ k & k \end{bmatrix} \begin{Bmatrix} X_1 \\ X_2 \end{Bmatrix} \quad (a)$$

or

$$\lambda\{X\} = [D]\{X\} \quad (b)$$

First mode—as a first approximation to $\{X\}$, we choose

$${}^1X = \begin{Bmatrix} 1 \\ 1 \end{Bmatrix} \quad (c)$$

The eigenvector, ${}^2\{X\}$, associated with Eq. (2.75a,b) is

$$R {}^2\{X\} = 3p^2 \frac{M}{k} \begin{Bmatrix} 0.667 \\ 1.000 \end{Bmatrix}; \quad \text{or} \quad \lambda {}^2\{X\} = 3 \frac{M}{k} \begin{Bmatrix} 0.667 \\ 1.000 \end{Bmatrix} \quad (d)$$

where the common factor, R is $3p^2 M/k$ (or $\lambda = 3M/k$) and the column vector, ${}^2\{X\}$, is $[0.667 \ 1.000]^T$. Because the ${}^2\{X\}$ value is different from the assumed vector ${}^1\{X\}$, the second assumed vector should be ${}^2\{X\}$, which is inserted in Eq. (2.75a,b) for the iteration process; consequently, the eigenvector is

$$R {}^3\{X\} = 2.667p^2 \frac{M}{k} \begin{Bmatrix} 0.625 \\ 1.000 \end{Bmatrix} \quad (e)$$

Again, the vector, ${}^3\{X\} = [0.625 \ 1.000]^T$, different from ${}^2\{X\}$, is used here. For the third assumed vector, ${}^4\{X\}$ becomes

$$R {}^4\{X\} = 2.623p^2 \frac{M}{k} \begin{Bmatrix} 0.619 \\ 1.000 \end{Bmatrix} \quad (f)$$

For further convergence, we use

$${}^4\{X\} = \begin{Bmatrix} 0.619 \\ 1.000 \end{Bmatrix} \quad (g)$$

and then we have

$$R {}^5\{X\} = 2.619p^2 \frac{M}{k} \begin{Bmatrix} 0.618 \\ 1.000 \end{Bmatrix}; \quad \text{or} \quad \lambda {}^5\{X\} = 2.619 \frac{M}{k} \begin{Bmatrix} 0.618 \\ 1.000 \end{Bmatrix} \quad (h)$$

If the required tolerance is ${}^q(X)_i - {}^{q-1}(X)_i \leq |0.001|$, the ${}^5(X)_1 - {}^4(X)_1 = 0.618 - 0.619 = |0.001|$. Therefore, the first normal mode can be determined from Eq. (h):

$$\{X\}_1 = \begin{Bmatrix} 0.618 \\ 1.000 \end{Bmatrix}$$

and the fundamental frequency can be determined from Eq. (2.77a) as

$$p_1^2 = \frac{{}^4(X)_2}{([D][M] {}^5\{X\})_2} = \frac{1}{2.619(M/k)} = 0.382 \frac{k}{M} \quad (i)$$

Alternately, the eigenvalue can be derived from Eq. (2.77b) as

$$\lambda_1 = \frac{([D] {}^5\{X\})_2}{{}^4\{X\}_2} = 2.619 \frac{M}{k} \quad \text{or} \quad p_1^2 = 0.382 \frac{k}{M} \quad (j)$$

from Eq. (2.78a) as

$$p_1^2 = \frac{0.619 + 1}{2.169(M/k)(0.618 + 1)} = 0.382 \frac{k}{M} \quad (k)$$

and from Eq. (2.78b) as

$$\lambda_1 = \frac{2.619(M/k)(0.618 + 1)}{0.619 + 1} = 2.617 \frac{M}{k} \quad \text{or} \quad p_1^2 = 0.382 \frac{k}{M} \quad (\text{l})$$

Second mode —for analysis of the second mode, the reduced dynamic matrix should be formulated according to Eq. (2.88) as

$$\begin{aligned} \lambda_1 \{X\}_1 \{X\}_1^T [M] &= 2.619 \frac{M}{k} \begin{Bmatrix} 0.618 \\ 1.000 \end{Bmatrix} \begin{Bmatrix} 0.618 \\ 1.000 \end{Bmatrix}^T \begin{bmatrix} M & 0 \\ 0 & M \end{bmatrix} \\ &= 2.619 \frac{M^2}{k} \begin{bmatrix} 0.382 & 0.618 \\ 0.618 & 1.000 \end{bmatrix} \end{aligned} \quad (\text{m})$$

and

$$\{X\}_1^T [M] \{X\}_1 = [0.618 \ 1.000] \begin{bmatrix} M & 0 \\ 0 & M \end{bmatrix} \begin{Bmatrix} 0.618 \\ 1.000 \end{Bmatrix} = 1.381 M \quad (\text{n})$$

Then the reduced dynamic matrix can be constructed as

$$\begin{aligned} [D]_2 &= ([\delta] [M])_2 = ([\delta] [M])_1 - \frac{\lambda_1}{\{X\}_1^T [M] \{X\}_1} \{X\}_1 \{X\}_1^T [M] \\ &= \begin{bmatrix} \frac{1}{k} & \frac{1}{k} \\ \frac{1}{k} & \frac{2}{k} \end{bmatrix} \begin{bmatrix} M & 0 \\ 0 & M \end{bmatrix} - \frac{2.619(M^2/k)}{1.381 M} \begin{bmatrix} 0.3819 & 0.618 \\ 0.618 & 1.000 \end{bmatrix} \\ &= \frac{M}{k} \begin{bmatrix} 0.2762 & -0.1713 \\ -0.1713 & 0.1047 \end{bmatrix} \end{aligned} \quad (\text{o})$$

Inserting Eq. (o) into Eq. (2.90) leads to

$$\begin{Bmatrix} X_1 \\ X_2 \end{Bmatrix} = p^2 \frac{M}{k} \begin{bmatrix} 0.2762 & -0.1713 \\ -0.1713 & 0.1047 \end{bmatrix} \begin{Bmatrix} X_1 \\ X_2 \end{Bmatrix} \quad (\text{p})$$

The iteration procedures can be similarly applied by first assuming that ${}^1\{X\} = [1 \ 1]^T$ for which the eigenvector is

$$R^2 \{X\} = 0.1049 p^2 \frac{M}{k} \begin{Bmatrix} 1.000 \\ -0.6349 \end{Bmatrix} \quad \text{or} \quad \lambda^2 \{X\} = 0.1049 \frac{M}{k} \begin{Bmatrix} 1.000 \\ -0.6349 \end{Bmatrix} \quad (\text{q})$$

Let the second assumed vector be ${}^2\{X\} = [1.0000 \ -0.6349]^T$; then the new column vector becomes

$$R^3 \{X\} = 0.3849 p^2 \frac{M}{k} \begin{Bmatrix} 1.0000 \\ -0.6178 \end{Bmatrix} \quad (\text{r})$$

where

$${}^3\{X\} = \begin{Bmatrix} 1.0000 \\ -0.6178 \end{Bmatrix} \quad (\text{s})$$

Since ${}^3\{X\}_2 - {}^2\{X\}_2 = [-0.6178 - (-0.6349)] = |0.0171| > |0.001|$, further convergence is

necessary. By using ${}^3\{X\}$, ${}^4\{X\}$ can be calculated as

$$R {}^4\{X\} = 0.3820 p^2 \frac{M}{k} \begin{Bmatrix} 1.000 \\ -0.6177 \end{Bmatrix} \quad (\text{t})$$

Now the difference between ${}^4\{X\}$ and ${}^3\{X\}$ is within the required tolerance; thus the second normal mode coordinates are

$$\{X\}_2 = \begin{Bmatrix} 1.000 \\ -0.618 \end{Bmatrix} \quad (\text{u})$$

The associated frequency from Eq. (2.77a) is

$$p_2^2 = \frac{{}^3(X)_1}{([δ][M]{}^4\{X\})_1} = \frac{1}{0.3820(M/k)} = 2.618 \frac{k}{M} \quad (\text{v})$$

and from Eq. (2.77b)

$$\lambda_2 = \frac{([D]{}^4\{X\})_1}{{}^3(X)_1} = \frac{0.3820 (M/k)}{1} = 0.3820 \frac{M}{k}, \quad \text{or} \quad p_2^2 = 2.618 \frac{k}{M} \quad (\text{w})$$

Note that $\{X\}_1$, $\{X\}_2$, p_1^2 , p_2^2 obtained by the iteration procedures can be checked satisfactorily with the results in Section 2.2.

Zero dynamic reduced matrix—if $[D]_2$ (or $([\delta][M])_2$), $\{X\}_2$, and p_2^2 (or λ_2) are inserted into Eq. (2.88), then a zero reduced dynamic matrix can be obtained as follows:

$$\begin{aligned} \lambda_2 \{X\}_2 \{X\}_2^T [M] &= \begin{Bmatrix} 1.000 \\ -0.6177 \end{Bmatrix} \begin{Bmatrix} 1.000 \\ -0.6177 \end{Bmatrix}^T \begin{bmatrix} M & 0 \\ 0 & M \end{bmatrix} \\ &= 0.3800 \frac{M^2}{k} \begin{bmatrix} 1.000 & -0.6177 \\ -0.6177 & 0.3815 \end{bmatrix} \end{aligned} \quad (\text{x})$$

$$\{X\}_2^T [M] \{X\}_2 = \begin{Bmatrix} 1.000 \\ -0.6177 \end{Bmatrix}^T \begin{bmatrix} M & 0 \\ 0 & M \end{bmatrix} \begin{Bmatrix} 1.000 \\ -0.6177 \end{Bmatrix} = 1.3814 M \quad (\text{y})$$

The reduced dynamic matrix becomes

$$\begin{aligned} [D]_3 &= ([\delta][M])_3 = \frac{M}{k} \begin{bmatrix} 0.2762 & -0.1713 \\ -0.1713 & 0.1047 \end{bmatrix} - \frac{0.3820(M^2/k)}{1.3814 M} \begin{bmatrix} 1.000 & -0.1677 \\ -0.1677 & 0.3815 \end{bmatrix} \\ &= \frac{M}{k} \begin{bmatrix} (0.2762 - 0.2765) - (0.1713 - 0.1708) \\ (-0.1713 + 0.1708) + (0.1047 - 0.1054) \end{bmatrix} = [0] \end{aligned} \quad (\text{z})$$

The zero matrix signifies that the third mode does not exist in the present example.

2.6.2. Proof of Iterative Solution

2.6.2.1. Proof of Convergence

The numerical method discussed in the previous section by using iteration procedures for eigensolution. Now, we can determine why the iterative solution can converge to the eigenvalue and eigenvector of the first mode; in other words, how we can be sure that the first solution is the fundamental frequency and normal mode.

Let us rewrite the dynamic matrix equation as follows:

$$\frac{1}{p^2} \{X\} - [\delta][M]\{X\} = 0 \quad (2.91)$$

where $[\delta][M]$ is an $n \times n$ nonsingular matrix. The distinct characteristic roots of Eq. (2.91) are

assumed to be

$$\left| \frac{1}{p_1^2} \right| > \left| \frac{1}{p_2^2} \right| > \dots > \left| \frac{1}{p_n^2} \right| \quad (2.92)$$

From Eq. (2.34) we have

$$[\Phi]^{-1} = [\Phi]^T [M] \quad (2.93)$$

or

$$[\Phi]^T = [\Phi]^{-1} [M]^{-1} \quad (2.94)$$

Also, we have shown in Eq. (2.38) that

$$[\Phi]^T [K] \Phi = \begin{bmatrix} 1 \\ p_1^2 \\ p_2^2 \\ \vdots \\ p_n^2 \end{bmatrix} \quad (2.95)$$

which can be inverted to

$$\begin{bmatrix} 1 \\ p_1^2 \\ p_2^2 \\ \vdots \\ p_n^2 \end{bmatrix} = [\Phi]^{-1} [K]^{-1} ([\Phi]^T)^{-1} \quad (2.96)$$

Substituting of Eq. (2.94) into the above and replacing $[K]^{-1}$ by $[\delta]$ yields

$$\begin{bmatrix} 1 \\ p_1^2 \\ p_2^2 \\ \vdots \\ p_n^2 \end{bmatrix} = [\Phi]^{-1} [\delta] [M] [\Phi] \quad (2.97)$$

Let $[g_i]$ denote an $n \times n$ diagonal matrix, which is associated with the left side of Eq. (2.97) by using 1 in place of $1/p_i^2$ and 0 in place of $1/p_j^2$ for every $i \neq j$. Then an identity matrix is obtained as

$$[I] = [g_1] + [g_2] + \dots + [g_n] \quad (2.98)$$

and Eq. (2.97) can be rewritten as

$$[\Phi]^{-1} [\delta] [M] [\Phi] = \frac{1}{p_1^2} [g_1] + \frac{1}{p_2^2} [g_2] + \dots + \frac{1}{p_n^2} [g_n] \quad (2.99)$$

or

$$[\delta] [M] = \frac{1}{p_1^2} [\Phi] [g_1] [\Phi]^{-1} + \frac{1}{p_2^2} [\Phi] [g_2] [\Phi]^{-1} + \dots + \frac{1}{p_n^2} [\Phi] [g_n] [\Phi]^{-1} \quad (2.100)$$

Let us introduce a new notation that is defined as

$$[G_i] = [\Phi] [g_i] [\Phi]^{-1}$$

Using the characteristics given in $[g_i]$, we can prove that

$$[g_i]^2 = [g_i] \quad \text{and} \quad [g_i] [g_j] = 0 \quad \text{where } i \neq j$$

Therefore

$$\begin{aligned} [G_i]^2 &= [\Phi] [g_i] [\Phi]^{-1} [\Phi] [g_i] [\Phi]^{-1} \\ &= [\Phi] [g_i] [g_i] [\Phi]^{-1} = [G_i] \end{aligned} \quad (2.101)$$

and

$$\begin{aligned} [G_i][G_j] &= [\Phi][g_i][\Phi]^{-1}[\Phi][g_j][\Phi]^{-1} \\ &= [\Phi][g_i][g_j][\Phi]^{-1} = [0] \end{aligned} \quad (2.102)$$

By using Eqs. (2.101) and (2.102), Eq. (2.100) can be reformulated as

$$\begin{aligned} ([\delta][M])^2 &= \left(\frac{1}{p_1^2}[G_1] + \frac{1}{p_2^2}[G_2] + \dots + \frac{1}{p_n^2}[G_n] \right) \left(\frac{1}{p_1^2}[G_1] + \frac{1}{p_2^2}[G_2] + \dots + \frac{1}{p_n^2}[G_n] \right) \\ &= \sum_{i,j} \frac{1}{p_i^2}[G_i] \frac{1}{p_j^2}[G_j] = \sum_i \frac{1}{p_i^4}[G_i] \end{aligned} \quad (2.103)$$

For r powers, the above equation becomes

$$([\delta][M])^r = \sum_i \frac{1}{p_i^{2r}}[G_i] \quad (2.104)$$

the expansion of which is

$$\frac{([\delta][M])^r}{p_1^{2r}} = [G_1] + \frac{1/p_2^{2r}}{1/p_1^{2r}}[G_2] + \dots + \frac{1/p_n^{2r}}{1/p_1^{2r}}[G_n] \quad (2.105)$$

Based on the conditions given in Eq. (2.92) (*i.e.* $|1/p_1^2| > |1/p_i^2|, i > 1$), when $r \rightarrow \infty$, all the terms on the right side of the above equation except the first term approach zero. Thus

$$([\delta][M])^r = \frac{1}{p_1^{2r}}[G_1] \quad (2.106)$$

or

$$([\delta][M])^{r+1} = \frac{1}{p_1^{2(r+1)}}[G_1] = \frac{1}{p_1^2}([\delta][M])^r \quad (2.107)$$

showing that, if we compute the successive power of $[\delta][M]$ until we reach a power of $([\delta][M])^{r+1}$, which is nearly equal to a scalar multiple of the proceeding power, $([\delta][M])^r$, then the scalar is the approximate value of $1/p_1^2$ as the largest characteristic root of Eq. (2.91). Therefore p_1 must be the smallest of all p 's and is the fundamental frequency. By using $[M]^{-1}[K]\{X\} - p^2\{X\} = \{0\}$ it can be proved that the iteration solution gives the highest frequency.

2.6.2.2. Iteration for Eigenvalues and Eigenvectors

Since we are interested in both natural frequencies and normal modes, the iteration procedures may be modified to obtain the eigenvalues (p 's) and eigenvectors ($\{X\}$) simultaneously. Let ${}^r\{X\}$ be any nonzero column vector so that $[\delta][M]{}^r\{X\} \neq \{0\}$. Define

$${}^r\{X\} = {}^r([\delta][M])^{-1}\{X\} \quad (2.108)$$

where r is the product of the matrix manipulations (or the number of iterations). Therefore, from Eq. (2.104), $([\delta][M])^r$ and ${}^r([\delta][M])$ are the same; substituting Eq. (2.104) into Eq. (2.108) yields

$$\begin{aligned} {}^r\{X\} &= \left(\frac{1}{p_1^{2r}}[G_1] + \frac{1}{p_2^{2r}}[G_2] + \dots + \frac{1}{p_n^{2r}}[G_n] \right)^{-1}\{X\} \\ &= \frac{1}{p_1^{2r}}[G_1]^{-1}\{X\} + \frac{1}{p_2^{2r}}[G_2]^{-1}\{X\} + \dots + \frac{1}{p_n^{2r}}[G_n]^{-1}\{X\} \end{aligned} \quad (2.109)$$

Dividing both sides by $1/p_1^{2r}$ yields

$${}^r\{X\} = \frac{1}{p_1^{2r}} [G_1] {}^1\{X\} \quad (2.110)$$

Following Eq. (2.107) leads to

$${}^{r+1}\{X\} = \frac{1}{p_1^{2(r+1)}} [G_1] {}^1\{X\} = \frac{1}{p_1^2} \frac{1}{p_1^{2r}} [G_1] {}^1\{X\} = \frac{1}{p_1^2} {}^r\{X\} \quad (2.111)$$

Thus, if we compute successive products, such as

$${}^2\{X\} = [\delta] [M] {}^1\{X\} \quad (2.112)$$

$${}^3\{X\} = [\delta] [M] {}^2\{X\} \quad (2.113)$$

until we find

$${}^{r+1}\{X\} = [\delta] [M] {}^r\{X\} \quad (2.114)$$

which is approximately a scalar multiple of the preceding vector, ${}^r\{X\}$, then the scalar factor is the approximate value of $1/p_1^2$. Thus p_1 and $\{X\}$ are the fundamental frequency and normal mode, respectively. Recall that in Section 2.6.1 the largest number in the column vector was used as 1 by removing the scalar factor from all the coordinates of $[\delta][M]\{X\}$ for the purpose of preventing the coordinates of $\{X\}$ from increasing without bound when the number of iteration increases.

2.6.3. Extraction Technique for Natural Frequencies

In some structural dynamic problems, only the natural frequency in a certain region is of interest, and it may not be the fundamental frequency. It can be time-consuming if the particular frequency is determined by means of the iteration method starting from the fundamental mode. Actually, the frequency can be directly obtained by using the *eigenvalue extraction* technique as follows. Let p_0 be the frequency to be extracted and p_v the frequency at the region of interest; then the new frequency can be expressed as

$$p^2 = p_0^2 \pm p_v^2 \quad (2.115)$$

Substituting the above into the dynamic matrix equation yields

$$[K]\{X\} = (p_0^2 \pm p_v^2)[M]\{X\} \quad (2.116)$$

Consider the positive sign for the case of the desired frequency greater than p_0 ; then

$$([K] - p_0^2[M])\{X\} = p_v^2[M]\{X\} \quad (2.117)$$

or in the condensed form of $[K]_v = [K] - p_0^2[M]$, the result is

$$[K]_v\{X\} = p_v^2[M]\{X\} \quad (2.118)$$

The matrix iteration method and the reduced dynamic matrix technique discussed previously can be directly applied to Eq. (2.118) for the frequency desired as well as for higher frequencies.

Note that the eigenvector associated with p^2 is the same as that corresponding to p_v^2 . This holds true because the actual frequency after extraction is p ; therefore the mode shape does not change. Also note that the method is useful for a structure having rigid-body motion; when an eigenvalue algorithm, such as iteration method, cannot be used to find zero eigenvalue, then the other eigensolutions cannot be calculated. Using the extraction technique, we can always shift the stiffness matrix by $[K] - p_0^2[M]$ and then find the eigensolutions.

2.6.4. Choleski's Decomposition Method

In the iteration method, the stiffness matrix, $[K]$, must be inverted to a flexibility matrix, $[\delta]$, in order to obtain the fundamental mode. Apparently, the inversion is time-consuming even with computer application. Matrix inversion can be avoided by using *Choleski's decomposition method*, presented in this section. In the following dynamic matrix equation

$$\frac{1}{p^2} [K] \{X\} = [M] \{X\} \quad (2.119)$$

$[K]$ can be decomposed as $[K] = [U]^T [\mathcal{D}_k] [U]$. The term $[U]$ is an upper triangular matrix with unit diagonal elements, and $[\mathcal{D}_k]$ is a diagonal matrix. Manipulating $[K] = [U]^T [\mathcal{D}_k] [U]$ yields

$$\left[\begin{array}{cccc} k_{11} & k_{12} & \dots & k_{1n} \\ k_{21} & k_{22} & \dots & k_{2n} \\ \vdots & \vdots & & \vdots \\ k_{n1} & k_{n2} & \dots & k_{nn} \end{array} \right] = \left[\begin{array}{ccccc} 1 & & & & \\ U_{12} & 1 & & & \\ U_{13} & U_{23} & 1 & & \\ \vdots & \vdots & \vdots & & \\ U_{1n} & U_{2n} & U_{3n} & \dots & 1 \end{array} \right] \left[\begin{array}{ccccc} D_{11} & & & & \\ & D_{22} & & & \\ & & D_{33} & & \\ & & & \ddots & \\ & & & & D_{nn} \end{array} \right]$$

Multiplying the matrices on the right side and equating the corresponding matrix elements on left side gives

$$\left. \begin{aligned} D_{11}U_{12} &= k_{12}; & D_{11} = k_{11} \\ &\dots & U_{12} = \frac{k_{12}}{D_{11}} \\ D_{11}U_{1n} &= k_{1n}; & U_{1n} = \frac{k_{1n}}{D_{11}} \\ D_{11}(U_{12})^2 + D_{22} &= k_{22}; & D_{22} = k_{22} - D_{11}(U_{12})^2 \\ U_{12}U_{13}D_{11} + U_{23}D_{22} &= k_{23}; & U_{23} = \frac{1}{D_{22}}(k_{23} - U_{12}U_{13}D_{11}) \\ U_{12}U_{14}D_{11} + U_{24}D_{22} &= k_{24}; & U_{24} = \frac{1}{D_{22}}(k_{24} - U_{12}U_{14}D_{11}) \\ &\dots & \dots \\ U_{13}^2D_{11} + U_{23}^2D_{22} + D_{33} &= k_{33}; & D_{33} = k_{33} - U_{13}^2D_{11} - U_{23}^2D_{22} \\ U_{13}U_{14}D_{11} + U_{23}U_{24}D_{22} + U_{34}D_{33} &= k_{34}; & U_{34} = \frac{1}{D_{33}}(k_{34} - U_{13}U_{14}D_{11} - U_{23}U_{24}D_{22}) \end{aligned} \right\} (2.121)$$

The above equations can be summarized as

$$D_{11} = k_{11} \quad (2.122)$$

$$U_{ij} = \frac{k_{ij}}{D_{11}}; \quad j \geq 2 \quad (2.123)$$

$$D_{ii} = k_{ii} - \sum_{r=1}^{i-1} U_{ri}^2 D_{rr}; \quad i \geq 2 \quad (2.124)$$

$$U_{ij} = \frac{1}{D_{ii}} \left(k_{ij} - \sum_{r=1}^{i-1} U_{ri} U_{rj} D_{rr} \right); \quad i \geq 2, \quad j \geq i+1 \quad (2.125)$$

Let Eq. (2.119) be decomposed as

$$[U]^T [D] [U] \frac{1}{p^2} \{X\}_q = [M] \{X\}_{q-1} \quad (2.126)$$

where $\{X\}_{q-1}$ is the column assumed or computed from the preceding step, $\{X\}_q$ is the unknown column to be determined, and q is the number of modes. Let

$$\frac{1}{p^2} \{X\}_q = \{Q\} \quad (2.127)$$

$$[M] \{X\}_{q-1} = \{V\} \quad (2.128)$$

Then

$$[D] [U] \{Q\} = \{W\} \quad (2.129)$$

$$[U]^T \{W\} = \{V\} \quad (2.130)$$

Since $\{V\}$ can be obtained from Eq. (2.128), Eq. (2.130) can be solved by forward substitution:

$$W_\ell = V_\ell - \sum_{m=1}^{\ell-1} U_{m\ell} W_m \quad (2.131)$$

By substituting $\{W\}$ in Eq. (2.129) for $\{Q\}$ through the use of backward substitution, we obtain

$$Q_\ell = \frac{W_\ell}{D_{\ell\ell}} - \sum_{m=\ell+1}^n U_{\ell m} Q_m \quad (2.132)$$

Here $\{Q\}$ can be normalized at the end of each cycle.

For the higher modes, we can similarly follow Eqs. (2.88) and (2.90) as

$$\{X\}_q^* = \{X\}_q - \sum_{\ell=1}^{q-1} S_\ell \{X\}_\ell \quad (2.133)$$

in which

$$S_\ell = \frac{1}{\{X\}_\ell^T [M] \{X\}_\ell} \{X\}_\ell^T [M] \{X\}_q; \quad \ell = 1, 2, \dots, q-1 \quad (2.134)$$

In Eq. (2.133), $\{X\}_q$ is any trial column and $\{X\}_q^*$ is the new column to be inserted in Eq. (2.128) for a new cycle. Illustration of the numerical procedure is shown in Example 2.6.2.

2.6.4.1. Iteration Method vs Choleski's Decomposition Method for Higher Modes

Since the calculation of higher modes for Choleski's decomposition method is based on the formulation of the iteration method as stated in Eq. (2.133), the similarity between these two formulations is shown as follows. The eigensolution for the q th mode can be obtained through iteration by combining Eqs. (2.88) and (2.89) as

$$[D]_q \{X\}_q = [D]_{q-1} \{X\}_q - \frac{\lambda_{q-1} \{X\}_{q-1} \{X\}_{q-1}^T [M] \{X\}_q}{\{X\}_{q-1}^T [M] \{X\}_{q-1}} \quad (2.135)$$

Since

$$[D]_q \{X\}_q = \lambda_q \{X\}_q \quad (2.136a)$$

$$[D]_{q-1} \{X\}_q = \lambda_{q-1} \{X\}_q \quad (2.136b)$$

Eq. (2.135) can be rewritten as

$$\{X\}_q = \frac{\lambda_{q-1}}{\lambda_q} \{X\}_q - \frac{(\lambda_{q-1}/\lambda_q) \{X\}_{q-1} \{X\}_{q-1}^T [M] \{X\}_q}{\{X\}_{q-1}^T [M] \{X\}_{q-1}} \quad (2.136c)$$

Let

$$\frac{\lambda_{q-1}}{\lambda_q} \{X\}_q = \{X\}'_q \quad (2.136d)$$

Then

$$\{X\}_q = \{X\}'_q - \frac{\{X\}_{q-1} \{X\}_{q-1}^T [M] \{X\}'_q}{\{X\}_{q-1}^T [M] \{X\}_{q-1}} \quad (2.137)$$

For the Choleski's decomposition method, the eigensolution of the q th mode is calculated using Eq. (2.133) as

$$\{X\}_q^* = \{X\}_q - \sum_{\ell=1}^{q-1} \frac{\{X\}_{\ell}^T [M] \{X\}_q \{X\}_{\ell}}{\{X\}_{\ell}^T [M] \{X\}_{\ell}} \quad (2.138)$$

Comparing Eq. (2.137) with Eq. (2.138) yields the following relationships:

$$\{X\}'_q = \{X\}_q \quad (2.139a)$$

$$q-1 = \ell \quad (2.139b)$$

$$\{X\}_{q-1}^T [M] \{X\}'_q = \{X\}_{\ell}^T [M] \{X\}_q \quad (2.139c)$$

Note that both $\{X\}_{q-1}^T [M] \{X\}'_q$ and $\{X\}_{\ell}^T [M] \{X\}_q$ are scalars which can be placed after $\{X\}_{q-1}$ and before $\{X\}_{\ell}$, respectively, as shown in Eqs. (2.137) and (2.138).

EXAMPLE 2.6.2 Find the natural frequencies and normal modes of the shear building shown in Fig. 2.14 by using Choleski's method of matrix decomposition, given that $\ell = 14$ ft (4.2672 m), $h = 22$ ft (6.7055 m), $M_1 = M_2 = M_3 = 0.8431 \text{ k sec}^2/\text{ft}$ ($12,304 \text{ N sec}^2/\text{m}$), $E = 30,000 \text{ ksi}$ ($206,842.8 \times 10^6 \text{ N/m}^2$), $I_3 = 238.4 \text{ in}^4$ ($9.9229 \times 10^{-5} \text{ m}^4$), $I_2 = 350.8 \text{ in}^4$ ($1.4601 \times 10^{-4} \text{ m}^4$), $I_1 = 476.1 \text{ in}^4$ ($1.98168 \times 10^{-4} \text{ m}^4$).

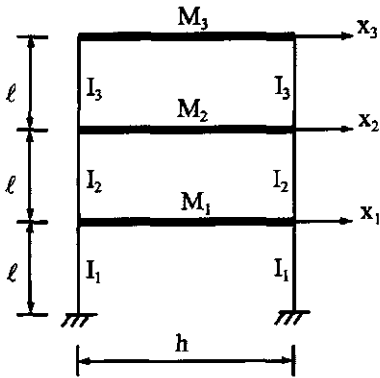


FIG. 2.14 Example 2.6.2.

Solution: For the given frame, the stiffness and mass matrices are

$$[K] = \begin{bmatrix} k_1 + k_2 & -k_2 & 0 \\ -k_2 & k_2 + k_3 & -k_3 \\ 0 & -k_3 & k_3 \end{bmatrix} = \begin{bmatrix} 1506.74 & -639.21 & 0 \\ -639.21 & 1073.61 & -434.4 \\ 0 & -434.4 & 434.4 \end{bmatrix} \quad (a)$$

$$[M] = \begin{bmatrix} M_1 & 0 & 0 \\ 0 & M_2 & 0 \\ 0 & 0 & M_3 \end{bmatrix} = \begin{bmatrix} 0.8431 & 0 & 0 \\ 0 & 0.8431 & 0 \\ 0 & 0 & 0.8431 \end{bmatrix} \quad (b)$$

where $k_1 = 24EI_1/\ell^3$, $k_2 = 24EI_2/\ell^3$, and $k_3 = 24EI_3/\ell^3$. Decomposition matrices $[D]$ and $[U]$ can be from $[K]$ by using Eqs. (2.122)–(2.125) as follows:

$$\begin{aligned} D_{11} &= k_{11} = 1506.74 \\ U_{12} &= k_{12}/D_{11} = -639.21/1506.74 = -0.4241 \\ U_{13} &= k_{13}/D_{11} = 0 \\ D_{22} &= k_{22} - U_{12}^2 D_{11} = 1073.61 - (-0.4241)^2 (1506.74) = 803.66 \\ U_{23} &= (k_{23} - U_{12} D_{11} U_{13})/D_{22} = -434.4/803.66 = -0.5419 \\ D_{33} &= k_{33} - D_{11} U_{13}^2 - D_{22} U_{23}^2 = 434.4 - 803.66 (-0.5419)^2 = 199.5 \end{aligned}$$

Thus

$$[D] = \begin{bmatrix} 1506.4 & 0 & 0 \\ 0 & 803.66 & 0 \\ 0 & 0 & 199.5 \end{bmatrix}; \quad [U] = \begin{bmatrix} 1.0 & -0.4241 & 0 \\ 0 & 1.0 & -0.5419 \\ 0 & 0 & 1.0 \end{bmatrix}$$

Knowing $[D]$ and $[U]$, the following four steps are employed for matrix iterations:

Step 1. Calculate $\{V\}$ from $[M]\{X\}_{q-1} = \{V\}$ as

$$V_1 = 0.8431 X_1; \quad V_2 = 0.8431 X_2; \quad V_3 = 0.8431 X_3 \quad (c)$$

Step 2. Calculate $\{W\}$ from $[U]^T \{W\} = \{V\}$ as

$$W_1 = V_1; \quad W_2 = V_2 + 0.4241 W_1; \quad W_3 = V_3 + 0.5419 W_2 \quad (d)$$

Step 3. Calculate $\{Q\}$ from

$$Q_\ell = \frac{W_\ell}{D_{\ell\ell}} - \sum_{m=\ell+1}^n U_{\ell m} Q_m$$

as

$$Q_3 = W_3/199.5; \quad Q_2 = (W_2 + 434.4 Q_3)/803.66; \quad Q_1 = (W_1 + 639.21 Q_2)/1506.74 \quad (e)$$

Step 4. Calculate p^2 and $\{X\}$ from Eq. (2.127) as

$$\frac{1}{p^2} \{X\} = \{Q\} \quad (f)$$

For the first iteration, let ${}^1\{X\} = [1 \ 1 \ 1]^T$; then Eqs. (c)–(e) become

$${}^1\{V\} = \begin{Bmatrix} 0.8431 \\ 0.8431 \\ 0.8431 \end{Bmatrix}; \quad {}^1\{W\} = \begin{Bmatrix} 0.8431 \\ 1.2009 \\ 1.4939 \end{Bmatrix}; \quad {}^1\{Q\} = \begin{Bmatrix} 2.9158 \\ 5.5521 \\ 7.4880 \end{Bmatrix} 10^{-3};$$

$$\frac{1}{p^2} {}^2\{X\} = 0.007488 \begin{Bmatrix} 0.3894 \\ 0.7414 \\ 1.0000 \end{Bmatrix}$$

For the second iteration, let ${}^2\{X\} = [0.3894 \ 0.7414 \ 1.000]^T$ the result is

$${}^2\{V\} = \begin{Bmatrix} 0.3283 \\ 0.6251 \\ 0.8431 \end{Bmatrix}; \quad {}^2\{W\} = \begin{Bmatrix} 0.3283 \\ 0.7644 \\ 1.2574 \end{Bmatrix}; \quad {}^2\{Q\} = \begin{Bmatrix} 2.0710 \\ 4.3665 \\ 6.3025 \end{Bmatrix} 10^{-3};$$

$$\frac{1}{p^2} {}^3\{X\} = 0.0063025 \begin{Bmatrix} 0.3286 \\ 0.2698 \\ 1.000 \end{Bmatrix}$$

For the third, forth, and fifth iterations, proceed likewise; the fifth iteration gives

$${}^5\{V\} = \begin{Bmatrix} 0.2691 \\ 0.5757 \\ 0.8431 \end{Bmatrix}; \quad {}^5\{W\} = \begin{Bmatrix} 0.2691 \\ 0.6899 \\ 0.2170 \end{Bmatrix}; \quad {}^5\{Q\} = \begin{Bmatrix} 1.9458 \\ 4.1641 \\ 6.1000 \end{Bmatrix} 10^{-3};$$

$$\frac{1}{p^2} {}^6\{X\} = 0.0061 \begin{Bmatrix} 0.3190 \\ 0.6826 \\ 1.0000 \end{Bmatrix}$$

${}^5\{X\}$ is not shown but its values are close to ${}^6\{X\}$. Thus the first natural frequency, p_1 , and the first normal mode, $\{X\}_1$, can be obtained as

$$p_1 = \sqrt{1/0.0061} = 12.803 \text{ rad/sec}, \quad \{X\} = [0.3190 \ 0.6826 \ 1.000]^T$$

For the second mode, begin with Eqs. (2.133) and (2.134) to sweep out the first mode and then employ the four steps described above for iteration. Thus,

$$\{X\}_1^T [M] \{X\}_1 = 1.3217$$

$$S_1 = \frac{1}{\{X\}_1^T [M] \{X\}_1} \{X\}_1^T [M] \{X\}_2 = [0.2032 \ 0.4354 \ 0.6379] \{X\}_2 \quad (g)$$

and

$$\{X\}_2^* = \{X\}_2 - S_1 \{X\}_1 = \begin{Bmatrix} 0.9352X_1 - 0.1389X_2 - 0.2034X_3 \\ -0.1389X_1 + 0.7028X_2 - 0.4354X_3 \\ -0.2034X_1 - 0.4354X_2 + 0.3621X_3 \end{Bmatrix} \quad (h)$$

Let $\{X\}_2 = [1.0 \quad 1.0 \quad -1.0]^T$; then $\{X\}_2^* = [0.997 \quad 0.993 \quad -1.000]^T$, which can be substituted in Eqs. (c)–(f) for the first iteration as

$${}^1\{V\} = \begin{Bmatrix} 0.8428 \\ 0.8425 \\ -0.8439 \end{Bmatrix}; \quad {}^1\{W\} = \begin{Bmatrix} 0.8428 \\ 1.2002 \\ -0.1935 \end{Bmatrix}; \quad {}^1\{Q\} = \begin{Bmatrix} 9.700 \\ 9.678 \\ -9.701 \end{Bmatrix} 10^{-4};$$

$$\frac{1}{p^2} {}^2\{X\}_2^* = 0.00097 \begin{Bmatrix} 0.9993 \\ 0.9976 \\ -1.000 \end{Bmatrix}$$

Performing subsequent iterations the results at the 5th and 6th iterations are

$$\frac{1}{p^2} {}^5\{X\}_2^* = 0.0009695 \begin{Bmatrix} 1.0000 \\ 0.9965 \\ -0.9992 \end{Bmatrix}; \quad \frac{1}{p^2} {}^6\{X\}_2^* = 0.0009694 \begin{Bmatrix} 1.0000 \\ 0.9964 \\ -0.9991 \end{Bmatrix}$$

Thus

$$p_2 = \sqrt{1/0.0009694} = 32.11 \text{ rad/sec}; \quad \{X\}_2 = [1.000 \quad 0.9964 \quad -0.9991]^T$$

For the third mode, Eq. (2.133) becomes

$$\{X\}_3^* = \{X\}_3 - S_1\{X\}_1 - S_2\{X\}_2 = \begin{Bmatrix} 0.6008X_1 - 0.4720X_2 + 0.1306X_3 \\ -0.4720X_1 + 0.3709X_2 - 0.1026X_3 \\ 0.1306X_1 - 0.1026X_2 + 0.0284X_3 \end{Bmatrix} \quad (\text{i})$$

in which $S_1\{X\}$ was calculated previously and S_2 is obtained from Eq. (2.134) as

$$S_2 = \frac{1}{\{X\}_2^T[M]\{X\}_2} \{X\}_2^T[M]\{X\}_3 = [0.3344 \quad 0.3331 \quad -0.3340]\{X\}_3 \quad (\text{j})$$

Let $\{X\}_3 = [1 \quad -1 \quad 1]^T$; then $\{X\}_3^* = [1 \quad -0.7855 \quad 0.2176]^T$. The first two cycles of iteration become

$${}^2\{V\} = \begin{Bmatrix} 0.8431 \\ -0.6622 \\ 0.1835 \end{Bmatrix}; \quad {}^2\{W\} = \begin{Bmatrix} 0.8431 \\ -0.3044 \\ 0.0185 \end{Bmatrix}; \quad {}^2\{Q\} = \begin{Bmatrix} 4.2008 \\ -3.2845 \\ 0.9289 \end{Bmatrix} 10^{-4};$$

$$\frac{1}{p^2} {}^3\{X\}_3^* = 0.0004201 \begin{Bmatrix} 1.000 \\ -0.7819 \\ 0.2211 \end{Bmatrix}$$

The above convergent solution yields

$$p_3 = \sqrt{1/0.0004201} = 48.79 \text{ rad/sec}; \quad \{X\}_3 = [1.000 \quad -0.7819 \quad 0.2211]^T$$

2.6.5. Generalized Jacobi Method

The Jacobi method has several versions. The one presented here is the *generalized Jacobi method*, based on the iteration technique and applied to solve the following eigenvalue problem:

$$[K][X] = [M][X]\left[\begin{smallmatrix} p \\ \vdots \\ p \end{smallmatrix}\right] \quad (2.140)$$

where $[X]$ and $\left[\begin{smallmatrix} p \\ \vdots \\ p \end{smallmatrix}\right]$ include all the modes. This approach is to find a series of orthogonal transformation matrices which will diagonalize the mass and stiffness matrices. The following transformation matrix is chosen in order to reduce the off-diagonal elements of $[K]$ and $[M]$ to zero.

$$[T]^{(r)} = \begin{bmatrix} 1 & & & & & & \\ & \ddots & & & & & \\ & & \ddots & & & & \\ & & & 1 & A & \dots & \\ & & & & B & 1 & \dots \\ & & & & & \ddots & \\ & & & & & & 1 \end{bmatrix} \begin{array}{l} \text{ith column} \\ \vdots \\ \text{jth column} \\ \text{ith row} \\ \vdots \\ \text{jth row} \\ \text{rows} \end{array} \quad (2.141)$$

where r represents the iteration number; A and B are constants to be determined in a manner that eliminates the off-diagonal elements. After premultiplying $[K]$ and $[M]$ by $[T]^{(r)T}$ and postmultiplying $[K]$ and $[M]$ by $[T]^{(r)}$, the $k_{ij}^{(r+1)}$ and $m_{ij}^{(r+1)}$ elements produce two equations

$$Ak_{ii}^{(r)} + (1 + AB)k_{ij}^{(r)} + Bk_{jj}^{(r)} = k_{ij}^{(r+1)} = 0 \quad (2.142)$$

and

$$Am_{ii}^{(r)} + (1 + AB)m_{ij}^{(r)} + Bm_{jj}^{(r)} = m_{ij}^{(r+1)} = 0 \quad (2.143)$$

Multiplying Eqs. (2.142) and (2.143) by m_{ij} and $-k_{ij}$, respectively, and adding the two new equations, lead to a single equation

$$A(k_{ii}m_{ij} - k_{ij}m_{ii}) + B(k_{ij}m_{ij} - k_{ij}m_{ij}) = 0 \quad (2.144)$$

which produces the solution (for simplicity, r , the iteration number has been omitted)

$$A = (k_{ij}m_{ij} - k_{ij}m_{ii}) \quad (2.145)$$

and

$$B = -(k_{ii}m_{ij} - k_{ij}m_{ii}) \quad (2.146)$$

Since Eqs. (2.142) and (2.143) are nonlinear, this is not a solution to either equation, but Eqs. (2.145) and (2.146) provide a means for a solution. Modifying these two equations to the form

$$A = \frac{(k_{ij}m_{ij} - k_{ij}m_{ii})}{C} = \frac{D}{C} \quad (2.147)$$

and

$$B = \frac{-(k_{ii}m_{ij} - k_{ij}m_{ii})}{C} = \frac{-E}{C} \quad (2.148)$$

and substituting the above into Eq. (2.144) yields

$$\frac{1}{C} [k_{ij}k_{jj}m_{ii} - k_{ii}k_{ij}m_{jj}] - \frac{k_{ij}}{C^2} [k_{ii}k_{ij}m_{ij}^2 - k_{ii}k_{ij}m_{ij}m_{jj} - k_{jj}k_{ij}m_{ii}m_{ij} + k_{ij}^2m_{jj}m_{ii}] + k_{ij} = 0 \quad (2.149)$$

which is a quadratic equation. Dividing by $(-k_{ij}/C^2)$ gives

$$-C^2 - C[k_{jj}m_{ii} - k_{ii}m_{jj}] + [k_{ii}k_{jj}m_{ij}^2 - k_{ii}k_{ij}m_{ij}m_{jj} - k_{jj}k_{ij}m_{ii}m_{ij} + k_{ij}^2m_{jj}m_{ii}] = 0 \quad (2.150)$$

or

$$C^2 + C[k_{jj}m_{ii} - k_{ii}m_{jj}] - [k_{ii}m_{ij} - m_{ii}k_{ij}][k_{jj}m_{ij} - m_{jj}k_{ij}] = 0 \quad (2.151)$$

and C can be written as

$$C = \frac{b}{2} + \text{sign of } b \sqrt{\left(\frac{b}{2}\right)^2 + c} \quad (2.152)$$

where

$$b = [k_{ii}m_{jj} - k_{jj}m_{ii}] \quad (2.153)$$

$$c = [k_{ii}m_{ij} - m_{ii}k_{ij}][k_{jj}m_{ij} - m_{jj}k_{ij}] = ED \quad (2.154)$$

Note that this transformation only zeros k_{ij} , k_{ji} , m_{ij} , and m_{ji} for this iteration. The next transformation will force these elements to become nonzero again. Although the elements become nonzero, convergence can be guaranteed. The proof can be found elsewhere. For a diagonal mass, one only needs to drop the off-diagonal element, m_{ij} , in A , B , b , and c of the above equations. The sign in Eq. (2.152) is determined in accordance with the sign of b . The solution is considered acceptable when

$$\frac{|p_i^{2(v+1)} - p_i^{2(v)}|}{p_i^{2(v+1)}} \leq 10^{-s} \quad i = 1, \dots, n \quad (2.155)$$

and

$$\left| \frac{(k_{ij}^{(r)})^2}{k_{ii}^{(r)}k_{jj}^{(r)}} \right| \leq 10^{-2s} \quad i = 1, \dots, n \quad j = 1, \dots, n \quad (2.156)$$

$$\left| \frac{(m_{ij}^{(r)})^2}{m_{ii}^{(r)}m_{jj}^{(r)}} \right| \leq 10^{-2s} \quad i = 1, \dots, n \quad j = 1, \dots, n \quad (2.157)$$

where 10^{-s} is a convergence tolerance, v is the sequence number for checking the convergence of frequencies, and r is the iteration cycle. Eqs. (2.156) and (2.157) are a means of testing whether the off-diagonal element are sufficiently close to zero. The eigenvectors are determined as the

multiplication of all the transformation matrices used as

$$[X] = [T]^{(1)}[T]^{(2)} \dots [T]^{(\ell)} \quad (2.158)$$

in which (ℓ) indicates the last iteration. Eq. (2.158) should be normalized with respect to the mass. Detailed procedures of the method may be summarized in the following seven steps.

1. Calculate coupling factors to determine whether the off-diagonal element needs to be reduced to zero or not. If both Eqs. (2.156) and (2.157) are less than or equal to a prescribed tolerance, then elements $k_{ij}^{(r+1)}$ and $m_{ij}^{(r+1)}$ need not be reduced to zero. Check other off-diagonal elements in a similar procedure.
2. If the off-diagonal element $[K]$ and $[M]$ need to be reduced to zero, then use matrix $[T]^{(r)}$ to transform matrices $[K]$ and $[M]$.
3. Define $[K]^{(1)} = [K]$ and $[M]^{(1)} = [M]$; then

$$\begin{aligned} [K]^{(2)} &= [T]^{(1)\top} [K]^{(1)} [T]^{(1)}, & [M]^{(2)} &= [T]^{(1)\top} [M]^{(1)} [T]^{(1)}, & [X] &= [T]^{(1)} [T]^{(2)} \\ [K]^{(3)} &= [T]^{(2)\top} [K]^{(2)} [T]^{(2)}, & [M]^{(3)} &= [T]^{(2)\top} [M]^{(2)} [T]^{(2)}, & [X] &= [T]^{(1)} [T]^{(2)} [T]^{(3)} \\ &\vdots & &\vdots & &\vdots \\ [K]^{(\ell+1)} &= [T]^{(\ell)\top} [K]^{(\ell)} [T]^{(\ell)}, & [M]^{(\ell+1)} &= [T]^{(\ell)\top} [M]^{(\ell)} [T]^{(\ell)}, & [X] &= [T]^{(1)} [T]^{(2)} \dots [T]^{(\ell)} \end{aligned}$$

4. For the procedures presented, when (r) approaches an infinite number of cycles, then $[K]^{(\ell)}$ and $[M]^{(\ell)}$ converge to diagonal form. The eigenvalues are obtained as

$$\left[\begin{array}{c} p^2 \\ \vdots \\ p^2 \end{array} \right]^{(v)} = \begin{bmatrix} \frac{k_{11}^{(\ell)}}{m_{11}^{(\ell)}} & & & 0 \\ & \ddots & & \\ 0 & & \frac{k_{nn}^{(\ell)}}{m_{nn}^{(\ell)}} & \end{bmatrix}_{n \times n} \quad (2.159)$$

Note that the elements in $\left[\begin{array}{c} p^2 \\ \vdots \\ p^2 \end{array} \right]$ are not in the order of modes.

5. Check the convergence of eigenvalues using Eq. (2.155).
6. If eigenvalues are not converged then repeat steps 1–5. If all eigenvalues satisfy the criterion then check whether there is any off-diagonal element required to be reduced to zero. Use step 1 to check.
7. If all criteria are satisfied, the eigenvectors are scaled by using the following formula

$$[X] = [T]^{(1)}[T]^{(2)} \dots [T]^{(\ell)} \text{ diag} \left(\frac{1}{\sqrt{M_i^{(\ell)}}} \right) = \begin{bmatrix} \frac{X_{11}}{\sqrt{m_{11}^{(\ell)}}} & \frac{X_{12}}{\sqrt{m_{22}^{(\ell)}}} & \dots & \frac{X_{1n}}{\sqrt{m_{nn}^{(\ell)}}} \\ \vdots & \vdots & \dots & \vdots \\ \frac{X_{n1}}{\sqrt{m_{11}^{(\ell)}}} & \frac{X_{n2}}{\sqrt{m_{22}^{(\ell)}}} & \dots & \frac{X_{nn}}{\sqrt{m_{nn}^{(\ell)}}} \end{bmatrix} \quad (2.160)$$

EXAMPLE 2.6.3 Rework Example 2.6.2 by using the generalized Jacobi method presented above. Let the convergence tolerance criterion, s , be 4.

Solution: Using the structural properties and d.o.f. given in Fig. 2.14, the stiffness and mass matrices may be taken directly from Eqs. (a) and (b) of Example 2.6.2 as

$$[K] = \begin{bmatrix} 1506.74 & -639.21 & 0 \\ & 1073.61 & -434.4 \\ \text{symm} & & 434.4 \end{bmatrix} = [K]^{(1)} \quad (\text{a})$$

$$[M] = \begin{bmatrix} 0.8431 & 0 & 0 \\ & 0.8431 & 0 \\ \text{symm} & & 0.8431 \end{bmatrix} = [M]^{(1)} \quad (\text{b})$$

The major iteration steps may be classified into two groups: (a) sweeping cycles in that each cycle has a number of iterations; and (b) iteration steps, as presented in the aforementioned procedures, that are within each sweeping cycle.

(a1) First sweeping cycle: For $i = 1, j = 2$, applying Eqs. (2.156) and (2.157) gives

$$\left| \frac{\left(k_{12}^{(1)} \right)^2}{k_{11}^{(1)} k_{22}^{(1)}} \right| = \left| \frac{(-639.21)^2}{(1506.74)(1073.61)} \right| = 0.2526 > 10^{-8}; \quad \frac{\left(m_{12}^{(1)} \right)^2}{m_{11}^{(1)} m_{22}^{(1)}} = 0$$

Elements k_{12} , k_{21} , m_{12} , and m_{21} are required to be reduced to zero in accordance with Eqs. (2.147), (2.148), and (2.152) as

$$\begin{aligned} E^{(1)} &= k_{11}^{(1)} m_{12}^{(1)} - m_{11}^{(1)} k_{12}^{(1)} = 1506.74(0) - 0.8431 (-639.21) = 538.92 \\ D^{(1)} &= k_{22}^{(1)} m_{12}^{(1)} - m_{22}^{(1)} k_{12}^{(1)} = 538.92 \\ b^{(1)} &= k_{11}^{(1)} m_{22}^{(1)} - k_{22}^{(1)} m_{11}^{(1)} = 365.17 \\ C^{(1)} &= \frac{b^{(1)}}{2} + \text{sign}(b^{(1)}) \sqrt{\left(\frac{b^{(1)}}{2} \right)^2 + D^{(1)} E^{(1)}} \\ &= \frac{365.17}{2} + \sqrt{\left(\frac{365.17}{2} \right)^2 + 538.92(538.92)} = 751.59 \quad (\text{c}) \\ A &= \frac{D^{(1)}}{C^{(1)}} = \frac{538.92}{751.59} = 0.717 \\ B &= \frac{-E^{(1)}}{C^{(1)}} = \frac{-538.92}{751.59} = -0.717 \end{aligned}$$

From Eq. (2.141)

$$[T]^{(1)} = \begin{bmatrix} 1 & 0.717 & 0 \\ -0.717 & 1 & 0 \\ 0 & 0 & 1 \end{bmatrix} \quad (\text{d})$$

Then

$$[K]^{(2)} = [T]^{(1)\top} [K]^{(1)} [T]^{(1)} = \begin{bmatrix} 1 & -0.717 & 0 \\ 0.717 & 1 & 0 \\ 0 & 0 & 1 \end{bmatrix} \begin{bmatrix} 1506.74 & -639.21 & 0 \\ -639.21 & 1073 & -434.4 \\ 0 & -434.4 & 434.4 \end{bmatrix} \quad (e)$$

$$\begin{bmatrix} 1 & 0.717 & 0 \\ -0.717 & 1 & 0 \\ 0 & 0 & 1 \end{bmatrix} = \begin{bmatrix} 2975.4 & 0 & 311.48 \\ 0 & 931.61 & -434.4 \\ 311.48 & -434.4 & 434.4 \end{bmatrix}$$

and

$$[M]^{(2)} = [T]^{(1)\top} [M]^{(1)} [T]^{(1)} = \begin{bmatrix} 1.2766 & 0 & 0 \\ 0 & 1.2766 & 0 \\ 0 & 0 & 0.8431 \end{bmatrix} \quad (f)$$

For $i = 1, j = 3$

$$\left| \frac{\left(k_{13}^{(2)} \right)^2}{k_{11}^{(2)} k_{33}^{(2)}} \right| = \left| \frac{(311.48)^2}{(2975.4)(434.4)} \right| = 0.075 > 10^{-8}; \quad \frac{\left(m_{13}^{(2)} \right)^2}{m_{11}^{(2)} m_{33}^{(2)}} = 0$$

$$E^{(2)} = k_{11}^{(2)} m_{13}^{(2)} - m_{11}^{(2)} k_{13}^{(2)} = -397.58$$

$$D^{(2)} = k_{33}^{(2)} m_{13}^{(2)} - m_{33}^{(2)} k_{13}^{(2)} = -262.59$$

$$b^{(2)} = k_{11}^{(2)} m_{33}^{(2)} - k_{33}^{(2)} m_{11}^{(2)} = 1953.96$$

$$C^{(2)} = \frac{b^{(2)}}{2} + \text{sign}(b^{(2)}) \sqrt{\left(\frac{b^{(2)}}{2}\right)^2 + D^{(2)} E^{(2)}} = 2006.01 \quad (g)$$

$$A = \frac{D^{(2)}}{C^{(2)}} = \frac{-262.59}{2006.01} = -0.1309, \quad B = \frac{-E^{(2)}}{C^{(2)}} = \frac{397.58}{2006.01} = 0.1982$$

$$[T]^{(2)} = \begin{bmatrix} 1 & 0 & -0.1309 \\ 0 & 1 & 0 \\ 0.1982 & 0 & 1 \end{bmatrix} \quad (h)$$

$$[K]^{(3)} = [T]^{(2)\top} [K]^{(2)} [T]^{(2)} = \begin{bmatrix} 3115.9 & -86.10 & 0 \\ -86.10 & 931.61 & -434.4 \\ 0 & -434.4 & 403.84 \end{bmatrix} \quad (i)$$

$$[M]^{(3)} = [T]^{(2)\top} [M]^{(2)} [T]^{(2)} = \begin{bmatrix} 1.3097 & 0 & 0 \\ 0 & 1.2766 & 0 \\ 0 & 0 & 0.8650 \end{bmatrix} \quad (\text{j})$$

$$[X] = [T]^{(1)} [T]^{(2)} = \begin{bmatrix} 1 & 0.717 & 0 \\ -0.717 & 1 & 0 \\ 0 & 0 & 1 \end{bmatrix} \begin{bmatrix} 1 & 0 & -0.1309 \\ 0 & 1 & 0 \\ 0.1982 & 0 & 1 \end{bmatrix} \quad (\text{k})$$

$$= \begin{bmatrix} 1 & 0.717 & -0.1309 \\ -0.717 & 1 & 0.9387 \\ 0.1982 & 0 & 1 \end{bmatrix}$$

For $i = 2, j = 3$

$$\left| \frac{\left(k_{23}^{(3)} \right)^2}{k_{22}^{(3)} k_{33}^{(3)}} \right| = 0.5016 > 10^{-8}; \quad \frac{\left(m_{23}^{(3)} \right)^2}{m_{22}^{(3)} m_{33}^{(3)}} = 0$$

$$E^{(3)} = k_{22}^{(3)} m_{33}^{(3)} - m_{22}^{(3)} k_{33}^{(3)} = 554.51$$

$$D^{(3)} = k_{33}^{(3)} m_{23}^{(3)} - m_{33}^{(3)} k_{23}^{(3)} = 375.76$$

$$b^{(3)} = k_{22}^{(3)} m_{33}^{(3)} - k_{33}^{(3)} m_{22}^{(3)} = 290.32$$

$$C^{(3)} = \frac{290.32}{2} + \sqrt{\left(\frac{290.32}{2} \right)^2 + (554.51)(375.76)} = 624.15 \quad (\text{l})$$

$$A = \frac{375.76}{624.15} = 0.602; \quad B = \frac{-554.51}{624.15} = -0.8884$$

$$[T]^{(3)} = \begin{bmatrix} 1 & 0 & 0 \\ 0 & 1 & 0.602 \\ 0 & -0.8884 & 1 \end{bmatrix} \quad (\text{m})$$

$$[K]^{(4)} = [T]^{(3)\top} [K]^{(3)} [T]^{(3)} = \begin{bmatrix} 3115.59 & -86.10 & -51.84 \\ -86.1 & 2022.3 & 0 \\ -51.84 & 0 & 218.45 \end{bmatrix} \quad (\text{n})$$

$$[M]^{(4)} = [T]^{(3)\top} [M]^{(3)} [T]^{(3)} = \begin{bmatrix} 1.3097 & 0 & 0 \\ \text{symm} & 1.9574 & 0 \\ & & 1.3276 \end{bmatrix} \quad (\text{o})$$

$$[X] = [T]^{(1)} [T]^{(2)} [T]^{(3)} = \begin{bmatrix} 1.0 & 0.8333 & 0.3008 \\ -0.717 & 0.9166 & 0.6959 \\ 0.1982 & -0.8885 & 1.0 \end{bmatrix} \quad (\text{p})$$

$$\begin{bmatrix} \backslash p_1^2 \end{bmatrix}^{(2)} = \begin{bmatrix} \frac{k_{11}^{(4)}}{m_{11}^{(4)}} & 0 \\ 0 & \frac{k_{22}^{(4)}}{m_{22}^{(4)}} \\ 0 & \frac{k_{33}^{(4)}}{m_{33}^{(4)}} \end{bmatrix} = \begin{bmatrix} 2378.86 & 0 & 0 \\ \text{symm} & 1032.10 & 0 \\ & & 164.54 \end{bmatrix} \quad (\text{q})$$

Check convergence of $\begin{bmatrix} \backslash p_1^2 \end{bmatrix}$ by using Eq. (2.155); then

$$\begin{aligned} \frac{|p_1^{2(2)} - p_1^{2(1)}|}{p_1^{2(2)}} &= \frac{|2378.86 - (k_{11}^{(1)}/m_{11}^{(1)})|}{2378.86} = \frac{|2378.86 - 1787.14|}{2378.86} \\ &= 0.2488 > 10^{-4} \text{ (no convergence)} \end{aligned}$$

(a2) Second sweeping cycle: for $i = 1, j = 2$ at the fifth iteration,

$$[X] = \begin{bmatrix} 0.97286 & 0.88207 & 0.30076 \\ -0.74689 & 0.88166 & 0.69581 \\ 0.22715 & -0.87883 & 1.0 \end{bmatrix} \quad (\text{r})$$

For $i = 1, j = 3$ at the sixth iteration

$$[X] = \begin{bmatrix} 0.96756 & 0.88207 & 0.31810 \\ -0.75914 & 0.88166 & 0.68258 \\ 0.20954 & -0.87883 & 1.00400 \end{bmatrix} \quad (\text{s})$$

For $i = 2, j = 3$ at the seventh iteration

$$\begin{aligned} [K]^{(7)} &= \begin{bmatrix} 3125.6 & 0.0445 & 0.66 \times 10^{-4} \\ & 2021.3 & 0 \\ \text{symm} & & 217.59 \end{bmatrix} \\ [M]^{(7)} &= \begin{bmatrix} 1.3122 & 0 & 0 \\ & 1.9625 & 0 \\ \text{symm} & & 1.3281 \end{bmatrix} \end{aligned}$$

$$[X] = \begin{bmatrix} 0.96756 & 0.88137 & 0.31941 \\ -0.75914 & 0.88016 & 0.68389 \\ 0.20954 & -0.88103 & 1.00270 \end{bmatrix} \quad (\text{t})$$

$$\begin{bmatrix} \backslash p_1^2 \end{bmatrix}^{(3)} = \begin{bmatrix} 2381.98 & 0 & 0 \\ \text{symm} & 1029.98 & 0 \\ & & 163.84 \end{bmatrix} \quad (\text{u})$$

Check the convergence:

$$\left| \frac{2381.98 - 2378.86}{2381.98} \right| = 1.314 \times 10^{-3} > 10^{-4} \text{ (no convergence)}$$

(a3) Third sweeping cycle at the 8th iteration,

$$\begin{aligned} [K]^{(8)} &= \begin{bmatrix} 3125.6 & 0 & 0.66 \times 10^{-6} \\ & 2021.3 & -0.166 \times 10^{-8} \\ \text{symm} & 0 & 217.59 \end{bmatrix} \\ [M]^{(8)} &= \begin{bmatrix} 1.3122 & 0 & 0 \\ & 1.9625 & 0 \\ \text{symm} & & 1.3281 \end{bmatrix} \\ [X] &= \begin{bmatrix} 0.96758 & 0.88135 & 0.31941 \\ -0.75913 & 0.88018 & 0.68389 \\ 0.20953 & -0.88104 & 1.00270 \end{bmatrix} \end{aligned} \quad (\text{v})$$

$$\left[\begin{smallmatrix} \backslash p^2 \\ \backslash p^2 \end{smallmatrix} \right]^{(4)} = \begin{bmatrix} 2381.98 & 0 & 0 \\ & 1029.98 & 0 \\ \text{symm} & & 163.84 \end{bmatrix} \quad (\text{w})$$

Check the convergence:

$$\left[\begin{smallmatrix} \backslash p^2 \\ \backslash p^2 \end{smallmatrix} \right]^{(4)} - \left[\begin{smallmatrix} \backslash p^2 \\ \backslash p^2 \end{smallmatrix} \right]^{(3)} = [0]$$

The solution is acceptable.

Note that the eigenvalues are not in the order of modes. The first, second and third eigenvalues are $p_1^2 = 163.84$, $p_2^2 = 1029.98$, and $p_3^2 = 2381.98$. Since $\sqrt{m_{11}^{(8)}} = \sqrt{1.3122} = 1.1455$, $\sqrt{m_{22}^{(8)}} = \sqrt{1.9625} = 1.4009$, $\sqrt{m_{33}^{(8)}} = \sqrt{1.3281} = 1.1524$; then applying Eq. (2.160) yields

$$[X] = \begin{bmatrix} \frac{0.96758}{1.1455} & \frac{0.88135}{1.4009} & \frac{0.31941}{1.1524} \\ \frac{-0.75913}{1.1455} & \frac{0.88018}{1.4009} & \frac{0.68389}{1.1524} \\ \frac{0.20953}{1.1455} & \frac{-0.88104}{1.4009} & \frac{1.0027}{1.1524} \end{bmatrix} = \begin{bmatrix} 0.84468 & 0.62913 & 0.27717 \\ -0.66270 & 0.62830 & 0.59344 \\ 0.18291 & -0.62891 & 0.87012 \end{bmatrix} \quad (\text{x})$$

where the order of modes should be determined according to the fundamental and higher frequencies associated with the columns in Eq. (w). Thus the final solutions of the natural frequencies and normal modes are

$$p_1 = 12.8; \quad \{X\}_1 = 0.87012 \begin{Bmatrix} 0.31854 \\ 0.68202 \\ 1.0 \end{Bmatrix} \quad (\text{y})$$

$$p_2 = 32.09; \quad \{X\}_2 = 0.62913 \begin{Bmatrix} 1.0 \\ 0.99868 \\ -0.99965 \end{Bmatrix} \quad (\text{z})$$

$$p_3 = 48.81; \quad \{X\}_3 = 0.84468 \begin{Bmatrix} 1.0 \\ -0.78456 \\ 0.21654 \end{Bmatrix} \quad (\text{aa})$$

The Jacobi method has the following special qualities: (1) simple and stable in numerical procedures; (2) applicable to symmetric matrix; and (3) capable of solving negative, zero, or positive eigenvalues. However, it must solve simultaneously for all the eigenvalues and corresponding eigenvectors. For a large structural system, if only some eigenpairs are needed, this method can be inefficient.

2.6.6. Sturm Sequence Method

The Sturm sequence method is presented with an outline of numerical procedures, which are then illustrated with an example. Some pertinent comments on the method are discussed afterwards. Readers can observe the general properties of the method more fully after the specifics are presented. Since the basic derivation and convergence proof of the method are somewhat lengthy, and well documented elsewhere, they are not presented here. For a typical eigenproblem shown below,

$$[K]_{n \times n} \{X\}_{n \times 1} = \lambda [M]_{n \times n} \{X\}_{n \times 1} \quad (2.161)$$

the solution procedures may be outlined in the following seven steps:

1. Choose any initial value, λ_0 .
2. Compute the leading principle minors of $[K] - \lambda[M]$, i.e.

$$P_r = |[K_r] - \lambda[M_r]|; \quad r = 0, 1, \dots, n. \quad (2.162)$$

The number of agreements in sign between consecutive members of the sequence, $P_r, r = 0, 1, 2, \dots, n$ is the number of eigenvalues greater than λ_0 .

3. Repeat step 2 to find a region where only the desired eigenvalue exists. Suppose λ_q is the q th eigenvalue. Then for $\ell \leq \lambda_q \leq u$ the number of eigenvalues greater than ℓ is $n - q + 1$, and the number of eigenvalues greater than u is $n - q$.
4. Employ a bisection procedure to find the new value of λ defined as

$$\rho = \frac{\ell + u}{2}$$

5. Compute the leading principle minors of $[K] - \rho[M]$, similar to step 2, to determine the number of eigenvalues greater than ρ . If it is $n - q + 1$, then replace ℓ by ρ .
6. Repeat steps 4 and 5 until the difference between ℓ and u is less than tolerance criterion ϵ ; the eigenvalue λ_q is then determined.
7. Calculate the associated eigenvector $\{X\}_q$, now that the eigenvalue λ_q is known, by evaluating the following singular matrix:

$$([K] - \lambda_q[M]) \{X\}_q = \{0\} \quad (2.163)$$

Let any element in $\{X\}_q$ be a number, say 1; then the rest of the elements can be expressed in terms of that element. It is preferable to have the largest number be 1.

EXAMPLE 2.6.4 A three-story shear building illustrate the iteration method in Example 2.6.2, and the Jacobi method in Example 2.6.3. The same building is now used to demonstrate the Sturm sequence numerical procedures.

Solution: As shown in the previous examples, stiffness and mass matrices are

$$[K] = \begin{bmatrix} 1506.74 & -639.21 & 0 \\ & 1073.61 & -434.4 \\ \text{symm} & & 434.4 \end{bmatrix} \text{ k/ft} \quad (\text{a})$$

$$[M] = \begin{bmatrix} 0.8431 & 0 & 0 \\ & 0.8431 & 0 \\ \text{symm} & & 0.8431 \end{bmatrix} \text{ ksec}^2/\text{ft} \quad (\text{b})$$

The seven steps outlined above are applied as follows:

1. Choose initial value, $\lambda_0 = 0$
2. Compute the leading principal minors.

$$P_0 = 1 \quad (\text{c})$$

$$P_1 = 1506.74 \quad (\text{d})$$

$$P_2 = \begin{vmatrix} 1506.74 & -639.21 \\ -639.21 & 1073.61 \end{vmatrix} = 1,209,061.68 \quad (\text{e})$$

$$P_3 = \det [K] = 240,889,505.0 \quad (\text{f})$$

The number of agreements in sign between P_r 's of Eqs. (c)–(f) is three (i.e. P_0 and P_1 , P_1 and P_2 , and P_2 and P_3). Therefore, the number of eigenvalues greater than 0 is three.

3. Try $\lambda_0 = 2500$, and repeat step 2; the result is

$$P_0 = 1 \quad (\text{g})$$

$$P_1 = |k_{11} - \lambda_0 M_1| = 1506.74 - 2500(0.8431) = -601.01 \quad (\text{h})$$

Similarly

$$P_2 = \left| \begin{bmatrix} k_{11} & k_{12} \\ k_{21} & k_{22} \end{bmatrix} - \lambda_0 \begin{bmatrix} M_1 & 0 \\ 0 & M_2 \end{bmatrix} \right| = \begin{vmatrix} -601.01 & -639.21 \\ -639.21 & 1034.14 \end{vmatrix} = 212,939.05 \quad (\text{i})$$

$$P_3 = |[K] - \lambda_0 [M]| = -242,908,965.0 \quad (\text{j})$$

Because the number of agreements in sign between P_r 's of Eqs. (g)–(j) is zero, all three eigenvalues are between 0 and 2500.

4. Use the bisection procedure to find the new λ as $\lambda_0 = (0 + 2500)/2 = 1250$
5. Repeat step 2

$$P_0 = 1; \quad P_1 = 452.865 \quad (\text{k}, \text{l})$$

$$P_2 = -399,652.13; \quad P_3 = 162,117,358.2 \quad (\text{m}, \text{n})$$

Since there is one agreement in sign between Eqs. (k) and (l), we have only one eigenvalue greater than 1250. Therefore $1250 < \lambda_3 < 2500$, and $0 < \lambda_1, \lambda_2 < 1250$. Try

$$\lambda = \frac{0 + 1250}{2} = 625.00 \quad (\text{o}, \text{p})$$

$$P_0 = 1; \quad P_1 = 979.80 \quad (\text{o}, \text{p})$$

$$P_2 = 127,041.66; \quad P_3 = -196,648,141.0 \quad (\text{q}, \text{r})$$

Two eigenvalues are greater than 625; thus $0 < \lambda_1 < 625$, and $625 < \lambda_2 < 1250$.

Cycle	Interval, lower, ℓ – upper, u	λ	P_0	P_1	P_2	P_3	Sign agreements for P_r
1	625–1250	937.5	1.0	716.33	–205,721	–61,936,560	2
2	937.5–1250	1093.75	1.0	584.6	–320,040	45,780,928	1
3	937.5–1093.75	1015.62	1.0	650.47	–267,219.1	–10,012,480	2
⋮	⋮	⋮	⋮	⋮	⋮	⋮	⋮
13	1029.97–1030.12	1030.04	1.0	638.31	–277,621.2	44,976	1
14	1029.97–1030.04	1030.01	1.0	638.34	–277,594	18,160	1
15	1029.97–1030.01	1029.98					

6. Suppose a second eigenvalue is needed. Steps 4 and 5 are repeated to find λ_2 ; the results as calculated appear in (s). Iteration tolerance is assumed to be $\epsilon = 0.05$. In the 15th cycle, $u - \ell = 1030.01 - 1029.97 = 0.04 < 0.05$; then the eigenvalue of the second mode is taken as

$$\lambda_2 = \frac{\ell + u}{2} = 1029.98; \quad p_2 = \sqrt{\lambda_2} = 32.09 \text{ rad/sec} \quad (\text{t})$$

Using similar procedures, eigenvalues of the first mode and third mode are found as

$$\begin{aligned} \lambda_1 &= 163.84; & p_1 &= 12.8 \text{ rad/sec} \\ \lambda_3 &= 2381.97; & p_3 &= 48.81 \text{ rad/sec} \end{aligned}$$

7. Find the eigenvector $\{X\}_1$, associated with λ_1 , by substituting the numerical values of $[K]$, λ , and $[M]$ into the following:

$$([K] - \lambda_1[M])\{X\}_1 = \begin{bmatrix} 1368.61 & -639.21 & 0 \\ \text{symm} & 935.78 & -434.4 \\ & & 296.27 \end{bmatrix} \begin{Bmatrix} X_1 \\ X_2 \\ X_3 \end{Bmatrix} = \begin{Bmatrix} 0 \\ 0 \\ 0 \end{Bmatrix} \quad (\text{u})$$

Let $X_3 = 1$; from the first row, $1368.61 X_1 - 639.21 X_2 = 0$

$$X_1 = \frac{639.21}{1368.61} X_2 = 0.4671 X_2$$

from the second row, $-639.21(0.4671 X_2) + 935.78(X_2) - 434.4(1) = 0$; then $X_2 = 0.6820$. Consequently, the final result is

$$\{X\}_1^T = [0.3185 \quad 0.6820 \quad 1] \quad (\text{v})$$

Some comments pertinent to numerical procedures are summarized as follows.

- The Sturm sequence method is suitable for calculating a limit number of eigenpairs. It is time-consuming to search for all individual eigenvalues. However, for large structural systems only a few fundamental modes are of practical use; the method is therefore very useful.
- In the numerical procedure, the determinant of $([K_r] - \lambda[M_r])$ is not necessarily calculated. Instead, the sign of $([K_r] - \lambda[M_r])$ is what we are interested in. For any positive definite $([K_r] - \lambda[M_r])$, we can transform it to the product of an upper triangular matrix $[S]$ and a lower triangular matrix $[L]$ as

$$[\tilde{K}] = [K] - \lambda[M] = [L][S] \quad (2.164)$$

where

$$[L] = \begin{bmatrix} 1 & & & \\ \ell_{21} & 1 & & 0 \\ \ell_{31} & \dots & 1 & \\ \vdots & & & \ddots \\ \ell_{n1} & \dots & \dots & \ell_{n,n-1} & 1 \end{bmatrix} \quad (2.165)$$

$$[S] = \begin{bmatrix} S_{11} & S_{12} & \dots & S_{1n} \\ S_{22} & & & \vdots \\ \ddots & & & \vdots \\ 0 & & & S_{nn} \end{bmatrix} \quad (2.166)$$

Using the Choleski decomposition technique, the elements of the above matrices can be found as

$$\left. \begin{array}{l} S_{1i} = \bar{k}_{1i} \quad i = 1, 2, \dots, n \\ \ell_{i1} = \bar{k}_{i1}/S_{11} \quad i = 1, 2, \dots, n \\ S_{ij} = \bar{k}_{ij} - \sum_{r=1}^{i-1} \ell_{ir} S_{rj} \quad i, j \geq 2 \\ \ell_{ji} = \frac{1}{S_{ii}} \left(\bar{k}_{ji} - \sum_{r=1}^{i-1} \ell_{jr} S_{ri} \right) \quad i \geq 2, \quad j \geq i+1 \end{array} \right\} \quad (2.167)$$

From Eq. (2.164), $\det [\bar{K}] = \det [L] \det [S]$ and, from Eq. (2.165), $\det [L_r] = 1$; therefore

$$\begin{aligned} \det ([K_r] - \lambda[M_r]) &= \det [S_r] = \prod_{i=1}^r S_{ii} \\ &= S_{11} S_{22} \dots S_{rr} \end{aligned} \quad (2.168)$$

By using the sign of S_{ii} , the sign of $\det ([K_r] - \lambda[M_r])$ can be easily determined.

3. Sturm sequence method can be applied to a structure having rigid body motion; that is $[K]$ can be singular but must be symmetric.

PART B ADVANCED TOPICS

2.7. EIGEN SOLUTION TECHNIQUES FOR UNSYMMETRIC MATRIX

2.7.1. Classification of Cases

The eigensolution techniques presented so far for symmetric matrix except the determinant method. There exist some cases of eigensolution problems for unsymmetric matrices.

2.7.1.1. Case A—Physical Model

This case can be typically described by using the soil-structure interaction shown in Fig. 2.15 in which k_1 , M_1 , and ρ_1 represent transverse stiffness, transverse mass, and rotational mass of the superstructure, respectively; k_2 and k_θ represent transverse stiffness and rotational stiffness of the soil, respectively; and M_2 and ρ_2 signify transverse mass and rotational mass of the foundation. The structure has three d.o.f., x_1 , x_2 , and x_3 , and may have three externally applied forces, $P_1(t)$, $P_2(t)$, and $P_3(t)$. To set up the dynamic equilibrium matrix, the accompanying

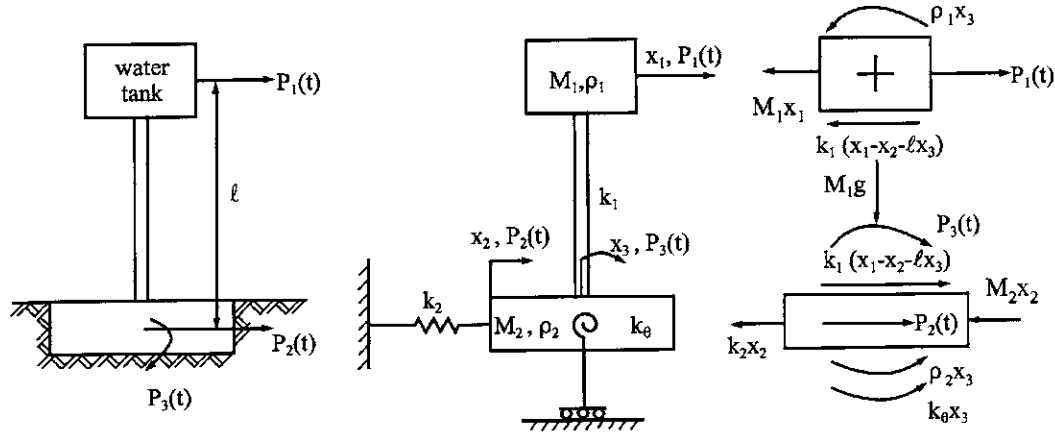


FIG. 2.15 Physical model.

free-body diagrams are used by applying

$$\begin{aligned} \Sigma F_x &= 0 \text{ at } M_1 \\ M_1 \ddot{x}_1 + k_1(x_1 - x_2 - \ell x_3) &= P_1(t) \end{aligned} \quad (2.169)$$

$$\begin{aligned} \Sigma F_x &= 0 \text{ at } M_2 \\ M_2 \ddot{x}_2 + k_2 x_2 - k_1(x_1 - x_2 - \ell x_3) &= P_2(t) \end{aligned} \quad (2.170)$$

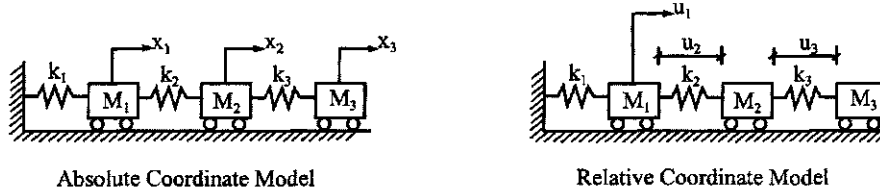
$$\begin{aligned} \Sigma M &= 0 \text{ at } \rho_2 \\ \rho_1 \ddot{x}_3 + \rho_2 \ddot{x}_3 + k_\theta x_3 + M_1 \ell \ddot{x}_1 - M_1 g(x_1 - x_2 - \ell x_3) &= P_3(t) + P_1(t)\ell \end{aligned} \quad (2.171)$$

where $\rho_1 = M_1 R^2 + M_1 \ell^2$, R is the *radius of gyration* about a gravity axis (i.e. central of M_1); $\rho_{cg} = M_1 R^2$; the term associated with $M_1 g$ represents a moment due to the superstructural weight that induces the moment. This is called *P-Δ effect*, which can be significant in the structural response for a structure having heavy weight such as a tall building. Using Eqs. (2.169)–(2.171), form the mass and stiffness matrices as

$$\begin{bmatrix} M_1 & 0 & 0 \\ 0 & M_2 & 0 \\ M_1 \ell & 0 & \rho_1 + \rho_2 \end{bmatrix} \begin{Bmatrix} \ddot{x}_1 \\ \ddot{x}_2 \\ \ddot{x}_3 \end{Bmatrix} + \begin{bmatrix} k_1 & -k_1 & -k_1 \ell \\ -k_1 & k_1 + k_2 & k_1 \ell \\ -M_1 g & M_1 g & k_\theta + M_1 g \ell \end{bmatrix} \begin{Bmatrix} x_1 \\ x_2 \\ x_3 \end{Bmatrix} = \begin{Bmatrix} P_1(t) \\ P_2(t) \\ P_3(t) + P_1(t)\ell \end{Bmatrix} \quad (2.172)$$

2.7.1.2. Case B—Coordinate Model

Here a coordinate system establishes the dynamic equilibrium matrix and allows a comparison of eigenvalues to determine the symmetric and unsymmetric case. Let the structure in Fig. 2.16 be assigned two different coordinate models of absolute coordinates x and relative coordinates u .

**FIG. 2.16** Coordinate model.

The relationship between x and u is $u_1 = x_1$, $u_2 = x_2 - x_1$ and $u_3 = x_3 - x_2$. Let $M_1 = M_2 = M_3 = M$, dynamic equilibrium matrix for the absolute coordinates is

$$\begin{bmatrix} M & 0 & 0 \\ \text{symm} & M & 0 \\ & M & M \end{bmatrix} \begin{Bmatrix} \ddot{x}_1 \\ \ddot{x}_2 \\ \ddot{x}_3 \end{Bmatrix} + \begin{bmatrix} k_1 + k_2 & -k_2 & 0 \\ k_2 + k_3 & k_2 + k_3 & -k_3 \\ 0 & 0 & k_3 \end{bmatrix} \begin{Bmatrix} x_1 \\ x_2 \\ x_3 \end{Bmatrix} = \begin{Bmatrix} 0 \\ 0 \\ 0 \end{Bmatrix} \quad (2.173)$$

Since

$$\begin{Bmatrix} x_1 \\ x_2 \\ x_3 \end{Bmatrix} = \begin{bmatrix} 1 & 0 & 0 \\ 1 & 1 & 0 \\ 1 & 1 & 1 \end{bmatrix} \begin{Bmatrix} u_1 \\ u_2 \\ u_3 \end{Bmatrix} \quad (2.174)$$

the dynamic equilibrium matrix for the relative coordinate system becomes

$$\begin{bmatrix} M & 0 & 0 \\ M & M & 0 \\ M & M & M \end{bmatrix} \begin{Bmatrix} \ddot{u}_1 \\ \ddot{u}_2 \\ \ddot{u}_3 \end{Bmatrix} + \begin{bmatrix} k_1 & -k_2 & 0 \\ 0 & k_2 & -k_3 \\ 0 & 0 & k_3 \end{bmatrix} \begin{Bmatrix} u_1 \\ u_2 \\ u_3 \end{Bmatrix} = \begin{Bmatrix} 0 \\ 0 \\ 0 \end{Bmatrix} \quad (2.175)$$

which is unsymmetric. Eigenvalues of both the symmetric and unsymmetric cases should be the same; the eigenvector can be transferred from one to the other.

2.7.1.3. Case C—Mathematical Model

This case is used mainly to evaluate eigensolutions with consideration of damping. Details are given in the next chapter.

2.7.2. Iteration Method

Besides using the determinant method to obtain the eigensolution of an unsymmetric matrix, a general approach—the iteration method—can be used. While its numerical procedures are similar to those in Eqs. (2.74a,b)–(2.77a,b), details are elaborated in this section. Let

$$[D] = [\delta][M], \quad \lambda = \frac{1}{p^2}$$

Then

$$[\delta][M]\{X\} = \frac{1}{p^2}\{X\}$$

which may be expressed as

$$[D]\{X\} = \lambda\{X\} \quad (2.176)$$

Note that $[D]$ is not symmetric.

2.7.2.1. Fundamental Mode

Let the trial vector ${}^1\{X\}$ be used at the left-hand side of Eq. (2.176); then

$${}^1\{Y\} = [D] {}^1\{X\} \quad (2.177)$$

Yet ${}^1\{Y\}$ is not the true eigenvector; therefore

$${}^1\{Y\} \approx \lambda {}^1\{X\} \quad (2.178)$$

If ${}^1\{Y\}$ is the true eigenvector, then eigenvalue λ can be obtained by dividing any element of vector ${}^1\{Y\}$ by the corresponding element of vector ${}^1\{X\}$. Since ${}^1\{Y\}$ is not the true eigenvector, all such ratios would not be equal. Therefore, the approximation of λ is obtained by taking the ratio of the sums of all elements in the vectors

$${}^1\lambda = \frac{\text{sum of elements of } {}^1\{Y\}}{\text{sum of elements of } {}^1\{X\}} \quad (2.179)$$

For convenience, the new trial eigenvector can be scaled to avoid unusually large or small numbers.

$${}^2\{X\} = {}^1\beta {}^1\{Y\} \quad (2.180)$$

Perform the next iteration ${}^2\{Y\} = [D] {}^2\{X\}$. Repeat this procedure as many times as necessary until reaching the desired degree of accuracy. The procedure will converge to the numerically largest eigenvalue λ (i.e. smallest p^2) and the associated eigenvector of the matrix $[D]$.

2.7.2.2. Higher Modes

In order to find the eigensolutions of higher modes, the orthogonality properties of unsymmetric matrix must be found. Here the derivation is first presented and then the numerical procedures. Let $[E] = [D]^T$ and let $\{X'\}$ and λ' be the eigenvector and eigenvalue associated with $[E]$; then we have

$$[D]\{X\}_i = \lambda_i\{X\}_i \quad (2.181)$$

$$[E]\{X'\}_j = \lambda'_j\{X'\}_j \quad (2.182)$$

where i and j represent two different modes. Premultiply Eq. (2.181) by $\{X'\}_j^T$ and Eq. (2.182) by $\{X\}_i^T$

$$\{X'\}_j^T [D] \{X\}_i = \lambda_i \{X'\}_j^T \{X\}_i \quad (2.183)$$

$$\{X\}_i^T [E] \{X'\}_j = \lambda'_j \{X\}_i^T \{X'\}_j \quad (2.184)$$

Transpose both sides of the above two equations:

$$\{X\}_i^T [E] \{X'\}_j = \lambda_i \{X\}_i^T \{X'\}_j \quad (2.185)$$

$$\{X'\}_j^T [D] \{X\}_i = \lambda'_j \{X'\}_j^T \{X\}_i \quad (2.186)$$

Compare Eq. (2.183) with Eq. (2.186), and Eq. (2.184) with Eq. (2.185),

$$(\lambda_i - \lambda'_j) \{X'\}_j^T \{X\}_i = 0 \quad (2.187)$$

$$(\lambda_i - \lambda'_j) \{X\}_i^T \{X'\}_j = 0 \quad (2.188)$$

If $i \neq j$ and $\lambda_i \neq \lambda_j$, we have the following two orthogonality conditions

$$\{X'\}_j^T \{X\}_i = 0 \quad (2.189)$$

$$\{X\}_i^T \{X'\}_j = 0 \quad (2.190)$$

Begin by finding the first mode of $\{X\}_1$ and λ_1 associated with $[D]$; next solve for $\{X'\}_1$, and λ'_1 corresponding to $[E]$. Use the orthogonality condition $\{X'\}_1^T \{X\}_2 = 0$ to modify $[D]$ to $[DD]$ from which $\{X\}_2$ and λ_2 are then established. For the third mode, we need $\{X'\}_2$ and λ'_2 , which can be obtained from $[EE]$. $[EE]$ should be modified from $[E]$; the modification is performed through $\{X\}_1^T \{X'\}_2 = 0$. This procedure can be applied for other higher modes, and is illustrated by the following example.

EXAMPLE 2.7.1 Find the eigensolutions of the single-story frame in Fig. 2.17 with a flexible foundation for which the mass and stiffness matrices are

$$[M] = \begin{bmatrix} 1 & 0 & 0 \\ 0 & 2 & 0 \\ 0 & 0 & 120 \end{bmatrix} \quad (a)$$

$$[K] = \begin{bmatrix} 500 & -500 & -6,000 \\ -500 & 100,500 & 6,000 \\ -6032.2 & 6032.2 & 192,000 \end{bmatrix} \quad (b)$$

For the first mode perform $[D] = [K]^{-1}[M]$

$$[D] = \begin{bmatrix} 0.00322034 & 0.00002 & 0.0120388 \\ 0.00001 & 0.00002 & 0 \\ 0.000100861 & 0 & 0.00100323 \end{bmatrix} \quad (c)$$

Follow Eqs. (2.177)–(2.180) and let ${}^1\{X\}^T = [1 \ 1 \ 1]$,

$${}^1\{Y\} = [D] {}^1\{X\}_1 = \begin{Bmatrix} 0.0152791 \\ 0.0000300 \\ 0.0011041 \end{Bmatrix} = 0.0152791 \begin{Bmatrix} 1.000 \\ 0.0019635 \\ 0.0722616 \end{Bmatrix} = 0.1052791 {}^2\{X\} \quad (d)$$

$${}^1\lambda = \frac{\text{sum of element of } {}^1\{Y\}}{\text{sum of element of } {}^1\{X\}} = \frac{0.0152791 + 0.00003 + 0.0011041}{1 + 1 + 1} = 5.47106 \times 10^{-3} \quad (e)$$

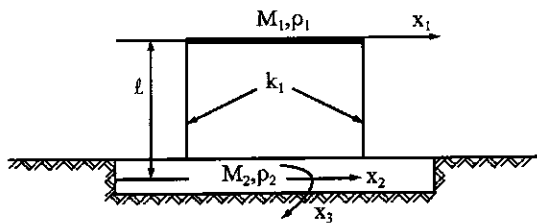


FIG. 2.17 Example 2.7.1.

Based on Eqs. (d) and (e), the iteration procedures may be summarized as:

Cycle (n)	Mode	${}^n\{Y\}(10^{-4})$	${}^{n+1}\{X\}$	${}^n\lambda(10^{-3})$	
2	X_1	40.9032	1.00000	3.9784	(f)
	X_2	0.1004	0.00245		
	X_3	1.7336	0.04238		
	\vdots	\vdots	\vdots	\vdots	
7	X_1	36.7491	1.00000	3.6749	
	X_2	0.1005	0.00274		
	X_3	1.3873	0.03775		

Solutions of the seventh and eighth cycles are identical; the iteration is stopped and the results are

$$\{X\}_1^T = [1 \quad 0.00274 \quad 0.03775] \quad (g)$$

$$\hat{\lambda} = 3.6749 \times 10^{-3}; \quad p_1 = \sqrt{\frac{1}{\hat{\lambda}_1}} = 16.4960 \text{ rad/sec} \quad (h)$$

For the second mode find $\{X'\}_1$ and λ'_1 , which may be found by using $[E] = [D]^T$. Try ${}^1\{X'\}^T = [1 \quad 1 \quad 1]$; then

$${}^1\{Y\} = [E] {}^1\{X'\} = \begin{Bmatrix} 0.003312 \\ 0.000040 \\ 0.013042 \end{Bmatrix} = 0.013042 \begin{Bmatrix} 0.255421 \\ 0.003067 \\ 1.000000 \end{Bmatrix} = 0.013042 {}^2\{X'\} \quad (i)$$

The other iteration may be summarized as follows:

Cycle (n)	Mode	${}^n\{Y\}(10^{-4})$	${}^{n+1}\{X'\}$	${}^n\lambda'(10^{-3})$	
2	X_1	9.2343	0.22643	3.9784	(j)
	X_2	0.0517	0.00127		
	X_3	40.7818	1.00000		
	\vdots	\vdots	\vdots	\vdots	
7	X_1	8.1554	0.22192	3.6749	
	X_2	0.04463	0.00121		
	X_3	36.7491	1.00000		

Again, the results of the seventh and eighth cycles are identical; then the solutions are

$$\{X'\}_1^T = [0.22192 \quad 0.00121 \quad 1] \quad (k)$$

$$\lambda'_1 = 3.6749 \times 10^{-3}; \quad p'_1 = \sqrt{\frac{1}{\lambda'_1}} = 16.4960 \quad (l)$$

Note that $\lambda'_1 = \lambda_1$ and $p'_1 = p_1$. Now use Eq. (k) in $\{X'\}_1^T \{X\}_2 = 0$, which yields $0.22192X_1 + 0.00121X_2 + X_3 = 0$. Express X_3 in terms of X_1 and X_2 as

$$X_3 = -0.22192X_1 - 0.00121X_2 \quad (m)$$

Use $[D]\{X\} = \lambda\{X\}$ where $[D]$ is given in Eq. (c), and substitute Eq. (m) for X_3 , leading to

$$\begin{bmatrix} 5.48689 \times 10^{-4} & 0 \\ 0.00001 & 0.00002 \end{bmatrix} \begin{Bmatrix} X_1 \\ X_2 \end{Bmatrix} = \lambda \begin{Bmatrix} X_1 \\ X_2 \end{Bmatrix} \quad (\text{n})$$

In symbolic form

$$[DD]\{X\} = \lambda\{X\} \quad (\text{o})$$

Let $^1\{X\}^T = [1 \ 1]$; then

$$^1\{Y\} = [DD] ^1\{X\}_2 = \begin{Bmatrix} 0.000548689 \\ 0.000030000 \end{Bmatrix} = 0.000548689 \begin{Bmatrix} 1.00000 \\ 0.54676 \end{Bmatrix} = 0.000548689 ^2\{X\} \quad (\text{p})$$

$$^1\lambda = \frac{0.00054869 + 0.00003}{1 + 1} = 0.000289344 \quad (\text{q})$$

After six cycles, the second-mode eigensolutions are

$$\{X\}_2^T = [1 \ 0.01891 \ -0.22194] \quad (\text{r})$$

$$\lambda_2 = 5.4869 \times 10^{-4}; \quad p_2 = \sqrt{\frac{1}{\lambda_2}} = 42.6910 \text{ rad/sec} \quad (\text{s})$$

For the third mode we need to find $\{X'\}_2$ and $[EE]$. Use $\{X\}_1^T \{X'\}_2 = 0$, where $\{X\}_1$ is given in Eq. (g); then we have $X'_1 + 0.00274X'_2 + 0.03775X'_3 = 0$. Thus,

$$X'_1 = -0.00274 X'_2 - 0.03775 X'_3 \quad (\text{t})$$

Substituting X'_1 into $[E]\{X'\} = \lambda'\{X'\}$ yields

$$\begin{bmatrix} 1.99452 \times 10^{-5} & -7.550 \times 10^{-7} \\ -3.29863 \times 10^{-5} & 5.48765 \times 10^{-4} \end{bmatrix} \begin{Bmatrix} X'_2 \\ X'_3 \end{Bmatrix} = \lambda' \begin{Bmatrix} X'_2 \\ X'_3 \end{Bmatrix} \quad (\text{u})$$

In symbolic form

$$[EE]\{X'\}_2 = \lambda'_2 \{X'\}_2 \quad (\text{v})$$

Let $\{X'\}_2^T = [1 \ 1]$; then

$$\begin{aligned} ^1\{Y\} &= [EE] ^1\{X'\}_2 = \begin{Bmatrix} 0.0000191902 \\ 0.000515779 \end{Bmatrix} = 0.000515779 \begin{Bmatrix} 0.0372063 \\ 1.0000000 \end{Bmatrix} \\ &= 0.00515779 ^2\{X'\} \end{aligned} \quad (\text{w})$$

$$^1\lambda' = \frac{0.0000191902 + 0.000515779}{1 + 1} = 0.000267484 \quad (\text{x})$$

After six cycles, the results are

$$\{X'\}_2^T = [-3.77484 \times 10^{-2} \ -0.001428 \ 1] \quad (\text{y})$$

$$\lambda'_2 = 5.48881 \times 10^{-4}; \quad p'_2 = 42.6863 \text{ rad/sec} \quad (\text{z})$$

To get the third-mode eigensolution, use $\{X'\}_1^T \{X\}_3 = 0$ and $\{X'\}_2^T \{X\}_3 = 0$, in which $\{X'\}_1^T$ and $\{X'\}_2^T$ are known. We then have two linear equations: $0.22192X_1 + 0.00121X_2 + X_3 = 0$ and $3.77484(10^{-2})X_1 + 0.001428X_2 - X_3 = 0$, from which X_3 can be eliminated and

$$X_1 = -0.010159111 X_2 \quad (\text{aa})$$

Substituting X_1 into $[DD]\{X\} = \lambda\{X\}$ of Eq. (n) yields

$$1.989841 \times 10^{-5} X_2 = \lambda_3 X_2 \quad (\text{bb})$$

Thus,

$$\lambda_3 = 1.989841 \times 10^{-5}; \quad p_3 = 224.1769 \text{ rad/sec} \quad (\text{cc})$$

Let $X_2 = 1$, the X_1 and X_3 can be calculated and the eigenvector becomes

$$\{X\}_3^T = [-0.010175 \quad 1 \quad 0.0010437] \quad (\text{dd})$$

Note that the eigensolution procedure shown in Eqs. (c)–(dd) is based on the *sweeping matrix* approach discussed in Section 2.6.1.

2.8. RESPONSE ANALYSIS FOR ZERO AND REPEATING EIGENVALUES

2.8.1. Zero and Repeating Eigenvalue Cases

Sample structural models shown in Fig. 2.18 represent cases having zero eigenvalue(s), multiple eigenvalue(s), or a combination of both. Case (a) represents a frame structure with roller supports which has a zero eigenvalue due to the rigid-body motion of the structure. Case (b) symbolizes two moving bodies connected by a spring; the system has two d.o.f., but one is a rigid-body motion with a zero eigenvalue. Case (c) is a simple model of an airplane in which M_1 and M_2 signify fuel tanks and M_2 is the airplane body; this structure has two rigid-body motions and zero eigenvalues. Case (d) is a column in a three-dimensional space; the motions of x_1 , x_2 , and x_3 in this particular case are uncoupled; the three eigenvalues could be the same or different depending on the stiffness of the column in the x -, y -, and z -directions. Case (e) represents a system that not only can have a zero eigenvalue, but can possibly have multiple eigenvalues. Case (f) represents a complex model for which some of the frequencies are repeating. Some of the cases are discussed in the following numerical examples.

2.8.2. Orthogonality Properties

From Fig. 2.18a, the stiffness matrix may be established as

$$[K] = \begin{bmatrix} k_1 & -k_1 & 0 \\ -k_1 & k_1 + k_2 & -k_2 \\ 0 & -k_2 & k_2 \end{bmatrix} \quad (\text{symm}) \quad (2.191)$$

which is a singular matrix (using row operation as: row 2 + row 1 + row 3 = 0). Therefore, one of the eigenvalues in $([K] - p^2[M])\{X\} = 0$ must be zero, and the associated eigenvector is a rigid-body motion. Similar behavior of rigid-body motion may be observed for the model in Fig. 2.18b. If a relative coordinate (say $u = x_1 - x_2$) is used to express the motion, then the system becomes one d.o.f and excludes rigid-body motion.

Orthogonality properties can be derived by using the same method as presented in Section 2.4

$$[D]\{X\}_i = \lambda_i\{X\}_i \quad (2.192)$$

$$[D]\{X\}_j = \lambda_j\{X\}_j \quad (2.193)$$

Premultiply the first equation by $\{X\}_j^T$ and the second by $\{X\}_i^T$; then transpose each of these two equations and recognize $[D] = [D]^T$ as symmetric matrix, leading to

$$(\lambda_i - \lambda_j)\{X\}_i^T\{X\}_j = 0 \quad (2.194)$$

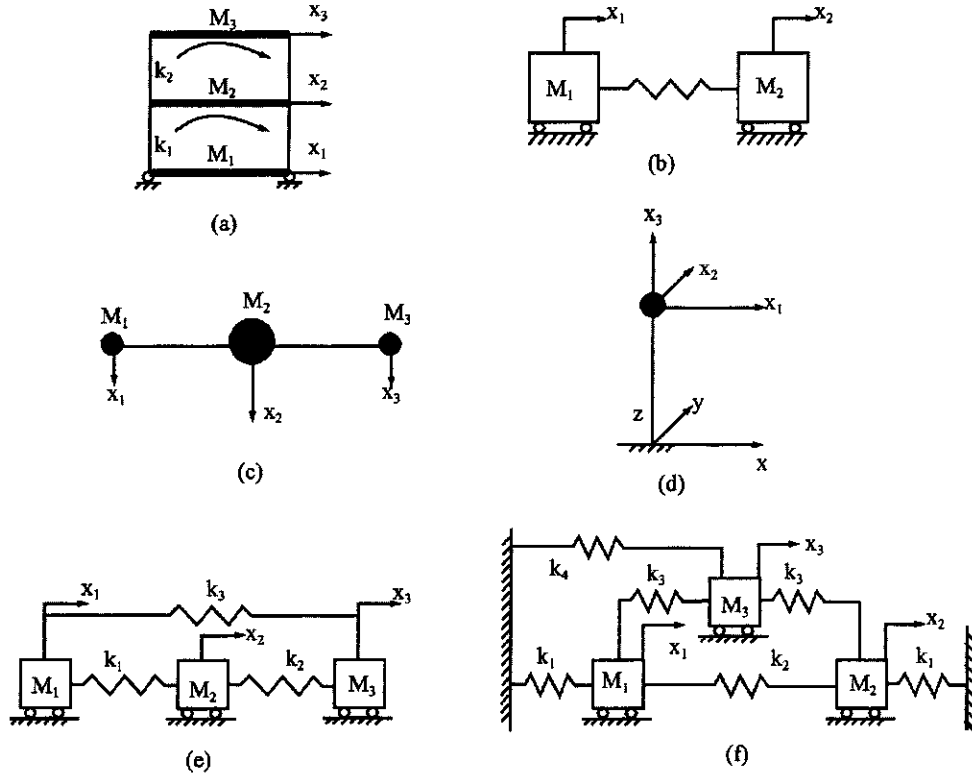


FIG. 2.18 Sample structural models.

If the eigenvalues are distinct, $\lambda_i \neq \lambda_j$, then $\{X\}_i^T \{X\}_j = 0$, as discussed in Section 2.5.4. Now

$$\lambda_i = \lambda_j, \quad \{X\}_i^T \{X\}_j = 0 \quad \text{or} \quad \{X\}_i^T \{X\}_j \neq 0 \quad (2.195)$$

In order to solve for response by modal analysis, the orthogonal matrix is needed to uncouple the motion equation. Therefore, it is essential to use

$$\{X\}_i^T \{X\}_j = 0; \quad i \neq j \quad (2.196)$$

Since $\{X\}_i^T \{X\}_j = 0$ is not always true, some way must be found to establish the orthogonality condition. A theorem in linear algebra states: *if an eigenvalue is repeated n times, then there are n linearly independent eigenvectors associated with these repeated eigenvalues*. Thus the orthogonality conditions can be found based on the characteristics of independent eigenvectors. Numerical procedures for Eqs. (2.195) and (2.196) are demonstrated in the next two examples.

EXAMPLE 2.8.1 Let the structural properties of Fig. 2.18d be $k_1 = k_2 = 600 \text{ k/ft}$, $k_3 = 2000 \text{ k ft/rad}$, $M_1 = M_2 = M_3 = 1.2 \text{ k sec}^2/\text{ft}$; find the eigenvalues and eigenvectors of the system.

Solution: The dynamic matrix equation, $[K]\{X\} - p^2[M]\{X\} = \{0\}$, of the vertical column in three-dimension space is

$$\left(\begin{bmatrix} k_1 & 0 & 0 \\ k_2 & k_3 & 0 \\ \text{symm} & & k_3 \end{bmatrix} - p^2 \begin{bmatrix} M_1 & 0 & 0 \\ M_2 & M_3 & 0 \\ \text{symm} & & M_3 \end{bmatrix} \right) \begin{Bmatrix} X_1 \\ X_2 \\ X_3 \end{Bmatrix} = \begin{Bmatrix} 0 \\ 0 \\ 0 \end{Bmatrix} \quad (\text{a})$$

Any appropriate eigensolution technique for symmetric matrix can be used to find the eigenvalues. For convenience, let us use the determinant method as follows:

$$|[D] - \lambda[I]| = \begin{vmatrix} 0.002 - \lambda & 0 & 0 \\ 0 & 0.002 - \lambda & 0 \\ \text{symm} & & 0.0006 - \lambda \end{vmatrix} \quad (\text{b})$$

$$= (0.002 - \lambda)(0.002 - \lambda)(0.0006 - \lambda) = 0$$

where $[D] = [K]^{-1}[M]$ and $\lambda = 1/p^2$. From Eq. (b)

$$\lambda_1 = 0.002; \quad \lambda_2 = 0.002; \quad \lambda_3 = 0.0006 \quad (\text{c})$$

Using λ_1 and λ_2 in $([D] - \lambda[I])\{X\} = 0$, we have $X_3 = 0$, and X_1 and X_2 can be any arbitrary value. In this case, $\{X\}_1$ and $\{X\}_2$ are arbitrarily chosen as

$$\{X\}_1^T = [1 \ 1 \ 0]; \quad \{X\}_2^T = [0 \ 1 \ 0] \quad (\text{d})$$

The eigenvector corresponding to λ_3 is

$$\{X\}_3^T = [0 \ 0 \ -1] \quad (\text{e})$$

Checking the orthogonality condition $\{X\}_i^T\{X\}_j = 0$ yields

$$\{X\}_1^T\{X\}_2 = 1; \quad \{X\}_1^T\{X\}_3 = 0; \quad \{X\}_2^T\{X\}_3 = 0 \quad (\text{f})$$

It is apparent that the first two modes are not orthogonal. By knowing that the eigenvectors corresponding to repeating eigenvalues are always independent; therefore, produce the orthogonal eigenvectors by using a linear combination of the original ones. Let * signify new eigenvector; then

$$^*\{X\}_1 = C_1\{X\}_1 + C_2\{X\}_2 \quad (\text{g})$$

$$^*\{X\}_2 = C_3\{X\}_1 + C_4\{X\}_2 \quad (\text{h})$$

For simplicity, take $C_1 = C_3 = 1$. The new eigenvectors should be orthogonal to each other as

$$^*\{X\}_1^T ^*\{X\}_2 = 1 + (1 + C_2)(1 + C_4) = 0 \quad (\text{i})$$

Let $C_2 = 0$ and then find $C_4 = -2$. Thus the true eigenvector of the second mode is

$$\{X\}_2^T = 1[1 \ 1 \ 0] - 2[0 \ 1 \ 0] = [1 \ -1 \ 0] \quad (\text{j})$$

It is apparent that $\{X\}_1$ and $\{X\}_2$ can be any vector on the X_1-X_2 plane due to the arbitrary selection of X_1 and X_2 , and consequently there are infinite pairs of $\{X\}_1$ and $\{X\}_2$ that maintain the orthogonality conditions.

EXAMPLE 2.8.2 For the structural model shown in Fig. 2.18e, find the sensitivity of k_3 which will cause the system to have repeating frequencies. For simplicity, let $M_1 = M_2 = M_3 = M$, $k_1 = k_2 = k$, and $k_3 = \varepsilon k$. ε is the sensitivity parameter.

Solution: The dynamic equilibrium matrix of $[K]\{X\} - p^2[M]\{X\} = \{0\}$ of this system may be written as

$$\left(\begin{bmatrix} (1+\varepsilon)k & -k & -\varepsilon k \\ -k & 2k & -k \\ -\varepsilon k & -k & (1+\varepsilon)k \end{bmatrix} - p^2 \begin{bmatrix} M & 0 & 0 \\ 0 & M & 0 \\ 0 & 0 & M \end{bmatrix} \right) \begin{Bmatrix} X_1 \\ X_2 \\ X_3 \end{Bmatrix} = \begin{Bmatrix} 0 \\ 0 \\ 0 \end{Bmatrix} \quad (a)$$

Let $\sigma = (Mp^2/k)$; the determinant of $([K] - p^2[M])$ becomes

$$\sigma[\sigma^2 - 2\sigma(2 + \varepsilon) + 3(1 + 2\varepsilon)] = 0 \quad (b)$$

from which

$$\sigma_1 = 0, \quad \sigma_{2,3} = (2 + \varepsilon) \pm \sqrt{(2 + \varepsilon)^2 - 3(1 + 2\varepsilon)} \quad (c)$$

Therefore, the first frequency associated with a rigid-body motion is zero. The second and third frequencies may be repeated if the terms in the square root of Eq. (c) vanish, that is

$$(2 + \varepsilon)^2 - 3(1 + 2\varepsilon) = 0 \quad (d)$$

from which $\varepsilon = 1$. Upon substitution of $\varepsilon = 1$ in Eq. (c), $\sigma_2 = \sigma_3 = 3$. It can now be concluded that where $k_1 = k_2 = k_3 = k$, the three natural frequencies are

$$p_1^2 = 0, \quad p_2^2 = p_3^2 = \frac{3k}{M} \quad (e)$$

Substituting the above into Eq. (a), and applying the linear combination technique to ensure orthogonality conditions, yields the correct eigenvectors as

$$\{X\}_1^T = [1 \quad 1 \quad 1]; \quad \{X\}_2^T = [1 \quad -2 \quad 1]; \quad \{X\}_3^T = [-1 \quad 0 \quad 1] \quad (f)$$

The mode shapes are shown in Fig. 2.19.

Note that the general solution of Eq. (c) is

$$\sigma_{2,3} = (2 + \varepsilon) \pm (\varepsilon - 1) = 3 \quad \text{or} \quad 2\varepsilon + 1 \quad (g)$$

Thus the second frequency is always $3k/M$, no matter what stiffness, k_3 , is used. When $\varepsilon = 1$, we have two repeating frequencies. Any other value of ε yields distinct frequencies.

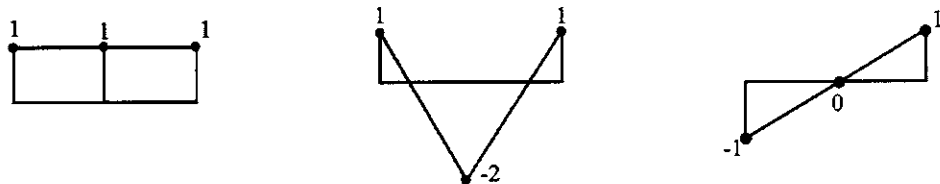


FIG. 2.19 Mode shapes for zero and repeating frequencies.

2.8.3. Response Analysis

From Eq. (2.66), the uncoupled equation is expressed as

$$[\bar{M}_v] \{\ddot{x}'\} + [\bar{M}_v] \left[\bar{p}_v^2 \right] \{x'\} = [X]^T \{F(t)\} \quad (2.197)$$

By knowing that the natural frequency corresponding to rigid-body motion is equal to zero, the second term on the left-hand side of the above equation should be dropped. Therefore, the response can be separated into two parts: rigid-body motion, $\{x\}_r$, and elastic motion, $\{x\}_e$.

$$\{x\} = \{x\}_r + \{x\}_e = [X]_r \{x'\}_r + [X]_e \{x'\}_e = [X] \{x'\} \quad (2.198)$$

where $[X]_r + [X]_e = [X]$, and $\{x'\}_r + \{x'\}_e = \{x'\}$. Rigid-body motion may be expressed as

$$\{\ddot{x}'\}_r = [\bar{M}_v]_r^{-1} [X]_r^T \{F(t)\} \quad (2.199)$$

$$\{x'\}_r = \int_0^t [\bar{M}_v]_r^{-1} [X]_r^T \{F(\Delta)\} d\Delta + \{\dot{x}'_0\}_r \quad (2.200)$$

$$\{x'\}_r = \int_0^t \int_0^\tau [\bar{M}_v]_r^{-1} [X]_r^T \{F(\Delta)\} d\Delta d\tau + t \{\dot{x}'_0\}_r + \{x'_0\}_r \quad (2.201)$$

Displacement associated with elastic motion was presented in Section 2.5.2. Follow Eq. (2.47), but use $[X]$ instead of $[\Phi]$; elastic displacement due to initial conditions for Eq. (2.197) becomes

$$\begin{aligned} \{x\}_{e(in)} &= [X]_e \{x'\}_{e(in)} = [X]_e [\bar{\cos} p t_v] \{x'_0\}_e + [X]_e [\bar{\sin} p t_v] [\bar{p}_v]^{-1} \{\dot{x}'_0\}_e \\ &= [\bar{\cos} p t_v] \{x_0\}_e + [\bar{\sin} p t_v] [\bar{p}_v]^{-1} \{\dot{x}_0\}_e \end{aligned} \quad (2.202)$$

Elastic displacement due to applied force is

$$\{x\}_{e(f)} = [X]_e \{x'\}_{e(f)} = [\bar{M}_v]_e^{-1} \int_0^A [\bar{\sin} p(t - \Delta)] [\bar{p}_v]^{-1} [X]_e^T \{F(\Delta)\} d\Delta \quad (2.203)$$

Total elastic displacement is

$$\{x\}_e = \{x\}_{e(in)} + \{x\}_{e(f)} \quad (2.204)$$

Numerical procedures are illustrated in the following examples.

EXAMPLE 2.8.3 The structure shown in Fig. 2.20 is subjected to a force $F \sin 2t$ applied at M_2 . Let $M_1 = M_3 = 1 \text{ k sec}^2/\text{ft}$, and $EI = 360,000 \text{ k ft}^2$; find the response. Assume the initial conditions are zero.

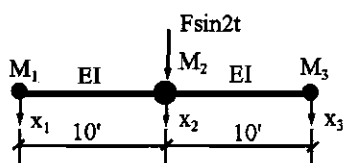


FIG. 2.20 Example 2.8.3.

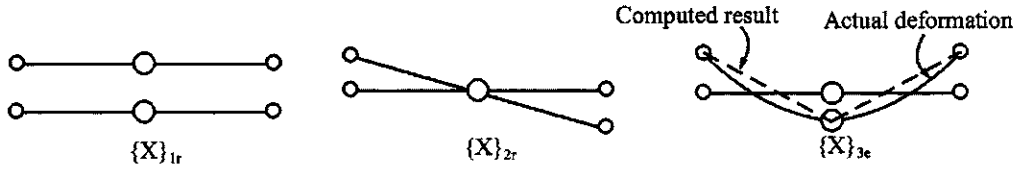


FIG. 2.21 Mode shapes of example 2.8.3.

Solution: For the d.o.f. assigned to the structure, the mass and stiffness matrices are

$$[M] = \begin{bmatrix} M_1 & 0 & 0 \\ 0 & M_2 & 0 \\ 0 & 0 & M_3 \end{bmatrix} = \begin{bmatrix} 1 & 0 & 0 \\ 0 & 2 & 0 \\ 0 & 0 & 1 \end{bmatrix} \quad (\text{a})$$

$$[K] = \frac{12EI}{L^3} = \begin{bmatrix} 1 & -2 & 1 \\ -2 & 4 & -2 \\ 1 & -2 & 1 \end{bmatrix} = \begin{bmatrix} 4320 & -8640 & 4320 \\ -8640 & 17,280 & -8640 \\ 4320 & -8640 & 4320 \end{bmatrix} \quad (\text{b})$$

Using the numerical procedures already presented, the eigensolutions become

$$\begin{aligned} p_1^2 &= 0, & p_2^2 &= 0, & p_3^2 &= 17,280 \\ [X]_{1r}^T &= [1 \ 1 \ 1], & [X]_{2r}^T &= [1 \ 0 \ -1], & [X]_{3e}^T &= [1 \ -1 \ 1] \end{aligned} \quad (\text{c})$$

The mode shape is shown in Fig. 2.21. Note that the third mode should be shown by dotted lines because the lumped mass is used. The solid line reveals actual elastic deformation. For the response, calculate

$$\begin{aligned} [\bar{M}_r] &= [X_{1r} \ X_{2r} \ X_{3e}]^T [M] [X_{1r} \ X_{2r} \ X_{3e}] \\ &= \begin{bmatrix} 4 & 0 & \vdots & 0 \\ 0 & 2 & \vdots & 0 \\ \vdots & \vdots & \ddots & \vdots \\ \text{symm} & \vdots & 4 & \end{bmatrix} = \begin{bmatrix} \bar{M}_r & \vdots & 0 \\ \vdots & \ddots & \vdots \\ \dots & \vdots & \dots \\ 0 & \vdots & \bar{M}_e \end{bmatrix} \end{aligned} \quad (\text{d})$$

From Eq. (2.201) with $\{\dot{x}'_0\} = \{x'_0\} = \{0\}$, the rigid-body motion is

$$\begin{aligned} \{x\}_r &= [X]_r \int_0^t \int_0^t [\bar{M}_r]_r^{-1} [X]_r^T \{F(\Delta)\} d\Delta d\tau \\ &= \begin{bmatrix} 1 & 1 \\ 1 & 0 \\ 1 & -1 \end{bmatrix} \int_0^t \int_0^t \begin{bmatrix} 4 & 0 \\ 0 & 2 \end{bmatrix}^{-1} \begin{bmatrix} 1 & 1 & 1 \\ 1 & 0 & -1 \end{bmatrix} \begin{Bmatrix} 0 \\ F \sin 2\Delta \\ 0 \end{Bmatrix} d\Delta d\tau \\ &= F \begin{Bmatrix} -0.0625 sn + 0.125t \\ -0.0625 sn + 0.125t \\ -0.0625 sn + 0.124t \end{Bmatrix} \end{aligned} \quad (\text{e})$$

where $sn = \sin 2t$. The elastic motion can be obtained from Eq. (2.202) as

$$\begin{aligned}\{x\}_e &= [X]_e [\bar{M}]_e^{-1} \int_0^t [\bar{\lambda} \sin p(t-\Delta)] [\bar{p}]^{-1} [X]_e^T \{F(\Delta)\} d\Delta \\ &= \begin{Bmatrix} 1 \\ -1 \\ 1 \end{Bmatrix} \frac{1}{4} \int_0^t \sin p(t-\Delta) \frac{1}{131.45} [1 \quad -1 \quad 1] \begin{Bmatrix} 0 \\ F \sin 2\Delta \\ 0 \end{Bmatrix} d\Delta \\ &= \begin{Bmatrix} -1.1577 sn_1 - 76.0922 sn \\ 1.1577 sn_1 - 76.0922 sn \\ -1.1577 sn_1 + 76.0922 sn \end{Bmatrix} F(10^{-4})\end{aligned}\quad (f)$$

where $sn_1 = \sin 131.45t$. The total response is found by adding Eq. (e) to Eq. (f).

EXAMPLE 2.8.4 Find the response of the structure shown in Fig. 2.20 due to the following initial conditions: $\{x_0\}_r^T = [1 \quad 2 \quad 1]$, $\{\dot{x}_0\}_r = \{0\}$, $\{x_0\}_e^T = [-1.5 \quad 1.5 \quad -1.5]$, and $\{\dot{x}_0\}_e^T = [2 \quad -2 \quad 2]$.

Solution: Since no external load is applied and $\{\dot{x}_0\}_r = \{0\}$, the rigid-body response corresponding to $\{x'_0\}$ is the last term of Eq. (2.201). Therefore

$$\{x\}_r^T = ([X]_r \{x'_0\}_r)^T = \{x_0\}_r^T = [1 \quad 2 \quad 1] \quad (a)$$

Elastic displacement response may be obtained from Eq. (2.202) as

$$\{x\}_{e(in)} = [\bar{\lambda} \cos pt] \{x_0\}_e + [\bar{\lambda} \sin pt] [\bar{p}]^{-1} \{\dot{x}_0\}_e \quad (b)$$

Substituting the appropriate terms into the above yields

$$[x]_{e(in)} = \begin{Bmatrix} -1.5 cs + 2 \frac{sn}{p_3} \\ 1.5 cs - 2 \frac{sn}{p_3} \\ -1.5 cs + 2 \frac{sn}{p_3} \end{Bmatrix} \quad (c)$$

where $cs = \cos p_3 t$, $sn = \sin p_3 t$, and $p_3 = 131.45$ rad. The total response is the summation of Eqs. (a) and (c).

EXAMPLE 2.8.5 The structure in Fig. 2.18f serves to illustrate a structural model with repeating frequencies and the effect of those frequencies on the response. Using the notations in the figure, let $M_1 = M_2 = M_3 = 1$, $k_1 = 0.143306$, $k_2 = 0.3125$, $k_3 = 0.044794$, $k_4 = 0.099112$, and the forcing function be $\{F(t)\}^T = [4 - 20t \quad 5 - 25t \quad 6 - 30t]$, which is sketched in Fig. 2.22.

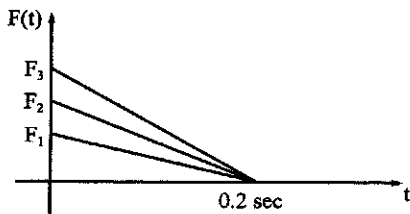


FIG. 2.22 Forcing function.

Solution: Based on the diagram in Fig. 2.18f, the mass and stiffness matrices are

$$[M] = \begin{bmatrix} M_1 & 0 & 0 \\ 0 & M_2 & 0 \\ 0 & 0 & M_3 \end{bmatrix}_{\text{symm}}, \quad [K] = \begin{bmatrix} k_1 + k_2 + k_3 & -k_2 & -k_3 \\ -k_2 & k_1 + k_2 + k_3 & -k_3 \\ -k_3 & -k_3 & 2k_3 + k_4 \end{bmatrix}_{\text{symm}} \quad (\text{a, b})$$

Substituting the given mass and stiffness coefficients and performing eigensolution procedures yields

$$p_1 = 0.35355; \quad p_2 = 0.5; \quad p_3 = 0.5 \quad (\text{c})$$

and

$$\{X\}_1^T = [0.707108 \quad 0.707108 \quad 1]; \quad \{X\}_2^T = [-1 \quad 1 \quad 0]; \quad \{X\}_3^T = [1 \quad 1 \quad -1.414214] \quad (\text{d})$$

Using Eqs. (2.49) and (2.50) gives the modal matrix as

$$[\Phi] = [\Phi_1 \quad \Phi_2 \quad \Phi_3] = \begin{bmatrix} 0.5 & -0.707107 & 0.5 \\ 0.5 & 0.707107 & 0.5 \\ 0.707107 & 0 & -0.707107 \end{bmatrix} \quad (\text{e})$$

From the given mass matrix and the above modal matrix, the following orthogonality conditions are satisfied

$$[\Phi]^T [M] [\Phi] = [I]; \quad [\Phi]^T [K] [\Phi] = [\lambda p^2] \quad (\text{f, g})$$

The element in Eq. (g) are associated with the frequencies already found in Eq. (c).

The displacement response without consideration of initial conditions is

$$\{x\} = [\Phi] \int_0^t [\lambda \sin p(t-\Delta)] [\lambda p]^{-1} [\Phi]^T \{F(\Delta)\} d\Delta \quad (\text{h})$$

Upon substitution, the displacements are

$$x_1 = a - b + c = \text{first mode} + \text{second mode} + \text{third mode} \quad (\text{i})$$

$$x_2 = a + b + c = \text{first mode} + \text{second mode} + \text{third mode} \quad (\text{j})$$

$$x_3 = d - e = \text{first mode} + 0 + \text{third mode} \quad (\text{k})$$

where

$$a = 0.5 \int_0^t \sin \sqrt{0.125} (t-\Delta) (24.7279 - 123.64\Delta) d\Delta \quad (\text{l})$$

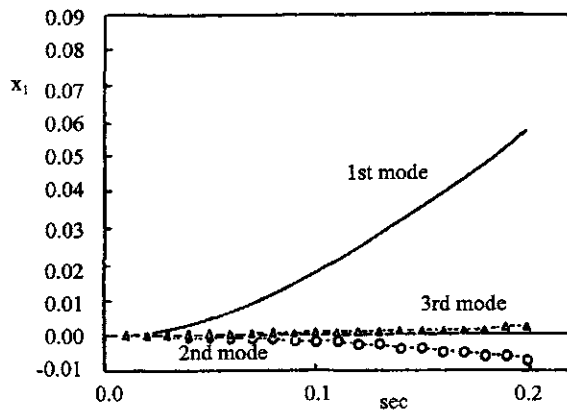


FIG. 2.23 Influence of modes on x_1 .

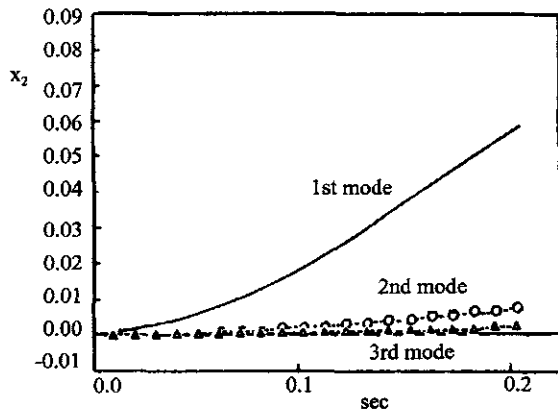


FIG. 2.24 Influence of modes on x_2 .

$$b = 0.707107 \int_0^t \sin 0.5(t-\Delta)(1.41421 - 7.07107\Delta) d\Delta \quad (m)$$

$$c = 0.5 \int_0^t \sin 0.5(t-\Delta)(0.514716 - 2.57358\Delta) d\Delta \quad (n)$$

$$d = 0.707107 \int_0^t \sin \sqrt{0.125}(t-\Delta)(24.7279 - 123.64\Delta) d\Delta \quad (o)$$

$$e = 0.707107 \int_0^t \sin 0.5(t-\Delta)(0.514716 - 2.57358\Delta) d\Delta \quad (p)$$

Integrating Eqs. (n)–(p), and then substituting the results into Eqs. (i), (j) and (k), yields the displacement response.

Influence of the individual modes on the response can be seen in Figs. 2.23–2.26, which are the results from Eqs. (i), (j) and (k), respectively. The first three figures show how much displacement

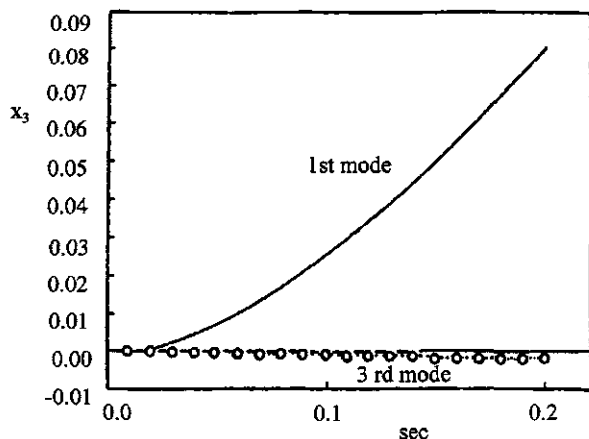


FIG. 2.25 Influence of modes on x_3 .

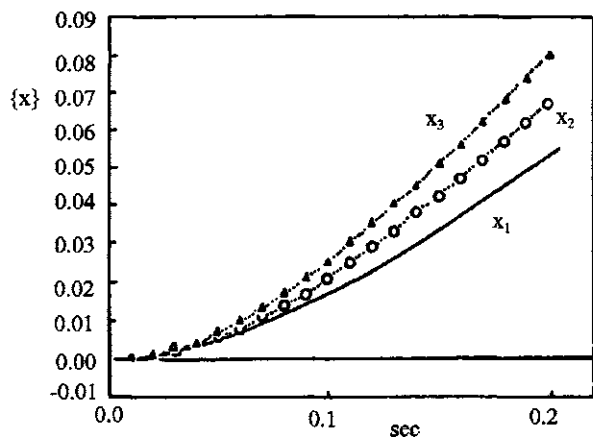


FIG. 2.26 Displacement of x_1 , x_2 , x_3 .

of x_1 , x_2 and x_3 is attributed to each of these modes. Clearly the first mode dominates all the displacements, and the second mode does not affect x_3 . Total displacements at each mass are shown in the last figure; they are obtained by combining the response of individual modes.

BIBLIOGRAPHY

1. KJ Bathe. Finite Element Procedures in Engineering Analysis. Englewood Cliffs, NJ: Prentice-Hall, 1982.
2. JM Biggs. Introduction to Structural Dynamics. New York: McGraw-Hill, 1964.
3. FY Cheng. Dynamics of frames with non-uniform elastic methods, ASCE J Struct Div 94(10):2411-2428, 1968.
4. FY Cheng, ed. Proceedings of International Symposium on Earthquake Structural Engineering (Vol I). Virginia US Department of Commerce, National Technical Information Service, NTIS no. PB290534, 1976 (658 pp).
5. FY Cheng, ed. Proceedings of International Symposium on Earthquake Structural Engineering (Vol II). Virginia: US Department of Commerce, National Technical Information Service, NTIS no. PB290535, 1976 (656 pp).

6. RR Craig Jr, CJ Chang. A review of substructure coupling methods for dynamic analysis. *Adv Engng Sci*, NASA CP-2001:393–408, 1976.
7. HH Goldstine, FJ Murray, J Von Neumann. The Jacobi method for real symmetric matrices. *J Assoc Comput Mach* 6:59–96, 1959.
8. KK Gupta. Solutions of eigenvalue problems by Sturm sequence method. *Int J Numer Meth Engng* 4:379–404, 1972.
9. RS Householder. *Principles of Numerical Analysis*. New York: McGraw-Hill, 1963.
10. CGJ Jacobi. Über ein leichtes Verfahren die in der Theorie der Säculärstörungen Vorkommenden Gleichungen numerisch aufzulösen. *Crelle's Journal* 30:51–94, 1846.
11. G Peters, JH Wilkinson. $Ax = \lambda Bx$ and the generalized eigenproblem. *SIAM J Numer Analy* 7:479–492, 1970.
12. VB Venkayya. Iterative Method for the Analysis of Large Structural Systems. Ohio: Wright-Patterson Air Force Base, Air Force Flight Dynamics Laboratory, Report AFFDL-TR-67-194, 1968.
13. JH Wilkinson. *The Algebraic Eigenvalue Problem*. Oxford: Clarendon Press, 1965.

3

Eigensolution Methods and Response Analysis for Proportional and Nonproportional Damping

PART A FUNDAMENTALS

3.1. INTRODUCTION

There are several kinds of damping, namely, *structural damping*, *coulumb damping*, *negative damping*, and *viscous damping*. Structural damping results from internal friction within the material or at connections of a structure. Coulumb damping is due to a body moving on a dry surface. Negative damping results from adding energy to a vibrating system instead of dissipating energy. Viscous damping results from a system vibrating in air or liquid of which examples are shock absorbers, hydraulic dashpots, and a body sliding on a lubricated surface. Viscous damping is commonly used in structural dynamics and is therefore presented in Chapter 1. The effect of damping on structural response is discussed in Sections 1.3 and 1.5. Four methods of evaluating damping coefficients are given in Sections 1.3.3, 1.6.1, and 1.6.2.

This chapter presents the methods of determining damping coefficients and response analysis of multiple-d.o.f. systems. The damping matrix can be symmetric or nonsymmetric, proportional or nonproportional. For nonproportional damping, the response analysis involves *complex eigensolutions*.

3.2. RESPONSE ANALYSIS FOR PROPORTIONAL DAMPING

3.2.1. Based on a Modal Matrix

A structural system of a discrete model is shown in Fig. 3.1, in which the resistance is due to the viscous damping in terms of $c\dot{x}$. c is the underdamping coefficient. The motion equations may be established by using the free-body diagrams as

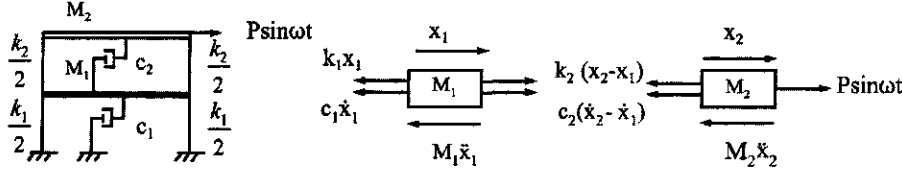


FIG. 3.1 Structural model for viscous damping.

$$M_1 \ddot{x}_1 + k_1 x_1 + c_1 \dot{x}_1 - k_2 x_2 + k_2 x_1 - c_2 \dot{x}_2 + c_2 \dot{x}_1 = 0 \quad (3.1)$$

$$M_2 \ddot{x}_2 + k_2 x_2 - k_2 x_1 + c_2 \dot{x}_2 - c_2 \dot{x}_1 = F(t) \quad (3.2)$$

in matrix notation

$$[M] \{ \ddot{x} \} + [C] \{ \dot{x} \} + [K] \{ x \} = \{ F(t) \} \quad (3.3)$$

where $[M]$, $[K]$, and $\{F(t)\}$ are established in a similar manner as shown in Chapter 2; the damping matrix is

$$[C] = \begin{bmatrix} c_1 + c_2 & -c_2 \\ -c_2 & c_2 \end{bmatrix} \quad (3.4)$$

By using the modal matrix $[\Phi]$ or normal mode matrix $[X]$ with the orthogonality conditions given in Sections 2.5.2 and 2.5.3, Eq. (3.3) may be decoupled as

$$\{ \ddot{x}' \} + [\Phi]^T [C] [\Phi] \{ \dot{x}' \} + \left[\begin{smallmatrix} p^2 \\ 0 \end{smallmatrix} \right] \{ x' \} = [\Phi]^T \{ F(t) \} \quad (3.5)$$

where $\{x\}$ is generalized response vector used in Eq. (2.41). Equation (3.5) may also be expressed as

$$\left[\begin{smallmatrix} \bar{M}_1 & 0 \\ 0 & \bar{M}_2 \end{smallmatrix} \right] \{ \ddot{x}' \} + [X]^T [C] [X] \{ \dot{x}' \} + \left[\begin{smallmatrix} p^2 \\ 0 \end{smallmatrix} \right] \{ x' \} = [X]^T \{ F(t) \} \quad (3.6)$$

Take the i th mode from Eq. (3.5),

$$\ddot{x}'_i + \{\Phi\}_i^T [C] \{\Phi\}_i \{ \dot{x}' \} + p_i^2 x'_i = \{\Phi\}_i^T \{ F(t) \} \quad (3.7)$$

or from Eq. (3.6),

$$\ddot{x}'_i + \{X\}_i^T [C] \{X\}_i \frac{1}{\bar{M}_i} \dot{x}'_i + p_i^2 x'_i = \frac{1}{\bar{M}_i} \{X\}_i^T \{ F(t) \} \quad (3.8)$$

Comparing Eq. (3.7) or (3.8) with Eq. (1.99), $\ddot{x} + 2\rho p \dot{x} + p^2 x = p^2 x_{st} \sin \omega t$, of a single-d.o.f. system, leads to

$$\{\Phi\}_i^T [C] \{\Phi\}_j = 2\rho_i p_i \delta_{ij} \quad (3.9)$$

or

$$\{X\}_i^T [C] \{X\}_j = 2\rho_i p_i \bar{M}_i \delta_{ij} \quad (3.10)$$

where δ_{ij} is the *Kronecker delta*

$$\delta_{ij} = \begin{cases} 1 & i=j \\ 0, & i \neq j \end{cases} \quad (3.11)$$

Thus Eq. (3.7) becomes

$$\ddot{x}'_i + 2\rho_i p_i \dot{x}'_i + p_i^2 x'_i = \{\Phi\}_i^T \{F(t)\} \quad (3.12)$$

Similarly for Eq. (3.8),

$$\ddot{x}'_i + 2\rho_i p_i \dot{x}'_i + p_i^2 x'_i = \frac{1}{M_i} \{X\}_i^T \{F(t)\} \quad (3.13)$$

For studying the characteristics of free vibration with proportional damping, drop $\{F(t)\}$ and consider the response due to initial conditions at $t = 0$. For instance, applying the similar procedures of Eqs. (1.41)–(1.45) to Eq. (3.12) for $\dot{x}'_i(0) = 0$, $x'_i(0) \neq 0$ yields modal displacement $x'_i(t)$ and velocity $\dot{x}'_i(t)$ at any time t as follows:

$$x'_i(t) = \frac{x'_i(0) e^{-\rho_i p_i t}}{\sqrt{1 - \rho_i^2}} \cos(\sqrt{1 - \rho_i^2} p_i t - \alpha_i) = A_{md} \cos(\sqrt{1 - \rho_i^2} p_i t - \alpha_i) \quad (3.13a)$$

$$\dot{x}'_i(t) = \frac{x'_i(0) p_i e^{-\rho_i p_i t}}{\sqrt{1 - \rho_i^2}} \cos\left(\sqrt{1 - \rho_i^2} p_i t + \frac{\pi}{2}\right) = A_{vd} \cos\left(\sqrt{1 - \rho_i^2} p_i t + \frac{\pi}{2}\right) \quad (3.13b)$$

which is condensed by employing $\sin \alpha_i = \rho_i$ and $\cos \alpha_i = \sqrt{(1 - \rho_i^2)}$; α_i is *phase angle* expressed as

$$\alpha_i = \tan^{-1} \frac{\rho_i}{\sqrt{1 - \rho_i^2}} \quad (3.13c)$$

In Eqs. (3.13a) and (3.13b) the damping effect on frequency is included.

The relationship between $x'_i(t)$ and $\dot{x}'_i(t)$ may be shown in Fig. 3.2. From the figure it can be seen that the velocity vector leads the displacement vector by an angle $(\pi/2) + \alpha_i$. Since the modal matrix, $[\Phi]$ (or $[X]$), is not a function of time as shown in Eq. (2.32), the displacement component of the i th mode, $\{x\}_i = \{\Phi\}_i x'_i(t)$, and the associated velocity also have the relationship $(\pi/2) + \alpha_i$.

The complete solution procedure of Eqs. (3.12) and (3.13) is identical to that used for a single-d.o.f. system, and the final results are

$$x'_i = e^{-\rho_i p_i t} (A \cos p_i t + B \sin p_i t) + \frac{\{\Phi\}_i^T}{p_i} \int_0^t e^{-\rho_i p_i (t-\Delta)} \{F(t)\} \sin p_i (t-\Delta) d\Delta \quad (3.14)$$

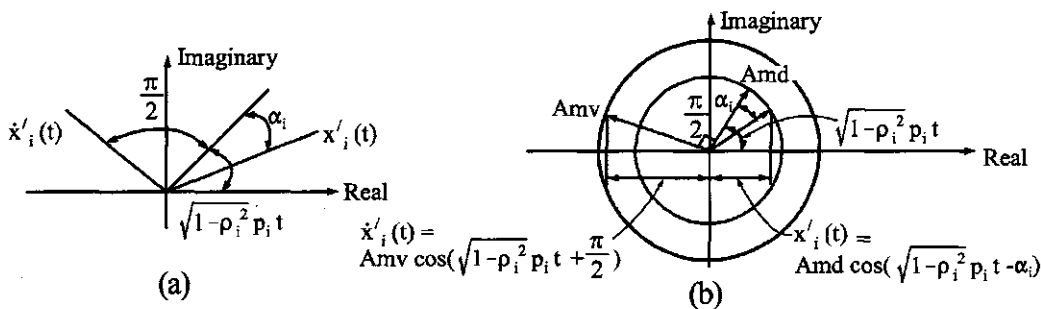


FIG. 3.2 Phase angle.

or

$$x'_i = e^{-\rho_i p_i t} (A \cos p_i t + B \sin p_i t) + \frac{\{X\}_i^T}{\bar{M}_i p_i} \int_0^t e^{-\rho_i p_i (t-\Delta)} (F(t)) \sin p_i (t-\Delta) d\Delta \quad (3.15)$$

Note that $[\Phi] = [X]/[\bar{M}^{1/2}]$. Eqs. (3.14) and (3.15) are based on modal matrix and normal mode, respectively. As discussed in Eq. (1.121b), for practical purposes, the damping effect on frequency p and on damping factor ρ is neglected in the above two equations; i.e. $p^* = \sqrt{(1 - \rho^2)p} = p$ and $\rho^* = \rho/\sqrt{(1 - \rho^2)} = \rho$. The procedure for finding the solution in the original coordinate $\{x\}$ should be identical to Eqs. (2.47)–(2.53).

3.2.2. Proportional Damping

Observing Eq. (3.9) or (3.10) reveals that the total damping of a structure is the sum of individual damping in each mode. Therefore one can use the methods presented in Chapter 1 to determine damping coefficients by measuring the decayed amplitude of mode shapes, such as logarithmic decrement technique, and then find the total damping.

From Eq. (1.31), $\rho = c/(2Mp) = c/[2\sqrt{(KM)}] = cp/(2K)$, it is apparent that damping factor, ρ , can be expressed in terms of mass, stiffness, or a combination of both. For a general expression, let

$$[C] = \alpha[M] + \beta[K] \quad (3.16)$$

which is substituted in Eq. (3.9) or (3.10) with consideration of orthogonality condition; then

$$\alpha + \beta p_i^2 = 2\rho_i p_i \quad (3.17)$$

Thus the damping factor can be determined for a given set of α and β as

$$\rho_i = \frac{\alpha}{2p_i} + \frac{\beta p_i}{2} \quad (3.18)$$

Examining α and β reveals the physical sense of ρ . If $\alpha = 0$, then

$$\rho_i = \frac{\beta p_i}{2} \quad (3.19)$$

which means that ρ_i is proportional to p_i . For higher modes of larger p_i , ρ_i will be larger; then the higher modes of a system will be damped faster than the lower modes. Since $[C] = \beta[K]$, the damping is proportional to stiffness and is called *relative damping* because it is associated with relative velocities of displacement coordinates.

Let $\beta = 0$; then

$$\rho_i = \frac{\alpha}{2p_i} \quad (3.20)$$

which means that ρ_i is inversely proportional to p_i . Therefore lower modes will be damped out more quickly than higher modes. Since $[C] = \alpha[M]$, which is associated with absolute velocity of displacement coordinates, the damping is called *absolute damping*. Damping expressed in Eq. (3.16) is called *proportional damping*.

EXAMPLE 3.2.1 For the structure given in Fig. 3.1, let $k_1 = k_2 = k = 1$, $M_1 = M_2 = M = 1$, $\alpha = 0.1$, and $\beta = 0.1$; find the damping matrix $[C]$ and then check the Kronecker delta.

Solution: The mass and stiffness matrices may be established

$$[M] = \begin{bmatrix} M & 0 \\ 0 & M \end{bmatrix}, \quad \text{and} \quad [K] = \begin{bmatrix} 2k & -k \\ -k & k \end{bmatrix} \quad (\text{a, b})$$

Substituting Eqs. (a) and (b) with the given values into Eq. (3.16) yields

$$[C] = 0.1 \begin{bmatrix} 1 & 0 \\ 0 & 1 \end{bmatrix} + 0.1 \begin{bmatrix} 2 & -1 \\ -1 & 1 \end{bmatrix} = \begin{bmatrix} 0.3 & -0.1 \\ -0.1 & 0.2 \end{bmatrix} \quad (\text{c})$$

Using the eigenvector, $\{X\}$, of the structure already obtained in Section 2.2.1, Eq. (3.10) may be expressed as

$$[X]^T [C] [X] = \begin{bmatrix} 0.61803 & 1 \\ 1 & -0.61804 \end{bmatrix} \begin{bmatrix} 0.3 & -0.1 \\ -0.1 & 0.2 \end{bmatrix} \begin{bmatrix} 0.61803 & 1 \\ 1 & -0.61804 \end{bmatrix} = \begin{bmatrix} 0.19098 & 0 \\ 0 & 0.50 \end{bmatrix} \quad (\text{d})$$

which satisfies the Kronecker delta.

3.3. EVALUATION OF DAMPING COEFFICIENTS AND FACTORS

3.3.1. Two Modes Required

From Eq. (3.18), $\rho_i = \alpha/(2p_i) + \beta p_i/2$; if ρ and p of any two modes of a vibrating system are known, say p_1, p_2 and ρ_1, ρ_2 , then α and β can be expressed as

$$\alpha = 2p_1 p_2 \frac{\rho_1 p_2 - \rho_2 p_1}{p_2^2 - p_1^2} \quad (3.21a)$$

$$\beta = \frac{2(\rho_2 p_2 - \rho_1 p_1)}{p_2^2 - p_1^2} \quad (3.21b)$$

Consequently, damping factors of other modes can also be determined by knowing the associated frequencies. Using α and β as calculated allows determination of the damping coefficients as $[C] = \alpha[M] + \beta[K]$.

EXAMPLE 3.3.1 For the shear building shown in Fig. 3.3, $M_1 = M_2 = M_3 = 1 \text{ k sec}^2/\text{in}$, $k = 1 \text{ k/in}$ and the frequencies are found as $p_1 = 0.44504$, $p_2 = 1.24698$, and $p_3 = 1.80194$. Experimental work yields the damping factors of the first two modes as $\rho_1 = 0.01063$ and $\rho_2 = 0.015$. Find ρ_3 and $[C]$.

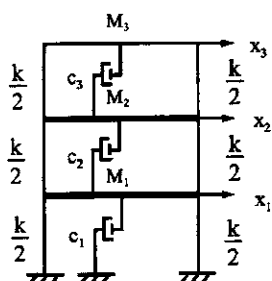


FIG. 3.3 Example 3.3.1

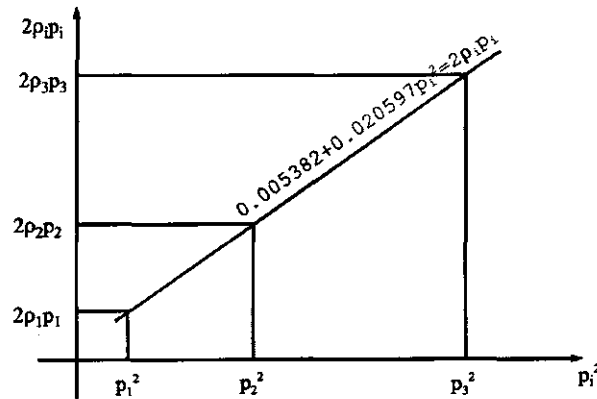


FIG. 3.4 Linear relationship of p_i^2 and $\rho_i p_i$.

Solution: Applying the given ρ and p of the first two modes to Eq. (3.21a,b) yields the following two equations:

$$\alpha = 2(0.44504)(1.24698) \frac{(0.01063)(1.24698) - (0.015)(0.44504)}{(1.24698)^2 - (0.44504)^2} = 0.005382 \quad (a)$$

$$\beta = \frac{2[(0.015)(1.24698) - (0.01063)(0.44504)]}{(1.24698)^2 - (0.44504)^2} = 0.020597 \quad (b)$$

Substituting α , β and p_3 into Eq. (3.18) yields

$$\rho_3 = \frac{0.005382}{(2)(1.80194)} + \frac{0.020597(1.80194)}{2} = 0.02005 \quad (c)$$

From Eq. (3.16) the damping matrix is calculated as

$$\begin{aligned} [C] &= 0.005382 \begin{bmatrix} 1 & 0 & 0 \\ 0 & 1 & 0 \\ 0 & 0 & 1 \end{bmatrix} + 0.020597 \begin{bmatrix} 2 & -1 & 0 \\ -1 & 2 & -1 \\ 0 & -1 & 1 \end{bmatrix} \\ &= \begin{bmatrix} 0.046576 & -0.020597 & 0 \\ 0.046576 & -0.020597 & 0 \\ \text{symm} & 0.025979 & \end{bmatrix} \end{aligned} \quad (d)$$

For proportional damping, $\rho_i p_i$ and p_i^2 always satisfy the linear relationship in Eq. (3.17) ($\alpha + \beta p_i^2 = 2 \rho_i p_i$). This example is, in fact, a case of proportional damping; the linear relationship is shown in Fig. 3.4.

Note that the experimental damping factors of several modes may not always satisfy Eq. (3.17). However, a curve-fitting technique can be used to find an approximate linear equation as shown in Fig. 3.5 from which \bar{p}_1^2 and \bar{p}_2^2 may be arbitrarily chosen and their corresponding $2\bar{\rho}_1\bar{p}_1$ and $2\bar{\rho}_2\bar{p}_2$ can then be established. By substituting these two pairs in Eq. (3.21a,b), α and β can be found.

When experimental data are not available, use the following steps to find α and β : (1) determine fundamental frequency and the associated damping factor; (2) assume a ratio of higher frequency to fundamental frequency and then find the associated damping factor; and (3) use the solutions obtained in steps 1 and 2 to find α and β .

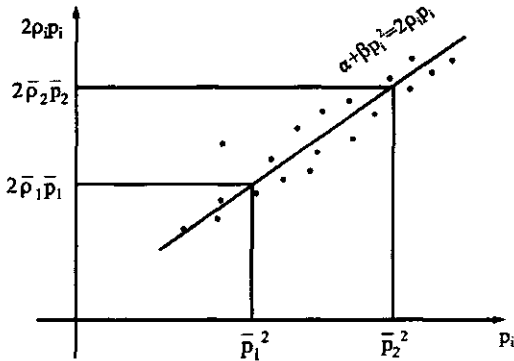


FIG. 3.5 Curve-fitting for linear relationship between p_i^2 and $2\rho_i \rho_i$.

Observe step 2. The optimum damping factor may be obtained by minimizing Eq. (3.18) as

$$\frac{d\rho_i}{dp_i} = -\frac{\alpha}{2p_i^2} + \frac{\beta}{2} = 0; \quad \frac{d^2\rho_i}{dp_i^2} = \frac{\alpha}{p_i^3} > 0$$

from which the associated frequency, $\bar{p} = p_i$, is

$$\bar{p} = \left(\frac{\alpha}{\beta}\right)^{1/2}$$

Substituting the above into Eq. (3.18) gives

$$\alpha = \bar{p} \bar{\rho}, \quad \beta = \bar{\rho}/\bar{p}$$

For a single-d.o.f. system, $\bar{p} = p = \sqrt{k/M}$ and $\bar{\rho} = \rho$; we then have $C = \alpha M + \beta k = \bar{p} \bar{\rho} M + \bar{\rho}/\bar{p} k = 2\bar{\rho} M p$.

Employing α and β in Eq. (3.18) yields the desired damping factor as

$$\rho_1 = \left(\frac{\bar{p}}{p_i} + \frac{p_i}{\bar{p}}\right) \frac{\bar{\rho}}{2} \quad (3.22a)$$

or

$$\rho_i = \left(\frac{T_i}{\bar{T}} + \frac{\bar{T}}{T_i}\right) \frac{\bar{\rho}}{2} \quad (3.22b)$$

The relationship between ρ_i and T_i/\bar{T} is shown in Fig. 3.6 for various $\bar{\rho}$'s, which indicates that buildings with smaller natural period may have damping factors two or three times higher than buildings with similar construction but larger natural period.

In Eq. (3.22a) \bar{p} may be taken as the lowest frequency of a structure. This value can be determined either by using the lower bound of response spectrum in the building codes (i.e. Uniform Building Code and International Building Code), such as $\bar{p} = 0.333(2\pi)$ rad/sec or $\bar{T} = 3$ sec, or by using the fundamental period equation recommended in the codes. The damping factor, $\bar{\rho}$, may be based on available data associated with building types given in Table 3.1. Both \bar{p} and $\bar{\rho}$ are taken as p_1 and ρ_1 , as indicated in step 1. By assuming \bar{p}/p_i (or T_i/\bar{T}), ρ_i can be derived from Eq. (3.22a); the value of \bar{p}/p_i gives the corresponding p_i as described in step 2. ρ_i and p_i are taken as ρ_2 and p_2 , which are substituted, along with ρ_1 and p_1 , in Eq. (3.21) for α and β to complete step 3.

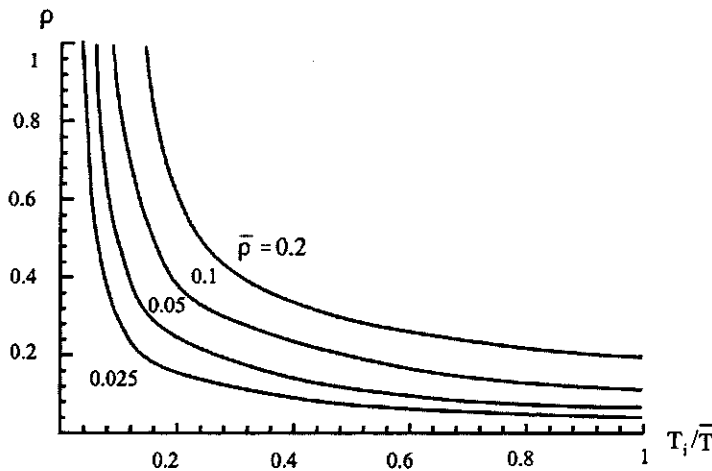


FIG. 3.6 T_i/\bar{T} vs ρ for various $\bar{\rho}$'s.

TABLE 3.1 Optimum Damping Factors

Building types	$\bar{\rho}$
Steel frame — welded connections and flexible walls	0.02
Steel frame — welded connections, normal floors and exterior cladding	0.05
Steel frame — bolted connections, normal floors and exterior cladding	0.10
Concrete frame — flexible internal walls	0.05
Concrete frame — flexible internal walls and exterior cladding	0.07
Concrete frame — concrete or masonry shear walls	0.10

EXAMPLE 3.3.2 Find α and β of a steel frame with welded connections, normal floors, and exterior cladding by using the upper-bound period of 3 sec shown in the UBC's response spectrum (see Fig. 7.31).

Solution: For the given problem, one may use

$$\bar{\rho} = 0.05, \quad \rho_1 = \bar{\rho}, \quad p_1 = \bar{p} = 0.333 (2\pi) \text{ rad/sec} \quad (\text{a})$$

Since the higher frequency is not given, we may assume a value of \bar{p}/p_i , say 0.5. Eq. (3.22a) and the assumed ratio give

$$\rho_i = \rho_2 = (0.5 + 2)(0.05)/2 = 0.0625 \quad (\text{b})$$

$$p_i = p_2 = 0.333 (2\pi)/0.5 = 0.6666 (2\pi) \quad (\text{c})$$

Substituting p_1 , ρ_1 , p_2 and ρ_2 into Eqs. (3.21a) and (3.21b) yields

$$\alpha = 2(0.3333)(0.6666) \frac{0.05(0.6666) - 0.0625(0.3333)}{(0.6666)^2 - (0.3333)^2} (2\pi) = 0.105 \quad (\text{d})$$

$$\beta = \frac{2[0.0625(0.6666) - 0.05(0.3333)]}{[(0.6666)^2 - (0.3333)^2]2\pi} = 0.024 \quad (\text{e})$$

3.3.2. All Modes Required

In Eq. (2.64), $[\bar{M}] = [X]^T [M] [X]$, from which

$$[\bar{M}]^{-1} [\bar{M}] = [\bar{M}]^{-1} [X]^T [M] [X] = ([X]^T [M] [X])^{-1} ([X]^T [M] [X]) = [X]^{-1} [X]$$

or

$$[X]^{-1} = [\bar{M}]^{-1} [X]^T [M]$$

Since

$$[\bar{C}] = [X]^T [C] [X] = [2\rho p \bar{M}] \quad (3.23)$$

then

$$[C] = ([X]^T)^{-1} [\bar{C}] [X]^{-1} = [M] [X] [2\rho p / \bar{M}] [X]^T [M] \quad (3.24)$$

Therefore damping coefficients can be found from either Eq. (3.24) or (3.25) using all the n modes of a system

$$[C] = \sum_{i=1}^n \left(\frac{2\rho_i p_i}{\bar{M}_i} \right) ([M] [X]_i) ([M] [X]_i)^T \quad (3.25)$$

3.3.3. Damping Factors from Damping Coefficients

Knowing the damping coefficients allows the calculation of the damping factors. The derivation may begin from a general motion equation, such as Eq. (3.23). For a free vibration, the equation at the r th row is

$$M_r \ddot{x}_r + \sum_{i=1}^n C_{ri} \dot{x}_i + \sum_{i=1}^n k_{ri} x_i = 0 \quad (3.26)$$

where $i = 1, 2, \dots, n$ (no. of d.o.f.), $r = 1, 2, \dots, n$ (no. of equations), and C_{ri} is the damping coefficient associated with the i th velocity in the r th equation. Observing Eqs. (2.12) and (2.13) yields the following relationship for any u th mode:

$$\frac{x_{iu}}{x_{ru}} = \frac{X^{(u)} a_i^{(u)}}{X^{(u)} a_r^{(u)}} \quad (3.27)$$

from which

$$x_{iu} = x_{ru} \left(\frac{a_i^{(u)}}{a_r^{(u)}} \right) \quad \text{and} \quad \dot{x}_{iu} = \dot{x}_{ru} \left(\frac{a_i^{(u)}}{a_r^{(u)}} \right) \quad (3.28)$$

Note that $a_i^{(u)}$ and $a_r^{(u)}$ are the u th normal modes which are typically signified by X_{iu} and X_{ru} , respectively. Upon substitution of Eq. (3.28) into Eq. (3.26),

$$M_r \ddot{x}_{ru} + \left(\sum_{i=1}^n C_{ri} \frac{X_{iu}}{X_{ru}} \right) \dot{x}_{ru} + \left(\sum_{i=1}^n k_{ri} \frac{X_{iu}}{X_{ru}} \right) x_{ru} = 0 \quad (3.29)$$

Analogous to a single d.o.f. system (Eq. 1.99), damping factors can be expressed as

$$\sum_{i=1}^n C_{ri} \frac{X_{iu}}{X_{ru}} = 2\rho_{ru} p_u M_r \quad (3.30)$$

EXAMPLE 3.3.3 For a two-d.o.f. vibrating system, the frequencies are $p_1 = 0.61803$ and $p_2 = 1.61802$; the first and second normal modes are $\{X\}_1 = [0.61803 \ 1]^T$ and $\{X\}_2 = [1 \ -0.61804]^T$; and the mass coefficients are M_1 (i.e. $M_{11} = 1$, M_2 (i.e. $M_{22} = 1$, $M_{12} = M_{21} = 0$). Find the damping factors from the damping coefficients given as

$$(a) \quad [C] = \begin{bmatrix} 0.3 & -0.1 \\ -0.1 & 0.2 \end{bmatrix} \quad \text{and} \quad (b) \quad [C] = \begin{bmatrix} 0.4 & 0.1 \\ 0.1 & 0.3 \end{bmatrix}$$

Solution: (a) Substituting the given data into Eq. (3.30) yields the following four equations

$$u = 1, \ r = 1, \quad 0.3 \left(\frac{0.61803}{0.61803} \right) - 0.1 \left(\frac{1}{0.61803} \right) = 2\rho_{11}(0.61803) \quad (1) \quad (a)$$

$$u = 1, \ r = 2, \quad -0.1 \left(\frac{0.61803}{1} \right) + 0.2 \left(\frac{1}{1} \right) = 2\rho_{21}(0.61803) \quad (1) \quad (b)$$

$$u = 2, \ r = 1, \quad 0.3 \left(\frac{1}{1} \right) - 0.1 \left(\frac{-0.61804}{1} \right) = 2\rho_{12}(1.61802) \quad (1) \quad (c)$$

$$u = 2, \ r = 2, \quad -0.1 \left(\frac{1}{-0.61804} \right) + 0.2 \left(\frac{-0.61804}{-0.61804} \right) = 2\rho_{22}(1.61802) \quad (1) \quad (d)$$

The solution for the above is

$$\rho_{11} = \rho_{21} = 0.1118 \quad \text{and} \quad \rho_{12} = \rho_{22} = 0.1118 \quad (e)$$

(b) Using the other set of damping coefficients yields

$$0.4 \left(\frac{0.61803}{0.61803} \right) + 0.1 \left(\frac{1}{0.61803} \right) = 2\rho_{11}(0.61803) \quad (1) \quad (f)$$

$$0.1 \left(\frac{0.61803}{1} \right) + 0.3 \left(\frac{1}{1} \right) = 2\rho_{21}(0.61803) \quad (1) \quad (g)$$

$$0.4 \left(\frac{1}{1} \right) + 0.1 \left(\frac{-0.61804}{1} \right) = 2\rho_{12}(1.61802) \quad (1) \quad (h)$$

$$0.1 \left(\frac{1}{-0.61804} \right) + 0.3 \left(\frac{-0.61804}{-0.61804} \right) = 2\rho_{22}(1.61802) \quad (1) \quad (i)$$

From Eqs. (f)–(i)

$$\rho_{11} = 0.4545; \quad \rho_{21} = 0.2927; \quad \rho_{12} = 0.1045; \quad \rho_{22} = 0.0427 \quad (j)$$

where ρ_{ij} represents the damping factor at the i th d.o.f. of the j th mode. Case (a) has the same damping factor for both modes, but Case (b) has different factors at each d.o.f. of individual mode.

3.4. DETERMINATION OF PROPORTIONAL AND NONPROPORTIONAL DAMPING

As discussed in Section 3.1, viscous damping can be classified as proportional or nonproportional damping. The response analysis technique for the former was discussed in the previous two sections; the analysis technique for the latter will be introduced in the next two sections. Here it is explained how to identify a damping matrix by whether it is proportional or not.

This identification poses a difficult problem and deserves further study. Quite often, we simply use Eq. (3.9) or (3.10) and let the Kronecker delta be satisfied. Thus the damping is treated as proportional in response analysis. In fact, proportional damping has to strictly satisfy Eq. (3.16) ($[C] = \alpha[M] + \beta[K]$); α and β determined from Eq. (3.18) must exhibit a linear relationship between ρ and p for all modes; and $[\bar{C}] = [X]^T[C][X]$ naturally becomes diagonal as a result of Eq. (3.16). One must note that $[\bar{C}]$ can be diagonal, but $[C]$ may still be nonproportional because

Eq. (3.18) is not satisfied for all modes. Physically, nonproportional damping can be due to different damping factors assigned to different d.o.f. of a system. For instance, engineers may use different construction materials at various floors of a building, employ a concentrated damper (such as a control system) at a certain structural level, or assign larger damping coefficients for the foundation than for the superstructure when foundation–structure interaction is encountered. A few examples are briefly presented to illustrate the characteristics of nonproportional damping.

EXAMPLE 3.4.1 For the structure in Example 3.3.1, the eigenvalues and eigenvectors are

$$\{p\} = \begin{Bmatrix} 0.44504 \\ 1.24698 \\ 1.80194 \end{Bmatrix}; \quad [X] = \begin{bmatrix} 0.445042 & 1.0 & 0.801938 \\ 0.801938 & 0.445042 & -1.0 \\ 1.0 & -0.801938 & 0.445042 \end{bmatrix}$$

and the damping factors are given as

$$\begin{aligned} \rho_{11} &= \rho_{21} = \rho_{31} = 0.251056 \\ \rho_{12} &= \rho_{22} = \rho_{32} = 0.409517 \\ \rho_{13} &= \rho_{23} = \rho_{33} = 0.559458 \end{aligned}$$

Find the damping coefficients and show the orthogonality condition.

Solution: Substituting the given data into Eq. (3.30) yields the following for $r = 1, u = 1, 2$, and 3:

$$\begin{bmatrix} X_{11}/X_{11} & X_{21}/X_{11} & X_{31}/X_{11} \\ X_{12}/X_{12} & X_{22}/X_{12} & X_{32}/X_{12} \\ X_{13}/X_{13} & X_{23}/X_{13} & X_{33}/X_{13} \end{bmatrix} \begin{Bmatrix} C_{11} \\ C_{12} \\ C_{13} \end{Bmatrix} = \begin{Bmatrix} 2\rho_{11}p_1M_1 \\ 2\rho_{12}p_2M_2 \\ 2\rho_{13}p_3M_3 \end{Bmatrix} \quad (a)$$

for $r = 2, u = 1, 2$, and 3

$$\begin{bmatrix} X_{11}/X_{21} & X_{21}/X_{21} & X_{31}/X_{21} \\ X_{12}/X_{22} & X_{22}/X_{22} & X_{32}/X_{22} \\ X_{13}/X_{23} & X_{23}/X_{23} & X_{33}/X_{23} \end{bmatrix} \begin{Bmatrix} C_{21} \\ C_{22} \\ C_{23} \end{Bmatrix} = \begin{Bmatrix} 2\rho_{21}p_1M_1 \\ 2\rho_{22}p_2M_2 \\ 2\rho_{23}p_3M_3 \end{Bmatrix} \quad (b)$$

for $r = 3, u = 1, 2$, and 3

$$\begin{bmatrix} X_{11}/X_{31} & X_{21}/X_{31} & X_{31}/X_{31} \\ X_{12}/X_{32} & X_{22}/X_{32} & X_{32}/X_{32} \\ X_{13}/X_{33} & X_{23}/X_{33} & X_{33}/X_{33} \end{bmatrix} \begin{Bmatrix} C_{31} \\ C_{32} \\ C_{33} \end{Bmatrix} = \begin{Bmatrix} 2\rho_{31}p_1M_1 \\ 2\rho_{32}p_2M_2 \\ 2\rho_{33}p_3M_3 \end{Bmatrix} \quad (c)$$

Substituting the given information into Eqs. (a)–(c) yields

$$[C] = \begin{bmatrix} 1.283 & -0.588 & 0 \\ -0.588 & 1.283 & -0.588 \\ 0 & -0.588 & 0.695 \end{bmatrix} \quad (d)$$

The orthogonality condition becomes

$$[X]^T[C][X] = \begin{bmatrix} 0.41143 & 0 & 0 \\ 0 & 1.88040 & 0 \\ 0 & 0 & 3.71220 \end{bmatrix} = 2 \begin{bmatrix} \rho_1 p_1 \bar{M}_1 & & \\ & \rho_2 p_2 \bar{M}_2 & \\ & & \rho_3 p_3 \bar{M}_3 \end{bmatrix} \quad (e)$$

in which

$$[\bar{M}] = [X]^T[M][X] = \begin{bmatrix} 1.84117 & 0 & 0 \\ 0 & 1.84117 & 0 \\ \text{symm} & & 1.84117 \end{bmatrix} \quad (f)$$

Substituting p_i already given and \bar{M}_i obtained above into Eq. (e) yields

$$\rho_1 = 0.25106, \quad \rho_2 = 0.40952, \quad \rho_3 = 0.55946 \quad (g)$$

Employing p_1, p_2, ρ_1, ρ_2 in Eqs. (3.21a) and (3.21b) leads to

$$\alpha = 0.107, \quad \beta = 0.588 \quad (h)$$

If $[C]$ is proportional damping, then p_3 and ρ_3 should satisfy Eq. (3.17) as

$$\alpha + \beta p_3^2 - 2p_3\rho_3 = 0.107 + 0.588(1.80194)^2 - 2(1.80194)(0.55946) = 0 \quad (i)$$

Therefore it can be concluded that $[C]$ is proportional damping.

EXAMPLE 3.4.2 For Example 3.4.1, let the damping factors differ as

$$\rho_{11} = \rho_{21} = \rho_{31} = 0.08460$$

$$\rho_{12} = \rho_{22} = \rho_{32} = 0.15245$$

$$\rho_{13} = \rho_{23} = \rho_{33} = 0.06784$$

Find the damping matrix and then show whether the damping is proportional or not.

Solution: Following the procedures presented in the previous example, one can obtain the following damping matrix and its orthogonality condition matrix in Eqs. (a) and (b), respectively.

$$[C] = \begin{bmatrix} 0.3 & 0.0 & -0.1 \\ 0.0 & 0.2 & -0.1 \\ -0.1 & -0.1 & 0.2 \end{bmatrix} \quad (a)$$

$$[\bar{C}] = [X]^T [C] [X] = \begin{bmatrix} 0.13864 & 0.0 & 0.0 \\ 0.0 & 0.70 & 0.0 \\ \text{symm} & & 0.45017 \end{bmatrix} \quad (b)$$

Although $[\bar{C}]$ is diagonal, $[C]$ may be either proportional or nonproportional damping. If $[C]$ is proportional, it should satisfy $[C] = \alpha[M] + \beta[K]$ which, after substitution of the given data, becomes

$$\begin{bmatrix} 0.3 & 0.0 & -0.1 \\ 0.0 & 0.2 & -0.1 \\ -0.1 & -0.1 & 0.2 \end{bmatrix} \stackrel{?}{=} \alpha \begin{bmatrix} 1 & 0 & 0 \\ 0 & 1 & 0 \\ 0 & 0 & 1 \end{bmatrix} + \beta \begin{bmatrix} 2 & -1 & 0 \\ -1 & 2 & -1 \\ 0 & -1 & 1 \end{bmatrix} \quad (c)$$

Since $C_{21} = C_{12} = 0, k_{12} = k_{21} = -1 \neq 0, C_{31} = C_{13} = -1, M_{13} = M_{31} = 0$, and $k_{13} = k_{31} = 0$, a pair of values cannot be found for α and β to satisfy $[C]$. It is concluded that $[C]$ is nonproportional damping.

PART B ADVANCED TOPICS

3.5. CHARACTERISTICS OF COMPLEX EIGENVALUES FOR NONPROPORTIONAL DAMPING

For convenience, rewrite the general motion equation of Eq. (3.3) as

$$[M]\{\ddot{x}\} + [C]\{\dot{x}\} + [K]\{x\} = \{F(t)\} \quad (3.31)$$

If $[C]$ is nonproportional damping, then each component of eigenvector $\{X\}$ is distinguished not only by amplitude but also by phase angle (for which the behavior is introduced in Section 3.8). Therefore $2n$ equations are required to determine all components of an n -d.o.f. system in each

mode. One additional equation needed to couple with Eq. (3.31) to solve the components is

$$[M]\{\ddot{x}\} - [M]\{\dot{x}\} = 0 \quad (3.32)$$

Combining the above two equations yields

$$\begin{bmatrix} [0] | [M] \\ \cdots \\ [M] | [C] \end{bmatrix} \begin{Bmatrix} \{\ddot{x}\} \\ \cdots \\ \{\dot{x}\} \end{Bmatrix} = \begin{bmatrix} -[M] | [0] \\ \cdots \\ [0] | [K] \end{bmatrix} \begin{Bmatrix} \dot{x} \\ \cdots \\ x \end{Bmatrix} = \begin{Bmatrix} 0 \\ \cdots \\ \{F(t)\} \end{Bmatrix} \quad (3.33)$$

or in symbolic form

$$[A]\{\dot{z}\} + [B]\{z\} = \{R\} \quad (3.34)$$

where

$$\{z\} = \begin{Bmatrix} \{\dot{x}\} \\ \cdots \\ \{x\} \end{Bmatrix}; \quad \{R\} = \begin{Bmatrix} 0 \\ \cdots \\ \{F(t)\} \end{Bmatrix} \quad (3.35a, b)$$

$\{z\}$ is called the *state vector*; both $[A]$ and $[B]$ are symmetric.

Assume that displacements and velocities of Eq. (3.34) have the form e^{pt} ; then

$$\{\dot{z}\} = p\{z\} \quad (3.36)$$

From Eq. (3.34) for $\{R\} = 0$

$$p[A]\{z\} = -[B]\{z\} \quad (3.37a)$$

or

$$p\{z\} = -[A]^{-1}[B]\{z\} = [D_1]\{z\} \quad (3.37b)$$

where

$$[D_1] = -[A]^{-1}[B] = -\begin{bmatrix} -[M]^{-1}[C][M]^{-1} & [M]^{-1} \\ [M]^{-1} & [0] \end{bmatrix} \begin{bmatrix} -[M] & [0] \\ [0] & [K] \end{bmatrix} = \begin{bmatrix} -[M]^{-1}[C] & -[M]^{-1}[K] \\ [I] & [0] \end{bmatrix} \quad (3.38a)$$

The complex frequency equation can be obtained as follows:

$$u(p) = |[D_1] - p[I]| \quad (3.38b)$$

Equations (3.37b) and (3.38b) may also be expressed as

$$\lambda\{z\} = [D]\{z\} \quad (3.39a)$$

$$u(\lambda) = |[D] - \lambda[I]| \quad (3.39b)$$

where

$$[D] = -[B]^{-1}[A] = -\begin{bmatrix} -[M]^{-1}|[0] \\ \cdots \\ [0]|[K]^{-1} \end{bmatrix} \begin{bmatrix} [0]|[M] \\ \cdots \\ [M]|[C] \end{bmatrix} = \begin{bmatrix} [0]|[I] \\ \cdots \\ -[K]^{-1}[M] | -[K]^{-1}[C] \end{bmatrix} \quad (3.40a)$$

and

$$\lambda = \frac{1}{p} \quad (3.40b)$$

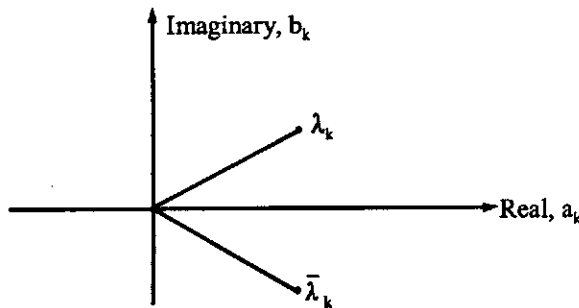


FIG. 3.7 Complex conjugate.

Note that Eq. (3.38a) is easier to handle than Eq. (3.40a) because the former needs only $[M]^{-1}$ while the latter needs both $[M]^{-1}$ and $[K]^{-1}$. Note also that Eq. (3.38a,b) is identical in form to Eq. (2.74a,b) of the undamped case. For damped vibration, proof of orthogonality of eigenvectors, iteration procedures for fundamental and higher modes, and proof of convergence are similar to those of the undamped case as presented in Chapter 2. However, the eigensolution method is different because $[D]$ or $[D_1]$ has an order $2n$. If $[K]$ is singular because of rigid-body displacement of a system, then rigid-body displacement can be removed from the system as explained in Section 2.8.

Solution of λ can be complex eigenvalues for underdamping and will involve conjugate pairs. If the k th and ℓ th eigenvalues are complex conjugate, then

$$\lambda_k = a_k + ib_k \quad (3.41)$$

$$\lambda_\ell = \bar{\lambda}_k = a_k - ib_k \quad (3.42)$$

for which the relationship is revealed in Fig. 3.7. Let the complex frequency be expressed as

$$p_k = \alpha_k + i\beta_k \quad (3.43)$$

Then from Eq. (3.41),

$$p_k = \frac{1}{a_k + ib_k} \quad (3.44)$$

Multiplying the above by $(a_k - ib_k)/(a_k - ib_k)$ leads to

$$p_k = \frac{a_k}{a_k^2 + b_k^2} - \frac{ib_k}{a_k^2 + b_k^2} = \alpha_k + i\beta_k \quad (3.45)$$

Therefore

$$\alpha_k = \frac{a_k}{a_k^2 + b_k^2} \quad (3.46)$$

$$\beta_k = \frac{-b_k}{a_k^2 + b_k^2} \quad (3.47)$$

Since the solution has time dependence,

$$z = e^{p_k t} = e^{\alpha_k t} e^{i\beta_k t} = e^{\alpha_k t} \cos(\beta_k t) + i e^{\alpha_k t} \sin(\beta_k t) \quad (3.48)$$

For a damped system, α_k is negative and β_k represents the frequency of damped free vibration.

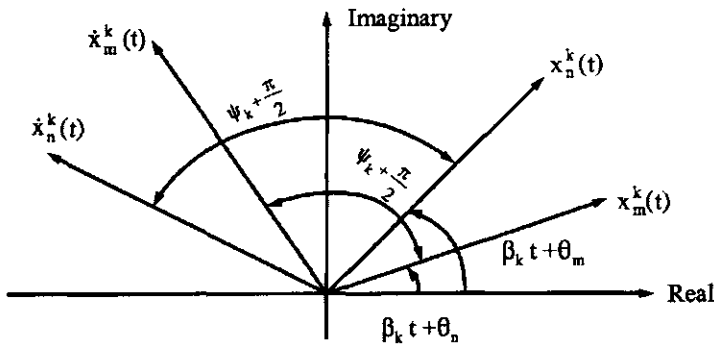


FIG. 3.8 Complex plane.

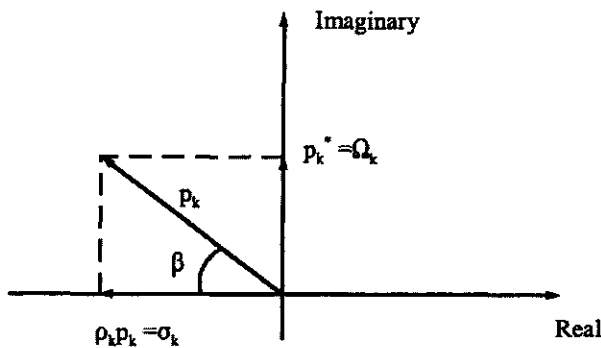


FIG. 3.9 Physical significance of complex frequency.

If the displacement, x_m ($m = 1, 2, 3, \dots, n$), is plotted as a rotating vector on a complex plane as shown in Fig. 3.8, its angular velocity is β_k . The velocities lead the corresponding displacements by a phase angle, $\psi_k + \pi/2$. When p_k is expressed in polar form

$$p_k = \alpha_k + i\beta_k = \sqrt{(\alpha_k)^2 + (\beta_k)^2} e^{i\psi_k} \quad (3.49)$$

and

$$\tan \psi_k = \frac{\beta_k}{\alpha_k} \quad (3.50)$$

Let σ_k be the real-part magnitude and Ω_k be the imaginary part magnitude of the complex frequency plane as shown in Fig. 3.9 for a single-d.o.f. case. The physical significance of σ_k and Ω_k can be inferred from the figure as the frequency, damped frequency, and damping factor in the following expressions:

- structural frequency without consideration of damping

$$p_k = \left[(\rho_k p_k)^2 + (p_k^*)^2 \right]^{1/2} = \left[(\rho_k p_k)^2 + \left(p_k \sqrt{1 - \rho_k^2} \right)^2 \right]^{1/2} \quad (3.51)$$

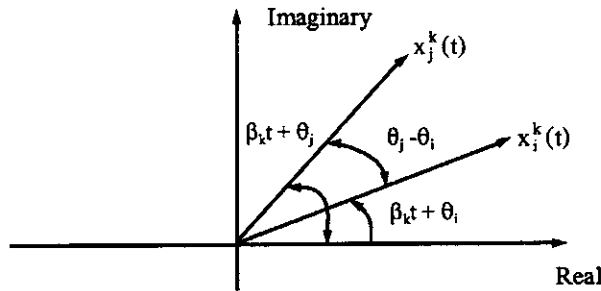


FIG. 3.10 Normalization of complex vectors.

- structural frequency with consideration of damping

$$p_k^* = \Omega_k = |\text{imaginary part}| \quad (3.52)$$

- damping factor

$$\rho_k = \frac{|\rho_k p_k|}{p_k} = |\cos \beta| \quad (3.53)$$

in which

$$\rho_k p_k = \sigma_k = |\text{real part}| \quad (3.54)$$

Thus the complex frequencies provide us with information on damping. The present method also applies to an undamped case for which σ is equal to zero, that is $\rho = 0$.

In general, x_m 's have different θ_m 's. For an undamped case, the eigensolution only yields the relative amplitudes of displacements but not phase angles. Therefore the relative magnitudes of complex displacements and the differences between phase angles, $|\theta_j - \theta_i|$, are determined only for a damped case. Consequently, normalization of complex vectors consists of not just scaling all magnitudes proportionally, but of rotating all components through the same angle in the complex plane as shown in Fig. 3.10.

EXAMPLE 3.5.1 Assume that the following two elements of a vector need to be normalized. Find the magnitude and phase angle.

$$x_1 = 1 + i, \quad x_2 = 5 - 3i$$

Solution: Expressing x_1 and x_2 in polar form

$$\tan \theta_1 = \frac{1}{1}, \quad \theta_1 = \frac{\pi}{4} \quad (a)$$

$$\tan \theta_2 = \frac{-3}{5}, \quad \theta_2 = -0.54 \quad (b)$$

$$x_1 = (1^2 + 1^2)^{\frac{1}{2}} e^{i\theta_1} = \sqrt{2} e^{i(\pi/4)} \quad (c)$$

$$x_2 = [5^2 + (-3)^2]^{\frac{1}{2}} e^{i\theta_2} = \sqrt{34} e^{-i(0.54)} \quad (d)$$

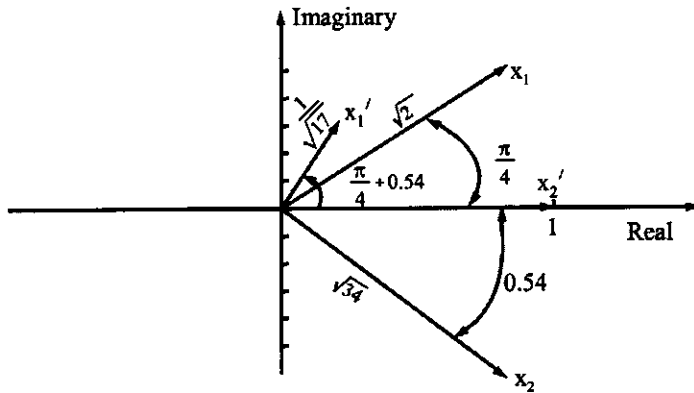


FIG. 3.11 Example 3.5.1.

Therefore the normalization yields

$$\frac{x_1}{x_2} = \sqrt{\frac{1}{17}} e^{i[(\pi/4)+0.54]}, \quad \frac{x_2}{x_2} = 1 \quad (e)$$

In a different approach

$$\begin{aligned} \frac{x_1}{x_2} &= \frac{1+i}{5-3i} = \frac{(1+i)(5+3i)}{(5)^2 - (3i)^2} = \frac{1}{17} + \frac{4}{17}i \\ \tan \theta &= 4, \quad \theta = 1.326 \end{aligned} \quad (f)$$

Therefore

$$\frac{x_1}{x_2} = \left[\left(\frac{1}{17} \right)^2 + \left(\frac{4}{17} \right)^2 \right] e^{i\theta} = \sqrt{\frac{1}{17}} e^{i[(\pi/4)+0.54]} \quad (g)$$

If normalized x_2 is signified by x'_2 , then not only does the magnitude of x_1 have to be reduced by $1/\sqrt{34}$, but also both eigenvectors have to be rotated by 0.54 rad or approximately 31° . Let normalized x_1 and x_2 be signified by x'_1 and x'_2 , respectively; then the relationship between $\{x\}$ and the normalized $\{x'\}$ is as shown in Fig. 3.11.

EXAMPLE 3.5.2 For the two-story shear building shown in Fig. 3.12 with $k_1 = k_2 = k = 800$ k/in and $M_1 = M_2 = M = 2$ k-sec²/in, find the eigenvalues and eigenvectors by using the state-vector approach.

Solution: The motion equation is

$$\begin{bmatrix} M_1 & 0 \\ 0 & M_2 \end{bmatrix} \begin{Bmatrix} \ddot{x}_1 \\ \ddot{x}_2 \end{Bmatrix} = - \begin{bmatrix} k_1 + k_2 & -k_2 \\ -k_2 & k_2 \end{bmatrix} \begin{Bmatrix} x_1 \\ x_2 \end{Bmatrix} \quad (a)$$

Let the state vector be

$$\{z\} = \begin{Bmatrix} x_1 \\ x_2 \\ \dot{x}_1 \\ \dot{x}_2 \end{Bmatrix} = \begin{Bmatrix} \{x\} \\ \dot{\{x\}} \end{Bmatrix} \quad (b)$$

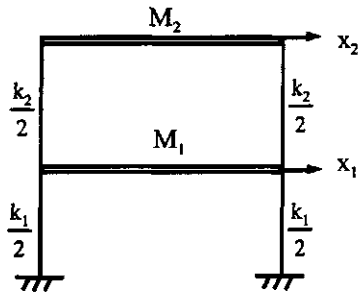


FIG. 3.12 Example 3.5.2—undamped case.

Then $\lambda\{z\} = [D]\{z\}$ in which

$$[D_1] = -[A]^{-1}[B] = \left[\begin{array}{cc|c} [0] & & [I] \\ \frac{-(2k)}{M} & \frac{k}{M} & [0] \\ \frac{k}{M} & -\frac{k}{M} & \end{array} \right] \quad (\text{c})$$

Note that the arrangement of x and \dot{x} in Eq. (b) is different from that of Eq. (3.35a). Using a simple determinant yields the following frequency equation:

$$u(p) = p^4 + 3p^2k/M + k^2/M \quad (\text{d})$$

from which

$$p_{1,2} = \pm 0.618\sqrt{k/M} i; \quad p_{3,4} = \pm 1.618\sqrt{k/M} i \quad (\text{e})$$

or

$$p_1 = |p_{1,2}| = 0.618\sqrt{\frac{k}{M}}; \quad p_2 = |p_{3,4}| = 1.618\sqrt{\frac{k}{M}} \quad (\text{f})$$

The eigenvalues in Eq. (e) may be interpreted in the complex plane shown in Fig. 3.13.

The eigenvectors can be obtained by substituting p_i , $i = 1, 2, 3, 4$, into

$$[pI - D]\{z\} = 0 \quad (\text{g})$$

where $[D]$ is given in Eq. (c). For instance, corresponding to $p_1 = 0.618\sqrt{k/M} i$, Eq. (g) becomes

$$\left[\begin{array}{cccc} 0.618\sqrt{k/M} i & 0 & -1 & 0 \\ 0 & 0.6180\sqrt{k/M} i & 0 & -1 \\ 2k/M & -k/M & 0.618\sqrt{k/M} i & 0 \\ -k/M & k/M & 0 & 0.618\sqrt{k/M} i \end{array} \right] \begin{bmatrix} z_1 \\ z_2 \\ \dot{z}_1 \\ \dot{z}_2 \end{bmatrix} = \begin{bmatrix} 0 \\ 0 \\ 0 \\ 0 \end{bmatrix} \quad (\text{h})$$

from which the first, second, and fourth rows yield $\dot{z}_1 = 0.618\sqrt{k/M}iz_1$, $\dot{z}_2 = 0.618\sqrt{k/M}iz_2$, $z_1 = -\sqrt{M/k}i\dot{z}_2$, respectively. Thus $\dot{z}_1 = 0.618\dot{z}_2$, $z_2 = -1.618\sqrt{M/k}i\dot{z}_2$, and $z_1 =$

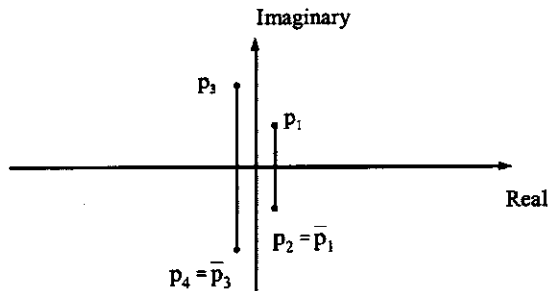


FIG. 3.13 Undamped case—complex eigenvalues.

$-\sqrt{M/k}i\dot{z}_2$. Let $\dot{z}_2 = 1$; then

$$\begin{bmatrix} z_1 \\ z_2 \\ \dot{z}_1 \\ \dot{z}_2 \end{bmatrix} = \begin{bmatrix} x_1 \\ x_2 \\ \dot{x}_1 \\ \dot{x}_2 \end{bmatrix} = \begin{bmatrix} -\sqrt{M/k}i \\ -1.618\sqrt{M/k}i \\ 0.618 \\ 1 \end{bmatrix} = \begin{bmatrix} 0.618 \\ 1 \\ 0.382\sqrt{k/M}i \\ 0.618\sqrt{k/M}i \end{bmatrix} \quad (\text{i})$$

Similarly, the eigenvectors corresponding to p_2, p_3 , and p_4 are given in columns 1, 2, and 3, of Eq. (j), respectively.

$$[z] = \begin{bmatrix} 0.618 & 1 & 1 \\ 1 & -0.618 & -0.618 \\ -0.382\sqrt{k/M}i & 1.618\sqrt{k/M}i & -1.618\sqrt{k/M}i \\ -0.618\sqrt{k/M}i & -\sqrt{k/M}i & \sqrt{k/M}i \end{bmatrix} \quad (\text{j})$$

The real modes are extracted from $p_{1,2}$ and $p_{3,4}$ as

$$\begin{bmatrix} z_1 \\ z_2 \end{bmatrix} = \begin{bmatrix} x_1 \\ x_2 \end{bmatrix} = \begin{bmatrix} 0.618 & 1 \\ 1.000 & -0.618 \end{bmatrix} \quad (\text{k})$$

EXAMPLE 3.5.3 Consider the two-d.o.f. damped system shown below of which the mass and stiffness are the same as given in the previous example: $M_1 = M_2 = 2 \text{ k sec}^2/\text{in}$ and $k_1 = k_2 = 800 \text{ k/in}$. For the present case, damping effects are assumed to be $\alpha = 0, \beta = 0.02$. Find the eigenvalues and eigenvectors.

Solution: Based on Eq. (3.31), we have

$$\begin{bmatrix} 2 & 0 \\ 0 & 2 \end{bmatrix} \begin{bmatrix} \ddot{x}_1 \\ \ddot{x}_2 \end{bmatrix} + \begin{bmatrix} 3.2 & -1.6 \\ -1.6 & 1.6 \end{bmatrix} \begin{bmatrix} \dot{x}_1 \\ \dot{x}_2 \end{bmatrix} + \begin{bmatrix} 1600 & -800 \\ -800 & 800 \end{bmatrix} \begin{bmatrix} x_1 \\ x_2 \end{bmatrix} = 0 \quad (\text{a})$$

Using state-vector form gives

$$\begin{bmatrix} \{\dot{x}\} \\ \{\ddot{x}\} \end{bmatrix} = \begin{bmatrix} [0] & [I] \\ -[M]^{-1}[K] & -[M]^{-1}[C] \end{bmatrix} \begin{bmatrix} \{x\} \\ \{\dot{x}\} \end{bmatrix}$$

or

$$\{\ddot{z}\} = [D_1]\{z\}$$

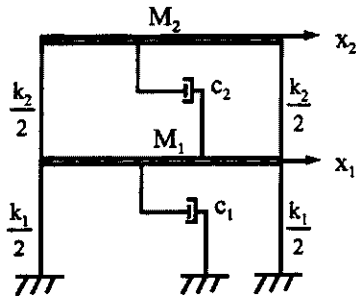


FIG. 3.14 Example 3.5.3—damped case.

in which

$$[D_1] = \left[\begin{array}{ccc|cc} 0 & 0 & | & 1 & 0 \\ 0 & 0 & | & 0 & 1 \\ \cdots & \cdots & | & \cdots & \cdots \\ -800 & 400 & | & -1.6 & 0.8 \\ 400 & -400 & | & 0.8 & -0.8 \end{array} \right] \quad (b)$$

The frequency equation is obtained as

$$u(p) = |D_1 - pI| = p^4 + 2.4p^3 + 1200.64p^2 + 640p + 160,000 = 0 \quad (c)$$

Thus

$$p_{1,2} = -0.153 \pm 12.360i \quad (d)$$

$$p_{3,4} = -1.047 \pm 32.344i \quad (e)$$

The frequencies are

$$p_1 = |p_{1,2}| = \sqrt{|(-0.153)^2 + (\pm 12.360)^2|} = 12.361 \text{ rad/sec} \quad (f)$$

$$p_2 = |p_{3,4}| = \sqrt{|(-1.047)^2 + (\pm 32.344)^2|} = 32.361 \text{ rad/sec} \quad (g)$$

Eqs. (d) and (e) can be interpreted as shown in Fig. 3.15.

From the figure it can be seen that p_1 and p_2 , p_3 and p_4 are complex conjugates. Because the system has damping, the eigenvalues do not lie entirely on the imaginary axis as they did with the undamped case in the previous example. Using the physical interpretation in Fig. 3.9 reveals the following:

- structural frequency without consideration of damping

$$p_k = [(\rho_k p_k)^2 + (p^*)^2]^{\frac{1}{2}} \quad (h)$$

Since $p_k^* = p_k \sqrt{1 - \rho_k^2}$, then

$$p_k = [(\rho_k p_k)^2 + p_k^2(1 - \rho_k^2)]^{\frac{1}{2}} = 12.361 \text{ and } 32.361$$

which were actually obtained in Eqs. (f) and (g).

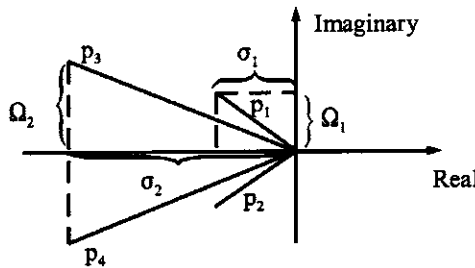


FIG. 3.15 Damped case—complex eigenvalues.

- structural frequency with consideration of damping

$$p_k^* = \text{damped frequency} = \Omega_k = |\text{imaginary part}| \\ = 12.360 \text{ and } 32.344 \quad (\text{i})$$

- damping factor

$$|\cos \beta| = \frac{|-\rho p|}{|p|} = \rho \quad (\text{j})$$

$$\rho p = \text{damping ratio} = \sigma = |\text{real part}| \quad (\text{k})$$

Thus for the present case

$$\rho_1 = \left| \frac{-0.153}{12.361} \right| = 0.01237; \quad \text{or } 1.237\% \text{ of critical} \quad (\text{l})$$

$$\rho_2 = \left| \frac{-1.047}{32.361} \right| = 0.03236; \quad \text{or } 3.236\% \quad (\text{m})$$

3.6. ITERATION METHOD FOR FUNDAMENTAL AND HIGHER MODES OF COMPLEX EIGENVALUES

The previous section presents some important characteristics of complex eigenvalues along with the determinant technique, which is useful for a small number of d.o.f. systems. This section covers the iteration method, which is a general complex eigensolution technique for multiple d.o.f. systems. Also included is the proof of orthogonality condition and the iteration for higher modes.

3.6.1. Fundamental Mode

Let eigenvector $\{z\}$ and eigenvalue λ in

$$\lambda\{z\} = [D]\{z\} \quad (3.55)$$

be expressed as

$$\{z\} = \{\varepsilon\} + i\{\sigma\} \quad (3.56)$$

and

$$\lambda = a + i b \quad (3.57)$$

Substitute $\{z\}$ and λ into Eq. (3.55), which is then separated into the following two parts:

- real part

$$[D]^r \{\varepsilon\} = a^r \{\varepsilon\} - b^r \{\sigma\} = ^{r+1} \{\varepsilon\} \quad (3.58)$$

- imaginary part

$$[D]^r \{\sigma\} = b^r \{\varepsilon\} + a^r \{\sigma\} = ^{r+1} \{\sigma\} \quad (3.59)$$

where superscript r at the upper left-hand corner signifies the iteration number. Rearrange the above two equations for vector $^r \{\sigma\}$

$$^r \{\sigma\} = \frac{a}{b} ^r \{\varepsilon\} - \frac{1}{b} ^{r+1} \{\varepsilon\} \quad (3.60)$$

$$^r \{\sigma\} = \frac{1}{a} ^{r+1} \{\sigma\} - \frac{b}{a} ^r \{\varepsilon\} \quad (3.61)$$

Eliminate $^r \{\sigma\}$ from the above equations:

$$\left(\frac{a}{b} + \frac{b}{a} \right) ^r \{\varepsilon\} - \frac{1}{b} ^{r+1} \{\varepsilon\} - \frac{1}{a} ^{r+1} \{\sigma\} = 0 \quad (3.62)$$

Replace r with $r + 1$ in Eq. (3.60) which is then substituted into the above

$$\left(\frac{a}{b} + \frac{b}{a} \right) ^r \{\varepsilon\} - \frac{1}{b} ^{r+1} \{\varepsilon\} - \frac{1}{b} ^{r+1} \{\varepsilon\} + \frac{1}{ab} ^{r+2} \{\varepsilon\} = 0 \quad (3.63)$$

Multiply the above by ab

$$(a^2 + b^2) ^r \{\varepsilon\} - 2a ^{r+1} \{\varepsilon\} + ^{r+2} \{\varepsilon\} = 0 \quad (3.64)$$

Replace r with $r + 1$

$$(a^2 + b^2) ^{r+1} \{\varepsilon\} - 2a ^{r+2} \{\varepsilon\} + ^{r+3} \{\varepsilon\} = 0 \quad (3.65)$$

Rewrite the above two equations for each component i

$$(a^2 + b^2) ^r \varepsilon_i - 2a ^{r+1} \varepsilon_i + ^{r+2} \varepsilon_i = 0 \quad (3.66)$$

$$(a^2 + b^2) ^{r+1} \varepsilon_i - 2a ^{r+2} \varepsilon_i + ^{r+3} \varepsilon_i = 0 \quad (3.67)$$

Performing [Eq. (3.67)] $(^{r+1} \varepsilon_i / ^{r+2} \varepsilon_i) -$ Eq. (3.66)] yields

$$(a^2 + b^2) = \frac{^{r+1} \varepsilon_i ^{r+3} \varepsilon_i - (^{r+2} \varepsilon_i)^2}{^r \varepsilon_i ^{r+2} \varepsilon_i - (^{r+1} \varepsilon_i)^2} \quad (3.68)$$

Similarly, multiply Eq. (3.66) by $^{r+1} \varepsilon_i / ^r \varepsilon_i$ and then subtract Eq. (3.67),

$$2a = \frac{^r \varepsilon_i ^{r+3} \varepsilon_i - ^{r+1} \varepsilon_i ^{r+2} \varepsilon_i}{^r \varepsilon_i ^{r+2} \varepsilon_i - (^{r+1} \varepsilon_i)^2} \quad (3.69)$$

By assuming the real trial vector $\{\varepsilon\}$ in Eq. (3.58) as

$$[D]^r \{\varepsilon\} = ^{r+1} \{\varepsilon\}$$

and operating iteration procedures on the above, $\{\varepsilon\}$ is found and then employed in Eqs. (3.68) and (3.69) for a and b as well as $\lambda = a + ib$. The frequency is consequently obtained through $p = 1/\lambda = \alpha + i\beta$, of which α and β are found by using a and b as shown in Eqs. (3.46) and (3.47) for any

k th mode. Substituting a , b , ${}^r\{\varepsilon\}$, and ${}^{r+1}\{\varepsilon\}$ into Eq. (3.60) yields the imaginary part, $i\{\sigma\}$, which is then combined with the known value of the real part to finally give the complex eigenvector as shown in Eq. (3.56).

3.6.2. Orthogonality Condition and Iteration for Higher Modes

In order to converge to the next higher mode by iteration, the complex trial vector must be orthogonal to the previous eigenvector and its conjugate. Let $\{z\}_1$ be the first mode and $\{z\}$ be the arbitrarily chosen mode; then orthogonality requires that

$$\{z\}_1^T [A] \{z\} = 0 \quad (3.70)$$

$$\{\bar{z}\}_1^T [A] \{z\} = 0 \quad (3.71)$$

where

$$\{z\}_1 = \{\varepsilon\}_1 + i\{\sigma\}_1 \quad (3.72)$$

$$\{\bar{z}\}_1 = \{\varepsilon\}_1 - i\{\sigma\}_1 \quad (3.73)$$

$$\{z\} = \{\varepsilon\} + i\{\sigma\} \quad (3.74)$$

Expanding Eqs. (3.70) and (3.71) into real and imaginary parts yields four equations of which two are given below that provide the real trial vector $\{\varepsilon\}$ needed for iteration:

$${}^r\{\varepsilon\}_1^T [A] \{\varepsilon\} = 0 \quad (3.75)$$

$${}^r\{\sigma\}_1^T [A] \{\varepsilon\} = 0 \quad (3.76)$$

Substitute Eq. (3.60) into Eq. (3.76) to eliminate ${}^r\{\sigma\}_1$

$$\frac{a}{b} {}^r\{\varepsilon\}_1^T [A] \{\varepsilon\} - \frac{1}{b} {}^{r+1}\{\varepsilon\}_1^T [A] \{\varepsilon\} = 0 \quad (3.77)$$

Considering Eq. (3.75) for the first term of the above, and given that $1/b$ cannot be zero, we have

$${}^{r+1}\{\varepsilon\}_1^T [A] \{\varepsilon\} = 0 \quad (3.78)$$

Thus, to ensure that the iteration on trial vector $\{\varepsilon\}$ converges to the next higher mode, $\{\varepsilon\}$ requires the following *orthogonality conditions*

$${}^r\{\varepsilon\}_1^T [A] \{\varepsilon\} = 0 \quad (3.79)$$

$${}^{r+1}\{\varepsilon\}_1^T [A] \{\varepsilon\} = 0 \quad (3.80)$$

Using the above two conditions yields two equations which are then expressed in the following condensed matrix as

$$[D'] \{\varepsilon\} = \{\varepsilon\} \quad (3.81)$$

Premultiply the above by $[D]$; the expressions for r th and $(r + 1)$ th iterations are

$$[D] [D'] {}^r\{\varepsilon\} = {}^{r+1}\{\varepsilon\} \quad (3.82)$$

Performing iteration procedures yields the next higher mode.

3.6.3. Step-by-Step Procedures

1. Assume real trial vector $\{\varepsilon\}$
2. Perform $[D] {}^r\{\varepsilon\} = {}^{r+1}\{\varepsilon\}$ [see Eq. (3.58)]

3. Calculate $\lambda = \alpha + i\beta$ and $p = \alpha + i\beta$ from Eqs. (3.42) and (3.45) in which

$$a^2 + b^2 = \frac{^{r+1}\varepsilon_i - ^{r+2}\varepsilon_i - (^{r+2}\varepsilon_i)^2}{^{r}\varepsilon_i - ^{r+2}\varepsilon_i - (^{r+1}\varepsilon_i)^2} \quad [\text{see Eq. (3.68)}]$$

$$2a = \frac{^{r}\varepsilon_i - ^{r+3}\varepsilon_i - ^{r+1}\varepsilon_i - ^{r+2}\varepsilon_i}{^{r}\varepsilon_i - ^{r+2}\varepsilon_i - (^{r+1}\varepsilon_i)^2} \quad [\text{see Eq. (3.69)}]$$

$$\alpha = \frac{a}{a^2 + b^2} \quad [\text{see Eq. (3.46)}]$$

$$\beta = \frac{-b}{a^2 + b^2} \quad [\text{see Eq. (3.47)}]$$

4. Obtain $\{z\} = {}^r\{\varepsilon\} + {}^r\{\sigma\}i$ in which

$${}^r\{\sigma\} = \frac{a}{b} {}^r\{\varepsilon\} - \frac{1}{b} {}^{r+1}\{\varepsilon\} \quad [\text{see Eq. (3.60)}]$$

5. Find $[D]$ $[D']$ for the next mode; $[D']$ is obtained by condensing the following two equations:

$${}^r\{\varepsilon\}_1^T [A] \{\varepsilon\} = 0 \quad [\text{see Eq. (3.79)}]$$

$${}^{r+1}\{\varepsilon\}_1^T [A] \{\varepsilon\} = 0 \quad [\text{see Eq. (3.80)}]$$

6. Perform the following for the second mode

$$[D] [D'] {}^r\{\varepsilon\} = {}^{r+1}\{\varepsilon\} \quad [\text{see Eq. (3.82)}]$$

7. Repeat the above six steps for the next higher mode.

EXAMPLE 3.6.1 For the structure shown in Fig. 3.16 with $M_1 = M_2 = M = 1$, $k_1 = k_2 = k = 1$, and damping coefficients $c_{11} = 0.4$, $c_{12} = 0.1$, $c_{21} = 0.1$, and $c_{22} = 0.3$, find the eigenvalue and eigenvector of the first mode by using the iteration method.

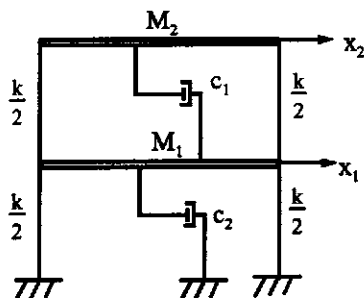


FIG. 3.16 Example 3.6.1.

TABLE 3.2 $\{\varepsilon\}$ for Example 3.6.1

ϵ	r									
	1	2	3	4	5	6	7	8	9	10
1	0	1	-0.50	-0.51	1.467	-0.824	-2.716	5.306	1.190	-15.205
2	0	0	-0.60	-0.28	2.202	-1.352	-4.430	8.258	2.612	-24.366
3	1	-0.5	-0.51	1.467	-0.824	-2.716	5.306	1.190	-15.204	13.546
4	0	-0.6	-0.28	2.202	-1.352	-4.430	8.258	2.612	-24.366	19.764

ϵ	r									
	11	12	13	14	15	16	17	18	19	
1	13.546	24.891	-62.545	3.364	159.508	-182.983	-216.302	713.618	-215.064	
2	19.764	41.973	-97.390	-3.137	257.503	-273.047	-373.593	1120.373	-248.944	
3	24.891	-62.545	3.364	159.508	-182.983	-216.302	713.618	-215.064	-1626.881	
4	41.973	-97.390	-3.137	257.503	-273.047	-373.593	1120.373	-248.944	-2651.064	

Solution: Using the given structural properties in Eq. (3.40a) yields

$$[D] = \begin{bmatrix} [0] & | & [I] \\ \cdots & | & \cdots \\ -[K]^{-1}[M] & | & -[K]^{-1}[C] \end{bmatrix} = \begin{bmatrix} 0 & 0 & | & 1 & 0 \\ 0 & 0 & | & 0 & 1 \\ \cdots & \cdots & | & \cdots & \cdots \\ -1 & -1 & | & -0.5 & -0.4 \\ -1 & -2 & | & -0.6 & -0.7 \end{bmatrix} \quad (a)$$

Following the six-step procedure and calculating

$$[D]^r \{\varepsilon\} = {}^{r+1}\{\varepsilon\} \quad (b)$$

give the numerical results listed in Tables 3.2 and 3.3. The notations in these two tables are self-explanatory except

$$\frac{A}{B} = a^2 + b^2 = \frac{{}^{r+1}\varepsilon_i {}^{r+3}\varepsilon_i - ({}^{r+2}\varepsilon_i)^2}{{}^r\varepsilon_i {}^{r+2}\varepsilon_i - ({}^{r+1}\varepsilon_i)^2} \quad (c)$$

$$\frac{C}{B} = 2a = \frac{{}^r\varepsilon_i {}^{r+3}\varepsilon_i - {}^{r+1}\varepsilon_i {}^{r+2}\varepsilon_i}{{}^r\varepsilon_i {}^{r+2}\varepsilon_i - ({}^{r+1}\varepsilon_i)^2} \quad (d)$$

Table 3.2 contains the calculations of and the corresponding cycle r . For instance, at the beginning, $r = 1$

$${}^1\{\varepsilon\} = [0 \ 0 \ 1 \ 0]^T \quad (e)$$

in which ε_3 is assumed to be 1 and $\varepsilon_1 = \varepsilon_2 = \varepsilon_4 = 0$. Apparently any other element could be chosen to be a nonzero number. From Eq. (b) we have

$${}^2\{\varepsilon\} = [1 \ 0 \ -0.5 \ -0.6]^T \quad (f)$$

which is given in the second column, signified by 2 ($r = 2$). The third elements ${}^1\varepsilon_3 = 1$ and ${}^2\varepsilon_3 =$

TABLE 3.3 a and b for Example 3.6.1

1	2	3	4	5	6
r	ϵ_3	B and A	$A/B = a^2 + b^2$	C	$C/B = 2a$
1	1	B_1	-0.760	A_1/B_1	1.3079
2	-0.5	$B_2 = A_1$	-0.994	A_2/B_2	1.7428
3	-0.51	$B_3 = A_2$	-1.732	A_3/B_3	2.6934
4	1.467	$B_4 = A_3$	-4.664	A_4/B_4	2.5195
5	-0.824	$B_5 = A_4$	-11.752	A_5/B_5	2.6709
6	-2.716	$B_6 = A_5$	-31.387	A_6/B_6	2.6155
7	5.306	$B_7 = A_6$	-82.093	A_7/B_7	2.6197
8	1.190	$B_8 = A_7$	-215.055	A_8/B_8	2.6130
9	-15.204	$B_9 = A_8$	-561.959	A_9/B_9	2.6102
10	13.546	$B_{10} = A_9$	-1466.828	A_{10}/B_{10}	2.6099
11	24.891	$B_{11} = A_{10}$	-3828.161	A_{11}/B_{11}	2.6090
12	-62.545	$B_{12} = A_{11}$	-9987.798	A_{12}/B_{12}	2.6090
13	3.364	$B_{13} = A_{12}$	-26058.506	A_{13}/B_{13}	2.6089
14	159.508	$B_{14} = A_{13}$	-67984.592	A_{14}/B_{14}	2.6089
15	-182.983	$B_{15} = A_{14}$	-177365.952	A_{15}/B_{15}	2.6089
16	-216.302	$B_{16} = A_{15}$	-462731.445	A_{16}/B_{16}	2.6089
17	713.617				
18	-215.064				
19	-1626.88				

-0.5 are recorded at rows 1 and 2 ($r = 1, 2$) of the second column of Table 3.3 under notation 2. Note that column 3 cannot be filled because ${}^{(r+2)}\epsilon_3$ from the third iteration is needed. Carrying another iteration yields

$${}^3\{\epsilon\} = [-0.5 \quad -0.6 \quad -0.51 \quad -0.28]^T \quad (g)$$

which is again recorded in Table 3.2 at $r = 3$. $\epsilon_3 = -0.51$ is recorded in the third row of column 2 in Table 3.3. Knowing ${}^1\epsilon_3 = 1$, ${}^2\epsilon_3 = -0.5$, and ${}^3\epsilon_3 = -0.51$, we find B_1 in column 3 at $r = 1$ as

$$B_1 = {}^1\epsilon_3 \cdot {}^3\epsilon_3 - ({}^2\epsilon_3)^2 = -0.76 \quad (h)$$

Similary, the fourth iteration yields

$${}^4\{\epsilon\} = [-0.51 \quad -0.28 \quad 1.467 \quad 2.202]^T \quad (i)$$

and

$$B_2 = {}^2\epsilon_3 \cdot {}^4\epsilon_3 - ({}^3\epsilon_3)^2 = -0.994 = A_1 \quad (j)$$

which are listed in column 3. Consequently columns 4, 5, and 6 contain the numerical results in

Eqs. (k), (l), and (m), respectively, as follows:

$$a^2 + b^2 = \frac{A_1}{B_1} = 1.3079 \quad (\text{k})$$

$$C_1 = {}^1\varepsilon_3 - {}^4\varepsilon_3 + {}^2\varepsilon_3 - {}^3\varepsilon_3 = 1.212 \quad (\text{l})$$

$$2a = \frac{C_1}{B_1} = -1.5947 \quad (\text{m})$$

The iterations continue until $a^2 + b^2$ and $2a$ converge as they did at the 15th and 16th iterations. Therefore

$$a_1 = \frac{2a}{2} = \frac{1}{2} \left(\frac{C_{15}}{B_{15}} \right) = -0.546 \quad (\text{n})$$

and

$$b_1 = [(a^2 + b^2) - a_1^2]^{\frac{1}{2}} = [(2.609) - (-0.546)^2]^{\frac{1}{2}} = \pm 1.520 \quad (\text{o})$$

Thus

$$\lambda_{1,2} = a_1 + ib_1 = -0.546 \pm 1.520i \quad (\text{p})$$

$$\alpha_1 = \frac{a_1}{a_1^2 + b_1^2} = \frac{-0.546}{2.608} = -0.209 \quad (\text{q})$$

$$\beta_1 = \frac{-b_1}{a_1^2 + b_1^2} = \frac{\mp 1.520}{2.608} = \mp 0.583 \quad (\text{r})$$

$$p_{1,2} = \alpha_1 + i\beta_1 = -0.209 \mp 0.583i \quad (\text{s})$$

The first frequency is obtained from Eq. (s) as $p_1 = [(0.209)^2 + (0.583i)^2]^{\frac{1}{2}} = 0.619$ rad/sec. The real part of the eigenvector is in column 15 ($r = 15$) of Table 3.2. The imaginary part of the eigenvector may be calculated by using Eq. (3.60) given in step 4 as

$$\begin{aligned} {}^{15}\{\sigma\} &= \frac{a_1}{b_1} {}^{15}\{\varepsilon\} - \frac{1}{b_1} {}^{16}\{\varepsilon\} \\ &= \frac{-0.546}{\pm 1.520} \begin{Bmatrix} 159.508 \\ 257.503 \\ -182.983 \\ -273.047 \end{Bmatrix} - \frac{1}{\pm 1.520} \begin{Bmatrix} -182.983 \\ -273.047 \\ -216.302 \\ -373.593 \end{Bmatrix} \\ &= \pm \begin{Bmatrix} 63.074 \\ 87.120 \\ 208.028 \\ 343.857 \end{Bmatrix} \end{aligned} \quad (\text{t})$$

Hence the eigenvector is

$$\{z\}_1 = {}^{15}\{\varepsilon\}_1 + {}^{15}\{\sigma\}_1 i = \begin{Bmatrix} 159.508 & \pm 63.074i \\ 257.503 & \pm 87.120i \\ -182.983 & \pm 208.028i \\ -273.04 & \pm 343.857i \end{Bmatrix} \quad (\text{u})$$

from which the first mode of $[z_1 \ z_2]^T$ is derived by letting $z_2 = 1$ as

$$\begin{Bmatrix} \dot{z}_1 \\ \dot{z}_2 \\ \dots \\ z_1 \\ z_2 \end{Bmatrix} = \begin{Bmatrix} (159.508 \pm 63.07i)(-273.04 \mp 343.857i) \\ (-273.04 \pm 343.857i)(-273.04 \mp 343.857i) \\ (257.503 \pm 87.120i)(-273.04 \mp 343.857i) \\ (-273.04 \pm 343.857i)(-273.04 \mp 343.857i) \\ (-182.983 \pm 208.028i)(-273.04 \mp 343.857i) \\ (-273.04 \pm 343.857i)(-273.04 \mp 343.857i) \end{Bmatrix} = \begin{Bmatrix} -0.113 \mp 0.374i \\ -0.209 \mp 0.583i \\ \dots \\ 0.630 \pm 0.032i \\ 1.0 \end{Bmatrix} \quad (v)$$

EXAMPLE 3.6.2 Use the structural data and solution of Example 3.6.1 to find the eigenvalue and eigenvector of the second mode.

Solution: Following step 5 in Section 3.6.3, calculate the orthogonality conditions as

$${}^{15}\{\varepsilon\}_1^T [A] \{\varepsilon\} = 0; \quad {}^{16}\{\varepsilon\}_1^T [A] \{\varepsilon\} = 0 \quad (a, b)$$

From Example 3.6.1,

$$\begin{aligned} {}^{15}\{\varepsilon\}_1^T &= [159.508 \quad 257.503 \quad -182.983 \quad -273.047] \\ {}^{16}\{\varepsilon\}_1^T &= [-182.983 \quad -273.047 \quad -216.302 \quad -373.593] \end{aligned} \quad (c)$$

$$[A] = \begin{bmatrix} 0 & 0 & 1 & 0 \\ 0 & 0 & 0 & 1 \\ 1 & 0 & 0.4 & 0.1 \\ 0 & 1 & 0.1 & 0.3 \end{bmatrix} \quad (d)$$

$${}^{15}\{\varepsilon\}_1^T [A] \{\varepsilon\} = -182.983\varepsilon_1 - 273.047\varepsilon_2 + 59.0101\varepsilon_3 + 157.2906\varepsilon_4 = 0 \quad (e)$$

$${}^{16}\{\varepsilon\}_1^T [A] \{\varepsilon\} = -216.302\varepsilon_1 - 373.593\varepsilon_2 - 306.8631\varepsilon_3 - 406.7551\varepsilon_4 = 0 \quad (f)$$

Condense Eqs. (e) and (f) by performing Eq. (e)/59.0101 + Eq. (f)/306.8631 and Eq. (e)/182.983 - Eq. (f)/216.302 which then yields Eqs. (g) and (h), respectively

$$\varepsilon_1 = -1.536\varepsilon_2 + 0.352\varepsilon_4 \quad (g)$$

$$\varepsilon_3 = -0.135\varepsilon_2 - 1.574\varepsilon_4 \quad (h)$$

Rewrite Eqs. (g) and (h); using $\varepsilon_2 = \varepsilon_2$ and $\varepsilon_4 = \varepsilon_4$ in matrix form leads to

$$\begin{bmatrix} 0 & -1.536 & 0 & 0.352 \\ 0 & 1 & 0 & 0 \\ 0 & -0.135 & 0 & -1.574 \\ 0 & 0 & 0 & 1 \end{bmatrix} \begin{Bmatrix} \varepsilon_1 \\ \varepsilon_2 \\ \varepsilon_3 \\ \varepsilon_4 \end{Bmatrix} = \begin{Bmatrix} \varepsilon_1 \\ \varepsilon_2 \\ \varepsilon_3 \\ \varepsilon_4 \end{Bmatrix} \quad (i)$$

TABLE 3.4 $\{\varepsilon\}$ for Example 3.6.2

ϵ	r						
	1	2	3	4	5	6	7
1	0	-1.574	0.035	0.599	-0.078	-0.221	0.054
2	0	1	-0.108	-0.372	0.081	0.134	-0.046
3	0	0.035	0.599	-0.078	-0.221	0.054	0.079
4	1	-0.108	-0.372	0.081	0.134	-0.046	-0.046

TABLE 3.5 a and b for Example 3.6.2

1	2	3	4	5	6
r	ϵ_4	<i>B and A</i>	$A/B = a^2 + b^2$	<i>C</i>	$C/B = 2a$
1	1	B_1	-0.383	A_1/B_1	0.3833
2	-0.108	$B_2 = A_1$	-0.147	A_2/B_2	0.3833
3	-0.372	$B_3 = A_2$	-0.056	A_3/B_3	0.3833
4	0.081	$B_4 = A_3$	-0.022	A_4/B_4	0.3833
5	0.134			C_1	0.0413
6	-0.046			C_2	0.0159
7	-0.046			C_3	0.0061

or

$$[D'] \{\varepsilon\} = \{\varepsilon\} \quad (\text{j})$$

Thus

$$[D] [D'] = \begin{bmatrix} 0 & -0.135 & 0 & -1.574 \\ 0 & 0 & 0 & 1 \\ 0 & 0.603 & 0 & 0.035 \\ 0 & -0.383 & 0 & -0.108 \end{bmatrix} \quad (\text{k})$$

in which $[D]$ is given in Eq. (a) of Example 3.6.1. Carrying out step 6 and then steps 1–3 gives the numerical results shown in Tables 3.4 and 3.5.

Since $a^2 + b^2$ and $2a$ converge at cycles 3 and 4, the solutions at $r = 3$ can be obtained in a similar manner as shown in Eq. (k) through Eq. (s) of the previous example. These solutions are

$$a_2 = \frac{2a}{2} = -0.054; \quad b_2 = [(a^2 + b^2) - a_2^2]^{\frac{1}{2}} = \pm 0.617 \quad (\text{l})$$

$$\alpha_2 = \frac{a_2}{a^2 + b^2} = -0.141; \quad \beta_2 = \frac{-b_2}{a^2 + b^2} = \mp 1.609 \quad (\text{m})$$

$$p_{3,4} = \alpha_2 + i\beta_2 = -0.141 \mp 1.609i \quad (\text{n})$$

The second natural frequency is $p_2 = |p_{3,4}| = 1.615$ rad/sec, and the mode shape may be obtained

from step 4 as

$$\begin{aligned} {}^3\{\sigma\} &= \frac{a_2}{b_2} {}^3\{\varepsilon\} - \frac{1}{b_2} {}^4\{\varepsilon\} = \frac{-0.054}{\pm 0.617} \begin{Bmatrix} 0.035 \\ -0.108 \\ 0.599 \\ -0.372 \end{Bmatrix} - \frac{1}{\pm 0.617} \begin{Bmatrix} 0.599 \\ -0.372 \\ -0.078 \\ 0.081 \end{Bmatrix} \\ &= \pm \begin{Bmatrix} -0.975 \\ 0.612 \\ 0.074 \\ -0.099 \end{Bmatrix} \end{aligned} \quad (\text{o})$$

Then

$$\{z\}_2 = {}^3\{\varepsilon\} + {}^3\{\sigma\} = \begin{Bmatrix} 0.035 \mp 0.975i \\ -0.108 \pm 0.612i \\ 0.599 \pm 0.074i \\ -0.372 \mp 0.099i \end{Bmatrix} \quad (\text{p})$$

Assume $x_1 = 1$; we have

$$\begin{aligned} \begin{Bmatrix} \dot{x}_1 \\ \dot{x}_2 \\ \cdots \\ x_1 \\ x_2 \end{Bmatrix} &= \begin{Bmatrix} \frac{(0.035 \mp 0.975i)(0.599 \mp 0.074i)}{(0.599 \mp 0.074i)(0.599 \pm 0.074i)} \\ \frac{(-0.108 \pm 0.612i)(0.599 \mp 0.074i)}{(0.599 \mp 0.074i)(0.599 \pm 0.074i)} \\ 1 \\ \frac{(-0.372 \mp 0.099i)(0.599 \mp 0.074i)}{(0.599 \mp 0.074i)(0.599 \pm 0.074i)} \end{Bmatrix} = \begin{Bmatrix} \frac{-0.051185 \mp 0.586615i}{0.364277} \\ \frac{-0.019404 \pm 0.37458i}{0.364277} \\ 1 \\ \frac{-0.230154 \mp 0.031773i}{0.364277} \end{Bmatrix} \\ &= \begin{Bmatrix} -0.141 \mp 1.609i \\ -0.053 \pm 1.028i \\ \cdots \\ 1 \\ -0.631 \mp 0.088i \end{Bmatrix} \end{aligned} \quad (\text{q})$$

EXAMPLE 3.6.3 Using the eigensolutions obtained in Examples 3.6.1 and 3.6.2, show the relationship between the two structural nodes for each mode.

Solution: From Examples 3.6.1 and 3.6.2, the eigensolutions are as follows:

$$p_1 = -0.209 - 0.583i; \quad \begin{Bmatrix} x_1^1 \\ x_2^1 \end{Bmatrix} = \begin{Bmatrix} 0.630 - 0.032i \\ 1.000 \end{Bmatrix} \quad (\text{a})$$

$$p_2 = -0.209 + 0.583i; \quad \begin{Bmatrix} x_1^2 \\ x_2^2 \end{Bmatrix} = \begin{Bmatrix} 0.630 + 0.032i \\ 1.000 \end{Bmatrix} \quad (\text{b})$$

$$p_3 = -0.141 - 1.609i; \quad \begin{Bmatrix} x_1^3 \\ x_2^3 \end{Bmatrix} = \begin{Bmatrix} 1.000 \\ -0.631 - 0.088i \end{Bmatrix} \quad (c)$$

$$p_4 = -0.141 + 0.088i; \quad \begin{Bmatrix} x_1^4 \\ x_2^4 \end{Bmatrix} = \begin{Bmatrix} 1.000 \\ -0.631 + 0.088i \end{Bmatrix} \quad (d)$$

Since $e^{\phi i} = \cos \phi + i \sin \phi$, $e^{p_i t}$ may be expressed in terms of p_1 and p_2 as

$$e^{(-0.209-0.583i)t} = e^{-0.209t} [\cos(-0.583t) + i \sin(-0.583t)] \quad (e)$$

$$e^{(-0.209+0.583i)t} = e^{-0.209t} [\cos(0.583t) + i \sin(0.583t)] \quad (f)$$

In Eqs. (e) and (f) the real parts can be shown on the real–imaginary plane as clockwise and counterclockwise, respectively. Similarly, clockwise rotation is for p_3 and counterclockwise for p_4 .

The eigenvector for p_1 is

$$\{x_1^1\} = \begin{Bmatrix} 0.630 - 0.032i \\ 1.000 \end{Bmatrix} \quad (g)$$

As $x_2^1 = 1.000$, x_1^1 can be expressed as

$$\begin{aligned} x_1^1 &= 0.630 - 0.032i = \sqrt{0.630^2 + 0.032^2} \angle \tan^{-1} \frac{-0.032}{0.630} \\ &= 0.6308 \angle 357.12^\circ \end{aligned} \quad (h)$$

Similarly, x_1^2 for p_2 is

$$\begin{aligned} x_1^2 &= 0.630 + 0.032i = \sqrt{0.630^2 + 0.032^2} \angle \tan^{-1} \frac{0.032}{0.630} \\ &= 0.6308 \angle 2.88^\circ \end{aligned} \quad (i)$$

Thus x_2^3 and x_2^4 are

$$\begin{aligned} x_2^3 &= \sqrt{0.631^2 + 0.088^2} \angle \tan^{-1} \frac{-0.088}{-0.631} \\ &= 0.637 \angle 187.95^\circ \end{aligned} \quad (j)$$

$$\begin{aligned} x_2^4 &= \sqrt{0.631^2 + 0.088^2} \angle \tan^{-1} \frac{0.088}{-0.631} \\ &= 0.637 \angle 172.05^\circ \end{aligned} \quad (k)$$

The relationships between x_1 and x_2 due to different phase angles are shown in Figs. 3.17 and 3.18.

EXAMPLE 3.6.4 Find the displacement response of free vibration associated with the first mode given in Example 3.6.1.

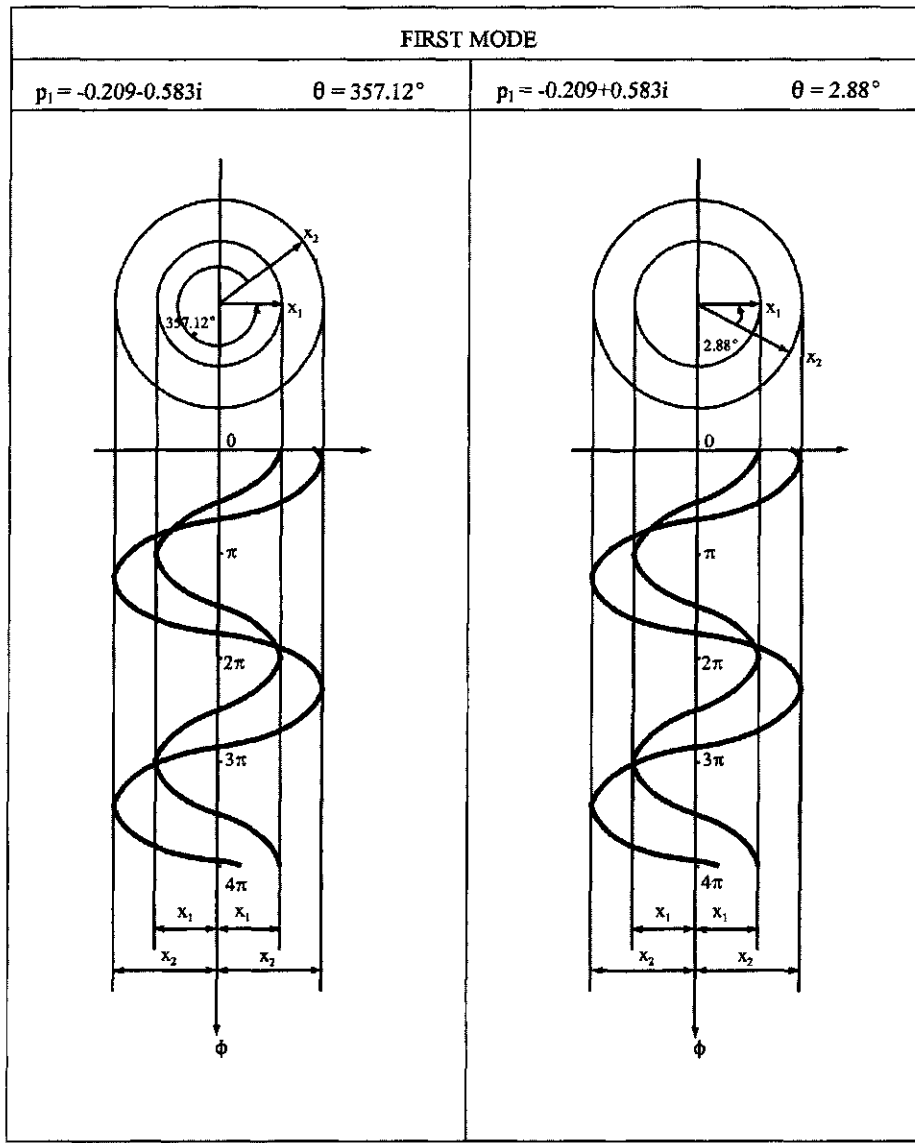


FIG. 3.17 Relationship between x_1 and x_2 of first mode

Solution: The general expression of displacement response may be expressed as

$$\{x\} = (a_1 + b_1 i) \begin{Bmatrix} 0.630 + 0.032i \\ 1 \end{Bmatrix} e^{(-0.546+1.52i)t} + (a_2 + b_2 i) \begin{Bmatrix} 0.630 - 0.032i \\ 1 \end{Bmatrix} e^{(-0.566-1.52i)t} \quad (a)$$

Let $A = a_1 + a_2$, $B = b_2 - b_1$, $\cos \Psi = \frac{A}{\sqrt{A^2+B^2}}$, $\sin \Psi = \frac{B}{\sqrt{A^2+B^2}}$; then

$$\{x\} = \sqrt{A^2 + B^2} e^{(-0.546t)} \begin{Bmatrix} 0.707 \cos(1.52t - \Psi + 2.9^\circ) \\ \cos(1.52t - \Psi) \end{Bmatrix} \quad (b)$$

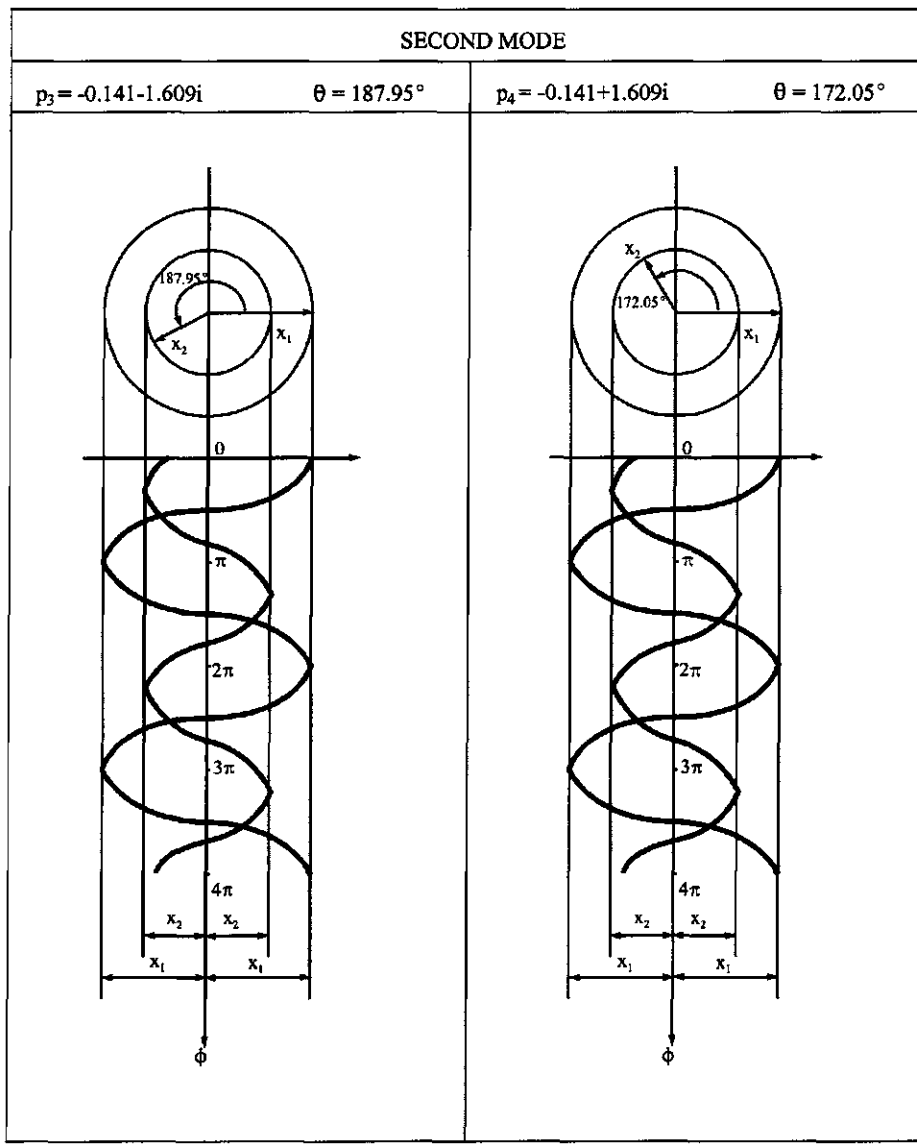


FIG. 3.18 Relationship between x_1 and x_2 of second mode

3.7. RESPONSE ANALYSIS WITH COMPLEX EIGENVALUES

The state vector for the general motion equation of a multiple-d.o.f. system was given in Eq. (3.34) as

$$\{A\} \{\dot{z}\} + [B] \{z\} = \{R\} \quad (3.83)$$

Response analysis is also derived from this equation. As presented in Section 2.5.2 of Chapter 2, Eq. (3.83) is uncoupled by constructing a *modal matrix* $[\Phi]$ from eigenvectors. Let

$$\{z\} = [\Phi] \{Y\} \quad (3.84)$$

where $\{Y\}$ is a new vector and $[\Phi]$ is established column by column of order $2n \times 2n$ with complex eigenvectors as follows:

$$\begin{aligned} [\Phi] &= \left[\{z\}_1 \{\bar{z}\}_1 \quad \{z\}_2 \{\bar{z}\}_2 \dots \{z\}_q \{\bar{z}\}_q \dots \{z\}_n \{\bar{z}\}_n \right] \\ &= \left[[\Phi]_1 [\Phi]_2 \dots [\Phi]_q \dots [\Phi]_n \right] \end{aligned} \quad (3.85)$$

By substituting Eq. (3.84) into Eq. (3.83) and premultiplying with $[\Phi]^T$, an uncoupled motion equation is obtained:

$$[\mathcal{G}] \{\dot{Y}\} + [\mathcal{H}] \{Y\} = \{Q\} \quad (3.86)$$

in which $[\mathcal{G}]$ and $[\mathcal{H}]$, diagonal matrices resulting from orthogonality conditions, and $\{Q\}$ are

$$[\mathcal{G}] = [\Phi]^T [A] [\Phi] \quad (3.87)$$

$$[\mathcal{H}] = [\Phi]^T [B] [\Phi] \quad (3.88)$$

$$\{Q\} = [\Phi]^T \{R\} \quad (3.89)$$

Since $[\Phi]$ is defined by $\{z\}$ and $\{\bar{z}\}$ as shown in Eq. (3.85), Eqs. (3.87) and (3.88) can be rewritten as

$$G_q = \{z\}_q^T [A] \{z\}_q \quad (3.90)$$

$$H_q = \{z\}_q^T [B] \{z\}_q \quad (3.91)$$

$$\bar{G}_q = \{\bar{z}\}_q^T [A] \{\bar{z}\}_q \quad (3.92)$$

$$\bar{H}_q = \{\bar{z}\}_q^T [B] \{\bar{z}\}_q \quad (3.93)$$

For free vibration, $\{Q\} = 0$; then $\{\dot{z}\} = p\{z\}$, and from Eq. (3.86)

$$H_q = -p_q G_q \quad (3.94)$$

Thus

$$\dot{Y}_q - p_q Y_q = \{z\}_q^T \{R\} / G_q = Q_q / G_q \quad (3.95)$$

$$\ddot{Y}_q - \bar{p}_q \ddot{Y}_q = \{\bar{z}\}_q^T \{R\} / \bar{G}_q = \bar{Q}_q / \bar{G}_q \quad (3.96)$$

By using *Laplace transform*,

$$\mathcal{L} Y_q(t) = \int_0^\infty e^{-st} Y_q(t) dt = Y_q(s) \quad (3.97)$$

$$\mathcal{L} \dot{Y}_q(t) = s Y_q(s) - Y_q(0) \quad (3.98)$$

$$\mathcal{L} Q_q(t) = Q_q(s) \quad (3.99)$$

Considering the initial displacement, $Y_q(0)$, to be zero, then the Laplace transform of Eq. (3.95) becomes

$$s Y_q(s) - p_q Y_q(s) = Q_q(s) / G_q \quad (3.100)$$

or

$$Y_q(s) = \frac{Q_q(s)}{G_q(s - p_q)} \quad (3.101)$$

Similarly for Eq. (3.96)

$$\bar{Y}_q(s) = \frac{\bar{Q}_q(s)}{\bar{G}_q(s - \bar{p}_q)} \quad (3.102)$$

The inverse transform can be written as

$$Y_q(t) = \frac{1}{G_q} \int_0^t e^{p_q(t-\Delta)} Q_q(\Delta) d\Delta \quad (3.103)$$

$$\bar{Y}_q(t) = \frac{1}{\bar{G}_q} \int_0^t e^{\bar{p}_q(t-\Delta)} \bar{Q}_q(\Delta) d\Delta \quad (3.104)$$

From Eqs. (3.84) and (3.85)

$$\begin{aligned} \{z(t)\}_{2n \times 1} &= \sum_{q=1}^n (\{z\}_q Y_q(t) + [\bar{z}]_q \bar{Y}_q(t)) \\ &= 2 \sum_{q=1}^n [\text{real part of } \{z\}_q Y_q(t)] \end{aligned} \quad (3.105)$$

Since $\{z\} = [\Phi] \{Y\}$ and

$$\{z\}_q = \left\{ \frac{p_q \{X\}_q}{\{X\}_q} \right\}_{2n \times 1} \quad (3.106)$$

we have

$$\begin{aligned} Q_q = \{z\}_q^T \{R\} &= \left\{ \frac{p_q \{X\}_q}{\{X\}_q} \right\}^T \left\{ \frac{\{0\}}{\{F(t)\}} \right\} = \{X\}_q^T \{F(t)\} \\ &= \sum_{k=1}^n X_q^k F_k(t) \end{aligned} \quad (3.107)$$

Consider only the displacement part of $\{z\}_q$ in terms of $\{X\}_q$; then Eq. (3.105) may be written as

$$\begin{aligned} \{z\}_{n \times 1} &= 2 \sum_{q=1}^n [\text{real part of } \{X\}_q Y_q(t)] \\ &= 2 \sum_{q=1}^n \left[\text{real part of } \frac{\{X\}_q}{G_q} \sum_{k=1}^n X_q^k \left(\int_0^t e^{p_q(t-\Delta)} F_k(\Delta) d\Delta \right) \right] \end{aligned} \quad (3.108)$$

In the above equation $\{X\}_q$, G_q , X_q^k , and p_q can be complex numbers. For convenience, the complex numbers may be expressed in terms of phase angles as

$$X = a + bi = |X|e^{j\theta}$$

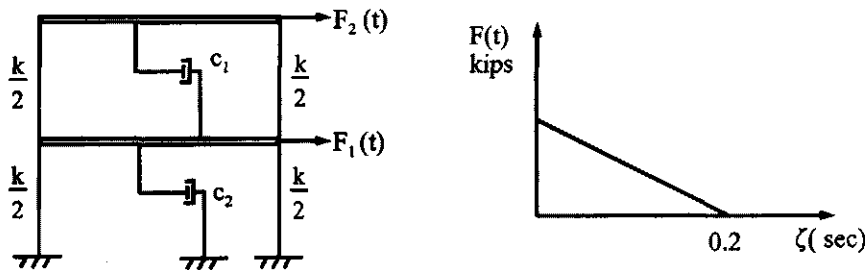


FIG. 3.19 Example 3.7.1.

Thus

$$X_q^m = |X_q^m| e^{i\theta_q^m} \quad (3.109)$$

$$G_q = |G_q| e^{i\phi_q} \quad (3.110)$$

$$X_q^k = |X_q^k| e^{i\theta_q^k} \quad (3.111)$$

$$p_q = \alpha_q + i\beta_q \quad (3.112)$$

The m th component of Eq. (3.108) becomes

$$x_m(t) = 2 \sum_{q=1}^n \left[\text{real part of } \frac{|X_q^m|}{|G_q|} \sum_{k=1}^n |X_q^k| \int_0^t e^{\alpha_q(t-\Delta)} e^{i(\beta_q(t-\Delta) + \theta_q^m - \phi_q + \theta_q^k)} F_k(\Delta) d\Delta \right] \quad (3.113)$$

Using $e^{i\theta} = \cos \theta + i \sin \theta$ and dropping the imaginary part yields the following displacement response expressed in real form:

$$x_m(t) = 2 \sum_{q=1}^n \frac{|X_q^m|}{|G_q|} \sum_{k=1}^n |X_q^k| \int_0^t e^{\alpha_q(t-\Delta)} \cos[\beta_q(t-\Delta) + \theta_q^m - \phi_q + \theta_q^k] F_k(\Delta) d\Delta \quad (3.114)$$

EXAMPLE 3.7.1 The shear building shown in Fig. 3.19 is subjected to impulsive forces whose forcing functions are $F_1(t) = 4(1 - 5\zeta)$ and $F_2(t) = 5(1 - 5\zeta)$. Structural properties and damping coefficients are the same as those in Example 3.6.1. Find the dynamic response equations and plot the numerical results. Note that the given damping is nonproportional.

Solution: Based on the given structural properties, matrix $[A]$ can be established from Eq. (3.33) as

$$[A] = \begin{bmatrix} [0] & | & [M] \\ \cdots & | & \cdots \\ [M] & | & [C] \end{bmatrix} = \begin{bmatrix} 0 & 0 & | & 1 & 0 \\ 0 & 0 & | & 0 & 1 \\ \cdots & \cdots & | & \cdots & \cdots \\ 1 & 0 & | & 0.4 & 0.1 \\ 0 & 1 & | & 0.1 & 0.3 \end{bmatrix} \quad (a)$$

The eigenvalues and eigenvectors, obtained in Examples 3.6.1 and 3.6.2, are summarized herein

with an additional term of eigenvectors expressed in polar form as (see Example 3.5.1)

$$\{z\}_1 = \begin{Bmatrix} -0.113 \mp 0.374i \\ -0.209 \mp 0.583i \\ 0.630 \mp 0.032i \\ 1 \end{Bmatrix} \quad \text{or} \quad \begin{cases} |\dot{x}_1^1| = 0.391, \quad \dot{\theta}_1^1 = 253.12^\circ \text{ or } 4.418 \\ |\dot{x}_1^2| = 0.619, \quad \dot{\theta}_1^2 = 250.24^\circ \text{ or } 4.367 \\ |\dot{x}_1^1| = 0.631, \quad \dot{\theta}_1^1 = 357.12^\circ \text{ or } 6.233 \\ |\dot{x}_1^2| = 1.0, \quad \dot{\theta}_1^2 = 0 \quad \text{or} \quad 0 \end{cases} \quad (\text{b})$$

$$\{z\}_2 = \begin{Bmatrix} -0.141 \mp 1.609i \\ -0.053 \pm 1.208i \\ 1 \\ -0.631 \mp 0.088i \end{Bmatrix} \quad \text{or} \quad \begin{cases} |\dot{x}_2^1| = 1.615, \quad \dot{\theta}_2^1 = 265.00^\circ \text{ or } 4.625 \\ |\dot{x}_2^2| = 1.029, \quad \dot{\theta}_2^2 = 92.95^\circ \text{ or } 1.622 \\ |\dot{x}_2^1| = 1.0, \quad \dot{\theta}_2^1 = 0 \quad \text{or} \quad 0 \\ |\dot{x}_2^2| = 0.637, \quad \dot{\theta}_2^2 = 187.95^\circ \text{ or } 3.280 \end{cases} \quad (\text{c})$$

Following the procedures discussed in previous examples

$$\alpha_1 = -0.209; \quad \beta_1 = \pm 0.583 \quad (\text{d})$$

$$\alpha_2 = -0.141; \quad \beta_2 = \pm 1.609 \quad (\text{e})$$

Using $[A]$ in Eq. (a), and the real and imaginary parts in Eqs. (b) and (c), the numerical results from Eq. (3.90) are calculated as follows:

$$\begin{aligned} G_j &= \{z\}_j^T [A] \{z\}_j = \{z_1 \ z_2 \ z_3 \ z_4\}_j^T [A] \{z_1 \ z_2 \ z_3 \ z_4\}_j \\ &= z_1 z_3 + z_2 z_4 + z_3(z_1 + 0.4z_3 + 0.1z_4) + z_4(z_2 + 0.1z_3 + 0.3z_4) \\ &= 2z_1 z_3 + 2z_2 z_4 + 0.2z_3 z_4 + 0.4z_3^2 + 0.3z_4^2 \end{aligned}$$

Thus

$$G_1 = \{z\}_1^T [A] \{z\}_1 = 0.047 + 1.621i \quad (\text{f})$$

or

$$|G_1| = 1.622; \quad \phi_1 = 88.35^\circ \quad (\text{g})$$

$$G_2 = \{z\}_2^T [A] \{z\}_2 = 0.358 + 4.490i \quad (\text{h})$$

or

$$|G_2| = 4.504; \quad \phi_2 = 85.45^\circ \quad (\text{i})$$

Substituting the above into Eq. (3.114) yields

$$\begin{aligned} x_1(t) &= \frac{2(0.631)}{1.622} \left[0.631 \int_0^t e^{-0.209(t-\Delta)} \cos[0.583(t-\Delta) + 6.233 - 1.542 + 6.233] F_1(\Delta) d\Delta \right. \\ &\quad \left. + \int_0^t e^{-0.209(t-\Delta)} \cos[0.583(t-\Delta) + 6.233 - 1.542 + 0] F_2(\Delta) d\Delta \right] \\ &\quad + \frac{2(1)}{4.504} \left[\int_0^t e^{-0.141(t-\Delta)} \cos[1.609(t-\Delta) + 0 - 1.491 + 0] F_1(\Delta) d\Delta \right. \\ &\quad \left. + 0.637 \int_0^t e^{-0.141(t-\Delta)} \cos[1.609(t-\Delta) + 0 - 1.491 + 3.003] F_2(\Delta) d\Delta \right] \end{aligned} \quad (\text{j})$$

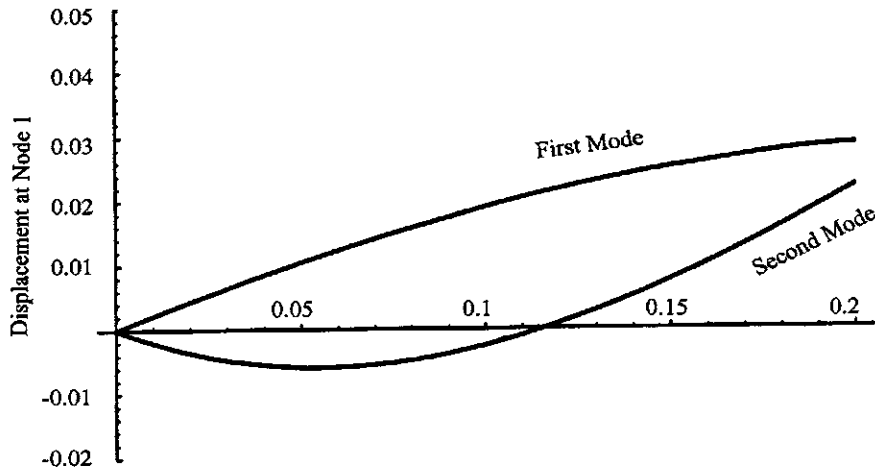


FIG. 3.20 Displacement x_1 of Example 3.7.1—nonproportional damping.

and

$$\begin{aligned}
 x_2(t) = & \frac{2(1)}{1.622} \left[0.631 \int_0^t e^{-0.209(t-\Delta)} \cos[0.583(t-\Delta) + 0 - 1.542 + 6.233] F_1(\Delta) d\Delta \right. \\
 & \left. + 1.0 \int_0^t e^{-0.209(t-\Delta)} \cos[0.583(t-\Delta) + 0 - 1.542 + 0] F_2(\Delta) d\Delta \right] \\
 & + \frac{2(0.637)}{4.504} \left[1.0 \int_0^t e^{-0.141(t-\Delta)} \cos[1.609(t-\Delta) + 3.003 - 1.491 + 0] F_1(\Delta) d\Delta \right. \\
 & \left. + 0.637 \int_0^t e^{-0.141(t-\Delta)} \cos[1.609(t-\Delta) + 3.003 - 1.491 + 3.003] F_2(\Delta) d\Delta \right]
 \end{aligned} \tag{k}$$

In Eqs. (j) and (k), $F_1(\Delta) = 4(1 - 5\Delta)$ and $F_2(\Delta) = 5(1 - 5\Delta)$. Numerical results are plotted in Figs. 3.20 and 3.21 for the first and second mode of $x_1(t)$ and $x_2(t)$, respectively.

EXAMPLE 3.7.2 Rework Example 3.7.1 with damping coefficients of $c_{11} = 0.3$, $c_{12} = -0.10$, $c_{21} = -0.1$, and $c_{22} = 0.2$. Find the response equations and plot the numerical results. Note that the given damping is proportional as shown in Example 3.2.1.

Solution: The procedures for eigensolutions are similar to those presented in Examples 3.6.1 and 3.6.2. Details are left to the reader as an exercise. The main results are summarized as follows:

$$[A] = \begin{bmatrix} 0 & 0 & 1 & 0 \\ 0 & 0 & 0 & 1 \\ 1 & 0 & 0.3 & -0.1 \\ 0 & 1 & -0.1 & 0.2 \end{bmatrix} \tag{a}$$

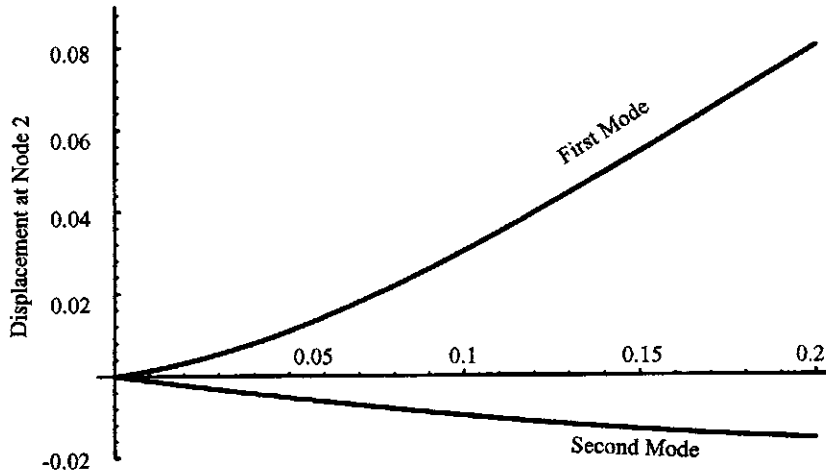


FIG. 3.21 Displacement x_2 of Example 3.7.1—nonproportional damping.

$$[D] = \begin{bmatrix} [0] & [I] \\ -[K]^{-1}[M] & -[K]^{-1}[C] \end{bmatrix} = \begin{bmatrix} 0 & 0 & 1 & 0 \\ 0 & 0 & 0 & 1 \\ -1 & -1 & -0.2 & -0.1 \\ -1 & -2 & -0.1 & -0.3 \end{bmatrix} \quad (\text{b})$$

$$|\lambda[I] - [D]| = \lambda^4 + 0.5\lambda^3 + 3.05\lambda^2 + 0.5\lambda + 1 = 0 \quad (\text{c})$$

$$\left. \begin{array}{l} \lambda_{1,2} = -0.18090 \pm 1.60789i; \\ \lambda_{3,4} = -0.06910 \pm 0.61416i; \end{array} \right. \quad \left. \begin{array}{l} p_{1,2} = -0.069 \mp 0.615i \\ p_{3,4} = -0.181 \mp 1.608i \end{array} \right\} \quad (\text{d})$$

and

$$\{z\}_1 = \begin{Bmatrix} -0.043 \mp 0.380i \\ -0.069 \mp 0.614i \\ 0.618 \\ 1 \end{Bmatrix}; \quad \{z\}_2 = \begin{Bmatrix} -0.181 \mp 1.608i \\ 0.112 \pm 0.994i \\ 1 \\ -0.618 \end{Bmatrix} \quad (\text{e}, \text{f})$$

$$\alpha_1 = -0.069; \quad \beta_1 = 0.615 \quad (\text{g})$$

$$\alpha_2 = -0.181; \quad \beta_2 = 1.608 \quad (\text{h})$$

$$G_j = \{z\}_j^T [A] \{z\}_j = 2z_1 z_3 + 2z_2 z_4 - 0.2z_3 z_4 + 0.3z_3^2 + 0.2z_4^2 \quad (\text{i})$$

for which

$$G_1 = \{z\}_1^T [A] \{z\}_1 = 1.698i \quad (\text{j})$$

or

$$|G_1| = 1.698; \quad \phi_1 = 90^\circ \quad (\text{k})$$

$$G_2 = [z]_2^T [A] [z]_2 = 4.444i \quad (\text{l})$$

or

$$|G_2| = 4.444; \quad \phi_2 = 90^\circ \quad (\text{m})$$

Thus using Eq. (3.114) yields the following displacement response

$$\begin{aligned} x_1(t) = & \frac{2(0.618)}{1.698} \left[0.618 \int_0^t e^{-0.069(t-\Delta)} \sin[0.615(t-\Delta)](4 - 20\Delta) d\Delta \right. \\ & \left. + 1 \int_0^t e^{-0.069(t-\Delta)} \sin[0.615(t-\Delta)](5 - 25\Delta) d\Delta \right] \\ & + \frac{2(1)}{4.444} \left[1 \int_0^t e^{-0.181(t-\Delta)} \sin[1.608(t-\Delta)](4 - 20\Delta) d\Delta \right. \\ & \left. - 0.618 \int_0^t e^{-0.181(t-\Delta)} \sin[1.608(t-\Delta)](5 - 25\Delta) d\Delta \right] \end{aligned} \quad (\text{n})$$

$$\begin{aligned} x_2(t) = & \frac{2(1)}{1.698} \left[0.618 \int_0^t e^{-0.069(t-\Delta)} \sin[0.615(t-\Delta)](4 - 20\Delta) d\Delta \right. \\ & \left. + 1 \int_0^t e^{-0.069(t-\Delta)} \sin[0.615(t-\Delta)](5 - 25\Delta) d\Delta \right] \\ & + \frac{2(0.618)}{4.444} \left[-1 \int_0^t e^{-0.181(t-\Delta)} \sin[1.608(t-\Delta)](4 - 20\Delta) d\Delta \right. \\ & \left. + 0.618 \int_0^t e^{-0.181(t-\Delta)} \sin[1.608(t-\Delta)](5 - 25\Delta) d\Delta \right] \end{aligned} \quad (\text{o})$$

The displacement corresponding to the first and second mode of $x_1(t)$ is shown in Fig. 3.22. $x_2(t)$ is similarly shown in Fig. 3.23.

3.8. RELATIONSHIP BETWEEN UNDAMPED, PROPORTIONAL DAMPING, AND NONPROPORTIONAL DAMPING

The iteration procedures for complex eigensolutions can be applied to undamped, proportional damping, and nonproportional damping as presented in Examples 3.5.2, 3.6.1 and 3.6.2, respectively. Since structural configuration, mass, and stiffness of these three examples are the same, the results are summarized in Table 3.6 for comparison.

The numerical results in Table 3.6 are plotted in Fig. 3.24. Note that for undamped and proportional damping, the difference between phase angles of each node is always equal to either zero or 180° . Therefore we can use a positive or negative sign to indicate the phase angles' difference.

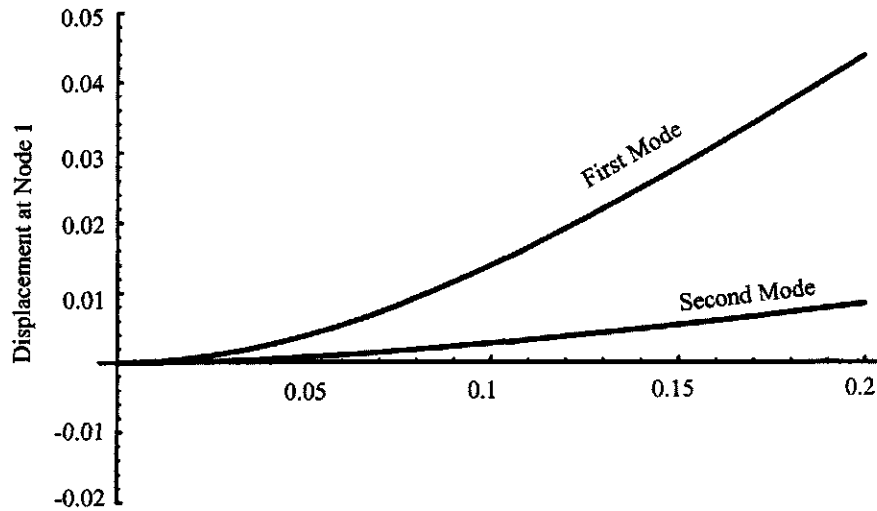


FIG. 3.22 Displacement x_1 in Example 3.7.2—proportional damping.

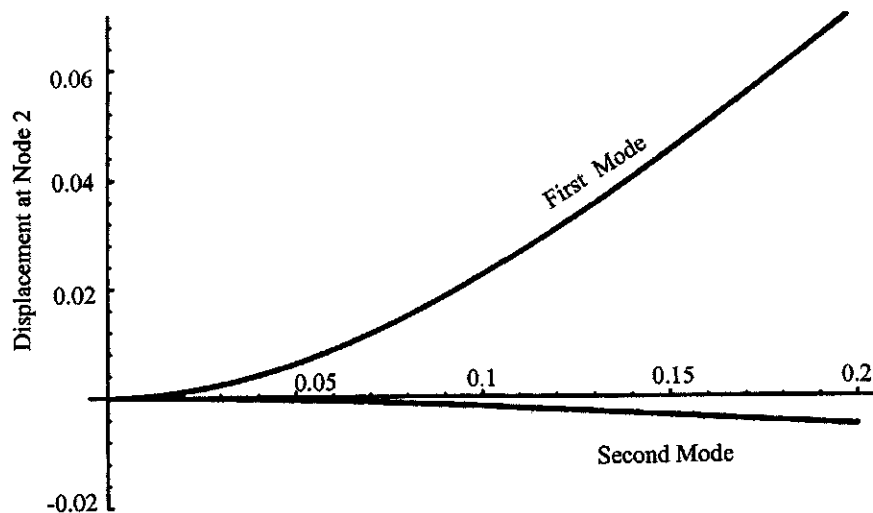


FIG. 3.23 Displacement x_2 in Example 3.7.2—proportional damping.

For nonproportional damping, however, the positive or negative signs, are not sufficient to identify the difference between phase angles. This is because at $t = t_0$ and $= t_0 + \Delta t$ each node can have the same sign and the different sign in a specific mode. Therefore, not only amplitude but also phase angle are necessary to identify a mode shape. For that reason, n additional equations are needed for a nonproportional damping system.

TABLE 3.6 Summary of Eigensolutions for Undamped, Proportional Damping, and Nonproportional Damping

		Undamped	Proportional Damping	Nonproportional Damping
p_1		$\pm 0.618i$	$-0.069 \mp 0.614i$	$-0.209 \mp 0.583i$
z_1^1	p_2	$\pm 1.618i$	$-0.181 \mp 1.608i$	$-0.141 \mp 1.609i$
	x_1^1	0.618	0.618	0.630 $\mp 0.032i$
	$ x_1^1 $	0.618	0.618	0.631
z_2^1	θ_1^1	0	0	$357.12^\circ, 2.88^\circ$
	x_2^1	1	1	1
	$ x_2^1 $	1	1	1
z_1^2	θ_2^1	0	0	0
	x_1^2	1	1	1
	$ x_1^2 $	1	1	1
z_2^2	θ_1^2	0	0	0
	x_2^2	-0.618	-0.618	$-0.631 \mp 0.088i$
	$ x_2^2 $	0.618	0.618	0.637
z_2^2	θ_2^2	180°	180°	$187.95^\circ, 172.05^\circ$

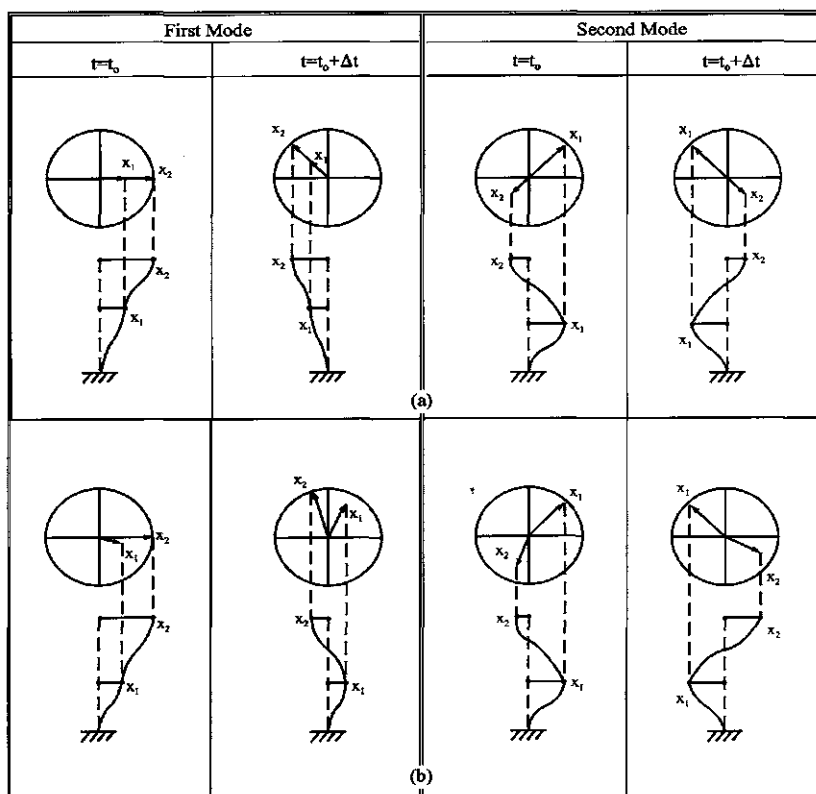


FIG. 3.24 Comparisons of eigenvectors: (a) undamped and proportional damping, (b) nonproportional damping.

BIBLIOGRAPHY

1. FY Cheng, ME Botkin. Second-order elasto-plastic analysis of tall buildings with damped dynamic excitations. In: Proceedings of Finite Element Method in Civil Engineering, McGill University, Montreal, 1972, pp 549–564.
2. FY Cheng, Zizhi Fu, eds. Computational Mechanics in Structural Engineering—Recent Developments and Future Trends. Oxford: Elsevier Science, 1992.
3. T Belytschko, WL Mindle. The treatment of damping in transient computations. In: PJ Torvik, ed. Damping Application for Vibration Control. New York ASME, Vol AMD 38, 1980, pp 123–132.
4. RA Frazer, WJ Duncan, AR Collar. Elementary Matrices. New York: Macmillan, 1946.
5. WC Hurty, MF Rubinstein. Dynamics of Structures. Englewood Cliffs, NJ: Prentice-Hall, 1946.
6. MR Lindeburgh. Seismic Design of Building Structures, 5th ed. Belmont, CA: Professional Publications, 1990.
7. Uniform Building Code. Whittier, CA: International Conference of Building Officials, 1997.
8. M Wakabayashi. Design of Earthquake-Resistant Buildings. New York: McGraw-Hill, 1986.
9. W Weaver, PR Johnson. Structural Dynamics by Finite Elements. Englewood Cliffs, NJ: Prentice-Hall, 1987.
10. International Building Code. Whittier, CA: International Conference of Building Officials, 2000.

4

Dynamic Stiffness and Energy Methods for Distributed Mass Systems

4.1. INTRODUCTION

The vibrations of structural frameworks composed of prismatic members with and without superimposed masses are discussed in this chapter. Members are considered to have bending deformation only, and structural joints are rigidly connected. Formulations and numerical examples are presented for eigensolutions, steady-state vibration, and response to general forcing functions with and without damping. The structures encountered are continuous beams and rigid frames that may have multiple d.o.f. in side-sway. Mathematical formulations are based on the dynamic stiffness method and the energy method.

4.2. DERIVATION OF BERNOULLI-EULER EQUATION

Let the typical prismatic beam shown in Fig. 4.1 be subjected to a time-dependent load, $w(x, t)$, i.e. the magnitude of the load varies continuously from section to section, and the direction varies with time. This load will cause motions of deflection, $y(x, t)$ (assume positive downward), velocity, $\partial y(x, t)/\partial t$, and acceleration, $\partial^2 y(x, t)/\partial t^2$, as well as internal forces of moment, $M(x, t)$, and shear, $V(x, t)$. From the accompanying free-body diagram, two equilibrium equations of $\Sigma F_y = 0$ and $\Sigma M = 0$ must be satisfied. The summation of the forces in the vertical direction is $\Sigma F_y = (m dx) \partial^2 y(x, t)/\partial t^2$, in which m is the mass per unit length. Substituting all the vertical forces yields

$$-V(x, t) + w(x, t)dx + V(x, t) + \frac{\partial V(x, t)}{\partial x} dx - m dx \frac{\partial^2 y(x, t)}{\partial t^2} = 0 \quad (4.1)$$

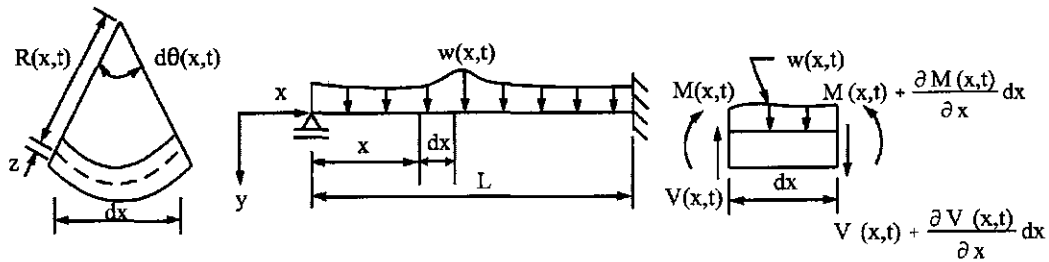


FIG. 4.1 Typical prismatic beam.

or in condensed form

$$\frac{\partial V(x, t)}{\partial x} = m \frac{\partial^2 y(x, t)}{\partial t^2} - w(x, t) \quad (4.2)$$

The summation of moments about the right side of the free-body diagram gives

$$V(x, t) dx + M(x, t) + m dx \frac{\partial^2 y(x, t)}{\partial t^2} \frac{dx}{2} - M(x, t) - \frac{\partial M(x, t)}{\partial x} dx - w(x, t) dx \frac{dx}{2} = 0 \quad (4.3)$$

Neglecting the higher-order terms involving $w(x, t)$ and m leads to

$$\frac{\partial M(x, t)}{\partial x} = V(x, t) \quad (4.4)$$

Substituting Eq. (4.2) into the above yields

$$\frac{\partial^2 M(x, t)}{\partial x^2} = m \frac{\partial^2 y(x, t)}{\partial t^2} - w(x, t) \quad (4.5)$$

For the case of free vibration, $w(x, t) = 0$, Eq. (4.5) becomes

$$\frac{\partial^2 M(x, t)}{\partial x^2} = m \frac{\partial^2 y(x, t)}{\partial t^2} \quad (4.6)$$

Curvature of the elastic curve $y(x, t)$ expressed in terms of the radius of curvature, $R(x, t)$, is

$$\frac{1}{R(x, t)} = - \frac{\partial^2 y(x, t)/\partial x^2}{\left[1 + \left(\frac{\partial y(x, t)}{\partial x} \right)^2 \right]^{3/2}} \quad (4.7)$$

Based on the small deflection theory, $(\partial y(x, t)/\partial x)^2$ can be neglected in comparison with unity; then Eq. (4.7) can be rewritten as

$$\frac{1}{R(x, t)} = - \frac{\partial^2 y(x, t)}{\partial x^2} \quad (4.8)$$

In the study of the mechanics of materials, the following relationship is derived from the curvature, bending moment, and flexural stiffness (EI) of a beam

$$\frac{1}{R(x, t)} = \frac{M(x, t)}{EI} \quad (4.9)$$

Comparing the above result with Eq. (4.8) yields

$$\frac{\partial^2 y(x, t)}{\partial x^2} = -\frac{M(x, t)}{EI} \quad (4.10)$$

Thus Eq. (4.6) becomes

$$EI \frac{\partial y(x, t)}{\partial x^4} + m \frac{\partial^2 y(x, t)}{\partial t^2} = 0 \quad (4.11)$$

To solve the partial differential equation, the method of separation of variables is employed,

$$y(x, t) = Y(x) \cdot g(t) \quad (4.12)$$

where $Y(x)$ is called the *shape function*, which is expressed in terms of x along a member, and $g(t)$ is the *time function*, which is related to the variable time of motion. Substituting Eq. (4.12) into Eq. (4.11) and then separating the variables leads to

$$\frac{EI(d^4 Y/dx^4)}{mY} = -\frac{d^2 g/dt^2}{g} \quad (4.13)$$

Since Y and g are dependent on x and t , respectively, Eq. (4.13) must be equal to a constant, say p^2 . Thus

$$\frac{d^4 Y}{dx^4} - \frac{p^2 m}{EI} Y = 0 \quad (4.14)$$

and

$$\frac{d^2 g}{dt^2} + p^2 g = 0 \quad (4.15)$$

Introducing a notation yields

$$\lambda^4 = \frac{p^2 m}{EI} \quad (4.16)$$

Equation (4.14) can be rewritten as

$$\frac{d^4 Y}{dx^4} - \lambda^4 Y = 0 \quad (4.17)$$

of which the characteristic roots are λ , $-\lambda$, $i\lambda$, and $-i\lambda$, and the complementary solution is

$$Y = C_1 e^{\lambda x} + C_2 e^{-\lambda x} + C_3 e^{i\lambda x} + C_4 e^{-i\lambda x} \quad (4.18)$$

Expressing it in trigonometric functions yields

$$Y = A \sin \lambda x + B \cos \lambda x + C \sinh \lambda x + D \cosh \lambda x \quad (4.19)$$

where A , B , C , and D are arbitrary constants and can be determined by using the boundary conditions of a member. Eq. (4.19) is called the *Bernoulli-Euler equation* and is based on consideration of bending deformation.

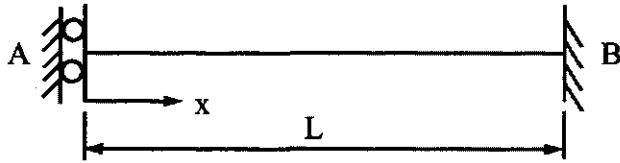


FIG. 4.2 Example 4.2.1.

Similarly, the general solution of Eq. (4.15) is

$$g = E \sin pt + F \cos pt \quad (4.20)$$

The constants E and F should be determined from the initial conditions of displacement and velocity at a given time. For determination of the natural frequencies of free vibration as shown in the following example, always use the shape function; the time function is not needed.

EXAMPLE 4.2.1 Find the natural frequencies of the prismatic beam shown in Fig. 4.2.

Solution: The boundary conditions of this beam include zero slope and zero shear at end $A(x = 0)$ as well as zero slope and zero deflection at end $B(x = L)$

$$\left. \begin{array}{l} \frac{\partial y}{\partial x}(0, t) = 0; \quad \frac{\partial^3 y}{\partial x^3}(0, t) = 0 \\ y(L, t) = 0; \quad \frac{\partial y}{\partial x}(L, t) = 0 \end{array} \right\} \text{for } t \geq 0 \quad (a)$$

These boundary conditions imply the following four conditions for $Y(x)$:

$$\left. \begin{array}{l} (1) \quad \frac{dY}{dx}(0) = 0 \\ (2) \quad \frac{d^3 Y}{dx^3}(0) = 0 \\ (3) \quad Y(L) = 0 \\ (4) \quad \frac{dY}{dx}(L) = 0 \end{array} \right\} \quad (b)$$

Conditions (1) and (2) give

$$A + C = 0 \quad (c)$$

$$-A + C = 0 \quad (d)$$

Conditions (3) and (4) imply that

$$A \sin \lambda L + B \cos \lambda L + C \sinh \lambda L + D \cosh \lambda L = 0 \quad (e)$$

$$A\lambda \cos \lambda L - B\lambda \sin \lambda L + C\lambda \cosh \lambda L + D\lambda \sinh \lambda L = 0 \quad (f)$$

Eqs. (c) and (d) give

$$A = C = 0 \quad (g)$$

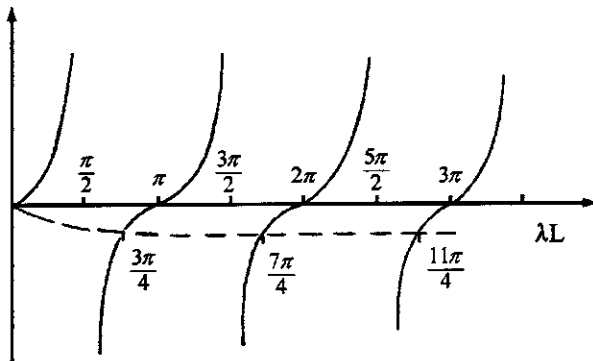


FIG. 4.3 Example 4.2.1.

and the result of Eqs. (e) and (f) is

$$B \cos \lambda L + D \cosh \lambda L = 0 \quad (h)$$

$$-B \sin \lambda L + D \sinh \lambda L = 0 \quad (i)$$

In order for the system to have a nontrivial solution, the determinant of the coefficients must be zero. Consequently, the *frequency equation* can be obtained as

$$-\tanh \lambda L = \tan \lambda L \quad (j)$$

The solution of $\lambda = 0$ in Eq. (j) need not be considered because it implies, according to Eq. (4.16), that $p = 0$ and, according to Eq. (4.16), that Y does not have any frequency parameter; therefore the beam is not vibrating. The results of Eq. (j) are plotted in Fig. 4.3, from which the solution may be approximately expressed as

$$\lambda L \approx \frac{3\pi}{4}; \quad \frac{7\pi}{4}; \quad \frac{11\pi}{4} \quad (k)$$

Substituting λL into Eq. (4.16) yields the natural frequency of the n th mode,

$$p_n \approx \left(\frac{4n-1}{4} \right)^2 \pi^2 \sqrt{\frac{EI}{mL^4}} \quad n = 1, 2, \dots, \infty \quad (l)$$

Using the arbitrary constants in Eqs. (g) and (h) (or Eq. (i)) leads to the following equation for determining the *characteristic modes* of the beam:

$$\begin{aligned} Y &= B \cos \lambda x - B \frac{\cos \lambda L}{\cosh \lambda L} \cosh \lambda x \\ &= B \left(\cos \lambda x - \frac{\cos h\lambda x}{\cosh \lambda L} \cos \lambda L \right) \end{aligned} \quad (m)$$

where B is arbitrary; λ , depending on which number of mode shapes is to be investigated, should be taken from Eq. (k).

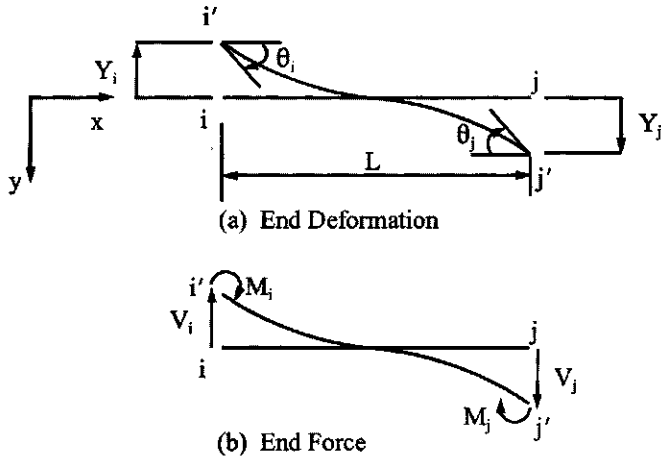


FIG. 4.4 Typical deformed member.

4.3. DERIVATION OF DYNAMIC STIFFNESS COEFFICIENTS

For the arbitrary member, “*ij*”, of a framework shown in Fig. 4.4, let the end moments, M_i, M_j , the end shears, V_i, V_j , and their associated end deflections, Y_i, Y_j , as well as the end slopes, θ_i, θ_j , be considered positive. According to the shape function derived in Eq. (4.19), the following boundary conditions can be established:

	End forces	End deformations	
$x = 0$	$\frac{d^2 Y}{dx^2} = -\frac{M_i}{EI}$	$\frac{dY}{dx} = \theta_i$	
$x = L$	$\frac{d^2 Y}{dx^2} = \frac{M_j}{EI}$	$\frac{dY}{dx} = \theta_j$	(4.21)
$x = 0$	$\frac{d^3 Y}{dx^3} = -\frac{V_i}{EI}$	$Y = -Y_i$	
$x = L$	$\frac{d^3 Y}{dx^3} = -\frac{V_j}{EI}$	$Y = Y_j$	

In order to obtain force-deformation relationships, the constant coefficients A, B, C , and D of Eq. (4.19) need to be solved in terms of end deformations. By doing so, M_i, M_j, V_i , and V_j can be shown in terms of θ_i, θ_j, Y_i , and Y_j .

The four end deformations can be expressed in terms of A, B, C , and D as follows:

	A	B	C	D	
θ_i	λ	0	λ	0	
θ_j	$\lambda \cos \lambda L$	$-\lambda \sin \lambda L$	$\lambda \cosh \lambda L$	$\lambda \sinh \lambda L$	
$-Y_i$	0	1	0	1	
Y_j	$\sin \lambda L$	$\cos \lambda L$	$\sinh \lambda L$	$\cosh \lambda L$	

Inverting Eq. (4.22) yields the following:

	θ_i	θ_j	Y_i	Y_j
A	$\frac{1 - \sinh \lambda L \sin \lambda L - \cos \lambda L \cosh \lambda L}{D\lambda}$	$\frac{\cos \lambda L - \cosh \lambda L}{D\lambda}$	$\frac{\cos \lambda L \sinh \lambda L + \cosh \lambda L \sin \lambda L}{D}$	$\frac{\sin \lambda L + \sinh \lambda L}{D}$
B =	$\frac{\cosh \lambda L \sin \lambda L - \sinh \lambda L \cos \lambda L}{D\lambda}$	$\frac{\sinh \lambda L - \sin \lambda L}{D\lambda}$	$\frac{\cosh \lambda L \cos \lambda L - \sinh \lambda L \sin \lambda L - 1}{D}$	$\frac{\cos \lambda L - \cosh \lambda L}{D}$
C	$\frac{1 + \sinh \lambda L \sin \lambda L - \cosh \lambda L \cos \lambda L}{D\lambda}$	$\frac{\cosh \lambda L - \cos \lambda L}{D\lambda}$	$\frac{-\cos \lambda L \sinh \lambda L - \cosh \lambda L \sin \lambda L}{D}$	$\frac{-\sin \lambda L - \sinh \lambda L}{D}$
D	$\frac{\sinh \lambda L \cos \lambda L - \cosh \lambda L \sin \lambda L}{D\lambda}$	$\frac{\sin \lambda L - \sinh \lambda L}{D\lambda}$	$\frac{\sinh \lambda L \sin \lambda L + \cosh \lambda L \cos \lambda L - 1}{D}$	$\frac{\cosh \lambda L - \cos \lambda L}{D}$

(4.23)

where $D = 2 - 2 \cosh \lambda L \cos \lambda L$. Similarly, the four conditions of end forces can be expressed in terms of arbitrary constants A , B , C , and D as follows:

	A	B	C	D
$-\frac{M_i}{EI}$	0	$-\lambda^2$	0	λ^2
$\frac{M_j}{EI} =$	$-\lambda^2 \sin \lambda L$	$-\lambda^2 \cos \lambda L$	$\lambda^2 \sinh \lambda L$	$\lambda^2 \cosh \lambda L$
$-\frac{V_i}{EI}$	$-\lambda^3$	0	λ^3	0
$-\frac{V_j}{EI}$	$-\lambda^3 \cos \lambda L$	$\lambda^3 \sin \lambda L$	$\lambda^3 \cosh \lambda L$	$\lambda^3 \sinh \lambda L$

Thus M_i , M_j , V_i , and V_j can be expressed in terms of θ_i , θ_j , Y_i , and Y_j , respectively, by eliminating constant coefficients. Flexural dynamic stiffness coefficients are shown in Eq. (4.25a, b):

$$\{Q_e\} = [K_e] \{q_e\} \quad (4.25a)$$

where $\{Q_e\} = [M_i \ M_j \ V_i \ V_j]^T$ and $\{q_e\} = [\theta_i \ \theta_j \ Y_i \ Y_j]^T$. In detailed form:

	θ_i	θ_j	Y_i	Y_j
M_i	$\frac{\sinh \phi \cos \phi - \cosh \phi \sin \phi}{G}$	$\frac{\sin \phi - \sinh \phi}{G}$	$\frac{\sinh \phi \sin \phi \left(\frac{\phi}{L}\right)}{G}$	$\frac{\cosh \phi - \cos \phi \left(\frac{\phi}{L}\right)}{G}$
$M_j =$		$\frac{\sinh \phi \cos \phi - \cosh \phi \sin \phi}{G}$	$\frac{\cosh \phi - \cos \phi \left(\frac{\phi}{L}\right)}{G}$	$\frac{\sinh \phi \sin \phi \left(\frac{\phi}{L}\right)}{G}$
V_i	symm		$\frac{(-\cos \phi \sinh \phi - \cosh \phi \sin \phi) \left(\frac{\phi}{L}\right)^2}{G}$	$\frac{-\sinh \phi - \sin \phi \left(\frac{\phi}{L}\right)^2}{G}$
V_j			$\frac{-\cos \phi \sinh \phi - \cosh \phi \sin \phi \left(\frac{\phi}{L}\right)^2}{G}$	

(4.25b)

where $\phi = \lambda L$, $G = [(\cosh \phi \cos \phi - 1)L]/\phi EI$. Let Eq. (4.25b) be represented by

	θ_i	θ_j	Y_i	Y_j	
M_i	$SM\theta_1$	$SM\theta_2$	SMY_1	SMY_2	
M_j	$=$	$SM\theta_2$	$SM\theta_1$	SMY_2	SMY_1
V_i		SMY_1	SMY_2	SVY_1	SVY_2
V_j		SMY_2	SMY_1	SVY_2	SVY_1

or

	θ	Y	
M	$=$	$SM\theta$	SMY
V		SMY	SVY

Eq. (4.26a,b) is treated later in this chapter as a symbol representing stiffness coefficients of formulating a structural stiffness matrix.

4.4. CHARACTERISTICS OF DYNAMIC STIFFNESS COEFFICIENTS

4.4.1. Numerals and Curves for Coefficients

The numerical values of six different dynamic stiffness coefficients are shown in Table 4.1. The values were calculated by varying the parameter, ϕ , between 0.05 and 6.50 (i.e. approximately between zero and 2π) at increments of 0.05. Coefficients are then plotted in Fig. 4.5. From the figure, the physical meaning can be interpreted as follows. For a given beam with both ends restrained, subjected to a unit steady-state rotation of $\theta_i e^{ipt}$ (for undamped harmonic motion, a structure's vibration varies with the forcing frequency, ω ; therefore, $p = \omega$), the moments and shears at the extreme case of low frequency, i.e. $\phi \rightarrow 0$, are finite, as $4EI/L$ at end i and $2EI/L$ at end j for moments, and $-6EI/L^2$ at both ends for shears. Similarly, the moments and shears at both ends, due to a unit displacement of $Y_i e^{ipt}$ at the limiting case of no vibration, are $-6EI/L^2$ and $12EI/L^3$, respectively. However, when the frequency of vibration increases to a value of $\phi = 3.926$ (corresponding to the natural frequency of a beam with one end rotated (i.e. hinged support) and the other end restrained), no moment is required at the rotated end to maintain its resonant behavior. Consequently, the stiffness, $SM\theta_1$, is zero. When ϕ equals 4.728, the vibrating mode shape is analogous to a beam with both ends restrained. In this case, the end moments of the beam are finite, but the end rotations are zero; therefore, the stiffness coefficients approach infinity.

TABLE 4.1 Flexural Dynamic Stiffness Coefficients

ϕ	$SVY_1\left(\frac{L^3}{EI}\right)$	$SVY_2\left(\frac{L^3}{EI}\right)$	$SM\theta_1\left(\frac{L}{EI}\right)$	$SM\theta_2\left(\frac{L}{EI}\right)$	$SMY_1\left(\frac{L^2}{EI}\right)$	$SMY_2\left(\frac{L^2}{EI}\right)$
0.05	12.000	12.000	4.0000	2.0000	-6.0000	-6.0000
0.10	12.000	12.000	4.0000	2.0000	-6.0000	-6.0000
0.15	12.000	12.000	4.0000	2.0000	-6.0000	-6.0000
0.20	11.999	12.000	4.0000	2.0000	-5.9999	-6.0001
0.25	11.999	12.001	4.0000	2.0000	-5.9998	-6.0001
0.30	11.997	12.001	3.9999	2.0001	-5.9996	-6.0003
0.35	11.994	12.002	3.9999	2.0001	-5.9992	-6.0005
0.40	11.990	12.003	3.9998	2.0002	-5.9987	-6.0008
0.45	11.985	12.005	3.9996	2.0003	-5.9979	-6.0013
0.50	11.977	12.008	3.9994	2.0004	-5.9967	-6.0019
0.55	11.966	12.012	3.9991	2.0007	-5.9952	-6.0028
0.60	11.952	12.017	3.9988	2.0009	-5.9932	-6.0040
0.65	11.934	12.023	3.9983	2.0013	-5.9906	-6.0055
0.70	11.911	12.031	3.9977	2.0017	-5.9874	-6.0074
0.75	11.882	12.041	3.9970	2.0023	-5.9834	-6.0098
0.80	11.848	12.053	3.9961	2.0029	-5.9785	-6.0127
0.85	11.806	12.067	3.9950	2.0037	-5.9726	-6.0162
0.90	11.756	12.084	3.9937	2.0047	-5.9656	-6.0203
0.95	11.697	12.105	3.9922	2.0058	-5.9573	-6.0253
1.00	11.628	12.129	3.9905	2.0072	-5.9475	-6.0310
1.05	11.548	12.157	3.9884	2.0087	-5.9362	-6.0377
1.10	11.455	12.189	3.9860	2.0105	-5.9231	-6.0455
1.15	11.349	12.226	3.9833	2.0125	-5.9082	-6.0544
1.20	11.228	12.268	3.9802	2.0149	-5.8911	-6.0645
1.25	11.091	12.316	3.9767	2.0175	-5.8717	-6.0760
1.30	10.936	12.370	3.9727	2.0205	-5.8498	-6.0890
1.35	10.762	12.431	3.9682	2.0239	-5.8252	-6.1036
1.40	10.568	12.499	3.9632	2.0277	-5.7976	-6.1200
1.45	10.351	12.575	3.9576	2.0319	-5.7669	-6.1382
1.50	10.110	12.659	3.9514	2.0366	-5.7328	-6.1586
1.55	9.8438	12.753	3.9445	2.0418	-5.6951	-6.1811
1.60	9.5499	12.857	3.9369	2.0475	-5.6534	-6.2060
1.65	9.2266	12.971	3.9285	2.0538	-5.6075	-6.2334
1.70	8.8719	13.097	3.9193	2.0608	-5.5571	-6.2636
1.75	8.4837	13.235	3.9092	2.0684	-5.5019	-6.2968
1.80	8.0599	13.387	3.8982	2.0768	-5.4415	-6.3331
1.85	7.5981	13.552	3.8862	2.0859	-5.3757	-6.3727
1.90	7.0960	13.733	3.8731	2.0958	-5.3040	-6.4160
1.95	6.5511	13.930	3.8588	2.1067	-5.2261	-6.4631
2.00	5.9608	14.144	3.8433	2.1184	-5.1417	-6.5143
2.05	5.3224	14.377	3.8265	2.1312	-5.0502	-6.5700
2.10	4.6331	14.630	3.8084	2.1451	-4.9512	-6.6304
2.15	3.8898	14.905	3.7887	2.1601	-4.8443	-6.6958
2.20	3.0895	15.202	3.7675	2.1764	-4.7289	-6.7667
2.25	2.2287	15.524	3.7447	2.1939	-4.6046	-6.8433
2.30	1.3041	15.872	3.7200	2.2129	-4.4707	-6.9261
2.35	.31185	16.248	3.6935	2.2334	-4.3267	-7.0156
2.40	-.75186	16.655	3.6649	2.2555	-4.1720	-7.1122
2.45	-1.8912	17.095	3.6341	2.2793	-4.0058	-7.2164

TABLE 4.1 Continued

ϕ	$SVY_1\left(\frac{L^3}{EI}\right)$	$SVY_2\left(\frac{L^3}{EI}\right)$	$SM\theta_1\left(\frac{L}{EI}\right)$	$SM\theta_2\left(\frac{L}{EI}\right)$	$SMY_1\left(\frac{L^2}{EI}\right)$	$SMY_2\left(\frac{L^2}{EI}\right)$
2.50	-3.1105	17.569	3.6011	2.3050	-3.8273	-7.3288
2.55	-4.4145	18.082	3.5656	2.3327	-3.6359	-7.4500
2.60	-5.8081	18.636	3.5275	2.3625	-3.4307	-7.5807
2.65	-7.2968	19.233	3.4865	2.3947	-3.2107	-7.7217
2.70	-8.8861	19.879	3.4426	2.4293	-2.9749	-7.8736
2.75	-10.582	20.576	3.3954	2.4666	-2.7222	-8.0375
2.80	-12.392	21.329	3.3447	2.5068	-2.4515	-8.2144
2.85	-14.322	22.144	3.2903	2.5501	-2.1615	-8.4052
2.90	-16.381	23.025	3.2319	2.5969	-1.8506	-8.6112
2.95	-18.577	23.978	3.1691	2.6473	-1.5175	-8.8338
3.00	-20.919	25.011	3.1016	2.7018	-1.1602	-9.0745
3.05	-23.417	26.131	3.0290	2.7607	-0.77688	-9.3349
3.10	-26.083	27.346	2.9509	2.8243	-0.36543	-9.6169
3.15	-28.929	28.667	2.8667	2.8933	.076568	-9.9228
3.20	-31.969	30.105	2.7759	2.9681	.55180	-10.255
3.25	-35.218	31.671	2.6779	3.0493	1.0633	-10.616
3.30	-38.694	33.381	2.5720	3.1375	1.6145	-11.009
3.35	-42.415	35.250	2.4573	3.2337	2.2092	-11.438
3.40	-46.405	37.299	2.3329	3.3386	2.8520	-11.907
3.45	-50.688	39.548	2.1977	3.4534	3.5480	-12.420
3.50	-55.294	42.024	2.0505	3.5792	4.3030	-12.984
3.55	-60.257	44.757	1.8897	3.7174	5.1241	-13.604
3.60	-65.614	47.783	1.7138	3.8698	6.0193	-14.290
3.65	-71.413	51.144	1.5206	4.0384	6.9980	-15.049
3.70	-77.708	54.890	1.3078	4.2254	8.0718	-15.892
3.75	-84.564	59.084	1.0724	4.4338	9.2542	-16.834
3.80	-92.059	63.799	8.1084	4.6670	10.562	-17.890
3.85	-100.29	69.127	.51891	4.9294	12.015	-19.080
3.90	-109.37	75.182	.19119	5.2262	13.638	-20.429
3.95	-119.46	82.108	-1.17904	5.5641	15.464	-21.967
4.00	-130.73	90.087	-.60034	5.9516	17.531	-23.734
4.05	-143.44	99.356	-.10838	6.3997	19.891	-25.782
4.10	-157.89	110.23	-1.6439	6.9230	22.613	-28.176
4.15	-174.52	123.12	-2.3004	7.5410	25.787	-31.009
4.20	-193.91	138.62	-3.0802	8.2805	29.539	-34.406
4.25	-216.88	157.55	-4.0214	9.1797	34.047	-38.542
4.30	-244.66	181.11	-5.1801	10.294	39.571	-43.678
4.35	-279.08	211.14	-6.6415	11.710	46.507	-50.210
4.40	-323.10	250.59	-8.5427	13.563	55.494	-58.774
4.45	-381.82	304.55	-11.119	16.089	67.622	-70.462
4.50	-464.71	382.49	-14.808	19.727	84.932	-87.313
4.55	-591.78	504.41	-20.539	25.403	111.73	-113.63
4.60	-813.86	721.13	-30.662	35.469	158.95	-160.36
4.65	-1308.7	1210.4	-53.407	58.155	264.84	-265.72
4.70	-3437.2	3333.1	-151.79	15.648	722.25	-722.58
4.75	5077.2	-5187.3	242.62	-238.00	-1110.5	1110.7
4.80	1414.6	-1531.0	73.219	-68.666	-323.03	232.85
4.85	801.16	-924.13	45.008	-40.525	-191.71	193.15
4.90	545.65	-675.41	33.375	-28.966	-137.43	139.51

TABLE 4.1 Continued

ϕ	$SVY_1\left(\frac{L^3}{EI}\right)$	$SVY_2\left(\frac{L^3}{EI}\right)$	$SM\theta_1\left(\frac{L}{EI}\right)$	$SM\theta_2\left(\frac{L}{EI}\right)$	$SMY_1\left(\frac{L^2}{EI}\right)$	$SMY_2\left(\frac{L^2}{EI}\right)$
4.95	403.83	-540.67	27.014	-22.682	-107.64	110.39
5.00	312.42	-456.62	22.994	-18.743	-88.720	92.175
5.05	247.67	-399.54	20.217	-16.050	-75.564	79.752
5.10	198.68	-358.53	18.178	-14.099	-65.827	70.780
5.15	159.73	-327.88	16.612	-12.625	-58.280	64.031
5.20	127.54	-304.34	15.367	-11.477	-52.214	58.800
5.25	100.07	-285.87	14.350	-10.560	-47.196	54.655
5.30	76.004	-271.19	13.500	-9.8160	-42.942	51.313
5.35	54.444	-259.41	12.775	-9.2024	-39.260	48.586
5.40	34.756	-249.91	12.147	-8.6908	-36.015	46.340
5.45	16.477	-242.26	11.595	-8.2606	-33.108	44.479
5.50	-737.65	-236.13	11.104	-7.8966	-30.467	42.934
5.55	-17.155	-231.29	10.660	-7.5873	-28.035	41.651
5.60	-32.984	-227.54	10.256	-7.3239	-25.770	40.590
5.65	-48.393	-224.76	9.8832	-7.0996	-23.637	39.721
5.70	-63.521	-222.83	9.5368	-6.9091	-21.607	39.019
5.75	-78.482	-221.67	9.2116	-6.7481	-19.659	38.465
5.80	-93.378	-221.23	8.9038	-6.6134	-17.771	38.045
5.85	-108.30	-221.44	8.6101	-6.5021	-15.928	37.748
5.90	-123.31	-222.29	8.3275	-6.4121	-14.115	37.563
5.95	-138.50	-223.75	8.0536	-6.3419	-12.320	37.485
6.00	-153.93	-225.81	7.7862	-6.2899	-10.530	37.509
6.05	-169.67	-228.46	7.5233	-6.2553	-8.7356	37.630
6.10	-185.78	-231.71	7.2632	-6.2373	-6.9251	37.849
6.15	-202.31	-235.57	7.0041	-6.2353	-5.0893	38.163
6.20	-219.35	-240.05	6.7444	-6.2490	-3.2181	38.574
6.25	-236.95	-245.19	6.4825	-6.2785	-1.3018	39.084
6.30	-255.19	-251.02	6.2169	-6.3237	.66989	39.606
6.35	-274.14	-257.58	5.9459	-6.3850	2.7076	40.418
6.40	-293.89	-264.93	5.6679	-6.4630	4.8227	41.243
6.45	-314.53	-273.13	5.3812	-6.5584	7.0275	42.192
6.50	-336.15	-282.26	5.0838	-6.6720	9.3354	43.269

4.4.2. Rayleigh's Dynamic Reciprocal Principle

In Eq. (4.25), the moment, M_i , at end i due to steady-state joint rotation, θ_i , is equal to the moment, M_j , due to the same steady-state joint rotation at end j , θ_j . Similarly, M_i due to θ_j is the same as M_j due to θ_i . This phenomenon of force-displacement relationships is similar to Rayleigh's dynamic reciprocal principle of displacement-force relationships. Rayleigh's principle may be stated as follows: *If i and j denote two points in a given structure, then the steady-state displacement at i produced by a harmonically varying load applied at j is equal to the steady-state displacement at j due to the same load applied at i .* The term displacement may be interpreted in a general sense as either linear or angular displacement, and the term load may be interpreted in the same general sense as either force or couple. Couples correspond to rotation, whereas forces correspond to linear displacements.

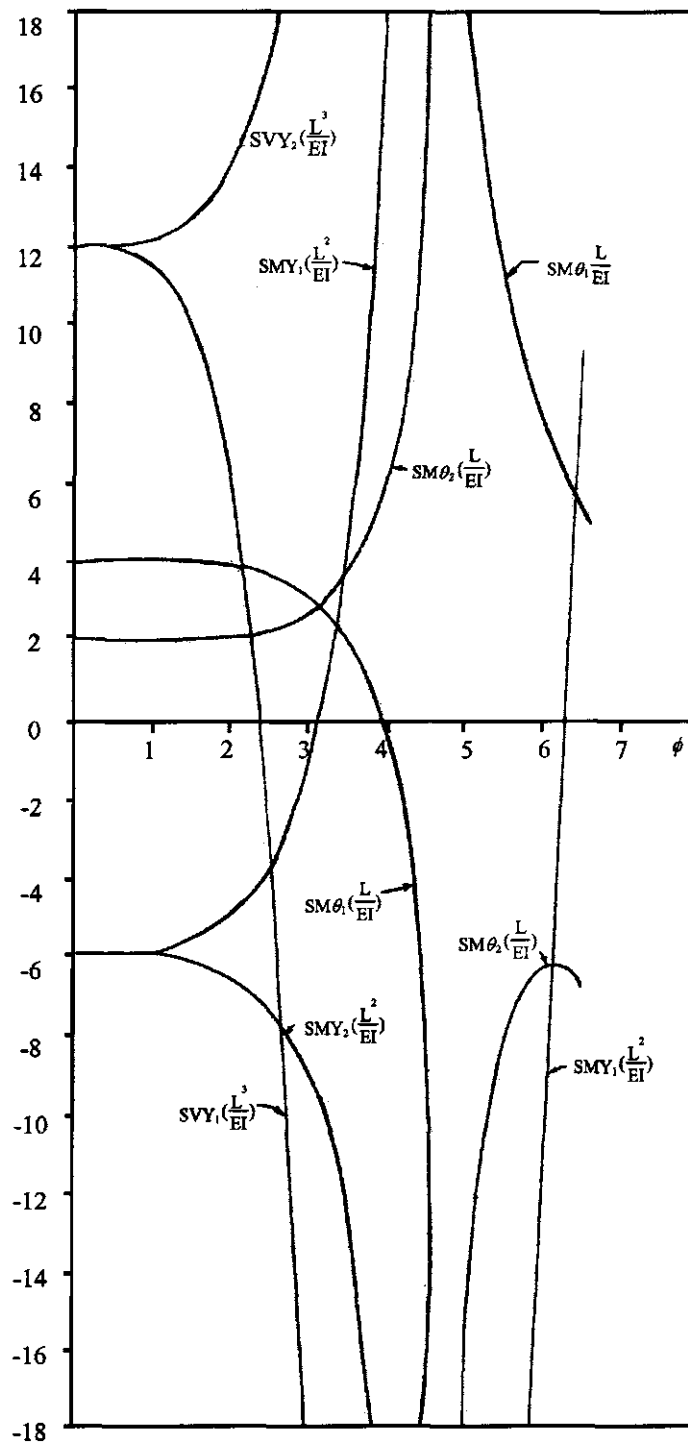


FIG. 4.5 Stiffness coefficients.

4.4.3. Müller-Breslau's Principle

By using Rayleigh's reciprocal relations, it can be readily proven that Müller-Breslau's principle is also applicable to the case of steady-state forced vibration. This principle states that *the influence line for any dynamic function, such as reaction, shear, bending moment, or torque, at some point, i, of a structure due to harmonically varying load can be obtained as the deflected shape of the structure due to a small unit displacement, either linear or angular, introduced at point i.*

It follows from this principle that the elastic curve of a fixed-end beam resulting from a unit rotation at one end represents an influence line for a fixed-end dynamic moment due to a unit-concentrated harmonically varying force on the beam. Similarly, the elastic curve of a beam resulting from a unit deflection at one end (no rotation at that end) represents an influence line for fixed-end dynamic shear due to a unit-concentrated harmonically varying force.

EXAMPLE 4.4.1 Prove that the dynamic stiffness coefficient, $SM\theta_1$, at the extreme condition of low frequency, ($\phi \rightarrow 0$), is equal to the static stiffness, $4EI/L$.

Solution: From Eq. (4.25)

$$SM\theta_1 = \frac{\sinh \phi \cos \phi - \cosh \phi \sin \phi}{\cosh \phi \cos \phi - 1} \frac{\phi EI}{L} \quad (a)$$

When ϕ is equal to zero, $SM\theta_1 = 0/0$ is an indeterminate form. The exact limit of $SM\theta_1$ can be found by using L'Hospital's rule to take the derivative of both the numerator and denominator with respect to ϕ and then let ϕ approach zero as a limit. The differentiation of Eq. (a) yields

$$SM\theta_1 = \frac{-2\phi \sin \phi \sinh \phi + \sinh \phi \cos \phi - \sin \phi \cosh \phi}{\sinh \phi \cos \phi - \cosh \phi \sin \phi} \frac{EI}{L} \quad (b)$$

which is still indeterminate when $\phi = 0$. Thus the L'Hospital operation must be performed on Eq. (b) and again yields an indeterminate result. Repeating the operation once more gives

$$SM\theta_1 = \frac{4\phi(\sinh \phi \cos \phi - \cosh \phi \sin \phi) + 16 \cosh \phi \cos \phi}{4 \cosh \phi \cos \phi} \frac{EI}{L} \quad (c)$$

which finally yields when ϕ approaches zero

$$SM\theta_1 = \frac{4EI}{L} \quad (d)$$

EXAMPLE 4.4.2 Numerical values of the stiffness coefficients corresponding to $\phi = 3$ can be obtained from Table 4.1 as follows: $SM\theta_1 = 3.1016 EI/L$, $SM\theta_2 = 2.7018 EI/L$, $SMY_1 = -1.1602 EI/L^2$, and $SMY_2 = -9.9745 EI/L^2$. These coefficients represent the moments and shears at both ends of the beam shown in Fig. 4.6 having a rotated end at i and a restrained end at j . Prove that the summation of all vertical forces, including the inertia force, is equal to zero.

Solution: The dynamic forces shown in Fig. 4.6 are based on the positive sign of the forces and deformations used for deriving stiffness coefficients. The summation of all vertical forces gives

$$g(t)SMY_1 - g(t)SMY_2 + \int_0^L m\ddot{y}(x, t) dx = 0 \quad (a)$$

Since the general expression of an elastic curve is

$$y(x, t) = Y(x)g(t) \quad (b)$$

the acceleration is the second derivation of $y(x, t)$ with respect to t

$$\ddot{y}(x, t) = -p^2 g(t)(A \sin \lambda x + B \cos \lambda x + C \sinh \lambda x + D \cosh \lambda x) \quad (c)$$

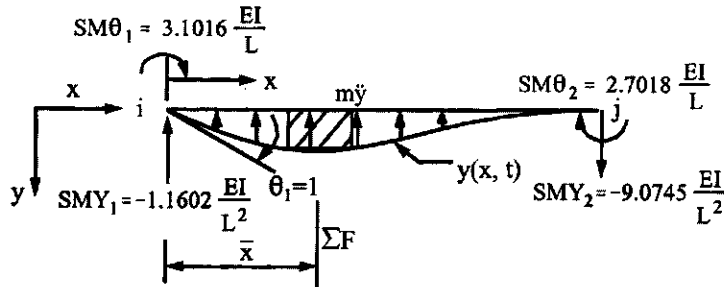


FIG. 4.6 Example 4.4.2.

Therefore, substituting Eq. (c) into the left-hand side of the following equation, using $p^2 = \lambda^4 EI/m$, and performing integration, we have

$$\int_0^L m\ddot{y}(x, t) dx = -g(t)\lambda^3 EI[A(1 - \cos \lambda L) + B \sin \lambda L + C(\cosh \lambda L - 1) + D \sinh \lambda L] \quad (d)$$

where λL is expressed in terms of ϕ , and A , B , C , and D should be determined by applying the boundary deformations, i.e. $\theta_i \neq 0$, $\theta_j = Y_i = Y_j = 0$, to the shape function. The solutions are actually given in the first column of Eq. (4.23), which are now substituted into Eq. (d) for $\theta_i = 1$; then

$$\int_0^L m\ddot{y} dx = g(t) \frac{\sin h \phi \sin \phi + \cos \phi - \cos h \phi}{1 - \cos h \phi \cos \phi} \frac{\phi^2 EI}{L^2} \quad (e)$$

For $\phi = 3$, $\sin 3 = 0.1410$, $\cos 3 = -0.9900$, $\sinh 3 = 10.0179$, and $\cosh 3 = 10.0677$, Eq. (e) becomes

$$g(t) \frac{(10.0179)(0.1410) - 0.9900 - 10.0677}{1 - (10.0677)(-0.9900)} \frac{9EI}{L^2} = -7.910 \frac{EI}{L^2} g(t) \quad (f)$$

Substituting Eq. (f) and the given values of SMY_1 and SMY_2 into Eq. (a) yields the desired result as follows:

$$-1.1602 \frac{EI}{L^2} g(t) - \left(-9.0745 \frac{EI}{L^2}\right) g(t) + \left(-7.910 \frac{EI}{L^2}\right) g(t) = 0 \quad (g)$$

The centroid of the inertia force is

$$\bar{x} = \frac{\int_0^L x m\ddot{y}(x, t) dx}{\int_0^L m\ddot{y}(x, t) dx} \quad (h)$$

Inserting x into Eq. (d), and then performing integration, yield $-3.2707 (EI/L)g(t)$. Substituting

the result along with Eq. (f) into Eq. (h) leads to

$$\bar{x} = \frac{-3.2707(EI/L)g(t)}{-7.910(EI/L^2)g(t)} = 0.413L \quad (i)$$

4.5. DYNAMIC STIFFNESS, LOAD, AND MASS MATRICES

4.5.1. Degree-of-Freedom of Plane Structural Systems

To formulate a structural stiffness matrix, the d.o.f. of the system must be known. In general, a plane elastic structure has three generalized displacements at each node, including the supports; the restraints that are imposed on the displacements by the supports are three for a fixed support, two for a hinged support, and one for a roller support. However, a rigid frame has one more restraint from each constituent member because the axial deformation is neglected. Let NFJ , NHJ , and NRJ be the number of fixed, hinged, and roller supports, respectively, and NJ and NM the number of structural joints and members, respectively.

Then total d.o.f., NP , of an elastic structure is

$$NP = 3NJ - (3NFJ + 2NHJ + NRJ) \quad (4.27a)$$

Total d.o.f. of a rigid frame is

$$NP = 3NJ - (3NFJ + 2NHJ + NRJ + NM) \quad (4.27b)$$

Total d.o.f. of a truss (two possible displacements at each joint) is

$$NP = 2NJ - (2NHJ + NRJ) \quad (4.27c)$$

The number of possible joint rotations, NPR , of a plane framework is the difference between the number of structural joints and the number of fixed supports (including guide support)

$$NPR = NJ - NFJ$$

Total d.o.f. in linear displacements, NPS , of an elastic structure is

$$NPS = 2NJ - (2NFJ + 2NHJ + NRJ) \quad (4.27d)$$

Total d.o.f. in side-sway of a rigid frame is

$$NPS = 2NJ - (2NFJ + 2NHJ + NRJ + NM) \quad (4.27e)$$

Let the structure given in Fig. 4.7a be subjected to harmonically varying forces and foundation movement of which the members are numbered 1–5. The d.o.f. in rotation, NPR , are assigned in the accompanying Fig. 4.7b as P_θ 's and X_θ 's, which signify externally rotational forces and displacements, respectively. Similarly, the d.o.f. in side-sway, NPS , are assigned as P_s 's and X_s 's for externally transverse forces and displacements, respectively. These actions are also called *generalized forces and displacements*. In Fig. 4.7b each member is assigned i and j , which represent the end forces and deformations of that member in conformity with the sign convention used for deriving stiffness coefficients as sketched in Fig. 4.4. Thus the positive moments and shears of individual members are assigned in Fig. 4.7c where the odd and even numbers represent i and j , respectively: for instance, 1 and 2 for member 1; 3 and 4 for member 2. Similarly the fixed-end moments, M_0 , and the fixed-end shears, V_0 , are designated as M_{03} , M_{04} , V_{03} and V_{04} for member 2, M_{05} , M_{06} , V_{05} , and V_{06} for member 3. Members 1 and 5 do not have fixed-end forces.

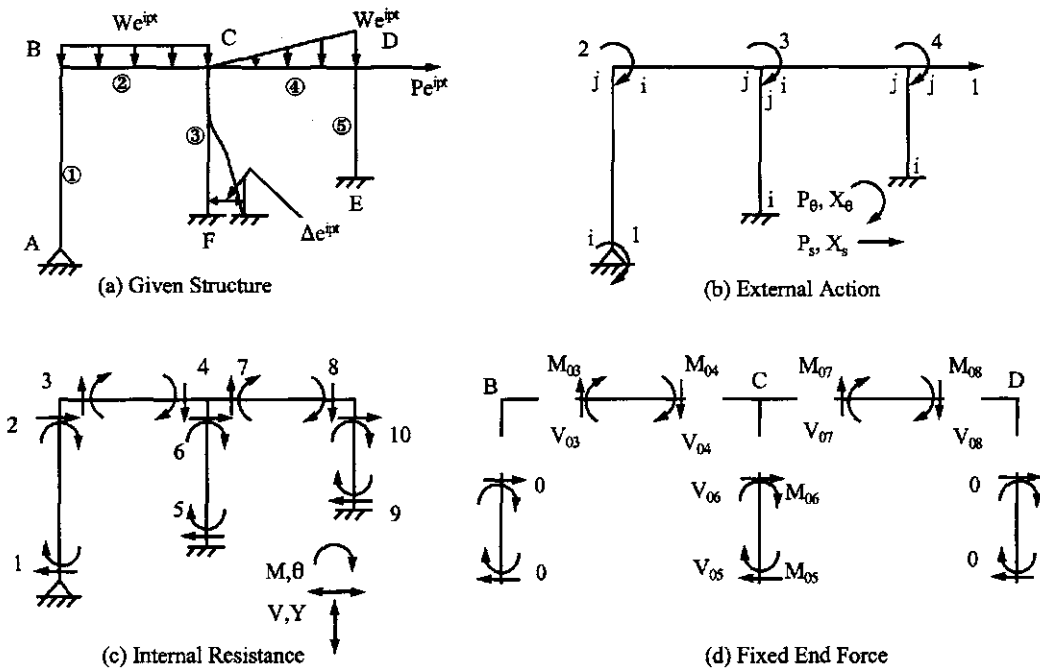


FIG. 4.7 Structure and diagrams.

For the frame, the d.o.f. in rotation is

$$NPR = NJ - NFJ = 6 - 2 = 4 \quad (4.28a)$$

and the d.o.f. in side-sway is

$$NPS = 2NJ - (2NFJ + 2NHJ + NRJ + NM) = 2(6) - [2(2) + 2(1) + 0 + 5] = 1 \quad (4.28b)$$

4.5.2. Equilibrium Matrices

Based on the diagrams shown in Fig. 4.7b and c, we may establish the equilibrium equations as:
at joint *A*

$$\Sigma M_A = 0; \quad P_{θ1} = M_1 \quad (4.29)$$

at joint *B*

$$\Sigma M_B = 0; \quad P_{θ2} = M_2 + M_3 \quad (4.30)$$

at joint *C*

$$\Sigma M_C = 0; \quad P_{θ3} = M_4 + M_6 + M_7 \quad (4.31)$$

at joint *D*

$$\Sigma M_D = 0; \quad P_{θ4} = M_8 + M_{10} \quad (4.32)$$

for member BCD

$$\Sigma F_x = 0; \quad P_{s1} = V_2 + V_6 + V_{10} \quad (4.33)$$

In notation, Eqs. (4.29)–(4.32) can be represented by

$$\{P_\theta\} = [A_\theta] \{M\} \quad (4.34a)$$

where

$$[A_\theta] = \begin{bmatrix} 1 & 0 & 0 & 0 & 0 & 0 & 0 & 0 & 0 & 0 \\ 0 & 1 & 1 & 0 & 0 & 0 & 0 & 0 & 0 & 0 \\ 0 & 0 & 0 & 1 & 0 & 1 & 1 & 0 & 0 & 0 \\ 0 & 0 & 0 & 0 & 0 & 0 & 0 & 1 & 0 & 1 \end{bmatrix} \quad (4.34b)$$

Eq. (4.33) becomes

$$\{P_s\} = [A_s] \{V\} \quad (4.35a)$$

and

$$[A_s] = [0 \ 1 \ 0 \ 0 \ 0 \ 1 \ 0 \ 0 \ 0 \ 1] \quad (4.35b)$$

$[A_\theta]$ and $[A_s]$ are *equilibrium matrices* for moments and shears, respectively. Note that the external loads, $\{P_\theta\}$ and $\{P_s\}$, and the internal forces, $\{M\}$ and $\{V\}$, have a time-function, e^{ipt} . Since e^{ipt} cannot be zero at anytime, t , it can be cancelled out and is therefore not shown in Eqs. (4.34a) and (4.35a). The same concept of not including e^{ipt} is applied to the following derivation of compatibility, structural stiffness, load, and system matrices.

4.5.3. Compatibility Matrices

Using kinematic analysis, the relationship between internal deformations (see Fig. 4.7c) and external displacements (see Fig. 4.7b), $\{\theta\}$ vs $\{X_\theta\}$ and $\{Y\}$ vs $\{X_s\}$, may be formulated as follows:

$$X_{\theta 1} \neq 0, \quad X_{\theta 2} = X_{\theta 3} = X_{\theta 4} = X_{s1} = 0, \quad \theta_1 = X_{\theta 1} \quad (4.36)$$

$$X_{\theta 2} \neq 0, \quad X_{\theta 1} = X_{\theta 3} = X_{\theta 4} = X_{s1} = 0, \quad \theta_2 = \theta_3 = X_{\theta 2} \quad (4.37)$$

$$X_{\theta 3} \neq 0, \quad X_{\theta 1} = X_{\theta 2} = X_{\theta 4} = X_{s1} = 0, \quad \theta_4 = \theta_6 = \theta_7 = X_{\theta 3} \quad (4.38)$$

$$X_{\theta 4} \neq 0, \quad X_{\theta 1} = X_{\theta 2} = X_{\theta 3} = X_{s1} = 0, \quad \theta_8 = \theta_{10} = X_{\theta 4} \quad (4.39)$$

$$X_{s1} \neq 0, \quad X_{\theta 1} = X_{\theta 2} = X_{\theta 3} = X_{\theta 4} = 0, \quad Y_2 = Y_6 = Y_{10} = X_{s1} \quad (4.40)$$

Expressing Eqs. (4.36)–(4.39) in matrix form gives

$$\{\theta\} = [B_\theta] \{X_\theta\} \quad (4.41a)$$

and

$$[B_\theta] = \begin{bmatrix} 1 & 0 & 0 & 0 \\ 0 & 1 & 0 & 0 \\ 0 & 1 & 0 & 0 \\ 0 & 0 & 1 & 0 \\ 0 & 0 & 0 & 0 \\ 0 & 0 & 1 & 0 \\ 0 & 0 & 1 & 0 \\ 0 & 0 & 0 & 1 \\ 0 & 0 & 0 & 0 \\ 0 & 0 & 0 & 1 \end{bmatrix} \quad (4.41b)$$

Similarly, Eq. (4.40) yields

$$\{Y\} = [B_s]\{X_s\} \quad (4.42a)$$

and

$$[B_s] = [0 \ 1 \ 0 \ 0 \ 0 \ 1 \ 0 \ 0 \ 0 \ 1]^T \quad (4.42b)$$

$[B_\theta]$ and $[B_s]$ are *compatibility matrices* or *kinematic matrices*.

4.5.4. Dynamic Stiffness Matrix

Similar to the expression of stiffness coefficients in Eq. (4.26), the internal forces of a system may be expressed as

$$\{M\} = [SM\theta]\{\theta\} + [SMY]\{Y\} \quad (4.43)$$

$$\{V\} = [SMY]\{\theta\} + [SVY]\{Y\} \quad (4.44)$$

where the dimensions of $[SM\theta]$, $[SMY]$, and $[SVY]$ are $2NM \times 2NM$ for a structure composed of NM members. Substituting Eqs. (4.41a) and (4.42a) into the above yields

$$\{M\} = [SM\theta][B_\theta]\{X_\theta\} + [SMY][B_s]\{X_s\} \quad (4.45)$$

$$\{V\} = [SMY][B_\theta]\{X_\theta\} + [SVY][B_s]\{X_s\} \quad (4.46)$$

Using the above expressions of internal forces in Eqs. (4.34a) and (4.35a), the relationship between external forces and external displacements takes the following form:

$$\begin{Bmatrix} P_\theta \\ P_s \end{Bmatrix} = \begin{bmatrix} A_\theta & | & 0 \\ 0 & | & A_s \end{bmatrix} \begin{bmatrix} SM\theta & | & SMY \\ SMY & | & SVY \end{bmatrix} \begin{bmatrix} B_\theta & | & 0 \\ 0 & | & B_s \end{bmatrix} \begin{Bmatrix} X_\theta \\ X_s \end{Bmatrix} \quad (4.47)$$

in which the *structural stiffness matrix* may be represented by

$$[K] = \begin{bmatrix} A_\theta & | & 0 \\ 0 & | & A_s \end{bmatrix} \begin{bmatrix} SM\theta & | & SMY \\ SMY & | & SVY \end{bmatrix} \begin{bmatrix} B_\theta & | & 0 \\ 0 & | & B_s \end{bmatrix} \quad (4.48)$$

Now the relationship between equilibrium matrices and compatibility matrices is examined. If a set of virtual displacements, $[X_\theta|X_s]_e^T$, is imposed on the nodal points of a system, the virtual work done on this system is

$$W = \begin{Bmatrix} X_\theta \\ X_s \end{Bmatrix}_e^T \begin{Bmatrix} P_\theta \\ P_s \end{Bmatrix} \quad (4.49)$$

Combining Eqs. (4.47) and (4.48) with Eq. (4.49) gives

$$W = \begin{Bmatrix} X_\theta \\ X_s \end{Bmatrix}_e^T [K] \begin{Bmatrix} X_\theta \\ X_s \end{Bmatrix} \quad (4.50)$$

The virtual deformations, corresponding to $[X_\theta|X_s]_e^T$, of all the constituent members are

$$\begin{Bmatrix} \theta \\ - \\ Y \end{Bmatrix}_e = \begin{bmatrix} B_\theta & | & 0 \\ - & - & - \\ 0 & | & B_s \end{bmatrix} \begin{Bmatrix} X_\theta \\ - \\ X_s \end{Bmatrix}_e \quad (4.51)$$

which gives the following strain energy gained in the system

$$U = \begin{Bmatrix} \theta \\ - \\ Y \end{Bmatrix}_e^T \begin{Bmatrix} M \\ - \\ V \end{Bmatrix} = \begin{Bmatrix} X_\theta \\ - \\ X_s \end{Bmatrix}_e^T \begin{bmatrix} B_\theta & | & 0 \\ - & - & - \\ 0 & | & B_s \end{bmatrix}^T \begin{bmatrix} SM\theta & | & SMY \\ - & - & - \\ SMY & | & SVY \end{bmatrix} \begin{bmatrix} B_\theta & | & 0 \\ - & - & - \\ 0 & | & B_s \end{bmatrix} \begin{Bmatrix} X_\theta \\ - \\ X_s \end{Bmatrix}_e \quad (4.52)$$

Since external work must be equal to internal energy, the equality between Eqs. (4.50) and (4.52) gives

$$[K] = \begin{bmatrix} B_\theta & | & 0 \\ - & - & - \\ 0 & | & B_s \end{bmatrix}^T \begin{bmatrix} SM\theta & | & SMY \\ - & - & - \\ SMY & | & SVY \end{bmatrix} \begin{bmatrix} B_\theta & | & 0 \\ - & - & - \\ 0 & | & B_s \end{bmatrix} \quad (4.53)$$

Note that both Eqs. (4.48) and (4.53) represent the structural stiffness matrix, if and only if they are equal

$$\begin{bmatrix} A_\theta & | & 0 \\ - & - & - \\ 0 & | & A_s \end{bmatrix} = \begin{bmatrix} B_\theta & | & 0 \\ - & - & - \\ 0 & | & B_s \end{bmatrix}^T \quad (4.54)$$

Thus, the transpose of the equilibrium matrix is equal to the compatibility matrix.

It must be pointed out that the above equations [Eqs. (4.48)–(4.53)] only serve to explain the mechanics of $[K]$ formulation. In practice, it is much more convenient to use either the *direct stiffness method* or *physical interpretation*. The direct stiffness method forms the stiffness of an individual member and then matches the local coordinates of that member with the global coordinates of the system. Physical interpretation means that by moving a unit displacement of each d.o.f. of a system, one at a time, we then find the unbalanced forces at the structural nodes due to the unit displacement. This establishes the stiffness in one column of $[K]$ corresponding to that d.o.f. The approach is particularly efficient in longhand procedures.

4.5.5. Dynamic Load Matrix

In Eq. (4.47), the external load matrix, $[P_\theta|P_s]^T$, is due to applied forces at the structural nodes or unbalanced forces at the nodes resulting from fixed-end moments and shears. Fig. 4.7d illustrates formulation procedures where the fixed-end moments, M_0 , and shears, V_0 , are sketched in positive direction at the member's ends. The fixed-end forces are then transferred to nodal points at which the unbalanced moments and shears are

$$P_{\theta 1} = 0 \quad (4.55)$$

$$-P_{\theta 2} = M_{03} \quad (4.56)$$

$$-P_{\theta 3} = M_{04} + M_{06} + M_{07} \quad (4.57)$$

$$-P_{\theta 4} = M_{08} \quad (4.58)$$

$$-P_{s1} = V_{06} - P \quad (4.59)$$

In matrix form

$$\begin{Bmatrix} P_{\theta 1} \\ P_{\theta 2} \\ P_{\theta 3} \\ P_{\theta 4} \\ \vdots \\ P_s \end{Bmatrix} = \begin{Bmatrix} 0 \\ -M_{03} \\ -M_{04} & -M_{06} & -M_{07} \\ -M_{08} \\ \vdots & \vdots & \vdots \\ -V_{06} & +P \end{Bmatrix} \quad (4.60)$$

which is the *dynamic load matrix*.

4.5.6. System Matrix Equation

The system matrix equation of a rigid frame with side-sway expresses the relationship between external loads and external displacements by using the dynamic stiffness matrix, which is then combined with the mass matrix derived from given members' rigid-body motion in the frame. For instance, members *BC* and *CD* in Fig. 4.7 have rigid-body motion resulting from displacement, $X_{s1}e^{ipt}$, which induces the following inertia forces:

$$m_2 L_2 \frac{d^2}{dt^2} (X_{s1} e^{ipt}) + m_4 L_4 \frac{d^2}{dt^2} (X_{s1} e^{ipt}) = -p^2 (m_2 L_2 + m_4 L_4) X_{s1} e^{ipt} \quad (4.61)$$

The system matrix equation of this two-bay, one-story frame should be a combination of Eqs. (4.47), (4.60), and (4.61) as follows:

$$\begin{Bmatrix} P_\theta \\ \vdots \\ P_s \end{Bmatrix} = \left(\begin{bmatrix} K_{11} & | & K_{12} \\ \vdots & \vdots & \vdots \\ K_{21} & | & K_{22} \end{bmatrix} - p^2 \begin{bmatrix} 0 & | & 0 \\ \vdots & \vdots & \vdots \\ 0 & | & M \end{bmatrix} \right) \begin{Bmatrix} X_\theta \\ \vdots \\ X_s \end{Bmatrix} \quad (4.62)$$

in which the load matrix is composed of lateral force directly applied to the structural node and fixed-end forces transferred to the nodes

$$\begin{Bmatrix} P_\theta \\ \vdots \\ P_s \end{Bmatrix} = -[0 \quad M_{03} \quad M_{04} + M_{06} + M_{07} \quad M_{08} \mid V_{06} - P]^T \quad (4.63)$$

The mass matrix is

$$[M] = [m_2 L_2 + m_4 L_4] \quad (4.64)$$

For a frame without side-sway, $\{P_s\}$ and $\{X_s\}$ should not be considered; then Eq. (4.62) becomes

$$\{P_\theta\} = [K_{11}] \{X_\theta\} \quad (4.65)$$

Similarly, for a frame without joint rotation, such as shear building, $\{P_\theta\}$ and $\{X_\theta\}$ can be omitted. Thus the system matrix equation becomes

$$\{P_s\} = ([K_{22}] - p^2 [M]) \{X_s\} \quad (4.66)$$

4.6. DERIVATION OF DYNAMIC FIXED-END MOMENTS AND FIXED-END SHEARS

The external loads or foundation movements of a structure are assumed to vary harmonically with time. The structure's response can therefore be treated as a steady-state vibration. If the load is applied to a member but not directly at a structural node, then we find the fixed-end moments

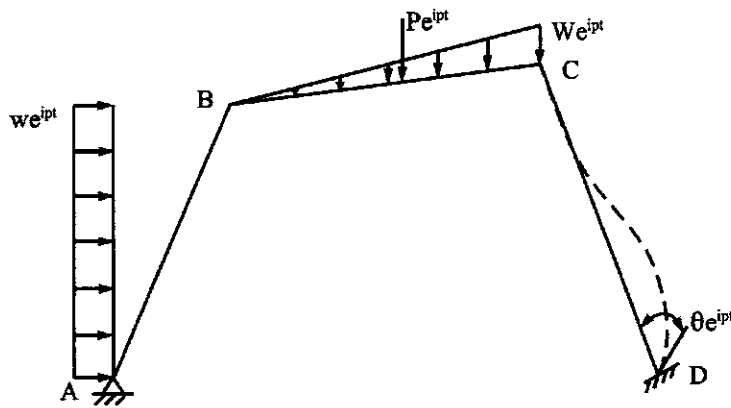


FIG. 4.8 Structure with various loadings.

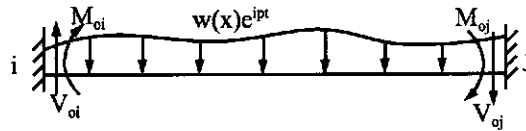


FIG. 4.9 Fixed-end beam.

and shears of the member and transfer them as unbalanced load to the structural nodes. The derivation of fixed-end forces is illustrated for the structure shown in Fig. 4.8, which is subjected to uniform load, triangular load, concentrated load, and foundation movement. The structure's load matrix is composed of unbalanced fixed-end moments and shears at structural nodal points *A*, *B*, *C*, and *D*.

4.6.1. Differential Equations

A typical fixed-end beam subjected to an arbitrarily distributed force, $w(x, t) = w(x)e^{ipt}$, is shown in Fig. 4.9, where the fixed-end moments, M_{0i} , M_{0j} , and fixed-end shears, V_{0i} , V_{0j} , at end *i* and end *j* are assumed to be in a positive direction. Note that the positive direction is the same as that used in deriving stiffness. The elastic curve of this beam can be obtained from the following nonhomogeneous differential equation with given boundary conditions

$$EI \frac{\partial^4 y(x, t)}{\partial x^4} + m \frac{\partial^2 y(x, t)}{\partial t^2} = w(x, t) \quad (4.67)$$

The derivation of this equation can be seen in Eqs. (4.1)–(4.11).

In view of harmonic excitations, the elastic curve varies harmonically in time, i.e.

$$y(x, t) = Y(x) e^{ipt} \quad (4.68)$$

Substituting Eq. (4.68) into Eq. (4.67) yields an ordinary differential equation

$$EI \frac{d^4 Y}{dx^4} - mp^2 Y = w(x) \quad (4.69)$$

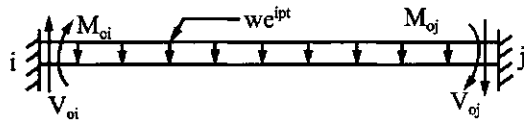


FIG. 4.10 Uniform load.

Using $\lambda^4 = mp^2/EI$ leads to

$$\frac{d^4 Y}{dx^4} - \lambda^4 Y = \frac{w(x)}{EI} \quad (4.70)$$

4.6.2. Uniform Load

Let us first study the case of the uniform load shown in Fig. 4.10 for which the differential equation is

$$\frac{d^4 Y}{dx^4} - \lambda^4 Y = \frac{w}{EI} \quad (4.71)$$

The complementary solution, Y_c , of Eq. (4.71) is the general expression of the shape function as shown in Eq. (4.19), and the particular solution, Y_p , can be obtained by trying the following polynomial equation:

$$Y_p = C_1 x^4 + C_2 x^3 + C_3 x^2 + C_4 x + C_5 \quad (4.72a)$$

Substituting Y_p into Eq. (4.71) yields

$$(24 - \lambda^4 x^4)C_1 - \lambda^4(C_2 x^3 + C_3 x^2 + C_4 x + C_5) = \frac{w}{EI} \quad (4.72b)$$

Compare both sides of the above equation,

$$C_1 = C_2 = C_3 = C_4 = 0 \quad \text{and} \quad C_5 = -\frac{w}{\lambda^4 EI} \quad (4.73)$$

Thus the complete solution of Eq. (4.71) is

$$Y = Y_c + Y_p = A \sin \lambda x + B \cos \lambda x + C \sinh \lambda x + D \cosh \lambda x - \frac{w}{\lambda^4 EI} \quad (4.74)$$

Using the boundary conditions in Eq. (4.75)

$$Y = 0 \quad \text{and} \quad \frac{dY}{dx} = 0 \quad \text{at } x = 0 \quad \text{and} \quad x = L \quad (4.75)$$

the arbitrary constants A , B , C , and D can be solved as

$$A = \frac{wL^4}{EI\phi^4} \left[\frac{\sin \phi + \sinh \phi - \cos \phi \sinh \phi - \cosh \phi \sin \phi}{2 - 2 \cos \phi \cosh \phi} \right] \quad (4.76)$$

$$B = \frac{wL^4}{EI\phi^4} \left[\frac{1 + \cos \phi - \cosh \phi - \cos \phi \cosh \phi + \sin \phi \sinh \phi}{2 - 2 \cos \phi \cosh \phi} \right] \quad (4.77)$$

$$C = \frac{wL^4}{EI\phi^4} \left[\frac{\cos \phi \sinh \phi + \sin \phi \cosh \phi - \sin \phi - \sinh \phi}{2 - 2 \cos \phi \cosh \phi} \right] \quad (4.78)$$

$$D = \frac{wL^4}{EI\phi^4} \left[\frac{1 - \cos \phi \cosh \phi - \sin \phi \sinh \phi - \cos \phi + \cosh \phi}{2 - 2 \cos \phi \cosh \phi} \right] \quad (4.79)$$

where $\phi = \lambda L$. The relationships between the fixed-end forces and deformations are

$$\frac{d^2 Y}{dx^2} \Big|_{x=0} = -\frac{M_{0i}}{EI} \quad \text{and} \quad \frac{d^2 Y}{dx^2} \Big|_{x=L} = \frac{M_{0j}}{EI} \quad (4.80)$$

$$\frac{d^3 Y}{dx^3} \Big|_{x=0} = -\frac{V_{0i}}{EI} \quad \text{and} \quad \frac{d^3 Y}{dx^3} \Big|_{x=L} = -\frac{V_{0j}}{EI} \quad (4.81)$$

Applying the above derivatives to Eq. (4.75) leads to M_{0i} , M_{0j} , V_{0i} , and V_{0j} expressed in terms of A , B , C , and D given by Eqs. (4.76)–(4.79). Consequently, the fixed-end moments and shears are

$$M_{0i} = \frac{wL^2}{\phi^2} \left[\frac{\cosh \phi - \cos \phi - \sin \phi \sinh \phi}{\cos \phi \cosh \phi - 1} \right] \quad (4.82)$$

$$V_{0i} = \frac{wL}{\phi} \left[\frac{\cos \phi \sinh \phi + \sin \phi \cosh \phi - \sin \phi - \sinh \phi}{\cos \phi \cosh \phi - 1} \right] \quad (4.83)$$

$$M_{0j} = -M_{0i} \quad (4.84)$$

$$V_{0j} = -V_{0i} \quad (4.85)$$

4.6.3. Triangular Load

A typical triangular load is shown in Fig. 4.11, for which the differential equation becomes

$$\frac{d^4 Y}{dx^4} - \lambda^4 Y = \frac{Wx}{EIL} \quad (4.86)$$

Substituting the polynomial equation from Eq. (4.72a) into the above yields

$$(24 - \lambda^4 x^4) C_1 - \lambda^4 (C_2 x^3 + C_3 x^2 + C_4 x + C_5) = \frac{Wx}{EIL} \quad (4.87)$$

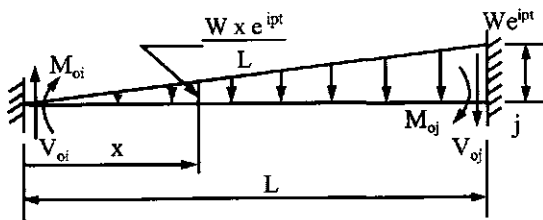
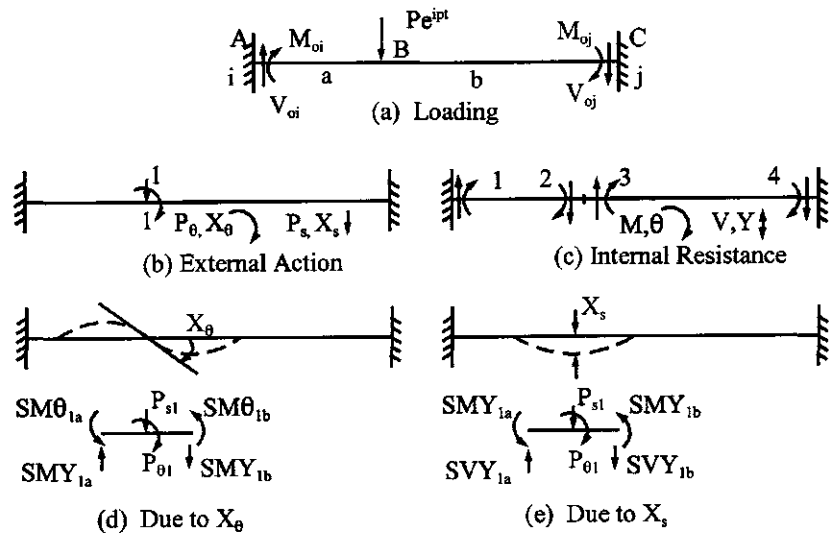


FIG. 4.11 Triangular load

**FIG. 4.12** Concentrated load.

Comparing both sides of the above equation leads to

$$C_1 = C_2 = C_3 = C_5 = 0 \quad \text{and} \quad C_4 = -\frac{W}{\lambda^4 EIL} \quad (4.88)$$

Thus the particular solution is

$$Y_p = -\frac{Wx}{\lambda^4 EIL} \quad (4.89)$$

and the complete solution is

$$Y = A \sin \lambda x + B \cos \lambda x + C \sinh \lambda x + D \cosh \lambda x - \frac{Wx}{\lambda^4 EIL} \quad (4.90)$$

By using the boundary conditions of deformations and forces shown in Eqs. (4.73), (4.80), and (4.81), the final solutions are

$$M_{0i} = \frac{WL^2}{\phi^3} \left[\frac{-\sinh \phi - \phi \cos \phi - \sin \phi \cosh \phi + \cos \phi \sinh \phi + \sin \phi + \phi \cosh \phi}{\cos \phi \cosh \phi - 1} \right] \quad (4.91)$$

$$M_{0j} = \frac{WL^2}{\phi^3} \left[\frac{\sin \phi \cosh \phi - \phi \sin \phi \sinh \phi + \sinh \phi - \cos \phi \sinh \phi - \sin \phi}{\cos \phi \cosh \phi - 1} \right] \quad (4.92)$$

$$V_{0i} = \frac{WL}{\phi^2} \left[\frac{\cosh \phi - \phi \sinh \phi - \phi \sin \phi - \cos \phi + \sin \phi \sinh \phi}{\cos \phi \cosh \phi - 1} \right] \quad (4.93)$$

$$V_{0j} = \frac{WL}{\phi^2} \left[\frac{-\phi \sinh \phi \cos \phi + \cosh \phi - \phi \cosh \phi \sin \phi + \sinh \phi \sin \phi - \cos \phi}{\cos \phi \cosh \phi - 1} \right] \quad (4.94)$$

4.6.4. Concentrated Load between Nodes

For a concentrated load acting at any point between two nodes (see Fig. 4.12a), we can treat the loading point as a node and then analyze the system composed of two members. However, for a concentrated load combined with other types of load (see member *BC* of Fig. 4.8), it is better to find the fixed-end moments and shears at the member ends and then transfer them onto unbalanced loads at nodes *B* and *C*. How to find fixed-end forces due to a concentrated load is illustrated as follows: consider the loading case in Fig. 4.12a for which diagrams for external action and internal resistance are given in Fig. 4.12b and c, respectively. Using the physical interpretation approach, the internal forces at node *B* are sketched on Fig. 4.12d and e, respectively. Note that the direction and subscripts of the internal forces are based on the stiffness coefficients and force-deformation relationship derived in Section 4.3. Thus the *dynamic system matrix* is

$$\begin{Bmatrix} P_{\theta 1} \\ - \\ P_{s1} \end{Bmatrix} = \begin{bmatrix} SM\theta_{1a} + SM\theta_{1b} & | & SMY_{1a} - SMY_{1b} \\ - & | & - \\ SMY_{1a} - SMY_{1b} & | & SVY_{1a} + SVY_{1b} \end{bmatrix} \begin{Bmatrix} X_{\theta 1} \\ - \\ X_{s1} \end{Bmatrix} = \begin{Bmatrix} 0 \\ - \\ P \end{Bmatrix} \quad (4.95)$$

where the first column of the stiffness matrix results from equilibrium conditions: $\Sigma M = 0$ and $\Sigma F = 0$, for $X_\theta = 1$ and $X_s = 0$; the second column represents equilibrium conditions due to $X_s = 1$ and $X_\theta = 0$. In symbolic form

$$[K] \begin{Bmatrix} X_{\theta 1} \\ - \\ X_{s1} \end{Bmatrix} = \begin{Bmatrix} 0 \\ - \\ P \end{Bmatrix} \quad (4.96)$$

from which the external displacements of the steady-state vibration can be calculated as follows:

$$\begin{Bmatrix} X_{\theta 1} \\ - \\ X_{s1} \end{Bmatrix} = [K]^{-1} \begin{Bmatrix} 0 \\ - \\ P \end{Bmatrix} = \frac{P}{|K|} \begin{Bmatrix} -SMY_{1a} + SMY_{1b} \\ SM\theta_{1a} + SM\theta_{1b} \end{Bmatrix} \quad (4.97)$$

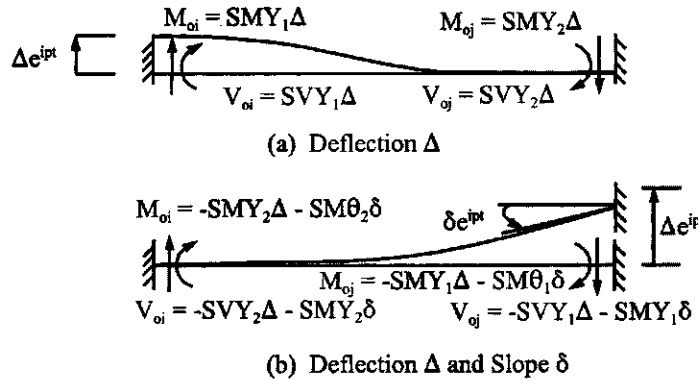
where $| \quad |$ is the symbol of the determinant. Using Eqs. (4.26) and (4.97) yields moments, M_{0i} , M_{0j} and shears, V_{0i} , V_{0j} , at the supports

$$\begin{aligned} M_{0i} &= SM\theta_{2a}X_{\theta 1} + SMY_{2a}X_{s1} \\ &= \frac{P}{|K|} [SM\theta_{2a}(-SMY_{1a} + SMY_{1b}) + SMY_{2a}(SM\theta_{1a} + SM\theta_{1b})] \end{aligned} \quad (4.98)$$

$$\begin{aligned} M_{0j} &= SM\theta_{2b}X_{\theta 1} - SMY_{2b}X_{s1} \\ &= \frac{P}{|K|} [SM\theta_{2b}(-SMY_{1a} + SMY_{1b}) - SMY_{2b}(SM\theta_{1a} + SM\theta_{1b})] \end{aligned} \quad (4.99)$$

$$\begin{aligned} V_{0i} &= SMY_{2a}X_{\theta 1} + SVY_{2a}X_{s1} \\ &= \frac{P}{|K|} [SMY_{2a}(-SMY_{1a} + SMY_{1b}) + SVY_{2a}(SM\theta_{1a} + SM\theta_{1b})] \end{aligned} \quad (4.100)$$

$$\begin{aligned} V_{0j} &= SMY_{2b}X_{\theta 1} - SVY_{2b}X_{s1} \\ &= \frac{P}{|K|} [SMY_{2b}(-SMY_{1a} + SMY_{1b}) - SVY_{2b}(SM\theta_{1a} + SM\theta_{1b})] \end{aligned} \quad (4.101)$$

**FIG. 4.13** Foundation movement.

4.6.5. Foundation Movement

Foundation movement due to harmonic motion may be displacement or rotation or a combination of both. Since no external load is applied, the differential equation without $w(x)/EI$ is identical to Eqs. (4.17) and (4.70) as

$$\frac{d^4 Y}{dx^4} - \lambda^4 Y = 0 \quad (4.102)$$

Obviously, the solution of the equation is the shape function, as in Eq. (4.19). Given any specific end movement, we can find internal forces for which the mathematical procedures are the same as those in Section 4.3 for deriving stiffness coefficients with two exceptions: first, the direction of a foundation movement may be different from the typical sign used in the stiffness derivation; second, the movement may be deflection only or a combination of deflection and rotation. Thus the stiffness coefficients in Eq. (4.25b) can be treated as fixed-end moments and shears due to individual end deformations. The analogy between the stiffness coefficients and the fixed-end moments and shears resulting from arbitrary foundation movements can be observed in Fig. (4.13). By comparison with Fig. 4.4, we note that Δ at i -end is positive; Δ and δ at the j -end are negative. Therefore, the fixed-end forces due to Δ at the i -end are the positive stiffness coefficients as shown in Fig. 4.13a. The fixed-end forces due to Δ and δ at the j -end, however, are the negative stiffness coefficients as shown in Fig. 4.13b.

4.7. NUMERICAL TECHNIQUE FOR EIGEN SOLUTIONS

When a structure is subjected to free vibration without external forces, the load matrix, $[P_\theta | P_s]^T$, vanishes and the system matrix equation in Eq. (4.62) becomes

$$\left(\begin{bmatrix} K_{11} & | & K_{12} \\ \hline K_{21} & | & K_{22} \end{bmatrix} - p^2 \begin{bmatrix} 0 & | & 0 \\ \hline 0 & | & M \end{bmatrix} \right) \begin{Bmatrix} X_\theta \\ X_s \end{Bmatrix} = 0 \quad (4.103)$$

of which the nontrivial solution can be obtained by making the determinant of the coefficients equal to zero

$$\left| \begin{bmatrix} K_{11} & | & K_{12} \\ \hline K_{21} & | & K_{22} \end{bmatrix} - p^2 \begin{bmatrix} 0 & | & 0 \\ \hline 0 & | & M \end{bmatrix} \right| = 0 \quad (4.104)$$

Recall that the mass matrix, $[M]$, is composed of inertia forces associated with rigid-body motion of swayed members of a framework. For a continuous beam or a rigid frame without side-sway, i.e. $\{X_s\} = 0$, Eqs. (4.103) and (4.104) should be modified accordingly,

$$[K_{11}] \{X_\theta\} = 0 \quad (4.105)$$

and

$$|[K_{11}]| = 0 \quad (4.106)$$

The above structural stiffness matrix and mass matrix are expressed in terms of the frequency parameter ϕ in which the frequency p is unknown. The frequency parameter ϕ varies for different members if the properties of the constituent members are not the same. Therefore, we must unify various ϕ 's into one unknown ϕ_1 so that Eqs. (4.104) and (4.106) can be solved on the basis of ϕ_1 for zero determinants. Then the frequencies p can be determined from ϕ_1 . Unification can be achieved by assuming that a member in a system is a reference member such that the properties of this reference member are proportional to the rest of the structural members in the following form:

$$\alpha_i = \frac{L_i}{L_1} \quad (4.107)$$

$$\beta_i = \frac{I_i}{I_1} \quad (4.108)$$

$$\gamma_i = \frac{m_i}{m_1} \quad (4.109)$$

where i indicates all structural members. Thus a general parameter ϕ_i can be expressed as

$$\phi_i = \alpha_i \sqrt{\beta_i} \sqrt{\frac{p^2 m_1 L_1^4}{EI_1}} = \delta_i \phi_1 \quad (4.110)$$

Elements for the mass matrix, $p^2[M]$, can be obtained by the following equation:

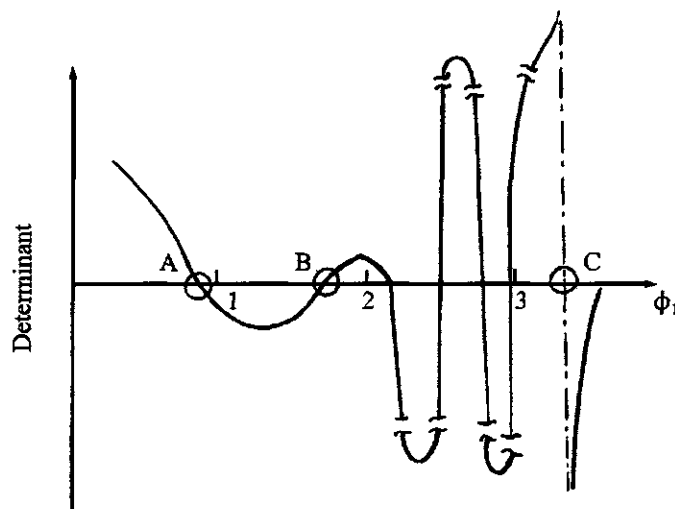
$$m_j L_j p^2 = \gamma_j \alpha_j \frac{\phi_1^4 EI_1}{L_1^2 L_j} \quad (4.111)$$

where j refers to the swayed members. Therefore, ϕ_1 is the only variable in Eqs. (4.103)–(4.106).

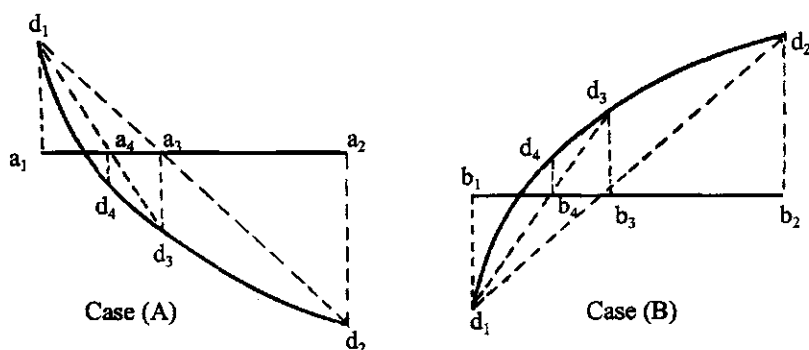
The process of evaluating the singularity of Eqs. (4.103) or (4.105) can become quite complicated, because the determinant function is usually continuous for fundamental frequencies but may be discontinuous for higher modes. The curve of the determinant vs ϕ_1 shown in Fig. 4.14a (actual example of a three-story one-bay frame) indicates that the determinant function is continuous for the first six frequencies. However, the determinant function of a two-span continuous beam may be continuous only for the first two frequencies.

In Fig. 4.14a, *inflectional points* (an inflectional point is where the determinant changes sign), A and B , can be defined as being in a *region of convergence* where the continuous curve intersects the ϕ_1 -axis; inflectional point, C , can be defined as being in a *region of divergence* where the discontinuous curve does not intersect the ϕ_1 -axis.

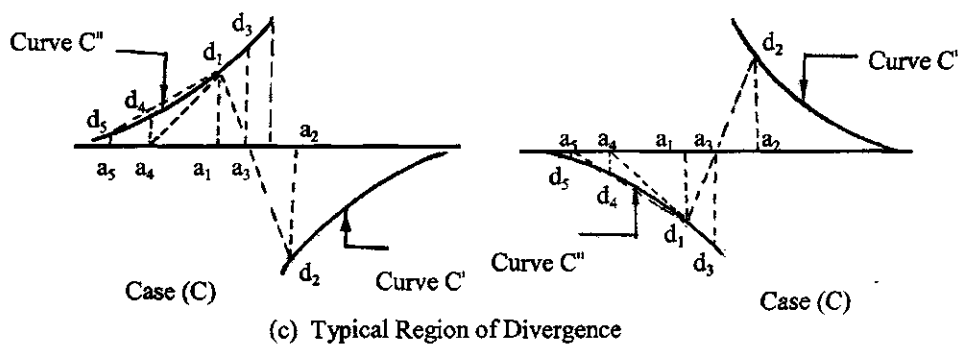
To search for an inflectional point, increase by increments the value of the control parameter, ϕ_1 , in the determinant function; when the sign of the determinant changes, there is the possibility of an inflectional point. This region is then examined for convergence or divergence. If there is convergence, an accurate frequency can be obtained; otherwise, the search continues for the next inflectional point. For further explanation, study Figs. 4.14b and c. In region A of Fig. 4.14b, d_1 and d_2 are two values of the determinant with opposite signs. By using these two values and their corresponding values of abscissa, a_1 and a_2 , a mean value of a_3 and its corresponding value of determinant d_3 can be obtained. By substituting the point (a_3, d_3) for (a_2, d_2) , which



(a) Determinant Function



(b) Typical Region of Convergence



(c) Typical Region of Divergence

FIG. 4.14 Possible determinant curves.

in the present case is further from (a_3, d_3) than (a_1, d_1) , a new mean value, (a_4, d_4) , can be found on the basis of (a_1, d_1) and (a_3, d_3) . By continuing the process and employing a certain criterion, an approximate singular matrix can be found. The criterion is a singular matrix taken at a particular ϕ_1 under two considerations: first, if the difference between the mean value a_i and the values of a_{i-1} and a_{i-2} , which are based on the computed value of a_i , is not greater than a tolerable value, say 10^{-5} ; second, if in this infinitesimal interval the values of the determinant change sign. A similar approach can be applied to region B.

The region of divergence might be either Case C or Case D as shown in Fig. 4.14c. For Case C, the mean values a_3 and d_3 obtained from a_1, d_1 , and a_2, d_2 can be either on curve C'' or C' . If on C'' , the determinant function goes backward to points (a_4, a_5) such that the previous frequency is evaluated. To avoid the repetition of calculating a frequency already found, a criterion is established by assuming that the difference between two successive frequencies cannot be less than or equal to a given number, say 2. Whenever this difference is less than or equal to 2, the parameter jumps over this region, and no frequency is determined. If the mean value a_3 is on curve C' , then the process continues as usual toward the next inflectional point. The same approach can be applied to Case D.

In the region of either convergence or divergence, the values of the determinant and the corresponding values of the parameter, ϕ_1 , may be printed so that the accuracy of convergence can be shown.

The eigenvector of any mode can be determined from Eq. (4.103) or (4.105) after the zero determinant of the coefficient matrix (stiffness matrix or stiffness and mass matrices) is obtained. After substituting the zero determinant parameter, ϕ_1 , into the coefficient matrix, the matrix can be changed to an upper (or lower) triangle as shown below:

$$\begin{bmatrix} X & X & \dots & X \\ & X & \dots & X \\ 0 & & \dots & \dots \\ & & & X \end{bmatrix} \begin{Bmatrix} X_1 \\ X_2 \\ \vdots \\ \vdots \\ X_n \end{Bmatrix} = 0 \quad (4.112)$$

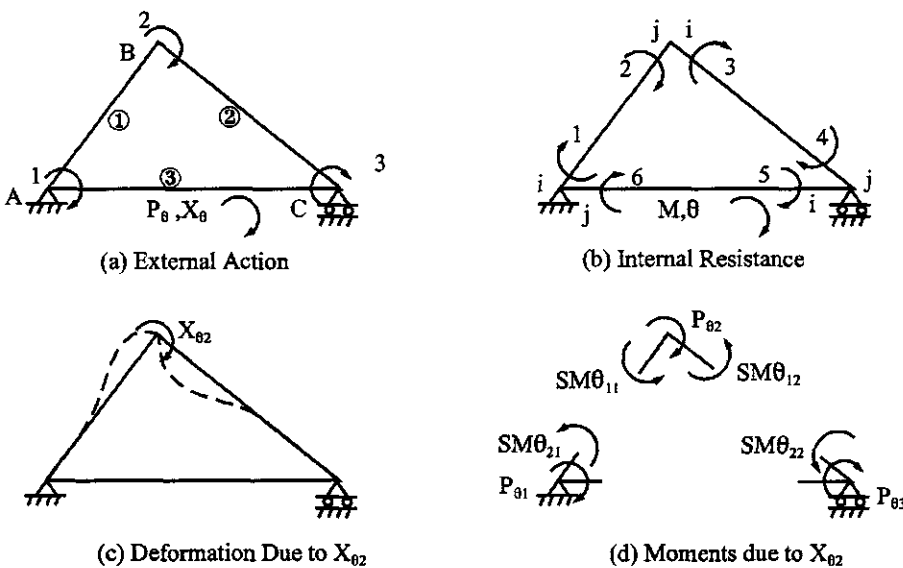


FIG. 4.15 Example 4.7.1.

The element at the bottom right-hand corner of the coefficient matrix has a small value because it is not practical to require the numerical procedure to yield an absolute zero determinant. Therefore, let $X_n = 1$; other X 's are then expressed in terms of X_n . The result is the eigenvector of a mode associated with the designated value of ϕ_1 .

EXAMPLE 4.7.1 Find the fundamental natural frequency of the triangular structure that is shown in Fig. 4.15 as a rigid frame without side-sway. Let the properties of the plane framework be as follows: $EI_1 = 189.887 \text{ k ft}^2$ (78.461 kN m^2), $L = 15 \text{ ft}$ (4.572 m), $m_1 = 1.8418 \times 10^{-4} \text{ k sec}^2/\text{ft}^2$ ($0.8992 \text{ kg sec}^2/\text{m}^2$), $EI_2 = 2.1073 EI_1$, $L_2 = 1.333L$, $m_2 = 1.28656 m_1$, $EI_3 = 3.832EI_1$, $L_3 = 1.667L_1$, and $m_3 = 1.571m_1$. By increasing the EI 's of all members 100 times and keeping the rest of the properties the same, compare the natural frequencies for the two values of flexural rigidity.

Solution: Because the structure is a rigid frame without side-sway, the nodal forces and their associated displacements are only $\{P_\theta\}$ and $\{X_\theta\}$, which are shown in Fig. 4.15a. The internal resistances, $\{M\}$, and their associated deformations, $\{\theta\}$, are shown in the accompanying figure. The diagram of internal resistance is numbered as 1–2 corresponding to member 1, 3–4 corresponding to member 2, and so on. Odd numbers (1, 3, 5, etc.) and even numbers (2, 4, 6, etc.) of the internal moments always coincide with i -ends and j -ends of the structural members, respectively. The i -end and j -end refer to the typical member shown in Fig. 4.4 for deriving stiffness coefficients. Let member 1 be taken as the reference member; then the structural system matrix is formulated according Eq. (4.106) as

$$[K_{11}] \{X_\theta\} = \begin{bmatrix} SM\theta_{11} + SM\theta_{13} & SM\theta_{21} & SM\theta_{23} \\ \text{symm} & SM\theta_{11} + SM\theta_{12} & SM\theta_{22} \\ & & SM\theta_{12} + SM\theta_{13} \end{bmatrix} \{X_\theta\} \quad (a)$$

Note that the first subscripts correspond to the stiffness coefficients' symbols; the second subscripts refer to the number of structural members. In order to unify the member properties, α , β , γ , and δ are calculated according to Eqs. (4.107)–(4.110).

Member i	$\alpha_i = \frac{L_i}{L_1}$	$\beta_i = \frac{I_i}{I_1}$	$\gamma_i = \frac{m_i}{m_1}$	$\delta_i = \alpha_i \sqrt{\frac{\gamma_i}{\beta_i}}$
1	1	1	1	1
2	1.3333	2.1073	1.2856	1.1784
3	1.6667	3.8320	1.5713	1.3337

(b)

Trying $\phi_1 = 2.6$ and 2.65 , we can find the frequency parameters of the other members, $\phi_i = \delta_i \phi_1$, for which the stiffness coefficients $SM\theta_{1i}$ and $SM\theta_{2i}$ of member i can be obtained from Table 4.1.

	$\phi_1 = 2.60$	$\phi_2 = \delta_2 \phi_1$	$\phi_3 = \delta_3 \phi_1$	$\phi_1 = 2.65$	$\phi_2 = \delta_2 \phi_1$	$\phi_3 = \delta_3 \phi_1$
		$= 3.06$	$= 3.47$		$= 3.12$	$= 3.53$
$SM\theta_{1i}$	$3.5275 \frac{EI}{L}$ (1)	$3.0100 \frac{EI}{L}$ (2)	$2.1447 \frac{EI}{L}$ (3)	$3.4865 \frac{EI}{L}$ (1)	$2.9121 \frac{EI}{L}$ (2)	$1.9414 \frac{EI}{L}$ (3)
$SM\theta_{2i}$	$2.3625 \frac{EI}{L}$ (1)	$2.7785 \frac{EI}{L}$ (2)	$3.4936 \frac{EI}{L}$ (3)	$2.3947 \frac{EI}{L}$ (1)	$2.8561 \frac{EI}{L}$ (2)	$3.6732 \frac{EI}{L}$ (3)

(c)

For the purpose of avoiding large numerical values in the determinant function, a common factor, such as EI/L , may not be included in the determinant and will not affect the final solution.

Therefore, we can modify the stiffness coefficients of member i in the following manner:

$$\frac{EI}{L}(i) = \frac{\beta_i}{\alpha_i} \frac{EI}{L}(1) \quad (d)$$

Consequently, Eq. (c) should be modified accordingly. Substituting the above numerical stiffness coefficients that correspond to $\phi_1 = 2.60$ into Eq. (a) yields Eqs. (e)–(g):

	$\phi_1 = 2.60$			$\phi_1 = 2.65$		
	$\frac{EI}{L}(1)$	$\frac{\beta_2}{\alpha_2} \frac{EI}{L}(1)$	$\frac{\beta_3}{\alpha_3} \frac{EI}{L}(1)$	$\frac{EI}{L}(1)$	$\frac{\beta_2}{\alpha_2} \frac{EI}{L}(1)$	$\frac{\beta_3}{\alpha_3} \frac{EI}{L}(1)$
$SM\theta_{1i}$	3.5275	4.7573	4.9310	3.4865	4.6025	4.4636
$SM\theta_{2i}$	2.3625	4.3914	8.0325	2.3947	4.5140	8.4454

$$[K_{11}] = \begin{bmatrix} 8.4585 & 2.3625 & 8.0325 \\ & 8.2848 & 4.3914 \\ \text{symm} & & 9.6883 \end{bmatrix} \frac{EI}{L}(1) \quad (f)$$

$$|[K_{11}]| = 92.58 \left(\frac{EI}{L}(1) \right)^3 \quad (g)$$

For $\phi_1 = 2.65$, Eqs. (e) and (f) may be similarly obtained of which the determinant is

$$|[K_{11}]| = -25.89 \left(\frac{EI}{L}(1) \right)^3 \quad (h)$$

Since the determinant solutions change the sign from positive to negative and the determinant value is finite, the zero determinant may be between $\phi_1 = 2.60$ and $\phi_1 = 2.65$. Using the linear interpretation technique, we can obtain the frequency parameter close to the location corresponding to the zero determinant,

$$\frac{2.65 - 2.60}{(92.58 + 25.89) \left(\frac{EI}{L}(1) \right)^3} = \frac{\phi_1 - 2.6}{92.58 \left(\frac{EI}{L}(1) \right)^3} \quad (i)$$

from which ϕ_1 is 2.6392.

Try $\phi_1 = 2.6392$; then

$$|[K_{11}]| = (783.11509 - 782.14837) \left(\frac{EI}{L}(1) \right)^3 = 0.966723 \left(\frac{EI}{L}(1) \right)^3 \quad (j)$$

Since the value of Eq. (j) is much smaller than those of Eqs. (g) and (h), we simply treat that as zero determinant, and no further convergence step is needed. Therefore the frequency is

$$p = \left(\frac{\phi_1}{L_1} \right)^2 \sqrt{\frac{EI_1}{m_1}} = \left(\frac{2.6392}{15} \right)^2 \sqrt{\frac{189.887}{1.8418 \times 10^{-4}}} = 31.0 \text{ rad/sec} \quad (k)$$

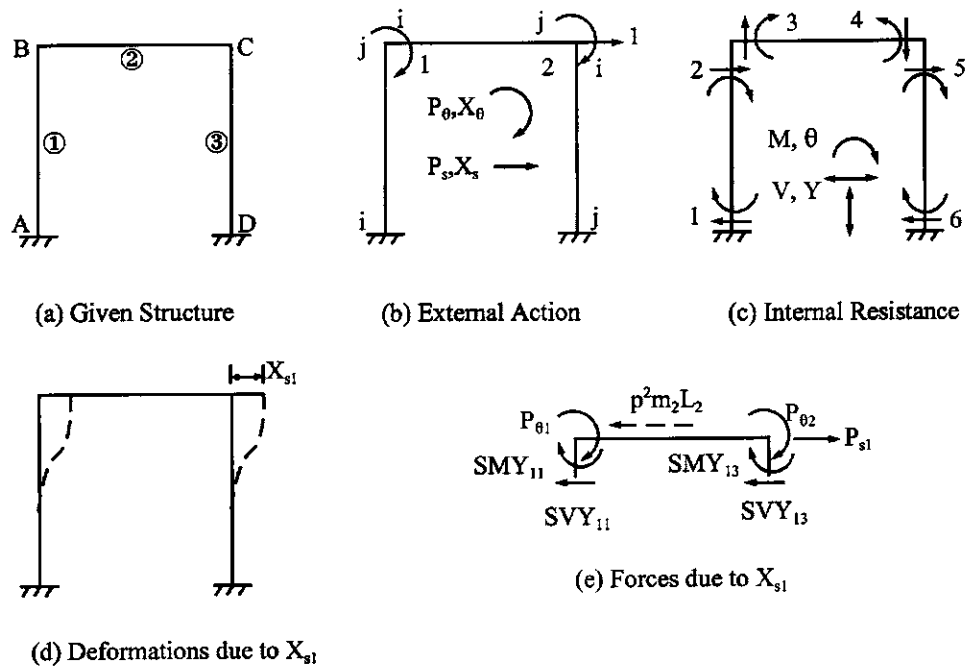


FIG. 4.16 Example 4.7.2.

For the eigenvector of the mode, substituting ϕ_1 into the stiffness coefficients, and then performing Gauss elimination on Eq. (a), we have

$$\begin{bmatrix} 8.066868 & 2.387536 & 8.352114 \\ 0 & 7.426967 & 2.013089 \\ 0 & 0 & 0.016136 \end{bmatrix} \begin{Bmatrix} X_{\theta 1} \\ X_{\theta 2} \\ X_{\theta 3} \end{Bmatrix} = 0 \quad (l)$$

Let $X_{\theta 3} = 1$; then find $X_{\theta 2}$ and $X_{\theta 1}$. The eigenvector is

$$[X_{\theta 1} \ X_{\theta 2} \ X_{\theta 3}]^T = [-0.95514 \ -0.27105 \ 1]^T \quad (m)$$

If the flexural rigidity of all members of the structure is increased 100 times and other properties of mass and length remain the same, then the coefficients of α , β , γ , and δ will be the same as shown in Eq. (b). Consequently the solution of the determinant will not change; the frequency, however, should be calculated as follows

$$p = \left(\frac{\phi_1}{L_1} \right)^2 \sqrt{\frac{100EI_1}{m_1}} = 31\sqrt{100} = 310 \text{ rad/sec} \quad (n)$$

Thus a general statement regarding the behavior of the flexural vibration of rigid frames can be made as follows: if the flexural rigidity, EI , of each member in a rigid frame without side-sway is increased by the factor β' , and the other members' properties are not changed, then the natural frequency for each mode will be increased by the factor $\sqrt{\beta'}$. Note that there is a similar effect, either increase or decrease, on natural frequencies if only the mass or length of each member of a rigid frame without side-sway is changed.

EXAMPLE 4.7.2 Formulate the dynamic system stiffness matrix of the rigid frame shown in Fig. 4.16. Evaluate the fundamental frequency on the basis of the following given member

properties: $m_1 = m_2 = m_3 = 0.00119 \text{ kg sec}^2/\text{m}$, $(6.88 \times 10^{-5} \text{ lb sec}^2/\text{in}) I_1 = I_2 = I_3 = 2.8578 \times 10^{-3} \text{ cm}^4$ ($6.866 \times 10^{-5} \text{ in}^4$), and $L_1 = L_2 = L_3 = 24.130 \text{ cm}$ (9.5 in).

Solution: According to Eqs. (4.27b) and (4.27e), $NP = 3$ and $NPS = 1$, for which the diagrams of external action and internal resistance are shown in Fig. 4.16b and c, respectively. The dynamic system matrix is formulated as

$$\begin{Bmatrix} P_{\theta 1} \\ P_{\theta 2} \\ \cdots \\ P_{s1} \end{Bmatrix} = \left(\begin{bmatrix} SM\theta_{11} + SM\theta_{12} & SM\theta_{22} & | & SMY_{11} \\ - & SM\theta_{12} + SM\theta_{13} & | & SMY_{13} \\ \text{symm} & & | & SVY_{11} + SVY_{13} \end{bmatrix} \right) \begin{Bmatrix} X_{\theta 1} \\ X_{\theta 2} \\ \cdots \\ X_{s1} \end{Bmatrix} \quad (a)$$

The third column of $[K]$ and that of the mass matrix can be physically interpreted from Fig. 4.16d and e as the unbalanced nodal forces and inertia force due to side-sway, X_{s1} . Since this is free vibration, the load matrix does not actually exist.

Because the properties of all the members are the same, the coefficients of α , β , γ , and δ should be equal to 1. If we try $\phi_1 = 1.75$, the stiffness coefficients in Eq. (a) may be obtained from Table 4.1 as follows:

$$SM\theta_{11} = SM\theta_{12} = SM\theta_{13} = 3.9092 \frac{EI}{L} \quad (b)$$

$$SM\theta_{22} = 2.0684 \frac{EI}{L} \quad (c)$$

$$SMY_{11} = SMY_{13} = -5.5019 \frac{EI}{L^2} \quad (d)$$

$$SVY_{11} = SVY_{13} = 8.4837 \frac{EI}{L^3} \quad (e)$$

The inertia force associated with rigid-body motion of member 2 is

$$m_2 L_2 p^2 = \phi_1^4 \frac{EI}{L^3} = (1.75)^4 \frac{EI}{L^3} \quad (f)$$

Substituting the above numerical values into Eq. (a) yields

$$\left(\begin{bmatrix} 7.8184 \frac{EI}{L} & 2.0684 \frac{EI}{L} & -5.5019 \frac{EI}{L^2} \\ & 7.8184 \frac{EI}{L} & -5.5019 \frac{EI}{L^2} \\ \text{symm} & & 16.9674 \frac{EI}{L^3} \end{bmatrix} - \begin{bmatrix} 0 & 0 & 0 \\ 0 & 0 & 0 \\ 0 & 0 & 9.36 \frac{EI}{L^3} \end{bmatrix} \right) \begin{Bmatrix} X_\theta \\ \cdots \\ X_s \end{Bmatrix} = 0 \quad (g)$$

The determinant of the coefficients in Eq. (g) yields

$$\left| \begin{array}{|ccc|} \hline & & \\ \phi_1 = 1.75 & = 84 \frac{(EI)^3}{L^5} \\ & & \end{array} \right| \quad (h)$$

For $\phi_1 = 1.8$, the determinant becomes

$$\left| \begin{array}{c} \\ \end{array} \right|_{\phi_1=1.8} = -23.5 \frac{(EI)^3}{L^5} \quad (i)$$

Applying the linear interpretation to Eqs. (h) and (i) gives

$$\frac{1.8 - 1.75}{(84 + 23.5)[(EI)^3/L^5]} = \frac{\phi_1 - 1.75}{84[(EI)^3/L^5]} \quad (j)$$

from which

$$\phi_1 = 1.7891 \quad (k)$$

The determinant for the new value is

$$\left| \begin{array}{c} \\ \end{array} \right|_{\phi_1=1.7891} = (5.44338 - 5.41903) \frac{(EI)^3}{L^5} = 0.02435 \frac{(EI)^3}{L^5} \quad (l)$$

which is taken as zero determinant. For the eigenvector of the mode, substituting ϕ_1 into the stiffness coefficients and then performing Gauss elimination on Eq. (a) leads to

$$\begin{bmatrix} 7.801361 & 2.074867 & -5.455118/L \\ 0 & 7.249525 & -4.004264/L \\ 0 & 0 & 0.038961/L^2 \end{bmatrix} \begin{Bmatrix} X_{\theta 1} \\ X_{\theta 2} \\ X_{s1} \end{Bmatrix} = 0 \quad (m)$$

Thus the eigenvector is

$$[X_{\theta 1} \ X_{\theta 2} \ X_{s1}]^T = [0.55235/L \ 0.55235/L \ 1]^T \quad (n)$$

The frequency can be calculated as

$$p = \frac{\phi_1^2}{L^2} \sqrt{\frac{EI}{m}} = \left(\frac{1.7891}{9.5} \right)^2 \sqrt{\frac{(30)10^6(6.866)10^{-5}}{(6.88)10^{-5}}} = 194 \text{ rad/sec} \quad (o)$$

EXAMPLE 4.7.3 The structure shown in Fig. 4.17a is analyzed by the lumped mass method as well as the dynamic stiffness method for the eigenvalues and eigenvectors of the first three modes. The frame has two different masses: Case A, structural weight only; and Case B, structural weight and a superimposed weight of 17.51 kN/m (1200 lb/ft) on each floor. Let $EI_1/L_1 = EI_4/L_4 = 9605.234 \text{ kN m}$ (7084.821 k ft), $EI_2/L_2 = EI_5/L_5 = 7077.329 \text{ kN m}$ (5220.328 k ft), $EI_3/L_3 = EI_6/L_6 = 4809.679 \text{ kN m}$ (3547.619 k ft), $EI_7/L_7 = EI_8/L_8 = EI_9/L_9 = 4354.827 \text{ kN m}$ (3212.121 k ft), $W_1 = W_4 = 0.846 \text{ kN/m}$ (58 lb/ft), $W_2 = W_5 = 0.657 \text{ kN/m}$ (45 lb/ft), $W_3 = W_6 = 0.452 \text{ kN/m}$ (31 lb/ft), $W_7 = W_8 = W_9 = 0.496 \text{ kN/m}$ (34 lb/ft), $E = 206,896.55 \text{ MPa}$ (30,000 ksi), and $g = 9.8145 \text{ m/sec}^2$ (32.2 ft/sec²).

Solution: The diagrams of external action and internal resistance are shown in Fig. 4.17b and c, respectively. The dynamic system matrix for both the dynamic stiffness method and the lumped mass method can be symbolically expressed as

$$\left(\begin{bmatrix} K_{11} & | & K_{12} \\ -- & | & -- \\ K_{21} & | & K_{22} \end{bmatrix} - p^2 \begin{bmatrix} 0 & | & 0 \\ - & | & - \\ 0 & | & M \end{bmatrix} \right) \begin{Bmatrix} X_{\theta} \\ -- \\ X_s \end{Bmatrix} = 0 \quad (a)$$

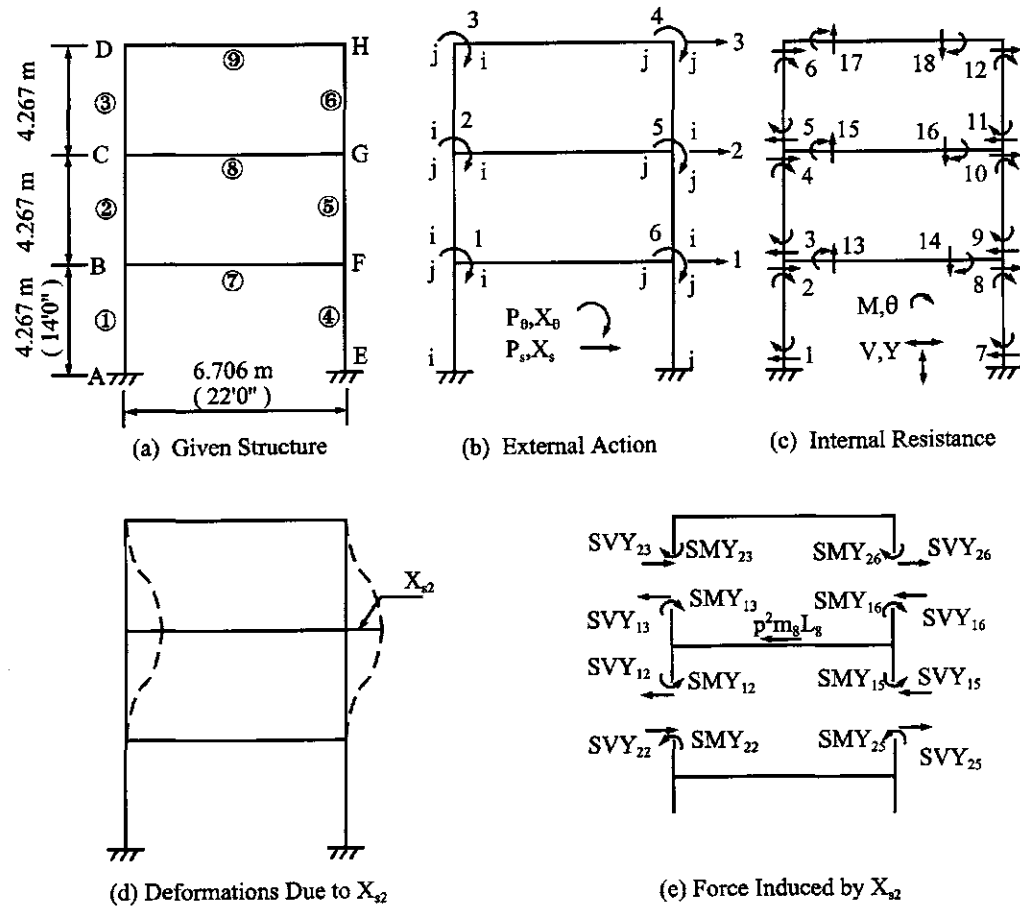


FIG. 4.17 Example 4.7.3.

(1) For the dynamic stiffness method, $[K]$ can be expressed as

$$\left[\begin{array}{cc|cc|cc|cc|cc} A & B & 0 & 0 & 0 & C & D & E & 0 \\ F & G & 0 & H & 0 & & I & J & K \\ L & M & 0 & 0 & 0 & & 0 & N & P \\ Q & R & 0 & & 0 & & 0 & T & U \\ V & W & & & X & Y & Z & & \\ & AA & & & BB & CC & 0 & & \\ \hline - & - & - & - & - & - & - & - & - \\ \text{symm} & & & & & & DD & EE & 0 \\ & & & & & & FF & GG & HH \end{array} \right] \left\{ \begin{array}{l} X_{\theta 1} \\ X_{\theta 2} \\ X_{\theta 3} \\ X_{\theta 4} \\ X_{\theta 5} \\ X_{\theta 6} \\ X_{s1} \\ X_{s2} \\ X_{s3} \end{array} \right\} = 0 \quad (b)$$

in which $A = SM\theta_{11} + SM\theta_{12} + SM\theta_{17}$; $B = SM\theta_{22}$; $C = SM\theta_{27}$; $D = SMY_{11} - SMY_{12}$; $E = SMY_{22}$; $F = SM\theta_{12} + SM\theta_{13} + SM\theta_{18}$; $G = SM\theta_{23}$; $H = SM\theta_{28}$; $I = -SMY_{22}$; $J = SMY_{12} - SMY_{13}$; $K = SMY_{23}$; $L = SM\theta_{13} + SM\theta_{19}$; $M = SM\theta_{29}$; $N = -SMY_{23}$; $P = SMY_{13}$; $Q = SM\theta_{19} + SM\theta_{16}$; $R = SM\theta_{26}$; $T = -SMY_{26}$; $U = SMY_{16}$; $V = SM\theta_{15} + SM\theta_{16} + SM\theta_{18}$; $W = SM\theta_{25}$; $X = -SMY_{25}$; $Y = SMY_{15} - SMY_{16}$; $Z = SMY_{26}$; $AA = SM\theta_{14} + SM\theta_{15} + SM\theta_{17}$; $BB = SMY_{14} - SMY_{15}$; $CC = SMY_{25}$; $DD = SVY_{11} + SVY_{12} + SVY_{14}$

$+ SVY_{15}$; $EE = -SVY_{22} - SVY_{25}$; $FF = SVY_{12} + SVY_{13} + SVY_{15} + SVY_{16}$; $GG = -SVY_{23} - SVY_{26}$; and $HH = SVY_{13} + SVY_{16}$. The eighth column of Eq. (b) can be physically interpreted from Fig. 4.17d and e. For the mass matrices, we have Case A of structural weight only,

$$p^2[M] = \frac{p^2}{g} \begin{bmatrix} W_7L_7 & 0 & 0 \\ 0 & W_8L_8 & 0 \\ 0 & 0 & W_9L_9 \end{bmatrix} \quad (\text{c})$$

and Case B of structural weight and superimposed weight,

$$p^2[M] = \frac{p^2}{g} \begin{bmatrix} (17.51 + W_7)L_7 & 0 & 0 \\ 0 & (17.51 + W_8)L_8 & 0 \\ 0 & 0 & (17.51 + W_9)L_9 \end{bmatrix} \quad (\text{d})$$

Note that the variables in Eqs. (c) and (d) must be unified in terms of a reference member. Consider Case B and let member 3 be used as a reference member; then a typical element associated with member 8 in Eq. (d) can be illustrated as follows:

$$\begin{aligned} m_8L_8p^2 &= \frac{m_8}{m_3} \frac{L_8}{L_3} \frac{\phi_1^4 EI_3}{I_3^3} = \frac{18.006}{0.452} \left(\frac{6.706}{4.267} \right) \frac{(206896.55)10^3(9.9194)10^5}{(4.267)^3} \phi_1^4 \\ &= 16,538.283 \phi_1^4 (\text{kN/m}) (1132.1727 \phi_1^4 (\text{k/ft})) \end{aligned} \quad (\text{e})$$

(2) For the lumped mass method, $[K]$ is similarly formulated as shown in Eqs. (a) and (b). Apparently the stiffness coefficients should be expressed in terms of $4EI/L$, $2EI/L$, $6EI/L^2$, and $12EI/L^3$, for $SM\theta_i$, $SM\theta_j$, SMY_i (or SMY_j), SVY_i (or SVY_j), respectively. For the mass matrices we have

Case A

$$p^2[M] = \frac{p^2}{g} \begin{bmatrix} W_7L_7 + HW_1 & 0 & 0 \\ 0 & W_8L_8 + HW_2 & 0 \\ 0 & 0 & W_9L_9 + HW_3 \end{bmatrix} \quad (\text{f})$$

Case B

$$p^2[M] = \frac{p^2}{g} \begin{bmatrix} (17.51 + W_7)L_7 + HW_1 & 0 & 0 \\ 0 & (17.51 + W_8)L_8 + HW_2 & 0 \\ 0 & 0 & (17.51 + W_9)L_9 + HW_3 \end{bmatrix} \quad (\text{g})$$

In Eqs. (f) and (g), $HW_1 = (2)(L/2)(W_1 + W_2)$, $HW_2 = (2)(L/2)(W_2 + W_3)$ and $HW_3 = (2)(L/2)W_3$ signify the masses lumped on the individual floors from the adjacent columns. For example, the columns' weight lumped on member 8 is one-half the weight of members 2, 3, 5, and 6 as

$$HW_2 = \frac{1}{2}(W_2L_2 + W_3L_3 + W_5L_5 + W_6L_6) = \frac{L}{2}(W_2 + W_3)2 \quad (\text{h})$$

Note that the d.o.f. of structural joints, $\{X_\theta\}$, are not included in the eigensolution procedures of the lumped mass model because they can be eliminated from Eq. (b) by matrix condensation as

$$\begin{bmatrix} K_{11} & K_{12} \\ K_{21} & K_{22} \end{bmatrix} \begin{Bmatrix} X_\theta \\ X_s \end{Bmatrix} = p^2 \begin{bmatrix} 0 & 0 \\ 0 & M \end{bmatrix} \begin{Bmatrix} X_\theta \\ X_s \end{Bmatrix} \quad (\text{i})$$

from which

$$[K]\{X_s\} = [K_{22} - K_{21}K_{11}^{-1}K_{12}]\{X_s\} = p^2[M]\{X_s\} \quad (j)$$

Once the eigenvector $\{X_s\}$ of a given mode is found, the joint rotations of that mode can then be obtained as

$$\{X_\theta\} = [-K_{11}^{-1}K_{12}]\{X_s\} \quad (k)$$

The frequencies (rad/sec) and normal modes are given in Eqs. (l) and (m), respectively.

Methods Cases	Dynamic stiffness			Lumped mass		
	1st	2nd	3rd	1st	2nd	3rd
Modes						
Case A	32.689	102.247	192.770	32.270	96.927	168.470
Case B	7.309	23.588	40.042	7.307	23.626	44.492

Methods Cases	Dynamic stiffness		Lumped mass		
	A	B	A	B	
1st mode	X_{s1}	0.27838	0.25553	0.27749	0.25710
	X_{s2}	0.70910	0.67522	0.70681	0.67747
	X_{s3}	1.00000	1.00000	1.00000	1.00000
2nd mode	X_{s1}	0.72392	0.94133	0.74337	0.94263
	X_{s2}	0.51851	1.00000	0.57159	1.00000
	X_{s3}	-1.00000	-0.94210	-1.00000	-0.94372
3rd mode	X_{s1}	0.99600	0.46542	1.00000	1.00000
	X_{s2}	-1.00000	-1.00000	-0.94649	-0.73140
	X_{s3}	0.65360	0.68924	0.63065	0.24080

Note that the first mode frequencies are almost the same for both analysis methods. Higher mode frequencies are also almost the same by both methods in the superimposed mass case only. Case A does not yield accurate frequencies of higher modes because the columns' masses lumped on the floors are estimated to be more than they actually exhibit. In Case B, the superimposed masses affect inertia forces significantly more than the structural masses of beams and columns. Therefore the inaccuracy of the lumped masses from columns does not show. The eigenvectors, however, are similar in both methods and are less sensitive than the frequencies to the distribution of lumped masses.

It is apparent that the lumped mass method is more suitable for buildings with heavy floor masses. The accuracy of this method diminishes for smaller ratios of floor mass to mass attached to columns. However, reasonable accuracy of eigenvalues of a structure without heavy floor masses can be obtained by this method only if we divide the structural members into multiple segments. Consequently, the dimensions of the problem and the need for computer storage increase. The dynamic stiffness method is indeed a better analytical technique for this type of problem, particularly for structures having prismatic members when higher modes are desired.

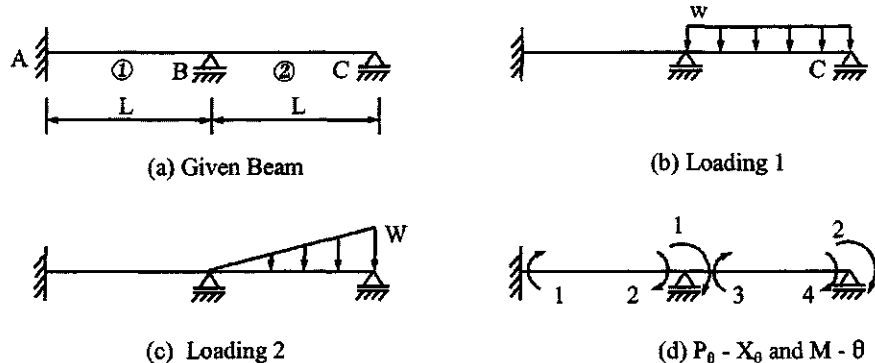


FIG. 4.18 Example 4.8.1.

4.8. STEADY-STATE RESPONSE ANALYSIS

For a structure subjected to harmonically varying forces or foundation movement, structural response may be treated as steady-state vibration. As discussed in Sections 1.4.1 and 1.4.2, the structure should vibrate at a given forcing frequency ω . Therefore, the natural frequency p in dynamic system matrix of Eq. (4.63) is replaced by ω from which the displacement response can be obtained as

$$\begin{Bmatrix} X_\theta \\ X_s \end{Bmatrix} = \left(\begin{bmatrix} K_{11} & K_{12} \\ K_{21} & K_{22} \end{bmatrix} - \omega^2 \begin{bmatrix} 0 & 0 \\ 0 & M \end{bmatrix} \right)^{-1} \begin{Bmatrix} P_\theta \\ P_s \end{Bmatrix} \quad (4.113)$$

Note that the internal forces of an individual member can be found when the external displacements are known. The procedure is to multiply the stiffness coefficients by the end deformations of that member.

EXAMPLE 4.8.1 The two-span beam shown in Fig. 4.18a is subjected to two loading conditions given in Fig. 4.18b and c, respectively. (A) Find the internal moments of the beam for a given forcing frequency $\omega = 119.93$ rad/sec. (B) Assume that the forcing frequency in loading condition 1 varies from $\omega = 44.05$ rad/sec ($\phi_1 = 2.0$) to 253.73 rad/sec ($\phi_1 = 4.8$); plot the moments M_1 and M_2 corresponding to ϕ_1 . Let $L = 3.048$ m (10 ft), $w = 29.188e^{i\omega t}$ kN/m ($2e^{i\omega t}$ k/ft), $W = 29.188e^{i\omega t}$ kN/m ($2e^{i\omega t}$ k/ft), and $EI_1 = 1868.1536$ kN m² (651,000 k in²), $EI_2 = 1274.1342$ kN m² (444,000 k in²), $m_1 = 0.1786$ kN sec²/m² (3.73227 lb sec²/ft²) and $m_2 = 0.1265$ kN sec²/m² (2.64369 lb sec²/ft²).

Solution: (A) Based on the diagram in the accompanying figure, the structural stiffness matrix of Eq. (4.65) may be expressed as

$$[K_{11}] = \begin{bmatrix} SM\theta_{11} + SM\theta_{12} & SM\theta_{22} \\ \text{symm} & SM\theta_{12} \end{bmatrix} \quad (a)$$

and the load matrix as

$$[P_\theta] = \begin{bmatrix} -M_{03}^1 \text{ [from Eq. (4.82)]} & -M_{03}^2 \text{ [from Eq. (4.91)]} \\ -M_{04}^1 \text{ [from Eq. (4.84)]} & -M_{04}^2 \text{ [from Eq. (4.92)]} \end{bmatrix} \quad (b)$$

where the superscript signifies the number of the loading condition.

Using member 1 as reference and harmonic motion of $\omega = 119.93 \text{ rad/sec}$ gives the frequency parameters

$$\phi_1 = \lambda_1 L = \sqrt{\frac{\omega^2 m_1}{EI_1}} L_1 = 3.301054 \quad (\text{c})$$

$$\phi_2 = \delta_2 \phi_1 = \alpha_2 \sqrt{\frac{\gamma_2}{\beta_2}} \phi_1 = 3.332435 \quad (\text{d})$$

the stiffness coefficients

$$SM\theta_{11} = 2.569677 EI_1/L_1 \quad (\text{e})$$

$$SM\theta_{12} = 2.498532 (\beta_2/\alpha_2) EI_1/L_1 = 1.704665 EI_1/L_1 \quad (\text{f})$$

$$SM\theta_{22} = 3.198813 (\beta_2/\alpha_2) EI_1/L_1 = 2.181677 EI_1/L_1 \quad (\text{g})$$

and the fixed-end moments of loading condition 1

$$M_{03}^1 = -29.194 \text{ kNm} (-21.533496 \text{ kft}) \quad (\text{h})$$

$$M_{04}^1 = -M_{03}^1 \quad (\text{i})$$

Substituting Eqs. (e)–(g) into Eq. (a), and Eqs. (h) and (i) into Eq. (b) yields the displacement response

$$\begin{Bmatrix} X_{\theta 1} \\ X_{\theta 2} \end{Bmatrix} = [K_{11}]^{-1} \{P_\theta\} = \begin{bmatrix} 0.675405 & -0.864705 \\ \text{symm} & 1.693894 \end{bmatrix} \frac{L_1}{EI_1} \begin{Bmatrix} 29.194 \\ -29.194 \end{Bmatrix} = \begin{Bmatrix} 44.96197 \\ 74.69574 \end{Bmatrix} \frac{L_1}{EI_1} \quad (\text{j})$$

and the internal moments

$$\begin{Bmatrix} M_1 \\ M_2 \\ M_3 \\ M_4 \end{Bmatrix} = \begin{Bmatrix} SM\theta_{21} X_{\theta 1} \\ SM\theta_{11} X_{\theta 1} \\ SM\theta_{12} X_{\theta 1} + SM\theta_{22} X_{\theta 2} + M_{03}^1 \\ SM\theta_{22} X_{\theta 1} + SM\theta_{12} X_{\theta 2} + M_{04}^1 \end{Bmatrix} = \begin{Bmatrix} 141.157 \\ 115.538 \\ -115.538 \\ 0 \end{Bmatrix} kN \cdot m \begin{pmatrix} 104.117474 \\ 85.220665 \\ -85.220665 \\ 0 \end{pmatrix} k \cdot ft \quad (\text{k})$$

(B) The variation of M_1 and M_2 for various forcing frequencies (or ϕ_1 's) is shown in Fig. 4.19.

EXAMPLE 4.8.2 The one-bay two-story rigid frame of Fig. 4.20a is subjected to a uniform load as shown. All the constituent members are the same: $L = 3.048 \text{ m}$ (19 ft), $I = 4070.743 \text{ cm}^4$ (97.8 in⁴), w (member weight) = 41.669 kg/m (28 lb/ft), and $E = 20,684.271 \text{ kN/cm}^2$ ($30 \times 10^6 \text{ lb/in}^2$). Assume $w = 14.594e^{i\omega t} \text{ kN/m}$ ($1 e^{i\omega t} \text{ k/ft}$). (A) Find the moments of 3 and 12 as well as shears of 4 and 8 corresponding to $\phi_1 = 1.1$; (B) make an equilibrium check of shears corresponding to P_{s2} ; and (C) plot M_3 and M_{12} for the frequency, ω , which varies from 2.45 rad/sec to 119.95 rad/sec.

Solution: Since all the members are the same, the coefficients of α , β , γ and δ should be equal to 1, and the stiffness coefficients of each member are identical. Any member can be taken as a reference member. The dynamic system matrix is formulated as

$$\begin{Bmatrix} -M_{03} \\ -M_{04} \\ 0 \\ 0 \\ \vdots \\ V_{03} \\ -V_{04} \end{Bmatrix} = \left(\begin{bmatrix} A & B & 0 & C & | & D & E \\ F & G & 0 & | & H & I \\ J & K & | & L & M \\ N & | & P & Q \\ \hline - & - & - & - & | & - & - \\ \text{symm} & & & & | & R & S \\ \hline & & & & | & T & \end{bmatrix} - \omega^2 \begin{bmatrix} 0 & & & & & \\ \vdash & \vdash & \vdash & \vdash & \vdash & 0 \\ \hline mL & & & & & mL \end{bmatrix} \right) \begin{Bmatrix} X_{\theta 1} \\ X_{\theta 2} \\ X_{\theta 3} \\ X_{\theta 4} \\ \vdots \\ X_{s1} \\ X_{s2} \end{Bmatrix} \quad (\text{a})$$

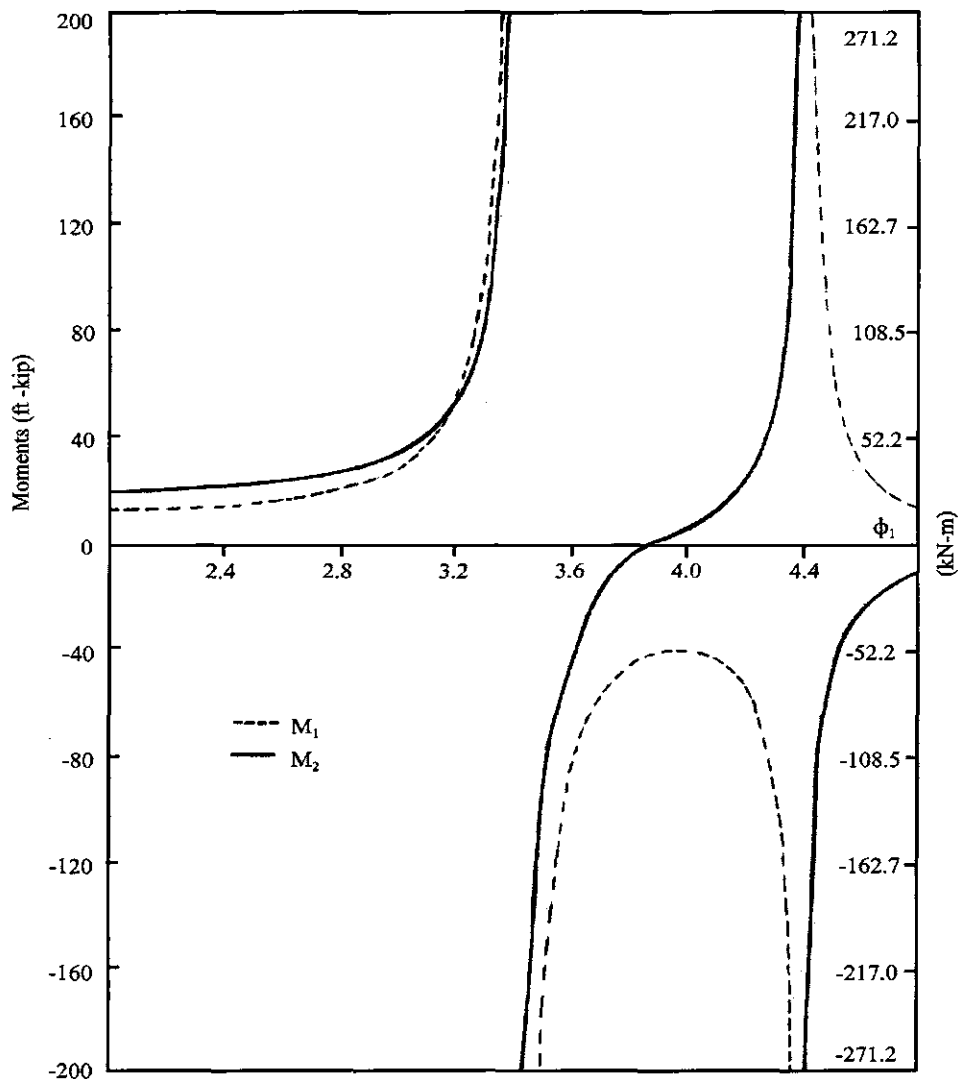


FIG. 4.19 Example 4.8.1— M_1 and M_2 of loading 1.

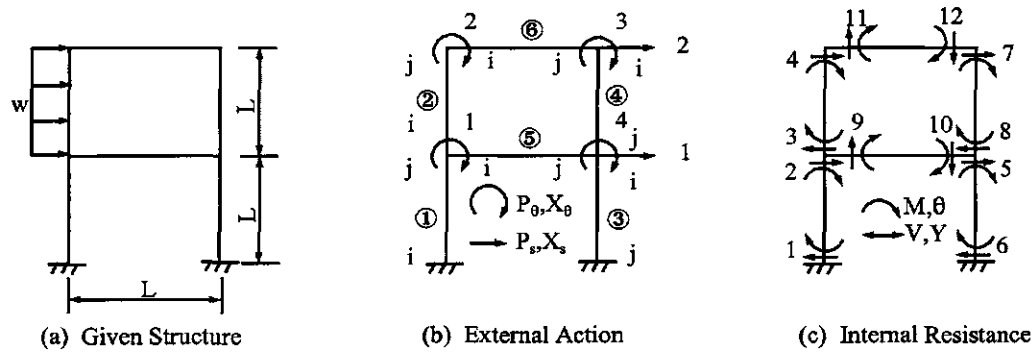


FIG. 4.20 Example 4.8.2.

(A) For $\phi = 1.1$, the coefficients, A , B , C , etc., of $[K]$ in Eq. (a) are composed of individual members' stiffness coefficients given in parentheses as:

$$\begin{aligned} A(SM\theta_{11} + SM\theta_{12} + SM\theta_{15}) &= N(SM\theta_{13} + SM\theta_{14} + SM\theta_{15}) = 3SM\theta_1 = 11.95806 \text{ EI/L}; \\ B(SM\theta_{22}) &= C(SM\theta_{25}) = G(SM\theta_{26}) = K(SM\theta_{24}) = SM\theta_2 = 2.01049 \text{ EI/L}; \\ D(SMY_{11} - SMY_{12}) &= P(SMY_{13} - SMY_{14}) = SMY_1 - SMY_1 = 0; \\ E(SMY_{22}) &= H(-SMY_{22}) = -L(-SM_{24}) = Q(SM_{24}) = SMY_2 = -6.04547 \text{ EI/L}^2; \\ F(SM\theta_{12} + SM\theta_{16}) &= J(SM\theta_{14} + SM\theta_{16}) = 2SM\theta_1 = 7.972043 \text{ EI/L}; \\ I(SMY_{12}) &= M(SMY_{14}) = SMY_1 = -5.923144 \text{ EI/L}^2; \\ R(SVY_{11} + SVY_{12} + SVY_{13} + SVY_{14}) &= 4SVY_1 = 45.82163 \text{ EI/L}^3; \\ S(-SVY_{22} - SVY_{24}) &= -2SVY_2 = -24.37790 \text{ EI/L}^3; \text{ and} \\ T(SVY_{12} + SVY_{14}) &= 2SVY_1 = 22.91081 \text{ EI/L}^3. \end{aligned}$$

Coefficients in the mass matrix are

$$\omega^2 = \frac{EI\phi^4}{mL^4} = \frac{8420.035(1.1)^4}{(3.048)^4(0.041669)} = 3425.455 \quad (b)$$

$$mL = 0.041669(3.048) = 0.127086 \text{ kN sec}^2/\text{m} (8.70863 \text{ lb sec}^2/\text{ft}) \quad (c)$$

Coefficients in the load matrix are

$$M_{03} = -M_{04} = [\text{Eq. (4.82) or (4.84)}] = -11.3275 \text{ kN m} (-8.35518 \text{ k ft}) \quad (d)$$

$$V_{03} = -V_{04} = [\text{Eq. (4.83) or (4.85)}] = 22.29 \text{ kN} (5.01020 \text{ k}) \quad (e)$$

Substituting the numerical values into Eq. (a) and then performing matrix inversion yield the displacement response is

$$\begin{Bmatrix} X_{\theta 1} \\ X_{\theta 2} \\ X_{\theta 3} \\ X_{\theta 4} \\ X_{s1} \\ X_{s2} \end{Bmatrix} = \begin{Bmatrix} 0.78037 \\ 0.27341 \\ 0.36215 \\ 0.72121 \\ 293.100 \\ 550.600 \end{Bmatrix} \times 10^{-2} \quad \text{rad} \quad (f)$$

The final results of M_3 , M_{12} are obtained by substituting the individual members' stiffness coefficients into Eqs. (g) and (h) as follows:

$$\begin{aligned} M_3 &= SM\theta_{12}X_{\theta 1} + SM\theta_{22}X_{\theta 2} - SMY_{12}X_{s1} + SMY_{22}X_{s2} + M_{03} \\ &= -54.557 \text{ kN m} (-40.24112 \text{ k ft}) \end{aligned} \quad (g)$$

$$M_{12} = SM\theta_{26}X_{\theta 2} + SM\theta_{16}X_{\theta 3} = 55.059 \text{ kN m} (40.61198 \text{ k ft}) \quad (h)$$

Shears due to rotations and deflections of members 2 and 4 are

$$V_4 = SMY_{22}X_{\theta 1} + SMY_{12}X_{\theta 2} - SVY_{22}X_{s1} + SVY_{12}X_{s2} + V_{04} = 1.6011 \text{ kN} (0.35996 \text{ k}) \quad (i)$$

$$V_8 = SMY_{24}X_{\theta 4} + SMY_{14}X_{\theta 3} - SVY_{24}X_{s1} + SVY_{14}X_{s2} = 22.364 \text{ kN} (5.02792 \text{ k}) \quad (j)$$

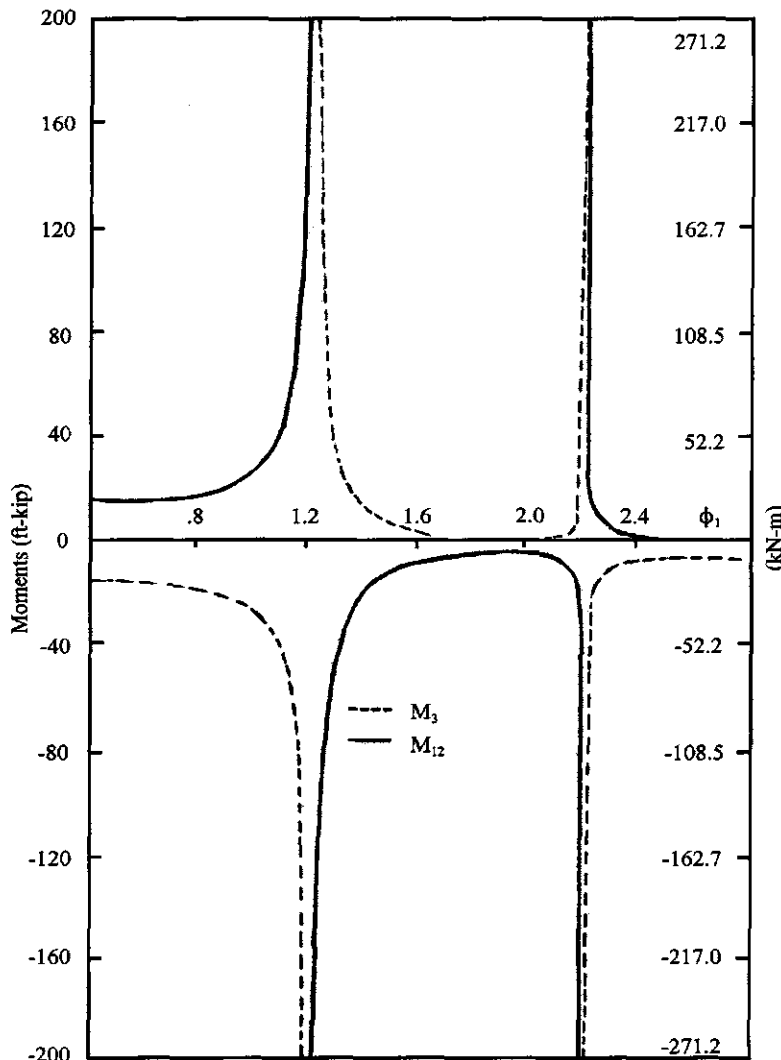


FIG. 4.21 Example 4.8.2— M_3 and M_{12} .

(B) The equilibrium check of shears corresponding to P_{s2} must include the following inertia force of the girder:

$$M\ddot{x}_{s2} = -\omega^2 m_6 L_6 X_{s2} = -(58.52739)^2 (0.127086) (0.05506) = -23.97 \text{ kN} \quad (-5.38898 \text{ k}) \quad (\text{k})$$

which acts in the same direction as P_{s2} . Total external and internal forces in the horizontal direction of member 6 must be zero. Thus

$$\Sigma F_x = M\ddot{x}_{s2} + V_4 + V_8 = -0.0049 \approx 0 \quad (\text{l})$$

(C) Moments M_3 and M_{12} are plotted in Fig. 4.21. By observing the resonant moments, the first two natural frequencies can be calculated as

$$p_1 = 72.524 \text{ rad/sec at } \phi_1 = 1.224 \quad (\text{m})$$

$$p_2 = 238.075 \text{ rad/sec at } \phi_1 = 2.218. \quad (\text{n})$$

4.9. RESPONSE FOR GENERAL FORCING FUNCTIONS WITH AND WITHOUT DAMPING

4.9.1. Kinetic and Strain Energy

The response analysis for a general type of dynamic force or ground excitation with and without damping may be formulated by using the *energy method*. One of the well-known formulation techniques is the following Lagrange's equation:

$$\frac{d}{dt} \left(\frac{\partial T}{\partial \dot{q}_k} \right) - \frac{\partial T}{\partial q_k} + \frac{\partial U}{\partial q_k} + \frac{\partial D}{\partial \dot{q}_k} = \frac{\partial W}{\partial q_k} \quad (4.114)$$

where T = kinetic energy, U = potential energy, D = work done due to damping forces, W = work done due to external forces, and the subscript k of q_k represents the k th normal mode associated with generalized coordinates, or sometimes referred to as the generalized response vector [q_k is the same as the x'_i used in Sections 2.5.2 and 3.2.1; see Eqs. (2.41), (2.66) and (3.5)]. The derivation of Eq. (4.114) is in Appendix A.

The dynamic deflection of point x at time t can be represented by the summation of modal components as

$$y(x, t) = \sum_i^n Y_i(x) q_i(t) \quad (4.115)$$

where $Y(x)$ = shape function or normal mode, and $i = 1, 2, \dots, n$, number of normal modes or generalized coordinates.

The expressions for velocity and curvature are

$$\dot{y}(x, t) = \sum_i^n \dot{q}_i(t) Y_i(x) \quad (4.116)$$

$$y''(x, t) = \sum_i^n q_i(t) Y''_i(x) \quad (4.117)$$

The kinetic energy can be expressed as

$$T = \frac{1}{2} m \int_0^L \left[\sum_i^n \dot{q}_i(t) Y_i(x) \right]^2 dx \quad (4.118)$$

For simplicity, the variables t and x are dropped. The squared term in Eq. (4.118) may be expanded as

$$\left[\sum_i^n \dot{q}_i Y_i \right]^2 = \left[\sum_i^n \dot{q}_i^2 Y_i^2 \right] + 2 \sum_i^n [\dot{q}_i Y_i] [\dot{q}_j Y_j] \quad (4.119)$$

From the orthogonality condition [see Eq. (4.132)], the second term in Eq. (4.119) is zero. Thus Eq. (4.118) becomes

$$T = \frac{1}{2} m \sum_i^n \dot{q}_i^2 \int_0^L Y_i^2 dx \quad (4.120)$$

Then

$$\frac{d}{dt} \frac{\partial T}{\partial \dot{q}_k} = \ddot{q}_k \int_0^L m Y_k^2 dx \quad (4.121)$$

The potential energy or strain energy can be expressed in terms of stress, σ , strain, ε , and integration over a volume,

$$U = \frac{1}{2} \int \sigma \varepsilon dv \quad (4.122)$$

From Fig. 4.1, the curvature is $1/R = d\theta/dx$. Since the total length of the fiber, $dx' = (R + z)d\theta$ or $(1 + z/R)dx$, and the original length of the fiber $dx = R d\theta$, the elongation is $e = dx' - dx = z/R(dx)$. Thus the strain is

$$\varepsilon = \frac{e}{dx} = \frac{z}{R} = y''z \quad (4.123)$$

Since $\sigma = Mz/I$

$$\sigma = E z y'' \quad (4.124)$$

Eq. (4.122) may now be expressed in terms of cross-sectional volume, v , as

$$U = \frac{1}{2} \int E(Y'')^2 z^2 dv = \frac{1}{2} \int EI (y'')^2 dx \quad (4.125)$$

Since $y = Yq$, then $\partial y''/\partial q_k = Y_k''$. Thus

$$\frac{\partial U}{\partial q_k} = \int EI y'' \frac{\partial y''}{\partial q_k} dx = \int EI Y_k'' \left[\sum_i^n Y_i'' q_i \right] dx \quad (4.126)$$

4.9.2. Orthogonality Condition

Recalling Eq. (4.14) for shape function Y_k , we can write

$$\int_0^L (EI Y_k'')'' dx = \int_0^L p_k^2 m Y_k dx \quad (4.127)$$

Multiplying the above by Y_m ($\neq Y_k$) and then integrating by parts twice for the left-hand side (LHS) yields

$$\begin{aligned} \int Y_m (EI Y_k''') dx &= Y_m (EI Y_k'''')|_0^L - \int_0^L Y_m' (EI Y_k''') dx \\ &= Y_m (EI Y_k''')|_0^L - Y_m' (EI Y_k'')|_0^L + \int_0^L Y_m'' (EI Y_k'') dx \end{aligned}$$

or

$$LHS = \left[Y_m (EI Y_k''') - Y_m' (EI Y_k'') \right]_0^L + \int_0^L Y_m'' (EI Y_k'') dx \quad (4.128)$$

Recognizing that the first two terms in the above will vanish for any combination of fixed, simply supported, or free ends, we have

$$\int_0^L Y_m'' (EI Y_k'') dx = m \int_0^L p_k^2 Y_m Y_k dx \quad (4.129)$$

Similarly, multiplying Eq. (4.127) of the m th mode by Y_k'' and following the above integrations yields

$$\int_0^L Y_k''(EI \cdot Y_m'') dx = \int_0^L m p_m^2 Y_m Y_k dx \quad (4.130)$$

Subtracting Eq. (4.130) from (4.129) gives

$$(p_k^2 - p_m^2) \int_0^L m Y_m Y_k dx = 0 \quad (4.131)$$

Since $p_k \neq p_m$, we have the following *orthogonality condition*:

$$\int_0^L Y_m Y_k dx = 0 \quad (4.132)$$

and

$$\int_0^L Y_m'' Y_k'' dx = 0 \quad (4.133)$$

Apply the results obtained from Eqs. (4.129) and (4.133) to Eq. (4.126), which can then be expressed as

$$\frac{\partial U}{\partial q_k} = p_k^2 q_k \int_0^L m Y_k^2 dx \quad (4.134)$$

4.9.3. Dissipated Energy and Work

The dissipated energy due to damping is

$$D = \frac{1}{2} c \int_0^L \dot{y}^2 dx = \frac{1}{2} c \int_0^L \left[\sum \dot{q}_i Y_i \right]^2 dx \quad (4.135)$$

from which

$$\frac{\partial D}{\partial \dot{q}_k} = c \dot{q}_k \int_0^L Y_k^2 dx \quad (4.136)$$

The work done by external dynamic force, $F(t,x) = F(x)f(t)$, is

$$W = \int_0^L F(t,x) \left[\sum q_i Y_i \right] dx \quad (4.137)$$

from which

$$\frac{\partial W}{\partial q_k} = f(t) \int_0^L F(x) Y_k dx \quad (4.138)$$

4.9.4. Response Equations

Substituting Eqs. (4.121), (4.134), (4.136) and (4.138) into Eq. (4.114) yields

$$\ddot{q}_k \int m Y_k^2 dx + p_k^2 q_k \int m Y_k^2 dx + c \dot{q}_k \int Y_k^2 dx = f(t) \int F(x) Y_k dx \quad (4.139a)$$

Recall that $c/m = 2\rho p$ [see Eq. (1.31)]; then Eq. (4.139a) can be expressed as the following uncoupled motion equation for the k th mode:

$$\ddot{q}_k + 2\rho p_k \dot{q}_k + p_k^2 q_k = \frac{f(t) \int_0^L F(x) Y_k dx}{\int_0^L m Y_k^2 dx} \quad (4.139b)$$

Let

$$\bar{M}_k = \int_0^L m Y_k^2 dx \quad (4.140)$$

$$F_k = \int_0^L F(x) Y_k dx \quad (4.141)$$

Then the integration of Eq. (4.139b) becomes

$$q_k = \frac{F_k}{\bar{M}_k p_k^2} A_k(t) \quad \text{or} \quad q_k = \frac{\sum_{\ell=1}^{NM} F_{k\ell}}{p_k^2 \sum_{\ell=1}^{NM} \bar{M}_{k\ell}} A_k(t) \quad (4.142)$$

where NM = total number of members of a structure and

$$A_k(t) = \frac{1}{\sqrt{1-\rho^2}} \int_0^L e^{\rho^* p^*(t-\Delta)} \sin p^* (t-\Delta) F(\Delta) d\Delta \quad (4.143)$$

Note that F_k is a general expression which can represent dynamic force or ground excitation. $A_k(t)$

can be simplified not to include the effect of damping on frequency [see Eq. (1.121b)]; then

$$A_k(t) = \int_0^L e^{-\rho p(t-\Delta)} \sin p(t-\Delta) F(\Delta) d\Delta \quad (4.144)$$

Let

$$Y_{stk} = \frac{F_k}{\bar{M}_k p_k^2} \quad \text{or} \quad Y_{stk} = \frac{\sum_{\ell=1}^{NM} F_{k\ell}}{p_k^2 \sum_{\ell=1}^{NM} \bar{M}_{k\ell}} \quad (4.145)$$

Then the total response is obtained by superimposing the modes shown in Eq. (4.115) as

$$y(x, t) = \sum_{k=1}^n Y_{stk} A_k(t) Y_k(x) \quad (4.146)$$

The moment and shear at time t are

$$M(x, t) = EIy''(x, t) = EI \sum_{k=1}^n Y_{stk} A_k(t) Y_k''(x) \quad (4.147)$$

$$V(x, t) = EIy'''(x, t) = EI \sum_{k=1}^n Y_{stk} A_k(t) Y_k'''(x) \quad (4.148)$$

Note that A_k is the *amplification factor* or *dynamic load factor* for the k th mode as introduced in Chapter 1 for various types of dynamic forces or ground excitation (response spectrum). Y_{stk} is the *pseudo-static displacement* at the k th mode, which is similar to x'_{si} in Eq. (2.62) of the lumped mass model. F_k is the *participation factor*, similar to X_{ri} F_r in Eq. (2.68) or X_{ri} M_r in Eq. (2.69).

EXAMPLE 4.9.1 A two-span continuous beam shown in Fig. 4.22 is subjected to a uniform impulse within the left span as $F(t, x) = 3000[1 - (t/0.1)]$ lb/in. Structural properties are $L = 150$ in, $EI = 6 \times 10^9$ lb/in 2 and $m = 0.2$ lb sec 2 /in 2 . Find the moments at support B and shears at supports A , B , and C . Check the equilibrium condition.

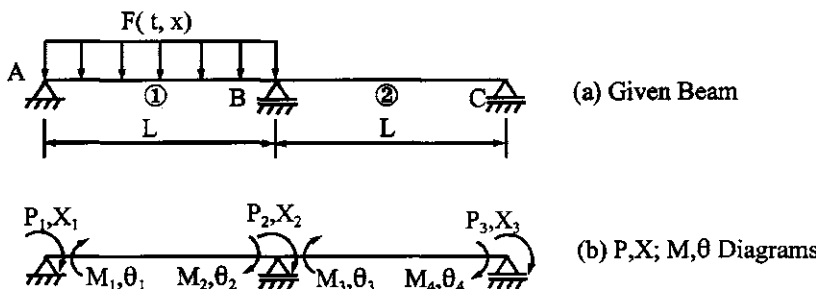


FIG. 4.22 Example 4.9.1.

Solution: Since the member properties are identical for both spans, the structural stiffness matrix may be expressed as

$$[K] = \begin{bmatrix} SM\theta_1 & SM\theta_2 & 0 \\ 2SM\theta_1 & SM\theta_2 & \\ \text{symm} & SM\theta_1 & \end{bmatrix} \quad (\text{a})$$

$\det [K] = 0$ yields as many frequencies as needed. For the first mode

$$\phi_1 = 3.1416; \quad \lambda_1 = \frac{\phi_1}{L} = 0.02094; \quad p_1 = \frac{\phi_1^2}{L^2} \sqrt{\frac{EI}{m}} = 75.97625 \text{ rad/sec} \quad (\text{b})$$

The stiffness coefficients corresponding to ϕ_1 are $SM\theta_1 = SM\theta_2 = 2.8816$. After substitution, $[K]\{X\}$ becomes

$$\begin{bmatrix} 2.8816 & 2.8816 & 0 \\ 5.7632 & 2.8816 & \\ \text{symm} & 2.8816 & \end{bmatrix} \begin{Bmatrix} X_1 \\ X_2 \\ X_3 \end{Bmatrix} = 0 \quad (\text{c})$$

from which the eigenvector is

$$\{X\} = [1 \quad -1 \quad 1]^T \quad (\text{d})$$

Substituting ϕ_1 , X_1 , and X_2 into Eq. (4.23) yields the constants in the shape function by using the eigenvector as boundary condition. Therefore

$$\begin{Bmatrix} A \\ B \\ C \\ D \end{Bmatrix} = \begin{bmatrix} 23.87324 & -23.87324 \\ 21.89540 & 21.89540 \\ 23.87324 & 23.87324 \\ -21.89540 & -21.89540 \end{bmatrix} \begin{Bmatrix} 1 \\ -1 \end{Bmatrix} \quad (\text{e})$$

from which

$$[A \quad B \quad C \quad D]^T = [47.74648 \quad 0 \quad 0 \quad 0]^T \quad (\text{f})$$

Thus the shape function of member 1 can be obtained by substituting Eq. (f) into Eq. (4.19) as

$$Y_{11} = 47.74648 \sin \lambda_1 x \quad (\text{g})$$

In a similar manner, the shape function of member 2 is

$$Y_{12} = -47.74648 \sin \lambda_1 x \quad (\text{h})$$

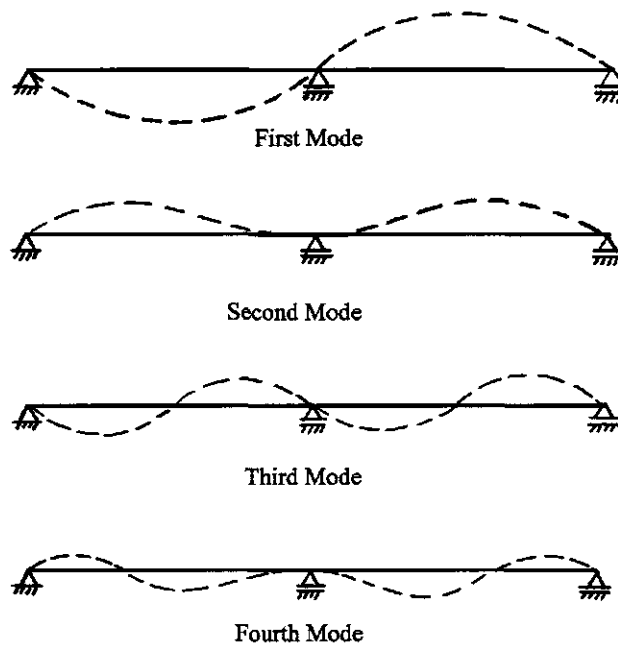
Using the above procedures will give the frequency parameters, ϕ 's frequencies, p 's, the associated eigenvectors, $\{X\}$, and the shape functions of the second, third, and fourth modes. The results are

$$\phi_2 = 3.92660; \quad \lambda_2 = 0.026177; \quad p_2 = 118.68938 \text{ rad/sec}; \quad \{X\}_2 = [-1 \quad 0 \quad 1]^T \quad (\text{i})$$

$$\phi_3 = 6.28318; \quad \lambda_3 = 0.0418879; \quad p_3 = 303.905 \text{ rad/sec}; \quad \{X\}_3 = [1 \quad 1 \quad 1]^T \quad (\text{j})$$

$$\phi_4 = 7.06858; \quad \lambda_4 = 0.0471239; \quad p_4 = 384.6268 \text{ rad/sec}; \quad \{X\}_4 = [-1 \quad 0 \quad 1]^T \quad (\text{k})$$

The mode shapes are shown in Fig. 4.23.

**FIG. 4.23** Mode shapes.

The coefficients A , B , C , and D of the shape function of member 1 are listed in Eq. (l) in the order of second, third, and fourth modes as

$$\begin{bmatrix} A \\ B \\ C \\ D \end{bmatrix} = \begin{bmatrix} -37.16499 & 23.87324 & -21.24624 \\ 0 & 0 & 0 \\ -1.035983 & 0 & 0.025582 \\ 0 & 0 & 0 \end{bmatrix} \quad (l)$$

Similarly, for member 2

$$\begin{bmatrix} A \\ B \\ C \\ D \end{bmatrix} = \begin{bmatrix} -26.28982 & 23.87324 & 15.02337 \\ 26.26940 & 0 & -15.02335 \\ 26.28982 & 0 & -15.02337 \\ -26.26940 & 0 & 15.02335 \end{bmatrix} \quad (m)$$

Shape functions for the second mode of members 1 and 2 are

$$Y_{21} = -37.16499 \sin \lambda_2 x - 1.035983 \sinh \lambda_2 x \quad (n)$$

$$Y_{22} = -26.28982 \sin \lambda_2 x + 26.26940 \cos \lambda_2 x + 26.28982 \sinh \lambda_2 x - 26.26940 \cosh \lambda_2 x \quad (o)$$

For the third mode

$$Y_{31} = 23.87324 \sin \lambda_3 x \quad (p)$$

$$Y_{32} = 23.87324 \sin \lambda_3 x \quad (q)$$

and the fourth mode

$$Y_{41} = -21.24624 \sin \lambda_4 x + 0.025582 \sinh \lambda_4 x \quad (\text{r})$$

$$Y_{42} = 15.02337 \sin \lambda_4 x - 15.02335 \cos \lambda_4 x - 15.02337 \sinh \lambda_4 x + 15.02335 \cosh \lambda_4 x \quad (\text{s})$$

Then, from Eq. (4.142)

$$q_k = \frac{\sum_{\ell=1}^2 F_{k\ell}}{p_k^2 \sum_{\ell=1}^2 \bar{M}_{k\ell}} A_k(t); \quad k = 1, 2, 3, 4 \quad (\text{t})$$

in which the amplification factor of impulse load, for $t \leq \zeta$, $\zeta = 0.1$ sec, is given in Eq. (1.81) as

$$A_k(t) = 1 - \cos p_k t + \frac{\sin p_k t}{p_k \zeta} - \frac{t}{\zeta} \quad (\text{u})$$

The maximum displacement of the first mode occurs during the pulse at 0.0379 sec, which is used for the response of other modes. The calculations are summarized as

k	$F_{k\ell}$		$\bar{M}_{k\ell}$		Y_{stk}	$A_k(t)$
	$\ell = 1$	$\ell = 2$	$\ell = 1$	$\ell = 2$		
1	13,678,350	0	34,195.8	34,195.8	0.034648	1.62095
2	-10,166,310	0	20,702.6	20,702.6	-0.017429	0.75110
3	0	0	8,549.0	8,549.0	0	0.09350
4	558,594	0	6,771.0	7,771.0	0.000279	1.07073

Substituting the results from Eq. (v) into Eqs. (4.146) and (4.147) yields the moments and shears of members 1 and 2. The moments at B for $t = 0.0379$ sec associated with the first, second and fourth modes are obtained by evaluating y'' of individual shape functions as

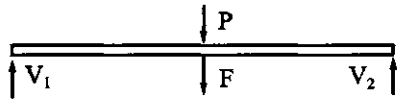
$$\begin{aligned} M_2 &= -EIy''(L) = -EI[Y_{st1}A_1 Y_{11}''(L) + Y_{st2}A_2 Y_{21}''(L) + Y_{st4}A_4 Y_{41}''(L)] \\ &= -EI[0.034648(1.62093)(0) + (-0.017429(0.75101)(-0.036)) \\ &\quad + 0.000279(1.070783)(0.06672)] = -4.912053(10^{-4})EI \end{aligned} \quad (\text{w})$$

$$\begin{aligned} M_3 &= EIy''(0) = EI[Y_{st1}A_1 Y_{12}''(0) + Y_{st2}A_2 Y_{22}''(0) + Y_{st4}A_4 Y_{42}''(0)] \\ &= EI[0.034648(1.62093)(0) + (-0.017429(0.75101)(-0.036)) \\ &\quad + 0.000279(1.070728)(0.066723)] = 4.912053(10^{-4})EI \end{aligned} \quad (\text{x})$$

Note that the third mode does not contribute to the structural response because $Y_{st3} = 0$. Note also that the equilibrium check on moments is satisfied at the joint. Following similar procedures, the shears of member 1 at $t = 0.0379$ sec associated with the first, second, and fourth modes are

$$V_1 = -EIy'''(0) = 147,813.5061 + 50,905.6642 - 3987.3606 = 194,731.8097 \text{ lb} \quad (\text{y})$$

$$V_2 = -EIy'''(L) = -147,813.5061 - 74,084.9888 - 5632.0954 = -227,530.59 \text{ lb} \quad (\text{z})$$

**FIG. 4.24** Forces on member.

In order to achieve an equilibrium check on shears, the inertia force must be found in the following manner:

$$\begin{aligned} F &= m \int_0^L \ddot{y} = m \int [Y_{st1} \ddot{A}_1 Y_{11}(x) + Y_{st2} \ddot{A}_2 Y_{21}(x) + Y_{st4} \ddot{A}_4 Y_{41}(x)] dx \\ &= (-911,849.069 - 108,249.7469 - 3454.1239)0.2 = -204,710.586 \text{ lb} \end{aligned} \quad (\text{aa})$$

where \ddot{A} is the second derivative with time t of the dynamic load factor; for the present case, $A_k(t) = 1 - \cos p_k t + [(\sin p_k t)/p_k \zeta] - (t/\zeta)$; then

$$\ddot{A}_1 = \frac{d^2 A_1}{dt^2} = p_1^2 \cos p_1 t - \frac{p_1 \sin p_1 t}{\zeta} \quad (\text{bb})$$

where t should be 0.0379. Total external force on the span is

$$P = F(x, t)L = 3000 \left(1 - \frac{0.0379}{0.1}\right) 150 = 279,450 \text{ lb} \quad (\text{cc})$$

The free-body diagram with all the forces given in Eqs. (y), (z), (aa) and (cc) is shown in Fig. 4.24; then

$$\Sigma F_y = V_1 + V_2 - P - F = 484,160.58 - 422,262.39 = 61,898.19 \text{ lb} \quad (\text{dd})$$

The final result should be zero. Apparently, we have only used first four modes, the inclusion of additional modes will yield more accurate results (see Problem 4.19 for comparison based on four modes and five modes).

Note that the procedure to find inertia force in Eqs. (aa) and (bb) can be simplified without using the second derivative of $A_k(t)$. From Eq. (4.139) for the undamped case, we may write

$$\ddot{q}_k = f(t) Y_{stk} p_k^2 - p_k^2 Y_{stk} A_k(t)$$

and

$$\ddot{y}(x, t) = \sum Y_i(x) \ddot{q}_i(t) = \sum Y_i(x) Y_{stk} p_k^2 [f(t) - A_k(t)] \quad (\text{ee})$$

Thus Eq. (aa) can be expressed as

$$\begin{aligned} F &= m \ddot{y}_1 + m \ddot{y}_2 + m \ddot{y}_4 = m \left\{ p_1^2 Y_{st1} [f(t) - A_1] \int Y_{11}(x) dx + p_2^2 Y_{st2} [f(t) - A_2] \right. \\ &\quad \left. \int Y_{21}(x) dx + p_4^2 Y_{st4} [f(t) - A_4] \int Y_{41}(x) dx \right\} \end{aligned} \quad (\text{ff})$$

where every term has already been calculated except the integration of shape function. To illus-

trate the first term,

$$m\ddot{y}_1 = (0.2)(75.97625)^2(0.034648)(0.621 - 1.62095) \int_0^{150} 47.74648 \sin \lambda_1 x dx \quad (\text{gg})$$

$$= -182,405.025 \text{ lb}$$

Similarly

$$m\ddot{y}_2 = -21,641.00308 \text{ lb} \quad (\text{hh})$$

and

$$m\ddot{y}_4 = -691.256988 \text{ lb} \quad (\text{ii})$$

Summation of Eqs. (gg), (hh), and (ii) yields the desired result of Eq. (ff) as

$$m\ddot{y}_1 + m\ddot{y}_2 + m\ddot{y}_4 = -182405.025 - 21641.00308 - 691.256988 = -204,736.85286 \text{ lb} \quad (\text{jj})$$

which is close to the result in Eq. (aa). But the computational effort for Eq. (ff) is much less than that for Eq. (aa).

BIBLIOGRAPHY

1. FY Cheng, WH Tseng, M Botkin. Matrix calculations of structural dynamic characteristics and response. Proceedings of International Conference on Earthquake Analysis of Structures I, Jassy, Romania, 1970, pp 85–101.
2. FY Cheng. Matrix analysis of complex dynamic structures. Proceedings of Fifth Symposium on Earthquake Engineering, India, 1974, pp 267–278.
3. FY Cheng. Comparative studies of seismic structural synthesis. Proceedings of Central American Conference on Earthquake Engineering, El Salvador, Vol II, 1978, pp 22–37.
4. FY Cheng, YT Yeh (eds). Proceedings of CCNAA-AIT Joint Seminar on Research and Application for Multiple Hazards Mitigation, National Science Foundation (US) and National Science Council (Taiwan), Vols I and II, 1988.
5. RW Clough, J Penzien. Dynamics of Structures. 2nd ed. New York: McGraw-Hill, 1977.
6. CH Norris, RJ Hansen, MJ Holley, Jr, JM Biggs, S Namyat, JK Nirrami. Structural Design for Dynamic Loads. New York: McGraw-Hill, 1959.
7. JJ Tuma, FY Cheng. Dynamic structural analysis. New York: McGraw-Hill, 1983.
8. CK Wang. Computer methods in advanced structural analysis. New York: Intext Educational, 1973.

5

Dynamic Stiffness Method for Coupling Vibration, Elastic Media and P-Δ Effect

PART A FUNDAMENTALS

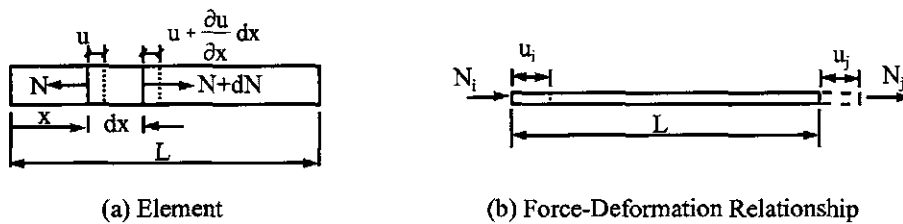
5.1. INTRODUCTION

Previous chapters treated only flexural vibration with bending deformation. This chapter undertakes the topics of longitudinal, torsional, and flexural vibrations with and without elastic media as well as coupling vibration. Flexural vibration further involves deformations due to bending and shear, rotatory inertia, and P-Δ effect. Coupling vibration herein implies that a structure vibrates in (a) longitudinal and flexural modes, (b) torsional and flexural modes, and (c) longitudinal, torsional, and flexural modes. Typical structures of plane trusses and elastic frames, plane grids, and space frames exemplify (a), (b) and (c), respectively. The effects of various parameters on vibration, such as the influence of bending and shear deformations, rotatory inertia, elastic media, and axial force on flexural frequencies, are derived in a closed form expressed in partial differential equations which are then used to obtain dynamic stiffness coefficients. Numerical examples are provided not only to illustrate calculation procedures but also to show the significant effects of coupling vibration and parameters on structural response.

5.2. LONGITUDINAL VIBRATION AND STIFFNESS COEFFICIENTS

Consider element dx of a longitudinal bar shown in Fig. 5.1a; the equilibrium equation of the element is

$$(m dx)\ddot{u} = N + dN - N \quad (5.1)$$

**FIG. 5.1** Longitudinal vibration.

where u = longitudinal displacement and N = axial force in tension. Since the axial force can be expressed in terms of area, A , and stress, $E\epsilon$, as $N = AE\epsilon = AE \partial u / \partial x$, Eq. (5.1) becomes

$$m dx \frac{\partial^2 u}{\partial t^2} = AE \frac{\partial^2 u}{\partial x^2} dx \quad \text{or} \quad \frac{\partial^2 u}{\partial t^2} = a^2 \frac{\partial^2 u}{\partial x^2} \quad (5.2)$$

where $a^2 = AE/m$. Using the separation of variables shown in Section 4.2 and substituting $u = X(x)g(t)$ into Eq. (5.2) yields

$$\frac{d^2 X}{dx^2} + \frac{p^2}{a^2} X = 0; \quad \frac{d^2 g}{dt^2} + p^2 g = 0 \quad (5.3)$$

of which the solutions are

$$X = C_1 \sin kx + C_2 \cos kx; \quad g = d_1 \sin pt + d_2 \cos pt \quad (5.4)$$

where

$$k = \sqrt{\frac{p^2 m}{AE}} \quad (5.5)$$

X and g are the shape function and time function, respectively.

Based on the following boundary conditions shown in Fig. 5.1b:

$$\begin{aligned} x = 0; \quad X &= u_i; \quad N_i = -AE \frac{dX}{dx} \\ x = L; \quad X &= u_j; \quad N_j = AE \frac{dX}{dx} \end{aligned} \quad (5.6)$$

the dynamic stiffness coefficients can be derived as

$$[SNU] = EAk \begin{bmatrix} \cot kL & -\csc kL \\ \text{symm} & \cot kL \end{bmatrix} = \begin{bmatrix} SNU_1 & SNU_2 \\ \text{symm} & SNU_1 \end{bmatrix} \quad (5.7)$$

in which SNU_1 and SNU_2 are symbolic notations.

5.3. LONGITUDINAL VIBRATION AND STIFFNESS COEFFICIENTS WITH ELASTIC MEDIA

Consider a prismatic bar encased in an elastic medium subjected to longitudinal vibration and let the spring constant be q and element length be dx ; then the equilibrium equation of $\Sigma F_x = 0$ is

$$AE \frac{\partial^2 u}{\partial x^2} - qu - m \frac{\partial^2 u}{\partial t^2} = 0 \quad (5.8)$$

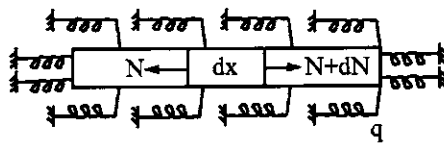


FIG. 5.2 Longitudinal vibrating bar encased in elastic medium.



FIG. 5.3 Example 5.3.1.

Note that q is expressed in terms of force per unit length and takes into account the width of the element. If $u = X(x)g(t)$, then Eq. 5.8 becomes

$$AE \frac{(d^2X/dx^2)}{mx} - \frac{q}{m} = \frac{d^2g/dt^2}{g} = -p^2 \quad (5.9)$$

from which

$$\frac{d^2X}{dx^2} + k^2X = 0 \quad \text{and} \quad \frac{d^2g}{dt^2} + p^2g = 0 \quad (5.10)$$

where

$$k = \sqrt{\frac{(mp^2 - q)}{AE}} \quad (5.11)$$

Since Eq. (5.10) is formally identical to Eq. (5.3), the stiffness coefficients given in Eq. (5.7) can likewise be used in this case by replacing the parameter k in Eq. (5.5) with that of Eq. (5.11).

EXAMPLE 5.3.1 The beam shown in Fig. 5.3 is subjected to harmonic force $F \sin \omega t$ and has the following structural properties: $A = 232.26 \text{ cm}^2$, $E = 206.84 \text{ GN/m}^2$, $L = 12.19 \text{ m}$, $\gamma = 76.973 \text{ kN/m}^3$, $q = m\omega^2/2$, $\omega = 330.84 \text{ rad/sec}$, and $F = 177.93 \text{ kN}$. Find the displacement at the free end and the reaction at the support end by using steady-state vibration analysis.

Solution: Based on the diagram shown in the accompanying figure, the system matrix equation

$$[F \sin \omega t] = [SNU_1] [X] \quad (a)$$

Let $\sin \omega t = 1$ for steady-state vibration; then

$$\{X\} = \frac{F}{EAk \cot kL} \quad (b)$$

in which

$$k = \sqrt{\frac{(m\omega^2 - q)}{AE}} \quad (c)$$

Using the given structural properties yields

$$m = \frac{\gamma A}{g} = \frac{76.973 (232.26) 10^{-4}}{9.81} = 0.1824 \text{ kN s}^2/\text{m}^2 \quad (\text{d})$$

$$q = \frac{m\omega^2}{2} = 9982.6427 \text{ kN/m}^2$$

$$k = \sqrt{\frac{(m\omega^2 - q)}{AE}} = \sqrt{\frac{q}{AE}} = \sqrt{\frac{9982.6427}{(0.023226)(206.84)10^6}} \\ = 0.045585 \text{ 1/m} \quad (\text{e})$$

and $kL = 0.55568$; then

$$\cot kL = 1.6105 \quad (\text{f})$$

The displacement at the free end is

$$X = \frac{F}{EAk \cot(kL)} = \frac{177.93}{(218,991.4197)(1.6105)} = 0.000504 \text{ m} \quad (\text{g})$$

The reaction at the support is

$$SNU_2 X = -EAk \csc(kL) X \\ = -218,991.4197 (1.89566) (0.000504) = -209.227 \text{ kN} \quad (\text{h})$$

5.4. DYNAMIC ANALYSIS OF TRUSSES AND ELASTIC FRAMES

According to the conventional definition of a statically loaded truss, the pin-connected members are either in tension or compression for the reason that external loads are applied at structural nodes only. When a *truss* vibrates, its constituent members not only have axial inertia forces but also transverse inertia forces; this is because overall vibration induces the members' mass to move in both longitudinal and transverse directions. In this case, one must consider the member's bending stiffness; even its slenderness ratio is normally very large. Since a truss member has both ends hinged, the inertia force is resisted at the structural nodes in two components: longitudinal force and shear. An *elastic structure* is a rigid connected framework in which the members also have longitudinal and flexural inertia forces. However, the inertia force of the member at an elastic structural node has three components of moment, shear, and axial force.

5.4.1. Dynamic Stiffness Coefficients of Pin-connected Member

Let a truss member of a vibrating system be shown in Fig. 5.4 in which the end-forces are $\{V\}$ and $\{N\}$ and their associated deformations are $\{Y\}$ and $\{u\}$, respectively. The member also has end-rotations, $\{\theta\}$, which are due to transverse inertia force; but no end-moments are associated with the rotations. For the longitudinal force-deformation relationship, $\{N\}$ vs $\{u\}$, the dynamic longitudinal stiffness is already presented in Eq. (5.7). The dynamic flexural stiffness coefficients of the member can be derived either by applying the boundary conditions (Fig. 5.4) directly to the shape function of Eq. (4.19) or by condensing Eq. (4.26b) on the basis that $\{M\} = 0$. Therefore

$$\{V\} = ([SY] - [SMY][SM\theta]^{-1}[SMY]) \{Y\} \quad (5.12)$$

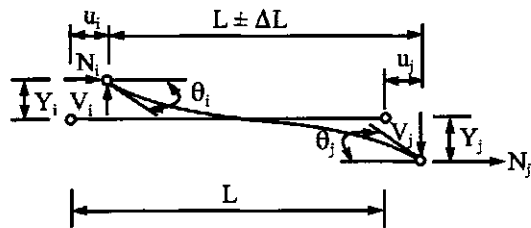


FIG. 5.4 Truss member of vibrating system.

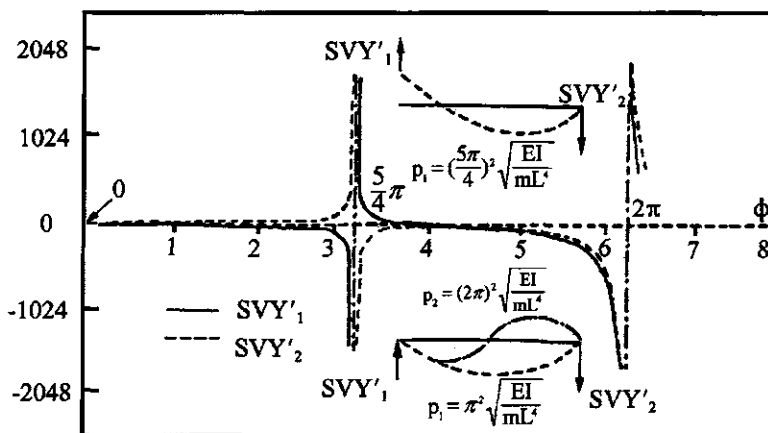


FIG. 5.5 Graphical description of SVY'_1 and SVY'_2 .

The final stiffness coefficients are

$$[SVY'] = \begin{bmatrix} cs' - c's & s' - s \\ \text{symm} & cs' - c's \end{bmatrix} \frac{\phi^3 EI}{2s'sL^3} = \begin{bmatrix} SVY'_1 & SVY'_2 \\ \text{symm} & SVY'_1 \end{bmatrix} \quad (5.13)$$

in which $s = \sin \phi$, $s' = \sinh \phi$, $c = \cos \phi$, $c' = \cosh \phi$, and

$$\phi = L\sqrt{p^2 m/EI} \quad (5.14)$$

The stiffness coefficients are graphically shown in Fig. 5.5 by varying ϕ to 2π . We may observe that when ϕ approaches zero as it does when there is no vibration, the stiffness coefficients are zero, corresponding to the static case. However, when $\phi = 5\pi/4$, the SVY'_1 is zero, and the ϕ corresponds to the resonance of a member having one end free and the other end hinged. Consequently, no exciting force is required at the free end to maintain the vibration. The sum of inertia force is then balanced by the reaction at the hinged end. When $\phi=\pi$ and 2π at the discontinuities, they represent the resonance of a member with both ends hinged; since the end deflections are zero, the stiffness coefficients become infinite. These ϕ 's are the frequency parameters of the first and second modes of the member.

5.4.2. Dynamic Stiffness Matrix of Trusses

The dynamic stiffness matrix may simply be called the stiffness matrix; it is, however, different from conventional statics because it includes frequency parameters. Formulation of a dynamic stiffness matrix, $[K]$, for plane or three-dimensional structures may use one of the following three techniques:

- (A) *Fundamental structural mechanics*—combine equilibrium matrix or compatibility matrix with stiffness coefficients as presented in Section 4.5.
- (B) *Physical interpretation*—displace the d.o.f. of a structure, one at a time, and then find the unbalanced forces at all structural nodes. The unbalanced forces induced by displacement associated with the system's d.o.f. represent the elements of a dynamic structural matrix.
- (C) *Direct element formulation*—formulate the stiffness matrix of each member, $[K^i]$, in the direction of global coordinates; then arrange the elements in $[K^i]$ by matching the number of local coordinates of the member with the system's global coordinates. Thus the structural stiffness is obtained as

$$[K] = \sum_{i=1}^{NM} [K^i] \quad (5.15)$$

where NM is the total number of members in a structure. These three techniques are briefly illustrated below. A *mapping technique* to formulate Eq. (5.15) is introduced in Section 8.12 for general three-dimensional building structures.

(A) *Fundamental structural mechanics*—Consider the truss shown in Fig. 5.6a. The external action (or possible forces applied at the structural nodes), $\{P_s\}$, and their associated displacements (or NP d.o.f. of global coordinates), $\{X_s\}$, are sketched in Fig. 5.6b. The internal resistances of $\{N\}$ and $\{V\}$ are designated in the accompanying Fig. 5.6c, where the signs are all positive identical to those used in stiffness derivations in Figs. 5.1 and 5.4. Let the possible external forces and internal forces be shown in the free-body diagram; then the equilibrium conditions at structural nodes B and C can be established as

$$\{P_s\}e^{ipt} = [A_n]\{N\} + [A_s]\{V\} \quad (5.16)$$

in which

$$[A_n] = \begin{bmatrix} 0 & 1 & 0 & 0 & 0 & 0 & 0 & 0 \\ 0 & 0 & 0 & 0 & -1 & 0 & 0 & c \\ 0 & 0 & 1 & 0 & 0 & 0 & 0 & 0 \\ 0 & 0 & 0 & 1 & 0 & 0 & 0 & s \end{bmatrix} \quad (5.17)$$

and

$$[A_s] = \begin{bmatrix} 0 & 0 & 1 & 0 & 0 & 0 & 0 & 0 \\ 0 & 0 & 0 & -1 & 0 & 0 & 0 & -s \\ 0 & 1 & 0 & 0 & 0 & 0 & 0 & 0 \\ 0 & 0 & 0 & 0 & 1 & 0 & 0 & c \end{bmatrix} \quad (5.18)$$

where $c = \cos \tau$ and $s = \sin \tau$. Following the proof in Section 4.5.4, the structural matrix equation

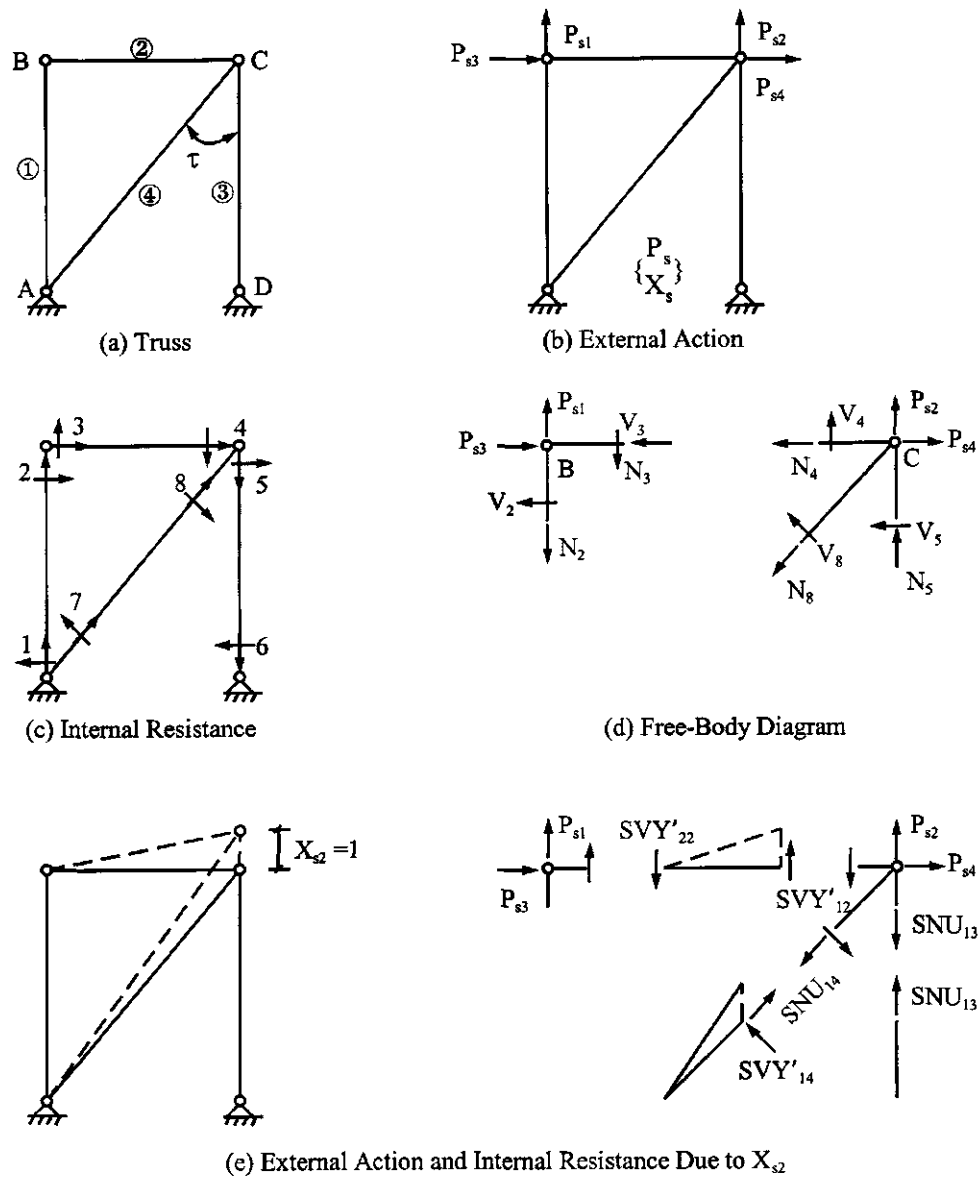


FIG. 5.6 Truss analysis.

of a truss can be formulated as

$$\begin{aligned} \{P_s\}e^{ipt} &= [A_n|A_s] \begin{bmatrix} SNU & | & 0 \\ -- & | & -- \\ 0 & | & SVY' \end{bmatrix} [A_n|A_s]^T \{X_s\} e^{ipt} \\ &= [[A_n][SNU][A_n]^T + [A_s][SVY'][A_s]^T] \{X_s\} e^{ipt} \\ &= [K] \{X_s\} e^{ipt} \end{aligned} \quad (5.19)$$

in which $[SNU]$ and $[SVY]$ are the diagonal *band submatrices* of the stiffness coefficients associated with the members of a system.

(B) *Physical interpretation*—displace each of $\{X_s\}$ in Fig. 5.6b one at a time, and then find the unbalanced forces at the structural nodes, B and C , caused by that displacement. For instance, let $X_{s1} = 1$ and the other X_s 's = 0; then

$$P_{sj} = K_{ij} \quad i = 1, 2, \dots, NP \quad (5.20)$$

where K_{ij} represents the unbalanced forces due to $X_{sj} = 1$, which in turn are the elements in the j th column of $[K]$ in global coordinates. If $j = 1$, then $X_{s2} = X_{s3} = X_{s4} = 0$, and $P_{s1} = SNU_{11} + SVY'_{12} = K_{11}$, $P_{s2} = -SVY'_{22} = K_{21}$, $P_{s3} = K_{31} = 0$, $P_{s4} = K_{41} = 0$, which form the first column of Eq. (5.21). In a similar manner, let $X_{s2} = 1$, without moving other d.o.f., as shown in Fig. 5.6c; then the unbalanced forces are expressed in the second column of $[K]$. Thus the complete structural stiffness is

$$[K] = \begin{bmatrix} SNU_{11} + SVY'_{12} & & & \\ -SVY'_{22} & SNU_{13} + SNU_{14}c^2 & & \\ 0 & SVY'_{12} + SVY'_{14}s^2 & & \\ 0 & 0 & SNU_{12} + SVY'_{11} & \\ 0 & SNU_{14}cs & SNU_{22} & SNU_{12} + SNU_{14}s^2 \\ -SVY'_{14}cs & -SVY'_{13} & +SVY'_{13} + SVY'_{14}c^2 & \end{bmatrix} \text{ symm } \quad (5.21)$$

(C) *Direct element formulation*—direct element formulation is to transform the local coordinate of a member into global coordinates. The members are assembled to form a structural stiffness matrix. In the transformation, the d.o.f. of global coordinates at supports can be handled in two ways: (1) assign d.o.f. to the supports as is usual with any structural node; then eliminate the row(s) and column(s) in the stiffness matrix, $[K]$, which are associated with the restraints from supporting conditions; or (2) assign NP d.o.f. to all the structure's free nodes with one redundant number, say 0 or 1. In the case of $NP+1$, the extra row and column of $[K]$ associated with the redundant d.o.f. can be disregarded in the solution procedure of dynamic response analysis.

Let the local and global coordinates of a truss member be assigned as shown in Fig. 5.7a and b, respectively. Typical transformation of a member at its end, p , is given in the accompanying Fig. 5.7c, from which

$$\begin{Bmatrix} u'_p \\ v'_p \end{Bmatrix} = \begin{bmatrix} \cos \phi & \sin \phi \\ -\sin \phi & \cos \phi \end{bmatrix} \begin{Bmatrix} u_p \\ v_p \end{Bmatrix} = [\nabla_p] \begin{Bmatrix} u_p \\ v_p \end{Bmatrix} \quad (5.22)$$

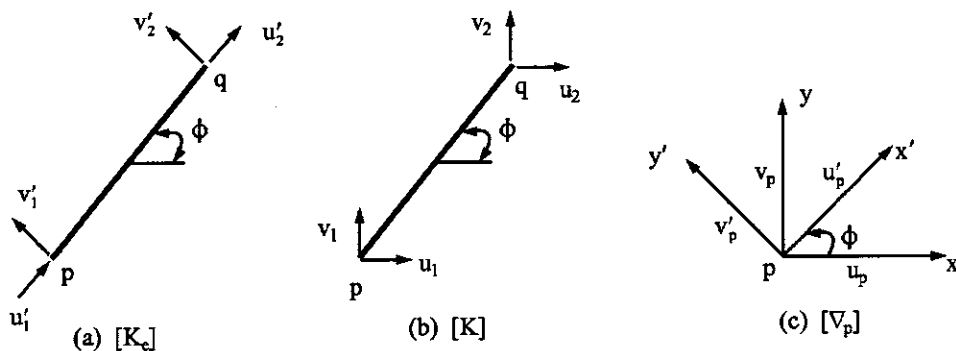


FIG. 5.7 Coordinate transformation of truss member.

Note that

$$[\nabla_p]^{-1} = [\nabla_p]^T \quad (5.23)$$

Dynamic stiffness coefficients of a truss member, comprising Eqs. (5.7) and (5.12), configure as follows for any member i according to the numbers assigned to the local d.o.f. shown in Fig. 5.7a.

$$[K_e] = \begin{bmatrix} SNU_1 & 0 & | & SNU_2 & 0 \\ 0 & SVY'_1 & | & 0 & -SVY'_2 \\ \hline SNU_2 & 0 & | & SNU_1 & 0 \\ 0 & -SVY'_2 & | & 0 & SVY'_1 \end{bmatrix} = \begin{bmatrix} S_{11} & | & S_{12} \\ \hline S_{21} & | & S_{22} \end{bmatrix} \quad (5.24)$$

which is then transformed into global coordinates as

$$[K^i] = \begin{bmatrix} \nabla_i^T S_{11} \nabla_i & | & \nabla_i^T S_{12} \nabla_i \\ \hline \text{symm} & | & \nabla_i^T S_{22} \nabla_i \end{bmatrix} \quad (5.25)$$

The structural stiffness is formed through member-by-member assemblage as given in Eq. (5.15),

$$[K] = \Sigma [K^i] \quad (5.26)$$

Note that $[K]$ comprises either all the d.o.f. including supports or NP plus one redundant number; it depends on how we assign the global d.o.f.

The external load matrix should also be transformed as

$$\{P_s\} e^{ipt} = [\nabla]^T \{P'_s\} e^{ipt} \quad (5.27)$$

in which $[\nabla]$ comprises $[\nabla_i]$ at the structural nodes, $\{P'_s\}$ represents forces in element's coordinates. Combining Eqs. (5.26) and (5.27) yields the same results as Eq. (5.19). Analysis of a truss with and without inclusion of transverse inertia force (SVY') can have significant differences in natural frequencies. This can be observed from the solutions of Problems 5.6 and 5.19.

5.4.3. Dynamic Stiffness Matrix of Elastic Frames

The three techniques of formulating $[K]$ in the previous article are also illustrated here for the elastic frame shown in Fig. 5.8. The structure has total d.o.f. of $NP = 6$ and linear d.o.f. of $NPS = 3$ as determined by using Eq. (4.27a, d). The d.o.f. of global and local coordinates are assigned in Figs. 5.8a and b, respectively.

(A) *Fundamental structural mechanics*—the equilibrium equations of an elastic system can be generally expressed as

$$\{P_\theta\} e^{ipt} = [A_\theta] \{M\} \quad (5.28)$$

$$\{P_s\} e^{ipt} = [A_s] \{V\} + [A_n] \{N\} \quad (5.29)$$

Based on the d.o.f. assigned in Fig. 5.8a and b, the equilibrium matrices are

$$[A_\theta] = \begin{bmatrix} 1 & 0 & 0 & 0 & 0 & 1 \\ 0 & 1 & 1 & 0 & 0 & 0 \\ 0 & 0 & 0 & 1 & 1 & 0 \end{bmatrix} \quad (5.30)$$

$$[A_s] = \begin{bmatrix} 0 & -c & c' & 0 & 0 & 0 \\ 0 & s & s' & 0 & 0 & 0 \\ 0 & 0 & 0 & -s' & 0 & 0 \end{bmatrix} \quad (5.31)$$

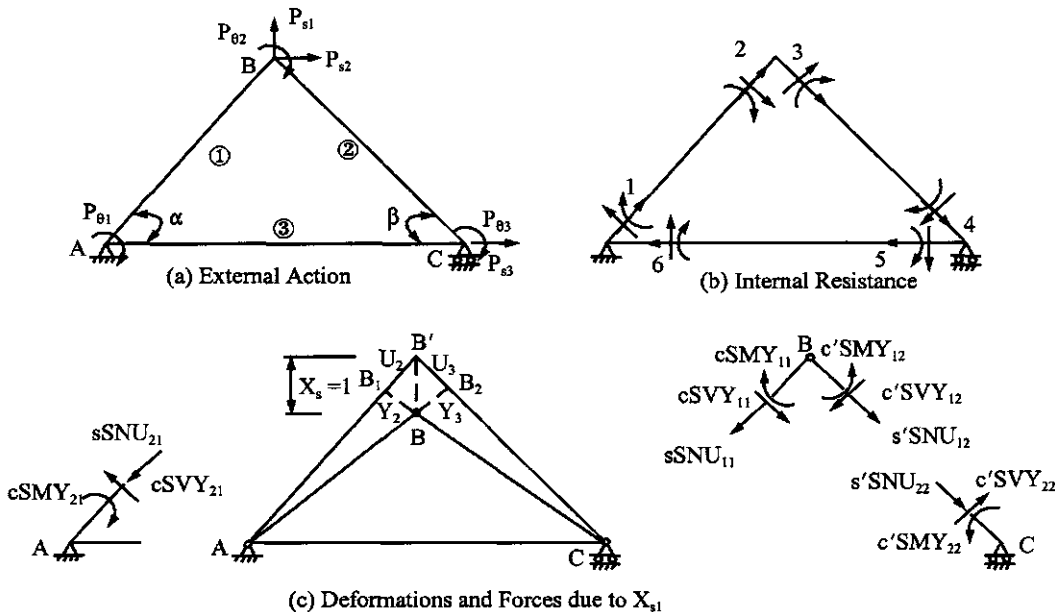


FIG. 5.8 Elastic frame analysis.

and

$$[A_n] = \begin{bmatrix} 0 & s & -s' & 0 & 0 & 0 \\ 0 & c & c' & 0 & 0 & 0 \\ 0 & 0 & 0 & c' & -1 & 0 \end{bmatrix} \quad (5.32)$$

where $s = \sin \alpha$, $s' = \sin \beta$, $c = \cos \alpha$, and $c' = \cos \beta$. In a similar manner shown in Eq. (5.19), the structural matrix equation of an elastic frame can be expressed as

$$\begin{Bmatrix} P_\theta \\ P_s \end{Bmatrix} e^{ipt} = \left(\begin{array}{c|c} [A_\theta][SM0][A_\theta]^T & [A_\theta][SMY][A_s]^T \\ \hline \text{symm} & [A_s][SVY][A_s]^T \end{array} \right) + \begin{Bmatrix} 0 \\ [A_n][SNU][A_n]^T \end{Bmatrix} \begin{Bmatrix} X_\theta \\ X_s \end{Bmatrix} e^{ipt} \\ = [K] \begin{Bmatrix} X_\theta \\ X_s \end{Bmatrix} e^{ipt} \quad (5.33)$$

in which $[SM0]$, $[SMY]$, $[SVY]$, and $[SNU]$ comprise NM submatrices. Each submatrix represents a member's dynamic stiffness as given in Eqs. (4.26) and (5.7). The arrangement of the submatrices is based on the relationship between global and local coordinates as shown in the equilibrium matrices.

(B) *Physical interpretation*—the structural stiffness matrix of the elastic frame is given in Eq. (5.34) which may be obtained by using any of these three techniques.

$$[K] = \begin{bmatrix} SM\theta_{11} + SM\theta_{13} & SM\theta_{21} & SM\theta_{23} & -cSMY_{21} & sSMY_{21} & 0 \\ SM\theta_{11} + SM\theta_{21} & SM\theta_{11} + SM\theta_{21} & SM\theta_{22} & -cSMY_{11} + c'SMY_{12} & sSMY_{11} + s'SMY_{12} & -s'SMY_{22} \\ SM\theta_{12} + SM\theta_{13} & SM\theta_{22} & c'SMY_{22} & c'SMY_{22} & s'SMY_{22} & -s'SMY_{12} \\ & & c^2SVY_{11} + c^2SVY_{12} & -s^2SVY_{11} + s^2SVY_{12} & -s^2SVY_{12} & -s^2SVY_{22} \\ & & +s^2SNU_{11} + s^2SNU_{12} & +s^2SNU_{11} - s^2SNU_{12} & -s^2SNU_{12} & -s^2SNU_{22} \\ & & & s^2SVY_{11} + s^2SVY_{12} & +c^2SNU_{11} + c^2SNU_{12} & +c^2SNU_{22} \\ & & & +c^2SNU_{11} + c^2SNU_{12} & s^2SNU_{11} + s^2SNU_{12} & s^2SNU_{22} \\ & & & & & +c^2SNU_{12} + SNU_{13} \end{bmatrix} \quad (5.34)$$

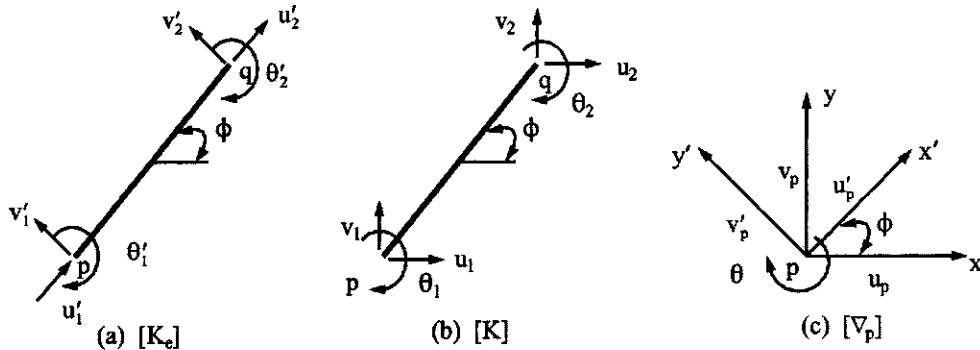


FIG. 5.9 Coordinate transformation of elastic member.

Note that the unbalanced forces due to the displacements of X_θ 's are moments and shears as shown in the first three columns of $[K]$ (or $K_{ij}, j = 1, 2, 3, i = 1, 2, \dots, 6$); the unbalanced forces due to the displacements of X_s 's are moments, shears, and axial forces $K_{ij}, j = 4, 5, 6$ and $i = 1, 2, \dots, 6$ in Eq. (5.34).

For illustration of the physical interpretation technique, let $X_{s1} = 1$, with other d.o.f. not moving, as shown in Fig. (5.8c); the members are then deformed as

$$\begin{aligned} Y_2 &= BB_1 = -\cos \alpha; & U_2 &= B_1 B' = \sin \alpha \\ Y_3 &= BB_2 = \cos \beta; & U_3 &= B_2 B' = -\sin \beta \end{aligned} \quad (5.35)$$

The negative sign with Y_2 in Eq. (5.35) is due to deflections at end 2 of member 1 opposite to the typical sign convention in Fig. 4.2. Similarly, U_3 is negative because end 3 is in tension, due to X_{s1} having moved, opposite to the typical sign convention in Fig. 5.1. Thus the internal forces resulting from the members' end-deformations are identified in the free-body diagrams by stiffness coefficients and their acting directions. The unbalanced forces at nodes A , B , and C can be obtained by using

$$\Sigma M = 0; \quad \Sigma F_x = 0; \quad \text{and} \quad \Sigma F_y = 0 \quad (5.36)$$

which yield the elements listed in the fourth column of $[K]$.

(C) *Direct element formulation*—let a typical elastic member be shown in Fig. 5.9; then the transformation at member end, p , can be established from the accompanying Fig. 5.9c as

$$\begin{Bmatrix} u'_p \\ v'_p \\ \theta'_p \end{Bmatrix} = \begin{bmatrix} \cos \phi & \sin \phi & 0 \\ -\sin \phi & \cos \phi & 0 \\ 0 & 0 & 1 \end{bmatrix} \begin{Bmatrix} u_p \\ v_p \\ \theta_p \end{Bmatrix} = [\nabla_p] \begin{Bmatrix} u_p \\ v_p \\ \theta_p \end{Bmatrix} \quad (5.37)$$

The stiffness coefficients of the elastic member should comprise the flexural stiffness in Eq. (4.26a) and the longitudinal stiffness in Eq. (5.7) as shown below:

$$[K_e] = \left[\begin{array}{ccc|ccc} SNU_1 & 0 & 0 & | & SNU_2 & 0 & 0 \\ 0 & SMY_1 & 0 & | & 0 & -SMY_2 & 0 \\ 0 & 0 & SM\theta_1 & | & 0 & 0 & SM\theta_2 \\ \hline SNU_2 & 0 & 0 & | & SNU_1 & 0 & 0 \\ 0 & -SMY_2 & 0 & | & 0 & SMY_1 & 0 \\ 0 & 0 & SM\theta_2 & | & 0 & 0 & SM\theta_1 \end{array} \right] \begin{bmatrix} S_{11} & | & S_{12} \\ \hline S_{21} & | & S_{21} \end{bmatrix} \quad (5.38)$$

Note that the sign and the coefficients' location in Eq. (5.38) are based on the coordinate system

given in Fig. (5.9a). Thus the stiffness coefficients in global coordinates are transformed by employing Eqs. (5.37) and (5.38) as symbolically expressed in Eq. (5.25). The structural stiffness matrix is then obtained by following the procedures presented in Eq. (5.26).

5.4.4. Coupling of Longitudinal and Flexural Vibration

When a plane structure is subjected to dynamic excitations, its constituent members may have longitudinal and flexural vibration. The vibration modes and frequencies may be coupled. *Coupling vibration* means that when a structural system is in vibration, all the constituent members vibrate in the same frequency for both the longitudinal and flexural motions. On the other hand, *uncoupling vibration* implies that longitudinal and flexural motions are independent of each other so the vibration mode of a system depends on whether the mode is associated with longitudinal or flexural frequency, but not affected by both. Whether a structure is in coupling or uncoupling motion depends on structural configuration, distribution of the structure's mass and stiffness, and modeling. The simple case may be observed from Example 5.4.1 and Problem 2.5. In the example, individual longitudinal and flexural modes vibrate independently; for the given problem, if the stiffness and mass of the frame are symmetric, then the vertical, lateral, and rocking motions do not affect each other. However, if the mass, stiffness, or structural configuration is not symmetric, then vertical, lateral, and rocking motions will vibrate simultaneously. Therefore these motions cannot be independent. The fundamental behavior of coupling vibration and the variables that induce this type of motion are discussed here and in Section 5.7.

To determine the natural frequencies of a coupling motion, Eqs. (4.107)–(4.110) are used to express the flexural vibration parameters of the constituent member, i , in terms of the reference member, 1, as

$$\phi_i = \alpha_i \sqrt{\frac{\gamma_i}{\beta_i}} \sqrt{\frac{P^2 m_1 L_1^4}{EI_1}} = \delta_i \phi_1 \quad (5.39)$$

Since vibration frequencies in both the longitudinal and transverse directions are the same, the frequency parameters in longitudinal stiffness of that member can be expressed in terms of ϕ_1 as

$$k_i L_i = L_i \sqrt{\frac{P^2 m_i}{A_i E}} = \frac{\delta_i^2 \phi_1^2}{\alpha_i L_1} \sqrt{\frac{\beta_i}{\varepsilon_i}} \quad (5.40)$$

and

$$EA_i k_i = \frac{EI_1 \delta_i^2 \phi_1^2}{\alpha_i^2 L_1^2} \sqrt{\beta_i \varepsilon_i} \quad (5.41)$$

where

$$\varepsilon_i = \frac{A_i}{I_1} \quad (5.42)$$

EXAMPLE 5.4.1 Find the natural frequencies of the first four modes of the beam shown in Fig. 5.10a with consideration of both longitudinal and flexural vibrations. The member properties are $L = 12.19 \text{ m}$, $A = 232.26 \text{ cm}^2$, $E = 206.84 \text{ GN/m}^2$, $\gamma = 76.973 \text{ kN/m}^3$, and $I = (1.01144)10^{-4} \text{ m}^4$. The slenderness ratio, L/R , of the beam is 184.76.

**FIG. 5.10** Example 5.4.1.

Solution: Let the beam be treated as a structure of two members for which a structural node and its d.o.f. are assigned at mid-span as shown in Fig. 5.10b. Based on the diagram, the structural stiffness matrix is

$$[K] = \begin{bmatrix} SM\theta_{11} + SM\theta_{12} & -SMY_{11} + SMY_{12} & 0 \\ -SMY_{11} + SMY_{12} & SVY_{11} + SVY_{12} & 0 \\ 0 & 0 & SNU_{11} + SNU_{12} \end{bmatrix} \quad (\text{a})$$

of which the determinant yields the following frequency equation:

$$|K| = [(SM\theta_{11} + SM\theta_{12})(SVY_{11} + SVY_{12}) - (-SMY_{11} + SMY_{12})^2](SNU_{11} + SNU_{12}) = 0 \quad (\text{b})$$

Thus

$$SNU_{11} + SNU_{12} = 0 \quad (\text{c})$$

or

$$(SM\theta_{11} + SM\theta_{12})(SVY_{11} + SVY_{12}) - (SMY_{11} + SMY_{12})^2 = 0 \quad (\text{d})$$

Eqs. (c) and (d) yield longitudinal and flexural frequencies, respectively. This vibration is uncoupled because the beam can vibrate in longitudinal and transverse modes independently.

Substituting longitudinal stiffness coefficients in Eq. (c) yields

$$2EAk \cot kL = 0 \quad (\text{e})$$

Thus the first four modes correspond to

$$kL = \frac{\pi}{2}; \quad \frac{3\pi}{2}; \quad \frac{5\pi}{2}; \quad \text{and} \quad \frac{7\pi}{2} \quad (\text{f})$$

Using the given member properties in the following

$$kL = L \sqrt{\frac{p^2 m}{EA}} \quad (\text{g})$$

the first four frequencies are obtained as

$$\begin{Bmatrix} p_1 \\ p_2 \\ p_3 \\ p_4 \end{Bmatrix} = \begin{Bmatrix} 661.27 \\ 1983.80 \\ 3306.34 \\ 4628.87 \end{Bmatrix} \text{ rad/sec} \quad (\text{h})$$

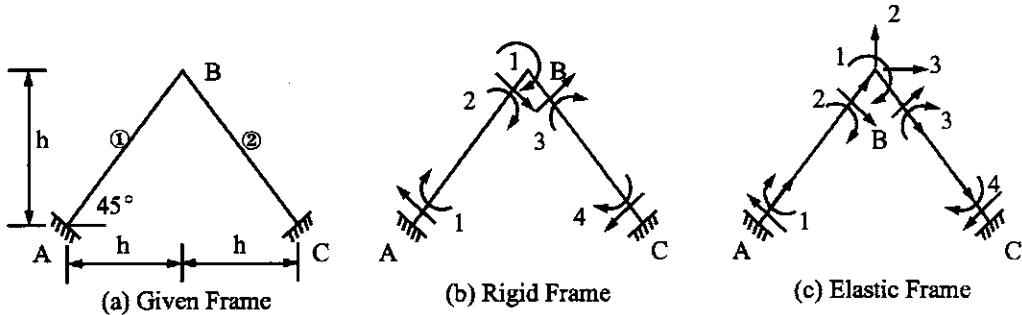


FIG. 5.11 Example 5.4.2.

Similarly, employing appropriate flexural stiffness coefficients in Eq. (d) and then substituting member properties, the following flexural frequency parameters, ϕ_{1i} , $i = 1, \dots, 4$, are found

$$\begin{Bmatrix} \phi_{11} \\ \phi_{12} \\ \phi_{13} \\ \phi_{14} \end{Bmatrix} = \begin{Bmatrix} 2.365020 \\ 3.926602 \\ 5.497804 \\ 7.068583 \end{Bmatrix} \quad (i)$$

From Eq. (4.110) or (5.14),

$$p_i = \frac{\phi_{1i}^2}{L^2} \sqrt{\frac{EI}{m}} \quad (j)$$

we have

$$\begin{Bmatrix} p_1 \\ p_2 \\ p_3 \\ p_4 \end{Bmatrix} = \begin{Bmatrix} 12.747 \\ 35.137 \\ 68.884 \\ 113.868 \end{Bmatrix} \text{ rad/sec} \quad (k)$$

Note that the frequencies in Eqs. (h) and (k) are not the same; their values depend on the parameters in Eqs. (g) and (j), respectively. Longitudinal frequencies are much higher on the order of 52, 56, 48, and 40 times the corresponding flexural frequencies.

EXAMPLE 5.4.2 In the two-bar frame shown in Fig. 5.11a, member properties are $L = 12.19$ m, $A = 232.26$ cm 2 , $E = 206.84$ GN/m 2 , $\gamma = 76.973$ kN/m 3 , $I = 10,114.423$ cm 4 , and $h = 8.6196$ m. The slenderness ratio of each member, L/R , is 184.72. Find the natural frequencies of the first five modes by considering (A) rigid frame with flexural vibration only, and (B) elastic frame with longitudinal and flexural vibration. Compare the results.

Solution: (A) The diagram for rigid frame analysis with one d.o.f. in rotation is shown in Fig. 5.11b. Although the members have dynamic stiffness coefficients associated with moments and shears, the stiffness matrix is due to unbalanced moments only. Thus the structural stiffness matrix can be simply obtained as

$$[K] = 2SM\theta_{11} \quad (a)$$

in which the zero determinant yields the frequency parameter of any mode n as ϕ_{1n} . Using the given EI and m , the corresponding frequency can be expressed as

$$p_n = \frac{\phi_{1n}^2}{L^2} \sqrt{\frac{EI}{m}} = 338.6448 \frac{\phi_{1n}^2}{L^2} \quad (b)$$

(B) The diagram for elastic frame analysis with three d.o.f. is shown in Fig. 5.11c. The structural stiffness matrix is

$$[K] = \begin{bmatrix} SM\theta_{11} + SM\theta_{12} & c(-SMY_{11} + SMY_{12}) & s(SMY_{11} + SMY_{12}) \\ & c^2(SVY_{11} + SVY_{12}) & sc(-SVY_{11} + SVY_{12}) \\ & +s^2(SNU_{11} + SNU_{12}) & +sc(SNU_{11} - SNU_{12}) \\ \text{symm} & & s^2(SVY_{11} + SVY_{12}) \\ & & +c^2(SNU_{11} + SNU_{12}) \end{bmatrix} \quad (c)$$

where $s = \sin 45^\circ$ and $c = \cos 45^\circ$. The determinant of $[K]$ yields a frequency equation in which longitudinal and flexural vibrations are coupled because the zero determinant cannot be evaluated by using these two groups of stiffness independently.

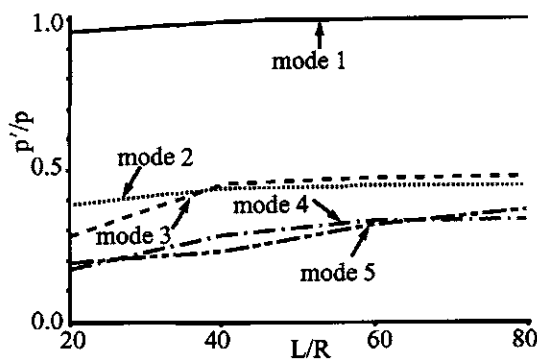
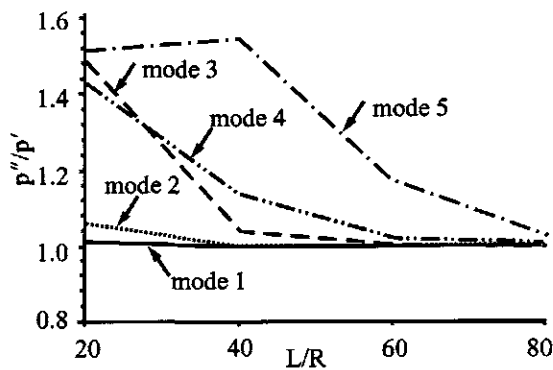
For the given structural properties, we find the parameters of longitudinal stiffness from Eqs. (5.40) and (5.41), in which the variable ϕ_1 is a function of flexural frequency. The singularity of $[K]$, as in the case of zero determinant, yields ϕ_{1n} , which is then substituted into Eq. (b) for the vibrating frequencies of the system. The results of Cases (A) and (B) are given in Eq. (d), where p_n is in rad/sec. It is apparent that the vibration is dominated by flexure in the first mode, and the coupling effect becomes significant for higher modes.

Case	Mode				
	First	Second	Third	Fourth	
A	ϕ_{1n}	3.92699	7.06858	10.21018	13.35176
	p_n	35.1444	113.8807	237.7539	406.2689
B	ϕ_{1n}	3.92576	4.72703	7.06324	7.83831
	p_n	35.1224	50.9229	113.6962	140.0172

EXAMPLE 5.4.3 Study the coupling effect of the structure given in the previous example. (A) Find the natural frequencies of flexure only, p , and of coupling effect, p' , for the first five modes by considering a wide range of slenderness ratios for the two identical members: $L/R = 20, 40, 60$, and 80 . (B) Study the influence of longitudinal frequency parameter on the coupling frequencies by letting the longitudinal dynamic stiffness be replaced by static stiffness as AE/L ; find the pseudo-coupling frequencies p'' , and compare them with p' obtained in (A).

Solution: (A) Employing the given structural properties in Eqs. (a) and (c) of the previous example, p and p' are first found and then tabulated in Eq. (a). The ratios of p'/p are plotted in Fig. 5.12.

Mode	$L/R = 20$		$L/R = 40$		$L/R = 60$		$L/R = 80$	
	p'	p	p'	p	p'	p	p'	p
1	2862.64	2998.04	742.17	749.51	331.67	333.12	186.91	187.38
2	3666.82	9713.64	1054.27	2428.41	477.17	1079.29	269.96	607.10
3	5638.55	20266.76	2264.11	5066.69	1059.12	2251.86	601.55	1266.67
4	5994.03	34657.30	2410.09	8664.33	1257.17	3850.81	730.51	2166.08
5	9998.64	52885.42	3035.93	13221.35	1861.46	5876.16	1211.67	3305.34

FIG. 5.12 p'/p vs L/R .FIG. 5.13 p''/p' vs L/R .

It is apparent that longitudinal vibration significantly influences the coupling frequencies in higher modes. A structure having smaller slenderness ratios displays more significant effects. At the fifth mode, the ratios of p'/p are 0.189 and 0.366, corresponding to $L/R = 20$ and 80, respectively. p' is always smaller than p .

(B) Replace SNU_{11} and SNU_{12} by AE/L in Eq. (c) of the structure's stiffness matrix given in the previous example; then consider axial deformation but not longitudinal frequencies. The frequency is called *pseudo-coupling frequency*, signified by p'' , which is tabulated in Eq. (b). The ratios of p''/p' and p''/p are shown in Figs. 5.13 and 5.14, respectively.

Mode	$L/R = 20$ p''	$L/R = 40$ p''	$L/R = 60$ p''	$L/R = 80$ p''	
1	2887.85	742.52	331.70	186.91	
2	3871.75	1057.62	477.45	270.01	
3	8380.78	2348.64	1063.92	602.29	(b)
4	8556.34	2739.30	1283.46	734.33	
5	15084.68	4680.52	2180.74	1244.95	

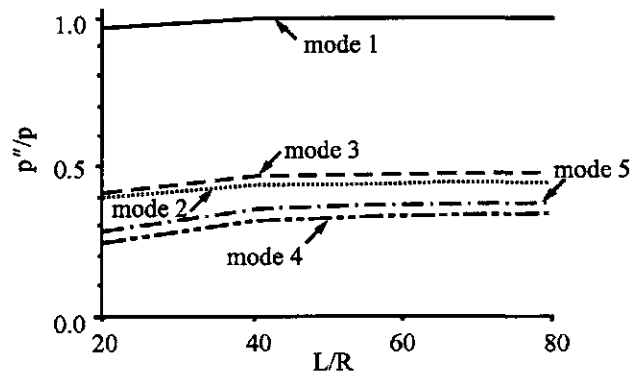
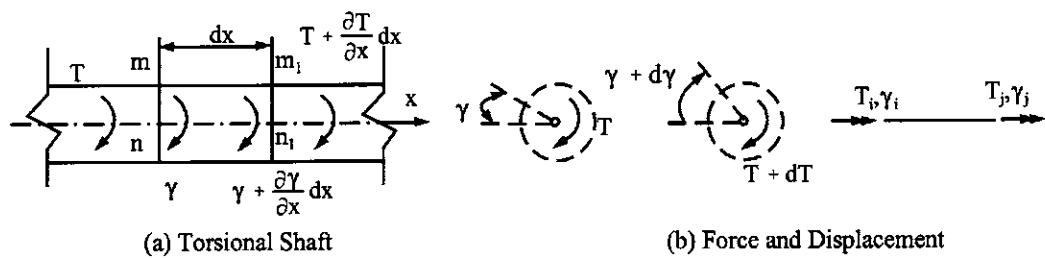
FIG. 5.14 p''/p vs L/R .

FIG. 5.15 Element subjected to torsion.

The above three figures reveal that: (1) p and p' are respectively upper and lower bounds of the frequencies; (2) the coupling effect on frequencies becomes more significant for higher modes and smaller slenderness ratios; and (3) the pseudo-coupling approach may be used for lower modes.

5.5. TORSIONAL VIBRATION AND STIFFNESS COEFFICIENTS

Consider an element, dx , of a circular shaft shown in Fig. 5.15. Let $\gamma = \gamma(x, t)$ be the angular displacement of the section mn at the time measured from the position of equilibrium. The angle of twist or angular displacement at $m_1 n_1$ at time t is $\gamma + (\partial\gamma/\partial x) dx$. If $T = T(x, t)$ signifies the *torque* or *twisting moment* at mn and time t , then the torque at $m_1 n_1$ at the same time is $T + (\partial T/\partial x) dx$. Let G = the shear modulus and the *polar moment of inertia* be

$$I_p = \int R^2 dA = I_x + I_y \quad (5.43a)$$

Then the *torsional inertia* may be expressed as

$$J = cI_p \quad (5.43b)$$

where R is radius of gyration and c is a constant. For an element of the member between mn and

m_1n_1 , the twisting moments are

$$T = GJ \frac{\partial \gamma}{\partial x} \quad (5.44a)$$

$$T + \frac{\partial T}{\partial x} dx = GJ \left(\frac{\partial \gamma}{\partial x} + \frac{\partial^2 \gamma}{\partial x^2} dx \right) \quad (5.44b)$$

Since the resulting torque acting on the element dx is equal to the element's mass moment of inertia multiplied by angular acceleration, the differential equation of motion of the element can be expressed as

$$\rho I_p \frac{\partial^2 \gamma}{\partial t^2} = GJ \frac{\partial^2 \gamma}{\partial x^2} \quad (5.45)$$

where ρ is unit mass per unit volume (or mass density). Using the separation of variables $\gamma = X(x)g(t)$ in the above yields

$$\frac{d^2 X}{dx^2} - \frac{p^2 \rho I_p}{GJ} X = 0 \quad (5.46a)$$

$$\frac{d^2 g}{dt^2} - p^2 g = 0 \quad (5.46b)$$

The solution of Eq. (5.46a) is

$$X = C_1 \cos(\psi X) + C_2 \sin(\psi x) \quad (5.47)$$

where

$$\psi = \sqrt{\frac{p^2 \rho I_p}{GJ}} \quad (5.48)$$

Using the sign convention shown in Fig. 5.15b leads to

$$x = 0, \quad X = \gamma_i; \quad T_i = -GJ \frac{dX}{dx} \quad (5.49)$$

and

$$x = L, \quad X = \gamma_j; \quad T_j = GJ \frac{dX}{dx} \quad (5.50)$$

Substituting Eq. (5.47) into Eqs. (5.49) and (5.50) then yields the following dynamic torsional stiffness coefficients

$$[ST\gamma] = \begin{bmatrix} ST\gamma_1 & ST\gamma_2 \\ \text{symm} & ST\gamma_1 \end{bmatrix} = GJ\psi \begin{bmatrix} \cot(\psi L) & -\csc(\psi L) \\ \text{symm} & \cot(\psi L) \end{bmatrix} \quad (5.51)$$

5.6. DYNAMIC STIFFNESS MATRIX OF GRID SYSTEMS

Grillage is a structure consisting of two sets of orthogonal or nonorthogonal beams rigidly connected at the intersections. A gridwork may be used for building floors, ship decks, bridge floor systems, missile ground facilities, electronically steerable radar systems, and so forth. In a *plane grid* system, the constituent members are subjected to both bending and torsion. General grid patterns are shown in Fig. 5.16. A typical member is given in Fig. 5.17, in which the member ends have moments M_i , M_j , shears V_i , V_j , and torques T_i , T_j . The dynamic stiffness coefficients and their sign convention are the same as those given in Eqs. (4.25b) and (5.51).

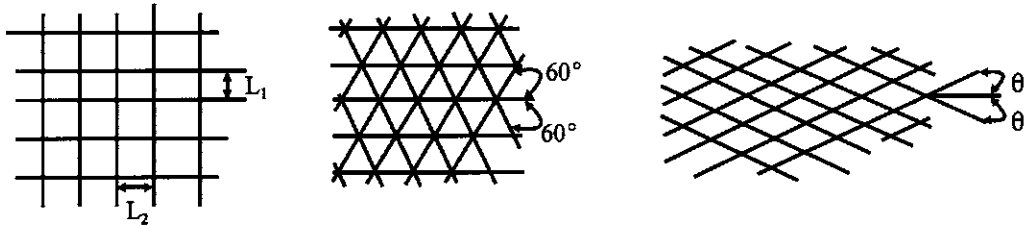


FIG. 5.16 General grid patterns.

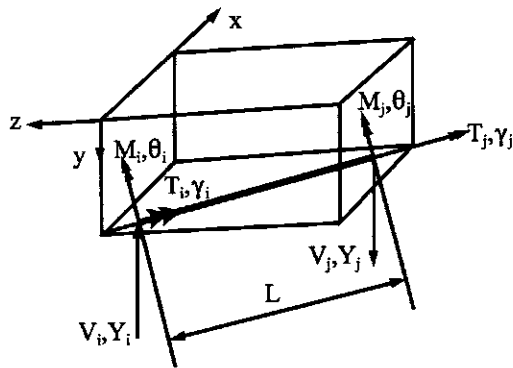


FIG. 5.17 Typical member of plane grillage.

The formulation of a dynamic stiffness matrix may be illustrated by using Fig. 5.18a with eight d.o.f. as shown in Fig. 5.18b: six rotations and two displacements. The rotations are positive in the clockwise direction, signified by right-hand rule, and the displacements are positive downward (perpendicular to the $x-z$ plane). The internal forces acting on the individual members are shown in Fig. 5.18c. From the accompanying figure of the free-body diagram at node G, the following equilibrium equations are derived as:

$$\left. \begin{aligned} \Sigma M_x &= 0 \\ P_{\theta 1} e^{ipt} &= cT_{11} + sM_{11} + cT_{10} + sM_{10} + cT_2 - sM_2 - sM_3 + cT_3 \end{aligned} \right\} \quad (5.52)$$

$$\left. \begin{aligned} \Sigma M_z &= 0 \\ P_{\theta 2} e^{ipt} &= -sT_{11} + cM_{11} - sT_{10} + cM_{10} + sT_2 + cM_2 + cM_3 + sT_3 \end{aligned} \right\} \quad (5.53)$$

$$\left. \begin{aligned} \Sigma F_y &= 0 \\ P_s 1 e^{ipt} &= -V_{11} + V_{10} + V_2 - V_3 \end{aligned} \right\} \quad (5.54)$$

where $c = \cos 30^\circ$ and $s = \sin 30^\circ$. Applying the three equilibrium conditions to the other two nodes, C and F, and then combining with Eqs. (5.52)–(5.54) yield the following equilibrium matrices:

$$\{P_\theta\} e^{ipt} = [A_\theta] \{M\} + [A_t] \{T\} \quad (5.55)$$

$$\{P_s\} e^{ipt} = [A_s] \{V\} \quad (5.56)$$

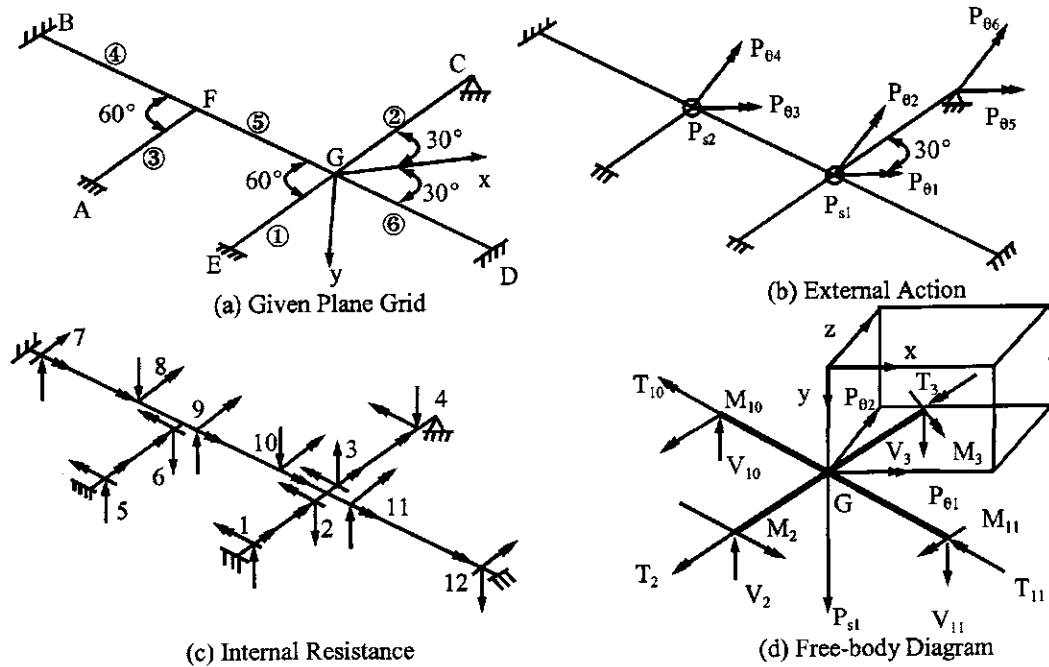


FIG. 5.18 Plane grid system.

in which

$$[A_\theta] = \begin{bmatrix} 0 & -s & -s & 0 & 0 & 0 & 0 & 0 & 0 & s & s & 0 \\ 0 & c & c & 0 & 0 & 0 & 0 & 0 & 0 & c & c & 0 \\ 0 & 0 & 0 & 0 & 0 & -s & 0 & s & s & 0 & 0 & 0 \\ 0 & 0 & 0 & 0 & 0 & c & 0 & c & c & 0 & 0 & 0 \\ 0 & 0 & 0 & -s & 0 & 0 & 0 & 0 & 0 & 0 & 0 & 0 \\ 0 & 0 & 0 & c & 0 & 0 & 0 & 0 & 0 & 0 & 0 & 0 \end{bmatrix} \quad (5.57)$$

$$[A_t] = \begin{bmatrix} 0 & c & c & 0 & 0 & 0 & 0 & 0 & 0 & c & c & 0 \\ 0 & s & s & 0 & 0 & 0 & 0 & 0 & 0 & -s & -s & 0 \\ 0 & 0 & 0 & 0 & c & 0 & c & c & 0 & 0 & 0 & 0 \\ 0 & 0 & 0 & 0 & 0 & s & 0 & -s & -s & 0 & 0 & 0 \\ 0 & 0 & 0 & 0 & 0 & 0 & 0 & 0 & 0 & 0 & 0 & 0 \\ 0 & 0 & 0 & 0 & 0 & 0 & 0 & 0 & 0 & 0 & 0 & 0 \end{bmatrix} \quad (5.58)$$

and

$$[A_s] = \begin{bmatrix} 0 & 1 & -1 & 0 & 0 & 0 & 0 & 0 & 0 & 1 & -1 & 0 \\ 0 & 0 & 0 & 0 & 0 & 1 & 0 & 1 & -1 & 0 & 0 & 0 \end{bmatrix} \quad (5.59)$$

Note that the first and second rows of Eqs. (5.57) and (5.58) are based on Eqs. (5.52) and (5.53), respectively. Likewise the first row of Eq. (5.59) is based on Eq. (5.54). By using a fundamental

structural mechanics approach, the dynamic stiffness matrix may be obtained as

$$\begin{Bmatrix} P_\theta \\ P_s \end{Bmatrix} e^{ipt} = \begin{bmatrix} A_\theta \text{ } SM0 \text{ } A_\theta^T & A_\theta \text{ } SMY \text{ } A_s^T \\ + A_t \text{ } ST\gamma \text{ } A_t^T & \text{symm} \quad A_s \text{ } SVY \text{ } A_s^T \end{bmatrix} \begin{Bmatrix} X_\theta \\ X_s \end{Bmatrix} e^{ipt} = [K] \begin{Bmatrix} X_\theta \\ X_s \end{Bmatrix} e^{ipt} \quad (5.60)$$

which is a general expression for all plane grid systems and can also be obtained by using the physical interpretation or the direct element formulation. General concepts of these formulations were presented in Section 5.4.2.

5.7. COUPLING OF TORSIONAL AND FLEXURAL VIBRATION

The dynamic structural stiffness matrix in Eq. (5.60) comprises flexural and torsional stiffness coefficients in which the frequency parameters ϕ (flexural) and ψ (torsional) must be unified so that the vibration frequencies of a system can be coupled. Let the ratio of polar moment of inertia and that of torsional inertia of member i to a reference member 1 be τ_i and σ_i , respectively, as

$$\tau_i = \frac{I_{pi}}{I_{p1}} \quad (5.61)$$

$$\sigma_i = \frac{J_i}{J_1} \quad (5.62)$$

Then the parameters in torsional stiffness coefficients of Eq. (5.48) may be unified in terms of flexural frequency parameter ϕ_1 ($\phi_i = \delta_i \phi_1$) as

$$GJ_i \psi_i = \left[\left(\frac{EG\rho I_1 I_{p1}}{m_1 L_1} \right) \left(\frac{\beta_i \tau_i}{\gamma_i \sigma_i} \right) \right]^{\frac{1}{2}} \frac{\delta_i^2 \phi_1^2}{\alpha_i^2 L_1^2} \quad (5.63a)$$

$$GJ_i \psi_i = \left[(EGJ_1 I_{p1}) \left(\sigma_i \beta_i \tau_i / \epsilon_i \right) \right]^{\frac{1}{2}} \frac{\delta_i^2 \phi_1^2}{\alpha_i^2 L_1^2} \quad (5.63b)$$

and

$$\psi_i L_i = \left[\left(\frac{E\rho I_1 I_{p1}}{Gm_1 L_1} \right) \left(\frac{\beta_i \tau_i}{\gamma_i \sigma_i} \right) \right]^{\frac{1}{2}} \frac{\delta_i^2 \phi_1^2}{\alpha_i L_1} \quad (5.64a)$$

$$\psi_i L_i = \left[(EI_{p1}/GJ_1) \left(\frac{\beta_i \tau_i}{\sigma_i \epsilon_i} \right) \right]^{\frac{1}{2}} \frac{\delta_i^2 \phi_1^2}{\alpha_i L_1} \quad (5.64b)$$

where α_i , β_i , and δ_i may be found from Eqs. (4.107)–(4.110). Note that Eqs. (5.63a) and (5.64a) are for a system having both structural and nonstructural mass while Eqs. (5.63b) and (5.64b) are for a system with structural mass only. Once the singularity of $[K]$ is obtained, the coupling frequency is then found from

$$p = \frac{\phi_1^2}{L_1^2} \left(\frac{EI_1}{m_1} \right)^{1/2} \quad (5.65)$$

EXAMPLE 5.7.1 For the prismatic beam given in Fig. 5.19a, find the frequencies of the first three modes. The member properties are $2L = 6.096$ m, $A = 77.419$ cm 2 , $I_x = 14.9843$ μm^4 , $I_p = J = 16.649$ μm^4 , $\gamma = 6.405$ kN/m 3 , $E = 206.843$ GPa, and $G = 82.737$ GPa. The slenderness ratio of this beam is 138.56.

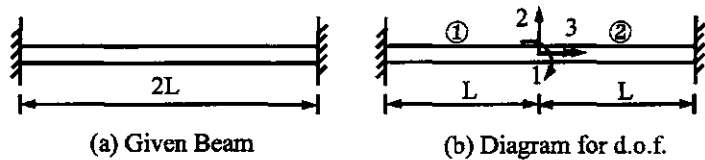


FIG. 5.19 Example 5.7.1.

Solution: Introduce a node at the midspan of the beam as shown in Fig. 5.19b, at which the assigned first two d.o.f. are associated with bending and the third with torsional motion. The structural stiffness matrix may be expressed as

$$[K] = \begin{bmatrix} SM\theta_{11} + SM\theta_{12} & -SMY_{11} + SMY_{12} & 0 \\ & SVY_{11} + SVY_{12} & 0 \\ \text{symm} & & ST\gamma_{11} + ST\gamma_{12} \end{bmatrix} \quad (a)$$

from which

$$|K| = \left[(SM\theta_{11} + SM\theta_{12})(SVY_{11} + SVY_{12}) - (-SMY_{11} + SMY_{12})^2 \right] (ST\gamma_{11} + ST\gamma_{12}) = 0 \quad (\text{b})$$

This is an uncoupled vibration. The torsional frequencies can be determined from the second term of Eq. (b),

$$ST\gamma_{11} + ST\gamma_{12} = 2GJ\psi \cot \psi L = 0 \quad (c)$$

or

$$\psi L = \frac{\pi}{2}, \quad \frac{3\pi}{2}, \quad \frac{5\pi}{2}, \dots$$

The corresponding torsional frequencies can be obtained from Eq. (5.48) as

$$p' = \frac{\psi L}{L} \sqrt{\frac{GJ}{\rho I_p}} = 1673.19, \quad 5019.58, \quad \text{and} \quad 8365.97 \text{ rad/sec} \quad (d)$$

Similarly, the flexural frequencies obtained from the first term of Eq. (b) are

$$p = 136.03, \quad 374.96, \quad \text{and} \quad 735.07 \text{ rad/sec} \quad (\text{e})$$

Note that the torsional frequencies are significantly larger than the flexural frequencies in the following order of magnitude

$$\frac{p'_i}{p_i} = 12.300, \quad 13.387, \quad \text{and} \quad 11.381, \quad i = 1, 2, 3 \quad (\text{f})$$

EXAMPLE 5.7.2 Find the first five frequencies of the following plane grid composed of two identical members. Consider (A) the coupling effect of bending and torsional vibration, (B) bending vibration only, and (C) the pseudo-coupling effect of bending vibration with static torsional stiffness of GJ/L . The member properties are: $A = 77.419 \text{ cm}^2$, $I_x = 14.9843 \mu\text{m}^4$, $I_p = J = 16.649 \mu\text{m}^4$, $\gamma = 76.921 \text{ kN/m}^3$, $E = 206.843 \text{ GPa}$, and $G = 82.737 \text{ GPa}$. The member length varies according to the slenderness ratio of 20, 40, 60, 80, and 100.

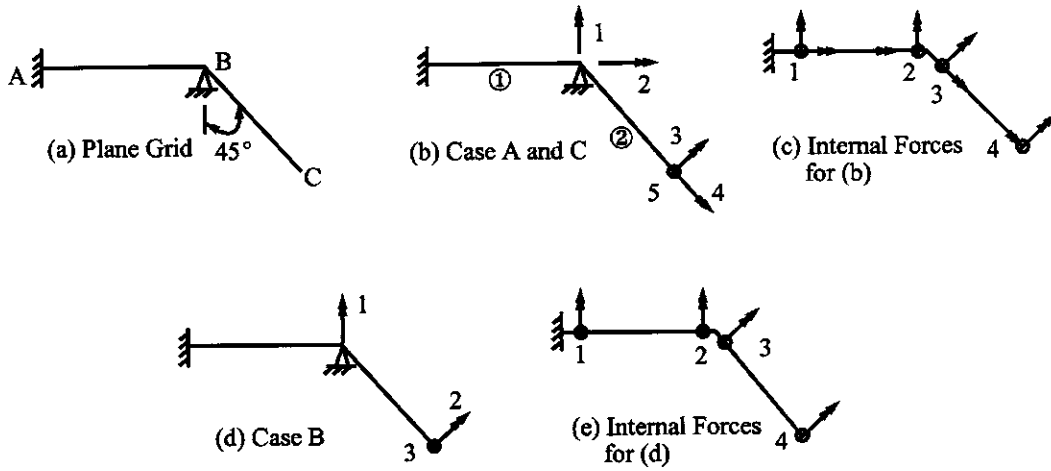


FIG. 5.20 Example 5.7.2.

Solution: (A) The d.o.f. are numbered in Fig. 5.20b with the first four rotational in a positive clockwise direction and the fifth transverse downward positive. The internal forces are numbered in Fig. 5.20c; each member end has bending, shear, and torsion. The dynamic stiffness matrix is formulated as

$$[K] = \begin{bmatrix} SM\theta_{11} + s^2SM\theta_{12} & scSM\theta_{12} & sSM\theta_{22} & -cST\gamma_{22} & sSMY_{22} \\ +c^2ST\gamma_{12} & -scST\gamma_{12} & cSM\theta_{22} & sST\gamma_{22} & cSMY_{12} \\ ST\gamma_{11} + c^2SM\theta_{12} & +s^2ST\gamma_{12} & SM\theta_{12} & 0 & SMY_{12} \\ +cSM\theta_{22} & cST\gamma_{22} & 0 & ST\gamma_{12} & 0 \\ symm & SMY_{12} & ST\gamma_{12} & SVY_{12} & \end{bmatrix} \quad (a)$$

where $s = \sin 45^\circ$ and $c = \cos 45^\circ$.

(B) For flexural vibration only without considering torsional effect, the d.o.f. and internal forces are similarly numbered in Figs. 5.20d and e, respectively. The dynamic stiffness matrix is

$$[K] = \begin{bmatrix} SM\theta_{11} + s^2SM\theta_{12} & sSM\theta_{22} & sSMY_{22} \\ sSM\theta_{12} & SM\theta_{12} & SMY_{12} \\ symm & SMY_{12} & SVY_{12} \end{bmatrix} \quad (b)$$

(C) In the case of pseudo-coupling vibration with consideration of dynamic flexural stiffness and static torsional stiffness, the d.o.f. diagrams and internal forces are the same as those used in (A). The stiffness matrix in Eq. (a), however, needs to be modified by replacing the dynamic torsional stiffness coefficients, $ST\gamma_1$ and $ST\gamma_2$, with static coefficient GJ/L .

Let p' be the frequency due to coupling flexural and torsional vibration of Case A, p be the frequency due to flexural vibration only of Case B, and p'' be the pseudo-coupling frequency due to flexural vibration with the static torsional stiffness of Case C. The results of p and p' (in rad/sec), from Cases A and B, for the first five modes and various slenderness ratios are given in Eq. (c). Comparisons of the frequencies are shown in Fig. 5.21. For Case C, p'' and p' comparisons are revealed in Fig. 5.22.

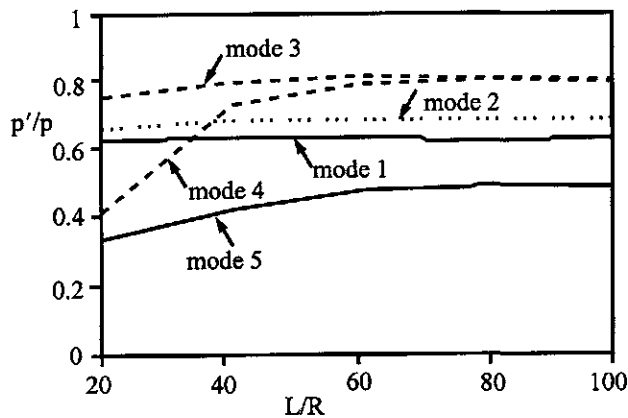


FIG. 5.21 p'/p vs L/R of Example 5.7.2.

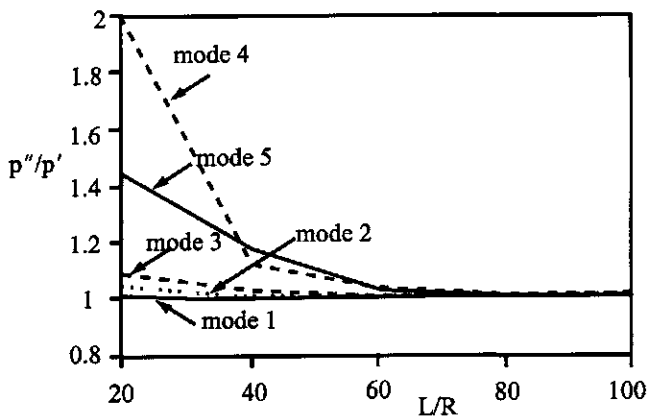


FIG. 5.22 p''/p' vs L/R of Example 5.7.2.

Mode	$L/R = 20$		$L/R = 40$		$L/R = 60$		$L/R = 80$		$L/R = 100$		(c)
	p'	p	p'	p	p'	p	p'	p	p'	p	
1	520.84	833.21	130.61	208.30	58.08	92.58	32.55	52.07	20.92	33.33	
2	2966.67	4499.49	771.16	1124.88	341.94	499.94	192.58	281.22	123.35	179.98	
3	4877.92	6480.55	1284.13	1620.14	583.53	720.06	328.70	405.04	210.43	259.22	
4	5939.58	14581.24	2627.18	3645.32	1271.47	1620.14	730.38	911.33	467.44	583.25	
5	10296.60	30422.59	3167.15	7605.67	1598.58	3380.30	921.55	1901.43	589.79	1216.90	

Significant observations from this example may be summarized as follows: (1) the coupling frequencies of flexural and torsional vibration are always smaller than those of flexural vibration only; the difference is sensitive to vibrating modes and to smaller slenderness ratios (when L/R is less than 50). (2) The difference between coupling frequencies and pseudo-coupling frequencies is significant for higher modes when the slenderness ratios is less than 50. (3) The first five mode shapes $\{X\}$ and $\{X'\}$ associated with p and p' , respectively, for $L/R = 100$

are given in Eqs (d)–(h). Other numerical examples show that the ratio of p'/p can be smaller or greater than 1, and mainly depends on whether system stiffness is responding to torsional or flexural vibration of a particular mode. The solutions of Problems 5.11 and 5.20 illustrate the situation in which some vibration modes are mainly influenced by torsional vibration.

$$\begin{aligned} \{X\}_1 &= [0.1003 & 0.2855 & 1.0]^T \\ \{X'\}_1 &= [0.0328 & 0.2135 & 0.24444 & 0.1264 & 1.0]^T \end{aligned} \quad (d)$$

$$\begin{aligned} \{X\}_2 &= [-0.8680 & 0.8932 & 1.0]^T \\ \{X'\}_2 &= [0.0858 & 1 & -0.8660 & 0.6556 & -0.1060]^T \end{aligned} \quad (e)$$

$$\begin{aligned} \{X\}_3 &= [-0.8617 & 0.5688 & 1.0]^T \\ \{X'\}_3 &= [1 & -0.2846 & 0.5166 & -0.9466 & -0.3352]^T \end{aligned} \quad (f)$$

$$\begin{aligned} \{X\}_4 &= [1 & 0.9988 & 0.6216]^T \\ \{X'\}_4 &= [-0.0109 & 1 & 0.7312 & 0.8868 & 0.0391]^T \end{aligned} \quad (g)$$

$$\begin{aligned} \{X\}_5 &= [-0.9999 & 1 & 0.4309]^T \\ \{X'\}_5 &= [-0.6544 & 0.3318 & -0.2375 & 1 & -0.2033]^T \end{aligned} \quad (h)$$

PART B ADVANCED TOPICS

5.8. BERNOULLI-EULER EQUATION WITH ELASTIC MEDIA

Consider a prismatic member shown in Fig. 5.23 subjected to transverse force, $w(x, t)$, and supported by elastic media (foundation) with a spring constant, q . Applying the equilibrium equations of $\Sigma F_y = 0$ and $\Sigma M = 0$ (neglect the higher order items) to the accompanying free-body diagram yields

$$-\frac{\partial V}{\partial x} = w(x, t) - qy - m\frac{\partial^2 y}{\partial t^2}; \quad \text{and} \quad \frac{\partial M}{\partial x} = V \quad (5.66)$$

Substituting $\partial^2 y / \partial x^2 = -M/EI$ into the above yields

$$EI\frac{\partial^4 y}{\partial x^4} + m\frac{\partial^2 y}{\partial t^2} + qy = w(x, t) \quad (5.67)$$

Let $w(x, t) = 0$ and use the separation of variables as $y = Y(x)g(t)$; then Eq. (5.67) may be written

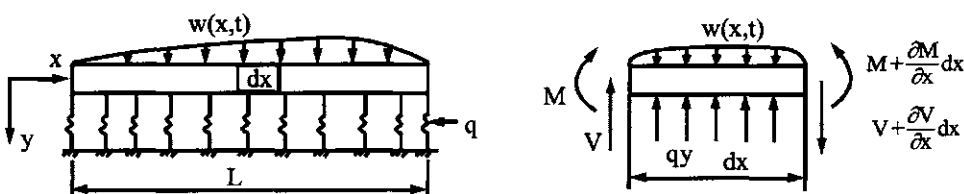


FIG. 5.23 Beam on elastic media.

as

$$\frac{EI(d^4y/dx^4)}{mY} + \frac{q}{m} = -\frac{d^2y/dt^2}{g} = p^2 \quad (5.68)$$

from which

$$\frac{d^4Y}{dx^4} - \zeta^4 Y = 0; \quad \text{and} \quad \frac{d^2g}{dt^2} + p^2 g = 0 \quad (5.69)$$

where

$$\zeta^4 = \frac{mp^2}{EI} - \frac{q}{EI} \quad (5.70)$$

Since the differential equations of Eq. (5.69) are formally identical to Eqs. (4.14) and (4.15), the stiffness coefficients, fixed-end forces, structural stiffness matrix, eigensolution techniques, and response analysis presented in Chapter 4 can be directly used for the problem depicted above.

5.9. BERNOULLI-EULER EQUATION WITH ELASTIC MEDIA AND P-Δ EFFECT

A beam shown in Fig. 5.24 supported by elastic media, q , is subjected to time-dependent transverse force, $w(x, t)$, and static axial force, P . From the free-body diagram, we may observe that the axial force, P , times the incremental deflection, $(\partial y/\partial x) dx$ (or Δ), gives additional moment, $P [(\partial y/\partial x) dx]$ (or $P-\Delta$). Since the incremental deflection results from the primary moment, the additional moment is called *second-order moment* due to the $P-\Delta$ effect. If P is in the opposite direction, then the vibration is affected by tensile force.

Taking the free-body diagram for equilibrium conditions of $\Sigma F_y = 0$ and $\Sigma M = 0$ gives

$$-\frac{\partial V}{\partial x} = w(x, t) - qy - m \frac{\partial^2 y}{\partial t^2} \quad (5.71)$$

and

$$V = \frac{\partial M}{\partial x} - P \frac{\partial y}{\partial x} \quad (5.72)$$

Employing the moment curvature relationship, $EI\partial^2y/\partial x^2 = -M$, in the above yields

$$EI \frac{\partial^4 y}{\partial x^4} + P \frac{\partial^2 y}{\partial x^2} + m \frac{\partial^2 y}{\partial t^2} + qy = w(x, t) \quad (5.73)$$

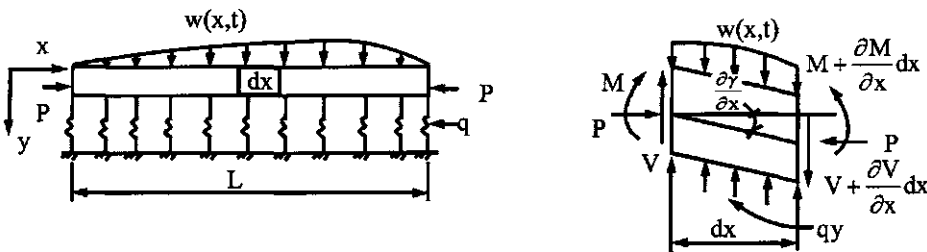


FIG. 5.24 Beam on elastic media with $P-\Delta$ effect.

Let $w(x,t) = 0$ and $y = Y(x)g(t)$; then Eq. (5.73) can be expressed as

$$\frac{EI(d^4y/dx^4)}{mY} + \frac{P(d^2Y/dx^2)}{mY} + \frac{q}{m} = -\frac{d^2g/dt^2}{g} = p^2 \quad (5.74)$$

from which

$$\frac{d^4Y}{dx^4} + \frac{P}{EI} \frac{d^2Y}{dx^2} - \lambda^4 Y = 0 \quad (5.75)$$

and

$$\frac{d^2g}{dt^2} + p^2 g = 0 \quad (5.76)$$

where

$$\lambda^4 = \frac{mp^2}{EI} - \frac{q}{EI} \quad (5.77)$$

Let the solution of Eq. (5.75) be $Y = e^{ax}$; we then have

$$e^{ax} \left(a^4 + \frac{P}{EI} a^2 - \lambda^4 \right) = 0 \quad (5.78)$$

of which the roots are

$$\begin{aligned} a_1 &= \alpha = \pm \sqrt{-\frac{P}{2EI} + \frac{1}{2} \left[\left(\frac{P}{EI} \right)^2 + 4\lambda^4 \right]^{\frac{1}{2}}} \\ a_2 &= -\alpha = \pm \sqrt{\frac{P}{2EI} + \frac{1}{2} \left[\left(\frac{P}{EI} \right)^2 + 4\lambda^4 \right]^{\frac{1}{2}}} \end{aligned} \quad (5.79)$$

and

$$\begin{aligned} a_3 &= \beta i = \pm i \sqrt{\frac{P}{2EI} + \frac{1}{2} \left[\left(\frac{P}{EI} \right)^2 + 4\lambda^4 \right]^{\frac{1}{2}}} \\ a_4 &= -\beta i = \pm i \sqrt{-\frac{P}{2EI} + \frac{1}{2} \left[\left(\frac{P}{EI} \right)^2 + 4\lambda^4 \right]^{\frac{1}{2}}} \end{aligned} \quad (5.80)$$

where $i = \sqrt{-1}$. If the axial force is in tension, then a negative sign should be placed before P . The solution of Eq. (5.75) is

$$Y = C_1 \sin \beta x + C_2 \cos \beta x + C_3 \sinh \alpha x + C_4 \cosh \alpha x \quad (5.81)$$

Using the typical beam of Fig. 4.4, leads to the following boundary conditions:

	End forces	End deformations
$x = 0$	$\frac{d^2Y}{dx^2} = -\frac{M_i}{EI}$	$\frac{dY}{dx} = \theta_i$
$x = L$	$\frac{d^2Y}{dx^2} = \frac{M_j}{EI}$	$\frac{dY}{dx} = \theta_j$
$x = 0$	$\frac{d^3Y}{dx^3} = -\frac{V_i}{EI} - \frac{P}{EI} \frac{dY}{dx}$	$Y = -Y_i$
$x = L$	$\frac{d^3Y}{dx^3} = -\frac{V_j}{EI} - \frac{P}{EI} \frac{dY}{dx}$	$Y = Y_j$

Following the procedures shown in Eqs. (4.22)–(4.25) yields the following dynamic stiffness coefficients:

$$[K_e] = \begin{bmatrix} SM\theta_1 & SM\theta_2 & SMY_1 & SMY_2 \\ & SM\theta_1 & SMY_2 & SMY_1 \\ \text{symm} & & SVY_1 & SVY_2 \\ & & & SVY_1 \end{bmatrix} \quad (5.83)$$

in which

$$\left. \begin{array}{l} SM\theta_1 = \left[\left(\frac{\alpha^2}{\beta} + \beta \right) cs' - \left(\frac{\alpha^3}{\beta^2} + \alpha \right) sc' \right] / D \\ SM\theta_2 = \left[\left(\frac{\alpha^3}{\beta^2} + \alpha \right) s - \left(\frac{\alpha^3}{\beta^2} + \beta \right) s' \right] / D \\ SMY_1 = \left[2\alpha^2 ss' + \left(\frac{\alpha^3}{\beta} - \alpha\beta \right) (cc' - 1) \right] / D \\ SMY_2 = \left[\left(\frac{\alpha^3}{\beta} + \alpha\beta \right) (c' - c) \right] / D \\ SVY_1 = - \left[\left(\alpha^2\beta + \frac{\alpha^4}{\beta} \right) cs' + (\alpha\beta^2 + \alpha^3) sc' \right] / D \\ SVY_2 = - \left[(\alpha\beta^2 + \alpha^3)s + \left(\alpha^2\beta + \frac{\alpha^4}{\beta} \right) s' \right] / D \end{array} \right\} \quad (5.84)$$

where $c = \cos \beta L$, $s = \sin \beta L$, $s' = \sinh \alpha L$, $c' = \cosh \alpha L$, $D = [(cc' - 1)2\alpha/\beta - (\alpha^2/\beta^2) - 1]ss'/(1/EI)$.

The above stiffness coefficients can be converged to the following five cases.

1. Flexural vibration with P - Δ effect but no elastic media—when elastic media are not included, then $q = 0$. λ in Eq. (5.77) has only the frequency parameter, p . Consequently the stiffness coefficients of Eq. (5.84) are modified for flexural vibration with the P - Δ effect.
2. Flexural vibration with elastic media but no P - Δ effect—when the P - Δ effect is neglected, then $P = 0$. Therefore α and β in Eqs. (5.79) and (5.80) have only the parameter λ which includes q and p as expressed in Eq. (5.77). This converges to the result presented in the previous section.
3. Flexural vibration without elastic media and P - Δ effect—when P and q are both neglected, then the modified stiffness coefficients are identical to those in Eq. (4.25b).
4. Static stability without elastic media—in this case q and p are dropped from Eq. (5.77); λ becomes zero and α and β in Eq. (5.79) include only the axial force P . If P is a compressive force, then the revised stiffness coefficients can be employed for stability analysis of buckling loads and buckling modes of a structure.
5. Static stability with elastic media—when the frequency parameter, p , is not considered, then the stiffness coefficients converge to the case for stability analysis (assume P is in compression) with elastic media.

Numerical procedures for eigensolutions, steady-state vibration, and response due to various types of dynamic excitations are the same as presented in Chapter 4.

5.10. TIMOSHENKO EQUATION (BENDING AND SHEAR DEFORMATION AND ROTATORY INERTIA)

5.10.1. Differential Equations

A member whose flexural vibration includes the effect of rotatory inertia, bending and shear deformation on the natural frequencies is called a *Timoshenko beam*. Timoshenko theory refers

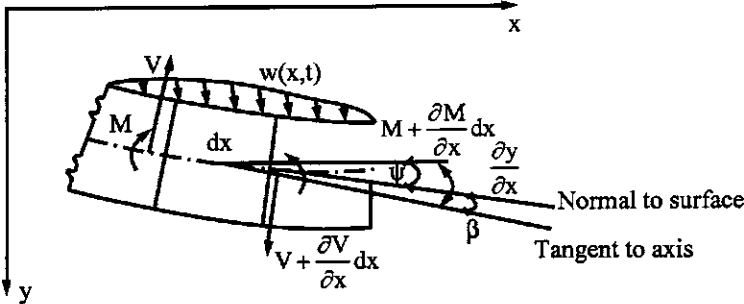


FIG. 5.25 Element of Timoshenko beam.

to the procedure of taking into account the aforementioned effect of the cross-sectional dimensions on the flexural vibration. Consider an element shown in Fig. 5.25. Let z be the distance measured at any point from the neutral axis; then the displacement of a fiber located at z is

$$y^a = -z \frac{\partial y}{\partial x} \quad (5.85)$$

Since y varies with time and distance, y^a must also vary with time and distance along the axis. Thus for every dx length of a beam, the cross-section dA has an inertia force

$$\frac{\gamma}{g} (dA) (dx) \ddot{y}^a \quad (5.86)$$

Since the displacements above and below the neutral axis are equal and opposite, the inertia forces at any cross-section are equal and opposite, and form a time-dependent couple which is *rotatory inertia* and has the following expression:

$$\int_{-z}^z \left[\left(\frac{\gamma}{g} dA \right) \left(-z \frac{\partial^3 y}{\partial x \partial t^2} \right) (z) (dx) \right] = -\frac{I\gamma}{g} \frac{\partial^3 y}{\partial x \partial t^2} dx \quad (5.87)$$

This couple is in the counterclockwise direction based on the sign convention in Fig. 5.25. Applying $\Sigma M = 0$ and $\Sigma F_y = 0$ yields

$$\frac{\partial M}{\partial x} = V - \frac{I\gamma}{g} \frac{\partial^3 y}{\partial x \partial t^2} \quad \text{and} \quad -\frac{\partial V}{\partial x} = w(x, t) - \frac{\gamma A}{g} \frac{\partial^2 y}{\partial t^2} \quad (5.88)$$

As shown in the figure, the total slope $\partial y / \partial x$ is a combination of the bending slope, ψ , and the shear slope, β

$$\frac{\partial y}{\partial x} = \psi + \beta \quad (5.89)$$

Using the bending and shear slopes, we can write

$$M = -EI \frac{\partial \psi}{\partial x} \quad \text{and} \quad V = \mu AG \beta = \mu AG \left(\frac{\partial y}{\partial x} - \psi \right) \quad (5.90)$$

where G is the shear modulus; μ is a constant called the *shear coefficient*, defined as the ratio of average shear stress on a section to the product of shear modulus and shear strain at the neutral axis of the member.

Since shear slope does not have opposite displacements above and below the neutral axis, no rotatory inertia is associated with the shear slope. Substituting Eq. (5.90) into Eq. (5.88) yields

$$EI \frac{\partial^2 \psi}{\partial x^2} + \mu AG \left(\frac{\partial y}{\partial x} - \psi \right) - \frac{I\gamma}{g} \frac{\partial^2 \psi}{\partial t^2} = 0 \quad (5.91)$$

and

$$\frac{\gamma A}{g} \frac{\partial^2 y}{\partial t^2} - \mu AG \left(\frac{\partial^2 y}{\partial x^2} - \frac{\partial \psi}{\partial x} \right) - w(x, t) = 0 \quad (5.92)$$

Eliminating either ψ or y from Eqs. (5.91) and (5.92) gives

$$EI \frac{\partial^4 y}{\partial x^4} + \frac{\gamma A}{g} \frac{\partial^2 y}{\partial t^2} - \left(\frac{\gamma I}{g} + \frac{EI}{g\mu} \frac{\gamma}{G} \right) \frac{\partial^4 y}{\partial x^2 \partial t^2} + \frac{\gamma I}{g} \frac{\gamma}{g\mu G} \frac{\partial^4 y}{\partial t^4} + \frac{EI}{\mu GA} \frac{\partial^2 w}{\partial x^2} + \frac{I\gamma}{g\mu AG} \frac{\partial^2 w}{\partial t^2} - w(x, t) = 0 \quad (5.93)$$

and

$$EI \frac{\partial^4 \psi}{\partial x^4} + \frac{\gamma A}{g} \frac{\partial^2 \psi}{\partial t^2} - \left(\frac{\gamma I}{g} + \frac{EI}{g\mu} \frac{\gamma}{G} \right) \frac{\partial^4 \psi}{\partial x^2 \partial t^2} + \frac{\gamma I}{g} \frac{\gamma}{g\mu G} \frac{\partial^4 \psi}{\partial t^4} - \frac{\partial w(x, t)}{\partial x} = 0 \quad (5.94)$$

Let

$$w(x, t) = 0 \quad (5.95)$$

$$\psi = \Psi e^{ipt} \quad (5.96)$$

$$y = Y e^{ipt} \quad (5.97)$$

$$\xi = \frac{x}{L} \quad (5.98)$$

Then

$$Y = C_1 \cosh b\alpha\xi + C_2 \sinh b\alpha\xi + C_3 \cos b\beta\xi + C_4 \sin b\beta\xi \quad (5.99)$$

$$\Psi = C'_1 \sinh b\alpha\xi + C'_2 \cosh b\alpha\xi + C'_3 \sin b\beta\xi + C'_4 \cos b\beta\xi \quad (5.100)$$

in which

$$\frac{\alpha}{\beta} = \frac{1}{\sqrt{2}} \left\{ \mp(r^2 + s^2) + \left[(r^2 - s^2)^2 + \frac{4}{b^2} \right]^{\frac{1}{2}} \right\}^{\frac{1}{2}} \quad (5.101)$$

$$b^2 = \frac{1}{EI} \frac{\gamma A}{g} L^4 p^2 \quad (5.102)$$

$$r^2 = \frac{I}{AL^2} \quad (5.103)$$

$$s^2 = \frac{EI}{\mu AGL^2} \quad (5.104)$$

$$C'_1 = \frac{b\alpha^2 + s^2}{L} C_1 = TC_1 \quad (5.105)$$

$$C'_2 = \frac{b\alpha^2 + s^2}{L} C_2 = TC_2 \quad (5.106)$$

$$C'_3 = -\frac{b\beta^2 - s^2}{L} C_3 = -UC_3 \quad (5.107)$$

$$C'_4 = \frac{b\beta^2 - s^2}{L} C_4 = UC_4 \quad (5.108)$$

where L = the length of the prismatic member.

The bending moment and shear of a Timoshenko beam can now be derived by applying the total derivative of Eq. (5.90) to Eqs. (5.99) and (5.100). Thus the end displacements Y, Ψ and end forces V, M of the beam may be obtained without considering external force W :

$$\begin{Bmatrix} Y \\ \Psi \\ V \\ M \end{Bmatrix} = \begin{bmatrix} \cosh b\alpha\xi & \sinh b\alpha\xi & \cos b\beta\xi & \sin b\beta\xi \\ T \sinh b\alpha\xi & T \cosh b\alpha\xi & -U \sin b\beta\xi & U \cos b\beta\xi \\ (u - GA\mu T) & (u - GA\mu T) & (-\eta + GA\mu U) & (\eta - GA\mu U) \\ \sinh b\alpha\xi & \cosh b\alpha\xi & \sin b\beta\xi & \cos b\beta\xi \\ -\Omega \cosh b\alpha\xi & -\Omega \sinh b\alpha\xi & \tau' \cos b\beta\xi & \tau' \sin b\beta\xi \end{bmatrix} \begin{Bmatrix} C_1 \\ C_2 \\ C_3 \\ C_4 \end{Bmatrix} \quad (5.109)$$

in which

$$u = GA\mu \frac{b\alpha}{L} \quad (5.110)$$

$$\eta = GA\mu \frac{b\beta}{L} \quad (5.111)$$

$$\Omega = EI \frac{b\alpha}{L} T \quad (5.112)$$

$$\tau' = EI \frac{b\beta}{L} U \quad (5.113)$$

5.10.2. Stiffness Coefficients

The derivation of the stiffness coefficients may use either the method presented previously or the following procedures. Let Eq. (5.109) be expressed in matrix notation,

$$\begin{Bmatrix} AG \\ \dots \\ AF \end{Bmatrix} = [s(\xi)] \{C\} \quad (5.114)$$

When $\xi = 0$, the integration constants, $\{C\}$, can be expressed in terms of end forces, $\{AF\}$, and end displacements, $\{AG\}$, at end i in the form

$$\{C\} = [s(0)]^{-1} \begin{Bmatrix} AG \\ \dots \\ AF \end{Bmatrix}_i \quad (5.115)$$

By substituting Eq. (5.115) into Eq. (5.114) for $\xi = 1$, the end displacements and end forces at end i and end j can be related as

$$\begin{Bmatrix} AG \\ \dots \\ AF \end{Bmatrix}_j = [s(1)][s(0)]^{-1} \begin{Bmatrix} AG \\ \dots \\ AF \end{Bmatrix}_i \quad (5.116)$$

which can be expanded as

$$\begin{Bmatrix} AG \\ \dots \\ AF \end{Bmatrix}_j = \begin{bmatrix} S_{11} & | & S_{12} \\ \dots & | & \dots \\ S_{21} & | & S_{22} \end{bmatrix} \begin{Bmatrix} AG \\ \dots \\ AF \end{Bmatrix}_i \quad (5.117)$$

such that the end forces, $\{AF\}_i$ and $\{AF\}_j$, can be expressed in terms of end displacements, $\{AG\}_i$ and $\{AG\}_j$, in the form

$$\{AF\}_i = [S_{12}]^{-1}\{AG\}_j - [S_{12}]^{-1}[S_{11}]\{AG\}_i \quad (5.118)$$

$$\{AF\}_j = [S_{22}][S_{12}]^{-1}\{AG\}_j + ([S_{21}] - [S_{22}][S_{12}]^{-1}[S_{11}])\{AG\}_i \quad (5.119)$$

The force-displacement relationship of Eqs. (5.118) and (5.119) must be expressed in accordance with the sign convention of the typical member shown in Fig. 4.4 for which the boundary conditions of a Timoshenko beam should be expressed as:

	End forces	End deformations
$\xi = 0$	$M_i = -\frac{EI}{L} \frac{d\Psi}{d\xi}$	$\Psi = \Psi_i$
$\xi = 1$	$M_j = \frac{EI}{L} \frac{d\Psi}{d\xi}$	$\Psi = \Psi_j$
$\xi = 0$	$V_i = GA\mu \left(\frac{dY}{d\xi} \frac{1}{L} - \Psi \right)$	$Y = -Y_i$
$\xi = 1$	$V_j = GA\mu \left(\frac{dY}{d\xi} \frac{1}{L} - \Psi \right)$	$Y = Y_j$

The final stiffness coefficients obtained from Eqs. (5.118)–(5.120) are symbolically written as

$$\begin{Bmatrix} M_i \\ M_j \\ V_i \\ V_j \end{Bmatrix} = \begin{bmatrix} SM0_1 & SM0_2 & SMY_1 & SMY_2 \\ M_1 & SM0_1 & SMY_2 & SMY_1 \\ V_i & SYV_1 & SYV_2 & SYV_1 \\ V_j & SYV_1 & SYV_2 & SYV_1 \end{bmatrix}_{\text{symm}} \begin{Bmatrix} \Psi_i \\ \Psi_j \\ Y_i \\ Y_j \end{Bmatrix} \quad (5.121)$$

Let $n = \sinh b\alpha$, $n' = \sin b\beta$, $c = \cosh b\alpha$, $c' = \cos b\beta$; then the coefficients are

$$SM0_1 = \frac{[-\alpha(\beta^2 - s^2)nc' + \beta(\alpha^2 + s^2)cn']EI}{bD} \frac{L}{L} \quad (5.122)$$

$$SM0_2 = \frac{[\alpha(\beta^2 - s^2)n - \beta(\alpha^2 + s^2)n']EI}{bD} \frac{L}{L} \quad (5.123)$$

$$SMY_1 = \frac{[\alpha\beta(2s^2 + \alpha^2 - \beta^2)(1 - cc') - (2\alpha^2\beta^2 - \alpha^2s^2 + \beta^2s^2)nn']EI}{b^2(\alpha^2 + \beta^2)\alpha\beta D} \frac{L}{L^2} \quad (5.124)$$

$$SMY_2 = \frac{(\beta^2 - s^2)(\alpha^2 + s^2)(-c + c')}{D} \frac{EI}{L^2} \quad (5.125)$$

$$SVY_1 = \frac{[\alpha(\beta^2 - s^2)cn' + \beta(\alpha^2 + s^2)nc']}{b\alpha\beta D} \frac{EI}{L^3} \quad (5.126)$$

$$SVY_2 = \frac{[\beta(\alpha^2 + s^2)n + \alpha(\beta^2 - s^2)n']}{b\alpha\beta D} \frac{EI}{L^3} \quad (5.127)$$

in which

$$D = \frac{2\alpha\beta(\beta^2 - s^2)(\alpha^2 + s^2)(1 - cc') + [(\alpha^2 - \beta^2)(\alpha^2\beta^2 - s^4) + 4\alpha^2\beta^2s^2]nn'}{b^2(\alpha^2 + \beta^2)\alpha\beta}$$

The dynamic stiffness coefficients shown above are based on Eq. (5.101) by assuming $b^2r^2s^2 \leq 1$. However, when the condition $b^2r^2s^2 > 1$ occurs, $n = \sinh b\alpha = i \sin b\alpha' = i m$; then

$$\alpha' = \sqrt{-1}\alpha \quad (5.128)$$

should be used. Thus the solution of Eqs. (5.93) and (5.94) becomes

$$Y = C_1 \cos b\alpha'\xi - C_2 \sqrt{-1} \sin b\alpha'\xi + C_3 \cos b\beta\xi + C_4 \sin b\beta\xi \quad (5.129)$$

$$\psi = -\sqrt{-1}C'_1 \sin b\alpha'\xi + C'_2 \cos b\alpha'\xi + C'_3 \sin b\beta\xi + C'_4 \cos b\beta\xi \quad (5.130)$$

in which the integration constants, C and C' , are formally identical to those given in Eqs. (5.105)–(5.108) with $\alpha'/\sqrt{-1}$ replacing α .

Using the procedure given in Eqs. (5.114)–(5.120) with the new notations of $m = \sin b\alpha'$ and $d = \cos b\alpha'$ leads to the following stiffness coefficients:

$$SM\theta_1 = \frac{1}{bD'} [\alpha'(\beta^2 - s^2)mc' + \beta(\alpha^2 + s^2)n'd] \frac{EI}{L} \quad (5.131)$$

$$SM\theta_2 = -\frac{1}{bD'} [\alpha'(\beta^2 - s^2)m + \beta(\alpha^2 + s^2)n'] \frac{EI}{L} \quad (5.132)$$

$$SMY_1 = \frac{[\alpha'(\beta^2 - s^2)(1 - dc') + (2\alpha^2\beta^2 - \alpha^2s^2 + \beta^2s^2)mn']}{\alpha'\beta b^2(\alpha^2 + \beta^2)D'} \frac{EI}{L^2} \quad (5.133)$$

$$SMY_2 = \frac{(\alpha^2 + s^2)(\beta^2 - s^2)}{D'} (c' - d) \frac{EI}{L^2} \quad (5.134)$$

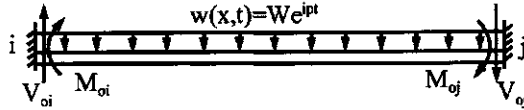
$$SVY_1 = \frac{[\alpha'(\beta^2 - s^2)dn' - \beta(\alpha^2 + s^2)mc']}{\alpha'\beta b D'} \frac{EI}{L^3} \quad (5.135)$$

and

$$SVY_2 = \frac{[-\beta(\alpha^2 + s^2)m + \alpha'(\beta^2 - s^2)n']}{\alpha'b\beta D'} \frac{EI}{L^3} \quad (5.136)$$

in which

$$D' = \frac{2\alpha'\beta(\beta^2 - s^2)(\alpha^2 + s^2)(1 - c'd) - [(\alpha^2 - \beta^2)(\alpha^2\beta^2 - s^4) + 4\alpha^2\beta^2s^2]n'm}{\alpha'\beta b(\alpha^2 + \beta^2)} \quad (5.137)$$

**FIG. 5.26** Uniform load.**5.10.3. Fixed-end Forces for Steady-State Vibration**

The derivation of fixed-end forces for a Timoshenko beam is illustrated for the beam shown in Fig. 5.26 subjected to uniformly distributed load $w(x,t)$. Boundary conditions of the beam are expressed in Eq. (5.138):

	End forces	End displacements	
$\xi = 0$	$M_{0i} = -\frac{EI}{L} \frac{d\Psi}{d\xi}$	$\Psi_i = 0$	
$\xi = 1$	$M_{0j} = \frac{EI}{L} \frac{d\Psi}{d\xi}$	$\Psi_j = 0$	(5.138)
$\xi = 0$	$V_{0i} = GA\mu \left(\frac{dY}{d\xi} \frac{1}{L} - \Psi \right)$	$Y_i = 0$	
$\xi = 1$	$V_{0j} = GA\mu \left(\frac{dY}{d\xi} \frac{1}{L} - \Psi \right)$	$Y_j = 0$	

For $b^2 r^2 s^2 \leq 1$

$$M_{0i} = \frac{WL^2}{D_1} \left\{ (\alpha^2 - \beta^2 + 2s^2)(1 - cc') + (\alpha^2 + \beta^2)(c - c') - \left[2\alpha\beta - \frac{s^2(\alpha^2 - \beta^2)}{\alpha\beta} \right] nn' \right\} \quad (5.139)$$

$$V_{0i} = \frac{WL(\alpha^2 - \beta^2)}{D_1 b} \left[\frac{(d-1)n}{\beta^2(\alpha^2 - s^2)} - \frac{(c'-1)m}{\alpha'(\beta^2 - s^2)} \right] \quad (5.140)$$

$$M_{0j} = -M_{0i}; \quad V_{0i} = -V_{0j} \quad (5.141)$$

in which

$$D_1 = 2(cc' - 1) + \left[\frac{\alpha(\beta^2 - s^2)}{\beta(\alpha^2 + s^2)} - \frac{\beta(\alpha^2 + s^2)}{\alpha(\beta^2 - s^2)} \right] nn' \quad (5.142)$$

For $b^2 r^2 s^2 > 1$

$$M_{0i} = \frac{WL^2}{D'_1} \left\{ [(2s^2 - \alpha'^2 - \beta^2)(1 - dc') + (\beta^2 - \alpha'^2)(d - c')] - \left[2\alpha'\beta - \frac{s^2(\alpha'^2 - \beta^2)}{\alpha'\beta} \right] mn' \right\} \quad (5.143)$$

$$V_{0i} = \frac{WL}{bD'_1} \left[\frac{(\alpha'^2 - \beta^2)(d-1)n'}{\beta(\alpha'^2 - s^2)} - \frac{(\alpha'^2 - \beta^2)(c'-1)m}{\alpha'(\beta^2 - s^2)} \right] \quad (5.144)$$

$$M_{0j} = -M_{0i}; \quad V_{0j} = -V_{0i} \quad (5.145)$$

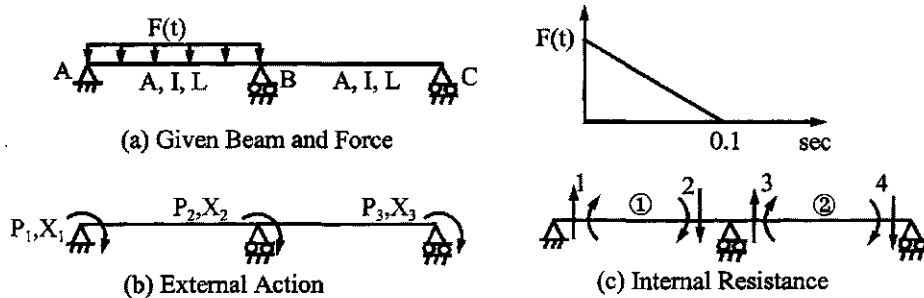


FIG. 5.27 Example 5.10.1.

in which

$$D'_1 = 2(dc' - 1) + \left[\frac{\beta(s^2 - \alpha'^2)}{\alpha'(\beta^2 - s^2)} - \frac{\alpha'(\beta^2 - s^2)}{\beta(\alpha'^2 - s^2)} \right] mn' \quad (5.146)$$

The numerical procedures for analyzing steady-state vibration are identical to those presented in Chapter 4, so they are not repeated here.

5.10.4. Response Analysis for General Forcing Functions

For general forcing functions of periodic excitations, impulsive loads, and earthquakes, the numerical procedures presented in Section 4.9 can be used for the present case. A sample problem is given below.

EXAMPLE 5.10.1 The continuous beam shown in Fig. 5.27 is subjected to an impulsive load of $F(t) = 3000(1-t/0.1)$ lb/in. Member properties are $I = 200 \text{ in}^4$, $A = 1.871 \text{ in}^2$, $E = 30 \times 10^6 \text{ lb/in}^2$, $G = 1.12 \times 10^7 \text{ lb/in}^2$, $\mu = 0.833$, $m = 0.2 \text{ lb sec}^2/\text{in}^2$, and $L = 150 \text{ in}$. Find the response by considering the first three modes. Note that this problem was solved in Example 4.9.1 with bending deformation only.

Solution: Based on the diagrams in Fig. 5.27b and c, we can formulate the system structural matrix as

$$[K] = \begin{bmatrix} SM\theta_{11} & SM\theta_{21} & 0 \\ 2SM\theta_{11} & SM\theta_{21} & \\ \text{symm} & SM\theta_{11} & \end{bmatrix} \quad (a)$$

in which stiffness coefficients are given in Eqs. (5.122) and (5.123) as well as Eq. (5.131) and (5.132). As pointed out earlier (Example 4.7.1), the second subscripts refer to member numbers. Eq. (a) is a condensed form with consideration of $SM\theta_{11} = SM\theta_{12}$, $SM\theta_{21} = SM\theta_{22}$ because the two members are identical. Note that the only variable in the stiffness coefficients is b , in which the frequency p is unknown as expressed in Eq. (5.102). By varying b in performing zero determinant of Eq. (a), one can find the first three eigenvalues as

$$b = 9.0409872; \quad 12.75753191; \quad 30.057537 \quad (b)$$

Then the frequency is obtained from

$$p_i = \frac{b_i}{L^2} \sqrt{\frac{EI}{m}}$$

Thus

$$p = 69.5967; \quad 98.1741; \quad 231.2822 \quad (\text{c})$$

The eigenvectors are

$$\{X\}_1 = [1 \quad -1 \quad 1]^T \quad (\text{d})$$

$$\{X\}_2 = [-1 \quad 0 \quad 1]^T \quad (\text{e})$$

$$\{X\}_3 = [1 \quad 1 \quad 1]^T \quad (\text{f})$$

Using Eqs. (5.99) and (5.100) for $\xi = 0$ at i end and $\xi = 1$ at j end, we have

$$\begin{Bmatrix} \Psi_i \\ \Psi_j \\ Y_i \\ Y_j \end{Bmatrix} = \begin{bmatrix} 0 & T & 0 & U \\ Tn & Tc & -Un' & Uc' \\ 1 & 0 & 1 & 0 \\ c & n & c' & n' \end{bmatrix} \begin{Bmatrix} C_1 \\ C_2 \\ C_3 \\ C_4 \end{Bmatrix} \quad (\text{g})$$

in which integration constants are based on the relationship expressed in Eqs. (5.105)–(5.108). Eq. (g) is a general equation which can be applied to different members for various modes.

For the first mode of members 1, the boundary condition is given in Eq. (d) as $\Psi_i = 1$, $\Psi_j = -1$, $Y_i = Y_j = 0$. Evaluate the coefficients in Eq. (g), which is then inverted as

$$\begin{Bmatrix} C_1 \\ C_2 \\ C_3 \\ C_4 \end{Bmatrix} = \begin{bmatrix} 0 & 0.0220297 & 0 & 0.0182941 \\ 0.193499 & 0.194749 & 0 & -0.0182941 \\ 1 & 0 & 1 & 0 \\ 8.840277 & 8.783536 & -1 & 0 \end{bmatrix}^{-1} \begin{Bmatrix} 1 \\ -1 \\ 0 \\ 0 \end{Bmatrix} = \begin{Bmatrix} (1.10743)10^{-4} \\ (-1.24066)10^{-4} \\ (-1.10743)10^{-4} \\ 54.6626 \end{Bmatrix} \quad (\text{h})$$

Substituting Eq. (h) into Eq. (5.99) yields the member's displacement shape function as

$$Y_{11}(\xi) = (1.10743)10^{-4}chx_1\xi - (1.24066)10^{-4}shx_1\xi - (1.10743)10^{-4}\cos x_2\xi + 54.6626 \sin x_2\xi \quad (\text{i})$$

in which $x_1 = b\alpha$, $x_2 = b\beta$, $sh = \sinh$, $ch = \cosh$. For the first mode of member 2, the boundaries are also based on Eq. (d) as $\Psi_i = -1$, $\Psi_j = 1$, $Y_i = Y_j = 0$. Since the two members' properties are identical, the coefficients in Eq. (h) can be used without change. Thus

$$[C_1 \quad C_2 \quad C_3 \quad C_4] = [(-1.10743)10^{-4} \quad (1.24066)10^{-4} \quad (1.10743)10^{-4} \quad -54.6626] \quad (\text{j})$$

The displacement shape function of this member is similar to Eq. (i) except that the coefficients should be replaced by those in Eq. (j).

In calculation of pseudo-static displacement, Eq. (4.145) may be expressed in the present case as

$$Y_{stk} = \frac{\sum_{\ell=1}^2 \int_0^1 F(\xi) Y_{k\ell}(\xi) d\xi}{p_k^2 \sum_{\ell=1}^2 m \int_0^1 Y_{1\ell}^2(\xi) d\xi} \quad (\text{k})$$

For convenience, the integration of shape functions in the denominator of Eq. (k) is expressed below in mathematical closed form, which can be used for different members and various mode

shapes

$$\begin{aligned} \int_0^1 Y^2(\xi) d\xi &= \int_0^1 (C_1 chx_1 \xi + C_2 shx_1 \xi + C_3 \cos x_2 \xi + C_4 \sin x_2 \xi)^2 d\xi \\ &= C_1^2 I_4 + C_2^2 I_3 + C_3^2 I_2 + C_4^2 I_1 + 2C_1 C_2 I_{10} + 2C_1 C_3 I_9 + 2C_1 C_4 I_7 + 2C_2 C_3 I_8 \\ &\quad + 2C_2 C_4 I_6 + 2C_3 C_4 I_5 \end{aligned} \quad (\text{l})$$

in which I 's are symbolic notations of the integration results. They are

$$I_1 = \left(\frac{1}{2} - \frac{1}{4x_2} \sin 2x_2 \right) \quad (\text{m})$$

$$I_2 = \left(\frac{1}{2} + \frac{1}{4x_2} \sin 2x_2 \right) \quad (\text{n})$$

$$I_3 = \left(-\frac{1}{2} + \frac{1}{4x_1} \operatorname{sh} 2x_1 \right) \quad (\text{o})$$

$$I_4 = \left(\frac{1}{2} + \frac{1}{4x_1} \operatorname{sh} 2x_1 \right) \quad (\text{p})$$

$$I_5 = \frac{1}{4x_2} (1 - \cos 2x_2) \quad (\text{q})$$

$$I_6 = \frac{1}{x_1^2 + x_2^2} (x_1 \sin x_2 chx_1 - x_2 \cos x_2 shx_1) \quad (\text{r})$$

$$I_7 = \frac{1}{x_1^2 + x_2^2} (x_1 \sin x_2 shx_1 - x_2 \cos x_2 chx_1 + 1) \quad (\text{s})$$

$$I_8 = \frac{1}{x_1^2 + x_2^2} (x_1 \cos x_2 chx_1 + x_2 \sin x_2 shx_1 - 1) \quad (\text{t})$$

$$I_9 = \frac{1}{x_1^2 + x_2^2} (x_1 \cos x_2 shx_1 + x_2 \sin x_2 chx_1) \quad (\text{u})$$

$$I_{10} = \frac{1}{4x_1} (ch_2 x_1 - 1) \quad (\text{v})$$

Substitute the numerical values ($x_1 = b\alpha = 2.869251$, $x_2 = b\beta = 3.141594$) of Eq. (m)–(v) and coefficients of Eq. (h) into (l); then

$$\int_0^1 Y_{11}^2(\xi) d\xi = 1493.998 \quad (\text{w})$$

The participation factor can be calculated as

$$F_{11} = \int_0^1 F(\xi) Y_{11}(\xi) d\xi = \int_0^1 (3000) Y_{11}(\xi) d\xi = 3000(34.79928) = 104,397.8 \quad (\text{x})$$

where $Y_{11}(\xi)$ is given in Eq. (i). Similarly for member 2

$$\int_0^1 Y_{12}^2(\xi) d\xi = 1493.998 \quad (\text{y})$$

$$F_{12} = \int_0^1 F(\xi) Y_{12}(\xi) d\xi = 0 \quad (\text{z})$$

in which $F(\xi)$ is zero for member 2.

The pseudo-dynamic mass of the two-span beam is

$$\bar{M}_1 = m \sum_{\ell=1}^2 \int_0^1 Y_{1\ell}^2(\xi) d\xi = 0.2(2)(1493.998) = 597.5992 \quad (\text{aa})$$

and the pseudo-static displacement of the first mode is

$$Y_{\text{st}1} = \frac{F_{11}}{p_1^2 \bar{M}_1} = \frac{104,397.8}{4843.6958(597.5992)} = 0.0361 \quad (\text{bb})$$

For the second mode, the calculations are carried out by following the above procedures for $x_1 = b\alpha = 3.339641$, $x_2 = b\beta = 3.796126$. The displacement shape functions are

$$Y_{21}(\xi) = (-7.18893)10^{-4}chx_1\xi - (1.95299)10^{-4}shx_1\xi + (7.18893)10^{-4} \cos x_2\xi - 45.208 \sin x_2\xi \quad (\text{cc})$$

$$Y_{22}(\xi) = -27.5224chx_1\xi + 27.5916shx_1\xi + 27.5224 \cos x_2\xi - 35.8655 \sin x_2\xi \quad (\text{dd})$$

Performing integration yields

$$\int_0^1 Y_{21}^2(\xi) d\xi = 1098.4 \quad (\text{ee})$$

$$F_{21} = \int_0^1 F(\xi) Y_{21}(\xi) d\xi = -84,331.59 \quad (\text{ff})$$

$$\int_0^1 Y_{22}^2(\xi) d\xi = 1021.504 \quad (\text{gg})$$

$$F_{22} = \int_0^1 F(\xi) Y_{22}(\xi) d\xi = 0 \quad (\text{hh})$$

$$\bar{M}_2 = m \sum_{\ell=1}^2 \int_0^1 Y_{2\ell}^2(\xi) d\xi = 0.2(1098.4 + 1021.504) = 423.9808 \quad (\text{ii})$$

$$Y_{\text{st}2} = \frac{F_{21}}{p_2^2 \bar{M}_2} = \frac{-84,331.59}{(9638.156)(423.9808)} = -0.02063 \quad (\text{jj})$$

The third mode does not affect response because the mode shape of member 1 is antisymmetric (see Example 4.9.1); therefore $F_{31} = 0$.

The displacement of member 1 may be calculated from Eq. (4.146) derived in Chapter 4 as

$$y_1(\xi, t) = \sum_{k=1}^n Y_{\text{st}k} A_k(t) Y_{k1}(\xi) \quad (\text{kk})$$

in which $A_1(t)$ and $A_2(t)$ are dynamic load factors corresponding to the first and second modes, respectively. $Y_{11}(\xi)$ is given in Eq. (i), and the moment and shear equations for member 1

are

$$M(\xi, t) = \sum_{k=1}^n Y_{stk} A_k(t) \left(-EI \frac{d\Psi}{dx} \right)_k \quad (\text{ll})$$

$$V(\xi, t) = \sum_{k=1}^n Y_{stk} A_k(t) \left[GA\mu \left(\frac{dY}{dx} - \Psi \right) \right]_k \quad (\text{mm})$$

in which Y and Ψ and their derivatives can be obtained from Eqs. (5.99) and (5.100).

For the first frequency found, we have

$$T = \frac{2\pi}{p_1} = 0.0903; \quad \frac{\zeta}{T_1} = \frac{0.1}{0.0903} = 1.1074 \quad (\text{nn})$$

From Fig. 1.17

$$A_1(t) = 1.60; \quad \frac{t_m}{T_1} = 0.455 \quad (\text{oo})$$

Then $t_m = 0.455(0.093) = 0.0411 < \zeta$, the time at which maximum response of the first mode occurs. Using the time to find second mode response, we then write Eq. (1.81) as

$$A_2(t) = 1 - \cos[(98.1741)(0.0411)] + \frac{\sin[(98.1741)(0.0411)]}{(98.1741)(0.1)} - \frac{0.0411}{0.1} = 1.364 \quad (\text{pp})$$

which can also be obtained from Fig. 1.17 at $t_m/T_2 = 0.642$.

Displacement at the midspan of member 1 can now be obtained from Eq. (kk) as

$$y(0.5) = 0.0361(1.6)[\text{Eq.(i)} \text{ at } \xi = 0.5] + (-0.02063)(1.1364)[\text{Eq.(cc)} \text{ at } \xi = 0.5] = 4.278 \text{ in} \quad (\text{qq})$$

Moment at the midspan can be calculated from Eq. (ll) as

$$\begin{aligned} M(0.5) &= \frac{(6)10^9}{150} \left\{ 1.60(0.0361) \left[-\frac{d\Psi}{dx} \right] \right. \\ &\quad \left. + 1.1364(-0.02063) \left[-\frac{d\Psi}{dx} \right] \right\} \\ &= 3,639,980.35 \text{ lb in} \end{aligned} \quad (\text{rr})$$

where Ψ in the first and the second term correspond to the first and second mode, respectively, of Eq. (5.100). Shear at the left end of the member is obtained by using Eq. (mm) as

$$\begin{aligned} V(0) &= (1.12)10^7(1.871)(0.833) \left\{ 1.6(0.0361) \left[\frac{1}{150} \left(\frac{dY}{dx} \right) - \Psi \right] \right. \\ &\quad \left. + (1.1364)(-0.020603) \left[\frac{1}{150} \left(\frac{dY}{dx} \right) - \Psi \right] \right\} \\ &= 222,814.20 \text{ lb} \end{aligned} \quad (\text{ss})$$

where Y and Ψ in the first and second term are associated with the first and second mode, respectively. Y is given in Eq. (5.99).

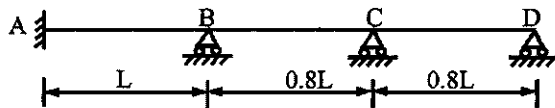


FIG. 5.28 Example 5.10.2.

5.10.5. Effect of Various Parameters on Frequencies

Various parameters of shear deformation, rotatory inertia, and shear factor can affect vibration frequencies. For a given beam, Bernoulli–Euler theory and Timoshenko theory yield upper and lower bounds of frequencies, respectively. A comparative study of frequencies is given in the following example.

EXAMPLE 5.10.2 The three-span, continuous, uniform beam shown in Fig. 5.28 is analyzed for natural frequencies. The given conditions are: $g = 32.2 \text{ ft/sec}^2$, $E = 30,000 \text{ kip/in}^2$, and $\gamma = 0.49 \text{ kip/ft}^3$, and $G = 12,000 \text{ ksi}$. Let the slenderness ratio, L/R , of span AB vary from 20, 30, 40, 50, to 60; then find the first five natural frequencies by considering: (A) bending deformation only; and (B) bending and shear deformation as well as rotatory inertia. In Case B, the values of μ are assumed to be 0.833 and $2/3$ for showing the effect of the shear factor on natural frequencies.

Solution: Let member AB be reference member 1; then the dimensionless parameters may be expressed as $\alpha_i = L_i/L_1$, $\beta_i = I_i/I_1$, $\Phi_i = A_i/A_1$. Thus

$$r_i^2 = \frac{\beta_i}{\alpha_i^2 \phi_i} \left(\frac{R}{L} \right)_1^2 \quad (a)$$

$$s_i^2 = \frac{E}{\mu G} r_i^2 \quad (b)$$

$$b_i^2 = \frac{\gamma}{Eg} \alpha_i^2 L_1^2 p^2 \frac{1}{r_i^2} = \frac{\gamma}{Eg} \alpha_i^2 L_1^2 p^2 \frac{\alpha_i^2 \phi_i}{\beta_i} \left(\frac{L}{R} \right)_1^2 \quad (c)$$

By changing member length, L , and keeping other member properties constant, then $\alpha_2 = \alpha_3 = 0.8$, $\beta_2 = \beta_3 = 1$, and $\Phi_2 = \Phi_3 = 1$ for various slenderness ratios of L/R . For a given L/R , we can evaluate the singularity of the structure's stiffness matrix by varying frequency parameter b_1 . The frequency is then found from

$$p = b_1 \sqrt{\frac{Eg}{\gamma}} \left(\frac{R}{L} \right)_1 \frac{1}{L_1} \quad (d)$$

Let p = frequencies of the Bernoulli–Euler theory and p^* = frequencies of the Timoshenko theory; then the ratio of frequencies, p^*/p , of the first five modes for various slenderness ratios of Cases A and B are shown in Fig. 5.29. Observation reveals that (1) Timoshenko theory yields lower frequencies than Bernoulli–Euler theory; (2) reduction is more pronounced for higher modes and lower slenderness ratios; and (3) the shear factor has a greater effect on higher modes while smaller μ reduces frequency more than larger μ .

5.11. TIMOSHENKO EQUATION WITH ELASTIC MEDIA AND P-Δ EFFECT

The Timoshenko equation is extended here with consideration of elastic support and axial force. Efforts are focused on derivation of differential equations, stiffness coefficients, and fixed-end forces. Sample numerical studies are also illustrated.

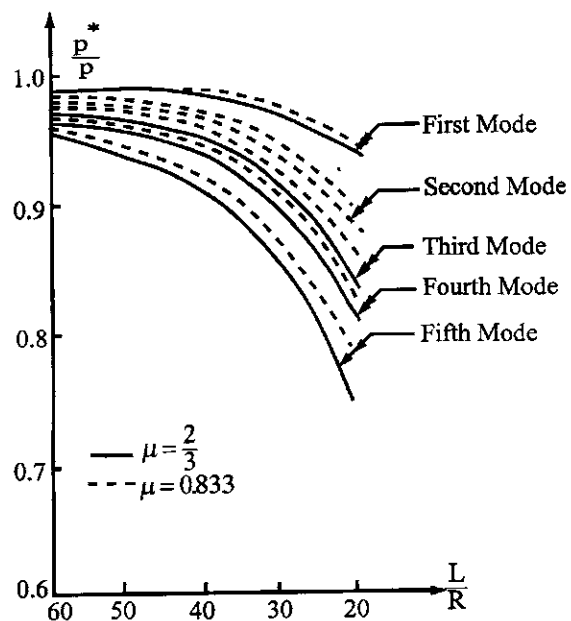


FIG. 5.29 Comparison of natural frequencies.

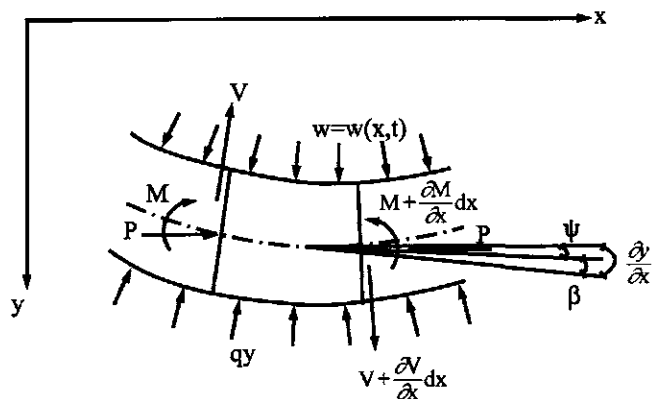


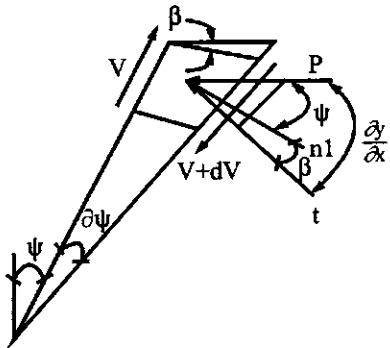
FIG. 5.30 Beam element.

5.11.1. Differential Equations

Consider the beam element shown in Fig. 5.30; equilibrium equations for the free-body diagram yield

$$\frac{\partial V}{\partial x} = \rho A \frac{\partial^2 y}{\partial t^2} - w + qy \quad (5.147)$$

$$V = \frac{\partial M}{\partial x} - P \frac{\partial y}{\partial x} + \rho I \frac{\partial^2 \psi}{\partial t^2} \quad (5.148)$$

**FIG. 5.31** Plane for axial force component.

where $\rho = \gamma/g$; other notations were defined previously.

Assume the component of axial load P on the cross-section is acting on the plane of the total slope as shown in Fig. 5.31; then $P \sin(\partial y/\partial x) \approx P \partial y/\partial x$. Shear deformation becomes

$$V + P \frac{\partial y}{\partial x} = \left(\frac{\partial y}{\partial x} - \psi \right) \phi \quad (5.149)$$

where

$$\phi = GA\mu \quad (5.150)$$

By eliminating ψ and y from Eqs. (5.147)–(5.150), the complete equations in y and ψ are obtained as

$$EI\zeta \frac{\partial^4 y}{\partial x^4} + \rho \left(A + \frac{qI}{\phi} \right) \frac{\partial^2 y}{\partial t^2} + \left(P - \frac{EIq}{\phi} \right) \frac{\partial^2 y}{\partial x^2} - I\rho \left(\zeta + \frac{EA}{\phi} \right) \frac{\partial^4 y}{\partial x^2 \partial t^2} + \frac{\rho^2 IA}{\phi} \frac{\partial^4 y}{\partial t^4} + qy - \frac{I}{\phi} \left(\rho \frac{\partial^2 w}{\partial t^2} - E \frac{\partial^2 w}{\partial x^2} \right) - w = 0 \quad (5.151)$$

$$EI\zeta \frac{\partial^4 \psi}{\partial x^4} + \rho \left(A + \frac{qI}{\phi} \right) \frac{\partial^2 \psi}{\partial t^2} + \left(P - \frac{EIq}{\phi} \right) \frac{\partial^2 \psi}{\partial x^2} - I\rho \left(\zeta + \frac{EA}{\phi} \right) \frac{\partial^4 \psi}{\partial x^2 \partial t^2} + \frac{\rho^2 IA}{\phi} \frac{\partial^4 \psi}{\partial t^4} + q\psi \frac{\partial w}{\partial x} = 0 \quad (5.152)$$

where

$$\zeta = 1 - \frac{P}{\phi} \quad (5.153)$$

Let $w = 0$; following the procedures in Eqs. (5.95)–(5.98) yields

$$Y(\xi) = C_1 \cosh b\alpha\xi + C_2 \sin b\alpha\xi + C_3 \cos b\beta\xi + C_4 \sin b\beta\xi \quad (5.154)$$

$$\Psi(\xi) = C'_1 \sinh b\alpha\xi + C'_2 \cosh b\alpha\xi + C'_3 \sin b\beta\xi + C'_4 \cos b\beta\xi \quad (5.155)$$

where

$$\frac{\alpha}{\beta} = \frac{1}{\sqrt{2}} \left[\mp r^2 T + \left(r^4 T^2 - \frac{4U}{b^2} \right)^{\frac{1}{2}} \right]^{\frac{1}{2}} \quad (5.156)$$

Depending on the values of $r^4 T^2$, $4U/b^2$ and $r^2 T^2$, there are three distinct cases for α and β : α and β are complex; α is imaginary and β is real; and α and β are real. However, the solutions derived for stiffness coefficients and fixed-end forces are valid for all cases [8]. Here, T , U , b^2 , s^2 , and r^2 are nondimensional parameters defined as

$$b^2 = \rho \frac{AL^4}{EI} p^2 \quad (5.157)$$

$$r^2 = \frac{I}{AL^2} \quad (5.158)$$

$$s^2 = \frac{EI}{\phi L^2} \quad (5.159)$$

$$T = \frac{\left[P - \frac{qEI}{\phi} \right]}{\zeta \rho p^2 I} + 1 + \frac{EA}{\zeta \phi} \quad (5.160)$$

$$U = \left(\frac{\rho I p^2}{\zeta \phi} - \frac{1}{\zeta} \right) + \frac{q}{A \zeta} \left(\frac{1}{\rho p^2} - \frac{I}{\phi} \right) \quad (5.161)$$

The constants are

$$C'_1 = \frac{b}{L\alpha} \left(\zeta \alpha^2 + s^2 - \frac{qL^2}{\phi b^2} \right) C_1 \quad (5.162)$$

$$C'_2 = \frac{b}{L\alpha} \left(\zeta \alpha^2 + s^2 - \frac{qL^2}{\phi b^2} \right) C_2 \quad (5.163)$$

$$C'_3 = \frac{-b}{L\beta} \left(\zeta \beta^2 - s^2 + \frac{qL^2}{\phi b^2} \right) C_3 \quad (5.164)$$

$$C'_4 = \frac{b}{L\beta} \left(\zeta \beta^2 - s^2 + \frac{qL^2}{\phi b^2} \right) C_4 \quad (5.165)$$

5.11.2. Stiffness Coefficients

The force-deformation relationships of a typical member are based on Fig. 4.4, for which the boundary conditions are

	End forces	End displacements	
$\xi = 0$	$M_i = \frac{-EI}{L} \frac{d\Psi}{d\xi}$	$\Psi = \Psi_i$	
$\xi = 1$	$M_j = \frac{EI}{L} \frac{d\Psi}{d\xi}$	$\Psi = \Psi_j$	(5.166)
$\xi = 0$	$V_i = \phi \left(\frac{\zeta}{L} \frac{dY}{d\xi} - \Psi \right)$	$Y = -Y_i$	
$\xi = 1$	$V_j = \phi \left(\frac{\zeta}{L} \frac{dY}{d\xi} - \Psi \right)$	$Y = Y_j$	

Following the procedures in Eqs. (5.114)–(5.119) yields the stiffness coefficients as

$$SM\theta_1 = \frac{EIb(\alpha\Lambda' + \beta B')(n'c\Lambda' - nc'B')}{|R'|L} \quad (5.167)$$

$$SM\theta_2 = \frac{EIb(\alpha\Lambda' + \beta B')(B'n - \Lambda'n')}{|R'|L} \quad (5.168)$$

$$SMY_1 = \frac{EIbB'\Lambda'[(1 - cc')(c\Lambda' - \beta B') - nn'(\alpha B' + \beta \Lambda')]}{|R'|L} \quad (5.169)$$

$$SMY_2 = \frac{EIbB'\Lambda'(c' - c)(\alpha\Lambda' + \beta B')}{|R'|L} \quad (5.170)$$

$$SVY_1 = \frac{\zeta b\phi(n'cB' + nc'\Lambda')(\beta\Lambda' - \alpha B')}{|R'|L} \quad (5.171)$$

$$SVY_2 = \frac{\zeta b\phi(n\Lambda' + n'B')(\beta\Lambda' - \alpha B')}{|R'|L} \quad (5.172)$$

in which $n = \sinh b\alpha$, $n' = \sinh b\beta$, $c = \cosh b\alpha$, $c' = \cosh b\beta$, and

$$|R'| = nn'(\Lambda'^2 - B'^2) + 2(1 - cc')\Lambda'B' \quad (5.173)$$

$$\Lambda' = \frac{b}{L\alpha} \left(\zeta\alpha^2 + s^2 - \frac{qL^2}{\phi b^2} \right) \quad (5.174)$$

$$B' = \frac{b}{L\beta} \left(\zeta\beta^2 - s^2 + \frac{qL^2}{\phi b^2} \right) \quad (5.175)$$

5.11.3. Fixed-end Forces

The fixed-end forces of a beam subjected to uniform load, We^{ipt} , and axial compression, P , shown in Fig. 5.32 can be obtained by using Eq. (5.166) with end deformations as $\Psi_i = \Psi_j = Y_i = Y_j = 0$. Thus

$$M_{0i} = \frac{EIbW\Lambda'B'[(1 - cc')(c\Lambda' - \beta B') - (\alpha B' + \beta \Lambda')nn' + (c - c')(\alpha\Lambda' + \beta B')]}{|R'|(q - \rho Ap^2)L} \quad (5.176)$$

$$V_{0i} = \frac{\zeta b\phi W(\alpha B' - \beta \Lambda')[n(1 - c')\Lambda' + n'(1 - c)B']}{|R'|(q - \rho Ap^2)L} \quad (5.177)$$

$$M_{0j} = -M_{0i} \quad (5.178)$$

$$V_{0j} = -V_{0i} \quad (5.179)$$

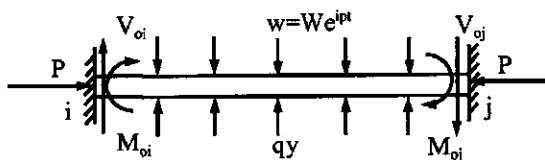


FIG. 5.32 Uniform forcing function.

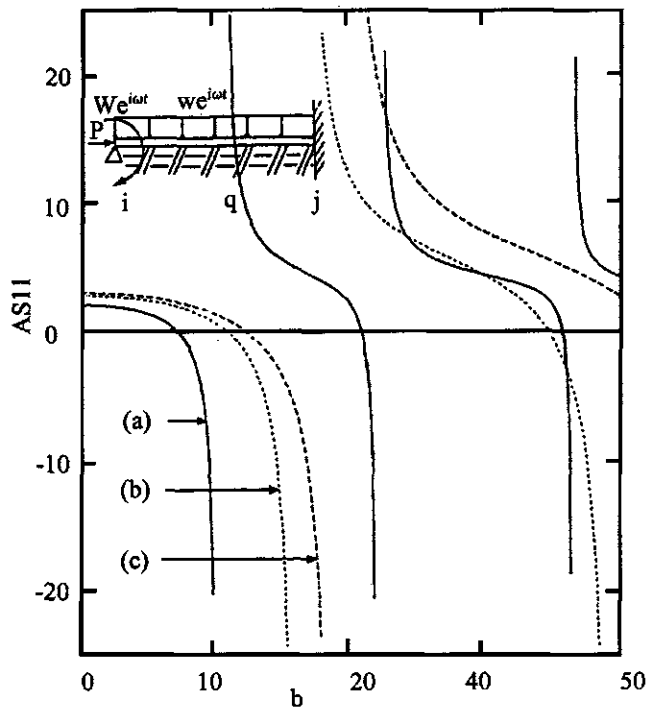


FIG. 5.33 Natural frequencies for $P/PE = 0.6$, $q = 0$ and various slenderness ratios: (a) $L/R = 10$; (b) $L/R = 20$; (c) $L/R = 40$.

5.11.4. Case Studies of the Effect of Various Parameters on Frequencies

For convenience in calculation, stiffness coefficients and fixed-end forces are expressed in terms of physical parameters such as P/PE , q/q_e , L/R , and b . $PE = \pi^2 EI/L$ is the lowest buckling load, or Euler buckling load, of a simply supported, single-span beam of length L subjected to axial load in the absence of an elastic foundation and vibration motion. $q_e = \pi^2 EI/L^4$ is the lowest eigenvalue or critical foundation constant of the same beam supported by an elastic foundation, but here the axial load is zero and vibration is not present.

A simple illustration can be observed from the beam shown in Fig. 5.33. The dynamic system matrix of the beam is

$$(W - M_{0i})e^{iot} = SM_{01}X_\theta e^{iot} \quad (5.180)$$

where W is the magnitude of the applied moment, M_{0i} is the fixed-end moment of the applied uniform load we^{iot} , ω is the forcing frequency, and X_θ is the joint rotation. Knowing the forcing frequency, ω , and the loading magnitudes of W and w , we may calculate X_θ of steady-state vibration from Eq. (5.180). When the external loads are not applied, we may calculate the natural frequencies by evaluating the zero determinant of the right-hand side of the equation. This calculation yields the stiffness-coefficient variation for different values of frequency parameter, b , as shown in Fig. 5.33. The graphs of $ASII$ [$ASII = SM_{01}/(EI/L)$] are plotted for three cases of slenderness ratios, $L/R = 10, 20, 40$, with $q = 0$, and $P = 0.66PE$, where $PE = \pi^2 EI/L^2$ is associated with the three slenderness ratios. Other parameters used are $v = 0.25$, $\mu = 2/3$, $\rho = 7839 \text{ kg/m}^3$, and $E = 212.95 \text{ kN/m}^2$. Fig. 5.33 shows two distinct characteristics: zero and infinite points. The former is associated with natural frequencies of the member shown in Fig. 5.33; the latter corresponds to the natural frequencies of the member with both ends fixed.

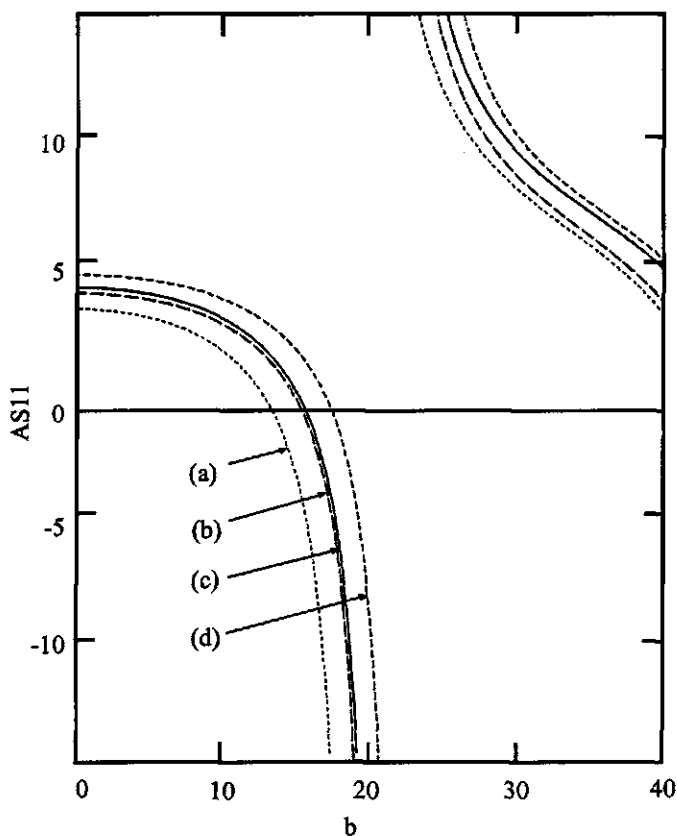


FIG. 5.34 Natural frequencies for $L/R = 40$ with various elastic media and axial load conditions: (a) $P/PE = 0.6, q = 0$; (b) $P/PE = 0.6, q/q_e = 0.6$; (c) $P = 0, q = 0$; (d) $P = 0, q/q_e = 0.6$.

Because the end-rotations are restrained, the end-moments must approach infinity when the natural frequency reaches resonance. Note that when L/R is reduced, the frequency parameter, b , decrease.

The effects of axial loads and elastic media on the natural frequencies and stiffness coefficients are shown in Fig. 5.34. It is apparent that axial force reduced stiffness and natural frequencies, while elastic media increases stiffness and natural frequencies.

These formulations of stiffness coefficients and fixed-end forces, as noted earlier, are discussed in terms of nondimensional parameters associated with the effects of transverse inertia, b , rotatory inertia, r , shear deformation, s , axial force, P , and elastic media, q . When individual effect is not considered, the associated parameter can be dropped. Therefore the formulation presented in this section can be converged to the results in Section 5.8 for $P = 0, r = 0$ and $s = 0$; in Section 5.9 for $r = 0, s = 0$; in Section 5.10 for $q = 0$ and $P = 0$; and in Chapter 4 for $r = s = q = P = 0$.

The numerical procedures for steady-state vibration and response analysis for various types of dynamic excitations presented previously can be directly applied to this section. Therefore they are not repeated here.

BIBLIOGRAPHY

1. FY, Cheng. Dynamics of prismatic and thin-walled member grids. Proceedings of Application of Finite Element Methods in Civil Engineering, ASCE, 1968, pp 339–373.

2. FY Cheng. Vibration of Timoshenko Beams and Frameworks. ASCE J Struct Div 3:551–271, 1970.
3. FY Cheng. Matrix Computer Methods in Structural Continuum Mechanics. University of Missouri-Rolla, MO: Extension Division Publication, 1970.
4. FY Cheng, WH Tseng, ME Botkin. Matrix calculations of structural dynamic characteristics and response. Proceedings of International Symposium on Earthquake Analysis of Structures, Jassy, Romania, Vol 1, 1970, pp 85–101.
5. FY Cheng, WH Tseng. Dynamic matrix of Timoshenko beam columns, ASCE J Struct Div 99(ST3):527–549, 1973.
6. FY Cheng. Dynamic matrices of beams on elastic foundation. Proceedings of International Symposium on Soil-Structures Interaction, India, 1977, pp 203–208.
7. FY Cheng, CP Pantelides. Static Timoshenko beam–columns on elastic media. ASCE J Struct Div 114(5): 1152–1172, 1988.
8. FY Cheng, CP Pantelides. Dynamic Timoshenko beam–columns on elastic media. ASCE J Struct Div 114(7): 1524–1550, 1988.
9. GR Cowper. The shear coefficients in Timoshenko's beam theory. Appl Mech 33:335–340, 1966.
10. M Hetenyi. Beams on Elastic Foundations. Ann Arbor, MI: University of Michigan Press, 1946.
11. TC Huang. The effect of rotary inertia and of shear deformation on the frequency and normal mode equations of uniform beams with simple end conditions. J Appl Mech 28:579–584, 1961.
12. RD Mindlin. Influence of rotary inertia and shear on flexural motions of isotropic, elastic plates. ASME Appl Mech Trans 73:31–38, 1951.
13. SP Timoshenko. On the correction for shear of the differential equation for transverse vibrations of prismatic bars. Phil Mag 6(41):744–746, 1921.
14. YS Ulfyand. The propagation of waves in the transverse vibration of bars and plates. Prikladnaya Matematika i Mekhanika 12:287–300, 1948.
15. HH West, M Mafi. Eigenvalue for beam–columns on elastic supports. J Struct Div 110(6):1305–1320, 1984.

6

Consistent Mass Method for Frames and Finite Elements

PART A FUNDAMENTALS

6.1. INTRODUCTION

Mathematical models for structural dynamic analysis may be generally classified into three approaches: lumped mass, dynamic stiffness (frequency-dependent stiffness), and *consistent mass (finite element)*. For computer application, all these are formulated by using the displacement (stiffness) matrix method. Lumped mass and dynamic stiffness approaches were already presented in previous chapters. The characteristics of these two approaches differ in that the motion equation for the lumped mass model consists of independent mass and stiffness matrices, while the dynamic stiffness model has mass implicitly combined with stiffness. The lumped mass and consistent mass approaches are similar in terms of motion equation: both of them have independent mass and stiffness matrices; their mass matrices, however, are not the same. Consistent mass may be considered an alliance of finite elements normally used in *continuum mechanics*. This method is often used for frameworks as well as plate structures.

The fundamental concept of finite element is able to model a structure or continuum by dividing it into a number of regions. Each region behaves as a structural member with nodes compatible to the nodes of neighboring regions. These regions are called *finite elements*. A plate shown in Fig. 6.1 represents a continuum where two regions are sketched with nodes 1, 2, ..., 9. the boundaries of neighboring elements at node 5 are compatible at the node but not necessarily compatible along the edges such as 4–5 or 5–8 and so on. Framed structures, however, are automatically discretized by the nature of their members and connections. We may say that finite element analysis is in the monarchy of structural matrix methods, and frameworks are special

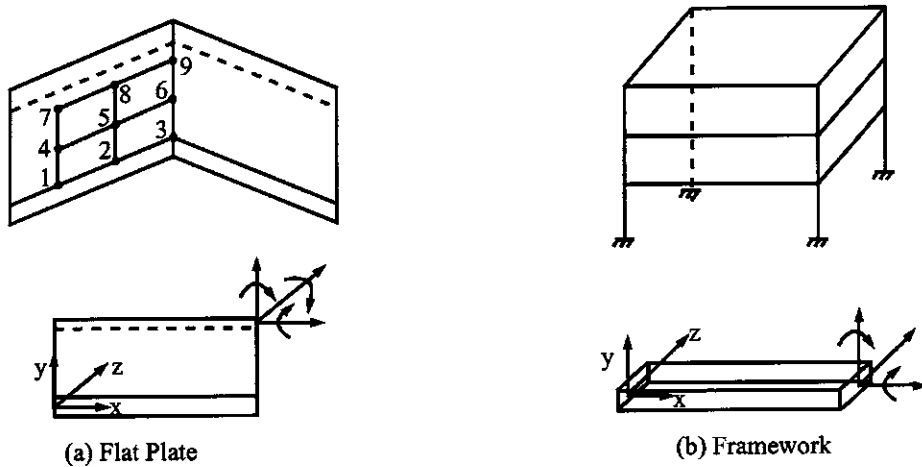


FIG. 6.1 Discretized elements. (a) Flat plate. (b) Framework.

cases of finite elements. Depending on the nature of structural problems and a structure's geometry, finite elements can be modeled as triangular, quadrilateral, axisymmetric solids, tetrahedrals, or other shapes.

The finite element approach has been recognized as a powerful tool in structural analysis and is therefore introduced in this chapter. Discussed herein are the fundamental concepts of finite element formulation (consistent mass) and their application to frameworks and plates. Also included are response analysis techniques and numerical comparisons between lumped mass, dynamic stiffness, and consistent mass models. Finite element formulation is illustrated by using two approaches: *generalized coordinates* and *natural coordinates*. The latter leads to *isoparametric elements*, which are currently in vogue in structural mechanics.

6.2. ENERGY METHOD FOR MOTION EQUATION

The governing motion equation of a structural system can be treated separately as two structural models: rigid frames and elastic frames. Motion characteristics of these two structural models can be illustrated by the gable frame shown in Fig. 6.2a, for which the rigid frame model has five d.o.f. (see Figs. 6.2b and d) and the elastic frame model has nine d.o.f. (see Fig. 6.2f). Fig. 6.2b and d represents two possibilities of assigning d.o.f. of sidesway for the rigid frame model. When the sidesway at node *B* of the rigid frames moves (see Fig. 6.2c), other d.o.f. do not move; the work of the external load, $P_1(t)$, must be transferred to nodes *B* and *D* because node *C* does not have linear d.o.f. and can move up or down. This side-sway movement induces member *BC* to have inertia force resulting from both deflection and axial rigid-body motion. However, when the d.o.f. of side-sway at *B* of Fig. 6.2d moves, member *BC* will not have axial rigid-body motion and $P_1(t)$ will not induce work because the vertical d.o.f. at node *C* must not be distorted (see Fig. 6.2e). Thus, the formulation of mass matrix and the external load's work of a rigid frame must include possible axial rigid-body motion of members, which is dependent on the assignment of d.o.f. of the system's side-sway. For the elastic frame shown in Fig. 6.2f, however, each node has three d.o.f. When the lateral d.o.f. at *B* is moved (see Fig. 6.2g), the inertia forces and work of $P_1(t)$ transfer into nodes at which the deformed members are connected. Since each node of a structure (i.e. two-dimensional plane structure) has three d.o.f. and each constituent member has three local d.o.f. at the member end, the structural formulation can be automatically generated through the relationship between local and global coordinates at the connecting nodes. For the sake of clarity, the governing motion equation is presented separately for rigid and elastic frames.

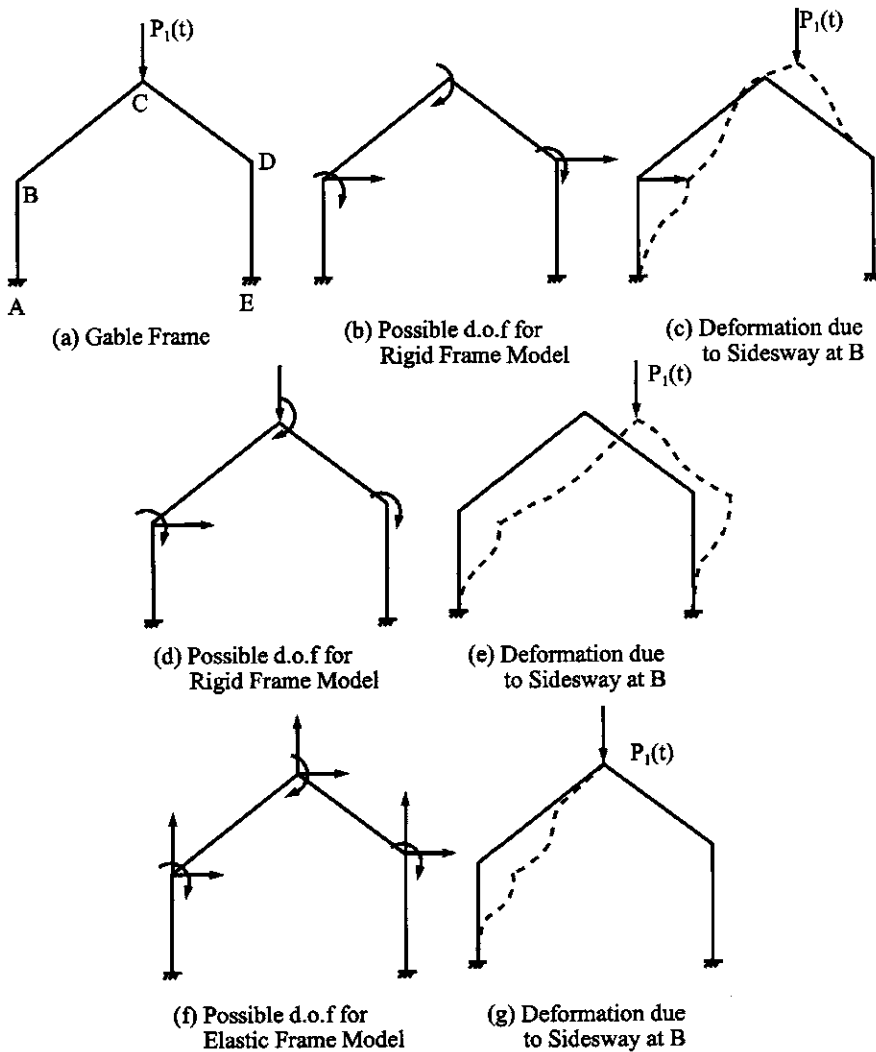


FIG. 6.2 Rigid and elastic frame models.

6.2.1. Rigid Frames

Let $y(x, t)$ be the transverse displacement of each point in the direction perpendicular to the axis of a structural element where x denotes the points of the coordinates of the structure. In addition to the transverse displacement, the structure has axial rigid-body motion resulting from side-sway. If $N_i(x)$ is chosen as *coordinate functions* of the structure and $q_i(t)$ represents the generalized coordinates, then the dynamic deflection of the structure can be expressed as

$$y(x, t) = \sum_{i=1}^n N_i(x) q_i(t) \quad (6.1)$$

where n is the number of generalized coordinates. For simplicity, the variables x and t are dropped from now on. Then the longitudinal displacement of the j th member of the structure can be given

as

$$u_j = \sum_{i=1}^{NP} \Delta_{ji} q_i \quad (6.2)$$

where Δ_{ji} is axial displacement of the j th member due to $q_i = 1$.

The kinetic energy of the structure can be represented by

$$T = \frac{1}{2} \int_v \rho(x) \left[\sum_{i=1}^n \frac{dq_i}{dt} N_i \right]^2 dv + \frac{1}{2} \sum_{j=1}^{MP} M_j \left[\sum_{i=1}^n \frac{dq_i}{dt} \Delta_{ji} \right]^2 \quad (6.3)$$

where $\rho(x)$ is the mass density per unit volume and MP is the total number of members having axial displacement.

The potential energy due to bending is

$$U = \frac{1}{2} \int EI(x) \left(\sum_{i=1}^n q_i \frac{d^2 N_i}{dx^2} \right)^2 dx \quad (6.4)$$

The work of the external load is

$$W = \int F(x, t) \sum_{i=1}^{NP} q_i N_i dx + \sum P_j \sum_{i=1}^n \Delta_{ji} q_i \quad (6.5)$$

where $F(x, t)$ is linear transverse load and P_j is axial force (static or dynamic) acting on the j th member. The second term in Eq. (6.5) is the work done by axial force times rigid-body motion in the member's longitudinal direction.

The dissipated energy due to viscous damping is

$$D = \frac{1}{2} \{\dot{q}\}^T [C] \{\dot{q}\} \quad (6.6)$$

where $[C]$ is a damping matrix, which is generally constructed using mass and stiffness, $[C] = \alpha[M] + \beta[K]$, as presented in Chapter 3.

Employing Lagrange's equation of Eq. (4.114), we have

$$\frac{d}{dt} \left(\frac{\partial T}{\partial \dot{q}_i} \right) + \frac{\partial(U - T)}{\partial q_i} + \frac{\partial D}{\partial \dot{q}_i} = \frac{\partial W}{\partial q_i} \quad (6.7)$$

Substituting Eqs. (6.3)–(6.6) into the above yields the following motion equation:

$$[M]\{\ddot{q}\} + [C]\{\dot{q}\} + [K]\{q\} = \{Q\} \quad (6.8)$$

where $[M]$ is the mass matrix, $[K]$ the stiffness matrix, and $\{Q\}$ represents generalized forces.

Let N_i be the *shape function* (also known as *displacement function*) of individual members, and be so defined: *the displacement shape of a member when one d.o.f. of that member has unit value and the other d.o.f. is zero*. Thus the displacement function of a structural system can be related to the members' shape functions through local coordinates (member) and global coordinates (system). The mass and stiffness coefficients of a typical member can be obtained by using a member's shape functions as

$$k_{ij} = \int EI(x) \frac{d^2 N_i}{dx^2} \frac{d^2 N_j}{dx^2} dx \quad (6.9)$$

$$m_{ij} = \int \rho(x) N_i N_j dv + \sum M_j \Delta_{ji} q_i \quad (6.10)$$

where $I(x)$ and $\rho(x)$, expressed as the function of x , signify that the formulation is applicable to a member with nonuniform cross-section. The generalized force can be found as

$$Q_i = \int F(x, t) N_i dx + \sum_j P_j \Delta_{ji} \quad (6.11)$$

By following procedures presented in Section 4.5 (similar procedures are in Sections 5.4 and 5.6), we can assemble k_{ij} , m_{ij} , and Q_i to form $[K]$, $[M]$, and $\{Q\}$ in Eq. (6.8).

6.2.2. Elastic Frames

A typical elastic frame model is shown in Fig. 6.2f where the members have axial deformations. Therefore rigid-body motion in the longitudinal direction of the members does not exist; consequently, the second term in Eqs. (6.3) and (6.5) should be dropped. For general consideration of a member in space (*three-dimensional*), the stiffness and mass coefficients as well as the generalized force can be formulated through the energy theorem (see Section 6.3.1 or [13]) as follows:

$$k_{ij} = \sum_r \int_v \sigma_i^r \varepsilon_j^r dv \quad (6.12)$$

$$m_{ij} = \sum_r \int_v \rho(x) N_i^r N_j^r dv \quad (6.13)$$

$$Q_i = \sum_r \int_v F(x, t) N_i^r dx \quad (6.14)$$

where $\sigma = \sigma(x)$ and $\varepsilon = \varepsilon(x)$ represent stress and strain, respectively, and the superscript, r , denotes the number of stresses and their associated strains, such as axial, bending, shear, and torsion. The integral is taken over the entire volume, v , of the member. This general formulation applies to various types of finite elements in continuum mechanics.

6.3. STIFFNESS, MASS AND GENERALIZED FORCE MATRICES FOR FRAME MEMBERS

6.3.1. Two-Force Member

Consider a tapered member subjected to longitudinal deformation as shown in Fig. 6.3, of which the cross-section varies along the member's longitudinal axis and may be expressed as

$$A(x) = A_1 \left(1 - \alpha \frac{x}{L}\right) \quad (6.15)$$

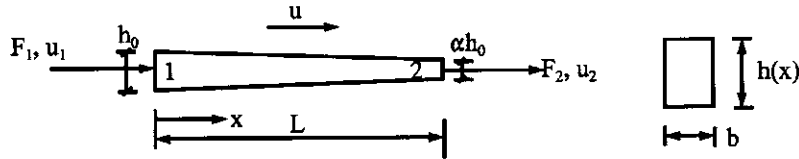


FIG. 6.3 Two-force member.

which represents various shapes of truss members. When

- $\alpha = 0$, prismatic member
- $\alpha = 1$, then $A_2 = 0$, wedge member
- $0 < \alpha < 1$, tapered shape with $A_2 < A_1$
- $\alpha < 0$, tapered shape with $A_2 > A_1$

The member has two d.o.f. of generalized coordinates, $\{q_e\}$, and their associated forces, $\{Q_e\}$, denoted as follows:

$$\{q_e\} = [q_1 \ q_2]^T = [u_1 \ u_2]^T \quad (6.16)$$

$$\{Q_e\} = [Q_1 \ Q_2]^T = [F_1 \ F_2]^T \quad (6.17)$$

6.3.1.1. Stiffness Matrix

Assume the *displacement function* of the member to be

$$u(x) = a_1 + a_2 x \quad (6.18)$$

Using the boundary conditions of deformation of the bar in the above equation yields

$$u(x) = N_1 \ q_1 + N_2 \ q_2 \quad (6.19)$$

in which the shape functions are

$$N_1 = 1 - \frac{x}{L}; \quad N_2 = \frac{x}{L} \quad (6.20)$$

The axial strain and stress are

$$\epsilon = \frac{\partial u(x)}{\partial x} = \frac{q_2 - q_1}{L} = \left[-\frac{1}{L} \quad \frac{1}{L} \right] [q_1 \ q_2]^T \quad (6.21)$$

$$\sigma = E\epsilon \quad (6.22)$$

Substituting Eqs. (6.21) and (6.22) into the following strain energy yields

$$U = \frac{1}{2} \int \epsilon \sigma \ dv = \frac{1}{2} \int \frac{1}{L} (q_2 - q_1) \frac{E}{L} (q_2 - q_1) dv \quad (6.23)$$

where dv is formulated by using Eq. (6.15) as

$$dv = A_1 \left(1 - \alpha \frac{x}{L} \right) dx$$

Then we have

$$U = \frac{EA_1}{2L} (q_2 - q_1)^2 \left(1 - \frac{\alpha}{2} \right) \quad (6.24)$$

From *Castigliano's first theorem*, we know that the partial derivative of the total energy of a structure, with respect to displacement at any point, is equal to the load applied at that point in the direction of the displacement. Thus

$$F_i = \frac{\partial U}{\partial q_i} \quad (6.25)$$

Substituting Eq. (6.24) into the above yields

$$\begin{Bmatrix} F_1 \\ F_2 \end{Bmatrix} = \frac{EA_1}{L} \left(1 - \frac{\alpha}{2}\right) \begin{bmatrix} 1 & -1 \\ -1 & 1 \end{bmatrix} \begin{Bmatrix} q_1 \\ q_2 \end{Bmatrix} \quad (6.26)$$

By definition of force-displacement relationship, we can conclude that Eq. (6.26) gives the stiffness matrix of the member as

$$[K_e] = \frac{EA_1}{L} \left(1 - \frac{\alpha}{2}\right) \begin{bmatrix} 1 & -1 \\ -1 & 1 \end{bmatrix} \quad (6.27)$$

Note that the second derivative of the strain energy yields stiffness coefficients. Also note that, using unit displacement in formulating ε , we can directly formulate a member's stiffness matrix (without using the procedures given in Eqs. (6.21)–(6.25) as

$$[K_e] = \int \varepsilon \sigma \, dv \quad (6.28)$$

Apparently when $\alpha = 0$, Eq. (6.27) becomes a stiffness matrix of a *prismatic member*. When $\alpha = 1$, Eq. (6.27) becomes

$$[K_e] = \frac{EA_1}{2L} \begin{bmatrix} 1 & -1 \\ -1 & 1 \end{bmatrix} \quad (6.29)$$

which means that $[K_e]$ of a *wedge member* is equivalent to using a prismatic member with the average height or area of the wedge shape.

The derivation presented above is an approximation. In order to examine the accuracy of the approximation, we may find the displacement of the member by applying an axial force, P , at end-2 with end-1 restrained. Thus, from Eq. (6.21),

$$\begin{aligned} u_2 &= \int \varepsilon \, dx = \int_0^L \frac{P}{A(x)E} \, dx \\ &= -\frac{PL}{\alpha EA_1} \ln\left(1 - \frac{\alpha x}{L}\right) \end{aligned} \quad (6.30)$$

For $\alpha = -1$, $A_2 = 2A_1$ (i.e. *tapered shape*),

$$u_2 = 0.6932 \frac{PL}{EA_1} \quad (6.31)$$

From Eq. (6.27) the approximate solution is

$$u_2 = \frac{2PL}{3EA_1} \quad (6.32)$$

Thus the exact solution is about 4% higher than the approximate one. Dividing the member into more segments will give a solution closer to the exact one.

6.3.1.2. Mass Matrix

The mass matrix of the member can be derived from Eq. (6.13) as

$$\{M_e\} = \int \rho A(x) [N]^T [N] dv = \frac{\rho A_1}{L^2} \int_0^L \left(1 - \alpha \frac{x}{L}\right) \begin{Bmatrix} L-x \\ x \end{Bmatrix} [L-x \ x]^T dA dx = \frac{\rho L A_1}{3} \begin{bmatrix} 1 - \frac{\alpha}{4} & \frac{1}{2} - \frac{\alpha}{4} \\ \text{symm} & 1 - \frac{\alpha}{4} \end{bmatrix} \quad (6.33)$$

By changing α , the above equation yields the mass matrix associated with the member of a given shape.

6.3.1.3. Generalized Force Matrix

For a uniformly distributed load acting along the member's length, $F(x, t) = F[1 - (t/\zeta)]$, the generalized force can be obtained from Eq. (6.14) as

$$\{Q_e\} = \int_0^L F(x, t) [N]^T dx = \frac{1}{L} F \left(1 - \frac{t}{\zeta}\right) \int_0^L [L-x \ x]^T dx = F \left(1 - \frac{t}{\zeta}\right) \frac{L}{2} [1 \ 1]^T \quad (6.34)$$

If the uniform load is applied to a portion of the member, say from node 1 to distance x , then

$$\{Q_e\} = \frac{F}{L} \left(1 - \frac{t}{\zeta}\right) \int_0^x [L-x \ x]^T dx = F \left(1 - \frac{t}{\zeta}\right) \frac{1}{2L} [x(2L-x) \ x^2]^T \quad (6.35)$$

6.3.2. Torsional Member

A torsional member of a uniform circular cross-section is shown in Fig. 6.4 with generalized coordinates and forces denoted by

$$\{q_e\} = [q_1 \ q_2]^T = [\gamma_1 \ \gamma_2]^T \quad (6.36)$$

$$\{Q_e\} = [Q_1 \ Q_2]^T = [T_1 \ T_2]^T \quad (6.37)$$

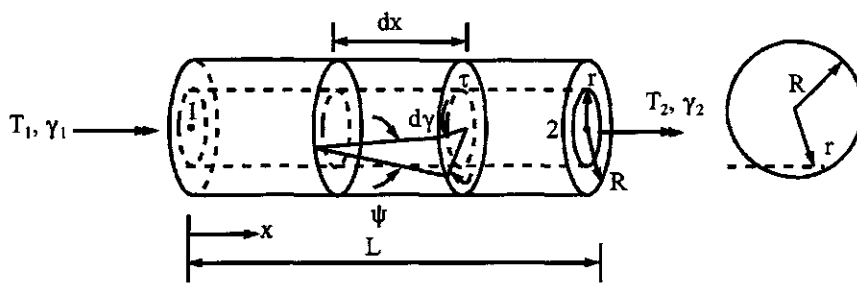


FIG. 6.4 Torsional member.

6.3.2.1. *Stiffness Matrix*

Assume the displacement function to be

$$\gamma(x) = a_1 + a_2 x \quad (6.38)$$

Using the boundary deformations of the bar, we have

$$\gamma(x) = N_1 q_1 + N_2 q_2 \quad (6.39)$$

where

$$N_1 = 1 - \frac{x}{L}; \quad N_2 = \frac{x}{L} \quad (6.40)$$

The shear strain at any point distant from the center, r , of the cross-section is

$$\psi = r \frac{d\gamma(x)}{dx} = \frac{r}{L} [-1 \quad 1] [q_1 \quad q_2]^T \quad (6.41)$$

For a cantilever member

$$\psi = \frac{Tr}{GJ} \quad (6.42)$$

where G is *shear modulus* and J is *polar moment of inertia*. The shear stress is

$$\tau = G\psi \quad (6.43)$$

From Eq. (6.28) with unit displacement, we have

$$[K_e] = \int \psi \tau \, dv = \frac{G}{L^2} [-1 \quad 1]^T [-1 \quad 1] \int_0^L \int_0^{2\pi} \int_0^R (r)^3 \, dx \, d\theta \, dr = \frac{GJ}{L} \begin{bmatrix} 1 & -1 \\ -1 & 1 \end{bmatrix} \quad (6.44)$$

where

$$J = \int_0^{2\pi} \int_0^R r^3 \, dr \, d\theta = \frac{\pi R^4}{2} \quad (6.45)$$

6.3.2.2. *Mass Matrix*

To obtain a consistent mass matrix, assume that the translational displacement at any point of the cross-section is $r\ddot{\gamma}(x)$; therefore, the acceleration may be expressed as $r\ddot{\gamma}(x)$. For the overall cross-section, *mass moment inertia* per unit length is

$$M_T = \int_0^{2\pi} \int_0^R \rho(r) r^3 \ddot{\gamma}(x) \, dr \, d\theta = \rho J \ddot{\gamma}(x) \quad (6.46)$$

Thus the consistent mass matrix of the member is

$$[M_e] = \int_0^L \rho J(x) [N]^T [N] \, dx = \frac{\rho J}{L^2} \int_0^L [L-x \quad x]^T [L-x \quad x] \, dx = \frac{\rho J L}{6} \begin{bmatrix} 2 & 1 \\ 1 & 2 \end{bmatrix} \quad (6.47)$$

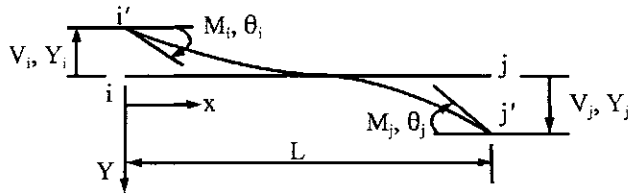


FIG. 6.5 Flexural element.

6.3.2.3. Generalized Force Matrix

For uniform torsional force, $T(x, t) = T[1 - (t/\zeta)]$, acting along the member, we have

$$\{Q_e\} = \int_0^L T(x, t) [N]^T dx = \frac{1}{L} T \left(1 - \frac{t}{\zeta}\right) \int_0^L [L - x \quad x]^T dx = T \left(1 - \frac{t}{\zeta}\right) \frac{L}{2} [1 \quad 1]^T \quad (6.48)$$

6.3.3. Flexural Member

For flexural vibration of a beam, the typical element is shown in Fig. 6.5. The generalized coordinates and forces are

$$\{Q_e\} = [Q_1 \quad Q_2 \quad Q_3 \quad Q_4]^T = [M_i \quad M_j \quad V_i \quad V_j]^T \quad (6.49)$$

$$\{q_e\} = [q_1 \quad q_2 \quad q_3 \quad q_4]^T = [\theta_i \quad \theta_j \quad Y_i \quad Y_j]^T \quad (6.50)$$

6.3.3.1. Stiffness Matrix

Displacement function is assumed to be

$$Y(x) = a_1 + a_2 x + a_3 x^2 + a_4 x^3 \quad (6.51)$$

Applying the following boundary conditions of the beam:

$$\begin{aligned} x = 0, \quad \frac{dY(0)}{dx} &= q_1; \quad Y(0) = -q_3 \\ x = L, \quad \frac{dY(L)}{dx} &= q_2; \quad Y(L) = q_4 \end{aligned}$$

to Eq. (6.51) yields

$$\begin{Bmatrix} q_1 \\ q_2 \\ q_3 \\ q_4 \end{Bmatrix} = \begin{bmatrix} 0 & 1 & 0 & 0 \\ 0 & 1 & 2L & 3L^2 \\ -1 & 0 & 0 & 0 \\ 1 & L & L^2 & L^3 \end{bmatrix} \begin{Bmatrix} a_1 \\ a_2 \\ a_3 \\ a_4 \end{Bmatrix} \quad (6.52)$$

of which the inverse gives

$$\begin{Bmatrix} a_1 \\ a_2 \\ a_3 \\ a_4 \end{Bmatrix} = \frac{1}{L^3} \begin{bmatrix} 0 & 0 & -L^3 & 0 \\ L^3 & 0 & 0 & 0 \\ -2L^2 & -L^2 & 3L & 3L \\ L & L & -2 & -2 \end{bmatrix} \begin{Bmatrix} q_1 \\ q_2 \\ q_3 \\ q_4 \end{Bmatrix} \quad (6.53)$$

Substituting Eq. (6.53) into Eq. (6.51) yields

$$Y(x) = [N_1 \ N_2 \ N_3 \ N_4][q] \quad (6.54)$$

in which the shape functions are

$$\left. \begin{aligned} N_1 &= x - \frac{2x^2}{L} + \frac{x^3}{L^2}; & N_2 &= -\frac{x^2}{L} + \frac{x^3}{L^2} \\ N_3 &= -1 + \frac{3x^2}{L^2} - \frac{2x^3}{L^3}; & N_4 &= \frac{3x^2}{L^2} - \frac{2x^3}{L^3} \end{aligned} \right\} \quad (6.55)$$

For a beam subject to bending moment, the curvature, stress, and strain are

$$Y'' = -\frac{M}{EI}; \quad \sigma = \frac{Mz}{I}; \quad \varepsilon = -Y''z \quad (6.56)$$

where z is the distance measured to any point from the neutral axis of the cross-section. Thus from Eq. (6.12), a stiffness coefficient can be obtained:

$$k_{ij} = E \int e_i e_j dv = E \int N_i'' N_j'' z^2 dv \quad (6.57)$$

For instance

$$k_{11} = E \int_0^L \int A (N_1'')^2 z^2 dA dx = EI \int_0^L \left(-\frac{4}{L} + \frac{6x}{L^2} \right)^2 dx = \frac{4EI}{L} \quad (6.58)$$

$$k_{32} = E \int_0^L \int A N_3'' N_2'' z^2 dA dx = EI \int_0^L \left(\frac{6}{L^2} - \frac{12x}{L^3} \right) \left(-\frac{2}{L} + \frac{6x}{L^2} \right) dx = -\frac{6EI}{L^2} \quad (6.59)$$

In summary, the stiffness matrix of the member is

$$[K_e] = \frac{EI}{L^3} \begin{bmatrix} 4L^2 & 2L^2 & | & -6L & -6L \\ & 4L^2 & | & -6L & -6L \\ --- & --- & | & --- & --- \\ \text{symm} & & | & 12 & 12 \\ & & & & 12 \end{bmatrix} = \begin{bmatrix} SM0 & | & SMY \\ --- & | & --- \\ \text{symm} & | & SVY \end{bmatrix} \quad (6.60)$$

in which the coefficients' array is identical to that of the dynamic stiffness shown in Eq. (4.26a,b). Therefore Eq. (6.60) also comprises the symbols $SM0$, SMY , and SVY .

6.3.3.2. Mass Matrix

Mass coefficients can be similarly obtained from Eq. (6.13). For illustration,

$$m_{11} = \int \rho(N_1)^2 dv = \rho A \int_0^L \left(x - \frac{2x^2}{L} + \frac{x^3}{L^2} \right)^2 dx = \frac{\rho AL^3}{105} \quad (6.61)$$

$$m_{32} = \int \rho N_3 N_2 dv = \rho A \int_0^L \left(-1 + \frac{3x^2}{L^2} - \frac{2x^3}{L^3} \right) \left(-\frac{x^2}{L} + \frac{x^3}{L^2} \right) dx = \frac{13}{420} \rho AL^2 \quad (6.62)$$

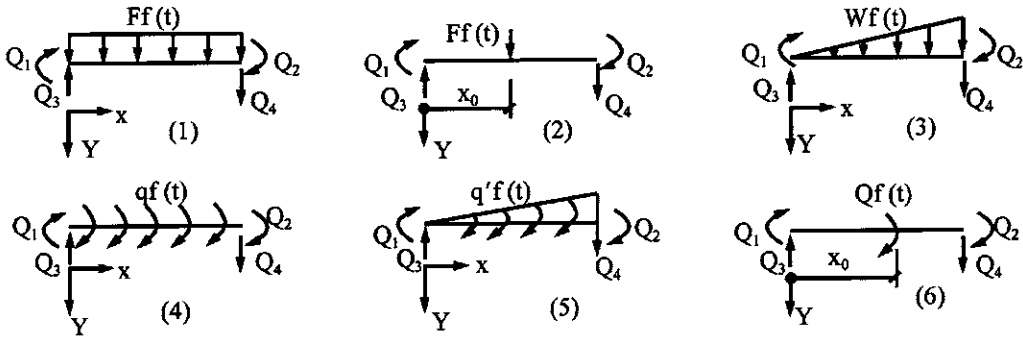


FIG. 6.6 Generalized forces of six loading cases.

The mass matrix of the beam is

$$[M_e] = \rho A L \begin{bmatrix} \frac{L^2}{105} & -\frac{L^2}{140} & | & -\frac{11L}{210} & \frac{13L}{420} \\ & \frac{L^2}{105} & | & \frac{13L}{420} & -\frac{11L}{210} \\ --- & --- & | & --- & --- \\ & & | & \frac{13}{35} & -\frac{9}{70} \\ \text{symm} & & | & & \frac{13}{35} \end{bmatrix} = \begin{bmatrix} MM0^t & | & MMY^t \\ \cdots & | & \cdots \\ \text{symm} & | & MVY^t \end{bmatrix} \quad (6.63)$$

For the sake of comparison with the Timoshenko member's mass matrix to be discussed in Sections 6.7 and 6.8, the above mass matrix is symbolically represented by $MM0^t$, MMY^t , and MVY^t . Recall that a Timoshenko beam has bending and shear deformation as well as transverse and rotatory inertia; here the superscript t signifies transverse inertia.

6.3.3.3. Generalized Force Matrix

The generalized forces of the six loading cases in Fig. 6.6 are derived and summarized in Table 6.1. For illustration, derivations of Q_1 are given in Eqs. (6.64)–(6.66) corresponding to cases 1, 2, and 4, respectively.

$$Q_1 = \int_0^L F(x, t) N_1 \, dx = \int_0^L Ff(t) \left(x - \frac{2x^2}{L} + \frac{x^3}{L^2} \right) \, dx = \frac{1}{12} FL^2 f(t) \quad (6.64)$$

$$Q_1 = F \left(x_0 - \frac{2x_0^2}{L} + \frac{x_0^3}{L^2} \right) f(t) = FL(r_0 - 2r_0^2 + r_0^3) f(t) \quad (6.65)$$

$$Q_1 = \int_0^L F(x, t) N'_1 \, dx = \int_0^L F(x, t) \left(1 - \frac{4x}{L} + \frac{3x^2}{L^2} \right) \, dx = 0 \quad (6.66)$$

In Eq. (6.65), $r_0 = x_0/L$.

EXAMPLE 6.3.1 Using the fundamental structural mechanics presented in Section 4.5, find the system matrix equation of the gable frame shown in Fig. 6.7a subjected to steady-state vibration with forcing frequency ω . Since the system matrix formulation for both the dynamic stiffness

TABLE 6.1. Equations of Generalized Forces

Cases	Q_1	Q_2	Q_3	Q_4
1	$\frac{1}{12}FL^2$	$-\frac{1}{12}FL^2$	$-\frac{1}{2}FL$	$\frac{1}{2}FL$
2	$FL(r_0 - 2r_0^2 + r_0^3)$	$-FL(r_0^2 - r_0^3)$	$-F(1 - 3r_0^2 + 2r_0^3)$	$F(3r_0^2 - 2r_0^3)$
3	$\frac{WL^2}{30}$	$-\frac{WL^2}{20}$	$-\frac{3WL}{20}$	$\frac{7WL}{20}$
4	0	0	q	q
5	$-\frac{1}{12}q'L$	$\frac{1}{12}q'L$	$\frac{1}{2}q'$	$\frac{1}{2}q'$
6	$Q(1 - 4r_0 + 3r_0^2)$	$-Q(2r_0 - 3r_0^2)$	$\frac{-6Q}{L}(-r_0 + r_0^2)$	$\frac{6Q}{L}(r_0 - r_0^2)$

Note: (1) $r_0 = x_0/L$; (2) all the coefficients should be multiplied by $f(t)$; (3) fixed-end forces should have a sign opposite to that given above.

method and the consistent mass method is similar, this example is based on the formulation procedures presented in Chapter 4 to illustrate the technique for a more complicated rigid frame than the one-story two-bay frame shown in Fig. 4.7.

Solution: The d.o.f. in rotation of the frame is determined from Eqs. (4.27b) and (4.27e) as

$$NP = 3NJ - (3NFJ + 2NHJ + NRJ + NM) = 3(5) - [3(2) + 0 + 0 + 4] = 5 \quad (a)$$

$$NPS = 2NJ - (2NFJ + 2NHJ + NRJ + NM) = 2(5) - [2(2) + 0 + 0 + 4] = 2 \quad (b)$$

Therefore, total d.o.f. is five with three in rotation ($NPR = NP - NPS$) and two in side-sway. The rotational d.o.f. are logically assigned to structural joints that can rotate; the side-sway d.o.f. must be assigned to joints which are so chosen that they can have *independent translational movement*. In other words, the displacement of any side-sway d.o.f. need not be expressed in terms of other d.o.f. The side-sway d.o.f. may be assigned to the gable frame in several ways; two possibilities are shown in Fig. 6.2b and d. For the present problem, take the case of Fig. 6.2b, for which the diagram of external action is shown Fig. 6.7b, where F 's are the possible longitudinal inertia forces associated with the displacements, U 's, of individual members due to linear rigid-body motion of the system. Internal moments and shears are numbered in Fig. 6.7c. Since no axial deformation is considered, the internal axial forces of individual members shown in Fig. 6.7d result from the equilibrium conditions at the joints.

Using notations in Section 4.5, the system matrix equation may be symbolically expressed as

$$\begin{aligned} e^{i\omega t} \begin{Bmatrix} P_\theta \\ \cdots \\ P_s \end{Bmatrix} &= \left(\begin{bmatrix} A_\theta \mid 0 \\ \cdots \\ 0 \mid A_s \end{bmatrix} [S] \begin{bmatrix} A_\theta \mid 0 \\ \cdots \\ 0 \mid A_s \end{bmatrix}^T - \omega^2 \begin{bmatrix} A_\theta \mid 0 \\ \cdots \\ 0 \mid A_s \end{bmatrix} [MS] \begin{bmatrix} A_\theta \mid 0 \\ \cdots \\ 0 \mid A_s \end{bmatrix}^T - \frac{[0]}{\omega^2 [D][ML][D]^T} \right) \\ &\quad \begin{bmatrix} X_\theta \\ \cdots \\ X_s \end{bmatrix} e^{i\omega t} \end{aligned} \quad (c)$$

for which the formulation of individual matrices is discussed below.

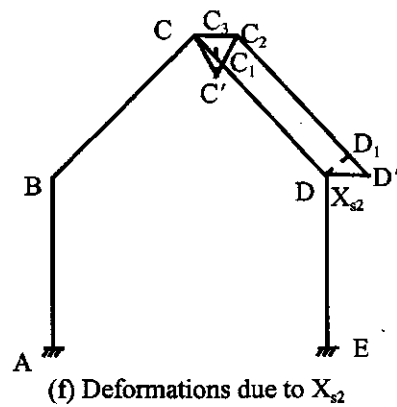
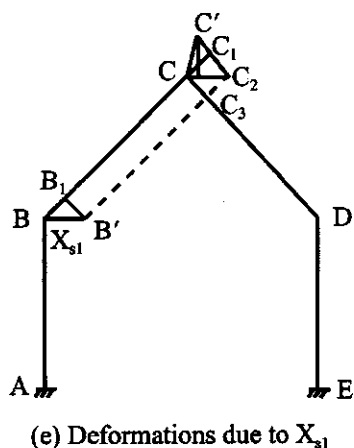
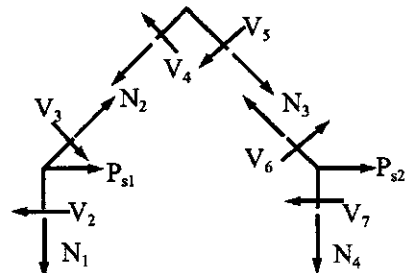
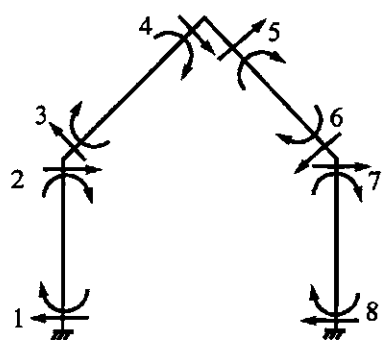
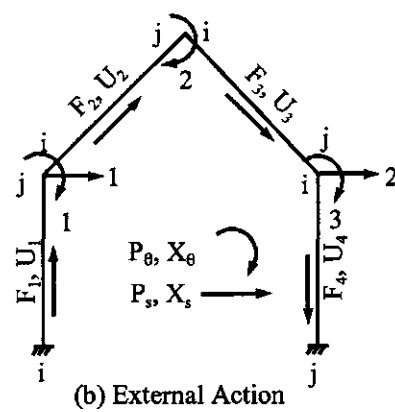
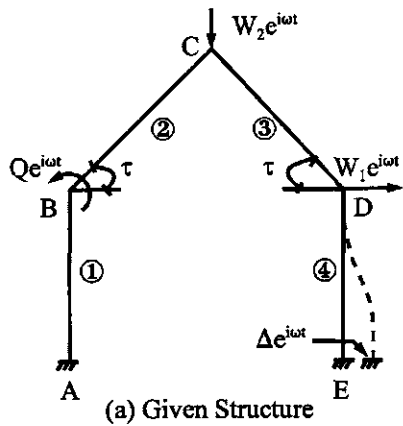


FIG. 6.7 General rigid frame. (a) Given structure. (b) External action. (c) Internal resistance. (d) Free-body diagram. (e) Deformation due to X_{s1} . (f) Deformation due to X_{s2} .

- $[A_\theta]$ is the equilibrium matrix of moments for the relationship between $\{P_\theta\}$ and $\{M\}$. From Fig. 6.7b and c, we obtain

$$[A_\theta] = \begin{bmatrix} 0 & 1 & 1 & 0 & 0 & 0 & 0 & 0 \\ 0 & 0 & 0 & 1 & 1 & 0 & 0 & 0 \\ 0 & 0 & 0 & 0 & 0 & 1 & 1 & 0 \end{bmatrix}_{NPR \times 2NM} \quad (d)$$

- $[S]$ is the stiffness coefficient matrix, which is arranged using the notations in Eq. (6.60) as follows:

$$[S] = \begin{bmatrix} \begin{bmatrix} \backslash & SM0 & \backslash \\ & & \backslash \end{bmatrix} & \begin{bmatrix} \backslash & SMY & \backslash \\ & & \backslash \end{bmatrix} \\ \text{symm} & \begin{bmatrix} \backslash & SVY & \backslash \\ & & \backslash \end{bmatrix} \end{bmatrix}_{2NM \times 2NM} \quad (e)$$

in which the submatrices are diagonal band matrices; NM equals the number of members.

- $[MS]$ is the mass coefficient matrix composed of individual members' coefficients given in Eq. (6.63)

$$[MS] = \begin{bmatrix} \begin{bmatrix} \backslash & MM0^t & \backslash \\ & & \backslash \end{bmatrix} & \begin{bmatrix} \backslash & MMY^t & \backslash \\ & & \backslash \end{bmatrix} \\ \text{symm} & \begin{bmatrix} \backslash & MVY^t & \backslash \\ & & \backslash \end{bmatrix} \end{bmatrix}_{2NM \times 2NM} \quad (f)$$

in which the submatrices are arranged like those shown in Eq. (e).

- $[A_s]$ is the equilibrium matrix of shears for the relationship between $\{P_s\}$ and $\{V\}$, as $\{P_s\} = [A_s]\{V\}$. In order to achieve the equilibrium of lateral force at a structural joint, note that the axial forces, $\{N\}$, are not independent and therefore must first be expressed in terms of the independent shears, $\{V\}$, which are then related to $\{P_s\}$. Consider the free-body diagram of joint C shown in Fig. 6.7d; $\Sigma F_x = 0$ gives

$$N_2 \cos \tau + V_4 \sin \tau + V_5 \sin \tau - N_3 \cos \tau = 0 \quad (g)$$

and $\Sigma F_y = 0$ yields

$$N_2 \sin \tau - V_4 \cos \tau + V_5 \cos \tau + N_3 \sin \tau = 0 \quad (h)$$

From Eqs. (g) and (h)

$$N_2 = V_4 \cot \tau - \frac{V_4 \sec \tau \csc \tau}{2} - V_5 \cot \tau + \frac{V_5 \cos 2\tau \csc \tau \sec \tau}{2} \quad (i)$$

$$N_3 = \frac{V_4 \csc \tau \sec \tau}{2} - \frac{V_5 \cos 2\tau \csc \tau \sec \tau}{2} \quad (j)$$

Thus the equilibrium conditions at joints *B* and *D* give

$$[A_s] = \begin{bmatrix} 0 & 1 & -\sin \tau & \frac{-\cos 2\tau \csc \tau}{2} & \frac{\csc \tau}{2} & 0 & 0 & 0 \\ 0 & 0 & 0 & \frac{\csc \tau}{2} & \frac{-\cos 2\tau \csc \tau}{2} & -\sin \tau & 1 & 0 \end{bmatrix}_{NPS \times 2NM} \quad (k)$$

- $[D]$ is the *inertia force matrix* for the relationship between nodal forces, $\{P_s\}$, and inertia forces, $\{F\}$, as $\{P_s\} = [D]\{F\}$. From Figs. 6.7b, e, and f we have $BB_1 = U_2 = X_{s1} \cos \tau$ and $D_1 D' = U_3 = X_{s2} \cos \tau$; thus

$$[D] = \begin{bmatrix} 0 & \cos \tau & 0 & 0 \\ 0 & 0 & \cos \tau & 0 \end{bmatrix}_{NPS \times NM} \quad (l)$$

- $[ML]$ is the mass matrix with diagonal elements, $m_i L_i$, to express inertia forces, $\{F\}$, in terms of longitudinal displacements, $\{U\}$, as $\{F\} = -\omega^2 [ML] \{U\}$; and $\{U\} = [D]^T \{X_s\}$. The positive direction of $\{F\}$ and $\{U\}$ is sketched in Fig. 6.7b.
- The external load matrix should be composed of applied loads and fixed-end forces. For the present problem

$$\begin{Bmatrix} P_\theta \\ P_s \end{Bmatrix} e^{i\omega t} = \begin{Bmatrix} -Q \\ 0 \\ -SMY_{24}\Delta - MMY_{24}^t\Delta \\ -\frac{1}{2}W_2 \cot \tau \\ W_1 + \frac{1}{2}W_2 \cot \tau - SVY_{24}\Delta - MVY_{24}^t\Delta \end{Bmatrix}_{NP \times LC} e^{i\omega t} \quad (m)$$

where *LC* signifies number of loading condition (see Example 4.8.1; here *LC* = 1); the fixed-end forces are due to the foundation movement at the member's *j*-end, for which the sign is negative. The generalized force vector due to the nodal force, W_2 , can be obtained by using the virtual work as

$$P_{s1} X_{s1} = -W_2 C'_3 C_3 \text{ (see Fig. 6.7e)} = -\frac{1}{2} W_2 X_{s1} \cot \tau \quad (n)$$

$$P_{s2} X_{s2} = W_2 C_3 C' \text{ (see Fig. 6.7f)} = \frac{1}{2} W_2 X_{s2} \cot \tau \quad (o)$$

Note that the procedures presented here are general and can be applied to various types of rigid frames such as continuous gable frames, towers, and vierendeel trusses. Readers are urged to learn how to formulate the compatibility matrices (i.e. $[A_s]^T$ and $[D]^T$) in the example in order to fully understand the kinematics (see Sections 4.5.3 and 4.5.4).

EXAMPLE 6.3.2 Based on the consistent mass method, find the displacements and internal forces of the beam shown in Fig. 6.8 subjected to a harmonic force $F(x, t) = W \cos \omega t$. Use the analytical techniques of (A) steady-state vibration and (B) modal matrix. Check the equilibrium condition of the solution. Let $L = 12 \text{ ft}$, $I = 13,824 \text{ in}^4$, $E = 30,000 \text{ ksi}$, $\gamma = 490 \text{ lb}/\text{ft}^3$, $A = 288 \text{ in}^2$, $W = 500 \text{ k/ft}$, and $\omega = 150 \text{ rad/sec}$.

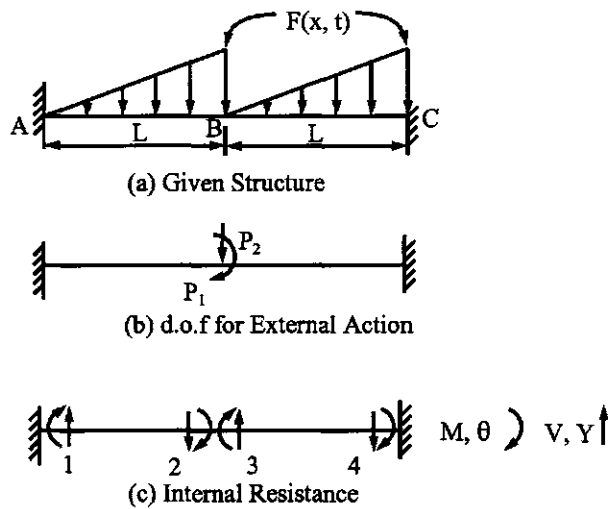


FIG. 6.8 Example 6.3.2. (a) Given structure. (b) d.o.f. for external action. (c) Internal resistance M , $\theta \not\propto V$, $Y \downarrow$.

Solution: Based on the diagrams given in Figs. 6.8b and c, the equilibrium matrices, $[A_\theta]$ and $[A_s]$, structural stiffness matrix, $[K]$, and mass matrix, $[M]$, are formulated as

$$[A_\theta] = [0 \quad 1 \quad 1 \quad 0]; \quad [A_s] = [0 \quad 1 \quad -1 \quad 0] \quad (a)$$

$$[S] = \frac{EI}{L} \begin{bmatrix} \begin{bmatrix} 4 & 2 & 0 & 0 \\ 4 & 0 & 0 & 0 \\ 4 & 2 & 4 & 0 \\ \text{symm} & & & \end{bmatrix} & \begin{bmatrix} -6/L & -6/L & 0 & 0 \\ -6/L & -6/L & 0 & 0 \\ -6/L & -6/L & -6/L & -6/L \\ \text{symm} & & & \end{bmatrix} \\ \begin{bmatrix} 12/L^2 & 12/L^2 & 0 & 0 \\ 12/L^2 & 12/L^2 & 0 & 0 \\ 12/L^2 & 12/L^2 & 12/L^2 & 12/L^2 \\ \text{symm} & & & \end{bmatrix} & \end{bmatrix} \quad (b)$$

$$[MS] = \rho AL \begin{bmatrix} \begin{bmatrix} L^2/105 & -L^2/140 & 0 & 0 \\ L^2/105 & L^2/105 & 0 & 0 \\ L^2/105 & L^2/105 & -L^2/140 & L^2/105 \\ \text{symm} & & & \end{bmatrix} & \begin{bmatrix} -11L/210 & 13L/420 & 0 & 0 \\ 13L/420 & -11L/210 & 0 & 0 \\ -11L/210 & -11L/210 & 13L/420 & -11L/210 \\ \text{symm} & & & \end{bmatrix} \\ \begin{bmatrix} 13/35 & -9/70 & 0 & 0 \\ 13/35 & 13/35 & 0 & 0 \\ 13/35 & 13/35 & -9/70 & 13/35 \\ \text{symm} & & & \end{bmatrix} & \end{bmatrix} \quad (c)$$

$$[K] = \begin{bmatrix} \frac{8EI}{L} & 0 \\ 0 & \frac{24EI}{L^3} \end{bmatrix} = \begin{bmatrix} 1920000 & 0 \\ 0 & 40000 \end{bmatrix} \quad (d)$$

$$[M] = \begin{bmatrix} \frac{2mL^3}{105} & 0 \\ 0 & \frac{26mL}{35} \end{bmatrix} = \begin{bmatrix} 1.0017 & 0 \\ 0 & 0.2713 \end{bmatrix} \quad (e)$$

The eigenvalues and eigenvectors are obtained as

$$p_1 = 383.97 \text{ rad/sec}; \quad p_2 = 1384.48 \text{ rad/sec} \quad (f)$$

$$[X] = \begin{bmatrix} 0 & 1 \\ 1 & 0 \end{bmatrix} \quad (g)$$

For the given load, we find the generalized forces for one member from Table 6.1 of Case 3 as

$$\begin{Bmatrix} Q_1 \\ Q_2 \\ Q_3 \\ Q_4 \end{Bmatrix} = \begin{Bmatrix} \frac{L}{30} \\ -\frac{L}{20} \\ -\frac{3}{20} \\ \frac{7}{20} \end{Bmatrix} WL \cos \omega t = \begin{Bmatrix} 2400 \text{ ft k} \\ -3600 \text{ ft k} \\ -900 \text{ k} \\ 2100 \text{ k} \end{Bmatrix} \cos \omega t \quad (h)$$

Change the above into fixed-end forces

$$\{F_0\} = -\{Q\} \quad (i)$$

as shown in Fig. 6.9.

The load matrix is

$$\begin{Bmatrix} P_1 \\ P_2 \end{Bmatrix} = \begin{Bmatrix} -1200 \\ 3000 \end{Bmatrix} \cos \omega t \quad (j)$$

(A) *Steady-state vibrational analysis*—substituting Eqs. (d), (e), (j) and the given forcing frequency into the following system matrix equation,

$$([K] - \omega^2[M])\{X\} \cos \omega t = \{P\} \cos \omega t \quad (k)$$

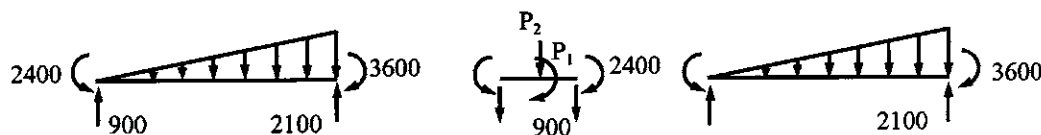


FIG. 6.9 Fixed-end forces.

and then performing inversion yields

$$\{X\} = ([K] - \omega^2[M])^{-1}\{P\} = \begin{Bmatrix} -6.324(10^{-4}) \text{ rad} \\ 0.0885 \text{ ft} \end{Bmatrix} \quad (l)$$

To calculate internal forces, we may conclude from the dynamic stiffness solutions presented in Chapters 4 and 5 that these forces stem from three sources: strain energy associated with stiffness, kinetic energy resulting from inertia force, and generalized force corresponding to fixed-end force (F.E.F.). Internal forces can be expressed as

$$\begin{Bmatrix} M \\ V \end{Bmatrix} = [S] \begin{Bmatrix} A_\theta & | & 0 \\ 0 & | & A_s \end{Bmatrix}^T \begin{Bmatrix} X_\theta \\ X_s \end{Bmatrix} \cos \omega t - \omega^2 [MS] \begin{Bmatrix} X_\theta \\ X_s \end{Bmatrix} \cos \omega t \pm \{\text{F.E.F.}\} \quad (m)$$

in which the first and second term on the right-hand side pertain to strain and kinetic energy, respectively. Consider the maximum response; let $\cos \omega t = 1$, where $\omega = 150 \text{ rad/sec}$ and $t = 0.0419 \text{ sec}$. Substituting stiffness and mass coefficients as well as fixed-end forces into Eq. (m) yields the following internal forces:

$$\begin{Bmatrix} M_1 \\ M_2 \\ M_3 \\ M_4 \\ V_1 \\ V_2 \\ V_3 \\ V_4 \end{Bmatrix} = \underbrace{\begin{Bmatrix} -10,923.56 \\ -11,227.13 \\ 10,012.87 \\ 1316.44 \\ 1845.89 \\ 1845.89 \\ -1694.11 \\ -1694.11 \end{Bmatrix}}_{\text{due to stiffness}} - \underbrace{\begin{Bmatrix} 275.46 \\ -464.26 \\ 450.00 \\ -264.77 \\ -95.43 \\ 273.35 \\ -266.85 \\ 91.57 \end{Bmatrix}}_{\text{due to inertia force}} + \underbrace{\begin{Bmatrix} -2400 \\ 3600 \\ -2400 \\ 3600 \\ 900 \\ -2100 \\ 900 \\ -2100 \end{Bmatrix}}_{\text{F.E.F.}} = \begin{Bmatrix} -13599.02 \text{ ft k} \\ -7162.87 \text{ ft k} \\ 7162.87 \text{ ft k} \\ 14181.21 \text{ ft k} \\ 2841.32 \text{ k} \\ -527.46 \text{ k} \\ -527.46 \text{ k} \\ -3885.68 \text{ k} \end{Bmatrix} \quad (n)$$

The resulting forces in Eq. (n) are shown in Fig. 6.10, for which the equilibrium conditions of $\sum M = 0$ and $\sum F_y = 0$ at B are apparently satisfied.

The deformations of member AB given in Eq. (l) are sketched in Fig. 6.11a for which the elastic curves due to deflection and rotation are shown in Figs. 6.11b and c, respectively. The displacement functions, Y 's, are represented by N_2 and N_4 which are given in Eq. (6.55). Since total displacement at any time, t , is

$$y(x, t) = Y(x)g(t) \quad (o)$$

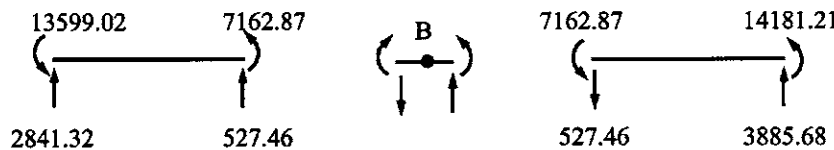


FIG. 6.10 Internal forces.

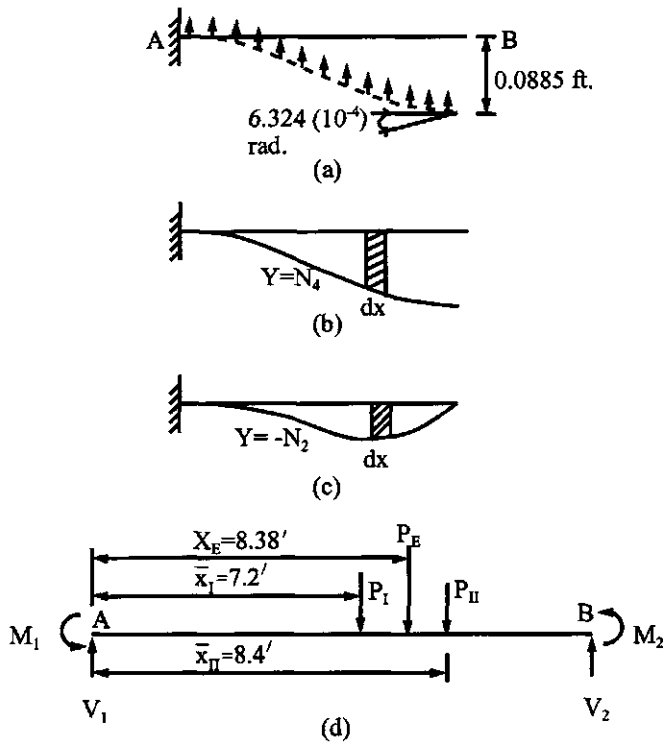


FIG. 6.11 Elastic curves and forces.

where $Y(x) = \sum N_i q_i$ and $g(t) = \cos \omega t$, the acceleration becomes

$$\ddot{y}(x, t) = \ddot{g}(t) Y(x) = -\omega^2 \cos \omega t [0.0885(N_4) - (6.3244)10^{-4}(N_2)] \quad (p)$$

The total inertia force of the member can be obtained by substituting Eq. (p) into the following equation:

$$P_E = \int_0^L \ddot{y}(x, t) \rho A \, dx \quad (q)$$

and then integrating. The inertia forces, P_I and P_{II} , associated with the deflection and rotation, respectively, are obtained as

$$P_E = P_I + P_{II} = (-363.622 - 5.197) \cos \omega t = -368.819 \cos \omega t \quad (r)$$

The centroids of the forces are

$$\left. \begin{aligned} X_E &= \frac{\int \ddot{y}(x)x \, dx}{\int \ddot{y} \, dx} = \frac{\int Y(x)x \, dx}{\int Y(x) \, dx} = \frac{4.515}{0.5386} = 8.38 \text{ ft} \\ \bar{X}_I &= \frac{\int x dA}{A} = \frac{\int x(-N_2) \, dx}{\int -N_2 \, dx} = \frac{86.4}{12} = 7.2 \text{ ft} \\ \bar{X}_{II} &= \frac{\int x(N_4) \, dx}{\int N_4 \, dx} = \frac{50.4}{6} = 8.4 \text{ ft} \end{aligned} \right\} \quad (s)$$

where $Y(x)$ is from Eq. (p). Note that the magnitude of slope and deflection at B of the elastic curve is not included because it will cancel itself as both numerator and denominator in the equations. Equilibrium conditions of the member are:

$$\Sigma F_y = 0$$

$$\begin{aligned} 2841.32 + 527.56 - 3000 - 363.622 - 5.197 \\ = 3368.78 - 3368.819 = -0.039 \end{aligned} \quad (\text{t})$$

$$\Sigma M = 0 \text{ about } A$$

$$\begin{aligned} 13599.02 + 7162.870 + 527.46(12) \\ - 3000(8) + 363.622(8.4) + 5.197(7.2) \\ = 27091.41 - 27091.84 = -0.43 \end{aligned} \quad (\text{u})$$

For $\cos \omega t = -1$, where $\omega = 150 \text{ rad/sec}$ at $t = 0.0209 \text{ sec}$, the displacements and internal forces are the same as those in Eqs. (l) and (n), respectively, except that the sign is opposite.

(B) *Modal matrix analysis*—from Eqs. (2.49) and (2.50), the displacement response is

$$\{x\} = [\Phi]\{x'\} = [\Phi] \int_0^t \begin{bmatrix} \sqrt{p(t-\Delta)} \\ 0 \\ \sqrt{p} \end{bmatrix} \begin{bmatrix} \sqrt{p} & 0 \\ 0 & \sqrt{p} \end{bmatrix}^{-1} [\Phi]^T \{F(\Delta)\} d\Delta \quad (\text{v})$$

For the given problem

$$[\Phi] = \begin{bmatrix} 0 & 0.9991 \\ 1.9199 & 0 \end{bmatrix} \quad (\text{w})$$

$$\{x'\} = \int_0^t \begin{bmatrix} \sin p_1(t-\Delta) & 0 \\ 0 & \sin p_2(t-\Delta) \end{bmatrix} \begin{bmatrix} 383.97 & 0 \\ 0 & 1384.48 \end{bmatrix}^{-1} \begin{Bmatrix} 5759.70 \\ -1198.98 \end{Bmatrix} \cos \omega \Delta d\Delta \quad (\text{x})$$

Consider $\cos \omega t = -1$; then $t = \Delta = 0.0209 \text{ sec}$. Thus

$$\{x'\} = \begin{Bmatrix} -0.03749 \\ 1.57983 \times 10^{-4} \end{Bmatrix} \quad (\text{y})$$

and

$$\{x\} = [\Phi]\{x'\} = \begin{Bmatrix} 1.57841 \times 10^{-4} \text{ rad} \\ -0.071981 \text{ ft} \end{Bmatrix} \quad (\text{z})$$

From Eq. (2.51), we may calculate accelerations at $\Delta = 0.0209 \text{ sec}$ as

$$\begin{aligned} \{\ddot{x}\} &= [\Phi][\Phi]^T\{F(\Delta)\} - [\Phi] \begin{bmatrix} \sqrt{p} & 0 \\ 0 & \sqrt{p^2} \end{bmatrix} [\Phi]^T \{M\}\{x\} \\ &= \begin{Bmatrix} 1197.872 \\ -11058.0 \end{Bmatrix} - \begin{Bmatrix} 302.547 \\ -10612.5 \end{Bmatrix} = \begin{Bmatrix} 895.325 \\ -445.5 \end{Bmatrix} \end{aligned} \quad (\text{aa})$$

The final forces at the members' ends due to strain energy, kinetic energy, and fixed-end forces can be calculated from

$$\begin{Bmatrix} M \\ \dots \\ V \end{Bmatrix} = [S] \begin{bmatrix} A_\theta & | & 0 \\ \dots & | & \dots \\ 0 & | & A_s \end{bmatrix}^T \begin{Bmatrix} X_\theta \\ \dots \\ X_s \end{Bmatrix} + [MS] \begin{bmatrix} A_\theta & | & 0 \\ \dots & | & \dots \\ 0 & | & A_s \end{bmatrix}^T \begin{Bmatrix} \ddot{x}_\theta \\ \dots \\ \ddot{x}_s \end{Bmatrix} \pm \{\text{F.E.F.}\} \quad (\text{bb})$$

Substituting Eqs. (a), (b), (e), (h), (z) and (aa) into above yields numerical values as follows:

$$\begin{Bmatrix} M_1 \\ M_2 \\ M_3 \\ M_4 \\ V_1 \\ V_2 \\ V_3 \\ V_4 \end{Bmatrix} = \underbrace{\begin{Bmatrix} 8713.49 \\ 8789.29 \\ -8486.17 \\ -8562.00 \\ -1458.56 \\ -1458.56 \\ 1420.68 \\ 1420.68 \end{Bmatrix}}_{\text{due to stiffness}} + \underbrace{\begin{Bmatrix} -396.76 \\ 550.71 \\ 346.17 \\ -275.90 \\ 142.37 \\ -265.94 \\ -145.18 \\ 100.53 \end{Bmatrix}}_{\text{due to inertia force}} + \underbrace{\begin{Bmatrix} 2400 \\ -3600 \\ 2400 \\ -3600 \\ -900 \\ 2100 \\ -900 \\ 2100 \end{Bmatrix}}_{\text{F.E.F.}} = \begin{Bmatrix} -10716.73 \text{ ft k} \\ 5740.00 \text{ ft k} \\ -5740.00 \text{ ft k} \\ -12437.90 \text{ ft k} \\ -2216.19 \text{ k} \\ 375.50 \text{ k} \\ 375.50 \text{ k} \\ 3621.21 \text{ k} \end{Bmatrix} \quad (\text{cc})$$

The inertia forces at $t = 0.0209$ sec are

$$\begin{aligned} P_E &= \int_0^L \ddot{y}(x, t) \rho A \, dx = P_I + P_{II} \\ &= \int_0^L (-895.325) N_2 \rho A \, dx + \int_0^L (445.5) N_4 \rho A \, dx \\ &= 326.99 + 81.38 = 408.37 \text{ k} \end{aligned} \quad (\text{dd})$$

The centroid of P_E is

$$X_E = \frac{\int [(-895.325)N_2 + (445.5)N_4]x \, dx}{\int [(-895.325)N_2 + (445.5)N_4] \, dx} = \frac{99819.036}{13418.082} = 7.439 \text{ ft} \quad (\text{ee})$$

All the final forces are shown in Fig. 6.12; the centroids of P_I and P_{II} are the same as those obtained previously, from which the equilibrium conditions of member AB give

$$\begin{aligned} \Sigma F_y &= 0 \\ 2216.19 + 375.5 + 326.99 + 81.38 - 3000 &= 0 \\ 3000.06 - 3000 &= 0.06 \end{aligned} \quad (\text{ff})$$

$$\Sigma M = 0 \text{ about } A$$

$$\begin{aligned} 10716.73 + 5740.0 + 81.38(8.4) + 375.5(12) + 326.99(7.2) - 3000(8) \\ = 24000.65 - 24000 = 0.65 \end{aligned} \quad (\text{gg})$$

Note that there is some difference between the solutions resulting from the steady-state analysis of (A) and those from the modal matrix analysis of (B). This is because the modal matrix approach is based on Duhamel's integral, which yields a transient response comprising both (1) the initial response due to the application of the harmonic force and (2) the response of

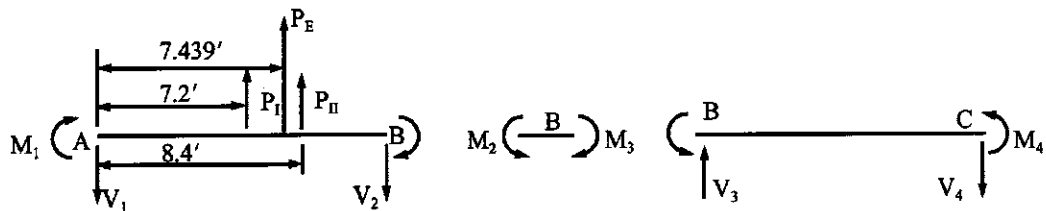


FIG. 6.12 Final forces of Case B.

the forced vibration. However, the steady-state analysis only yields the response of the forced vibration. As stated in Section 1.4.1, the initial response due to application of force will diminish during the first few cycles of vibration when damping is considered.

Note also that the stress at a member's cross-section, according to the consistent mass analysis, should stem from three components: deformation, fixed forces combined with externally applied load, and inertia force. It is easy to include all three components in calculating displacements and internal forces, but difficult to include inertia force in calculating stress. This is because the complicated procedures shown in Example 6.3.2 must be used to determine the concentrated inertia force and its location and then to find the moment at a given cross-section. To avoid complication and still achieve reasonable accuracy, we may divide a member into numerous elements and then calculate the stress on the basis of deformation only.

6.4. EIGENVALUE COMPARISONS AMONG LUMPED MASS, DYNAMIC STIFFNESS AND CONSISTENT MASS METHODS

Three models of lumped mass (Chapters 2 and 3), dynamic stiffness (Chapters 4 and 5), and consistent mass (presented earlier in this chapter) are now applied to typical frameworks for eigenvalue comparison. Let us consider bending deformation only and find natural frequencies of the one-bay one-story framework shown in Fig. 6.13a by using (A) the lumped mass method, (B) the consistent mass method, and (C) the dynamic stiffness method. For (A) and (B) the structural members are divided into three, six and nine elements, respectively, and the masses of (A) are lumped at the center of the divided segments. Dynamic stiffness, lumped mass, and consistent mass models are shown in Fig. 6.13b, c, and d, respectively. Assume that all members are identical with $m = 0.04837 \text{ kg s}^2/\text{m}^2$, $I = 0.00286 \text{ cm}^4$, $E = 20,684.27 \text{ kN/cm}^2$, and $L = 0.2413 \text{ m}$.

Eigenvalues of the first three modes are shown in Table 6.2 for comparison with the accurate solution by the dynamic stiffness method. Observation of the solutions reveals that the lumped mass method needs six elements for the first two modes and nine for the third mode, while the consistent mass method needs three elements for the first mode and six for the second and third modes. The lumped mass model can give eigenvalues higher or lower than the dynamic stiffness's solution depending on how much mass is lumped at each node of the structure. The consistent mass model always gives frequencies higher than the dynamic stiffness.

The consistent mass and dynamic stiffness methods are further compared through eigenvalues of a typical one-bay three-story rigid frame shown in Fig. 6.14a. Assume that all the members are identical with $A = 1.5483 \cdot 10^{-2} \text{ m}^2$, $I = 3.99582 \cdot 10^{-5} \text{ m}^4$, $E = 20,684.27 \text{ kN/cm}^2$, and $\gamma = 7849.045 \text{ kg/m}^3$. Consider the nine structural members as nine elements for both methods.

Let the slenderness ratio of the individual members be L/R . Then changing L/R by increasing the member length but not changing its cross-sectional area, we can find the natural angular frequencies corresponding to the various values of L/R as shown in Table 6.3.

Comparison of the results shows that, for the first three modes with the same number of elements, consistent mass and dynamic stiffness give similar solutions. Consistent mass yields higher values than dynamic stiffness in the fourth mode (i.e. about 12% higher). Variation of

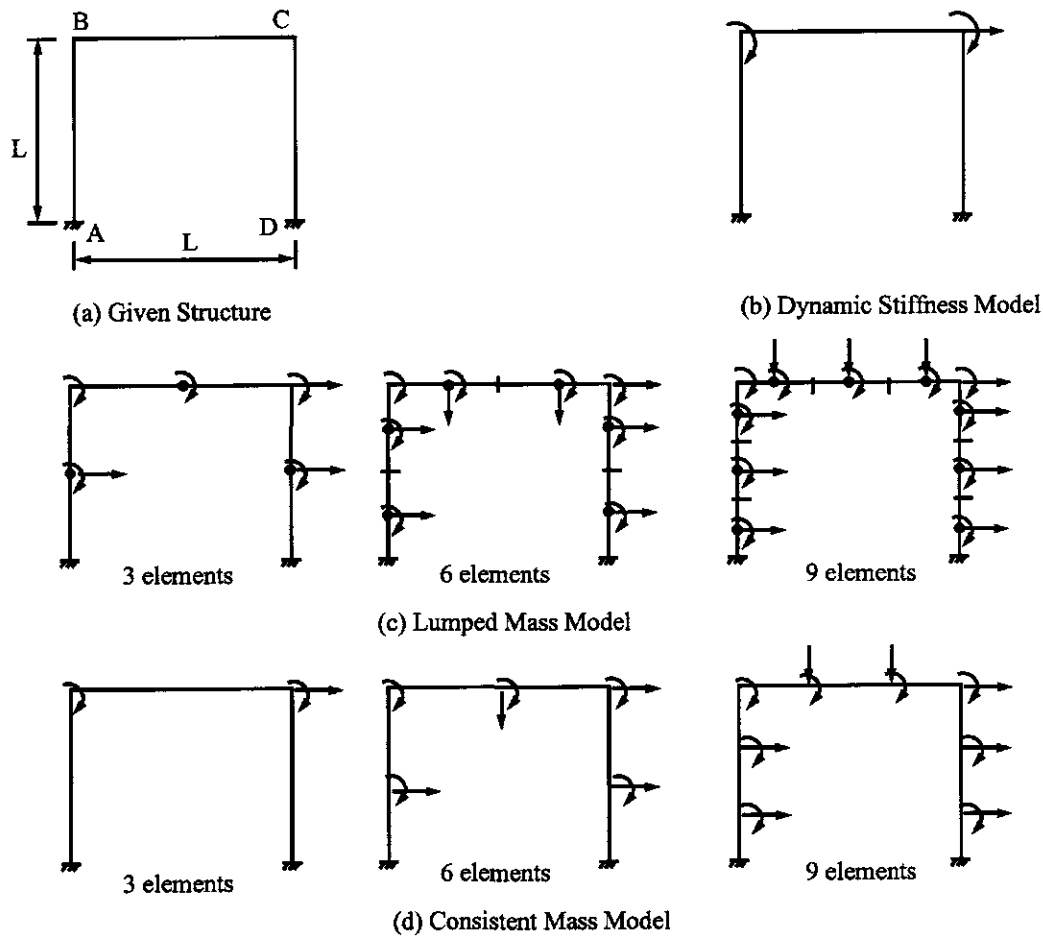


FIG. 6.13 Modeling for three analysis methods. (a) Given structure. (b) Dynamic stiffness model (c) Lumped mass model (d) Consistent mass model.

TABLE 6.2. Comparison of Eigenvalues by Lumped Mass, Consistent Mass and Dynamic Stiffness

Methods	Number of elements	First mode (rad/sec)	Second mode (rad/sec)	Third mode (rad/sec)
Lumped mass	3	210.5	531.2	840.0
	6	195.8	762.5	1323.6
	9	194.5	765.7	1265.0
Consistent mass	3	194.5	891.7	1988.6
	6	194.3	771.7	1264.9
	9	194.3	767.8	1254.2
Dynamic stiffness	3	194.3	766.8	1250.7

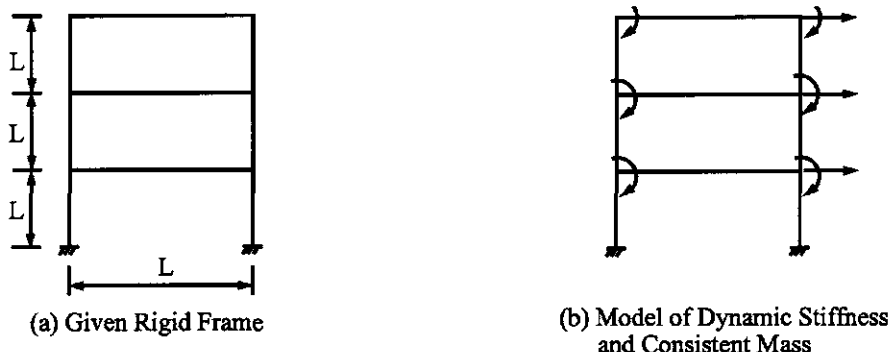


FIG. 6.14 Rigid frame model. (a) Given rigid frame. (b) Model of dynamic stiffness and consistent mass.

TABLE 6.3. Comparison of Eigenvalues by Consistent Mass and Dynamic Stiffness

Cases	<i>L/R</i>	First mode (rad/sec)	Second mode (rad/sec)	Third mode (rad/sec)	Fourth mode (rad/sec)
Consistent mass	40	60.1	199.2	359.2	732.1
	80	15.0	49.8	89.8	183.0
	120	6.7	22.1	39.9	81.3
Dynamic stiffness	40	60.1	199.0	358.4	653.8
	80	15.0	49.7	89.6	163.4
	120	6.7	22.1	39.8	72.6

slenderness ratio does not affect the consistency of the comparison. Note that, for the structure having more members than the one-story one-bay frame (see Fig. 6.14), the consistent mass method does not need to divide the constituent members into segments to yield an accurate solution. Also note that smaller frequencies are with larger slenderness ratios because of smaller flexural rigidity.

The consistent mass model does not yield accurate solutions for higher modes because the shape functions, which are based on four generalized coordinates in deriving the mass and stiffness coefficients of a typical member, cannot be flexible enough to represent the deformed shape of higher modes. Consequently, the rigidity resulting from modeling can give greater value of frequencies as observed in the fourth mode. For the same reason, the lumped mass method also yields larger rigidity in structural modeling.

PART B ADVANCED TOPICS

6.5. STIFFNESS, MASS AND GENERALIZED FORCE MATRICES FOR FINITE ELEMENTS

A flat plate may be subjected to in-plane or out-of-plane forces. It should therefore be modeled either as an in-plane or a bending element. The stress-strain relationship of an element can be plane stress or plane strain. *Plane stress* is a condition that prevails in a plate in its plane ($x-y$ plane), loaded only in the plane without any restraint in the z -direction perpendicular to the $x-y$ plane. *Plane strain* means the deformation in z -direction is zero and the deformation

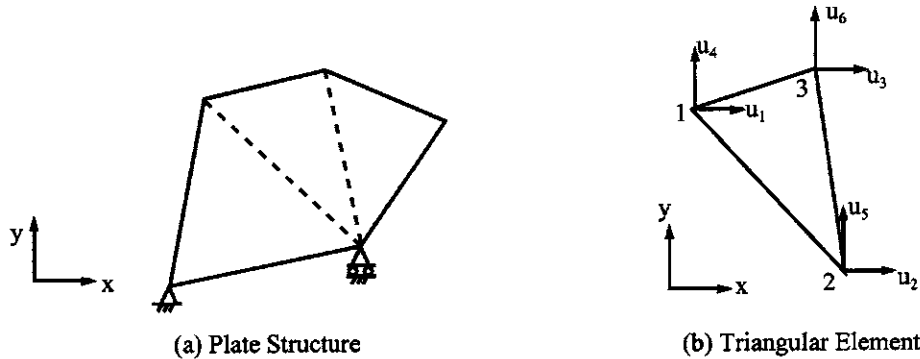


FIG. 6.15 Triangular element modeling. (a) Plate structure. (b) Triangular element.

in its plane ($x-y$) is a function of x and y but not of z . Plane strain is usually applied to the member for which the geometry and loading do not vary significantly in the longitudinal direction (z -direction) such as strip footings, cylinders, tunnels, walls, and dams. Material presented here is confined to in-plane elements for both plane stress and plane strain.

A plate subjected to in-plane or out-of-plane force can be modeled as a triangular, rectangular, or quadrilateral element. Triangular and quadrilateral elements can effectively represent various geometric configurations of a physical problem.

Finite element formulation and calculation can be based on *generalized coordinates* or *natural coordinates*. The generalized coordinate is fundamental and provides the basis of understanding the finite element formulation. The natural coordinate finite element, commonly called the *isoparametric element*, is more effective in practical analysis. As introductory material, this discussion includes only the triangular element for generalized coordinates and the quadrilateral for natural coordinates. Standard texts on finite elements are available for further study.

6.5.1. Finite Element Formulation—Generalized Coordinates

A plate structure shown in Fig. 6.15a is discretized into three triangular elements. Let a typical triangular element, as shown in Fig. 6.15b, have the following generalized forces and coordinates

$$\{Q_e\} = [Q_1 \ Q_2 \ Q_3 \ Q_4 \ Q_5 \ Q_6]^T = [F_1 \ F_2 \ F_3 \ F_4 \ F_5 \ F_6]^T \quad (6.67)$$

$$\{q_e\} = [q_1 \ q_2 \ q_3 \ q_4 \ q_5 \ q_6]^T = [u_1 \ u_2 \ u_3 \ u_4 \ u_5 \ u_6]^T \quad (6.68)$$

Displacement function of the element is

$$u_x = a_1 + a_2x + a_3y \quad (6.69)$$

$$u_y = a_4 + a_5x + a_6y \quad (6.70)$$

The displacement function selected is general because it satisfies the basic requirements of finite element formulation: the number of constants is equal to the number of coordinates; the function allows the element to have rigid-body motion; and the element displacements are not dependent on the orientation of the coordinate axes.

Displacements at the element's nodes may be expressed as

$$\begin{Bmatrix} u_1 \\ u_2 \\ u_3 \\ u_4 \\ u_5 \\ u_6 \end{Bmatrix} = \begin{bmatrix} 1 & x_1 & y_1 & 0 & 0 & 0 \\ 1 & x_2 & y_2 & 0 & 0 & 0 \\ 1 & x_3 & y_3 & 0 & 0 & 0 \\ 0 & 0 & 0 & 1 & x_1 & y_1 \\ 0 & 0 & 0 & 1 & x_2 & y_2 \\ 0 & 0 & 0 & 1 & x_3 & Y_3 \end{bmatrix} \begin{Bmatrix} a_1 \\ a_2 \\ a_3 \\ a_4 \\ a_5 \\ a_6 \end{Bmatrix} \quad (6.71)$$

and in symbolic form

$$\{u\} = [c]\{a\} = \begin{bmatrix} c_1 & | & 0 \\ \cdots & | & \cdots \\ 0 & | & c_1 \end{bmatrix} \{a\} \quad (6.72)$$

from which

$$\{a\} = [c]^{-1}\{u\} \quad (6.73)$$

The determinant of submatrix $[c_1]$ is

$$|c_1| = \begin{vmatrix} 1 & x_1 & y_1 \\ 1 & x_2 & y_2 \\ 1 & x_3 & y_3 \end{vmatrix} = (x_2 - x_3)(y_3 - y_1) - (x_3 - x_1)(y_2 - y_3) = x_{23}y_{31} - x_{31}y_{23} = 2A \quad (6.74)$$

in which

$$x_{ij} = x_i - x_j; \quad y_{ij} = y_i - y_j \quad (6.75)$$

and A = area of the triangular element. Thus

$$[c_1]^{-1} = \begin{bmatrix} 1 & x_1 & y_1 \\ 1 & x_2 & y_2 \\ 1 & x_3 & y_3 \end{bmatrix}^{-1} = \frac{1}{2A} \begin{bmatrix} x_2y_3 - x_3y_2 & x_3y_1 - x_1y_3 & x_1y_2 - x_2y_1 \\ y_2 - y_3 & y_3 - y_1 & y_1 - y_2 \\ x_3 - x_2 & x_1 - x_3 & x_2 - x_1 \end{bmatrix} \quad (6.76)$$

and

$$[c]^{-1} = \begin{bmatrix} c_1^{-1} & | & 0 \\ \cdots & | & \cdots \\ 0 & | & c_1^{-1} \end{bmatrix} \quad (6.77)$$

Substituting Eqs. (6.76) and (6.77) into Eq. (6.73), which is then substituted into Eqs. (6.69) and (6.70), yields the displacement function of the element as

$$\begin{aligned} u_x &= [N_1 \ N_2 \ N_3][q_1 \ q_2 \ q_3]^T \\ &= \frac{1}{2A} [(x_2y_3 - x_3y_2 + y_{23}x + x_{32}y)u_1 + (x_3y_1 - x_1y_3 + y_{31}x + x_{13}y)u_2 \\ &\quad + (x_1y_2 - x_2y_1 + y_{12}x + x_{21}y)u_3] \end{aligned} \quad (6.78)$$

$$\begin{aligned} u_y &= [N_4 \ N_5 \ N_6][q_4 \ q_5 \ q_6]^T \\ &= \frac{1}{2A} [(x_2y_3 - x_3y_2 + y_{23}x + x_{32}y)u_4 + (x_3y_1 - x_1y_3 + y_{31}x + x_{13}y)u_5 \\ &\quad + (x_1y_2 - x_2y_1 + y_{12}x + x_{21}y)u_6] \end{aligned} \quad (6.79)$$

The strain–displacement relationship is

$$\{\varepsilon\} = \begin{Bmatrix} \varepsilon_x \\ \varepsilon_y \\ \varepsilon_{xy} \end{Bmatrix} = \begin{Bmatrix} \frac{\partial u_x}{\partial x} \\ \frac{\partial u_y}{\partial y} \\ \frac{\partial u_x}{\partial y} + \frac{\partial u_y}{\partial x} \end{Bmatrix} = \frac{1}{2A} \begin{bmatrix} y_{23} & y_{31} & y_{12} & 0 & 0 & 0 \\ 0 & 0 & 0 & x_{32} & x_{13} & x_{21} \\ x_{32} & x_{13} & x_{21} & y_{23} & y_{31} & y_{12} \end{bmatrix} \begin{Bmatrix} u_1 \\ u_2 \\ u_3 \\ u_4 \\ u_5 \\ u_6 \end{Bmatrix} = [b] \{u\} \quad (6.80)$$

which indicates that the assumption of linearly varying displacement [see Eqs. (6.69) and (6.70) within the element leads to constant strains, and hence, by Hooke's law, leads also to constant stresses. From the elasticity, the stress–strain relationship of plane stress is

$$\{\sigma\} = \frac{1}{E} \begin{bmatrix} 1 & -\mu & 0 \\ -\mu & 1 & 0 \\ 0 & 0 & 2(1+\mu) \end{bmatrix} \begin{Bmatrix} \sigma_x \\ \sigma_y \\ \sigma_{xy} \end{Bmatrix} = [B]\{\sigma\} \quad (6.81)$$

where μ is *Poisson's ratio* which may be 0.3 for steel and 0.15 for concrete [10]. The inverse of $[B]$ is

$$[B]^{-1} = \frac{E}{1-\mu^2} \begin{bmatrix} 1 & \mu & 0 \\ \mu & 1 & 0 \\ 0 & 0 & \frac{1-\mu}{2} \end{bmatrix} = [D] \quad (6.82)$$

Thus the stress–strain relationship may now be expressed as

$$\{\sigma\} = [D][b]\{u\} \quad (6.83)$$

Finally, the stiffness matrix can be formulated by using Eq. (6.12) as

$$[K_e]_{6 \times 6} = \int_v \{\sigma\}^T \{\varepsilon\} dv = [b]^T [D] [b] \int_v dv \quad (6.84)$$

or

$$[K_e] = \frac{Et}{4A(1-\mu^2)} \begin{bmatrix} y_{23}^2 + nx_{32}^2 & y_{31}^2 + nx_{13}^2 & y_{12}^2 + nx_{21}^2 & & & & \text{symm} \\ y_{31}y_{23} + nx_{13}x_{32} & y_{31}y_{12} + nx_{21}x_{13} & ny_{12}x_{32} + nx_{21}y_{23} & x_{32}^2 + ny_{23}^2 & & & \\ y_{12}y_{23} + nx_{21}x_{32} & y_{31}y_{12} + nx_{21}x_{13} & ny_{12}x_{32} + nx_{21}y_{23} & x_{32}^2 + ny_{23}^2 & & & \\ ny_{23}x_{13} + nx_{31}x_{32} & ny_{31}x_{13} + nx_{13}x_{31} & ny_{12}x_{13} + nx_{21}y_{31} & x_{32}x_{13} + ny_{23}y_{31} & x_{13}^2 + ny_{31}^2 & & \\ ny_{23}x_{21} + nx_{32}y_{12} & ny_{31}x_{21} + nx_{13}y_{12} & ny_{12}x_{21} + nx_{21}y_{12} & x_{32}x_{21} + ny_{23}y_{12} & x_{21}x_{13} + ny_{31}y_{12} & x_{21}^2 + ny_{12}^2 & \end{bmatrix} \quad (6.85)$$

in which t is the plate thickness and

$$n = \frac{1-\mu}{2}$$

For plane-strain problems, $[D]$ in Eq. (6.84) is replaced by

$$[D] = \frac{E}{(1+\mu)(1-2\mu)} \begin{bmatrix} 1-\mu & \mu & 0 \\ \mu & 1-\mu & 0 \\ 0 & 0 & \frac{1-2\mu}{2} \end{bmatrix} \quad (6.86)$$

Consequently, the stiffness coefficients should be modified accordingly.

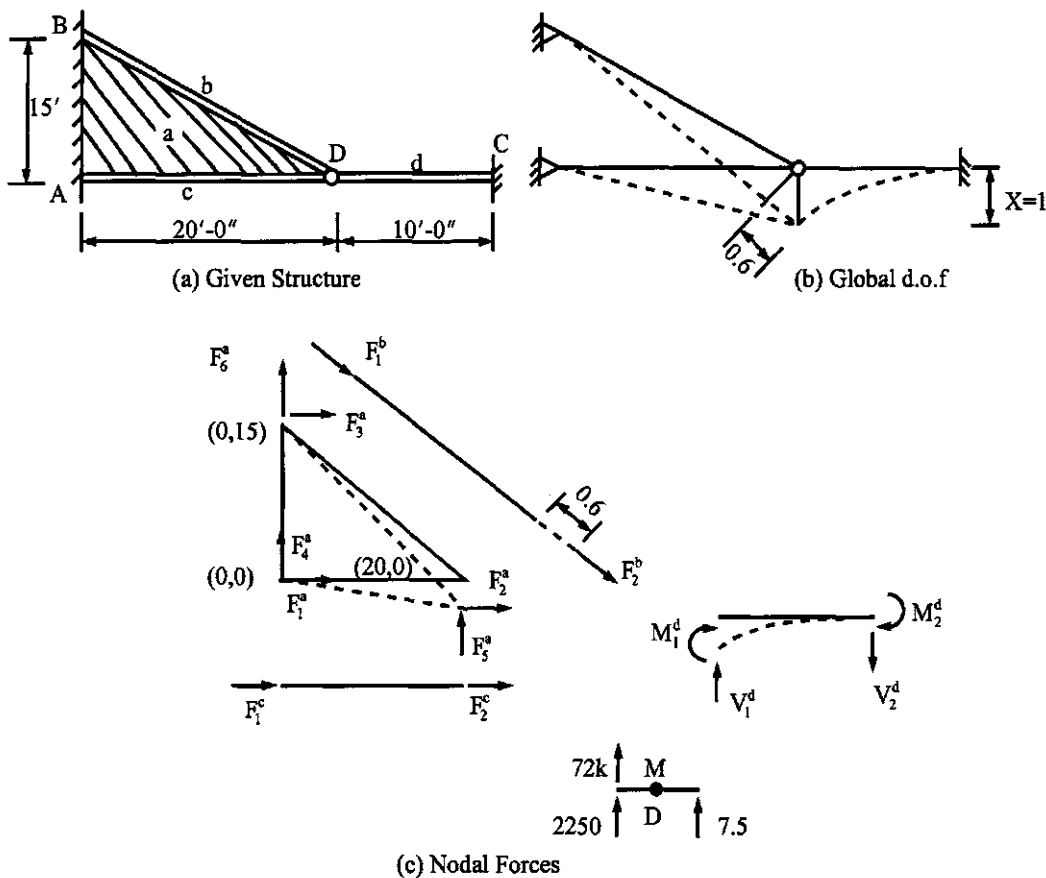


FIG. 6.16 Example 6.5.1. (a) Given structure. (b) Global d.o.f. (c) Nodal forces.

The generalized force may be obtained in the manner presented in Section 6.3 as

$$Q_i = \int_A F(x, y, t) N_i \, dA \quad (6.87)$$

where N_i is given in Eqs. (6.78) and (6.79).

The consistent mass coefficients may also be obtained by using the general procedure as

$$m_{ij} = \int_V \rho(x, y) N_i N_j \, dy \quad (6.88)$$

Since N_i and N_j each has several complicated terms, the integration becomes awkward for plate elements. Lumped mass is generally used in practical analyses.

EXAMPLE 6.5.1 Formulate the stiffness matrix, $[K]$, and lumped mass matrix, $[M]$, of the structure composed of plate element, a , truss elements, b and c , and beam element, d , as shown in Fig. 6.16. Thickness of the plate is 0.5 in and Poisson's ratio is 0.25, the cross-sectional area of the truss elements is 2 in², and the moment of inertia of the beam is 144 in⁴. The beam is

rigid in the axial direction and has a mass, $40 \text{ k s}^2/\text{in}$, including its own weight, lumped at node D . Plate and truss elements have a unit weight of 490 lb/ft^3 . Modulus of elasticity of the elements is $30,000 \text{ ksi}$.

Solution: Since the beam element is rigid in the axial direction, it has no axial deformation and the structure has only one d.o.f. as shown in Fig. 6.16b. The nodal forces of the constituent members due to the unit global displacement are shown in Fig. 6.16c.

Member a—the nodal forces due to the unit displacement are

$$\left. \begin{aligned} F_1^a &= -k_{15}^a; & F_2^a &= -k_{25}^a \\ F_3^a &= -k_{35}^a; & F_4^a &= -k_{45}^a \\ F_5^a &= -k_{55}^a; & F_6^a &= -k_{65}^a \end{aligned} \right\} \quad (\text{a})$$

where the stiffness coefficients are given in the fifth column (or fifth row) of Eq. (6.85). Since F_1^a , F_3^a , F_4^a , and F_6^a are transmitted to the supports, they are not needed for the present problem. F_2^a is zero due to the axial restraint of the beam.

The stiffness coefficient needed to be evaluated is

$$k_{55}^a = \frac{Et}{4A(1-\mu^2)} (x_{13}^2 + ny_{31}^2) \quad (\text{b})$$

where

$$A = \frac{1}{2}(x_{23}y_{31} - x_{31}y_{23}) = \frac{1}{2}[(x_2 - x_3)(y_3 - y_1) - (x_3 - x_1)(y_2 - y_3)] = \frac{1}{2}[20(15) - (0)] = 150 \text{ ft}^2 \quad (\text{c})$$

$$n = \frac{1-\mu}{2} = \frac{1-0.25}{2} = 0.375 \quad (\text{d})$$

$$k_{55}^a = \frac{30,000(0.5)}{4(150)(144)[1-(0.25)^2]} [0 + 0.375(15)^2(144)] = 2250 \text{ k/in} \quad (\text{e})$$

Note that stiffness coefficients, $k_{i,j}$, in Eqs. (a) and (b) are based on notations used for elements (i.e. in local coordinates), which can nonetheless be treated as a structural system's stiffness coefficients, $K_{i,j}^l$, because the global d.o.f., X , is the same as the local d.o.f., u^5 .

Members b and c— F_1^b is transmitted to the support and

$$F_2^b = \frac{AE}{L} u_2 = \frac{2(30,000)}{25(12)} (0.6) = 120 \text{ k} \quad (\text{f})$$

$$F_1^c = F_2^c = 0 \quad (\text{g})$$

Member d— M_1^d is zero due to the center hinge; M_2^d and V_2^d are transmitted to the support; and

$$V_1^d = -\frac{3EI}{L^3} = -\frac{3(30,000)(144)}{(10 \times 12)^3} = -7.5 \text{ k} \quad (\text{h})$$

Mass—the mass at node D is assumed to be equivalent to one-third of the triangular element, one-half of the truss member, and the given mass of the beam

$$M = \frac{0.490}{32.3} \left[\frac{150(0.5)}{2(3)} + \frac{2(25)}{2} + \frac{2(20)}{2} + 40 \right] = 1.484 \text{ k-s}^2/\text{in} \quad (\text{i})$$

Motion equation—the nodal forces and the mass at D are shown in Fig. 6.16c, for which the motion equation is

$$1.484\ddot{x} + 2329.5x = 0 \quad (\text{j})$$

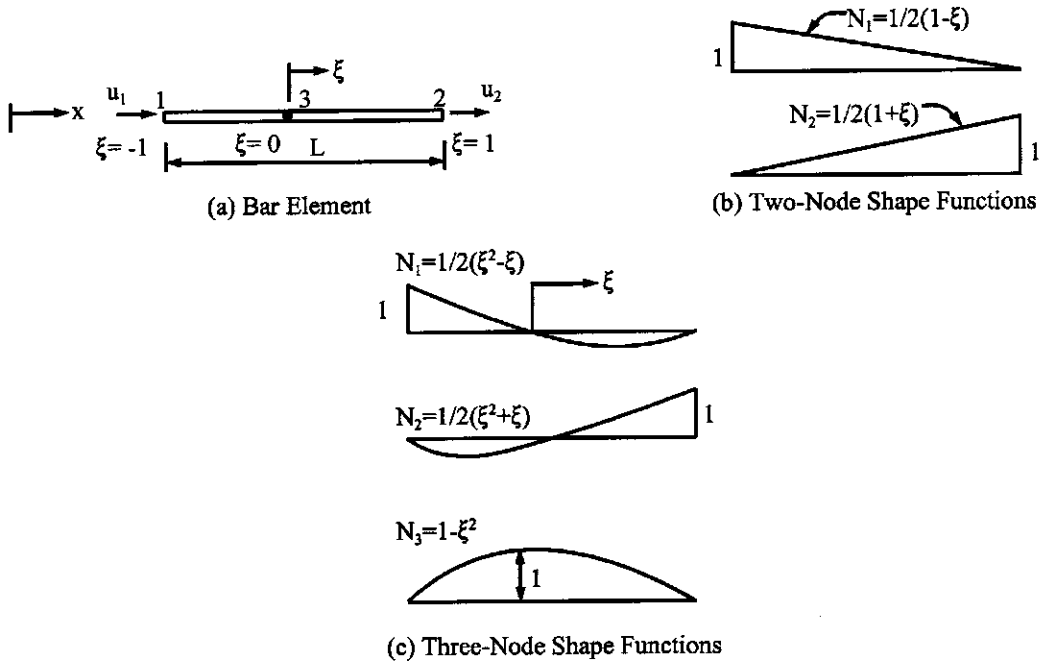


FIG. 6.17 Shape functions for bar element. (a) Bar element. (b) Two-node shape function. (c) Three-node shape function.

Solution techniques for eigenvalues and responses presented in the lumped mass and the consistent mass methods can be directly applied to finite element structures.

6.5.2. Finite Element Formulation—Natural Coordinates

6.5.2.1. Natural Coordinates and their Fundamental Concept

Natural coordinates are dimensionless and are expressed with reference to the element rather than with reference to the global coordinate system in which the element resides. As noted, finite element modeling based on the natural coordinates is called *isoparametric finite element*, which is powerful and efficient in application. The relationship between generalized coordinates and natural coordinates may be illustrated by using a truss (bar) element formulation as follows.

Let a bar element be shown in Fig. 6.17 in which ξ is at any arbitrary point of the element defined as a natural coordinate. $\xi = -1$ and $+1$ at nodes 1 and 2, respectively. The variation for two nodes and three nodes is shown in Figs. 6.17b and c, respectively. Consider the two-node case shown in Fig. 6.17b; we have

$$x = \frac{1}{2}(1 - \xi)x_1 + \frac{1}{2}(1 + \xi)x_2 = \sum_{i=1}^2 N_i x_i = \{N\}^T \{x\} \quad (6.89)$$

where N_i is called the *interpolation function* or *shape function*, for which a general derivation procedure will be discussed later in this section.

The displacement of the bar can also be expressed as

$$u = [N]^T \begin{Bmatrix} u_1 \\ u_2 \end{Bmatrix} = [N]^T \{q\} \quad (6.90)$$

The element is isoparametric because the interpolation function is used for both x and u . If the shape function used for x in Eq. (6.89) is of a higher degree than the shape function used for u in Eq. (6.90), then the element is called *subparametric*; otherwise, the element is called *superparametric*.

For derivation of stiffness coefficients, from Eqs. (6.89) and (6.90)

$$\varepsilon = \frac{\partial u}{\partial \xi} \frac{\partial \xi}{\partial x} \quad (6.91)$$

$$\frac{\partial u}{\partial \xi} = \frac{1}{2}(u_2 - u_1) \quad (6.92)$$

In general, $\partial u / \xi$ is not obtained directly; we must first calculate $\partial x / \partial \xi$ and then find its inverse. For the present simple case

$$\frac{\partial x}{\partial \xi} = \frac{1}{2}(x_2 - x_1) = \frac{L}{2}; \quad dx = \frac{L}{2}d\xi = Jd\xi \quad (6.93)$$

where J is called the *Jacobian*: it reflects a scale factor that describes physical length dx with a reference length $d\xi$. Substituting Eqs. (6.92) and (6.93) into Eq. (6.91) yields

$$\varepsilon = \frac{1}{L}(u_2 - u_1) = \begin{bmatrix} -\frac{1}{L} & \frac{1}{L} \end{bmatrix} \begin{Bmatrix} u_1 \\ u_2 \end{Bmatrix} = \begin{bmatrix} \frac{\partial N_1}{\partial \xi} & \frac{\partial N_2}{\partial \xi} \end{bmatrix} \begin{Bmatrix} u_1 \\ u_2 \end{Bmatrix} = [B] \{u\} \quad (6.94)$$

The stiffness of the prismatic bar is

$$[K_e] = \int \varepsilon E \varepsilon dv = E \int_{-1}^1 [B]^T [B] AJ d\xi = \frac{AE}{L} \begin{bmatrix} 1 & -1 \\ -1 & 1 \end{bmatrix} \quad (6.95)$$

The generalized forces are

$$\{Q_e\} = \int_{-1}^1 [N]^T \{\bar{F}(x, t)\} AJ d\xi + \int_{-1}^1 [N]^T \{F(x, t)\} J d\xi \quad (6.96)$$

where $\{\bar{F}(x, t)\}$ is a known body force and $\{F(x, t)\}$ is a distributed surface load.

The mass matrix is

$$[M_e] = \int_{-1}^1 \rho(x) [N]^T [N] JA d\xi \quad (6.97)$$

6.5.2.2. Interpolation Scheme

The shape function can be obtained by means of several techniques [2]. Below is the Lagrange's interpolation technique of curve-fitting. Let the true curve be "a" and the interpolating curve be "b" as shown in Fig. 6.18.

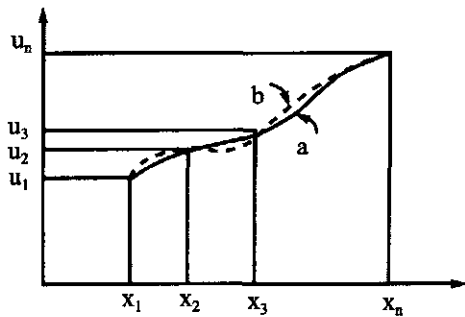


FIG. 6.18 Interpolating curve.

The expression of curve *b* is

$$u = \sum N_i u_i \quad (6.98)$$

where

$$N_i = \frac{\prod_{j=1}^n (x - x_j)}{\prod_{\substack{j=1 \\ j \neq i}}^n (x_i - x_j)} \quad (6.99)$$

in which Π denotes a product of the indicated binomials, $(x-x_j)$ or (x_i-x_j) , over the indicated range *j*. For instance

$$N_n = \frac{(x - x_1)(x - x_2) \cdots (x - x_{n-1})}{(x_n - x_1)(x_n - x_2) \cdots (x_n - x_{n-1})} \quad (6.100)$$

The equation can be used for both physical coordinates and natural coordinates. For a two-dimensional problem

$$u = \sum_{i=1}^m \sum_{j=1}^n N_i(x) N_j(y) u_{ij} \quad (6.101)$$

where u_{ij} is the value of u at $x = x_i$ and $y = y_j$.

6.5.2.3. Gauss Method for Numerical Integral

As shown earlier in this section, the stiffness, load, and mass matrices involve an integral over the natural coordinates and Jacobian scale factor. For two- and three-dimensional elements, these matrices cannot be integrated in closed form and are thus obtained using a numerical integral. Among many numerical integration schemes, the most appropriate for finite element work is the Gauss method, commonly referred to as *Gaussian quadrature* [15].

Consider the following equation originally given in Eq. (6.89):

$$f(x) = x = \frac{1}{2}(1 - \xi)x_1 + \frac{1}{2}(1 + \xi)x_2 \quad (6.102)$$

Since ξ is a function of x , we may write

$$g(\xi) = \frac{1}{2}(1 - \xi)x_1 + \frac{1}{2}(1 + \xi)x_2 \quad (6.103)$$

The definite integral of Eqs. (6.102) and (6.103) is

$$I = \int_{x_1}^{x_2} f(x) dx \quad (6.104)$$

or

$$I = \int_{-1}^1 g(\xi) J d\xi \quad (6.105)$$

where $J d\xi$ is obtained from

$$\frac{dx}{d\xi} = \frac{1}{2}(x_2 - x_1)$$

or

$$dx = \frac{1}{2}(x_2 - x_1)d\xi = J d\xi$$

In practice, the integration of Eq. (6.105) is obtained by numerically evaluating $g = g(\xi)$ at n locations (or *sampling points*); for each ξ_i , we find g_i and then multiply g_i by a *weight factor* W_i . Thus

$$I = \int_{-1}^1 g(\xi) d\xi = \sum_{i=1}^n W_i g(\xi_i) = W_1 g(\xi_1) + W_2 g(\xi_2) + \cdots + W_n g(\xi_n) \quad (6.106)$$

Eqs. (6.104) and (6.106) are graphically shown in Fig. 6.19 where the accompanying figures, Figs. 6.19b and c, represent two and three sampling points, respectively.

The numerical values of some sampling points and weight factors for Gauss numerical integration over $\xi = -1$ to $\xi = +1$ are listed in Table 6.4. For instance, let

$$g(\xi) = 6 + 2\xi^2$$

for $n = 1$, then $\xi_1 = 0$, and $W_1 = 2$; the result is

$$I = 2(6) = 12$$

for $n = 2$, then $\xi_1 = -\xi_2 = 1/\sqrt{3}$, and $W_1 = W_2 = 1$

$$I = (1)\left[6 + 2\left(\frac{1}{\sqrt{3}}\right)^2\right] + (1)\left[6 + 2\left(-\frac{1}{\sqrt{3}}\right)^2\right] = 13.333$$

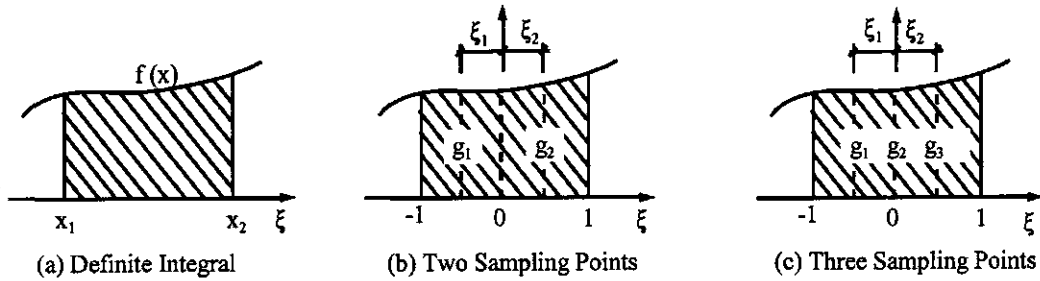


FIG. 6.19 Schemes for integral.

TABLE 6.4. Numerical Values of ξ_i and W_i

n	$\pm \xi_i$	W_i
1	0	2
2	$\pm \frac{1}{\sqrt{3}}$	1
3	$\pm \sqrt{0.6}$ 0	$5/9$ $8/9$
4	$\pm \left[\frac{3 + 2\sqrt{1.2}}{7} \right]^{\frac{1}{2}}$ $\pm \left[\frac{3 - 2\sqrt{1.2}}{7} \right]^{\frac{1}{2}}$	$\frac{1}{2} - \frac{1}{6\sqrt{1.2}}$ $\frac{1}{2} + \frac{1}{6\sqrt{1.2}}$

Here the solution associated with $n = 2$ is exact. In general, Gaussian quadrature is exact for polynomials of $2n-1$; that is, two and three sampling points are needed respectively for third and fourth order polynomials. Use of more than n points still produces exact results.

For a two-dimensional problem, $g = g(\xi, \eta)$, we can use Gaussian product rule as

$$I = \int_{-1}^1 \int_{-1}^1 g(\xi, \eta) d\xi d\eta \approx \int_{-1}^1 \left[\sum_i W_i g(\xi_i, \eta) \right] d\eta \approx \sum_i \sum_j W_i W_j g(\xi_i, \eta_j) \quad (6.107)$$

6.5.2.4. Quadrilateral Element

Quadrilateral element offers versatility, being suitable for rectangular as well as triangular elements. Sample cases are shown in Fig. 6.20.

A quadrilateral element can have straight or curved edges. Consider the straight-edged quadrilateral element shown in Fig. 6.21; it has four nodes with axes ξ and η passing through the geometric center or mid-point, P . ξ and η are dimensionless natural coordinates and the

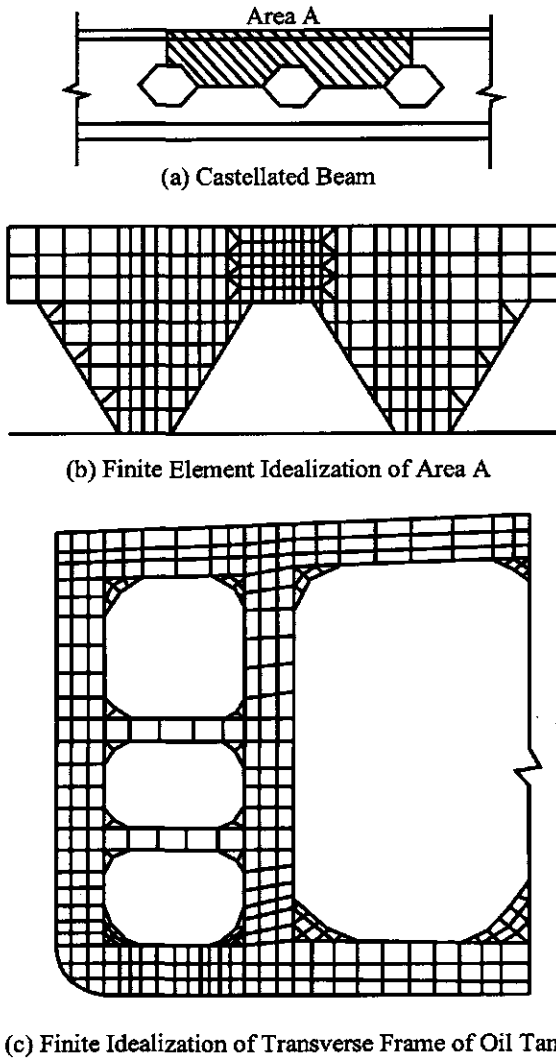


FIG. 6.20 Sample finite element idealization. (a) Castellated beam. (b) Finite element idealization of Area A. (c) Finite idealization of transverse frame of oil tank.

mid-point is defined as

$$x_P = \frac{1}{4}(x_1 + x_2 + x_3 + x_4); \quad y_P = \frac{1}{4}(y_1 + y_2 + y_3 + y_4)$$

where x_i and y_i correspond to the node numbers. Note that the geometric center does not necessarily coincide with the element's centroid.

Any location of the element on the $x-y$ plane can be expressed using Eq. (6.101) as discussed in Eqs. (6.89) and (6.90); then

$$\begin{Bmatrix} x \\ y \end{Bmatrix} = \begin{bmatrix} N_1 & 0 & N_2 & 0 & N_3 & 0 & N_4 & 0 \\ 0 & N_1 & 0 & N_2 & 0 & N_3 & 0 & N_4 \end{bmatrix} \begin{bmatrix} x_1 & y_1 & x_2 & y_2 & x_3 & y_3 & x_4 & y_4 \end{bmatrix}^T \quad (6.108)$$

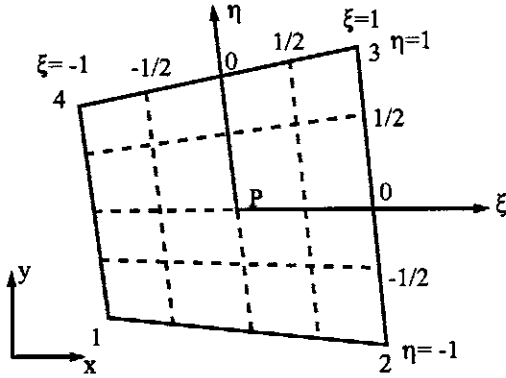


FIG. 6.21 Quadrilateral element.

or in symbolic form

$$x = \sum_{i=1}^4 N_i x_i; \quad y = \sum_{i=1}^4 N_i y_i \quad (6.109)$$

Similarly, the displacement at any point of the element on the x - y plane can also be expressed as

$$u = \sum_{i=1}^4 N_i u_i; \quad v = \sum_{i=1}^4 N_i v_i \quad (6.110)$$

where the shape functions can be determined by using the interpolation scheme shown in Eqs. (6.99) and (6.101) as

$$\left. \begin{aligned} N_1 &= N_1(\xi)N_2(\eta) = \frac{\xi - 1}{-1 - 1} \frac{\eta - 1}{-1 - 1} = \frac{1}{4}(1 - \xi)(1 - \eta) \\ N_2 &= N_2(\xi)N_2(\eta) = \frac{\xi - (-1)}{1 - (-1)} \frac{\eta - 1}{-1 - 1} = \frac{1}{4}(1 + \xi)(1 - \eta) \\ N_3 &= N_3(\xi)N_3(\eta) = \frac{\xi - (-1)}{1 - (-1)} \frac{\eta - (-1)}{1 - (-1)} = \frac{1}{4}(1 + \xi)(1 + \eta) \\ N_4 &= N_4(\xi)N_4(\eta) = \frac{\xi - 1}{-1 - 1} \frac{\eta - (-1)}{1 - (-1)} = \frac{1}{4}(1 - \xi)(1 + \eta) \end{aligned} \right\} \quad (6.111)$$

Although the above shape functions can be obtained by inspection, the illustration shows how to apply Lagrange's interpolation to an element with many nodes.

The strain-displacement relationship yields

$$\begin{Bmatrix} \varepsilon_x \\ \varepsilon_y \\ \varepsilon_{xy} \end{Bmatrix} = \begin{Bmatrix} \frac{\partial u}{\partial x} \\ \frac{\partial v}{\partial y} \\ \frac{\partial u}{\partial y} + \frac{\partial v}{\partial x} \end{Bmatrix} = \begin{bmatrix} \frac{\partial N_i}{\partial x} & 0 \\ 0 & \frac{\partial N_i}{\partial y} \\ \frac{\partial N_i}{\partial y} & \frac{\partial N_i}{\partial x} \end{bmatrix} \begin{Bmatrix} u_i \\ v_i \end{Bmatrix} \quad (6.112)$$

or in symbolic form

$$\{\varepsilon\} = [B]\{\delta\} \quad (6.113)$$

Since N_i is a function of ξ and η , we cannot obtain $\partial N_i / \partial x$ directly, but the *chain rule* for differentiation gives

$$\frac{\partial N_i}{\partial \xi} = \frac{\partial N_i}{\partial x} \frac{\partial x}{\partial \xi} + \frac{\partial N_i}{\partial y} \frac{\partial y}{\partial \xi} \quad (6.114)$$

$$\frac{\partial N_i}{\partial \eta} = \frac{\partial N_i}{\partial x} \frac{\partial x}{\partial \eta} + \frac{\partial N_i}{\partial y} \frac{\partial y}{\partial \eta} \quad (6.115)$$

In matrix form

$$\begin{Bmatrix} N_{i'\xi} \\ N_{i'\eta} \end{Bmatrix} = \begin{bmatrix} x'_{\xi} & y'_{\xi} \\ x'_{\eta} & y'_{\eta} \end{bmatrix} \begin{Bmatrix} N_{i'x} \\ N_{i'y} \end{Bmatrix} = [J] \begin{Bmatrix} N_{i'x} \\ N_{i'y} \end{Bmatrix} \quad (6.116)$$

where

$$[J] = \begin{bmatrix} \Sigma N_{i'\xi} x_i & \Sigma N_{i'\xi} y_i \\ \Sigma N_{i'\eta} x_i & \Sigma N_{i'\eta} y_i \end{bmatrix} = \begin{bmatrix} J_{11} & J_{12} \\ J_{21} & J_{22} \end{bmatrix} \quad (6.117)$$

The symbols used above are: $N_{i'\xi}$ represents the differentiation of N_i with respect to ξ ; x_ξ means the differentiation of x with respect to ξ ; and $[J]$ is the Jacobian matrix. Thus from Eq. (6.116)

$$\begin{Bmatrix} N_{i'x} \\ N_{i'y} \end{Bmatrix} = [J]^{-1} \begin{Bmatrix} N_{i'\xi} \\ N_{i'\eta} \end{Bmatrix} \quad (6.118)$$

The inverse of $[J]$ is usually performed by cofactor method as

$$[J]^{-1} = \frac{1}{\det[J]} \begin{bmatrix} J_{22} & -J_{12} \\ -J_{21} & J_{11} \end{bmatrix} \quad (6.119)$$

which can be used for different types of quadrilateral elements. For those having curved edges with higher order function, $[J]$ is always a 2×2 matrix. For hexahedrons, the Jacobian matrix is 3×3 ; the cofactor technique can still be used. This technique is therefore popular for computer application. Note that the order of numbering an element's nodes can vary, such as 1234 (see Fig. 6.21) and 2541 (see Fig. 6.1), but the numbers must go counterclockwise in order to have the Jacobian be positive.

For plane stress or plane strain problems, the stiffness of an element with uniform thickness can be derived as

$$[K_e] = \int \int [B]^T [D] [B] t \, dx \, dy = \int \int [B]^T [D] [B] t \, \det[J] \, d\xi \, d\eta \quad (6.120)$$

where $\det[J]$ is the *magnification factor* transforming area $dx \, dy$ into $d\xi \, d\eta$. $[K_e]$ is obtained by *Gaussian quadrature* as

$$[K_e] = t \sum_{j=1}^n \sum_{i=1}^n W_i W_j [B_{i,j}]^T [D] [B_{i,j}] \det[J_{i,j}] \quad (6.121)$$

where $[B_{i,j}]$ and $\det[J_{i,j}]$ are evaluated at each integration point corresponding to coordinates ξ_i and η_j .

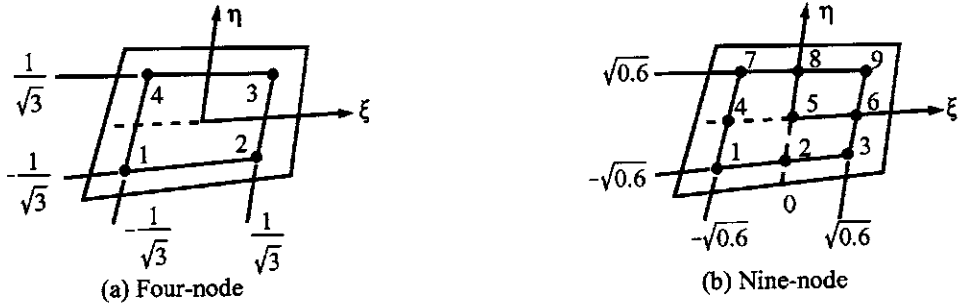


FIG. 6.22 Four-node and nine-node quadrilaterals.

For the four-node and nine-node quadrilateral elements shown in Fig. 6.22, the sampling points and weight factors are given in Table 6.4; numerical integrations become

$$I = \sum_{i=1}^2 \sum_{j=1}^2 W_i W_j g(\xi_i, \eta_j) = (1)(1)(g_1 + g_2 + g_3 + g_4) \quad (6.122)$$

$$\begin{aligned} I = \sum_{i=1}^3 \sum_{j=1}^3 W_i W_j g(\xi_i, \eta_j) &= \left(\frac{5}{9}\right)(g_1 + g_3 + g_7 + g_9) + \left(\frac{5}{9}\right)\left(\frac{8}{9}\right)(g_2 + g_4 + g_6 + g_8) \\ &\quad + \left(\frac{8}{9}\right)\left(\frac{8}{9}\right)(g_5) \end{aligned} \quad (6.123)$$

where g_i represents $g(\xi_i, \eta_i)$.

The mass matrix is

$$[M_e] = \rho t \int_{-1}^1 \int_{-1}^1 [N]^T [N] \det[J] d\xi d\eta \approx \rho t \sum_{j=1}^n \sum_{i=1}^n W_i W_j N_{i,j}^T N_{i,j} \det[J_{i,j}] \quad (6.124)$$

and the generalized force matrix due to body force should be

$$\{Q_e\} = t \int \int [N]^T \{F(x, t)\} \det[J] d\xi d\eta \approx t \sum_{j=1}^n \sum_{i=1}^n W_i W_j N_{i,j}^T F(x, t)_{i,j} \det[J_{i,j}] \quad (6.125)$$

EXAMPLE 6.5.2 Find the stiffness, mass, and generalized force matrix for one of the triangles of the plate structure shown in Fig. 6.23. Use the quadrilateral element just presented with $E = 30(10^6)$ psi and $\mu = 0.25$. The plate has body force, $w(x, t) = P \sin \omega t$; constant thickness, $t = 1$ in; and mass density, ρ .

Solution: The plate can be analyzed by using rectangular or triangular element models as shown in Figs. 6.23b and c, for which quadrilateral element formulation can be directly applied. Here a triangular model illustrates how to employ the quadrilateral element for the present problem.

Element 1 of Fig. 6.23c is shown in the accompanying figure d; by collapsing side 3–4 of the four-node quadrilateral element in Fig. 6.23e, a triangle is obtained, as shown in the accompanying figure f. From Eqs. (6.108)–(6.111), we have

$$\begin{aligned} x &= \frac{1}{4}(1-\xi)(1-\eta)x_1 + \frac{1}{4}(1+\xi)(1-\eta)x_2 + \frac{1}{4}(1+\xi)(1+\eta)x_3 + \frac{1}{4}(1-\xi)(1+\eta)x_4 \\ &= N_1 x_1 + N_2 x_2 + N_3 x_3 + N_4 x_4 \end{aligned} \quad (a)$$

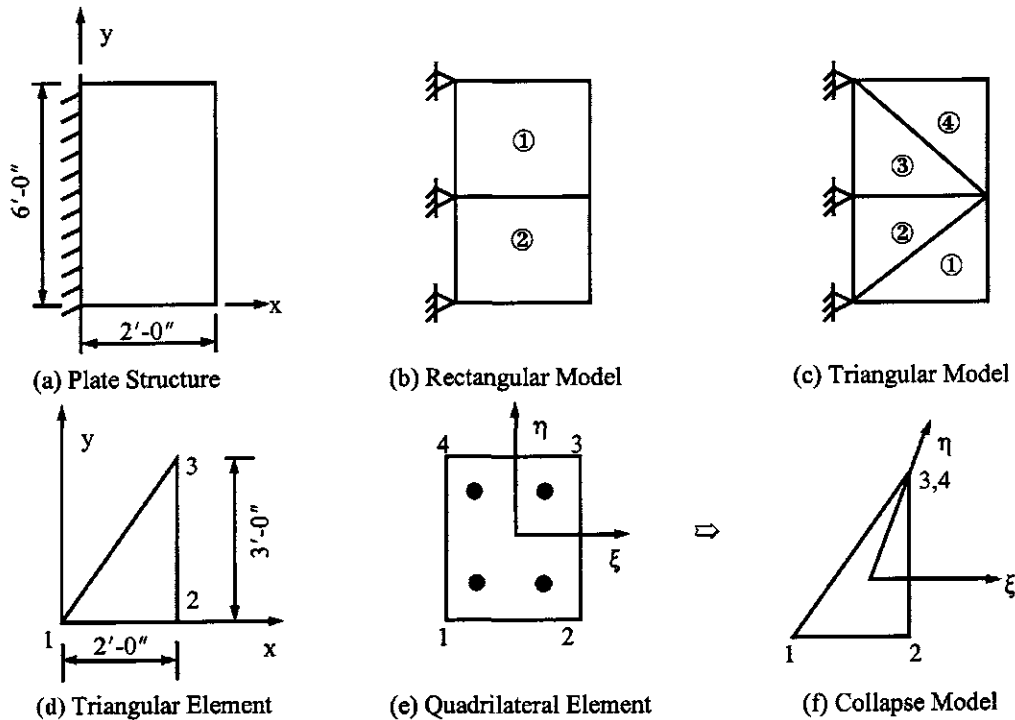


FIG. 6.23 Example 6.5.2. (a) Plate structure. (b) Rectangular model. (c) Triangular model. (d) Triangular element. (e) Quadrilateral element. (f) Collapse model.

and

$$y = N_1 y_1 + N_2 y_2 + N_3 y_3 + N_4 y_4 \quad (\text{b})$$

Since $x_3 = x_4$ and $y_3 = y_4$ at the collapsed side, Eqs. (a) and (b) become

$$x = \frac{1}{4}(1 - \xi)(1 - \eta)x_1 + \frac{1}{4}(1 + \xi)(1 - \eta)x_2 + \frac{1}{4}(1 + \eta)x_3 = N_1 x_1 + N_2 x_2 + N_3 x_3 \quad (\text{c})$$

$$y = \frac{1}{4}(1 - \xi)(1 - \eta)y_1 + \frac{1}{4}(1 + \xi)(1 - \eta)y_2 + \frac{1}{4}(1 + \eta)y_3 = N_1 y_1 + N_2 y_2 + N_3 y_3 \quad (\text{d})$$

(A) Stiffness matrix—the general expression of a quadrilateral element is

$$[K_e] = \sum_{j=1}^4 \sum_{i=1}^4 W_i W_j [B_{i,j}]^T [D] [B_{i,j}] t \det[J_{i,j}] \quad (\text{e})$$

where $W_i = W_j = 1$, and

$$[D] = \frac{E}{1 - \mu^2} \begin{bmatrix} 1 & \mu & 0 \\ \mu & 1 & 0 \\ 0 & 0 & \frac{1 - \mu}{2} \end{bmatrix} \quad (\text{f})$$

The individual matrices in Eq. (e) are obtained by employing Eqs. (c) and (d) in quadrilateral

element formulation as

$$[J] = \begin{bmatrix} N_{1'\xi} & N_{2'\xi} & N_{3'\xi} \\ N_{1'\eta} & N_{2'\eta} & N_{3'\eta} \end{bmatrix} \begin{bmatrix} x_1 & y_1 \\ x_2 & y_2 \\ x_3 & y_3 \end{bmatrix} = \begin{bmatrix} \frac{1}{4}(\eta - 1) & \frac{1}{4}(1 - \eta) & 0 \\ \frac{1}{4}(\xi - 1) & \frac{1}{4}(\xi - 1) & \frac{1}{2} \end{bmatrix} \begin{bmatrix} x_1 & y_1 \\ x_2 & y_2 \\ x_3 & y_3 \end{bmatrix} \quad (g)$$

$$[B] = \begin{bmatrix} N_{i'x} & 0 \\ 0 & N_{i'y} \\ N_{i'y} & N_{i'x} \end{bmatrix} = \begin{bmatrix} N_{1'x} & 0 & N_{2'x} & 0 & N_{3'x} & 0 \\ 0 & N_{1'y} & 0 & N_{2'y} & 0 & N_{3'y} \\ N_{1'y} & N_{1'x} & N_{2'y} & N_{2'x} & N_{3'y} & N_{3'x} \end{bmatrix} \quad (h)$$

in which

$$\begin{bmatrix} N_{1'x} & N_{2'x} & N_{3'x} \\ N_{1'y} & N_{2'y} & N_{3'y} \end{bmatrix} = [J]^{-1} \begin{bmatrix} N_{1'\xi} & N_{2'\xi} & N_{3'\xi} \\ N_{1'\eta} & N_{2'\eta} & N_{3'\eta} \end{bmatrix} \quad (i)$$

Let us consider sampling point 3 at $\xi_3 = 0.57735$ and $\eta_3 = 0.57735$; then

$$[J_{3,3}] = \begin{bmatrix} -0.105662 & 0.105662 & 0 \\ -0.105662 & -0.394337 & 0.5 \end{bmatrix} \begin{bmatrix} 0 & 0 \\ 24 & 0 \\ 24 & 36 \end{bmatrix} = \begin{bmatrix} 2.5359 & 0 \\ 2.5359 & 18 \end{bmatrix} \quad (j)$$

$$[J_{3,3}]^{-1} = \begin{bmatrix} 0.394337 & 0 \\ -0.055556 & 0.055556 \end{bmatrix}; \quad \det[J_{3,3}] = 45.6462 \quad (k)$$

$$\begin{bmatrix} N_{1'x} & N_{2'x} & N_{3'x} \\ N_{1'y} & N_{2'y} & N_{3'y} \end{bmatrix} = \begin{bmatrix} 0.394337 & 0 \\ -0.055556 & 0.055556 \end{bmatrix} \begin{bmatrix} -0.105662 & 0.105662 & 0 \\ -0.105662 & -0.394337 & 0.5 \end{bmatrix} \quad (l)$$

$$= \begin{bmatrix} -0.041667 & 0.041667 & 0 \\ 0 & -0.027778 & 0.027778 \end{bmatrix}$$

$$[B_{3,3}] = \begin{bmatrix} -0.041667 & 0 & 0.041667 & 0 & 0 & 0 \\ 0 & 0 & 0 & -0.027778 & 0 & 0.027778 \\ 0 & -0.041667 & -0.027778 & 0.041667 & 0.027778 & 0 \end{bmatrix} \quad (m)$$

$$[D] = \frac{30(10^6)}{1 - (0.25)^2} \begin{bmatrix} 1 & 0.25 & 0 \\ 0.5 & 1 & 0 \\ 0 & 0 & 0.375 \end{bmatrix} \quad (n)$$

Substituting Eqs. (j)–(n) into Eq. (e),

$$[K_e]_a = [B_{3,3}]^T [D] [B_{3,3}] t \det[J_{3,3}] = \begin{bmatrix} 2.5359 & 0 & -2.5359 & 0.4227 & 0 & -0.4227 \\ & 0.9510 & 0.6340 & -0.9510 & -0.634 & 0 \\ & & 2.9586 & 1.0566 & -0.4227 & 0.4227 \\ & & & 2.0780 & 0.6340 & -1.1271 \\ & & & & 0.4227 & 0 \\ & & & & & 1.1271 \end{bmatrix} 10^6 \quad (o)$$

In a similar manner, we may calculate

$[K_e]_b$ at point 2 for $\xi_2 = 0.57735$, $\eta_2 = -0.57735$

$[K_e]_c$ at point 4 for $\xi_4 = -0.57735$, $\eta_4 = 0.57735$

$[K_e]_d$ at point 1 for $\xi_1 = -0.57735$, $\eta_1 = -0.57735$

The stiffness coefficients of element 1 are finally obtained as

$$[K_e] = [K_e]_a + [K_e]_b + [K_e]_c + [K_e]_d = \begin{bmatrix} 24.0 & 0 & -24.0 & 4.0 & 0 & 4.0 \\ 9.0 & 6.0 & -9.0 & -6.0 & 0 & 0 \\ & 28.0 & -10.0 & -4.0 & 4.0 & \\ & & 19.67 & 6.0 & -10.67 & \\ \text{symm} & & & 4.0 & 0 & \\ & & & & 10.67 & \end{bmatrix} 10^6 \text{ lbs/in}$$

(p)

(B) *Mass matrix*—from Eq. (6.124) with $W_i = W_j = 1$, we have

$$[M_e] = \rho t [N]^T [N] \det[J] = \rho t \det[J] \begin{bmatrix} N_1^2 & 0 & N_1 N_2 & 0 & N_1 N_3 & 0 \\ N_1^2 & 0 & N_1 N_2 & 0 & N_1 N_3 & \\ & N_2^2 & 0 & N_2 N_3 & 0 & \\ & & N_2^2 & 0 & N_2 N_3 & \\ \text{symm} & & & N_3^2 & 0 & \\ & & & & N_3^2 & \end{bmatrix} \quad (q)$$

For sampling point 3, $\zeta_3 = 0.57735$, $\eta_3 = 0.57735$, the shape functions in Eqs. (c) and (d) are calculated as

$$N_1 = 0.044658; \quad N_2 = 0.166667; \quad N_3 = 0.788675 \quad (r)$$

Upon substitution, Eq. (q) becomes

$$[M_e]_a = \rho t [N_{3,3}]^T [N_{3,3}] \det[J_{3,3}] = \rho \begin{bmatrix} 9.1035(10^{-2}) & 0 & 0.33975 & 0 & 1.607698 & 0 \\ & 9.1035(10^{-2}) & 0 & 0.33975 & 0 & 1.607698 \\ & & 1.26795 & 0 & 6 & 0 \\ & & & 1.26795 & 0 & 6 \\ \text{symm} & & & & 28.3923 & 0 \\ & & & & & 28.3923 \end{bmatrix} \quad (s)$$

where $\det[J_{3,3}]$ is from Eq. (j). Similarly, we can calculate $[M_e]_b$, $[M_e]_c$, and $[M_e]_d$ corresponding to sampling points 2, 4, and 1, respectively. The final mass matrix is

$$[M_e] = [M_e]_a + [M_e]_b + [M_e]_c + [M_e]_d = \rho \begin{bmatrix} 112.0525 & 0 & 45.4641 & 0 & 42 & 0 \\ & 112.0525 & 0 & 45.4641 & 0 & 42 \\ & & 112.0525 & 0 & 42 & 0 \\ & & & 112.0525 & 0 & 42 \\ \text{symm} & & & & 72 & 0 \\ & & & & & 72 \end{bmatrix} \quad (t)$$

(C) *Generalized force matrix*—from Eq. (6.125)

$$\{Q_e\} = t [N]^T \{P \sin \omega t\} \det[J] = t \det[J] \begin{bmatrix} N_1 & 0 \\ 0 & N_1 \\ N_2 & 0 \\ 0 & N_2 \\ N_3 & 0 \\ 0 & N_3 \end{bmatrix} \begin{Bmatrix} P \sin \omega t \\ P \sin \omega t \end{Bmatrix} \quad (u)$$

For sampling point 3 at $\xi_3 = \eta_3 = 0.57735$; N_1 , N_2 , and N_3 are given in Eq. (c); $\det [J]$ is in Eq. (k). Upon substitution, Eq. (u) yields

$$\{Q_e\}_a = [2.0385 \quad 2.0385 \quad 7.6077 \quad 7.6077 \quad 36 \quad 36]^T P \sin \omega t \quad (v)$$

Following the same procedures, the generalized force matrix is obtained as

$$\begin{aligned} \{Q_e\} &= \{Q_e\}_a + \{Q_e\}_b + \{Q_e\}_c + \{Q_e\}_d \\ &= [172.3923 \quad 172.3923 \quad 172.3923 \quad 172.3923 \quad 144 \quad 144]^T P \sin \omega t \end{aligned} \quad (w)$$

6.6. MOTION EQUATION WITH P-Δ EFFECT

As presented in Chapter 5, when a member is subjected to a compressive force, P , the force times the member's deflection, Δ , yields additional moment which is called *second-order moment* due to the $P-\Delta$ effect. For the dynamic stiffness method, the $P-\Delta$ is implicitly expressed in the stiffness coefficient. For consistent mass and lumped mass methods, the $P-\Delta$ effect is formulated separately from stiffness in a *geometric matrix*. The geometric matrix is important in response analysis for large deflection problems with material and geometric nonlinearity. This section presents the formulation of geometric matrix to be included in motion equations for eigenvalues and response analysis of linear systems. Nonlinear analysis with $P-\Delta$ effect will be presented in Chapter 9.

6.6.1. Potential Energy and Motion Equation

Consider a member subjected to axial compression, P , as shown in Fig. 6.24. The influence of axial force on bending deformation can be taken into account by studying the *potential energy* due to relative axial displacement

$$\Delta = \int_0^L d\Delta \quad (6.126)$$

in which

$$d\Delta = ds - dx \quad (6.127)$$

Since $(ds)^2 = (dx)^2 + (dy)^2$, then

$$ds = dx \left[1 + \left(\frac{dy}{dx} \right)^2 \right]^{\frac{1}{2}} \quad (6.128)$$

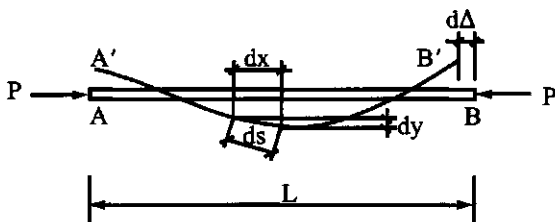


FIG. 6.24 P-Δ effect on bending deformation.

Using *binomial expansion*,

$$ds = dx \left[1 + \frac{1}{2} \left(\frac{dy}{dx} \right)^2 - \frac{1}{8} \left(\frac{dy}{dx} \right)^4 + \dots \right]$$

neglecting higher-order terms,

$$ds = dx \left[1 + \frac{1}{2} \left(\frac{dy}{dx} \right)^2 \right] \quad (6.129)$$

Substituting Eqs. (6.127) and (6.129) into Eq. (6.126) yields

$$\Delta = \int_0^L \frac{1}{2} \left(\frac{dy}{dx} \right)^2 dx \quad (6.130)$$

Thus the potential energy may be expressed as

$$V = \frac{1}{2} \int_0^L P \left(\frac{dy}{dx} \right)^2 dx \quad (6.131)$$

For a member with the following displacement function,

$$y(x, t) = \sum_{i=1}^n N_i(x) q_i(t) \quad (6.132)$$

the expression of potential energy becomes

$$V = \frac{1}{2} \sum_{i=1}^n \sum_{j=1}^n P \int_0^L \left(\frac{\partial N_i}{\partial x} \right) \left(\frac{\partial N_j}{\partial x} \right) q_i q_j \quad (6.133)$$

of which the second derivative yields a coefficient denoted by

$$\frac{\partial^2 V}{\partial q_i \partial q_j} = k_{qij} = P \int_0^L N_i N'_j dx \quad (6.134)$$

For the general expression of Lagrange's equation of either a member or a system, the potential energy can be included in Eq. (6.7) as

$$\frac{d}{dt} \left(\frac{\partial T}{\partial \dot{q}_i} \right) - \frac{\partial T}{\partial q_i} + \frac{\partial U}{\partial q_i} - \frac{\partial V}{\partial q_i} + \frac{\partial D}{\partial \dot{q}_i} = \frac{\partial W}{\partial q_i} \quad (6.135)$$

Applying Eq. (6.135) to a system with *kinetic energy*, T , *strain energy*, U , *dissipated energy*, D , and *work of external load*, W , given in Section 6.2, as well as the potential energy just derived, we have

$$[M]\{\ddot{q}\} + [C]\{\dot{q}\} + [K]\{q\} - [K_g]\{q\} = \{Q\} \quad (6.136)$$

The system matrices above are assembled from members' matrices through the compatibility con-

dition as shown in Sections 4.5, 5.4, and 5.6

$$\left. \begin{array}{l} [M] = \Sigma[M^i] \\ [K] = \Sigma[K^i] \\ [K_g] = \Sigma[K_g^i] \\ [C] = \alpha[M] + \beta([K] - [K_g]) \end{array} \right\} \quad (6.137)$$

where $[M^i]$, $[K^i]$, and $[K_g^i]$ are element matrices of member i in global coordinates; $[K_g]$ is the *geometric matrix*, for which the coefficient is derived in Eq. (6.134). The negative sign of $[K_g]$ is associated with compressive force. If a member has tensile force, then a positive sign should be used for $[K_g]$ of that member. The negative sign shows that compressive force reduces structural stiffness and consequently induces the structure to have larger deflections and smaller natural frequencies.

6.6.2. Geometric Matrix with Rotation and Deflection

The geometric matrix of a member can be derived by substituting the shape functions of Eq. (6.55) into Eq. (6.134) which yields

$$[K_{eg}] = P \begin{bmatrix} \frac{2L}{15} & -\frac{L}{30} & | & -\frac{1}{10} & -\frac{1}{10} \\ \frac{2L}{15} & | & -\frac{1}{10} & -\frac{1}{10} \\ --- & --- & | & --- & --- \\ \text{symm} & | & \frac{6}{5L} & \frac{6}{5L} & | & \frac{6}{5L} \end{bmatrix} = \begin{bmatrix} GM0 & | & GMY \\ \text{-----} & | & \text{-----} \\ \text{symm} & | & GVY \end{bmatrix} \quad (6.138)$$

in which submatrices are symbolically denoted by $GM0$, GMY , and GVY . This denotation gives the submatrices the same coefficients array in the stiffness matrix of Eq. (6.60) and allows ease of comparison with Timoshenko member's geometric matrix later in Sections 6.7 and 6.8. For illustration, two coefficients in Eq. (6.138) are derived in detail as follows:

$$\begin{aligned} k_{g11} &= P \int_0^L (N'_1)^2 dx = P \int_0^L \left(1 - \frac{4x}{L} + \frac{3x^2}{L^2}\right)^2 dx = \frac{2PL}{15} \\ k_{g12} &= P \int_0^L N'_1 N'_2 dx = P \int_0^L \left(1 - \frac{4x}{L} + \frac{3x^2}{L^2}\right) \left(-\frac{2x}{L} + \frac{3x^2}{L^2}\right) dx = -\frac{PL}{30} \end{aligned}$$

6.6.3. Geometric Matrix (String Stiffness) with Deflection

Observation of Eq. (6.138) reveals that compressive force influences both deflection and rotation. For lumped mass analysis of large building structures, the model may be simplified as a rigid bar such that axial force will only influence deflection but not rotation, as shown in Fig. 6.25.

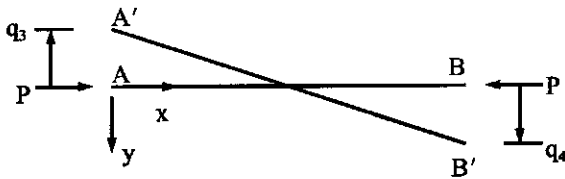


FIG. 6.25 P- Δ effect on rigid bar.

The displacement function of the member may be expressed as

$$Y = \left(\frac{x}{L} - 1\right)q_3 + \frac{x}{L}q_4 = N_3q_3 + N_4q_4 \quad (6.139)$$

of which the shape functions are

$$N_3 = \frac{x}{L} - 1; \quad N_4 = \frac{x}{L} \quad (6.140)$$

Substituting Eq. (6.140) into Eq. (6.134) yields

$$[K_{eg}] = P \begin{bmatrix} 0 & 0 & | & 0 & 0 \\ 0 & 0 & | & 0 & 0 \\ \cdots & \cdots & | & \cdots & \cdots \\ & & | & \frac{1}{L} & \frac{1}{L} \\ \text{symm} & & | & \frac{1}{L} & \end{bmatrix} = \begin{bmatrix} 0 & | & 0 \\ \cdots & | & \cdots \\ \text{symm} & | & GVY \end{bmatrix} \quad (6.141)$$

For illustration

$$k_{g33} = P \int_0^L (N_3)^2 dx = P \int_0^L \left(\frac{1}{L}\right)^2 dx = \frac{P}{L}$$

$$k_{g34} = P \int_0^L N'_3 N'_4 dx = P \int_0^L \left(\frac{1}{L}\right) \left(\frac{1}{L}\right) dx = \frac{P}{L}$$

Eq. (6.141) is commonly used for lumped mass model of such structures as trusses and tall buildings. Since we normally consider linear inertia force (i.e. associated with displacement) and neglect rotatory inertia of a lumped mass, the rotational d.o.f. of a building can be condensed from ($[K] - [K_g]$). What then remains is the d.o.f. coinciding with linear inertia forces. This numerical strategy can significantly reduce computer time in eigensolutions and response analyses. To distinguish from the geometric matrix derived in Eq. (6.138), $[K_{eg}]$ in Eq. (6.141) is sometimes called the *string stiffness matrix*.

6.7. TIMOSHENKO PRISMATIC MEMBER WITH P- Δ EFFECT

6.7.1. Displacement and Shape Functions

Consider a typical member shown in Fig. 6.26a with generalized coordinates and generalized forces represented by q_i and Q_i , respectively; the member is similarly shown in Fig. 6.5. For Fig. 6.26b, take the equilibrium condition of the moment, $Q_{mx} = Q_1 + Q_3x$, and then use $d^2 Y_b / dx^2$

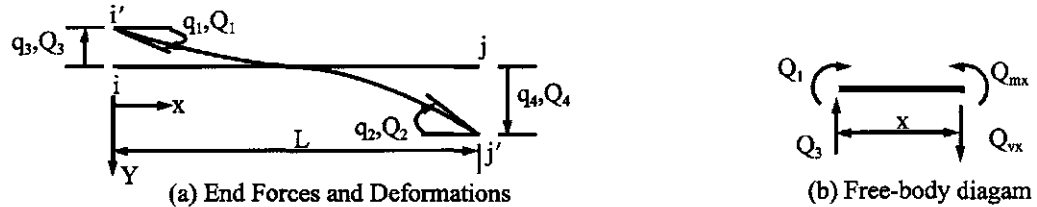


FIG. 6.26 Timoshenko member. (a) End forces and deformations. (b) Free-body diagram.

$= -Q_{mx}/EI$; we obtain

$$EIY_b'' = -Q_1 - Q_3x$$

where E = modulus of elasticity, I = moment of inertia of a cross-section, and Y_b = displacement due to bending deformation only. Integration yields

$$EIY_b' = -Q_1x - Q_3x^2/2 + C_1 \quad (6.142a)$$

Let $Y = Y_b + Y_s$ and $Y' = Y_b' + Y_s'$, where Y_s is displacement due to shear; then

$$Y_s' = \frac{Q_3}{GA\mu} \quad (6.142b)$$

and

$$EIY' = EIY_b' + EI \frac{Q_3}{GA\mu} \quad (6.143)$$

where G = shear modulus, A = cross-sectional area, and μ = shear coefficient. Integration of the above becomes

$$EIY = \frac{EIQ_3}{GA\mu}x - \frac{Q_1x^2}{2} - \frac{Q_3x^3}{6} + C_1x + C_2 \quad (6.144)$$

The displacement, Y , in Eq. (6.144) can be applied to a member with substitution of that member's boundary conditions. Let us consider the displacement due to q_4 , when $q_1 = q_2 = q_3 = 0$, for which the boundary conditions are

$$\left. \begin{array}{l} x = 0, \quad Y(0) = 0 \quad \text{and} \quad Y_b'(0) = 0 \\ x = L, \quad Y(L) = q_4 \quad \text{and} \quad Y_b'(L) = 0 \end{array} \right\} \quad (6.145)$$

Applying the boundary conditions at $x = L$ to Eqs. (6.142a) and (6.144) yields

$$\begin{aligned} C_1 &= Q_1L + Q_3L^2/2 \\ C_2 &= -\frac{EIQ_3L}{GA\mu} - \frac{1}{2}Q_1L^2 - \frac{1}{3}Q_3L^3 + EIq_4 \end{aligned}$$

Consequently, the displacement expression of Eq. (6.144) becomes

$$EIY = \frac{EIQ_3}{GA\mu}(x - L) - \frac{1}{2}Q_1x^2 - \frac{1}{6}Q_3x^3 + \left(Q_1L + \frac{1}{2}Q_3L^2 \right)x - \frac{1}{2}Q_1L^2 - \frac{1}{3}Q_3L^3 + EIq_4 \quad (6.146)$$

Applying the boundary conditions at $x = 0$ to Eq. (6.146) gives

$$Y(0) = 0, \quad -\frac{Q_3}{GA\mu} EIL - \frac{1}{2} Q_1 L^2 - \frac{1}{3} Q_3 L^3 + EI q_4 = 0 \quad (6.147)$$

$$Y'_b(0) = 0, \quad Q_1 L + \frac{1}{2} Q_3 L^2 = 0 \quad (6.148)$$

Note that $Q_3/GA\mu$ in Eq. (6.146) is associated with shear slope; because bending slope and shear slope are expressed separately as $Y' = Y'_b + Y'_s$, the derivative of Eq. (6.146) for the bending slope of Eq. (6.148) does not include $Q_3/GA\mu$. The effect of shear deformation can be obtained by solving Eqs. (6.147) and (6.148), and represented by

$$\phi = \frac{12EI}{GA\mu L^2} \quad (6.149)$$

Then

$$Q_1 = \frac{-6EI}{(1+\phi)L^2} q_4; \quad Q_3 = \frac{12EI}{(1+\phi)L^3} q_4 \quad (6.150)$$

Eq. (6.146) finally becomes

$$Y_4 = \frac{1}{1+\phi} [\phi + 3r^2 - 2r^3 + \phi(r-1)^*] q_4 = (N_{b4} + N_{s4})q_4 = N_4 q_4 \quad (6.151)$$

where N_{b4} is associated with bending slope, N_{s4} is due to shear slope, and

$$r = \frac{x}{L}$$

The term (N_{s4}) marked with an asterisk (*) is the displacement due to shear linked with $Q_3/GA\mu$ shown in Eq. (6.143). Note that the shape function comprises bending and shear slope; thus, the bending shape is influenced by both bending and shear. For other shape functions, we have

$$Y_1 = \frac{L}{1+\phi} \left[r - r^2 \left(2 + \frac{1}{2}\phi - r \right) + \phi r - \frac{1}{2}\phi r^* \right] q_1 = (N_{b1} + N_{s1})q_1 = N_1 q_1 \quad (6.152)$$

$$Y_2 = \frac{-L}{1+\phi} \left[\frac{1}{2}\phi + r^2 \left(1 - \frac{1}{2}\phi \right) - r^3 + \left(\frac{1}{2}\phi r - \frac{1}{2}\phi \right)^* \right] q_2 = (N_{b2} + N_{s2})q_2 = N_2 q_2 \quad (6.153)$$

$$Y_3 = -\frac{1}{1+\phi} [-r^2(3-2r) + 1 + \phi(1-r)^*] q_3 = (N_{b3} + N_{s3})q_3 = N_3 q_3 \quad (6.154)$$

If the shear effect is not considered, then ϕ and the term marked with an asterisk (i.e. N_s) should be dropped from Eqs. (6.151)–(6.154) which become shape functions due to bending deformation only, as shown in Eq. (6.55).

6.7.2. Stiffness Matrix

Let bending and shear strains be expressed as $\varepsilon_b = \sigma/E = z/R = -Y''_b z$, $\varepsilon_s = Y'_s$ (see Eq. (6.142a)), respectively, where R is the radius of curvature and z is the distance from the fiber location to the neutral axis of a cross-section. From Eq. (6.12),

$$k_{ij} = E \int_v \varepsilon_{bi} \varepsilon_{bj} dv + G \int_v \varepsilon_{si} \varepsilon_{sj} dv = E \int_v Y''_{bi} Y''_{bj} z^2 dv + G \int_v Y'_{si} Y'_{sj} dv \quad (6.155)$$

For illustration, consider the derivation of k_{11} ; then from Eq. (6.152), we have

$$Y''_{b1} = \frac{1}{(1+\phi)L}(-4-\phi+6r)$$

$$Y'_{s1} = \frac{-\phi}{2(1+\phi)}$$

Upon substitution, Eq. (6.155) becomes

$$k_{11} = \frac{E}{(1+\phi)^2 L^2} \int_0^L \int_A (-4-\phi+6r)^2 z^2 L dA dr + \frac{G\phi^2}{4(1+\phi)^2} \int_0^L A \mu L dr = \frac{4(1+\phi/4)}{(1+\phi)} \frac{EI}{L} \quad (6.156)$$

Similarly, for k_{31} ,

$$Y''_{b3} = -\frac{1}{(1+\phi)L^2}(-6+12r)$$

$$Y'_{s3} = \frac{\phi}{(1+\phi)L}$$

Thus Eq. (6.155) yields

$$k_{31} = \frac{-6}{(1+\phi)} \frac{EI}{L^2} \quad (6.157)$$

The stiffness coefficients of a member may be summarized as

$$[K_e] = \begin{bmatrix} 4(1+\phi/4) & 2(1-\phi/2) & -6/L & -6/L \\ & 4(1+\phi/4) & -6/L & -6/L \\ & & 12/L^2 & 12/L^2 \\ & & & 12/L^2 \end{bmatrix} \frac{1}{1+\phi} \frac{EI}{L} \quad (6.158)$$

in which ϕ is dropped when only bending deformation is considered; then Eq. (6.158) becomes Eq. (6.60). Note that the notations used in this section are consistent with those used previously (see Figs. 4.4, 6.5, and 6.26). The stiffness coefficients derived above may also be symbolically expressed as [see Eqs. (4.26) and (6.60)].

$$[K_e] = \begin{bmatrix} SM\theta_1 & SM\theta_2 & | & SMY_1 & SMY_2 \\ & SM\theta_1 & | & SMY_2 & SMY_1 \\ --- & --- & | & --- & --- \\ & & | & SVY_1 & SVY_2 \\ symm & & & & | & SVY_1 \end{bmatrix} = \begin{bmatrix} SM\theta & | & SMY \\ --- & | & --- \\ symm & | & SVY \end{bmatrix} \quad (6.159)$$

6.7.3. Mass Matrix

As discussed in Section 5.10.1, the Timoshenko beam has two components of inertia force: transverse and rotatory. In the consistent mass method, the mass matrix associated with these two components may be derived by following Eq. (6.13) as

$$[M_e] = \rho \int_v [N]^T [N] dv \quad (6.160)$$

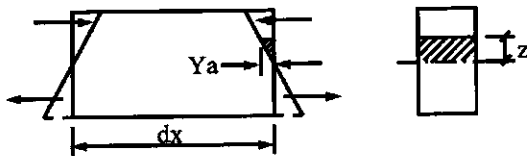


FIG. 6.27 Couple due to rotatory inertia.

in which

$$[N] = \begin{bmatrix} N_1 & N_2 & N_3 & N_4 \\ N_{a1} & N_{a2} & N_{a3} & N_{a4} \end{bmatrix} \quad (6.161)$$

where N_1-N_4 are given in Eqs. (6.151)–(6.154); $N_{a1}-N_{a4}$ are the shape functions in the longitudinal direction above and below the neutral axis of the cross-section of a member. Let z be the distance measured at any point from neutral axis; then the displacement of a fiber located at z shown in Fig. 6.27 is

$$Y_a = -z \frac{dY}{dx} \quad (6.162)$$

which is a horizontal displacement. During vibration the displacement induces horizontal inertia force acting to the right, say, below the neutral axis. There is an equal and opposite force above the axis. These two forces form a couple due to rotatory inertia. Substituting Eqs. (6.151)–(6.154) into Eq. (6.162), we can find the corresponding Y_a . For instance, employing Eq. (6.152) gives

$$Y_{a1} = -\frac{z}{L} \frac{dY_1}{dr} = \frac{-z}{1+\phi} (1 - 4r + \phi - r\phi + 3r^2) q_1 = z \bar{N}_{a1} q_1 = N_{a1} q_1 \quad (6.163)$$

Note that the derivative of Y_1 has not included the term marked with * as

$$\frac{1}{2} \phi r^*$$

because it is associated with shear slope which does not induce rotatory inertia. In a similar manner, we can find

$$Y_{a2} = \frac{-z}{1+\phi} (3r^2 - 2r + \phi r) q_2 = z \bar{N}_{a2} q_2 = N_{a2} q_2 \quad (6.164)$$

$$Y_{a3} = \frac{z}{(1+\phi)L} (-6r + 6r^2) q_3 = z \bar{N}_{a3} q_3 = N_{a3} q_3 \quad (6.165)$$

$$Y_{a4} = \frac{-z}{(1+\phi)L} (6r - 6r^2) q_4 = z \bar{N}_{a4} q_4 = N_{a4} q_4 \quad (6.166)$$

Employing N_i and N_{ai} in Eq. (6.161) which is then substituted into Eq. (6.160), we have a typical

member's mass matrix as

$$[M_e] = \rho \int_v \underbrace{\begin{bmatrix} N_1^2 & N_1N_2 & N_1N_3 & N_1N_4 \\ & N_2^2 & N_2N_3 & N_2N_4 \\ & & N_3^2 & N_3N_4 \\ & & & N_4^2 \end{bmatrix}}_{\text{symm}} dv + \rho \int_v \underbrace{\begin{bmatrix} N_{a1}^2 & N_{a1}N_{a2} & N_{a1}N_{a3} & N_{a1}N_{a4} \\ & N_{a2}^2 & N_{a2}N_{a3} & N_{a2}N_{a4} \\ & & N_{a3}^2 & N_{a3}N_{a4} \\ & & & N_{a4}^2 \end{bmatrix}}_{\text{symm}} dv$$

$$\quad [M^t] \quad [M^r] \quad (6.167)$$

where $[M^t]$ and $[M^r]$ are mass matrices corresponding to transverse inertia and rotatory inertia, respectively. In symbolic form

$$[M_e^t] = \begin{bmatrix} MM0_1^t & MM0_2^t & | & MMY_1^t & MMY_2^t \\ & MM0_1^T & | & MMY_2^t & MMY_1^t \\ --- & --- & | & --- & --- \\ & & | & M V Y_1^t & M V Y_2^t \\ & & & symm & | & M V Y_1^t \end{bmatrix} = \begin{bmatrix} MM0^t & | & MMY^t \\ --- & | & --- \\ symm & | & M V Y^t \end{bmatrix} \quad (6.168)$$

and

$$[M_e^r] = \begin{bmatrix} MM0_1^r & MM0_2^r & | & MMY_1^r & MMY_2^r \\ & MM0_1^r & | & MMY_2^r & MMY_1^r \\ ---- & ---- & | & ---- & ---- \\ & & | & M V Y_1^r & M V Y_2^r \\ & & & symm & | & M V Y_1^r \end{bmatrix} = \begin{bmatrix} MM0^r & | & MMY^r \\ --- & | & --- \\ symm & | & M V Y^r \end{bmatrix} \quad (6.169)$$

The coefficients of $[M_e^t]$ are

$$\left. \begin{aligned} MM0_1^t &= \frac{mL^3}{(1+\phi)^2} \left(\frac{1}{120}\phi^2 + \frac{1}{60}\phi + \frac{1}{105} \right) \\ MM0_2^t &= \frac{-mL^3}{(1+\phi)^2} \left(\frac{1}{120}\phi^2 + \frac{1}{60}\phi + \frac{1}{140} \right) \\ MMY_1^t &= \frac{-mL^2}{(1+\phi)^2} \left(\frac{1}{24}\phi^2 + \frac{11}{120}\phi + \frac{11}{210} \right) \\ MMY_2^t &= \frac{mL^2}{(1+\phi)^2} \left(\frac{1}{24}\phi^2 + \frac{3}{40}\phi + \frac{13}{420} \right) \\ M V Y_1^t &= \frac{mL}{(1+\phi)^2} \left(\frac{1}{3}\phi^2 + \frac{7}{10}\phi + \frac{13}{35} \right) \\ M V Y_2^t &= \frac{-mL}{(1+\phi)^2} \left(\frac{1}{6}\phi^2 + \frac{3}{10}\phi + \frac{9}{70} \right) \end{aligned} \right\} \quad (6.170)$$

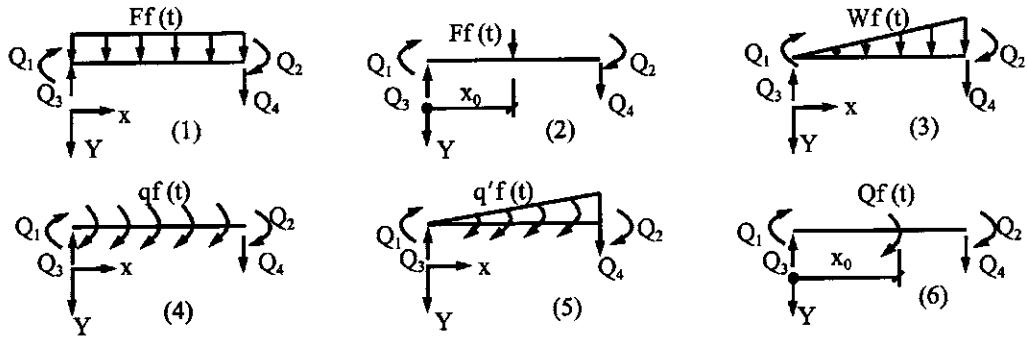


FIG. 6.28 Generalized forces of six loading cases.

For $[M_e^r]$, the coefficients are

$$\left. \begin{aligned} MM\theta_1^r &= \frac{\rho IL}{(1+\phi)^2} \left(\frac{1}{3}\phi^2 + \frac{1}{6}\phi + \frac{2}{15} \right) \\ MM\theta_2^r &= \frac{\rho IL}{(1+\phi)^2} \left(\frac{1}{6}\phi^2 - \frac{1}{6}\phi - \frac{1}{30} \right) \\ MMY_1^r = MMY_2^r &= \frac{\rho I}{(1+\phi)^2} \left(\frac{1}{2}\phi - \frac{1}{10} \right) \\ MVY_1^r = MVY_2^r &= \frac{\rho I}{L(1+\phi)^2} \frac{6}{5} \end{aligned} \right\} \quad (6.171)$$

If rotatory inertia is neglected, we can simply let $[M_e^r] = 0$. If shear deformation and rotatory inertia are both neglected, then $[M_e^r] = 0$ and ϕ in $[M_e^r]$ should also be zero; consequently, Eq. (6.170) converges to Eq. (6.3), where the mass matrix results from bending deformation.

6.7.4. Generalized Force Matrix

The generalized forces of six loading cases shown in Fig. 6.28 are summarized in Table 6.5. Note that the given loading cases are identical to those shown in Fig. 6.6; consequently the derivation is similar to that of Eqs. (6.64)–(6.66) and is not repeated here. When $\phi = 0$, the coefficients in Table 6.5 become those of Table 6.1.

6.7.5. Geometric Matrix

The geometric matrix may be formulated by following Eq. (6.134) as

$$k_{gij} = P \int_0^L N'_i N'_j dx \quad (6.172)$$

Substituting the shape functions of Eqs. (6.151)–(6.154) into the above yields a geometric matrix.

TABLE 6.5. Generalized Forces of Six Loading Cases of Timoshenko Beam

Cases	Q_1	Q_2	Q_3	Q_4
1	$\frac{1}{12}FL^2$	$-\frac{1}{12}FL^2$	$-\frac{1}{2}FL$	$\frac{1}{2}FL$
2	$\frac{FL}{1+\phi} \left[\left(1 + \frac{\phi}{2}\right)r_0 + r_0^3 - \left(2 + \frac{\phi}{2}\right)r_0^2 \right]$	$-\frac{FL}{1+\phi} \left[\frac{\phi}{2}r_0 + \left(1 - \frac{\phi}{2}\right)r_0^2 - r_0^3 \right]$	$-\frac{F}{1+\phi} [1 + (1 - r_0)\phi] - 3r_0^2 + 2r_0^3$	$\frac{F}{1+\phi} [\phi r_0 + 3r_0^2 - 2r_0^3]$
3	$\frac{wL^2}{1+\phi} \left(\frac{\phi}{24} + \frac{1}{30} \right)$	$-\frac{wL^2}{1+\phi} \left(\frac{\phi}{24} + \frac{1}{20} \right)$	$-\frac{wL}{1+\phi} \left(\frac{3}{20} + \frac{\phi}{6} \right)$	$\frac{wL}{1+\phi} \left(\frac{\phi}{3} + \frac{7}{20} \right)$
4	0	0	q	q
5	$\frac{q'L}{1+\phi} \left(\frac{1}{12} + \frac{\phi}{12} \right)$	$\frac{1}{12}q'L$	$\frac{q'}{2}$	$\frac{q'}{2}$
6	$\frac{Q}{1+\phi} \left[1 + \frac{\phi}{2} - 4r_0 - \phi r_0^3 + 3r_0^2 \right]$	$-\frac{Q}{1+\phi} \left[\frac{\phi}{2} + 2r_0 - \phi r_0 - 3r_0^2 \right]$	$-\frac{Q}{L(1+\phi)} (-\phi - 6r_0 + 6r_0^2)$	$\frac{Q}{L(1+\phi)} (\phi + 6r_0 - 6r_0^2)$

Note: (1) $r_0 = x_0/L$; (2) all the coefficients should be multiplied by $f(t)$; (3) fixed-end forces should have a sign opposite to that given above.

For instance

$$\begin{aligned} k_{g11} &= P \int_0^L (N'_1)^2 dx = P \int_0^L \left\{ \frac{L}{1+\phi} \left[\left(1 + \frac{1}{2}\phi\right) - (4 + \phi)r + 3r^2 \right] \right\}^2 L dr \\ &= \frac{PL}{60(1+\phi)^2} (5\phi^2 + 10\phi + 8) \end{aligned} \quad (6.173)$$

which is also k_{g22} . Other coefficients may be similarly derived as

$$k_{g12} = \frac{-PL}{60(1+\phi)^2} (5\phi^2 + 10\phi + 2) \quad (6.174)$$

$$k_{g13} = k_{g14} = k_{g23} = k_{g24} = \frac{-P}{10(1+\phi)^2} \quad (6.175)$$

$$k_{g33} = k_{g34} = k_{g44} = \frac{P}{60(1+\phi)L} (60\phi^2 + 120\phi + 72) \quad (6.176)$$

Expressing the coefficients in a matrix,

$$[K_{eg}] = \begin{bmatrix} k_{g11} & k_{g12} & k_{g13} & k_{g14} \\ & k_{g22} & k_{g23} & k_{g24} \\ & & k_{g33} & k_{g34} \\ \text{symm} & & & k_{g44} \end{bmatrix} = \begin{bmatrix} GM0 & | & GMY \\ \text{---} & | & \text{---} \\ \text{symm} & | & GVY \end{bmatrix} \quad (6.177)$$

If the effect of shear deformation is not considered, then $\phi = 0$; the coefficients in Eq. (6.177) become those given in Eq. (6.138).

6.8. TIMOSHENKO TAPERED MEMBER WITH P- Δ EFFECT

The beam element shown in Fig. 6.29a represents a typical *tapered member* with variable bending stiffness, EI_i and EI_j , at ends i and j , respectively. Distribution of mass, rotatory inertia, and axial load is also shown in the figure. Stiffness, mass, generalized force, and geometric matrices of the element are presented below with consideration of rotatory inertia as well as shear and bending deformations.

6.8.1. Stiffness Matrix

To adapt the general expression of the stiffness coefficients given in Eq. (6.12) to the present problem, the formulation may be expressed as

$$k_{ij} = E \int_v \varepsilon_{bi} \varepsilon_{bj} dv + G \int_v \varepsilon_{si} \varepsilon_{sj} dv = EI_i L \int_0^1 N''_{bi} N''_{bj} dr + (EI_j - EI_i)L \int_0^1 N''_{bi} N''_{bj} r dr + G\mu LA \int_0^1 N'_i N'_j dr \quad (6.178)$$

for which the shape functions are given in Eqs. (6.151)–(6.154); variation of area is not considered in the volume integration associated with the shear deformation term. To illustrate, derive k_{33} and k_{31} as

$$k_{33} = \frac{EI_i}{L^3(1+\phi)^2} \int_0^1 (-6 + 12r)^2 dr + \frac{(EI_j - EI_i)}{L^3(1+\phi)^2} \int_0^1 (-6 + 12r)^2 r dr + \frac{G\mu A\phi^2}{L(1+\phi)^2} \int_0^1 dr = \frac{12EI}{(1+\phi)L^3} \quad (6.179)$$

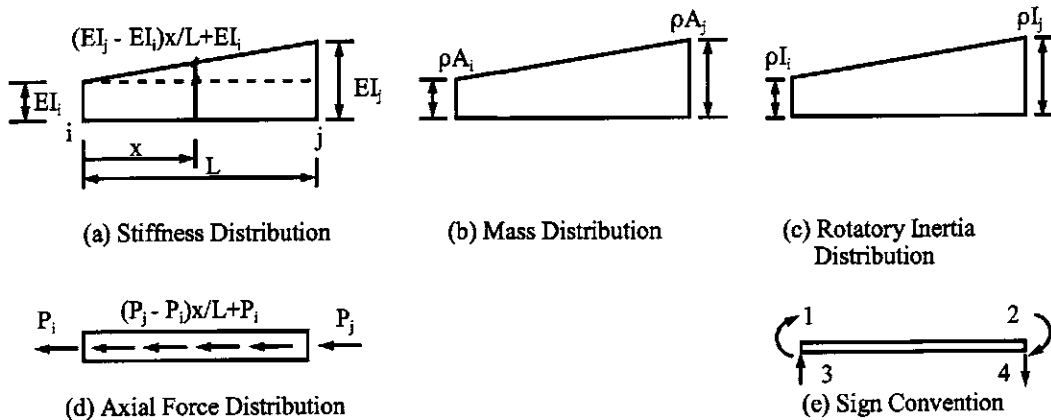


FIG. 6.29 Tapered beam. (a) Stiffness distribution. (b) Mass distribution. (c) Rotary inertia distribution. (d) Axial force distribution. (e) Sign convention.

where $GA\mu$ is replaced by $12\overline{EI}/\phi L^2$ and $\overline{EI} = (EI_i + EI_j)/2$

$$\begin{aligned} k_{31} = & -\frac{EI_i}{L^2(1+\phi)^2} \int_0^1 (-4-\phi+6r)(-6+12r) dr - \frac{(EI_j-EI_i)}{L^2(1+\phi)^2} \int_0^1 r(-4-\phi+6r)(-6+12r) dr \\ & - \frac{GA\mu\phi^2}{2(1+\phi)^2} \int_0^1 dr = -\frac{2\overline{EI}}{(1+\phi)L^2}(3+A_1) \end{aligned} \quad (6.180)$$

where $A_1 = (EI_i - EI_j)/(EI_i + EI_j)$.

Other stiffness coefficients can likewise be derived, and the final results are arranged according to Eq. (6.158) as follows:

$$[K_e] = \frac{2\overline{EI}}{(1+\phi)L^3} \begin{bmatrix} L^2(2+A_1+\phi/2) & L^2(1-\phi/2) & -L(3+A_1) & -L(3+A_1) \\ \text{symm} & L^2(2-A_1+\phi/2) & -L(3-A_1) & -L(3-A_1) \\ & & 6 & 6 \\ & & & 6 \end{bmatrix} \quad (6.181)$$

When $EI_i = EI_j$, then $A_1 = 0$ and $\overline{EI} = EI$; consequently, Eq. (6.181) becomes Eq. (6.158).

6.8.2. Mass Matrix

Using the basic expression of mass coefficients shown in Eq. (6.13), the shape functions in Eqs. (6.151)–(6.154), and $\rho A = \rho A_i + \rho(A_j - A_i)x/L$, we can employ Eq. (6.167) to express the transverse inertia as

$$m_{ij}^t = \int \rho A N_i N_j L dr = \rho A_i L \int_0^1 N_i N_j dr + (\rho A_j - \rho A_i) L \int_0^1 N_i N_j r dr \quad (6.182)$$

and the rotatory inertia [using the shape functions in Eqs. (6.163)–(6.166)] as

$$\begin{aligned} m_{ij}^r = & \int \int \rho L N_{ai} N_{aj} dA dr = \int \int \rho L \bar{N}_{ai} \bar{N}_{aj} z^2 dA dr \\ = & \rho I_i \int_0^1 \bar{N}_{ai} \bar{N}_{aj} dr + (\rho I_j - \rho I_i) \int_0^1 \bar{N}_{ai} \bar{N}_{aj} r dr \end{aligned} \quad (6.183)$$

For illustration,

$$\begin{aligned} m_{33}^t = & \frac{\rho A_i L}{(1+\phi)^2} \int_0^1 [1 + (1-r)\phi - r^2(3-2r)]^2 dr + \frac{(\rho A_j - \rho A_i)L}{(1+\phi)^2} \int_0^1 r[1 + (1-r)\phi - r^2(3-2r)]^2 dr \\ = & \frac{\rho A_i L}{(1+\phi)^2} \left(\frac{1}{4}\phi^2 + \frac{8\phi}{15} + \frac{10}{35} \right) + \frac{\rho A_j L}{(1+\phi)^2} \left(\frac{1}{12}\phi^2 + \frac{\phi}{6} + \frac{3}{35} \right) \end{aligned} \quad (6.184)$$

$$\begin{aligned}
m_{33}^r &= \frac{1}{(1+\phi)^2 L} \int \int \rho (-6r + 6r^2)^2 z^2 dA dr = \frac{36}{(1+\phi)^2 L} \int_0^1 \rho I r (-4 + r^2)^2 dr \\
&= \frac{36}{(1+\phi)^2 L} \left[\rho I_i \int_0^1 (-4 + r^2)^2 dr + (\rho I_j - \rho I_i) \int_0^1 (-r + r^2)^2 r dr \right] \\
&= \frac{3\rho I_i}{5(1+\phi)^2 L} + \frac{3\rho I_j}{5(1+\phi)^2 L}
\end{aligned} \tag{6.185}$$

The final results of the transverse inertia expressed in symbolic form of Eq. (6.168) are

$$[M_e^t] = \begin{bmatrix} MM\theta_1^t & MM\theta_2^t & | & MMY_1^t & MMY_2^t \\ & \overline{MM}\theta_1^t & | & \overline{MM}Y_2^t & \overline{MM}Y_1^t \\ --- & --- & | & --- & --- \\ \text{symm} & & | & MVY_1^t & MVY_2^t \\ & & & & \overline{MV}Y_1^t \end{bmatrix} = \begin{bmatrix} MM\theta^t & | & MMY^t \\ --- & | & --- \\ \text{symm} & | & MVY^t \\ & & \overline{MV}Y_1^t \end{bmatrix} \tag{6.186}$$

in which

$$\begin{aligned}
MM\theta_1^t &= \frac{\rho A_i L^3}{(1+\phi)^2} \left(\frac{\phi^2}{240} + \frac{\phi}{105} + \frac{1}{168} \right) + \frac{\rho A_j L^3}{(1+\phi)^2} \left(\frac{\phi^2}{240} + \frac{\phi}{140} + \frac{1}{280} \right) \\
MM\theta_2^t &= \frac{-\rho A_i L^3}{(1+\phi)^2} \left(\frac{\phi^2}{240} + \frac{\phi}{120} + \frac{1}{280} \right) - \frac{\rho A_j L^3}{(1+\phi)^2} \left(\frac{\phi^2}{240} + \frac{\phi}{120} + \frac{1}{280} \right) \\
\overline{MM}\theta_1^t &= \frac{\rho A_i L^3}{(1+\phi)^2} \left(\frac{\phi^2}{240} + \frac{\phi}{140} + \frac{1}{280} \right) + \frac{\rho A_j L^3}{(1+\phi)^2} \left(\frac{\phi^2}{240} + \frac{\phi}{105} + \frac{1}{168} \right) \\
MMY_1^t &= \frac{-\rho A_i L^2}{(1+\phi)^2} \left(\frac{\phi^2}{40} + \frac{5\phi}{84} + \frac{1}{28} \right) - \frac{\rho A_j L^2}{(1+\phi)^2} \left(\frac{\phi^2}{60} + \frac{9\phi}{280} + \frac{1}{60} \right) \\
MMY_2^t &= \frac{\rho A_i L^2}{(1+\phi)^2} \left(\frac{\phi^2}{60} + \frac{9\phi}{280} + \frac{1}{70} \right) + \frac{\rho A_j L^2}{(1+\phi)^2} \left(\frac{\phi^2}{40} + \frac{3\phi}{70} + \frac{1}{60} \right) \\
\overline{MM}Y_1^t &= \frac{-\rho A_i L^2}{(1+\phi)^2} \left(\frac{\phi^2}{60} + \frac{9\phi}{280} + \frac{1}{60} \right) - \frac{\rho A_j L^2}{(1+\phi)^2} \left(\frac{\phi^2}{40} + \frac{5\phi}{84} + \frac{1}{28} \right) \\
\overline{MM}Y_2^t &= \frac{\rho A_i L^3}{(1+\phi)^2} \left(\frac{\phi^2}{40} + \frac{3\phi}{70} + \frac{1}{60} \right) + \frac{\rho A_j L^2}{(1+\phi)^2} \left(\frac{\phi^2}{60} + \frac{9\phi}{280} + \frac{1}{70} \right) \\
MVY_1^t &= \frac{\rho A_i L}{(1+\phi)^2} \left(\frac{\phi^2}{4} + \frac{8\phi}{15} + \frac{1}{7} \right) + \frac{\rho A_j L}{(1+\phi)^2} \left(\frac{\phi^2}{12} + \frac{\phi}{6} + \frac{3}{35} \right) \\
MVY_2^t &= \frac{-\rho A_i L}{(1+\phi)^2} \left(\frac{\phi^2}{12} + \frac{3\phi}{20} + \frac{9}{140} \right) - \frac{\rho A_j L}{(1+\phi)^2} \left(\frac{\phi^2}{12} + \frac{3\phi}{20} + \frac{9}{140} \right) \\
\overline{MV}Y_1^t &= \frac{\rho A_i L}{(1+\phi)^2} \left(\frac{\phi^2}{12} + \frac{\phi}{6} + \frac{3}{35} \right) + \frac{\rho A_j L}{(1+\phi)^2} \left(\frac{\phi^2}{4} + \frac{8\phi}{15} + \frac{2}{7} \right)
\end{aligned} \tag{6.187}$$

Note that the coefficients denoted with and without superbar are not the same. Therefore $\overline{MM}\theta_1^t \neq MM\theta_1^t$. When $\rho A_i = \rho A_j = \rho A$, then Eq. (6.187) becomes Eq. (6.170).

The rotatory inertia coefficients, when expressed identically to Eq. (6.169), are written the following symbolic form:

$$[\mathbf{M}_e^r] = \begin{bmatrix} MM0_1^r & MM0_2^r & | & MMY_1^r & MMY_2^r \\ & \overline{MM0}_1^r & | & \overline{MMY}_2^r & \overline{MMY}_1^r \\ \cdots & \cdots & | & \cdots & \cdots \\ & | & M V Y_1^r & M V Y_2^r \\ \text{symm} & | & & \overline{M V Y}_1^r \end{bmatrix} = \begin{bmatrix} MM0^r & | & MMY^r \\ \cdots & | & \cdots \\ \text{symm} & | & M V Y^r \end{bmatrix} \quad (6.188)$$

in which

$$\left. \begin{aligned} MM0_1^r &= \frac{\rho I_i L}{(1+\phi)^2} \left(\frac{\phi^2}{4} + \frac{\phi}{5} + \frac{1}{10} \right) + \frac{\rho I_j L}{(1+\phi)^2} \left(\frac{\phi^2}{12} - \frac{\phi}{30} + \frac{1}{30} \right) \\ MM0_2^r &= \frac{\rho I_i L}{(1+\phi)^2} \left(\frac{\phi^2}{12} - \frac{\phi}{12} - \frac{1}{60} \right) + \frac{\rho I_j L}{(1+\phi)^2} \left(\frac{\phi^2}{12} - \frac{\phi}{12} - \frac{1}{60} \right) \\ \overline{MM0}_1^r &= \frac{\rho I_i L}{(1+\phi)^2} \left(\frac{\phi^2}{12} - \frac{\phi}{30} + \frac{1}{30} \right) + \frac{\rho I_j L}{(1+\phi)^2} \left(\frac{\phi^2}{4} + \frac{\phi}{5} + \frac{1}{10} \right) \\ MMY_1^r &= MMY_2^r = \frac{\rho I_i}{(1+\phi)^2} \left(\frac{3\phi}{10} \right) + \frac{\rho I_j}{(1+\phi)^2} \left(\frac{\phi}{5} - \frac{1}{10} \right) \\ \overline{MMY}_1^r &= \overline{MMY}_2^r = \frac{\rho I_i}{(1+\phi)^2} \left(\frac{\phi}{5} - \frac{1}{10} \right) + \frac{\rho I_j}{(1+\phi)^2} \left(\frac{3\phi}{10} \right) \\ M V Y_1^r &= M V Y_2^r = \overline{M V Y}_1^r = \frac{\rho I_i}{L(1+\phi)^2} \left(\frac{3}{5} \right) + \frac{\rho I_j}{L(1+\phi)^2} \left(\frac{3}{5} \right) \end{aligned} \right\} \quad (6.189)$$

When $\rho I_i = \rho I_j = \rho I$ and $\rho A_i = \rho A_j = \rho A$, then Eq. (6.189) becomes Eq. (6.171).

6.8.3. Generalized Force Matrix

Since the shape functions used in the stiffness and mass derivations for the tapered beam are based on those of a prismatic member, these functions are approximate and commonly acceptable in practical applications. For consistency, the same shape functions should be used for deriving the generalized force matrix of a tapered beam, which apparently is the same as that of a prismatic beam. The generalized force for various loading cases given in Table 6.5 can be directly applied here.

6.8.4. Geometric Matrix

Following Eqs. (6.134) and (6.172), we can formulate the coefficients of the geometric matrix as

$$k_{gij} = \int_0^1 P_i N'_j L dr + \int_0^1 (P_j - P_i) N'_i N'_j L r dr \quad (6.190)$$

For illustration

$$\begin{aligned}
 k_{g33} &= \int_0^1 \frac{P_i L}{L^2(1+\phi)^2} (-\phi - 6r + 6r^2)^2 dr + \int_0^1 (P_j - P_i) \frac{1}{(1+\phi)^2 L} (-\phi - 6r + 6r^2)^2 r dr \\
 &= \frac{P_i}{60L(1+\phi)^2} \left(\frac{\phi^2}{30} + \frac{\phi}{60} + 36 \right) + \frac{P_j}{60L(1+\phi)^2} \left(\frac{\phi^2}{30} + \frac{\phi}{60} + 36 \right)
 \end{aligned} \tag{6.191}$$

The expression of the geometric matrix in symbolic notation is

$$[K_{eg}] = \begin{bmatrix} GM\theta_1 & GM\theta_2 & GMY_1 & GMY_2 \\ \overline{GM}\theta_1 & \overline{GM}Y_2 & \overline{GM}Y_1 & \\ GYY_1 & GYY_2 & \\ \text{symm} & & \overline{G}\overline{V}Y_1 \end{bmatrix} \tag{6.192}$$

in which

$$\left. \begin{aligned}
 GM\theta_1 &= \frac{P_i L}{60(1+\phi)^2} \left(\frac{5}{2}\phi^2 + 7\phi + 6 \right) + \frac{P_j L}{60(1+\phi)^2} \left(\frac{5}{2}\phi^2 + 3\phi + 2 \right) \\
 GM\theta_2 &= -\frac{L}{60(1+\phi)^2} \left(\frac{5}{2}\phi^2 + 5\phi + 1 \right) (P_i + P_j) \\
 \overline{GM}\theta_1 &= \frac{P_i L}{60(1+\phi)^2} \left(\frac{5}{2}\phi^2 + 3\phi + 2 \right) + \frac{P_j L}{60(1+\phi)^2} \left(\frac{5}{2}\phi^2 + 7\phi + 6 \right) \\
 GMY_1 = GMY_2 &= \frac{P_i}{60(1+\phi)^2} (5\phi^2 + 8\phi) - \frac{P_j}{60(1+\phi)^2} (5\phi^2 + 8\phi + 6) \\
 \overline{GM}Y_1 = \overline{GM}Y_2 &= -\frac{P_i}{60(1+\phi)^2} (5\phi^2 + 8\phi + 6) + \frac{P_j}{60(1+\phi)^2} (5\phi^2 + 8\phi) \\
 GYY_1 = GYY_2 = \overline{G}\overline{V}Y_1 &= \frac{1}{60L(1+\phi)^2} (30\phi^2 + 60\phi + 36)(P_i + P_j)
 \end{aligned} \right\} \tag{6.193}$$

When $P_i = P_j = P$, Eq. (6.193) converges to the coefficients in Eqs. (6.173)–(6.176).

The matrices of a typical element derived in Sections 6.6, 6.7, and 6.8 are expressed in closed form with the same sign convention used in previous chapters. Therefore, the system matrix formulation and numerical procedures of eigensolution and response analysis already presented can be directly used here.

6.9. COMMENTS ON LUMPED MASS, CONSISTENT MASS, AND DYNAMIC STIFFNESS MODELS

The three well-known models of lumped mass, consistent mass, and dynamic stiffness were presented in previous chapters as well as this chapter for free and forced vibration with and without damping. The significant characteristics of these models may be summarized as follows:

- For a structure having the same number of divided segments or elements, dynamic stiffness and lumped mass models yield, respectively, the lower- and upper-bound of natural frequency of a given mode, while consistent mass gives a solution closer to but somewhat greater than that of dynamic stiffness.

- The three models can give a closer eigenvalue for fundamental mode but quite different results for higher modes. This behavior is particularly true for lumped mass case. In order to have accurate solutions, a larger number of divided segments is necessary to lump the masses, which in turn will create more unknowns in eigensolutions. Therefore, the dynamic stiffness model can be advantageous for some structures such as Example 4.7.1.
- The natural frequency of lumped mass and consistent mass models is explicitly expressed in the mass matrix. Therefore the eigensolution techniques, currently in vogue and presented in Chapters 2 and 3, can be applied to both models. The dynamic stiffness model, however, has natural frequency implicitly expressed in stiffness. Consequently, special eigensolution techniques are needed for this method, such as the determinant technique in Chapter 4.
- Due to lumped mass nature, the inertia force associated with rotational d.o.f. is usually small in comparison to that associated with linear d.o.f. and therefore can be neglected. Consequently, the number of eigensolution unknowns can be remarkably reduced by using matrix condensation of structural stiffness to eliminate the rotational d.o.f. of large structural systems such as tall buildings. Note further that the lumped mass method ably serves to model structures with constituent members having nonuniform cross-sections as well as those with structural and nonstructural masses irregularly distributed.

BIBLIOGRAPHY

1. JS Archer. Consistent formulations for structural analysis using finite-element techniques. *J Am Inst Aeronaut Astronaut (AIAA)* 3:1910–1918, 1965.
2. KJ Bathe. *Finite Element Procedures in Engineering Analysis*. Englewood Cliffs, NJ: Prentice-Hall, 1982.
3. FY Cheng, WH Tseng, ME Botkin. Matrix calculations of structural dynamic characteristics and response. *Proceedings of International Conference on Earthquake Analysis of Structures*, Vol I, Jassy, Romania, 1970, pp 85–101.
4. FY Cheng. Dynamic response of nonlinear space frames by finite element method. *Proceedings of International Association of Space Structures*, Architecture Institute of Japan, 1972, pp 817–826.
5. FY Cheng. Dynamic matrices of beams on elastic foundation. *Proceedings of International Symposium on Soil Structure Interaction*, Vol I, 1977, pp 203–208.
6. FY Cheng, E Uzgider, P Kitipitayangkul. Analysis of space frames subject to multicomponent earthquakes. *Proceedings of Conferencia Centro Americana De Ingenieria Sismica*, San Salvador, 1978, pp 105–116.
7. FY Cheng, ed. *Proceedings of 11th Analysis and Computation Conference*, Structures Congress XII, ASCE, Atlanta, GA, 1994.
8. FY Cheng, ed. *Proceedings of 12th Analysis and Computation Conference*, ASCE, Chicago, IL, 1996.
9. WK Cheng, MU Hosain, VV Veis. Analysis of castellated beams by finite element method. *Proceedings of Conference on Finite Element Method in Civil Engineering*, McGill University, Canada, 1972, pp 1105–1140.
10. RD Cook, DS Malkus, ME Plesha. *Concepts and Applications of Finite Element Analysis*. 3rd ed. New York: Wiley, 1989.
11. RH Gallagher. *Finite Element Analysis Fundamentals*. Englewood Cliffs, NJ: Prentice-Hall, 1975.
12. JM Gere, SP Timoshenko. *Mechanics of Materials*. 2nd ed. Monterey, CA: Brooks/Cole, 1984.
13. BM Iron. Engineering applications of numerical integration in stiffness methods. *J AIAA* 4(11):2035–2037, 1966.
14. CY Luo, FT Cheng. Accurate response analysis of seismic distributed mass systems. *Proceedings of 10th Conference on Electronic Computation*, ASCE, (FY Cheng, ed.) 1991, pp 122–130.
15. JS Przemieniecki. *Theory of Matrix Structural Analysis*. New York: McGraw-Hill, 1968.
16. EMQ Røren. Finite element analysis of ship structures. In: I Holland, K Bell, eds. *Finite Element Methods in Stress Analysis*, TAPIR, Technical University of Norway, Trondheim, 1969.
17. AH Stroud, D Secrest. *Gaussian Quadrature Formulas*. Englewood Cliffs, NJ: Prentice-Hall, 1966.
18. W Weaver Jr, PR Johnston. *Structural Dynamics by Finite Elements*. Englewood Cliffs, NJ: Prentice-Hall, 1987.

7

Numerical Integration Methods and Seismic Response Spectra for Single- and Multi-Component Seismic Input

PART A FUNDAMENTALS

7.1. INTRODUCTION

In Chapter 1 we discussed Duhamel's integral method for dynamic response of a single d.o.f. system, and introduced maximum response of a single d.o.f. system by using response spectra and shock spectra (see Figs. 1.28 and 1.30). In Chapter 2 Duhamel's integral method as well as response spectra were further applied to multiple d.o.f. systems. In this chapter, additional numerical integration methods along with their stability and accuracy are introduced. These methods are general in that they can be used for irregular loading patterns, such as earthquake ground motion, and for structures whose members change from elastic to inelastic during response.

Since maximum structural response is usually needed in structural design, sophisticated *response spectra* and *design spectra* are developed in this chapter. Included are elastic spectra, inelastic spectra, modal combination techniques, and spectra for multicomponent seismic input. The multicomponent input comprises three translational directions, x , y , and z , which are used to form main, intermediate and minor principal directions and three rotationals. The derivations of *rotational ground records* and *principal components* are presented in detail.

7.2. EARTHQUAKES AND THEIR EFFECTS ON STRUCTURES

7.2.1 Earthquake Characteristics

An earthquake is an oscillatory, sometimes violent movement of the earth's surface that follows a release of energy in the earth's crust. This energy can be generated by sudden dislocation of

segments in the crust, volcanic eruption, or man-made explosion. Most destructive earthquakes, however, are caused by dislocation of the crust. When subjected to geologic forces from plate tectonics, the crust strains, and the rock in the crust is stressed and stores strain energy. When stress exceeds the rock's ultimate strength, the rock breaks and quickly moves into new positions. In the process of breaking, strain energy is released and seismic waves are generated. These waves travel from the source of the earthquake, known as the *hypocenter* or *focus*, to the surface and underground. The *epicenter* is the point on the earth's surface directly above the hypocenter, as shown in Fig. 7.1. An earthquake's location is commonly described by the geographic position of its epicenter and its focal depth. The *focal depth* of an earthquake is the distance from epicenter to focus. These terms are illustrated in Fig. 7.1.

Seismic waves are of three types: *compression*, *shear*, and *surface waves*. Only compression waves can pass through the earth's molten core. Because compression waves, also known as *longitudinal waves*, travel at great speeds (5800 m/sec, or 19,000 ft/sec) and ordinarily reach the surface first, they are known as *P-waves* (primary waves). P-wave velocity is

$$v_p = \sqrt{\frac{2G + \lambda}{\rho}} \quad (7.1)$$

in which $\lambda = vE/[(1 + v)(1 - 2v)]$, where v is Poisson's ratio, G is the shear modulus, E is the modulus of elasticity, and ρ is mass density. Shear waves (transverse waves) (3000 m/sec, or 10,000 ft/sec) do not travel as rapidly as P-waves. Because they ordinarily reach the surface later, they are known as *S-waves* (secondary waves). S-wave velocity is

$$v_s = \sqrt{\frac{G}{\rho}} \quad (7.2)$$

While S-waves travel more slowly than P-waves, they transmit more energy and cause the majority of damage to structures. *Surface waves*, also known as *R-waves* (Rayleigh waves) or *L-waves* (Love waves), may or may not form. They arrive after the primary and secondary waves. R-waves move at approximately 2700 m/sec or 9000 ft/sec. Rayleigh waves move both horizontally and vertically in the direction of movement in a manner similar to ocean waves. Configurations of P-, S-, and R-waves are shown in Fig. 7.2.

7.2.2. Intensity, Magnitude, and Acceleration of Earthquakes

There are two scales to measure earthquakes. One is *intensity*, referred to as the Modified Mercalli Intensity Scale, a measurement of the degree of shaking caused by an earthquake at a given location. The other is *magnitude*, referred to as the Richter Magnitude Scale, a measurement of the amplitude of an earthquake. Magnitude can be translated into the amount of energy

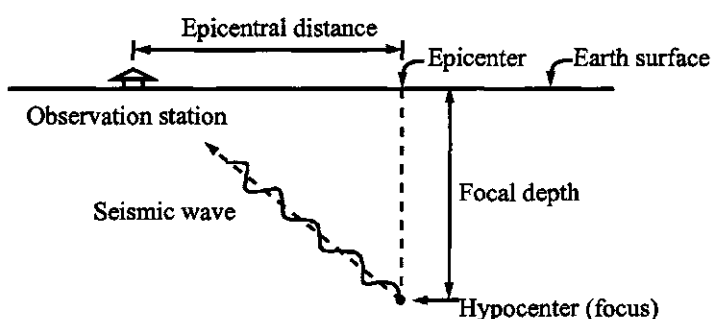


FIG. 7.1 Earthquake terminology.

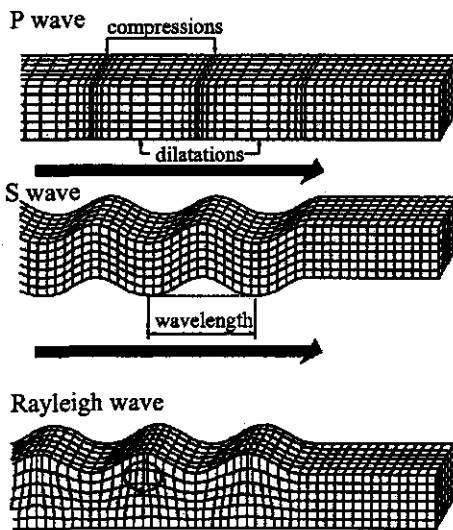


FIG. 7.2 Types of seismic waves.

released by an earthquake. Force generated by an earthquake is usually expressed in terms of gravitational acceleration.

7.2.2.1. Intensity

The intensity of an earthquake is based on damage and observed effects on people, buildings, and other objects. It varies from one place to another within a disturbed region. An earthquake in a densely populated area that results in severe damage and loss of life may have the same magnitude (see the next section) as one in a remote area that does not cause much damage, but the intensity of the earthquake in a densely populated area is much higher than in a remote area.

The Mercalli scale was developed in 1902 by Italian priest and geologist Giuseppe Mercalli, and later modified by American seismologists H.O. Wood and Frank Neumann to include descriptions of damage to more modern structures. The Modified Mercalli scale consists of 12 increasing levels of intensity expressed as Roman numerals following the initials MM. Numerical values are based on direct experience of people and structural damage observed. An abridgement of the MM scale, as prepared by Wood and Neumann, follows:

- I. Not felt except by a very few under especially favorable conditions.
- II. Felt only by a few persons at rest, especially on upper floors of buildings. Delicately suspended objects may swing.
- III. Felt quite noticeably indoors, especially on upper floors of buildings, but many people do not recognize it as an earthquake. Standing vehicles may rock slightly. Vibration similar to a truck passing.
- IV. During the day felt indoors by many, outdoors by a few. At night, some awakened. Dishes, windows, and doors disturbed; walls make cracking sound. Sensation like heavy truck striking building. Standing vehicles rock noticeably.
- V. Felt by nearly everyone; many awakened. Some dishes, windows, etc., broken. Unstable objects overturned. Disturbance of trees, poles, and other tall objects sometimes noticed. Pendulum clocks may stop.
- VI. Felt by all; many frightened and run outdoors. Some heavy furniture moves; few instances of fallen plaster or damaged chimneys. Overall damage slight.

- VII. Everybody runs outdoors. Damage negligible in buildings of good design and construction; damage slight to moderate in well-built ordinary structures; considerable damage in poorly built structures. Some chimneys broken. Noticed by persons driving vehicles.
- VIII. Damage slight in specially designed structures; considerable damage in ordinary substantial buildings with partial collapse. Damage great in poorly built structures. Panel walls thrown out of frame structures. Fall of chimneys, factory stacks, columns, monuments, and walls. Heavy furniture overturned. Sand and mud ejected in small amounts. Changes in well water. Disturbs persons driving vehicles.
- IX. Damage considerable in specially designed structures; well-designed frame structures thrown out of plumb. Damage great in substantial buildings with partial collapse. Buildings shifted off foundations. Ground cracked conspicuously. Underground pipes broken.
- X. Some well-built wooden structures destroyed; most masonry and frame structures destroyed along with foundations; ground badly cracked. Rails bent. Landslides considerable from riverbanks and steep slopes. Sand and mud shift. Water splashes over bank.
- XI. Few, if any, masonry structures remain standing. Bridges destroyed. Rails bent greatly. Broad fissures in ground. Underground pipelines completely out of service. Earth slumps and land slips in soft ground.
- XII. Damage total. Wave motion seen on ground surface. Lines of sight and level distorted. Objects thrown in the air.

7.2.2.2. *Magnitude*

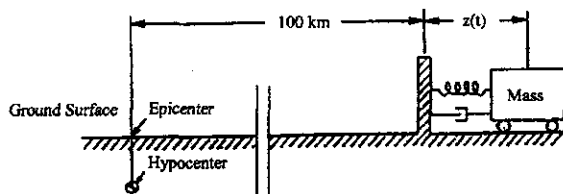
Earthquake magnitude is directly measured by instruments called *seismograms*. This technique was developed by Charles F. Richter in 1934. The Richter scale is actually open-ended. It technically has no upper or lower limit. The smallest earthquakes generally measure above zero; the largest ever recorded measured 8.9. The magnitude, M , of an earthquake is determined from the logarithm of the amplitude recorded by a seismometer as

$$M = \log_{10} \left(\frac{A}{A_0} \right) \quad (7.3)$$

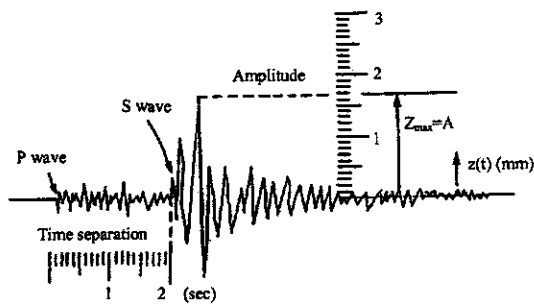
in which A is the maximum amplitude of the seismometer trace (see Fig. 7.3). A_0 is a constant equal to 0.001 mm resulting from the seismometer reading produced by a standard calibration earthquake. Because Richter magnitude, M , is a logarithmic scale, each whole-number increase in magnitude represents a 10-fold increase in measured amplitude. For example, an earthquake measuring 6.0 on the Richter scale has ground waves 10 times stronger than an earthquake measuring 5.0 on the same scale. People can slightly detect a measurement of 2.0. A 5.0 magnitude earthquake can damage structures, and those measuring 6.0 can inflict severe damage. Earthquakes measuring between 7.0 and 8.0 can be catastrophic.

Equation (7.3) assumes that a distance of 100 km separates the seismometer and the epicenter. For other distances, the Richter magnitude should be modified. In such cases, the nomograph of Fig. 7.4 with the following procedure can be used to calculate magnitude.

1. Determine the time between the arrival of the P- and S-waves. For example, the time difference between P- and S-waves in Fig. 7.3(b) is 2 sec.
2. Determine the maximum amplitude of oscillation A . In Fig. 7.3(b), $A = Z_{\max} = 1.7$ mm.
3. Connect the arrival time difference on the left scale and amplitude on the right scale with a straight line.
4. Read the Richter magnitude on the center scale. For example, the Richter magnitude is 2.9 for the earthquake shown in Fig. 7.3(b).
5. Read the distance separating the seismometer and the epicenter on the left scale. From Fig. 7.4, the distance is about 80 km for the earthquake shown in Fig. 7.3(b).



(a) Definition of Richter Magnitude



(b) Typical Seismometer Amplitude

FIG. 7.3 Seismograph and seismometer amplitude recording. (a) Definition of Richter magnitude. (b) Typical Seismometer amplitude.

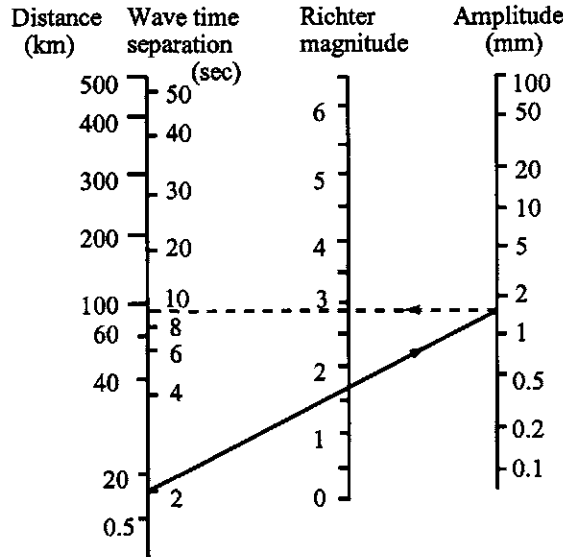


FIG. 7.4 Richter magnitude correction technique.

While one seismometer can approximate distance to the epicenter, it takes three seismometers to reliably locate the epicenter. As shown in Fig. 7.5, three seismometers designated C1, C2, and C3 are located at sites 1, 2, and 3, respectively. Approximate distances to the epicenter measured from C1, C2, and C3 are a , b , and c . From this figure, the epicenter based on seismometers C1 and C2 is located at either point A or B. However, if seismometer C3 exists and is applied, the epicenter can be located with certainty at point B.

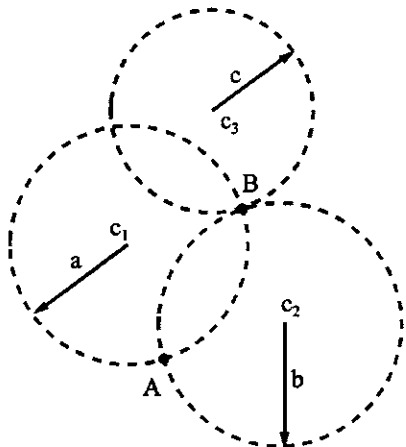


FIG. 7.5. Epicenter location.

7.2.2.3. Peak Ground Acceleration

Peak ground acceleration (PGA), measured by a seismometer or accelerometer, is one of the most important characteristics of an earthquake. PGA represents a maximum measured value and is commonly expressed in terms of gravitational acceleration, g , although it can be given in various units as length (ft, m, or in) per second squared. Thus, $\text{PGA} = (\text{acceleration in ft/sec}^2 / 32.2)$ represents a fraction of g which has a unit of ft/sec^2 .

Earthquake acceleration records used to analyze a structure at a given location may not be directly obtained from instrumentation on that site. However, earthquake records from a neighboring station may be modified to find the acceleration needed by using appropriate acceleration attenuation formulations such as

$$a_1 = a \left(\frac{R_2 + 0.0606e^{0.7M}}{R_1 + 0.0606e^{0.7M}} \right)^{1.09} \quad (7.4)$$

where a_1 is modified acceleration; a = peak acceleration in g (gravity acceleration) obtained from a neighboring instrumentation station; M = magnitude of earthquake at that station; R_1 = distance from epicenter to structure being analyzed, in kilometers; and R_2 = distance from epicenter to instrumentation station, also in kilometers. For the Mission-Gothic Undercrossing collapse during the 1994 Northridge earthquake, an instrumentation station at Sylmar County Hospital parking lot was about 18 km from the epicenter, R_2 ; the bridge was about 7.5 km from the epicenter, R_1 ; and the magnitude of the earthquake was 6.7, M . Therefore, the modifying coefficient is obtained as $a_1/a = 1.16$. This coefficient was used to amplify the parking lot's earthquake records for N-S, E-W, and vertical components in the bridge analysis.

7.2.3. Relationship Between Seismic Zone, Acceleration, Magnitude, and Intensity

The primary factors affecting structural damage due to earthquake are: (1) *earthquake characteristics*, such as peak ground acceleration, duration of strong shaking, and frequency content; (2) *site characteristics*, such as distance and geology between epicenter and structure, soil conditions at the site, and natural period of the site; and (3) *structural characteristics*, such as natural period and damping of the structure, and seismic provisions included in the design.

In order to design a structure to withstand the effects of an earthquake, many seismic codes have evolved a simplified model based on seismic zones. This method is to correlate the zone with approximate ground acceleration, Richter magnitudes, and Modified Mercalli Intensity Scale

as shown in Table 7.1. The seismic zones and their corresponding *effective peak ground accelerations* (EPGA) are from the 1994 Uniform Building Code. PGA and EPGA can be related to each other but are not necessarily the same. When very high frequencies are present in ground motion, the EPGA can be significantly less than PGA. EPGA includes the effect of ground motion frequencies as well as duration (more on the subject is presented in Section 10.9.4).

The relationship between earthquake magnitude, intensity, and annual incidence is shown in Table 7.2.

7.2.4. Earthquake Principal Components

As noted in Section 7.2.1, earthquake motions are considered as several types of waves propagating through the earth's crust. These waves mix together and cause random ground motion. For dynamic analysis of structures, it is usual to consider two horizontal components (N-S, E-W) and sometimes three components: two horizontal (N-S, E-W) and one vertical. Studies of the correlative character of translational components have shown that, in general, the N-S, E-W, and vertical components are statistically correlated. However, there is a set of three orthogonal axes along which the ground translational components, called *earthquake principal components*, are not correlated. These three independent components are called *main*, *intermediate*, and *minor principal components*. They represent the maximum, intermediate, and minimum acceleration of motion, respectively. The orientation of the main principal component, \ddot{u}_x , is along the epicentral direction (see Fig. 7.6) in which \ddot{u}_y and \ddot{u}_z represent the intermediate and minor principal components. For a three-dimensional structure subjected

TABLE 7.1 Seismic Zone, Effective Peak Ground Acceleration, Peak Ground Acceleration, Magnitude, and Intensity

Zone	Effective peak ground acceleration	Peak ground acceleration	Maximum magnitude	MM intensity
1	0.075 g	0.08 g	4.75	Minor damage corresponding to MM V and VI
2A	0.15 g	0.16 g	5.75	Moderate damage corresponding to MM VII
2B	0.20 g			
3	0.3 g	0.33 g	7.00	Major damage corresponding to MM VIII and higher

TABLE 7.2 Magnitude, Intensity, and Expected Annual Incidence

Richter Magnitude	MM Intensity	Expected Annual Incidence
Below 3.0	I	1,000,000
3.0-3.9	II-III	49,000
4.0-4.9	IV-V	6,200
5.0-5.9	VI-VII	800
6.0-6.9	VII-VIII	120
7.0-7.9	IX-X	18
8.0-8.9	XI-XII	Fewer than 1

Source: Magnitude and intensity: measures of earthquake size and severity. Earthq Information Bulletin, September–October 1974.

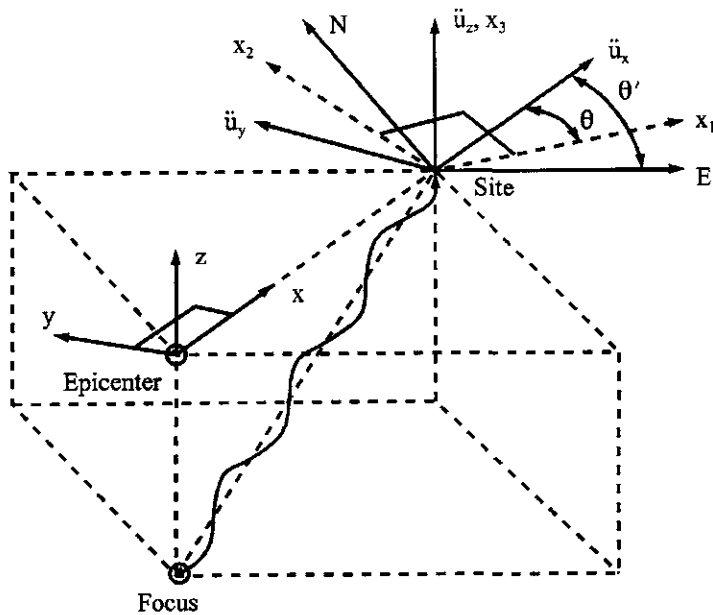


FIG. 7.6 Earthquake principal components.

to multi-component seismic input, structural response is dependent on the orientation (i.e. reference area x_1, x_2, x_3) of the structure with respect to the earthquake principal component's direction. A structure should be capable of resisting earthquake motion from any possible direction.

As shown in Fig. 7.6, earthquake principal acceleration records can be calculated from N–S, E–W, and vertical acceleration records. The relationships of earthquake principal components to N–S, E–W, and vertical components are as follows:

$$\left. \begin{aligned} \ddot{u}_x(t) &= \ddot{u}_{E-W}(t) \cos \theta' + \ddot{u}_{N-S}(t) \sin \theta' \\ \ddot{u}_y(t) &= -\ddot{u}_{E-W}(t) \sin \theta' + \ddot{u}_{N-S}(t) \cos \theta' \\ \ddot{u}_z(t) &= \ddot{u}_{\text{vertical}}(t) \end{aligned} \right\} \quad (7.5)$$

in which θ' is the angle from the \ddot{u}_{E-W} component to the \ddot{u}_x component. \ddot{u}_{E-W} , \ddot{u}_{N-S} , and $\ddot{u}_{\text{vertical}}$ are actual acceleration records in the E–W, N–S, and vertical directions, respectively. Similarly, principal velocity records, \dot{u}_x , \dot{u}_y , and \dot{u}_z , can be obtained by

$$\left. \begin{aligned} \dot{u}_x(t) &= \dot{u}_{E-W}(t) \cos \theta' + \dot{u}_{N-S}(t) \sin \theta' \\ \dot{u}_y(t) &= -\dot{u}_{E-W}(t) \sin \theta' + \dot{u}_{N-S}(t) \cos \theta' \\ \dot{u}_z(t) &= \dot{u}_{\text{vertical}}(t) \end{aligned} \right\} \quad (7.6)$$

For the 18 May, 1940 El Centro earthquake, the orientation of the main principal component was reported to be 26° clockwise measured from the north direction, or $\theta' = 64^\circ$ [19]. Therefore, the main and intermediate principal components of that earthquake can be obtained by substituting $\theta' = 64^\circ$ into Eq. (7.5) as

$$\ddot{u}_x(t) = \ddot{u}_{E-W}(t) \cos(64^\circ) + \ddot{u}_{N-S}(t) \sin(64^\circ) \quad (7.7)$$

$$\ddot{u}_y(t) = -\ddot{u}_{E-W}(t) \sin(64^\circ) + \ddot{u}_{N-S}(t) \cos(64^\circ) \quad (7.8)$$

7.3. NUMERICAL INTEGRATION AND STABILITY

The dynamic response of a multiple-d.o.f. system subjected to the three components of earthquake excitation can be obtained by solving the following motion equation:

$$[M]\{\ddot{x}(t)\} + [C]\{\dot{x}(t)\} + [K]\{x(t)\} = \{F(t)\} \quad (7.9)$$

in which $\{\ddot{x}(t)\}$ signifies N-S, E-W, and vertical earthquake accelerations. The solution of Eq. (7.9) can be obtained by numerical integration techniques. The three well-known numerical techniques, Newmark, Wilson-θ, and Runge-Kutta fourth-order, are discussed next.

7.3.1. Newmark Integration Method

The Newmark integration method assumes that, during an incremental time, Δt , acceleration varies linearly as shown in Fig. 7.7. Average acceleration from t to $t + \Delta t$ is $\{\ddot{x}\}_{\text{avg}} = \frac{1}{2}(\{\ddot{x}(t)\} + \{\ddot{x}(t + \Delta t)\})$. Thus the velocity vector at $t + \Delta t$ can be expressed as

$$\begin{aligned} \{\dot{x}(t + \Delta t)\} &= \{\dot{x}(t)\} + \Delta t\{\ddot{x}\}_{\text{avg}} \\ &= \{\dot{x}(t)\} + \frac{\Delta t}{2}(\{\ddot{x}(t)\} + \{\ddot{x}(t + \Delta t)\}) \end{aligned} \quad (7.10)$$

The displacement vector at $t + \Delta t$ can be obtained from Eq. (7.10) as $\{x(t + \Delta t)\} = \{x(t)\} + \Delta t\{\dot{x}\}_{\text{avg}}$ in which $\{\dot{x}\}_{\text{avg}} = \frac{1}{2}(\{\dot{x}(t)\} + \{\dot{x}(t + \Delta t)\})$ or

$$\{x(t + \Delta t)\} = \{x(t)\} + \{\dot{x}(t)\}\Delta t + \frac{(\Delta t)^2}{4}(\{\ddot{x}(t)\} + \{\ddot{x}(t + \Delta t)\}) \quad (7.11)$$

Equations (7.10) and (7.11) represent the *Newmark trapezoidal rule* or the *average acceleration method*. The general Newmark integration may be expressed as

$$\{\dot{x}(t + \Delta t)\} = \{\dot{x}(t)\} + [(1 - \delta)(\ddot{x}(t)) + \delta(\ddot{x}(t + \Delta t))]\Delta t \quad (7.12)$$

$$\{x(t + \Delta t)\} = \{x(t)\} + \{\dot{x}(t)\}\Delta t + \left[\left(\frac{1}{2} - \alpha \right) (\ddot{x}(t)) + \alpha (\ddot{x}(t + \Delta t)) \right] (\Delta t)^2 \quad (7.13)$$

where α and δ are parameters that can be determined to obtain integration accuracy and stability. When $\delta = \frac{1}{2}$ and $\alpha = \frac{1}{4}$, Eqs. (7.12) and (7.13) correspond to the average acceleration method. When $\delta = \frac{1}{2}$ and $\alpha = 1/6$, Eqs. (7.12) and (7.13) are then associated with the *linear acceleration method*.

From Eq. (7.13),

$$\{\ddot{x}(t + \Delta t)\} = \frac{1}{\alpha \Delta t^2} \left[\{x(t + \Delta t)\} - \{x(t)\} - \Delta t\{\dot{x}(t)\} - \Delta t^2 \left(\frac{1}{2} - \alpha \right) \{\ddot{x}(t)\} \right] \quad (7.14)$$

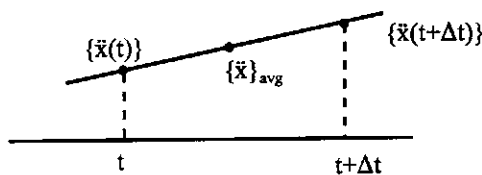


FIG. 7.7 Linear variation of acceleration.

Substituting Eq. (7.14) into Eq. (7.12) leads to

$$\{\ddot{x}(t + \Delta t)\} = \{\dot{x}(t)\} + \left[(1 - \delta)\{\ddot{x}(t)\} + \delta \left\{ \frac{1}{\alpha \Delta t^2} \left[\{x(t + \Delta t)\} - \{x(t)\} \right. \right. \right. \\ \left. \left. \left. - \Delta t\{\dot{x}(t)\} - \Delta t^2 \left(\frac{1}{2} - \alpha \right) \{\ddot{x}(t)\} \right] \right\} \right] \Delta t \quad (7.15)$$

Employing Eqs. (7.14) and (7.15) in Eq. (7.9) at $t + \Delta t$ gives

$$[M] \left\{ \frac{1}{\alpha \Delta t^2} \{x(t + \Delta t)\} - \frac{1}{\alpha \Delta t^2} \{x(t)\} - \frac{1}{\alpha \Delta t} \{\dot{x}(t)\} - \frac{1}{\alpha} \left(\frac{1}{2} - \alpha \right) \{\ddot{x}(t)\} \right\} + [C] \left\{ \{\dot{x}(t)\} + (1 - \delta) \Delta t \{\ddot{x}(t)\} \right. \\ \left. + \frac{\delta}{\alpha \Delta t} \{x(t + \Delta t)\} - \frac{\delta}{\alpha \Delta t} \{x(t)\} - \frac{\delta}{\alpha} \{\dot{x}(t)\} - \frac{\delta \Delta t}{\alpha} \left(\frac{1}{2} - \alpha \right) \{\ddot{x}(t)\} \right\} + [K] \{x(t + \Delta t)\} \\ = \{F(t + \Delta t)\} \quad (7.16)$$

Based on time-increment approach, response parameters are known at t but unknown at $t + \Delta t$; collecting appropriate terms in the above yields

$$\left(\frac{1}{\alpha \Delta t^2} [M] + \frac{\delta}{\alpha \Delta t} [C] + [K] \right) \{x(t + \Delta t)\} = \{F(t + \Delta t)\} + [M] \left[\frac{1}{\alpha \Delta t^2} \{x(t)\} + \frac{1}{\alpha \Delta t} \{\dot{x}(t)\} + \frac{1}{\alpha} \left(\frac{1}{2} - \alpha \right) \right. \\ \left. \{\ddot{x}(t)\} \right] + [C] \left[\frac{\delta}{\alpha \Delta t} \{x(t)\} + \left(\frac{\delta}{\alpha} - 1 \right) \{\dot{x}(t)\} + \left(\frac{\delta \Delta t}{\alpha} \left(\frac{1}{2} - \alpha \right) - (1 - \delta) \Delta t \right) \{\ddot{x}(t)\} \right] \quad (7.17)$$

Let

$$a_0 = \frac{1}{\alpha \Delta t^2}, \quad a_1 = \frac{\delta}{\alpha \Delta t}, \quad a_2 = \frac{1}{\alpha \Delta t}, \quad a_3 = \frac{1}{2\alpha} - 1, \quad a_4 = \frac{\delta}{\alpha} - 1, \text{ and } a_5 = \frac{\Delta t}{2} \left(\frac{\delta}{\alpha} - 2 \right)$$

Eq. (7.17) becomes

$$(a_0[M] + a_1[C] + [K]) \{x(t + \Delta t)\} = \{F(t + \Delta t)\} + [M](a_0 \{x(t)\} + a_2 \{\dot{x}(t)\} + a_3 \{\ddot{x}(t)\}) \\ + [C](a_1 \{x(t)\} + a_4 \{\dot{x}(t)\} + a_5 \{\ddot{x}(t)\}) \quad (7.18)$$

or

$$[\bar{K}](x(t + \Delta t)) = \{\bar{F}\} \quad (7.18a)$$

from which $\{x(t + \Delta t)\}$ can be obtained. Substituting $\{x(t + \Delta t)\}$ in Eq. (7.14) leads to

$$\{\ddot{x}(t + \Delta t)\} = a_0 [\{x(t + \Delta t)\} - \{x(t)\}] - a_2 \{\dot{x}(t)\} - a_3 \{\ddot{x}(t)\} \quad (7.19)$$

Employing $\{\ddot{x}(t + \Delta t)\}$ from Eq. (7.19) in Eq. (7.12), we have

$$\{\dot{x}(t + \Delta t)\} = \{\dot{x}(t)\} + a_6 \{\ddot{x}(t)\} + a_7 \{\ddot{x}(t + \Delta t)\} \quad (7.20)$$

where $a_6 = \Delta t(1 - \delta)$ and $a_7 = \delta \Delta t$. When $\alpha = 1/6$ and $\delta = 1/2$, the Newmark integration method becomes the linear acceleration method; Eqs. (7.18), (7.19), and (7.20) are then expressed as Eqs. (7.20a), (7.21), and (7.22), respectively.

$$\left(\frac{6}{\Delta t^2} [M] + \frac{3}{\Delta t} [C] + [K] \right) \{x(t + \Delta t)\} = \{F(t + \Delta t)\} - [M]\{A\} - [C]\{B\} \quad (7.20a)$$

or

$$[\bar{K}]\{x(t + \Delta t)\} = \{\bar{F}(t + \Delta t)\} \quad (7.20b)$$

$$\begin{aligned} \{\ddot{x}(t + \Delta t)\} &= \frac{6}{\Delta t^2} [\{x(t + \Delta t)\} - \{x(t)\}] - \frac{6}{\Delta t} \{\dot{x}(t)\} - 2\{\ddot{x}(t)\} \\ &= \frac{6}{\Delta t^2} \{x(t + \Delta t)\} + \{A\} \end{aligned} \quad (7.21)$$

$$\begin{aligned} \{\dot{x}(t + \Delta t)\} &= \{\dot{x}(t)\} + \frac{\Delta t}{2} \left[\{\ddot{x}(t)\} + \frac{6}{\Delta t^2} \{x(t + \Delta t)\} - \frac{6}{\Delta t^2} \{x(t)\} - \frac{6}{\Delta t} \{\dot{x}(t)\} - 2\{\ddot{x}(t)\} \right] \\ &= \frac{3}{\Delta t} \{x(t + \Delta t)\} + \{B\} \end{aligned} \quad (7.22)$$

in which

$$\{A\} = -\frac{6}{\Delta t^2} \{x(t)\} - \frac{6}{\Delta t} \{\dot{x}(t)\} - 2\{\ddot{x}(t)\} \quad (7.23)$$

and

$$\{B\} = -2\{\dot{x}(t)\} - \frac{\Delta t}{2} \{\ddot{x}(t)\} - \frac{3}{\Delta t} \{x(t)\} \quad (7.24)$$

EXAMPLE 7.3.1 Let $\{\Delta x\} = \{x(t + \Delta t)\} - \{x(t)\}$, $\{\Delta \dot{x}\} = \{\dot{x}(t + \Delta t)\} - \{\dot{x}(t)\}$, and $\{\Delta \ddot{x}\} = \{\ddot{x}(t + \Delta t)\} - \{\ddot{x}(t)\}$. Derive Eqs. (7.20a), (7.21), and (7.22) of the linear acceleration method in incremental form.

Solution: Since the displacement response is due to time increment Δt , the external force should also be expressed incrementally. Thus Eq. (7.20a) should be written as

$$\left(\frac{6}{\Delta t^2} [M] + \frac{3}{\Delta t} [C] + [K] \right) \{\Delta x\} = (\{F(t + \Delta t)\} - \{F(t)\}) - [M]\{A\} - [C]\{B\} \quad (a)$$

From Eq. (7.21),

$$\begin{aligned} \{\Delta \ddot{x}\} &= \{\ddot{x}(t + \Delta t)\} - \{\ddot{x}(t)\} = \frac{6}{\Delta t^2} \{x(t + \Delta t)\} + \{A\} - \{\ddot{x}(t)\} \\ &= \frac{6}{\Delta t^2} \{x(t + \Delta t)\} - \frac{6}{\Delta t^2} \{x(t)\} - \frac{6}{\Delta t} \{\dot{x}(t)\} - 2\{\ddot{x}(t)\} - \{\ddot{x}(t)\} \\ &= \frac{6}{\Delta t^2} \{\Delta x\} + \{C\} \end{aligned} \quad (b)$$

in which

$$\{C\} = -\frac{6}{\Delta t} \{\dot{x}(t)\} - 3\{\ddot{x}(t)\} \quad (c)$$

From Eq. (7.22)

$$\begin{aligned} \{\Delta \dot{x}\} &= \{\dot{x}(t + \Delta t)\} - \{\dot{x}(t)\} = \frac{3}{\Delta t} \{x(t + \Delta t)\} + \{B\} - \{\dot{x}(t)\} \\ &= \frac{3}{\Delta t} \{x(t + \Delta t)\} - 2\{\dot{x}(t)\} - \frac{\Delta t}{2} \{\ddot{x}(t)\} - \frac{3}{\Delta t} \{x(t)\} - \{\dot{x}(t)\} \\ &= \frac{3}{\Delta t} \{\Delta x\} + \{D\} \end{aligned} \quad (d)$$

in which

$$\{D\} = -3\{\dot{x}(t)\} - \frac{\Delta t}{2}\{\ddot{x}(t)\} \quad (e)$$

7.3.2. Wilson- θ Method

The Wilson- θ method is an extension of the linear acceleration method in which a linear variation of acceleration from time t to $t + \Delta t$ is assumed. In the Wilson- θ method, acceleration is assumed to be linear from time t to $t + \theta\Delta t$, with $\theta \geq 1$ ($\theta = 1$ is the linear acceleration method), as shown in Fig. 7.8. Let $\{\Delta x\}$, $\{\Delta \dot{x}\}$, and $\{\Delta \ddot{x}\}$ be expressed as

$$\left. \begin{aligned} \{\Delta x\} &= \{x(t + \Delta t)\} - \{x(t)\} \\ \{\Delta \dot{x}\} &= \{\dot{x}(t + \Delta t)\} - \{\dot{x}(t)\} \\ \{\Delta \ddot{x}\} &= \{\ddot{x}(t + \Delta t)\} - \{\ddot{x}(t)\} \end{aligned} \right\} \quad (7.25)$$

The incremental velocity vector from t to $t + \tau$ can be expressed as

$$\begin{aligned} \{\Delta \dot{x}_\tau\} &= \{\dot{x}(t + \tau)\} - \{\dot{x}(t)\} = \frac{1}{2}[\{\ddot{x}(t)\} + \{\ddot{x}(t + \tau)\}]\tau \\ &= \frac{1}{2}\left[\{\ddot{x}(t)\} + \{\ddot{x}(t)\} + ((\{\ddot{x}(t + \Delta t)\} - \{\ddot{x}(t)\})\frac{\tau}{\Delta t})\right]\tau \\ &= \{\ddot{x}(t)\}\tau + \frac{\tau^2}{2\Delta t}[\{\ddot{x}(t + \Delta t)\} - \{\ddot{x}(t)\}] \\ &= \{\ddot{x}(t)\}\tau + \frac{\tau^2}{2\Delta t}\{\Delta \ddot{x}\} \end{aligned} \quad (7.26)$$

Integrating Eq. (7.26), we have

$$\int_0^\tau [\dot{x}(t + \tau)] d\tau - \int_0^\tau [\dot{x}(t)] d\tau = \int_0^\tau [\ddot{x}(t)\tau] d\tau + \int_0^\tau \frac{\tau^2}{2\Delta t} \{\Delta \ddot{x}\} d\tau$$

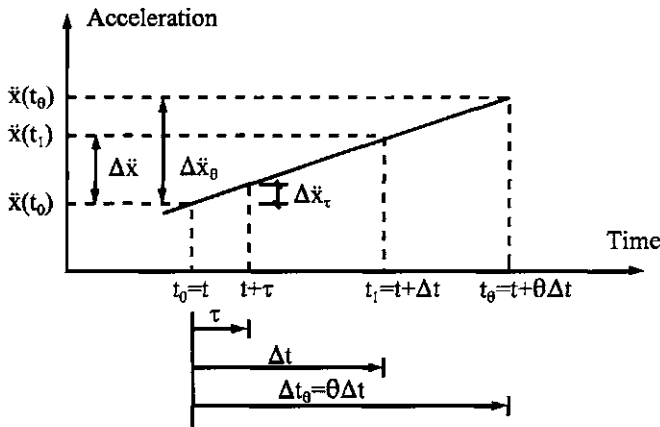


FIG. 7.8 Wilson- θ integration method.

After integration and rearrangement,

$$\{x(t + \tau)\} = \{x(t)\} + \tau\{\dot{x}(t)\} + \frac{\tau^2}{2}\{\ddot{x}(t)\} + \frac{\tau^3}{6\Delta t}\{\Delta\ddot{x}\} \quad (7.27)$$

or

$$\{\Delta x_\tau\} = \tau\{\dot{x}(t)\} + \frac{\tau^2}{2}\{\ddot{x}(t)\} + \frac{\tau^3}{6\Delta t}\{\Delta\ddot{x}\} \quad (7.27a)$$

Since the Wilson-θ method assumes linear variation of acceleration from t to $t + \theta\Delta t$, Eqs. (7.26) and (7.27a) can also be expressed as Eqs. (7.27b) and (7.27c), respectively, with $t \leq \tau \leq t + \theta\Delta t$.

$$\{\Delta\dot{x}_\tau\} = \{\ddot{x}(t)\}\tau + \frac{\tau^2}{2\theta\Delta t}\{\Delta\ddot{x}_\theta\} \quad (7.27b)$$

$$\{\Delta x_\tau\} = \tau\{\dot{x}(t)\} + \frac{\tau^2}{2}\{\ddot{x}(t)\} + \frac{\tau^3}{6\theta\Delta t}\{\Delta\ddot{x}_\theta\} \quad (7.27c)$$

When $\tau = \theta\Delta t$, let $\Delta t_\theta = \theta\Delta t$; Eqs. (7.27b) and (7.27c) are reduced to

$$\{\Delta\dot{x}_\theta\} = \{\ddot{x}(t)\}\Delta t_\theta + \frac{1}{2}\{\Delta\ddot{x}_\theta\}\Delta t_\theta \quad (7.28)$$

$$\{\Delta x_\theta\} = \{\dot{x}(t)\}\Delta t_\theta + \frac{1}{2}\{\ddot{x}(t)\}(\Delta t_\theta)^2 + \frac{1}{6}\{\Delta\ddot{x}_\theta\}(\Delta t_\theta)^2 \quad (7.29)$$

From Eq. (7.29)

$$\begin{aligned} \{\Delta\ddot{x}_\theta\} &= \frac{6}{(\Delta t_\theta)^2} \left[\{\Delta x_\theta\} - \{\dot{x}(t)\}\Delta t_\theta - \frac{1}{2}\{\ddot{x}(t)\}(\Delta t_\theta)^2 \right] \\ &= \frac{6}{(\Delta t_\theta)^2}\{\Delta x_\theta\} - \frac{6}{\Delta t_\theta}\{\dot{x}(t)\} - 3\{\ddot{x}(t)\} \end{aligned} \quad (7.30)$$

Substituting Eq. (7.30) into Eq. (7.28) results in

$$\begin{aligned} \{\Delta\dot{x}_\theta\} &= \{\ddot{x}(t)\}\Delta t_\theta + \frac{3}{\Delta t_\theta}\{\Delta x_\theta\} - 3\{\dot{x}(t)\} - \frac{3\Delta t_\theta}{2}\{\ddot{x}(t)\} \\ &= \frac{3}{\Delta t_\theta}\{\Delta x_\theta\} - 3\{\dot{x}(t)\} - \frac{\Delta t_\theta}{2}\{\ddot{x}(t)\} \end{aligned} \quad (7.31)$$

Based on Eq. (7.9), the incremental equation of motion can be expressed as

$$[M]\{\Delta\dot{x}_\theta\} + [C]\{\Delta\dot{x}_\theta\} + [K]\{\Delta x_\theta\} = \{\Delta F_\theta\} \quad (7.32)$$

in which

$$\{\Delta F_\theta\} = \theta\{\Delta F\} = \theta[\{F(t + \Delta t)\} - \{F(t)\}]$$

Substituting Eqs. (7.30) and (7.31) into Eq. (7.32) leads to

$$[\tilde{K}]\{\Delta x_\theta\} = \{\Delta \tilde{F}\} \quad (7.33)$$

where

$$[\tilde{K}] = [K] + \frac{6}{(\Delta t_\theta)^2}[M] + \frac{3}{\Delta t_\theta}[C] \quad (7.34)$$

and

$$\{\Delta\bar{F}\} = \{\Delta F_\theta\} + [M]\{Q\} + [C]\{R\} \quad (7.35)$$

in which

$$\{\Delta F_\theta\} = \theta\{\Delta F\} \quad (7.36)$$

$$\{Q\} = \frac{6}{\Delta t_\theta} \{\dot{x}(t)\} + 3\{\ddot{x}(t)\} \quad (7.37)$$

$$\{R\} = 3\{\dot{x}(t)\} + \frac{\Delta t_\theta}{2} \{\ddot{x}(t)\} \quad (7.38)$$

Equation (7.33) is solved for $\{\Delta x_\theta\}$ as

$$\{\Delta x_\theta\} = [\bar{K}]^{-1}\{\Delta F\} \quad (7.39)$$

Then the incremental acceleration vector, $\{\Delta\ddot{x}_\theta\}$, can be obtained from Eq. (7.30) and $\{\Delta\ddot{x}\}$ is determined by the following formula:

$$\{\Delta\ddot{x}\} = \frac{1}{\theta}\{\Delta\ddot{x}_\theta\} \quad (7.40)$$

The incremental velocity vector, $\{\Delta\dot{x}\}$, and displacement vector, $\{\Delta x\}$, are obtained from Eqs. (7.26) and (7.27) at $\tau = \Delta t$, respectively. Total displacement, velocity, and acceleration vectors are determined from

$$\{x(t + \Delta t)\} = \{x(t)\} + \{\Delta x\} \quad (7.41)$$

$$\{\dot{x}(t + \Delta t)\} = \{\dot{x}(t)\} + \{\Delta\dot{x}\} \quad (7.42)$$

$$\{\ddot{x}(t + \Delta t)\} = \{\ddot{x}(t)\} + \{\Delta\ddot{x}\} \quad (7.43)$$

7.3.3. General Numerical Integration Related to Newmark and Wilson-θ Methods

Displacement-response formulas shown in Eqs. (7.11), (7.13), and (7.27) may be related to a *general integration* expression, written as

$$x_{n+1} = \sum_{L=n-k}^n A_L x_L + \sum_{L=n-k}^{n+1} B_L \dot{x}_L + \sum_{L=n-k}^{n+1} C_L \ddot{x}_L + R; \quad k = 0 - n \quad (7.44)$$

where x , \dot{x} , and \ddot{x} represent displacement, velocity, and acceleration, respectively; n represents the n th time step; x_{n+1} represents displacement at time $(n+1)h$ in which h is the time interval; R is a remainder term (or error term) signifying the error in the expression; and A_L , B_L , and C_L are constants, some of which may equal zero. By inspection of Eq. (7.44), the equation has $m = 5 + 3k$ constants in which 5 represents five coefficients of A_0 , B_0 , C_0 , B_{n+1} and C_{n+1} . For instance,

$k = 0$

$$x_{n+1} = A_n x_n + B_n \dot{x}_n + B_{n+1} \dot{x}_{n+1} + C_n \ddot{x}_n + C_{n+1} \ddot{x}_{n+1} + R \quad (7.44a)$$

$k = n$

$$\begin{aligned} x_{n+1} = & A_0 x_0 + A_1 x_1 + A_2 x_2 + \dots + A_n x_n \\ & + B_0 \dot{x}_0 + B_1 \dot{x}_1 + B_2 \dot{x}_2 + \dots + B_n \dot{x}_n + B_{n+1} \dot{x}_{n+1} \\ & + C_0 \ddot{x}_0 + C_1 \ddot{x}_1 + C_2 \ddot{x}_2 + \dots + C_n \ddot{x}_n + C_{n+1} \ddot{x}_{n+1} + R \end{aligned} \quad (7.44b)$$

By a suitable choice of the values for these constants, Eq. (7.44) can be made exact in the special case where x is a polynomial of order $m - 1$, i.e. $x = t^{m-1}$. With this exactness, the remainder R equals zero. If Eq. (7.44) is exact for a polynomial of order $m - 1$, it is likewise exact for

$$x = 1, t, t^2, \dots, t^{m-1} \quad (7.45)$$

To evaluate the m constants, we can set x equal to each of the values in Eq. (7.45) and make a substitution in Eq. (7.44) with remainder term $R = 0$. This procedure yields m simultaneous equations involving the set of m coefficients A_L, B_L , and C_L . A solution of these equations provides the required values for the coefficients.

If $x = t^m$ is substituted into Eq. (7.44), R is not equal to zero and the value of R is designated as $R = E_m$. Therefore, Eq. (7.44), which is exact for polynomials up to an order $m - 1$, has a truncation error E_m when $x = t^m$. It is of interest to estimate the truncation error term when x is a polynomial of order higher than m , or x is a function other than a polynomial. To obtain an expression for the remainder R , we start with the Taylor series and let $a = (n - k)h$. Then

$$\begin{aligned} x(t) &= x(a) + (t - a)x'(a) + \frac{(t - a)^2}{2!}x''(a) + \dots \\ &\quad + \frac{(t - a)^{m-1}}{(m - 1)!}x^{(m-1)}(a) + \frac{1}{(m - 1)!} \int_a^t x^{(m)}(s)(t - s)^{m-1} ds \end{aligned} \quad (7.46)$$

Here x' is the same as \dot{x} , and x'' is the same as \ddot{x} ; \dot{x} and \ddot{x} were used previously in this section. Eq. (7.46) can be expressed as

$$x(t) = \sum_{j=0}^{m-1} \frac{x^{(j)}(a)}{j!}(t - a)^j + \frac{1}{(m - 1)!} \int_a^t x^{(m)}(s)(t - s)^{m-1} ds \quad (7.47)$$

Let $t = (n + 1)h = b$, $i = n - k$. We now substitute Eq. (7.47) into both sides of Eq. (7.44), that is, for x_{n+1} (left side) and for x_L , \dot{x}_L , and \ddot{x}_L (right side). The error in Eq. (7.44) is the difference between the two sides of the equation. As noted previously, Eq. (7.44) is exact when x is expressed as shown in Eq. (7.45). Therefore, the corresponding polynomial terms are cancelled out and we have only the integral term to be substituted into the two sides of Eq. (7.44). This becomes

$$\begin{aligned} \frac{1}{(m - 1)!} \int_a^b x^{(m)}(s)(b - s)^{m-1} ds &= \sum_{L=i}^n A_L \int_a^{t_L} \frac{1}{(m - 1)!} x^{(m)}(s)(t_L - s)^{m-1} ds \\ &\quad + \sum_{L=i}^{n+1} \frac{B_L}{(m - 1)!} \frac{d}{dt_L} \int_a^{t_L} x^{(m)}(s)(t_L - s)^{m-1} ds \\ &\quad + \sum_{L=i}^{n+1} \frac{C_L}{(m - 1)!} \frac{d^2}{dt_L^2} \int_a^{t_L} x^{(m)}(s)(t_L - s)^{m-1} ds + R \end{aligned} \quad (7.48)$$

or

$$\begin{aligned} R &= \frac{1}{(m - 1)!} \int_a^b x^{(m)}(s)(b - s)^{m-1} ds - \sum_{L=i}^n A_L \int_a^{t_L} \frac{1}{(m - 1)!} x^{(m)}(s)(t_L - s)^{m-1} ds \\ &\quad - \sum_{L=i}^{n+1} \frac{B_L}{(m - 1)!} \frac{d}{dt_L} \int_a^{t_L} x^{(m)}(s)(t_L - s)^{m-1} ds - \sum_{L=i}^{n+1} \frac{C_L}{(m - 1)!} \frac{d^2}{dt_L^2} \int_a^{t_L} x^{(m)}(s)(t_L - s)^{m-1} ds \end{aligned} \quad (7.48a)$$

in which t_L represents time at Lh . In order to eliminate the cumbersome notations at the upper limit t_L in the integrals, the following is introduced for $m > 0$

$$(t-s)_+^m = \begin{cases} 0 & \text{if } t-s \leq 0 \\ (t-s)^m & \text{if } t-s > 0 \end{cases} \quad (7.48b)$$

Using this notation, the upper limit in the integrals of Eq. (7.48a) is increased from t_L to b as follows:

$$\begin{aligned} R &= \frac{1}{(m-1)!} \int_a^b x^{(m)}(s) \left[(b-s)^{m-1} - \sum_{L=i}^n A_L (t_L - s)_+^{m-1} - \sum_{L=i}^{n+1} B_L \frac{d(t_L - s)_+^{m-1}}{dt_L} - \sum_{L=i}^{n+1} C_L \frac{d^2(t_L - s)_+^{m-1}}{dt_L^2} \right] ds \\ &= \int_a^b x^{(m)}(s) G(s) ds \end{aligned} \quad (7.49)$$

in which

$$\begin{aligned} G(s) &= \frac{1}{(m-1)!} \left[(b-s)^{m-1} - \sum_{L=i}^n A_L (t_L - s)_+^{m-1} - \sum_{L=i}^{n+1} B_L (m-1)(m-2)(t_L - s)_+^{m-2} \right. \\ &\quad \left. - \sum_{L=i}^{n+1} C_L (m-1)(m-2)(t_L - s)_+^{m-3} \right] \end{aligned} \quad (7.49a)$$

The particular function $x(t) = t^m$ enables us to compute the integral of $G(s)$ from Eq. (7.49) as

$$R(t^m) = \int_a^b x^{(m)}(s) G(s) ds = \int_a^b \frac{d^m(t^m)}{dt^m} G(s) ds = m! \int_a^b G(s) ds = E_m \neq 0 \quad (7.50)$$

where $R(t^m)$ is the R value at $x=t^m$ and $t=b$.

If x is not a function other than a polynomial, then, by the *mean-value theorem*, we can further write Eq. (7.49) as

$$R = \int_a^b x^{(m)}(s) G(s) ds = x^{(m)}(\xi) \int_a^b G(s) ds; \quad a < \xi < b \quad (7.51)$$

The mean-value concept is shown in Fig. 7.9 where area A is assumed to be equal to area B . Thus

$$\begin{aligned} A &= \int_a^b x^{(m)}(s) G(s) ds = B \\ &= x^{(m)}(\xi) G(\xi) (b-a) = x^{(m)}(\xi) \int_a^b G(s) ds \end{aligned} \quad (7.52)$$

From Eqs. (7.50) and (7.51), the remainder R can be expressed as

$$R = \frac{E_m}{m!} x^{(m)}(\xi); \quad a \leq \xi \leq b \quad (7.53)$$

in which $a=(n-k)h$, $b=(n+1)h$, and $x^{(m)}(\xi)$ is the value of the m th differential of x at $t=\xi$. In general, parameter ξ is not known, and it may not be possible to obtain a precise value for

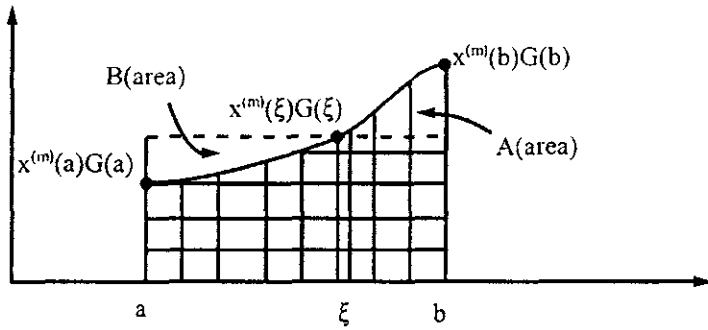


FIG. 7.9 Mean-value theorem.

R. But Eq. (7.53) can often be used to provide an upper limit on R. An estimate of the truncation error term may be helpful in choosing one formula [Eq. (7.44)] over the other.

EXAMPLE 7.3.2 Derive the Newmark integration formulas by the general method of Section 7.3.4 and compare the formulas derived with Eqs. (7.12) and (7.13). Also calculate the remainder R for displacement and velocity expressions.

Solution: Similar to Eq. (7.44), the velocity expression is written as

$$\dot{x}_{n+1} = a_1 \dot{x}_n + a_2 \ddot{x}_n + a_3 \ddot{x}_{n+1} \quad (\text{a})$$

If $x=1$, $\dot{x}=0$, and $\ddot{x}=0$, then Eq. (a) is satisfied with $x=1$. Since the total constants are 3 ($m=3$), namely a_1 , a_2 , and a_3 , we use two of them to make Eq. (a) exact for $x=t$ and t^2 , and leave one of the constants slack. When $x=t$, $\dot{x}=1$, and $\ddot{x}=0$, Eq. (a) becomes

$$1 = a_1 + 0 + 0; \quad a_1 = 1 \quad (\text{b})$$

When $x=t^2$, $\dot{x}=2t$, and $\ddot{x}=2$, (a) becomes

$$2t_{n+1} = (1)(2t)_n + 2a_2 + 2a_3$$

By using the notation, $h = \Delta t$, $t_{n+1} = (n+1)\Delta t$, the above may be written as

$$2(n+1)h = 2(nh) + 2a_2 + 2a_3 \quad (\text{c})$$

Therefore

$$a_2 + a_3 = h$$

Let $a_3 = \delta h$, where δ is an arbitrary constant; we get

$$a_2 = h - a_3 = h - \delta h = (1 - \delta)h \quad (\text{d})$$

Substituting Eqs. (b) and (d) into Eq. (a) yields

$$\begin{aligned} \dot{x}_{n+1} &= \dot{x}_n + (1 - \delta)h\ddot{x}_n + \delta h\ddot{x}_{n+1} \\ &= \dot{x}_n + [(1 - \delta)\dot{x}_n + \delta \ddot{x}_{n+1}]h \end{aligned} \quad (\text{e})$$

Eq. (e) has the same expression as Eq. (7.12). Now the velocity expression is written as

$$\dot{x}_{n+1} = \dot{x}_n + [(1 - \delta)\dot{x}_n + \delta \ddot{x}_{n+1}]h + R \quad (\text{f})$$

The remainder term R is obtained by substituting $x=t^3$ in Eq. (f). When $x=t^3$, $\dot{x}=3t^2$, and

$\ddot{x} = 6t$, Eq. (f) becomes

$$3(n+1)^2h^2 = 3n^2h^2 + h(1-\delta)6(nh) + \delta h(6(n+1)h) + E_3 \quad (\text{g})$$

or

$$E_3 = h^2(3 - 6\delta) \quad (\text{h})$$

Using Eqs. (7.53) and (h)

$$R = \frac{E_3}{3!}x^{(3)}(\xi) = h^2\left(\frac{1}{2} - \delta\right)x^{(3)}(\xi) \quad (\text{i})$$

For displacement, use the following expression

$$x_{n+1} = b_1x_n + b_2\dot{x}_n + b_3\ddot{x}_n + b_4\dddot{x}_{n+1} \quad (\text{j})$$

When $x = 1$, t , t^2 , and t^3 , Eq. (j) is then exact. Therefore

$$x = 1; \quad \text{then } b_1 = 1 \quad (\text{k})$$

$$x = t, \quad (n+1)h = (1)nh + b_2 + 0 + 0; \quad \text{then } b_2 = h \quad (\text{l})$$

$$x = t^2, \quad (n+1)^2h^2 = (1)n^2h^2 + 2nh^2 + 2(b_3 + b_4); \quad \text{then } 2(b_3 + b_4) = h^2 \quad (\text{m})$$

Letting $b_4 = \alpha h^2$, where α is an arbitrary value, gives

$$b_3 = \left(\frac{1}{2} - \alpha\right)h^2 \quad (\text{n})$$

Substituting Eqs. (k), (l), and (n) into Eq. (j) leads to

$$x_{n+1} = x_n + h\dot{x}_n + \left[\left(\frac{1}{2} - \alpha\right)\ddot{x}_n + \alpha\ddot{x}_{n+1}\right]h^2 \quad (\text{o})$$

which gives the same expression as Eq. (7.13). Now the displacement expression is written as

$$x_{n+1} = x_n + h\dot{x}_n + \left[\left(\frac{1}{2} - \alpha\right)\ddot{x}_n + \alpha\ddot{x}_{n+1}\right]h^2 + R \quad (\text{p})$$

The remainder term R in Eq. (p) can be obtained by substituting $x = t^3$ in the equation. When $x = t^3$, $\dot{x} = 3t^2$, and $\ddot{x} = 6t$, Eq. (p) becomes

$$\begin{aligned} E_3 &= (n+1)^3h^3 - n^3h^3 - 3h^3n^2 - h^2\left(\frac{1}{2} - \alpha\right)(6nh) - 6(n+1)(h^3)\alpha \\ &= h^3(1 - 6\alpha) \end{aligned} \quad (\text{q})$$

and

$$R = \frac{E_3}{3!}x^{(3)}(\xi) = h^3\left(\frac{1}{6} - \alpha\right)x^{(3)}(\xi) \quad (\text{r})$$

7.3.4. Runge-Kutta Fourth-Order Method

The Runge-Kutta fourth-order method is designed to approximate the Taylor series numerical solutions of first-order differential equations. In Eq. (7.9), the motion equation is of the

second-order and can be expressed as

$$\{\ddot{x}(t)\} = [M]^{-1}(\{F(t)\} - [K]\{x(t)\} - [C]\{\dot{x}(t)\}) \quad (7.54)$$

or in symbolic form

$$\{\ddot{x}(t)\} = \{f(t, x(t), \dot{x}(t))\} \quad (7.55)$$

In order to reduce Eq. (7.54) from second-order to first-order, let $v = \dot{x}$. Then Eq. (7.55) can be transformed into two first-order differential equations as

$$\{\dot{v}(t)\} = \{f(t, x, v)\} \quad (7.56)$$

and

$$\{\dot{x}(t)\} = \{F(t, x)\} \quad (7.57)$$

We can use Runge-Kutta fourth-order formulas to solve Eqs. (7.56) and (7.57). Derivations of Runge-Kutta fourth-order formulas are detailed as follows.

Given the first-order differential equation, $y' = dy/dx = f(x, y) = f$, with initial conditions $y(x_0) = y_0$, the solution $y(x_0 + h)$ can be expressed in the form of the Taylor series as

$$y(x_0 + h) = y_0 + hy'_0 + \frac{h^2}{2!}y''_0 + \frac{h^3}{3!}Y'''_0 + \frac{h^4}{4!}y^{iv}_0 + \dots \quad (7.58)$$

in which $h = (x - x_0)$.

Since $y' = f$, the total differential, dy' , is $dy' = (\partial f / \partial y) dx$; y'' can be expressed as

$$y'' = \frac{dy'}{dx} = \frac{\partial f}{\partial x} + \frac{\partial f}{\partial y} \frac{dy}{dx} = f_x + f_y f \quad (7.59)$$

Similarly

$$\begin{aligned} y''' &= \frac{dy''}{dx} = \frac{\partial y''}{\partial x} + \frac{\partial y''}{\partial y} \frac{dy}{dx} \\ &= \frac{\partial(f_x + f_y f)}{\partial x} + \frac{\partial(f_x + f_y f)}{\partial y} \frac{dy}{dx} \\ &= f_{xx} + 2f_{xy} + f^2 f_{yy} + f_y f_x + f_y f_y \end{aligned} \quad (7.60)$$

Let $D = \partial/\partial x + f(\partial/\partial y)$ as an operator; then $D^2 = [(\partial/\partial x) + f(\partial/\partial y)]^2 = \partial^2/\partial x^2 + 2f[(\partial^2/\partial x \partial y)] + f^2(\partial^2/\partial y^2)$, and

$$D^3 = \frac{\partial^3}{\partial x^3} + 3f \frac{\partial^3}{\partial x^2 \partial y} + 3f^2 \frac{\partial^3}{\partial x \partial y^2} + f^3 \frac{\partial^3}{\partial y^3}.$$

Thus

$$\left. \begin{aligned} y' &= f \\ y'' &= f_x + f_y = Df \\ y''' &= f_{xx} + 2f_{xy} + f^2 f_{yy} + f_y(f_x + f_y) = D^2 f + f_y Df \end{aligned} \right\} \quad (7.61)$$

Similarly

$$D^3 f = \frac{\partial^3 f}{\partial x^3} + 3f \frac{\partial^3 f}{\partial x^2 \partial y} + 3f^2 \frac{\partial^3 f}{\partial x \partial y^2} + f^3 \frac{\partial^3 f}{\partial y^3}$$

Then we have

$$y^{iv} = \frac{\partial(D^2f + f_y Df)}{\partial x} + \frac{\partial(D^2f + f_y Df)}{\partial y} \frac{dy}{dx} = D^3f + f_y D^2f + f_y^2 Df + 3Df Df_y \quad (7.62)$$

Substituting Eqs. (7.61) and (7.62) into Eq. (7.58) yields

$$\begin{aligned} y(x_0 + h) - y(x_0) &= hy'_0 + \frac{h^2}{2!} y''_0 + \frac{h^3}{3!} y'''_0 + \frac{h^4}{4!} y^{iv}_0 + \dots \\ &\approx hy'_0 + \frac{h^2}{2!} y''_0 + \frac{h^3}{3!} y'''_0 + \frac{h^4}{4!} y^{iv}_0 \\ &= \left[hf + \frac{h^2}{2!} Df + \frac{h^3}{3!} (D^2f + f_y Df) \right. \\ &\quad \left. + \frac{h^4}{4!} (D^3f + f_y D^2f + f_y^2 Df + 3Df Df_y) \right]_{x=x_0} \end{aligned} \quad (7.63)$$

in which terms whose order is higher than four are omitted. Eq. (7.63) thus has a truncation error of h^5 . Since $f = dy/dx$ or $dy = f dx$, Eq. (7.58) can also be expressed as

$$\begin{aligned} y(x_0 + h) &= y(x_0) + \int_{x_0}^{x_0+h} \frac{dy}{dx} dx \\ &= y(x_0) + \int_{x_0}^{x_0+h} f(x, y) dx \end{aligned} \quad (7.64)$$

By using mean-value theorem, the integral of Eq. (7.64) can further be expressed as

$$\begin{aligned} y(x_0 + h) - y(x_0) &= \int_0^{x_0+h} f(x, y) dx \\ &= hf(x_0 + \theta h, y(x_0 + \theta h)) \end{aligned} \quad (7.65)$$

in which $0 < \theta < h$. Note that Eqs. (7.65) and (7.63) are equivalent. Therefore, we first set the equivalence which is then assumed to be expressed in a linear equation as

$$hf(x_0 + \theta h, y(x_0 + \theta h)) = y(x_0 + h) - y(x_0) = \mu_1 k_1 + \mu_2 k_2 + \mu_3 k_3 + \mu_4 k_4 \quad (7.66)$$

in which

$$\left. \begin{array}{l} k_1 = hf(x_0, y_0) = hf_0 \\ k_2 = hf(x_0 + \alpha h, y_0 + \beta k_1) \\ k_3 = hf(x_0 + \alpha_1 h, y_0 + \beta_1 k_1 + \gamma_1 k_2) \\ k_4 = hf(x_0 + \alpha_2 h, y_0 + \beta_2 k_1 + \gamma_2 k_2 + \delta_2 k_3) \end{array} \right\} \quad (7.67)$$

where $\mu_1, \mu_2, \mu_3, \mu_4, \alpha, \beta, \alpha_1, \alpha_2, \beta_1, \beta_2, \gamma_1, \gamma_2$, and δ_2 are the constants to be determined by applying Taylor series theorem to expand $f(x_0, y_0)$, $f(x_0 + \alpha h, y_0 + \beta k_1)$, $f(x_0 + \alpha_1 h, y_0 + \beta_1 k_1 + \gamma_1 k_2)$, and $f(x_0 + \alpha_2 h, y_0 + \beta_2 k_1 + \gamma_2 k_2 + \delta_2 k_3)$ in Eq. (7.67). Before expanding them, the Taylor series for

function of two variables is summarized as follows:

$$f(x_0 + \alpha_r, y_0 + \beta_r) = \left[f(x, y) + D_r f(x, y) + \frac{D_r^2 f(x, y)}{2!} + \frac{D_r^3 f(x, y)}{3!} + \frac{D_r^4 f(x, y)}{4!} + \dots \right]_{x=x_0} \quad (7.68)$$

in which the operator is defined as

$$D_r = \alpha_r \frac{\partial}{\partial x} + \beta_r \frac{\partial}{\partial y} \quad (7.69)$$

where α_r and β_r are scalars. Based on the Taylor series expressed in Eq. (7.68), k_1, k_2, k_3 , and k_4 of Eq. (7.67) can be further expressed as

$$k_1 = hf(x_0, y_0) = hf_0 \quad (7.70)$$

$$\begin{aligned} k_2 &= hf(x_0 + \alpha h, y_0 + \beta k_1) \\ &= h \left[f + D_{11} f + \frac{D_{11}^2 f}{2!} + \frac{D_{11}^3 f}{3!} + \frac{D_{11}^4 f}{4!} + \dots \right]_{x=x_0} \\ &= h \left[f + h D_{11} f + \frac{h^2}{2!} D_{11}^2 f + \frac{h^3}{3!} D_{11}^3 f + \frac{h^4}{4!} D_{11}^4 f + \dots \right]_{x=x_0} \end{aligned} \quad (7.70a)$$

where $D_{11} = (\alpha h) \partial/\partial x + (\beta k_1) \partial/\partial y$ and $D_{11} = D_{11}/h$. Similarly, let $D_{21} = \alpha_1 h (\partial/\partial x) + (\beta_1 k_1 + \gamma_1 k_2) (\partial/\partial y)$ and $D_2 = \alpha_1 (\partial/\partial x) + (\beta_1 + \gamma_1) f_0 (\partial/\partial y)$. Then

$$\begin{aligned} D_{21} &= \alpha_1 h \frac{\partial}{\partial x} + (\beta_1 k_1 + \gamma_1 k_2) \frac{\partial}{\partial y} \\ &= h \left(\alpha_1 \frac{\partial}{\partial x} + \beta_1 f_0 \frac{\partial}{\partial y} \right) + \gamma_1 k_2 \frac{\partial}{\partial y} \\ &= h D_2 + \gamma_1 (k_2 - h f_0) \frac{\partial}{\partial y} \\ &= h D_2 + \gamma_1 \left[h^2 D_{11} f + \frac{h^3}{2!} D_{11}^2 f + \frac{h^4}{3!} D_{11}^3 f + \frac{h^5}{4!} D_{11}^4 f + \dots \right]_{x=x_0} \frac{\partial}{\partial y} \\ &= h D_2 + h^2 \gamma_1 \left[D_{11} f + \frac{h}{2!} D_{11}^2 f + \frac{h^2}{3!} D_{11}^3 f + \dots \right]_{x=x_0} \frac{\partial}{\partial y} \end{aligned} \quad (7.71)$$

$$\begin{aligned} D_{31} &= \alpha_2 h \frac{\partial}{\partial x} + (\beta_2 k_1 + \gamma_2 k_2 + \delta_2 k_3) \frac{\partial}{\partial y} \\ &= h D_3 + [\gamma_2 (k_2 - h f_0) + \delta_2 (k_3 - h f_0)] \frac{\partial}{\partial y} \end{aligned}$$

From Eq. (7.71), k_3 can be expanded as

$$\begin{aligned}
 k_3 &= hf(x_0 + \alpha_1 h, y_0 + \beta_1 k_1 + \gamma_1 k_2) \\
 &= h \left[f + D_{21}f + \frac{D_{21}^2 f}{2!} + \frac{D_{21}^3 f}{3!} + \frac{D_{21}^4 f}{4!} + \dots \right]_{x=x_0} \\
 &= h \left\{ \left[f + hD_{21}f + \frac{h^2}{2!} D_{21}^2 f + \frac{h^3}{3!} D_{21}^3 f + \frac{h^4}{4!} D_{21}^4 f + \dots \right] \right. \\
 &\quad \left. + h^2 \gamma_1 \left[f_y D_{11}f + \frac{h}{2!} f_y D_{11}^2 f + h D_{11}f D_{21}f_y + \frac{h^2}{3!} f_y D_{11}^3 f + \dots \right] \dots \right\}
 \end{aligned} \tag{7.72}$$

For k_4 , substitute k_2 and k_3 of Eqs. (7.70) and (7.72) into D_{31} as

$$\begin{aligned}
 D_{31} &= hD_3 + h^2 \left\{ \gamma_2 \left[D_{11}f + \frac{h}{2!} D_{11}^2 f + \frac{h^2}{3!} D_{11}^3 f + \frac{h^3}{4!} D_{11}^4 f + \dots \right] + \delta_2 \left[D_{21}f + \frac{h}{2} (D_{21}^2 f + 2\gamma_1 f_y D_{11}f) \right. \right. \\
 &\quad \left. \left. + \frac{h^2}{3!} D_{21}^3 f + \frac{h}{2!} \gamma_1 f_y D_{21}^2 f + h^2 \gamma_1 D_{11}f D_{21}f_y + \dots \right] \right\}_{x=x_0} \frac{\partial}{\partial y}
 \end{aligned}$$

Consequently

$$\begin{aligned}
 k_4 &= hf(x_0 + \alpha_2 h, y_0 + \beta_2 k_1 + \gamma_2 k_2 + \delta_2 k_3) \\
 &= h \left[f + D_{31}f + \frac{D_{31}^2 f}{2!} + \frac{D_{31}^3 f}{3!} + \frac{D_{31}^4 f}{4!} + \dots \right]_{x=x_0} \\
 &= h \left\{ f + hD_{31}f + h^2 f_y \left[\gamma_2 \left(D_{11}f + \frac{h}{2!} D_{11}^2 f + \frac{h^2}{3!} D_{11}^3 f + \dots \right) \right. \right. \\
 &\quad \left. \left. + \delta_2 \left(D_{21}f + h\gamma_1 f_y D_{11}f + \frac{h}{2!} D_{21}^2 f + \frac{h^2}{2} \gamma_1 f_y D_{11}^2 f \right. \right. \right. \\
 &\quad \left. \left. \left. + h^2 \gamma_1 D_{11}f D_{21}f_y + \frac{h^2}{3!} D_{21}^3 f + \dots \right) \right] \right. \\
 &\quad \left. + \frac{1}{2!} \left(h^2 D_{31}^2 f + 2h^3 D_{31}f_y \left[\gamma_2 \left(D_{11}f + \frac{h}{2} D_{11}^2 f + \dots \right) \right. \right. \right. \\
 &\quad \left. \left. \left. + \delta_2 \left(D_{21}f + \frac{h}{2!} D_{21}^2 f + h\gamma_1 f_y D_{11}f + \dots \right) \right] \right. \right. \\
 &\quad \left. \left. \left. + h^4 f_{yy} \left[\gamma_2^2 D_{11}^2 f + 2\gamma_2 \delta_2 D_{11}f D_{21}f + \delta_2^2 (D_{21}f)^2 + \dots \right] \right] \right) \\
 &\quad \left. + \frac{1}{3!} (h^3 D_{31}^3 f + 3h^4 D_{31}^2 f_y [\gamma_2 D_{11}f + \delta_2 D_{21}f + \dots]) \right. \\
 &\quad \left. + \frac{1}{4!} (h^4 D_{31}^4 f + \dots) + \dots \right\}_{x=x_0}
 \end{aligned} \tag{7.73}$$

Now substitute Eqs. (7.70), (7.70a), (7.72), and (7.73) into Eq. (7.66); compare the developed form of Eq. (7.66) with Eq. (7.63); then equate the coefficients of the corresponding terms. This com-

parison leads to a set of equations having 13 parameters as shown below:

$$\left. \begin{array}{l} \mu_1 + \mu_2 + \mu_3 + \mu_4 = 1 \\ \mu_2 D_1 f + \mu_3 D_2 f + \mu_4 D_3 f = \frac{1}{2!} D^2 f \\ \mu_2 D_1^2 f + \mu_3 D_2^2 f + \mu_4 D_3^2 f = (2!) \left(\frac{1}{3!} \right) D^2 f \\ \mu_2 D_1^3 f + \mu_3 D_2^3 f + \mu_4 D_3^3 f = (3!) \left(\frac{1}{4!} \right) D^3 f \\ \mu_3 \gamma_1 D_1 f + \mu_4 (\gamma_2 D_1 f + \delta_2 D_2 f) = \left(\frac{1}{3!} \right) D f \\ \mu_3 \gamma_1 D_1^2 f + \mu_4 (\gamma_2 D_1^2 f + \delta_2 D_2^2 f) = (2!) \left(\frac{1}{4!} \right) D^2 f \\ \mu_3 \gamma_1 D_1 f D_2 f_y + \mu_4 (\gamma_2 D_1 f D_3 f_y + \delta_2 D_2 f D_3 f_y) = \left(\frac{3}{4!} \right) D f D f_y \\ \mu_4 \gamma_1 \delta_2 D_1 f = \left(\frac{1}{4!} \right) D f \end{array} \right\} \quad (7.74)$$

in which

$$\left. \begin{array}{l} D = \frac{\partial}{\partial x} + f_0 \frac{\partial}{\partial y} \\ D_1 = \alpha \frac{\partial}{\partial x} + \beta f_0 \frac{\partial}{\partial y} \\ D_2 = \alpha_1 \frac{\partial}{\partial x} + (\beta_1 + \gamma_1) f_0 \frac{\partial}{\partial y} \\ D_3 = \alpha_2 \frac{\partial}{\partial x} + (\beta_2 + \gamma_2 + \delta_2) f_0 \frac{\partial}{\partial y} \end{array} \right\} \quad (7.74a)$$

For Eq. (7.74) to be applicable to all functions f , the ratio, $(D_r^j f)/(D^j f)$ ($r, j = 1, 2, 3$), must be constant. Therefore, the ratios of D_1/D , D_2/D , D_3/D are constant if $\alpha = \beta$, $\alpha_1 = \beta_1 + \gamma_1$, and $\alpha_2 = \beta_2 + \gamma_2 + \delta_2$ in Eq. (7.75). Thus

$$\left. \begin{array}{l} D_1 = \alpha D \\ D_2 = \alpha_1 D \\ D_3 = \alpha_2 D \end{array} \right\} \quad (7.75)$$

Inserting Eq. (7.75) into Eq. (7.74) yields

$$\left. \begin{array}{l} \mu_1 + \mu_2 + \mu_3 + \mu_4 = 1 \\ \mu_2 \alpha D f + \mu_3 \alpha_1 D f + \mu_4 \alpha_2 D f = \frac{1}{2} D f \\ \mu_2 \alpha^2 D^2 f + \mu_3 \alpha_1^2 D^2 f + \mu_4 \alpha_2^2 D^2 f = \frac{1}{3} D^2 f \\ \mu_2 \alpha^3 D^3 f + \mu_3 \alpha_1^3 D^3 f + \mu_4 \alpha_2^3 D^3 f = \frac{1}{4} D^3 f \\ \mu_3 \gamma_1 \alpha D f + \mu_4 (\gamma_2 \alpha D f + \delta_2 \alpha_1 D f) = \frac{1}{6} D f \\ \mu_3 \gamma_1 \alpha^2 D^2 f + \mu_4 (\gamma_2 \alpha^2 D^2 f + \delta_2 \alpha_1^2 D^2 f) = \frac{1}{12} D^2 f \\ \mu_3 \gamma_1 \alpha D f \alpha_1 D f_y + \mu_4 (\gamma_2 \alpha D f \alpha_2 D f_y + \delta_2 \alpha_1 D f \alpha_2 D f_y) = \frac{1}{8} D f D f_y \\ \mu_4 \gamma_1 \delta_2 \alpha D f = \frac{1}{24} D f \end{array} \right\} \quad (7.76)$$

or

$$\left. \begin{array}{l} \mu_1 + \mu_2 + \mu_3 + \mu_4 = 1 \\ \mu_2 \alpha + \mu_3 \alpha_1 + \mu_4 \alpha_2 = \frac{1}{2} \\ \mu_2 \alpha^2 + \mu_3 \alpha_1^2 + \mu_4 \alpha_2^2 = \frac{1}{3} \\ \mu_2 \alpha^3 + \mu_3 \alpha_1^3 + \mu_4 \alpha_2^3 = \frac{1}{4} \\ \mu_3 \gamma_1 \alpha + \mu_4 (\alpha \gamma_2 + \alpha_1 \delta_2) = \frac{1}{6} \\ \mu_3 \gamma_1 \alpha^2 + \mu_4 (\alpha^2 \gamma_2 + \alpha_1^2 \delta_2) = \frac{1}{12} \\ \mu_3 \gamma_1 \alpha \alpha_1 + \mu_4 (\alpha \alpha_2 \gamma_2 + \alpha_1 \alpha_2 \delta_2) = \frac{1}{8} \\ \mu_4 \alpha \gamma_1 \delta_2 = \frac{1}{24} \end{array} \right\} \quad (7.77)$$

Equation (7.77) is a set of eight equations with 10 unknown parameters: $\mu_1, \mu_2, \mu_3, \mu_4, \alpha, \alpha_1, \alpha_2, \gamma_1, \gamma_2$, and δ_2 . The equation thus has two d.o.f. Therefore, we can set two unknown arbitrary values. Taking $\alpha = 1/2$ and $\delta_2 = 1$ gives eight equations and eight unknowns. The results are

$$\left. \begin{array}{l} \alpha = 1/2 \\ \alpha_1 = 1/2 \\ \alpha_2 = 1 \\ \gamma_1 = 1/2 \\ \gamma_2 = 0 \\ \mu_1 = 1/6 \\ \mu_2 = 1/3 \\ \mu_3 = 1/3 \\ \mu_4 = 1/6 \end{array} \right\} \quad (7.78)$$

Consequently

$$\left. \begin{array}{l} \alpha = \beta = 1/2 \\ \alpha_1 = \beta_1 + \gamma_1 = \beta_1 + 1/2 = 1/2, \quad \beta_1 = 0 \\ \alpha_2 = \beta_2 + \gamma_2 + \delta_2 = \beta_2 + 0 + 1 = 1, \quad \beta_2 = 0 \end{array} \right\} \quad (7.79)$$

Substituting Eqs. (7.78) and (7.79) into Eqs. (7.67) and (7.66) yields

$$\left. \begin{array}{l} k_1 = hf(x_0, y_0) \\ k_2 = hf(x_0 + h/2, y_0 + k_1/2) \\ k_3 = hf(x_0 + h/2, y_0 + k_2/2) \\ k_4 = hf(x_0 + h, y_0 + k_3) \end{array} \right\} \quad (7.80)$$

and

$$\begin{aligned} y(x_0 + h) - y(x_0) &= \mu_1 k_1 + \mu_2 k_2 + \mu_3 k_3 + \mu_4 k_4 \\ &= 1/6[k_1 + 2k_2 + 2k_3 + k_4] \end{aligned} \quad (7.80a)$$

which is called the *Runge–Kutta fourth-order formula*. As noted previously, the Runge–Kutta fourth-order method is designed to approximate the solutions of first-order differential equations

such as Eqs. (7.56) and (7.57). Therefore, based on Eq. (7.80a), $v(t + \Delta t)$ can be expressed as

$$v(t + \Delta t) = v(t) + \frac{1}{6}(k_1 + 2k_2 + 2k_3 + k_4) \quad (7.81)$$

in which

$$\left. \begin{aligned} k_1 &= (\Delta t)f(t, x(t), v(t)) \\ k_2 &= (\Delta t)f\left(t + \frac{\Delta t}{2}, x(t) + \frac{q_1}{2}, v(t) + \frac{k_1}{2}\right) \\ k_3 &= (\Delta t)f\left(t + \frac{\Delta t}{2}, x(t) + \frac{q_2}{2}, v(t) + \frac{k_2}{2}\right) \\ k_4 &= (\Delta t)f(t + \Delta t, x(t) + q_3, v(t) + k_3) \end{aligned} \right\} \quad (7.82)$$

Similar to Eq. (7.81)

$$x(t + \Delta t) = x(t) + \frac{1}{6}(q_1 + 2q_2 + 2q_3 + q_4) \quad (7.83)$$

where

$$\left. \begin{aligned} q_1 &= (\Delta t)F(v(t)) = (\Delta t)v(t) \\ q_2 &= (\Delta t)F\left(v(t) + \frac{k_1}{2}\right) = (\Delta t)\left(v(t) + \frac{k_1}{2}\right) \\ q_3 &= (\Delta t)F\left(v(t) + \frac{k_2}{2}\right) = (\Delta t)\left(v(t) + \frac{k_2}{2}\right) \\ q_4 &= (\Delta t)F(v(t) + k_3) = (\Delta t)(v(t) + k_3) \end{aligned} \right\} \quad (7.84)$$

Now substitute Eq. (7.84) into Eqs. (7.82) and (7.83),

$$\left. \begin{aligned} k_1 &= (\Delta t)f(t, x(t), v(t)) \\ k_2 &= (\Delta t)f\left(t + \frac{\Delta t}{2}, x(t) + \frac{\Delta t}{2}v(t), v(t) + \frac{k_1}{2}\right) \\ k_3 &= (\Delta t)f\left(t + \frac{\Delta t}{2}, x(t) + \frac{\Delta t}{2}\left(v(t) + \frac{k_1}{2}\right), v(t) + \frac{k_2}{2}\right) \\ &= (\Delta t)f\left(t + \frac{\Delta t}{2}, x(t) + \frac{\Delta t}{2}v(t) + \frac{\Delta t}{4}k_1, v(t) + \frac{k_2}{2}\right) \\ k_4 &= (\Delta t)f\left(t + \Delta t, x(t) + \Delta t\left(v(t) + \frac{k_2}{2}\right), v(t) + k_3\right) \\ &= (\Delta t)f\left(t + \Delta t, x(t) + (\Delta t)v(t) + \frac{\Delta t}{2}k_2, v(t) + k_3\right) \end{aligned} \right\} \quad (7.85)$$

and

$$\begin{aligned} x(t + \Delta t) &= x(t) + \frac{1}{6}(q_1 + 2q_2 + 2q_3 + q_4) \\ &= x(t) + \frac{1}{6}\left[\Delta t v(t) + 2\Delta t\left(v(t) + \frac{k_1}{2}\right) + 2\Delta t\left(v(t) + \frac{k_2}{2}\right) + \Delta t(v(t) + k_3)\right] \\ &= x(t) + \frac{\Delta t}{6}[6v(t) + k_1 + k_2 + k_3] \\ &= x(t) + \Delta t \dot{x}(t) + \frac{\Delta t}{6}(k_1 + k_2 + k_3) \end{aligned} \quad (7.86)$$

From Eqs. (7.81), (7.85), and (7.86), the numerical solution for the motion equation of Eq. (7.9) based on the Runge–Kutta fourth-order method can be summarized as

$$\{x(t + \Delta t)\} = \{x(t)\} + \Delta t\{\dot{x}(t)\} + \frac{\Delta t}{6}(\{k_1\} + \{k_2\} + \{k_3\}) \quad (7.87)$$

$$\{\dot{x}(t + \Delta t)\} = \{\dot{x}(t)\} + \frac{1}{6}(\{k_1\} + 2\{k_2\} + 2\{k_3\} + \{k_4\}) \quad (7.88)$$

in which

$$\begin{aligned} \{k_1\} &= \Delta t[f(t, x(t), \dot{x}(t))] \\ &= \Delta t[M]^{-1}(\{F(t)\} - [K]\{x(t)\} - [C]\{\dot{x}(t)\}) \end{aligned} \quad (7.89)$$

$$\begin{aligned} \{k_2\} &= (\Delta t)\left\{f\left(t + \frac{\Delta t}{2}, x(t) + \frac{\Delta t}{2}v(t), v(t) + \frac{k_1}{2}\right)\right\} \\ &= (\Delta t)[M]^{-1}\left(\left\{F\left(t + \frac{\Delta t}{2}\right)\right\} - [K]\left(\{x(t)\} + \frac{\Delta t}{2}\{\dot{x}(t)\}\right) - [C]\left(\{\dot{x}(t)\} + \frac{1}{2}\{k_1\}\right)\right) \end{aligned} \quad (7.90)$$

$$\begin{aligned} \{k_3\} &= (\Delta t)\left\{f\left(t + \frac{\Delta t}{2}, x(t) + \frac{\Delta t}{2}v(t), v(t) + \frac{\Delta t}{4}k_1, v(t) + \frac{k_2}{2}\right)\right\} \\ &= (\Delta t)[M]^{-1}\left(\left\{F\left(t + \frac{\Delta t}{2}\right)\right\} - [K]\left(\{x(t)\} + \frac{\Delta t}{2}\{\dot{x}(t)\} + \frac{\Delta t}{4}\{k_1\}\right) \right. \\ &\quad \left.- [C]\left(\{\dot{x}(t)\} + \frac{1}{2}\{k_2\}\right)\right) \end{aligned} \quad (7.91)$$

$$\begin{aligned} \{k_4\} &= (\Delta t)\left\{f\left(t + \Delta t, x(t) + \Delta tv(t), v(t) + \frac{\Delta t}{2}k_2, v(t)k_3\right)\right\} \\ &= (\Delta t)[M]^{-1}\left(\{F(t + \Delta t)\} - [K]\left(\{x(t)\} + \Delta t\{\dot{x}(t)\} + \frac{\Delta t}{2}\{k_2\}\right) \right. \\ &\quad \left.- [C]\left(\{\dot{x}(t)\} + \{k_3\}\right)\right) \end{aligned} \quad (7.92)$$

Runge–Kutta formulation is a self-starting method for it only requires the functional values at a previous point. The method has a truncation error of order (h^3) .

EXAMPLE 7.3.3 The framework shown in Fig. 7.10 is subjected to lateral force, $F(t) = F_0(1 - t/\zeta)$, in which $F_0 = 45$ lb (200.170 N) and $\zeta = 0.03$ sec. Assume that the columns are massless and the girder is infinitely rigid. The lumped mass on the girder is $M = 0.5823$ lb sec²/in. (10.119 kg sec²/m). Let $h = 60$ in (1.524 m), $E = 30 \times 10^6$ psi (206.843×10^9 N/m²), $I = 5$ in⁴ (20.811×10^{-7} m⁴), and damping ratio $\rho = 0.1$. Using Newmark, Wilson-θ, and Runge–Kutta fourth-order methods, find the displacement response of the girder for $\Delta t = 0.005$ sec. Also find the exact solution by Duhamel's integrals. Use $\theta = 1.4$ for the Wilson method, and $\alpha = 1/6$ and $\delta = 1/2$ for the Newmark method (the merit of using the numerical values of θ , α , and δ is discussed in Section 7.3.5).

Solution: The differential equation for a single-d.o.f. system is

$$M\ddot{x} + C\dot{x} + Kx = F(t) \quad (a)$$

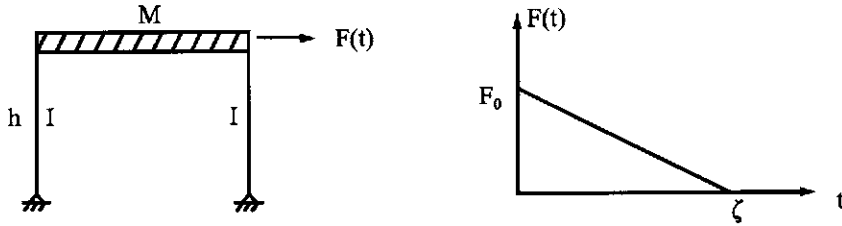


FIG. 7.10 Example 7.3.3.

in which

$$M = 0.5823 \text{ lb sec}^2/\text{in}; \quad K = 3E(2I)/h^3 = \frac{3(30 \times 10^6)(2 \times 5)}{(60)^3} = 4166.7 \text{ lb/in}$$

$$C = \rho C_{cr} = 2\rho\sqrt{KM} = 2(0.1)\sqrt{(4166.7)(0.58230)} = 9.8515 \text{ lb sec/in}$$

and

$$F(t) = 45(1 - t/0.03) \text{ lb}$$

Typical calculations at $t=0$ and 0.005 sec are illustrated as follows.

(a) *Newmark method with $\alpha = 1/6$ and $\delta = 1/2$* —At $t=0$, $x=\dot{x}=0$

$$\ddot{x} = F(t=0)/M = 45/0.5823 = 77.280 \text{ in/sec}^2$$

At $t = 0.005$ sec, from Eqs. (7.23) and (7.24),

$$A = -\frac{6 \times (0)}{(\Delta t)^2} - \frac{6\dot{x}(0)}{\Delta t} - 2\ddot{x}(0) = 0 - 2(77.280) = -154.560$$

$$B = -2\dot{x}(0) - \frac{\Delta t}{2}\ddot{x}(0) - \frac{3}{\Delta t}x(0) = \frac{-0.005}{2}(77.280) = -0.1932$$

From Eqs. (7.20a) and (7.20b)

$$\bar{K} = \frac{6M}{\Delta t^2} + \frac{3C}{\Delta t} + K = \frac{6(0.5823)}{(0.005)^2} + 3(9.8515)/0.005 + 4166.7 = 149,830$$

and

$$\bar{F} = F(0.005) - (M)(A) - (C)(B) = 37.5 - (0.5823)(-154.560) - (9.8515)(-0.1932) = 129.4033$$

Thus

$$x(0.005) = \bar{F}/\bar{K} = 129.4033/149830 = 0.8637 \times 10^{-3} \text{ in} \quad (\text{b})$$

From Eqs. (7.22) and (7.21),

$$\dot{x}(0.005) = \frac{3}{\Delta t}x(0.005) + B = \frac{3(0.8637 \times 10^{-3})}{0.005} + (-0.1932) = 0.3250 \text{ in/sec} \quad (\text{c})$$

$$\ddot{x}(0.005) = \frac{6}{\Delta t^2}x(0.005) + A = \frac{6(0.8637 \times 10^{-3})}{(0.005)^2} + (-154.56) = 52.7045 \text{ in/sec}^2 \quad (\text{d})$$

Successive responses at various time intervals can be similarly calculated. The entire results from $t=0$ through $t=0.03$ sec are listed in Table 7.3.

(b) Wilson-0 method with $\theta = 1.4$ —at $t = 0$, $x = \dot{x} = 0$

$$\ddot{x} = F(t = 0)/M = 45/0.5823 = 77.280 \text{ in/sec}^2$$

At $t = 0.005$ sec, from Eqs. (7.36), (7.37) and (7.38),

$$\Delta F_\theta = \theta \Delta F = 1.4(37.5 - 45) = -10.5 \text{ lb}$$

$$\Delta t_\theta = \theta \Delta t = 1.4(0.005) = 0.007 \text{ sec}$$

$$Q = \frac{6}{\Delta t_\theta} \dot{x}(0) + 3\ddot{x}(0) = 3(77.280) = 231.84$$

$$R = 3\dot{x}(0) + \frac{\Delta t_\theta}{2} \ddot{x}(0) = \frac{0.007}{2} (77.280) = 0.2704$$

From Eqs. (7.34) and (7.35),

$$\begin{aligned}\bar{K} &= K + \frac{6}{(\Delta t_\theta)^2} M + \frac{3}{\Delta t_\theta} C \\ &= 4166.7 + \frac{6}{(0.007)^2} (0.5823) + \frac{3}{0.007} (9.8515) = 79,690.8122\end{aligned}$$

$$\begin{aligned}\Delta \bar{F} &= \Delta F_\theta + (M)(Q) + (C)(R) \\ &= -10.5 + (0.5823)(231.84) + (9.8515)(0.2704) = 127.165\end{aligned}$$

$$\Delta x_\theta = \Delta \bar{F}/\bar{K} = 1.5957 \times 10^{-3}$$

From Eq. (7.30)

$$\begin{aligned}\Delta \ddot{x}_\theta &= \frac{6}{(\Delta t_\theta)^2} \Delta x_\theta - \frac{6}{\Delta t_\theta} \dot{x}(0) - 3\ddot{x}(0) \\ &= \frac{6}{(0.007)^2} (1.5957 \times 10^{-3}) - 0 - 3(77.280) = -36.4444 \\ \Delta \ddot{x}(0.005) &= \Delta \ddot{x}_\theta / \theta = -36.4444 / 1.4 = -26.0317\end{aligned}$$

From Eqs. (7.26) and (7.27) with $\tau = \Delta t = 0.005$ sec

$$\begin{aligned}\Delta \dot{x}(0.005) &= \dot{x}(0)\Delta t + \frac{\Delta t}{2} \Delta \ddot{x}(0.005) \\ &= 77.280(0.005) + \frac{0.005}{2} (-26.0317) = 0.3213 \text{ in/sec}\end{aligned}$$

$$\begin{aligned}\Delta x(0.005) &= \dot{x}(0)\Delta t + \frac{(\Delta t)^2}{2} \ddot{x}(0) + \frac{\Delta t^2}{6} \Delta \ddot{x}(0.005) \\ &= \frac{(0.005)^2}{2} (77.280) + \frac{(0.005)^2}{6} (-26.0317) = 0.8575 \times 10^{-3} \text{ in}\end{aligned}$$

From Eqs. (7.41), (7.42), and (7.43)

$$x(0.005) = x(0) + \Delta x(0.005) = 0.8575 \times 10^{-3} \text{ in} \quad (\text{e})$$

$$\dot{x}(0.005) = \dot{x}(0) + \Delta \dot{x}(0.005) = 0.3213 \text{ in/sec} \quad (\text{f})$$

$$\ddot{x}(0.005) = \ddot{x}(0) + \Delta \ddot{x}(0.005) = 77.280 - 26.0317 = 51.2482 \text{ in/sec}^2 \quad (\text{g})$$

The entire results from $t = 0$ through $t = 0.03$ sec are listed in Table 7.3.

(c) *Runge-Kutta fourth-order method*—at $t = 0$, $x = \dot{x} = 0$

$$\ddot{x} = F(t = 0)/M = 77.280 \text{ in/sec}^2$$

At $t = 0.005$ sec, k_1 , k_2 , k_3 , and k_4 in Eqs. (7.89)–(7.92) can be calculated as

$$\begin{aligned} k_1 &= \Delta t M^{-1}(F(0) - Kx(0) - C\dot{x}(0)) = 0.005(45 - 0 - 0)/0.5823 = 0.3864 \\ k_2 &= \Delta t M^{-1} \left[F(0.0025) - K \left(x(0) + \frac{\Delta t}{2} \dot{x}(0) \right) - C \left(\dot{x}(0) + \frac{k_1}{2} \right) \right] \\ &= \left(\frac{0.005}{0.5823} \right) \left[41.25 - 4166.7(0) - 9.8515 \left(0 + \frac{0.3864}{2} \right) \right] = 0.3379 \\ k_3 &= \Delta t M^{-1} \left[F(0.0025) - K \left(x(0) + \frac{\Delta t}{2} \dot{x}(0) + \frac{\Delta t}{4} k_1 \right) - C \left(\dot{x}(0) + \frac{k_2}{2} \right) \right] \\ &= (0.005/0.5823) \left[41.25 - 4166.7 \left(\frac{0.005}{4} \right) (0.3864) - 9.8515 \left(\frac{1}{2} \right) (0.3379) \right] = 0.3226 \\ k_4 &= \Delta t M^{-1} \left[F(0.005) - K \left(x(0) + \Delta t \dot{x}(0) + \frac{\Delta t}{2} k_2 \right) - C(\dot{x}(0) + k_3) \right] \\ &= (0.005/0.5823) \left[37.5 - 4166.7 \left(\frac{1}{2} \right) (0.005) (0.3379) - 9.8515(0.3226) \right] = 0.2645 \end{aligned}$$

From Eqs. (7.87) and (7.88),

$$\begin{aligned} x(0.005) &= x(0) + \Delta t \dot{x}(0) + \frac{\Delta t}{6} (k_1 + k_2 + k_3) \\ &= 0 + 0 + \left(\frac{0.005}{6} \right) (0.3864 + 0.3379 + 0.3226) = 0.8724 \times 10^{-3} \text{ in} \end{aligned} \quad (\text{h})$$

$$\begin{aligned} \dot{x}(0.005) &= \dot{x}(0) + \frac{1}{6} (k_1 + 2k_2 + 2k_3 + k_4) \\ &= \frac{1}{6} (0.3864 + 2(0.3379 + 0.3226) + 0.2645) = 0.3286 \text{ in/sec} \end{aligned} \quad (\text{i})$$

From Eq. (7.54)

$$\begin{aligned} \ddot{x}(0.005) &= M^{-1}[F(0.005) - Kx(0.005) - C\dot{x}(0.005)] \\ &= \frac{1}{0.5823} [37.5 - 4166.7(0.0008724) - 9.8515(0.3286)] \\ &= 52.5979 \text{ in/sec}^2 \end{aligned} \quad (\text{j})$$

(d) *Duhamel's integrals*—from Eq. (1.121a), the Duhamel's integral with damping factor $\rho < 0.15$ can be expressed as

$$\begin{aligned} x &= \frac{1}{\sqrt{KM(1-\rho^2)}} \int_0^\Delta e^{(-\rho/\sqrt{1-\rho^2})p^*(t-\Delta)} F(\Delta) \sin p^*(t-\Delta) d\Delta \\ &= \frac{c}{p^*(d^2+1)} \left\{ \left(1 - \frac{t}{\zeta} \right) - \frac{2d}{\zeta p^*(d^2+1)} - \left[1 - \frac{d}{\zeta p^*(d^2+1)} \right] e^{dp^*t} (cs - dsn) + \frac{e^{dp^*t} (dc s + sn)}{\zeta p^*(d^2+1)} \right\} \end{aligned} \quad (\text{k})$$

in which

$$c = \frac{F(0)}{\sqrt{KM(1-\rho^2)}}, \quad d = \frac{-\rho}{\sqrt{1-\rho^2}}, \quad cs = \cos p^*t, \quad sn = \sin p^*t, \quad p^* = \sqrt{(1-\rho^2)p}, \text{ and}$$

$$p = \sqrt{\frac{K}{M}} = \sqrt{\frac{4166.7}{0.5823}} = 84.5907$$

For x at $t=0.005$ sec, $\sqrt{(1-\rho^2)} = \sqrt{1-(0.1)^2} = 0.9949$, $p^* = 84.1666$, $sn = 0.4085$, $cs = 0.9127$, $d = -0.1/0.9949 = -0.1005$, and $c = 45/\sqrt{[(4166.7)(0.5823)(0.9949)^2]} = 0.9181$. From Eq. (k)

$$x(0.005) = \frac{0.9181}{84.1666[(-0.1005)^2 + 1]} \left\{ 0.833 - \frac{2(-0.1005)}{(0.03)(84.1666)(1.0101)} - \left[1 - \left(\frac{-0.1005}{2.5505} \right) \right] \right.$$

$$\left. (e^{-0.0422})(0.9538) + \frac{e^{-0.0422}(0.3167)}{(0.03)(84.1666)(1.0101)} \right\}$$

$$= 0.8734 \times 10^{-3} \text{ in} \quad (l)$$

A summary of the displacement response obtained by these four methods is given in the Table 7.3. It is apparent that the incremental time interval can affect results of the calculation. How to choose a suitable Δt is discussed in the next section.

7.3.5. Numerical Stability and Error of Newmark and Wilson-θ Methods

7.3.5.1. Numerical Stability

Stability of a numerical integration method requires that any error in displacement, velocity, and acceleration at time t does not grow for different incremental time intervals used in the integration. Therefore, the response of an undamped system subjected to an initial condition should be a harmonic motion with constant amplitude, which must not be amplified when different Δt 's are employed in the analysis. Stability of an integration method can thus be determined by examining the behavior of the numerical solution for arbitrary initial conditions based on the following recursive relationship.

$$\{X(t + \Delta t)\} = [A]\{X(t)\} \quad (7.93)$$

where $\{X(t + \Delta t)\}$ and $\{X(t)\}$ signify the displacement, velocity, and acceleration vector at time $t = \Delta t$ and t ; and $[A]$ is an integration approximation matrix. Each quantity in Eq. (7.93) depends on the specific integration method used (see Examples 7.3.4 and 7.3.5).

If we start at time t , and take n time steps, Eq. (7.93) may be expressed as

$$\{X(t + n\Delta t)\} = [A]^n\{X(t)\} \quad (7.94)$$

To investigate the stability of an integration method, we use the decomposed form of matrix $[A]$ in

TABLE 7.3 Displacement Response of Example 7.3.3, Multiplied by 10^{-3}

Time	Newmark method	Wilson-θ method	Runge-Kutta	Duhamel integrals
0	0	0	0	0
0.005	0.8637	0.8575	0.8724	0.8734
0.01	3.0168	2.9738	3.0446	3.0457
0.015	5.6980	5.5863	5.7404	5.7441
0.02	8.1179	7.9355	8.1579	8.1621
0.025	9.5931	9.3855	9.6074	9.6108
0.03	9.6515	9.5130	9.6185	9.6198

Eq. (7.94) as

$$[A]^n = [\Phi][\lambda^n][\Phi]^{-1} \quad (7.95)$$

where $[\lambda^n]$ is a diagonal matrix with eigenvalues $\lambda_1^n, \lambda_2^n, \lambda_3^n$ in the diagonal position; and $[\Phi]$ is the modal matrix with eigenvectors Φ_1, Φ_2 , and Φ_3 .

Now define the spectral radius of matrix $[A]$ as

$$r(A) = \max|\lambda_i|; \quad i = 1, 2, 3 \quad (7.96)$$

Then, from Eq. (7.95), we must have

$$r(A) \leq 1 \quad (7.97)$$

in order to keep the $[A]^n$ in Eq. (7.95) from growing without bound. The condition of Eq. (7.97) is known as the *stability criterion* for a given method. The bound of $[A]^n$ and Eq. (7.97) may be proved as follows. Let the inverse of $[\Phi]$ be $[\mathcal{Q}]$; then

$$[\mathcal{Q}][\Phi] = \begin{cases} 1, & i = j \\ 0, & i \neq j \end{cases}$$

Since $[A][\Phi] = [\lambda][\Phi]$, we have

$$\begin{aligned} [\Phi]^{-1}[A][\Phi] &= \begin{bmatrix} \lambda_1 Q_1 \Phi_1 & \dots & \lambda_m Q_1 \Phi_m \\ \vdots & & \vdots \\ \lambda_1 Q_m \Phi_1 & \dots & \lambda_m Q_m \Phi_m \end{bmatrix} \\ &= [\lambda] \end{aligned} \quad (9.97a)$$

Thus,

$$[A] = [\Phi][\lambda][\Phi]^{-1}$$

For the n th power,

$$[\lambda^n] = \begin{bmatrix} \lambda_1^n & & 0 \\ & \lambda_2^n & \\ \text{symm} & & \lambda_m^n \end{bmatrix} \quad (7.97b)$$

$[\lambda^n]$ is bounded as long as

$$r(A) = \max\{|\lambda_1|, |\lambda_2|, \dots, |\lambda_m|\} \leq 1$$

Therefore

$$|\lambda^n| = |\lambda_1|^n |\lambda_2|^n \cdots |\lambda_m|^n \leq (1)(1)(1) \cdots (1) = 1$$

and

$$\begin{aligned} [A]^n &= ([\Phi][\lambda][\Phi]^{-1})^n = [\Phi][\lambda][\Phi]^{-1}[\Phi][\lambda][\Phi]^{-1} \cdots \\ &= [\Phi][\lambda^n][\Phi]^{-1} \end{aligned} \quad (7.98)$$

If $[\lambda^n]$ is bounded, then $[A]^n$ is also bounded.

EXAMPLE 7.3.4 For a single-d.o.f. system with natural frequency p and damping ratio ρ , find the integration approximation matrix $[A]$ for the Wilson-θ method.

Solution: The differential equation of the single-d.o.f. system is

$$\ddot{x}(t + \theta\Delta t) + 2\rho p \dot{x}(t + \theta\Delta t) + p^2 x(t + \theta\Delta t) = 0 \quad (\text{a})$$

Let τ denote the increase in time from time t , where $0 \leq \tau \leq \theta\Delta t$. Then, for the time interval t to $t + \theta\Delta t$, we have

$$\ddot{x}(t + \tau) = \ddot{x}(t) + (\ddot{x}(t + \Delta t) - \ddot{x}(t)) \frac{\tau}{\Delta t} \quad (\text{b})$$

From Eqs. (7.26) and (7.27)

$$\dot{x}(t + \tau) = \dot{x}(t) + \ddot{x}(t)\tau + \frac{\tau^2}{2\Delta t}(\ddot{x}(t + \Delta t) - \ddot{x}(t)) \quad (\text{c})$$

and

$$x(t + \tau) = x(t) + \dot{x}(t)\tau + \frac{\tau^2}{2} \ddot{x}(t) + \frac{\tau^3}{6\Delta t}(\ddot{x}(t + \Delta t) - \ddot{x}(t)) \quad (\text{d})$$

When $\tau = \Delta t$, Eqs. (c) and (d) become

$$\dot{x}(t + \Delta t) = \dot{x}(t) + \frac{\Delta t}{2}(\ddot{x}(t + \Delta t) + \ddot{x}(t)) \quad (\text{e})$$

$$x(t + \Delta t) = x(t) + \dot{x}(t)\Delta t + \frac{\Delta t^2}{6}(\ddot{x}(t + \Delta t) + 2\ddot{x}(t)) \quad (\text{f})$$

Substituting Eqs. (b)–(d) into Eq. (a) with $\tau = \theta\Delta t$ leads to

$$\begin{aligned} & \ddot{x}(t) + \theta\ddot{x}(t + \Delta t) - \theta\ddot{x}(t) + 2\rho p \left[\dot{x}(t) + \ddot{x}(t)\theta\Delta t + \frac{\theta^2\Delta t}{2}(\ddot{x}(t + \Delta t) - \ddot{x}(t)) \right] \\ & + p^2 \left[x(t) + \dot{x}(t)\theta\Delta t + \frac{\theta^2\Delta t^2}{2} \ddot{x}(t) + \frac{\theta^3\Delta t^2}{6} \ddot{x}(t + \Delta t) - \frac{\theta^3\Delta t^2}{6} \ddot{x}(t) \right] = 0 \end{aligned} \quad (\text{g})$$

Collecting terms gives

$$\begin{aligned} & \left(\theta + \rho p \theta^2 \Delta t + \frac{p^2 \theta^3 \Delta t^2}{6} \right) \ddot{x}(t + \Delta t) \\ & = - \left[1 - \theta + 2\rho p \theta \Delta t - \rho p \theta^2 \Delta t + \frac{p^2 \theta^2 \Delta t^2}{2} - \frac{p^2 \theta^3 \Delta t^2}{6} \right] \ddot{x}(t) \\ & \quad - [2\rho p + p^2 \theta \Delta t] \dot{x}(t) - p^2 x(t) \\ & = -A\dot{x}(t) - B\ddot{x}(t) - Cx(t) = D\ddot{x}(t + \Delta t) \end{aligned}$$

where

$$\begin{aligned} A &= 2\rho p + p^2 \theta \Delta t \\ B &= 1 - \theta + 2\rho p \theta \Delta t - \rho p \theta^2 \Delta t + \frac{p^2 \theta^2 \Delta t^2}{2} - \frac{p^2 \theta^3 \Delta t^2}{6} \\ C &= p^2 \\ D &= 0 + \rho p \theta^2 \Delta t + \frac{p^2 \theta^3 \Delta t^2}{6} \end{aligned}$$

Therefore

$$\ddot{x}(t + \Delta t) = \left(\frac{-B}{D} \right) \ddot{x}(t) + \left(\frac{-A}{D} \right) \dot{x}(t) + \left(\frac{-C}{D} \right) x(t) \quad (\text{h})$$

in which

$$\frac{-B}{D} = 1 - \frac{E\theta^2}{3} - \frac{1}{\theta} - F\theta \quad (\text{i})$$

$$\frac{-A}{D} = \frac{1}{\Delta t}(-E\theta - 2F) \quad (\text{j})$$

$$\frac{-C}{D} = \frac{-E}{\Delta t^2} \quad (\text{k})$$

where

$$E = \left[\frac{\theta}{p^2 \Delta t^2} + \frac{\rho \theta^2}{p \Delta t} + \frac{\theta^3}{6} \right]^{-1} \quad (\text{l})$$

and

$$F = \frac{\rho E}{p \Delta t} \quad (\text{m})$$

Substituting Eq. (h) into Eq. (e) yields

$$\ddot{x}(t + \Delta t) = \frac{\Delta t}{2} \left(1 - \frac{B}{D} \right) \ddot{x}(t) + \left(1 + \frac{\Delta t}{2} \left(\frac{-A}{D} \right) \right) \dot{x}(t) + \frac{\Delta t}{2} \left(\frac{-C}{D} \right) x(t) \quad (\text{n})$$

in which

$$\frac{\Delta t}{2} \left(1 - \frac{B}{D} \right) = \Delta t \left(1 - \frac{1}{2\theta} - \frac{E\theta^2}{6} - \frac{F\theta}{2} \right) \quad (\text{o})$$

$$1 + \frac{\Delta t}{2} \left(\frac{-A}{D} \right) = 1 - \frac{E\theta}{2} - F \quad (\text{p})$$

$$\frac{\Delta t}{2} \left(\frac{-C}{D} \right) = \frac{-E}{2\Delta t} \quad (\text{q})$$

Substituting Eq. (h) into Eq. (f) leads to

$$x(t + \Delta t) = \frac{\Delta t^2}{6} \left[\frac{-B}{D} + 2 \right] \ddot{x}(t) + \left[\Delta t + \frac{\Delta t^2}{6} \left(-\frac{A}{D} \right) \right] \dot{x}(t) + \left[1 + \frac{\Delta t^2}{6} \left(\frac{-C}{D} \right) \right] x(t) \quad (\text{r})$$

in which

$$\frac{\Delta t^2}{6} \left[\frac{-B}{D} + 2 \right] = \Delta t^2 \left(\frac{1}{2} - \frac{E\theta^2}{18} - \frac{1}{6\theta} - \frac{F\theta}{6} \right) \quad (\text{s})$$

$$\Delta t + \frac{\Delta t^2}{6} \left(-\frac{A}{D} \right) = \Delta t \left(1 - \frac{E\theta}{6} - \frac{F}{3} \right) \quad (\text{t})$$

$$1 + \frac{\Delta t^2}{6} \left(\frac{-C}{D} \right) = 1 - \frac{E}{6} \quad (\text{u})$$

Using Eqs. (h), (n) and (r), the recursive relationship given in Eq. (7.93) is established as

$$\begin{Bmatrix} \ddot{x}(t + \Delta t) \\ \dot{x}(t + \Delta t) \\ x(t + \Delta t) \end{Bmatrix} = [A] \begin{Bmatrix} \ddot{x}(t) \\ \dot{x}(t) \\ x(t) \end{Bmatrix} \quad (\text{v})$$

where

$$[A] = \begin{bmatrix} 1 - \frac{E\theta^2}{3} - \frac{1}{\theta} - F\theta & -\frac{1}{\Delta t}(E\theta + 2F) & \frac{-E}{\Delta t^2} \\ \Delta t \left(1 - \frac{1}{2\theta} - \frac{E\theta^2}{6} - \frac{F\theta}{2} \right) & 1 - \frac{E\theta}{2} - F & \frac{-E}{2\Delta t} \\ \Delta t^2 \left(\frac{1}{2} - \frac{1}{6\theta} - \frac{E\theta^2}{18} - \frac{F\theta}{6} \right) & \Delta t \left(1 - \frac{E\theta}{6} - \frac{F}{3} \right) & 1 - \frac{E}{6} \end{bmatrix} \quad (\text{w})$$

EXAMPLE 7.3.5 Rework Example 7.3.4 for the Newmark method.

Solution: The differential equation of the single-d.o.f. system is

$$\ddot{x}(t + \Delta t) + 2\rho p \dot{x}(t + \Delta t) + p^2 x(t + \Delta t) = 0 \quad (\text{a})$$

From Eqs. (7.12) and (7.13), $\dot{x}(t + \Delta t)$ and $x(t + \Delta t)$ can be expressed as

$$\dot{x}(t + \Delta t) = \dot{x}(t) + [(1 - \delta)\ddot{x}(t) + \delta\ddot{x}(t + \Delta t)]\Delta t \quad (\text{b})$$

$$x(t + \Delta t) = x(t) + \dot{x}(t)\Delta t + \left[\left(\frac{1}{2} - \alpha \right) \ddot{x}(t) + \alpha \ddot{x}(t + \Delta t) \right] (\Delta t)^2 \quad (\text{c})$$

Substitute Eqs. (b) and (c) into Eq. (a),

$$\begin{aligned} & \ddot{x}(t + \Delta t) + 2\rho p [\dot{x}(t) + \Delta t((1 - \delta)\ddot{x}(t) + \delta\ddot{x}(t + \Delta t))] \\ & + p^2 \left[x(t) + \dot{x}(t)\Delta t + \left(\left(\frac{1}{2} - \alpha \right) \ddot{x}(t) + \alpha \ddot{x}(t + \Delta t) \right) \Delta t^2 \right] = 0 \end{aligned} \quad (\text{d})$$

Rearrange Eq. (d),

$$\begin{aligned} & (1 + 2\rho p \Delta t \delta + p^2 \Delta t^2 \alpha) \ddot{x}(t + \Delta t) \\ & = - \left[2\rho p \Delta t (1 - \delta) + p^2 \Delta t^2 \left(\frac{1}{2} - \alpha \right) \right] \ddot{x}(t) - [2\rho p + p^2 \Delta t] \dot{x}(t) - p^2 x(t) \end{aligned}$$

or

$$D\ddot{x}(t + \Delta t) = -A\ddot{x}(t) - B\dot{x}(t) - Cx(t) \quad (\text{e})$$

where

$$\begin{aligned} A &= 2\rho p \Delta t (1 - \delta) + p^2 \Delta t^2 \left(\frac{1}{2} - \alpha \right) \\ B &= 2\rho p + p^2 \Delta t \\ C &= p^2 \\ D &= 1 + 2\rho p \Delta t \delta + p^2 \Delta t^2 \alpha \end{aligned}$$

Therefore

$$\ddot{x}(t + \Delta t) = \left(\frac{-A}{D} \right) \ddot{x}(t) + \left(\frac{-B}{D} \right) \dot{x}(t) + \left(\frac{-C}{D} \right) x(t) \quad (\text{f})$$

in which

$$-\frac{A}{D} = -\left(\frac{1}{2} - \alpha\right)E - 2(1 - \delta)F \quad (\text{g})$$

$$-\frac{B}{D} = \frac{1}{\Delta t}(-E - 2F) \quad (\text{h})$$

$$-\frac{C}{D} = \frac{-E}{\Delta t^2} \quad (\text{i})$$

where

$$E = \left(\frac{1}{p^2 \Delta t^2} + \frac{2\rho\delta}{p\Delta t} + \alpha \right)^{-1}$$

and

$$F = \frac{\rho E}{p\Delta t}$$

Substitute Eq. (f) into Eq. (b),

$$\ddot{x}(t + \Delta t) = \Delta t \left[1 - \delta + \delta \left(\frac{-A}{D} \right) \right] \ddot{x}(t) + \left[1 + \delta \Delta t \left(\frac{-B}{D} \right) \right] \dot{x}(t) + \Delta t \delta \left(\frac{-C}{D} \right) x(t) \quad (\text{j})$$

in which

$$\Delta t \left[1 - \delta + \delta \left(\frac{-A}{D} \right) \right] = \Delta t \left[1 - \delta - \left(\frac{1}{2} - \alpha \right) \delta E - 2(1 - \delta) \delta F \right] \quad (\text{k})$$

$$1 + \delta \Delta t \left(\frac{-B}{D} \right) = 1 - E\delta - 2\delta F \quad (\text{l})$$

$$\Delta t \delta \left(\frac{-C}{D} \right) = \frac{1}{\Delta t} (-E\delta) \quad (\text{m})$$

Substitute Eq. (f) into Eq. (c)

$$x(t + \Delta t) = \Delta t^2 \left[\frac{1}{2} - \alpha + \alpha \left(\frac{-A}{D} \right) \right] \ddot{x}(t) + \left[\Delta t + \Delta t^2 \alpha \left(\frac{-B}{D} \right) \right] \dot{x}(t) + \left[1 + \Delta t^2 \alpha \left(\frac{-C}{D} \right) \right] x(t) \quad (\text{n})$$

in which

$$\Delta t^2 \left(\frac{1}{2} - \alpha + \alpha \left(\frac{-A}{D} \right) \right) = \Delta t^2 \left[\frac{1}{2} - \alpha - \left(\frac{1}{2} - \alpha \right) \alpha E - 2(1 - \delta) \alpha F \right] \quad (\text{o})$$

$$\Delta t + \Delta t^2 \left(\frac{-B}{D} \right) = \Delta t [1 - \alpha E - 2\alpha F] \quad (\text{p})$$

$$1 + \Delta t^2 \alpha \left(\frac{-C}{D} \right) = 1 - \alpha E \quad (\text{q})$$

Using Eqs. (f), (j), and (n) yields the following recursive relationship as shown in Eq. (7.93):

$$\begin{Bmatrix} \ddot{x}(t + \Delta t) \\ \dot{x}(t + \Delta t) \\ x(t + \Delta t) \end{Bmatrix} = [A] \begin{Bmatrix} \ddot{x}(t) \\ \dot{x}(t) \\ x(t) \end{Bmatrix} \quad (\text{r})$$

where

$$[A] = \begin{bmatrix} -\left(\frac{1}{2} - \alpha\right)E - 2(1 - \delta)F & \frac{-1}{\Delta t}(E + 2F) & \frac{-E}{\Delta t^2} \\ \Delta t \left[1 - \delta - \left(\frac{1}{2} - \alpha\right)\delta E - (1 - \delta)\delta F\right] & 1 - E\delta - 2\delta F & \frac{-E\delta}{\Delta t} \\ \Delta t^2 \left[\frac{1}{2} - \alpha - \left(\frac{1}{2} - \alpha\right)\alpha E - 2(1 - \delta)\alpha F\right] & \Delta t(1 - \alpha E - 2\alpha F) & (1 - \alpha E) \end{bmatrix} \quad (s)$$

EXAMPLE 7.3.6 Assuming a single-d.o.f. undamped system having natural frequency $p = 2\pi$ rad/sec, find the spectral radii for (A) the Newmark method with $\alpha = \frac{1}{6}$ and $\delta = \frac{1}{2}$ as well as $\alpha = \frac{1}{4}$ and $\delta = \frac{1}{2}$, and (B) the Wilson-θ method with $\theta = 1.4$ and $\theta = 1.36$. The spectral radii are calculated from $\Delta t/T = 0.001$ to $\Delta t/T = 100$ in which $T = 2\pi/p = 1$ sec.

Solution: (A) for Newmark method, the E and F values in Example 7.3.5 are

$$\begin{aligned} E &= \left(\frac{1}{p^2 \Delta t^2} + \frac{2\rho\delta}{p\Delta t} + \alpha \right)^{-1} = \left(\frac{1}{4(\pi)^2 \Delta t^2} + \frac{1}{6} \right)^{-1} \\ &= 3.9478 \times 10^{-5} \end{aligned} \quad (a)$$

$$F = \frac{\rho E}{p\Delta t} = 0 \quad (b)$$

in which $\alpha = 1/6$, $\delta = 0.5$, and $\Delta t = 0.001$ (1) = 0.001 sec. Substituting the above numerical numbers into Eq. (s) of Example 7.3.5 yields

$$[A] = \begin{bmatrix} -1.3159 \times 10^{-5} & -0.03947 & 39.4781 \\ 4.9999 \times 10^{-4} & 0.9999 & -0.0197 \\ 3.3332 \times 10^{-7} & 9.9999 \times 10^{-4} & 0.9999 \end{bmatrix} \quad (c)$$

The eigenvalues of matrix $[A]$ are

$$\lambda_1 = 0.1316 \times 10^{-4}; \quad \lambda_2 = 0.9999; \quad \text{and} \quad \lambda_3 = 0.9999 \quad (d)$$

From Eq. (7.97)

$$r(A) = \max |\lambda_i| = 0.9999 < 1 \quad (e)$$

Therefore, when $\Delta t/T = 0.001$, the Newmark method with $\alpha = 1/6$ and $\delta = 1/2$ (linear acceleration method) is stable.

(B) For the Wilson-θ method, with $\theta = 1.36$, $\Delta t = 100$ sec, the E and F values in Example 7.3.4 are

$$\begin{aligned} E &= \left[\frac{\theta}{p^2 \Delta t^2} + \frac{\rho\theta^2}{p\Delta t} + \frac{\theta^3}{6} \right]^{-1} = \left(\frac{1.36}{4\pi^2 (\Delta t)^2} + 0 + \frac{(1.36)^3}{6} \right)^{-1} \\ &= 2.3852 \end{aligned} \quad (f)$$

$$F = \frac{\rho E}{p\Delta t} = 0 \quad (g)$$

Substituting E , θ , and F into Eq. (w) of Example 7.3.4 leads to

$$[A] = \begin{bmatrix} -1.2058 & -0.03243 & -0.2385 \times 10^{-3} \\ -10.2935 & -0.6219 & -0.0119 \\ 1323.55 & 45.9347 & 0.6024 \end{bmatrix} \quad (h)$$

Performing $\det([A] - \lambda[I]) = 0$ results in

$$\lambda_1 = -1.0358; \quad \lambda_2 = -0.2587; \quad \text{and} \quad \lambda_3 = 0.0692 \quad (i)$$

Thus

$$r(A) = \text{Max}|\lambda_i| = 1.0358 > 1 \quad (j)$$

Therefore, when $\Delta t/T = 100$, the Wilson- θ method with $\theta = 1.36$ is unstable.

Numerical results for the Newmark method ($\alpha = 1/6$, $\delta = 1/2$ and $\alpha = 1/4$, $\delta = 1/2$) and Wilson- θ method ($\theta = 1.36$ and 1.4) from $\Delta t/T = 0.001$ to $\Delta t/T = 100$ are plotted in Fig. 7.11. It can be seen that the spectral radius for Newmark method with $\alpha = 1/6$ and $\delta = 1/2$ is stable [$r(A) \leq 1$] at approximately $\Delta t/T < 0.55$ and becomes unstable [$r(A) > 1$] at $\Delta t/T \geq 0.55$. The stability of this method depends on the magnitude of Δt , and is called the *conditional stability* method. However, the spectral radii for $\alpha = 1/4$ and $\delta = 1/2$ from $\Delta t/T = 0.001$ –100 are all less than or equal to 1 [$r(A) \leq 1$]; this case is called *unconditional stability* because it does not depend on the magnitude of Δt . Figure 7.11 also shows that the Wilson- θ method with $\theta = 1.4$ is unconditionally stable. Note that it becomes conditionally stable with $\theta = 1.36$ since the spectral radius is greater than 1 when $\Delta t/T$ is approximately greater than 4. For unconditional stability,

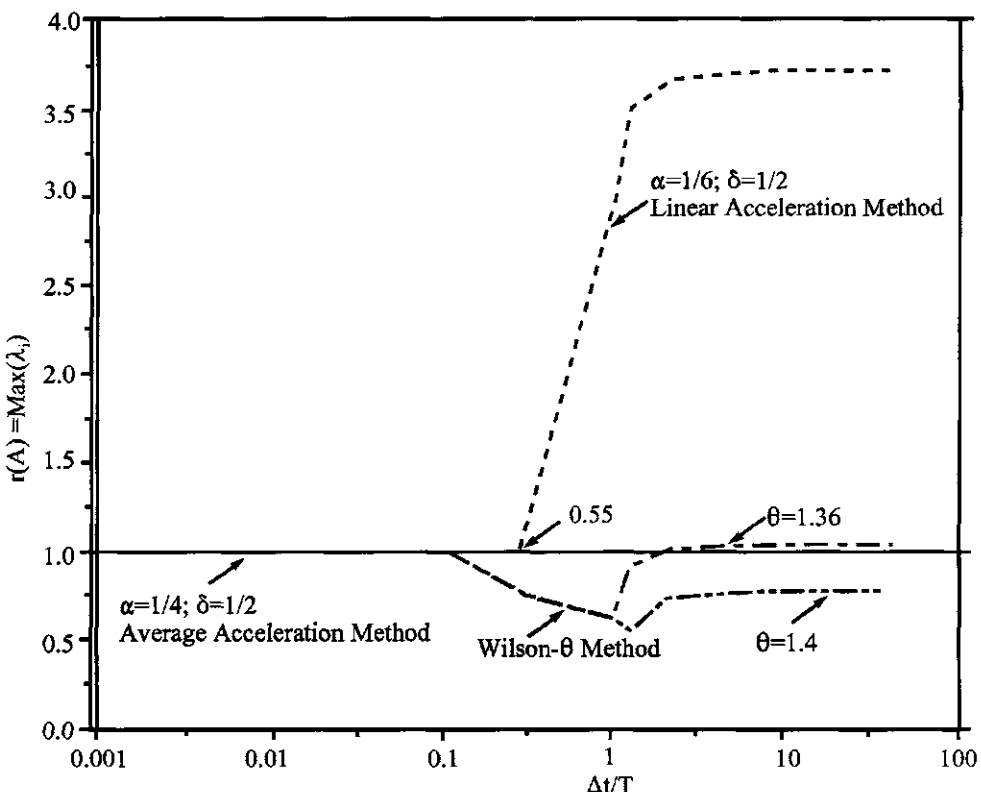


FIG. 7.11 Spectral radii for Newmark method and Wilson- θ method.

the solution is not divergent even if time increment Δt is large. To assure solution stability, $\theta = 1.4$ is usually used for the Wilson-θ method, and $\alpha = 1/4$ and $\delta = 1/2$ or $\alpha = 1/6$, $\delta = 1/2$ and $\Delta t/T \leq 0.55$ (Fig. 7.11) are used for the Newmark method.

7.3.5.2. Numerical Error

Numerical error, sometimes referred to as *computational error*, is due to the incremental time-step expressed in terms of $\Delta t/T$. Such errors result not from the stability behavior just discussed but from two other sources: (1) externally applied force or excitation, and (2) d.o.f. of a vibrating system. A forcing function, particularly an irregular one such as earthquake ground motion, is composed of a number of forcing periods (or frequencies). A larger Δt may exclude a significant part of a forcing function. That part is associated with smaller periods, a forcing function's higher modes. This error may occur for both single- and multiple-d.o.f. vibrating systems. Therefore, Δt must be selected small enough to ensure solution accuracy by including the first few significant vibrating modes in the analysis.

Numerical error reflects two characteristics: *amplitude decay* and *period elongation*. This behavior can be illustrated by using a free undamped vibration problem such as

$$M\ddot{x} + Kx = 0; \quad x_0 = a, \dot{x}_0 = 0$$

for which the exact solution ($x = a \cos pt$) and numerical results are compared in Fig. 7.12. Studies indicate that linear acceleration and average acceleration methods do not present amplitude decay. Depending on $\Delta t/T$ used, the Wilson-θ method gives both amplitude decay and period elongation. Among the three methods, linear acceleration has the least period elongation when $\Delta t/T < 0.55$ is within the stability limit (Fig. 7.11).

For reasonable accuracy, $\Delta t/T = 0.1$ is recommended, where T is the natural period of highest mode considered in the analysis. Properly selecting the number of modes depends on an individual problem. A suggested approach is to follow the building code's modal analysis. The code stipulates that at least the lowest three modes of vibration, or all modes of vibration with periods greater than 0.4 sec, whichever is greater, the number of modes shall equal the number of stories. (Note that structures less than three stories high are an exception to this rule.) Generally, we use one Δt and another slightly smaller Δt to find solutions continuously, until two successive solutions are reasonably close.

7.3.6. Numerical Stability of the Runge-Kutta Fourth-Order Method

The stability of this method should be examined on the basis of a first-order differential equation since the method is designed to approximate the Taylor series in the first-order form as

$$y'(t) = \frac{dy(t)}{dt} = py(t) = f(y(t)) \quad (7.99)$$

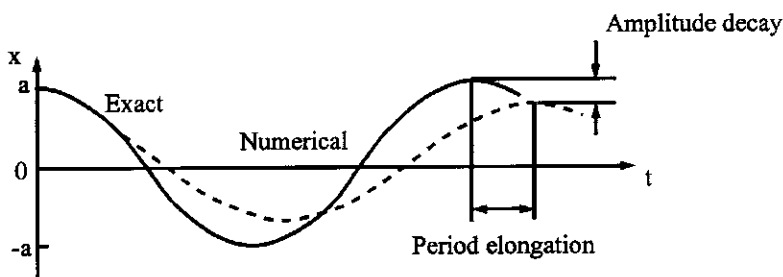


FIG. 7.12 Amplitude decay and period elongation.

where p is a constant. Based on Eqs. (7.80) and (7.80a)

$$y(t + \Delta t) = y(t) + \frac{1}{6}k_1 + \frac{1}{3}k_2 + \frac{1}{3}k_3 + \frac{1}{6}k_4 \quad (7.100)$$

in which

$$\left. \begin{aligned} k_1 &= \Delta t f(y(t)) \\ k_2 &= \Delta t f\left(y(t) + \frac{k_1}{2}\right) \\ k_3 &= \Delta t f\left(y(t) + \frac{k_2}{2}\right) \\ k_4 &= \Delta t f(y(t) + k_3) \end{aligned} \right\} \quad (7.101)$$

Substituting Eq. (7.101) into (7.100) leads to

$$\begin{aligned} y(t + \Delta t) &= y(t) + \frac{1}{6}\Delta t[p y(t)] + \frac{1}{3}\Delta t p \left[y(t) + \frac{k_1}{2} \right] + \frac{1}{3}\Delta t p \left[y(t) + \frac{k_2}{2} \right] \\ &\quad + \frac{1}{6}\Delta t p [y(t) + k_3] \\ &= \left[1 + \Delta t p + \frac{1}{2}\Delta t^2 p^2 + \frac{1}{6}\Delta t^3 p^3 + \frac{1}{24}\Delta t^4 p^4 \right] y(t) \\ &= \mu y(t) \end{aligned} \quad (7.102)$$

In order to keep $y(t + \Delta t)$ from growing without bound, the following criterion should be satisfied:

$$|\mu| \leq 1 \quad (7.103)$$

or

$$[1 + (\Delta t p) + \frac{1}{2}(\Delta t p)^2 + \frac{1}{6}(\Delta t p)^3 + \frac{1}{24}(\Delta t p)^4] \leq 1 \quad (7.104)$$

The real roots or real stability boundaries are

$$\Delta t p \leq 0 \quad \text{and} \quad \Delta t p \geq -2.785, \quad \text{when } p < 0 \quad (7.105)$$

When $p > 0$, the Runge–Kutta method is unconditionally stable with error as small as $(\Delta t)^5$, as shown in Eq. (7.63).

EXAMPLE 7.3.7 Use the Runge–Kutta fourth-order method to solve the first-order differential equation $y'(t) = -y(t)$ with $\Delta t = 0.5$, 2.0, and 3.0. The initial condition is $y(0) = 1$. Compare numerical results with the exact solution of $y(t) = e^{-t}$ in the range of $t = 0$ through $t = 25$.

Solution: From Eqs. (7.100) and (7.101)

$$y(t + \Delta t) = y(t) + \frac{1}{6}k_1 + \frac{1}{3}k_2 + \frac{1}{3}k_3 + \frac{1}{6}k_4 \quad (a)$$

and

$$\left. \begin{aligned} k_1 &= \Delta t f(y(t)) = \Delta t [p y(t)] = p \Delta t y(t) \\ k_2 &= \Delta t f\left(y(t) + \frac{k_1}{2}\right) = \Delta t \left[p \left(y(t) + \frac{k_1}{2} \right) \right] = p \Delta t y(t) + p \frac{k_1}{2} \Delta t \\ k_3 &= \Delta t f\left(y(t) + \frac{k_2}{2}\right) = p \Delta t y(t) + p \frac{k_2}{2} \Delta t \\ k_4 &= \Delta t f(y(t) + k_3) = \Delta t [p(y(t) + k_3)] = p \Delta t y(t) + p \Delta t k_3 \end{aligned} \right\} \quad (b)$$

Using $\Delta t = 0.5$

$$\begin{aligned}k_1 &= p\Delta t y(t) = (-1)(0.5)y(0) = (-1)(0.5)(1) = -0.5 \\k_2 &= p\Delta t y(t) + p\Delta t \frac{k_1}{2} = (-0.5) - (0.5)\left(\frac{-0.5}{2}\right) = -0.375 \\k_3 &= p\Delta t y(t) + p\Delta t \frac{k_2}{2} = (-0.5) - (0.5)\left(\frac{-0.375}{2}\right) = -0.4062 \\k_4 &= p\Delta t y(t) + p\Delta t k_3 = (-0.5) - (0.5)(-0.4062) = -0.2968\end{aligned}$$

From Eq. (a)

$$\begin{aligned}y(0.5) &= y(0) + \frac{1}{6}k_1 + \frac{1}{3}k_2 + \frac{1}{3}k_3 + \frac{1}{6}k_4 \\&= 1 + \frac{1}{6}(-0.5) + \frac{1}{3}(-0.375) + \frac{1}{3}(-0.4062) + \frac{1}{6}(-0.2968) \\&= 0.6067\end{aligned}\tag{c}$$

The exact solution at $t = 0.5$ is $e^{-0.5} = 0.6065$. Ratio of the exact to the numerically calculated value, R , is

$$\text{Ratio} = \frac{0.6065}{0.6067} = 0.9996\tag{d}$$

Results for $\Delta t = 0.5$, 2.0, and 3.0 are compared in Table 7.4 and plotted in Fig. 7.13.

Table 7.4 shows that response $y(t)$ with $\Delta t = 0.5$ is close to the exact solution. With Δt at 2.0, response $y(t)$ exhibits a large error relative to the exact solution (see Fig. 7.13), but it is not divergent and the numerical analysis is stable. With Δt at 3.0, response $y(t)$ increases and becomes divergent; the numerical analysis is unstable. Thus, when $p < 0$, Runge–Kutta fourth-order method is a conditional stability method.

For the first-order differential equation in Example 7.3.7, where $y(t) = e^t$ and $y'(t) = y(t)$, (i.e. $p = 1$) the numerical results for $\Delta t = 0.5$, 2.0, and 3.0 are plotted in Fig. 7.14. This figure shows that numerical error increases if a larger Δt is used. But response $y(t)$ with a larger Δt is not divergent, and the Runge–Kutta fourth-order method is an unconditional stability method when $p > 0$.

Note that numerical integrations are essential in dynamic response. If external excitations cannot be expressed in a mathematical form applicable to direct integration, then numerical procedures are a powerful tool. These procedures demonstrate their importance in other situations as well. When a structure's stiffness changes during response, such as stiffness degrading due to development of plastic hinges, structural frequency consequently changes. Response analyses based on modal matrix formulation become unreliable and numerical integrations should be used.

TABLE 7.4 Comparison of Numerical Results for $y(t) = e^{-t}$

$\Delta t = 0.5$		$\Delta t = 2$		$\Delta t = 3$	
Time, t	Ratio	Time, t	Ratio	Time, t	Ratio
0	1	0	1	0	1
0.5	0.9996	2	0.4060	3	0.0362
1	0.9992	4	0.1648	6	0.0013
2.5	0.9980	6	0.0669	9	0.4747×10^{-4}
5.0	0.9960	10	0.0110	12	0.1718×10^{-5}
10.0	0.9921	16	0.7383×10^{-3}	18	0.2253×10^{-8}
20.0	0.9842	20	0.1217×10^{-3}	21	0.8160×10^{-10}
25.0	0.9803	24	0.2×10^{-4}	24	0.2954×10^{-11}

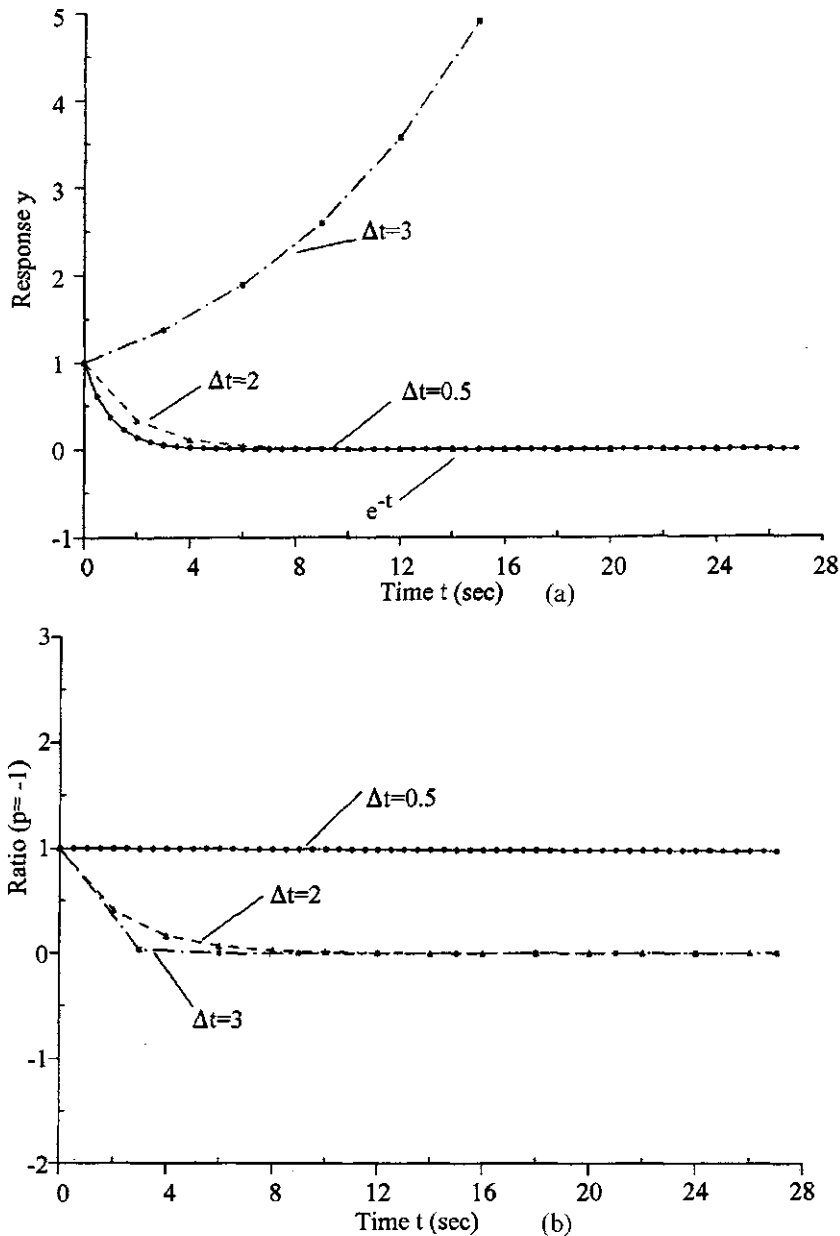


FIG. 7.13 Stability evaluation of $y'(t) = -y(t)$ for Runge-Kutta fourth-order method. (a) Stability observation. (b) Error observation.

In the case of degrading or softening stiffness, Δt can be decreased as natural period increases; but the value of Δt recommended previously can still be used.

7.4. SEISMIC RESPONSE SPECTRA FOR ANALYSIS AND DESIGN

In Section 7.3, the dynamic response of structures at any time can be obtained by numerical integration methods. As noted in previous chapters, structural response can also be analyzed by using response spectrum methods. Based on numerical techniques presented in Section 7.3, here more

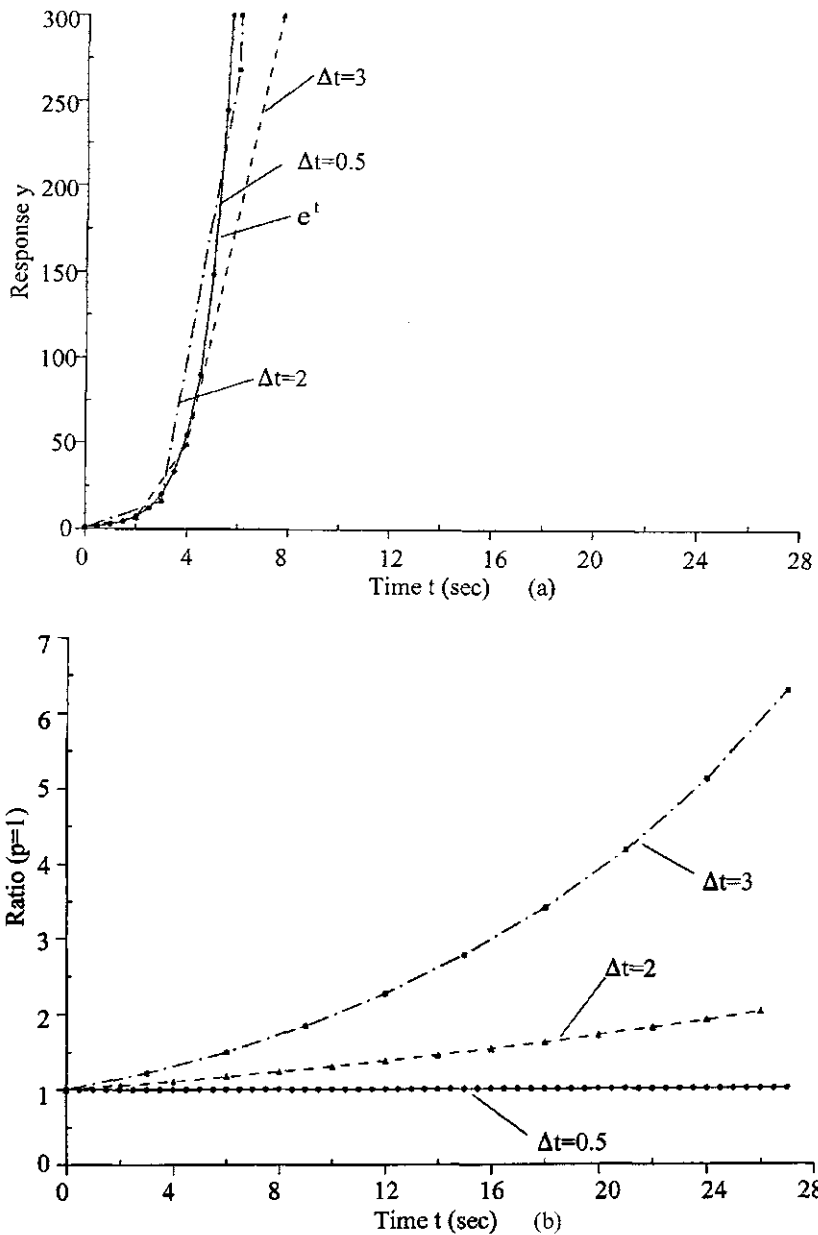


FIG. 7.14. Stability evaluation of $y'(t) = y(t)$ for Runge-Kutta fourth-order method. (a) Stability observation. (b) Error observation.

comprehensive procedures are developed for computing and constructing response spectra. The relationship between *response spectrum* and *design spectrum* is also elaborated.

7.4.1. Response Spectra, Pseudo-Spectra and Principal-Component Spectra

Acceleration, velocity, and displacement spectra plotted in tripartite logarithm are shown in Fig. 1.30, while different plots of these individual spectra are shown in Fig. 7.15. As observed from

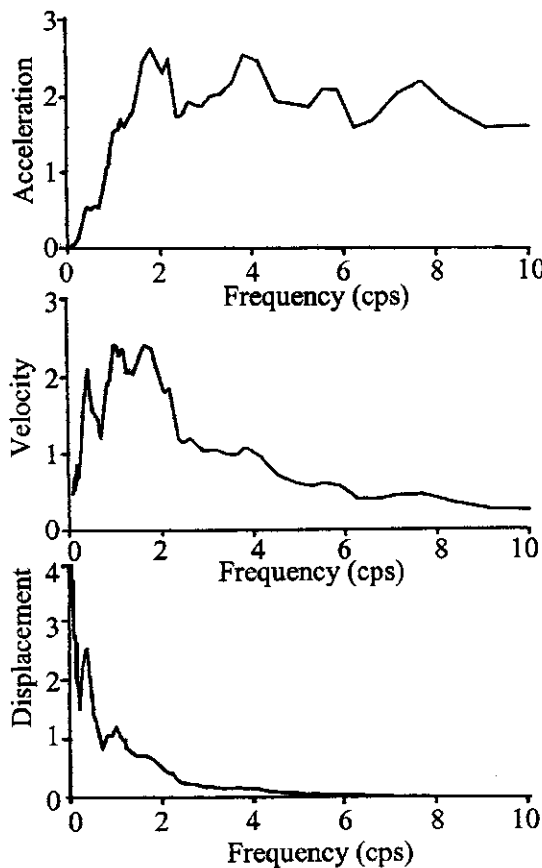


FIG. 7.15 Typical acceleration, velocity, and displacement response spectra for N-S component of El Centro Earthquake, 18 May, 1940.

the former, the latter also shows that, at large frequencies, relative displacement is small whereas acceleration is relatively large. At intermediate frequencies, velocity is substantially larger than at the high or low end of the spectrum. Note that the three spectral quantities can be shown by a single curve on a graph with three different scales called a *tripartite logarithmic plot*. Tripartite plots can differ in how their axes are arranged (as discussed later for Fig. 7.16).

Response spectra can be generated by using numerical integration methods to repeatedly solve the motion equation for a single d.o.f. system with different natural frequencies and damping ratios [see Eq. (a) in Example 7.3.3]. Peak response can be obtained as

$$x(p_i, \rho) = \max|x(t, p_i, \rho)| \quad (7.106)$$

$$\dot{x}(p_i, \rho) = \max|\dot{x}(t, p_i, \rho)| \quad (7.107)$$

$$\ddot{x}(p_i, \rho) = \max|\ddot{x}(t, p_i, \rho)| \quad (7.108)$$

For review purposes, Eq. (7.106) can be solved by numerical integration of Duhamel's integrals as

$$x = \frac{1}{p^*} \int_0^t \ddot{x}_g e^{-\rho p(t-\Delta)} \sin p^*(t - \Delta) d\Delta \quad (7.109)$$

where p^* represents a damped circular frequency, including the damping effect on structural natu-

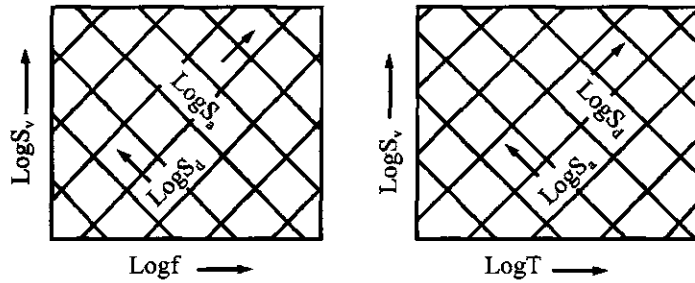


FIG. 7.16 Typical tripartite plots.

ral frequency as shown below,

$$p^* = p\sqrt{1 - \rho^2}$$

Equation (7.107) can be obtained by differentiating Eq. (7.109) with the following typical form:

$$\frac{d}{dx} \int_0^t f(t, \Delta) d\Delta = f(t, t) + \int_0^t \frac{df(t, \Delta)}{dt} d\Delta$$

and then substituting Eq. (7.109) in the above

$$\begin{aligned} \dot{x} &= \frac{1}{p^*} \ddot{x}_g e^{-\rho p(t-\Delta)} \sin p^*(t-\Delta)|_{\Delta=t} + \frac{1}{p^*} \int_0^t \ddot{x}_g [(-\rho p)e^{-\rho p(t-\Delta)} \sin p^*(t-\Delta) \\ &\quad + e^{-\rho p(t-\Delta)} p^* \cos p^*(t-\Delta)] d\Delta \\ &= -\rho p x + \int_0^t \ddot{x}_g e^{-\rho p(t-\Delta)} \cos p^*(t-\Delta) d\Delta \end{aligned} \quad (7.110)$$

which yields Eq. (7.107).

For Eq. (7.108), first divide the mass, M , on both sides of Eq. (1.122) and apply $C/M = 2\rho p$, which gives

$$\ddot{x} + 2\rho p \dot{x} + p^2 x = -\ddot{x}_g \quad (7.111)$$

Knowing x , \dot{x} , and \ddot{x}_g , we then find Eq. (7.108) in the following form:

$$\ddot{x} = -\ddot{x}_g - 2\rho p \dot{x} - p^2 x \quad (7.112)$$

Combining the relative acceleration of mass and the ground acceleration yields total mass acceleration,

$$\ddot{x}_t = \ddot{x} + \ddot{x}_g = -2\rho p \dot{x} - p^2 x \quad (7.113)$$

Let a single-d.o.f. system's *absolute maximum velocity* due to ground motion be S_v

$$S_v = \left| \int_0^t \ddot{x}_g e^{-\rho p(t-\Delta)} \sin p^*(t-\Delta) d\Delta \right| \quad (7.114)$$

Peak displacement and acceleration of the system are then

$$S_d = \frac{S_v}{p} \quad (7.115)$$

$$S_a = pS_v = p^2 S_d \quad (7.116)$$

or

$$\begin{aligned} S_v &= \frac{2\pi}{T} S_d = \frac{T}{2\pi} S_a \\ &= 2\pi f S_d = \frac{1}{2\pi f} S_a \end{aligned} \quad (7.117)$$

from which

$$\log S_v = -\log T + \log(2\pi S_d) \quad (7.118a)$$

or

$$\log S_v = \log(2\pi f) + \log S_d \quad (7.118b)$$

and

$$\log S_v = \log T + \log \left(\frac{S_a}{2\pi} \right) \quad (7.119a)$$

or

$$\log S_v = -\log(2\pi f) + \log S_a \quad (7.119b)$$

Equations (7.118a) and (7.119b) can respectively be expressed in the following linear form:

$$Y = X + C_1 \quad \text{and} \quad Y = X + C_2$$

Note that when X ($\log T$) increases and C_1 ($\log 2\pi S_d$) remains constant, then Y ($\log S_v$) decreases. Similarly, when X ($\log T$) increases and C_2 ($\log S_a/2\pi$) remains unchanged, then Y ($\log S_v$) increases. Relationships among $\log S_v$, $\log f$, $\log S_d$, and $\log S_a$ can be similarly established. The linear expression forms a tripartite plot with $\tan(-45^\circ) = -1$ and $\tan(45^\circ) = 1$ as shown in Fig. 7.16. S_v , S_a , and S_d are called *pseudo-velocity*, *pseudo-acceleration*, and *pseudo-displacement*, respectively, which constitute a pseudo-response spectrum. Numerical values of Eqs. (7.114)–(7.116) [same as Eq. (7.117)] are plotted in Figs. 7.17 and 7.18 (solid lines) with notations of S_v vs f and S_v vs T for the N–S component of El Centro earthquake, 18 May, 1940 with 30 sec (see Fig. 1.29). A damping factor of 5% is considered.

Observing the curves, some general behavior may be summarized as follows:

1. Curves are jagged at different frequencies or periods due to the randomness of seismic input. Studies of various earthquake records indicate that the jaggedness is quite sensitive to structural period but much less so to damping. In the figures, $\ddot{x}_g(0.319g)$, \dot{x}_g (13.04 in/sec), and x_g (8.4 in) represent maximum values of the earthquake (\dot{x}_g and x_g are obtained directly from \ddot{x}_g) which are used here for reference.
2. When the frequency is large (or short period), S_d is small and S_a approaches to \ddot{x}_g . This is because for a stiff structure with short period, the mass moves as a rigid body along with ground motion. Consequently, the structure has little deformation, and the mass acceleration is almost equal to ground acceleration, \ddot{x}_g .
3. When the frequency is small (or long period) for a flexible structure with little stiffness but much mass, S_d approaches to x_g and S_a is small. This behavior can be physically interpreted as a nearly immobile mass, but the structure's foundation moves along with the ground.

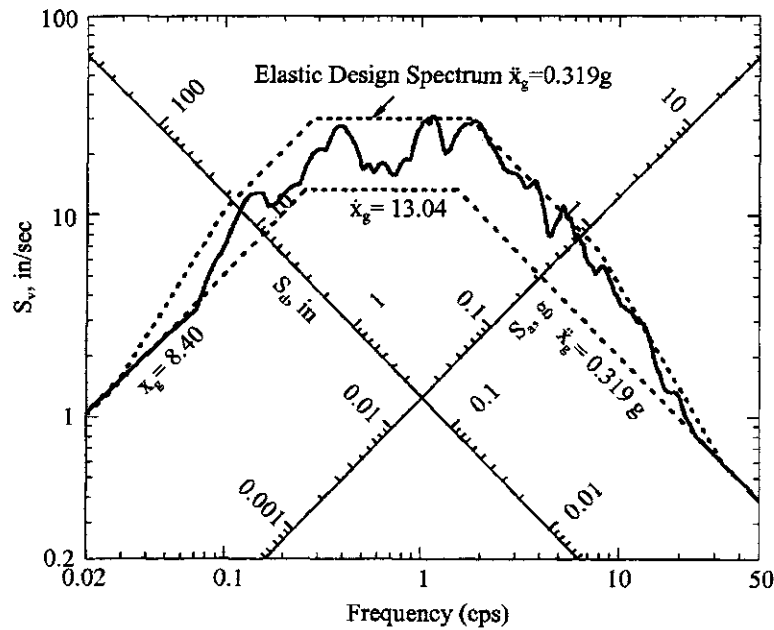


FIG. 7.17 Response spectrum S_v vs f for N-S component of 18 May, 1940 El Centro Earthquake.

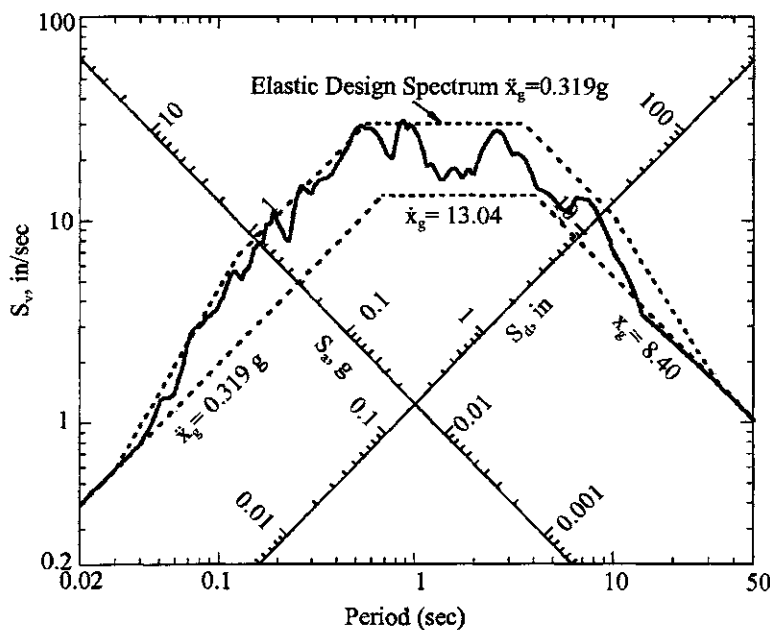


FIG. 7.18 Response spectrum S_v vs T for N-S component of 18 May, 1940 El Centro Earthquake.

4. For regions associated with intermediate frequency or period, velocity S_v is sensitive to f or T and ρ .

Note that the response spectra and pseudo-response spectra are established by using available earthquake records. In reality, these spectra are not appropriate for designing new structures

subject to future earthquakes of unknown characteristics. For a given region, such as El Centro, California, response spectra developed from the earthquakes which occurred at different times have different jaggedness. A *design spectrum* is needed to satisfy the safety requirements of new construction or the safety evaluation of existing structures. Researchers studied a large number of earthquake records for different soil profiles of rock, soft rock, and various sediments and determined amplification factors for various nonexceedence probabilities in terms of percentile. The amplification factors are based on damping ratios and sensitivity regions of acceleration, velocity, and displacement.

The elastic design spectrum shown in Figs. 7.17 and 7.18 is based on 18 May, 1940 El Centro earthquake with 84.1 percentile of nonexceedence probability and 5% damping. This percentile means the spectrum amplification factors, which are used to construct the elastic design spectrum, are obtained from a cumulative probability of 84.1%. That is, 84.1% of actual spectral values corresponding to the specified damping ratio can be expected to fall at or below the smoothed maximum ground motion values multiplied by the spectrum amplification factors. Amplification factors are 2.7 in the acceleration-sensitive region ($f=2.86\text{--}8$ or $T=0.125\text{--}0.349$), 2.3 in the velocity-sensitive region ($f=0.28\text{--}2$, or $T=0.5\text{--}3.57$), and 2.0 in the displacement-sensitive region ($f=0.03\text{--}0.1$ or $T=10\text{--}33$). Between $f=8$ and 33, the amplification factor gradually changes from 2.71 to 1 and between $f=0.1$ and 0.03, the factor changes from 2 to 1.

Comparisons between the velocities from Eq. (7.110) (\dot{x}) and Eq. (7.114) (S_v), between the relative acceleration from Eq. (7.112) (\ddot{x}) and pseudo-acceleration from Eq. (7.116) (S_a), and between the total acceleration from Eq. (7.113) (\ddot{x}_t) and pseudo-acceleration, S_a from Eq. (7.116) (S_a) are shown in Figs. 7.19–7.21, respectively. Note that the comparison between displacement x and pseudo-displacement S_d is not shown because they are identical for Eqs. (7.109), and (7.115) in absolute value. A significant difference exists between \dot{x} and S_v . This is because \dot{x} is based on Eq. (7.110), identical to Eq. (7.114) (S_v) only if the first term on the right-hand side of Eq. (7.110) is zero or if damping is not considered in both equations. Physically, for a long-period structure, the ground moves but the mass moves only a little. In this case, S_d is almost equal to x_g , which implies a small S_v . Also note that some differences exist between \ddot{x} and S_a (see Fig. 7.20) as well as between \ddot{x}_t and S_a (see Fig. 7.21).

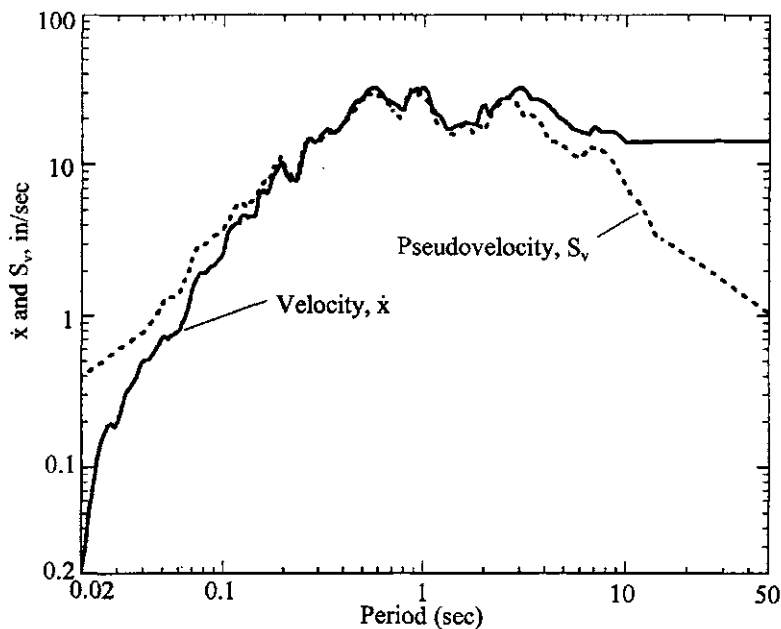


FIG. 7.19 Comparison between \dot{x} and S_v .

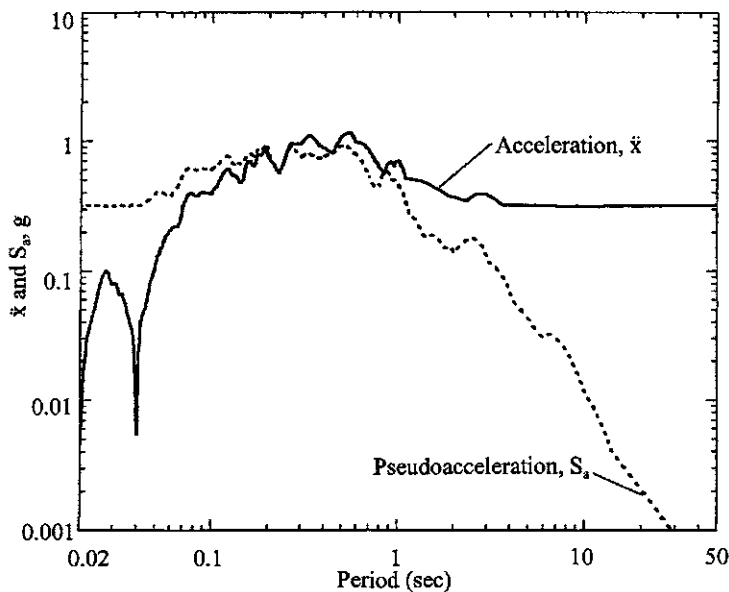


FIG. 7.20 Comparison between \ddot{x} and S_a .

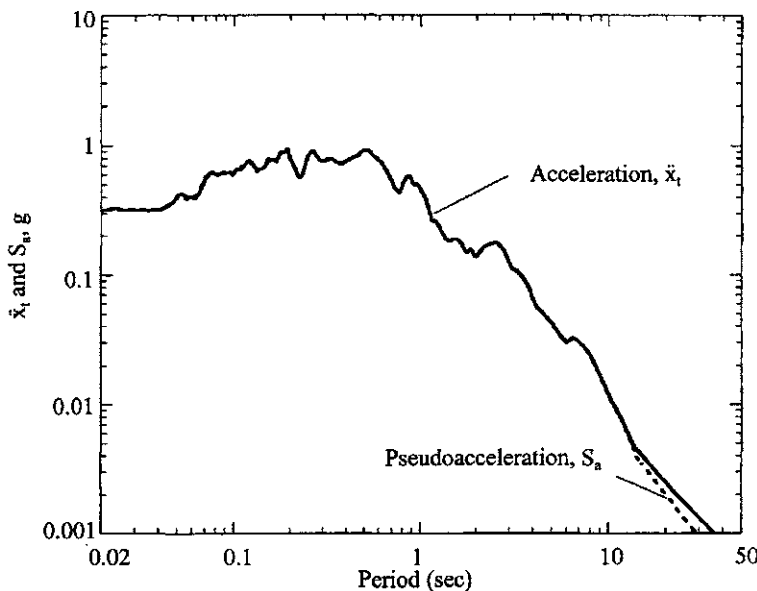


FIG. 7.21 Comparison between \ddot{x}_t and S_a .

Note further that \ddot{x}_t and S_a are different for various damping ratios. They are equal for the undamped case only. For a long period, both \ddot{x}_t and S_a approach to zero but at different rates of change. S_a is faster than \ddot{x}_t because of the denominator T^2 in S_a .

The above observations lead to the following conclusions:

1. x , \dot{x} , and \ddot{x}_t , (or \ddot{x}) and S_d , S_v , S_a are not respectively identical (except x and S_d). To distinguish them, the former are called *response spectra* and the latter *pseudo-spectra*, which means that they are approximations of response spectra.

2. Both spectra have jaggedness which shows the characteristics of a particular earthquake. For a given construction site, earthquakes occurring at different times do not have identical jaggedness. Therefore, for general structural design purposes, we must develop a spectrum that is representative of earthquake characteristics in a given region. This spectrum is defined as a *design spectrum* and should comprise a set of smooth curves or a set of straight lines with different damping factors. Detailed discussion of design spectrum is presented in Sections 7.4.2–7.4.6.

In response spectrum development, it is interesting to reveal response spectra of principal components. Displacement response spectra vs period (S_p vs T) for three *principal components*, *main*, *intermediate*, and *minor* of the 18 May, 1940 El Centro earthquake are shown in Figs. 7.22, 7.23, and 7.24, respectively. S_p is also denoted by R_p . The response spectra are based on Eq. (7.5). Note that the displacements at $T=1$, $\rho=0$ associated with main, intermediate, and minor principal components are about 6.2 in, 5 in, and 0.13 in, respectively.

As noted previously, response spectra for a specific earthquake record can be used to obtain the response of a structure subjected to that earthquake, but these spectra are not well-suited for design. For practical application, several design spectra are introduced in the following articles.

7.4.2. Housner's Average Design Spectra

Housner's average design spectra (see Fig. 7.25) are based on the characteristics of the two horizontal components of four earthquake ground motions recorded at El Centro in 1934 and 1940, Olympia in 1949, and Tehachapi in 1952 [13]. Spectra of individual earthquakes are generated, then normalized, averaged, and smoothed. The normalized spectra shown in Fig. 7.25 have the following characteristics: undamped velocity associated with long period has a value of

Scale factors	Ground motion
2.7	El Centro, 18 May, 1940
1.9	El Centro, 30 December, 1940
1.9	Olympia, 13 April, 1949
1.6	Taft, 31 July, 1952
1.5	Vernon, 10 March, 1933

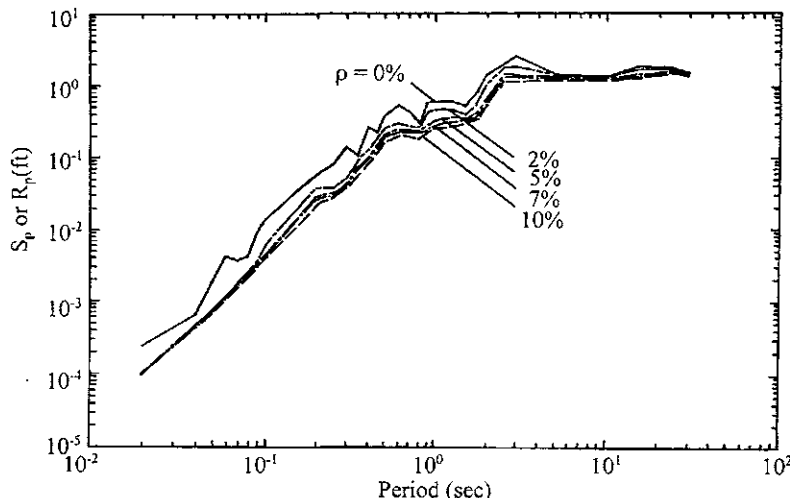


FIG. 7.22 Displacement response spectrum (S_p or R_p) for main principal component.

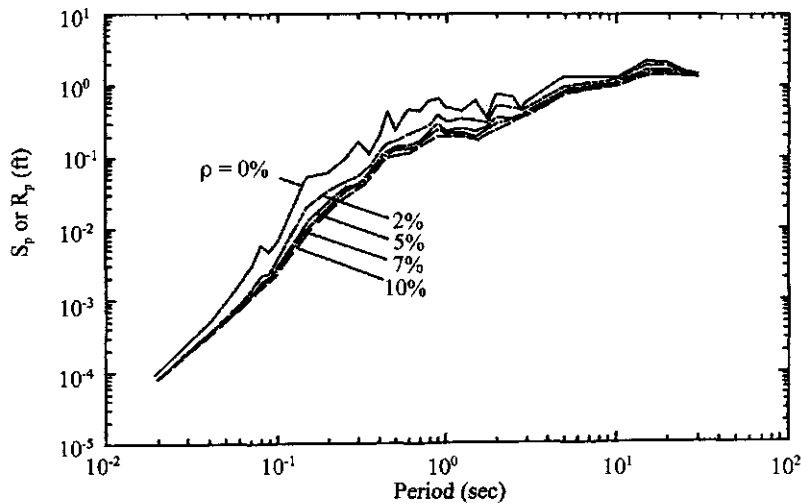


FIG. 7.23 Displacement response spectrum (S_p or R_p) for intermediate principal component.

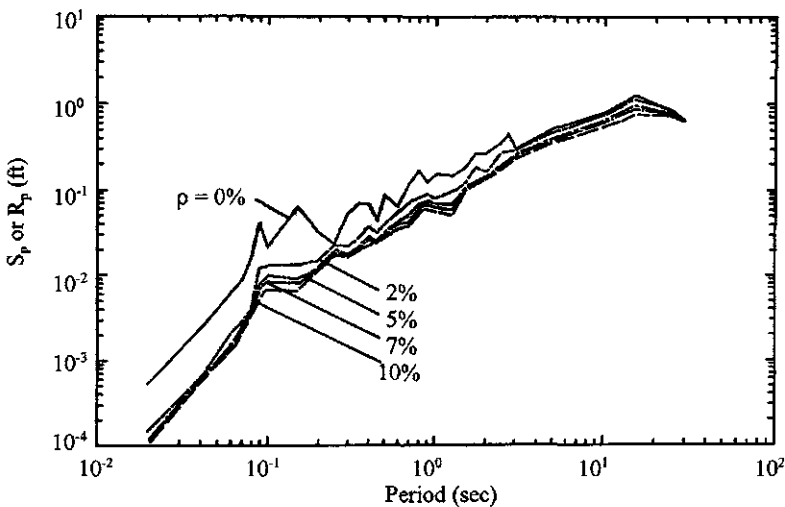


FIG. 7.24 Displacement response spectrum (S_p or R_p) for minor principal component.

1 ft/sec; undamped acceleration is close to 22 ft/sec² at peak, around 2 ft/sec² at long period, and 4 ft/sec² at zero period. Ordinates should be multiplied by the scale factors shown in the table above to bring them into agreement with the specific ground motion.

Magnitude equivalent to the 1940 El Centro earthquake is expected to recur an average of every 70 years at that site. Smaller earthquakes are expected to occur there more often. Figure 7.25 can be used for other recurrence intervals at El Centro by applying the multiplier in the table below [15].

Multipliers	Recurrence intervals in years
2.77	2
1.83	20
1.5	32
1.0	70

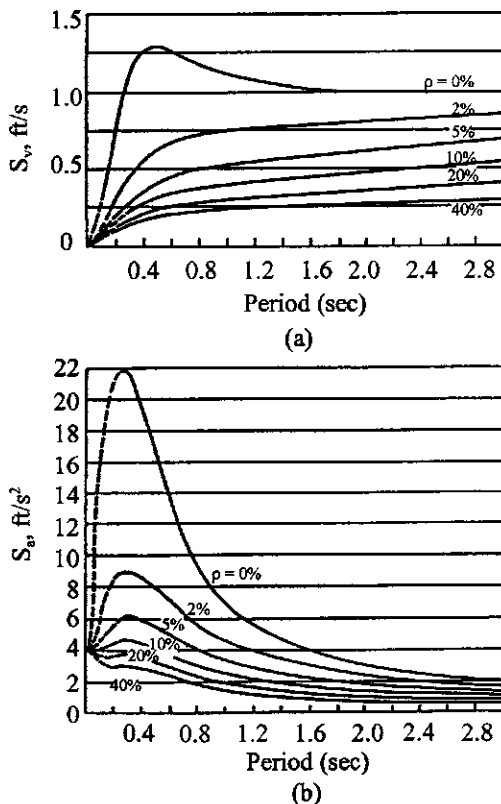


FIG. 7.25 Housner's smoothed averaged design spectra.

7.4.3. Newmark Elastic Design Spectra

Newmark elastic design spectra are shown in Fig. 7.26, where typical values of peak ground acceleration, velocity, and displacement with $1.0g$, 48 in/sec, and 36 in, are used to construct normalized design spectra for firm ground. These maximum values should be scaled down when ground acceleration is other than $1.0g$. In the elastic design spectra, three regions sensitive to acceleration, velocity, and displacement are respectively at the high, intermediate, and low frequency ranges, as presented previously in Fig. 7.17.

In this figure, spectral ordinates corresponding to different damping factors are obtained by multiplying ground acceleration, velocity, and displacement by the amplifications associated with a given damping (see Table 7.5). Spectral displacement, spectral velocity, and spectral acceleration are plotted parallel to maximum ground displacement, ground velocity, and ground acceleration, respectively. Frequencies at the intersections of the spectral displacement and velocity and of the spectral velocity and acceleration define the three amplified regions of the spectrum. At a frequency of approximately 6 Hz, spectral accelerations taper down to the maximum ground acceleration. It is assumed that the spectral acceleration for 2% damping intersects the maximum ground acceleration at a frequency of 30 Hz. Tapered spectral-acceleration lines for other dampings are parallel to the one for 2%. The normalized response spectra in Fig. 7.26 can be used in design by scaling ordinates to the design acceleration at the site.

EXAMPLE 7.4.1 A single-d.o.f. system has a natural period $T=1$ sec and damping factor $\rho=0.1$. Use the Newmark elastic design spectrum to determine maximum acceleration, maximum relative displacement, and maximum velocity for an earthquake with a maximum ground acceleration equal to $0.32g$.

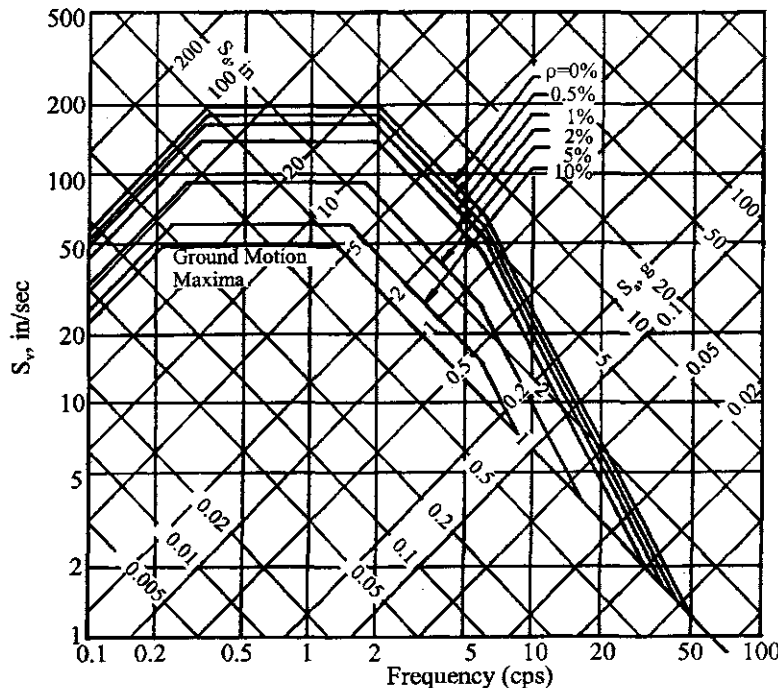


FIG. 7.26 Newmark elastic design spectra normalized to $1.0g$.

TABLE 7.5 Values of Spectrum Amplification Factors

Percent of critical damping	Amplification factor for		
	Displacement	Velocity	Acceleration
0	2.5	4.0	6.4
0.5	2.2	3.6	5.8
1	2.0	3.2	5.2
2	1.8	2.8	4.3
5	1.4	1.9	2.6
7	1.2	1.5	1.9
10	1.1	1.3	1.5
20	1.0	1.1	1.2

Solution: From the Newmark elastic design spectra in Fig. 7.26 with frequency $f = 1/T = 1 \text{ Hz}$ and 10% critical damping, maximum displacement, maximum velocity, and maximum acceleration are

$$\begin{aligned} S_d &= 9.5 (0.32) = 3.04 \text{ in} \\ S_v &= 60 (0.32) = 19.2 \text{ in/sec} \\ S_a &= 0.95 (0.32) = 0.304g \end{aligned}$$

7.4.4. Newmark Inelastic Design Spectra

Structures subjected to severe earthquake ground motion experience deformations beyond the elastic range. Inelastic deformations depend on load-deformation characteristics of the structure

and often result in stiffness deterioration. A simple model that approximates the inelastic behavior of structural systems is the elasto-plastic model shown in Fig. 7.27b where x_y represents yield displacement and x_m signifies maximum displacement. (More inelastic models are discussed in Chapter 9.)

Figure 7.27b displays two material models: the *elasto-plastic model* (or elastic perfectly plastic) shown by $oabcde$ and the *equivalent elastic model* defined by $oABC$. Q_y and x_y represent yielding force and deformation, respectively. The fundamental behavior of an elasto-plastic model is as follows. When a structural member's internal force is less than Q_y , the member is elastic or linear; the member force cannot be more than Q_y , but its deformation can be more than yielding deformation x_y . If a member is assumed to behave with a linear force-deformation relationship beyond yielding level as shown in $oABC$, it is an equivalent, not a real, elastic model. From the figure, *yield reduction factor*, Y_r , *force reduction factor*, F_r , and *ductility factor*, μ , may be defined as

$$Y_r = \frac{Q_e}{Q_y}, \quad F_r = \frac{Q_e}{Q_e} \quad (7.120)$$

$$\mu = \frac{x_m}{x_y} \quad (7.120a)$$

Then

$$F_r = \frac{1}{Y_r} = \frac{x_y}{x_e} \quad (7.121)$$

Combining Eqs. (7.120) and (7.121) yields

$$\frac{x_m}{x_e} = \mu \quad F_r = \frac{\mu}{Y_r} \quad (7.122)$$

From Fig. 7.29a, the motion equation of a single-d.o.f. system with mass M , damping factor ρ , and frequency p is

$$\ddot{x} + 2\rho p\dot{x} + p^2 x_y \bar{Q} = -\ddot{x}_g \quad (7.123)$$

in which the third term on the left-hand side is due to a resistance force, $Q(x)$, a function of

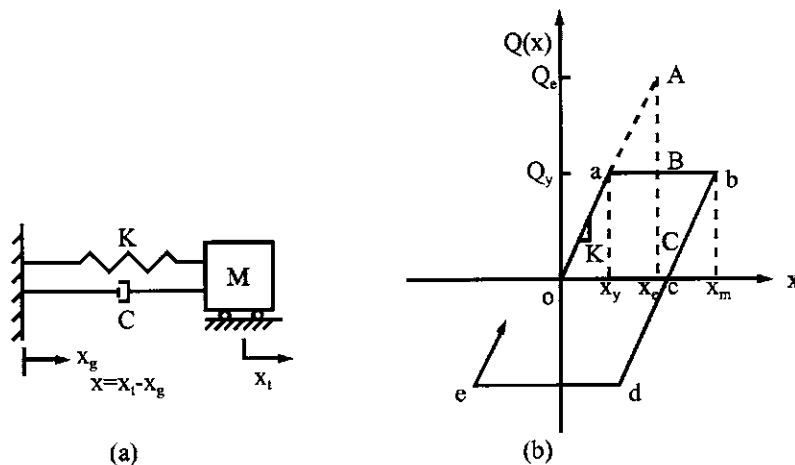


FIG. 7.27 Elasto-plastic model for single-d.o.f. system.

deformation, x , resulting from

$$\frac{Q(x)}{M} = \frac{\bar{Q}Q_y}{M} = \frac{Kx_y}{M} \bar{Q} = p^2 x_y \bar{Q} \quad (7.124)$$

where \bar{Q} is a simple notation as $\bar{Q} = Q(x)/Q_y$; $Q_y = Kx_y$.

The response spectrum of an inelastic system may be established by using Fig. 7.28 as follows.

1. Select damping factor ρ .
2. Select ductility factor μ .
3. Select a range of frequencies between $f = 0.02$ and 50 cps (or period) with small increment of f in the following calculations:
 - (a) Find the peak elastic response x_e from

$$M\ddot{x} + C\dot{x} + Kx = -M\ddot{x}_g$$

and then calculate the peak resistance of the equivalent elastic system,

$$Q_e = Kx_e$$

- (b) Find the inelastic response $x(t)$ of the elasto-plastic system from the motion equation given in (a) for which yielding resistance is defined by

$$Q_y = F_r Q_e$$

where F_r is gradually increased from 0.001 to 1 ; at each increment find the peak deformation as

$$x_m = \max|x(t)|$$

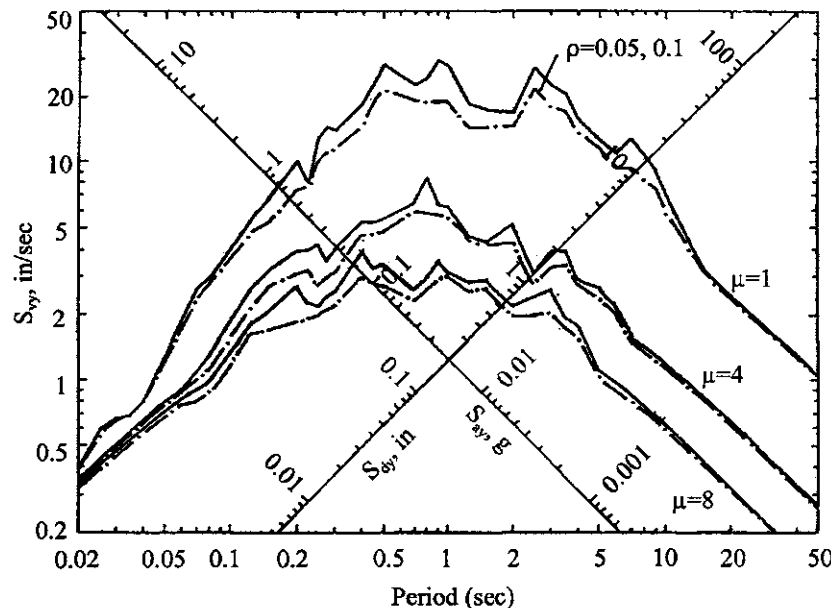


FIG. 7.28 Inelastic design spectra for ground motion $\ddot{x}_g = 1g$, $\dot{x}_g = 48$ in/sec, $x_g = 36$ in, and $\rho = 0.05$.

when

$$\left| \frac{x_m}{x_e} - \mu F_r \right| = 0 \quad (7.125)$$

or less than a tolerance ϵ ; then F_r is determined. Consequently $Q_y(F_r Q_e)$, $x_y(F_r x_e)$, x_m are known.

- (c) Find velocity and acceleration corresponding to the correct solution of x_m by using any numerical method presented previously, such as Newmark integration. Results are plotted in a spectrum associated with a frequency.
- 4. Repeat step 3 for another incremental frequency.
- 5. Repeat step 2 for another ductility.

With the same percentile of nonexceedence probability and amplification factors, elastic design spectrum ($\mu=1$) is plotted in Fig. 7.28. Inelastic design spectra associated with $\mu=4$ and 8 are also plotted in the figure where pseudo-displacement, pseudo-velocity, and pseudo-acceleration are obtained at yielding deformation as

$$S_{dy} = x_y; \quad S_{vy} = p x_y; \quad S_{ay} = p^2 x_y \quad (7.126)$$

Observing Fig. 7.28 leads to some general conclusions.

- 1. Both ductility and damping have little influence on the acceleration-sensitive regions corresponding to larger frequency (shorter period), nor on the displacement-sensitive region associated with smaller frequency (longer period).
- 2. Both damping and ductility have significant influence on the velocity-sensitive region with an intermediate range of frequencies or periods.

Although elasto-plastic models can be used to predict structural response by numerical integration methods, the computations are time-consuming and costly. This is especially true when they have to be repeated with a number of earthquake acceleration records to arrive at representative response values for design. *Inelastic design spectra* are given in Fig. 7.29 (frequency vs S_{vy} and period vs S_{vy}), which looks similar to spectra for the elastic system in Figs. 7.17 and 7.18 (frequency vs S_v and period vs S_v). Here, amplification factors are 2.7 in the acceleration-sensitive region, 2.3 in the velocity-sensitive region, and 2.0 in the displacement sensitive region. We thus have 2.7g for line E, 110.4 ($2.3 \times 48 = 110.4$) for line D, and 72 ($2 \times 36 = 72$) for line C in Fig. 7.29a or for lines C, D, and E in Fig. 7.29b. These values are based on 84.1 percentile and 5% damping. Lines associated with elastic response ($\mu = 1$) in Fig. 7.29 are displaced downward by an amount from the ductility factor μ .

Rules for construction of an inelastic design spectrum are summarized as follows.

- 1. Draw lines A' , B' , C' and D' parallel to lines A , B , C and D by dividing the ordinates of A , B , C and D with a specified ductility ratio μ (say 4 or 8 in the figure). The reason is that, for this frequency region, the response is somewhat affected by a constant value of μ as observed from Fig. 7.28.
- 2. Divide the ordinate of E on elastic spectrum segment de by $\sqrt{(2\mu - 1)}$ to locate point E' , i.e. move e to e' ; then draw a line from e' with 45° to intersect line D' at point d' . Here the rationale comes from the conservation of energy method, i.e. total energy absorbed by the spring of an inelastic system is the same as that of an elastic system; both systems have the same frequency. This is based on Fig. 7.27 and can be expressed as

$$\frac{1}{2} Q_e x_e = \frac{1}{2} Q_y x_y + (x_m - x_y) Q_y \quad (7.127)$$

or

$$Q_e x_e = x_y Q_y (2\mu - 1) \quad (7.128)$$

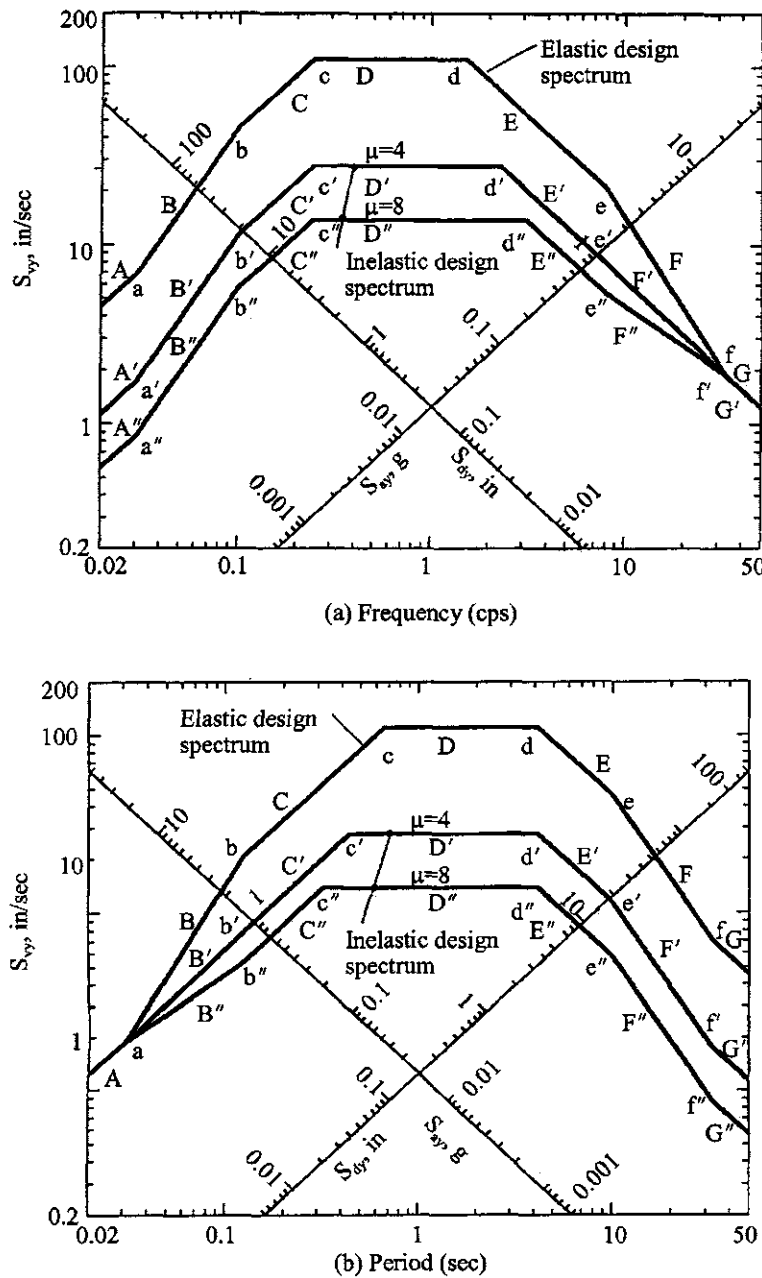


FIG. 7.29 Typical inelastic design spectrum for $\mu = 4$ and 8, and $\rho = 0.05$.

Since

$$Q_e = Kx_e; \quad Q_y = Kx_y \quad (7.129)$$

Substituting Eq. (7.129) into Eq. (7.128) yields

$$\frac{x_e}{x_y} = \sqrt{2\mu - 1} \quad (7.130)$$

Therefore

$$\frac{Q_e}{Q_y} = \sqrt{2\mu - 1} \quad (7.131)$$

Since both Q_e and Q_y are based on elastic systems, we may write $Q_e = M S_{ay}$, $Q_y = M S'_{ay}$, and derive the final correction factor in the acceleration-sensitive region

$$S'_{ay} = \frac{S_{ay}}{\sqrt{2\mu - 1}} \quad (7.132)$$

3. In a region with very large frequency, points f and f' are the same while G and G' coincide, which implies that a very stiff structure should be designed as an elastic system.

Ductility is an important parameter in structural design. It is necessary to distinguish ductility demand, ductility capacity, and allowable ductility. *Ductility demand* represents a requirement on the design of a system that its ductility capacity should exceed ductility demand. *Ductility capacity* means the ability to deform beyond the elastic limit. Suppose the peak deformation of an elasto-plastic system, with $F_r = Q_y/Q_e = 0.5$, is x_m of 2.5 in, for which the equivalent linear model has displacement $x_e = 1.75$ in. We can calculate the ductility demand of the system by using Eq. (7.122) as

$$\mu = \frac{x_m}{x_e} \frac{1}{F_r} = \frac{2.5}{1.75} \frac{1}{0.5} = 2.86$$

Allowable ductility means the ductility capacity that can be attained from the materials and the details used in a structure. For a given allowable ductility, period, and damping of a structure with weight W , we find yielding strength Q_y , in order to limit ductility demand to allowable ductility, by using Eq. (7.126),

$$Q_y = K x_y = \frac{S_{ay}}{p^2} K = \frac{S_{ay}}{g} W \quad (7.133)$$

Thus

$$x_m = \mu x_y = \mu \frac{S_{ay}}{p^2} \quad (7.134)$$

For a specific earthquake excitation, a structural designer should design and detail to achieve deformation capacity x_m .

EXAMPLE 7.4.2 For a single-d.o.f. system with structural weight W , frequency 5 cps, and damping factor 0.05, find the force Q_y and displacement x_m for which the structure should be designed in the following three cases: (1) within elastic limit; (2) with allowable ductility of 2; and (3) with allowable ductility of 4. Assume an earthquake with a peak acceleration of 0.32g.

Solution: From Fig. 7.29, S_{ay} of elastic response at $f=5$ ($T=0.2$) can be obtained from line E in the amount of $2.7g$ which should be scaled down to $S_{ay} = (0.32)(2.7g) = 0.864g$. Solutions of individual cases are calculated as follows.

Case 1 of elastic case—from Eqs. (7.133) and (7.134)

$$Q_e = \frac{S_{ay}}{g} W = 0.864 W \quad (a)$$

$$x_m = x_e = \frac{S_{ay}}{p^2} = \frac{0.864(386.4)}{[2\pi(5)]^2} = 0.338 \text{ in} \quad (b)$$

x_m may also be obtained directly from Fig. 7.29a or b at $S_{dy} = 1.06$, which is then multiplied by 0.32.

Case 2 for $\mu=2$

$$Q_y = \frac{Q_e}{\sqrt{2\mu - 1}} = \frac{0.864W}{1.732} = 0.5W \quad (c)$$

$$x_m = \frac{\mu x_e}{\sqrt{2\mu - 1}} = \frac{0.676}{1.732} = 0.39 \text{ in} \quad (d)$$

which cannot be obtained from Fig. 7.29a or b since it does not have the design response for $\mu = 2$.

Case 3 for $\mu = 4$ —we may calculate the response in a manner similar to that shown in Eqs. (c) and (d) as

$$Q_y = \frac{0.864W}{\sqrt{2(4) - 1}} = 0.327W \quad (e)$$

$$x_m = \frac{4(0.338)}{\sqrt{(2)(4) - 1}} = 0.511 \text{ in} \quad (f)$$

The solution in Eq. (f) can be obtained from Fig. 7.29a on line E' or Fig. 7.29b on line C' with $S_{dy}=0.4$. Thus

$$x_m = 0.4(0.32)(4) = 0.512 \text{ in} \quad (g)$$

EXAMPLE 7.4.3 Calculate maximum acceleration, maximum velocity, and maximum displacement of the single-d.o.f. system in Example 7.4.1; assume that the structure has design ductility ratio $\mu = 4.0$.

Solution: From the inelastic design spectra in Fig. 7.29a with frequency $f = 1 \text{ Hz}$, 5% critical damping, and $\mu = 4$, the maximum displacement S_{dy} , maximum velocity S_{vy} , and maximum acceleration S_{ay} are

$$S_{dy} = 5 \times 0.32 = 1.60 \text{ in}$$

$$S_{vy} = 27.5 \times 0.32 = 8.8 \text{ in/sec}$$

$$S_{ay} = 0.31 \times 0.32 = 0.099g$$

7.4.5. Site-Dependent Spectra and UBC-94 Design Spectra

7.4.5.1. Site Dependent Spectra

In 1976, a study of the influence of soil conditions on response spectra was published [20]. It shows that soil conditions can substantially affect spectral shapes. The study included a total of 104 ground motions obtained from 23 earthquake records with peak ground accelerations greater than $0.05g$. The records were representative of four site conditions: rock, stiff soils less than about 150 ft deep, deep cohesionless soil with depths greater than about 250 ft, and soft to medium stiff clay with associated strata of sand or gravel. Response spectra for 5% damping were normalized to the peak ground acceleration of the records and averaged at various periods. Average spectra of the four site conditions are presented in Fig. 7.30. The ordinate in this figure represents acceleration amplification. Normalized spectral ordinates for rock are substantially below those for soft to medium clay and for deep cohesionless soil.

7.4.5.2. UBC-94 Design Spectra

The Uniform Building Code or UBC (International Conference of Building Officials, 1994), recommends the design spectra with site-dependent effects shown in Fig. 7.31. Soil profile types in the design spectra are divided into three categories: types S_1 , S_2 , and S_3 . Type S_1 is for rock and stiff soils, type S_2 is for deep cohesionless or stiff clay soils, and type S_3 is for soft to medium clays and sands.

Recommended design spectra for Fig. 7.31 are constructed on the basis of 5% damping. To obtain the acceleration, the ordinates must be multiplied by the value of the *effective peak ground accelerations* (EPGA). For vertical motion, the spectral value may be determined by multiplying

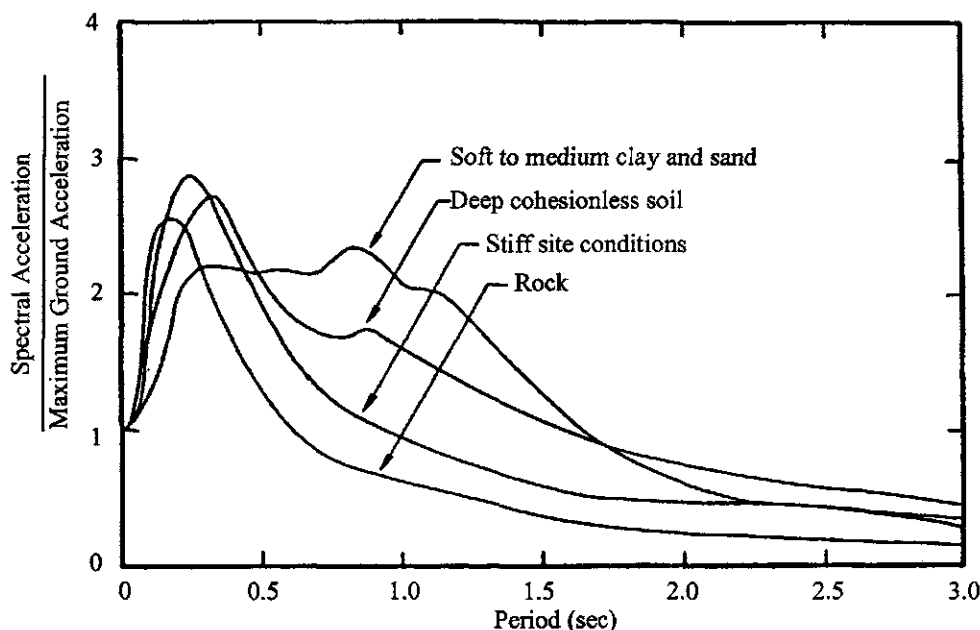


FIG. 7.30 Average acceleration spectra with 5% damping.

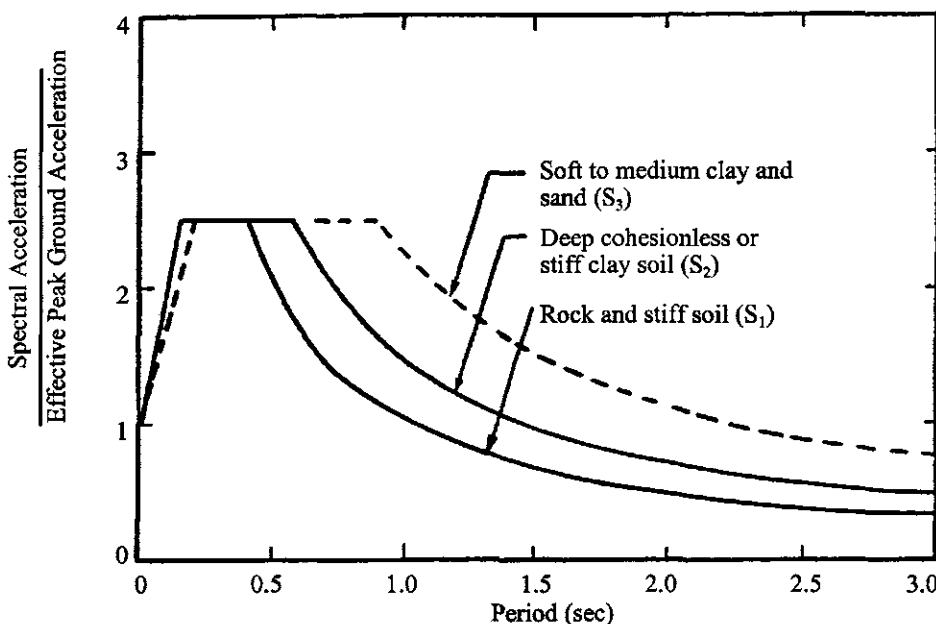


FIG. 7.31 UBC-94 normalized design spectra.

the spectral acceleration of horizontal motion by a factor of 0.67. The relationship between *peak ground acceleration* (PGA), EPGA, and seismic zone is introduced in Section 7.2.3. Spectra include both *near* and *distant earthquakes*, and are averaged as well as normalized with respect to PGA. The averaged curve is then smoothed to eliminate irregularities that could cause large

For convenience of computer programming, the curve-fitting polynomial functions of the spectral curves for soil profile types S_1 , S_2 , and S_3 are given as follows:

1. Soil profile type S_1

$$(S_a)_i = 1 + 10 T_i; \quad \text{for } T_i \leq 0.15 \text{ sec} \quad (7.135)$$

$$(S_a)_i = 2.5; \quad \text{for } 0.15 < T_i \leq 0.4 \text{ sec} \quad (7.136)$$

$$\begin{aligned} (S_a)_i &= 2.4291 - 3.9693(T_i - 0.4) + 3.4752(T_i - 0.4)^2 \\ &\quad - 1.4541(T_i - 0.4)^3 + 0.2252(T_i - 0.4)^4; \\ &\quad \text{for } 0.4 < T_i \leq 3.0 \text{ sec} \end{aligned} \quad (7.137)$$

2. Soil profile type S_2

$$(S_a)_i = 1 + 10 T_i; \quad \text{for } T_i \leq 0.15 \text{ sec} \quad (7.138)$$

$$(S_a)_i = 2.5; \quad \text{for } 0.15 < T_i \leq 0.57 \text{ sec} \quad (7.139)$$

and

$$\begin{aligned} (S_a)_i &= 2.5844 - 2.9449(T_i - 0.5) + 1.8397(T_i - 0.5)^2 \\ &\quad - 0.5847(T_i - 0.5)^3 + 0.0737(T_i - 0.5)^4; \\ &\quad \text{for } 0.57 < T_i \leq 3.0 \text{ sec} \end{aligned} \quad (7.140)$$

3. Soil profile type S_3

$$(S_a)_i = 1 + 7.5 T_i; \quad \text{for } T_i \leq 0.2 \text{ sec} \quad (7.141)$$

$$(S_a)_i = 2.5; \quad \text{for } 0.2 \text{ sec} < T_i \leq 0.8 \text{ sec} \quad (7.142)$$

and

$$\begin{aligned} (S_a)_i &= 0.9[2.4989 - 2.4919(T_i - 0.9) \\ &\quad + 1.8436(T_i - 0.9)^2 - 0.8017(T_i - 0.9)^3 \\ &\quad + 0.1435(T_i - 0.9)^4]; \\ &\quad \text{for } 0.8 \text{ sec} < T_i \leq 3.0 \text{ sec} \end{aligned} \quad (7.143)$$

All spectral shapes presented in Fig. 7.31 have an upper bound of 3.0 sec for the corresponding natural period. It is assumed that for any period longer than 3.0 sec, spectral acceleration corresponding to a period of 3.0 sec can be used.

7.4.6. Various Definitions of Ductility

There are several definitions of ductility according to various physical deformations which may be summarized as follows.

1. *Based on load displacement*—here ductility is based on the ratio of maximum absolute displacement (or deflection) of a member or system to the yielding displacement of that member or system as

$$\mu = \frac{|x_m|}{x_y} \quad (7.144)$$

which is already described in Eq. (7.120a) and Fig. (7.27).

2. *Based on moment rotation*—here ductility is defined in terms of rotation as

$$\mu = \frac{|\theta_{\max}|}{\theta_y} = \frac{\theta_y + \alpha}{\theta_y} = 1 + \frac{\alpha}{\theta_y} \quad (7.145)$$

where $|\theta_{\max}|$ is maximum absolute structural nodal rotation, θ_y is yielding rotation, and α is plastic rotation as shown in Fig. 7.32.

3. *Ductility based on moment curvature*—ductility can also be expressed in terms of curvature

$$\mu = \frac{|\phi_{\max}|}{\phi_y} = 1 + \frac{\phi_0}{\phi_y} \quad (7.146)$$

where $|\phi_{\max}|$ is maximum absolute curvature, ϕ_0 is plastic curvature, and ϕ_y is curvature at yield (see Fig. 7.33).

4. *Ductility based on moment energy*—structural deformation behavior depends mainly on variations in external excitation. When a structure is subjected to coupling horizontal and vertical earthquake ground motion, deformation exhibits irregular patterns as shown in Fig. 7.34 [1]. It is convenient to express ductility in terms of the internal force of a

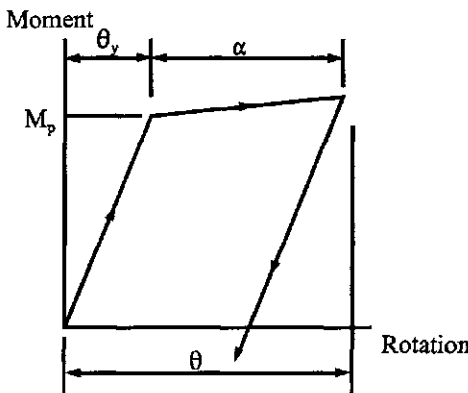


FIG. 7.32 Ductility based on moment rotation.

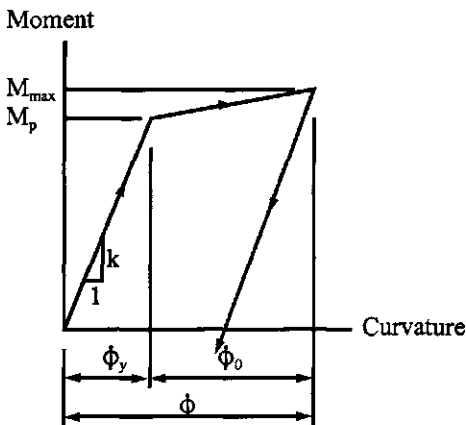


FIG. 7.33 Ductility based on moment curvature.

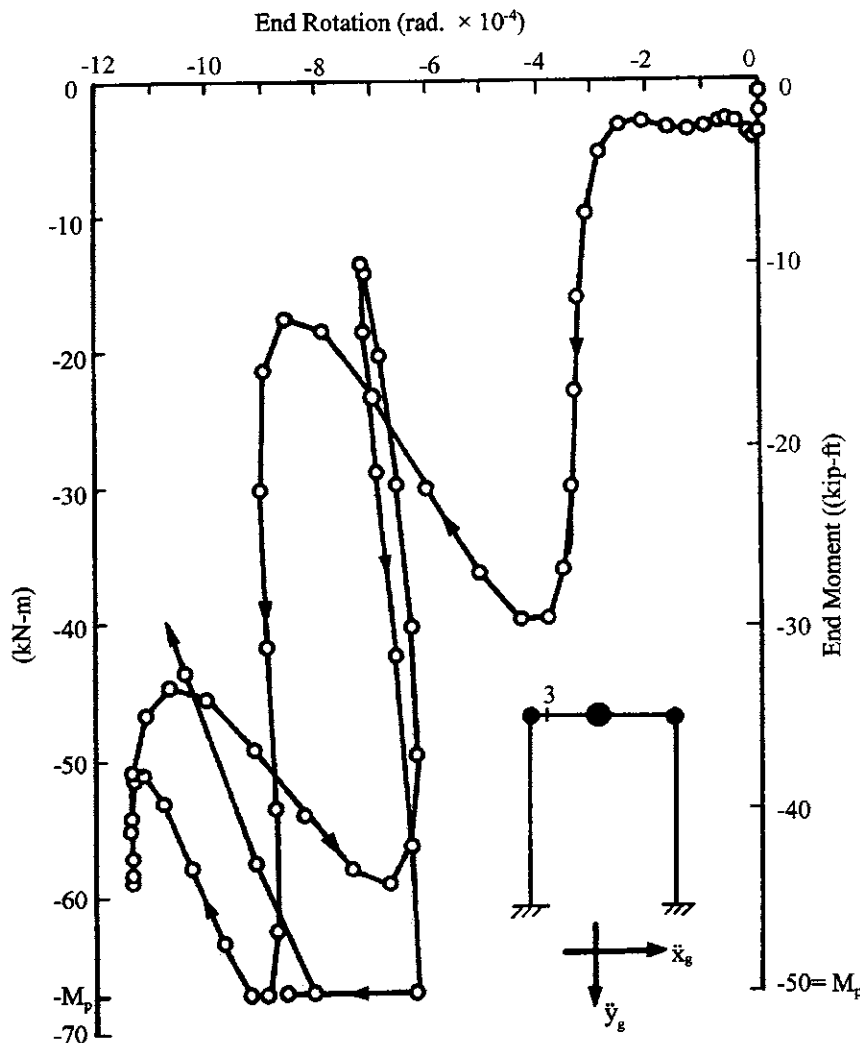


FIG. 7.34 Moment-rotation relationship of node 3 for coupling horizontal and vertical ground motion of 18 May, 1940 El Centro Earthquake.

member and the internal energy associated with this force as

$$\mu = 1 + \frac{E_{ds}}{E_{tes}} \quad (7.147)$$

where E_{ds} is dissipated strain energy of a member-end during a half-cycle of nodal rotation and E_{tes} is total elastic strain energy in the member under consideration. Symbolic notations are shown in Fig. 7.35. For the irregular moment rotation relationship shown in Fig. 7.34, energy should be calculated by using incremental procedures to find cumulative results.

Note that the ductility of a structural system may be defined as the ratio of deflection (or rotation) at the system's ultimate collapse to deflection (or rotation) when the system suffers its first yield.

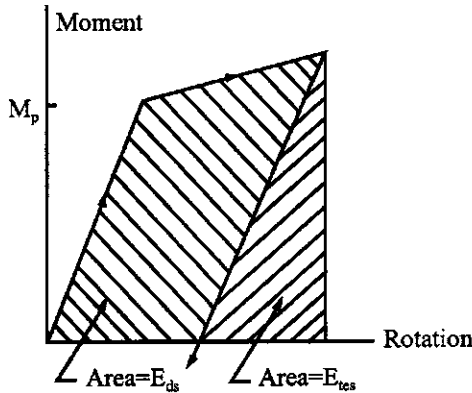


FIG. 7.35 Ductility based on moment energy.

PART B ADVANCED TOPICS

7.5. TORSIONAL RESPONSE SPECTRA

As mentioned in Section 7.2.4, earthquake ground motion is considered to have three translational components and three rotational components. In general, rotational components have not been part of dynamic structural analysis, but their effect is significant and should be considered for safety's sake of critical structures such as nuclear power plants.

Since most strong motion seismographs are designed to record three translational motions only, no actual record of rotational earthquakes is available. Therefore, the following articles describe how to generate seismic rotational records from translational ones, and how to compute torsional response spectra from rotational records.

7.5.1. Ground Rotational Records Generation

Assuming the soil is an elastic medium and earthquake waves propagate in the direction of x , wave motion is known to be governed by the following partial differential equation:

$$a^2 \frac{\partial^2 u(x, t)}{\partial x^2} = \frac{\partial^2 u(x, t)}{\partial t^2} \quad (7.148)$$

in which $u(x, t)$ represents displacement of soil particles moving in the x direction, “ a ” represents shear wave (S-wave) velocity, and t represents time. The solution of Eq. (7.148) can be obtained by using *D'Alembert's method* as follows. Let $\ell = x + at$ and $m = x - at$. Then

$$\frac{\partial u}{\partial x} = \frac{\partial u}{\partial \ell} \frac{\partial \ell}{\partial x} + \frac{\partial u}{\partial m} \frac{\partial m}{\partial x} = \frac{\partial u}{\partial \ell} + \frac{\partial u}{\partial m} \quad (7.149)$$

$$\begin{aligned} \frac{\partial^2 u}{\partial x^2} &= \frac{\partial}{\partial x} \left(\frac{\partial u}{\partial \ell} + \frac{\partial u}{\partial m} \right) = \frac{\partial}{\partial \ell} \left(\frac{\partial u}{\partial \ell} + \frac{\partial u}{\partial m} \right) \frac{\partial \ell}{\partial x} + \frac{\partial}{\partial m} \left(\frac{\partial u}{\partial \ell} + \frac{\partial u}{\partial m} \right) \frac{\partial m}{\partial x} \\ &= \frac{\partial^2 u}{\partial \ell^2} + 2 \frac{\partial^2 u}{\partial \ell \partial m} + \frac{\partial^2 u}{\partial m^2} \end{aligned} \quad (7.150)$$

$$\frac{\partial u}{\partial t} = \frac{\partial u}{\partial \ell} \frac{\partial \ell}{\partial t} + \frac{\partial u}{\partial m} \frac{\partial m}{\partial t} = a \left(\frac{\partial u}{\partial \ell} - \frac{\partial u}{\partial m} \right) \quad (7.151)$$

$$\begin{aligned}\frac{\partial^2 u}{\partial t^2} &= \frac{a \partial \left[\frac{\partial u}{\partial \ell} - \frac{\partial u}{\partial m} \right]}{\partial t} = a \left[\frac{\partial \left(\frac{\partial u}{\partial \ell} - \frac{\partial u}{\partial m} \right)}{\partial \ell} \frac{\partial \ell}{\partial t} + \frac{\partial \left(\frac{\partial u}{\partial \ell} + \frac{\partial u}{\partial m} \right)}{\partial m} \frac{\partial m}{\partial t} \right] \\ &= a^2 \left(\frac{\partial^2 u}{\partial \ell^2} - 2 \frac{\partial^2 u}{\partial \ell \partial m} + \frac{\partial^2 u}{\partial m^2} \right)\end{aligned}\quad (7.152)$$

Substituting Eqs. (7.150), and (7.152) into Eq. (7.48) leads to

$$a^2 \left[\frac{\partial^2 u}{\partial \ell^2} + 2 \frac{\partial^2 u}{\partial \ell \partial m} + \frac{\partial^2 u}{\partial m^2} \right] = a^2 \left[\frac{\partial^2 u}{\partial \ell^2} - 2 \frac{\partial^2 u}{\partial \ell \partial m} + \frac{\partial^2 u}{\partial m^2} \right] \quad (7.153)$$

which yields

$$\frac{\partial^2 u}{\partial \ell \partial m} = 0 \quad (7.154)$$

Integrating Eq. (7.154) with respect to m gives

$$\frac{\partial u}{\partial \ell} = h(\ell) \quad (7.155)$$

where $h(\ell)$ is a function of ℓ . Integrating Eq. (7.155) with respect to ℓ gives

$$\begin{aligned}u &= \int h(\ell) d\ell + f(m) \\ &= g(\ell) + f(m) \\ &= g(x + at) + f(x - at)\end{aligned}\quad (7.156)$$

where g and f are the functions of ℓ and m , respectively. If we consider only the transmission of movement in the positive x direction, then Eq. (7.156) reduces to

$$u(x, t) = f(x - at) \quad (7.157)$$

or

$$u(x, t) = f\left(t - \frac{x}{a}\right) \quad (7.157a)$$

To explain $f(x - at)$ as the wave moving toward the positive x direction, we introduce a travel-time curve as shown in Fig. 7.36. In this figure, a wave travels from points A' and B' to points B' and C' . Then the following relationship can be observed:

$$f(x_1) = f(x_2) \quad (7.157b)$$

or

$$f(x_2 - a(t_2 - t_1)) = f(x_2) \quad (7.157c)$$

If t_1 is the initial time or $t_1 = 0$, Eq. (7.157c) leads to

$$f(x) = f(x - at) \quad (7.157d)$$

Therefore $f(x - at)$ represents wave displacement of f at location x and at time t . Comparing Eqs. (7.157) and (7.157a), $f(x - at)$ is equal to $f(t - x/a)$. This relationship can be illustrated in Fig. 7.37. This figure shows t and x can express each other, i.e. $x = at$ or $t = x/a$. Therefore a wave can be expressed as $f(x - at)$ or $f(t - x/a)$.

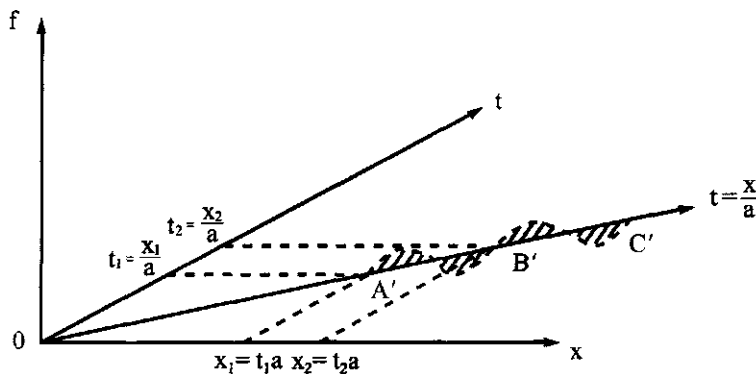


FIG. 7.36 Wave travel-time curve.

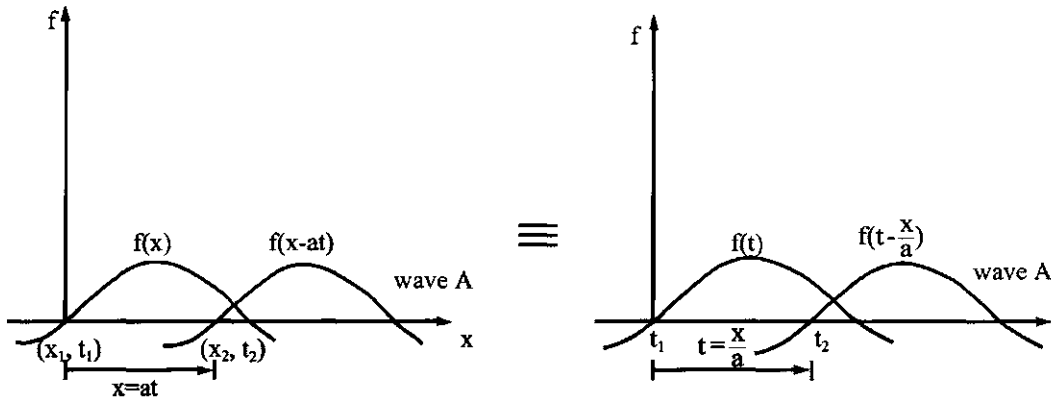


FIG. 7.37 Wave motions.

Consider a wave propagating along the ξ direction as shown in Fig. 7.38. From Eq. (7.157a), we may express soil particle movement as

$$u(\xi, t) = f\left(t - \frac{\xi}{a}\right) \quad (7.158)$$

In Fig. 7.38, the earthquake's *main*, *intermediate*, and *minor components* are along the x , y , and z directions, respectively. Displacement ξ can be expressed as

$$\xi = x \cos \alpha + y \cos \beta + z \cos \gamma \quad (7.159)$$

Substituting Eq. (7.159) into Eq. (7.158) yields

$$u(x, y, z, t) = f\left[t - \left(\frac{x}{C_x} + \frac{y}{C_y} + \frac{z}{C_z}\right)\right] \quad (7.160)$$

in which $C_x = a/\cos \alpha$, $C_y = a/\cos \beta$, $C_z = a/\cos \gamma$. C_x , C_y , and C_z are the velocities with which the wave travels in the x , y , and z directions, respectively. To explain the meaning of C_x , C_y , and C_z , we assume that the wave motion acts like a rigid plate moving parallel to its previous position (see Fig. 7.39). In this figure, a plane wave will travel from point M to point N in a unit of time, and this distance is equal to a . Along the x axis, in the same unit of time, C_x is the velocity with a magnitude of $C_x = a/\cos \alpha$. Similarly, C_z can be expressed as $C_z = a/\cos \gamma$. Because $u(x, y, z, t)$

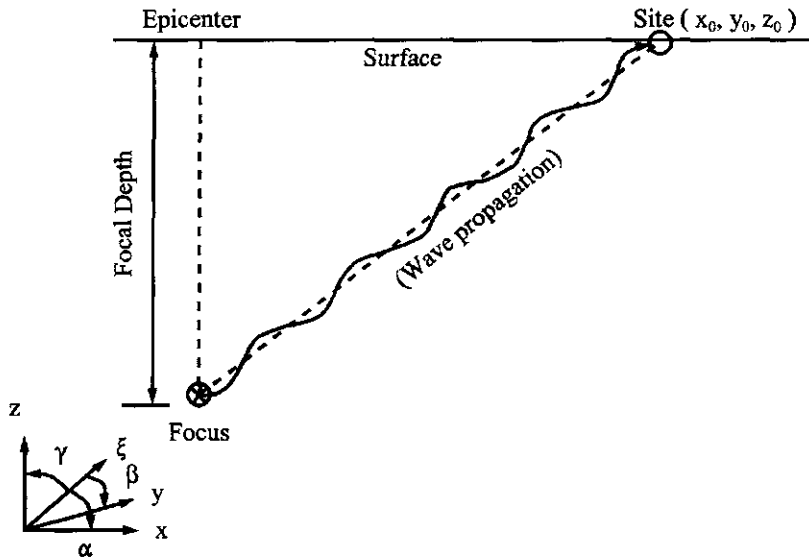


FIG. 7.38 Wave propagation in ξ direction.

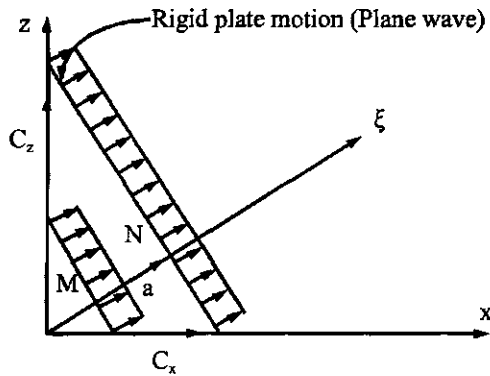


FIG. 7.39 Rigid plane motion (assume $\beta = 90^\circ$).

represents a wave motion, $u(x, y, z, t)$ may be written as

$$u(x, y, z, t) = F(x, y, z) e^{i\tilde{\psi}(x, y, z, t)} \quad (7.161)$$

Let the site location (Fig. 7.38) be (x_0, y_0, z_0) , and the amplitude at that site be F_0 . Assume that, in the vicinity of the site, the variation of F remains sufficiently unchanged that F equals the constant F_0 (assume no dissipation of vibratory energy in the soil medium). We may then call F the amplitude. In a small vicinity of x_0, y_0, z_0, t_0 , the variation of u can thus be expressed as

$$u(\delta x, \delta y, \delta z, \delta t) = F_0 \exp \left(i \left[\tilde{\psi}_0 + \left(\frac{\partial \tilde{\psi}}{\partial t} \right)_{t_0} \delta t + \left(\frac{\partial \tilde{\psi}}{\partial x} \right)_{x_0} \delta x + \left(\frac{\partial \tilde{\psi}}{\partial y} \right)_{y_0} \delta y + \left(\frac{\partial \tilde{\psi}}{\partial z} \right)_{z_0} \delta z \right] \right) \quad (7.162)$$

where δ represents the variation symbol and $\tilde{\psi}_0 = \tilde{\psi}(x_0, y_0, z_0, t_0)$. Let

$$A_0 = F_0 e^{i\tilde{\psi}_0} \quad (7.163)$$

$$\frac{\partial \tilde{\psi}}{\partial t}|_{t_0} = \omega \quad (7.164)$$

$$\frac{\partial \tilde{\psi}}{\partial x}|_{x_0} = -k_x; \quad \frac{\partial \tilde{\psi}}{\partial y}|_{y_0} = -k_y; \quad \frac{\partial \tilde{\psi}}{\partial z}|_{z_0} = -k_z \quad (7.165)$$

Replacing variation δt by t , δx by x , etc., Eq. (7.162) can be expressed as

$$u(x, y, z, t) = A_0 e^{i[\omega t - (k_x x + k_y y + k_z z)]} \quad (7.166)$$

If we treat the wave as harmonic with frequency ω , the Fourier integral can be employed to represent $u(x, y, z, t)$ as

$$\begin{aligned} u(x, y, z, t) &= f \left[t - \left(\frac{x}{C_x} + \frac{y}{C_y} + \frac{z}{C_z} \right) \right] \\ &= \int_{-\infty}^{\infty} A(\omega) \exp \left[i\omega \left(t - \left(\frac{x}{C_x} + \frac{y}{C_y} + \frac{z}{C_z} \right) \right) \right] d\omega \\ &= A_0 \exp \left(i\omega \left[t - \left(\frac{x}{C_x} + \frac{y}{C_y} + \frac{z}{C_z} \right) \right] \right) \end{aligned} \quad (7.167)$$

Comparing Eqs. (7.166) and (7.167) gives

$$\frac{\omega}{C_x} = k_x; \quad \frac{\omega}{C_y} = k_y; \quad \frac{\omega}{C_z} = k_z \quad (7.168)$$

From Eq. (7.166), ground displacements along x , y , and z direction can be expressed as

$$u_x = A_0 \cos \alpha e^{i[\omega t - (k_x x + k_y y + k_z z)]} = A_x e^{i[\omega t - (k_x x + k_y y + k_z z)]} \quad (7.169)$$

$$u_y = A_0 \cos \beta e^{i[\omega t - (k_x x + k_y y + k_z z)]} = A_y e^{i[\omega t - (k_x x + k_y y + k_z z)]} \quad (7.170)$$

$$u_z = A_0 \cos \gamma e^{i[\omega t - (k_x x + k_y y + k_z z)]} = A_z e^{i[\omega t - (k_x x + k_y y + k_z z)]} \quad (7.171)$$

From Eq. (7.169)

$$\frac{\partial u_x}{\partial y} = -iA_x k_y e^{i[\omega t - (k_x x + k_y y + k_z z)]} \quad (7.172)$$

$$\frac{\partial u_x}{\partial t} = iA_x \omega e^{i[\omega t - (k_x x + k_y y + k_z z)]} \quad (7.173)$$

From Eq. (7.173), A_x can be expressed as

$$A_x = \frac{(\partial u_x / \partial t)}{i\omega e^{i[\omega t - (k_x x + k_y y + k_z z)]}} \quad (7.174)$$

Substituting Eq. (7.174) into Eq. (7.172) yields

$$\frac{\partial u_x}{\partial y} = \frac{(-ik_y)(\partial u_x / \partial t) e^{i[\omega t - (k_x x + k_y y + k_z z)]}}{i\omega e^{i[\omega t - (k_x x + k_y y + k_z z)]}} = -\frac{k_y}{\omega} \left(\frac{\partial u_x}{\partial t} \right) = -\frac{1}{C_y} \left(\frac{\partial u_x}{\partial t} \right) \quad (7.175)$$

Similarly

$$\frac{\partial u_x}{\partial z} = -\frac{1}{C_z} \frac{\partial u_x}{\partial t} \quad (7.176)$$

$$\frac{\partial u_y}{\partial x} = -\frac{1}{C_x} \frac{\partial u_y}{\partial t} \quad (7.177)$$

$$\frac{\partial u_y}{\partial z} = -\frac{1}{C_z} \frac{\partial u_y}{\partial t} \quad (7.178)$$

$$\frac{\partial u_z}{\partial x} = -\frac{1}{C_x} \frac{\partial u_z}{\partial t} \quad (7.179)$$

$$\frac{\partial u_z}{\partial y} = -\frac{1}{C_y} \frac{\partial u_z}{\partial t} \quad (7.180)$$

For simplicity, assume shear wave velocities are the same in all directions and are equal to C , i.e. $C_x = C_y = C_z = C = a$. Then Eqs. (7.175)–(7.180) can be expressed as

$$\frac{\partial u_i}{\partial j} = -\frac{1}{C} \frac{\partial u_i}{\partial t} = -\frac{1}{C} \dot{u}_i; \quad i \neq j \quad (7.181)$$

From the fundamental theory of elasticity, rotational deformation can be expressed as

$$\left. \begin{aligned} \phi_x &= \frac{1}{2} \left(\frac{\partial u_z}{\partial y} - \frac{\partial u_y}{\partial z} \right) \\ \phi_y &= \frac{1}{2} \left(\frac{\partial u_x}{\partial z} - \frac{\partial u_z}{\partial x} \right) \\ \phi_z &= \frac{1}{2} \left(\frac{\partial u_y}{\partial x} - \frac{\partial u_x}{\partial y} \right) \end{aligned} \right\} \quad (7.182)$$

in which ϕ_i represents rotational deformation in the i th direction. The derivation of Eq. (7.182) based on theory of elasticity is shown in Appendix B. Substituting Eq. (7.181) into (7.182), we can obtain the ground rotational components expressed in terms of the translational components [7, 8, 16, 22]. The three components of rotational deformations can be written as

$$\left. \begin{aligned} \phi_x &= \frac{1}{2C} (\dot{u}_y - \dot{u}_z) \\ \phi_y &= \frac{1}{2C} (\dot{u}_z - \dot{u}_x) \\ \phi_z &= \frac{1}{2C} (\dot{u}_x - \dot{u}_y) \end{aligned} \right\} \quad (7.183)$$

Once ground rotational deformations have been generated, ground rotational velocities and accelerations can be obtained by the differentiation of translational records as follows:

$$\left. \begin{aligned} \dot{\phi}_x &= \frac{1}{2C} (\ddot{u}_y - \ddot{u}_z) \\ \dot{\phi}_y &= \frac{1}{2C} (\ddot{u}_z - \ddot{u}_x) \\ \dot{\phi}_z &= \frac{1}{2C} (\ddot{u}_x - \ddot{u}_y) \end{aligned} \right\} \quad (7.184)$$

$$\left. \begin{aligned} \ddot{\phi}_x &= \frac{1}{2C} (\ddot{u}_y - \ddot{u}_z) \\ \ddot{\phi}_y &= \frac{1}{2C} (\ddot{u}_z - \ddot{u}_x) \\ \ddot{\phi}_z &= \frac{1}{2C} (\ddot{u}_x - \ddot{u}_y) \end{aligned} \right\} \quad (7.185)$$

7.5.2. Construction of Torsional Response Spectra

Ground rotational components, as noted, can be obtained from Eqs. (7.183), (7.184), and (7.185). Thus torsional response spectra can be generated using any of the previous numerical integration methods to repeatedly solve the following motion equation for a single-d.o.f. oscillator with different frequency value, p , and damping factor (ratio) ρ . Note that p and ω can be analogous for steady-state vibration of undamped harmonic motion because the structure's vibration (frequency p) varies with forcing frequency, ω . Therefore we can use p instead of ω in the derivation hereafter. Thus

$$\ddot{\Omega}_i(t) + 2\rho p \dot{\Omega}_i(t) + p^2 \Omega_i(t) = -\ddot{\phi}_i(t); \quad i = x, y, z \quad (7.186)$$

where $\Omega_i(t)$ represents relative rotation of the oscillator in the i th earthquake principal component direction; $\ddot{\phi}_i(t)$ represents ground rotational acceleration in the i th principal component direction. As shown in Eq. (7.185), $\ddot{\phi}_i(t)$ can be obtained by taking the second derivative of Eq. (7.183). Therefore \ddot{u}_x , \ddot{u}_y , and \ddot{u}_z must be calculated by taking the first derivative of ground acceleration records, \ddot{u}_x , \ddot{u}_y , and \ddot{u}_z , with respect to time. However, \ddot{u}_x , \ddot{u}_y , and \ddot{u}_z may be inaccurate because \ddot{u}_x , \ddot{u}_y , and \ddot{u}_z already vary highly with time. Since a structure's total rotational displacement is equal to the sum of relative rotational displacement and ground rotational displacement (see Fig. 7.40), relative rotational displacement can be expressed as

$$\Omega_i(t) = \psi_i(t) - \phi_i(t); \quad i = x, y, z \quad (7.187)$$

where $\psi_i(t)$ represents total rotation of the oscillator in the i th principal component direction. Substituting Eq. (7.187) into Eq. (7.186), the equation of motion can be written as

$$\ddot{\psi}_i(t) + 2\rho p \ddot{\psi}_i(t) + p^2 \psi_i(t) = 2\rho p \dot{\phi}_i(t) + p^2 \phi_i(t); \quad i = x, y, z \quad (7.188)$$

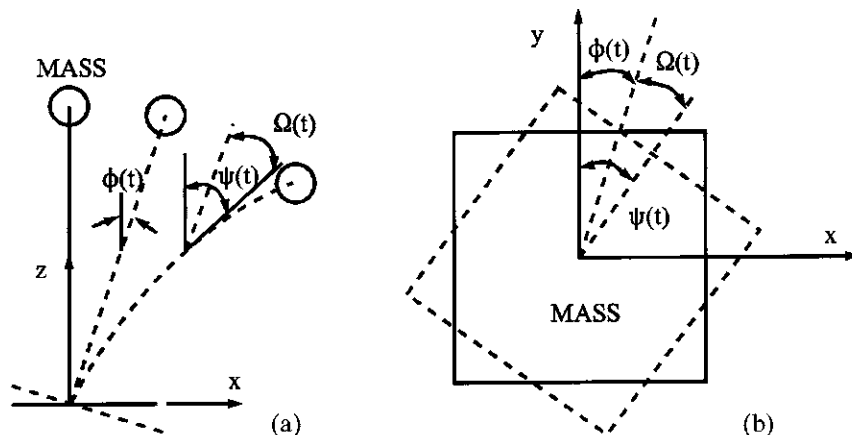


FIG. 7.40 Ground rotational components. (a) In horizontal direction (rotation about y - axis). (b) In vertical direction (rotation about z -axis).

where $\dot{\phi}(t)$ and $\phi(t)$ represent ground rotational velocity and rotational displacement in the i th principal component direction, respectively. Eq (7.188) avoids the step of calculating the first derivative of ground acceleration records, \ddot{u}_x , \ddot{u}_y , and \ddot{u}_z with respect to time. From Eqs. (7.187) and (7.188), one can find relative rotational displacement, $\Omega(t)$, at any instant. Torsional spectral quantity, S_t^i , (or in another notation R_t^i), can be obtained in a similar manner for Eq. (1.123a) as

$$S_t^i = R_t^i = \Omega_i(t)|_{\max} \quad (7.189)$$

in which subscript t represents torsional spectrum and superscript i represents i th ground rotational component. Based on Eq. (7.189), typical torsional spectra for 18 May, 1940 El Centro earthquake, in the minor principal component direction (vertical), are shown in Fig. 7.41. Torsional response spectra for main and intermediate principal component directions are shown in Figs. 7.42 and 7.43, respectively.

7.6. RESPONSE SPECTRUM ANALYSIS OF A MULTIPLE d.o.f. SYSTEM

The motion equation of a multiple d.o.f. system with consideration of ground translation and rotation can be written as

$$[M]\{\ddot{x}\} + [C]\{\dot{x}\} + [K]\{x\} = \{F\} = -[M]\{I_n\}\ddot{x}_g \quad (7.190)$$

where \ddot{x}_g represents the earthquake acceleration component; $\{I_n\}$ is the system *influence coefficient vector*, which represents the displacement vector from a unit support movement (translation and rotation) as illustrated in Fig. 7.44. Let

$$\{x(t)\} = [X]\{x'(t)\} = \sum_{n=1}^N \{X\}_n x'_n(t); \quad N = \text{number of modes considered} \quad (7.191)$$

in which $[X]$ is the modal matrix (see Section 2.5.3), $\{x'_n(t)\}$ is the generalized response vector, $\{X\}_n$ is the n th normal mode vector, and $x'_n(t)$ is the generalized modal response corresponding to the n th

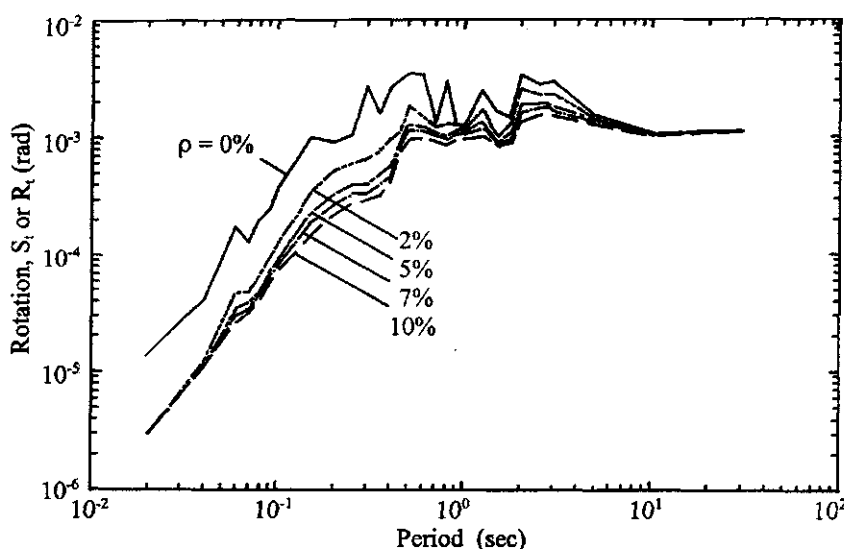


FIG. 7.41 Torsional response spectra (S_t or R_t) for 18 May, 1940 El Centro Earthquake (vertical direction).

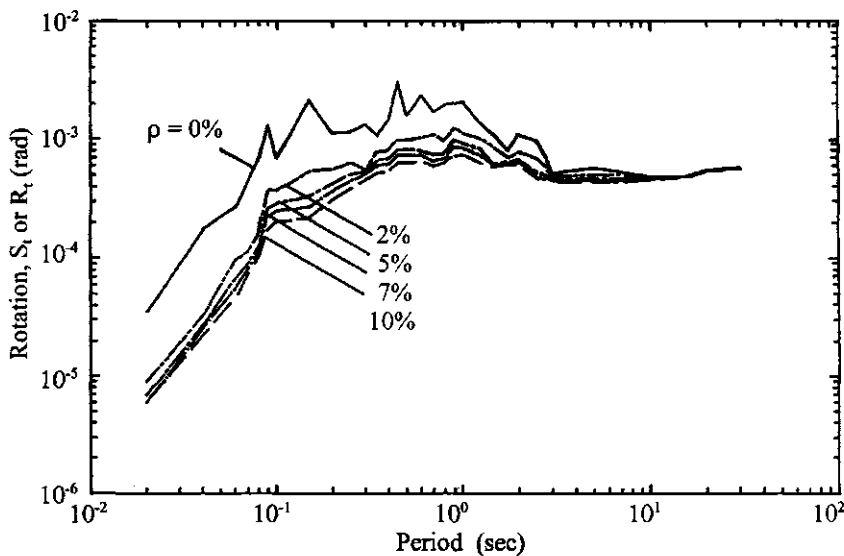


FIG. 7.42 Torsional response spectra (S_t or R_t) for 18 May, 1940 El Centro Earthquake (main principal component direction).

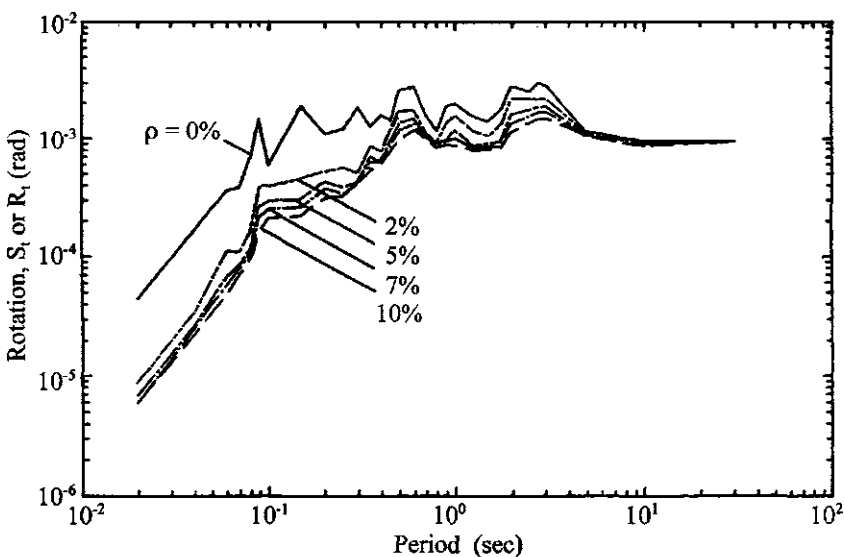


FIG. 7.43 Torsional response spectra (S_t or R_t) for 18 May, 1940 El Centro Earthquake (intermediate principal component direction).

mode. Equation (7.191) can also be expressed in modal matrix, $[\Phi]$, with normalization as discussed in Section 2.5.2.

Substituting Eq. (7.191) into Eq. (7.190) yields

$$[M][X]\{\ddot{x}'\} + [C][X]\{\dot{x}'\} + [K][X]\{x\} = \{F\} \quad (7.192)$$

Multiplying the above equation by the transpose of any normal mode vector, $\{X\}_n$, corresponding

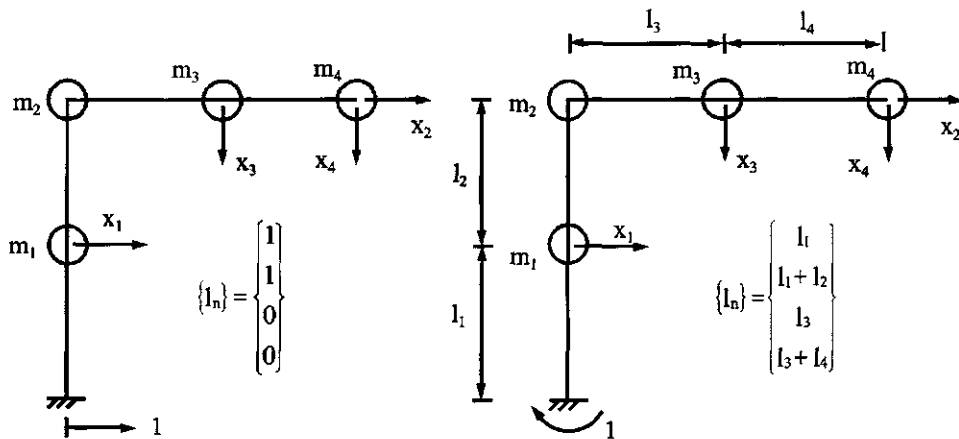


FIG. 7.44 Influence coefficient vector. (a) Ground translation. (b) Ground rotation.

to the n th mode, gives

$$[X]_n^T [M] [X] \{ \ddot{x}' \} + [X]_n^T [C] [X] \{ \dot{x}' \} + [X]_n^T [K] [X] \{ x' \} = [X]_n^T \{ F \} \quad (7.193)$$

Using the orthogonality conditions of normal modes leads to

$$\left. \begin{aligned} & \{ X \}_n^T [M] \{ X \}_m = 0 \\ & \{ X \}_n^T [K] \{ X \}_m = 0 \\ & \{ X \}_n^T [C] \{ X \}_m = 0 \end{aligned} \right\} \quad (7.194)$$

Equation (7.193) can be uncoupled to the following generalized form:

$$M_n \ddot{x}'_n + C_n \dot{x}'_n + K_n x'_n = P_n; \quad n = 1-N \quad (7.195)$$

where M_n is identical to $[M]_{nn}$ in Eqs. (2.64) and (3.6). The generalized properties for the n th mode in Eq. (7.195) are given as

$$M_n = \{ X \}_n^T [M] \{ X \}_n = \text{generalized mass} \quad (7.196)$$

$$C_n = \{ X \}_n^T [C] \{ X \}_n = 2\rho_n p_n M_n = \text{generalized damping} \quad (7.197)$$

$$K_n = \{ X \}_n^T [K] \{ X \}_n = p_n^2 M_n = \text{generalized stiffness} \quad (7.198)$$

$$P_n = \{ X \}_n^T \{ F \} = \text{generalized loading} \quad (7.199)$$

in which ρ_n and p_n represent the n th mode's damping ratio and natural frequency, respectively. From the above equations, Eq. (7.195) can be further simplified

$$\ddot{x}'_n + 2\rho_n p_n \dot{x}'_n + p_n^2 = \frac{P_n}{M_n} = \frac{\{ X \}_n^T [M] \{ I_n \} \ddot{x}_g}{M_n} \quad (7.200)$$

Response of the n th mode in Eq. (7.200) at time t can be obtained as

$$x'_n(t) = \frac{\{ X \}_n^T [M] \{ I_n \}}{M_n p_n} \int_0^t \ddot{x}_g(\Delta) e^{-\rho_n p_n(t-\Delta)} \sin p_n(t-\Delta) d\Delta = \frac{\{ X \}_n^T [M] \{ I_n \}}{M_n p_n} V_n(t) \quad (7.201)$$

in which $V_n(t)$ [similar to A_{mi} in Eq. (2.62) represents the integral

$$V_n(t) = \left| \int_0^t \ddot{x}_g(\Delta) e^{-\rho_n p_n(t-\Delta)} \sin p_n(t-\Delta) d\Delta \right| \quad (7.202)$$

From Eq. (7.114), the velocity response spectrum is

$$(S_v)_n = \left| \int_0^t \ddot{x}_g(t) e^{-\rho_n p_n(t-\Delta)} \sin p_n(t-\Delta) d\Delta \right|_{\max} = |V_n(t)|_{\max} \quad (7.203)$$

Therefore Eq. (7.201) can be expressed as

$$x'_n = \frac{\{X\}_n^T [M] \{I_n\}}{M_n p_n} (S_v)_n = \frac{\{X\}_n^T [M] \{I_n\}}{M_n} R(p_n) \quad (7.204)$$

in which $R(p_n)$ is the *displacement spectral value* from S_d , S_p , or S_t corresponding to p_n . Based on Eqs. (7.191) and (7.203), the maximum response of a multiple-d.o.f. system corresponding to the n th mode, $\{x\}_n$, can be expressed as

$$\begin{aligned} \{x\}_n &= \{X\}_n x'_n = \{X\}_n \frac{\{X\}_n^T [M] \{I_n\}}{\{X\}_n^T [M] \{X\}_n} R(p_n) \\ &= \{X\}_n \gamma_n R(p_n) \end{aligned} \quad (7.205)$$

in which γ_n is called the *participation factor* for the n th mode [see Eqs. (2.63) and (2.69)]. Using Eq. (7.205), maximum modal response is obtained for each mode. The question then arises, as discussed in Section 2.5.3, how these modal maxima should be combined for the best estimate of maximum total response. The response expression of Eq. (7.191) provides accurate results only as long as $\{x(t)\}$ is evaluated concurrently with time. However, in response spectrum analysis, time is removed from this equation. Maximum response values for individual modes cannot possibly occur at the same time. Therefore, a combination of modal maxima such as

$$\{x\} = \sum_{n=1}^N \{x\}_n \quad (7.206)$$

is too conservative for design application. There are two modal combination methods, based on probability theory, which give a more reasonable estimate of maximum structural response. These two methods are described as follows.

7.6.1. SRSS Modal Combination Method

As introduced in Example 2.5.5, the *square-root-of-the-sum-of-the-squares* (SRSS) method can be expressed as

$$x^k = \sqrt{\sum_{n=1}^N (x^k)_n^2}; \quad N = \text{number of modes considered} \quad (7.207)$$

in which superscript k represents the k th d.o.f. of the structural system. This method of combination is known to give a good approximation of the response for frequencies distinctly separated in neighboring modes (see Section 10.9.1).

7.6.2. CQC Modal Combination Method

In general, the *complete-quadratic-combination* (CQC) method may offer a significant improvement in estimating maximum structural response [23]. The CQC combination is expressed as

$$x^k = \sqrt{\sum_{i=1}^N \sum_{j=1}^N x_i^k \alpha_{ij} x_j^k} = \left[\sum_{i=1}^N (x_i^k)^2 + \sum_{j=1}^N \sum_{i=1}^N x_i^k \alpha_{ij} x_j^k \right]^{\frac{1}{2}}; \quad i, j = 1-N \quad (7.208)$$

where α_{ij} is called the *cross-correlation coefficient*, indicating the cross-correlation between modes i and j . α_{ij} is a function of model frequency and damping ratio of a structure, and can be expressed as

$$\alpha_{ij} = \frac{8\rho^2(1+q)q^{3/2}}{(1-q^2)^2 + 4\rho^2q(1+q)^2} \quad (7.209)$$

and

$$q = p_j/p_i \quad (7.210)$$

The correlation coefficient diminishes when q is small, i.e. p_j and p_i are distinctly separate, particularly when damping is small, such as $\rho = 0.05$ or less. The CQC method is significant only for a narrow range of q . Note that when α_{ij} is small, the second term of Eq. (7.208) can be neglected; consequently CQC is reduced to SRSS given in Eq. (7.207).

Similar to Eq. (7.205), the *maximum effective earthquake force* can be obtained from the maximum modal acceleration vector multiplied by the system's mass matrix:

$$\{Q\}_n = \{X\}_n \frac{[M]\{X\}_n^T [M]\{I_n\}}{\{X\}_n^T [M]\{X\}_n} (S_a)_n \quad (7.211)$$

where $(S_a)_n$ is the *acceleration spectral value* corresponding to the n th mode; $\{Q\}_n$ also represents the *maximum base shear* of the structure due to the n th mode. The modal combination for $\{Q\}_n$ is the same as that for $\{x\}_n$ by using either the SRSS or the CQC method.

EXAMPLE 7.6.1 A one-story building shown in Fig. 7.45 is subjected to the 18 May, 1940 El Centro earthquake, for which the ground main principal component is assumed in the direction of structural reference axis x . The mass and stiffness matrices are

$$[M] = \begin{bmatrix} 259375 & 0 & 0 \\ & 2250 & 0 \\ \text{symm} & & 2250 \end{bmatrix}; \quad [K] = \begin{bmatrix} 53383.3465 & 534.3746 & 365.6252 \\ & 168.7499 & 0 \\ \text{symm} & & 168.7498 \end{bmatrix}$$

in which the units are in kip, ft, and sec. The damping ratio is assumed to be 7%. The natural frequency and modal vector corresponding to each mode are $p_1 = 0.2640$ rad/sec ($T_1 = 23.8$ sec), $p_2 = 0.2738$ rad/sec ($T_2 = 22.94$ sec), $p_3 = 0.4594$ rad/sec ($T_3 = 13.67$ sec),

$$\{X\}_1 = \begin{bmatrix} -0.0222 \\ 1 \\ 0.6842 \end{bmatrix}; \quad \{X\}_2 = \begin{bmatrix} 0 \\ -0.6842 \\ 1 \end{bmatrix}; \quad \text{and} \quad \{X\}_3 = \begin{bmatrix} 0.5730 \\ 1 \\ 0.6842 \end{bmatrix}$$

Based on the main principal component (see Fig. 7.22), the corresponding response spectral values for p_1 , p_2 , and p_3 are $R(p_1) = 1.5411$ ft, $R(p_2) = 1.5323$ ft, and $R(p_3) = 1.2652$ ft. Using SRSS and CQC methods, find the structural response associated with d.o.f. D_1 , D_2 , and D_3 .

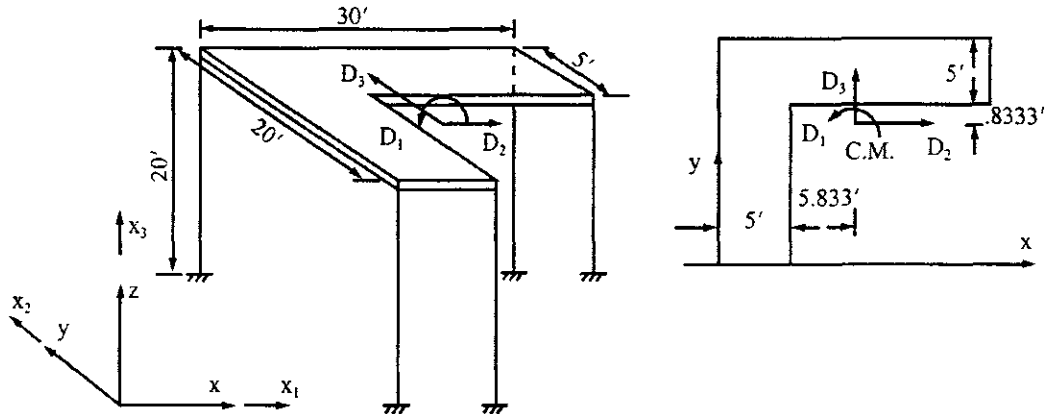


FIG. 7.45 One-story shear building for Example 7.6.1.

Solution: Influence coefficient vector, $\{I_n\}$, and $[X]^T [M] [X]$ are

$$\{I_n\} = \begin{Bmatrix} 0 \\ 1 \\ 0 \end{Bmatrix} \quad (a)$$

$$\begin{aligned} [X]^T [M] &= \begin{bmatrix} -0.0222 & 1 & 0.6842 \\ 0 & -0.6842 & 1 \\ 0.5730 & 1 & 0.6842 \end{bmatrix} \begin{bmatrix} 259375 & 0 & 0 \\ 0 & 2250 & 0 \\ 0 & 0 & 2250 \end{bmatrix} \\ &= \begin{bmatrix} -0.5758 & 0.225 & 0.154 \\ 0 & -0.154 & 0.225 \\ 14.860 & 0.225 & 0.153 \end{bmatrix} 10^4 \end{aligned} \quad (b)$$

$$[X]^T [M] \{I_n\} = \begin{bmatrix} 2250 \\ -1540 \\ 2250 \end{bmatrix} \quad (c)$$

$$[X]^T [M] [X] = \begin{bmatrix} 3432 & 0 & 0 \\ 0 & 3303 & 0 \\ 0 & 0 & 88470 \end{bmatrix} \quad (d)$$

From Eq. (7.205), the participation factors γ_1 , γ_2 , and γ_3 are evaluated as

$$\gamma_n = \frac{\{X\}_n^T [M] \{I_n\}}{\{X\}_n^T [M] [X]_n} \quad (e)$$

$$\gamma_1 = \frac{2250}{3432} = 0.6556 \quad (f)$$

$$\gamma_2 = \frac{-1540}{3303} = -0.4662 \quad (g)$$

$$\gamma_3 = \frac{2250}{88470} = 0.0254 \quad (h)$$

The maximum response vector due to each mode can then be calculated as

$$\begin{aligned}\{x\}_1 &= [X]_1 \gamma_1 R(p_1) \\ &= \begin{bmatrix} -0.0222 \\ 1 \\ 0.6842 \end{bmatrix} (0.6556) (1.5411) = \begin{bmatrix} -0.0224 \\ 1.0103 \\ 0.6913 \end{bmatrix} \text{ rad ft ft}\end{aligned}\quad (\text{i})$$

$$\begin{aligned}\{x\}_2 &= [X]_2 \gamma_2 R(p_2) \\ &= \begin{bmatrix} 0 \\ -0.6842 \\ 1 \end{bmatrix} (-0.4662) (1.5323) = \begin{bmatrix} 0 \\ 0.4888 \\ -0.7143 \end{bmatrix} \text{ rad ft ft}\end{aligned}\quad (\text{j})$$

$$\begin{aligned}\{x\}_3 &= [X]_3 \gamma_3 R(p_3) \\ &= \begin{bmatrix} 0.5730 \\ 1 \\ 0.6842 \end{bmatrix} (0.0254) (1.2652) = \begin{bmatrix} 0.0184 \\ 0.0321 \\ 0.0220 \end{bmatrix} \text{ rad ft ft}\end{aligned}\quad (\text{k})$$

For the SRSS method—total maximum response values are calculated from Eq. (7.207)

$$\{x\} = \sqrt{(\{x\}_1)^2 + (\{x\}_2)^2 + (\{x\}_3)^2} = \sqrt{\begin{bmatrix} 8.4032 \times 10^{-4} \\ 1.2608 \\ 0.9887 \end{bmatrix}} = \begin{bmatrix} 0.0290 \\ 1.1228 \\ 0.9943 \end{bmatrix} \text{ rad (} D_1 \text{) ft (} D_2 \text{) ft (} D_3 \text{)}\quad (\text{l})$$

For CQC method—cross-correlation coefficients are calculated from Eq. (7.209)

$$\alpha_{ij} = \frac{8\rho^2(1+q)q^{3/2}}{(1-q^2)^2 + 4\rho^2q(1+q)^2}, \quad \text{where } q = p_j/p_i \quad (\text{m})$$

for which

$$\begin{aligned}\alpha_{12} &= \frac{8(0.07)^2(1+0.9641)(0.9641)^{1.5}}{(1-(0.9641)^2)^2 + 4(0.07)^2(0.9641)(1.9641)^2}; \quad q = \frac{p_1}{p_2} = \frac{0.2640}{0.2738} = 0.9641 \\ &= \frac{0.0728}{(4.9543 \times 10^{-3} + 0.0729)} = 0.9362\end{aligned}$$

Similarly

$$\begin{aligned}\alpha_{13} &= 0.0564 \\ \alpha_{23} &= 0.0646\end{aligned}$$

From Eq. (7.208), total maximum response values are calculated as

$$x^k = \sqrt{\sum_{i=1}^N \sum_{j=1}^N x_i^k \alpha_{ij} x_j^k} \quad (\text{n})$$

or

$$(x^k)^2 = (x_1^k \alpha_{11} x_1^k) + 2(x_1^k \alpha_{12} x_2^k) + 2(x_1^k \alpha_{13} x_3^k) \\ + 2(x_2^k \alpha_{23} x_3^k) + (x_2^k \alpha_{22} x_2^k) + (x_3^k \alpha_{33} x_3^k)$$

Thus

$$\{x\}^2 = \begin{bmatrix} 5.0176 \times 10^{-4} & +0 & -4.6492 \times 10^{-5} & +0 & +0 & +3.3856 \times 10^{-4} \\ 1.0207 & +0.9247 & +3.6582 \times 10^{-3} & +2.0272 \times 10^{-3} & +0.2389 & +1.0304 \times 10^{-3} \\ 0.4779 & -0.9246 & +1.7155 \times 10^{-3} & -2.0303 \times 10^{-3} & +0.5102 & +4.8400 \times 10^{-4} \end{bmatrix} \\ = \begin{bmatrix} 7.9383 \times 10^{-4} \\ 2.1910 \\ 0.0636 \end{bmatrix} \quad (o)$$

from which

$$\{x\} = \begin{bmatrix} 0.0282 \\ 1.4803 \\ 0.2524 \end{bmatrix} \begin{array}{l} \text{rad} \\ \text{ft} \\ \text{ft} \end{array} \quad (p)$$

7.6.3 Structural Response Due to Multiple-Component Seismic Input

In the previous sections, we introduced response spectrum analysis for multiple-d.o.f. systems with a single seismic component input. For multiple-component earthquake input, Eq. (7.205) should be modified as

$$\{x\}_{ji} = \{X\}_j \gamma_{ij} R_i(p_j) \quad (7.212)$$

where $\{x\}_{ji}$ is structural response for the j th mode due to ground principal component applied at structural i th reference axis direction (see Fig. 7.6); $R_i(p_j)$ is a displacement spectral quantity corresponding to ground principal component in the structural i th reference axis direction for the j th mode [see Eq. (7.215) for inclusion of ground rotation]; and γ_{ij} is the participation factor of the j th mode in the structural i th reference axis direction. Similar to Eq. (7.205), γ_{ij} can be expressed as

$$\gamma_{ij} = \frac{\{X\}_j^T [M] \{I_n\}_i}{\{X\}_j^T [M] \{X\}_j} \quad (7.213)$$

in which $\{I_n\}_i$ is the system influence coefficient vector corresponding to the i th structural reference axis direction. Response vector of the j th mode due to multiple-component seismic input effects can be expressed as

$$\{x\}_j = \sum_{i=1}^N \{x\}_{ji}; \quad N = \text{number of ground components considered} \quad (7.214)$$

Once Eq. (7.214) is calculated, structural maximum response can be evaluated using the SRSS method, Eq. (7.207), or the CQC method, Eq. (7.208).

EXAMPLE 7.6.2 Rework Example 7.6.1 for a structure subjected to ground main principal component and intermediate principal component in the structural x and y reference axis directions, respectively. Displacement response spectral values for p_1 , p_2 , and p_3 are $R_x(p_1) = 1.5411$ ft, $R_x(p_2) = 1.5323$ ft, $R_x(p_3) = 1.2652$ ft, $R_y(p_1) = 1.3688$ ft, $R_y(p_2) = 1.3844$ ft, and $R_y(p_3) = 1.3925$ ft.

Solution: From Eqs. (i), (j), and (k) in Example 7.6.1,

$$\{x\}_{1x} = [-0.0224 \quad 1.0103 \quad 0.6913]^T \quad (a)$$

$$\{x\}_{2x} = [0 \quad 0.4888 \quad -0.7143]^T \quad (b)$$

$$\{x\}_{3x} = [0.0184 \quad 0.0321 \quad 0.02220]^T \quad (c)$$

The influence coefficient vector $\{I_n\}_y$ of the structure is

$$\{I_n\}_y = \begin{bmatrix} 0 \\ 0 \\ 1 \end{bmatrix} \quad (d)$$

$$[X]^T [M] [I_n]_y = 10^4 \begin{bmatrix} -0.5765 & 0.225 & 0.154 \\ 0 & -0.154 & 0.225 \\ 14.860 & 0.225 & 0.153 \end{bmatrix} \begin{bmatrix} 0 \\ 0 \\ 1 \end{bmatrix} = \begin{bmatrix} 1540 \\ 2250 \\ 1539 \end{bmatrix} \quad (e)$$

From Eq. (d) in Example 7.6.1,

$$[X]^T [M] [X] = \begin{bmatrix} 3432 & 0 & 0 \\ 0 & 3303 & 0 \\ 0 & 0 & 88470 \end{bmatrix} \quad (f)$$

Using Eq. (7.213) gives the participation factors as

$$\gamma_{ij} = \frac{\{X\}_j^T [M] [I_n]_i}{\{X\}_j^T [M] [X]} \quad (g)$$

$$\gamma_{y1} = \frac{1540}{3432} = 0.4486 \quad (h)$$

$$\gamma_{y2} = \frac{2250}{3303} = 0.6811 \quad (i)$$

$$\gamma_{y3} = \frac{1539}{88470} = 0.0174 \quad (j)$$

$$\{x\}_{1y} = \{X\}_1 \gamma_{y1} R_y(p_1) = \begin{bmatrix} -0.0222 \\ 1 \\ 0.6842 \end{bmatrix} (0.4486) (1.3688) = \begin{bmatrix} -0.0136 \\ 0.6140 \\ 0.4201 \end{bmatrix} \quad (k)$$

$$\{x\}_{2y} = \{X\}_2 \gamma_{y2} R_y(p_2) = \begin{bmatrix} 0 \\ -0.6842 \\ 1 \end{bmatrix} (0.6811) (1.3844) = \begin{bmatrix} 0 \\ -0.6451 \\ 0.9429 \end{bmatrix} \quad (l)$$

$$\{x\}_{3y} = \{X\}_3 \gamma_{y3} R_y(p_3) = \begin{bmatrix} 0.5730 \\ 1 \\ 0.6842 \end{bmatrix} (0.0174) (1.3925) = \begin{bmatrix} 0.0138 \\ 0.0242 \\ 0.0165 \end{bmatrix} \quad (m)$$

From Eq. (7.214), the response vector of each mode due to the two principal components can be calculated as

$$\{x\}_1 = \{x\}_{1x} + \{x\}_{1y} = [-0.0361 \quad 1.6244 \quad 1.1114]^T \quad (n)$$

$$\{x\}_2 = \{x\}_{2x} + \{x\}_{2y} = [0 \quad -0.1563 \quad 0.2285]^T \quad (o)$$

$$\{x\}_3 = \{x\}_{3x} + \{x\}_{3y} = [0.0323 \quad 0.0564 \quad 0.0385]^T \quad (p)$$

For the SRSS method,

$$\{x\} = \sqrt{(\{x\}_1)^2 + (\{x\}_2)^2 + (\{x\}_3)^2} = \sqrt{\begin{bmatrix} 2.3480 \times 10^{-3} \\ 2.6665 \\ 1.2890 \end{bmatrix}} = \begin{bmatrix} 0.0484 \\ 1.6329 \\ 1.1353 \end{bmatrix} \text{ rad ft ft} \quad (\text{q})$$

For the CQC method,

$$(x^k)^2 = (x_1^k \alpha_{11} x_1^k) + (x_2^k \alpha_{22} x_2^k) + (x_3^k \alpha_{33} x_3^k) + 2(x_1^k \alpha_{12} x_2^k) + 2(x_1^k \alpha_{13} x_3^k) + 2(x_2^k \alpha_{23} x_3^k) \quad (\text{r})$$

Thus

$$\begin{aligned} \{x\}^2 &= \begin{bmatrix} 1.2960 \times 10^{-3} & +0 & +1.0368 \times 10^{-3} & +0 & +(-6.5379 \times 10^{-5})2 & +0 \\ 2.6384 & +0.0244 & +3.1697 \times 10^{-3} & +(-0.2377)2 & +(5.1577 \times 10^{-3})2 & +(-5.6846 \times 10^{-4})2 \\ 1.2352 & +0.0523 & +1.4823 \times 10^{-3} & +(0.2379)2 & +(2.4133 \times 10^{-3})2 & +(5.6855 \times 10^{-4})2 \end{bmatrix} \\ &= \begin{bmatrix} 2.2021 \times 10^{-3} \\ 2.1998 \\ 1.7706 \end{bmatrix} \end{aligned} \quad (\text{s})$$

from which

$$\{x\} = \begin{bmatrix} 0.0470 \\ 1.4832 \\ 1.3306 \end{bmatrix} \text{ rad ft ft} \quad (\text{t})$$

Note that the response spectrum analysis introduced here can also be applied to ground rotational components. Based on Eq. (7.205), modal response due to ground rotational components can be expressed as

$$\{\bar{x}\}_{ji} = \{X\}_j \frac{\{X\}_j^T [M] \{I_n\}_i}{\{X\}_j^T [M] \{X\}_j} R_t^i(p_j) = \{X\}_j \gamma_{ij} R_t^i(p_j) \quad (7.215)$$

in which $\{\bar{x}\}_{ji}$ is structural response for the j th mode due to the ground rotational component applied along the structural i th reference axis direction; $R_t^i(p_j)$ is rotational spectral quantity corresponding to the ground principal rotational component in the structural i th reference axis direction for the j th mode. Similar to Eq. (7.214), the response vector of the j th mode due to multiple rotational component seismic input can be expressed as

$$\{\bar{x}\}_j = \sum_{i=1}^N \{\bar{x}\}_{ji}; \quad N = \text{number of ground rotational components} \quad (7.216)$$

Therefore, the response of the k th degree of freedom in the system due to translational and rotational seismic components becomes

$$x_{\text{total}}^k = \sqrt{\sum_{n=1}^M (x_n^k)^2 + \sum_{n=1}^M (\bar{x}_n^k)^2}; \quad M = \text{number of modes} \quad (7.217)$$

7.7. MAXIMUM (WORST-CASE) RESPONSE ANALYSIS FOR SIX SEISMIC COMPONENTS

For three-dimensional structures subjected to multiple-component seismic input, the response is dependent on the orientation of the structure with respect to ground principal component directions. For rectangular and symmetric structures whose *mass center* coincides with the *rigidity*

center, the response could be maximum. This is because the ground principal components can be applied along the structure's principal directions (i.e. in the long and short direction of the building). For a structure without symmetric characteristics (such as configuration and stiffness) whose mass center does not coincide with its rigidity center, the *maximum response* (or *worst-case response*) may be obtained by repeatedly applying input ground components to the structure using different input angles. However, this process is time-consuming and costly. A new technique is applied to the SRSS and CQC methods in the next two sections to obtain the critical seismic input angle for maximum response. Also included are numerical examples to illustrate the significance of this technique [7,8,21].

7.7.1. Based on SRSS Method

Let \ddot{u}_{x_1} , \ddot{u}_{x_2} , and \ddot{u}_{x_3} be the accelerations of the seismic components along the structural reference axes, x_1 , x_2 , and x_3 , respectively (see Fig. 7.6), and $\{I_n\}_1$, $\{I_n\}_2$, and $\{I_n\}_3$ be the influence coefficient vectors corresponding to x_1 , x_2 , and x_3 directions, respectively. Assume the main, intermediate, and minor seismic principal components, \ddot{u}_x , \ddot{u}_y and \ddot{u}_z , are aligned with axes x , y , and z as shown in Fig. 7.6. Then the seismic components in structural reference axes, x_1 , x_2 , and x_3 can be expressed in terms of seismic principal components by the directional cosine transformation

$$\begin{Bmatrix} \ddot{u}_{x_1} \\ \ddot{u}_{x_2} \\ \ddot{u}_{x_3} \end{Bmatrix} = \begin{Bmatrix} d_1 & d_2 & 0 \\ -d_2 & d_1 & 0 \\ 0 & 0 & 1 \end{Bmatrix}^T \begin{Bmatrix} \ddot{u}_x \\ \ddot{u}_y \\ \ddot{u}_z \end{Bmatrix} \quad (7.218)$$

where $d_1 = \cos \theta$ and $d_2 = \sin \theta$. θ represents the angle between seismic component \ddot{u}_x and structural axis x_1 as shown in Fig. 7.6. Based on Eqs. (7.212) and (7.218), the modal response vector can be expressed as

$$\{x\}_{ji} = \begin{cases} \{X\}_j \gamma_{ij} [R_x(p_j)d_1 - R_y(p_j)d_2] \\ \{X\}_j \gamma_{ij} [R_x(p_j)d_2 + R_y(p_j)d_1] \\ \{X\}_j \gamma_{ij} R_z(p_j) \end{cases} \quad (7.219)$$

where $\{x\}_{ji}$ is the j th modal response vector due to the i th seismic component of \ddot{x}_1 ; \ddot{x}_2 , \ddot{x}_3 ; $\{X\}_j$ is the j th normal mode vector; γ_{ij} is the participation factor for the j th mode in the x_i direction; and $R_x(p_j)$, $R_y(p_j)$ and $R_z(p_j)$ are the response spectral quantities of the j th mode due to excitations $\ddot{u}_x(t)$, $\ddot{u}_y(t)$, and $\ddot{u}_z(t)$, respectively. The participation factor, γ_{ij} , can be expressed as

$$\gamma_{ij} = \frac{\{X\}_j^T [M] \{I_n\}_i}{\{X\}_j^T [M] \{X\}_j}; \quad i = x_1, x_2, x_3 \quad (7.220)$$

From Eq. (7.219) a response quantity of the k th d.o.f., x_{ji}^k , can be written in terms of the modal parameters

$$x_{ji}^k = \begin{cases} X_j^k \gamma_{ij} [R_x(p_j)d_1 - R_y(p_j)d_2] \\ X_j^k \gamma_{ij} [R_x(p_j)d_2 + R_y(p_j)d_1] \\ X_j^k \gamma_{ij} R_z(p_j) \end{cases} \quad (7.221)$$

where X_j^k is the k th component of the j th normal mode vector. Thus the j th modal response for the k th d.o.f. can be expressed as

$$x_j^k = \sum_i x_{ji}^k; \quad i = x_1, x_2, x_3 \quad (7.222)$$

Substituting Eq. (7.221) into Eq. (7.222) yields

$$(x_j^k)^2 = \{d\}^T [R_j^k] \{d\} + \{D_j^k\}^T \{d\} + E_j^k \quad (7.223)$$

where

$$\{d\}^T = [d_1 \ d_2] \quad (7.223a)$$

$$[R_j^k] = \begin{bmatrix} (R_j^k)_{11} & (R_j^k)_{12} \\ (R_j^k)_{12} & (R_j^k)_{22} \end{bmatrix} \quad (7.223b)$$

$$(R_j^k)_{11} = (X^k)_j^2 [R_x(p_j)\gamma_{1j} + R_y(p_j)\gamma_{2j}]^2 \quad (7.223c)$$

$$(R_j^k)_{12} = (X^k)_j^2 \gamma_{1j}\gamma_{2j} [R_x^2(p_j) - R_y^2(p_j)] + (X^k)_j^2 R_x(p_j)R_y(p_j)[\gamma_{2j}^2 - \gamma_{1j}^2] \quad (7.223d)$$

$$(R_j^k)_{22} = (X^k)_j^2 [R_x(p_j)\gamma_{2j} - R_y(p_j)\gamma_{1j}]^2 \quad (7.223e)$$

$$\{D_j^k\}^T = [(D_j^k)_1 \ (D_j^k)_2] \quad (7.223f)$$

$$(D_j^k)_1 = 2(X^k)_j^2 R_z(p_j) [\gamma_{2j}\gamma_{3j} R_y(p_j) + \gamma_{1j}\gamma_{3j} R_x(p_j)] \quad (7.223g)$$

$$(D_j^k)_2 = 2(X^k)_j^2 R_z(p_j) [\gamma_{2j}\gamma_{3j} R_x(p_j) - \gamma_{1j}\gamma_{3j} R_y(p_j)] \quad (7.223h)$$

$$E_j^k = (X^k)_j^2 R_z^2(p_j) \gamma_{3j}^2 \quad (7.223i)$$

Using the SRSS modal combination approach, the response for the k th d.o.f. x^k , can be obtained by

$$(x^k)^2 = \sum_{j=1}^N (x_j^k)^2; \quad N = \text{number of modes considered} \quad (7.224)$$

or

$$(x^k)^2 = \{d\}^T [R^k] \{d\} + \{D^k\}^T \{d\} + E^k \quad (7.225)$$

where

$$[R^k] = \begin{bmatrix} R_{11}^k & R_{12}^k \\ R_{12}^k & R_{22}^k \end{bmatrix} \quad (7.225a)$$

$$\{D^k\}^T = [D_1^k \ D_2^k] = \sum_{j=1}^N \left[(D_j^k)_1 \ (D_j^k)_2 \right] \quad (7.225b)$$

$$E^k = \sum_{j=1}^N E_j^k \quad (7.225c)$$

$$R_{ln}^k = \sum_{j=1}^N (R_j^k)_{ln}; \quad \ell, n = 1, 2 \quad (7.225d)$$

Equation (7.225) leads to

$$(x^k)^2 = R_{11}^k \cos^2 \theta + 2R_{12}^k \sin \theta \cos \theta + R_{22}^k \sin^2 \theta + D_1^k \cos \theta + D_2^k \sin \theta + E^k \quad (7.226)$$

Since the magnitude of structural response is dependent on structural orientation with respect to seismic input, for a particular orientation the structural response could be maximum. To obtain maximum response, taking the first derivative with respect to θ in Eq. (7.226) yields

$$[R_{22}^k - R_{11}^k] \sin(2\theta) + 2R_{12}^k \cos(2\theta) - D_1^k \sin \theta + D_2^k \cos \theta = 0 \quad (7.227)$$

from which the *critical seismic input angle* θ_{cr} can be obtained. Therefore, maximum response for the k th d.o.f., x^k , can be found by substituting θ_{cr} into Eq. (7.226). Another approach to solving the critical seismic input angle is based on eigensolution procedures. For simple illustration, let the seismic vertical component be neglected; then the second and third terms on the right side of Eq. (7.225) become zero. For maximum response of the k th d.o.f., Eq. (7.225) can be expressed in the following *Lagrange multiplier* form

$$L(\lambda) = \{d\}^T [R^k] \{d\} - \lambda (\{d\}^T \{d\} - 1) \quad (7.228)$$

Taking a partial derivative with respect to $\{d\}$, we have

$$[R^k] \{d\} - \lambda \{d\} = \{0\} \quad (7.229)$$

which is an eigenpair problem and yields two eigenvalues, λ_1 and λ_2 , and two eigenvectors, $\{d\}_1$, and $\{d\}_2$. Each of the eigenpair should satisfy Eq. (7.229). Therefore

$$[R^k] \{d\}_i - \lambda_i \{d\}_i = \{0\}; \quad i = 1, 2 \quad (7.230)$$

from which

$$\lambda_i = \{d\}_i^T [R^k] \{d\}_i \quad (7.231)$$

From Eq. (7.225) and Eq. (7.231), one may observe that the larger eigenvalue is equal to the square of the maximum response, and the corresponding eigenvector is the critical seismic input direction.

EXAMPLE 7.7.1 Find the maximum (worst-case) response of d.o.f. D_1 in Example 7.6.2, and find the corresponding critical seismic input angle for D_1 by the SRSS method. Employ three modes in the calculation.

Solution: For Eq. (7.225d) and $k = 1$, R_{11}^1 , R_{12}^1 , R_{22}^1 can be calculated from Eqs. (7.226d–f) as

$$\begin{aligned} R_{11}^1 &= \sum_{j=1}^3 (R_j^1)_{11} \\ &= (X^1)_1^2 [R_x(p_1)\gamma_{11} + R_y(p_1)\gamma_{21}]^2 + (X^1)_2^2 [R_x(p_2)\gamma_{12} + R_y(p_2)\gamma_{22}]^2 \\ &\quad + (X^1)_3^2 [R_x(p_3)\gamma_{13} + R_y(p_3)\gamma_{23}]^2 \\ &= (-0.0222)^2 [1.5411(0.6556) + 1.3688(0.4486)]^2 + (0) \\ &\quad + (0.5730)^2 [1.2652(0.0254) + 1.3925(0.0174)]^2 \\ &= 2.3436 \times 10^{-3} \end{aligned} \quad (a)$$

$$\begin{aligned} R_{12}^1 &= \sum_{j=1}^3 (R_j^1)_{12} \\ &= (X^1)_1^2 \gamma_{11} \gamma_{21} [R_x^2(p_1) - R_y^2(p_1)] + (X^1)_1^2 R_x(p_1) R_y(p_1) [\gamma_{21}^2 - \gamma_{11}^2] \\ &\quad + (X^1)_2^2 \gamma_{12} \gamma_{22} [R_x^2(p_2) - R_y^2(p_2)] + (X^1)_2^2 R_x(p_2) R_y(p_2) [\gamma_{22}^2 - \gamma_{12}^2] \\ &\quad + (X^1)_3^2 \gamma_{13} \gamma_{23} [R_x^2(p_3) - R_y^2(p_3)] + (X^1)_3^2 R_x(p_3) R_y(p_3) [\gamma_{23}^2 - \gamma_{13}^2] \\ &= (-0.0222)^2 (0.6556) (0.4486) [(1.5411)^2 - (1.3688)^2] \\ &\quad + (-0.0222)^2 (1.5411) (1.3688) [(0.4486)^2 - (0.6556)^2] + 0 \\ &\quad + (0.5730)^2 (0.0254) (0.0174) [(1.2652)^2 - (1.3925)^2] \\ &\quad + (0.5730)^2 (1.2652) (1.3925) [(0.0174)^2 - (0.0254)^2] \\ &= -4.1346 \times 10^{-4} \end{aligned} \quad (b)$$

$$\begin{aligned}
R_{22}^1 &= \sum_{j=1}^3 (R_j^1)_{22} = (X^1)_1^2 [R_x(p_1)\gamma_{21} - R_y(p_1)\gamma_{11}]^2 + (X^1)_2^2 [R_x(p_2)\gamma_{22} - R_y(p_2)\gamma_{12}]^2 \\
&\quad + (X^1)_3^2 [R_x(p_3)\gamma_{23} - R_y(p_3)\gamma_{13}]^2 \\
&= (-0.0222)^2 [1.5411(0.4486) - 1.3688(0.6556)]^2 + 0 \\
&\quad + (0.5730)^2 [1.2652(0.0174) - 1.3925(0.0254)]^2 \\
&= 7.9907 \times 10^{-5}
\end{aligned} \tag{c}$$

From Eqs. (a)–(c), $[R^1]$ of Eq. (7.225a) can be expressed as

$$[R^1] = \begin{bmatrix} 2.3481 \times 10^{-3} & -4.1346 \times 10^{-4} \\ -4.1346 \times 10^{-4} & 7.9907 \times 10^{-5} \end{bmatrix} \tag{d}$$

Since the seismic vertical component is not considered here, Eq. (7.229) can be used to calculate maximum response of d.o.f. D_1

$$[R^1]\{d\} - \lambda\{d\} = \{0\} \tag{e}$$

or

$$\begin{vmatrix} 2.3481 \times 10^{-3} - \lambda & -4.1346 \times 10^{-4} \\ -4.1346 \times 10^{-4} & 7.9907 \times 10^{-5} - \lambda \end{vmatrix} \tag{f}$$

Thus

$$\lambda_1 = 0.0024; \quad \lambda_2 = 0.6888 \times 10^{-5} \tag{g}$$

Substituting $\lambda_1 = 0.0024$ into Eq. (e) yields

$$-7.3597 \times 10^{-5} d_1 - 4.1346 \times 10^{-4} d_2 = 0 \tag{h}$$

from which

$$d_1 = -5.6179 d_2 \tag{i}$$

Since

$$d_1^2 + d_2^2 = 1 \tag{j}$$

Eqs. (i) and (j) give

$$\left. \begin{array}{l} d_1 = 0.9845 \\ d_2 = -0.1752 \end{array} \right\} \tag{k}$$

Thus the worst-case response of d.o.f. D_1 is equal to

$$(\lambda_1)^{1/2} = (0.0024)^{1/2} = 0.0492 \text{ rad} \tag{l}$$

and the corresponding critical seismic input angle is

$$\theta_{cr} = \sin^{-1}(d_2) = \sin^{-1}(-0.1752) = -10.09^\circ \tag{m}$$

θ_{cr} is shown in Fig. 7.46.

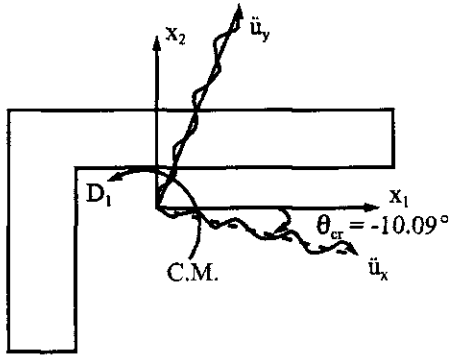


FIG. 7.46 Critical seismic input angle for d.o.f. D_1 .

7.7.2. Based on CQC Method

Since the k th component of the j th modal response vector, x_j^k , can be obtained by using Eq. (7.222), the structural response of the k th d.o.f. may now be expressed as

$$(x^k)^2 = \sum_{m=1}^N \sum_{j=1}^N x_j^k \alpha_{mj} x_m^k; \quad m, j = \text{mode number} \quad N = \text{number of modes considered} \quad (7.232)$$

where α_{mj} represents the cross-modal coefficient of the m th and j th modes. Equation (7.232) may be similarly expanded as Eq. (7.223a)

$$(x^k)^2 = \sum_{m=1}^N \sum_{j=1}^N \left(\{d\}^T [R_{jm}^k] \{d\} + \{D_{jm}^k\}^T \{d\} + E_{jm}^k \right) \quad (7.233)$$

where

$$[R_{jm}^k] = \begin{bmatrix} (R_{jm}^k)_{11} & (R_{jm}^k)_{12} \\ (R_{jm}^k)_{12} & (R_{jm}^k)_{22} \end{bmatrix} \quad (7.233a)$$

$$(R_{jm}^k)_{11} = \alpha_{mj} X_j^k X_m^k [R_x(p_j) \gamma_{1j} (R_x(p_m) \gamma_{1m} + R_y(p_m) \gamma_{2m}) + R_y(p_j) \gamma_{2j} (R_x(p_m) \gamma_{1m} + R_y(p_m) \gamma_{2m})] \quad (7.233b)$$

$$(R_{jm}^k)_{12} = (0.5) \alpha_{mj} X_j^k X_m^k \{ [R_x(p_j) R_x(p_m) - R_y(p_j) R_y(p_m)] (\gamma_{1j} \gamma_{2m} + \gamma_{2j} \gamma_{1m}) + [R_x(p_j) R_y(p_m) + R_y(p_j) R_x(p_m)] (\gamma_{2j} \gamma_{2m} - \gamma_{1j} \gamma_{1m}) \} \quad (7.233c)$$

$$(R_{jm}^k)_{22} = \alpha_{mj} X_j^k X_m^k [R_x(p_j) \gamma_{2j} (R_x(p_m) \gamma_{2m} - R_y(p_m) \gamma_{1m}) + R_y(p_j) \gamma_{1j} (R_y(p_m) \gamma_{1m} - R_x(p_m) \gamma_{2m})] \quad (7.233d)$$

$$\{D_{jm}^k\}^T = \left[\begin{pmatrix} D_{jm}^k \end{pmatrix}_1 \quad \begin{pmatrix} D_{jm}^k \end{pmatrix}_2 \right] \quad (7.233e)$$

$$\begin{aligned} \left(D_{jm}^k \right)_1 &= \alpha_{mj} X_j^k X_m^k \{ R_z(p_m) \gamma_{3m} [\gamma_{1j} R_x(p_j) + \gamma_{2j} R_y(p_j)] \\ &\quad + R_z(p_j) \gamma_{3j} [\gamma_{1m} R_x(p_m) + \gamma_{2m} R_y(p_m)] \} \end{aligned} \quad (7.233f)$$

$$\begin{aligned} \left(D_{jm}^k \right)_2 &= \alpha_{mj} X_j^k X_m^k \{ R_z(p_m) \gamma_{3m} [\gamma_{2j} R_x(p_m) - \gamma_{1j} R_y(p_j)] \\ &\quad + R_z(p_j) \gamma_{3j} [\gamma_{2m} R_x(p_m) - \gamma_{1m} R_y(p_m)] \} \end{aligned} \quad (7.233g)$$

$$E_{jm}^k = \alpha_{mj} X_j^k X_m^k R_z(p_j) R_z(p_m) \gamma_{3j} \gamma_{3m} \quad (7.233h)$$

Equation (7.233) can also be expressed in the manner shown in Eq. (7.225a) in which

$$R_{11}^k = \sum_{m=1}^N \sum_{j=1}^N \left(D_{jm}^k \right)_{11} \quad (7.234)$$

$$R_{12}^k = \sum_{m=1}^N \sum_{j=1}^N \left(D_{jm}^k \right)_{12} \quad (7.235)$$

$$R_{22}^k = \sum_{m=1}^N \sum_{j=1}^N \left(D_{jm}^k \right)_{22} \quad (7.236)$$

$$D_\ell^k = \sum_{m=1}^N \sum_{j=1}^N \left(D_{jm}^k \right)_\ell; \quad \ell = 1, 2 \quad (7.237)$$

$$E^k = \sum_{m=1}^N \sum_{j=1}^N E_{jm}^k \quad (7.238)$$

After substituting Eqs. (7.234)–(7.238) into Eq. (7.227), the critical seismic input angle and maximum response can be determined by following the procedures in Eq. (7.226).

EXAMPLE 7.7.2 Rework Example 7.7.1 using the CQC method.

Solution: From Eq. (7.225a)

$$[R^k] = \sum_{m=1}^N \sum_{j=1}^N \left[R_{jm}^k \right] = \begin{bmatrix} R_{11}^k & R_{12}^k \\ R_{21}^k & R_{22}^k \end{bmatrix} \quad (a)$$

where

$$\left[R_{jm}^k \right] = \begin{bmatrix} R_x(p_j) R_x(p_m) \gamma_{1j} \gamma_{1m} \\ + R_x(p_j) R_y(p_m) \gamma_{1j} \gamma_{2m} \\ + R_y(p_j) R_x(p_m) \gamma_{2j} \gamma_{1m} \\ + R_y(p_j) R_y(p_m) \gamma_{2j} \gamma_{2m} \\ \frac{1}{2} [R_x(p_j) R_x(p_m) - R_y(p_j) R_y(p_m)] & R_x(p_j) R_x(p_m) \gamma_{2j} \gamma_{2m} \\ (\gamma_{1j} \gamma_{2m} + \gamma_{2j} \gamma_{1m}) & -R_x(p_j) R_y(p_m) \gamma_{2j} \gamma_{1m} \\ + \frac{1}{2} [R_x(p_j) R_y(p_m) + R_y(p_j) R_x(p_m)] & -R_y(p_j) R_x(p_m) \gamma_{1j} \gamma_{2m} \\ (\gamma_{2j} \gamma_{2m} - \gamma_{1j} \gamma_{1m}) & +R_y(p_j) R_y(p_m) \gamma_{1j} \gamma_{1m} \end{bmatrix} \alpha_{mj} X_j^k X_m^k \quad (b)$$

in which detailed expressions can be found in Eqs. (7.234)–(7.236). Numerical values are thus calculated as follows:

$$\begin{aligned}
 R_{11}^1 &= \alpha_{11} X_1^1 X_1^1 [R_x(p_1)R_x(p_1)\gamma_{11}\gamma_{11} + R_x(p_1)R_y(p_1)\gamma_{11}\gamma_{21} + R_y(p_1)R_x(p_1)\gamma_{21}\gamma_{11} + R_y(p_1)R_y(p_1)\gamma_{21}\gamma_{21}] \\
 &\quad + 2\alpha_{12} X_2^1 X_1^1 [R_x(p_2)R_x(p_1)\gamma_{12}\gamma_{11} + R_x(p_2)R_y(p_1)\gamma_{12}\gamma_{21} + R_y(p_2)R_x(p_1)\gamma_{22}\gamma_{11} + R_y(p_2)R_y(p_1)\gamma_{22}\gamma_{21}] \\
 &\quad + 2\alpha_{13} X_3^1 X_1^1 [R_x(p_3)R_x(p_1)\gamma_{13}\gamma_{11} + R_x(p_3)R_y(p_1)\gamma_{13}\gamma_{21} + R_y(p_3)R_x(p_1)\gamma_{23}\gamma_{11} + R_y(p_3)R_y(p_1)\gamma_{23}\gamma_{21}] \\
 &\quad + 2\alpha_{23} X_3^1 X_2^1 [R_x(p_3)R_x(p_2)\gamma_{13}\gamma_{12} + R_x(p_3)R_y(p_2)\gamma_{13}\gamma_{22} + R_y(p_3)R_x(p_2)\gamma_{23}\gamma_{12} + R_y(p_3)R_y(p_2)\gamma_{23}\gamma_{22}] \\
 &\quad + \alpha_{22} X_2^1 X_2^1 [R_x(p_2)R_x(p_2)\gamma_{12}\gamma_{12} + R_x(p_2)R_y(p_2)\gamma_{12}\gamma_{22} + R_y(p_2)R_x(p_2)\gamma_{22}\gamma_{12} + R_y(p_2)R_y(p_2)\gamma_{22}\gamma_{22}] \\
 &\quad + \alpha_{33} X_3^1 X_3^1 [R_x(p_3)R_x(p_3)\gamma_{13}\gamma_{13} + R_x(p_3)R_y(p_3)\gamma_{13}\gamma_{23} + R_y(p_3)R_x(p_3)\gamma_{23}\gamma_{13} + R_y(p_3)R_y(p_3)\gamma_{23}\gamma_{23}] \\
 &= (-0.0222)^2 [(1.5411)^2 (0.6556)] \\
 &\quad + (1.5411)(1.3688)(0.6556)(0.4486)2 + (1.3688)^2 (0.4486)^2] + 0 \\
 &\quad + 2(0.0564)(0.5730)(-0.0222)[(1.2652)(1.5411)(0.0254)(0.6556) \\
 &\quad + (1.2652)(1.3688)(0.0254)(0.4486) + (1.3925)(1.5411)(0.0174)(0.6556) \\
 &\quad + (1.3925)(1.3688)(0.0174)(0.4486)] + 0 + 0 \\
 &\quad + (0.5730)^2 [(1.2652)^2 (0.0254)^2 + (1.2652)(1.3925)(0.0254)(0.0174)2 \\
 &\quad + (1.3925)^2 (0.0174)^2] \\
 &= 0.2216 \times 10^{-2}
 \end{aligned} \tag{c}$$

$$\begin{aligned}
 R_{12}^1 &= \alpha_{11} X_1^1 X_1^1 \left\{ 0.5 [R_x^2(p_1) - R_y^2(p_1)] (\gamma_{11}\gamma_{21} + \gamma_{21}\gamma_{11}) + 0.5 [R_x(p_1)R_y(p_1) + R_y(p_1)R_x(p_1)] (\gamma_{21}^2 - \gamma_{11}^2) \right\} \\
 &\quad + 0 \\
 &\quad + 2\alpha_{13} X_3^1 X_1^1 \left\{ 0.5 [R_x(p_3)R_x(p_1) - R_y(p_3)R_y(p_1)] (\gamma_{13}\gamma_{21} + \gamma_{23}\gamma_{11}) + \frac{1}{2} [R_x(p_3)R_y(p_1) + R_y(p_3)R_x(p_1)] (\gamma_{23}\gamma_{21} - \gamma_{13}\gamma_{11}) \right\} \\
 &\quad + 0 \\
 &\quad + 0 \\
 &\quad + \alpha_{33} X_3^1 X_3^1 \left\{ 0.5 [R_x^2(p_3) - R_y^2(p_3)] (\gamma_{13}\gamma_{23} + \gamma_{23}\gamma_{13}) + 0.5 [R_x(p_3)R_y(p_3) + R_y(p_3)R_x(p_3)] (\gamma_{23}^2 - \gamma_{13}^2) \right\} \\
 &= (-0.0222)^2 [0.5[(1.5411)^2 - (1.3688)^2] [2(0.6556)(0.4486)] \\
 &\quad + 0.5(2)(1.5411)(1.3688)[(0.4486)^2 - (0.6556)^2]] \\
 &\quad + 2(0.0564)(0.5730)(-0.0222) \{ 0.5[1.2652(1.5411) - 1.3925(1.3688)] \\
 &\quad [(0.0254)0.4486 + 0.0174(0.6556)] + 0.5[1.2652(1.3688) \\
 &\quad + 1.3925(1.5411)][(0.0174)0.4486 - 0.0254(0.6556)] \} \\
 &\quad + (0.5730)^2 \{ 0.5[(1.2652)^2 - (1.3925)^2] [2(0.0254)(0.0174)] \\
 &\quad + 0.5(1.2652)(1.3925)2[(0.0174)^2 - (0.0254)^2] \} \\
 &= -3.896 \times 10^{-4}
 \end{aligned} \tag{d}$$

$$\begin{aligned}
 R_{22}^1 &= \alpha_{11} X_1^1 X_1^1 [R_x(p_1)R_x(p_1)\gamma_{21}\gamma_{21} - R_x(p_1)R_y(p_1)\gamma_{21}\gamma_{11} - R_y(p_1)R_x(p_1)\gamma_{11}\gamma_{21} + R_y(p_1)R_y(p_1)\gamma_{11}\gamma_{11}] \\
 &\quad + 0 \\
 &\quad + 2\alpha_{13} X_3^1 X_1^1 [R_x(p_3)R_x(p_1)\gamma_{23}\gamma_{21} - R_x(p_3)R_y(p_1)\gamma_{23}\gamma_{11} - R_y(p_3)R_x(p_1)\gamma_{13}\gamma_{21} + R_y(p_3)R_y(p_1)\gamma_{13}\gamma_{11}] \\
 &\quad + \alpha_{33} X_3^1 X_3^1 [R_x(p_3)R_x(p_3)\gamma_{23}\gamma_{23} - R_x(p_3)R_y(p_3)\gamma_{23}\gamma_{13} - R_y(p_3)R_x(p_3)\gamma_{13}\gamma_{23} + R_y(p_3)R_y(p_3)\gamma_{13}\gamma_{13}] \\
 &= (-0.0222)^2 [(1.5411)^2 (0.4486)^2 - 2(1.5411)(1.3688)(0.6556)(0.4486) \\
 &\quad + (1.3688)^2 (0.6556)^2] + 0 \\
 &\quad + 2(0.0564)(0.5730)(-0.0222)[(1.2652)(1.5411)(0.0174)(0.4486) \\
 &\quad - (1.2652)(1.3688)(0.0174)(0.6556) - (1.3925)(1.5411)(0.0254)(0.4486) \\
 &\quad + (1.3925)(1.3688)(0.0254)(0.6556)] \\
 &\quad + (0.5730)^2 [(1.2652)^2 (0.0174)^2 - 2(1.2652)(1.3925)(0.0174)(0.0254) \\
 &\quad + (1.3925)^2 (0.0254)^2] \\
 &= 7.5938 \times 10^{-5}
 \end{aligned} \tag{e}$$

From Eqs. (c)–(e), $[R^1]$ of Eq. (a) can be expressed as

$$[R^1] = \begin{bmatrix} 0.2216 \times 10^{-2} & -3.896 \times 10^{-4} \\ -3.896 \times 10^{-4} & 7.5938 \times 10^{-5} \end{bmatrix} \quad (f)$$

Similar to Example 7.7.1, the maximum response of d.o.f. D_1 can be calculated as

$$[R^1]\{d\} - \lambda\{d\} = \{0\} \quad (g)$$

or

$$\begin{vmatrix} 0.2216 \times 10^{-2} - \lambda & -3.896 \times 10^{-4} \\ -3.896 \times 10^{-4} & 7.5938 \times 10^{-5} - \lambda \end{vmatrix} = 0 \quad (h)$$

which yields

$$\lambda_1 = 0.2285 \times 10^{-2}; \quad \lambda_2 = 0.7274 \times 10^{-5} \quad (i)$$

Employing $\lambda_1 = 0.2285 \times 10^{-2}$ in Eq. (g) gives

$$d_1 = -5.6382d_2 \quad (j)$$

Since

$$d_1^2 + d_2^2 = 1 \quad (k)$$

from Eqs. (j) and (k)

$$\left. \begin{array}{l} d_1 = 0.9848 \\ d_2 = -0.1746 \end{array} \right\} \quad (l)$$

Thus the worst-case response of d.o.f. D_1 is equal to

$$(\zeta_1)^{1/2} = (0.2285 \times 10^{-2})^{1/2} = 0.0478 \text{ rad} \quad (m)$$

Seismic input direction relative to the structural reference axis is

$$\theta_{cr} = \sin^{-1}(d_2) = \sin^{-1}(-0.1746) = -10.05^\circ \quad (n)$$

Note that if ground rotational components are also considered in the response analysis, then the structural response $\{\bar{x}\}$ due to rotational components is assumed to be based on the input angle of θ_{cr} . Response can be evaluated in a manner similar to Eq. (7.232). Consequently, maximum structural response due to multiple seismic components can be obtained by combining response values due to translational and rotational components

$$x_{\text{total}}^k = \sqrt{(x^k)^2 + (\bar{x}^k)^2} \quad (7.239)$$

EXAMPLE 7.7.3 Apply three ground principal rotational components to the structure in Example 7.7.2 with main principal components acting along the critical input angle, $\theta_{cr} = -10.05^\circ$. Find the response values of d.o.f. D_1 due to (A) ground rotational components and (B) both ground translational and rotational components. Torsional response spectra for ground main, intermediate, and minor rotational components are shown in Figs. 7.41–7.43 from which we have

$$\begin{aligned} \left[\begin{array}{l} R_t^x(p_1) = 0.774 \\ R_t^x(p_2) = 0.773 \\ R_t^x(p_3) = 0.769 \end{array} \right] 10^{-3}; \quad & \left[\begin{array}{l} R_t^y(p_1) = 1.063 \\ R_t^y(p_2) = 1.061 \\ R_t^y(p_3) = 1.026 \end{array} \right] 10^{-3}; \quad & \left[\begin{array}{l} R_t^z(p_1) = 1.373 \\ R_t^z(p_2) = 1.371 \\ R_t^z(p_3) = 1.339 \end{array} \right] 10^{-3} \end{aligned}$$

Solutions: Influence coefficient vectors $\{I_n\}_{x1}$, $\{I_n\}_{x2}$ and $\{I_n\}_{x3}$ corresponding to structural reference axes x_1 , x_2 , and x_3 directions (see Fig. 7.45) are

$$\{I_n\}_{x1} = \begin{bmatrix} 0 \\ 0 \\ -20 \end{bmatrix}; \quad \{I_n\}_{x2} = \begin{bmatrix} 0 \\ 20 \\ 0 \end{bmatrix}; \quad \{I_n\}_{x3} = \begin{bmatrix} 1 \\ 0 \\ 0 \end{bmatrix} \quad (a)$$

The influence coefficient vector $\{I_n\}_x$ due to ground main rotational component input at an angle $\theta_{cr} = -10.05^\circ$ is shown in Fig. 7.47.

Therefore, the influence coefficient vector corresponding to the ground main rotational component is

$$\{I_n\}_x = 0.9848\{I_n\}_{x1} + (-0.174)\{I_n\}_{x2} = \begin{bmatrix} 0 \\ -3.4800 \\ -19.6962 \end{bmatrix} \quad (b)$$

$\{I_n\}_y$ due to the ground intermediate rotational component is

$$\{I_n\}_y = (0.174)\{I_n\}_{x1} + (0.9848)\{I_n\}_{x2} = \begin{bmatrix} 0 \\ 19.6962 \\ -3.4800 \end{bmatrix} \quad (c)$$

$\{I_n\}_z$ due to ground minor rotational component is

$$\{I_n\}_z = \{I_n\}_{x3} = \begin{bmatrix} 1 \\ 0 \\ 0 \end{bmatrix} \quad (d)$$

$$[X]^T [M] \{I_n\}_x = 10^4 \begin{bmatrix} -0.5765 & 0.225 & 0.1540 \\ 0 & -0.154 & 0.2250 \\ 0.1486 \times 10^2 & 0.225 & 0.1539 \end{bmatrix} \begin{bmatrix} 0 \\ -3.4800 \\ -19.6962 \end{bmatrix} = \begin{bmatrix} -38162.1480 \\ -38957.2500 \\ -38142.4518 \end{bmatrix} \quad (e)$$

$$[X]^T [M] \{I_n\}_y = [X]^T [M] \begin{bmatrix} 0 \\ 19.6962 \\ -3.4800 \end{bmatrix} = \begin{bmatrix} 38957.250 \\ -38162.148 \\ 38960.730 \end{bmatrix} \quad (f)$$

$$[X]^T [M] \{I_n\}_z = [X]^T [M] \begin{bmatrix} 1 \\ 0 \\ 0 \end{bmatrix} = \begin{bmatrix} -0.5765 \times 10^4 \\ 0 \\ 0.1486 \times 10^6 \end{bmatrix} \quad (g)$$

$$[X]^T [M] [X] = \begin{bmatrix} 3432 & 0 & 0 \\ 0 & 3303 & 0 \\ 0 & 0 & 88470 \end{bmatrix} \quad (h)$$

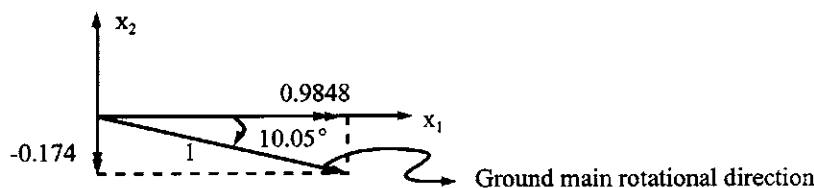


FIG. 7.47 Components of ground main rotational component direction.

Using Eq. (7.195) yields the following participation factors, γ 's, and rotational responses, $\{\bar{x}\}$.

$$\left. \begin{array}{l} \gamma_{x1} = -38162.148/3432 = -11.1195 \\ \gamma_{x2} = -38957.25/3303 = -11.7945 \\ \gamma_{x3} = -38142.4518/88470 = -0.4311 \end{array} \right\} \quad (\text{i})$$

$$\left. \begin{array}{l} \gamma_{y1} = 38957.25/3432 = 11.3511 \\ \gamma_{y2} = -38162.148/3303 = -11.5537 \\ \gamma_{y3} = 38960.73/88470 = 0.4403 \end{array} \right\} \quad (\text{j})$$

$$\left. \begin{array}{l} \gamma_{z1} = -5765/3432 = -1.6797 \\ \gamma_{z2} = 0/3303 = 0 \\ \gamma_{z3} = 0.1486 \times 10^6/88470 = 1.6796 \end{array} \right\} \quad (\text{k})$$

and

$$\{\bar{x}\}_{1x} = \{X\}_1 \gamma_{x1} R_t^x(p_1) = \begin{bmatrix} -0.0222 \\ 1 \\ 0.6842 \end{bmatrix} (-11.1195)(0.774 \times 10^{-3}) = \begin{bmatrix} 0.1912 \\ -8.6064 \\ -5.8885 \end{bmatrix} 10^{-3} \quad (\text{l})$$

$$\{\bar{x}\}_{2x} = \{X\}_2 \gamma_{x2} R_t^x(p_2) = \begin{bmatrix} 0 \\ -0.6842 \\ 1 \end{bmatrix} (-11.7945)(0.773 \times 10^{-3}) = \begin{bmatrix} 0 \\ 6.2382 \\ -9.1171 \end{bmatrix} 10^{-3} \quad (\text{m})$$

$$\{\bar{x}\}_{3x} = \{X\}_3 \gamma_{x3} R_t^x(p_3) = \begin{bmatrix} 0.5730 \\ 1 \\ 0.6842 \end{bmatrix} (-0.4311)(0.769 \times 10^{-3}) = \begin{bmatrix} -1.8998 \\ -3.3154 \\ -2.2684 \end{bmatrix} 10^{-4} \quad (\text{n})$$

$$\{\bar{x}\}_{1y} = \{X\}_1 \gamma_{y1} R_t^y(p_1) = \begin{bmatrix} -0.0222 \\ 1 \\ 0.6842 \end{bmatrix} (11.3511)(1.063 \times 10^{-3}) = \begin{bmatrix} -2.6817 \times 10^{-4} \\ 0.0120 \\ 8.2557 \times 10^{-3} \end{bmatrix} \quad (\text{o})$$

$$\{\bar{x}\}_{2y} = \{X\}_2 \gamma_{y2} R_t^y(p_2) = \begin{bmatrix} 0 \\ -0.6842 \\ 1 \end{bmatrix} (-11.5537)(1.061 \times 10^{-3}) = \begin{bmatrix} 0 \\ 8.3877 \times 10^{-3} \\ -0.0122 \end{bmatrix} \quad (\text{p})$$

$$\{\bar{x}\}_{3y} = \{X\}_3 \gamma_{y3} R_t^y(p_3) = \begin{bmatrix} 0.5730 \\ 1 \\ 0.6842 \end{bmatrix} (0.4403)(1.026 \times 10^{-3}) = \begin{bmatrix} 2.5890 \\ 4.5182 \\ 3.0914 \end{bmatrix} 10^{-4} \quad (\text{q})$$

$$\{\bar{x}\}_{1z} = \{X\}_1 \gamma_{z1} R_t^z(p_1) = \begin{bmatrix} -0.0222 \\ 1 \\ 0.6842 \end{bmatrix} (-1.6797)(1.373 \times 10^{-3}) = \begin{bmatrix} 0.0525 \\ -2.3063 \\ -1.5780 \end{bmatrix} 10^{-3} \quad (\text{r})$$

$$\{\bar{x}\}_{2z} = \{X\}_2 \gamma_{z2} R_t^z(p_2) = \begin{bmatrix} 0 \\ 0 \\ 0 \end{bmatrix} \quad (s)$$

$$\{\bar{x}\}_{3z} = \{X\}_3 \gamma_{z3} R_t^z(p_3) = \begin{bmatrix} 0.5730 \\ 0 \\ 0.6842 \end{bmatrix} (1.6796)(1.339 \times 10^{-3}) = \begin{bmatrix} 1.2887 \\ 2.2490 \\ 1.5388 \end{bmatrix} 10^{-3} \quad (t)$$

The response vector of each mode due to these three principal components can be written as

$$\{\bar{x}\}_1 = \{\bar{x}\}_{1x} + \{\bar{x}\}_{1y} + \{\bar{x}\}_{1z} = \begin{bmatrix} -2.5635 \times 10^{-2} \\ 1.0873 \\ 0.7892 \end{bmatrix} 10^{-3} \quad (u)$$

$$\{\bar{x}\}_2 = \{\bar{x}\}_{2x} + \{\bar{x}\}_{2y} + \{\bar{x}\}_{2z} = \begin{bmatrix} 0 \\ 0.0146 \\ -0.0213 \end{bmatrix} \quad (v)$$

$$\{\bar{x}\}_3 = \{\bar{x}\}_{3x} + \{\bar{x}\}_{3y} + \{\bar{x}\}_{3z} = \begin{bmatrix} 1.3576 \\ 2.3693 \\ 1.6211 \end{bmatrix} 10^{-3} \quad (w)$$

Using the CQC method yields the following response of d.o.f. D_1

$$(\bar{x}^k)^2 = (\bar{x}_1^k \alpha_{11} \bar{x}_1^k) + 2(\bar{x}_1^k \alpha_{12} \bar{x}_2^k) + 2(\bar{x}_1^k \alpha_{13} \bar{x}_3^k) + 2(\bar{x}_2^k \alpha_{23} \bar{x}_3^k) + (\bar{x}_2^k \alpha_{23} \bar{x}_2^k) + (\bar{x}_3^k \alpha_{33} \bar{x}_3^k) \quad (x)$$

Thus

$$\begin{aligned} (\bar{x}^{D_1})^2 &= 6.5719 \times 10^{-10} + 0 + 2(-2.5635 \times 10^{-5})(0.0564)(1.3576 \times 10^{-3}) \\ &\quad + 0 + 0 + (1.8433 \times 10^{-6}) \\ &= 1.8400 \times 10^{-6} \\ \bar{x}^{D_1} &= 0.0013 \text{ rad} \end{aligned} \quad (y)$$

The response of d.o.f. D_1 due to both ground translational and rotational components is then obtained by using Eq. (7.239) as

$$\begin{aligned} x_{\text{total}}^{D_1} &= \sqrt{(x^{D_1})^2 + (\bar{x}^{D_1})^2} \\ &= \sqrt{(0.2285 \times 10^{-2}) + (1.8400 \times 10^{-6})} \\ &= 0.0478 \text{ rad} \end{aligned} \quad (z)$$

7.8. COMPOSITE TRANSLATIONAL SPECTRUM AND TORSIONAL SPECTRUM

The previous section describes the (worst-case) response of a structural system subjected to multiple-component seismic input. One response spectrum for each of the six spectra (three seismic translational and three rotational principal components) is needed. Critical seismic input angle, θ_{cr} , must be calculated in order to determine the maximum structural response. In this section, we will introduce a simplified approach, called a *composite response spectrum*, one for the three translational principal components and one for the three torsional principal components, to eval-

ate the structure's worst-case response. This approach does not depend on seismic input direction, and the results are close to those derived by the rigorous method presented in the previous section.

7.8.1. Construction of the Composite Response Spectrum

The composite translational spectrum is constructed by estimating the response peak of the oscillator subjected to input of the three translational principal components. The motion equation of the oscillator can be written as

$$\ddot{r}_i(t) + 2\rho p_n \dot{r}_i(t) + p_n^2 r_i(t) = \ddot{u}_i(t); \quad i = x, y, z \quad (7.240)$$

where x , y , and z represent ground principal component directions; $r_i(t)$ represents the relative displacement of the oscillator or mass in the i th principal direction; and $\ddot{u}_i(t)$ represents ground acceleration records in the i th principal direction, i.e. main, intermediate or minor. Total relative displacement at any instant is calculated using the root-mean-square technique as

$$r(t) = [r_x^2(t) + r_y^2(t) + r_z^2(t)]^{1/2} \quad (7.241)$$

The composite translational spectral quantity is obtained by finding the maximum value of $r(t)$ in the entire earthquake record for a given p_n and ρ

$$S_c = R_d(p_n) = r(t)|_{\max} \quad (7.242)$$

The composite translational spectrum denoted by S_c or R_d for the 1940 El Centro earthquake's three translational principal components is shown in Fig. 7.48.

Similar to Eqs. (7.241) and (7.242), the composite torsional spectrum can be constructed from the total relative rotational displacement at any instant as

$$\Omega(t) = [\Omega_x^2(t) + \Omega_y^2(t) + \Omega_z^2(t)]^{1/2} \quad (7.243)$$

in which $\Omega_i(t)$ represents the total relative rotational displacement in the i th component direction. Thus the composite torsional spectrum, $S_r = R_r(p_n)$, becomes

$$S_r = R_r(p_n) = \Omega(t)|_{\max} \quad (7.244)$$

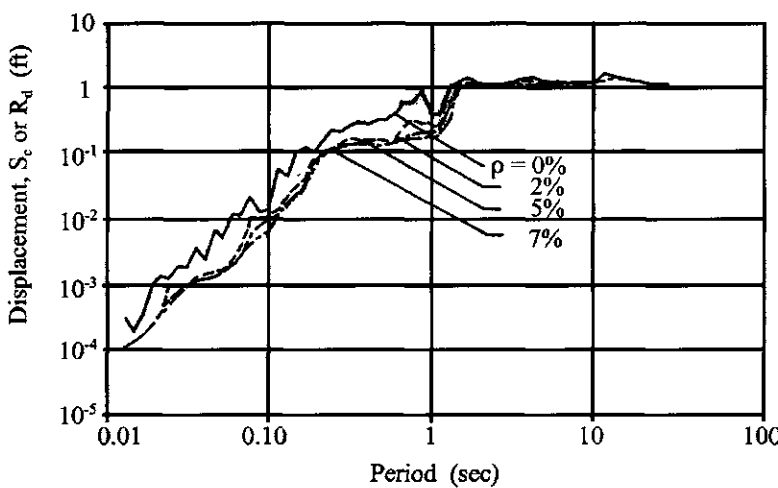


FIG. 7.48 Composite translational spectrum (S_c or R_d) for 18 May, 1940 El Centro Earthquake.

The composite torsional spectrum constructed using the 1940 El Centro earthquake's three rotational principal components is shown in Fig. 7.49.

7.8.2. Composite Spectral Modal Analysis

Similar to Eq. (7.205), the structural responses for the j th mode can be approximately expressed as

$$\{x\}_{ji} = \{X\}_j \gamma_{ij} [\Lambda_i R_d(p_j)] \quad (7.245)$$

where $\{x\}_{ji}$ is the j th modal response vector due to ground component input in the structural i th reference axis direction; Λ_i is the *spectral distribution factor* corresponding to ground principal translational component applied at the structural i th direction ($\Lambda_i = 1.0$ is used for main, intermediate principal components, and 0.5 for minor principal component); and $R_d(p_j)$ is the *composite translational spectral value* for the j th mode. Similarly, the j th modal response vector due to ground rotational components can be approximately expressed as

$$\{\bar{x}\}_{ji} = \{x\}_j \gamma_{ij} [\Lambda_i R_r(p_j)] \quad (7.246)$$

where $\Lambda_i = 1.0$ is used for all principal components; and $R_r(p_j)$ is the *composite torsional spectral quantity* corresponding to the j th mode. The structural response due to multiple seismic components can be expressed as

$$x_{\text{total}}^k = \sqrt{\sum_{i=1}^N (x^k)_i^2 + \sum_{i=1}^N (\bar{x}^k)_i^2}; \quad N = \text{no. of ground components considered} \quad (7.247)$$

EXAMPLE 7.8.1 Rework Example 7.7.2 with the composite translational spectra. Spectral values corresponding to p_1 , p_2 , and p_3 may be obtained from Fig. 7.48. Here the values are from computer output as $R_d(p_1) = 2.0782$ ft; $R_d(p_2) = 2.0596$ ft; and $R_d(p_3) = 1.8723$ ft.

Solution: From Eq. (7.245)

$$\{x\}_{ji} = \{X\}_j \gamma_{ij} [\Lambda_i R_d(p_j)]; \quad \Lambda_i = 1 \text{ in this example} \quad (a)$$

where $\{x\}_{ji}$ represents the j th modal response vector due to ground component input at structural

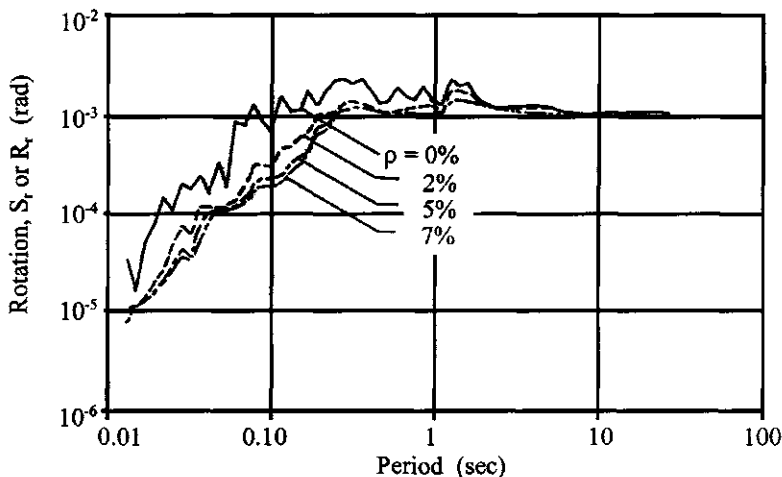


FIG. 7.49 Composite torsional spectrum (S_r or R_r) for 18 May, 1940 El Centro Earthquake.

*i*th reference axis direction. Thus

$$\{x\}_{11} = \{X\}_1 \gamma_{11} R_d(p_1) = \begin{bmatrix} -0.0222 \\ 1 \\ 0.6842 \end{bmatrix} (0.6556) (2.0782) = \begin{bmatrix} -0.0302 \\ 1.3624 \\ 0.9322 \end{bmatrix} \quad (\text{b})$$

$$\{x\}_{12} = \{X\}_1 \gamma_{21} R_d(p_1) = \begin{bmatrix} -0.0222 \\ 1 \\ 0.6842 \end{bmatrix} (0.4486) (2.0782) = \begin{bmatrix} -0.0207 \\ 0.9322 \\ 0.6378 \end{bmatrix} \quad (\text{c})$$

$$\{x\}_{21} = \{X\}_2 \gamma_{12} R_d(p_2) = \begin{bmatrix} 0 \\ -0.6842 \\ 1 \end{bmatrix} (-0.4662) (2.0596) = \begin{bmatrix} 0 \\ 0.6569 \\ -0.9601 \end{bmatrix} \quad (\text{d})$$

$$\{x\}_{22} = \{X\}_2 \gamma_{22} R_d(p_2) = \begin{bmatrix} 0 \\ -0.6842 \\ 1 \end{bmatrix} (0.6811) (2.0596) = \begin{bmatrix} 0 \\ -0.9598 \\ 1.4027 \end{bmatrix} \quad (\text{e})$$

$$\{x\}_{31} = \{X\}_3 \gamma_{13} R_d(p_3) = \begin{bmatrix} 0.5730 \\ 1 \\ 0.6842 \end{bmatrix} (0.0254) (1.8723) = \begin{bmatrix} 0.0272 \\ 0.0476 \\ 0.0325 \end{bmatrix} \quad (\text{f})$$

$$\{x\}_{32} = \{X\}_3 \gamma_{23} R_d(p_3) = \begin{bmatrix} 0.5730 \\ 1 \\ 0.6842 \end{bmatrix} (0.0174) (1.8723) = \begin{bmatrix} 0.0186 \\ 0.0325 \\ 0.0222 \end{bmatrix} \quad (\text{g})$$

For the CQC method

$$x_i^k = \sqrt{\sum_{m=1}^M \sum_{j=1}^M x_{mi}^k \alpha_{mj} x_{ji}^k}; \quad \begin{array}{l} M = \text{number of modes considered} \\ i = \text{structural } i\text{th reference axis} \end{array} \quad (\text{h})$$

The response, x_1^k , for the k th component due to ground component input at the structural reference axis x_1 (i.e. first structural reference axis) is

$$(x_1^k)^2 = x_{11}^k \alpha_{11} x_{11}^k + x_{21}^k \alpha_{22} x_{21}^k + x_{31}^k \alpha_{33} x_{31}^k + 2x_{11}^k \alpha_{12} x_{21}^k + 2x_{11}^k \alpha_{13} x_{31}^k + 2x_{21}^k \alpha_{23} x_{31}^k \quad (\text{i})$$

Thus

$$\begin{aligned} \{x_1\}^2 &= \\ &\begin{bmatrix} 9.1204 \times 10^{-4} & +0 & +7.3984 \times 10^{-4} & +0 & -9.2658 \times 10^{-5} & +0 \\ 1.8564 & +0.4316 & +2.2658 \times 10^{-3} & +1.6761 & +7.3156 \times 10^{-3} & +4.0405 \times 10^{-3} \\ 0.8690 & +0.9220 & +1.0563 \times 10^{-3} & -1.6760 & +3.4174 \times 10^{-3} & -4.0319 \times 10^{-3} \end{bmatrix} \\ &= \begin{bmatrix} 1.5592 \times 10^{-3} \\ 3.9778 \\ 0.1154 \end{bmatrix} \end{aligned} \quad (\text{j})$$

The response, x_2^k , for the k th component due to ground component input at the structural reference axis x_2 (i.e. second structural reference axis) is

$$\{x_2^k\}^2 = x_{12}^k \alpha_{11} x_{12}^k + x_{22}^k \alpha_{22} x_{22}^k + x_{32}^k \alpha_{33} x_{32}^k + 2x_{12}^k \alpha_{12} x_{22}^k + 2x_{12}^k \alpha_{13} x_{32}^k + 2x_{22}^k \alpha_{23} x_{32}^k \quad (k)$$

Thus

$$\begin{aligned} \{x_2\}^2 &= \\ &\left[\begin{array}{cccccc} 4.2849 \times 10^{-4} & +0 & +3.4969 \times 10^{-4} & +0 & -4.3664 \times 10^{-5} & +0 \\ 0.8692 & +0.9212 & +1.0628 \times 10^{-3} & -1.6755 & +3.4283 \times 10^{-3} & -4.0300 \times 10^{-3} \\ 0.4069 & +1.9678 & +4.9729 \times 10^{-4} & +1.6755 & +1.6046 \times 10^{-3} & +4.0417 \times 10^{-3} \end{array} \right] \\ &= \left[\begin{array}{c} 7.3452 \times 10^{-4} \\ 0.1154 \\ 4.0564 \end{array} \right] \end{aligned} \quad (l)$$

The total response vector is

$$\{D\} = \sqrt{\{x_1\}^2 + \{x_2\}^2} = \begin{bmatrix} 0.0479 \\ 2.0231 \\ 2.0424 \end{bmatrix} \begin{array}{l} \text{rad} \\ \text{ft} \\ \text{ft} \end{array} \quad (m)$$

7.9. OVERVIEW

This chapter consists of seven major themes: (1) introduction to fundamentals of earthquake motion; (2) numerical integration methods and assessment of their stability and accuracy; (3) construction of various spectra such as elastic and inelastic response spectra, design spectra, and principal component spectra; (4) definition of ductilities and their application in design; (5) ground rotation; (6) construction of response spectra including the effects of ground translational and rotational motion; and (7) modal combination techniques of SSRS and CQC. For the convenience of readers, numerical examples are given with more detailed steps than normally found in a standard text. Some well-known algorithms are documented in computer program lists in Appendices G, H and I. Detailed mathematical derivation of ground rotation is shown in Appendix B. This chapter is intended to be self-contained, presenting fundamental as well as advanced topics for both beginners and those more familiar with the subject matter.

BIBLIOGRAPHY

1. FY Cheng, KB Oster. Ultimate instability of earthquake structures. ASCE J Struct Engng 102:961–972, 1976.
2. FY Cheng, KB Oster. Dynamic instability and ultimate capacity of inelastic systems parametrically excited by earthquakes (Part II). NSF Report. National Technical Information Service, US Department of Commerce, Virginia, NTIS no. PB261097/AS, 1976 (313pp).
3. FY Cheng, P Kitipitayangkul. Investigation of effect of 3-D parametric earthquake motions on stability of elastic and inelastic building systems. NSF Report. National Technical Information Service, US Department of Commerce, Virginia, NTIS no. PB80-176936, 1979 (392pp).
4. FY Cheng, P Kitipitayangkul. Multicomponent earthquake analysis of mixed structural systems. B Kato, LW Lu, eds. US-Japan Seminar on Composite Structures and Mixed Structural Systems, Developments in Composite and Mixed Construction. Tokyo:Gihodo Shuppan Co. Ltd, 1980, pp 337–347.
5. FY Cheng, DS Juang. Assessment of ATC-03 for steel structures based on optimization algorithm. Proceedings of 8th World Conference on Earthquake Engineering, Vol. 5, San Francisco, CA, 1984, pp 425–442.

6. FY Cheng, DS Juang. Optimum design of braced and unbraced frames subjected to static, seismic and wind forces with UBC, ATC-3 and TJ-11. NSF Report. National Technical Information Service, US Department of Commerce, Virginia, NTIS no. PB 87-162988/AS, 1985 (376pp).
7. FY Cheng, JF Ger. Maximum response of buildings to multi-seismic input. Dynamics of Structures. ASCE, 1987, pp 397–410.
8. FY Cheng, JF Ger. Response analysis of 3-D pipeline structures with consideration of six-component seismic input. Proceedings of Symposium on Recent Developments in Lifeline Earthquake Engineering, American Society of Mechanical Engineers (ASME) and Japan Society of Mechanical Engineers (JSME), Vol. I, 1989, pp 257–271.
9. FY Cheng, JF Ger. The effect of multicomponent seismic excitation and direction on response behavior of 3-D structures. Proceedings of 4th US National Conference on Earthquake Engineering, Earthquake Engineering Research Institute (EERI), Vol. 2, 1990, pp 5–14.
10. FY Cheng, MS Sheu, eds. Urban Disaster Mitigation: the Role of Engineering and Technology. Oxford, Elsevier Science, 1995.
11. FY Cheng, KY Lou. Assessment of a bridge collapse and its design parameters for northridge earthquake. In: FY Cheng, Y Wang, eds. Post-Earthquake Rehabilitation and Reconstruction. Oxford: Elsevier Science, 1996.
12. AK Chopra. Dynamics of Structures. Englewood Cliffs, NJ: Prentice-Hall, 1995.
13. GW Housner. Behavior of Structures during Earthquakes. ASCE J Engng Mech 85(EM4):109–129, 1959.
14. International Conference of Building Officials. Uniform Building Code. Whittier, CA :ICBO, 1994.
15. MR Lindeburg. Seismic Design of Building Structures. 5th ed. Belmont, CA: Professional Publications, 1990.
16. NM Newmark. Torsion in symmetrical buildings. Proceedings of 4th World Conference on Earthquake Engineering, Vol. A3, Santiago, 1969, pp 19–32.
17. NM Newmark, WJ Hall. Earthquake Spectra and Design. Oakland, CA: Earthquake Engineering Research Institute, 1982.
18. CF Richter. Elementary Seismology. San Francisco, CA: Freeman, 1958.
19. J Penzien, M Watabe. Characteristics of 3-dimensional earthquake ground motion. J Earthq Engng Struct Dyn 3:365–373, 1975.
20. HB Seed, C Ugas, J Lysmer. Site dependent spectra for earthquake-resistant design. Bull Seismol Soc Am 66(1):221–244, 1976.
21. MP Singh, GA Mohsen. Maximum response of nonproportionally and proportionally damped structural systems under multicomponent earthquakes. Report NSF/CEE-83029. Blacksburg, VA: Polytechnic Institute and State University, 1983.
22. WK Tso, TI Hsu. Torsional spectrum for earthquake motion. J Earthq Engng Struct Dyn 6:375–382, 1978.
23. EL Wilson, AD Kiureghian, EP Bayo. A replacement for the SRSS method in seismic analysis. J Earthq Engng and Struct Dyn 9:187–194, 1981.
24. HO Wood, F Neumann. Modified Mercalli Intensity Scale of 1931. Bull Seismol Soc of Am 21(4):277–283, 1931.

8

Formulation and Response Analysis of Three-Dimensional Building Systems with Walls and Bracings

PART A FUNDAMENTALS

8.1. INTRODUCTION

Previous chapters emphasized fundamental concepts of structural dynamics such as dynamic response behavior, mathematical models (lumped mass, distributed mass, and consistent mass), closed-form integration and numerical integration techniques, as well as response and design spectra. These fundamentals can be applied to various types of structures in different engineering disciplines including aerospace, mechanical, and civil. This chapter focuses on civil engineering building structures which have beams, beam-columns, bracing elements, shear walls, floor slabs, and rigid zones at structural joints. Here, stiffness matrices for each element, assembly of system matrix, and condensation are discussed in depth with consideration of restrained, constrained, and free d.o.f. Because the structural configuration is three-dimensional (3D), vector formulation is introduced for generalized coordinate transformation.

8.2. JOINTS, MEMBERS, COORDINATE SYSTEMS, AND DEGREE OF FREEDOM (D.O.F)

A structural *joint* or structural *node* is defined as the point where two or more structural elements (members) connect; structural support is also considered as a node. In Fig. 8.1 a structure has 14 joints, numbered 1–14.

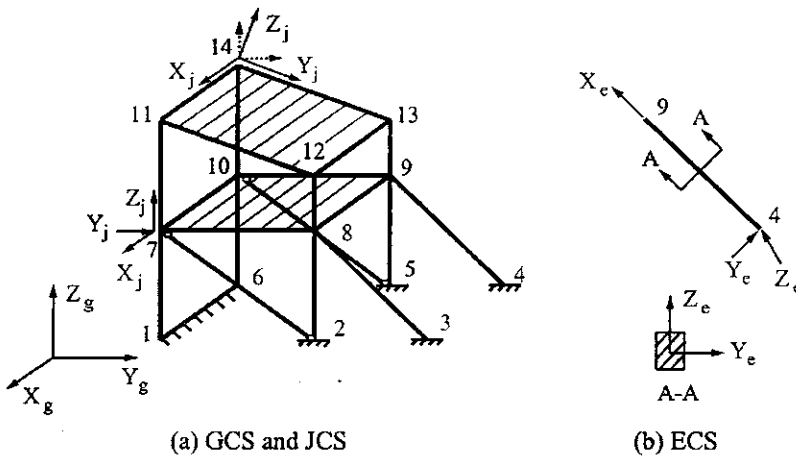


FIG. 8.1 GCS, JCS, ECS and members in a building structure.

A *member* is the basic element of a structure. The assembly of all members forms a *structural model*. A basic building structure has beam–columns, bracing elements, shear walls, and slab elements. As shown in Fig. 8.1a, member 1–6–10–7 is a shear wall, members 2–7 and 5–10 are bracing elements (pinned connections), members 7–8–9–10 and 11–12–13–14 are slabs, and other members are beam–columns. A structural model is established by first defining the location and orientation of each joint; then the elements that connect the joints are located and oriented. To define a structural model, three coordinate systems are essential: global, joint, and element.

The *global coordinate system* (GCS) is used to represent the location of a structure in Cartesian coordinates with three perpendicular X_g , Y_g , and Z_g axes, (right-hand rule) as shown in Fig. 8.1a. The location of the origin, while arbitrary, is usually put at the base of the structure.

The *joint coordinate system* (JCS) is defined by the X_j , Y_j , and Z_j axes (right-hand rule) of a given joint. The JCS may not be parallel to the GCS, and can vary for different joints. In Fig. 8.1a, joints 7 and 14 have two JCSs. For joint 14, the JCS can be either parallel to the GCS (dashed line) or in any reasonable direction (solid line).

The *element coordinate system* (ECS) is defined by the X_e , Y_e , and Z_e axes (right-hand rule) for a given element. Generally, the X_e axis is the same as the element's axis while the Y_e and Z_e axes coincide with the principal axes of the element's cross-sectional area. The original point of the coordinate system is at the geometric centroid of the cross-section of an element (see Fig. 8.1b).

Each joint is assumed to have six d.o.f. The first three are translational and correspond to the joint's X_j , Y_j , and Z_j axes. The remaining three are rotational about the joint's X_j , Y_j , and Z_j axes.

Note that, for simple building geometry, the JCS can be assumed to be parallel to the GCS. By doing so, it is easier to define nodal coordinates and to analyze the system. For complex structural configuration, the JCS may not necessarily be parallel to the GCS. Also note that, in the floor slabs of a building, in-plane stiffness is usually assumed to be infinitely rigid and out-of-plane stiffness to be flexible and negligible.

8.3. COORDINATE TRANSFORMATION BETWEEN JCS AND GCS: METHODS 1 AND 2

For analysis of general 3D structural systems, coordinate transformation between the JCS and GCS is important. Therefore two methods are introduced in this section; their detailed derivations are given in Appendix D. Sample structural configurations are shown in Fig. 8.2. Figure 8.3 shows the transformation between the JCS and GCS. Let the orientation of the JCS at a given joint be

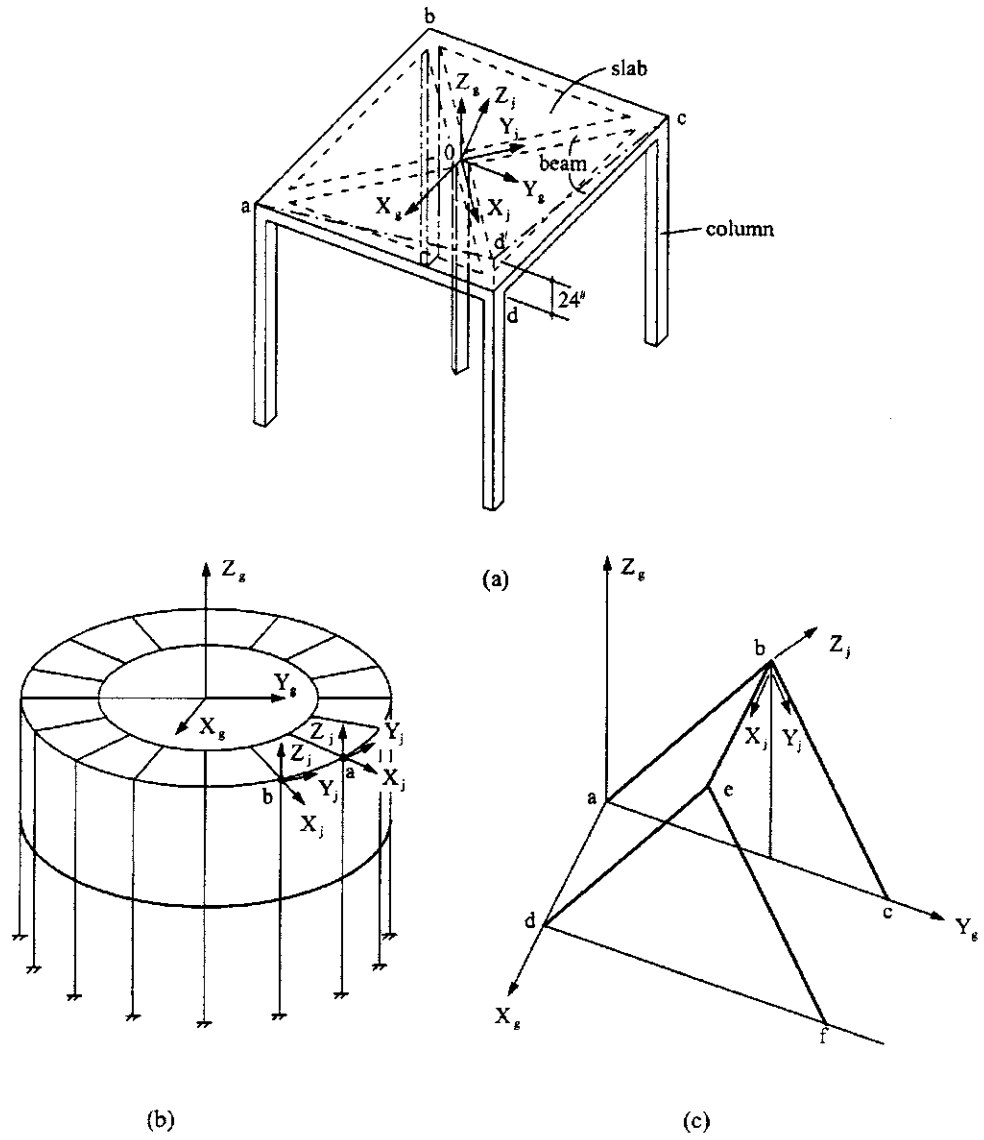


FIG. 8.2 GCS and JCS transformation for sample cases.

defined by two vectors \vec{V}_{xj} and \vec{V}_{yj} , which are parallel to X_j and Y_j axes of the coordinates of JCS, respectively. The third vector \vec{V}_{zj} , in the direction of Z_j axis, is the cross product of \vec{V}_{xj} and \vec{V}_{yj} as $\vec{V}_{zj} = \vec{V}_{xj} \times \vec{V}_{yj}$. An introduction to vector analysis is given in Appendix C.

Method 1

Expressing the three vectors in a symbolic matrix yields

$$\{\vec{V}_j\} = \begin{Bmatrix} \vec{V}_{xj} \\ \vec{V}_{yj} \\ \vec{V}_{zj} \end{Bmatrix} = \begin{bmatrix} C_{11} & C_{12} & C_{13} \\ C_{21} & C_{22} & C_{23} \\ C_{31} & C_{32} & C_{33} \end{bmatrix} \begin{Bmatrix} \vec{i} \\ \vec{j} \\ \vec{k} \end{Bmatrix} = [C_j] \begin{Bmatrix} \vec{i} \\ \vec{j} \\ \vec{k} \end{Bmatrix}; [C_j] = \begin{bmatrix} \cos \alpha_1 & \cos \beta_1 & \cos \gamma_1 \\ \cos \alpha_2 & \cos \beta_2 & \cos \gamma_2 \\ \cos \alpha_3 & \cos \beta_3 & \cos \gamma_3 \end{bmatrix} \quad (8.1)$$

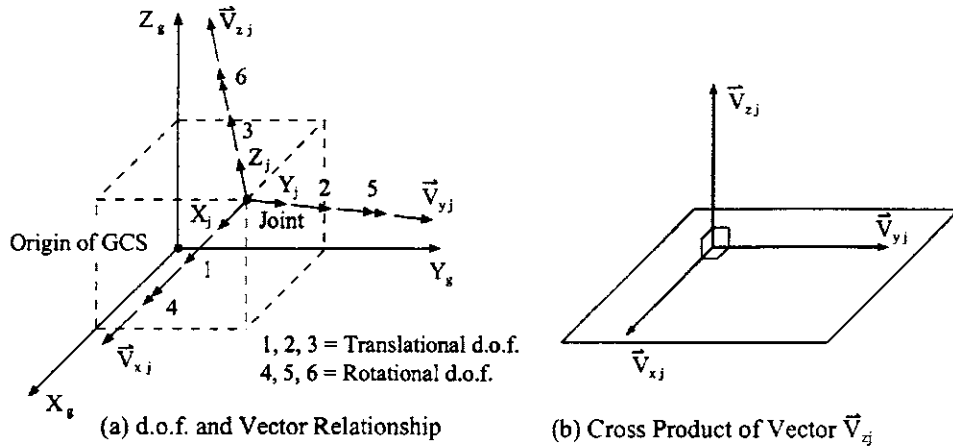


FIG. 8.3 Relationship between JCS and GCS.

where \vec{i} , \vec{j} , and \vec{k} are unit vectors parallel to the X_g , Y_g , and Z_g axes, respectively; $[C_j]$ is the transformation matrix between the JCS and GCS in which the angles for α 's, β 's, and γ 's are shown in Fig. 8.4a. In summary, α_1 , α_2 , and α_3 are measured from X_g to X_j and Y_j , and Z_j , respectively; β_1 , β_2 , and β_3 are measured from Y_g to X_j and Y_j , and Z_j , respectively; and γ_1 , γ_2 , and γ_3 are measured from Z_g to X_j and Y_j , and Z_j , respectively. A detailed derivation of Eq. (8.1) is given in Appendix D.

Method 2

The joint transformation matrix, $[C_j]$, in Eq. (8.1) can also be expressed in Eq. (8.1a) as

$$[C_j] = \begin{bmatrix} \cos \beta \cos \gamma & \sin \beta & \cos \beta \sin \gamma \\ -\cos \phi \sin \beta \cos \gamma - \sin \phi \sin \gamma & \cos \phi \cos \beta & -\sin \gamma \cos \phi \sin \beta + \sin \phi \cos \gamma \\ \cos \gamma \sin \phi \sin \beta - \sin \gamma \cos \phi & -\sin \phi \cos \beta & \sin \phi \sin \beta \sin \gamma + \cos \phi \cos \gamma \end{bmatrix} \quad (8.1a)$$

where γ is the angle between X_g and the projection of X_j in the X_g-Z_g plane, β is the angle measured from the X_j projection in the X_g-Z_g plane to X_j , and ϕ is the rotation of X_j . Facing the X_j axis, ϕ is defined as positive when it rotates in the counterclockwise direction. These angles are shown in Fig. 8.4. Detailed derivation of Eqs. (8.1) and (8.1a) also appears in Appendix D. Identification of these two methods is further elaborated at the end of that Appendix.

EXAMPLE 8.3.1 For the structural configuration shown in Fig. 8.2a, find the transformation matrix $[C_j]$ by using Eqs. (8.1a) of methods 1 and 2, respectively.

Solution: Let the structural floor, with four corners signified by a , b , c , and d , be shown on the X_g-Z_g plane in Fig. 8.5a, where Z_g is perpendicular to the plane and pointing upward with the sign \odot . This sign is also used for the Z_j axis, although it is not perpendicular to the X_g-Y_g plane.

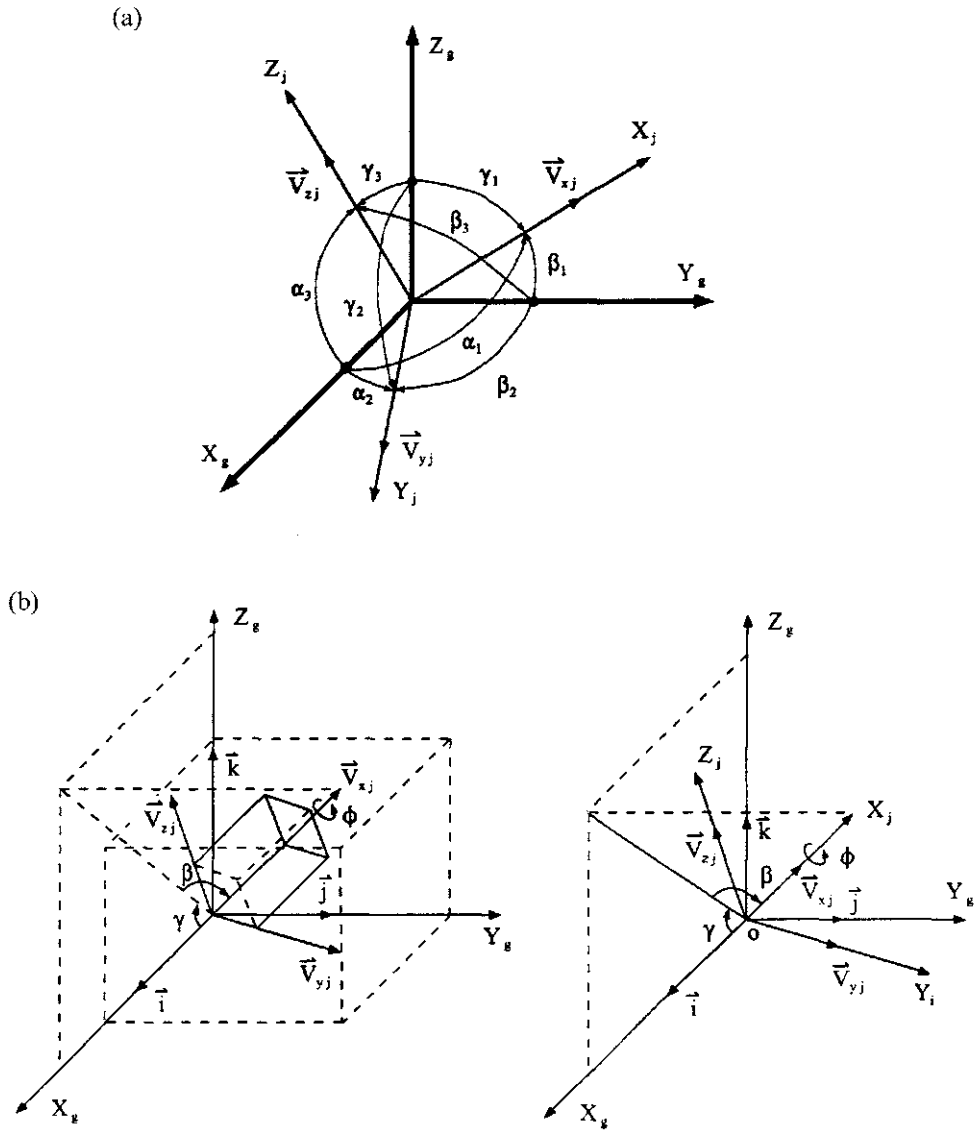


FIG. 8.4 Transformation between JCS and GCS. Angle notation for transformation of (a) Method 1 and (b) Method 2.

Method 1

Let the angles between the GCS and JCS be shown in Fig. 8.5b and let X_j be along line \overline{od} and Y_j along line \overline{oc} ; line then coordinates of point d be $(50, 50, -24)$. Therefore

$$\begin{aligned} \overline{od} &= \sqrt{(50)^2 + (50)^2 + (24)^2} = 74.673 \text{ in} \\ C_{11} &= \cos \alpha_1 = \frac{50}{\overline{od}} = 0.670; \quad C_{12} = \cos \beta_1 = \frac{50}{\overline{od}} = 0.670; \quad C_{13} = \cos \gamma_1 = -\frac{24}{\overline{od}} = -0.321 \end{aligned} \quad (\text{a})$$

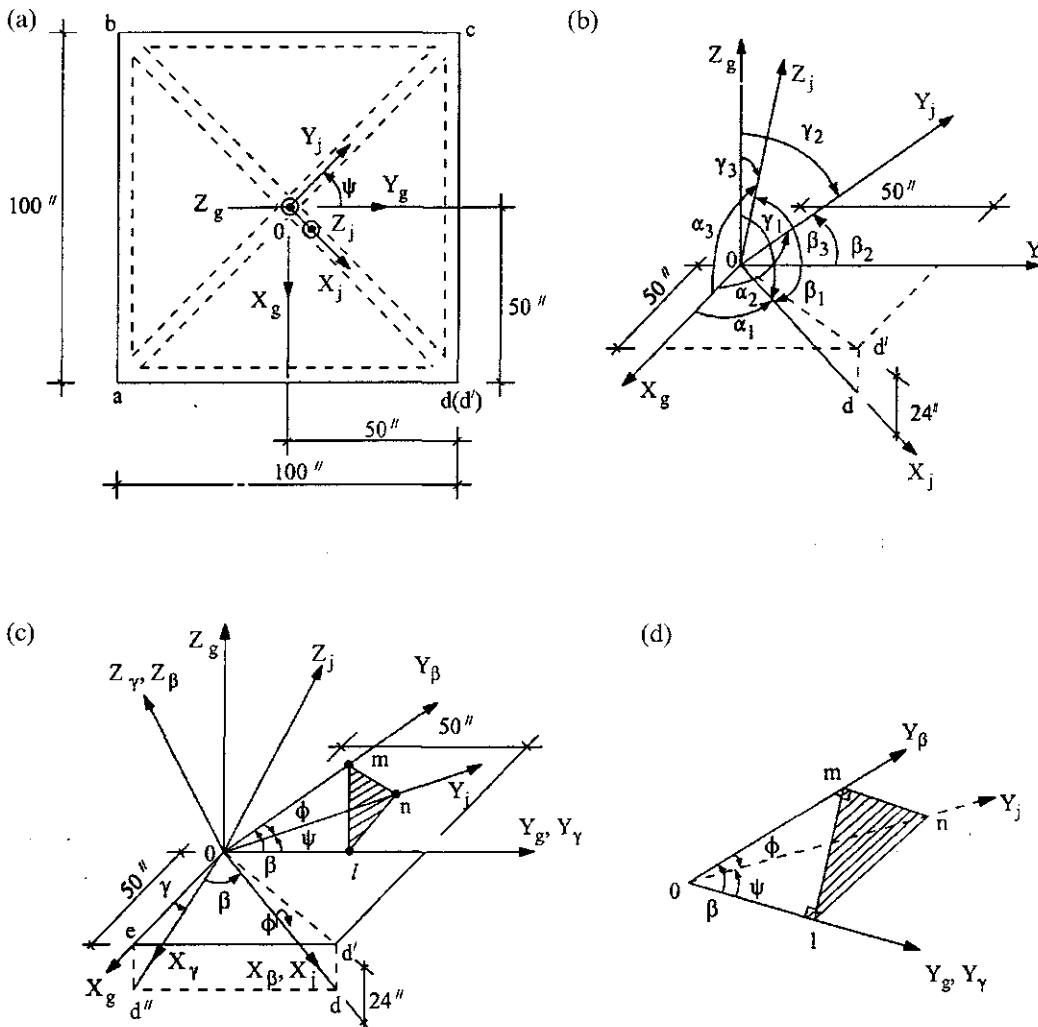


FIG. 8.5 Transformation between JCS and GCS. (a) \$X_g\$-\$Z_g\$. (b) Angles for Method 1. (c) Angles for Method 2. (d) Amplified projection of \$lmn\$.

The coordinates of point \$c\$ are \$(-50, 50, 0)\$; we then have

$$\begin{aligned} \overline{oc} &= \sqrt{(50)^2 + (50)^2 + (0)^2} = 70.711 \text{ in} \\ C_{21} &= \cos \alpha_2 = -\frac{50}{70.711} = -0.707; \quad C_{22} = \cos \beta_2 = \frac{50}{70.711} = 0.707; \\ C_{23} &= \cos \gamma_2 = \frac{0}{70.711} = 0 \end{aligned} \quad \left. \right\} \quad (b)$$

Angles α_3 , β_3 , and γ_3 can be obtained by using a vector cross product as

$$\begin{aligned} Z_j &= X_j \times Y_j = \begin{vmatrix} \vec{i} & \vec{j} & \vec{k} \\ 0.670 & 0.670 & -0.321 \\ -0.707 & 0.707 & 0 \end{vmatrix} \\ &= \begin{vmatrix} 0.670 & -0.321 \\ 0.707 & 0 \end{vmatrix} \vec{i} - \begin{vmatrix} 0.670 & -0.321 \\ -0.707 & 0 \end{vmatrix} \vec{j} + \begin{vmatrix} 0.670 & 0.670 \\ -0.707 & 0.707 \end{vmatrix} \vec{k} \\ &= 0.227 \vec{i} + 0.227 \vec{j} + 0.947 \vec{k} \end{aligned} \quad (c)$$

from which

$$C_{31} = \cos \alpha_3 = 0.227; \quad C_{32} = \cos \beta_3 = 0.227; \quad C_{33} = \cos \gamma_3 = 0.974 \quad (d)$$

Note that the derivation of Eq. (c) is given in Example E-1 in Appendix E. Combining Eqs. (a), (b), and (d) yields numerical values of Eq. (8.1) as

$$[C_j] = \begin{bmatrix} 0.670 & 0.670 & -0.321 \\ -0.707 & 0.707 & 0 \\ 0.227 & 0.227 & 0.947 \end{bmatrix} \quad (e)$$

Method 2

The GCS and JCS relationship for this method is shown in Fig. 8.5c and d, from which we can observe how angles β , ϕ , γ and ψ relate. The relationship among angles β , ϕ , γ , and ψ is determined by the following three steps: (1) proof of right triangle lmn , (2) demonstration of right triangle mlo , and (3) establishment of β , ϕ , and γ relationships.

(1) Assume that point n is an arbitrary point on the Y_j axis. \overline{ol} is the projection of \overline{on} ; therefore $\angle lno$ is a right angle. \overline{om} is the projection of \overline{on} so $\angle nmo$ is a right angle. Since the Y_β axis has rotated an angle β away from the Y_g axis, X_β , Y_β , and Y_g axes are in $X_\beta-Y_g$ plane. Because the X_β axis is perpendicular to the $Y_\beta-Z_\beta$ plane and Y_j rotates an angle ϕ due to the rotation of X_β , Y_j is still on the $Y_\beta-Z_\beta$ plane. In fact, the $X_\beta-Y_\beta$ plane is perpendicular to the $Y_\beta-Z_\beta$ plane; therefore $\angle lmn$ is a right angle.

(2) Now \overline{nl} , \overline{mn} , and \overline{ml} may be expressed as follows:

$$\overline{ml}^2 = \overline{nl}^2 - \overline{mn}^2 = \overline{on}^2 \sin^2 \psi - \overline{on}^2 \sin^2 \phi \quad (f)$$

To show mlo to be a right triangle, let us assume $\angle mlo$ is a right angle. Thus

$$\begin{aligned} \overline{om}^2 - \overline{ol}^2 &= \overline{om}^2 \cos^2 \phi - \overline{on}^2 \cos^2 \psi = \overline{on}^2 (\sin^2 \psi - \sin^2 \phi) \\ &= \overline{ml}^2 \end{aligned} \quad (g)$$

which proves the assumption is correct and \overline{ol} is the projection of \overline{om} .

(3) Relationships for β , ϕ , and ψ can be established as

$$\overline{ol} = \overline{on} \cos \psi; \quad \overline{ol} = \overline{om} \cos \beta = \overline{on} \cos \phi \cos \beta; \quad \overline{on} \cos \psi = \overline{on} \cos \phi \cos \beta$$

Thus

$$\cos \psi = \cos \phi \cos \beta \quad (h)$$

In this problem, \overline{od}'' is the projection of line \overline{od} on the X_g-Z_g plane, and X_γ is in the direction of line \overline{od}'' . Angle γ is

$$\gamma = \sin^{-1} \left(\frac{\overline{ed}''}{\overline{od}} \right) = -25.641^\circ \quad (\text{i})$$

where

$$\overline{ed}'' = \overline{d'd} = -24; \quad \overline{od} = \sqrt{(50)^2 + (50)^2 + (24)^2} = 74.726$$

Since

$$\overline{od}'' = \sqrt{(\overline{oe})^2 + (\overline{ed}'')^2} = \sqrt{(50)^2 + (24)^2} = 55.462$$

we have β between lines \overline{od} and \overline{od}'' as

$$\beta = \cos^{-1} \left(\frac{\overline{od}''}{\overline{od}} \right) = 42.035^\circ \quad (\text{j})$$

Angle ϕ can be determined from Eq. (h), in which ψ is given as 45° ; thus

$$\phi = \cos^{-1} \left(\frac{\cos \psi}{\cos \beta} \right) = \pm 17.824^\circ \quad (\text{k})$$

ϕ should be negative according to the positive-sign definition. Using the angles found in Eqs. (i), (j), and (k) in Eq. (8.1a) yields the same result shown in Eq. (e).

8.4. FORCE TRANSFORMATION BETWEEN SLAVE JOINT AND MASTER JOINT

The deformation of one structural component or element can be very small relative to the deformation of adjacent components or elements. Thus the component or element with small deformation may be idealized as a rigid body. Two joints on the rigid body are *constrained*, such that the deformation of one (called a *slave joint*) can be represented by the deformation of the other (called a *master joint*). Deformation of the slave joint is dependent on that of the master joint, and the d.o.f. for the slave joint can be transferred to the master joint. Consequently, the total d.o.f. in a structure is reduced. The transformation of d.o.f. for both 3D and planar constraints is described below.

Let joint m be the master joint and joint s be the slave joint. Also, let the coordinate orientation of both joints be identical. By definition, these two joints are connected by a rigid body. Thus the forces at the slave joint can be transferred to the master joint, and the displacement of the former can be expressed in terms of the latter. Typical notations are shown in Fig. 8.6 in which F_{js} and M_{js} signify transverse forces and moments at slave joint, respectively; F_{jm} and M_{jm} signify transverse forces and moments at master joint, respectively. For instance, F_{jmx} represents the force at the master joint in the JCS X -direction and M_{jmz} represents the moment at the master joint about the JCS Z -axis. Likewise, F_{jsx} represents the force at the slave joint in the JCS X -direction and M_{jsz} represents the moment at the slave joint about the JCS Z -axis. Summing the forces acting on the slave joint related to the master joint for a 3D rigid body yields

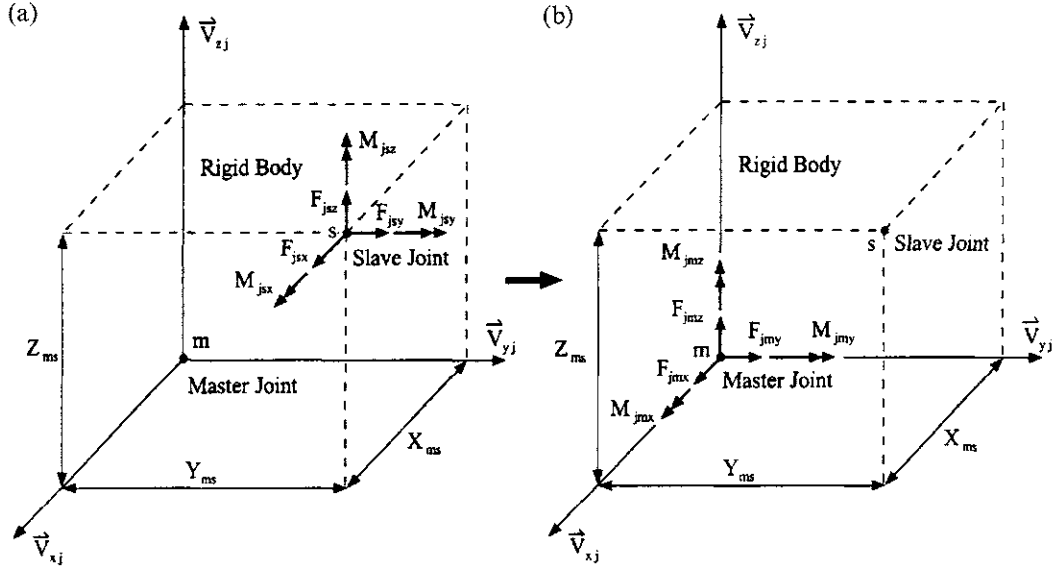


FIG. 8.6 Rigid-Body Constraint. (a) Before transformation. (b) After transformation.

the force transformation

$$\begin{Bmatrix} F_{jm_x} \\ F_{jm_y} \\ F_{jm_z} \\ M_{jm_x} \\ M_{jm_y} \\ M_{jm_z} \end{Bmatrix} = \begin{bmatrix} 1 & 0 & 0 & 0 & 0 & 0 \\ 0 & 1 & 0 & 0 & 0 & 0 \\ 0 & 0 & 1 & 0 & 0 & 0 \\ 0 & -Z_{ms} & Y_{ms} & 1 & 0 & 0 \\ Z_{ms} & 0 & -X_{ms} & 0 & 1 & 0 \\ -Y_{ms} & X_{ms} & 0 & 0 & 0 & 1 \end{bmatrix} \begin{Bmatrix} F_{js_x} \\ F_{js_y} \\ F_{js_z} \\ M_{js_x} \\ M_{js_y} \\ M_{js_z} \end{Bmatrix} \quad (8.2)$$

or

$$\{F_{jm}\} = [T_{ms}]\{F_{js}\} \quad (8.3)$$

where $[T_{ms}]$ is called *constraint matrix* and expresses the relationship between the forces $\{F_{jm}\}$ acting on the master joint and those $\{F_{js}\}$ acting on the slave joint. A similar transformation for displacement (see Section 4.5) can be derived as

$$\{\delta_{jm}\} = [T_{ms}]^T\{\delta_{js}\} \quad (8.4)$$

where $\{\delta_{jm}\}$ represents displacement of the master joint, and $\{\delta_{js}\}$ represents displacement of the slave joint.

In Eq. (8.2) X_{ms} , Y_{ms} , and Z_{ms} are the distance between master joint and slave joint in the JCS. Recall that the joint's coordinates are defined in the GCS. Transferring the coordinates of both joints from GCS into JCS and then subtracting yields

$$\begin{Bmatrix} X_{ms} \\ Y_{ms} \\ Z_{ms} \end{Bmatrix} = [C_j] \begin{Bmatrix} X_{gs} - X_{gm} \\ Y_{gs} - Y_{gm} \\ Z_{gs} - Z_{gm} \end{Bmatrix} \quad (8.5)$$

where X_{gm} represents the global X coordinate of master joint m , and Z_{gs} represents the global Z coordinate of slave joint s . The coordinate relationship between JCS and GCS is shown in Fig. 8.7. The transformation matrix $[C_j]$ is expressed in Eqs. (8.1) and (8.1a).

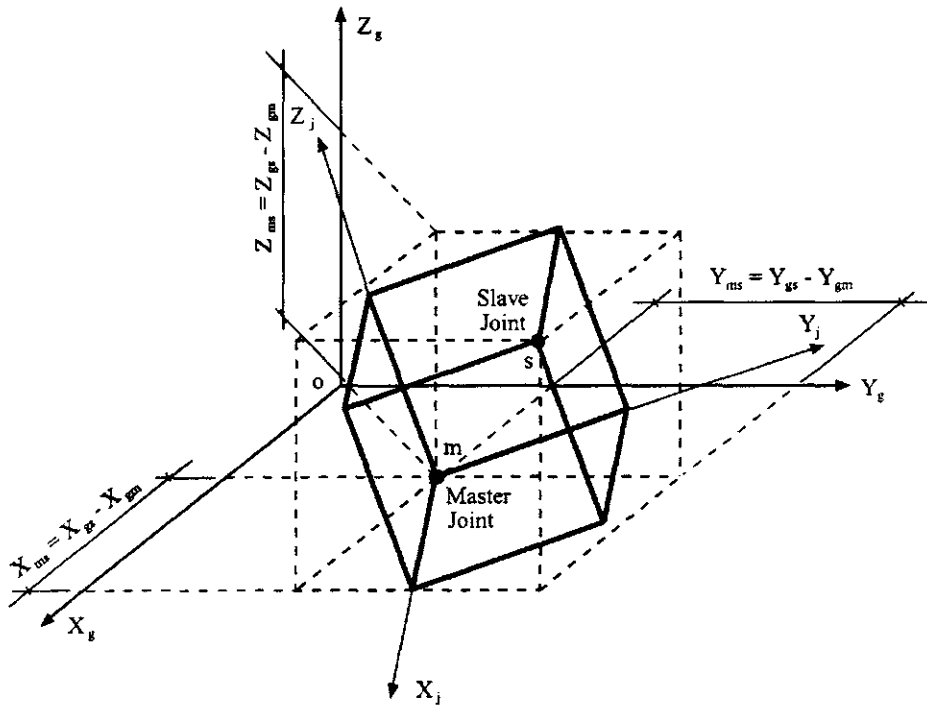


FIG. 8.7 Notations for coordinate transformation.

A slab in a building structure is very stiff in the plane of the floor, but flexible out of the plane. Thus a *planar constraint* is used to treat the floor slab's diaphragm stiffness as a rigid body. Figure 8.8a shows the floor slab's $X_j - Y_j$ plane in which neither moments about the X_j and Y_j axes nor force in the Z_j axis can be transferred from the slave joint to the master joint due to out-of-plane flexibility. Since both master joint and slave joint are structural nodes having d.o.f., the forces not transferable from the slave joint should remain there and be included in structural analysis. Force transformation for Fig. 8.8b can now be expressed as

$$\begin{Bmatrix} F_{jm_x} \\ F_{jm_y} \\ F_{jm_z} \\ M_{jm_x} \\ M_{jm_y} \\ M_{jm_z} \end{Bmatrix} = \begin{bmatrix} 1 & 0 & 0 & 0 & 0 & 0 \\ 0 & 1 & 0 & 0 & 0 & 0 \\ 0 & 0 & 1 & 0 & 0 & 0 \\ 0 & 0 & 0 & 1 & 0 & 0 \\ 0 & 0 & 0 & 0 & 1 & 0 \\ -Y_{ms} & X_{ms} & 0 & 0 & 0 & 1 \end{bmatrix} \begin{Bmatrix} F_{js_x} \\ F_{js_y} \\ F_{js_z} \\ M_{js_x} \\ M_{js_y} \\ M_{js_z} \end{Bmatrix} \quad (8.6)$$

8.5. SYSTEM d.o.f. AS RELATED TO COORDINATE AND FORCE TRANSFORMATION

Global degrees of freedom (global d.o.f.), also known as *structural system d.o.f.* or simply *structural d.o.f.*, represent and describe a structure's motion. The structural system d.o.f. can be defined as: (1) restrained not movable, such as at the support; (2) constrained-movable but needing to be transformed, such as from slave to master; and (3) free (movable) with or without mass lumped at the joint. This d.o.f. classification can be applied to both static and dynamic analyses. For dynamic analysis, free d.o.f. without mass inertia effect can be expressed in terms of d.o.f. associ-

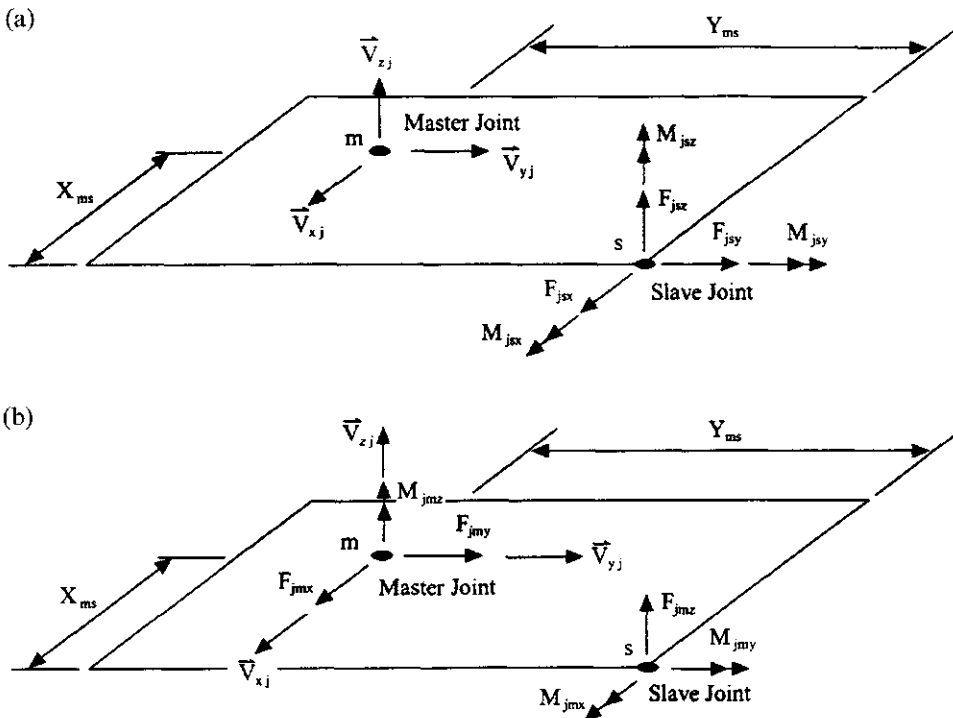


FIG. 8.8 Force transformation of a floor slab. (a) Master and slave joints at floor plane, (b) Force transformation.

ated with the mass inertia effect by elimination or condensation. Once joints are defined and constraints identified, global d.o.f. can be numbered. Global d.o.f. comprise condensed d.o.f. (free d.o.f. without mass), restrained d.o.f., and free d.o.f. (with mass).

EXAMPLE 8.5.1 Formulate a constraint matrix, $[T_{ms}]$, to relate slave joint 6 to master joint 12 as well as slave joint 106 to master joint 111 of the structure shown in Fig. 8.9. For each joint, the JCS has the same direction as the GCS. The $X-Y$ planar constraint is assumed for each slab, and each slab's mass center (MC) is assumed to be a master joint such as 11, 12, and 111. The assigned joint numbers are shown in the same figure. For convenience, joints are numbered 1–100 starting at the top floor; moving downward, each floor has its nodal number increased by 100.

Solution: From Eq. (8.5), the distance from slave joint 6 to master joint 12 is

$$\begin{Bmatrix} X_{ms} \\ Y_{ms} \\ Z_{ms} \end{Bmatrix} = [C_j] \begin{Bmatrix} X_{gs} - X_{gm} \\ Y_{gs} - Y_{gm} \\ Z_{gs} - Z_{gm} \end{Bmatrix} = \begin{bmatrix} 1 & 0 & 0 \\ 0 & 1 & 0 \\ 0 & 0 & 1 \end{bmatrix} \begin{Bmatrix} 480 - 400 \\ 0 - 80 \\ 320 - 320 \end{Bmatrix} = \begin{Bmatrix} 80 \\ -80 \\ 0 \end{Bmatrix} \quad (a)$$

Note that the GCS and JCS are the same for this problem; no transformation is needed and $[C_j]$ of Eq. (8.1) or Eq. (8.1a) becomes an identity matrix. Thus the transformation for $m=12$ and $s=6$

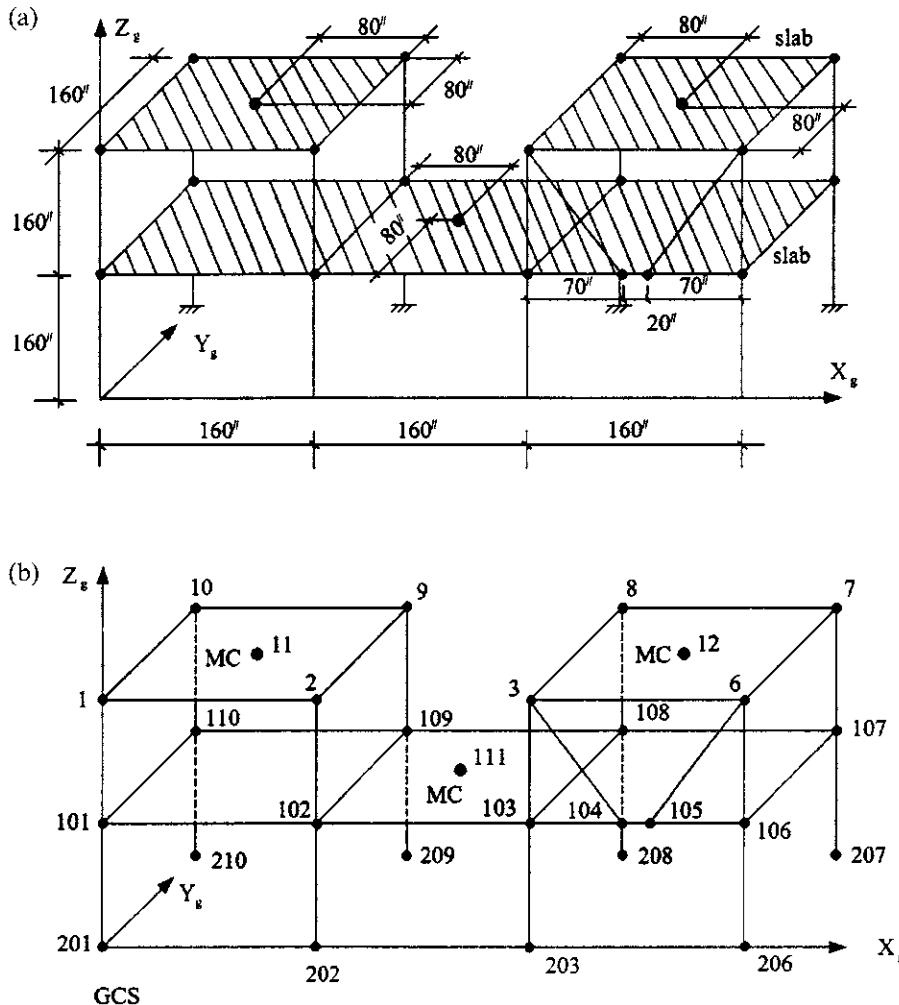


FIG. 8.9 Two-story building. (a) Configuration of two-story buildings. (b) Joint numbers.

can be obtained from Eq. (8.6) as

$$\{F_{jm}\} = \begin{Bmatrix} F_{jm_x} \\ F_{jm_y} \\ F_{jm_z} \\ M_{jm_x} \\ M_{jm_y} \\ M_{jm_z} \end{Bmatrix} = \begin{bmatrix} 1 & 0 & 0 & 0 & 0 & 0 \\ 0 & 1 & 0 & 0 & 0 & 0 \\ 0 & 0 & 1 & 0 & 0 & 0 \\ 0 & 0 & 0 & 1 & 0 & 0 \\ 0 & 0 & 0 & 0 & 1 & 0 \\ 80 & 80 & 0 & 0 & 0 & 1 \end{bmatrix} \begin{Bmatrix} F_{js_x} \\ F_{js_y} \\ F_{js_z} \\ M_{js_x} \\ M_{js_y} \\ M_{js_z} \end{Bmatrix} = [T_{ms}] \{F_{js}\} \quad (b)$$

in which F_{jm_z} , M_{jm_x} , and M_{jm_y} are independent forces at joint 6 (which is also a structural node), since they cannot be transferred to master joint 12. Similarly, slave joint 106 and master joint 111 have the following relationship:

$$\begin{Bmatrix} X_{ms} \\ Y_{ms} \\ Z_{ms} \end{Bmatrix} = \begin{bmatrix} 1 & 0 & 0 \\ 0 & 1 & 0 \\ 0 & 0 & 1 \end{bmatrix} \begin{Bmatrix} 480-240 \\ 0-80 \\ 160-160 \end{Bmatrix} = \begin{Bmatrix} 240 \\ -80 \\ 0 \end{Bmatrix} \quad (c)$$

$$\{F_{jm}\} = \begin{bmatrix} 1 & 0 & 0 & 0 & 0 & 0 \\ 0 & 1 & 0 & 0 & 0 & 0 \\ 0 & 0 & 1 & 0 & 0 & 0 \\ 0 & 0 & 0 & 1 & 0 & 0 \\ 0 & 0 & 0 & 0 & 1 & 0 \\ 80 & 240 & 0 & 0 & 0 & 1 \end{bmatrix} \{F_{js}\} = [T_{ms}] \{F_{js}\} \quad (d)$$

8.6. BEAM-COLUMNS

8.6.1. Coordinate Transformation between ECS and JCS or GCS: Methods 1 and 2

8.6.1.1. Method 1

A typical beam-column element (see Fig. 8.10) has two joints, *start-joint A* and *end-joint B*. This element has three axes, X_e , Y_e , and Z_e , and can exhibit bending about the Y_e and Z_e axes, torsion about the X_e axis, and axial deformation along the X_e axis. Depending on structural modeling, some deformations may be neglected with consideration of a constrained condition. For instance, an element attached to a rigid plane slab in the X_e-Z_e plane should have neither axial deformation in the X_e axis nor bending about the Y_e -axis. Stiffness of the element can be elastic and/or inelastic. Elastic stiffness is discussed in Section 8.6.2 and inelastic in Chapter 9.

Let X_{gs} , Y_{gs} , and Z_{gs} be the coordinates of *start-joint A*, and X_{ge} , Y_{ge} , Z_{ge} be the coordinates of *end-joint B*. The distance between *A* and *B* is

$$D_{se} = \sqrt{(X_{ge} - X_{gs})^2 + (Y_{ge} - Y_{gs})^2 + (Z_{ge} - Z_{gs})^2} \quad (8.7)$$

Define \vec{V}_x as a unit vector from start-joint to end-joint in GCS:

$$\vec{V}_x = \frac{(X_{ge} - X_{gs})\vec{i} + (Y_{ge} - Y_{gs})\vec{j} + (Z_{ge} - Z_{gs})\vec{k}}{D_{se}} \quad (8.8)$$

Note that the GCS and JCS coincide, so designated for convenience. Vector \vec{V}_x defines the orientation of the element's local X_e axis. Choose vector \vec{V}_{xy} such that \vec{V}_x and \vec{V}_{xy} both lie on the element's local X_e-Y_e plane. For a girder, the local X_e-Y_e plane is usually defined in

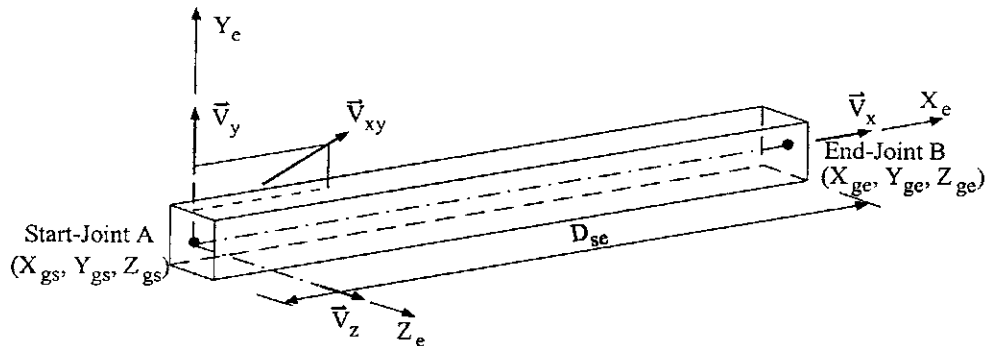


FIG. 8.10 ECS of beam-column element.

the plane of the web. Thus

$$\vec{V}_z = \frac{\vec{V}_x \times \vec{V}_{xy}}{|\vec{V}_{xy}|} \quad (8.9)$$

and

$$\vec{V}_y = \vec{V}_z \times \vec{V}_x \quad (8.10)$$

where \vec{V}_y and \vec{V}_z are unit vectors which define the orientation of the element's local Y_e and Z_e axes, respectively (see Appendix F).

Unit vectors \vec{V}_x , \vec{V}_y , and \vec{V}_z define the *element coordinate system* (ECS), denoted by X_e , Y_e , Z_e , with its origin at joint A. Those three unit vectors, defining the orientation of the ECS, are written in matrix form as

$$\{V_e\} = \begin{Bmatrix} \vec{V}_x \\ \vec{V}_y \\ \vec{V}_z \end{Bmatrix} = \begin{bmatrix} C_{11} & C_{12} & C_{13} \\ C_{21} & C_{22} & C_{23} \\ C_{31} & C_{32} & C_{33} \end{bmatrix} \begin{Bmatrix} \vec{i} \\ \vec{j} \\ \vec{k} \end{Bmatrix} = [C_e] \begin{Bmatrix} \vec{i} \\ \vec{j} \\ \vec{k} \end{Bmatrix} \quad (8.11)$$

where $[C_e]$ is a direction cosine matrix for ECS; \vec{i} , \vec{j} , and \vec{k} are unit vectors in the GCS.

To determine the transformation matrix in Eq. (8.11), coordinates of a member at four points, A, B, m, and n, are needed (see Fig. 8.11). Points A and B are used to compute unit vector \vec{V}_x in Eq. 8.11 where Aa is on the X_g-Z_g plane with angle γ between the Aa and X_g axis; Aa and AB are on the same plane with angle β ; α_1 , β_1 , and γ_1 are for direction cosines ($\cos \alpha_1$, $\cos \beta_1$, $\cos \gamma_1$) of vector \vec{V}_x ; m and n are used to determine unit vector \vec{V}_z along Z_e direction in Eq. (8.12). Unit vector \vec{V}_y along the Y_e direction is then determined in Eq. (8.10).

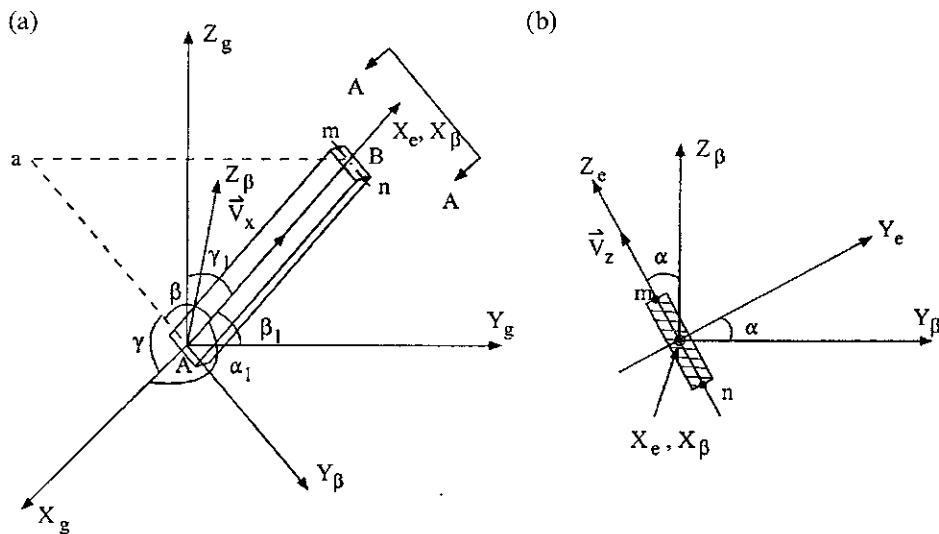


FIG. 8.11 Member orientation relative to GCS.

8.6.1.2. Method 2

Sometimes the input for a computer program requires only coordinates A and B along with angle α of the member's web relative to Z_β (see Fig. 8.11b). Coordinates A and B define the member's location in GCS; angle α depicts the orientation of the member's web in the ECS. Then the derivation of the element's transformation matrix is similar to Eq. (8.1a), applicable to both JCS vs GCS and ECS vs GCS.

The relationship between GCS and ECS may be expressed as

$$\begin{Bmatrix} \vec{V}_x \\ \vec{V}_y \\ \vec{V}_z \end{Bmatrix} = [C_e] \begin{Bmatrix} \vec{i} \\ \vec{j} \\ \vec{k} \end{Bmatrix}$$

in which

$$[C_e] = \begin{bmatrix} c_x & c_y & c_z \\ -\frac{1}{m}(c_x c_y \cos \alpha + c_z \sin \alpha) & m \cos \alpha & \frac{1}{m}(c_x \sin \alpha - c_y c_z \cos \alpha) \\ \frac{1}{m}(c_x c_y \sin \alpha - c_z \cos \alpha) & -m \sin \alpha & \frac{1}{m}(c_y c_z \sin \alpha + c_x \cos \alpha) \end{bmatrix} \quad (8.12)$$

$$\cos \alpha_1 = c_x = \frac{X_{ge} - X_{gs}}{D_{se}} \quad (8.13)$$

$$\cos \beta_1 = c_y = \frac{Y_{ge} - Y_{gs}}{D_{se}} \quad (8.14)$$

$$\cos \gamma_1 = c_z = \frac{Z_{ge} - Z_{gs}}{D_{se}} \quad (8.15)$$

$$m = \sqrt{c_x^2 + c_z^2} \quad (8.16)$$

Appendix E gives a detailed derivation of Eq. (8.12).

8.6.2. Beam-Column Stiffness in the ECS

Figure 8.12 shows a beam-column element which has 12 d.o.f., three translational and three rotational at each end. In matrix form, local forces $\{F_e\}$ and displacements $\{\delta_e\}$ in the ECS are

$$\{F_e\} = [F_{xa} \ F_{ya} \ F_{za} \ M_{xa} \ M_{ya} \ M_{za} \ F_{xb} \ F_{yb} \ F_{zb} \ M_{xb} \ M_{yb} \ M_{zb}]^T \quad (8.17)$$

$$\{\delta_e\} = [\delta_{xa} \ \delta_{ya} \ \delta_{za} \ \theta_{xa} \ \theta_{ya} \ \theta_{za} \ \delta_{xb} \ \delta_{yb} \ \delta_{zb} \ \theta_{xb} \ \theta_{yb} \ \theta_{zb}]^T \quad (8.18)$$

The stiffness matrix of a beam-column element corresponding to \vec{V}_y and \vec{V}_z directions can be expressed as

$$\begin{Bmatrix} M_{ya} \\ M_{yb} \end{Bmatrix} = \begin{bmatrix} B & D \\ D & B \end{bmatrix} \begin{Bmatrix} \theta_{ya} \\ \theta_{yb} \end{Bmatrix} \quad (8.19)$$

and

$$\begin{Bmatrix} M_{za} \\ M_{zb} \end{Bmatrix} = \begin{bmatrix} A & C \\ C & A \end{bmatrix} \begin{Bmatrix} \theta_{za} \\ \theta_{zb} \end{Bmatrix} \quad (8.20)$$

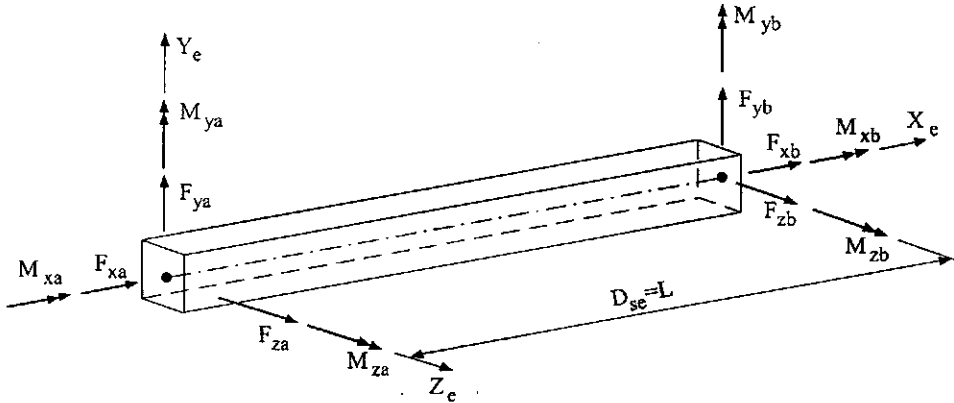


FIG. 8.12 Element's local d.o.f.

in which

$$\begin{aligned} B &= \frac{4EI_y}{L}; & D &= \frac{2EI_y}{L} \\ A &= \frac{4EI_z}{L}; & C &= \frac{2EI_z}{L} \end{aligned}$$

where I and E are the cross section's moment of inertia and modulus of elasticity, respectively; θ_{ya} and θ_{yb} represent rotations in the \vec{V}_y direction, and θ_{za} and θ_{zb} represent those in the \vec{V}_z direction (see Fig. 8.12). The torsional stiffness is

$$\begin{Bmatrix} M_{xa} \\ M_{xb} \end{Bmatrix} = \frac{JG}{L} \begin{bmatrix} 1 & -1 \\ -1 & 1 \end{bmatrix} \begin{Bmatrix} \theta_{xa} \\ \theta_{xb} \end{Bmatrix} = \begin{bmatrix} Q & -Q \\ -Q & Q \end{bmatrix} \begin{Bmatrix} \theta_{xa} \\ \theta_{xb} \end{Bmatrix} \quad (8.21)$$

where J is the cross section's polar moment of inertia and G is the shear modulus of elasticity. The axial stiffness is

$$\begin{Bmatrix} F_{xa} \\ F_{xb} \end{Bmatrix} = \frac{EA}{L} \begin{bmatrix} 1 & -1 \\ -1 & 1 \end{bmatrix} \begin{Bmatrix} \delta_{xa} \\ \delta_{xb} \end{Bmatrix} = \begin{bmatrix} H & -H \\ -H & H \end{bmatrix} \begin{Bmatrix} \delta_{xa} \\ \delta_{xb} \end{Bmatrix} \quad (8.22)$$

where A is the cross-sectional area. Combining the stiffness terms of Eqs. (8.19)–(8.22) yields the local element stiffness matrix

$$\begin{Bmatrix} F_{xa} \\ M_{xa} \\ M_{ya} \\ M_{za} \\ F_{xb} \\ M_{xb} \\ M_{yb} \\ M_{zb} \end{Bmatrix} = \begin{bmatrix} H & 0 & 0 & 0 & -H & 0 & 0 & 0 \\ 0 & Q & 0 & 0 & 0 & -Q & 0 & 0 \\ 0 & 0 & B & 0 & 0 & 0 & D & 0 \\ 0 & 0 & 0 & A & 0 & 0 & 0 & C \\ -H & 0 & 0 & 0 & H & 0 & 0 & 0 \\ 0 & -Q & 0 & 0 & 0 & Q & 0 & 0 \\ 0 & 0 & D & 0 & 0 & 0 & B & 0 \\ 0 & 0 & 0 & C & 0 & 0 & 0 & A \end{bmatrix} \begin{Bmatrix} \delta_{xa} \\ \theta_{xa} \\ \theta_{ya} \\ \theta_{za} \\ \delta_{xb} \\ \theta_{xb} \\ \theta_{yb} \\ \theta_{zb} \end{Bmatrix} \quad (8.23)$$

or

$$\{\bar{F}\} = [S_I] \{\bar{\delta}\} \quad (8.24)$$

As Fig. 8.12 illustrates, the following relationships can be derived by summing moments at ends A

and B :

$$\begin{aligned} \sum M_{yA} &= 0 = M_{ya} + M_{yb} - F_{zb}L \\ F_{zb} &= \frac{M_{ya} + M_{yb}}{L} \end{aligned} \quad (8.25)$$

$$\begin{aligned} \sum M_{yB} &= 0 = M_{ya} + M_{yb} + F_{za}L \\ F_{za} &= \frac{-M_{ya} - M_{yb}}{L} \end{aligned} \quad (8.26)$$

$$\begin{aligned} \sum M_{zA} &= 0 = M_{za} + M_{zb} + F_{yb}L \\ F_{yb} &= \frac{-M_{za} - M_{zb}}{L} \end{aligned} \quad (8.27)$$

$$\begin{aligned} \sum M_{zB} &= 0 = M_{za} + M_{zb} - F_{ya}L \\ F_{ya} &= \frac{M_{za} + M_{zb}}{L} \end{aligned} \quad (8.28)$$

Rewriting Eqs. (8.25)–(8.28) in matrix form yields

$$\{F_e\} = \left\{ \begin{array}{c} F_{xa} \\ F_{ya} \\ F_{za} \\ M_{xa} \\ M_{ya} \\ M_{za} \\ F_{xb} \\ F_{yb} \\ F_{zb} \\ M_{xb} \\ M_{yb} \\ M_{zb} \end{array} \right\} = \frac{1}{L} \left[\begin{array}{ccccccc} L & 0 & 0 & 0 & 0 & 0 & 0 \\ 0 & 0 & 0 & 1 & 0 & 0 & 0 \\ 0 & 0 & -1 & 0 & 0 & 0 & -1 \\ 0 & L & 0 & 0 & 0 & 0 & 0 \\ 0 & 0 & L & 0 & 0 & 0 & 0 \\ 0 & 0 & 0 & L & 0 & 0 & 0 \\ 0 & 0 & 0 & 0 & L & 0 & 0 \\ 0 & 0 & 0 & -1 & 0 & 0 & 0 \\ 0 & 0 & 1 & 0 & 0 & 0 & 1 \\ 0 & 0 & 0 & 0 & 0 & L & 0 \\ 0 & 0 & 0 & 0 & 0 & 0 & L \end{array} \right] \left\{ \begin{array}{c} F_{xa} \\ M_{xa} \\ M_{ya} \\ M_{za} \\ F_{xb} \\ M_{xb} \\ M_{yb} \\ M_{zb} \end{array} \right\} = [A_e] \left\{ \begin{array}{c} F_{xa} \\ M_{xa} \\ M_{ya} \\ M_{za} \\ F_{xb} \\ M_{xb} \\ M_{yb} \\ M_{zb} \end{array} \right\} \quad (8.29)$$

Substituting Eq. (8.24) in Eq. (8.29) leads to

$$\{F_e\} = [A_e][S_I][A_e]^T\{\delta_e\} = [K_e]\{\delta_e\} \quad (8.30)$$

where $\{\delta_e\} = \{\delta_{xa} \ \delta_{ya} \ \delta_{za} \ \theta_{xa} \ \theta_{ya} \ \theta_{za} \ \delta_{xb} \ \delta_{yb} \ \delta_{zb} \ \theta_{xb} \ \theta_{yb} \ \theta_{zb}\}^T$ [see Eq. (8.18)]. The basis for using transpose matrix $[A_e]^T$ was established in Section 4.5.4 and shown in Eq. (4.54). Thus the beam–column element's stiffness in ECS takes the form

$$[K_e] = \left[\begin{array}{cccccccccc} H & 0 & 0 & 0 & 0 & 0 & -H & 0 & 0 & 0 & 0 & 0 \\ S_{22} & 0 & 0 & 0 & S_{26} & 0 & -S_{22} & 0 & 0 & 0 & 0 & S_{26} \\ S_{33} & 0 & -S_{35} & 0 & 0 & 0 & -S_{33} & 0 & 0 & -S_{35} & 0 & 0 \\ Q & 0 & 0 & 0 & 0 & 0 & 0 & -Q & 0 & 0 & 0 & 0 \\ B & 0 & 0 & 0 & 0 & S_{35} & 0 & D & 0 & 0 & 0 & 0 \\ & & & A & 0 & -S_{26} & 0 & 0 & 0 & C & 0 & 0 \\ & & & H & 0 & 0 & 0 & 0 & 0 & 0 & 0 & 0 \\ & & & S_{22} & 0 & 0 & 0 & 0 & -S_{26} & 0 & 0 & 0 \\ & & & S_{33} & 0 & 0 & S_{35} & 0 & 0 & 0 & 0 & 0 \\ & & & Q & 0 & 0 & 0 & 0 & 0 & 0 & 0 & 0 \\ & & & B & 0 & 0 & 0 & 0 & 0 & 0 & 0 & 0 \\ & & & & & & & & & & A & 0 \end{array} \right] \text{ symm} \quad (8.31)$$

where

$$S_{22} = \frac{2(A + C)}{L^2} \quad (8.32)$$

$$S_{26} = \frac{A + C}{L} \quad (8.33)$$

$$S_{33} = \frac{2(B + D)}{L^2} \quad (8.34)$$

$$S_{35} = \frac{B + D}{L} \quad (8.35)$$

8.6.3. Beam-Column Stiffness in the JCS or GCS Based on Method 1

Transformation of d.o.f. from ECS to GCS consists of two steps. First, the d.o.f. at each of the two joints (*A* and *B*) are rotated from ECS to GCS and then to JCS. For simplicity, let GCS and JCS coincide. Second, the constraint transformation moves d.o.f. from each of the slave joints to the corresponding master joints in GCS.

In step one, the transformation between global forces and element forces in ECS is expressed as

$$\{F_e\} = \begin{bmatrix} [C_e]_A & 0 & 0 & 0 \\ 0 & [C_e]_A & 0 & 0 \\ 0 & 0 & [C_e]_B & 0 \\ 0 & 0 & 0 & [C_e]_B \end{bmatrix} \{F_g\} = [\bar{C}_e] \{F_g\} \quad (8.36)$$

where $[C_e]$ is shown in Eq. (8.11); $\{F_e\} = [F_{xa} \ F_{ya} \ F_{za} \ M_{xa} \ M_{ya} \ M_{za} \ F_{xb} \ F_{yb} \ F_{zb} \ M_{xb} \ M_{yb} \ M_{zb}]^T$ comprises the element forces in ECS shown in Eq. (8.29); $\{F_g\}$ represents the same forces in GCS; and $[C_e]$ is the direction cosine matrix of ECS. Rotating the element forces, $\{F_e\}$, to global forces, $\{F_g\}$, is achieved by

$$\{F_g\} = [\bar{C}_e]^T \{F_e\} \quad (8.37)$$

and rotating the global forces to joint forces, $\{F_j\}$, by

$$\{F_j\} = \begin{bmatrix} [C_j]_A & 0 & 0 & 0 \\ 0 & [C_j]_A & 0 & 0 \\ 0 & 0 & [C_j]_B & 0 \\ 0 & 0 & 0 & [C_j]_B \end{bmatrix} \{F_g\} = [\bar{C}_j] \{F_g\} \quad (8.38)$$

where $[C_j]$ is defined in Eq. (8.1). Substituting Eq. (8.37) into (8.38) leads to

$$\{F_j\} = [\bar{C}_j] [\bar{C}_e]^T \{F_e\} \quad (8.39)$$

In step two of constraint transformation for each joint of a rigid in-plane but flexible out-of-plane floor model, horizontal forces and torsion must be transferred from the slave joint to the master joint. Let $[T_{ms}]_A$ and $[T_{ms}]_B$ be the constraint transformation, as shown in Eq. (8.6), for joints *A* and *B*, respectively. Forces acting on the master joints, $\{F_{jm}\}$, can be expressed as

$$\{F_{jm}\} = \begin{bmatrix} [T_{ms}]_A & 0 \\ 0 & [T_{ms}]_B \end{bmatrix} \{F_j\} = [\bar{T}_{ms}] \{F_j\} \quad (8.40)$$

If constraints are not present, this transformation matrix $[\bar{T}_{ms}]$ reduces to an identity matrix. Combining Eqs. (8.39) and (8.40) yields the transformation from element forces, $\{F_e\}$, to forces acting on the master joints as

$$\{F_{jm}\} = [\bar{T}_{ms}] [\bar{C}_j] [\bar{C}_e]^T \{F_e\} = [A] \{F_e\} \quad (8.41)$$

Similarly, transformation for the deformation (see Section 4.5.4) is given by

$$\{\delta_e\} = [A]^T \{\delta_{jm}\} \quad (8.42)$$

The stiffness matrix of the i th member is then transformed from ECS to JCS as

$$[K^i] = [A] [K_e] [A]^T \quad (8.43)$$

If the JCS and GCS are assumed to coincide, then $[\bar{C}_j]$ in Eq. (8.38) becomes an identity matrix and $[K^i]$ shown above represents the transformation from ECS to GCS. Note that the forces that cannot be transferred from slave joint to MC stay at the joint. Thus a slave joint has a dual role, serving as master joint for those forces not transferable.

EXAMPLE 8.6.1 Assume that the structure in Example 8.5.1 has the following properties: columns are box sections $15 \times 13 \times 0.5$ in; bracing members are $W 8 \times 67$; and beams are $W 12 \times 26$. Cross-sectional properties of columns, beams, and bracing members, as well as their ECS, are shown in Fig. 8.13a. Member numbers of the system are given in Fig. 8.13b. Find the element stiffness matrix, $[K^{11}]$, of member 11 corresponding to global d.o.f.

Solution: For member 11, global coordinates at the starting point and end point are

$$(X_{gs}, Y_{gs}, Z_{gs}) = (480, 0, 160) \quad (a)$$

$$(X_{ge}, Y_{ge}, Z_{ge}) = (480, 0, 320) \quad (b)$$

From Eqs. (8.7) and (8.8)

$$D_{se} = \sqrt{(X_{ge} - X_{gs})^2 + (Y_{ge} - Y_{gs})^2 + (Z_{ge} - Z_{gs})^2} = 160 \quad (c)$$

$$\vec{V}_x = \frac{(X_{ge} - X_{gs})\vec{i} + (Y_{ge} - Y_{gs})\vec{j} + (Z_{ge} - Z_{gs})\vec{k}}{D_{se}} = 0\vec{i} + 0\vec{j} + \vec{k} \quad (d)$$

As shown in Example E-1 of Appendix E, we may choose a vector $\vec{V}_{xy} = 1\vec{i} + 0\vec{j} + 0\vec{k}$; then

$$\vec{V}_z = \frac{\vec{V}_x \times \vec{V}_{xy}}{|\vec{V}_{xy}|} = \vec{V}_x \times \vec{V}_{xy} = \begin{vmatrix} \vec{i} & \vec{j} & \vec{k} \\ 0 & 0 & 1 \\ 1 & 0 & 0 \end{vmatrix} = 0\vec{i} + \vec{j} + 0\vec{k} \quad (e)$$

$$\vec{V}_y = \vec{V}_z \times \vec{V}_x = \begin{vmatrix} \vec{i} & \vec{j} & \vec{k} \\ 0 & 1 & 0 \\ 0 & 0 & 1 \end{vmatrix} = \vec{i} + 0\vec{j} + 0\vec{k} \quad (f)$$

From Eq. (8.11), the orientation of ECS in GCS can be expressed as

$$\{\vec{V}_e\} = \begin{Bmatrix} \vec{V}_x \\ \vec{V}_y \\ \vec{V}_z \end{Bmatrix} = \begin{bmatrix} 0 & 0 & 1 \\ 1 & 0 & 0 \\ 0 & 1 & 0 \end{bmatrix} \begin{Bmatrix} \vec{i} \\ \vec{j} \\ \vec{k} \end{Bmatrix} = [C_e] \begin{Bmatrix} \vec{i} \\ \vec{j} \\ \vec{k} \end{Bmatrix} \quad (g)$$

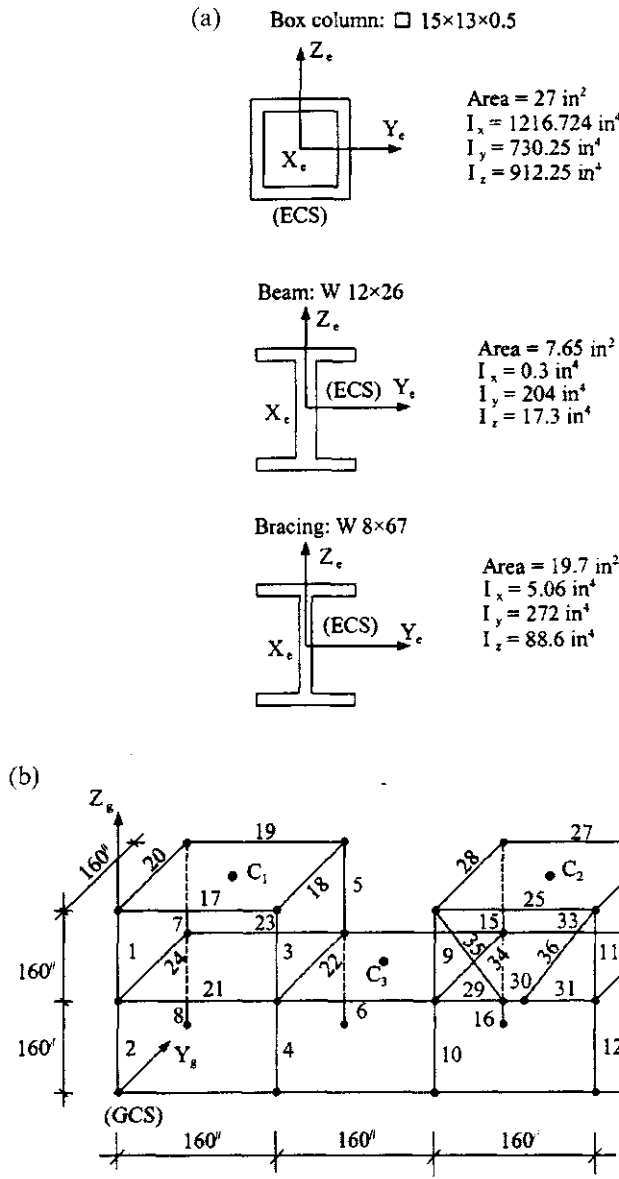


FIG. 8.13 Two-story building. (a) Element properties and ECS. (b) Member numbers.

Furthermore, from Eq. (8.41)

$$[A] = \{\bar{T}_{ms}\} [\bar{C}_j] [\bar{C}_e]^T \quad (h)$$

in which

$$[\bar{C}_e]^T = \begin{bmatrix} [C_e]^T_A & 0 & 0 & 0 \\ 0 & [C_e]^T_A & 0 & 0 \\ 0 & 0 & [C_e]^T_B & 0 \\ 0 & 0 & 0 & [C_e]^T_B \end{bmatrix} \quad (i)$$

$$[\bar{C}_j] = \begin{bmatrix} [C_j]_A & 0 & 0 & 0 \\ 0 & [C_j]_A & 0 & 0 \\ 0 & 0 & [C_j]_B & 0 \\ 0 & 0 & 0 & [C_j]_B \end{bmatrix} \quad (j)$$

$$[\bar{T}_{ms}] = \begin{bmatrix} [T_{ms}]_A & 0 \\ 0 & [T_{ms}]_B \end{bmatrix} \quad (k)$$

where $[T_{ms}]$ is shown in Eq. (8.11). For joint A , $Y_{ms} = Y_{gs} - Y_{gm} = -80$, $X_{ms} = X_{gs} - X_{gm} = 480 - 240 = 240$; for joint B , $Y_{ms} = -80$ and $X_{ms} = 80$. Thus numerical values for Eqs. (i), (j), and (k) are

$$[\bar{C}_j] = \begin{bmatrix} \diagdown & & \\ & I & \\ & & \diagdown \end{bmatrix} \quad (l)$$

$$[C_e]^T_A = [C_e]^T_B = \begin{bmatrix} 0 & 0 & 1 \\ 1 & 0 & 0 \\ 0 & 1 & 0 \end{bmatrix}^T \quad (m)$$

$$[T_{ms}]_A = \begin{bmatrix} 1 & 0 & 0 & 0 & 0 & 0 \\ 0 & 1 & 0 & 0 & 0 & 0 \\ 0 & 0 & 1 & 0 & 0 & 0 \\ 0 & 0 & 0 & 1 & 0 & 0 \\ 0 & 0 & 0 & 0 & 1 & 0 \\ 80 & 240 & 0 & 0 & 0 & 1 \end{bmatrix} \quad (n)$$

$$[T_{ms}]_B = \begin{bmatrix} 1 & 0 & 0 & 0 & 0 & 0 \\ 0 & 1 & 0 & 0 & 0 & 0 \\ 0 & 0 & 1 & 0 & 0 & 0 \\ 0 & 0 & 0 & 1 & 0 & 0 \\ 0 & 0 & 0 & 0 & 1 & 0 \\ 80 & 80 & 0 & 0 & 0 & 1 \end{bmatrix} \quad (o)$$

After substitution, Eq. (h) yields

$$[A] = \left[\begin{array}{cccccc|ccccccccc} 0 & 1 & 0 & 0 & 0 & 0 & | & 0 & 0 & 0 & 0 & 0 & 0 & 0 & 0 \\ 0 & 0 & 1 & 0 & 0 & 0 & | & 0 & 0 & 0 & 0 & 0 & 0 & 0 & 0 \\ 1 & 0 & 0 & 0 & 0 & 0 & | & 0 & 0 & 0 & 0 & 0 & 0 & 0 & 0 \\ 0 & 0 & 0 & 0 & 1 & 0 & | & 0 & 0 & 0 & 0 & 0 & 0 & 0 & 0 \\ 0 & 0 & 0 & 0 & 0 & 1 & | & 0 & 0 & 0 & 0 & 0 & 0 & 0 & 0 \\ 0 & 80 & 240 & 1 & 0 & 0 & | & 0 & 0 & 0 & 0 & 0 & 0 & 0 & 0 \\ \hline 0 & 0 & 0 & 0 & 0 & 0 & | & 0 & 1 & 0 & 0 & 0 & 0 & 0 & 0 \\ 0 & 0 & 0 & 0 & 0 & 0 & | & 0 & 0 & 1 & 0 & 0 & 0 & 0 & 0 \\ 0 & 0 & 0 & 0 & 0 & 0 & | & 1 & 0 & 0 & 0 & 0 & 0 & 0 & 0 \\ 0 & 0 & 0 & 0 & 0 & 0 & | & 0 & 0 & 0 & 0 & 0 & 1 & 0 & 0 \\ 0 & 0 & 0 & 0 & 0 & 0 & | & 0 & 0 & 0 & 0 & 0 & 0 & 0 & 1 \\ 0 & 0 & 0 & 0 & 0 & 0 & | & 0 & 80 & 80 & 1 & 0 & 0 & 0 & 0 \end{array} \right] \quad (p)$$

From Eqs. (8.23) and (8.31), the element stiffness matrix has the following coefficients:

$$\begin{aligned}
 H &= \frac{AE}{L} = (27)29000/160 = 4893.75 \\
 B &= \frac{4EI_y}{L} = (4)(29000)730.25/160 = 529,431.25 \\
 D &= \frac{B}{2} = 264,715.625; \quad A = \frac{4EI_z}{L} = (4)(29000)912.25/160 = 661,381.25 \\
 C &= \frac{A}{2} = 330,690.625; \quad Q = \frac{GJ}{L} = (13000)1216.7/160 = 98,858.865 \\
 S_{22} &= \frac{2(A+C)}{L^2} = 77.505; \quad S_{26} = \frac{A+C}{L} = 6200.449 \\
 S_{33} &= \frac{2(B+D)}{L^2} = 62.042; \quad S_{35} = \frac{B+D}{L} = 4963.417
 \end{aligned}$$

The stiffness matrix corresponding to global d.o.f. is obtained by Eq. (8.43) as

$$\begin{aligned}
 [K^{11}]_{12 \times 12} &= [A][K_e][A]^T \\
 &= \left[\begin{array}{cccc|cccc|cccc}
 S_{22} & 0 & 0 & 0 & S_{26} & 80S_{22} & | & -S_{22} & 0 & 0 & 0 & S_{26} & -80S_{22} \\
 S_{33} & 0 & -S_{35} & 0 & 240S_{33} & | & 0 & -S_{33} & 0 & -S_{35} & 0 & 0 & -80S_{33} \\
 H & 0 & 0 & 0 & | & 0 & | & 0 & 0 & -H & 0 & 0 & 0 \\
 B & 0 & -240S_{35} & | & 0 & S_{35} & | & 0 & D & 0 & 80S_{35} \\
 A & 80S_{26} & | & -S_{26} & 0 & 0 & | & 0 & 0 & C & -80S_{26} & \\
 & (80)^2 S_{22} & & & & & & & & & -640S_{22} \\
 & +(240)^2 S_{33} & | & -80S_{22} & -240S_{33} & 0 & | & -240S_{35} & 80S_{26} & -19200S_{33} & \\
 & +Q & & & & & & & & & -Q \\
 \cdots & \cdots & \cdots & \cdots & \cdots & | & \cdots & \cdots & \cdots & \cdots & \cdots & \cdots & \\
 & & & & & | & S_{22} & 0 & 0 & 0 & -S_{26} & 80S_{22} \\
 & & & & & | & S_{33} & 0 & S_{35} & 0 & 0 & 80S_{33} \\
 & & & & & | & & H & 0 & 0 & 0 \\
 & & & & & | & & & B & 0 & 80S_{35} \\
 & & & & & | & & & & A & -80S_{26} & \\
 & & & & & | & & & & & 6400S_{22} \\
 & & & & & | & & & & & +6400S_{33} \\
 & & & & & & & & & & +Q
 \end{array} \right] \quad (q)
 \end{aligned}$$

for which the force vector is $\{F_{jm}\} = [F_{Amx} \ F_{Amy} \ F_{Amz} \ M_{Amx} \ M_{Amy} \ M_{Amz} \ F_{Bmx} \ F_{Bmy} \ F_{Bmz} \ M_{Bmx} \ M_{Bmy} \ M_{Bmz}]^T$, where A and B signify nodal numbers 106 and 6, respectively (see Figs. 8.9b and 8.13). Note that F_{Amx} and F_{Amy} are transferred to master joint C_3 where M_{Amz} is torsion induced by these two forces; F_{Amz} , M_{Amx} , M_{Amy} and M_{Amz} are not transferable and stay at joint A (node 106), acting as a master joint. A similar explanation covers the forces at joint B (node 6).

8.6.4. Beam–Column Geometric Matrix (String Stiffness) in ECS and JCS or GCS Based on Method 1

In order to be consistent with lumped mass formulation, the $P-\Delta$ effect should be based on the *string stiffness* model (see Section 6.6.3). The *geometric matrix* is often called the *geometric stiffness matrix* because its inclusion can decrease or increase a system's stiffness (see Section 6.6). The model used here considers the $P-\Delta$ effect that induces shear in an element. An element is idealized as a rigid bar with an axial load P as shown in Fig. 8.14. Axial load, P , is positive

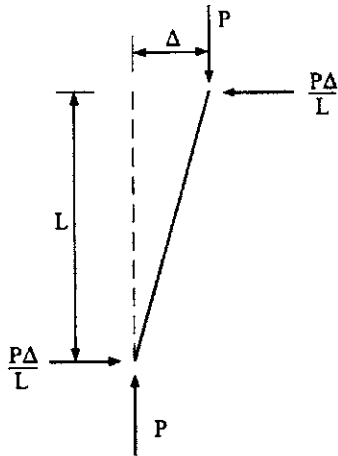


FIG. 8.14 $P-\Delta$ effect for beam–column element.

when the member is in compression. The shear at each end of a member, due to equilibrium condition, is $P\Delta/L$. Thus the element geometric stiffness matrix is

$$[K_{eg}] = \frac{P}{L} \begin{bmatrix} 0 & 0 & 0 & 0 & 0 & 0 & 0 & 0 & 0 & 0 & 0 & 0 \\ 0 & 1 & 0 & 0 & 0 & 0 & 0 & -1 & 0 & 0 & 0 & 0 \\ 0 & 0 & 1 & 0 & 0 & 0 & 0 & 0 & -1 & 0 & 0 & 0 \\ 0 & 0 & 0 & 0 & 0 & 0 & 0 & 0 & 0 & 0 & 0 & 0 \\ 0 & 0 & 0 & 0 & 0 & 0 & 0 & 0 & 0 & 0 & 0 & 0 \\ 0 & 0 & 0 & 0 & 0 & 0 & 0 & 0 & 0 & 0 & 0 & 0 \\ 0 & 0 & 0 & 0 & 0 & 0 & 0 & 0 & 0 & 0 & 0 & 0 \\ 0 & 0 & 0 & 0 & 0 & 0 & 0 & 0 & 0 & 0 & 0 & 0 \\ 0 & -1 & 0 & 0 & 0 & 0 & 0 & 1 & 0 & 0 & 0 & 0 \\ 0 & 0 & -1 & 0 & 0 & 0 & 0 & 0 & 1 & 0 & 0 & 0 \\ 0 & 0 & 0 & 0 & 0 & 0 & 0 & 0 & 0 & 0 & 0 & 0 \\ 0 & 0 & 0 & 0 & 0 & 0 & 0 & 0 & 0 & 0 & 0 & 0 \end{bmatrix} \quad (8.44)$$

Since the element's d.o.f. for $[K_{eg}]$ in Eq. (8.44) is the same for $[K_e]$ in Eq. (8.31), the geometric stiffness in the JCS or GCS can be obtained as follows:

$$[K_g^i] = [A][K_{eg}][A]^T \quad (8.45)$$

8.7. SHEAR WALLS

8.7.1. Shear-Wall ECS and GCS Relationship Based on Method 1

A shear-wall element's coordinate system is shown in Fig. 8.15 where the four joints at the corners of the element are denoted by $J1-J4$. The global coordinates of each joint are X_{g1}, Y_{g1}, Z_{g1} through X_{g4}, Y_{g4}, Z_{g4} . Vectors \vec{V}_{xt} at the top and \vec{V}_{xb} at the bottom of the wall are

$$\vec{V}_{xt} = (X_{g1} - X_{g2})\hat{i} + (Y_{g1} - Y_{g2})\hat{j} + (Z_{g1} - Z_{g2})\hat{k} \quad (8.46)$$

$$\vec{V}_{xb} = (X_{g4} - X_{g3})\hat{i} + (Y_{g4} - Y_{g3})\hat{j} + (Z_{g4} - Z_{g3})\hat{k} \quad (8.47)$$

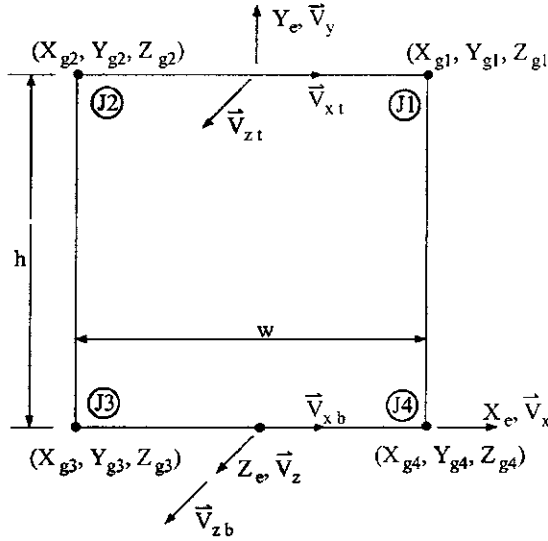


FIG. 8.15 Shear-wall element coordinate system.

Define a vector $\vec{V}_{y'}$ along with the average longitudinal axis of the wall; then

$$\begin{aligned}\vec{V}_{y'} = & \left[\frac{X_{g1} + X_{g2}}{2} - \frac{X_{g3} + X_{g4}}{2} \right] \hat{i} + \left[\frac{Y_{g1} + Y_{g2}}{2} - \frac{Y_{g3} + Y_{g4}}{2} \right] \hat{j} \\ & + \left[\frac{Z_{g1} + Z_{g2}}{2} - \frac{Z_{g3} + Z_{g4}}{2} \right] \hat{k}\end{aligned}\quad (8.48)$$

Height (also defined as length) of the wall is

$$h = |\vec{V}_{y'}| \quad (8.49)$$

Normalizing $\vec{V}_{y'}$, yields

$$\vec{V}_y = \frac{\vec{V}_{y'}}{h} \quad (8.50)$$

Define vectors \vec{V}_{zb} and \vec{V}_{zt} , which are perpendicular to the wall, as

$$\vec{V}_{zb} = \vec{V}_{xb} \times \vec{V}_y ; \quad \vec{V}_{zt} = \vec{V}_{xt} \times \vec{V}_y \quad (8.51)$$

Since the wall is planar, \vec{V}_{zb} and \vec{V}_{zt} are parallel. Also $|\vec{V}_{zb}| = |\vec{V}_{zt}|$ because the wall has a constant width w . Therefore $|\vec{V}_{zb}| = |\vec{V}_{zt}|$, and the single unit vector perpendicular to the plane of the wall can be defined as

$$\vec{V}_z = \frac{\vec{V}_{zb}}{|\vec{V}_{zb}|} \quad (8.52)$$

while vector \vec{V}_x , perpendicular to the in-plane length of the wall, is

$$\vec{V}_x = \vec{V}_y \times \vec{V}_z \quad (8.53)$$

Three unit vectors, \vec{V}_x , \vec{V}_y , and \vec{V}_z , define the element's coordinate system, denoted by X_e , Y_e , Z_e , with the origin midway between joints $J3$ and $J4$. The three unit vectors defining the ECS orientation are written in matrix form similar to Eq. (8.11) as

$$\{V_e\} = \begin{Bmatrix} \vec{V}_x \\ \vec{V}_y \\ \vec{V}_z \end{Bmatrix} = \begin{bmatrix} C_{11} & C_{12} & C_{13} \\ C_{21} & C_{22} & C_{23} \\ C_{31} & C_{32} & C_{33} \end{bmatrix} \begin{Bmatrix} \vec{i} \\ \vec{j} \\ \vec{k} \end{Bmatrix} = [C_e] \begin{Bmatrix} \vec{i} \\ \vec{j} \\ \vec{k} \end{Bmatrix} \quad (8.54)$$

where $[C_e]$ is the direction cosine matrix for the ECS; \vec{i} , \vec{j} , and \vec{k} are unit vectors in GCS.

8.7.2. Shear-Wall Stiffness in the ECS

As shown in Fig. 8.16, the element has 10 translational d.o.f: d.o.f. 1 and 8 represent in-plane lateral deformation; d.o.f. 2, 4, 6, and 9 represent axial and rotational deformation; and d.o.f. 3, 5, 7 and 10 are used to formulate the out-of-plane geometric matrix for 3D system analysis. Out-of-plane stiffness, however, is not considered. (Section 8.7.4 treats in-plane and out-of-plane geometric matrices.) In matrix form, the ECS local forces and displacements are

$$\{F_e\} = [F_1 \ F_2 \ F_3 \ F_4 \ F_5 \ F_6 \ F_7 \ F_8 \ F_9 \ F_{10}]^T \quad (8.55)$$

$$\{\delta_e\} = [\delta_1 \ \delta_2 \ \delta_3 \ \delta_4 \ \delta_5 \ \delta_6 \ \delta_7 \ \delta_8 \ \delta_9 \ \delta_{10}]^T \quad (8.56)$$

α and β as shown in Fig. 8.16 represent a fraction of the wall's height at the top and bottom, respectively. Length α depends on the ratio of rigidity at the bottom of the wall to rigidity at the top of the wall or simply on relative rotation as

$$\alpha = \frac{h}{1 + \left| \frac{\theta_B}{\theta_A} \right|} \quad (8.57)$$

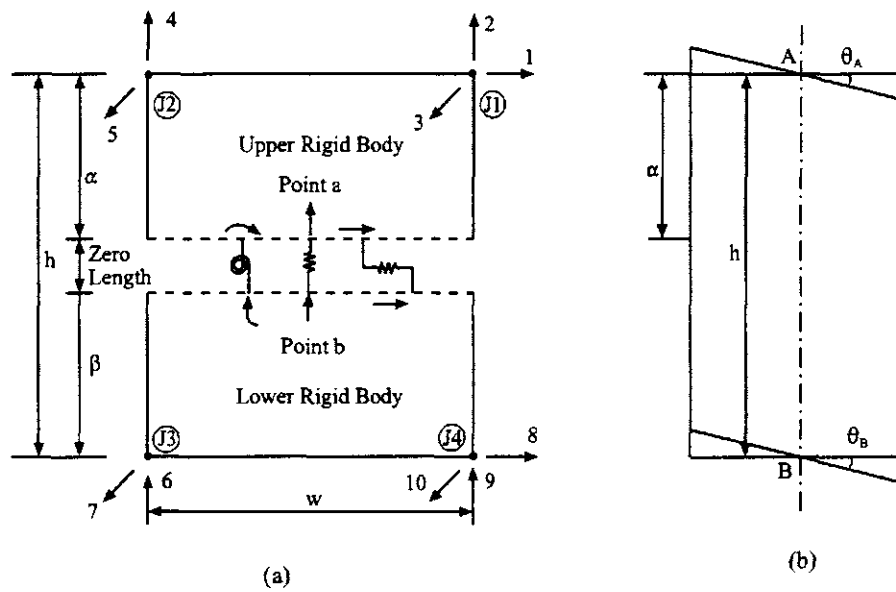


FIG. 8.16 Shear-wall element.

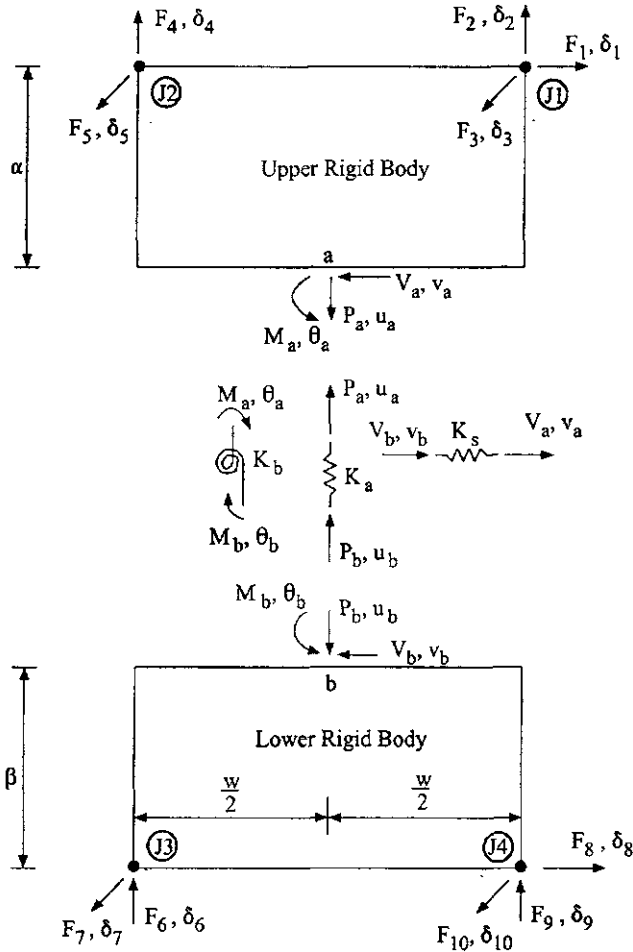


FIG. 8.17 Shear-wall forces and deformations.

For instance, if end *A* is free and end *B* is fixed, then $\theta_B = 0$, $\alpha = h$; if end *A* is fixed, then $\theta_A = 0$, $|\theta_B/\theta_A| = \infty$, and $\alpha = 0$; if $\theta_A = \theta_B$, then $\alpha = h/2$; and if $\theta_A = 2\theta_B$, then $|\theta_B/\theta_A| = 1/2$ and $\alpha = 2h/3$.

To develop a generalized formulation of shear-wall stiffness for both elastic analysis (this chapter) and inelastic analysis (Chapter 9), a rigid-body spring model is used to express the force-deformation relationship [4].

Let a free-body diagram of the shear wall element in Fig. 8.16 be shown in Fig. 8.17. The force-deformation relationship for each spring is

$$M_a = K_b \theta_u = \frac{K_b}{h} (\theta_a - \theta_b) = -M_b \quad (8.58)$$

$$V_a = K_s V_u = \frac{K_s}{h} (v_a - v_b) = -V_b \quad (8.59)$$

and

$$P_a = K_a u_u = \frac{K_a}{h} (u_a - u_b) = -P_b \quad (8.60)$$

where

- $K_a = EA$, axial stiffness of unit-height wall for which the derivation is u (axial deformation) $= Ph/EA$, $P/u = EA/h$; therefore $Ph/u = EA$;
- $K_b = EI$, bending stiffness of unit-height wall because $M = EI\phi$; ϕ is curvature $= \theta/h$ or $1/R$ (see Fig. 4.1);
- $K_s = GA/\kappa$, shear stiffness of unit-height wall because shear rotation $\beta = V\kappa/GA$ [see Eq. (5.90)]; lateral displacement due to shear rotation is $v = \beta h$; therefore $Vh/v = GA/\kappa$;
- $\theta_a, \theta_b =$ flexural rotations at top and bottom of bending spring, respectively;
- $\theta_u =$ relative unit rotation;
- $v_a, v_b =$ lateral shear deformation at top and bottom of shear spring, respectively;
- $v_u =$ relative unit shear deformation;
- $u_a, u_b =$ axial deformation at top and bottom of axial spring, respectively;
- $u_u =$ relative unit axial deformation;
- $M_a, M_b =$ moments at top and bottom of bending spring, respectively;
- $V_a, V_b =$ shears at top and bottom of shear spring, respectively;
- $P_a, P_b =$ axial force at top and bottom of axial spring, respectively;
- $G =$ shear modulus;
- $I =$ moment of inertia;
- $A =$ cross-sectional area; and
- $\kappa = 1.2$ numerical factor for using average shear [$\kappa = 1/\mu$; μ is given in Eq. (5.90)].

Rewriting Eqs. (8.58)–(8.60) in matrix form yields

$$\begin{Bmatrix} M_a \\ M_b \\ V_a \\ V_b \\ P_a \\ P_b \end{Bmatrix} = \begin{bmatrix} 1 & 0 & 0 \\ -1 & 0 & 0 \\ 0 & 1 & 0 \\ 0 & -1 & 0 \\ 0 & 0 & 1 \\ 0 & 0 & -1 \end{bmatrix} \begin{Bmatrix} M_a \\ V_a \\ P_a \end{Bmatrix} = [A_1] \begin{Bmatrix} M_a \\ V_a \\ P_a \end{Bmatrix} \quad (8.61)$$

and

$$\begin{aligned} \begin{Bmatrix} M_a \\ V_a \\ P_a \end{Bmatrix} &= \begin{bmatrix} K_b & & \\ & K_s & \\ & & K_a \end{bmatrix} \left(\frac{1}{h}\right) \begin{Bmatrix} \theta_a - \theta_b \\ v_a - v_b \\ u_a - u_b \end{Bmatrix} \\ &= \frac{1}{h} \begin{bmatrix} K_b & & \\ & K_s & \\ & & K_a \end{bmatrix} \begin{bmatrix} 1 & -1 & 0 & 0 & 0 & 0 \\ 0 & 0 & 1 & -1 & 0 & 0 \\ 0 & 0 & 0 & 0 & 1 & -1 \end{bmatrix} \begin{Bmatrix} \theta_a \\ \theta_b \\ v_a \\ v_b \\ u_a \\ u_b \end{Bmatrix} \quad (8.62) \\ &= [S_I] [A_1]^T \begin{Bmatrix} \theta_a \\ \theta_b \\ v_a \\ v_b \\ u_a \\ u_b \end{Bmatrix} \end{aligned}$$

From summation of forces and moments in Fig. 8.17, the relationship between spring forces and element forces is

$$\sum F_{x\ top} = 0 = F_1 - V_a; \quad F_1 = V_a \quad (8.63)$$

$$\sum M_{J1} = 0 = M_a - wF_4 + P_a \frac{w}{2} - \alpha V_a; \quad F_4 = \frac{M_a}{w} + \frac{P_a}{2} - \frac{\alpha}{w} V_a \quad (8.64)$$

$$\sum M_{J2} = 0 = M_a + wF_2 - P_a \frac{w}{2} - \alpha V_a; \quad F_2 = \frac{-M_a}{w} + \frac{P_a}{2} + \frac{\alpha}{w} V_a \quad (8.65)$$

$$\sum F_{x\ btm} = 0 = F_8 - V_b; \quad F_8 = V_b \quad (8.66)$$

$$\sum M_{J4} = 0 = M_b - wF_6 + \frac{w}{2} P_b + \beta V_b; \quad F_6 = \frac{M_b}{w} + \frac{P_b}{2} + \frac{\beta}{w} V_b \quad (8.67)$$

$$\sum M_{J3} = 0 = M_b + wF_9 - \frac{w}{2} P_b + \beta V_b; \quad F_9 = \frac{-M_b}{w} + \frac{P_b}{2} - \frac{\beta}{w} V_b \quad (8.68)$$

Combining Eqs. (8.63)–(8.68) in matrix form gives

$$\{F_e\} = \begin{Bmatrix} F_1 \\ F_2 \\ F_3 \\ F_4 \\ F_5 \\ F_6 \\ F_7 \\ F_8 \\ F_9 \\ F_{10} \end{Bmatrix} = \frac{1}{2w} \begin{bmatrix} 0 & 0 & 2w & 0 & 0 & 0 \\ -2 & 0 & 2\alpha & 0 & w & 0 \\ 0 & 0 & 0 & 0 & 0 & 0 \\ 2 & 0 & -2\alpha & 0 & w & 0 \\ 0 & 0 & 0 & 0 & 0 & 0 \\ 0 & 2 & 0 & 2\beta & 0 & w \\ 0 & 0 & 0 & 0 & 0 & 0 \\ 0 & 0 & 0 & 2w & 0 & 0 \\ 0 & -2 & 0 & -2\beta & 0 & w \\ 0 & 0 & 0 & 0 & 0 & 0 \end{bmatrix} \begin{Bmatrix} M_a \\ M_b \\ V_a \\ V_b \\ P_a \\ P_b \end{Bmatrix} = [A_2] \begin{Bmatrix} M_a \\ M_b \\ V_a \\ V_b \\ P_a \\ P_b \end{Bmatrix} \quad (8.69)$$

Substituting Eq. (8.61) into Eq. (8.69) leads to

$$\{F_e\} = [A_2][A_1] \begin{Bmatrix} M_a \\ V_a \\ P_a \end{Bmatrix} = [A_e] \begin{Bmatrix} M_a \\ V_a \\ P_a \end{Bmatrix} \quad (8.70)$$

Shear-wall stiffness is then given by

$$[K_e] = [A_e][S_I][A_e]^T \quad (8.71)$$

Since there is no bending or shear stiffness perpendicular to the wall (see Fig. 8.17), the stiffness terms associated with d.o.f. 3, 5, 7, and 10 are zero. To prevent a singular stiffness matrix, the out-of-plane d.o.f. must be restrained when analyzing a planar frame. The shear wall element in Fig. 8.17 depicts a general case for 3D building structures.

EXAMPLE 8.7.1 Find the stiffness matrix $[K_e]$ for the wall shown in Fig. 8.18a. Let the concrete's modulus of elasticity $E_c = 30,000 \text{ N/mm}^2$, its Poisson's ratio $\nu = 0.2$, and the steel's modulus of elasticity $E_s = 210,000 \text{ N/mm}^2$. Other member properties are given in the figure. Verify the correctness of the stiffness coefficients obtained.

Solution: The wall is analyzed by means of the *transformed section method* for which

$$G = \frac{E_c}{2(1+\nu)} = \frac{30,000}{2(1+0.2)} = 12,500 \text{ N/mm}^2, n = \frac{E_s}{E_c} = \frac{210,000}{30,000} = 7$$

$$A = A_c + (n-1)A_s = 1000(100) + 100(10)(7-1) = 1.06(10)^5 \text{ mm}^2$$

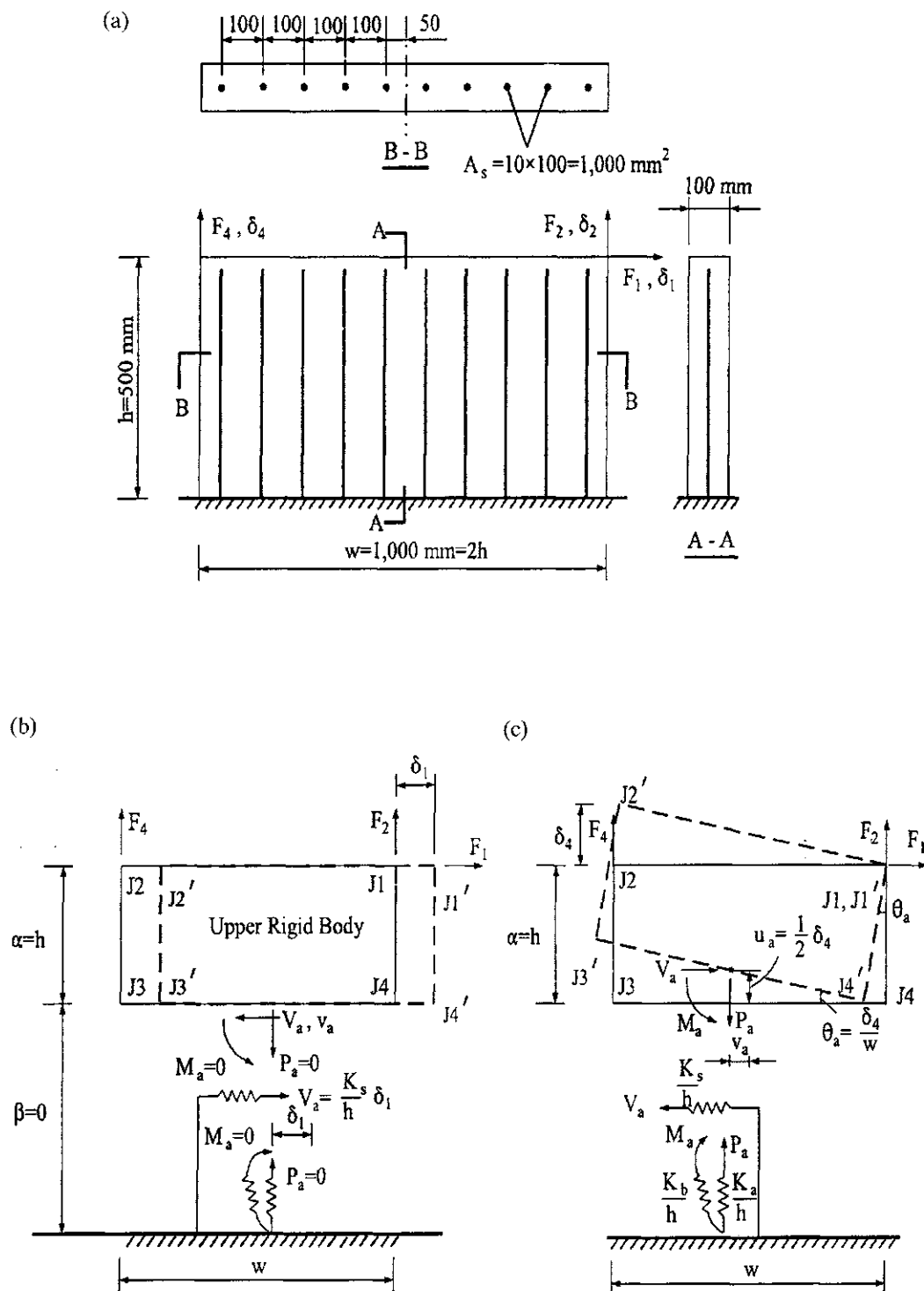


FIG. 8.18 Shear wall in Example 8.7.1. (a) Wall properties. (b) Due to δ_1 . (c) Due to δ_4 .

$$\begin{aligned}
I &= \frac{1}{12}(100)(1000)^3 + (7-1)[(2)(100)(50)^2 + (2)(100)(150)^2 + 2(100)(250)^2 + 2(100)(350)^2 \\
&\quad + 2(100)(450)^2] = 8.828(10)^9 \text{ mm}^4 \\
K_b &= E_c I = (30,000)(8.828)(10)^9 = 2.648(10)^{14} \text{ N mm}^2, \\
K_s &= \frac{GA}{\kappa} = \frac{(12,500)(1.06)(10)^5}{1.2} = 1.104(10)^9 \text{ N} \\
K_a &= E_c A = 30,000(1.06)(10)^5 = 3.18(10)^9 \text{ N}
\end{aligned}$$

From Eq. (8.61),

$$[A_1] = \begin{bmatrix} 1 & 0 & 0 \\ -1 & 0 & 0 \\ 0 & 1 & 0 \\ 0 & -1 & 0 \\ 0 & 0 & 1 \\ 0 & 0 & -1 \end{bmatrix} \quad (a)$$

Since the element's free d.o.f. are only 1, 2, and 4, and the wall is fixed so that $\alpha = h$ and $\beta = 0$, $[A_2]$ in Eq. (8.69) is reduced to

$$[A_2] = \begin{bmatrix} 0 & 0 & 1 & 0 & 0 & 0 \\ -\frac{1}{w} & 0 & \frac{h}{w} & 0 & \frac{1}{2} & 0 \\ \frac{1}{w} & 0 & -\frac{h}{w} & 0 & \frac{1}{2} & 0 \end{bmatrix} \quad (b)$$

Then

$$[A_2][A_1] = \begin{bmatrix} 0 & 1 & 0 \\ -\frac{1}{w} & \frac{1}{2} & \frac{1}{2} \\ \frac{1}{w} & -\frac{1}{2} & \frac{1}{2} \end{bmatrix} \quad (c)$$

Thus

$$\begin{aligned}
[K_e] &= [A_2][A_1][S_I][[A_2][A_1]]^T \\
&= \frac{1}{h} \begin{bmatrix} K_s & \frac{1}{2}K_s & -\frac{1}{2}K_s \\ \frac{K_b}{w^2} + \frac{1}{4}K_s + \frac{1}{4}K_a & -\frac{K_b}{w^2} - \frac{1}{4}K_s + \frac{1}{4}K_a \\ \text{symm} & \frac{K_b}{w^2} + \frac{1}{4}K_s + \frac{1}{4}K_a \end{bmatrix} \\
&= \frac{1}{500} \begin{bmatrix} 1.104 & 0.552 & -0.552 \\ \text{symm} & 1.336 & 0.254 \\ & & 1.336 \end{bmatrix} (10)^9
\end{aligned} \quad (d)$$

Stiffness coefficients in Eq. (d) can be verified by the accompanying figures b and c as follows. When $\delta_1 \neq 0$, $\delta_2 = \delta_4 = 0$, as shown in Fig. 8.18b.

$$\sum F_x = 0; \quad F_1 = V_a = \frac{K_s}{h} \delta_1 \quad (e)$$

$$\sum M_{J2} = 0; \quad F_2 = \frac{h}{w} V_a = \left(\frac{h}{w}\right) \frac{K_s}{h} \delta_1 = \frac{K_s}{2h} \delta_1 \quad (f)$$

$$\sum M_{J1} = 0; \quad F_4 = -\frac{h}{w} V_a = -\frac{K_s}{2h} \delta_1 \quad (g)$$

Eqs. (e), (f), and (g) represent elements in the first column of Eq. (d).

Similarly, when $\delta_4 \neq 0$, $\delta_1 = \delta_2 = 0$, the equilibrium conditions of Fig. 8.18c yield

$$\begin{aligned} \sum F_x = 0; \quad F_1 = -V_a = -\frac{K_s h}{h w} \delta_4 = -\frac{K_s}{2h} \delta_4 \\ \sum M_{J2} = 0; \quad F_2 w + V_a h - P_a \frac{w}{2} + M_a = 0; \quad V_a = \left(\frac{K_a}{h}\right) \frac{\delta_4}{2}; \quad M_a = \left(\frac{K_b}{h}\right) \frac{\delta_4}{w} \end{aligned} \quad (h)$$

Then

$$F_2 = \left(-\frac{K_b}{hw^2} - \frac{K_s}{4h} + \frac{K_a}{4h}\right) \delta_4 \quad (i)$$

$$\sum M_{J1} = 0; \quad F_4 w - V_a h - P_a \frac{w}{2} - M_a = 0$$

$$F_4 = \left(\frac{K_b}{hw^2} + \frac{K_s}{4h} + \frac{K_a}{4h}\right) \delta_4 \quad (j)$$

Eqs. (h), (i), and (j) are identical to the third column of Eq. (d).

8.7.3. Shear-Wall Stiffness in the JCS or GCS Based on Method 1

Similar to the formulation of beam–column stiffness, we rotate the element forces from the ECS to the GCS, which are then expressed in the JCS. Referring to Eqs. (8.37) and (8.38), let the element forces at joint i , $\{F_{ei}\}$, be expressed in global forces at that joint $\{F_{gi}\}$, i.e. $[F_{gix} \ F_{giy} \ F_{giz}]^T$ (in X_g , Y_g , Z_g axes). Use the element direction cosine matrix as

$$\{F_{gi}\} = [C_{ei}]^T \{F_{ei}\} \quad (8.72)$$

and express the global forces at joint i , $\{F_{gi}\}$, as joint forces in the following form:

$$\{F_{ji}\} = [C_{ji}] \{F_{gi}\} \quad (8.73)$$

where $[C_{ji}]$ is the direction cosine of JCS for joint i . Since the wall is thick relative to its length and width, deformation in the X -direction is negligible. If joints $J1$ and $J4$ in Fig. 8.15 are considered to have independent displacement in the X -direction, then there is no independent d.o.f. in that direction. In other words, $J2$ and $J1$ are dependent on each other, as are $J3$ and $J4$. Therefore

transformation matrix $[A_3]$ is used to create dummy d.o.f. at these joints.

$$\begin{Bmatrix} F_{e1} \\ F_{e2} \\ F_{e3} \\ F_{e4} \end{Bmatrix} = \begin{Bmatrix} F_{j1x} \\ F_{j1y} \\ F_{j1z} \\ F_{j2x} \\ F_{j2y} \\ F_{j2z} \\ F_{j3x} \\ F_{j3y} \\ F_{j3z} \\ F_{j4x} \\ F_{j4y} \\ F_{j4z} \end{Bmatrix} = \begin{bmatrix} 1 & 0 & 0 & 0 & 0 & 0 & 0 & 0 & 0 & 0 \\ 0 & 1 & 0 & 0 & 0 & 0 & 0 & 0 & 0 & 0 \\ 0 & 0 & 1 & 0 & 0 & 0 & 0 & 0 & 0 & 0 \\ 0 & 0 & 0 & 0 & 0 & 0 & 0 & 0 & 0 & 0 \\ 0 & 0 & 0 & 1 & 0 & 0 & 0 & 0 & 0 & 0 \\ 0 & 0 & 0 & 0 & 1 & 0 & 0 & 0 & 0 & 0 \\ 0 & 0 & 0 & 0 & 0 & 1 & 0 & 0 & 0 & 0 \\ 0 & 0 & 0 & 0 & 0 & 0 & 1 & 0 & 0 & 0 \\ 0 & 0 & 0 & 0 & 0 & 0 & 0 & 1 & 0 & 0 \\ 0 & 0 & 0 & 0 & 0 & 0 & 0 & 0 & 1 & 0 \\ 0 & 0 & 0 & 0 & 0 & 0 & 0 & 0 & 0 & 1 \end{bmatrix} \begin{Bmatrix} F_1 \\ F_2 \\ F_3 \\ F_4 \\ F_5 \\ F_6 \\ F_7 \\ F_8 \\ F_9 \\ F_{10} \end{Bmatrix} = [A_3] \{F_e\} \quad (8.74)$$

where notation $\{F_{ei}\} = [F_{j1x} \ F_{j1y} \ F_{j1z}]^T$ represents forces on joint $J1$ in the ECS; similarly, $\{F_{ej}\}$ represents forces at joint Ji (see Fig. 8.15). Rotating the forces at each of the wall's four joints from ECS to JCS yields

$$\begin{Bmatrix} F_{j1} \\ F_{j2} \\ F_{j3} \\ F_{j4} \end{Bmatrix} = \begin{bmatrix} [C_{j1} C_{e1}^T] & 0 & 0 & 0 \\ 0 & [C_{j2} C_{e2}^T] & 0 & 0 \\ 0 & 0 & [C_{j3} C_{e3}^T] & 0 \\ 0 & 0 & 0 & [C_{j4} C_{e4}^T] \end{bmatrix} \begin{Bmatrix} F_{e1} \\ F_{e2} \\ F_{e3} \\ F_{e4} \end{Bmatrix} = [A_4] \begin{Bmatrix} F_{e1} \\ F_{e2} \\ F_{e3} \\ F_{e4} \end{Bmatrix} \quad (8.75)$$

where $\{F_{ji}\}$ represents forces acting in the X_j , Y_j , and Z_j directions at joint $J1$ in the JCS and likewise at the other three joints. Recalling the constraint transformation equation $[T_{ms}]_i$ for slave joint i , Eq. (8.6) takes the form

$$[T_{ms}]_i = \begin{bmatrix} [I] & [0] \\ [XYZ]_i & [I] \end{bmatrix} \quad (8.76)$$

The second column of $[T_{ms}]_i$ pertains to rotational d.o.f. at the slave joint. Since $\{F_{ji}\}$ for the wall element contains only translational d.o.f. (see Figs. 8.15 and 8.17), the second column is omitted and the constraint equation becomes

$$\begin{Bmatrix} F_{jm_x} \\ F_{jm_y} \\ F_{jm_z} \\ M_{jm_x} \\ M_{jm_y} \\ M_{jm_z} \end{Bmatrix} = \begin{bmatrix} 1 & 0 & 0 \\ 0 & 1 & 0 \\ 0 & 0 & 1 \\ 0 & 0 & 0 \\ 0 & 0 & 0 \\ -Y_{ms} & X_{ms} & 0 \end{bmatrix} \begin{Bmatrix} F_{js_x} \\ F_{js_y} \\ F_{js_z} \end{Bmatrix} \quad (8.77)$$

For a typical slab-wall joint, Ji , the slave–master joint relationship is

$$[T'_{ms}]_i = \begin{bmatrix} [I] \\ [XYZ]_i \end{bmatrix} \quad (8.78)$$

For instance, the constraint transformation of $J1$ in Fig. 8.19 is

$$\begin{Bmatrix} F_{jm_x} \\ F_{jm_y} \\ F_{jm_z} \\ M_{jm_x} \\ M_{jm_y} \\ M_{jm_z} \end{Bmatrix} = \begin{bmatrix} 1 & 0 & 0 \\ 0 & 1 & 0 \\ 0 & 0 & 1 \\ 0 & 0 & 0 \\ 0 & 0 & 0 \\ -Y_{ms} & X_{ms} & 0 \end{bmatrix} \begin{Bmatrix} F_1 \sin \theta \\ F_1 \cos \theta \\ F_2 \end{Bmatrix} \quad (8.79)$$

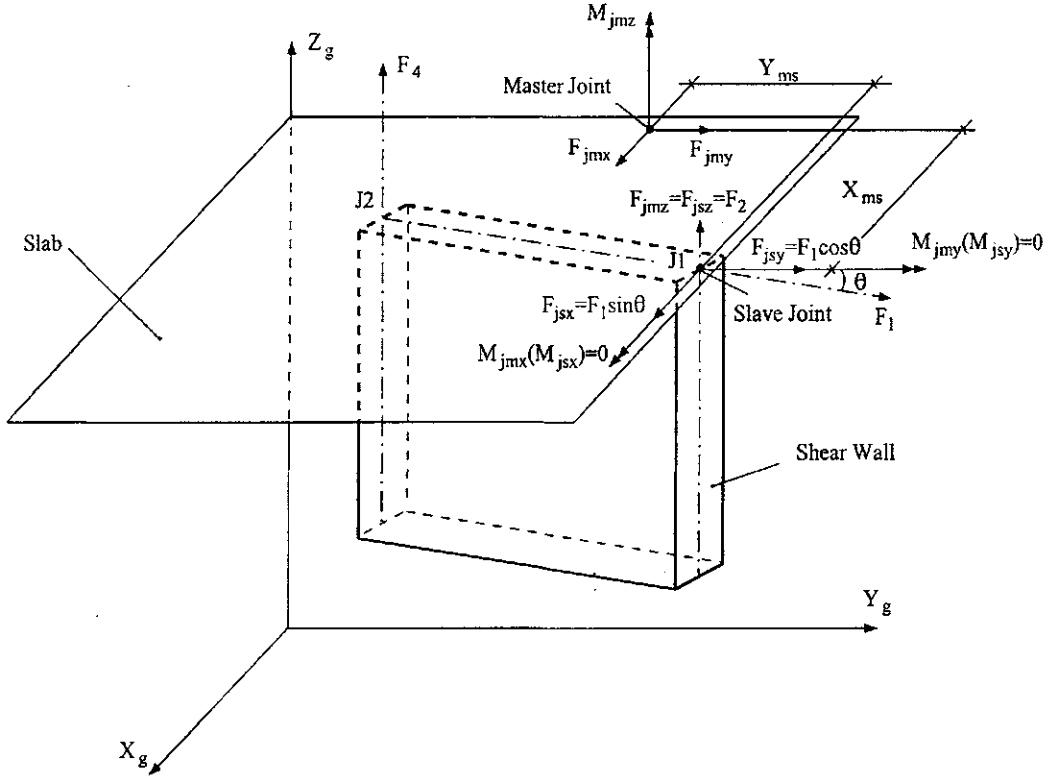


FIG. 8.19 Slave–master joint relationship of slab–wall joint.

Note that the relationship between notations $\{F_{jm}\}$ and $\{F_{js}\}$ shown in Fig. 8.8b is the same as that in Fig. 8.19. In the latter figure, F_{jsx} and F_{jsy} at $J1$ merely show from where they result. These two forces are then transferred to and induce torsion in the master joint [see Eq. (8.79)]. Thus the master joint assigned at the floor slab has three independent forces. Although the slave joint also has three independent forces, two of them are zero as *dummy d.o.f.*: $M_{jmx}(M_{jsx})=0$; $M_{jmy}(M_{jsy})=0$. These three are part of the nodal forces in a structural system.

Combining the transformation for all four joints yields

$$\begin{Bmatrix} F_{j1m} \\ F_{j2m} \\ F_{j3m} \\ F_{j4m} \end{Bmatrix} = \begin{bmatrix} [T'_{ms}]_1 & 0 & 0 & 0 \\ 0 & [T'_{ms}]_2 & 0 & 0 \\ 0 & 0 & [T'_{ms}]_3 & 0 \\ 0 & 0 & 0 & [T'_{ms}]_4 \end{bmatrix} \begin{Bmatrix} F_{j1} \\ F_{j2} \\ F_{j3} \\ F_{j4} \end{Bmatrix} = [A_5] \begin{Bmatrix} F_{j1} \\ F_{j2} \\ F_{j3} \\ F_{j4} \end{Bmatrix} \quad (8.80)$$

where $\{F_{jm}\} = [F_{jmx} \ F_{jmy} \ F_{jmz} \ M_{jmx} \ M_{jmy} \ M_{jmz}]$ represents the transformation at joint i . Substituting Eq. (8.74) into Eq. (8.75), which is then substituted into Eq. (8.80), leads to

$$\begin{Bmatrix} F_{j1m} \\ F_{j2m} \\ F_{j3m} \\ F_{j4m} \end{Bmatrix} = [A_5][A_4][A_3]\{F_e\} = [A]\{F_e\} \quad (8.81)$$

Using Eq. (8.70) in the above to replace internal forces at the wall's nodes, $\{F_e\}$, with spring forces,

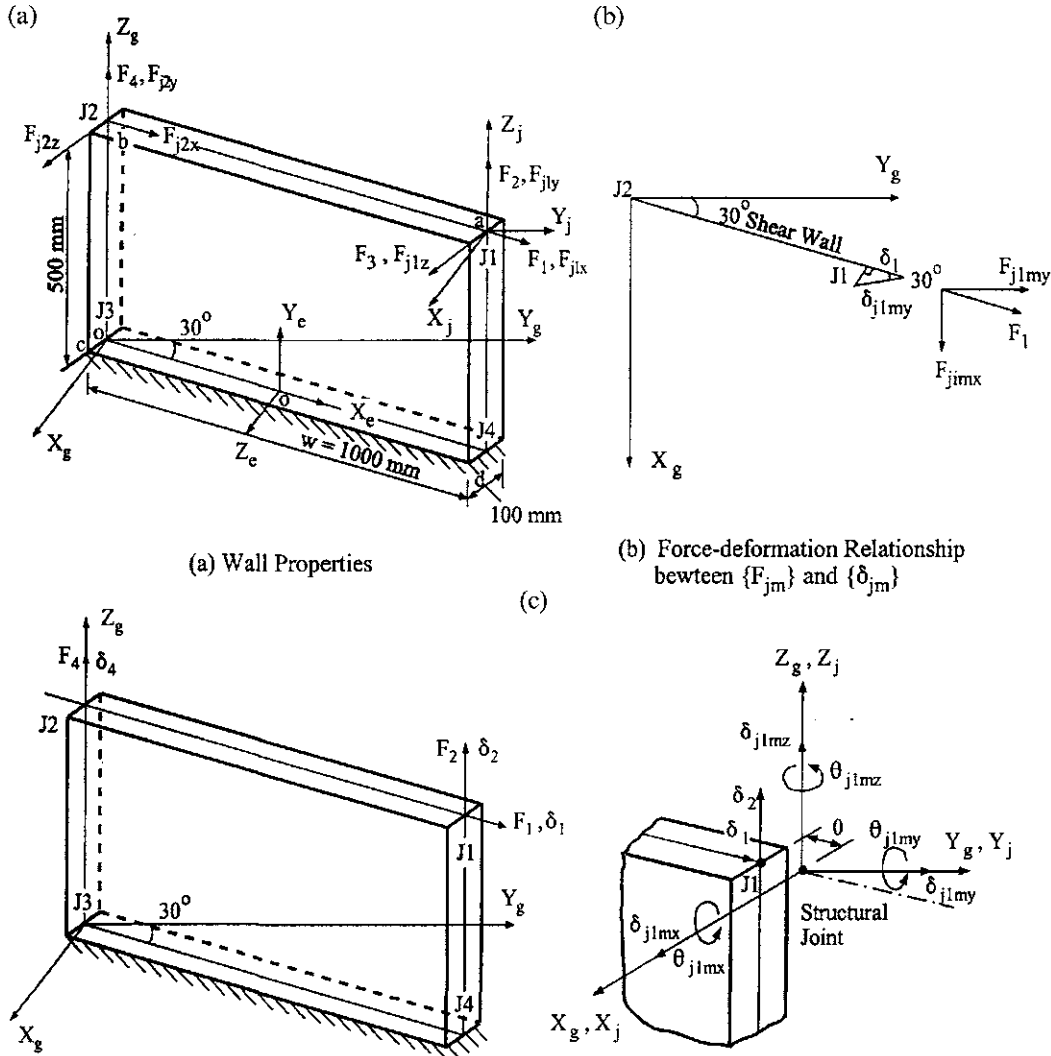


FIG. 8.20 Example 8.7.2. (a) Wall properties. (b) Force-deformation relationship between $\{F_{jm}\}$ and $\{\delta_{jm}\}$. (c) Relationship between joint d.o.f. and dummy d.o.f.

$[M_a \ V_a \ P_a]^T$, we have

$$\begin{Bmatrix} F_{j1m} \\ F_{j2m} \\ F_{j3m} \\ F_{j4m} \end{Bmatrix} = [A][A_e] \begin{Bmatrix} M_a \\ V_a \\ P_a \end{Bmatrix} \quad (8.82)$$

For deformation of the springs, the transformation is expressed as

$$\begin{Bmatrix} \theta_a \\ v_a \\ u_a \end{Bmatrix} = [[A][A_e]]^T \begin{Bmatrix} \delta_{j1m} \\ \delta_{j2m} \\ \delta_{j3m} \\ \delta_{j4m} \end{Bmatrix} \quad (8.83)$$

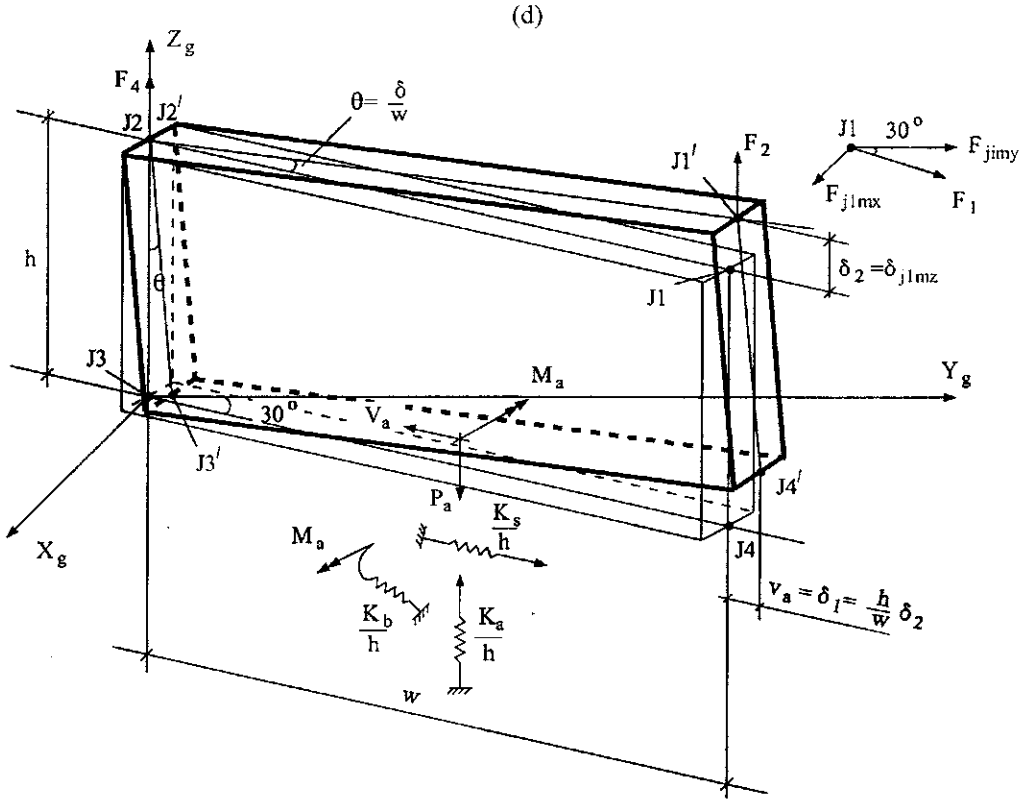


FIG. 8.20 Example 8.7.2. (d) Forces and deformations due to δ_{j1mx} .

where $[\delta_{jm}] = [\delta_{jm_x} \delta_{jm_y} \delta_{jm_z} \theta_{jm_x} \theta_{jm_y} \theta_{jm_z}]$ after transformation. The stiffness matrix of the wall is finally obtained in the JCS as

$$[K^t] = [A][K_e][A]^T \quad (8.84)$$

If the JCS and GCS are assumed to coincide, then $[C_{ji}]$ in Eq. (8.73) becomes an identity matrix. $[K^t]$ in Eq. (8.84) is the wall's stiffness matrix in the GCS.

EXAMPLE 8.7.2 The orientation of the shear wall given in Example 8.7.1 is shown in Fig. 8.20a where X_g , Y_g , and Z_g are global coordinates; F_1 , F_2 , and F_4 , are the wall's joint forces in ECS; and F_{j2x} , F_{j1z} , and F_{j2z} are dummy d.o.f. in the ECS for transformation purposes. The orientation of the ECS is based on Fig. 8.15. Find $\{F_{jm}\} = [K^t]\{\delta_{jm}\}$. Check the correctness of the stiffness coefficients.

Solution: From the spring stiffness matrix derived in Eq. (8.62) and numerical values obtained from Example 8.7.1, we have

$$[S_I] = \frac{1}{h} \begin{bmatrix} K_b & 0 & 0 \\ \text{symm} & K_s & 0 \\ & 0 & K_a \end{bmatrix} = \frac{1}{500} \begin{bmatrix} 2.648(10)^5 & 0 & 0 \\ \text{symm} & 1.104 & 0 \\ & 0 & 3.18 \end{bmatrix} 10^9 \quad (a)$$

From Eq. (8.61),

$$[A_1] = \begin{bmatrix} 1 & 0 & 0 \\ -1 & 0 & 0 \\ 0 & 1 & 0 \\ 0 & -1 & 0 \\ 0 & 0 & 1 \\ 0 & 0 & -1 \end{bmatrix} \quad (\text{b})$$

Because the shear wall is fixed at the bottom, the wall's free d.o.f. are only 1, 2 and 4; $\alpha=h$, $\beta=0$; $[A_2]$ in Eq. (8.69) is therefore reduced to

$$[A_2] = \begin{bmatrix} 0 & 0 & 1 & 0 & 0 & 0 \\ -\frac{1}{w} & 0 & \frac{h}{w} & 0 & \frac{1}{2} & 0 \\ \frac{1}{w} & 0 & -\frac{h}{w} & 0 & \frac{1}{2} & 0 \end{bmatrix} \quad (\text{c})$$

From Eq. (8.74), the relationship between $[F_{j1x} \ F_{j1y} \ F_{j1z} \ F_{j2x} \ F_{j2y} \ F_{j2z}]^T$ and $[F_1 \ F_2 \ F_4]^T$ is

$$[A_3] = \begin{bmatrix} 1 & 0 & 0 \\ 0 & 1 & 0 \\ 0 & 0 & 0 \\ 0 & 0 & 0 \\ 0 & 0 & 1 \\ 0 & 0 & 0 \end{bmatrix} \quad (\text{d})$$

Global forces at joint i , in terms of joint forces at that joint, are expressed in Eq. (8.73), $\{F_{ji}\} = [C_{ji}]\{F_{gi}\}$. Since the JCS is parallel to GCS as shown in Fig. 8.20, $[C_{ji}]$ ($i=1, 2$) becomes

$$[C_{j1}] = [C_{j2}] = \begin{bmatrix} 1 & 0 & 0 \\ 0 & 1 & 0 \\ 0 & 0 & 1 \end{bmatrix} \quad (\text{e})$$

For expressing element forces (in the ECS) in terms of global force (in the GCS), we need the following calculations.

For line $od=1000$ mm, $X_{g4}-X_{g3}=1000 \cos 60^\circ-0=500$ mm, $Y_{g4}-Y_{g3}=1000 \cos 30^\circ-0=866$ mm, $Z_{g4}-Z_{g3}=0-0=0$, and

$$D_{g43}=\sqrt{(X_{g4}-X_{g3})^2+(Y_{g4}-Y_{g3})^2+(Z_{g4}-Z_{g3})^2}=1000 \text{ mm} \quad (\text{f})$$

vector \vec{od} is

$$C_{11}=\frac{X_{g4}-X_{g3}}{D_{g43}}=\frac{500}{1000}=0.5, \ C_{12}=\frac{Y_{g4}-Y_{g3}}{D_{g43}}=\frac{866}{1000}=0.866, \ C_{13}=\frac{Z_{g4}-Z_{g3}}{D_{g43}}=0 \quad (\text{g})$$

For line $ob=500$ mm, $X_{g2}-X_{g3}=0-0=0$, $Y_{g2}-Y_{g3}=0-0=0$, $Z_{g2}-Z_{g3}=500-0=500$ mm, and

$$D_{g23}=\sqrt{(X_{g2}-X_{g3})^2+(Y_{g2}-Y_{g3})^2+(Z_{g2}-Z_{g3})^2}=500 \text{ mm} \quad (\text{h})$$

vector \vec{od} is

$$C_{21}=\frac{X_{g2}-X_{g3}}{D_{g23}}=\frac{0}{500}=0, \ C_{22}=\frac{Y_{g2}-Y_{g3}}{D_{g23}}=0, \ C_{23}=\frac{Z_{g2}-Z_{g3}}{D_{g23}}=\frac{500}{500}=1 \quad (\text{i})$$

For line $oc = 50$ mm, $X_{gc} - X_{g3} = 50 \cos 30^\circ - 0 = 43.3$ mm, $Y_{gc} - Y_{g3} = 50 \cos 120^\circ - 0 = -25$ mm, $Z_{gc} - Z_{g3} = 0 - 0$, and

$$D_{gc3} = \sqrt{(X_{gc} - X_{g3})^2 + (Y_{gc} - Y_{g3})^2 + (Z_{gc} - Z_{g3})^2} = 50 \text{ mm} \quad (\text{j})$$

vector \vec{oc} is

$$C_{31} = \frac{X_{gc} - X_{g3}}{D_{gc3}} = \frac{43.3}{50} = 0.866, \quad C_{32} = \frac{Y_{gc} - Y_{g3}}{D_{gc3}} = \frac{-25}{50} = -0.5, \quad C_{33} = \frac{Z_{gc} - Z_{g3}}{D_{gc3}} = 0 \quad (\text{k})$$

Thus, at joint $J1$, we have

$$\{F_{e1}\} = [C_{e1}] \{F_{g1}\} = \begin{Bmatrix} F_{j1x} \\ F_{j1y} \\ F_{j1z} \end{Bmatrix} = \begin{bmatrix} C_{11} & C_{12} & C_{13} \\ C_{21} & C_{22} & C_{23} \\ C_{31} & C_{32} & C_{33} \end{bmatrix} \begin{Bmatrix} F_{xg1} \\ F_{yg1} \\ F_{zg1} \end{Bmatrix} = \begin{bmatrix} 0.5 & 0.866 & 0 \\ 0 & 0 & 1 \\ 0.866 & -0.5 & 0 \end{bmatrix} \begin{Bmatrix} F_{xg1} \\ F_{yg1} \\ F_{zg1} \end{Bmatrix} \quad (\text{l})$$

Due to fixity at the bottom of the shear wall, $[A_4]$ in Eq. (8.75) is reduced to

$$[A_4] = \begin{bmatrix} [C_{j1}][C_{e1}]^T & 0 \\ 0 & [C_{j2}][C_{e2}]^T \end{bmatrix} \quad (\text{m})$$

where $[C_{j1}] = [C_{j2}] = [I]$ and

$$[C_{j1}][C_{e1}]^T = [C_{j2}][C_{e2}]^T = \begin{bmatrix} 0.5 & 0 & 0.866 \\ 0.866 & 0 & -0.5 \\ 0 & 1 & 0 \end{bmatrix} \quad (\text{n})$$

Assuming the master joint is at $(0, 0, 500)$ of the GCS, we have $[X_{gm} \ Y_{gm} \ Z_{gm}]^T = [0 \ 0 \ 500]^T$ and

$$\begin{Bmatrix} X_{gs} \\ Y_{gs} \\ Z_{gs} \end{Bmatrix}_1 = \begin{Bmatrix} 1000 \sin 30^\circ \\ 1000 \cos 30^\circ \\ 500 \end{Bmatrix} = \begin{Bmatrix} 500 \\ 866 \\ 500 \end{Bmatrix} \quad (\text{o})$$

Using Eq. (8.5) yields

$$\begin{Bmatrix} X_{ms} \\ Y_{ms} \\ Z_{ms} \end{Bmatrix}_1 = \begin{bmatrix} 1 & 0 & 0 \\ 0 & 1 & 0 \\ 0 & 0 & 1 \end{bmatrix} \begin{Bmatrix} 500 - 0 \\ 866 - 0 \\ 500 - 500 \end{Bmatrix} = \begin{Bmatrix} 500 \\ 866 \\ 0 \end{Bmatrix} \quad (\text{p})$$

Thus $[T'_{ms}]$ for $J1$ from Eq. (8.77) is

$$[T'_{ms}]_1 = \begin{bmatrix} 1 & 0 & 0 \\ 0 & 1 & 0 \\ 0 & 0 & 1 \\ 0 & 0 & 0 \\ 0 & 0 & 0 \\ -Y_{ms1} & X_{ms1} & 0 \end{bmatrix} = \begin{bmatrix} 1 & 0 & 0 \\ 0 & 1 & 0 \\ 0 & 0 & 1 \\ 0 & 0 & 0 \\ 0 & 0 & 0 \\ -866 & 500 & 0 \end{bmatrix} \quad (\text{q})$$

Similarly for $J2$

$$[T'_{ms}]_2 = \begin{bmatrix} 1 & 0 & 0 \\ 0 & 1 & 0 \\ 0 & 0 & 1 \\ 0 & 0 & 0 \\ 0 & 0 & 0 \\ -Y_{ms2} & X_{ms2} & 0 \end{bmatrix} = \begin{bmatrix} 1 & 0 & 0 \\ 0 & 1 & 0 \\ 0 & 0 & 1 \\ 0 & 0 & 0 \\ 0 & 0 & 0 \\ 0 & 0 & 0 \end{bmatrix} \quad (r)$$

$$\begin{Bmatrix} X_{gs} \\ Y_{gs} \\ Z_{gs} \end{Bmatrix}_2 = \begin{Bmatrix} 0 \\ 0 \\ 500 \end{Bmatrix}; \quad \begin{Bmatrix} X_{ms} \\ Y_{ms} \\ Z_{ms} \end{Bmatrix}_2 = \begin{bmatrix} 1 & 0 & 0 \\ 0 & 1 & 0 \\ 0 & 0 & 1 \end{bmatrix} \begin{Bmatrix} 0-0 \\ 0-0 \\ 500-500 \end{Bmatrix} = \begin{Bmatrix} 0 \\ 0 \\ 0 \end{Bmatrix} \quad (s)$$

From Eq. (8.80), we have

$$[A_s] = \begin{bmatrix} 1 & 0 & 0 & 0 & 0 & 0 \\ 0 & 1 & 0 & 0 & 0 & 0 \\ 0 & 0 & 1 & 0 & 0 & 0 \\ 0 & 0 & 0 & 0 & 0 & 0 \\ 0 & 0 & 0 & 0 & 0 & 0 \\ -866 & 500 & 0 & 0 & 0 & 0 \\ 0 & 0 & 0 & 1 & 0 & 0 \\ 0 & 0 & 0 & 0 & 1 & 0 \\ 0 & 0 & 0 & 0 & 0 & 1 \\ 0 & 0 & 0 & 0 & 0 & 0 \\ 0 & 0 & 0 & 0 & 0 & 0 \\ 0 & 0 & 0 & 0 & 0 & 0 \end{bmatrix} \quad (t)$$

Finally the stiffness matrix is obtained from Eq. (8.81) and (8.84) as

$$\{F_{jm}\} = [K^i]\{\delta_{jm}\} = [A][K_e][A]^T\{\delta_{jm}\}$$

$$= \left\{ \begin{array}{l} F_{j1mx} \\ F_{j1my} \\ F_{j1mz} \\ M_{j1mx} \\ M_{j1my} \\ M_{j1mz} \\ F_{j2mx} \\ F_{j2my} \\ F_{j2mz} \\ M_{j2mx} \\ M_{j2my} \\ M_{j2mz} \end{array} \right\} = 10^5 \left[\begin{array}{ccccccccc} 5.520 & 9.561 & 5.520 & 0 & 0 & 0 & 0 & -5.520 & 0 & 0 & 0 \\ 16.66 & 9.561 & 0 & 0 & 0 & 0 & 0 & -9.561 & 0 & 0 & 0 \\ & & 26.72 & 0 & 0 & 0 & 0 & 5.084 & 0 & 0 & 0 \\ & & & 0 & 0 & 0 & 0 & 0 & 0 & 0 & 0 \\ & & & & 0 & 0 & 0 & 0 & 0 & 0 & 0 \\ & & & & & 0 & 0 & 0 & 0 & 0 & 0 \\ & & & & & & 0 & 0 & 0 & 0 & 0 \\ & & & & & & & 0 & 0 & 0 & 0 \\ & & & & & & & & 26.72 & 0 & 0 \\ & & & & & & & & & 0 & 0 \\ & & & & & & & & & & 0 \end{array} \right] \left\{ \begin{array}{l} \delta_{j1mx} \\ \delta_{j1my} \\ \delta_{j1mz} \\ \theta_{j1mx} \\ \theta_{j1my} \\ \theta_{j1mz} \\ \delta_{j2mx} \\ \delta_{j2my} \\ \delta_{j2mz} \\ \theta_{j2mx} \\ \theta_{j2my} \\ \theta_{j2mz} \end{array} \right\} \quad (u)$$

From systems analysis procedure, the d.o.f. associated with a slave joint are assigned to a master joint. In this case, forces at $J2$ are transferred from $J1$ by d.o.f. identification (see Example 8.12.1). F_{j1mz} is not transferable and stays at $J1$; M_{j1mx} , M_{j1my} , and M_{j1mz} are dummy forces assigned to nodal d.o.f. for structural stiffness formulation of a 3D building structure. The cor-

rectness of the coefficients in Eq. (u) is checked by first noting that the moments and rotations are associated with dummy d.o.f. (For the purpose of connecting a wall's node to a typical structural joint of the six d.o.f., see accompanying Fig. 8.20c.) Therefore no stiffness coefficients exist in Eq. (u). Other stiffness coefficients are checked as follows:

$K_{1,2}$ and $K_{2,2}$ due to δ_{j1my} (see Fig. 8.20b)

$$F_1 = (K_s/h)\delta_1 = (1.104)10^9/500\delta_1 = 22.08(10)^5\delta_1; \quad \delta_1 = \delta_{j1my} \cos 30^\circ \quad (v)$$

$$F_{j1mx} = F_1 \sin 30^\circ = F_1 \sin 30^\circ \cos 30^\circ \delta_{j1my} = (9.561)10^5\delta_{j1my} = K_{1,2}\delta_{j1my} \quad (w)$$

$$F_{j1my} = F_1 \cos 30^\circ = F_1 \cos 30^\circ \delta_{j1my} = 16.66(10)^5\delta_{j1my} = K_{2,2}\delta_{j1my} \quad (x)$$

$K_{1,3}$ and $K_{2,3}$ due to δ_{j1mz} (see Fig. 8.20d)

$$\delta_1 = (h/w)\delta_{j1mz}; \quad F_1 = V_a = (K_s/h)\delta_1 = (1.104)10^9/2(500)\delta_{j1mz} = 11.04(10)^5\delta_{j1mz} \quad (y)$$

$$F_{j1mx} = F_1 \sin 30^\circ = 5.52(10)^5\delta_{j1my} = K_{1,3}\delta_{j1mz} \quad (z)$$

$$F_{j1my} = F_1 \cos 30^\circ = 9.561(10)^5\delta_{j1mx} = K_{2,3}\delta_{j1mz} \quad (aa)$$

8.7.4. Shear-Wall Geometric Matrix (String Stiffness) in the JCS or GCS Based on Method 1

To be consistent with lumped mass formulation, the geometric matrix of shear walls is formulated in *string stiffness*. A wall is idealized as a rigid body in the plane of the wall with d.o.f. 1 and 8 as shown in Fig. 8.21a. Axial load P is positive when the wall is in compression. Since the wall's out-of-plane stiffness is not considered, the vertical ends of the wall (perpendicular to its plane) are idealized as two rigid bars so they can move independently in accordance with deformation of other elements connected to them. As shown in Fig. 8.21b, one rigid bar has d.o.f. 3 and 10; the other has 5 and 7. Both bars share an axial load with $P/2$. Thus the element geometric matrix in the ECS is

$$[K_{eg}] = \frac{P}{2h} \begin{bmatrix} 2 & 0 & 0 & 0 & 0 & 0 & 0 & -2 & 0 & 0 \\ 0 & 0 & 0 & 0 & 0 & 0 & 0 & 0 & 0 & 0 \\ 0 & 0 & 1 & 0 & 0 & 0 & 0 & 0 & 0 & -1 \\ 0 & 0 & 0 & 0 & 0 & 0 & 0 & 0 & 0 & 0 \\ 0 & 0 & 0 & 0 & 1 & 0 & -1 & 0 & 0 & 0 \\ 0 & 0 & 0 & 0 & -1 & 0 & 0 & 0 & 0 & 0 \\ 0 & 0 & 0 & 0 & 0 & 0 & 1 & 0 & 0 & 0 \\ -2 & 0 & 0 & 0 & 0 & 0 & 0 & 2 & 0 & 0 \\ 0 & 0 & 0 & 0 & 0 & 0 & 0 & 0 & 0 & 0 \\ 0 & 0 & -1 & 0 & 0 & 0 & 0 & 0 & 0 & 1 \end{bmatrix} \quad (8.85)$$

The following geometric matrix is obtained by transferring the ECS to JCS or GCS, depending on whether JCS and GCS are assumed to coincide

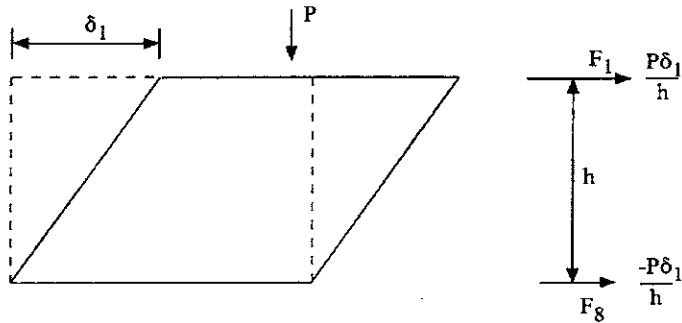
$$[K_g^i] = [A][K_{eg}][A]^T \quad (8.86)$$

8.8. BRACING ELEMENTS

8.8.1. Bracing-Element ECS and GCS Relationship Based on Method 1

A bracing element consists of two joints, A and B , as shown in Fig. 8.22. Orientation of the bracing element is defined by ECS. Locations of both the start-joint A and end-joint B are defined in the GCS. Let X_{gs} , Y_{gs} , Z_{gs} be the coordinates of joint A , and X_{ge} , Y_{ge} , Z_{ge} be the coordinates of

(a)



(b)

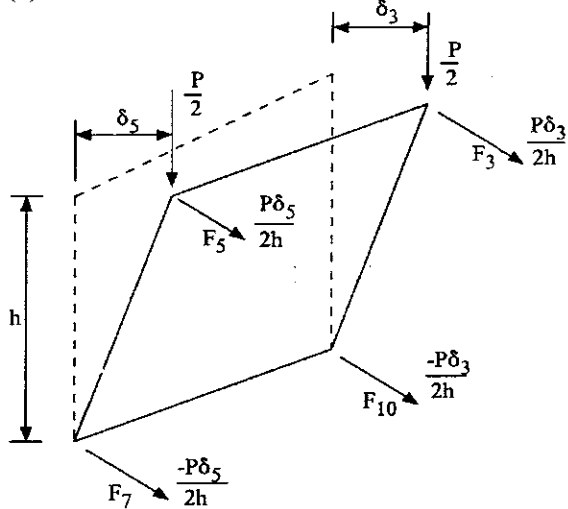


FIG. 8.21 $P-\Delta$ effect on shear wall. (a) In-plane deformation. (b) Out-of-plane deformation.

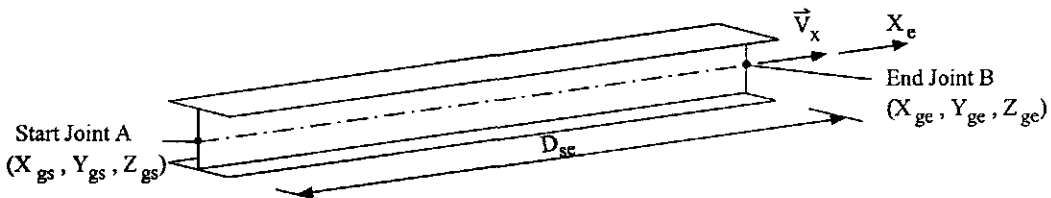


FIG. 8.22 ECS of bracing element.

joint *B*. The distance between *A* and *B* is given by

$$D_{se} = \sqrt{(X_{ge} - X_{gs})^2 + (Y_{ge} - Y_{gs})^2 + (Z_{ge} - Z_{gs})^2} \quad (8.87)$$

The unit vector, \vec{V}_x , from the start joint to the end joint is

$$\vec{V}_x = \frac{(X_{ge} - X_{gs})\hat{i} + (Y_{ge} - Y_{gs})\hat{j} + (Z_{ge} - Z_{gs})\hat{k}}{D_{se}} \quad (8.88)$$

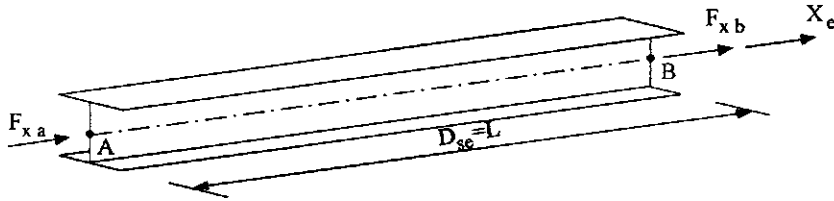


FIG. 8.23 Local d.o.f. for bracing element.

Vector \vec{V}_x defines the orientation of the member's local X_e axis. Let the origin of X_e be at joint A . The vector that defines the orientation of the element coordinate system can be written as

$$\{V_e\} = \vec{V}_x = [C_{11} \quad C_{12} \quad C_{13}] \begin{Bmatrix} \vec{i} \\ \vec{j} \\ \vec{k} \end{Bmatrix} = [C_e] \begin{Bmatrix} \vec{i} \\ \vec{j} \\ \vec{k} \end{Bmatrix} \quad (8.89)$$

where $[C_e]$ is the direction cosine matrix of the ECS (see Example 8.8.1); \vec{i} , \vec{j} , and \vec{k} are unit vectors of the GCS. The element has two d.o.f. as shown in Fig. 8.23; its forces and displacements in the ECS are

$$\{F_e\} = [F_{xa} \quad F_{xb}]^T \quad (8.90a)$$

$$\{\delta_e\} = [\delta_{xa} \quad \delta_{xb}]^T \quad (8.90b)$$

8.8.2. Bracing-Element Stiffness in ECS

Stiffness of a bracing element corresponding to the \vec{V}_x direction can be expressed as

$$\{F_e\} = \begin{Bmatrix} F_{xa} \\ F_{xb} \end{Bmatrix} = K_{br} \begin{bmatrix} 1 & -1 \\ -1 & 1 \end{bmatrix} \begin{Bmatrix} \delta_{xa} \\ \delta_{xb} \end{Bmatrix} = [K_e] \{\delta_e\} \quad (8.91)$$

where K_{br} represents the axial stiffness coefficient. For the elastic case, $K_{br} = AE/L$; for the inelastic case, K_{br} is based on the hysteresis rules discussed in Chapter 9.

8.8.3. Bracing-Element Stiffness in the JCS or GCS Based on Method 1

Since the procedure of transformation between the forces in the JCS or GCS and those in the ECS is similar to that used for beam–column elements in Section 8.6.3, it is presented only briefly here. For the relationship between ECS and GCS, we have

$$\{F_e\} = \begin{bmatrix} [C_e] & 0 \\ 0 & [C_e] \end{bmatrix} \{F_g\} = [\bar{C}_e] \{F_g\} \quad (8.92)$$

where $\{F_e\}$ and $\{F_g\}$ represent the forces in the ECS and GCS, respectively; and $[\bar{C}_e]$ is the direction cosine matrix of the ECS. Thus rotating the element forces to global forces yields

$$\{F_g\} = [\bar{C}_e]^T \{F_e\} \quad (8.93)$$

Expressing the joint forces, $\{F_j\}$, in terms of the global forces gives

$$\{F_j\} = \begin{bmatrix} [C_j]_A & 0 \\ 0 & [C_j]_B \end{bmatrix} \{F_g\} = [\bar{C}_j] \{F_g\} \quad (8.94)$$

Substituting Eq. (8.93) into the above leads to

$$\{F_j\} = [\bar{C}_j][\bar{C}_e]^T \{F_e\} \quad (8.95)$$

Constraint transformation of the forces from slave joint to master joint is illustrated by Fig. 8.24. F_{jsz} at the slave joint cannot be transferred to the master joint and stays as F_{jmz} ; F_{jsx} and F_{jsy} are transferred to the master joint as F_{jm_x} and F_{jm_y} , respectively, and also induce torsional moment, M_{jm_z} . Two dummy d.o.f. are $M_{jm_x}(M_{js_x})=0$, $M_{jm_y}(M_{js_y})=0$. Symbols (M_{js_x}) and (M_{js_y}) imply that dummy moments M_{jm_x} and M_{jm_y} correspond to M_{js_x} and M_{js_y} , respectively. The resulting transformation is

$$\begin{bmatrix} F_{jm_x} \\ F_{jm_y} \\ F_{jm_z} \\ M_{jm_x} \\ M_{jm_y} \\ M_{jm_z} \end{bmatrix} = \begin{bmatrix} 1 & 0 & 0 \\ 0 & 1 & 0 \\ 0 & 0 & 1 \\ 0 & 0 & 0 \\ 0 & 0 & 0 \\ -(Y_{gs} - Y_{gm}) & (X_{gs} - X_{gm}) & 0 \end{bmatrix} \begin{bmatrix} F_{js_x} \\ F_{js_y} \\ F_{js_z} \end{bmatrix} \quad (8.96)$$

$$= \begin{bmatrix} 1 & 0 & 0 \\ 0 & 1 & 0 \\ 0 & 0 & 1 \\ 0 & 0 & 0 \\ 0 & 0 & 0 \\ -Y_{ms} & X_{ms} & 0 \end{bmatrix} \begin{bmatrix} F_{js_x} \\ F_{js_y} \\ F_{js_z} \end{bmatrix} = [T'_{ms}] \begin{bmatrix} F_{js_x} \\ F_{js_y} \\ F_{js_z} \end{bmatrix}$$

which is identical to Eq. (8.77) and is therefore similarly expressed [see also Eq. (8.40)] as

$$\{F_{jm}\} = [\bar{T}'_{ms}] \{F_j\} \quad (8.97)$$

where

$$[\bar{T}'_{ms}] = \begin{bmatrix} [T'_{ms}]_A & 0 \\ 0 & [T'_{ms}]_B \end{bmatrix}$$

Distances Y_{gs} , Y_{gm} , X_{gs} , and X_{gm} are shown in Fig. 8.24b and can be used in Eq. 8.5 for Y_{ms} and X_{ms} as

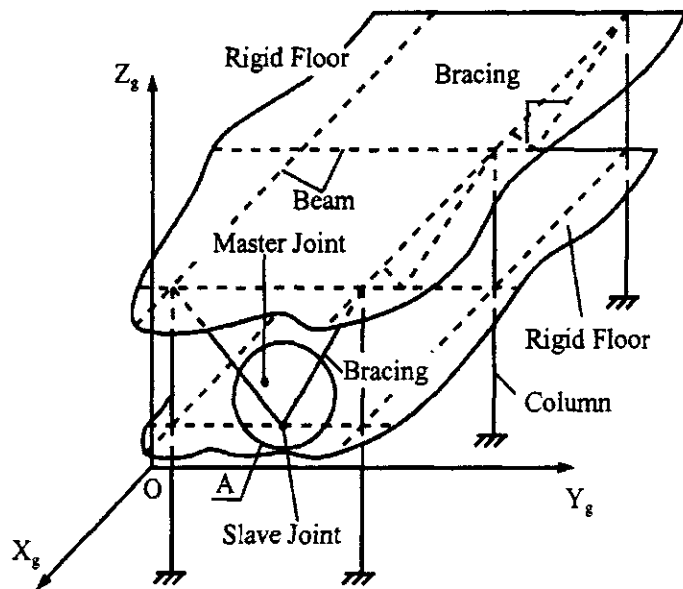
$$\begin{bmatrix} Y_{ms} \\ Y_{ms} \\ Z_{ms} \end{bmatrix} = [C_j] \begin{bmatrix} X_{gs} - X_{gm} \\ Y_{gs} - Y_{gm} \\ Z_{gs} - Z_{gm} \end{bmatrix} \quad (8.98)$$

Formulation of the stiffness matrix expressed in the JCS or GCS (if the JCS and GCS coincide, then the stiffness matrix is the GCS) uses Eqs. (8.41)–(8.43). The result is

$$[K^i] = [A][K_e][A]^T \quad (8.99)$$

Note that the $P-\Delta$ effect is not considered for bracing members. The $P-\Delta$ effect of the beam-column or shear wall, as presented earlier, is based on the following consideration: axial force on a member is obtained from the load either directly applied to the member or lumped on the member from the floor load, or both. A bracing member's force can only be obtained

(a)



(b)

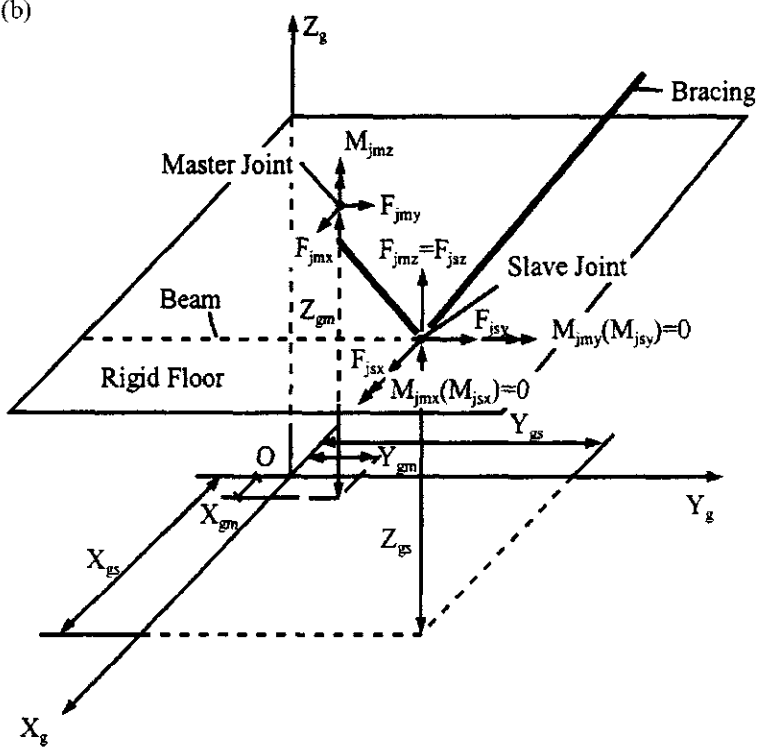


FIG. 8.24 Relationship between master and slave joints of bracing element. (a) Arbitrary master joint in relation to bracing-element's slave joint. (b) Detail at Section A.

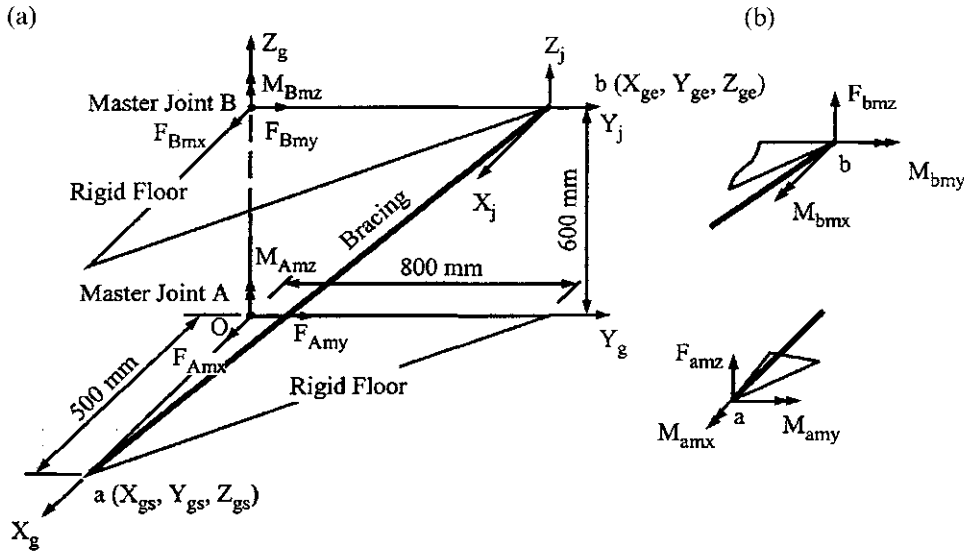


FIG. 8.25 Example 8.8.1. (a) Forces transferred to *A* and *B*. (b) Forces staying at *a* and *b*.

after first-order structural analysis. For simplicity, this force is not included in geometric matrix formulation, which therefore is not presented (see Section 9.7 for *geometric nonlinear* analysis after *first-order analysis*).

EXAMPLE 8.8.1 Determine the stiffness matrix in GCS of the bracing element shown in Fig. 8.25. The member is $W8 \times 67$ for which $A = 12,710 \text{ mm}^2$ and $E = 210,000 \text{ N/mm}^2$. Coordinates of points *A* and *B* are: $X_{gs} = 500 \text{ mm}$, $Y_{gs} = Z_{gs} = 0$, $X_{ge} = 0$, $Y_{ge} = 800 \text{ mm}$, and $Z_{ge} = 600 \text{ mm}$.

Solution: For Eq. (8.89), $[C_e]$ is obtained as follows:

$$\begin{aligned}
 D_{se} &= \sqrt{(X_{ge} - X_{gs})^2 + (Y_{ge} - Y_{gs})^2 + (Z_{ge} - Z_{gs})^2} = \sqrt{(-500)^2 + (800)^2 + (600)^2} = 1118.034 \text{ mm} \\
 C_{11} &= \frac{X_{ge} - X_{gs}}{D_{se}} = \frac{0 - 500}{1118.034} = -0.447 \\
 C_{12} &= \frac{Y_{ge} - Y_{gs}}{D_{se}} = \frac{800 - 0}{1118.034} = 0.716 \\
 C_{13} &= \frac{Z_{ge} - Z_{gs}}{D_{se}} = \frac{600}{1118.034} = 0.537 \\
 [C_e]_a &= [-0.447 \quad 0.716 \quad 0.537] \tag{a}
 \end{aligned}$$

Similarly

$$[C_e]_b = [C_e]_a \tag{b}$$

Assume the JCS is parallel to the GCS; then

$$[C_j]_a = [C_j]_b = \begin{bmatrix} 1 & 0 & 0 \\ 0 & 1 & 0 \\ 0 & 0 & 1 \end{bmatrix} \quad (c)$$

The floor slab is in the $X_g - Y_g$ plane and the master joints are assumed to be at A and B of the lower and upper floors. Let the GCS originate at A . Force transformation for the bracing element is then expressed as

at joint A

$$\begin{Bmatrix} X_{ms} \\ Y_{ms} \\ Z_{ms} \end{Bmatrix} = [C_j] \begin{Bmatrix} X_{gs} - X_{gm} \\ Y_{gs} - Y_{gm} \\ Z_{gs} - Z_{gm} \end{Bmatrix} = \begin{bmatrix} 1 & 0 & 0 \\ 0 & 1 & 0 \\ 0 & 0 & 1 \end{bmatrix} \begin{Bmatrix} 500 - 0 \\ 0 - 0 \\ 0 - 0 \end{Bmatrix} = \begin{Bmatrix} 500 \\ 0 \\ 0 \end{Bmatrix} \quad (d)$$

and

$$[T'_{ms}]_A = \begin{bmatrix} 1 & 0 & 0 & 0 & 0 & 0 \\ 0 & 1 & 0 & 0 & 0 & 500 \\ 0 & 0 & 1 & 0 & 0 & 0 \end{bmatrix}^T \quad (e)$$

at joint B

$$\begin{Bmatrix} X_{ms} \\ Y_{ms} \\ Z_{ms} \end{Bmatrix} = [C_j] \begin{Bmatrix} X_{gs} - X_{gm} \\ Y_{gs} - Y_{gm} \\ Z_{gs} - Z_{gm} \end{Bmatrix} = \begin{bmatrix} 1 & 0 & 0 \\ 0 & 1 & 0 \\ 0 & 0 & 1 \end{bmatrix} \begin{Bmatrix} 0 - 0 \\ 800 - 0 \\ 600 - 600 \end{Bmatrix} = \begin{Bmatrix} 0 \\ 800 \\ 0 \end{Bmatrix} \quad (f)$$

and

$$[T'_{ms}]_B = \begin{bmatrix} 1 & 0 & 0 & 0 & 0 & -800 \\ 0 & 1 & 0 & 0 & 0 & 0 \\ 0 & 0 & 1 & 0 & 0 & 0 \end{bmatrix}^T \quad (g)$$

Thus from Eq. (8.41),

$$\begin{aligned} [A] &= [\bar{T}_{ms}] [\bar{C}_j] [\bar{C}_e]^T = \begin{bmatrix} [T'_{ms}]_A & 0 \\ 0 & [T'_{ms}]_B \end{bmatrix} \begin{bmatrix} [C_j]_a & 0 \\ 0 & [C_j]_b \end{bmatrix} \begin{bmatrix} [C_e]_a^T & 0 \\ 0 & [C_e]_b^T \end{bmatrix} \\ &= \begin{bmatrix} -0.447 & 0.716 & 0.537 & 0 & 0 & 358 & 0 & 0 & 0 & 0 & 0 & 0 \\ 0 & 0 & 0 & 0 & 0 & 0 & -0.447 & 0.716 & 0.537 & 0 & 0 & 357.6 \end{bmatrix}^T \end{aligned} \quad (h)$$

The stiffness coefficient of the bracing member is

$$K_{br} = \frac{AE}{L} = \frac{AE}{D_{se}} = \frac{(12,710)(210,000)}{1118.034} = (2.387)10^6 \text{ N/mm} \quad (i)$$

The stiffness matrix in GCS is then obtained from Eq. (8.99) as

$$\left\{ \begin{array}{l} F_{Amx} \\ F_{Amy} \\ F_{amz} \\ M_{amx} \\ M_{amy} \\ M_{amz} \\ F_{Bmx} \\ F_{Bmy} \\ F_{bmz} \\ M_{bmx} \\ M_{bmy} \\ M_{bmz} \end{array} \right\} = 10^5 \left[\begin{array}{ccccccccccccc} 4.769 & -7.640 & -5.730 & 0 & 0 & -3820 & -4.769 & 7.640 & 5.730 & 0 & 0 & 3816 \\ 12.24 & 9.178 & 0 & 0 & 6119 & 7.639 & -12.24 & -9.178 & 0 & 0 & -6112 \\ 6.883 & 0 & 0 & 4589 & 5.730 & -9.178 & -6.883 & 0 & 0 & -4584 \\ 0 & 0 & 0 & 0 & 0 & 0 & 0 & 0 & 0 & 0 & 0 \\ 0 & 0 & 0 & 0 & 0 & 0 & 0 & 0 & 0 & 0 & 0 \\ 3059(10)^3 & 3820 & -6119 & -4589 & 0 & 0 & -3056(10)^3 \\ 4.769 & -7.640 & -5.730 & 0 & 0 & -3816 \\ 12.24 & 9.178 & 0 & 0 & 6112 \\ 6.883 & 0 & 0 & 4584 \\ 0 & 0 & 0 & 0 & 0 \\ 0 & 0 & 0 & 0 & 0 \\ 3.052(10)^6 \end{array} \right] \quad (j)$$

Note that joints *a* and *b* are structural nodes at which the forces that cannot be transferred to the master joints should stay. Thus each of these two nodes has three forces remaining. For instance, node *a* has F_{amz} , M_{amx} , M_{amz} . Among them, only vertical force F_{amz} exists (as nonzero) and the bending moments are zero, which are assigned here as dummy to match the structural system's d.o.f.

8.9. STRUCTURAL CHARACTERISTICS OF 3-D BUILDING SYSTEMS

As a comprehensive illustration of formulating structural stiffness matrix, a 3D one-story building comprising various structural components is shown in Fig. 8.26 with structural nodes numbered 1–8. Structural components include an in-plane rigid floor on the X_g - Y_g plane, a wall in the vertical direction along the Z_g -axis, column 2–6 vertical, column 1–5 slanted, and a bracing member connecting nodes 1 and 6. Note that the floor has a mass center (MC) which is also a master joint. The MC may signify a master joint without mass lumped on it. These structural components are further studied here with consideration of building characteristics through the second method of coordinate transformation.

8.10. RIGID ZONE BETWEEN MEMBER END AND JOINT CENTER

In structural analysis, we usually consider (as in previous chapters) that a structural member is connected to a structural joint, and member length is measured from center line to center line of joints to which the member is connected. In reality, structural members intersect at the joints, and member ends are at the surface where the member connects, such as a beam's connection to a column. Therefore member length should be measured from a surface (i.e. member end), but not from the center of a joint. Deformation between surface and center line due to rigidity

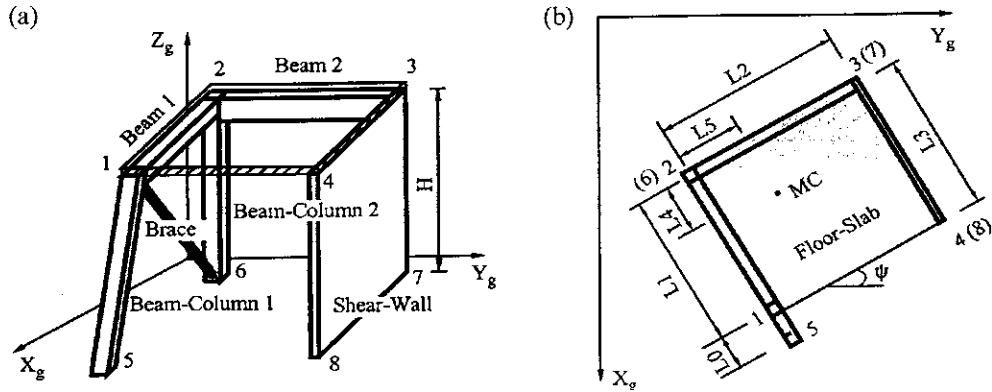


FIG. 8.26 Three-dimensional building configuration. (a) Elevation. (b) Floor plane.

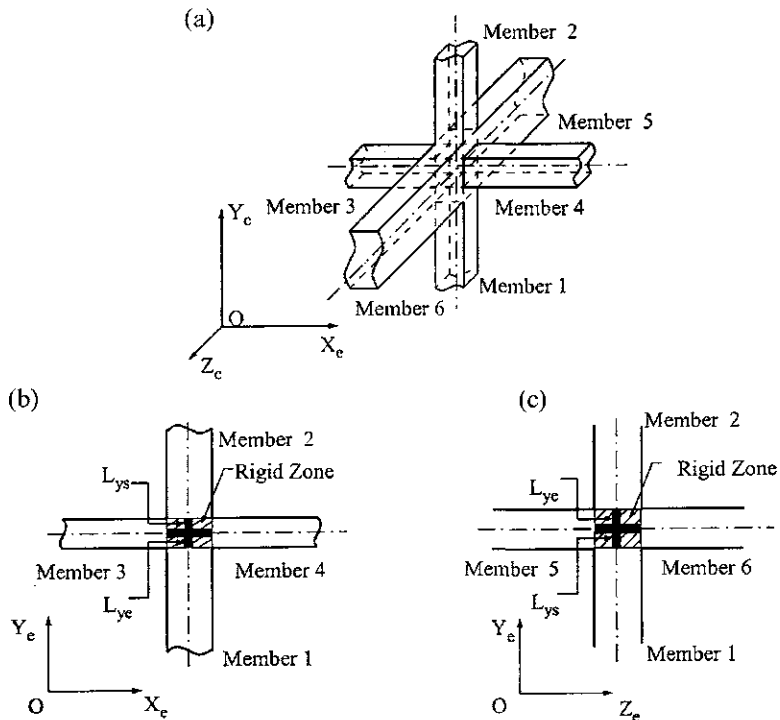


FIG. 8.27 Rigid zones of structural connection. (a) Structural connection. (b) Rigid Zones in \$X_e - Y_e\$ plane. (c) Rigid zones in \$Z_e - Y_e\$ plane.

of connections (such as a slab) is complex and may be defined as a *rigid zone*. A typical rigid zone is shown in Fig. 8.27; it is assumed to have no deformation and to move as a rigid body with the member end connected to that zone.

Figure 8.27a shows a joint of six members (elements) for which the rigid zones of members 1 and 2 are displayed in Fig. 8.27b and c, where \$L_{ys}\$ and \$L_{ye}\$ express the length of rigid zones in the \$X_e - Y_e\$ plane, respectively; \$L_{zs}\$ and \$L_{ze}\$ express the length of rigid zones in the \$Z_e - Y_e\$ plane, respectively. Subscripts \$s\$ and \$e\$ stand for the start joint and end joint of a member (see Fig. 8.28). \$X_e\$, \$Y_e\$, and \$Z_e\$ axes are the element coordinates of the ECS.

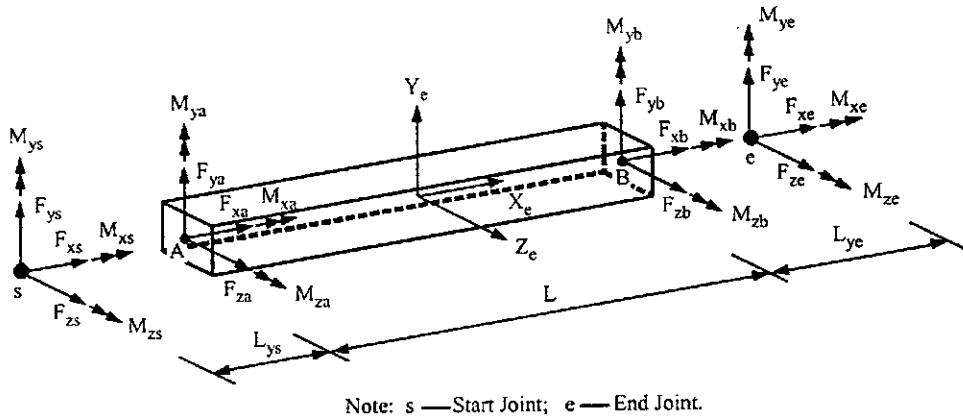


FIG. 8.28 Force transformation from member end to joint center.

8.11. BUILDING-STRUCTURE-ELEMENT STIFFNESS WITH RIGID ZONE

8.11.1. Beam-Column Stiffness in ECS Based on Method 2

With consideration of the rigid zone, the beam-column element stiffness in the ECS shown in Fig. 8.12 and derived in Eq. (8.31) should be modified to transfer member-end forces $\{F_e\}$ to structural joints. A typical 3D beam-column element is shown in Fig. 8.28, for which the moments at start joint s due to F_{ya} and at end joint e due to F_{yb} are

$$M_{zs} = F_{ya}L_{ys}; \quad M_{ze} = -F_{yb}L_{ye}$$

Similarly, the moments due to F_{za} and F_{zb} are

$$M_{ys} = -F_{za}L_{zs}; \quad M_{ye} = F_{zb}L_{ze}$$

By summing the forces and moments at the joints,

$$\{F'_e\} = \begin{Bmatrix} F_{xs} \\ F_{ys} \\ F_{zs} \\ M_{xs} \\ M_{ys} \\ M_{zs} \\ F_{xe} \\ F_{ye} \\ F_{ze} \\ M_{xe} \\ M_{ye} \\ M_{ze} \end{Bmatrix} = \begin{bmatrix} 1 & 0 & 0 & 0 & 0 & 0 & 0 & 0 & 0 & 0 & 0 & 0 \\ 0 & 1 & 0 & 0 & 0 & 0 & 0 & 0 & 0 & 0 & 0 & 0 \\ 0 & 0 & 1 & 0 & 0 & 0 & 0 & 0 & 0 & 0 & 0 & 0 \\ 0 & 0 & 0 & 1 & 0 & 0 & 0 & 0 & 0 & 0 & 0 & 0 \\ 0 & 0 & -L_{zs} & 0 & 1 & 0 & 0 & 0 & 0 & 0 & 0 & 0 \\ 0 & L_{ys} & 0 & 0 & 0 & 1 & 0 & 0 & 0 & 0 & 0 & 0 \\ 0 & 0 & 0 & 0 & 0 & 0 & 1 & 0 & 0 & 0 & 0 & 0 \\ 0 & 0 & 0 & 0 & 0 & 0 & 0 & 1 & 0 & 0 & 0 & 0 \\ 0 & 0 & 0 & 0 & 0 & 0 & 0 & 0 & 1 & 0 & 0 & 0 \\ 0 & 0 & 0 & 0 & 0 & 0 & 0 & 0 & 0 & 1 & 0 & 0 \\ 0 & 0 & 0 & 0 & 0 & 0 & 0 & L_{ze} & 0 & 1 & 0 & 0 \\ 0 & 0 & 0 & 0 & 0 & 0 & 0 & 0 & 0 & 0 & 1 & 0 \end{bmatrix} \begin{Bmatrix} F_{xa} \\ F_{ya} \\ F_{za} \\ M_{xa} \\ M_{ya} \\ M_{za} \\ F_{xb} \\ F_{yb} \\ F_{zb} \\ M_{xb} \\ M_{yb} \\ M_{zb} \end{Bmatrix} = [T_{je}] \{F_e\}$$

(8.100)

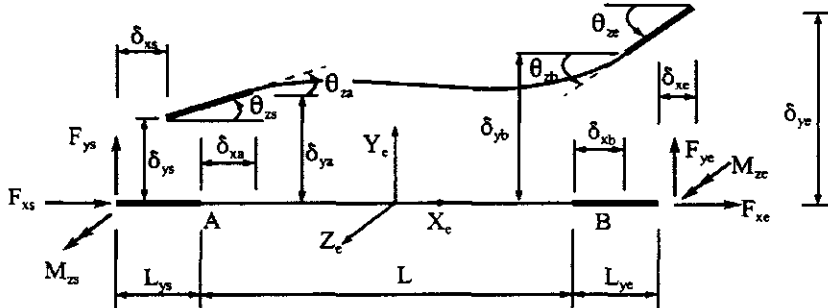


FIG. 8.29 Compatibility condition between joint center and member end.

or

$$\{F'_e\} = [T_{je}] \{F_e\} \quad (8.101)$$

where $[T_{je}]$ is *rigid-zone transfer matrix*. Note that if the rigid-zone at the member's end is not considered or is negligible, the transformation matrix $[T_{je}]$ reduces to an identity matrix.

The compatibility condition between the joint center and the member end is illustrated in Fig. 8.29 for deformations in the X_e - Y_e plane from which

$$\delta_{xa} = \delta_{xs} + L_{ys} \cos \theta_{zs} - L_{ys} \approx \delta_{xs} \quad (8.102a)$$

$$\delta_{ya} = \delta_{ys} + L_{ys} \sin \theta_{zs} \approx \delta_{ys} + L_{ys} \theta_{zs} \quad (8.102b)$$

$$\theta_{za} = \theta_{zs} \quad (8.102c)$$

$$\delta_{xb} = \delta_{xe} - L_{ye} \cos \theta_{ze} + L_{ye} \approx \delta_{xe} \quad (8.103a)$$

$$\delta_{yb} = \delta_{ye} - L_{ye} \sin \theta_{ze} \approx \delta_{ye} - L_{ye} \theta_{ze} \quad (8.103b)$$

$$\theta_{zb} = \theta_{ze} \quad (8.103c)$$

Eqs. (8.102a-c) correspond to columns 1, 2, and 6 in Eq. (8.100), respectively; Eqs. (8.103a-c) are also respectively identical to columns 7, 8, and 12 in that equation. Similarly, the compatibility condition of the member in the X_e - Z_e plane is the basis for the rest of the columns in Eq. (8.100). Thus the deformation relationship between member end δ_e and joint center δ'_e is

$$\{\delta_e\} = [T_{je}]^T \{\delta'_e\} \quad (8.104)$$

The element stiffness matrix at the joint center in the ECS is thus modified from Eq. (8.30) as

$$\{F'_e\} = [T_{je}] [K_e] [T_{je}]^T \{\delta'_e\} \quad (8.105)$$

Using $[K_e] = [A_e] [S_I] [A_e]^T$ [see Eq. (8.30)] in the above yields

$$[K'_e] = [T_{je}] [A_e] [S_I] [A_e]^T [T_{je}]^T = [A'_e] [S_I] [A'_e]^T \quad (8.106)$$

If a rigid zone is not considered, then $[A'_e] = [A_e]$ and $[K'_e] = [K_e]$.

Transformation from the joint's d.o.f. to global d.o.f. is similar to transformation from the member-end's d.o.f. to global d.o.f. without a rigid zone. Note that the transformation technique of Method 2 presented in appendices G and H is applied here to general 3D building structures.

8.11.2. Beam–Column Stiffness in GCS Based on Method 2

The beam–column stiffness derived in Section 8.6 is expressed in the JCS or GCS and is given in terms of various transformation matrices. The stiffness matrix is now presented in detailed form with all transformations done in the GCS. This form is convenient for system stiffness assembly in classroom teaching as well as for computer facilities with less storage capacity. The stiffness is thus ready for use without manipulation of transformation matrices. More importantly, its detailed form provides a means of understanding the physical sense of individual stiffness coefficients, which will be discussed later for beam–columns and other elements. This discussion of stiffness includes various parameters such as angles between member axis and joint axis, between joint axis and GCS, as well as rigid zones. An individual parameter can be dropped from the general expression if it is not to be considered.

Combining Eqs. (8.41)–(8.43) with Eq. (8.105), we obtain the stiffness matrix of a beam–column with rigid zone in the JCS as

$$[K^i] = [\bar{T}_{ms}][\bar{C}_j][\bar{C}_e]^T[T_{je}][K_e]([\bar{T}_{ms}][\bar{C}_j][\bar{C}_e]^T[T_{je}])^T \quad (8.107)$$

Let

$$[A'] = [\bar{T}_{ms}][\bar{C}_j][\bar{C}_e]^T[T_{je}] \quad (8.108)$$

Then

$$[K^i] = [A'][K_e][A']^T \quad (8.109)$$

If the rigid zone is not considered, then $[A'] = [A]$, which is the same as that expressed in Eq. (8.41).

To illustrate a general case, let a beam–column be arbitrarily oriented in a space as shown in Fig. 8.30 (see Fig. E-2 in Appendix E). The element transformation matrix between ECS and JCS is derived in Appendix E with the following result:

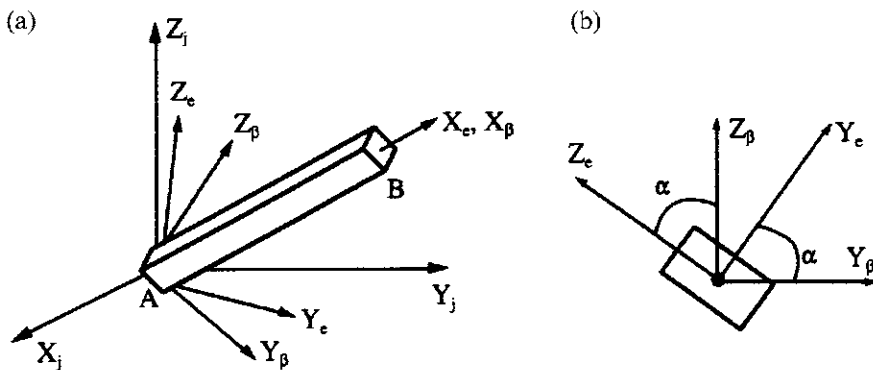


FIG. 8.30 Beam–column element in space. (a) Beam–column in space. (b) Angle α .

$$\begin{aligned}
 [C_e] &= \begin{bmatrix} l_1 & l_2 & l_3 \\ m_1 & m_2 & m_3 \\ n_1 & n_2 & n_3 \end{bmatrix} \\
 &= \begin{bmatrix} c_x & c_y & c_z \\ -\frac{1}{m}(c_x c_y \cos \alpha + c_z \sin \alpha) & m \cos \alpha & \frac{1}{m}(c_x \sin \alpha - c_y c_z \cos \alpha) \\ \frac{1}{m}(c_x c_y \sin \alpha - c_z \cos \alpha) & -m \sin \alpha & \frac{1}{m}(c_y c_z \sin \alpha + c_x \cos \alpha) \end{bmatrix} \quad (8.110)
 \end{aligned}$$

The transformation between the JCS and GCS is derived in Appendix D, for which the result is given in Eq. (8.1a) and repeated as follows:

$$\begin{aligned}
 [C_j]_A &= \begin{bmatrix} i_{1A} & i_{2A} & i_{3A} \\ j_{1A} & j_{2A} & j_{3A} \\ k_{1A} & k_{2A} & k_{3A} \end{bmatrix} \\
 &= \begin{bmatrix} \cos \beta \cos \gamma & \sin \beta & \cos \beta \sin \gamma \\ -\cos \phi \sin \beta \cos \gamma - \sin \phi \sin \gamma & \cos \phi \cos \beta & -\sin \gamma \cos \phi \sin \beta + \sin \phi \cos \gamma \\ \cos \gamma \sin \phi \sin \beta - \sin \gamma \cos \phi & -\sin \phi \cos \beta & \sin \phi \sin \beta \sin \gamma + \cos \phi \cos \gamma \end{bmatrix}_A \quad (8.111a)
 \end{aligned}$$

and

$$\begin{aligned}
 [C_j]_B &= \begin{bmatrix} i_{1B} & i_{2B} & i_{3B} \\ j_{1B} & j_{2B} & j_{3B} \\ k_{1B} & k_{2B} & k_{3B} \end{bmatrix} \\
 &= \begin{bmatrix} \cos \beta \cos \gamma & \sin \beta & \cos \beta \sin \gamma \\ -\cos \phi \sin \beta \cos \gamma - \sin \phi \sin \gamma & \cos \phi \cos \beta & -\sin \gamma \cos \phi \sin \beta + \sin \phi \cos \gamma \\ \cos \gamma \sin \phi \sin \beta - \sin \gamma \cos \phi & -\sin \phi \cos \beta & \sin \phi \sin \beta \sin \gamma + \cos \phi \cos \gamma \end{bmatrix}_B \quad (8.111b)
 \end{aligned}$$

Note that angles β , γ , and ϕ at A are not necessarily the same as at B . Transformation matrix $[A']$ and global element matrix $[K']$ for this general case are given in Appendix F.

In a building structure, the center line of a column is usually perpendicular to the X_g-Y_g plane of the GCS as shown in Fig. 8.31. Therefore the direction cosines of axis X_e are $c_x=0$, $c_y=0$, $c_z=1$. In order to use the aforementioned cosines, the orientation of the GCS must be the same as shown in Fig. 8.31. Assuming that the JCS coincides with the GCS, we have $\beta=0$, $\gamma=0$ and $\phi=0$. Substituting the known values into Eqs. (8.110) and (8.111a or b), $[C_e]$ and $[C_j]$ are modified as

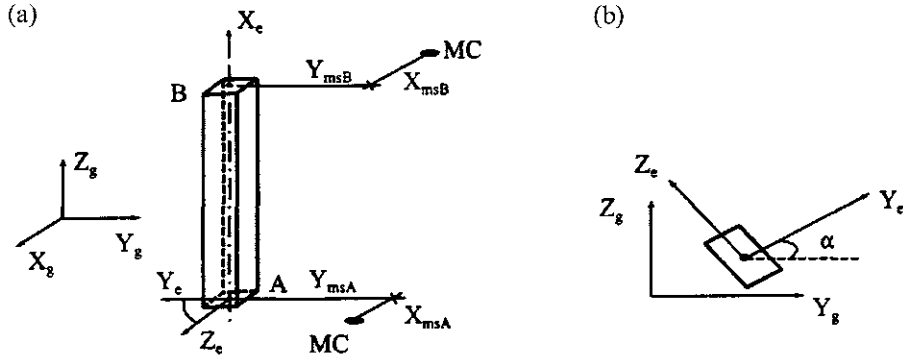


FIG. 8.31 Beam-column element. (a) ECS and GCS. (b) Angle α .

$$\begin{aligned}
 [C_e] &= \begin{bmatrix} c_x & c_y & c_z \\ \frac{-c_x c_y \cos \alpha - c_z \sin \alpha}{m} & m \cos \alpha & \frac{-c_y c_z \cos \alpha + c_x \sin \alpha}{m} \\ \frac{c_x c_y \sin \alpha - c_z \cos \alpha}{m} & -m \sin \alpha & \frac{c_y c_z \sin \alpha + c_x \cos \alpha}{m} \end{bmatrix} \\
 &= \begin{bmatrix} 0 & 0 & 1 \\ -\sin \alpha & \cos \alpha & 0 \\ -\cos \alpha & -\sin \alpha & 0 \end{bmatrix}
 \end{aligned} \tag{8.112}$$

and

$$\begin{aligned}
 [C_j] &= \begin{bmatrix} \cos \beta \cos \gamma & \sin \beta & \cos \beta \sin \gamma \\ -\cos \phi \sin \beta \cos \gamma - \sin \phi \sin \gamma & \cos \phi \cos \beta & -\sin \gamma \cos \phi \sin \beta + \sin \phi \cos \gamma \\ \cos \gamma \sin \phi \sin \beta - \sin \gamma \cos \phi & -\sin \phi \cos \beta & \sin \phi \sin \beta \sin \gamma + \cos \phi \cos \gamma \end{bmatrix} \\
 &= \begin{bmatrix} 1 & 0 & 0 \\ 0 & 1 & 0 \\ 0 & 0 & 1 \end{bmatrix}
 \end{aligned} \tag{8.113}$$

The stiffness matrix can be obtained by using the procedure shown in Eq. (8.109) or substituting the known parameters of $i_1 = 0$, $i_2 = 0$, $i_3 = 1$, $m_1 = -\sin \alpha$, $m_2 = \cos \alpha$, $m_3 = 0$, $n_1 = -\cos \alpha$, $n_2 = -\sin \alpha$, $n_3 = 0$, $i_{1A} = i_{1B} = j_{2A} = j_{2B} = k_{3A} = k_{3B} = 1$, $i_{2A} = i_{2B} = i_{3A} = i_{3B} = j_{1A} = j_{1B} = j_{3A} = j_{3B} = k_{1A} = k_{1B} = k_{2A} = k_{2B} = 0$ into Eqs. (F-1) and (F-2) in Appendix F. For example

$$\begin{aligned}
 A_{13} &= i_{1A}n_1 + i_{2A}n_2 + i_{3A}n_3 = (1)(-\cos \alpha) + (0)(-\sin \alpha) + (0)(0) = -\cos \alpha \\
 A_{32} &= k_{1A}m_1 + k_{2A}m_2 + k_{3A}m_3 = (0)(-\sin \alpha) + (0)\cos \alpha + (1)(0) = 0 \\
 A_{63} &= -Y_{msA}i_{1A}n_1 - Y_{msA}i_{2A}n_2 - Y_{msA}i_{3A}n_3 + X_{msA}j_{1A}n_1 + X_{msA}j_{2A}n_2 + X_{msA}j_{3A}n_3 - L_{zs}A_{32} \\
 &= Y_{msA}(1)\cos \alpha - Y_{msA}(0)(-\sin \alpha) - Y_{msA}(0)(0) + X_{msA}(0)(-\cos \alpha) \\
 &\quad + X_{msA}(1)(-\sin \alpha) + X_{msA}(0)(0) - L_{zs}(0) = Y_{msA}\cos \alpha - X_{msA}\sin \alpha
 \end{aligned}$$

Calculating each item of Eq. (F-1), $[A']$ becomes

$$\left\{ \begin{array}{l} F_{Amx} \\ F_{Amy} \\ F_{Amz} \\ M_{Amx} \\ M_{Amy} \\ M_{Amz} \\ F_{Bmx} \\ F_{Bmy} \\ F_{Bmz} \\ M_{Bmx} \\ M_{Bmy} \\ M_{Bmz} \end{array} \right\} = [A'] \left\{ \begin{array}{l} F_{xa} \\ F_{ya} \\ F_{za} \\ M_{xa} \\ M_{ya} \\ M_{za} \\ F_{xb} \\ F_{yb} \\ F_{zb} \\ M_{xb} \\ M_{yb} \\ M_{zb} \end{array} \right\} = \left[\begin{array}{ccccccccccccc} 0 & -sn & -cs & 0 & 0 & 0 & 0 & 0 & 0 & 0 & 0 & 0 & 0 & 0 & 0 \\ 0 & cs & -sn & 0 & 0 & 0 & 0 & 0 & 0 & 0 & 0 & 0 & 0 & 0 & 0 \\ 1 & 0 & 0 & 0 & 0 & 0 & 0 & 0 & 0 & 0 & 0 & 0 & 0 & 0 & 0 \\ 0 & -cs L_{ys} & sn L_{zs} & 0 & -sn & -cs & 0 & 0 & 0 & 0 & 0 & 0 & 0 & 0 & 0 \\ 0 & -sn L_{ys} & -cs L_{zs} & 0 & cs & -sn & 0 & 0 & 0 & 0 & 0 & 0 & 0 & 0 & 0 \\ 0 & A_{62} & A_{63} & 1 & 0 & 0 & 0 & 0 & 0 & 0 & 0 & 0 & 0 & 0 & 0 \\ 0 & 0 & 0 & 0 & 0 & 0 & 0 & -sn & -cs & 0 & 0 & 0 & 0 & 0 & 0 \\ 0 & 0 & 0 & 0 & 0 & 0 & 0 & cs & -sn & 0 & 0 & 0 & 0 & 0 & 0 \\ 0 & 0 & 0 & 0 & 0 & 0 & 1 & 0 & 0 & 0 & 0 & 0 & 0 & 0 & 0 \\ 0 & 0 & 0 & 0 & 0 & 0 & 0 & cs L_{ye} & -sn L_{ze} & 0 & -sn & -cs & 0 & 0 & 0 \\ 0 & 0 & 0 & 0 & 0 & 0 & 0 & sn L_{ye} & cs L_{ze} & 0 & cs & -sn & 0 & 0 & 0 \\ 0 & 0 & 0 & 0 & 0 & 0 & 0 & B_{62} & B_{63} & 1 & 0 & 0 & 0 & 0 & 0 \end{array} \right] \left\{ \begin{array}{l} F_{xa} \\ F_{ya} \\ F_{za} \\ M_{xa} \\ M_{ya} \\ M_{za} \\ F_{xb} \\ F_{yb} \\ F_{zb} \\ M_{xb} \\ M_{yb} \\ M_{zb} \end{array} \right\} \quad (8.114)$$

where $sn = \sin \alpha$, $cs = \cos \alpha$, and

$$\begin{aligned} A_{62} &= sn Y_{msA} + cs X_{msA}; & A_{63} &= cs Y_{msA} - sn X_{msA} \\ B_{62} &= sn Y_{msB} + cs X_{msB}; & B_{63} &= cs Y_{msB} - sn X_{msB} \end{aligned}$$

The coefficients $-sn$, (seventh row and eighth column) and $sn L_{ye}$, (11th and eighth column) of Eq. (8.114) correspond to B_{12} and B_{52} , respectively, in Eq. (F-1). Similarly, the coefficient $-cs$ (first row and third column) of Eq. (8.114) is associated with A_{13} in Eq. (F-1). Coefficients in Eq. (8.114) can be explained either in terms of force transformation or deformation transformation. For example, $A_{7,9}$ [row 7 and column 9 in Eq. (8.114)] and $A_{11,8}$ [row 11 and column 8 in Eq. (8.114)] are illustrated with deformation transformation in Fig. 8.32 based on $[B']^T = [A']$; $A_{7,9}$ and $A_{11,8}$ are illustrated with force transformation in Fig. 8.32b.

For $A_{7,9}$ and $A_{11,8}$ based on deformation transformation (see Fig. 8.32a),

If $\delta_{Bmx} \neq 0$, other displacements = 0; $\delta_{zb} = -\cos \alpha \delta_{Bmx} = B_{13} \delta_{Bmx} = A_{7,9} \delta_{Bmx}$.
If $\theta_{Bmy} \neq 0$, other displacements = 0; $\delta_{yb} = L_{ye} \sin \alpha \theta_{Bmy} = B_{52} \theta_{Bmy} = A_{11,8} \theta_{Bmy}$.

For $A_{7,9}$ and $A_{11,8}$ based on force transformation (see Fig. 8.32b)

If $F_{zb} \neq 0$, other forces = 0; $F_{Bmx} = -\cos \alpha F_{zb} = B_{13} F_{zb} = A_{7,9} F_{zb}$.

If $F_{yb} \neq 0$, other forces = 0; $F_{Bmy} = L_{ye} \sin \alpha F_{yb} = B_{52} F_{yb} = A_{11,8} F_{yb}$.

As discussed previously, notation B as used above refers to the coefficients in Eq. (F-1).

Similarly, the stiffness matrix is simplified from Eq. (F-2) as

$$\begin{aligned}
 & \left\{ \begin{array}{l} F_{Amx} \\ F_{Amy} \\ F_{Amz} \\ M_{Amx} \\ M_{Amy} \\ M_{Amz} \\ F_{Bmx} \\ F_{Bmy} \\ F_{Bmz} \\ M_{Bmx} \\ M_{Bmy} \\ M_{Bmz} \end{array} \right\} = [K^i] \left\{ \begin{array}{l} \delta_{Amx} \\ \delta_{Amy} \\ \delta_{Amz} \\ \theta_{Amx} \\ \theta_{Amy} \\ \theta_{Amz} \\ \delta_{Bmx} \\ \delta_{Bmy} \\ \delta_{Bmz} \\ \theta_{Bmx} \\ \theta_{Bmy} \\ \theta_{Bmz} \end{array} \right\} \\
 & = \left[\begin{array}{cccccccccccc} K_{1,1} & K_{1,2} & 0 & K_{1,4} & K_{1,5} & K_{1,6} & K_{1,7} & K_{1,8} & 0 & K_{1,10} & K_{1,11} & K_{1,12} \\ K_{2,1} & 0 & K_{2,4} & K_{2,5} & K_{2,6} & K_{2,7} & K_{2,8} & 0 & K_{2,10} & K_{2,11} & K_{2,12} & \\ K_{3,1} & & 0 & 0 & 0 & 0 & 0 & K_{3,9} & 0 & 0 & 0 & \\ K_{4,1} & & & K_{4,5} & K_{4,6} & K_{4,7} & K_{4,8} & 0 & K_{4,10} & K_{4,11} & K_{4,12} & \\ K_{5,1} & & & K_{5,5} & K_{5,6} & K_{5,7} & K_{5,8} & 0 & K_{5,10} & K_{5,11} & K_{5,12} & \\ K_{6,1} & & & K_{6,6} & K_{6,7} & K_{6,8} & 0 & K_{6,10} & K_{6,11} & K_{6,12} & \\ K_{7,1} & & & K_{7,7} & K_{7,8} & 0 & K_{7,10} & K_{7,11} & K_{7,12} & \\ K_{8,1} & & & K_{8,8} & 0 & K_{8,10} & K_{8,11} & K_{8,12} & \\ \text{symm} & & & & & K_{9,9} & 0 & 0 & 0 & \\ & & & & & & K_{10,10} & K_{10,11} & K_{10,12} & \\ & & & & & & K_{11,11} & K_{11,12} & \\ & & & & & & & K_{12,12} & \end{array} \right] \left\{ \begin{array}{l} \delta_{Amx} \\ \delta_{Amy} \\ \delta_{Amz} \\ \theta_{Amx} \\ \theta_{Amy} \\ \theta_{Amz} \\ \delta_{Bmx} \\ \delta_{Bmy} \\ \delta_{Bmz} \\ \theta_{Bmx} \\ \theta_{Bmy} \\ \theta_{Bmz} \end{array} \right\} \quad (8.115)
 \end{aligned}$$

To show how the stiffness elements in Eq. 8.115 are obtained from Eq. F-2, we illustrate the following two elements:

$$\begin{aligned}
 K_{1,1} &= A_{11}^2 H + A_{12}^2 S_{22} + A_{13}^2 S_{33} = (0) H + (-sn)^2 S_{22} + (-cs)^2 S_{33} = sn^2 S_{22} + cs^2 S_{33} \\
 K_{1,2} &= A_{11} H A_{21} + A_{12} S_{22} A_{22} + A_{13} S_{33} A_{23} = (0) H(0) + (-sn) S_{22} \\
 &\quad cs + (-cs) S_{33} (-sn) = sn cs (S_{33} - S_{22})
 \end{aligned}$$

Other elements of Eq. (8.115) can be obtained by using the same procedure. Results are

$$\begin{aligned}
 K_{1,4} &= sn cs (S_{22} L_{ys} - S_{33} L_{zs} - S_{35} + S_{26}); \quad K_{1,5} = sn^2 (S_{22} L_{ys} + S_{26}) + cs^2 (S_{33} L_{zs} + S_{35}) \\
 K_{1,6} &= sn cs X_{msA} (S_{33} - S_{22}) - sn^2 S_{22} Y_{msA} - cs^2 S_{33} Y_{msA}; \quad K_{1,7} = -K_{1,1} \\
 K_{1,8} &= -K_{1,2}; \quad K_{1,10} = sn cs (S_{22} L_{yc} - S_{33} L_{ze} - S_{35} + S_{26}) \\
 K_{1,11} &= sn^2 (S_{22} L_{yc} + S_{26}) + cs^2 (S_{33} L_{ze} + S_{35}); \quad K_{1,12} = -sn cs X_{msB} (S_{33} - S_{22}) + sn^2 S_{22} Y_{msB} + cs^2 S_{33} Y_{msB} \\
 K_{2,2} &= cs^2 S_{22} + sn^2 S_{33}; \quad K_{2,4} = -cs^2 (S_{22} L_{ys} + S_{26}) - sn^2 (S_{33} L_{zs} + S_{35}) \\
 K_{2,5} &= -K_{1,4}; \\
 K_{2,6} &= sn cs Y_{msA} (S_{22} - S_{33}) + sn^2 S_{33} X_{msA} + cs^2 S_{22} X_{msA}; \quad K_{2,7} = K_{1,8} \\
 K_{2,8} &= -K_{2,2}; \quad K_{2,10} = -cs^2 (S_{22} L_{yc} + S_{26}) - sn^2 (S_{33} L_{ze} + S_{35}) \\
 K_{2,11} &= -K_{1,10}; \quad K_{2,12} = sn cs Y_{msB} (S_{33} - S_{22}) - sn^2 S_{33} X_{msB} - cs^2 S_{22} X_{msB} \\
 K_{3,3} &= -K_{3,9} = K_{9,9} = H \\
 K_{4,4} &= cs^2 (L_{ys}^2 S_{22} + 2L_{ys} S_{26} + A) + sn^2 (L_{zs}^2 S_{33} + 2L_{zs} S_{35} + B) \\
 K_{4,5} &= cssn (L_{ys}^2 S_{22} + 2L_{ys} S_{26} + A - L_{zs}^2 S_{33} - 2L_{zs} S_{35} - B) \\
 K_{4,6} &= -X_{msA} [cs^2 (L_{ys} S_{22} + S_{26}) + sn^2 (L_{zs} S_{33} + S_{35})] + cssn Y_{msA} (L_{zs} S_{33} + S_{35} - L_{ys} S_{22} - S_{26}) \\
 K_{4,7} &= -K_{1,4}; \quad K_{4,8} = -K_{2,4}
 \end{aligned}$$

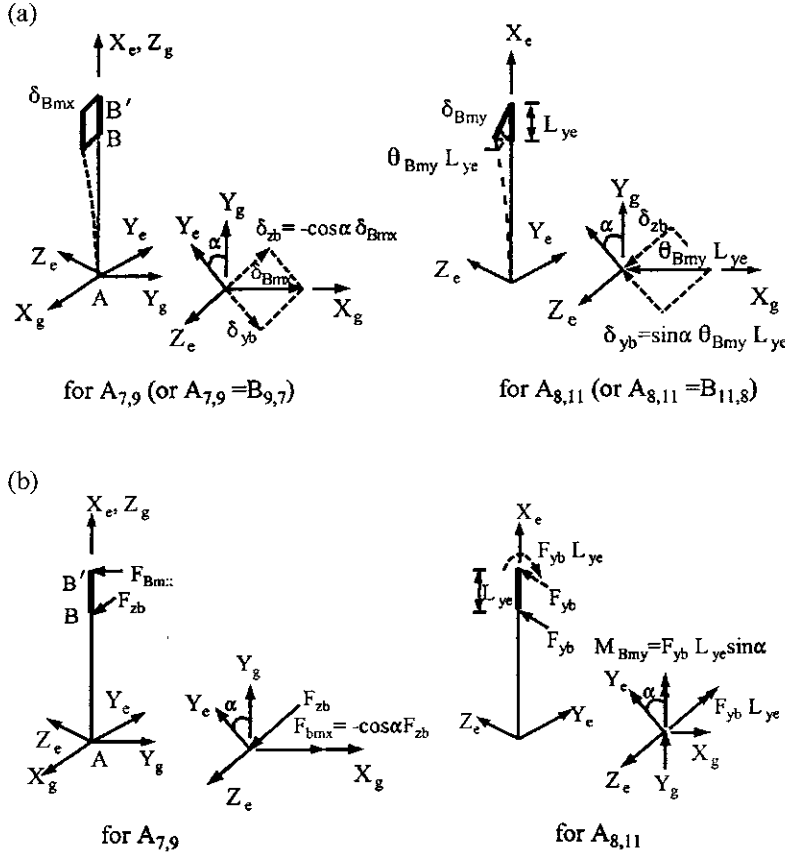


FIG. 8.32 Coefficient verification of beam-column's transformation matrix. (a) Deformation transformation. (b) Force transformation.

$$\begin{aligned}
 K_{4,10} &= cs^2(L_{ye}L_{ys}S_{22} + L_{ye}S_{26} + L_{ys}S_{26} + C) + sn^2(L_{ze}L_{zs}S_{33} + L_{ze}S_{35} + L_{zs}S_{35} + D) \\
 K_{4,11} &= scs(L_{ye}L_{ys}S_{22} - L_{ze}L_{zs}S_{33} + S_{26}L_{ys} - S_{35}L_{zs} + S_{26}L_{ye} - S_{35}L_{ze} + C - D) \\
 K_{4,12} &= X_{msB}[cs^2(L_{ys}S_{22} + S_{26}) + sn^2(L_{zs}S_{33} + S_{35})] + cssn Y_{msB}(-L_{zs}S_{33} - S_{35} + L_{ys}S_{22} + S_{26}) \\
 K_{5,5} &= cs^2(L_{zs}^2S_{33} + 2L_{zs}S_{35} + B) + sn^2(L_{ys}^2S_{22} + 2L_{ys}S_{26} + A) \\
 K_{5,6} &= -Y_{msA}[sn^2(L_{ys}S_{22} + S_{26}) + cs^2(L_{zs}S_{33} + S_{35})] + cssn X_{msA}(L_{zs}S_{33} + S_{35} - L_{ys}S_{22} - S_{26}) \\
 K_{5,7} &= -cs^2(S_{33}L_{zs} + S_{35}) - sn^2(S_{22}L_{ys} + S_{26}); \quad K_{5,8} = K_{1,4} \\
 K_{5,10} &= K_{4,11} \\
 K_{5,11} &= sn^2(L_{ye}L_{ys}S_{22} + L_{yo}S_{26} + L_{ys}S_{26} + C) + cs^2(L_{ze}L_{zs}S_{33} + L_{ze}S_{35} + L_{zs}S_{35} + D) \\
 K_{5,12} &= Y_{msB}[sn^2(L_{ys}S_{22} + S_{26}) + cs^2(L_{zs}S_{33} + S_{35})] + cssn X_{msB}(L_{ys}S_{22} - S_{35} - L_{zs}S_{33} + S_{26}) \\
 K_{6,6} &= cs^2(S_{22}X_{msA}^2 + S_{33}Y_{msA}^2) + Q + sn^2(S_{22}Y_{msA}^2 + S_{33}X_{msA}^2) + 2cssn X_{msA} Y_{msA} (S_{22} - S_{33}) \\
 K_{6,7} &= -K_{1,6}; \quad K_{6,8} = -K_{2,6} \\
 K_{6,10} &= -X_{msA}[cs^2(L_{ye}S_{22} + S_{26}) + sn^2(L_{ze}S_{33} + S_{35})] + cssn Y_{msA}(L_{ze}S_{33} + S_{35} - L_{ye}S_{22} - S_{26}) \\
 K_{6,11} &= -Y_{msA}[sn^2(L_{ye}S_{22} + S_{26}) + cs^2(L_{ze}S_{33} + S_{35})] + cssn X_{msA}(L_{ze}S_{33} + S_{35} - L_{ye}S_{22} - S_{26}) \\
 K_{6,12} &= -X_{msA}X_{msB}(cs^2S_{22} + sn^2S_{33}) - Y_{msA}Y_{msB}(sn^2S_{22} + cs^2S_{33}) - Q + cssn(Y_{msA}X_{msB} + X_{msA}Y_{msB})(S_{33} - S_{22}) \\
 K_{7,7} &= K_{1,1}; \quad K_{7,8} = K_{1,2} \\
 K_{7,10} &= -K_{1,10}; \quad K_{7,11} = -K_{1,11} \\
 K_{7,12} &= -K_{1,12}; \quad K_{8,8} = K_{2,2} \\
 K_{8,10} &= -K_{2,10}; \quad K_{8,11} = -K_{2,11} \\
 K_{8,12} &= -K_{2,12}; \\
 K_{10,10} &= cs^2(L_{ye}^2S_{22} + 2L_{ye}S_{26} + A) + sn^2(L_{ze}^2S_{33} + 2L_{ze}S_{35} + B)
 \end{aligned}$$

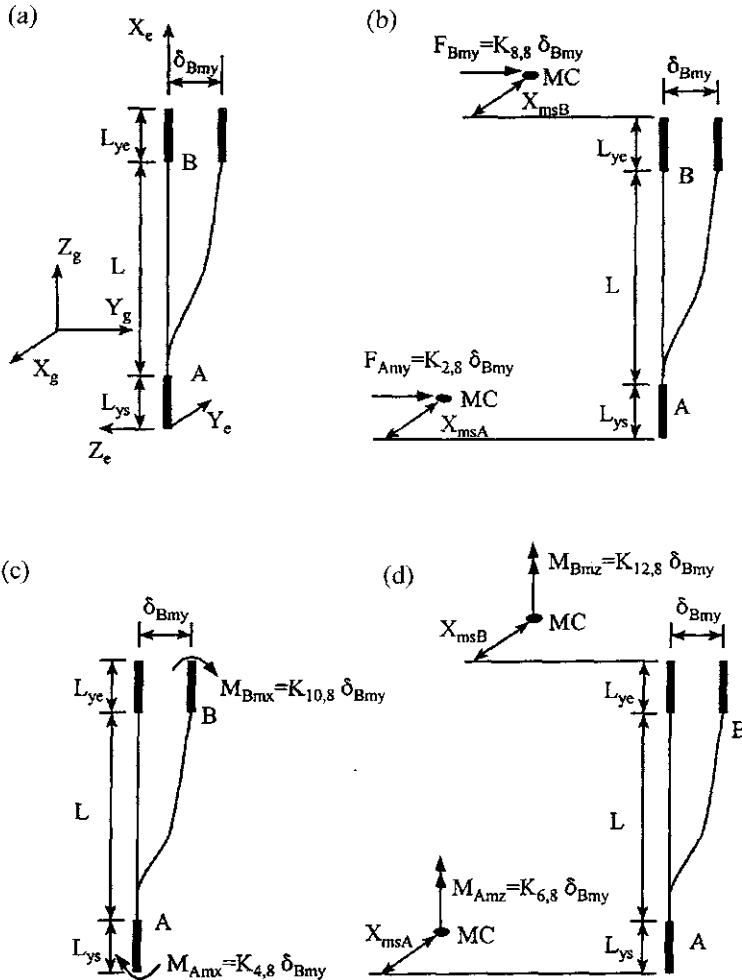


FIG. 8.33 Verification of beam–column stiffness matrix coefficients. (a) Displacement δ_{Bmy} . (b) For $K_{2,8}$ and $K_{8,8}$. (c) For $K_{4,8}$ and $K_{10,8}$. (d) For $K_{6,8}$ and $K_{12,8}$.

$$\begin{aligned}
 K_{10,11} &= csn(L_{ye}^2 S_{22} + 2L_{ye} S_{26} + A - L_{ze}^2 S_{33} - 2L_{ze} S_{35} - B) \\
 K_{10,12} &= X_{msB} [cs^2(L_{ye} S_{22} + S_{26}) + sn^2(L_{ze} S_{33} + S_{35})] + csn Y_{msB} (-L_{ze} S_{33} - S_{35} + L_{ye} S_{22} + S_{26}) \\
 K_{11,11} &= cs^2(L_{ze}^2 S_{33} + 2L_{ze} S_{35} + B) + sn^2(L_{ye}^2 S_{22} + 2L_{ye} S_{26} + A) \\
 K_{11,12} &= Y_{msB} [sn^2(L_{ye} S_{22} + S_{26}) + cs^2(L_{ze} S_{33} + S_{35})] + csn X_{msB} (L_{ye} S_{22} - S_{35} - L_{ze} S_{33} + S_{26}) \\
 K_{12,12} &= cs^2(S_{22} X_{msB}^2 + S_{33} Y_{msB}^2) + Q + sn^2(S_{22} Y_{msB}^2 + S_{33} X_{msB}^2) + 2csn X_{msB} Y_{msB} (S_{22} - S_{33})
 \end{aligned}$$

Note that \$A\$, \$B\$, \$C\$, \$D\$, \$H\$, \$Q\$, and \$S\$ as used above are defined in Eqs. (8.19)–(8.22) and (8.32)–(8.35).

The physical meaning of the coefficients in Eq. (8.115) can be explained from Fig. 8.33. For simplicity, assume that the member's major and minor axes are parallel to the GCS; therefore angle \$\alpha=0\$ in Fig. 8.31. Let displacement \$\delta_{Bmy}\neq 0\$; the others in Eq. (8.115) are zero. Forces caused by displacement \$\delta_{Bmy}\$ are shown in Fig. 8.33b–d, in which MC is mass center and/or master joint. The latter implies a master joint without lumped mass.

In Fig. 8.33, displacement \$\delta_{Bmy}\$ induces horizontal forces and moments at member ends \$A\$ and \$B\$. Consider only the forces. At each end, the force is \$S_{22}\delta_{Bmy}\$ (see Eq. (8.32) for \$S_{22}\$), which transfers to the joint center and also induces moment at the center. Force and moment are finally transferred to MC.

Forces transferred to MC, represented by \$K_{2,8}\$ and \$K_{8,8}\$ as shown in Fig. 8.33b, are

$$F_{A\text{my}} = -S_{22}\delta_{B\text{my}} = K_{2,8}\delta_{B\text{my}}; \quad F_{B\text{my}} = S_{22}\delta_{B\text{my}} = K_{8,8}\delta_{B\text{my}}$$

Forces also induce moments at the joint center. These moments, represented by $K_{4,8}$ and $K_{10,8}$ as shown in Fig. 8.33c, are

$$M_{A\text{mx}} = -L_{ys}S_{22}\delta_{B\text{my}} = K_{4,8}\delta_{B\text{my}}; \quad M_{B\text{mx}} = -L_{ye}S_{22}\delta_{B\text{my}} = K_{10,8}\delta_{B\text{my}}$$

Note that these two moments stay at the joint center. This center is also treated as master joint for the forces or moments not transferable, as discussed in Section 8.4. The force transferred to the joint center then induces torsional moment at MC, represented by $K_{6,8}$ and $K_{12,8}$ as shown in Fig. 8.33d.

$$M_{A\text{mz}} = X_{\text{ms}A}S_{22}\delta_{B\text{my}} = K_{6,8}\delta_{B\text{my}}; \quad M_{B\text{mz}} = -X_{\text{ms}B}S_{22}\delta_{B\text{my}} = K_{12,8}\delta_{B\text{my}}$$

8.11.3. Beam–Column Geometric Matrix (String Stiffness) in JCS or GCS Based on Method 2

The geometric matrix of a beam–column without rigid zone in ECS is notated in Eq. (8.44). When the geometric matrix is in the JCS or GCS and the rigid zone is considered, the matrix should be modified from Eq. (8.45) as

$$[K_g^i] = [A'][K_{eg}][A']^T \quad (8.116)$$

in which $[A']$ is given in Eq. (8.108) for the general case of a member's orientation in space. If the direction of the X_e axis of the ECS coincides with the Z_j axis of the JCS as well as Z_g of the GCS (see Figs. 8.30 and 8.31), then Eqs. (8.112)–(8.114) can be modified and the geometric matrix is expressed in the GCS as

$$\begin{aligned} & \left\{ \begin{array}{l} F_{A\text{mx}} \\ F_{A\text{my}} \\ F_{A\text{mz}} \\ M_{A\text{mx}} \\ M_{A\text{my}} \\ M_{A\text{mz}} \\ F_{B\text{mx}} \\ F_{B\text{my}} \\ F_{B\text{mz}} \\ M_{B\text{mx}} \\ M_{B\text{my}} \\ M_{B\text{mz}} \end{array} \right\} = [K_g^i] \left\{ \begin{array}{l} \delta_{A\text{mx}} \\ \delta_{A\text{my}} \\ \delta_{A\text{mz}} \\ \theta_{A\text{mx}} \\ \theta_{A\text{my}} \\ \theta_{A\text{mz}} \\ \delta_{B\text{mx}} \\ \delta_{B\text{my}} \\ \delta_{B\text{mz}} \\ \theta_{B\text{mx}} \\ \theta_{B\text{my}} \\ \theta_{B\text{mz}} \end{array} \right\} \\ & = \begin{bmatrix} K_{g1,1} & 0 & 0 & K_{g1,4} & K_{g1,5} & K_{g1,6} & K_{g1,7} & 0 & 0 & K_{g1,10} & K_{g1,11} & K_{g1,12} \\ K_{g2,2} & 0 & K_{g2,4} & K_{g2,5} & K_{g2,6} & 0 & K_{g2,8} & 0 & K_{g2,10} & K_{g2,11} & K_{g2,12} & \\ & 0 & 0 & 0 & 0 & 0 & 0 & 0 & 0 & 0 & 0 & 0 \\ & & K_{g4,4} & K_{g4,5} & K_{g4,6} & K_{g4,7} & K_{g4,8} & 0 & K_{g4,10} & K_{g4,11} & K_{g4,12} & \\ & & & K_{g5,5} & K_{g5,6} & K_{g5,7} & K_{g5,8} & 0 & K_{g5,10} & K_{g5,11} & K_{g5,12} & \\ & & & & K_{g6,6} & K_{g6,7} & K_{g6,8} & 0 & K_{g6,10} & K_{g6,11} & K_{g6,12} & \\ & & & & K_{g7,7} & 0 & 0 & K_{g7,10} & K_{g7,11} & K_{g7,12} & \\ & & & & K_{g8,8} & 0 & K_{g8,10} & K_{g8,11} & K_{g8,12} & \\ & & & & & & 0 & 0 & 0 & 0 & \\ & & & & & & & K_{g10,10} & K_{g10,11} & K_{g10,12} & \\ & & & & & & & K_{g11,11} & K_{g11,12} & \\ & & & & & & & & K_{g12,12} & \end{bmatrix} \left\{ \begin{array}{l} \delta_{A\text{mx}} \\ \delta_{A\text{my}} \\ \delta_{A\text{mz}} \\ \theta_{A\text{mx}} \\ \theta_{A\text{my}} \\ \theta_{A\text{mz}} \\ \delta_{B\text{mx}} \\ \delta_{B\text{my}} \\ \delta_{B\text{mz}} \\ \theta_{B\text{mx}} \\ \theta_{B\text{my}} \\ \theta_{B\text{mz}} \end{array} \right\} \end{aligned} \quad (8.117)$$

symm

in which

$$\begin{aligned}
 K_{g1,1} &= -K_{g1,7} = K_{g7,7} = K_{g2,2} = -K_{g2,8} = K_{g8,8} = P/L; & K_{g1,4} &= Psncs(L_{ys} - L_{zs})/L \\
 K_{g1,5} &= P(sn^2L_{ys} + cs^2L_{zs})/L; & K_{g1,6} &= -PY_{msA}/L \\
 K_{g1,12} &= PY_{msB}/L; & K_{g1,10} &= Psncs(L_{ye} - L_{ze})/L \\
 K_{g1,11} &= P(sn^2L_{ye} + cs^2L_{ze})/L; & K_{g2,4} &= -P(cs^2L_{ys} + sn^2L_{zs})/L \\
 K_{g2,5} &= -K_{g1,4}; & K_{g2,6} &= PX_{msA}/L \\
 K_{g2,10} &= -P(cs^2L_{ye} + sn^2L_{ze})/L; & K_{g2,11} &= Psncs(L_{ye} - L_{ze})/L \\
 K_{g2,12} &= -PX_{msB}/L; & K_{g4,4} &= P(cs^2L_{ys}^2 + sn^2L_{zs}^2)/L \\
 K_{g4,5} &= Psncs(L_{ys}^2 - L_{zs}^2)/L \\
 K_{g4,6} &= P[-snchsY_{msA}(L_{ys} - L_{zs}) - X_{msA}(cs^2L_{ys} + sn^2L_{zs})]/L \\
 K_{g4,7} &= -K_{g1,4}; & K_{g4,8} &= -K_{g2,4} \\
 K_{g4,10} &= P(cs^2L_{ys}L_{ye} + sn^2L_{zs}L_{ze})/L; & K_{g4,11} &= Psncs(L_{ys}L_{ye} - L_{zs}L_{ze})/L \\
 K_{g4,12} &= P[(snchsY_{msB}(L_{ys} - L_{zs}) + X_{msB}(cs^2L_{ys} + sn^2L_{zs})]/L \\
 K_{g5,5} &= P(sn^2L_{ys}^2 + cs^2L_{zs}^2)/L \\
 K_{g5,6} &= P[-snchsX_{msA}(L_{ys} - L_{zs}) - Y_{msA}(sn^2L_{ys} + cs^2L_{zs})]/L \\
 K_{g5,7} &= -K_{g1,5}; & K_{g5,8} &= -K_{g2,5} \\
 K_{g5,10} &= K_{g4,11}; & K_{g5,11} &= P(sn^2L_{ys}L_{ye} + cs^2L_{zs}L_{ze})/L \\
 K_{g5,12} &= P[snchsX_{msB}(L_{ys} - L_{zs}) + Y_{msB}(sn^2L_{ys} + cs^2L_{zs})]/L \\
 K_{g6,6} &= P(Y_{msA}^2 + X_{msA}^2)/L; & K_{g6,7} &= PY_{msA}/L \\
 K_{g6,8} &= -PX_{msA}/L \\
 K_{g6,10} &= P[-snchsY_{msA}(L_{ye} - L_{ze}) - X_{msA}(cs^2L_{ye} + sn^2L_{ze})]/L \\
 K_{g6,11} &= P[-snchsX_{msA}(L_{ye} - L_{ze}) - Y_{msA}(sn^2L_{ye} + cs^2L_{ze})]/L \\
 K_{g6,12} &= P(-Y_{msA}Y_{msB} - X_{msA}X_{msB})/L; & K_{g7,10} &= -K_{g2,11} \\
 K_{g7,11} &= -K_{g1,11}; & K_{g7,12} &= -K_{g1,12} \\
 K_{g8,10} &= -K_{g2,10}; & K_{g8,11} &= K_{g1,10} \\
 K_{g8,12} &= -K_{g2,12}; & K_{g10,10} &= P(cs^2L_{ye}^2 + sn^2L_{ze}^2)/L \\
 K_{g10,11} &= Psncs(L_{ye}^2 - L_{ze}^2)/L \\
 K_{g10,12} &= P[snchsY_{msB}(L_{ye} - L_{ze}) + X_{msB}(cs^2L_{ye} + sn^2L_{ze})]/L \\
 K_{g11,11} &= P(sn^2L_{ye}^2 + cs^2L_{ze}^2)/L \\
 K_{g11,12} &= P[snchsX_{msB}(L_{ye} - L_{ze}) + Y_{msB}(sn^2L_{ye} + cs^2L_{ze})]/L \\
 K_{g12,12} &= P(Y_{msB}^2 + X_{msB}^2)/L
 \end{aligned}$$

The physical meaning of the sample coefficients in Eq. (8.117) is explained by Fig. 8.34. For simplicity, it is assumed that $\alpha=0$ (see Fig. 8.31), which means member principal axes coincide with the ECS. Therefore $K_{g2,8}=-P/L$, $K_{g4,8}=(P/L)L_{ys}$, $K_{g6,8}=-(P/L)X_{msA}$, $K_{g8,8}=P/L$, $K_{g10,8}=(P/L)L_{ye}$, and $K_{g12,8}=(P/L)X_{msB}$. MC's of the mass center and/or master joint are at the top and bottom floor of the column.

In Fig. 8.34, displacement δ_{Bmy} induces horizontal force (shear) $(P/L)\delta_{Bmy}$ at each of the member ends, *A* and *B*. This force is transferred to the joint center and causes moment at the center. Then the joint center force is transferred to MC and also induces torsion at MC. Transferred forces are signified by the geometric matrix coefficients shown in the figure.

For Fig. 8.34b

$$F_{Amy} = -P/L\delta_{Bmy} = K_{g2,8}\delta_{Bmy}; \quad F_{Bmy} = P/L\delta_{Bmy} = K_{g8,8}\delta_{Bmy}$$

For Fig. 8.34c

$$M_{Amx} = -L_{ys}P/L\delta_{Bmy} = K_{g4,8}\delta_{Bmy}; \quad M_{Bmx} = -L_{ye}P/L\delta_{Bmy} = K_{g10,8}\delta_{Bmy}$$

For Fig. 8.34d

$$M_{Amz} = X_{msA}P/L\delta_{Bmy} = K_{g6,8}\delta_{Bmy}; \quad M_{Bmz} = -X_{msB}P/L\delta_{Bmy} = K_{g12,8}\delta_{Bmy}$$

Note that the moments shown in Fig. 8.34c are not transferable and stay at joint centers that are part of the structural nodes; these nodes are treated as master joints.

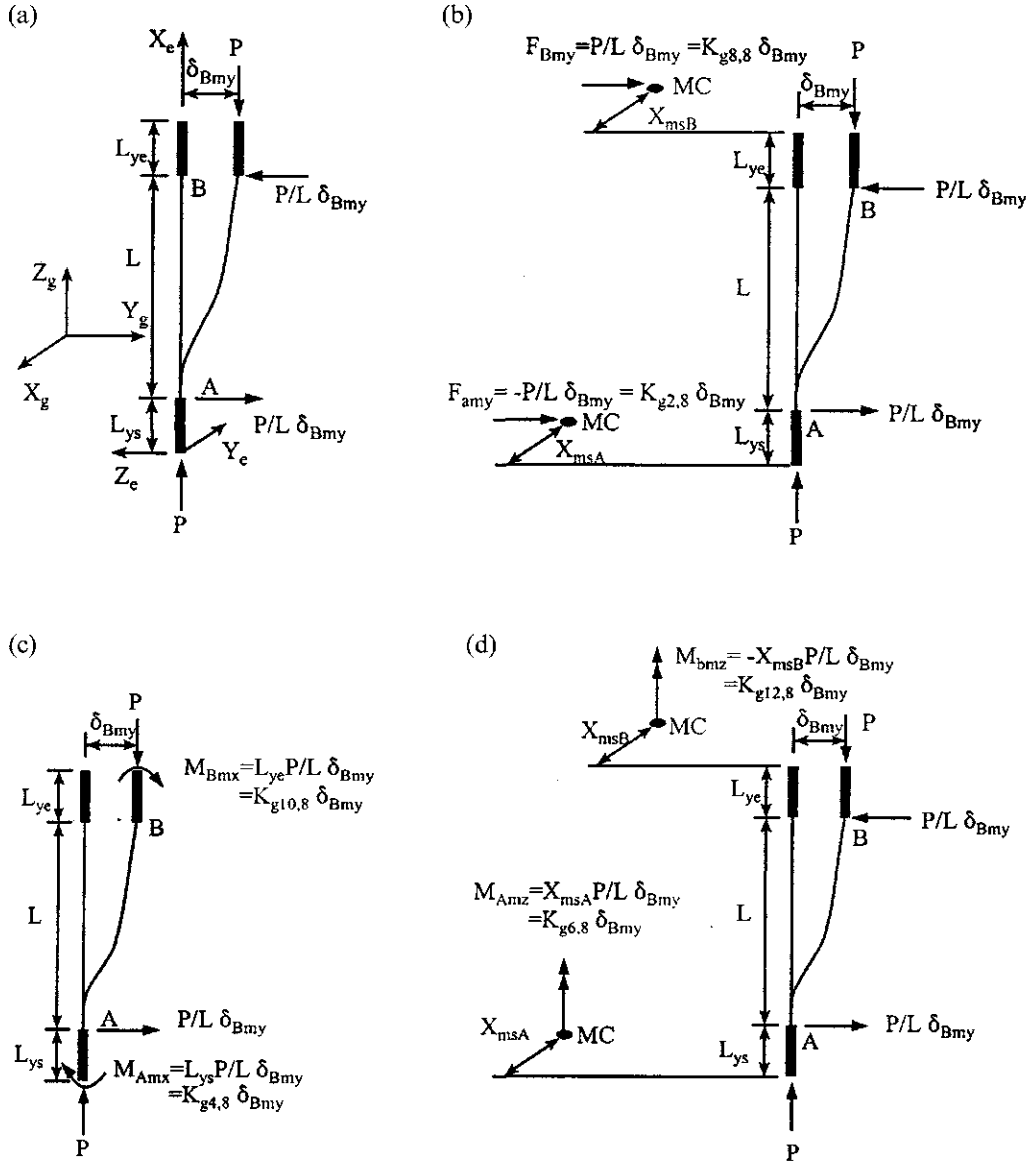


FIG. 8.34 Verification of beam–column geometric matrix coefficients. (a) Axial load P . b) For $K_{g2,8}$ and $K_{g8,8}$. (c) For $K_{g4,8}$ and $K_{g10,8}$. (d) For $K_{g6,8}$ and $K_{g12,8}$.

8.11.4. Beam Stiffness in the GCS Based on Method 2

For a building structure, a floor slab is usually in the X_g-Y_g plane and a beam is attached to the floor slab as shown in Fig. 8.26. The connection of these two elements is further illustrated in Fig. 8.35. Since the floor slab is rigid in its plane, the beam's axial deformation and rotation about its Z_e axis are zero. Since the slab is flexible out of its plane (i.e. slab's out-of-plane bending is negligible), bending of the slab about the beam's Y_e exists, but is solely due to beam stiffness.

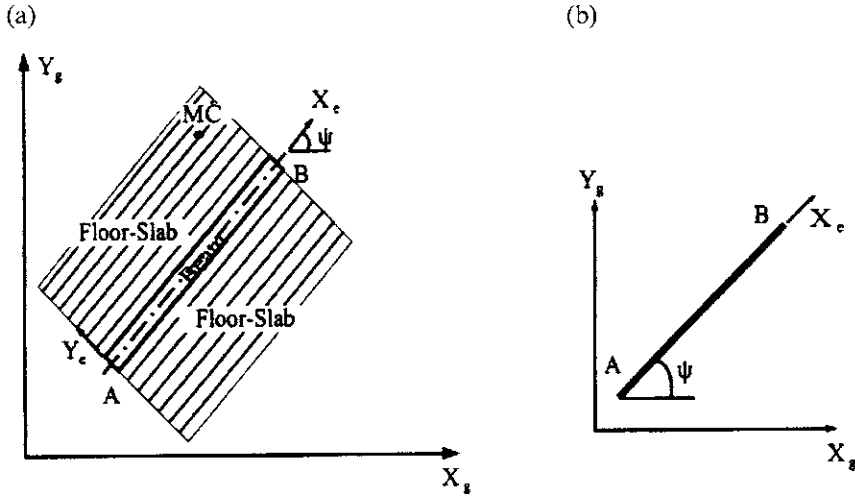


FIG. 8.35 Beam connected to rigid floor slab. (a) Beam connected to rigid floor slab. (b) Angle ψ .

Assuming MC is as shown in the figure, the force-deformation relationship of the beam element is

$$\begin{aligned} & [F_{Amx} \ F_{Amy} \ F_{Amz} \ M_{Amx} \ M_{Amy} \ M_{Amz} \ F_{Bmx} \ F_{Bmy} \ F_{Bmz} \ M_{Bmx} \ M_{Bmy} \ M_{Bmz}]^T \\ & = [K^i] [\delta_{Amx} \ \delta_{Amy} \ \delta_{Amz} \ \theta_{Amx} \ \theta_{Amy} \ \theta_{Amz} \ \delta_{Bmx} \ \delta_{Bmy} \ \delta_{Bmz} \ \theta_{Bmx} \ \theta_{Bmy} \ \theta_{Bmz}]^T \end{aligned} \quad (8.118)$$

For the beam shown in Fig. 8.35, direction cosines of axis \$X_e\$ are \$c_x = \cos \psi\$, \$c_y = \sin \psi\$, \$c_z = 0\$, which leads to \$l_1 = \cos \psi\$, \$l_2 = \sin \psi\$, \$l_3 = 0\$, \$m_1 = -\sin \psi\$, \$m_2 = \cos \psi\$, \$m_3 = 0\$, \$n_1 = 0\$, \$n_2 = 0\$, and \$n_3 = 1\$. As noted for Eq. (8.112), the above cosines are based on the orientation of global coordinates shown in this figure. Let JCS coincide with GCS (\$\beta = \gamma = \phi = 0\$); then \$[C_j]\$ of Eq. (8.111) becomes an identity matrix. A general expression of beam stiffness matrix \$[K^i]\$ can be obtained by using the same procedure shown in Section 8.11.2, or by substituting the known parameters into Eqs. (F-1) and (F-2) in Appendix F. Since the beam's web is usually perpendicular to the floor plane and no bending is allowed in that plane, it can be assumed that \$L_{ys} = L_{ye} = 0\$. This is because \$L_{ys}\$ and \$L_{ye}\$ are in the rigid plane of the floor slab. Substituting the known parameters into Eqs. (F-1) and (F-2), we have

$$\begin{aligned} A_{12} &= i_{1A} m_1 + i_{2A} m_2 + i_{3A} m_3 = (1) (-\sin \psi) + (0) (\cos \psi) + (0) (0) = -\sin \psi \\ A_{13} &= i_{1A} n_1 + i_{2A} n_2 + i_{3A} n_3 = (1) (0) + (0) (0) + (0) (1) = 0 \\ A_{42} &= A_{13} L_{ys} = (0) (0) = 0 \\ A_{43} &= -A_{12} L_{zs} = -(-\sin \psi) L_{zs} = \sin \psi L_{zs} \\ A_{11} &= i_{1A} l_1 + i_{2A} l_2 + i_{3A} l_3 = (1) (\cos \psi) + (0) (\sin \psi) + (0) (0) = \cos \psi \end{aligned}$$

The matrix array of the above elements in Eqs. (F-1) and (8.119) can be identified as \$A_{12} = A_{4,5}\$; \$A_{13} = A_{4,6}\$; \$A_{42} = A_{4,2}\$; \$A_{43} = A_{4,3}\$; \$A_{11} = A_{4,4}\$. Notations on the left and right of the equals sign denote the elements in Eqs. (F-1) and (8.119), respectively. As discussed, axial

deformations and rotations about the X_g-Y_g plane of a beam are zero due to rigidity of the floor slab in its plane. Therefore the elements associated with these deformations and rotations are zero. The matrix array of these zero elements in Eqs. (F-1) and (8.119) is identified as $A_{11}=A_{1,1}=A_{12}=A_{1,2}=A_{13}=A_{1,3}=A_{21}=A_{2,1}=A_{22}=A_{2,2}=A_{23}=A_{2,3}=0$ [where $A_{i,j}$ is the element in Eq. (8.119)] for member end A, and similarly for member end B. Calculating each item of Eq. (F-1) by using the above approach, we obtain the following transformation $[A']$ for a beam element.

$$\begin{aligned} & \left\{ \begin{array}{l} F_{Amx} \\ F_{Amy} \\ F_{Amz} \\ M_{Amx} \\ M_{Amy} \\ M_{Amz} \\ F_{Bmx} \\ F_{Bmy} \\ F_{Bmz} \\ M_{Bmx} \\ M_{Bmy} \\ M_{Bmz} \end{array} \right\} = [A'] \left\{ \begin{array}{l} F_{xa} \\ F_{ya} \\ F_{za} \\ M_{xa} \\ M_{ya} \\ M_{za} \\ F_{xb} \\ F_{yb} \\ F_{zb} \\ M_{xb} \\ M_{yb} \\ M_{zb} \end{array} \right\} \\ & = \begin{bmatrix} 0 & 0 & 0 & 0 & 0 & 0 & 0 & 0 & 0 & 0 & 0 & 0 \\ 0 & 0 & 0 & 0 & 0 & 0 & 0 & 0 & 0 & 0 & 0 & 0 \\ 0 & 0 & 1 & 0 & 0 & 0 & 0 & 0 & 0 & 0 & 0 & 0 \\ 0 & 0 & \sin \psi L_{zs} & \cos \psi & -\sin \psi & 0 & 0 & 0 & 0 & 0 & 0 & 0 \\ 0 & 0 & -\cos \psi L_{zs} & \sin \psi & \cos \psi & 0 & 0 & 0 & 0 & 0 & 0 & 0 \\ 0 & 0 & 0 & 0 & 0 & 0 & 0 & 0 & 0 & 0 & 0 & 0 \\ 0 & 0 & 0 & 0 & 0 & 0 & 0 & 0 & 0 & 0 & 0 & 0 \\ 0 & 0 & 0 & 0 & 0 & 0 & 0 & 0 & 0 & 0 & 0 & 0 \\ 0 & 0 & 0 & 0 & 0 & 0 & 0 & 1 & 0 & 0 & 0 & 0 \\ 0 & 0 & 0 & 0 & 0 & 0 & 0 & \cos \psi L_{ze} & \sin \psi & -\sin \psi & 0 & 0 \\ 0 & 0 & 0 & 0 & 0 & 0 & 0 & \sin \psi & \cos \psi & \cos \psi & 0 & 0 \\ 0 & 0 & 0 & 0 & 0 & 0 & 0 & 0 & 0 & 0 & 0 & 0 \end{bmatrix} \left\{ \begin{array}{l} F_{xa} \\ F_{ya} \\ F_{za} \\ M_{xa} \\ M_{ya} \\ M_{za} \\ F_{xb} \\ F_{yb} \\ F_{zb} \\ M_{xb} \\ M_{yb} \\ M_{zb} \end{array} \right\} \end{aligned} \quad (8.119)$$

Coefficients in Eq. (8.119) can be explained either in terms of force transformation or deformation transformation. For example, $A_{5,3} = -\cos \psi L_{zs}$ [row 5 and column 3 in Eq. (8.119)] and $A_{5,5} = \cos \psi$ [row 5 and column 5 of Eq. (8.119)] in deformation transformation, based on $[B']^T = [A']$, are illustrated in Fig. 8.36a as

If $\theta_{Amy} \neq 0$, other displacements = 0

$$\delta_{za} = -\cos \psi L_{zs} \theta_{Amy} = A_{5,3} \theta_{Amy}; \quad \theta_{ya} = \cos \psi \theta_{Amy} = A_{5,5} \theta_{Amy}$$

For force transformation based on $[A']$, the illustration is shown in Fig. 8.36b as

If $F_{za} \neq 0$, other forces = 0

$$M_{Amy} = -L_{zs} \cos \psi F_{za} = A_{5,3} F_{za}.$$

If $M_{ya} \neq 0$, other forces = 0

$$M_{Amy} = \cos \psi M_{ya} = A_{5,5} M_{ya}.$$

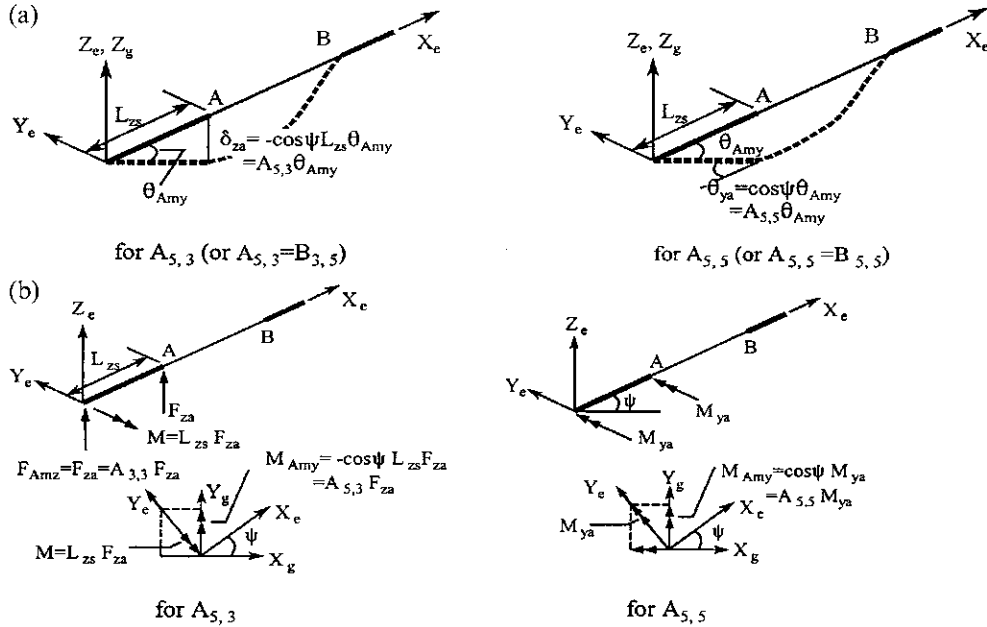


FIG. 8.36 Coefficient verification of beam's transformation matrix. (a) Deformation transformation. (b) Force transformation.

Similarly, the stiffness matrix can be obtained as

$$\begin{aligned}
 & \left\{ \begin{array}{l} F_{Amx} \\ F_{Amy} \\ F_{Amz} \\ M_{Amx} \\ M_{Amy} \\ M_{Amz} \\ F_{Bmx} \\ F_{Bmy} \\ F_{Bmz} \\ M_{Bmx} \\ M_{Bmy} \\ M_{Bmz} \end{array} \right\} = [K^i] \left\{ \begin{array}{l} \delta_{Amx} \\ \delta_{Amy} \\ \delta_{Amz} \\ \theta_{Amx} \\ \theta_{Amy} \\ \theta_{Amz} \\ \delta_{Bmx} \\ \delta_{Bmy} \\ \delta_{Bmz} \\ \theta_{Bmx} \\ \theta_{Bmy} \\ \theta_{Bmz} \end{array} \right\} \\
 & = \left[\begin{array}{ccccccccccccc} 0 & 0 & 0 & 0 & 0 & 0 & 0 & 0 & 0 & 0 & 0 & 0 & 0 & 0 \\ 0 & 0 & 0 & 0 & 0 & 0 & 0 & 0 & 0 & 0 & 0 & 0 & 0 & 0 \\ K_{3,3} & K_{3,4} & K_{3,5} & 0 & 0 & 0 & K_{3,9} & K_{3,10} & K_{3,11} & 0 & 0 & 0 & \delta_{Amx} \\ K_{4,4} & K_{4,5} & 0 & 0 & 0 & K_{4,9} & K_{4,10} & K_{4,11} & 0 & 0 & 0 & \delta_{Amy} \\ K_{5,5} & 0 & 0 & 0 & K_{5,9} & K_{5,10} & K_{5,11} & 0 & 0 & 0 & 0 & 0 & \delta_{Amz} \\ 0 & 0 & 0 & 0 & 0 & 0 & 0 & 0 & 0 & 0 & 0 & 0 & 0 \\ 0 & 0 & 0 & 0 & 0 & 0 & 0 & 0 & 0 & 0 & 0 & 0 & 0 \\ 0 & 0 & 0 & 0 & 0 & 0 & 0 & 0 & 0 & 0 & 0 & 0 & 0 \\ K_{9,9} & K_{9,10} & K_{9,11} & 0 & 0 & 0 & K_{9,11} & 0 & 0 & 0 & 0 & 0 & \delta_{Bmx} \\ K_{10,10} & K_{10,11} & 0 & 0 & 0 & K_{10,11} & 0 & 0 & 0 & 0 & 0 & 0 & \delta_{Bmy} \\ K_{11,11} & 0 & 0 & 0 & 0 & 0 & 0 & 0 & 0 & 0 & 0 & 0 & 0 \\ 0 & 0 & 0 & 0 & 0 & 0 & 0 & 0 & 0 & 0 & 0 & 0 & 0 \end{array} \right] \left\{ \begin{array}{l} \delta_{Amx} \\ \delta_{Amy} \\ \delta_{Amz} \\ \theta_{Amx} \\ \theta_{Amy} \\ \theta_{Amz} \\ \delta_{Bmx} \\ \delta_{Bmy} \\ \delta_{Bmz} \\ \theta_{Bmx} \\ \theta_{Bmy} \\ \theta_{Bmz} \end{array} \right\} \quad (8.120)
 \end{aligned}$$

in which

$$\begin{aligned}
 K_{3,3} &= -K_{3,9} = K_{9,9} = S_{33}; & K_{3,4} &= \sin\psi(S_{33}L_{zs} + S_{35}) \\
 K_{3,5} &= -\cos\psi(S_{33}L_{zs} + S_{35}); & K_{3,10} &= \sin\psi(S_{33}L_{ze} + S_{35}) \\
 K_{3,11} &= -\cos\psi(S_{33}L_{ze} + S_{35}); & K_{4,4} &= \sin^2\psi(L_{zs}^2S_{33} + 2L_{zs}S_{35} + B) + \cos^2\psi Q \\
 K_{4,5} &= -\sin\psi\cos\psi(L_{zs}^2S_{33} + 2L_{zs}S_{35} - Q + B); & K_{4,9} &= -K_{3,4} \\
 K_{4,10} &= \sin^2\psi(L_{zs}L_{ze}S_{33} + L_{zs}S_{35} + L_{ze}S_{35} + D) - \cos^2\psi Q \\
 K_{4,11} &= -\sin\psi\cos\psi(L_{zs}L_{ze}S_{33} + L_{zs}S_{35} + L_{ze}S_{35} + Q + D) \\
 K_{5,5} &= \cos^2\psi(L_{zs}^2S_{33} + 2L_{zs}S_{35} + B) + \sin^2\psi Q \\
 K_{5,9} &= -K_{3,5}; & K_{5,10} &= K_{4,11} \\
 K_{5,11} &= \cos^2\psi(L_{zs}L_{ze}S_{33} + L_{zs}S_{35} + L_{ze}S_{35} + D) - \sin^2\psi Q \\
 K_{9,10} &= -K_{3,10}; & K_{9,11} &= -K_{3,11} \\
 K_{10,10} &= \sin^2\psi(L_{ze}^2S_{33} + 2L_{ze}S_{35} + B) + \cos^2\psi Q; & K_{10,11} &= -\sin\psi\cos\psi(L_{ze}^2S_{33} + \\
 & 2L_{ze}S_{35} - Q + B) \\
 K_{11,11} &= \cos^2\psi(L_{ze}^2S_{33} + 2L_{ze}S_{35} + B) + \sin^2\psi Q
 \end{aligned}$$

As presented earlier, notations B , D , Q , and S employed here are defined in Eqs. (8.19)–(8.22) and (8.32)–(8.35).

The physical meaning of the coefficients in Eq. (8.120) is shown in Fig. 8.37 for a sample deformation δ_{Amz} where, for convenience of graphic illustration, we let $\psi=0$. This deformation induces forces and moments that lead to the following stiffnesses $K_{3,3}=S_{33}$, $K_{4,3}=0$, $K_{5,3}=-(S_{33}L_{zs}+S_{35})$, $K_{9,3}=-S_{33}$, $K_{10,3}=0$, and $K_{11,3}=-(S_{33}L_{ze}+S_{35})$.

8.11.5. Bracing-Element Stiffness in the JCS or GCS Based on Method 2

For a two-force bracing element, neither rigid zone nor major and minor axes (see Figs. 8.11 and 8.26) exist. Therefore they should not be considered in stiffness formulation. Let a bracing member be oriented in space as shown in Fig. 8.38, where MC is located at lower and upper floors relative to member ends A and B, respectively. Using the general transformation matrix of a beam–column shown in Eq. (8.110), we only need to consider axial displacement (or force) transformation of the member. Thus the transformation matrix at A and B can be directly modified from Eq. (8.110) as

$$[\bar{C}_e] = \begin{bmatrix} [C_e]_A & 0 \\ 0 & [C_e]_B \end{bmatrix} = \begin{bmatrix} c_x & c_y & c_z & 0 & 0 & 0 \\ 0 & 0 & 0 & c_x & c_y & c_z \end{bmatrix} \quad (8.121)$$

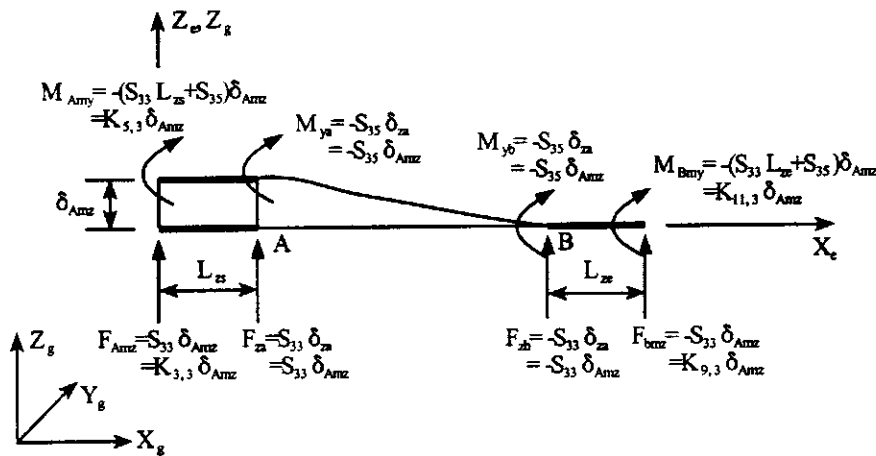


FIG. 8.37 Verification of beam's stiffness coefficients.

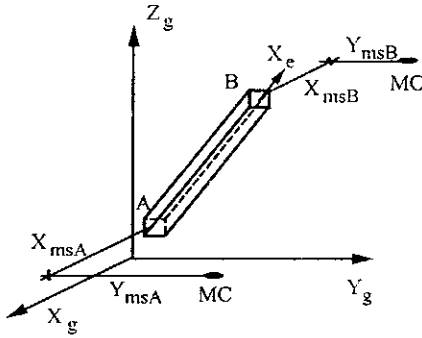


FIG. 8.38 Bracing element.

Similar to beam-columns and beams, the cosines are based on the GCS orientation shown in Fig. 8.38. The transformation matrix between the JCS and GCS, $[C_j]$, is given in Eq. (8.111a,b). Constraint matrices $[T'_{ms}]_A$ and $[T'_{ms}]_B$ may be obtained by Eq. (8.97) as

$$\{F_{jm}\} = \begin{bmatrix} [T'_{ms}]_A & 0 \\ 0 & [T'_{ms}]_B \end{bmatrix} \{F_{js}\} = [\bar{T}_{ms}] \{F_{js}\} \quad (8.122)$$

where

$$\begin{aligned} \{F_{jm}\} &= [F_{Amx} \ F_{Amy} \ F_{Amz} \ M_{Amx} \ M_{Amy} \ M_{Amz} \ F_{Bmx} \ F_{Bmy} \ F_{Bmz} \ M_{Bmx} \ M_{Bmy} \ M_{Bmz}]^T \\ \{F_{js}\} &= [F_{Asx} \ F_{Asy} \ F_{Asz} \ F_{Bsx} \ F_{Bs} \ F_{Bs}]^T \end{aligned}$$

Note that F_{Asz} and F_{Bs} are not transferable to MC and stay at the member ends. Transformation matrix $[A]$, which transforms an element's forces in ECS to GCS by using Eq. (8.108) (without rigid zone $[A']=[A]$) can be expressed as

$$\begin{bmatrix} F_{Amx} \\ F_{Amy} \\ F_{Amz} \\ M_{Amx} \\ M_{Amy} \\ M_{Amz} \\ F_{Bmx} \\ F_{Bmy} \\ F_{Bmz} \\ M_{Bmx} \\ M_{Bmy} \\ M_{Bmz} \end{bmatrix} = [\bar{T}_{ms}] [\bar{C}_j] [\bar{C}_e] [T_{je}] \begin{bmatrix} F_{xa} \\ F_{zb} \end{bmatrix} = [A] \begin{bmatrix} F_{xa} \\ F_{xb} \end{bmatrix} = \begin{bmatrix} A_{11} & 0 \\ A_{21} & 0 \\ A_{31} & 0 \\ 0 & 0 \\ 0 & 0 \\ 0 & 0 \\ A_{61} & 0 \\ 0 & B_{11} \\ 0 & B_{21} \\ 0 & B_{31} \\ 0 & 0 \\ 0 & 0 \\ 0 & B_{61} \end{bmatrix} \begin{bmatrix} F_{xa} \\ F_{xb} \end{bmatrix} \quad (8.123)$$

where

$$[T_{je}] = [I]$$

$$[\bar{C}_j] = \begin{bmatrix} [C_j]_A & 0 \\ 0 & [C_j]_B \end{bmatrix}$$

$$\begin{aligned} A_{11} &= i_{1A}c_x + i_{2A}c_y + i_{3A}c_z; & A_{21} &= j_{1A}c_x + j_{2A}c_y + j_{3A}c_z \\ A_{31} &= k_{1A}c_x + k_{2A}c_y + k_{3A}c_z \\ A_{61} &= c_x(X_{msA}j_{1A} - Y_{msA}i_{1A}) + c_y(X_{msA}j_{2A} - Y_{msA}i_{2A}) + c_z(X_{msA}j_{3A} - Y_{msA}i_{3A}) \\ B_{11} &= i_{1B}c_x + i_{2B}c_y + i_{3B}c_z; & B_{21} &= j_{1B}c_x + j_{2B}c_y + j_{3B}c_z \\ B_{31} &= k_{1B}c_x + k_{2B}c_y + k_{3B}c_z \\ B_{61} &= c_x(X_{msB}j_{1B} - Y_{msB}i_{1B}) + c_y(X_{msB}j_{2B} - Y_{msB}i_{2B}) + c_z(X_{msB}j_{3B} - Y_{msB}i_{3B}) \end{aligned}$$

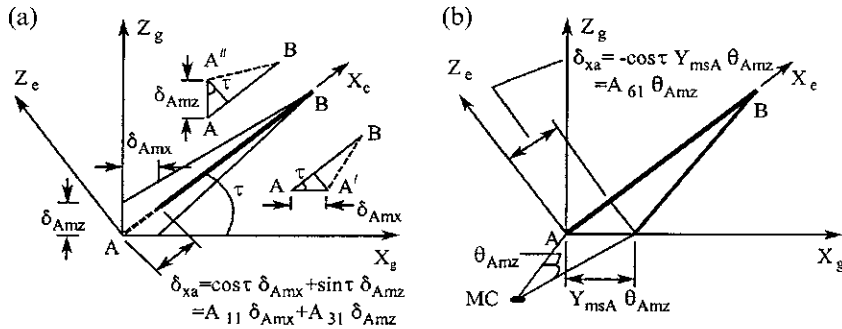


FIG. 8.39 Coefficient verification of bracing member's compatibility matrix. (a) For A_{11} and A_{12} . (b) For A_{61} .

The physical interpretation of coefficients in $[A]$ is shown in Fig. 8.39. In the figure, we assume that the GCS coincides with the JCS; then $[C_j] = [I]$. Furthermore, member AB is assumed to be in the $X_g - Z_g$ plane with angle τ ; therefore $\beta = 0$, $\gamma = \tau$, $\phi = 0$, $c_x = \cos \tau$, $c_y = 0$, and $c_z = \sin \tau$. Using $[B]^T = [A]$ yields $B_{1,1} = A_{1,1} = A_{11} = c_x$, $B_{1,2} = A_{2,1} = A_{21} = c_y$, $B_{1,3} = A_{3,1} = A_{31} = c_z$, and $B_{1,6} = A_{6,1} = A_{61} = -c_x Y_{msA}$. Note that the subscripts of A_{ij} and $A_{i,j}$ are the same; ij (i.e. 11, 21, 31, 61) refers to the notation used in Eq. (8.123), and i,j (i.e. 1,1; 2,1; 3,1; 6,1) signifies the matrix array of row and column numbers in order to identify the deform matrix coefficients $B_{i,j}$.

Using the general expression in Eq. (8.109), we obtain the following global element stiffness matrix:

$$\begin{aligned}
 & \left\{ \begin{array}{l} F_{Amx} \\ F_{Amy} \\ F_{Amz} \\ M_{Amx} \\ M_{Amy} \\ M_{Amz} \\ F_{Bmx} \\ F_{Bmy} \\ F_{Bmz} \\ M_{Bmx} \\ M_{Bmy} \\ M_{Bmz} \end{array} \right\} = [K^i] \left\{ \begin{array}{l} \delta_{Amx} \\ \delta_{Amy} \\ \delta_{Amz} \\ \theta_{Amx} \\ \theta_{Amy} \\ \theta_{Amz} \\ \delta_{Bmx} \\ \delta_{Bmy} \\ \delta_{Bmz} \\ \theta_{Bmx} \\ \theta_{Bmy} \\ \theta_{Bmz} \end{array} \right\} \\
 & = \left[\begin{array}{cccccccccc} K_{1,1} & K_{1,2} & K_{1,3} & 0 & 0 & K_{1,6} & K_{1,7} & K_{1,8} & K_{1,9} & 0 & 0 & K_{1,12} \\ K_{2,2} & K_{2,3} & 0 & 0 & K_{2,6} & K_{2,7} & K_{2,8} & K_{2,9} & 0 & 0 & K_{2,12} & \delta_{Amx} \\ & K_{3,3} & 0 & 0 & K_{3,6} & K_{3,7} & K_{3,8} & K_{3,9} & 0 & 0 & K_{3,12} & \delta_{Amy} \\ & & 0 & 0 & 0 & 0 & 0 & 0 & 0 & 0 & 0 & 0 & \delta_{Amz} \\ & & & 0 & 0 & 0 & 0 & 0 & 0 & 0 & 0 & 0 & \theta_{Amx} \\ & & & & K_{6,6} & K_{6,7} & K_{6,8} & K_{6,9} & 0 & 0 & K_{6,12} & \theta_{Amy} \\ & & & & K_{7,7} & K_{7,8} & K_{7,9} & 0 & 0 & K_{7,12} & \theta_{Amz} \\ & & & & K_{8,8} & K_{8,9} & 0 & 0 & K_{8,12} & \theta_{Bmx} \\ & & & & & & K_{9,9} & 0 & 0 & K_{9,12} & \theta_{Bmy} \\ & & & & & & & 0 & 0 & 0 & \theta_{Bmz} \\ & & & & & & & & 0 & 0 & 0 & \theta_{Bmz} \\ & & & & & & & & & K_{12,12} & \theta_{Bmz} \end{array} \right] \left\{ \begin{array}{l} \delta_{Amx} \\ \delta_{Amy} \\ \delta_{Amz} \\ \theta_{Amx} \\ \theta_{Amy} \\ \theta_{Amz} \\ \delta_{Bmx} \\ \delta_{Bmy} \\ \delta_{Bmz} \\ \theta_{Bmx} \\ \theta_{Bmy} \\ \theta_{Bmz} \end{array} \right\} \quad (8.124)
 \end{aligned}$$

symm

in which

$$\begin{aligned}
 K_{1,1} &= K_{br}a_1a_1; & K_{1,2} &= K_{br}a_1a_2; & K_{1,3} &= K_{br}a_1a_3 \\
 K_{1,6} &= K_{br}a_1a_4; & K_{1,7} &= -K_{br}a_1a_5; & K_{1,8} &= -K_{br}a_1a_6 \\
 K_{1,9} &= -K_{br}a_1a_7; & K_{1,12} &= -K_{br}a_1a_8; & K_{2,2} &= K_{br}a_2a_2 \\
 K_{2,3} &= K_{br}a_2a_3; & K_{2,6} &= K_{br}a_2a_4; & K_{2,7} &= -K_{br}a_2a_5 \\
 K_{2,8} &= -K_{br}a_2a_6; & K_{2,9} &= -K_{br}a_2a_7; & K_{2,12} &= -K_{br}a_2a_8 \\
 K_{3,3} &= K_{br}a_3a_3; & K_{3,6} &= K_{br}a_3a_4; & K_{3,7} &= -K_{br}a_3a_5 \\
 K_{3,8} &= -K_{br}a_3a_6; & K_{3,9} &= -K_{br}a_3a_7; & K_{3,12} &= -K_{br}a_3a_8 \\
 K_{6,6} &= K_{br}a_4a_4; & K_{6,7} &= -K_{br}a_4a_5; & K_{6,8} &= -K_{br}a_4a_6 \\
 K_{6,9} &= -K_{br}a_4a_7; & K_{6,12} &= -K_{br}a_4a_8; & K_{7,7} &= K_{br}a_5a_5 \\
 K_{7,8} &= K_{br}a_5a_6; & K_{7,9} &= K_{br}a_5a_7; & K_{7,12} &= K_{br}a_5a_8 \\
 K_{8,8} &= K_{br}a_6a_6; & K_{8,9} &= K_{br}a_6a_7; & K_{8,12} &= K_{br}a_6a_8 \\
 K_{9,9} &= K_{br}a_7a_7; & K_{9,12} &= K_{br}a_7a_8; & K_{12,12} &= K_{br}a_8a_8 \\
 a_1 &= i_{1A}c_x + i_{2A}c_y + i_{3A}c_z; & a_2 &= j_{1A}c_x + j_{2A}c_y + j_{3A}c_z; & a_3 &= k_{1A}c_x + k_{2A}c_y + k_{3A}c_z \\
 a_4 &= -c_x Y_{msA}i_{1A} + c_x X_{msA}j_{1A} - c_y Y_{msA}i_{2A} + c_y X_{msA}j_{2A} - c_z Y_{msA}i_{3A} + c_z X_{msA}j_{3A} \\
 a_5 &= i_{1B}c_x + i_{2B}c_y + i_{3B}c_z; & a_6 &= j_{1B}c_x + j_{2B}c_y + j_{3B}c_z; & a_7 &= k_{1B}c_x + k_{2B}c_y + k_{3B}c_z \\
 a_8 &= -c_x Y_{msB}i_{1B} + c_x X_{msB}j_{1B} - c_y Y_{msB}i_{2B} + c_y X_{msB}j_{2B} - c_z Y_{msB}i_{3B} + c_z X_{msB}j_{3B}
 \end{aligned}$$

Note that Eq. (8.124) can be directly obtained from Eq. (F-2) of the beam–column element by letting $I_y = I_z = J = \alpha = L_{ys} = L_{zs} = L_{ye} = L_{ze} = 0$. For $c_x = \cos \tau$, $c_y = 0$, $c_z = \sin \tau$ (the GCS coincides with the JCS), the coefficients may be simplified as

$$\begin{aligned}
 K_{1,1} &= a_1^2 K_{br} = (i_{1A}c_x + i_{2A}c_y + i_{3A}c_z)^2 K_{br} = [(1)\cos \tau + (0)(0) + (0)\sin \tau]^2 K_{br} = \cos^2 \tau K_{br} \\
 K_{2,1} &= 0; & K_{3,1} &= \sin \tau \cos \tau K_{br}; & K_{6,1} &= -\cos^2 \tau Y_{msA} K_{br} \\
 K_{7,1} &= -\cos^2 \tau K_{br}; & K_{8,1} &= 0; & K_{9,1} &= -\sin \tau \cos \tau K_{br} \\
 K_{12,1} &= \cos^2 \tau Y_{msB} K_{br}
 \end{aligned}$$

The above coefficients are physically interpreted in Fig. 8.40 with the following derivations due to displacement δ_{Amx}

$$\begin{aligned}
 F_{xa} &= K_{br}\delta_{xa} = K_{br} \cos \tau \delta_{Amx}; & F_{xb} &= -K_{br}\delta_{xa} = -K_{br} \cos \tau \delta_{Amx} \\
 F_{Amx} &= \cos \tau F_{xa} = \cos^2 \tau K_{br}\delta_{Amx} = K_{1,1}\delta_{Amx}; & F_{Amz} &= \sin \tau F_{xa} = \sin \tau \cos \tau K_{br}\delta_{Amx} = K_{3,1}\delta_{Amx} \\
 M_{Amx} &= -Y_{msA}F_{Amx} = -\cos^2 \tau Y_{msA}K_{br}\delta_{Amx} = K_{6,1}\delta_{Amx}; & F_{Bmx} &= \cos \tau F_{xb} = -\cos^2 \tau K_{br}\delta_{Amx} = K_{7,1}\delta_{Amx} \\
 F_{Bmz} &= \sin \tau F_{xb} = -\sin \tau \cos \tau K_{br}\delta_{Amx} = K_{9,1}\delta_{Amx}; & M_{Bmz} &= -Y_{msB}F_{Bmx} = \cos^2 \tau Y_{msB}K_{br}\delta_{Amx} = \\
 & K_{12,1}\delta_{Amx}
 \end{aligned}$$

8.11.6. Shear-Wall Stiffness in the JCS or GCS Based on Method 2

A shear wall is usually perpendicular to the $X_g - Y_g$ plane of GCS as shown in Fig. 8.41. When this is the case, Eq. 8.110 becomes

$$[C_e] = \begin{bmatrix} \cos \lambda & \sin \lambda & 0 \\ 0 & 0 & 1 \\ \sin \lambda & -\cos \lambda & 0 \end{bmatrix} = \begin{bmatrix} n_x & n_y & 0 \\ 0 & 0 & 1 \\ n_y & -n_x & 0 \end{bmatrix} \quad (8.125)$$

Since the shear wall ECS is different from the beam–column ECS, we should switch the position of column 1 with column 2, and row 1 with row 2 of Eq. (8.110) to get the transformation between ECS and GCS. Eq. (8.125) is obtained from Eq. (8.110) by substituting $c_x = c_y = 0$, $c_z = 1$, and $\alpha = -\lambda$ after the switch.

The transformation between ECS and JCS is given in Eq. (8.75). For normal building configuration, the JCS usually coincides with the GCS; therefore $[C_j] = [I]$. Coordinate transformation

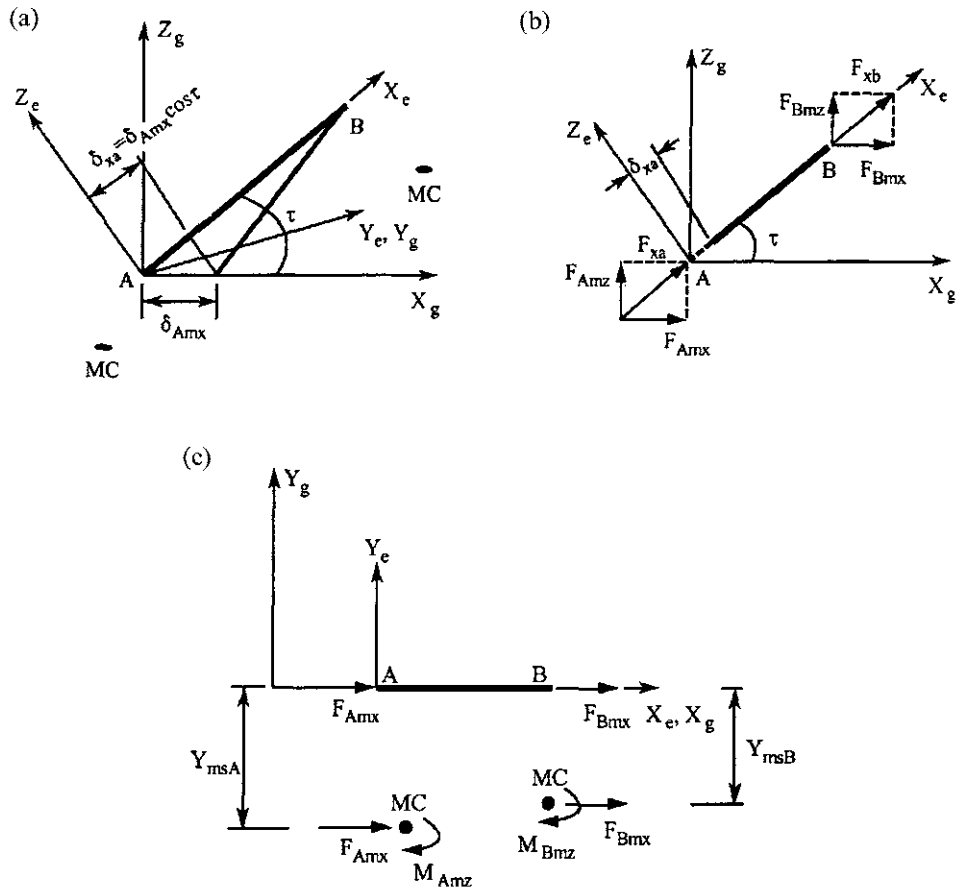


FIG. 8.40 Verification of bracing member's stiffness coefficients. (a) Deformation δ_{amx} . (b) For $K_{1,1}$, $K_{3,1}$, $K_{7,1}$, and $K_{9,1}$ (c) For $K_{6,1}$ and $K_{12,1}$.

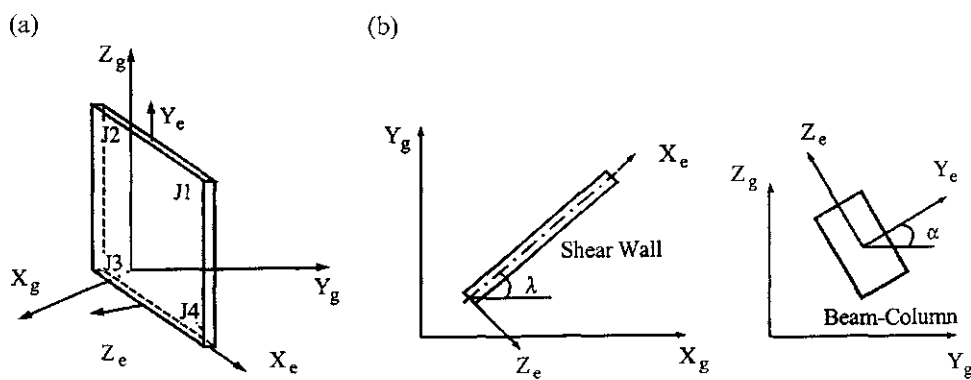


FIG. 8.41 Shear wall element in space. (a) Shear wall. (b) Relationship between λ and α angles.

matrix $[A_4]$ [Eq. (8.75)] can be written as

$$[A_4] = \begin{bmatrix} [C_e]^T & 0 & 0 & 0 \\ 0 & [C_e]^T & 0 & 0 \\ 0 & 0 & [C_e]^T & 0 \\ 0 & 0 & 0 & [C_e]^T \end{bmatrix} \quad (8.126)$$

The element stiffness matrix of shear wall in ECS is defined in Eq. 8.71 as

$$[K_e] = [A_e][S_I][A_e]^T \quad (8.127)$$

in which $[A_e]$ is presented in Eq. (8.70) as

$$[A_e] = [A_2][A_1] = \frac{1}{2w} \begin{bmatrix} 0 & 2w & 0 \\ -2 & 2\alpha & w \\ 0 & 0 & 0 \\ 2 & -2\alpha & w \\ 0 & 0 & 0 \\ -2 & -2\beta & -w \\ 0 & 0 & 0 \\ 0 & -2w & 0 \\ 2 & 2\beta & -w \\ 0 & 0 & 0 \end{bmatrix} \quad (8.128)$$

Substituting Eq. (8.128) into Eq. (8.127) leads to

$$\begin{Bmatrix} F_1 \\ F_2 \\ F_3 \\ F_4 \\ F_5 \\ F_6 \\ F_7 \\ F_8 \\ F_9 \\ F_{10} \end{Bmatrix} = [K_e] \begin{Bmatrix} \delta_1 \\ \delta_2 \\ \delta_3 \\ \delta_4 \\ \delta_5 \\ \delta_6 \\ \delta_7 \\ \delta_8 \\ \delta_9 \\ \delta_{10} \end{Bmatrix} = \begin{bmatrix} k_{11} & k_{12} & 0 & -k_{12} & 0 & -k_{13} & 0 & -k_{11} & k_{13} & 0 \\ & k_{22} & 0 & k_{23} & 0 & k_{24} & 0 & -k_{12} & k_{25} & 0 \\ & & 0 & 0 & 0 & 0 & 0 & 0 & 0 & 0 \\ & & & k_{22} & 0 & k_{25} & 0 & k_{12} & k_{24} & 0 \\ & & & & 0 & 0 & 0 & 0 & 0 & 0 \\ & & & & & k_{66} & 0 & k_{13} & k_{67} & 0 \\ & & & & & & 0 & 0 & 0 & 0 \\ & & & & & & & k_{11} & -k_{13} & 0 \\ & & & & & & & & k_{66} & 0 \\ & & & & & & & & & 0 \end{bmatrix} \begin{Bmatrix} \delta_1 \\ \delta_2 \\ \delta_3 \\ \delta_4 \\ \delta_5 \\ \delta_6 \\ \delta_7 \\ \delta_8 \\ \delta_9 \\ \delta_{10} \end{Bmatrix} \quad (8.129)$$

in which

$$\begin{aligned} k_{11} &= K_s/h; & k_{12} &= (K_s\alpha)/(hw) \\ k_{13} &= (K_s\beta)/(hw); & k_{22} &= (4K_b + 4\alpha^2 K_s + w^2 K_a)/(4hw^2) \\ k_{23} &= (-4K_b - 4\alpha^2 K_s + w^2 K_a)/(4hw^2); & k_{24} &= (4K_b - 4\alpha K_s\beta - w^2 K_a)/(4hw^2) \\ k_{25} &= (-4K_b + 4\alpha K_s\beta - w^2 K_a)/(4hw^2); & k_{66} &= (4K_b + 4\beta^2 K_s + w^2 K_a)/(4hw^2) \\ k_{67} &= (-4K_b - 4\beta^2 K_s + w^2 K_a)/(4hw^2) \end{aligned}$$

The transformation matrix is developed in Eq. (8.81) as

$$\begin{Bmatrix} F_{j1m} \\ F_{j2m} \\ F_{j3m} \\ F_{j4m} \end{Bmatrix} = [A] \{F_e\} = [A_5][A_4][A_3]\{F_e\} = \begin{bmatrix} A_{11} \\ A_{22} \end{bmatrix} \{F_e\} \quad (8.130)$$

where $[A]$ is divided into two submatrices for convenience in expressing $[K]$ later; and

$$\{F_{jm}\} = [F_{jm_x} \ F_{jm_y} \ F_{jm_z} \ M_{jm_x} \ M_{jm_y} \ M_{jm_z}]_J^T; \quad J = 1, 2, 3, 4 \quad (8.131a)$$

$$\{F_e\} = [F_1 \ F_2 \ F_3 \ F_4 \ F_5 \ F_6 \ F_7 \ F_8 \ F_9 \ F_{10}]^T \quad (8.131b)$$

where J represents the wall's four corners, $J1$, $J2$, $J3$, and $J4$. In Eq. (8.130), $[A_3]$, $[A_4]$, and $[A_5]$ expressed in general form are given in Eqs. (8.74), (8.75), and (8.80), respectively. For the present case, $[A_4]$ is defined in Eq. (8.126); $[A_5]$ is

$$[A_5] = \begin{bmatrix} [T'_{ms}]_1 & 0 & 0 & 0 \\ 0 & [T'_{ms}]_2 & 0 & 0 \\ 0 & 0 & [T'_{ms}]_3 & 0 \\ 0 & 0 & 0 & [T'_{ms}]_4 \end{bmatrix}; \quad [T'_{ms}]_J = \begin{bmatrix} 1 & 0 & 0 \\ 0 & 1 & 0 \\ 0 & 0 & 1 \\ 0 & 0 & 0 \\ 0 & 0 & 0 \\ -Y_{ms,J} & X_{ms,J} & 0 \end{bmatrix}; \quad J = 1, 2, 3, 4 \quad (8.132)$$

Submatrices of Eq. (8.130) are defined as

$$[A_{11}] = \begin{bmatrix} n_x & 0 & n_y & 0 & 0 & 0 & 0 & 0 & 0 & 0 \\ n_y & 0 & -n_x & 0 & 0 & 0 & 0 & 0 & 0 & 0 \\ 0 & 1 & 0 & 0 & 0 & 0 & 0 & 0 & 0 & 0 \\ 0 & 0 & 0 & 0 & 0 & 0 & 0 & 0 & 0 & 0 \\ 0 & 0 & 0 & 0 & 0 & 0 & 0 & 0 & 0 & 0 \\ -Y_{ms1}n_x + X_{ms1}n_y & 0 & -Y_{ms1}n_y - X_{ms1}n_x & 0 & 0 & 0 & 0 & 0 & 0 & 0 \\ 0 & 0 & 0 & 0 & 0 & n_y & 0 & 0 & 0 & 0 \\ 0 & 0 & 0 & 0 & 0 & -n_x & 0 & 0 & 0 & 0 \\ 0 & 0 & 0 & 0 & 1 & 0 & 0 & 0 & 0 & 0 \\ 0 & 0 & 0 & 0 & 0 & 0 & 0 & 0 & 0 & 0 \\ 0 & 0 & 0 & 0 & 0 & 0 & 0 & 0 & 0 & 0 \\ 0 & 0 & 0 & 0 & 0 & 0 & 0 & 0 & 0 & 0 \end{bmatrix} \quad (8.133)$$

and

$$[A_{22}] = \begin{bmatrix} 0 & 0 & 0 & 0 & 0 & 0 & n_y & 0 & 0 & 0 \\ 0 & 0 & 0 & 0 & 0 & 0 & -n_x & 0 & 0 & 0 \\ 0 & 0 & 0 & 0 & 0 & 1 & 0 & 0 & 0 & 0 \\ 0 & 0 & 0 & 0 & 0 & 0 & 0 & 0 & 0 & 0 \\ 0 & 0 & 0 & 0 & 0 & 0 & 0 & 0 & 0 & 0 \\ 0 & 0 & 0 & 0 & 0 & 0 & -Y_{ms3}n_y - X_{ms3}n_x & 0 & 0 & 0 \\ 0 & 0 & 0 & 0 & 0 & 0 & 0 & n_x & 0 & n_y \\ 0 & 0 & 0 & 0 & 0 & 0 & 0 & n_y & 0 & -n_x \\ 0 & 0 & 0 & 0 & 0 & 0 & 0 & 0 & 1 & 0 \\ 0 & 0 & 0 & 0 & 0 & 0 & 0 & 0 & 0 & 0 \\ 0 & 0 & 0 & 0 & 0 & 0 & 0 & 0 & 0 & 0 \\ 0 & 0 & 0 & 0 & 0 & 0 & -Y_{ms4}n_x + X_{ms4}n_y & 0 & -Y_{ms4}n_y - X_{ms4}n_x & 0 \end{bmatrix} \quad (8.134)$$

The global element stiffness matrix of a shear wall is

$$\begin{Bmatrix} F_{j1m} \\ F_{j2m} \\ F_{j3m} \\ F_{j4m} \end{Bmatrix} = [K^i] \begin{Bmatrix} \delta_{j1m} \\ \delta_{j2m} \\ \delta_{j3m} \\ \delta_{j4m} \end{Bmatrix} = [A][K_e][A]^T \begin{Bmatrix} \delta_{j1m} \\ \delta_{j2m} \\ \delta_{j3m} \\ \delta_{j4m} \end{Bmatrix} = \begin{bmatrix} K_{11} & K_{12} \\ K_{21} & K_{22} \end{bmatrix} \begin{Bmatrix} \delta_{j1m} \\ \delta_{j2m} \\ \delta_{j3m} \\ \delta_{j4m} \end{Bmatrix} \quad (8.135)$$

where the force vector, $\{F_{j,m}\}$, is defined in Eq. (8.131a) and the displacement vector is

$$\{\delta_{j,Jm}\} = [\delta_{jm_x} \quad \delta_{jm_y} \quad \delta_{jm_z} \quad \theta_{jm_x} \quad \theta_{jm_y} \quad \theta_{jm_z}]_J^T; \quad J = 1, 2, 3, 4. \quad (8.136)$$

In Eq. (8.135), the submatrices are written as

and $[K_{21}] = [K_{12}]^T$

$$[K_{22}] = \begin{bmatrix} 0 & 0 & 0 & 0 & 0 & 0 & 0 & 0 & 0 & 0 & 0 & 0 \\ 0 & 0 & 0 & 0 & 0 & 0 & 0 & 0 & 0 & 0 & 0 & 0 \\ K_{15,15} & 0 & 0 & 0 & K_{15,19} & K_{15,20} & K_{15,21} & 0 & 0 & K_{15,24} \\ 0 & 0 & 0 & 0 & 0 & 0 & 0 & 0 & 0 & 0 & 0 & 0 \\ 0 & 0 & 0 & 0 & 0 & 0 & 0 & 0 & 0 & 0 & 0 & 0 \\ 0 & 0 & 0 & 0 & 0 & 0 & 0 & 0 & 0 & 0 & 0 & 0 \\ K_{19,19} & K_{19,20} & K_{19,21} & 0 & 0 & K_{19,24} \\ K_{20,20} & K_{20,21} & K_{20,24} \\ K_{21,21} & 0 & 0 & K_{21,24} \\ \text{symm} & & & 0 & 0 & 0 \\ & & & 0 & 0 & 0 \\ & & & & & K_{24,24} \end{bmatrix} \quad (8.139)$$

In matrix $[K^i]$, the stiffness coefficients are

$$\begin{aligned} K_{1,1} &= -K_{1,19} = K_{19,19} = n_x k_{11} n_x; & K_{1,2} &= -K_{1,20} = -K_{2,19} = K_{19,20} = n_x k_{11} n_y \\ K_{1,3} &= -K_{1,9} = -K_{3,19} = K_{9,19} = n_x k_{12}; & K_{1,6} &= -K_{6,19} = -n_x k_{11} (Y_{ms1} n_x - X_{ms1} n_y) \\ K_{1,15} &= -K_{1,21} = -K_{15,19} = K_{19,21} = -n_x k_{13}; & K_{1,24} &= -K_{19,24} = n_x k_{11} (Y_{ms4} n_x - X_{ms4} n_y) \\ K_{2,2} &= -K_{2,20} = K_{20,20} = n_y k_{11} n_y; & K_{2,3} &= -K_{2,9} = -K_{3,20} = K_{9,20} = n_y k_{12} \\ K_{2,6} &= -K_{6,20} = -n_y k_{11} (Y_{ms1} n_x - X_{ms1} n_y); & K_{2,15} &= -K_{2,21} = -K_{15,20} = K_{20,21} = -n_y k_{13} \\ K_{2,24} &= -K_{20,24} = n_y k_{11} (Y_{ms4} n_x - X_{ms4} n_y); & K_{3,3} &= K_{9,9} = k_{22} \\ K_{3,6} &= -K_{6,9} = -k_{12} (Y_{ms1} n_x - X_{ms1} n_y); & K_{3,9} &= k_{23} \\ K_{3,15} &= K_{9,21} = k_{24}; & K_{3,21} &= K_{9,15} = k_{25} \\ K_{3,24} &= -K_{9,24} = k_{12} (Y_{ms4} n_x - X_{ms4} n_y); & K_{6,6} &= k_{11} (Y_{ms1} n_x - X_{ms1} n_y)^2 \\ K_{6,15} &= -K_{6,21} = k_{13} (Y_{ms1} n_x - X_{ms1} n_y); & K_{6,24} &= -k_{11} (Y_{ms1} n_x - X_{ms1} n_y) (Y_{ms4} n_x - X_{ms4} n_y) \\ K_{15,15} &= K_{21,21} = k_{66}; & K_{15,21} &= k_{67} \\ K_{15,24} &= -K_{21,24} = -k_{13} (Y_{ms4} n_x - X_{ms4} n_y); & K_{24,24} &= k_{11} (Y_{ms4} n_x - X_{ms4} n_y)^2 \end{aligned}$$

Physical interpretation of the stiffness coefficients is shown in Fig. 8.42. We illustrate coefficients $K_{1,1}$, $K_{2,1}$, $K_{3,1}$, and $K_{6,1}$ in Eq. (8.137) by assuming $\delta_{1mx} \neq 0$; other displacements are zero. The forces at J1 and MC (master joint) are

$$\begin{aligned} F_{1mx} &= \cos \lambda F_1 = \cos \lambda k_{11} \delta_{j1} = \cos \lambda k_{11} \cos \lambda \delta_{1mx} = K_{1,1} \delta_{1mx} \\ F_{1my} &= \sin \lambda F_1 = \sin \lambda k_{11} \delta_{j1} = \sin \lambda k_{11} \cos \lambda \delta_{1mx} = K_{2,1} \delta_{1mx} \\ F_{1mz} &= F_2 = k_{12} \delta_{j1} = k_{12} \cos \lambda \delta_{1mx} = K_{3,1} \delta_{1mx} \\ M_{1mz} &= -F_{1mx} Y_{ms1} + F_{1my} X_{ms1} = -\cos \lambda k_{11} (Y_{ms1} \cos \lambda - X_{ms1} \sin \lambda) \delta_{1mx} = K_{6,1} \delta_{1mx} \end{aligned}$$

Note that a rigid zone is not included in the stiffness because joints J1–J4 of the wall are at the joint center, and rigid zone effect should not be considered.

8.11.7. Shear-Wall Geometric Matrix (String Stiffness) in the JCS or GCS Based on Method 2

The global element geometric matrix of a shear wall is defined by Eq. (8.86) where the transformation matrix $[A] = [A_5] [A_4] [A_3]$ is the same as Eq. (8.130). When $[A_4]$ is used as given in Eq. (8.75), then the geometric matrix is expressed in terms of the JCS. When Eq. (8.126) is employed for $[A_4]$ (i.e. $[C_j] = [I]$), then the global geometric matrix $[K_g^i]$ of a shear wall is obtained as

$$\begin{Bmatrix} F_{j1m} \\ F_{j2m} \\ F_{j3m} \\ F_{j4m} \end{Bmatrix} = [K_g^i] \begin{Bmatrix} \delta_{j1m} \\ \delta_{j2m} \\ \delta_{j3m} \\ \delta_{j4m} \end{Bmatrix} = \begin{bmatrix} K_{g11} & K_{g12} \\ K_{g21} & K_{g22} \end{bmatrix} \begin{Bmatrix} \delta_{j1m} \\ \delta_{j2m} \\ \delta_{j3m} \\ \delta_{j4m} \end{Bmatrix} \quad (8.140)$$

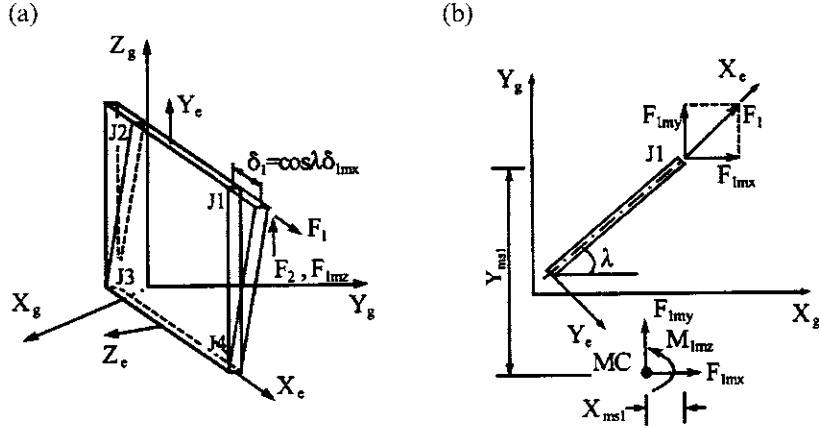


FIG. 8.42 Verification of shear-wall stiffness coefficients. (a) For $K_{3,1}$. (b) For $K_{1,1}$, $K_{2,1}$, and $K_{6,1}$.

Coefficients of the submatrices are given in Eqs. (8.141)–(8.143) as

$$[K_{g11}] = \begin{bmatrix} K_{g1,1} & K_{g1,2} & 0 & 0 & 0 & K_{g1,6} & 0 & 0 & 0 & 0 & 0 & 0 \\ K_{g2,2} & 0 & 0 & 0 & 0 & K_{g2,6} & 0 & 0 & 0 & 0 & 0 & 0 \\ 0 & 0 & 0 & 0 & 0 & 0 & 0 & 0 & 0 & 0 & 0 & 0 \\ 0 & 0 & 0 & 0 & 0 & 0 & 0 & 0 & 0 & 0 & 0 & 0 \\ 0 & 0 & 0 & 0 & 0 & 0 & 0 & 0 & 0 & 0 & 0 & 0 \\ 0 & 0 & 0 & 0 & 0 & 0 & 0 & 0 & 0 & 0 & 0 & 0 \\ K_{g6,6} & 0 & 0 & 0 & 0 & 0 & 0 & 0 & 0 & 0 & 0 & 0 \\ K_{g7,7} & K_{g7,8} & 0 & 0 & 0 & 0 & K_{g7,12} & 0 & 0 & 0 & 0 & 0 \\ K_{g8,8} & 0 & 0 & 0 & 0 & K_{g8,12} & 0 & 0 & 0 & 0 & 0 & 0 \\ 0 & 0 & 0 & 0 & 0 & 0 & 0 & 0 & 0 & 0 & 0 & 0 \\ 0 & 0 & 0 & 0 & 0 & 0 & 0 & 0 & 0 & 0 & 0 & 0 \\ K_{g12,12} & 0 & 0 & 0 & 0 & 0 & 0 & 0 & 0 & 0 & 0 & 0 \end{bmatrix} \quad (8.141)$$

$$[K_{g12}] = \begin{bmatrix} 0 & 0 & 0 & 0 & 0 & 0 & K_{g1,19} & K_{g1,20} & 0 & 0 & 0 & K_{g1,24} \\ 0 & 0 & 0 & 0 & 0 & 0 & K_{g2,19} & K_{g2,20} & 0 & 0 & 0 & K_{g2,24} \\ 0 & 0 & 0 & 0 & 0 & 0 & 0 & 0 & 0 & 0 & 0 & 0 \\ 0 & 0 & 0 & 0 & 0 & 0 & 0 & 0 & 0 & 0 & 0 & 0 \\ 0 & 0 & 0 & 0 & 0 & 0 & 0 & 0 & 0 & 0 & 0 & 0 \\ 0 & 0 & 0 & 0 & 0 & 0 & K_{g6,19} & K_{g6,20} & 0 & 0 & 0 & K_{g6,24} \\ K_{g7,13} & K_{g7,14} & 0 & 0 & 0 & K_{g7,18} & 0 & 0 & 0 & 0 & 0 & 0 \\ K_{g8,13} & K_{g8,14} & 0 & 0 & 0 & K_{g8,18} & 0 & 0 & 0 & 0 & 0 & 0 \\ 0 & 0 & 0 & 0 & 0 & 0 & 0 & 0 & 0 & 0 & 0 & 0 \\ 0 & 0 & 0 & 0 & 0 & 0 & 0 & 0 & 0 & 0 & 0 & 0 \\ 0 & 0 & 0 & 0 & 0 & 0 & 0 & 0 & 0 & 0 & 0 & 0 \\ K_{g12,13} & K_{g12,14} & 0 & 0 & 0 & K_{g12,18} & 0 & 0 & 0 & 0 & 0 & 0 \end{bmatrix} \quad (8.142)$$

$[K_{g21}] = [K_{g12}]^T$, and

$$[K_{g22}] = \begin{bmatrix} K_{g13,13} & K_{g13,14} & 0 & 0 & 0 & K_{g13,18} & 0 & 0 & 0 & 0 & 0 & 0 \\ K_{g14,14} & 0 & 0 & 0 & 0 & K_{g14,18} & 0 & 0 & 0 & 0 & 0 & 0 \\ 0 & 0 & 0 & 0 & 0 & 0 & 0 & 0 & 0 & 0 & 0 & 0 \\ 0 & 0 & 0 & 0 & 0 & 0 & 0 & 0 & 0 & 0 & 0 & 0 \\ 0 & 0 & 0 & 0 & 0 & 0 & 0 & 0 & 0 & 0 & 0 & 0 \\ K_{g18,18} & 0 & 0 & 0 & 0 & 0 & 0 & 0 & 0 & 0 & 0 & 0 \\ K_{g19,19} & K_{g19,20} & 0 & 0 & 0 & K_{g19,24} & 0 & 0 & 0 & 0 & 0 & 0 \\ K_{g20,20} & 0 & 0 & 0 & 0 & K_{g20,24} & 0 & 0 & 0 & 0 & 0 & 0 \\ 0 & 0 & 0 & 0 & 0 & 0 & 0 & 0 & 0 & 0 & 0 & 0 \\ \text{symm} & & & & & & & & & & & K_{g24,24} \end{bmatrix} \quad (8.143)$$

where

$$\begin{aligned} K_{g1,1} &= -K_{g1,19} = K_{g19,19} = (2n_x^2 + n_y^2)P/(2h) \\ K_{g1,2} &= -K_{g1,20} = -K_{g2,19} = -K_{g7,8} = K_{g7,14} = K_{g8,13} = -K_{g13,14} = K_{g19,20} = n_x n_y P/(2h) \\ K_{g1,6} &= -K_{g6,19} = (n_x X_{ms1} n_y - 2Y_{ms1} n_x^2 - Y_{ms1} n_y^2)P/(2h) \\ K_{g1,24} &= -K_{g19,24} = (-n_y X_{ms4} n_x + 2Y_{ms4} n_x^2 + Y_{ms4} n_y^2)P/(2h) \\ K_{g2,2} &= -K_{g2,20} = K_{g20,20} = (n_x^2 + 2n_y^2)P/(2h) \\ K_{g2,6} &= -K_{g6,20} = (-n_y Y_{ms1} n_x + 2X_{ms1} n_y^2 + X_{ms1} n_x^2)P/(2h) \\ K_{g2,24} &= -K_{g20,24} = (n_y Y_{ms4} n_x - 2X_{ms4} n_y^2 - X_{ms4} n_x^2)P/(2h) \\ K_{g6,6} &= (2Y_{ms1} n_x^2 - 2Y_{ms1} n_x X_{ms1} n_y + 2X_{ms1} n_y^2 + Y_{ms1}^2 n_y^2 + X_{ms1}^2 n_x^2)P/(2h) \\ K_{g6,24} &= [-Y_{ms1} Y_{ms4} (2n_x^2 + n_y^2) + n_x n_y (X_{ms1} Y_{ms4} + Y_{ms1} X_{ms4}) - X_{ms1} X_{ms4} (2n_y^2 + n_x^2)]P/(2h) \\ K_{g7,7} &= -K_{g7,13} = K_{g13,13} = n_y^2 P/(2h) \\ K_{g7,12} &= -K_{g12,13} = n_y (Y_{ms2} n_y + X_{ms2} n_x)P/(2h) \\ K_{g7,18} &= -K_{g13,18} = n_y (Y_{ms3} n_y + X_{ms3} n_x)P/(2h) \\ K_{g8,8} &= -K_{g8,14} = K_{g14,14} = n_x^2 P/(2h) \\ K_{g8,12} &= -K_{g12,14} = (n_x Y_{ms2} n_y + X_{ms2} n_x^2)P/(2h) \\ K_{g8,18} &= -K_{g14,18} = -n_x (Y_{ms3} n_y + X_{ms3} n_x)P/(2h) \\ K_{g12,12} &= (Y_{ms2} n_y + X_{ms2} n_x)^2 P/(2h) \\ K_{g12,18} &= -(Y_{ms2} n_y + X_{ms2} n_x)(Y_{ms3} n_y + X_{ms3} n_x)P/(2h) \\ K_{g18,18} &= (Y_{ms3} n_y + X_{ms3} n_x)^2 P/(2h) \\ K_{g24,24} &= [Y_{ms4}^2 (2n_x^2 + n_y^2) - 2n_x n_y X_{ms4} Y_{ms4} + X_{ms4}^2 (2n_y^2 + n_x^2)]P/(2h) \end{aligned}$$

Physical interpretation of the geometric matrix coefficients derived above is shown in Fig. 8.43 for both in-plane ($\delta_{lmx} \neq 0$ only) and out-of-plane deformation ($\delta_{lmy} \neq 0$ only). In Fig. 8.43, we assume that $\lambda = 0$ which results in $n_x = 1$ and $n_y = 0$. Therefore

$$\begin{aligned} K_{g1,1} &= (2n_x^2 + n_y^2) \frac{P}{2h} = \frac{P}{h}; \quad K_{g2,2} = (2n_y^2 + n_x^2) \frac{P}{2h} = \frac{P}{2h} \\ K_{g6,1} &= (n_x X_{ms1} n_y - 2Y_{ms1} n_x^2 - Y_{ms1} n_y^2) \frac{P}{2h} = -\frac{P}{h} Y_{ms1} \\ K_{g6,2} &= (-n_x Y_{ms1} n_y + 2X_{ms1} n_y^2 + X_{ms1} n_x^2) \frac{P}{2h} = \frac{P}{2h} X_{ms1} \end{aligned}$$

MC is the master joint.

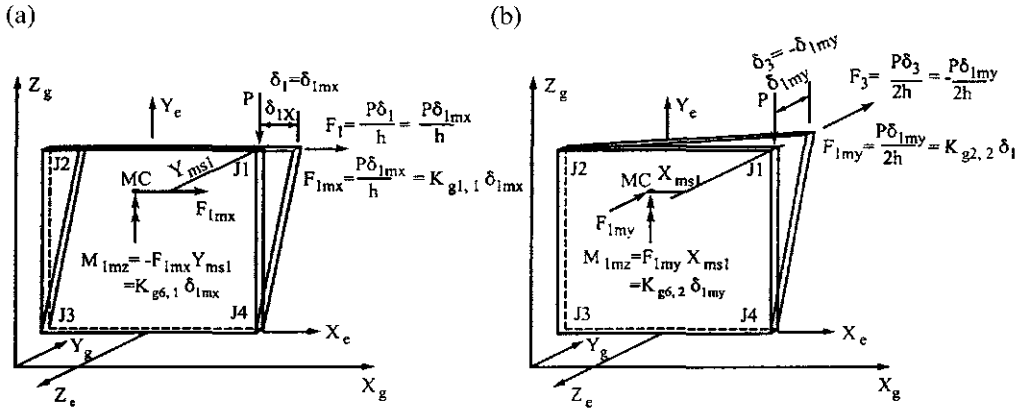


FIG. 8.43 Verification of shear-wall geometric matrix coefficients. (a) In-plane deformation for $K_{g1,1}$ and $K_{g6,1}$. (b) Out-of-plane deformation for $K_{g2,2}$ and $K_{g6,2}$.

PART B ADVANCED TOPICS

8.12. ASSEMBLY OF STRUCTURAL GLOBAL STIFFNESS MATRIX

The assembly technique for structural global stiffness is based on direct element formulation, introduced in Section 5.4.2 for trusses and Section 5.4.3 for elastic frames. Here the formulation is augmented by the *mapping* concept: map an element's d.o.f. with global d.o.f. so that a summation of individual element's stiffness, geometric, and mass matrices can directly form the system matrices (structural global matrices). This mapping concept and the symmetric characteristics of a structural matrix allow the use of sophisticated techniques for minimum storage of computer data, efficient procedure of system assembly, and optimum numerical calculations such as matrix inversion. These techniques include *skyline* or *band matrix* as well as *half band*, *linear array* of system matrix coefficients, and *matrix condensation*. This section focuses on two methods of building structure assembly. The first, called *general system assembly* (GSA), is based on direct element formulation to obtain the system matrix member by member. Then the system matrix is condensed to keep the d.o.f. at each floor's master joints and mass center for dynamic analysis. The second, called *floor-by-floor assembly* (FFA), is also based on the direct element approach, but assembly and condensation are simultaneously obtained on each floor, usually starting at the top and proceeding downward.

8.12.1. General System Assembly (GSA)

A 3D structure can have three general coordinate systems as shown in Fig. 8.44: the GCS (X_g , Y_g , Z_g), JCS (X_{mj} , Y_{mj} , Z_{mj} and X_j , Y_j , Z_j), and ECS (X_e , Y_e , Z_e). The orientation of a slave JCS (X_j , Y_j , Z_j) should be identical to its master JCS (X_{mj} , Y_{mj} , Z_{mj}).

The stiffness at a structural joint comes from the members connected to that joint. Assembly of a structural global stiffness matrix can be completed by a *coding method* based on the mapping concept. This method consists of three steps: (1) formulate the i th element stiffness matrix $[K_e]$ in ECS; (2) transform matrix $[K_e]$ into a global element stiffness matrix $[K^i]$ (or $[K'^i]$ with consideration of the rigid zone); (3) code the global element matrix and add it directly to the global stiffness matrix of a structure. A similar procedure can be applied to formulate other global matrices such as a geometric matrix. In Sections 8.6–8.8, we introduced the element stiffness matrices in the ECS of beam–column, bracing, and shear-wall members without a rigid zone. The geometric matrix (string stiffness) is also introduced for the P–Δ effect on beam–columns and shear walls. These element stiffness and geometric matrices are then expressed in JCS or GCS by using

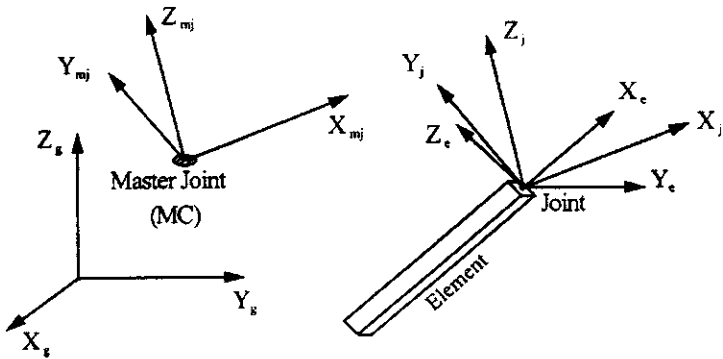


FIG. 8.44 Coordinate systems for 3D structural analysis.

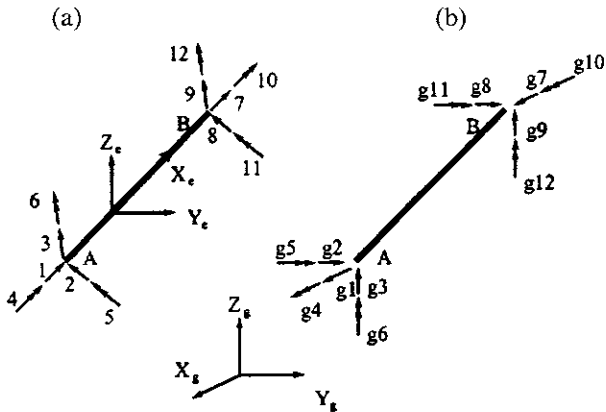


FIG. 8.45 Element and global d.o.f. of element i . (a) Element d.o.f. (b) Global d.o.f.

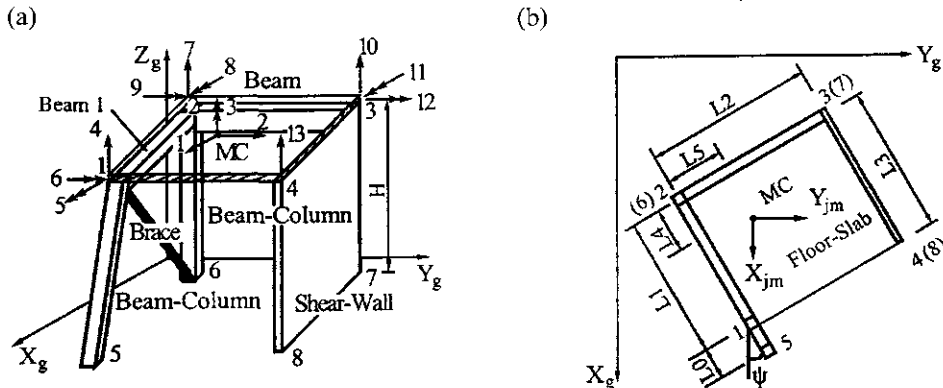
transformation matrix of Method 1 (vector formulation). In Section 8.11, the aforementioned matrices are formulated using the transformation matrix of Method 2 (direct transformation) with consideration of the rigid zone. In this section, we use the coding method to assemble global stiffness matrix $[K]$ of a structure. Note that constraint in the X_g-Y_g plane is included for rigid in-plane stiffness of floor slabs.

To assemble a global stiffness matrix $[K]$ of a structure by the coding method, Fig. 8.45a shows the element (local) d.o.f. of beam–column element i , and Fig. 8.45b shows global d.o.f. of the element. The relationship between the element and global d.o.f. systems is displayed in Table 8.1, in which the notations for element forces and deformations are based on Eqs. (8.17) and (8.18), respectively.

If the global d.o.f. is restrained, then the corresponding global d.o.f. is assigned a value of zero. Based on the relationship in Table 8.1, each $K_{i,j}$ of matrix $[K^i]$ can be directly added to system matrix $[K]$. For example, element stiffness coefficient $K_{5,7}$ corresponds to $K_{g5,g7}$ in global d.o.f. system. If $g5=11$ and $g7=20$, then $K_{5,7}$ is added to $K_{11,20}$ according to the matrix array (row and column of 11 and 20) of $[K]$; if $g5=0$ or/and $g7=0$, then $K_{5,7}$ should be neglected.

TABLE 8.1 Relationship between Element d.o.f. and Global d.o.f. for Element i

Element Forces	F_{xa}	F_{ya}	F_{za}	M_{xa}	M_{ya}	M_{za}	F_{xb}	F_{yb}	F_{zb}	M_{xb}	M_{yb}	M_{zb}
Element Deformations	δ_{xa}	δ_{ya}	δ_{za}	θ_{xa}	θ_{ya}	θ_{za}	δ_{xb}	δ_{yb}	δ_{zb}	θ_{xb}	θ_{yb}	θ_{zb}
Element d.o.f.	1	2	3	4	5	6	7	8	9	10	11	12
Global d.o.f.	g_1	g_2	g_3	g_4	g_5	g_6	g_7	g_8	g_9	g_{10}	g_{11}	g_{12}

**FIG. 8.46** One-story building. (a) Global d.o.f. (b) Structural plane.

Global stiffness matrix $[K]$ of a structure is the sum of the stiffness matrix of each element. It can be expressed as

$$[K] = \sum_{i=1}^{NM} [K^i] \quad (8.144)$$

where NM is the total number of members of a structure.

EXAMPLE 8.12.1 Find the global stiffness matrix $[K]$ for the one-story building shown in Fig. 8.46, which has two beam-columns, two beams, one bracing, and one shear wall. No rigid zone is considered.

Solution: Let the orientation of the JCS coincide with that of the GCS. The global element stiffness matrices defined in Section 8.11 can be directly used. When the JCS and GCS do not have the same orientation, the stiffness coefficients in Appendix F should be used. The analytical method is the same, but the coefficients in stiffness matrix $[K^i]$ have different values. This is because the transformation matrix $[C_i]$ (Eq. 8.111a,b) is no longer an identical matrix. When designating the GCS, it is important to make its orientation the same as that of most other elements in the ECS in order to reduce the amount of calculation. In this example, the GCS is chosen at angle ψ with the structural system to demonstrate a general analytical procedure. If $\psi = 0$, then the coefficients of $[K^i]$ are less complicated.

The structure is fixed at its base for which the global d.o.f. are shown in Fig. 8.46a. A total of 13 global d.o.f. represent relative forces and deformations given in Table 8.2. Thus the stiffness matrix of this structure is 13 by 13.

TABLE 8.2 Global d.o.f. of Given System

Global d.o.f.	1	2	3	4	5	6	7	8	9	10	11	12	13
Forces	F_x	F_y	M_z	F_{z1}	M_{x1}	M_{y1}	F_{z2}	M_{x2}	M_{y2}	F_{z3}	M_{x3}	M_{y3}	F_{z4}
Deformations	δ_x	δ_y	θ_z	δ_{z1}	θ_{x1}	θ_{y1}	δ_{z2}	θ_{x2}	θ_{y2}	δ_{z3}	θ_{x3}	θ_{y3}	δ_{z4}

TABLE 8.3 Relationship between Element d.o.f. and Global d.o.f. of Beam–Column 1

Element d.o.f.	1	2	3	4	5	6	7	8	9	10	11	12
Global d.o.f.	0	0	0	0	0	0	1	2	4	5	6	3

For beam–column 1, the numbering of its two ends is $A=5$ and $B=1$. The relationship between element d.o.f. and global d.o.f. is given in Table 8.3. Member length can be obtained from Eq. (8.7) as

$$D_{se} = \sqrt{(X_{g1} - X_{g5})^2 + (Y_{g1} - Y_{g5})^2 + (Z_{g1} - Z_{g5})^2} \quad (a)$$

Direction cosines of X_e axis are defined in Eqs. (8.13)–(8.15) as

$$c_x = \frac{X_{g1} - X_{g5}}{D_{se}}, \quad c_y = \frac{Y_{g1} - Y_{g5}}{D_{se}}, \quad c_z = \frac{Z_{g1} - Z_{g5}}{D_{se}} \quad (b)$$

Therefore for Eq. (8.110), we have

$$[C_e] = \begin{bmatrix} l_1 & l_2 & l_3 \\ m_1 & m_2 & m_3 \\ n_1 & n_2 & n_3 \end{bmatrix} = \begin{bmatrix} c_x & c_y & c_z \\ \frac{-c_x c_y \cos \alpha - c_z \sin \alpha}{m} & m \cos \alpha & \frac{-c_y c_z \cos \alpha + c_x \sin \alpha}{m} \\ \frac{c_x c_y \sin \alpha - c_z \cos \alpha}{m} & -m \sin \alpha & \frac{c_y c_z \sin \alpha + c_x \cos \alpha}{m} \end{bmatrix} \quad (c)$$

where $m = (c_x^2 + c_z^2)^{1/2}$. If the JCS coincides with the GCS [see Eq. (8.111)], then

$$[C_j] = \begin{bmatrix} i_1 & i_2 & i_3 \\ j_1 & j_2 & j_3 \\ k_1 & k_2 & k_3 \end{bmatrix} = \begin{bmatrix} 1 & 0 & 0 \\ 0 & 1 & 0 \\ 0 & 0 & 1 \end{bmatrix} \quad (d)$$

Substituting the known parameters of Eqs. (b), (c), and (d), length D_{se} and $L_{ys} = L_{zs} = L_{ye} = L_{ze} = 0$, $X_{msB} = X_1 - X_{mc}$, and $Y_{msB} = Y_1 - Y_{mc}$ (where X_1 and Y_1 are the global coordinate values of node 1, and X_{mc} and Y_{mc} are the global coordinate values of the mass center), into Eq. (8.107) or (F-2) in Appendix F, the stiffness matrix of beam–column 1 is

$$[K^{e1}] = \begin{bmatrix} K_{11}^{e1} & K_{12}^{e1} \\ K_{21}^{e1} & K_{22}^{e1} \end{bmatrix} \quad (e)$$

where $[K_{11}^{e1}]$, $[K_{12}^{e1}]$, and $[K_{21}^{e1}]$ correspond to restrained global d.o.f.; they do not contribute to global

stiffness matrix $[K]$. $[K_{22}^{cl}]$ is given as

$$[K_{22}^{cl}] = \begin{bmatrix} K_{7,7}^{cl} & K_{7,8}^{cl} & K_{7,9}^{cl} & K_{7,10}^{cl} & K_{7,11}^{cl} & K_{7,12}^{cl} \\ K_{8,7}^{cl} & K_{8,8}^{cl} & K_{8,9}^{cl} & K_{8,10}^{cl} & K_{8,11}^{cl} & K_{8,12}^{cl} \\ K_{9,7}^{cl} & K_{9,8}^{cl} & K_{9,9}^{cl} & K_{9,10}^{cl} & K_{9,11}^{cl} & K_{9,12}^{cl} \\ K_{10,7}^{cl} & K_{10,8}^{cl} & K_{10,9}^{cl} & K_{10,10}^{cl} & K_{10,11}^{cl} & K_{10,12}^{cl} \\ \text{symm} & & & K_{11,11}^{cl} & K_{11,12}^{cl} & \\ & & & & K_{12,12}^{cl} & \end{bmatrix} \quad (f)$$

Based on Table 8.3, we can put $[K^{cl}]$ into the global stiffness matrix as follows

$$[K] = \begin{bmatrix} K_{7,7}^{cl} & K_{7,8}^{cl} & K_{7,12}^{cl} & K_{7,9}^{cl} & K_{7,10}^{cl} & K_{7,11}^{cl} & 0 & 0 & 0 & 0 & 0 & 0 & 0 \\ K_{8,7}^{cl} & K_{8,8}^{cl} & K_{8,12}^{cl} & K_{8,9}^{cl} & K_{8,10}^{cl} & K_{8,11}^{cl} & 0 & 0 & 0 & 0 & 0 & 0 & 0 \\ K_{12,7}^{cl} & K_{12,8}^{cl} & K_{12,12}^{cl} & K_{9,12}^{cl} & K_{10,12}^{cl} & K_{11,12}^{cl} & 0 & 0 & 0 & 0 & 0 & 0 & 0 \\ K_{9,7}^{cl} & K_{9,8}^{cl} & K_{9,9}^{cl} & K_{9,10}^{cl} & K_{9,11}^{cl} & K_{10,11}^{cl} & 0 & 0 & 0 & 0 & 0 & 0 & 0 \\ K_{10,7}^{cl} & K_{10,8}^{cl} & K_{10,9}^{cl} & K_{10,10}^{cl} & K_{10,11}^{cl} & K_{11,11}^{cl} & 0 & 0 & 0 & 0 & 0 & 0 & 0 \\ & & & & K_{11,7}^{cl} & 0 & 0 & 0 & 0 & 0 & 0 & 0 & 0 \\ & & & & & & 0 & 0 & 0 & 0 & 0 & 0 & 0 \\ & & & & & & & 0 & 0 & 0 & 0 & 0 & 0 \\ & & & & & & & & 0 & 0 & 0 & 0 & 0 \\ & & & & & & & & & 0 & 0 & 0 & 0 \\ & & & & & & & & & & 0 & 0 & 0 \\ & & & & & & & & & & & 0 & 0 \\ & & & & & & & & & & & & 0 \\ & & & & & & & & & & & & & 0 \end{bmatrix} \quad (g)$$

For beam 2, one end is $A = 2$ and the other is $B = 3$. The relationship between element d.o.f. and global d.o.f. is given in Table 8.4.

The angle between the X_e axis and X_g is ψ ; the length is $L_{b2} = L_2$. Substituting the known parameters into Eq. (8.120) yields the following stiffness matrix for beam 2:

$$[K^{b2}] = \begin{bmatrix} 0 & 0 & 0 & 0 & 0 & 0 & 0 & 0 & 0 & 0 & 0 & 0 & 0 \\ 0 & 0 & 0 & 0 & 0 & 0 & 0 & 0 & 0 & 0 & 0 & 0 & 0 \\ K_{3,3}^{b2} & K_{3,4}^{b2} & K_{3,5}^{b2} & 0 & 0 & 0 & K_{3,9}^{b2} & K_{3,10}^{b2} & K_{3,11}^{b2} & 0 & & & \\ K_{4,4}^{b2} & K_{4,5}^{b2} & 0 & 0 & 0 & K_{4,9}^{b2} & K_{4,10}^{b2} & K_{4,11}^{b2} & 0 & & & \\ K_{5,5}^{b2} & 0 & 0 & 0 & K_{5,9}^{b2} & K_{5,10}^{b2} & K_{5,11}^{b2} & 0 & & & & \\ 0 & 0 & 0 & 0 & 0 & 0 & 0 & 0 & 0 & & & & \\ 0 & 0 & 0 & 0 & 0 & 0 & 0 & 0 & 0 & & & & \\ 0 & 0 & 0 & 0 & 0 & 0 & 0 & 0 & 0 & & & & \\ \text{symm} & & & & K_{9,9}^{b2} & K_{9,10}^{b2} & K_{9,11}^{b2} & 0 & & & & \\ & & & & K_{10,10}^{b2} & K_{10,11}^{b2} & K_{11,11}^{b2} & 0 & & & & \\ & & & & & & & 0 & & & & & \end{bmatrix} \quad (h)$$

TABLE 8.4 Relationship between Element d.o.f. and Global d.o.f. of Beam 2

Element d.o.f.	1	2	3	4	5	6	7	8	9	10	11	12
Global d.o.f.	1	2	7	8	9	3	1	2	10	11	12	3

TABLE 8.5 Relationship between Element d.o.f. and Global d.o.f. of Bracing Member

Element d.o.f.	1	2	3	4	5	6	7	8	9	10	11	12
Global d.o.f.	0	0	0	0	0	0	1	2	4	5	6	3

Based on Table 8.4, the above stiffness matrix of beam 2 can be put into global stiffness matrix $[K]$ which becomes

$$[K] = \begin{bmatrix} K_{7,7}^{c1} & K_{7,8}^{c1} & K_{7,12}^{c1} & K_{7,9}^{c1} & K_{7,10}^{c1} & K_{7,11}^{c1} & 0 & 0 & 0 & 0 & 0 & 0 & 0 \\ K_{8,8}^{c1} & K_{8,12}^{c1} & K_{8,9}^{c1} & K_{8,10}^{c1} & K_{8,11}^{c1} & 0 & 0 & 0 & 0 & 0 & 0 & 0 & 0 \\ K_{12,12}^{c1} & K_{9,12}^{c1} & K_{10,12}^{c1} & K_{11,12}^{c1} & 0 & 0 & 0 & 0 & 0 & 0 & 0 & 0 & 0 \\ K_{9,9}^{c1} & K_{9,10}^{c1} & K_{9,11}^{c1} & 0 & 0 & 0 & 0 & 0 & 0 & 0 & 0 & 0 & 0 \\ K_{10,10}^{c1} & K_{10,11}^{c1} & 0 & 0 & 0 & 0 & 0 & 0 & 0 & 0 & 0 & 0 & 0 \\ K_{11,11}^{c1} & 0 & 0 & 0 & 0 & 0 & 0 & 0 & 0 & 0 & 0 & 0 & 0 \\ K_{3,3}^{b2} & K_{3,4}^{b2} & K_{3,5}^{b2} & K_{3,9}^{b2} & K_{3,10}^{b2} & K_{3,11}^{b2} & 0 & & & & & & \\ K_{4,4}^{b2} & K_{4,5}^{b2} & K_{4,9}^{b2} & K_{4,10}^{b2} & K_{4,11}^{b2} & 0 & & & & & & & \\ K_{5,5}^{b2} & K_{5,9}^{b2} & K_{5,10}^{b2} & K_{5,11}^{b2} & 0 & & & & & & & & \\ K_{9,9}^{b2} & K_{9,10}^{b2} & K_{9,11}^{b2} & 0 & & & & & & & & & \\ K_{10,10}^{b2} & K_{10,11}^{b2} & 0 & & & & & & & & & & \\ K_{11,11}^{b2} & 0 & & & & & & & & & & & 0 \end{bmatrix} \quad (i)$$

For the bracing member, one end is $A=6$ and the other is $B=1$. The relationship between element d.o.f. and global d.o.f. is given in Table 8.5. $[C_e]$ and $[C_j]$ are calculated according to Eqs. (a)–(d) for which $\alpha=\psi$. These results along with $X_{msB}=X_1-X_{mc}$ and $Y_{msB}=Y_1-Y_{mc}$ are then substituted into Eq. (8.124), and the bracing's stiffness matrix may be expressed as

$$[K^r] = \begin{bmatrix} K_{11}^r & K_{12}^r \\ K_{21}^r & K_{22}^r \end{bmatrix} \quad (j)$$

where $[K_{11}^r]$, $[K_{12}^r]$, and $[K_{21}^r]$ correspond to restrained global d.o.f.; they do not contribute to global stiffness matrix $[K]$. $[K_{22}^r]$ is expressed as

$$[K_{22}^r] = \begin{bmatrix} K_{7,7}^r & K_{7,8}^r & K_{7,9}^r & 0 & 0 & K_{7,12}^r \\ K_{8,8}^r & K_{8,9}^r & 0 & 0 & K_{8,12}^r \\ K_{9,9}^r & 0 & 0 & K_{9,12}^r \\ 0 & 0 & 0 & & & \\ \text{symm} & & 0 & 0 & & \\ & & & & K_{12,12}^r & \end{bmatrix} \quad (k)$$

TABLE 8.6 Relationship between Element d.o.f. and Global d.o.f. of Shear Wall

Element d.o.f.	1	2	3	4	5	6	7	8	9	10	11	12
Global d.o.f.	1	2	10	11	12	3	1	2	13	0	0	3
Element d.o.f.	13	14	15	16	17	18	19	20	21	22	23	24
Global d.o.f.	0	0	0	0	0	0	0	0	0	0	0	0

Based on Table 8.5, we add the bracing's stiffness matrix to global stiffness matrix $[K]$

$$[K] = \begin{bmatrix} K_{7,7}^{cl} + K_{7,7}^r & K_{7,8}^{cl} + K_{7,8}^r & K_{7,12}^{cl} + K_{7,12}^r & K_{7,9}^{cl} + K_{7,9}^r & K_{7,10}^{cl} & K_{7,11}^{cl} & 0 & 0 & 0 & 0 & 0 & 0 & 0 \\ K_{8,8}^{cl} + K_{8,8}^r & K_{8,12}^{cl} + K_{8,12}^r & K_{8,9}^{cl} + K_{8,9}^r & K_{8,10}^{cl} & K_{8,11}^{cl} & 0 & 0 & 0 & 0 & 0 & 0 & 0 & 0 \\ K_{12,12}^{cl} + K_{12,12}^r & K_{9,12}^{cl} + K_{9,12}^r & K_{10,12}^{cl} & K_{11,12}^{cl} & 0 & 0 & 0 & 0 & 0 & 0 & 0 & 0 & 0 \\ K_{9,9}^{cl} + K_{9,9}^r & K_{9,10}^{cl} & K_{9,11}^{cl} & 0 & 0 & 0 & 0 & 0 & 0 & 0 & 0 & 0 & 0 \\ K_{10,10}^{cl} & K_{10,11}^{cl} & 0 & 0 & 0 & 0 & 0 & 0 & 0 & 0 & 0 & 0 & 0 \\ K_{11,11}^{cl} & 0 & 0 & 0 & 0 & 0 & 0 & 0 & 0 & 0 & 0 & 0 & 0 \\ K_{3,3}^{b2} & K_{3,4}^{b2} & K_{3,5}^{b2} & S_{3,9}^{b2} & K_{3,10}^{b2} & K_{3,11}^{b2} & 0 & & & & & & \\ K_{4,4}^{b2} & K_{4,5}^{b2} & K_{4,9}^{b2} & K_{4,10}^{b2} & K_{4,11}^{b2} & 0 & & & & & & & \\ K_{3,5}^{b2} & K_{3,9}^{b2} & K_{5,10}^{b2} & K_{3,11}^{b2} & 0 & & & & & & & & \\ K_{9,9}^{b2} & K_{9,10}^{b2} & K_{9,11}^{b2} & 0 & & & & & & & & & \\ K_{10,10}^{b2} & K_{10,11}^{b2} & 0 & & & & & & & & & & \\ K_{11,11}^{b2} & 0 & & & & & & & & & & & \\ 0 & & & & & & & & & & & & \end{bmatrix} \quad (l)$$

For the shear wall, its four joints are numbered $J1 = 3$, $J2 = 4$, $J3 = 8$, and $J4 = 7$. The relationship between element d.o.f. and global d.o.f. is given in Table 8.6. Substituting $n_x = \sin \psi$ and $n_y = \cos \psi$ in Eq. (8.125) and other parameters into Eqs. (8.137)–(8.139) yields $[K_{11}^w]$, $[K_{12}^w]$, and $[K_{22}^w]$. $[K_{12}^w]$, $[K_{21}^w]$, and $[K_{22}^w]$ correspond to restrained global d.o.f., and have no effect on the global stiffness matrix $[K]$. $[K_{11}^w]$ is

$$[K_{11}^w] = \begin{bmatrix} K_{1,1}^w & K_{1,2}^w & K_{1,3}^w & 0 & 0 & K_{1,6}^w & 0 & 0 & K_{1,9}^w & 0 & 0 & 0 \\ K_{2,2}^w & K_{2,3}^w & 0 & 0 & K_{2,6}^w & 0 & 0 & K_{2,9}^w & 0 & 0 & 0 \\ K_{3,3}^w & 0 & 0 & K_{3,6}^w & 0 & 0 & K_{3,9}^w & 0 & 0 & 0 & 0 & 0 \\ 0 & 0 & 0 & 0 & 0 & 0 & 0 & 0 & 0 & 0 & 0 & 0 \\ 0 & 0 & 0 & 0 & 0 & 0 & 0 & 0 & 0 & 0 & 0 & 0 \\ K_{6,6}^w & 0 & 0 & K_{6,9}^w & 0 & 0 & 0 & 0 & 0 & 0 & 0 & 0 \\ 0 & 0 & 0 & 0 & 0 & 0 & 0 & 0 & 0 & 0 & 0 & 0 \\ 0 & 0 & 0 & 0 & 0 & 0 & 0 & 0 & 0 & 0 & 0 & 0 \\ \text{symm} & & & & & K_{9,9}^w & 0 & 0 & 0 & 0 & 0 & 0 \\ & & & & & 0 & 0 & 0 & 0 & 0 & 0 & 0 \\ & & & & & 0 & 0 & 0 & 0 & 0 & 0 & 0 \end{bmatrix} \quad (m)$$

Based on Table 8.6, we can add the wall's stiffness matrix to global stiffness matrix $[K]$ as follows

THREE-DIMENSIONAL BUILDING SYSTEMS

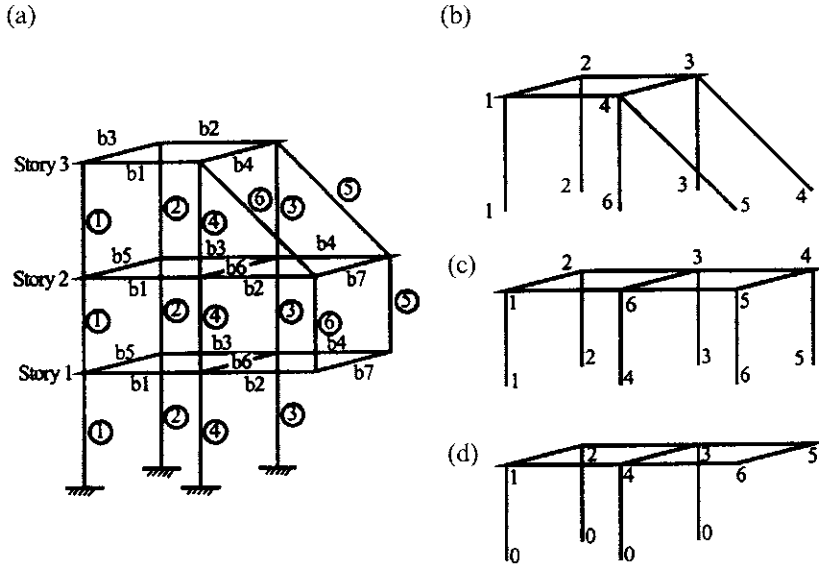


FIG. 8.47 Numbering system for FFA. (a) Three-story building. (b) Story 3. (c) Story 2. (d) Story 1.

Using the same procedure, we can further add global element stiffness matrices of beam 1 and beam–column 2 to global stiffness matrix $[K]$ for which the complete result is given in Eq. (o). Note that global geometric matrix $[K_g]$ for this structure can be established by using the same procedure.

8.12.2. Floor-by-Floor Assembly (FFA)

8.12.2.1. Assembly Procedure

For a building structure, it is more convenient to assemble the global structural stiffness matrix floor-by-floor. Each story is treated as a substructure. The global d.o.f. number for each story begins with 1 at the top of that story. Global d.o.f. numbers at the bottom of a column, bracing or shear-wall are based on their connection: if connected to the base (assuming fixed connection), the number is zero; if connected to a lower story, it is taken as the number of the connected node. Figure 8.47 explains the numbering procedure.

At node i of story j , the first global d.o.f. is calculated as

$$f_{ij}^{(1)} = \sum_{k=1}^{j-1} (3 * NM_k + 3) + 3 + 3(i-1) + 1 \quad (8.145)$$

where NM_k is the largest number of nodes at the k th story. Equation (8.145) is based on the assumption that in-plane stiffness of the floor-slab is rigid. Therefore each floor has three common d.o.f.: two horizontal displacements and one torsion numbered 1, 2, and 3. With this assumption, each node has only three independent d.o.f. and the k th floor has $3 * NM_k + 3$ d.o.f. In the equation, the first term, $\sum_{k=1}^{j-1} (3 * NM_k + 3)$, represents total d.o.f. of previous $j-1$ stories; the second term, 3, signifies the d.o.f at MC of the story considered; the third term, $3(i-1)$, represents the d.o.f of the $(i-1)$ nodes or joints; and the last term, 1, signifies the first d.o.f of node i . For the structure shown in Fig. 8.47, NM_k ($k = 1, 2, 3$) are

$$NM_1 = 6; \quad NM_2 = 6; \quad NM_3 = 4 \quad (8.146)$$

TABLE 8.7 Relationship between Element d.o.f. and Global d.o.f. of Column 3

Element d.o.f.	1	2	3	4	5	6	7	8	9	10	11	12
Global d.o.f.	22	23	31	32	33	24	43	44	52	53	54	45

The first d.o.f. of node 3 on the third story is

$$f_{3,3}^{(1)} = (3 * 6 + 3) + (3 * 6 + 3) + 3 + 3(3 - 1) + 1 = 52 \quad (8.147)$$

The other two d.o.f. of joint 3 are added to Eq. (8.147) as $f_{3,3}^{(2)} = f_{3,3}^{(1)} + 1$ and $f_{3,3}^{(3)} = f_{3,3}^{(2)} + 1$. Similarly, the first d.o.f. of node 3 on the second story is

$$f_{3,2}^{(1)} = (3 * 6 + 3) + 3 + 3(3 - 1) + 1 = 31 \quad (8.148)$$

The first d.o.f. of the master joint at each floor can be calculated as

$$f_{m,j}^{(1)} = \sum_{k=1}^{j-1} (3 * NM_k + 3) + 1 \quad (8.149)$$

Therefore the first d.o.f. of the master joint at the second and third story is

$$f_{m,3}^{(1)} = (3 * 6 + 3) + (3 * 6 + 3) + 1 = 43 \quad (8.150)$$

$$f_{m,2}^{(1)} = (3 * 6 + 3) + 1 = 22 \quad (8.151)$$

As discussed, global d.o.f. of an element are determined by its connecting nodes. For column 3 at the third story of Fig. 8.47, the top node of the column is 3, which corresponds to global d.o.f. (43, 44, 45, 52, 53, 54); the bottom node 3 is at the second floor, which corresponds to global d.o.f. (22, 23, 24, 31, 32, 33). Underlined d.o.f. are at the master joints. The relationship between global and element d.o.f. of column 3 is given in Table 8.7.

Based on the relationship between global and element d.o.f., an element can be assembled into the global stiffness matrix of a structure using the same procedures as demonstrated in Section 8.12.1.

FFA is useful for tall buildings. A tall building may have more than 1000 nodes; however, the number of structural nodes at each story is far fewer. Thus the elimination of d.o.f. not associated with lumped mass can be carried out floor-by-floor, considerably reducing computational effort and data storage. To demonstrate the advantage of FFA solution procedures for both static and dynamic analysis, a building system's stiffness matrix is briefly described below.

The global stiffness matrix of an n -story building structure takes the following form:

$$[K] = \begin{bmatrix} [K_{1,1}] & [K_{1,2}] & 0 & 0 & \dots & 0 & 0 \\ [K_{2,1}] & [K_{2,2}] & 0 & 0 & \dots & 0 & 0 \\ & \dots & \dots & & & & \\ & \dots & \dots & & & & \\ \text{symm} & & & [K_{n-1,n-1}] & [K_{n-1,n}] & & \\ & & & & [K_{n,n}] & & \end{bmatrix} \quad (8.152)$$

The global displacement vector is

$$\{\Delta\} = [\{\Delta\}_1^T \{\Delta\}_2^T \dots \{\Delta\}_i^T \dots \{\Delta\}_n^T]^T \quad (8.153)$$

in which displacements at the i th story are

$$\{\Delta\}_i = [\delta_x \quad \delta_y \quad \theta_z \quad \delta_{z1} \quad \theta_{x1} \quad \theta_{y1} \quad \dots \quad \delta_{zL} \quad \theta_{xL} \quad \theta_{yL}]_i^T \quad (8.154)$$

where δ_x , δ_y , and θ_z are displacements at the master joint; δ_{zj} , θ_{xj} and θ_{yj} are displacements at the j th node (joint); and L is the largest number of nodes (i.e. NM_k) at the i th story. The structure's load vector is

$$\{R\} = [\{R\}_1^T \quad \{R\}_2^T \dots \{R\}_i^T \dots \{R\}_n^T]^T \quad (8.155)$$

in which the i th story load vector is

$$\{R\}_i = [F_x \quad F_y \quad M_z \quad F_{z1} \quad M_{x1} \quad M_{y1} \quad \dots \quad F_{zL} \quad M_{xL} \quad M_{yL}]_i^T \quad (8.156)$$

where F_x , F_y , and M_z are the loads at the master joint; F_{zj} , M_{xj} and M_{yj} are the loads at the j th node. The equilibrium equation of the structure is

$$[K]\{\Delta\} = \{R\} \quad (8.157)$$

which is a general expression of force-displacement relationship for a structural system. The brief outline given in Eqs (8.152)–(8.157) is the foundation for GSA. These equations, however, can be simplified for FFA as follows.

8.12.2.2. Solution Procedure

The procedure for FFA is summarized in the following six steps.

Step 1—form the stiffness matrix of the n th story, which is the building's top floor.

$$\begin{bmatrix} K_{11}^{(n)} & K_{12}^{(n)} \\ K_{21}^{(n)} & K_{22}^{(n)} \end{bmatrix} \begin{Bmatrix} \Delta_{n-1} \\ \Delta_n \end{Bmatrix} = \begin{Bmatrix} R_{n-1} \\ R_n \end{Bmatrix}; \quad \left(\text{let } [K]_n = \begin{bmatrix} K_{11}^{(n)} & K_{12}^{(n)} \\ K_{21}^{(n)} & K_{22}^{(n)} \end{bmatrix} \right) \quad (8.158)$$

Step 2—the equilibrium equation for the n th story, from the second row of Eq. (8.158), is

$$[K_{21}^{(n)}]\{\Delta\}_{n-1} + [K_{22}^{(n)}]\{\Delta\}_n = \{R\}_n \quad (8.159)$$

Rewrite Eq. (8.159) as

$$\begin{aligned} \{\Delta\}_n &= [K_{22}^{(n)}]^{-1}\{R\}_n - [K_{22}^{(n)}]^{-1}[K_{21}^{(n)}]\{\Delta\}_{n-1} \\ &= \{R'\}_n - [K']_n\{\Delta\}_{n-1} \end{aligned} \quad (8.160)$$

in which

$$\{R'\}_n = [K_{22}^{(n)}]^{-1}\{R\}_n; \quad [K']_n = [K_{22}^{(n)}]^{-1}[K_{21}^{(n)}]$$

Step 3—form the stiffness matrix of the $(n-1)$ th story. Note that $\{R_{n-1}\}$ can be either applied at the n th story or the $(n-1)$ th story. For the present formulation, $\{R_{n-1}\}$ is applied at the n th story as shown in Eq. (8.158). Thus

$$\begin{bmatrix} K_{11}^{(n-1)} & K_{12}^{(n-1)} \\ K_{21}^{(n-1)} & K_{22}^{(n-1)} \end{bmatrix} \begin{Bmatrix} \Delta_{n-2} \\ \Delta_{n-1} \end{Bmatrix} = \begin{Bmatrix} R_{n-2} \\ 0 \end{Bmatrix}; \quad \left(\text{let } [K]_{n-1} = \begin{bmatrix} K_{11}^{(n-1)} & K_{12}^{(n-1)} \\ K_{21}^{(n-1)} & K_{22}^{(n-1)} \end{bmatrix} \right) \quad (8.161)$$

From the first row of Eq. (8.158)

$$[K_{11}^{(n)}]\{\Delta\}_{n-1} + [K_{12}^{(n)}]\{\Delta\}_n = \{R\}_{n-1}$$

and the second row of Eq. (8.161)

$$[K_{21}^{(n-1)}]\{\Delta\}_{n-2} + [K_{22}^{(n-1)}]\{\Delta\}_{n-1} = \{0\}$$

Combining the above two equations yields

$$[K_{21}^{(n-1)}]\{\Delta\}_{n-2} + ([K_{22}^{(n-1)}] + [K_{11}^{(n)}])\{\Delta\}_{n-1} + [K_{12}^{(n)}]\{\Delta\}_n = \{R\}_{n-1} \quad (8.162)$$

Substituting Eq. (8.160) into Eq. (8.162) to eliminate $\{\Delta_n\}$ yields

$$[K_{21}^{(n-1)}]\{\Delta\}_{n-2} + ([K_{22}^{(n-1)}] + [K_{11}^{(n)}])\{\Delta\}_{n-1} + [K_{12}^{(n)}](\{R'\}_n - [K']_n\{\Delta\}_{n-1}) = \{R\}_{n-1} \quad (8.163)$$

Let

$$[K']_{n-1} = ([K_{22}^{(n-1)}] + [K_{11}^{(n)}] - [K_{12}^{(n)}])[K']_n^{-1}[K_{21}^{(n-1)}] \quad (8.164)$$

and

$$\{R'\}_{n-1} = ([K_{22}^{(n-1)}] + [K_{11}^{(n)}] - [K_{12}^{(n)}])[K']_n^{-1}(\{R\}_{n-1} - [K_{12}^{(n)}]\{R'\}_n) \quad (8.165)$$

Equation (8.163) can then be rewritten as

$$\{\Delta\}_{n-1} = \{R'\}_{n-1} - [K']_{n-1}\{\Delta\}_{n-2} \quad (8.166)$$

Step 4—repeat step 3 for stories $n-2$ through 2.

$$\{\Delta\}_2 = \{R'\}_2 - [K']_2\{\Delta\}_1 \quad (8.167)$$

Step 5—form the stiffness matrix of the first story.

$$[K]_1 = \begin{bmatrix} K_{11}^{(1)} & K_{12}^{(1)} \\ K_{21}^{(1)} & K_{22}^{(1)} \end{bmatrix} \quad (8.168)$$

Assume that the structure is fixed at its base, and the displacements at ground level are zero. The equilibrium equation at the first story becomes

$$[K_{12}^{(2)}]\{\Delta\}_2 + ([K_{22}^{(1)}] + [K_{11}^{(1)}])\{\Delta\}_1 = \{R\}_1 \quad (8.169)$$

If ground floor displacements are not zero, then Eq. (8.169) should be revised based on the known displacements. Substituting Eq. (8.167) into Eq. (8.169) to eliminate $\{\Delta\}_2$ yields

$$[K_{12}^{(2)}]\{R'\}_2 + ([K_{22}^{(1)}] + [K_{11}^{(1)}] - [K_{12}^{(2)}][K']_2)\{\Delta\}_1 = \{R\}_1 \quad (8.170)$$

Let

$$[K']_1 = [K_{22}^{(1)}] + [K_{11}^{(1)}] - [K_{12}^{(2)}][K']_2 \quad (8.171)$$

and

$$\{R'\}_1 = \{R\}_1 - [K_{12}^{(2)}]\{R'\}_2 \quad (8.172)$$

Then Eq. (8.170) can be rewritten as

$$[K']_1\{\Delta\}_1 = \{R'\}_1 \quad (8.173)$$

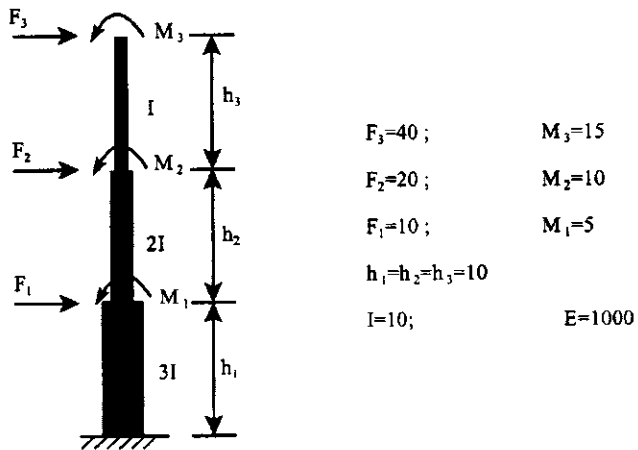


FIG. 8.48 Three-story building model.

Step 6—obtain displacements from the first story to the top of a building by backward substitution. From Eq. (8.173), $\{\Delta\}_1$ is

$$\{\Delta\}_1 = [K']_1^{-1} \{R'\}_1 \quad (8.174)$$

Substituting $\{\Delta\}_1$ into Eq. (8.167) yields

$$\{\Delta\}_2 = \{R'\} - [K']_2 \{\Delta\}_1 \quad (8.175)$$

Repeat the same procedure to obtain other floor displacements as $\{\Delta\}_3, \dots, \{\Delta\}_n$.

EXAMPLE 8.12.2 Using the numerical procedures presented in Eqs. (8.158)–(8.175), find the displacements of the three-story structure shown in Fig. 8.48. Consider horizontal and rotational displacements and neglect vertical displacement at each floor.

Solution: *Step 1*—form the stiffness matrix of the third story:

$$\begin{aligned}
 [K]_3 &= \begin{bmatrix} K_{11}^{(3)} & K_{12}^{(3)} \\ K_{21}^{(3)} & K_{22}^{(3)} \end{bmatrix} \\
 &= \begin{bmatrix} \frac{12EI}{L^3} & \frac{6EI}{L^2} & \frac{-12EI}{L^3} & \frac{6EI}{L^2} \\ \frac{6EI}{L^2} & \frac{4EI}{L} & \frac{-6EI}{L^2} & \frac{2EI}{L} \\ \frac{-12EI}{L^3} & \frac{-6EI}{L^2} & \frac{12EI}{L^3} & \frac{-6EI}{L^2} \\ \frac{6EI}{L^2} & \frac{2EI}{L} & \frac{-6EI}{L^2} & \frac{4EI}{L} \end{bmatrix} = \begin{bmatrix} 120 & 600 & | & -120 & 600 \\ 600 & 4000 & | & -600 & 2000 \\ --- & --- & | & --- & --- \\ -120 & -600 & | & 120 & -600 \\ 600 & 2000 & | & -600 & 4000 \end{bmatrix} \quad (a) \\
 \{R\}_3 &= \begin{Bmatrix} 40 \\ 15 \end{Bmatrix} \quad (b)
 \end{aligned}$$

Step 2—the equilibrium equation for the third story is

$$\begin{bmatrix} -120 & -600 \\ 600 & 2000 \end{bmatrix} \{\Delta\}_2 + \begin{bmatrix} 120 & -600 \\ -600 & 4000 \end{bmatrix} \{\Delta\}_3 = \begin{Bmatrix} 40 \\ 15 \end{Bmatrix} \quad (\text{c})$$

Following Eq. (8.160), we have

$$\begin{aligned} \{\Delta\}_3 &= \begin{bmatrix} 120 & -600 \\ -600 & 4000 \end{bmatrix}^{-1} \left(\begin{Bmatrix} 40 \\ 15 \end{Bmatrix} - \begin{bmatrix} -120 & -600 \\ 600 & 2000 \end{bmatrix} \{\Delta\}_2 \right) \\ &= \begin{Bmatrix} 1.408 \\ 0.215 \end{Bmatrix} - \begin{bmatrix} -1 & -10 \\ 0 & -1 \end{bmatrix} \{\Delta\}_2 \end{aligned} \quad (\text{d})$$

Step 3—form the stiffness matrix and load matrix of the second story:

$$[K]_2 = \begin{bmatrix} K_{11}^{(2)} & K_{12}^{(2)} \\ K_{21}^{(2)} & K_{22}^{(2)} \end{bmatrix} = \begin{bmatrix} 240 & 1200 & | & -240 & 1200 \\ 1200 & 8000 & | & -1200 & 4000 \\ --- & --- & | & --- & --- \\ -240 & -1200 & | & 240 & -1200 \\ 1200 & 4000 & | & -1200 & 8000 \end{bmatrix} \quad (\text{e})$$

$$\{R\}_2 = \begin{Bmatrix} 20 \\ 10 \end{Bmatrix} \quad (\text{f})$$

From Eq. (8.162)

$$\begin{aligned} &\begin{bmatrix} -240 & -1200 \\ 1200 & 4000 \end{bmatrix} \{\Delta\}_1 + \left(\begin{bmatrix} 240 & -1200 \\ -1200 & 8000 \end{bmatrix} + \begin{bmatrix} 120 & 600 \\ 600 & 4000 \end{bmatrix} \right) \{\Delta\}_2 \\ &+ \begin{bmatrix} -120 & 600 \\ -600 & 2000 \end{bmatrix} \{\Delta\}_3 = \begin{Bmatrix} 20 \\ 10 \end{Bmatrix} \end{aligned} \quad (\text{g})$$

and from Eq. (8.164),

$$\begin{aligned} [K_{22}^{(2)}] + [K_{12}^{(3)}] - [K_{11}^{(3)}][K']_3 &= \begin{bmatrix} 240 & -1200 \\ -1200 & 8000 \end{bmatrix} + \begin{bmatrix} 120 & 600 \\ 600 & 4000 \end{bmatrix} \\ &- \begin{bmatrix} -120 & 600 \\ -600 & 2000 \end{bmatrix} \begin{bmatrix} -1 & -10 \\ 0 & -1 \end{bmatrix} = \begin{bmatrix} 240 & -1200 \\ -1200 & 8000 \end{bmatrix} \end{aligned} \quad (\text{h})$$

$$[K']_2 = \begin{bmatrix} 240 & -1200 \\ -1200 & 8000 \end{bmatrix}^{-1} \begin{bmatrix} -240 & -1200 \\ 1200 & 4000 \end{bmatrix} = \begin{bmatrix} -1 & -10 \\ 0 & -1 \end{bmatrix} \quad (\text{i})$$

Substituting the above into Eq. (8.165) yields

$$\{R'\}_2 = \begin{bmatrix} 240 & -1200 \\ -1200 & 8000 \end{bmatrix}^{-1} \left(\begin{Bmatrix} 20 \\ 10 \end{Bmatrix} - \begin{bmatrix} -120 & 600 \\ -600 & 2000 \end{bmatrix} \begin{Bmatrix} 1.408 \\ 0.215 \end{Bmatrix} \right) = \begin{Bmatrix} 2.0625 \\ 0.3625 \end{Bmatrix} \quad (\text{j})$$

Using Eq. (8.166) results in

$$\{\Delta\}_2 = \begin{Bmatrix} 2.0625 \\ 0.3625 \end{Bmatrix} - \begin{bmatrix} -1 & -10 \\ 0 & -1 \end{bmatrix} \{\Delta\}_1 \quad (\text{k})$$

Step 4—skip this step for the three-story building.

Step 5—form the stiffness matrix of the first story and its equilibrium equation:

$$[K]_1 = \begin{bmatrix} K_{11}^{(1)} & K_{12}^{(1)} \\ K_{21}^{(1)} & K_{22}^{(1)} \end{bmatrix} = \left[\begin{array}{cc|cc} 360 & 1800 & -360 & 1800 \\ 1800 & 12,000 & -1800 & 6000 \\ \cdots & \cdots & \cdots & \cdots \\ -360 & -1800 & 360 & -1800 \\ 1800 & 6000 & -1800 & 12,000 \end{array} \right] \quad (\text{l})$$

$$\begin{bmatrix} -240 & 1200 \\ -1200 & 4000 \end{bmatrix} \{\Delta\}_2 + \left(\begin{bmatrix} 360 & -1800 \\ -1800 & 12,000 \end{bmatrix} + \begin{bmatrix} 240 & 1200 \\ 1200 & 8000 \end{bmatrix} \right) \{\Delta\}_1 = \begin{Bmatrix} 10 \\ 5 \end{Bmatrix} \quad (\text{m})$$

Substituting Eq. (k) into Eq. (m) to eliminate $\{\Delta\}_2$ yields

$$[K']_1 = \begin{bmatrix} 600 & -600 \\ -600 & 20000 \end{bmatrix} + \begin{bmatrix} -240 & 1200 \\ -1200 & 4000 \end{bmatrix} \begin{Bmatrix} 1 & 10 \\ 0 & 1 \end{Bmatrix} = \begin{bmatrix} 360 & -1800 \\ -1800 & 12,000 \end{bmatrix} \quad (\text{n})$$

$$\{R'\}_1 = \begin{Bmatrix} 10 \\ 5 \end{Bmatrix} - \begin{bmatrix} -240 & 1200 \\ -1200 & 4000 \end{bmatrix} \begin{Bmatrix} 2.0625 \\ 0.3625 \end{Bmatrix} = \begin{Bmatrix} 70 \\ 1030 \end{Bmatrix} \quad (\text{o})$$

$$\begin{bmatrix} 360 & -1800 \\ -1800 & 12,000 \end{bmatrix} \{\Delta\}_1 = \begin{Bmatrix} 70 \\ 1030 \end{Bmatrix} \quad (\text{p})$$

Step 6—find displacements by backward substitution:

$$\{\Delta\}_1 = \begin{Bmatrix} \delta_1 \\ \theta_1 \end{Bmatrix} = \begin{bmatrix} 360 & -1800 \\ -1800 & 12,000 \end{bmatrix}^{-1} \begin{Bmatrix} 70 \\ 1030 \end{Bmatrix} = \begin{Bmatrix} 2.4944 \\ 0.46 \end{Bmatrix} \quad (\text{q})$$

$$\{\Delta\}_2 = \begin{Bmatrix} \delta_2 \\ \theta_2 \end{Bmatrix} = \begin{Bmatrix} 2.0625 \\ 0.3625 \end{Bmatrix} - \begin{bmatrix} -1 & -10 \\ 0 & -1 \end{bmatrix} \begin{Bmatrix} 2.4944 \\ 0.46 \end{Bmatrix} = \begin{Bmatrix} 9.1569 \\ 0.8225 \end{Bmatrix} \quad (\text{r})$$

$$\{\Delta\}_3 = \begin{Bmatrix} \delta_3 \\ \theta_3 \end{Bmatrix} = \begin{Bmatrix} 1.408 \\ 0.215 \end{Bmatrix} - \begin{bmatrix} -1 & -10 \\ 0 & -1 \end{bmatrix} \begin{Bmatrix} 9.1569 \\ 0.8225 \end{Bmatrix} = \begin{Bmatrix} 18.7899 \\ 1.0375 \end{Bmatrix} \quad (\text{s})$$

8.13. MASS MATRIX ASSEMBLY

From Fig. 8.49, the relationship between the lumped mass of master joint MC (mass center) and the lumped mass of a slave joint (nodes 1, 2, 3, and 4) can be expressed as

$$\begin{aligned} [M]_{\text{master}} &= [T_{\text{ms}}] [M]_{\text{slave}} [T_{\text{ms}}]^T \\ &= \begin{bmatrix} m_x & 0 & 0 & 0 & 0 & -m_x Y_{\text{ms}} \\ m_y & 0 & 0 & 0 & 0 & m_y X_{\text{ms}} \\ m_z & 0 & 0 & 0 & 0 & 0 \\ \text{symm} & 0 & 0 & 0 & 0 & 0 \\ & & & & & m_x Y_{\text{ms}}^2 + m_y X_{\text{ms}}^2 \end{bmatrix} \end{aligned} \quad (8.176)$$

where X_{ms} and Y_{ms} are defined in Fig. 8.49 in terms of a typical slave joint, such as joint 2; matrix

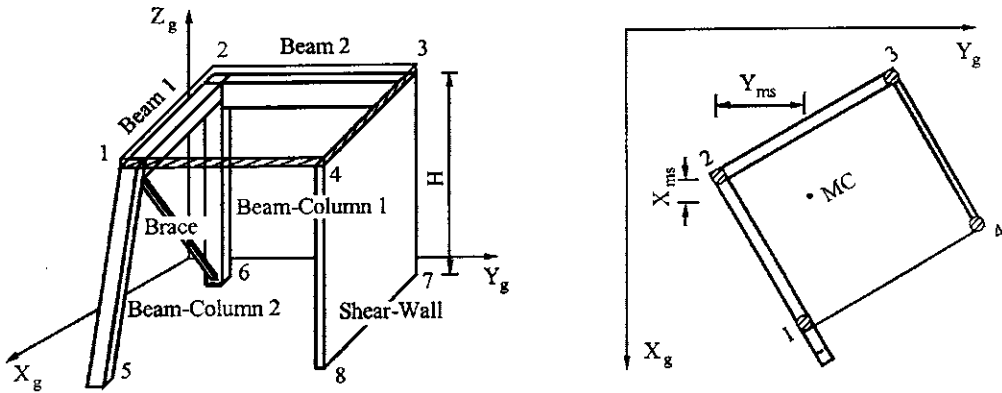


FIG. 8.49 Relationship between master joint and slave joint.

$[T_{ms}]$ is given in Eq. (8.6) and the lumped mass matrix of a slave joint is

$$[M]_{\text{slave}} = \begin{bmatrix} m_x & 0 & 0 & 0 & 0 & 0 \\ 0 & m_y & 0 & 0 & 0 & 0 \\ 0 & 0 & m_z & 0 & 0 & 0 \\ 0 & 0 & 0 & 0 & 0 & 0 \\ 0 & 0 & 0 & 0 & 0 & 0 \\ 0 & 0 & 0 & 0 & 0 & 0 \end{bmatrix} \quad (8.177)$$

If vertical inertia force is not considered, then let $m_z = 0$, and the d.o.f. of δ_z can be eliminated from the stiffness matrix. Since rotatory inertia is small and negligible, θ_x and θ_y can also be eliminated. After excluding d.o.f. of δ_z , θ_x , θ_y from Eq. (8.176), the result is

$$[M]_{\text{master}} = \begin{bmatrix} m_x & 0 & -m_x Y_{ms} \\ 0 & m_y & m_y X_{ms} \\ \text{symm} & m_x Y_{ms}^2 + m_y X_{ms}^2 & \end{bmatrix} \quad (8.178)$$

For the i th floor with L joints, the mass matrix of a system is

$$[M_i] = \begin{bmatrix} \sum_{j=1}^L m_{xj} & 0 & \sum_{j=1}^L (-m_{xj} Y_{msj}) & 0 & \dots & \dots & 0 \\ \sum_{j=1}^L m_{yj} & \sum_{j=1}^L (m_{yj} X_{msj}) & 0 & \dots & \dots & \dots & 0 \\ \sum_{j=1}^L (m_{xj} Y_{msj}^2 + m_{yj} X_{msj}^2) & 0 & \dots & \dots & \dots & \dots & 0 \\ 0 & \dots & \dots & 0 & \dots & \dots & 0 \\ \dots & \dots & \dots & 0 & \dots & \dots & 0 \\ \dots & \dots & \dots & 0 & \dots & \dots & 0 \end{bmatrix} \quad (8.179)$$

Note that the MC of a floor should be located at either the rigidity center or the mass center of the floor. Eq. (8.179) is based on the assumption that MC is at the rigidity center. If MC is at the mass center, then Eq. (8.179) becomes a diagonal matrix, which is usually preferred in dynamic

analysis. Thus

$$\begin{aligned}\sum_{j=1}^L (-m_{xj} Y_{msj}) &= 0 \\ \sum_{j=1}^L (m_{yj} X_{msj}) &= 0\end{aligned}$$

Recall that the mass matrix does not include d.o.f. where inertia force is neglected. These d.o.f. should be excluded from the stiffness matrix to reduce computer storage and improve computational efficiency. Rewrite the structural global stiffness matrix [Eq. (8.144)] as

$$[K] = \begin{bmatrix} [K_{mm}] & [K_{ms}] \\ [K_{sm}] & [K_{ss}] \end{bmatrix} \quad (8.180)$$

where $[K_{mm}]$ is the submatrix corresponding to the master joints with lumped-mass inertia forces, and $[K_{ss}]$ is the submatrix corresponding to slave joints without lumped mass. Arrange the mass matrix to match the above stiffness matrix, which becomes

$$[M] = \begin{bmatrix} [M]_m & [0] \\ [0] & [0]_s \end{bmatrix} \quad (8.181)$$

where $[M]_m$ is a diagonal matrix

$$\text{diag}([M]_m) = [M_1 \ M_1 \ J_1 \ M_2 \ \dots \ J_{n-1} \ M_n \ M_n \ J_n] \quad (8.182)$$

in which n is the number of stories; M_j and M_i are the masses associated with translational d.o.f. of δ_{xj} and δ_{yj} , and J_j is the torsional mass for $\delta_{\theta j}$ at the j th floor. It is assumed that vertical inertia forces of columns are neglected and the masses at each floor are lumped at the mass center of that floor. Substituting Eqs. (8.181) and (8.182) into the following eigensolution matrix,

$$([K] - p^2[M])\{X\} = \{0\} \quad (8.183)$$

yields

$$\begin{bmatrix} [K_{mm}] & [K_{ms}] \\ [K_{sm}] & [K_{ss}] \end{bmatrix} \begin{Bmatrix} X_m \\ X_s \end{Bmatrix} - p^2 \begin{bmatrix} [M]_m & [0] \\ [0] & [0]_s \end{bmatrix} \begin{Bmatrix} X_m \\ X_s \end{Bmatrix} = \begin{Bmatrix} 0 \\ 0 \end{Bmatrix} \quad (8.184)$$

from which

$$[K_{mm}]\{X_m\} + [K_{ms}]\{X_s\} - p^2[M]_m\{X_m\} = \{0\} \quad (8.185)$$

and

$$[K_{sm}]\{X_m\} + [K_{ss}]\{X_s\} = \{0\} \quad (8.186)$$

Displacements at slave joints can be expressed in terms of master joints (mass centers) as

$$[X_s] = -[K_{ss}]^{-1}[K_{sm}]\{X_m\} \quad (8.187)$$

Thus $\{X_s\}$ can be eliminated by substituting Eq. (8.187) into (8.185)

$$([K_{mm}] - [K_{ms}][K_{ss}]^{-1}[K_{sm}])\{X_m\} - p^2[M]_m\{X_m\} = \{0\} \quad (8.188)$$

Let

$$[K]_m = [K_{mm}] - [K_{ms}][K_{ss}]^{-1}[K_{sm}] \quad (8.189)$$

Then the eigensolution matrix in Eq. (8.183) can be reduced to

$$([K]_m - p^2 [M]_m) \{X_m\} = \{0\} \quad (8.190)$$

To find $[K]_m$, we may use Eq. (8.189) directly or employ the following *numerical elimination technique*.

Let the load be equal to 1 at the position corresponding to δ_x of the first mass center. No other load exists, so the displacement vector is $\{\Delta\}_{\delta x1}$. Then let the unit load be applied to δ_y of the same mass center. Other loads are zero, so $\{\Delta\}_{\delta y1}$; then $\{\Delta\}_{\theta z1}$. Repeating the same procedure for other mass centers, the result is $\{\Delta\}_{\delta x2}$, $\{\Delta\}_{\delta y2}$, $\{\Delta\}_{\theta z2}$, ..., $\{\Delta\}_{\delta xn}$, $\{\Delta\}_{\delta yn}$, $\{\Delta\}_{\theta zn}$. Keep only the displacements corresponding to the mass center in the above displacement vectors. Then put them together; we obtain

$$[\Delta]_m = [\{\Delta\}_{\delta x1} \ \{\Delta\}_{\delta y1} \ \{\Delta\}_{\theta z1} \dots \{\Delta\}_{\delta xn} \ \{\Delta\}_{\delta yn} \ \{\Delta\}_{\theta zn}]_{3n \times 3n} \quad (8.191)$$

$[\Delta]_m$ is a $3n$ by $3n$ matrix, and

$$[K]_m = [\Delta]_m^{-1} \quad (8.192)$$

In finding $[\Delta]_m$, there is no need to find the displacement vectors of the mass center one by one. Instead a load matrix $[R]$ can be constructed. Solve the equation $[K] \{\Delta\} = \{R\}$, and the $[\Delta]_m$ matrix can be obtained simultaneously.

EXAMPLE 8.13.1 Find $[K_m]$ corresponding to $\{\delta_x\}$ of the structure shown in Fig. 8.48 of Example 8.12.2 by using FFA. Eliminate $\{\Delta\}_{\theta z}$ and neglect $\{\Delta\}_{\delta y}$.

Solution: To find $\{\Delta\}_{\delta x}$ of the three-story building, the load matrix is

$$[R] = \begin{bmatrix} [R]_3 \\ [R]_2 \\ [R]_1 \end{bmatrix}; \quad [R]_3 = \begin{bmatrix} 1 & 0 & 0 \\ 0 & 0 & 0 \end{bmatrix}; \quad [R]_2 = \begin{bmatrix} 0 & 1 & 0 \\ 0 & 0 & 0 \end{bmatrix}; \quad [R]_1 = \begin{bmatrix} 0 & 0 & 1 \\ 0 & 0 & 0 \end{bmatrix} \quad (a)$$

Using the above load matrix $[R]_3$ in Eq. (d) of Example 8.12.2 gives

$$\begin{aligned} [\Delta]_3 &= \begin{bmatrix} 120 & -600 \\ -600 & 4000 \end{bmatrix}^{-1} \left(\begin{bmatrix} 1 & 0 & 0 \\ 0 & 0 & 0 \end{bmatrix} - \begin{bmatrix} -120 & -600 \\ 600 & 2000 \end{bmatrix} \{\Delta\}_2 \right) \\ &= \begin{bmatrix} 0.003 & 0 & 0 \\ 0.005 & 0 & 0 \end{bmatrix} - \begin{bmatrix} -1 & -10 \\ 0 & -1 \end{bmatrix} \{\Delta\}_2 \end{aligned} \quad (b)$$

Using $[R]_2$ given above in Eq. (j) of Example 8.12.2 gives

$$\begin{aligned} [R']_2 &= \begin{bmatrix} 240 & -1200 \\ -1200 & 8000 \end{bmatrix}^{-1} \left(\begin{bmatrix} 0 & 1 & 0 \\ 0 & 0 & 0 \end{bmatrix} - \begin{bmatrix} -120 & 600 \\ -600 & 2000 \end{bmatrix} \begin{bmatrix} 0.033 & 0 & 0 \\ 0.005 & 0 & 0 \end{bmatrix} \right) \\ &= \begin{bmatrix} 0.0417 & 0.0167 & 0 \\ 0.0075 & 0.0025 & 0 \end{bmatrix} \end{aligned} \quad (c)$$

which is substituted into Eq. (k) of that example; then

$$[\Delta]_2 = \begin{bmatrix} 0.0417 & 0.0167 & 0 \\ 0.0075 & 0.0025 & 0 \end{bmatrix} - \begin{bmatrix} -1 & -10 \\ 0 & -1 \end{bmatrix} \{\Delta\}_1 \quad (d)$$

Employing $[R]_1$ in Eq. (o) of that example gives

$$\begin{aligned}[R']_1 &= \begin{bmatrix} 0 & 0 & 1 \\ 0 & 0 & 0 \end{bmatrix} - \begin{bmatrix} -240 & 1200 \\ -1200 & 4000 \end{bmatrix} \begin{bmatrix} 0.0417 & 0.0167 & 0 \\ 0.0075 & 0.0025 & 0 \end{bmatrix} \\ &= \begin{bmatrix} 1 & 1 & 1 \\ 20 & 10 & 0 \end{bmatrix}\end{aligned}\quad (\text{e})$$

which is employed in Eq. (q) of that example, leading to

$$\begin{aligned}[\Delta]_1 &= \begin{bmatrix} \delta_{23} & \delta_{22} & \delta_{21} \\ \theta_{23} & \theta_{22} & \theta_{21} \end{bmatrix} = \begin{bmatrix} 360 & -1800 \\ -1800 & 12000 \end{bmatrix} \begin{bmatrix} 1 & 1 & 1 \\ 20 & 10 & 0 \end{bmatrix} \\ &= \frac{1}{9} \begin{bmatrix} 0.4000 & 0.250 & 0.100 \\ 0.0075 & 0.045 & 0.015 \end{bmatrix}\end{aligned}\quad (\text{f})$$

Using $\{\Delta\}_1$ just obtained in Eq. (d) above, we have

$$[\Delta]_2 = \begin{bmatrix} \delta_{23} & \delta_{22} & \delta_{21} \\ \theta_{23} & \theta_{22} & \theta_{21} \end{bmatrix} = \frac{1}{9} \begin{bmatrix} 1.5250 & 0.8500 & 0.250 \\ 0.1425 & 0.0675 & 0.015 \end{bmatrix}\quad (\text{g})$$

Similarly from Eq. (b),

$$[\Delta]_3 = \begin{bmatrix} \delta_{33} & \delta_{32} & \delta_{31} \\ \theta_{33} & \theta_{32} & \theta_{31} \end{bmatrix} = \frac{1}{9} \begin{bmatrix} 3.25 & 1.5250 & 0.400 \\ 1.47 & 0.0675 & 0.015 \end{bmatrix}\quad (\text{h})$$

Combining Eqs. (f)–(h) yields

$$\begin{bmatrix} [\Delta]_1 \\ [\Delta]_2 \\ [\Delta]_3 \end{bmatrix} = \begin{bmatrix} \delta_{13} & \delta_{12} & \delta_{11} \\ \theta_{13} & \theta_{12} & \theta_{11} \\ \delta_{23} & \delta_{22} & \delta_{21} \\ \theta_{23} & \theta_{22} & \theta_{21} \\ \delta_{33} & \delta_{32} & \delta_{31} \\ \theta_{33} & \theta_{32} & \theta_{31} \end{bmatrix} = \frac{1}{9} \begin{bmatrix} 0.400 & 0.250 & 0.100 \\ 0.075 & 0.045 & 0.015 \\ 1.525 & 0.850 & 0.250 \\ 0.142 & 0.0675 & 0.015 \\ 3.250 & 1.525 & 0.400 \\ 1.470 & 0.0675 & 0.015 \end{bmatrix}\quad (\text{i})$$

Eliminate rotational displacement from the above; then the rest of the elements in matrix form $[\Delta]_m$ corresponding horizontal displacements become

$$[\Delta]_m = \frac{1}{9} \begin{bmatrix} 0.10 & 0.25 & 0.40 \\ 0.25 & 0.85 & 1.52 \\ 0.40 & 1.52 & 3.25 \end{bmatrix}\quad (\text{j})$$

which is a *flexibility matrix* whose inversion is a stiffness matrix,

$$[K]_m = [\Delta]_m^{-1} = \begin{bmatrix} 411.17 & -190.59 & 38.82 \\ & 155.29 & -49.41 \\ & \text{symm} & 21.18 \end{bmatrix}\quad (\text{k})$$

Note that either the flexibility matrix in Eq. (j) or the stiffness matrix in Eq. (k) can be used for eigensolutions as discussed in Section 2.6.

8.14. LOADING MATRIX ASSEMBLY

For structural system analysis, a stiffness matrix is formed in association with d.o.f. at the structural joints. Each joint has member(s) connected to it. Therefore the loads which act on member(s) but not on joints must be transferred to the corresponding joints by using fixed-end forces.

8.14.1. Vertical Static or Harmonic Forces

For vertical loads in gravity direction acting on a beam or a member, the fixed-end forces including moments and shears are found and then transferred to joints as unbalanced forces. This procedure was applied to steady-state vibration introduced in Section 4.5.5 for dynamic stiffness and in Section 6.3 for consistent mass method. For the structural model presented in this chapter, the positive direction of unbalanced forces at a structural system's joint should be the same as the system's positive d.o.f. For a beam connected to a floor slab which is rigid in its plane (see Fig. 8.35), axial forces along X_e and bending about Z_e are neglected. Thus the unbalanced forces due to a vertical load are only aligned with the Z_e -axis of the member and should be transferred to the member's structural joints. For member i , the unbalanced forces can be expressed as

$$\begin{aligned}\{R_{ti}\} &= [F_{xs} \quad F_{ys} \quad F_{zs} \quad M_{xs} \quad M_{ys} \quad M_{zs} \quad F_{xe} \quad F_{ye} \quad F_{ze} \quad M_{xe} \quad M_{ye} \quad M_{ze}]^T \\ &= [0 \quad 0 \quad F_{ozs} \quad 0 \quad -M_{oyz} \quad 0 \quad 0 \quad 0 \quad F_{oze} \quad 0 \quad M_{oye} \quad 0]^T\end{aligned}\quad (8.193)$$

To put the local unbalanced loads into the global load vector, the following transformation is necessary:

$$\{R_i\} = [\bar{C}_j] [\bar{C}_e]^T \{R_{ti}\} \quad (8.194)$$

where $[\bar{C}_j]$ and $[\bar{C}_e]$ were defined previously for different types of members, such as the beam-column in Eq. (8.39). After finding the internal forces $\{F_e\}_i$ of the i th member resulting from deformations (displacements), the actual internal forces of the member are obtained as

$$\{F_e\}'_i = \{F_e\}_i \pm \{R_{ti}\} \quad (8.195)$$

in which the positive (+) or negative sign (-) of $\{R_{ti}\}$ adjusts the fixed-end force's direction. For instance, the two fixed-end moments of a beam are opposite to each other; when the counter-clockwise direction is positive, the clockwise direction is negative. The global load vector of a structure can be expressed as

$$\{R\} = \sum_{i=1}^{NM} \{R_i\} \quad (8.196)$$

where NM is the total number of structural members. When using the FFA method, $\{R\}$ based on Eq. (8.155) can be written as

$$\{R\} = [\{R\}_1^T \dots \{R\}_i^T \dots \{R\}_n^T]^T \quad (8.197)$$

where

$$\{R\}_i = [0 \quad 0 \quad 0 \quad R_1 \quad M_{x1} \quad M_{y1} \quad \dots \quad R_L \quad M_{xL} \quad M_{yL}]^T \quad (8.198)$$

EXAMPLE 8.14.1 The two-story building structure shown in Fig. 8.50 is subjected to harmonic forces $q_1 \cos \omega t$ and $q_2 \cos \omega t$ acting vertically on beam b_1 and b_2 , respectively. Form load matrix $\{R\}$ for steady-state vibration response.

Solution: For steady-state vibration response, the time function $\cos \omega t$ is assumed to be a unit value. Thus, the fixed-end shears and moments for beam b_1 can be expressed as (see Fig. 8.35 for sign convention):

$$\left. \begin{aligned} F_{oz1} &= \frac{q_1 L}{2}; & F_{oz2} &= \frac{q_1 L}{2} \\ M_{oy1} &= -\frac{q_1 L^2}{12}; & M_{oy2} &= \frac{q_1 L^2}{12} \end{aligned} \right\} \quad (a)$$

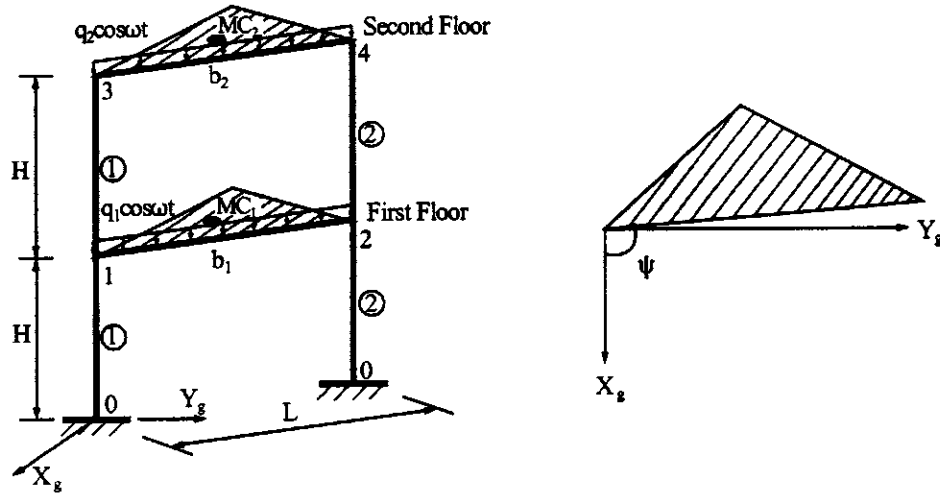


FIG. 8.50 Two-story building structure.

and

$$\{R_{t1}\} = \left[0 \ 0 \ \frac{q_1 L}{2} \ 0 \ \frac{-q_1 L^2}{12} \ 0 \ 0 \ 0 \ \frac{q_1 L}{2} \ 0 \ \frac{q_1 L^2}{12} \ 0 \right]^T \quad (b)$$

Similarly for beam b_2

$$\{R_{t2}\} = \left[0 \ 0 \ \frac{q_2 L}{2} \ 0 \ \frac{-q_2 L^2}{12} \ 0 \ 0 \ 0 \ \frac{q_2 L}{2} \ 0 \ \frac{q_2 L^2}{12} \ 0 \right]^T \quad (c)$$

Each floor is parallel to the $X_g - Y_g$ plane; thus from Eq. (8.110), $c_x = \cos \psi$, $c_y = \sin \psi$, $c_z = 0$, $l_1 = \cos \psi$, $l_2 = \sin \phi$, $l_3 = 0$, $m_1 = -\sin \psi$, $m_2 = \cos \psi$, $m_3 = 0$, $n_1 = n_2 = 0$, $n_3 = 1$, we have

$$[C_e] = \begin{bmatrix} \cos \psi & \sin \psi & 0 \\ -\sin \psi & \cos \psi & 0 \\ 0 & 0 & 1 \end{bmatrix} \quad (d)$$

$$[\bar{C}_{e1}] = \begin{bmatrix} [C_e]_1 & 0 & 0 & 0 \\ 0 & [C_e]_1 & 0 & 0 \\ 0 & 0 & [C_e]_2 & 0 \\ 0 & 0 & 0 & [C_e]_2 \end{bmatrix} = [\bar{C}_{e2}] \quad (e)$$

Assume the GCS is parallel to the JSC; then $[\bar{C}_{j1}] = [I]$; and

$$\begin{aligned} [\bar{C}_{j2}] &= [\bar{C}_{j1}] = [I]_{12 \times 12} \\ \{R_{t1}\} &= [\bar{C}_{j1}] [\bar{C}_{e1}]^T \{R_{t1}\} \end{aligned} \quad (f)$$

$$= \left[0 \ 0 \ \frac{q_1 L}{2} \ \frac{-q_1 L^2 \sin \psi}{12} \ \frac{-q_1 L^2 \cos \psi}{12} \ 0 \ 0 \ 0 \ \frac{q_1 L}{2} \ \frac{q_1 L^2 \sin \psi}{12} \ \frac{q_1 L^2 \cos \psi}{12} \ 0 \right]^T \quad (g)$$

Thus

$$\begin{aligned}\{R_{t2}\} &= [\bar{C}_{f2}] [\bar{C}_{e2}]^T \{R_{t2}\} \\ &= \left[0 \quad 0 \quad \frac{q_2 L}{2} \quad \frac{-q_2 L^2 \sin \psi}{12} \quad \frac{-q_2 L^2 \cos \psi}{12} \quad 0 \quad 0 \quad 0 \quad \frac{q_2 L}{2} \quad \frac{q_2 L^2 \sin \psi}{12} \quad \frac{q_2 L^2 \cos \psi}{12} \quad 0 \right] \quad (h)\end{aligned}$$

As shown in Example 8.12.1, the relationship between element and global d.o.f. of b_1 and b_2 can be established in Eqs. (i) and (j), respectively.

Element d.o.f. of b_1	1	2	3	4	5	6	7	8	9	10	11	12	(i)
Global d.o.f.	1	2	4	5	6	3	1	2	7	8	9	3	
Element d.o.f. of b_2	1	2	3	4	5	6	7	8	9	10	11	12	(j)
Global d.o.f.	10	11	13	14	15	12	10	11	16	17	18	12	

Thus the final load matrix in GCS is

$$\begin{aligned}\{R\} &= \left[0 \quad 0 \quad 0 \quad \frac{q_1 L}{2} \quad \frac{-q_1 L^2 \sin \psi}{12} \quad \frac{-q_1 L^2 \cos \psi}{12} \quad \frac{q_1 L}{2} \quad \frac{q_1 L^2 \sin \psi}{12} \quad \frac{q_1 L^2 \cos \psi}{12} \right. \\ &\quad \left. 0 \quad 0 \quad 0 \quad \frac{q_2 L}{2} \quad \frac{-q_2 L^2 \sin \psi}{12} \quad \frac{-q_2 L^2 \cos \psi}{12} \quad \frac{q_2 L}{2} \quad \frac{q_2 L^2 \sin \psi}{12} \quad \frac{q_2 L^2 \cos \psi}{12} \right]^T \quad (k)\end{aligned}$$

8.14.2. Lateral Wind Forces

For general lateral forces, we can use the procedure discussed in Section 8.14.1 to transform non-joint to joint loads as unbalanced fixed-end forces. For wind load acting on a building structure's surface, we usually find equivalent forces lumped on floor levels that are transformed to respective MCs. At the top story, the lumped force equals the distributed forces on half the story; for the other stories, the lumped force equals the distributed forces acting on the upper and lower half of each individual floor. A lumped force transferred to MC can induce torsion which is equal to the force multiplied by its eccentricity measured from the lumped force's location to MC. Figure 8.51 explains this in more detail.

For triangular distributed wind forces, W_{xi} and W_{yi} are force magnitudes at the i th story height (Fig. 8.51b). Let d_{xi} and d_{yi} be eccentricities measured from the lumped-force location to the master joint of the i th story; typical lumped forces and torsions at the top and i th stories are given in Eq. (8.199a–f).

$$F_{xn} = W_{xn} \frac{h_n}{2} S_n \quad (8.199a)$$

$$F_{yn} = W_{yn} \frac{h_n}{2} L_n \quad (8.199b)$$

$$M_{zn} = F_{xn} d_{yn} + F_{yn} d_{xn} \quad (8.199c)$$

$$F_{xi} = W_{xi} \frac{1}{2} (h_{i+1} S_{i+1} + h_i S_i) \quad (8.199d)$$

$$F_{yi} = W_{yi} \frac{1}{2} (h_{i+1} L_{i+1} + h_i L_i) \quad (8.199e)$$

$$M_{zi} = F_{xi} d_{yi} + F_{yi} d_{xi} \quad (8.199f)$$

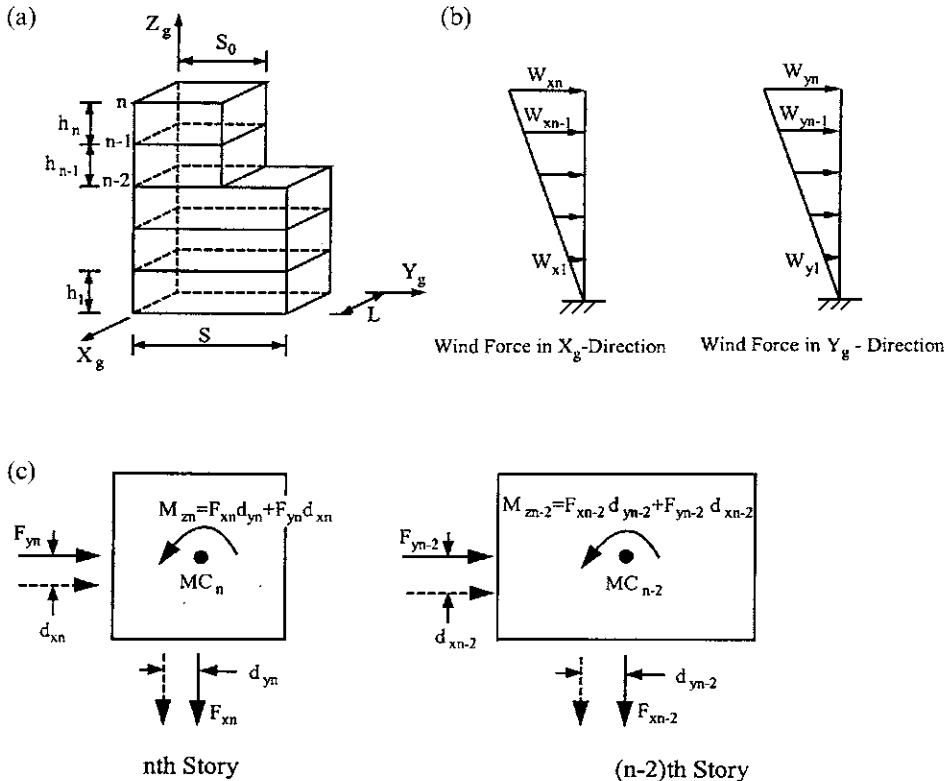


FIG. 8.51 Lumped forces transferred to MC. (a) Building structure. (b) Wind forces. (c) Loads at master joints.

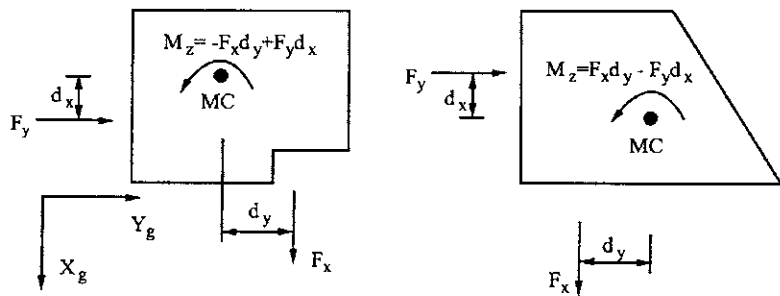


FIG. 8.52 Torsion direction.

The direction of torsion depends on the force direction relative to X_g and Y_g axes and the eccentricity. Sample torsion equations are shown in Fig. 8.52, where forces are positive; torsion is positive in the counterclockwise direction. The wind force vector is composed of transferred forces and torsion at MC of each floor.

EXAMPLE 8.14.2 For a two-story building structure in Example 8.14.1, two lumped forces, P_1 and P_2 , are applied at the first and second floors, respectively (see Fig. 8.53). Form the loading matrix $\{R\}$.

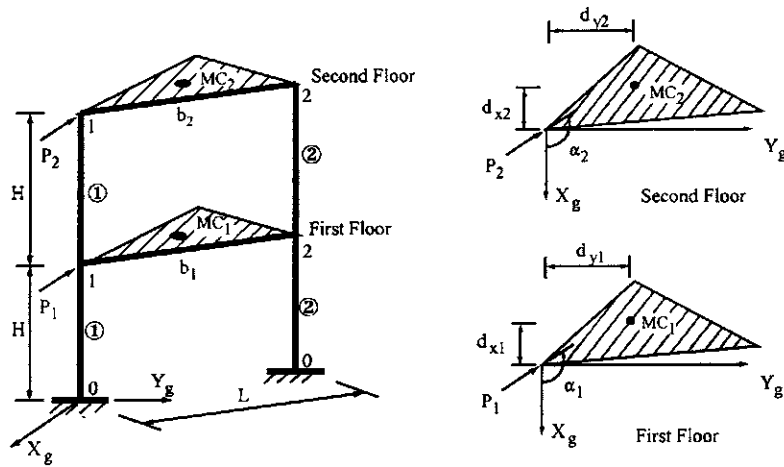


FIG. 8.53 Example 8.14.2.

Solution: Based on the solution of Example 8.14.1, the global d.o.f. are 18. The d.o.f. are 1, 2, 3 at master joint MC₁ and 10, 11, 12 at MC₂. For MC₁ at d.o.f. 1, 2, 3

$$F_{x1} = P_1 \sin \alpha_1 \quad (a)$$

$$F_{y1} = P_1 \cos \alpha_1 \quad (b)$$

$$M_{z1} = F_{x1}d_{y1} + F_{y1}d_{x1} = P_1(d_{y1} \sin \alpha_1 + d_{x1} \cos \alpha_1) \quad (c)$$

For MC₂ at d.o.f. 10, 11, 12

$$F_{x2} = P_2 \sin \alpha_2 \quad (d)$$

$$F_{y2} = P_2 \cos \alpha_2 \quad (e)$$

$$M_{z2} = F_{x2}d_{y2} + F_{y2}d_{x2} = P_2(d_{y2} \sin \alpha_2 + d_{x2} \cos \alpha_2) \quad (f)$$

Thus the loading matrix is

$$\{R\} = \begin{bmatrix} P_1 \sin \alpha_1 & P_1 \cos \alpha_1 & P_1(d_{y1} \sin \alpha_1 + d_{x1} \cos \alpha_1) & 0 & 0 & 0 & 0 & 0 & 0 \\ P_2 \sin \alpha_2 & P_2 \cos \alpha_2 & P_2(d_{y2} \sin \alpha_2 + d_{x2} \cos \alpha_2) & 0 & 0 & 0 & 0 & 0 & 0 \end{bmatrix}^T \quad (g)$$

Note that if α (α_1 or α_2) $< 90^\circ$, then $\cos \alpha > 0$ and F_x (F_{x1} or F_{x2}) > 0 ; if α (α_1 or α_2) $> 90^\circ$, then $\cos \alpha < 0$ and F_x (F_{x1} or F_{x2}) < 0 .

8.14.3. Lateral Dynamic Loads

For lateral dynamic loads acting on the building structure shown in Fig. 8.54, the acting load does not pass through the mass center (say *i*th story); torsion at that story is then induced by the lateral load as

$$M_{imz}(t) = F_i(t) (-\sin \theta_i d_y + \cos \theta_i d_x) \quad (8.200)$$

Horizontal loads which act at the mass center are

$$F_{imx}(t) = -F_i(t) \sin \theta_i \quad (8.201a)$$

$$F_{imy}(t) = F_i(t) \cos \theta_i \quad (8.201b)$$

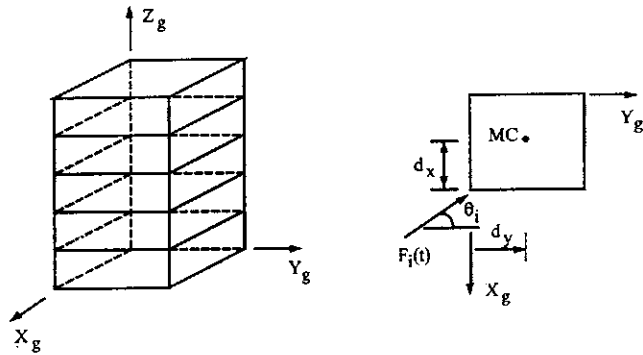


FIG. 8.54 Lateral dynamic loads.

At each story, load vectors corresponding to δ_x , δ_y , and θ_z are

$$\{F_{mi}(t)\} = \begin{Bmatrix} \{F_{imx}(t)\} \\ \{F_{imy}(t)\} \\ \{M_{imz}(t)\} \end{Bmatrix} = \begin{Bmatrix} -\sin \theta_i \\ \cos \theta_i \\ -\sin \theta_i d_y + \cos \theta_i d_x \end{Bmatrix} F_i(t) \quad (8.202)$$

The lateral dynamic load vector for an n -story building structure is

$$\{R(t)\} = \begin{Bmatrix} \{F_{m1}(t)\} \\ \dots \\ \{F_{mi}(t)\} \\ \dots \\ \{F_{mn}(t)\} \end{Bmatrix} \quad (8.203)$$

8.14.4. Seismic Excitations

Building structures subjected to seismic excitations can be analyzed by means of: (1) pseudo-dynamic procedure based on response spectra, (2) time-history response using numerical integration, or (3) equivalent lateral force procedure. Method 1 and 2 are discussed in earlier chapters, notably Chapter 7; method 3, based on building code recommendations, is covered in Chapter 10. For pseudo-dynamic procedure, the lateral pseudo-dynamic loads at each story are obtained for each of the modes included in the analysis; shear and moment at the base or any floor are then obtained for the individual modes by using equilibrium requirements. Using modal combination technique SRSS, CQC or ABSSUM (summation of individual absolute value of individual modes) yields the peak value of base shear and overturning moment. For instance, with SRSS the peak value of base shear for m modes is

$$V_b = (V_{b1}^2 + V_{b2}^2 + \dots + V_{bm}^2)^{\frac{1}{2}} \quad (8.204)$$

Similarly, the value of a member's internal forces or a structure's story drift is determined by combining the peak value of individual modal contributions with the same response (member force or story drift).

After the lateral pseudo-dynamic loads at each story are obtained, the seismic load vector is

$$\{R(t)\} = [\{R\}_1^T \dots \{R\}_i^T \dots \{R\}_n^T]^T \quad (8.205)$$

Since the seismic forces are acting on the mass center at each floor, the lateral force vector at i th

floor is

$$\{R\}_i = [F_{xs} \ F_{ys} \ 0 \ 0 \ \dots \ 0]^T \quad (8.206)$$

For time-history response analysis, the load vector is based on mass matrix and seismic acceleration records and may be expressed as

$$\{R(t)\} = -[M] \{\ddot{x}_g(t)\} \quad (8.207)$$

The dynamic equilibrium matrix for a structural system is

$$[M] \{\ddot{x}(t)\} + [C] \{\dot{x}(t)\} + [K_m] \{x(t)\} = \{R(t)\} \quad (8.208)$$

where $[M]$ and $[K_m]$ are given in Eqs. (8.207) and (8.208), respectively. Damping matrix, $[C]$, can be computed based on Section 3.3 in Chapter 3 as

$$[C] = \alpha[M] + \beta[K_m] \quad (8.209)$$

EXAMPLE 8.14.3 A two-story building structure is subjected to earthquake accelerations of N-S component $\ddot{u}_{N-S}(t)$ and E-W component $\ddot{u}_{E-W}(t)$, as shown in Fig. 8.55. Assume that MC_1 and MC_2 are mass centers of the first and second floor, respectively. Formulate the mass matrix $[M]$ and loading matrix $\{R(t)\}$.

Solution: Using Eq. (7.5) in Chapter 7 with the given accelerations in E-W and N-S directions, we obtain accelerations along the X_g and Y_g axes as

$$\ddot{u}_x(t) = \ddot{u}_{E-W}(t) \cos \theta' + \ddot{u}_{N-S}(t) \sin \theta' \quad (a)$$

$$\ddot{u}_y(t) = -\ddot{u}_{E-W}(t) \sin \theta' + \ddot{u}_{N-S}(t) \cos \theta' \quad (b)$$

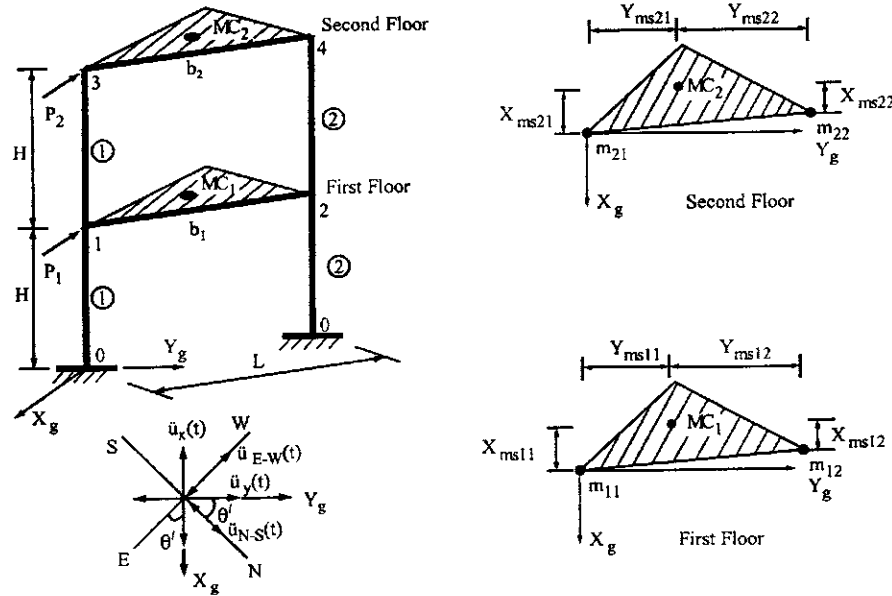


FIG. 8.55 Example 8.14.3.

The mass matrix for first and second floor is obtained from Eq. (8.178) as

$$[M] = \begin{bmatrix} [M_1] & 0 \\ 0 & [M_2] \end{bmatrix} \quad (c)$$

where

$$[M_1] = \begin{bmatrix} m_{11} + m_{12} & 0 & 0 \\ 0 & m_{11} + m_{12} & 0 \\ 0 & 0 & m_{11}(X_{ms11}^2 + Y_{ms11}^2) + m_{12}(X_{ms12}^2 + Y_{ms12}^2) \end{bmatrix} \quad (d)$$

and

$$[M_2] = \begin{bmatrix} m_{21} + m_{22} & 0 & 0 \\ 0 & m_{21} + m_{22} & 0 \\ 0 & 0 & m_{21}(X_{ms21}^2 + Y_{ms21}^2) + m_{22}(X_{ms22}^2 + Y_{ms22}^2) \end{bmatrix} \quad (e)$$

The load vector is

$$\{R(t)\} = -[M]\{\ddot{x}_g\} = -\begin{bmatrix} [M_1] & 0 \\ 0 & [M_2] \end{bmatrix} \begin{Bmatrix} \ddot{u}(t) \\ \ddot{u}_y(t) \\ 0 \\ \ddot{u}_x(t) \\ \ddot{u}_y(t) \\ 0 \end{Bmatrix} \quad (f)$$

8.15. ANALYSIS AND RESPONSE BEHAVIOR OF SAMPLE STRUCTURAL SYSTEMS

This section comprises two numerical examples. The first one demonstrates how to model a 2D structure based on 3D elements and then provides detailed analysis of a plane beam-column and shear-wall system. The second one involves a 3D structure subjected to multicomponent seismic input, which shows how significantly the interacting seismic input affects structural response.

EXAMPLE 8.15.1 A 2D beam-column and shear-wall structure is subjected to two concentrated forces as shown in Fig. 8.56. The beam-column has elastic modulus, $E = 29,000$ ksi; cross-section area, $A = 19.1$ in 2 ; and in-plane moment of inertia in the plane of bending, $I = 174$ in 4 . The shear wall has $K_a = 7000$ k, $K_b = (1.35)10^9$ k in 2 , and $K_s = (2.67)10^5$ k. Formulate the structural stiffness matrix by using the 3D elements presented previously and then find system displacements and member deformations and forces. Neither rigid zone nor second-order effect is considered.

Solution: Since the wall is fixed at the support, $\alpha = h$ and $\beta = 0$ should be used for stiffness coefficients. As a 2D structural system, only three in-plane d.o.f. exist at each joint: one horizontal displacement, one vertical displacement, and one bending. The others are restrained. Thus the dimension of the beam-column stiffness matrix is 6 by 6 where joints 4 and 5 are connected with a rigid-body bar. Assume that one of the principal planes of the beam-column cross-section is parallel to the X_g-Z_g plane, and that the JCS is parallel to the GCS. The in-plane stiffness matrix in the GCS of beam-columns can be established using Eq. (8.115). For member 1, the restrained d.o.f. are: $\delta_{3mx} = \theta_{3my} = \theta_{3mz} = \delta_{6mx} = \theta_{6my} = \theta_{6mz} = 0$; the stiffness matrix in the

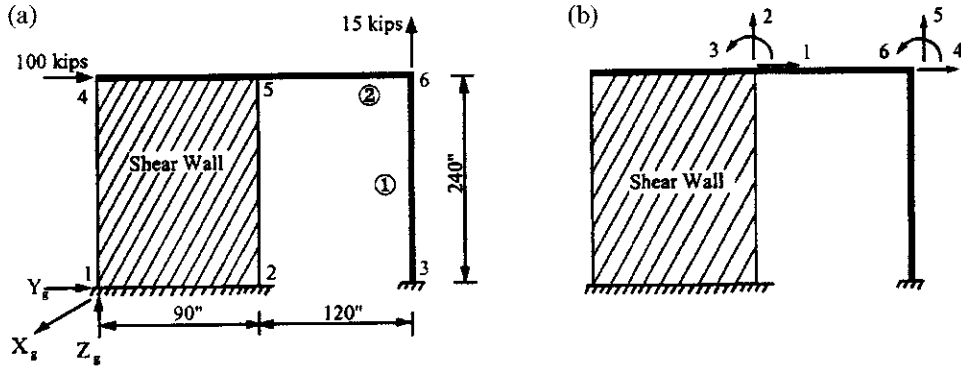


FIG. 8.56 Two-dimensional beam–column and shear-wall system. (a) Given structure. (b) Global d.o.f.

GCS is

$$\begin{Bmatrix} F_{3my} \\ F_{3mz} \\ M_{3mx} \\ F_{6my} \\ F_{6mz} \\ M_{6mx} \end{Bmatrix} = \begin{bmatrix} K_{2,2} & 0 & K_{2,4} & K_{2,8} & 0 & K_{2,10} \\ K_{3,3} & 0 & 0 & K_{3,9} & 0 & 0 \\ K_{4,4} & K_{4,8} & 0 & K_{4,10} & 0 & 0 \\ K_{8,8} & 0 & K_{8,10} & 0 & 0 & 0 \\ K_{9,9} & 0 & K_{9,10} & 0 & 0 & 0 \\ K_{10,10} & 0 & K_{10,10} & 0 & 0 & 0 \end{bmatrix} \begin{Bmatrix} \delta_{3my} \\ \delta_{3mz} \\ \theta_{3mx} \\ \delta_{6my} \\ \delta_{6mz} \\ \theta_{6mx} \end{Bmatrix} \quad (a)$$

Substituting the known conditions into Eq. (8.115) leads to

$$[K^1] = \begin{bmatrix} \frac{12EI}{L_1^3} & 0 & \frac{6EI}{L_1^2} & \frac{-12EI}{L_1^3} & 0 & \frac{6EI}{L_1^2} \\ \frac{EA}{L_1} & 0 & 0 & \frac{-EA}{L_1} & 0 & 0 \\ \frac{4EI}{L_1} & \frac{-6EI}{L_1^2} & 0 & \frac{2EI}{L_1} & 0 & 0 \\ \frac{12EI}{L_1^3} & 0 & \frac{-6EI}{L_1^2} & 0 & \frac{2EI}{L_1} & 0 \\ \frac{EA}{L_1} & 0 & \frac{4EI}{L_1} & 0 & \frac{-6EI}{L_1^2} & 0 \\ \frac{4EI}{L_1} & 0 & 0 & \frac{6EI}{L_1^2} & 0 & 0 \end{bmatrix} \quad (b)$$

Similarly for beam–column 2, $\delta_{5mx} = \theta_{5my} = \theta_{5mz} = \delta_{6mx} = \theta_{6my} = \theta_{6mz} = 0$, we have

$$\begin{Bmatrix} F_{5my} \\ F_{5mz} \\ M_{5mx} \\ F_{6my} \\ F_{6mz} \\ M_{6mx} \end{Bmatrix} = \begin{bmatrix} K_{2,2} & 0 & K_{2,4} & K_{2,8} & 0 & 0 \\ K_{3,3} & K_{3,4} & 0 & K_{3,9} & K_{3,10} & 0 \\ K_{4,4} & 0 & K_{4,9} & K_{4,10} & 0 & 0 \\ K_{8,8} & 0 & 0 & K_{9,10} & 0 & 0 \\ K_{9,9} & K_{9,10} & 0 & K_{10,10} & 0 & 0 \\ K_{10,10} & 0 & 0 & K_{10,10} & 0 & 0 \end{bmatrix} \begin{Bmatrix} \delta_{5my} \\ \delta_{5mz} \\ \theta_{5mx} \\ \delta_{6my} \\ \delta_{6mz} \\ \theta_{6mx} \end{Bmatrix} \quad (c)$$

and

$$[K^2] = \begin{bmatrix} \frac{EA}{L_2} & 0 & 0 & \frac{-EA}{L_2} & 0 & 0 \\ 0 & \frac{12EI}{L_2^3} & \frac{6EI}{L_2^2} & 0 & \frac{-12EI}{L_2^3} & \frac{6EI}{L_2^2} \\ 0 & \frac{6EI}{L_2^2} & \frac{4EI}{L_2} & 0 & \frac{-6EI}{L_2^2} & \frac{2EI}{L_2} \\ 0 & 0 & \frac{2EI}{L_2} & \frac{EA}{L_2} & 0 & 0 \\ 0 & \frac{2EI}{L_2} & 0 & 0 & \frac{12EI}{L_2^3} & \frac{-6EI}{L_2^2} \\ 0 & 0 & \frac{-6EI}{L_2^2} & \frac{4EI}{L_2} & 0 & 0 \end{bmatrix} \quad (\text{d})$$

The stiffness matrix of the shear wall can be obtained from Eqs. (8.137)–(8.139). Based on the numbering system shown in Fig. 8.56 and that of a typical wall given in Eq. (8.136), the restrained d.o.f. are

$$\text{at } J=1, \delta_{5mx}=0, \delta_{5my}=0, \delta_{5mz}=0; \quad \text{at } J=2, \delta_{4mx}=0, \delta_{4my}=0, \delta_{4mz}=0 \quad (\text{e})$$

$$\text{at } J=3, \delta_{1mx}=0, \delta_{1my}=0, \delta_{1mz}=0; \quad \text{at } J=4, \delta_{2mx}=0, \delta_{2my}=0, \delta_{2mz}=0. \quad (\text{f})$$

Since the wall is fixed at the base, its stiffness matrix is $[K_{11}]$ as given in Eq. (8.137). Considering restrained d.o.f. of Eq. (e), $[K_{11}]$ may be expressed as

$$\begin{Bmatrix} F_{j1m} \\ F_{j2m} \end{Bmatrix} = [K_{11}] \begin{Bmatrix} \delta_{j1m} \\ \delta_{j2m} \end{Bmatrix} \quad (\text{g})$$

where

$$[\delta_{j1m} \quad \delta_{j2m}]^T = [\delta_{5my} \quad \delta_{5mz} \quad \delta_{5mx} \quad \delta_{4my} \quad \delta_{4mz} \quad \delta_{4mx}]^T \quad (\text{h})$$

$$[K_{11}] = \begin{bmatrix} K_{2,2} & K_{2,3} & 0 & 0 & K_{2,9} & 0 \\ K_{3,2} & K_{3,3} & 0 & 0 & K_{3,9} & 0 \\ 0 & 0 & 0 & 0 & 0 & 0 \\ 0 & 0 & 0 & 0 & 0 & 0 \\ \text{symm} & & K_{9,9} & 0 & & \\ & & 0 & & & \end{bmatrix} = \begin{bmatrix} k_{11} & k_{12} & 0 & 0 & -k_{12} & 0 \\ k_{21} & k_{22} & 0 & 0 & k_{23} & 0 \\ 0 & 0 & 0 & 0 & 0 & 0 \\ 0 & 0 & 0 & 0 & 0 & 0 \\ \text{symm} & & k_{22} & 0 & & \\ & & 0 & & & 0 \end{bmatrix} \quad (\text{i})$$

in which the stiffness coefficients k , such as k_{11}, k_{12} , are given in Eq. (8.129).

Since node 5 is the master joint of the wall and the rigid bar on the wall (see Fig. 8.56), transformation between the slave joint at node 4 and the master joint is obtained from Eq. (8.2), with consideration of restrained d.o.f., as

$$[T_{ms}] = \begin{bmatrix} [T_{ms}]_5 & 0 \\ 0 & [T_{ms}]_4 \end{bmatrix} = \begin{bmatrix} 1 & 0 & 0 & 0 & 0 & 0 \\ 0 & 1 & 0 & 0 & 0 & 0 \\ 0 & 0 & 1 & 0 & 0 & 0 \\ 0 & 0 & 0 & 1 & 0 & 0 \\ 0 & 0 & 0 & 0 & 1 & 0 \\ 0 & 0 & 0 & 0 & Y_{ms} & 1 \end{bmatrix} \quad (\text{j})$$

Note that the displacement vector of Eq. (j) is $[\delta_{5my} \quad \delta_{5mz} \quad \delta_{5mx} \quad \delta_{4sy} \quad \delta_{4sz} \quad \delta_{4sx}]^T$. The parameters used in Eq. (8.2) are: at node 4, $X_{ms} = X_{gs} - X_{gm} = 0$; $Y_{ms} = Y_{gs} - Y_{gm} = 0 - 90 = -90$ in; $Z_{ms} = Z_{gs} - Z_{gm} = 240 - 240 = 0$; and at node 5, $X_{ms} = X_{gs} - X_{gm} = 0$; $Y_{ms} = Y_{gs} - Y_{gm} = 90 - 90 = 0$; $Z_{ms} = Z_{gs} - Z_{gm} = 240 - 240 = 0$. Submatrix $[K_{11}]$ of the shear-wall stiffness matrix

becomes

$$[K_{11}] = [T_{ms}][K_{11}][T_{ms}]^T = \begin{bmatrix} k_{11} & k_{12} & 0 & 0 & -k_{12} & -k_{12} Y_{ms} \\ k_{22} & k_{22} & 0 & 0 & k_{23} & k_{23} Y_{ms} \\ 0 & 0 & 0 & 0 & 0 & 0 \\ 0 & 0 & 0 & 0 & 0 & 0 \\ \text{symm} & & k_{22} & k_{22} & k_{22} Y_{ms} & k_{22} Y_{ms}^2 \end{bmatrix} \quad (\text{k})$$

in which the displacements at the slave joint (node 4) are transferred to the master joint (node 5). Thus the displacement vector is $\{\delta_m\} = [\delta_{5my} \ \delta_{5mz} \ \theta_{5mx} \ \delta_{6my} \ \delta_{6mz} \ \theta_{6mx}]^T$. The global stiffness matrix of the structure is

$$[K] = \begin{bmatrix} \frac{EA}{L_2} + k_{11} & 0 & -k_{12} Y_{ms} & \frac{-EA}{L_2} & 0 & 0 \\ 0 & \frac{12EI}{L_2^3} + (k_{22} + k_{23}) & \frac{6EI}{L_2^2} + (k_{22} + k_{23}) Y_{ms} & 0 & \frac{-12EI}{L_2^3} & \frac{6EI}{L_2^2} \\ -k_{12} Y_{ms} & \frac{6EI}{L_2^2} + (k_{22} + k_{23}) Y_{ms} & \frac{4EI}{L_2} + k_{22} Y_{ms}^2 & 0 & \frac{-6EI}{L_2^2} & \frac{2EI}{L_2} \\ \frac{-EA}{L_2} & 0 & 0 & \frac{EA}{L_2} + \frac{12EI}{L_1^2} & 0 & \frac{-6EI}{L_1^2} \\ 0 & 0 & 0 & 0 & \frac{12EI}{L_2^2} + \frac{EA}{L_1} & \frac{-6EI}{L_2^2} \\ 0 & 0 & 0 & \frac{-6EI}{L_1^2} & \frac{4EI}{L_2} + \frac{4EI}{L_1} & \end{bmatrix} \quad (\text{l})$$

From Fig. 8.56, we have $L_1 = w = 240$ in, $L_2 = 120$ in, $Y_{ms} = -90$ in. Substituting the known data into Eq. (l) yields

$$[K] = \begin{bmatrix} 5728.3333 & 0 & 267,000.00 & -4615.833 & 0 & 0 \\ 64.2083 & 790.0001 & 0 & -35.0416 & 2102.5 & \\ 0 & 69,932,262.48 & 0 & -2102.5 & 84,100 & \\ & & 4620.2135 & 0 & -525.625 & \\ \text{symm} & & & 2342.9583 & -2102.5 & \\ & & & & 252,300 & \end{bmatrix} \quad (\text{m})$$

The load vector is

$$\{R\} = [F_{5my} \ F_{5mz} \ M_{5mx} \ F_{6my} \ F_{6mz} \ M_{6mx}]^T = [100 \ 0 \ 0 \ 0 \ 15 \ 0]^T \quad (\text{n})$$

Structural displacements are then found as

$$\{\Delta\} = \left\{ \begin{array}{c} \Delta_5 \\ \Delta_6 \end{array} \right\} = \left\{ \begin{array}{c} \delta_{5my} \\ \delta_{5mz} \\ \theta_{5mx} \\ \delta_{6my} \\ \delta_{6mz} \\ \theta_{6mx} \end{array} \right\} = [K]^{-1}\{R\} = \left\{ \begin{array}{c} 1.0605 \\ -0.0897 \\ -0.0041 \\ 1.0600 \\ 0.0053 \\ 0.0044 \end{array} \right\} \quad (\text{o})$$

which is shown in Fig. 8.57a.

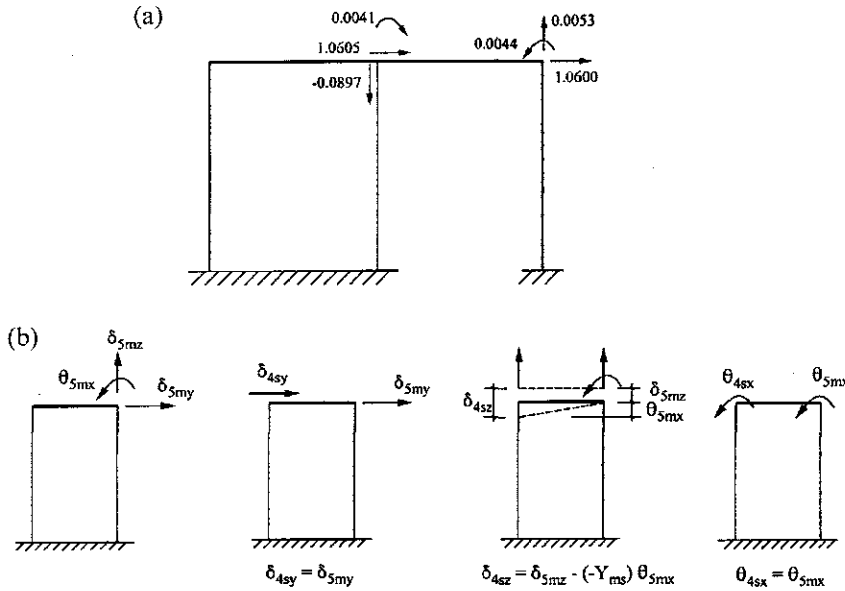


FIG. 8.57 Displacement details. (a) Displacements. (b) Relationship between Wall's master and slave joints.

From Fig. 8.57b, displacements of joint 4 are

$$\{\Delta_4\} = \begin{bmatrix} 1 & 0 & 0 \\ 0 & 1 & 0 \\ 0 & Y_{ms} & 1 \end{bmatrix}^T \{\Delta_5\} = \begin{Bmatrix} 1.0605 \\ 0.2751 \\ -0.0041 \end{Bmatrix} \quad (p)$$

The internal forces of beam-column 1 can be obtained as

$$\begin{aligned} \begin{Bmatrix} F_{3y} \\ F_{3z} \\ M_{3x} \\ F_{6y} \\ F_{6z} \\ M_{6x} \end{Bmatrix} &= [K^1] \begin{Bmatrix} \Delta_3 \\ \Delta_6 \end{Bmatrix} = \begin{bmatrix} \frac{841}{192} & 0 & \frac{4205}{8} & \frac{-841}{192} & 0 & \frac{4205}{8} \\ 2307.917 & 0 & 0 & 2307.917 & 0 & 0 \\ & 84,100 & \frac{-4205}{8} & 0 & 42,050 & 0 \\ & \frac{841}{192} & 0 & \frac{-4205}{8} & 0 & 0 \\ & \text{symm} & & 2307.917 & 0 & 0 \\ & & & & 84100 & 0 \end{bmatrix} \begin{Bmatrix} 0 \\ 0 \\ 0 \\ 1.0600 \\ 0.0053 \\ 0.0044 \end{Bmatrix} \\ &= \begin{Bmatrix} -2.36 \\ -12.30 \\ -374.17 \\ 2.36 \\ 12.30 \\ -191.21 \end{Bmatrix} \quad (q) \end{aligned}$$

Similarly, the internal forces of beam-column 2 are

$$\begin{Bmatrix} F_{5y} \\ F_{5z} \\ M_{5x} \\ F_{6y} \\ F_{6z} \\ M_{6x} \end{Bmatrix} = [K^2] \begin{Bmatrix} \Delta_5 \\ \Delta_6 \end{Bmatrix} = \begin{bmatrix} 4615.8333 & 0 & 0 & -4615.8333 & 0 & 0 \\ 0 & \frac{841}{24} & 2102.5 & 0 & \frac{-841}{24} & 2102.5 \\ 0 & 2102.5 & 168,200 & 0 & 2102.5 & 0 \\ 0 & 0 & 0 & 4615.8333 & 0 & 0 \\ 0 & 0 & 0 & 0 & \frac{841}{24} & 0 \\ 0 & 0 & 0 & 0 & 0 & 168,200 \end{bmatrix} \text{ symm } \quad (r)$$

$$\begin{Bmatrix} 1.0605 \\ -0.0897 \\ -0.0041 \\ 1.0600 \\ 0.0053 \\ 0.0044 \end{Bmatrix} = \begin{Bmatrix} -2.36 \\ -2.70 \\ -515.57 \\ -2.36 \\ 2.70 \\ 191.21 \end{Bmatrix}$$

Based on the displacement of joints 4 and 5 and the structure's fixed condition, the displacements of the four joints of the shear wall can be expressed from local d.o.f. in Fig. 8.16 as

$$\{\Delta_w\} = \begin{Bmatrix} \delta_1 \\ \delta_2 \\ \delta_4 \\ \delta_6 \\ \delta_8 \\ \delta_9 \end{Bmatrix} = \begin{Bmatrix} 1.0605 \\ -0.0897 \\ 0.2751 \\ 0 \\ 0 \\ 0 \end{Bmatrix} \quad (s)$$

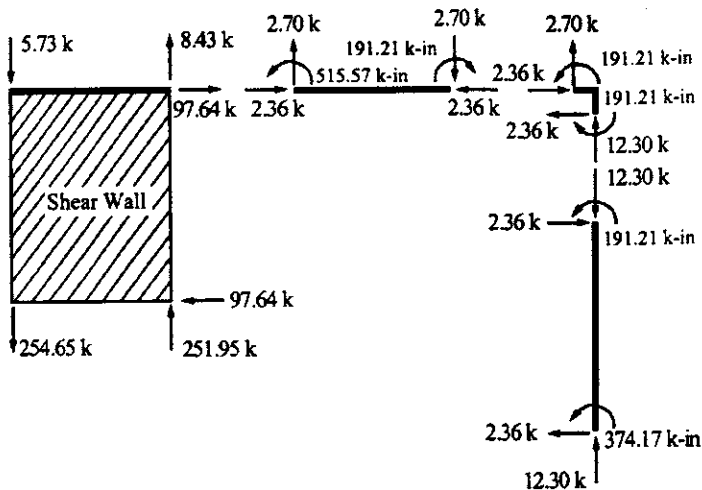
Using Eq. (8.129), the shear-wall internal forces are

$$\begin{Bmatrix} F_1 \\ F_2 \\ F_4 \\ F_6 \\ F_8 \\ F_9 \end{Bmatrix} = [K_e]\{\Delta_w\}$$

$$= \begin{bmatrix} 1112.5 & 2966.667 & -2966.667 & 0 & -1112.5 & 0 \\ 2966.667 & 8612.8472 & -8598.264 & 687.153 & -2966.6672 & -701.736 \\ -2966.667 & -8598.264 & 8612.847 & -701.736 & 2966.667 & 687.153 \\ 0 & 687.153 & -701.736 & (3.9375)10^{10} & 0 & -687.153 \\ -1112.5 & -2966.6672 & 2966.667 & 0 & 1112.5 & 0 \\ 0 & -701.736 & 687.153 & -687.153 & 0 & (3.9375)10^{10} \end{bmatrix} \text{ symm } \quad (t)$$

$$\begin{Bmatrix} 1.0605 \\ -0.0897 \\ 0.2751 \\ 0 \\ 0 \\ 0 \end{Bmatrix} = \begin{Bmatrix} 97.64 \\ 8.43 \\ -5.73 \\ -254.65 \\ -97.64 \\ 251.95 \end{Bmatrix}$$

(a)



(b)

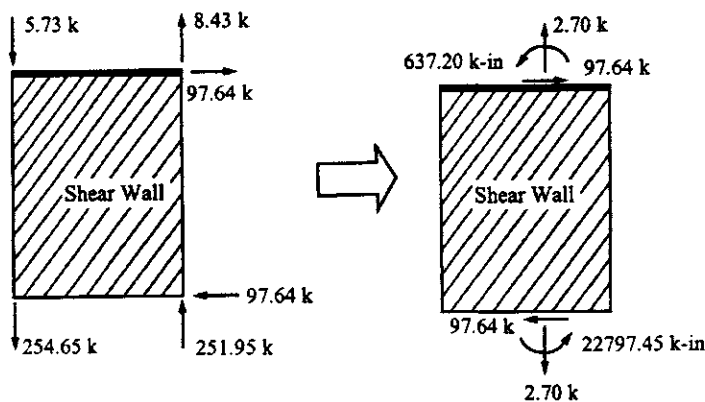


FIG. 8.58 Members' internal forces from Example 8.15.1. (a) Internal forces at members. (b) Transformation of shear-wall internal forces.

Internal forces are given in Fig. 8.58a from which the equilibrium conditions are illustrated at the members and the joints. Shear-wall internal forces are transferred to the wall's center line, as shown in Fig. 8.58b, according to the equilibrium principle.

EXAMPLE 8.15.2 A pipeline structural model is shown in Fig. 8.59a with 36 d.o.f. Member thickness, t , and radius, r , are 0.5 in and 20 in, respectively. The structural reference axes are aligned with the coordinates x_1 , x_2 , and x_3 . Structural properties are: damping ratio = 5% in all modes; elastic modulus = 3000 ksi; member mass = $0.0066 \text{ k sec}^2/\text{ft}^2$ and liquid mass = $0.016 \text{ k sec}^2/\text{ft}^2$. Thus the lumped masses are calculated as $M_1 = 0.805 \text{ k sec}^2/\text{ft}$ and $M_2 = 0.23 \text{ k sec}^2/\text{ft}$. Rotational masses of inertia at points B , C , D , E , F , and G are 1.92, 0.38, 0.192, 0.192, 0.38 and $1.92 \text{ k sec}^2\text{-ft}$ in the x_1 direction, respectively; 1.725, 0.192, 0.38, 0.38, 0.192 and $1.725 \text{ k sec}^2\text{-ft}$ in the x_2 direction, respectively; 1.92, 0.192, 0.192, 0.192, 0.192 and $1.92 \text{ k sec}^2\text{-ft}$ in the x_3 direction, respectively.

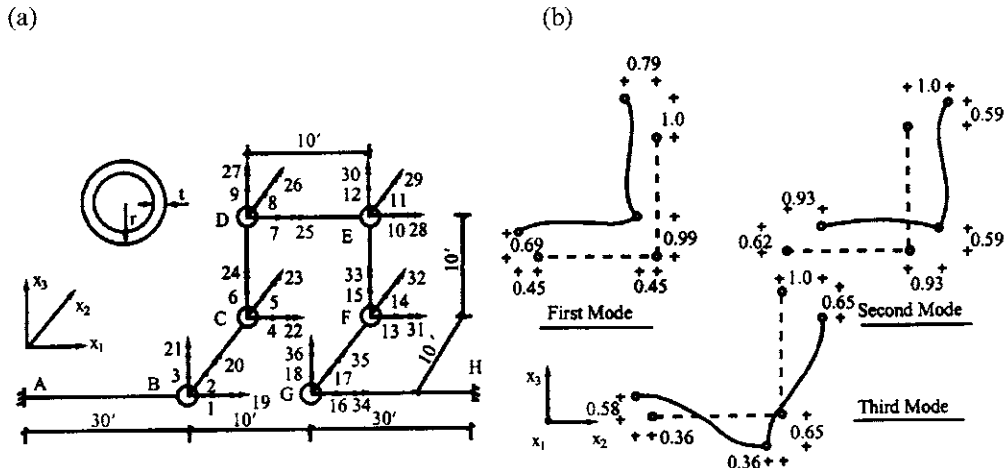


FIG. 8.59 Pipeline structure and mode shapes. (a) 3D pipeline structure. (b) First three mode shapes.

(A) Find the first three vibration modes and then observe coupling behavior of the modes. (B) Obtain the structural responses by using time-history analysis for seismic input of 1D, 2D, and 3D respectively corresponding to the N-S component, the N-S and E-W components, and to the N-S, E-W, and vertical components of the 18 May, 1940 El Centro earthquake records. For 1D analysis, N-S earthquake input is applied in the x_1 direction; for 2D analysis, earthquake records of N-S and E-W are respectively applied along the x_1 and x_2 directions simultaneously. Similarly for 3D analysis, N-S, E-W and vertical components are respectively applied to x_1 , x_2 , and x_3 directions simultaneously. (C) Find the responses by respectively applying ground main (\ddot{u}_x), intermediate (\ddot{u}_y), and minor (\ddot{u}_z) principal components [see Section 7.2.4 and Eq. (7.5)] in x_1 , x_2 , and x_3 simultaneously based on time-history analysis. This result, identified as Type 1, is then compared with the 3D result, identified as Type 2, obtained from (B) above.

Solution: (A) The first three modes are shown in Fig. 8.59b which reveals that structural translational motion and torsional motion are strongly coupled in each of the three fundamental modes.

(B) Comparing 1D, 2D, and 3D responses in Fig. 8.60a shows that 2D and 3D responses are much greater than 1D and that the 3D results are somewhat greater than the 2D, but not as striking when compared to 1D.

(C) Comparing the Type 1 and 2 responses in Fig. 8.60b shows that using major, intermediate, and minor seismic input components yields greater responses than those resulting from N-S, E-W, and vertical ground motion.

8.16. OVERVIEW

This chapter treats concepts and techniques of formulating and analyzing 3D building structures with greater scope than even a self-contained text. Since coordinate transformations for ECS, JCS, and GCS are important in 3D structural analysis, they are carefully presented with two different comprehensive approaches that hardly mentioned in other texts. A structural joint's rigid zones, shear walls, and in-plane rigid floor slabs are key in modeling building systems. Therefore, significant effort is devoted to deriving stiffness and geometric matrices and to interpreting the physical meaning of the element coefficients of these matrices. Structural stiffness matrix assembly and solution procedures, unique for tall buildings, are depicted in detail along with a comparison to the conventional approach for general 3D structures. These features cannot readily be found in a single source. Extensive examples illustrate formulation concepts and numerical procedures. Note that the material in this chapter is written as part of the computer

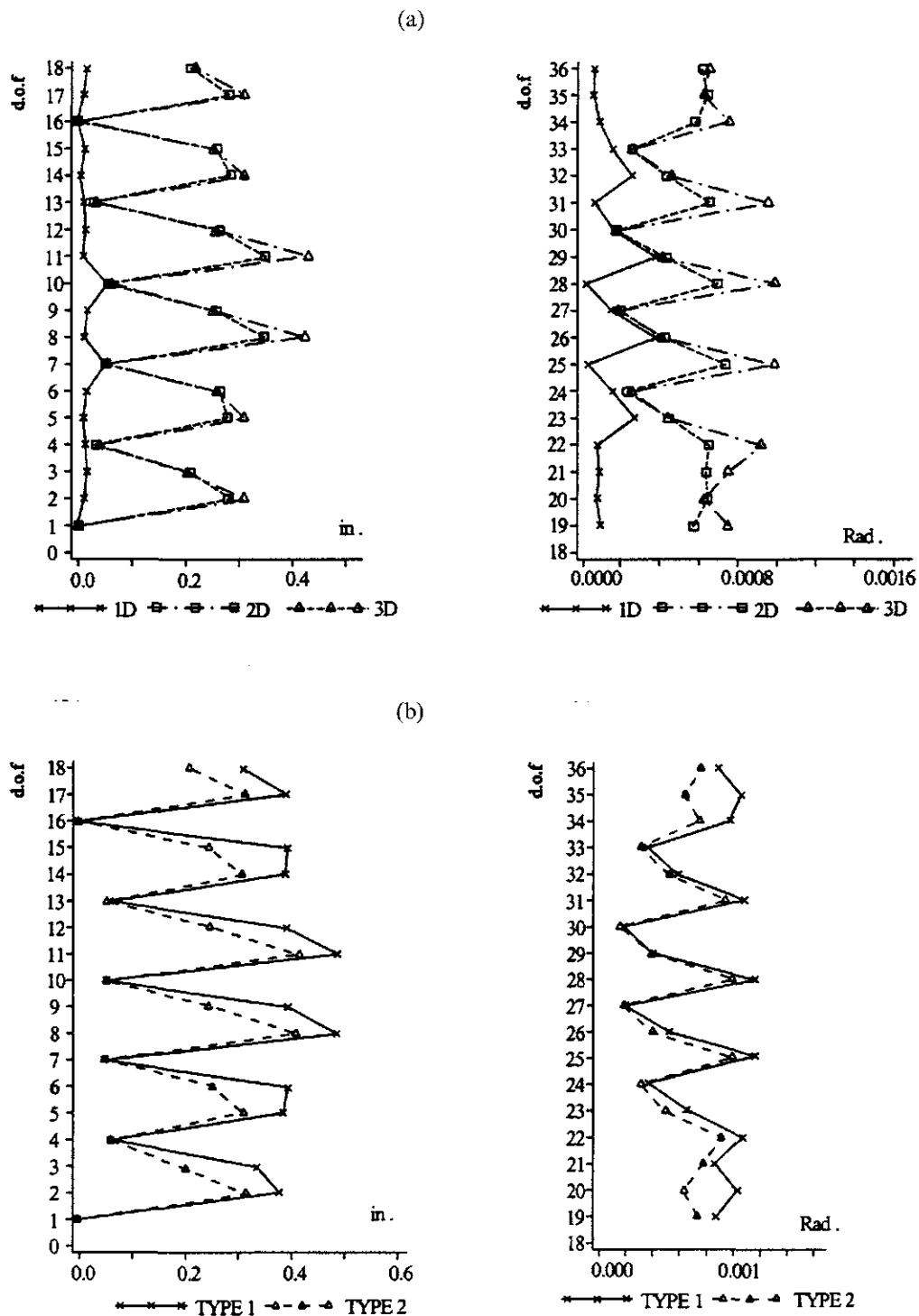


FIG. 8.60 Response comparison of 3D pipeline structure subjected to 18 May, 1940 El Centro Earthquake. (a) Response comparison for 1D, 2D, and 3D seismic input. (b) Comparison of type of response for major, intermediate and minor seismic input component (type 1) and response for 3D seismic input (type 2).

program INRESB-3D [1,5–7], which is widely available. This program can be used to analyze not only 3D but also 2D structures for both elastic and inelastic response due to static and/or dynamic forces, or static load and seismic excitations. Also note that there are references cited here to guide the reader seeking to fill the gap between the author's original work and the condensed form presented in this chapter. Publications on the subject by other researchers can be found in this author's reports cited here.

BIBLIOGRAPHY

1. FY Cheng, P Kitipitayangkul. INRESB-3D: A computer program for inelastic analysis of RC and steel buildings subjected to 3-D ground motion. NSF Report. National Technical Information Service, U.S. Department of Commerce, Virginia, NTIS no. PB80-165944, 1979 (101pp).
2. FY Cheng. Inelastic analysis of 3-D mixed steel and reinforced concrete seismic building systems. In: Computational Methods in Nonlinear Structural and Solid Mechanics. Oxford: Pergamon Press, 1980, pp 189–196.
3. FY Cheng, GE Mertz. INRESB-3D-SUP user's manual: a computer program for inelastic seismic analysis of 3-D RC and steel buildings. NSF Report. National Technical Information Service, U.S. Department of Commerce, Virginia, NTIS no. PB90-122225, 1989 (197pp).
4. FY Cheng, GE Mertz, MS Sheu, JF Ger. Computed versus observed inelastic seismic response of low-rise RC shear walls, ASCE J Struct Engng, 119(11):3255–3275, 1993.
5. FY Cheng, JF Ger, D Li and JS Yang. INRESB-3D-SUPII user's manual: General purpose program for inelastic analysis of RC and steel building systems for 3D static and dynamic loads and seismic excitations (based on supercomputer and PC). NSF Report. National Technical Information Service, U.S. Department of Commerce, Virginia, NTIS no. PB97-123624, 1996 (237pp).
6. FY Cheng, JF Ger, D Li and JS Yang. INRESB-3D-SUPII program listing for supercomputer: general purpose program for inelastic analysis of RC and steel building systems for 3D static and dynamic loads and seismic excitations. NSF Report. National Technical Information Service, U.S. Department of Commerce, Virginia, NTIS no. PB97-123616, 1996 (114pp).
7. FY Cheng, JF Ger, D Li, JS Yang. INRESB-3D-SUPII program listing for PC: inelastic analysis of RC and steel building systems for 3D static and dynamic loads and seismic excitations. NSF Report. National Technical Information Service, U.S. Department of Commerce, Virginia, NTIS no. PB97-121362 1996 (109pp).
8. FY Cheng, ed. Proceedings of 12th Analysis and Computation Conference, ASCE, Chicago, IL, 1996.
9. FY Cheng, YY Wang, eds. Post-Earthquake Rehabilitation and Reconstruction. Oxford: Elsevier Science, 1996.
10. FY Cheng, YX Gu, eds. Computational Mechanics in Structural Engineering: Recent Advances. Oxford: Elsevier Science, 1998.
11. FY Cheng, KY Lou, LH Sheng. Damage of Mission Gothic Undercrossing and Bull Creek Canyon Channel Bridge during the Northridge Earthquake. Proceedings of Structural Engineers World Congress (CD-ROM), paper no. T-110-5, San Francisco, CA, 1998.
12. DM Davis. The effect of reinforced concrete building modeling on dynamic and stability characteristics. M.S. Thesis, University of Missouri-Rolla, MO, 1985.
13. JF Ger, FY Cheng. Post-buckling and hysteresis models of open-web girders. ASCE J Struct Engng 119(3):831–851, 1993.
14. JF Ger, FY Cheng. Collapse behavior of Pino-Suarez building during 1985 Mexico earthquake. ASCE J Struct Engng 119(3):852–870, 1993.
15. KY Lou, FY Cheng. Post-earthquake assessment of bridge collapse and design parameters. Proceedings of 11th World Conference on Earthquake Engineering (CD-ROM), paper no. 1316, Acapulco, 1996.

9

Various Hysteresis Models and Nonlinear Response Analysis

PART A FUNDAMENTALS

9.1. INTRODUCTION

The previous chapters focused on elastic structures with emphasis on mathematical models, analytical methodologies and numerical procedures as well as response characteristics. When a structure is subjected to dynamic force or ground motion, its constituent members may deform beyond their elastic limit, such as yielding stress of steel or crack stress of concrete. If we assume that the members continue to behave elastically, then their response behavior is based on *linear* or *elastic analysis* as presented previously. When the stress-strain relationship beyond the elastic stage is considered, the response then results from *nonlinear* or *inelastic analysis*. Analytical techniques and response behavior of inelastic structures are discussed here. Note that nonlinear analysis always encompasses linear analysis because of elastic material behavior at the early loading stage.

Linear and nonlinear analysis can be conducted with consideration of *small* or *large deflection*. Large deflection implies that structural configuration deforms markedly, which results in change of originally assumed directions of forces and displacements. The direction of members' internal forces in a structure after large deformation is not the same as that used in formulation for this structure with small deformation. Consequently, equilibrium equations between internal forces (shears, axial forces, etc.) and external loads (applied force, inertia force, etc.) and the compatibility condition between internal deformations and external displacements at each structural node should be modified at various loading stages. Large deflection formulation is generally considered in inelastic analysis, but is sometimes used in elastic cases for material with a small modulus of elasticity. Note that the geometric stiffness matrix or stringer matrix due to the $P-\Delta$ effect presented previously can be included in either small or large deflection formulation. Naturally, $P-\Delta$ effect becomes more pronounced for large deflections.

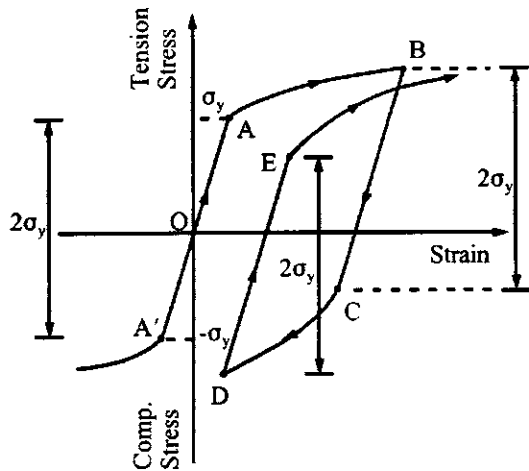


FIG. 9.1 Material nonlinearity.

When inelastic material behavior is considered in formulating the force-deformation relationship of a structural member, the relationship is called the *hysteresis model*. In this chapter, four well-known hysteresis models of *elasto-plastic*, *bilinear*, *curvilinear*, and *Ramberg-Osgood* are introduced; numerical procedures for response analysis of members' forces and structural displacements are illustrated; various effects of $P-\Delta$, large deflection, and material nonlinearity on structural response behavior are shown; and a correctness check of inelastic numerical solutions based on equilibrium and compatibility requirements is demonstrated.

9.1.1. Material Nonlinearity and Stress-Strain Models

A typical stress-strain relationship of structural steel is shown in Fig. 9.1. The linear relationship between O and A is defined as elastic behavior. After initial yielding, σ_y , the slope of the stress-strain curve is not constant and material behavior becomes inelastic. Unloading path $B-C$ and reloading path $D-E$ are elastic, and form straight lines parallel to the initial elastic path $O-A$. Absolute values of the initial yield points in tension A and in compression A' are the same, but the values change for subsequent points B and C or D and E . A stress magnitude of $2\sigma_y$ is observed for \overline{AA} , \overline{BC} , and \overline{DE} , which is known as the *Bauschinger effect* [2].

For practical purposes, some simplified models are often used. Most typical are those shown in Fig. 9.2 as *elasto-plastic*, *bilinear*, *curvilinear*, and *Ramberg-Osgood*.

9.1.2. Bauschinger Effect on Moment-Curvature Relationship

The Bauschinger effect can also be observed in the moment-curvature ($M-\phi$) relationship of a structural member. This relationship is determined by the material stress-strain relationship and the cross-section shape of that member. Figure 9.3a shows a rectangular cross-section with width b and depth d . Assuming the stress-strain relationship follows the elasto-plastic stress-strain model, stress and strain distributions on the cross-section at different loading stages are shown in Fig. 9.3b. Moment-curvature relationships corresponding to each loading stage are sketched in Fig. 9.3c. As shown in Fig. 9.3b, at stage (1) the stresses on the cross-section at both compression and tension sides are less than the yielding stress, σ_y , and the slope of the moment-curvature is equal to EI . When stresses at the extreme fibers of the cross-section reach yielding stress, σ_y , as shown at stage (2), the corresponding moment is called the *initial yield moment*, M_y . Continued increase of the moment will develop yielding stresses on more of the cross-section area, as is the case at stage (3).

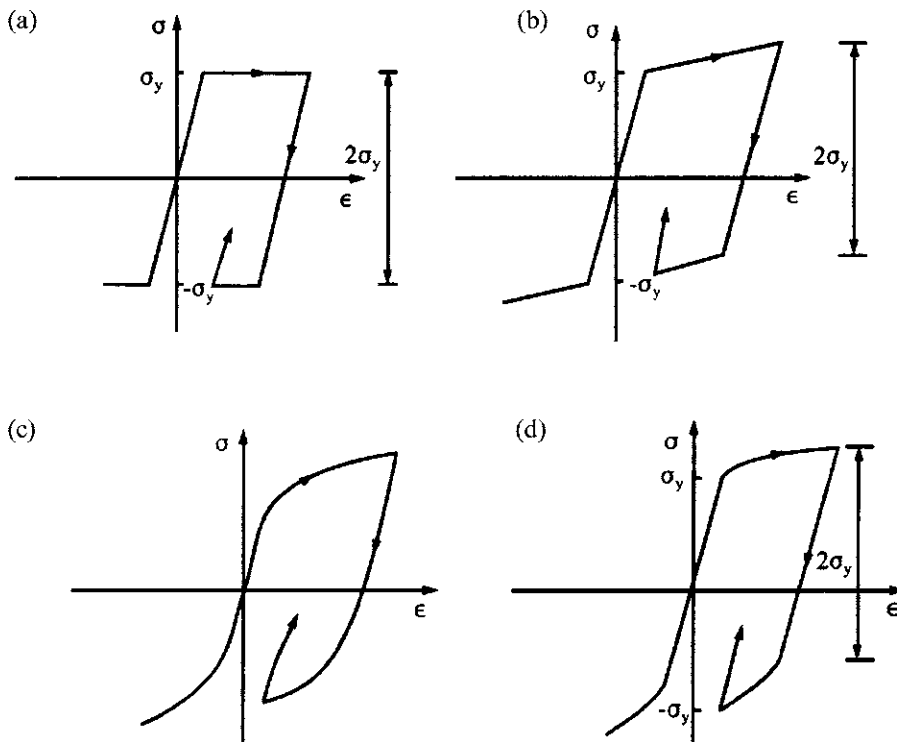


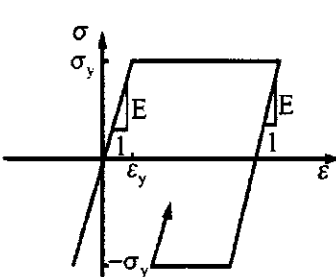
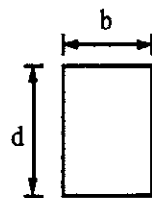
FIG. 9.2 Simplified stress-strain models. (a) Elasto-plastic. (b) Bilinear. (c) Curvilinear. (d) Ramberg-Osgood.

At stage (4) the entire cross-section yields, so the moment cannot increase further. Any additional deformation makes the cross-section rotate like a center hinge with a constant moment. The hinge is a *plastic hinge* and the moment is *plastic moment*, normally signified by M_p . Note that at stage (3) strain distribution is linear but stress distribution is not linear. Therefore the nonlinear moment-curvature relationship develops as shown in Fig. 9.3c. Once the cross-section reaches its plastic moment, stress distribution is unchanged even though strain increases continually at stage (5). Strain decreases at stage (6); decreased strain results in a linear stress-strain relationship. Thus the slope of the moment-curvature curve becomes the initial slope as EI . Using the strain and stress distributions shown at stages (7) and (8) yields the linear moment-curvature relationship at both stages. Further decrease of strain yields negative plastic moment at stage (9). The linear segment with magnitude of $2M_y$ from stages (5)–(8) shows the Bauschinger effect on the moment-curvature relationship.

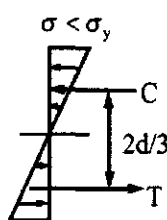
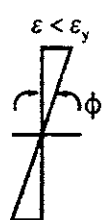
9.2. ELASTO-PLASTIC HYSTERESIS MODEL

Observe from the previous section that when a structure is subjected to strong cyclic motions, a nonlinear moment-curvature relationship develops (see Fig. 9.3c). For elasto-plastic stress-strain material, the nonlinear moment-curvature relationship can be simplified by using branches I and II (solid lines) for linear and nonlinear behavior, respectively, as shown in Fig. 9.4. In this *elasto-plastic hysteresis* model the bending stiffness associated with branches I and II is EI and zero, respectively. M_p is the plastic moment (also referred to as *ultimate moment*) of the member.

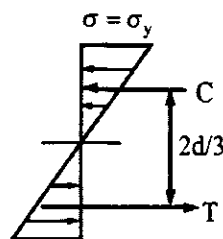
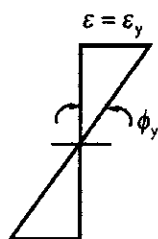
(a)



(b)



$$\begin{aligned}\epsilon &= \frac{d}{2}\phi, \quad \sigma = E\epsilon \\ \sigma &= \phi\left(\frac{d}{2}\right)E \\ C &= T = \frac{\sigma bd}{2(2)} = \frac{bd^2}{8}E\phi \\ M &= C\left(\frac{2}{3}d\right) = E\left(\frac{bd^3}{12}\right)\phi = EI\phi\end{aligned}$$

Stage 1

$$\begin{aligned}M_y &= C\left(\frac{2}{3}d\right) = \frac{bd}{4}\sigma_y\left(\frac{2}{3}\right)d \\ &= \left(\frac{bd^2}{6}\right)\sigma_y = S\sigma_y\end{aligned}$$

Stage 2Stage 3

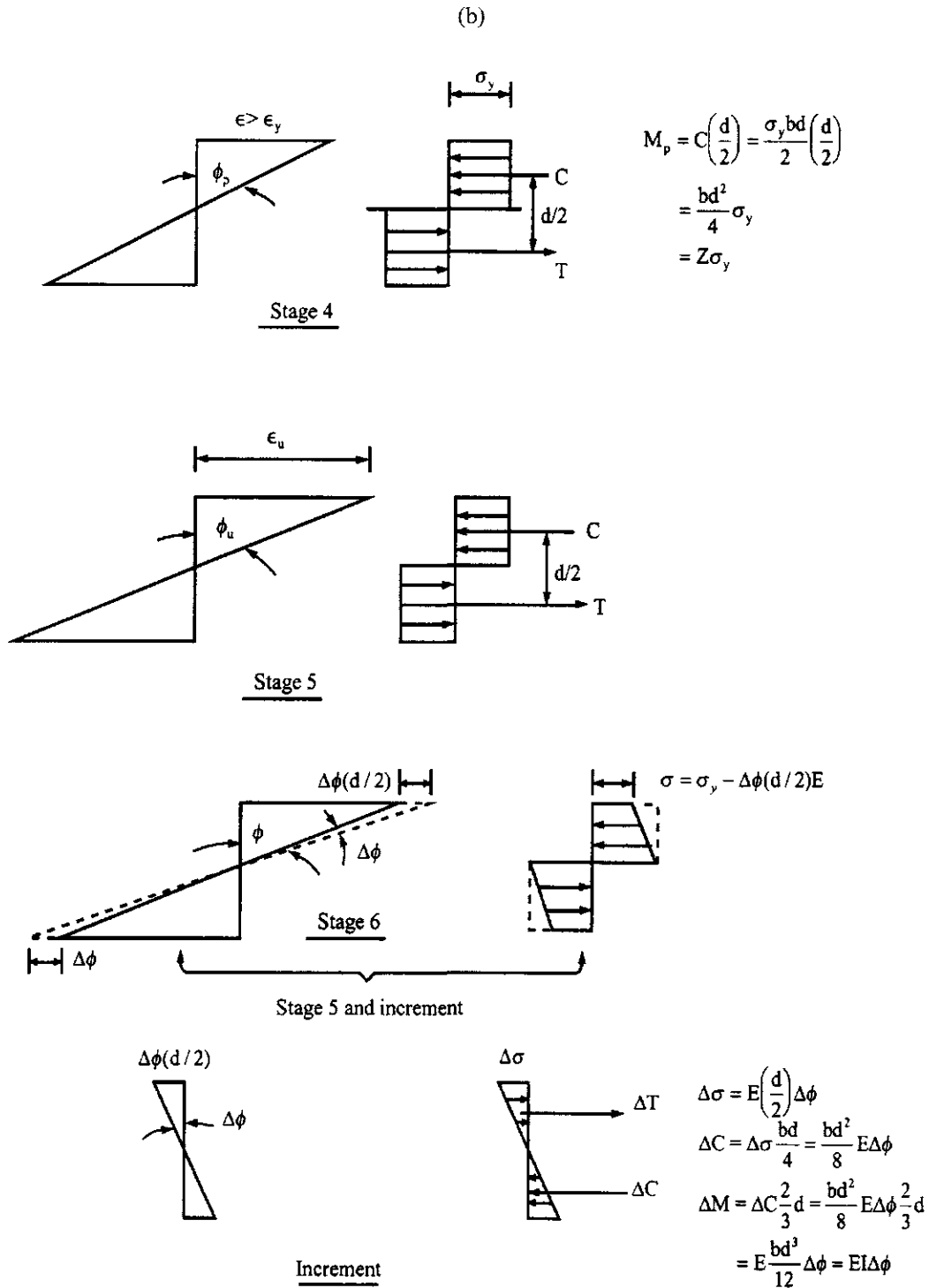


FIG. 9.3 Bauschinger effect on moment-curvature relationship. (a) Cross-section and stress-strain relationship. (b) Stress and strain distribution at loading stages 1–9.

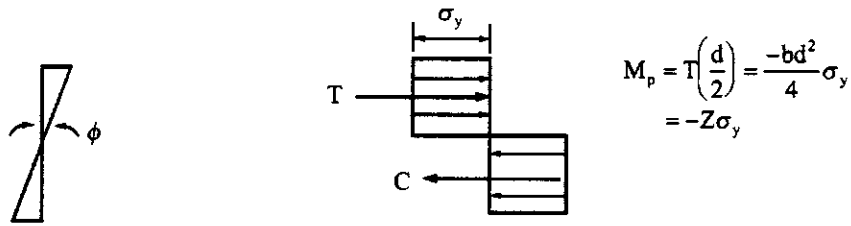
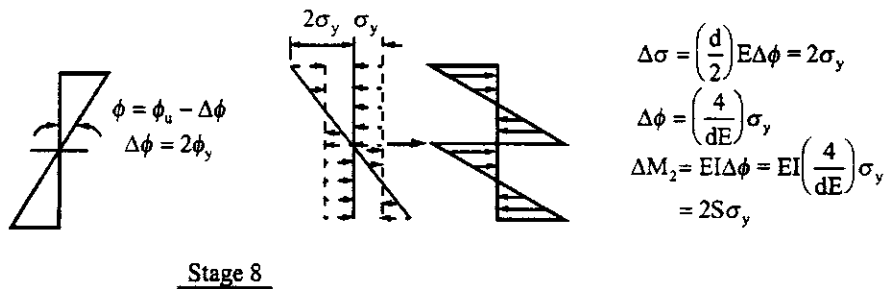
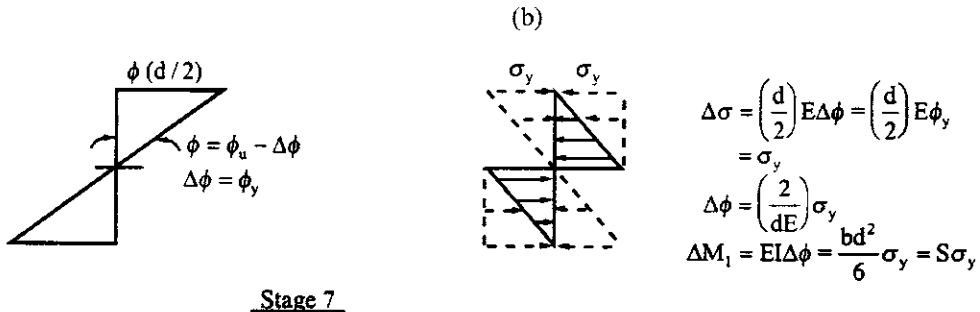


FIG. 9.3 Continued.

9.2.1. Stiffness Matrix Formulation

The elasto-plastic model in Fig. 9.4 shows that, when the moment reaches the *ultimate moment* capacity of a member, the plastic moment cannot increase but the rotation of the plastic hinge at the cross-section can increase. For a member without considering gravity dead load, as is the case with dynamic or seismic analysis, the outcome is as follows. A plastic hinge develops at the member's end where the magnitude of the moment is greater than at other locations. The member end behaves like a real center hinge with a constant ultimate moment, M_p . When the member-end rotates in reverse, the moment decreases elastically and the plastic hinge disappears. Elastic behavior remains unchanged until the moment reaches ultimate moment capacity. Consequently, a plastic hinge forms again.

Plastic hinge formation in a member has three possibilities: a hinge at the i -end, the j -end or both ends (see i and j in Fig. 9.5). Force-deformation relationships associated with elastic state and the three states of yield condition are discussed as follows.

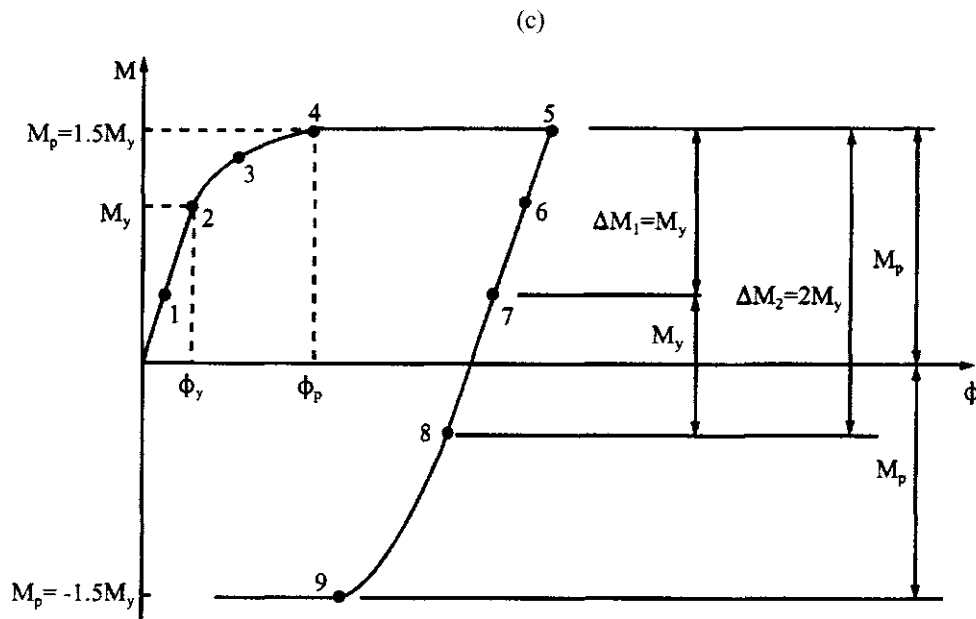


FIG. 9.3 Bauschinger effect on moment-curvature relationship. (c) Moment-curvature relationship

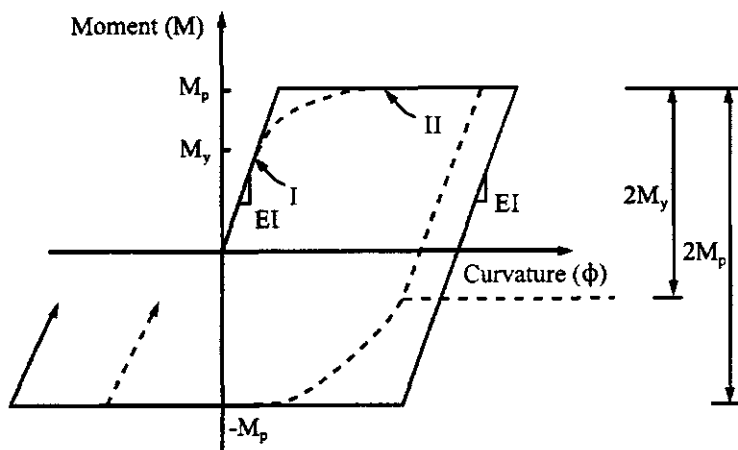


FIG. 9.4 Elasto-plastic moment-curvature relationship.

(A) *Both ends linear*—since the member is still elastic, the member stiffness matrix is

$$\begin{Bmatrix} \Delta M_i \\ \Delta M_j \\ \Delta V_i \\ \Delta V_j \end{Bmatrix} = 4EI \begin{bmatrix} 1/L & 1/2L & -3/2L^2 & -3/2L^2 \\ 1/L & 1/L & -3/2L^2 & -3/2L^2 \\ 3/L^3 & 3/L^3 & 3/L^3 & 3/L^3 \end{bmatrix}_{\text{symm}} \begin{Bmatrix} \Delta \theta_i \\ \Delta \theta_j \\ \Delta Y_i \\ \Delta Y_j \end{Bmatrix} \quad (9.1)$$

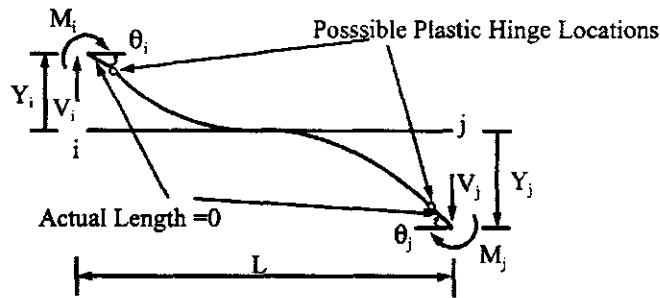


FIG. 9.5 Nonlinear beam.

(B) *i-end nonlinear and j-end linear*—since the plastic hinge develops at the *i*-end, the member can be treated as a beam with one end restrained and the other end supported by a hinge. Using any conventional structural analysis technique, such as *moment-area* or *conjugate beam*, the following stiffness coefficients of the member can be found:

$$\begin{Bmatrix} \Delta M_i \\ \Delta M_j \\ \Delta V_i \\ \Delta V_j \end{Bmatrix} = 3EI \begin{bmatrix} 0 & 0 & 0 & 0 \\ 0 & 1/L & -1/L^2 & -1/L^2 \\ 0 & 1/L^3 & 1/L^3 & 1/L^3 \\ 0 & 0 & 0 & 0 \end{bmatrix} \begin{Bmatrix} \Delta\theta_i \\ \Delta\theta_j \\ \Delta Y_i \\ \Delta Y_j \end{Bmatrix} \quad (9.2)$$

(C) *i-end linear and j-end nonlinear*—similar to the preceding state of yield, notations become

$$\begin{Bmatrix} \Delta M_i \\ \Delta M_j \\ \Delta V_i \\ \Delta V_j \end{Bmatrix} = 3EI \begin{bmatrix} 1/L & 0 & -1/L^2 & -1/L^2 \\ 0 & 0 & 0 & 0 \\ 0 & 1/L^3 & 1/L^3 & 1/L^3 \\ 0 & 0 & 0 & 0 \end{bmatrix} \begin{Bmatrix} \Delta\theta_i \\ \Delta\theta_j \\ \Delta Y_i \\ \Delta Y_j \end{Bmatrix} \quad (9.3)$$

(D) *Both ends nonlinear*—when a beam has hinges at both ends, the bending stiffness of the member vanishes; therefore

$$\begin{Bmatrix} \Delta M_i \\ \Delta M_j \\ \Delta V_i \\ \Delta V_j \end{Bmatrix} = [0] \begin{Bmatrix} \Delta\theta_i \\ \Delta\theta_j \\ \Delta Y_i \\ \Delta Y_j \end{Bmatrix} \quad (9.4)$$

9.3. BILINEAR HYSTERESIS MODEL

Expanding on Section 9.1.1, the moment-curvature relationship of a member can be idealized as a *bilinear model*, shown in Fig. 9.6, if the material stress-strain relationship is assumed to be bilinear (see Fig. 9.2b). Initial elastic slope and subsequent inelastic slope of the bilinear moment-curvature curve are EI and EI_1 , respectively; I_1 can be in terms of I . The Bauschinger effect on the moment magnitude of $2M_p$ also exists between two subsequent plastic hinges as signified by points *B* and *C* in Fig. 9.6. The moment-rotation relationship of a member shown in Fig. 9.7a is given in Fig. 9.7b, which is composed of two imaginary components as linear component and elasto-plastic component, sketched in Figs. 9.7c and 9.7d, respectively.

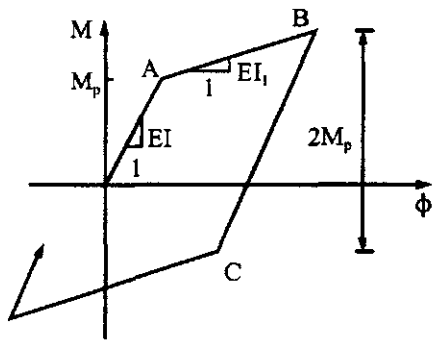


FIG. 9.6 Bilinear moment–curvature relationship.

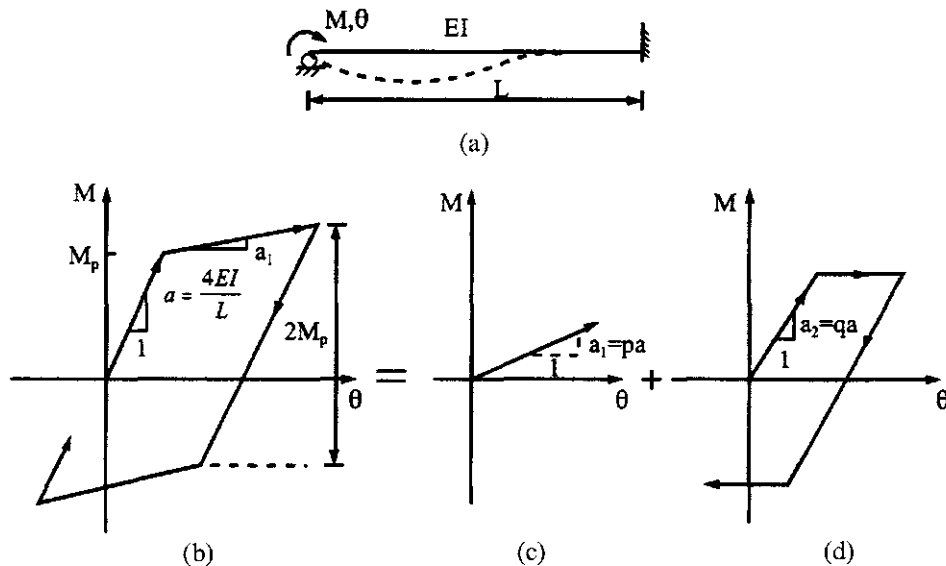


FIG. 9.7 Bilinear moment–rotation. (a) Structural member. (b) Bilinear hysteresis loop. (c) Linear component. (d) Elasto-plastic component.

Initial stiffness of the hysteresis loop and of the elastic, elasto-plastic components is a , a_1 , a_2 , respectively, where $a = a_1 + a_2$, $a_1 = pa$, $a_2 = qa$, and $p + q = 1$. p is the fraction of stiffness apportioned to the linear component and q is the fraction of stiffness apportioned to the elasto-plastic component. The second slope a_1 of the hysteresis loop is the same as the initial slope of the linear component.

9.3.1. Stiffness Matrix Formulation

Based on the moment–rotation in Fig. 9.7, assume that an inelastic member has two equivalent components, elastic and elasto-plastic, as shown in Fig. 9.8. In the latter figure, θ_i and θ_j are joint rotations (also member-end rotations); α_i and α_j are plastic angles at each end of the elasto-plastic component. For purposes of illustration, α 's and θ 's are not shown in the same

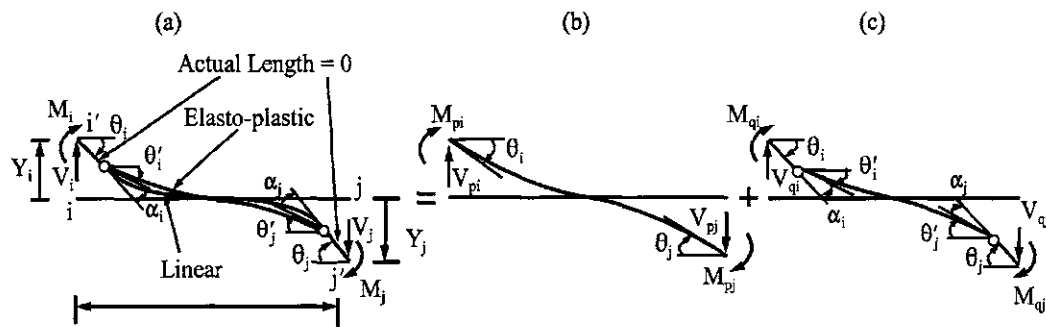


FIG. 9.8 Bilinear beam. (a) Nonlinear beam. (b) Linear component. (c) Elasto-plastic component.

location, although they actually are. End rotations of the elasto-plastic component become

$$\theta'_i = \theta_i - \alpha_i \quad \theta'_j = \theta_j - \alpha_j \quad (9.5a)$$

or in incremental form

$$\Delta\theta'_i = \Delta\theta_i - \Delta\alpha_i \quad \Delta\theta'_j = \Delta\theta_j - \Delta\alpha_j \quad (9.5b)$$

Incremental forces and deformations at both ends of these two components in Fig. 9.8b and 9.8c may be expressed in terms of stiffness coefficients as

(I) *Linear component*

$$\begin{Bmatrix} \Delta M_{pi} \\ \Delta M_{pj} \\ \Delta V_{pi} \\ \Delta V_{pj} \end{Bmatrix} = p \begin{bmatrix} a & b & -c & -c \\ & a & -c & -c \\ \Delta Y_i & & d & d \\ & & & d \end{bmatrix} \begin{Bmatrix} \Delta\theta_i \\ \Delta\theta_j \\ \Delta Y_i \\ \Delta Y_j \end{Bmatrix} \quad (9.6)$$

in which $a = 4EI/L$, $b = 2EI/L$, $c = 6EI/L^2$ and $d = 12EI/L^3$; and

(II) *Elasto-plastic component*

$$\begin{Bmatrix} \Delta M_{qi} \\ \Delta M_{qj} \\ \Delta V_{qi} \\ \Delta V_{qj} \end{Bmatrix} = q \begin{bmatrix} a & b & -c & -c \\ & a & -c & -c \\ \Delta Y_i & & d & d \\ & & & d \end{bmatrix} \begin{Bmatrix} \Delta\theta'_i \\ \Delta\theta'_j \\ \Delta Y_i \\ \Delta Y_j \end{Bmatrix} \quad (9.7)$$

Moments and shears of the nonlinear beam are the combination of the end forces of the components according to the state of yield. *State of yield* may be one of the following four conditions including elastic state at the beginning: (A) both ends linear; (B) *i*-end nonlinear and *j*-end linear, (C) *i*-end linear and *j*-end nonlinear; and (D) both ends nonlinear. Force-deformation relationships associated with the above conditions are examined separately as follows.

(A) *Both ends linear*—since the member is still elastic, plastic hinges do not exist; Eq. (9.5a) and b) yields

$$\alpha_i = \alpha_j = 0; \quad \theta'_i = \theta_i; \quad \text{and} \quad \theta'_j = \theta_j \quad (9.8a)$$

or in incremental form

$$\Delta\alpha_i = \Delta\alpha_j = 0; \quad \Delta\theta'_i = \Delta\theta_i; \quad \text{and} \quad \Delta\theta'_j = \Delta\theta_j \quad (9.8b)$$

The incremental force-deformation relationship may be expressed either directly in elastic stiffness or by combining Eqs. (9.6) and (9.7) with $p+q=1$

$$\begin{Bmatrix} \Delta M_i \\ \Delta M_j \\ \Delta V_i \\ \Delta V_j \end{Bmatrix} = \begin{Bmatrix} \Delta M_{pi} \\ \Delta M_{pj} \\ \Delta V_{pi} \\ \Delta V_{pj} \end{Bmatrix} + \begin{Bmatrix} \Delta M_{qi} \\ \Delta M_{qj} \\ \Delta V_{qi} \\ \Delta V_{qj} \end{Bmatrix} = \begin{bmatrix} a & b & -c & -c \\ & a & -c & -c \\ & & d & d \\ & & & \text{symm} \end{bmatrix} \begin{Bmatrix} \Delta \theta_i \\ \Delta \theta_j \\ \Delta Y_i \\ \Delta Y_j \end{Bmatrix} \quad (9.9)$$

(B) *i-end nonlinear and j-end linear*—from Eq. (9.5a and b),

$$\alpha_i \neq 0; \quad \alpha_j = 0; \quad \theta'_i = \theta_i - \alpha_i; \quad \text{and } \theta'_j = \theta_j \quad (9.10)$$

or

$$\Delta \alpha_i \neq 0; \quad \Delta \alpha_j = 0; \quad \Delta \theta'_i = \Delta \theta_i - \Delta \alpha_i; \quad \text{and } \Delta \theta'_j = \Delta \theta_j \quad (9.11)$$

Combining Eqs. (9.6) and (9.7) gives

$$\begin{Bmatrix} \Delta M_i \\ \Delta M_j \\ \Delta V_i \\ \Delta V_j \end{Bmatrix} = \begin{bmatrix} a & b & -c & -c \\ & a & -c & -c \\ & & d & d \\ & & & \text{symm} \end{bmatrix} \begin{Bmatrix} \Delta \theta_i \\ \Delta \theta_j \\ \Delta Y_i \\ \Delta Y_j \end{Bmatrix} + \begin{Bmatrix} -a \\ -b \\ c \\ c \end{Bmatrix} q \Delta \alpha_i \quad (9.12)$$

Since the moment at the *i*-end of the elasto-plastic component is constant, the increase in moment ΔM_i at the end of the member must be due to ΔM_{pi} of the linear component, i.e.

$$\Delta M_i = \Delta M_{pi} \quad (9.13)$$

which means that ΔM_{pi} of Eq. (9.6) is equal to ΔM_i of Eq. (9.12). This equality yields

$$\Delta \alpha_i = \Delta \theta_i + \frac{b}{a} \Delta \theta_j - \frac{c}{a} \Delta Y_i - \frac{c}{a} \Delta Y_j = \Delta \theta_i + \frac{1}{2} \Delta \theta_j - \frac{3}{2L} (\Delta Y_i + \Delta Y_j) \quad (9.14)$$

Substituting the above into Eq. (9.12) gives the desired result,

$$\begin{Bmatrix} \Delta M_i \\ \Delta M_j \\ \Delta V_i \\ \Delta V_j \end{Bmatrix} = \begin{bmatrix} pa & pb & -pc & -pc \\ & pa + qe & -pc - qf & -pc - qf \\ & & pd + qg & pd + qg \\ & & & \text{symm} \end{bmatrix} \begin{Bmatrix} \Delta \theta_i \\ \Delta \theta_j \\ \Delta Y_i \\ \Delta Y_j \end{Bmatrix} + \begin{Bmatrix} -b \\ -a \\ c \\ c \end{Bmatrix} q \Delta \alpha_i \quad (9.15)$$

in which $e = 3EI/L$, $f = 3EI/L^2$, and $g = 3EI/L^3$.

(C) *i-end linear and j-end nonlinear*—similar to the preceding state of yield, we have

$$\Delta \alpha_i = 0; \quad \Delta \alpha_j \neq 0; \quad \Delta \theta'_i = \Delta \theta_i; \quad \text{and } \Delta \theta'_j = \Delta \theta_j - \Delta \alpha_j \quad (9.16)$$

Substituting the above into Eq. (9.7), which is then combined with Eq. (9.6), yields

$$\begin{Bmatrix} \Delta M_i \\ \Delta M_j \\ \Delta V_i \\ \Delta V_j \end{Bmatrix} = \begin{bmatrix} a & b & -c & -c \\ & a & -c & -c \\ & & d & d \\ & & & \text{symm} \end{bmatrix} \begin{Bmatrix} \Delta \theta_i \\ \Delta \theta_j \\ \Delta Y_i \\ \Delta Y_j \end{Bmatrix} + \begin{Bmatrix} -b \\ -a \\ c \\ c \end{Bmatrix} q \Delta \alpha_j \quad (9.17)$$

Using $\Delta M_j = \Delta M_{pj}$ in Eqs. (9.6) and (9.17) gives

$$\Delta \alpha_j = \frac{1}{2} \Delta \theta_i + \Delta \theta_j - \frac{3}{2L} (\Delta Y_i + \Delta Y_j) \quad (9.18)$$

Consequently, Eq. (9.17) becomes

$$\begin{Bmatrix} \Delta M_i \\ \Delta M_j \\ \Delta V_i \\ \Delta V_j \end{Bmatrix} = \begin{bmatrix} pa + qe & pb & -pc - qf & -pc - qf \\ & pa & -pc & -pc \\ & & pd + qg & pd + qg \\ & & \text{symm} & pd + qg \end{bmatrix} \begin{Bmatrix} \Delta \theta_i \\ \Delta \theta_j \\ \Delta Y_i \\ \Delta Y_j \end{Bmatrix} \quad (9.19)$$

(D) *Both ends nonlinear*—since both ends have plastic hinges, $\Delta\alpha_i \neq 0$, $\Delta\alpha_j \neq 0$, we may directly substitute Eq. (9.5b) into Eq. (9.7) and then combine Eqs. (9.6) and (9.7) as

$$\begin{Bmatrix} \Delta M_i \\ \Delta M_j \\ \Delta V_i \\ \Delta V_j \end{Bmatrix} = \begin{bmatrix} a & b & -c & -c \\ & a & -c & -c \\ & & d & d \\ & \text{symm} & & d \end{bmatrix} \begin{Bmatrix} \Delta \theta_i \\ \Delta \theta_j \\ \Delta Y_i \\ \Delta Y_j \end{Bmatrix} + q \begin{bmatrix} -a & -b \\ -b & -a \\ c & c \\ c & c \end{bmatrix} \begin{Bmatrix} \Delta \alpha_i \\ \Delta \alpha_j \end{Bmatrix} \quad (9.20)$$

Equating $\Delta M_i = \Delta M_{pi}$ and $\Delta M_j = \Delta M_{pj}$ in Eqs. (9.6) and (9.20) yields

$$\Delta \alpha_i = \Delta \theta_i - \frac{1}{L}(\Delta Y_i + \Delta Y_j) \quad (9.21)$$

$$\Delta \alpha_j = \Delta \theta_j - \frac{1}{L}(\Delta Y_i + \Delta Y_j) \quad (9.22)$$

Thus Eq. (9.20) may be expressed as

$$\begin{Bmatrix} \Delta M_i \\ \Delta M_j \\ \Delta V_i \\ \Delta V_j \end{Bmatrix} = p \begin{bmatrix} a & b & -c & -c \\ & a & -c & -c \\ & & d & d \\ & \text{symm} & & d \end{bmatrix} \begin{Bmatrix} \Delta \theta_i \\ \Delta \theta_j \\ \Delta Y_i \\ \Delta Y_j \end{Bmatrix} \quad (9.23)$$

which are actually the incremental forces of the linear component as shown in Eq. (9.6).

Note that when $p=0$, then $q=1$. The bilinear model presented above becomes the elasto-plastic model introduced in the previous section, and the stiffness coefficients in Eqs. (9.15), (9.19), and (9.23) become identical to those in Eqs. (9.2), (9.3), and (9.4), respectively.

9.4. CONVERGENCE TECHNIQUES AT OVERSHOOTING REGIONS

9.4.1. State of Yield and Time-Increment Technique

In nonlinear dynamic analysis, the criteria for establishing the state of yield at time t (the beginning of a time increment) are based on the bending moment at time t and the last incremental bending moment prior to time t . These criteria are shown in Fig. 9.9 as

If $ML(t) < M(t) < MU(t)$

then the state of yield is linear

If $\left\{ \begin{array}{l} M(t) \geq MU(t) \text{ and } \Delta M(t) > 0 \\ M(t) \leq ML(t) \text{ and } \Delta M(t) < 0 \end{array} \right\}$

then the state of yield is nonlinear

If $\left\{ \begin{array}{l} M(t) \geq MU(t) \text{ and } \Delta M(t) < 0 \\ M(t) \leq ML(t) \text{ and } \Delta M(t) > 0 \end{array} \right\}$

then backtracking has occurred and the state of yield is linear in which $M(t)$ = total bending at time t ; $MU(t)$ = upper yield bending moment at time t ; $ML(t)$ = lower yield bending moment at time t ; $\Delta M(t)$ = current moment $M(t)$ subtracted from previously calculated moment (the last

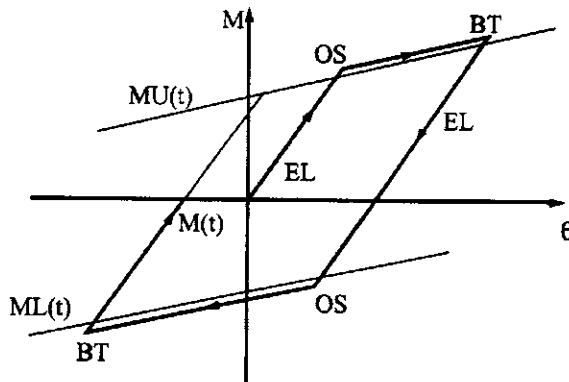


FIG. 9.9 State of yield.

incremental bending moment prior to time t); OS = overshooting, the yield limit upon entering the nonlinear state; BT = backtracking, the limit upon returning to the linear state; and EL = elastic linear range. When a system has a number of yield joints, it is necessary to check the state of yield for each joint at the beginning of each time increment. When using a predetermined incremental time Δt , turning points at overshooting and backtracking often do not occur at the theoretical point. If this situation arises, reasonable accuracy can be achieved by reducing the time increment at OS and BT . For a large structure with many structural elements, several of them may exhibit a stiffness change in a single time step. In such cases, this approach leads to excessive computation time. To achieve computational efficiency, an *unbalanced force technique* is introduced in the following section.

9.4.2. Unbalanced Force Technique

Consider a beam element of a bilinear hysteresis model and assume that the moment-rotation curve at the element's i -end is as shown in Fig. 9.10. Note that the moment-rotation curve need not be a bilinear shape because the moment at end i will be influenced by the rotation at end j . Assume that point A is on the loading curve and has a rotation, θ_{a0} , and a moment, M_{a0} . When an incremental rotation, $\Delta\theta_a$, is applied, member stiffness at the current stage is used to determine the end moment which then has a value of M_{a1} . Moment M_{a1} , however, is greater than the actual internal moment M'_{a1} corresponding to rotation θ_{a1} . The actual moment may be calculated as

$$M'_{a1} = M_{a1} - (M_{a1} - M_p - y) = M_{a1} - [(M_{a1} - M_p)(1 - p)] \quad (9.24)$$

Now the unbalanced force at end i is $\Delta U_a = M_{a1} - M'_{a1}$, and the unbalanced force at end j is similarly calculated as $\Delta U_b = M_{b1} - M'_{b1}$. At every time step, the element's unbalanced forces at each end are obtained, and are then treated as joint loads of a structure for the next time step. The total structure's unbalanced force vector can be expressed as

$$\{\Delta U = [\Delta U_1 \quad \Delta U_2 \quad \dots \quad \Delta U_m]^T; \quad m = \text{total joint number} \quad (9.25)$$

This approach is fairly simple to execute. Yet it provides a reasonable approximation of actual nonlinear dynamic response.

EXAMPLE 9.4.1 Applying the incremental linear acceleration method with state of yield technique, find the dynamic response of the framework given in Fig. 9.11a and then plot the response history of moment vs deflection and moment vs time. Use the bilinear hysteresis model for all members. Assume $EI = 1000 \text{ k in}^2$ (2.8697 kN m^2), $M = 2 \times 10^{-4} \text{ k sec}^2/\text{in}$ (35.0236 N

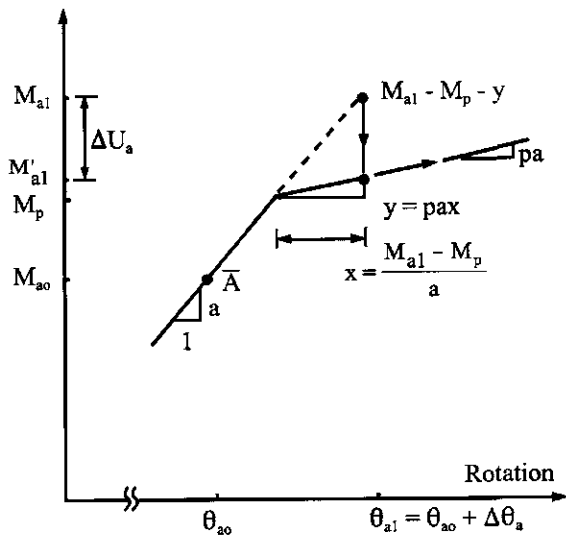


FIG. 9.10 Member's unbalanced force.

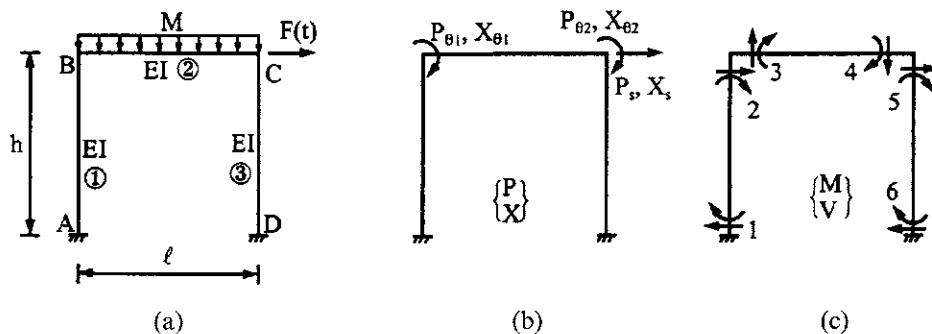


FIG. 9.11 One-story building of Example 9.4.1. (a) Given structure. (b) External action. (c) Internal resistance.

sec^2/m), $h = 10 \text{ ft}$ (3.048m), $\ell = 20 \text{ ft}$ (6.096m), $F(t) = 0.02 \sin(\pi t)\text{k}$ [$88.96 \sin(\pi t)\text{N}$], $p = 0.05$, and ultimate moment capacity $M_p = 0.2 \text{ k}$ in (22.59584 N m). The initial conditions are $x_0 = \dot{x}_0 = \ddot{x}_0 = 0$.

Solution: Let the stiffness matrix of i element be expressed as

$$[K_e^i] = \begin{bmatrix} k_{11}^i & k_{12}^i & k_{13}^i & k_{14}^i \\ k_{21}^i & k_{22}^i & k_{23}^i & k_{24}^i \\ k_{31}^i & k_{32}^i & k_{33}^i & k_{34}^i \\ k_{41}^i & k_{42}^i & k_{43}^i & k_{44}^i \end{bmatrix} \quad (\text{a})$$

Using the diagrams shown in Fig. 9.11b and c, the motion equation can be formulated as

$$\begin{bmatrix} 0 & 0 & | & 0 \\ 0 & 0 & | & 0 \\ \cdots & \cdots & | & \cdots \\ 0 & 0 & | & M \end{bmatrix} \begin{Bmatrix} \Delta\ddot{x}_{\theta 1} \\ \Delta\ddot{x}_{\theta 2} \\ \cdots \\ \Delta\ddot{x}_s \end{Bmatrix} + \begin{bmatrix} k_{22}^1 + k_{11}^1 & k_{12}^2 & | & k_{24}^1 \\ & k_{22}^2 + k_{11}^3 & | & k_{13}^3 \\ \text{symm} & \cdots & | & k_{44}^1 + k_{33}^3 \end{bmatrix} \begin{Bmatrix} \Delta x_{\theta 1} \\ \Delta x_{\theta 2} \\ \cdots \\ \Delta x_s \end{Bmatrix} = \begin{Bmatrix} 0 \\ 0 \\ \cdots \\ \Delta F(t) \end{Bmatrix} \quad (b)$$

in which $M = 2 \times 10^{-4}$ k sec²/in, $\Delta F(t) = 0.02 \sin \pi \Delta t$, $k_{22}^1 = a_1 = k_{11}^3 = a_3 = 4EI/h = 33.3333$ k/in, $k_{11}^2 = k_{22}^2 = a_2 = 4EI/\ell = 16.6667$ k/in, $k_{12}^2 = b_2 = 2EI/\ell = 8.3333$ k/in, $k_{24}^1 = c_1 = k_{13}^3 = -c_3 = -6EI/h^2 = -0.41667$ k, and $k_{44}^1 = d_1 = k_{33}^3 = d_3 = 12EI/h^3 = 0.0069445$ k/in. Note that the subscripts of a, b, c, d represent the member numbers. For convenience, let Eq. (b) be expressed symbolically as

$$\begin{bmatrix} 0 & | & 0 \\ \cdots & | & M \end{bmatrix} \begin{Bmatrix} \Delta\ddot{x}_{\theta} \\ \cdots \\ \Delta\ddot{x}_s \end{Bmatrix} + \begin{bmatrix} K_{11} & | & K_{12} \\ K_{21} & | & K_{22} \end{bmatrix} \begin{Bmatrix} \Delta x_{\theta} \\ \cdots \\ \Delta x_s \end{Bmatrix} = \begin{Bmatrix} 0 \\ \cdots \\ \Delta F(t) \end{Bmatrix} \quad (c)$$

where

$$\begin{bmatrix} K_{11} & | & K_{12} \\ \cdots & | & \cdots \\ K_{21} & | & K_{22} \end{bmatrix} = \begin{bmatrix} 50 & 8.3333 & -0.41667 \\ \cdots & 50 & -0.41667 \\ \text{symm} & \cdots & 0.01389 \end{bmatrix} \quad (d)$$

By matrix condensation, Eq. (c) becomes

$$M\Delta\ddot{x}_s + K\Delta x_s = \Delta F(t) \quad (e)$$

in which

$$K = K_{22} - K_{21}K_{11}^{-1}K_{12} = 0.007936 \text{ k/in} \quad (f)$$

Note that the modified K in Eq. (f) can be obtained either by using matrix condensation as shown above or by using Gauss elimination on the original structural stiffness in Eq. (d). Now Eq. (e) may be rewritten as

$$(2)10^{-4}\Delta\ddot{x}_s + 0.007936\Delta x_s = \Delta F(t) \quad (g)$$

After Δx_s has been found from Eq. (g), the joint rotations can be calculated as

$$\begin{Bmatrix} \Delta x_{\theta 1} \\ \Delta x_{\theta 2} \end{Bmatrix} = -K_{11}^{-1}K_{12}\Delta x_s = \begin{Bmatrix} 0.0071429 \\ 0.0071429 \end{Bmatrix} \Delta x_s \quad (h)$$

Internal forces are then

$$\left. \begin{aligned} \Delta M_1 &= k_{12}^1\Delta x_{\theta 1} + k_{14}^1\Delta x_s = b_1\Delta x_{\theta 1} - c_1\Delta x_s; & \Delta M_2 &= k_{22}^1\Delta x_{\theta 1} + k_{24}^1\Delta x_s = a_1\Delta x_{\theta 1} - c_1\Delta x_s \\ \Delta M_3 &= k_{11}^2\Delta x_{\theta 1} + k_{12}^2\Delta x_{\theta 2} = a_2\Delta x_{\theta 1} + b_2\Delta x_{\theta 2}; & \Delta M_4 &= k_{21}^2\Delta x_{\theta 1} + k_{22}^2\Delta x_{\theta 2} = b_2\Delta x_{\theta 1} + a_2\Delta x_{\theta 2} \\ \Delta M_5 &= k_{11}^3\Delta x_{\theta 2} + k_{13}^3\Delta x_s = a_3\Delta x_{\theta 2} - c_3\Delta x_s; & \Delta M_6 &= k_{21}^3\Delta x_{\theta 2} + k_{23}^3\Delta x_s = b_3\Delta x_{\theta 2} - c_3\Delta x_s \end{aligned} \right\} \quad (i)$$

Incremental linear acceleration formulae are used here and, for convenience, can be summarized as follows:

$$\underbrace{\left[\frac{6}{(\Delta t)^2} M + K \right]}_{\bar{K}} \Delta x_s = \underbrace{\Delta F(t) - MA}_{\Delta \bar{F}} \quad (j)$$

$$\left. \begin{aligned} A &= -\frac{6}{\Delta t} \dot{x}_{s(n-1)} - 3\ddot{x}_{s(n-1)}; & B &= -3\dot{x}_{s(n-1)} - \frac{\Delta t}{2} \ddot{x}_{s(n-1)} \\ x_s &= x_{s(n-1)} + \Delta x_s; & \dot{x}_s &= \dot{x}_{s(n-1)} + \frac{3}{\Delta t} \Delta x_s + B \\ \ddot{x}_s &= \ddot{x}_{s(n-1)} + \frac{6}{\Delta t^2} \Delta x_s + A; & \{x_\theta\} &= \{x_\theta\}_{(n-1)} + \{\Delta x_\theta\} \end{aligned} \right\} \quad (k)$$

in which n represents current calculated results and $n-1$ signifies a time-step immediately preceding the current time step.

Using Eqs. (j) and (k), we may find the dynamic responses shown in Table 9.1. Detailed calculations are illustrated at $t=0.3$ sec for which the initial conditions at $t=0.2$ sec are

$$x_{s(n-1)} = 0.3637 \text{ in}; \quad \dot{x}_{s(n-1)} = 5.1157 \text{ in/sec}; \quad \ddot{x}_{s(n-1)} = 44.343 \text{ in/sec}^2$$

Following Eqs. (j) and (k), we have

$$\begin{aligned} A &= -\frac{6}{\Delta t} \dot{x}_{s(n-1)} - 3\ddot{x}_{s(n-1)} = -\frac{6}{0.1} (5.1157) - 3(44.343) = -439.97 \\ B &= -3\dot{x}_{s(n-1)} - \frac{\Delta t}{2} \ddot{x}_{s(n-1)} = -17.564 \\ \bar{K} &= \frac{6}{(\Delta t)^2} M + K = \frac{6}{(0.1)^2} (2)(10^{-4}) + 0.007936 = 0.1279 \\ \Delta F(t) &= 0.02 \sin(0.3\pi) - 0.02 \sin(0.2\pi) = (4.42463)(10^{-3}) \\ \Delta \bar{F} &= \Delta F(t) - MA \\ &= (4.42463)(10^{-3}) - (2)(10^{-4})(-439.97) = 0.0924 \end{aligned}$$

and displacement responses

$$\Delta x_s = \Delta \bar{F} / \bar{K} = 0.7224 \text{ in} \quad (l)$$

$$\left. \begin{aligned} x_s &= x_{s(n-1)} + \Delta x_s = 1.0861 \text{ in} \\ \dot{x}_s &= \dot{x}_{s(n-1)} + \frac{3}{\Delta t} \Delta x_s + B = 9.2229 \text{ in/sec} \\ \ddot{x}_s &= \ddot{x}_{s(n-1)} + \frac{6}{(\Delta t)^2} \Delta x_s + A = 37.801 \text{ in/sec}^2 \end{aligned} \right\} \quad (m)$$

$$\begin{Bmatrix} \Delta x_{\theta 1} \\ \Delta x_{\theta 2} \end{Bmatrix} = -K_{11}^{-1} K_{12} \Delta x_s = \begin{Bmatrix} 0.0071429 \\ 0.0071429 \end{Bmatrix} \Delta x_s = \begin{Bmatrix} 0.00516 \\ 0.00516 \end{Bmatrix} \quad (n)$$

$$\begin{Bmatrix} x_{\theta 1} \\ x_{\theta 2} \end{Bmatrix} = \begin{Bmatrix} x_{\theta 1} \\ x_{\theta 2} \end{Bmatrix}_{(n-1)} + \begin{Bmatrix} \Delta x_{\theta 1} \\ \Delta x_{\theta 2} \end{Bmatrix} = \begin{Bmatrix} 0.0077 \\ 0.0077 \end{Bmatrix} \text{ rad} \quad (o)$$

BLE 9.1 Dynamic Response of Example 9.4.1

Δt (sec)	A	B	$\Delta \bar{F}$ (k)	\bar{K} (k/in)	x_s (in)	\dot{x}_s (in/sec)	$(\dot{x}_s)^2$ (in/sec ²)	$x_{\theta 1} = x_{\omega}$ rad	$M_1 = M_3 = M_4 = -M_2 = -M_5$ (k in)
0.1	0	0	0.0062	0.1279	0.0483	1.4492	28.985	0.0003	-0.0144
0.1	-173.91	-5.797	0.0403	0.1279	0.3637	5.1157	44.343	0.0026	-0.1083
0.1	-439.97	-17.564	0.0924	0.1279	1.0861	9.2229	37.801	0.0077	-0.3232
0.05	-746.91	-16.455	0.1517	0.4879	0.6748	7.3225	43.928	0.0048	-0.2008
0.05	-1010.48	-23.066	0.2041	0.4821	1.0982	9.6627	49.682	0.0066	-0.2081
0.05	-1038.58	-30.230	0.2633	0.4821	1.6445	12.2088	52.155	0.0090	-0.2175
0.025	-2468.11	-29.609	0.4945	1.9220	1.3555	10.9226	51.350	0.0077	-0.2125
0.0125	-5398.34	-33.098	1.0801	7.6821	1.4961	11.5707	51.865	0.0084	-0.2149
0.00625	-10642.7	-32.937	2.1287	30.7221	1.4248	11.2474	51.622	0.0081	-0.2137
0.1	-829.78	-36.325	0.1682	0.1204	2.8222	16.8428	60.262	0.0180	-0.2345
0.1	-1191.36	-53.541	0.2386	0.1204	4.8043	22.7646	58.168	0.0322	-0.2640
0.1	-1540.41	-71.203	0.3065	0.1204	7.3501	27.9345	45.219	0.0504	-0.3019
0.1	-1811.75	-86.065	0.3590	0.1204	10.3317	31.3179	22.439	0.0717	-0.3463
0.1	-1946.39	-95.075	0.3844	0.1204	13.5248	32.0355	-8.085	0.0945	-0.3938
0.1	-1897.88	-95.702	0.3737	0.1204	16.6291	29.4625	-43.379	0.1166	-0.4400
0.1	-1637.61	-86.218	0.3213	0.1204	19.2976	23.2980	-79.907	0.1357	-0.4797
0.1	-1158.24	-65.902	0.2256	0.1204	21.1705	13.6069	-113.896	0.1491	-0.5076
0.1	-474.89	-35.134	0.0897	0.1204	21.9165	0.8288	-141.721	0.1544	-0.5187
0.1	375.43	4.599	-0.0791	0.1204	21.2599	-14.2705	-160.272	0.1497	-0.5089
0.01	-72.11	-1.778	0.0140	12.0004	21.9044	-0.5999	-144.039	0.1543	-0.5187
0.01	792.06	2.512	-0.1588	12.0004	21.9044	-2.0514	-146.260	0.1543	-0.5185
0.1	468.11	9.002	-0.0974	0.1279	21.1560	-14.4464	-132.892	0.1490	-0.2920
0.1	1265.48	49.985	-0.2551	0.1279	19.1613	-24.3024	-64.223	0.1348	0.3016
0.05	2132.28	46.662	-0.4277	0.4879	20.2794	-20.3817	-104.505	0.1427	-0.0311
0.025	3865.87	45.001	-0.7739	1.9274	20.7546	-17.6132	-120.436	0.1461	-0.1726
0.0125	8815.64	53.592	-1.7634	7.6879	20.5525	-19.0711	-112.834	0.1445	-0.1362

Using the incremental moments' expressions given in Eq. (i), moments can be calculated as

$$\begin{aligned} M_1 &= M_{1(n-1)} + \Delta M_1 \\ &= -0.1083 + 16.6667(0.00516) + (-0.41667)(0.7224) \\ &= -0.3232 \text{ k in} = M_6 \end{aligned} \quad (\text{p})$$

$$\begin{aligned} M_2 &= M_{2(n-1)} + \Delta M_2 = -0.0649 + 33.3333(0.00516) + (-0.41667)(0.7224) \\ &= -0.1939 \text{ k in} = M_5 \end{aligned} \quad (\text{q})$$

$$\begin{aligned} M_3 &= M_{3(n-1)} + \Delta M_3 = 0.0649 + 16.6667(0.00516) + 8.3333(0.00516) \\ &= 0.1939 \text{ k in} = M_4 \end{aligned} \quad (\text{r})$$

Some other key aspects of Table 9.1 are explored as follows.

(A) At $t=0.3$ —at the OS point, M_1 and M_6 are greater than M_p . Reducing the time increment to $\Delta t=0.05$ and using initial conditions at $t=0.2$, we have, at $t=0.25$, $M_1=M_6=-0.2008$ k in. Let the difference between the calculated moment M_c and the ultimate moment M_p be the tolerance as $\epsilon=0.002$. Then

$$M_c - M_p = 0.2008 - 0.2 < \epsilon$$

Thus the solution at $t=0.25$ is accepted as correct. This tolerance also applies to the difference between the moment at current step, n , and the previous time step, $n-1$. Since nodes 1 and 6 become nonlinear, the stiffness of members (1) and (3) must be changed in motion equation (b) according to yield conditions described in Eqs. (9.15) and (9.19). Stiffness coefficients in Eq. (b) are changed as

$$\left. \begin{array}{l} k_{11}^2 + k_{22}^1 = a_2 + pa_1 + qe_1 = 4EI/\ell + 4EI_p/h + 3EI_q/h = 42.0834 \\ k_{12}^2 = b_2 = 2EI/\ell = 8.3333 \\ k_{24}^1 = -pc_1 - qf_1 = -6EI_p/h^2 - 3EI_q/h^2 = -0.21875 \\ k_{22}^2 + k_{11}^3 = a_2 + pa_3 + qe_3 = 4EI/\ell + 4EI_p/h + 3EI_q/h = 42.0834 \\ k_{13}^3 = -pc_3 - qf_3 = -6EI_p/h^2 - 3EI_q/h^2 = -0.21875 \\ k_{44}^1 + k_{33}^3 = p(d_1 + d_3) + q(g_1 + g_3) = 24EI_p/h^3 + 6EI_q/h^3 = 0.0039931 \end{array} \right\} \quad (\text{s})$$

With similar operations applied to Eqs. (c)–(f), (g) becomes

$$(2)10^{-4}\Delta\ddot{x}_s + 0.00209482\Delta x_s = \Delta(0.02 \sin \pi t) \quad (\text{t})$$

Incremental joint rotations and incremental moments may be calculated from

$$\begin{Bmatrix} \Delta x_{\theta 1} \\ \Delta x_{\theta 2} \end{Bmatrix} = \begin{Bmatrix} 0.0043388 \\ 0.0043388 \end{Bmatrix} \Delta x_s \quad (\text{u})$$

$$\left. \begin{aligned} \Delta M_1 &= k_{12}^1 \Delta x_{\theta 1} + k_{14}^1 \Delta x_s = pb_1 \Delta x_{\theta 1} - pc_1 \Delta x_s = 0.8333 \Delta x_{\theta 1} - 0.020833 \Delta x_s \\ \Delta M_2 &= k_{22}^1 \Delta x_{\theta 1} + k_{24}^1 \Delta x_s = (pa_1 + qe_1) \Delta x_{\theta 1} - (pc_1 + qf_1) \Delta x_s = 25.4167 \Delta x_{\theta 1} - 0.21875 \Delta x_s \\ \Delta M_3 &= k_{11}^2 \Delta x_{\theta 1} + k_{12}^2 \Delta x_{\theta 2} = a_2 \Delta x_{\theta 1} + b_2 \Delta x_{\theta 2} = 16.6667 \Delta x_{\theta 1} + 8.3333 \Delta x_{\theta 2} \end{aligned} \right\} \quad (v)$$

Other moments can be similarly expressed as above.

(B) At $t=0.35$ —again, at the OS point, M_1-M_6 are greater than M_p . By changing the time increment, we finally reach a solution satisfying tolerance criterion ε at $t=0.33125$ sec. At the end of $t=0.33125$, all nodes become nonlinear. Use the predetermined time increment $\Delta t=0.1$ for the next cycle.

(C) At $t=0.43125$ —since all nodes are nonlinear, stiffness coefficients in Eq. (b) should be modified as

$$\left. \begin{aligned} k_{11}^2 + k_{22}^1 &= k_{22}^2 + k_{11}^3 = p(a_1 + a_2) + p(a_2 + a_3) = 2.5 \\ k_{12}^2 &= pb_2 = 0.41667 \\ k_{24}^1 &= k_{13}^3 = -pc_1 = -pc_3 = -0.020833 \\ k_{44}^1 + k_{33}^3 &= p(d_1 + d_3) = 0.0006944 \end{aligned} \right\} \quad (w)$$

Motion equation, incremental rotations and moments may now be expressed in Eqs. (x), (y), and (z), respectively.

$$(2) 10^{-4} \Delta \ddot{x}_s + 0.0003968 \Delta x_s = \Delta F(t) \quad (x)$$

$$\left. \begin{aligned} \Delta x_{\theta 1} \\ \Delta x_{\theta 2} \end{aligned} \right\} = \left. \begin{aligned} 7.1429 \times 10^{-3} \\ 7.1429 \times 10^{-3} \end{aligned} \right\} \Delta x_s \quad (y)$$

$$\left. \begin{aligned} \Delta M_1 &= k_{12}^1 \Delta x_{\theta 1} + k_{14}^1 \Delta x_s = pb_1 \Delta x_{\theta 1} - pc_1 \Delta x_s = 0.8333 \Delta x_{\theta 1} - 0.020833 \Delta x_s \\ \Delta M_2 &= k_{22}^1 \Delta x_{\theta 1} + k_{24}^1 \Delta x_s = pa_1 \Delta x_{\theta 1} - pc_1 \Delta x_s = 1.66667 \Delta x_{\theta 1} - 0.020833 \Delta x_s \\ \Delta M_3 &= k_{11}^2 \Delta x_{\theta 1} + k_{12}^2 \Delta x_{\theta 2} = pa_2 \Delta x_{\theta 1} + pb_2 \Delta x_{\theta 2} = 0.8333 \Delta x_{\theta 1} + 0.41667 \Delta x_{\theta 2} \end{aligned} \right\} \quad (z)$$

Note that Eqs. (w)–(z) are used for the period $t=0.43125$ to 1.33125 .

(D) At $t=1.33125$ —moments are less than those at the preceding time. This signifies that $\{\Delta M\}$ changes sign [i.e. $\Delta M_1 = -0.5089 - (-0.5187) = 0.0098$, $\Delta M_2 = -0.3798 - (-0.3848) = -0.0059$] and the structure is moving backwards. Consequently, backtracking has occurred. In order to obtain an accurate solution, we may change time increments at $t=1.23125$ with $\Delta t=0.01$ sec for $t=1.24125$ sec. In comparison with those at $t=1.23125$ sec, $\Delta M_1 = -0.5187 - (0.5187) = 0$ and $\Delta M_2 = -0.3848 - (-0.3848) = 0$. This result indicates that the correction is acceptable. To gain insight into the correction, actual computer results (not shown in the table) are $\Delta M_1 = -0.00001732$ and $\Delta M_2 = -0.00001039$, which have the same sign as $t=1.23125$. This implies that the members' deformations are still increasing on the right track. By increasing $\Delta t=0.01$ sec, incremental moments at $t=1.25125$ are $\Delta M_1 = -0.5185 - (-0.5187) = 0.0002$ and $\Delta M_2 = -0.3847 - (-0.3848) = 0.0001$, of which the sign is different from the preceding time and the difference is within tolerance. Correct backtracking may thus be assumed at $t=1.25125$; at the end of this time, the structure is assumed to be elastic. Consequently, numerical values in Eqs. (f)–(h) should be used for further analysis.

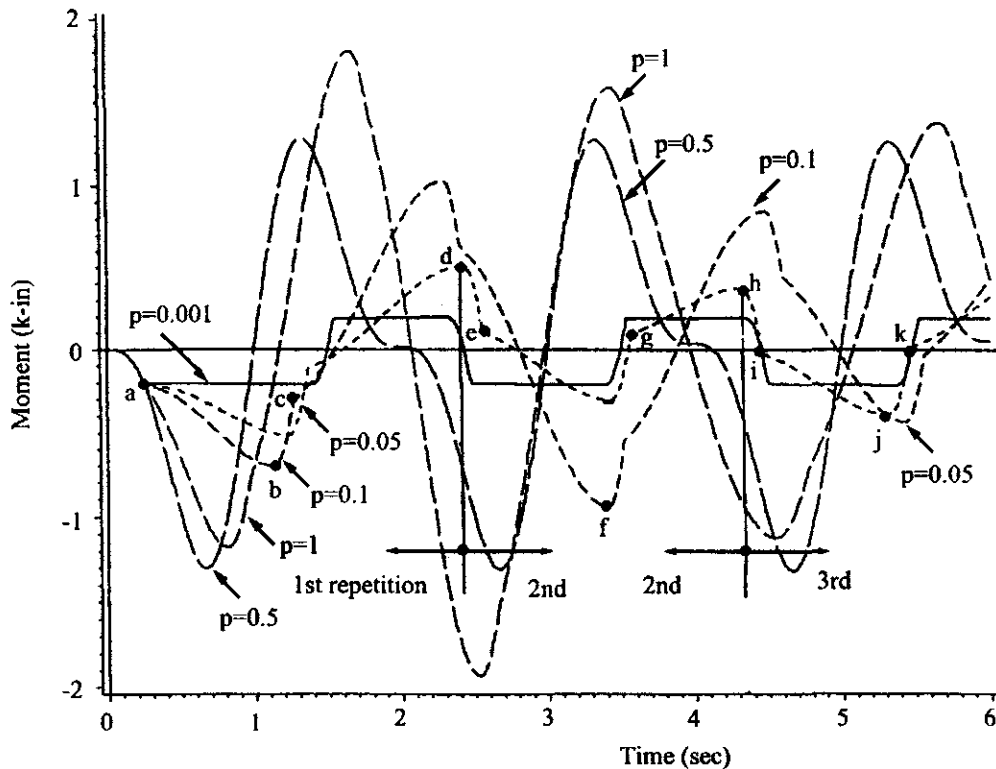


FIG. 9.12 Effects of p 's on M_1 vs time of Example 9.4.1; $oabcd$, $defgh$, $hijk$ signify repetitions 1, 2, 3, respectively, for $p = 0.05$ shown in FIG. 9.13.

(E) At $t = 1.44125$ —overshooting arises again. Procedures shown in (A) should be similarly used for an accurate solution. How various p 's of $p = 1, 0.5, 0.1, 0.05, 0.001$ affect M_1 vs time, M_1 vs x_s , and x_s vs time is shown in Figs. 9.12–9.14, respectively. Note that $p = 1$ is an elastic response and $p = 0.001$ corresponds approximately to an elasto-plastic response. The elastic response may also be obtained by using $x_s = -1.673 \sin(6.2922t) + 3.3543 \sin(\pi t)$ resulting from $x_s = A \cos pt + B \sin pt + 100 \sin(\pi)/(p^2 - \pi^2)$; $A = 0$; and $B = -1.673$ for $x = \dot{x} = 0$ at $t = 0$. Thus the numerical integration solution includes transient vibration [see Eq. (1.59)].

EXAMPLE 9.4.2 Find the dynamic response of the framework given in Example 9.4.1 by using incremental linear acceleration method with unbalanced force technique.

Solution: Using the linear acceleration method with time increment $\Delta t = 0.1$ sec, structural displacements and internal forces at $t = 0.1$ and 0.2 sec are elastic and are the same as those in Table 9.1 of Example 9.4.1. At $t = 0.3$ sec, M_1 and M_6 are greater than the ultimate moment capacity, M_p , and need to be corrected.

The relationship between forces (moments and shears) and deformations (rotations and deflections) of a member corresponding to various plastic hinge conditions shown in Eqs. (9.9), (9.15), (9.19) and (9.23) can be expressed in terms of moments and relative rotations. Shears are expressed in terms of moments based on equilibrium conditions of a member, and rotations and deflections are combined into relative rotations as shown in Fig. 9.15.

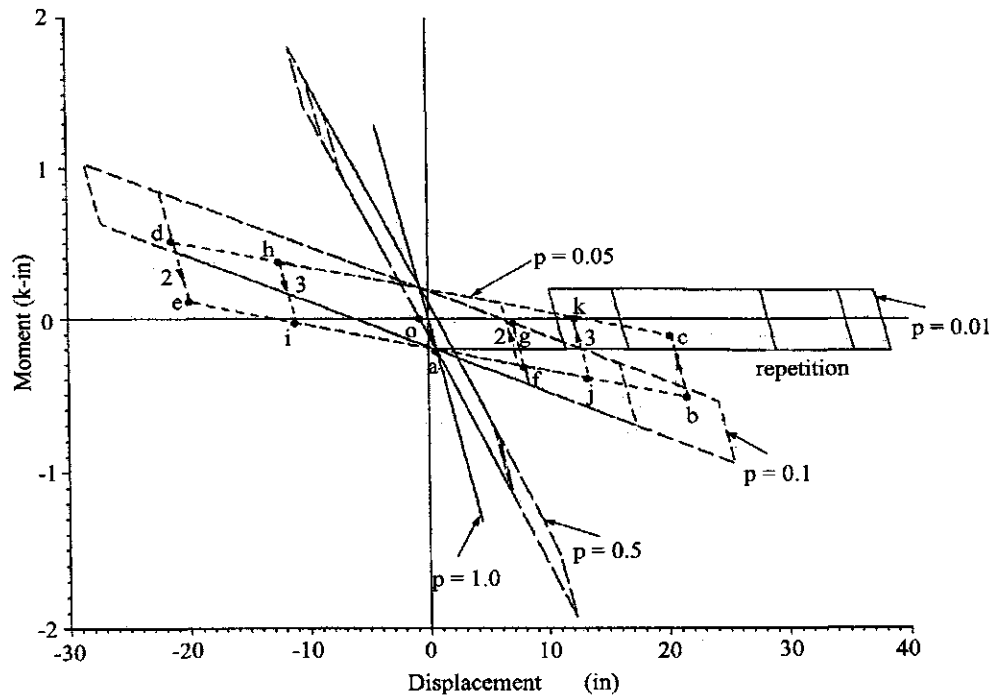


FIG. 9.13 Effects of p 's on M_1 vs x_s of Example 9.4.1.

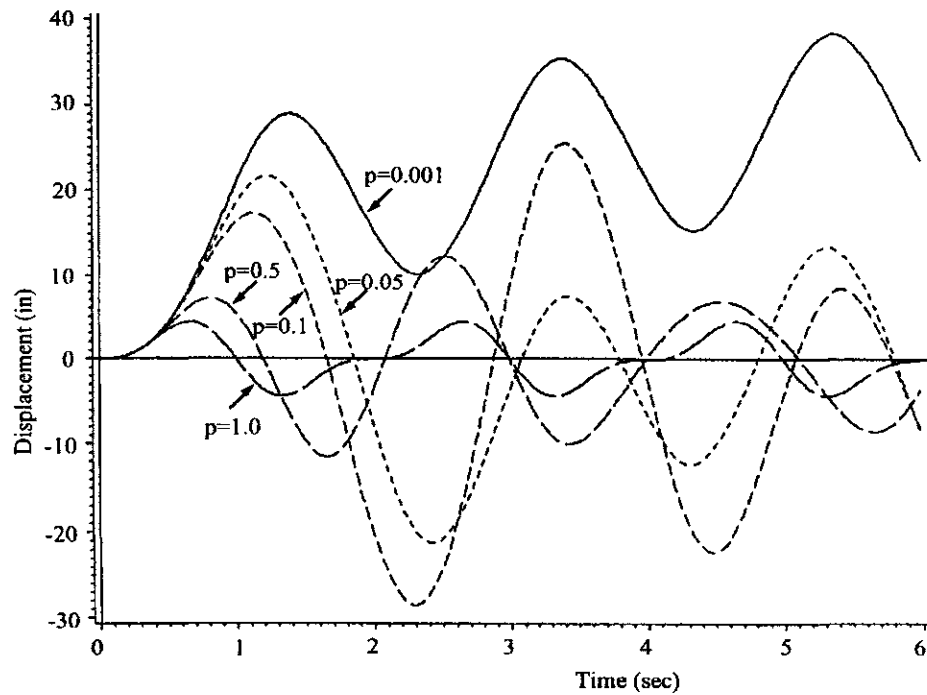


FIG. 9.14 Effects of p 's on x_s vs time of Example 9.4.1.

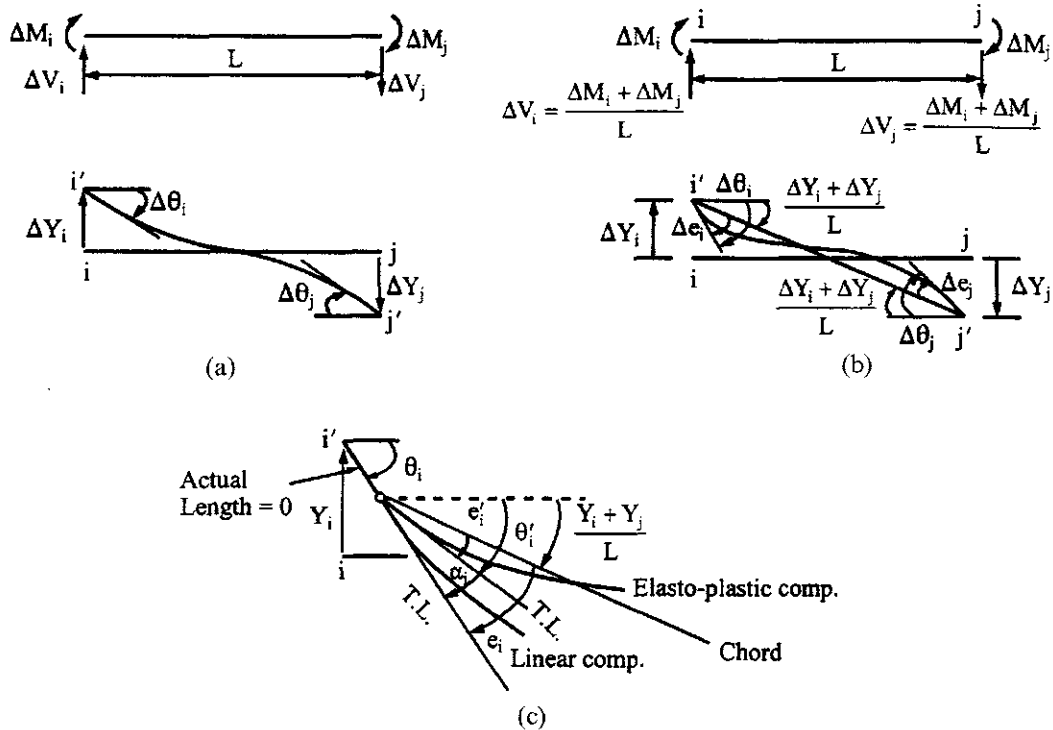


FIG. 9.15 Relationship between four- and two-d.o.f. of a member. (a) Four independent forces and deformations. (b) Two independent forces and deformations. (c) Detailed deformations at i-end of (b) in total form.

When the *i*-end is nonlinear and the *j*-end is linear, the moments in Eq. (9.15) can be expressed as

$$\begin{aligned}\Delta M_i &= pa\Delta\theta_i + pb\Delta\theta_j - pc\Delta Y_i - pd\Delta Y_j = pa\left(\Delta\theta_i - \frac{\Delta Y_i + \Delta Y_j}{L}\right) + pb\left(\Delta\theta_j - \frac{\Delta Y_i + \Delta Y_j}{L}\right) \\ &= pa\Delta e_i + pb\Delta e_j\end{aligned}\quad (\text{a})$$

$$\begin{aligned}\Delta M_j &= pb\Delta\theta_i + (pa + qc)\Delta\theta_j - (pc + qf)\Delta Y_i - (pd + qg)\Delta Y_j \\ &= pb\left(\Delta\theta_i - \frac{\Delta Y_i + \Delta Y_j}{L}\right) + (pa + qc)\left(\Delta\theta_j - \frac{\Delta Y_i + \Delta Y_j}{L}\right) \\ &= pb\Delta e_i + (pa + qc)\Delta e_j\end{aligned}\quad (\text{b})$$

$$\begin{aligned}\Delta V_i &= -pc\Delta\theta_i - (pc + qf)\Delta\theta_j + (pd + qg)\Delta Y_i + (pd + qg)\Delta Y_j \\ &= -pc\left(\Delta\theta_i - \frac{\Delta Y_i + \Delta Y_j}{L}\right) - (pc + qf)\left(\Delta\theta_j - \frac{\Delta Y_i + \Delta Y_j}{L}\right) \\ &= -pc\Delta e_i - (pc + qf)\Delta e_j\end{aligned}\quad (\text{c})$$

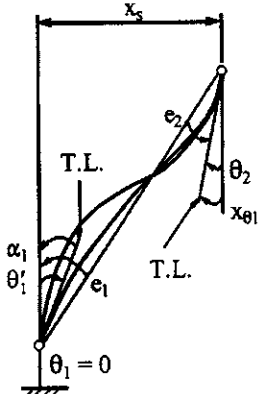


FIG. 9.16 Relationship between deformations.

From the equilibrium condition of Eqs. (a) and (b)

$$\begin{aligned}\Delta V_i &= \frac{\Delta M_i + \Delta M_j}{L} = \frac{(pa + pb)}{L} \Delta e_i + \frac{(pb + pa + qe)}{L} \Delta e_j \\ &= pc \Delta e_i + (pc + qf) \Delta e_j\end{aligned}\quad (d)$$

Note that the sign of shear in Eq. (c) is opposite to that of Eq. (d), which is due to the equilibrium condition of moments and is consistent with the sign shown in Fig. 9.15a and b.

Relative deformations of members 1 and 3 are shown in Fig. 9.16 from which angle e , between the chord and the tangent line, can be calculated as

$$\left. \begin{array}{l} \text{at } t = 0.3 \text{ sec} \\ e_1 = -\frac{x_s}{h} = -\frac{1.0861}{120} = -9.051(10^{-3}) \text{ rad} \\ e_2 = \theta_2 - \frac{x_s}{h} = 7.7(10^{-3}) - 9.051(10^{-3}) \\ = -1.351(10^{-3}) \text{ rad} \\ \text{at } t = 0.2 \text{ sec} \\ e_1 = -\frac{x_s}{h} = -\frac{0.3637}{120} = -3.031(10^{-3}) \text{ rad} \end{array} \right\} \quad (e)$$

Unbalanced forces for members 1 and 3 can be obtained from Fig. 9.17 as

$$k_1 = \frac{M_1(t=0.3) - M_1(t=0.2)}{e_1(t=0.3) - e_1(t=0.2)} = \frac{-0.3232 - (-0.1083)}{-9.051(10^{-3}) - (-3.031)(10^{-3})} = 35.6977 \quad (f)$$

$$k_2 = pk_1 = (0.05)35.6977 = 1.7849 \text{ k in/rad} \quad (g)$$

$$\begin{aligned}x &= \frac{M_p - M_1(t=0.3)}{k_1} = \frac{-0.2 - (-0.3232)}{35.6977} = 3.4512(10^{-3}) \\ M'_1(t=0.3) &= M_p - k_2 x = -0.2 - 6.160(10^{-3}) \\ &= -0.20616 \text{ k in}\end{aligned} \quad (h)$$

The member's unbalanced moment is $\Delta M_1 = M_1 - M'_1$; thus $\Delta M_1 = -0.3232 - (-0.2062) = -0.1170 \text{ k in}$. Unbalanced shear of the member is

$$\Delta V = \Delta M_1/h = -9.750(10^{-4}) \text{ k} \quad (i)$$

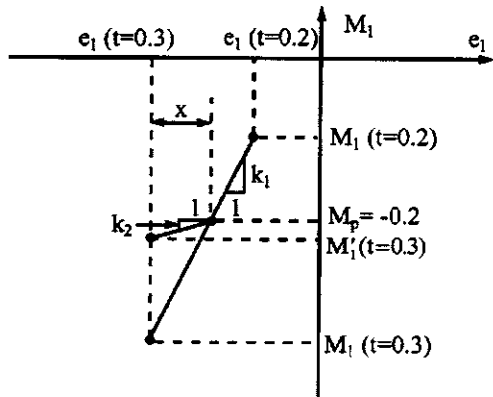


FIG. 9.17 Member force correction.

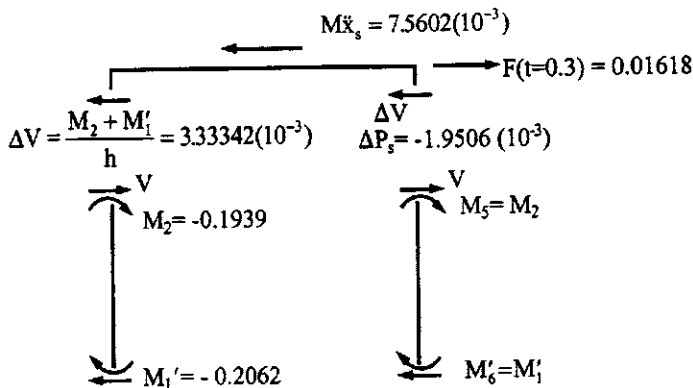


FIG. 9.18 Equilibrium check for Example 9.4.2.

Unbalanced lateral force of the structure is then

$$\Delta P_s = 2\Delta V = -1.9506(10^{-3}) \text{ k} \quad (j)$$

which should satisfy the equilibrium condition of the structure as shown in Eq. (k) based on Fig. 9.18.

$$\Sigma F_x = 0, \quad -7.5602(10^{-3}) - (2)3.33342(10^{-3}) - 1.9506(10^{-3}) + 0.01618 = 0 \quad (k)$$

The response analysis continues for $t=0.4$ sec with initial conditions at $t=0.3$ sec as

$$\left. \begin{aligned} x_s &= 1.0861 \text{ in} \\ \dot{x}_s &= 9.2229 \text{ in/sec} \\ \ddot{x}_s &= 37.801 \text{ in/sec}^2 \\ \Delta F(t)|_{t=0.3}^{t=0.4} &= 0.02 \sin(0.4\pi) - 0.02 \sin(0.3\pi) = 2.84077(10^{-3}) \end{aligned} \right\} \quad (l)$$

Member 1 has i -end nonlinear and j -end linear, and member 3 has i -end linear and j -end nonlinear. Repeat the procedures shown above for the rest of the calculations. The dynamic response for the time increment of $\Delta t = 0.01$ sec is listed in Table 9.2. Comparing Table 9.2 with Table 9.1 reveals the difference between their responses. Apparently the smaller Δt used in the unbalanced force technique gives more accurate results.

TABLE 9.2 Dynamic Response of Example 9.4.2 with $\Delta t = 0.01$ sec

sec)	x_s (in)	\dot{x}_s (in/sec)	\ddot{x}_s (in/sec 2)	$x_{\theta 1} = x_{\theta 2}$ (rad)	$M_1 = M_6$ (k in)	$M_3 = M_4 = -M_2 = -M_5$ (k in)
0.0511	1.5068	28.8749	0.36481(10^{-3})	-0.0152	0.0091	
0.3790	5.3013	43.7401	0.27069(10^{-2})	-0.1128	0.0677	
1.1305	9.8143	48.9784	0.68131(10^{-2})	-0.2968	0.1703	
2.3710	15.1607	58.1338	0.014864	-0.3731	0.2085	
4.1845	21.1298	59.4301	0.027817	-0.4001	0.2247	
6.5830	26.6803	49.7767	0.044950	-0.4358	0.2461	
9.4707	30.7411	29.8431	0.065576	-0.4788	0.2719	
12.6497	32.3646	1.4124	0.088284	-0.5261	0.3003	
15.8380	30.8304	-32.7904	0.11106	-0.5735	0.3287	
18.6964	25.7271	-69.3636	0.13147	-0.6160	0.3543	
20.8624	17.0035	-104.5627	0.14695	-0.6483	0.3736	
21.9869	4.9847	-134.6708	0.15498	-0.6650	0.3836	
21.7757	-9.4072	-145.0190	0.15347	-0.5767	0.3307	
20.1658	-22.1393	-111.8493	0.14356	-0.1446	0.0829	

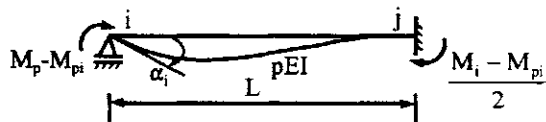


FIG. 9.19 Linear component.

9.4.3. Equilibrium and Compatibility Checks for Numerical Solutions

After the bending moments are found, we may calculate deformations at each end of individual members. Moments and deformations can then be used for compatibility and equilibrium checks. Deformations may be derived according to the state of yield as shown below.

(A) *Both ends linear*—from Eq. (9.9), the moment–rotation relationship in total form may be expressed as

$$\begin{Bmatrix} M_i \\ M_j \end{Bmatrix} = \begin{bmatrix} a & b \\ b & a \end{bmatrix} \begin{Bmatrix} e_i \\ e_j \end{Bmatrix} \quad (9.26)$$

in which $b = a/2$, $a = 4EI/L$, and e is the rotation measured from chord to tangent line, positive in the clockwise direction, as shown in Fig. 9.15. Thus

$$\begin{Bmatrix} e_i \\ e_j \end{Bmatrix} = \begin{bmatrix} 4/3a & -2/3a \\ -2/3a & 4/3a \end{bmatrix} \begin{Bmatrix} M_i \\ M_j \end{Bmatrix} \quad (9.27)$$

(B) *i-end nonlinear and j-end linear*—from Fig. 9.15c, the angle beyond θ'_j is $\alpha_i = \theta_i - \theta'_j$, which is due to the moment above M_{pi} as $M_i - M_{pi}$. Since the angle results from an elastic component, we may use the conjugate beam method to find α_i as shown in Fig. 9.19 for which

$$\alpha_i = \frac{M_i - M_{pi}}{pEI} \frac{L}{2} \left(\frac{2}{3} \right) - \frac{M_i - M_{pi}}{2pEI} \frac{L}{2} \left(\frac{1}{3} \right) = \frac{M_i - M_{pi}}{pa}; \quad \alpha_j = 0 \quad (9.28)$$

where M_{pi} is the plastic moment at the *i*-end.

From Eq. (9.12), the total moment–rotation relationship may be expressed as

$$\begin{aligned} M_i &= a\theta_i + b\theta_j - cY_i - cY_j - qa\alpha_i = ae_i + be_j - qa\alpha_i \\ &= a(e_i - q\alpha_i) + be_j \end{aligned} \quad (9.29)$$

and

$$M_j = b(e_i - q\alpha_i) + ae_j \quad (9.30)$$

Substituting Eq. (9.28) into Eqs. (9.29) and (9.30) yields

$$e_i = \frac{4M_i}{3a} - \frac{2M_j}{3a} + \frac{q(M_i - M_{pi})}{pa}; \quad e_j = \frac{4M_j}{3a} - \frac{2M_i}{3a} \quad (9.31)$$

From Fig. 9.15c

$$e'_i = e_i - \alpha_i = \frac{M_{pi}}{a} + \frac{1}{3a}(M_i - 2M_j); \quad e'_j = e_j \quad (9.32)$$

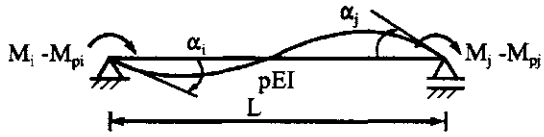


FIG. 9.20 Both ends nonlinear.

(C) *i-end linear and j-end nonlinear*—similar to case (B)

$$\alpha_i = 0; \quad \alpha_j = \frac{M_j - M_{pj}}{pa} \quad (9.33)$$

$$e_i = \frac{4M_i}{3a} - \frac{2M_j}{3a}; \quad e_j = \frac{4M_j}{3a} - \frac{2M_i}{3a} + \frac{q(M_j - M_{pj})}{pa} \quad (9.34)$$

and

$$e'_i = e_i; \quad e'_j = e_j - \alpha_j = \frac{M_{pj}}{a} + \frac{1}{3a}(M_j - 2M_i) \quad (9.35)$$

(D) *Both ends nonlinear*—let the positive moments of the elasto-plastic component be as shown in Fig. 9.20 where M_{pi} is usually equal to M_{pj} but the direction may be different. By using the conjugate beam method, the plastic angles are

$$\alpha_i = \frac{4(M_i - M_{pi})}{3pa} - \frac{2(M_j - M_{pj})}{3pa}; \quad \alpha_j = \frac{4(M_j - M_{pj})}{3pa} - \frac{2(M_i - M_{pi})}{3pa} \quad (9.36)$$

From Eq. (9.20), the total moment–rotation relationship can be similarly derived as shown in Eqs. (9.29) and (9.30)

$$M_i = a(e_i - q\alpha_i) + b(e_j - q\alpha_j); \quad M_j = b(e_i - q\alpha_i) + a(e_j - q\alpha_j) \quad (9.37)$$

Substituting Eq. (9.36) into Eq. (9.37) and then solving for e_i and e_j results in

$$e_i = \frac{4M_i}{3a} - \frac{2M_j}{3a} + \frac{q}{p} \left[\frac{4(M_i - M_{pi})}{3a} - \frac{2(M_j - M_{pj})}{3a} \right] \quad (9.38)$$

$$e_j = \frac{4M_j}{3a} - \frac{2M_i}{3a} + \frac{q}{p} \left[\frac{4(M_j - M_{pj})}{3a} - \frac{2(M_i - M_{pi})}{3a} \right] \quad (9.39)$$

Consequently

$$e'_i = e_i - \alpha_i = \frac{4M_{pi}}{3a} - \frac{2M_{pj}}{3a}; \quad e'_j = e_j - \alpha_j = \frac{4M_{pj}}{3a} - \frac{2M_{pi}}{3a} \quad (9.40)$$

The above is based on the assumption that both ends of the member become nonlinear simultaneously and $|M_i| = |M_j|$. If $|M_i| \geq |M_j|$, then one end becomes nonlinear sooner than the other. Thus the carry-over process of the moments on the linear component can be quite complicated during joint plastification.

EXAMPLE 9.4.3 Using Example 9.4.1, make the equilibrium and compatibility checks for the dynamic responses at $t=0.3$ sec as shown in Table 9.1.

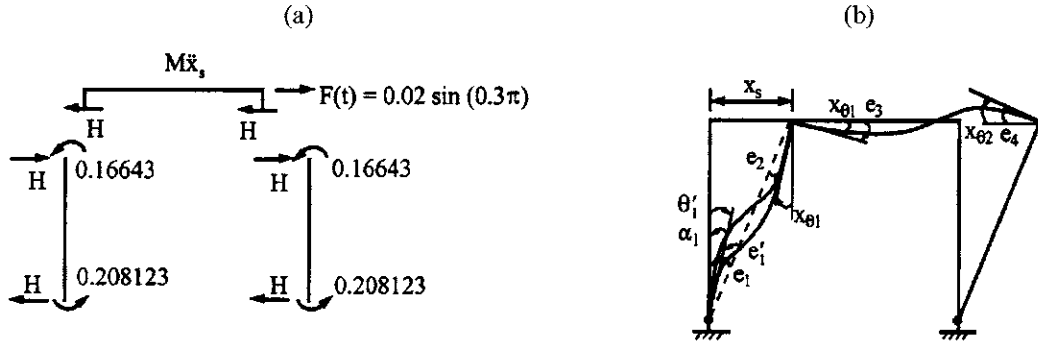


FIG. 9.21 Example 9.4.3. (a) Internal forces. (b) Deformations.

Solution: According to computer output, the dynamic responses at $t=0.3$ sec are

$$x_1 = x_{\theta_2} = 0.665722 \times 10^{-2} \text{ rad}; x_s = 1.09824 \text{ in}; \ddot{x}_s = 49.682 \text{ in/sec}^2 \quad (\text{a})$$

$$M_1 = M_6 = -0.208123 \text{ k in}; M_{p1} = M_{p6} = -0.2000 \text{ k in} \quad (\text{b})$$

$$M_2 = M_5 = -M_3 = -M_4 = -0.16643 \text{ k in} \quad (\text{c})$$

For the equilibrium check, the condition of $\sum M = 0$ at the joints is satisfactory by inspecting the above moments; the condition of $\sum F = 0$ may be applied to the girder shown in Fig. 9.21a for which

$$H = (0.208123 + 0.16643)/120 = 0.0031212 \text{ k} \quad (\text{d})$$

and

$$M\ddot{x}_s + 2H = F(t) \quad (\text{e})$$

yields

$$(2)10^{-4}(49.682) + 2(0.0031212) = 0.016179 \text{ k} \approx F(t = 0.3) = 0.016180 \quad (\text{f})$$

The compatibility check may be studied by using the accompanying figure of deformations where members (1) and (2) correspond to the states of yield of (B) (i -end nonlinear and j -end linear) and (A) (both ends linear), respectively.

Using Eq. (9.28) for member (2), we write

$$e_3 = \frac{4M_3}{3a_2} - \frac{2M_4}{3a_2} = \frac{2(0.16643)}{3(16.6667)} = 0.0066572 \text{ rad} \approx x_{\theta_1} \quad (\text{g})$$

$$e_4 = \frac{4M_4}{3a_2} - \frac{2M_3}{3a_2} = \frac{2(0.16643)}{3(16.6667)} = 0.0066572 \text{ rad} \approx x_{\theta_2} \quad (\text{h})$$

which are the same as given in Eq. (a). For member (1), applying Eqs. (9.29), (9.31) and (9.32)

yields

$$\alpha_1 = \frac{M_1 - M_{p1}}{pa_1} = \frac{-0.208123 - (-0.2000)}{0.05(33.3333)} = -0.004874 \text{ rad}; \quad \alpha_2 = 0 \quad (\text{i})$$

$$\begin{aligned} e_1 &= \frac{4M_1}{3a_1} - \frac{2M_2}{3a_1} + \frac{q(M_1 - M_{p1})}{pa_1} = \frac{4(-0.208123)}{3(33.3333)} - \frac{2(-0.16643)}{3(33.3333)} \\ &\quad + \frac{0.95(-0.208123 + 0.2000)}{0.05(33.3333)} \\ &= -0.00962644 \text{ rad.} \end{aligned} \quad (\text{j})$$

$$e_2 = \frac{4M_2}{3a_1} - \frac{2M_1}{3a_1} = \frac{4(-0.16643)}{3(33.3333)} - \frac{2(-0.208123)}{3(33.3333)} = -0.00249478 \text{ rad} \quad (\text{k})$$

$$\theta'_1 = \theta_1 - \alpha_1 = 0 - (-0.004374) = 0.004374 \quad (\text{l})$$

$$e'_1 = e_1 - \alpha_1 = -0.00962644 - (0.004374) = -0.005252 \quad (\text{m})$$

The above deformations are shown in Fig. 9.21b from which

$$x_{\theta 1} = -(e_1 - e_2) = -[(-0.00962644) - (-0.00249478)] = 0.007132 \text{ rad} \quad (\text{n})$$

$$x_s = (-e_1)h = 0.00962644(120) = 1.15517 \text{ in} \quad (\text{o})$$

Note that the final values in Eqs. (n) and (o) based on hand calculation are slightly different from the computer output given in Eq. (a).

9.5. CURVILINEAR HYSTERESIS MODEL

A curvilinear beam is shown in Fig. 9.22, where the notations are the same as those used in Fig. 9.8 of the bilinear beam defined in Section 9.3. This model consists of a *central beam* and a *nonlinear spring* at each end. The moment beyond the ultimate capacity of the central beam is assumed to be carried by the nonlinear spring signified by S_j , which actually represents the yield characteristics of the beam. For generalization, let S_i and S_j be the yield characteristics at end- i and end- j of the member, respectively. Moments, rotations, plastic angles, and yield characteristics may be related to each other as shown in Fig. 9.23.

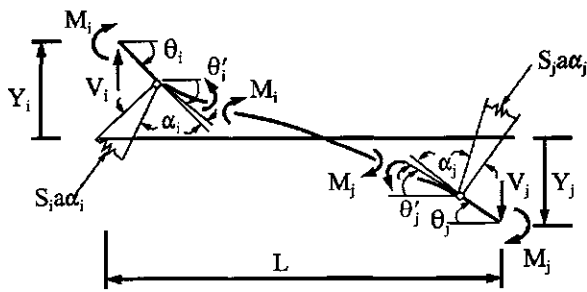


FIG. 9.22 Curvilinear beam.

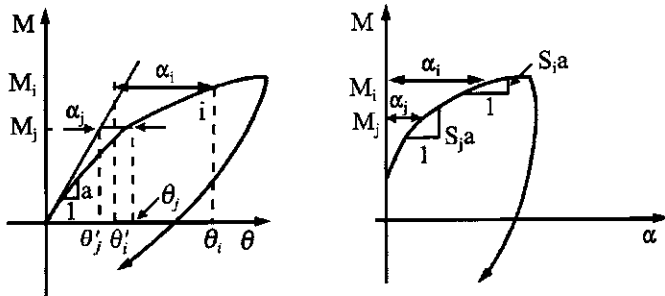


FIG. 9.23 M vs θ and M vs α .

9.5.1. Stiffness Matrix Formulation

From Fig. 9.22, we may express the plastic angles and force-deformation relationship in the following incremental forms associated with the central beam:

$$\Delta\theta'_i = \Delta\theta_i - \Delta\alpha_i; \quad \Delta\theta'_j = \Delta\theta_j - \Delta\alpha_j \quad (9.41)$$

$$\begin{Bmatrix} \Delta M_i \\ \Delta M_j \\ \Delta V_i \\ \Delta V_j \end{Bmatrix} = \begin{bmatrix} a & b & -c & -c \\ & a & -c & -c \\ \Delta\theta'_i & & d & d \\ \Delta\theta'_j & & & d \end{bmatrix} \begin{Bmatrix} \Delta\theta'_i \\ \Delta\theta'_j \\ \Delta Y_i \\ \Delta Y_j \end{Bmatrix} \quad (9.42)$$

where a , b , c , and d are the stiffness coefficients identical to those defined in Eq. (9.6).

Since the magnitude of plastic angles depends upon yielding conditions, Eq. (9.42) is reformulated according to the states of yield given in Section 9.3.

(A) *Both ends linear*—since $\Delta\alpha_i = \Delta\alpha_j = 0$, Eq. (9.41) becomes

$$\Delta\theta'_i = \Delta\theta_i; \quad \Delta\theta'_j = \Delta\theta_j \quad (9.43)$$

Consequently, Eq. (9.42) yields

$$\begin{Bmatrix} \Delta M_i \\ \Delta M_j \\ \Delta V_i \\ \Delta V_j \end{Bmatrix} = \begin{bmatrix} a & b & -c & -c \\ & a & -c & -c \\ \Delta\theta_i & & d & d \\ \Delta\theta_j & & & d \end{bmatrix} \begin{Bmatrix} \Delta\theta_i \\ \Delta\theta_j \\ \Delta Y_i \\ \Delta Y_j \end{Bmatrix} \quad (9.44)$$

(B) *i-end nonlinear and j-end linear*—since $\Delta\alpha_i \neq 0$ and $\Delta\alpha_j = 0$, we have

$$\Delta\theta'_i = \Delta\theta_i - \Delta\alpha_i; \quad \Delta\theta'_j = \Delta\theta_j \quad (9.45)$$

The incremental moment at the *i*-end may be expressed as

$$\Delta M_i = S_i a \Delta\alpha_i \quad (9.46)$$

which is equal to the moment, ΔM_i , of the central beam given in Eq. (9.42). Thus

$$a \Delta\theta'_i + b \Delta\theta'_j - c \Delta Y_i - c \Delta Y_j = S_i a \Delta\alpha_i \quad (9.47)$$

Substituting Eq. (9.45) into the above yields

$$\Delta\alpha_i = \frac{1}{1+S_i} \left[\Delta\theta_i + \frac{1}{2}\Delta\theta_j - \frac{3}{2L}(\Delta Y_i + \Delta Y_j) \right] \quad (9.48)$$

Substituting Eqs. (9.45) and (9.48) into Eq. (9.42) yields Eq. (9.49)

$$\begin{Bmatrix} \Delta M_i \\ \Delta M_j \\ \Delta V_i \\ \Delta V_j \end{Bmatrix} = \frac{1}{1+S_i} \begin{bmatrix} S_i a & S_i b & -S_i c & -S_i c \\ (\frac{3}{4}+S_i)a & -(\frac{1}{2}+S_i)c & -(\frac{1}{2}+S_i)c \\ (\frac{1}{4}+S_i)d & (\frac{1}{4}+S_i)d & (\frac{1}{4}+S_i)d \\ \text{symm} & & (\frac{1}{4}+S_i)d \end{bmatrix} \begin{Bmatrix} \Delta\theta_i \\ \Delta\theta_j \\ \Delta Y_i \\ \Delta Y_j \end{Bmatrix} \quad (9.49)$$

in which the first row is used to demonstrate how it is condensed from the following equation:

$$\Delta M_i = a \left[\Delta\theta_i - \frac{1}{1+S_i} \left[\left(\Delta\theta_i + \frac{1}{2}\Delta\theta_j - \frac{3}{2L}(\Delta Y_i + \Delta Y_j) \right) \right] + b\Delta\theta_j - c(\Delta Y_i + \Delta Y_j) \right]$$

(C) *i-end linear and j-end nonlinear*—similar to (B), Eqs. (9.45)–(9.49) may be changed as

$$\Delta\theta'_i = \Delta\theta_i; \quad \Delta\theta'_j = \Delta\theta_j - \Delta\alpha_j \quad (9.50)$$

$$\Delta M_j = S_j a \Delta\alpha_j \quad (9.51)$$

$$\Delta\alpha_j = \frac{1}{1+S_j} \left[\frac{1}{2}\Delta\theta_i + \Delta\theta_j - \frac{3}{2L}(\Delta Y_i + \Delta Y_j) \right] \quad (9.52)$$

and finally

$$\begin{Bmatrix} \Delta M_i \\ \Delta M_j \\ \Delta V_i \\ \Delta V_j \end{Bmatrix} = \frac{1}{1+S_j} \begin{bmatrix} (\frac{3}{4}+S_j)a & S_j b & -(\frac{1}{2}+S_j)c & -(\frac{1}{2}+S_j)c \\ S_j a & -S_j c & -S_j c \\ (\frac{1}{4}+S_j)d & (\frac{1}{4}+S_j)d & (\frac{1}{4}+S_j)d \\ \text{symm} & & (\frac{1}{4}+S_j)d \end{bmatrix} \begin{Bmatrix} \Delta\theta_i \\ \Delta\theta_j \\ \Delta Y_i \\ \Delta Y_j \end{Bmatrix} \quad (9.53)$$

(D) *Both ends nonlinear*—since both ends have plastic hinges, moments beyond the ultimate moment are

$$\Delta M_i = S_i a \Delta\alpha_i; \quad \Delta M_j = S_j a \Delta\alpha_j \quad (9.54)$$

which are equal to the respective moments in Eq. (9.42) as

$$a\Delta\theta'_i + b\Delta\theta'_j - c(\Delta Y_i + \Delta Y_j) = S_i a \Delta\alpha_i \quad (9.55)$$

$$b\Delta\theta'_i + a\Delta\theta'_j - c(\Delta Y_i + \Delta Y_j) = S_j a \Delta\alpha_j \quad (9.56)$$

Substituting Eq. (9.41) into the above and then solving for $\Delta\alpha_i$ and $\Delta\alpha_j$ gives

$$\Delta\alpha_i = \frac{1}{A} \left[\left(1 + \frac{4}{3}S_j\right)\Delta\theta_i + \frac{2}{3}S_j\Delta\theta_j - \frac{2}{L} \left(\frac{1}{2} + S_j\right) (\Delta Y_i + \Delta Y_j) \right] \quad (9.57)$$

$$\Delta\alpha_j = \frac{1}{A} \left[\frac{2}{3}S_i\Delta\theta_i + \left(1 + \frac{4}{3}S_i\right)\Delta\theta_j - \frac{2}{L} \left(\frac{1}{2} + S_i\right) (\Delta Y_i + \Delta Y_j) \right] \quad (9.58)$$

in which

$$A = 1 + \frac{4}{3}(S_i + S_j + S_iS_j) \quad (9.59)$$

Using Eqs. (9.41) and (9.57)–(9.59) in Eq. (9.42) yields the desired solution

$$\begin{Bmatrix} \Delta M_i \\ \Delta M_j \\ \Delta V_i \\ \Delta V_j \end{Bmatrix} = \frac{1}{A} \begin{bmatrix} S_i(1 + \frac{4}{3}S_j)a & \frac{2}{3}S_iS_ja & -\frac{2}{3}S_i(1 + 2S_j)c & -\frac{2}{3}S_i(1 + 2S_j)c \\ S_j(1 + \frac{4}{3}S_i)a & S_j(1 + \frac{4}{3}S_i)a & -\frac{2}{3}S_j(1 + 2S_i)c & -\frac{2}{3}S_j(1 + 2S_i)c \\ \text{symm} & & \frac{1}{3}(S_i + S_j + 4S_iS_j)d & \frac{1}{3}(S_i + S_j + 4S_iS_j)d \\ & & \frac{1}{3}(S_i + S_j + 4S_iS_j)d & \end{bmatrix} \begin{Bmatrix} \Delta\theta_i \\ \Delta\theta_j \\ \Delta Y_i \\ \Delta Y_j \end{Bmatrix} \quad (9.60)$$

EXAMPLE 9.5.1 Use the curvilinear hysteresis model shown in Fig. 9.24 to find the dynamic response of the framework given in Example 9.4.1 at time equal to 0.4 sec by linear acceleration method with consideration of unbalanced force technique. The structural response at $t=0.3$ sec is

$$\begin{aligned} x_s &= 1.0861338 \text{ in}; & \dot{x}_s &= 9.222907 \text{ in/sec}; & \ddot{x}_s &= 37.80112 \text{ in/sec}^2; \\ x_{\theta 1} &= x_{\theta 2} = 7.758179 (10^{-3}) \text{ rad}; & M_1 &= M_6 = -0.3232 \text{ k in}; \\ M_2 &= M_5 = -M_3 = -M_4 = -0.19395 \text{ k in}; & e_1(t=0.3 \text{ sec}) &= -9.051 (10^{-3}) \text{ rad}; \\ \text{and } e_1(t=0.2 \text{ sec}) &= -3.031(10^{-3}) \text{ rad} \end{aligned}$$

Solution: Using procedures similar to Example 9.4.2, the unbalanced force of member 1 may be calculated from the given initial values shown in Fig. 9.25 as

$$\begin{aligned} k_1 &= \frac{M_1(t=0.3) - M_1(t=0.2)}{e_1(t=0.3) - e_1(t=0.2)} = \frac{-0.3232 - (-0.1083)}{-9.051(10^{-3}) - (-3.031)(10^{-3})} \\ &= 35.6977 \end{aligned} \quad (a)$$

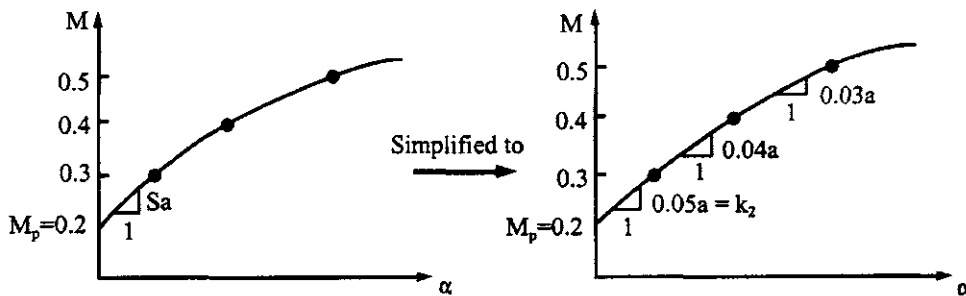


FIG. 9.24 Curvilinear model for Example 9.5.1.

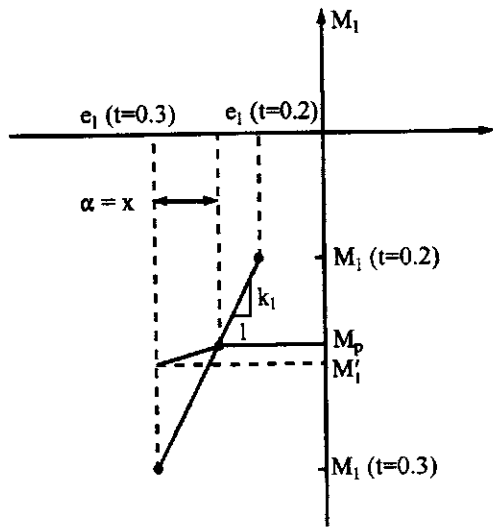


FIG. 9.25 Member force correction for Example 9.5.1.

and

$$x = \frac{M_p - M_1(t = 0.03)}{k_1} = \frac{-0.2 - (-0.3232)}{35.6977} = 3.45(10^{-3}) = \alpha \quad (b)$$

From Fig. 9.24

$$k_2 = 0.05a = (0.05) \frac{4EI}{h} = 1.6667 \quad (c)$$

$$\begin{aligned} M'_1(t = 0.3) &= M_p + k_2\alpha = -0.2 + (1.6667)(-3.45(10^{-3})) \\ &= -0.20575 \text{ k in} \end{aligned} \quad (d)$$

The member's unbalanced moment, $\Delta M_a = M_1 - M'_1$, is

$$\Delta M_a = M_1(t = 0.3) - M'_1(t = 0.3) = -0.11745 \text{ k in} \quad (e)$$

Then the member's unbalanced shear can be obtained as

$$\Delta V = \frac{\Delta M_a}{h} = -9.79(10^{-4}) \text{ k} \quad (f)$$

and finally the system's unbalanced nodal force becomes

$$\Delta U = 2\Delta V = -1.958(10^{-3}) \text{ k} \quad (g)$$

which should satisfy the equilibrium condition of $\sum F_x = 0$ as shown in Example 9.4.2.

To calculate the response at $t = 0.4$ sec, use the given response at $t = 0.3$ sec as initial value. Now member 1 has *i*-end nonlinear and *j*-end linear; member 3 has *i*-end linear and *j*-end nonlinear; and member 2 has both ends linear. The element stiffness matrix of member 1 can

be calculated from Eq. (9.49) for which

$$\left. \begin{aligned} S_i &= 0.05; & a &= 33.3333 \text{ k in}; & b &= 16.667 \text{ k in} \\ c &= 0.41667 \text{ k}; & \text{and } d &= (6.9445) 10^{-3} \text{ k/in} \end{aligned} \right\} \quad (h)$$

Similarly, we calculate element stiffnesses of members 2 and 3 and the structural stiffness as well as its condensed matrix. Then the motion equation becomes

$$2(10^{-4})\Delta\ddot{x}_s + 2.0778(10^{-3})\Delta x_s = 0.02[\sin(0.4\pi) - \sin(0.3\pi)] - 1.958(10^{-3}) \quad (i)$$

which can be used for subsequent responses with Δt of time increment in the linear acceleration method as shown in Example 9.4.1.

9.5.2. Stiffness Comparison Between Bilinear and Curvilinear Models

Bilinear and curvilinear models are compared to find the relationship of p and q in bilinear and S in curvilinear stiffness coefficients. A curvilinear model represents a moment–rotation curve with multiple linearized slopes. This comparative study is to identify the similarity or difference between these two models for a moment–rotation curve having two slopes only. Comparison is conducted for the four deformation conditions described in the previous two sections.

(A) *Both ends linear*—since the member is elastic, the stiffness coefficients should be the same for both models. That is why Eq. (9.9) of the bilinear and Eq. (9.44) of the curvilinear model are identical. In this case $p = 1$, $q = 0$, $S = \infty$ and $\Delta\alpha = 0$.

(B) *i-end nonlinear and j-end linear*—this comparison can be made by examining the equality of individual stiffness coefficients as

$$(k_{ij})_{\text{bilinear}} = (k_{ij})_{\text{curvilinear}} \quad (9.61)$$

For instance, let the coefficients of Eqs. (9.15) and (9.49) be

$$(k_{11})_{\text{bilinear}} = pa = (k_{11})_{\text{curvilinear}} = \frac{S_i a}{1 + S_i} \quad (9.62)$$

Then

$$p = \frac{S_i}{1 + S_i}; \quad q = \frac{1}{1 + S_i} \quad (9.63)$$

or

$$S_i = \frac{p}{1 - p} = \frac{p}{q} \quad (9.64)$$

Eqs. (9.63) and (9.64) can also be obtained by applying Eq. (9.61) to all other stiffness coefficients. Eq. (9.64) indicates that S is equivalent to the ratio of the linear component to the elasto-plastic component.

Since p and q can take values between 0.0 and 1.0, S varies from 1 to ∞ when

$$p = 0, \quad q = 1; \quad \text{then } S = 0 \quad (9.65)$$

which corresponds to the elasto-plastic model. When

$$p = 1, \quad q = 0; \quad \text{then } S = \infty \quad (9.66)$$

which is the elastic case. Since the rotational spring has infinite stiffness, the model becomes completely elastic. This behavior can be observed directly for all stiffness coefficients by letting S_i

approach infinity and applying l'Hospital's rule; for instance

$$k_{11} = \lim_{S_i \rightarrow \infty} \frac{S_i a}{1 + S_i} = \lim_{S_i \rightarrow \infty} \frac{a}{1} = a = \frac{4EI}{L} \quad (9.67)$$

$$k_{33} = \lim_{S_i \rightarrow \infty} \frac{(1/4 + S_i)d}{1 + S_i} = d = \frac{12EI}{L^3} \quad (9.68)$$

(C) *i-end linear and j-end nonlinear*—the derivation is identical to that of (B). Therefore

$$p = \frac{S_j}{1 + S_j}; \quad q = \frac{1}{1 + S_j} \quad (9.69)$$

Substituting Eq. (9.69) into Eq. (9.19) of the bilinear model yields Eq. (9.53) of the curvilinear model's stiffness coefficients.

(D) *Both ends nonlinear*—to verify stiffnesses of the bilinear model and the curvilinear model with both ends nonlinear, stiffness coefficients of both models should be identical. Thus

$$[K_e] [Eq. (9.60) of the curvilinear model] = [K_e] [Eq. (9.23) of the bilinear model] \quad (9.70)$$

From the symmetric matrix of Eq. (9.20), we have four distinct elements: $k_{11}=k_{22}$, $k_{12}=k_{21}$, $k_{13}=k_{14}=k_{23}=k_{24}$, and $k_{23}=k_{24}=k_{43}=k_{44}$. Consequently the coefficients in Eq. (9.60) must be proven to have similar characteristics. For k_{11} and k_{22}

$$S_i(1 + \frac{4}{3}S_j)a = S_j(1 + \frac{4}{3}S_i)a \quad (9.71)$$

which gives a constant relationship signified by S

$$S_i = S_j = S \quad (9.72)$$

Substitute S into Eq. (9.60) and then let

$$k_{ij} [Eq. (9.23) of bilinear] = k_{ij} [Eq. (9.60) of curvilinear] \quad (9.73)$$

which yields the following results:

$$p = \frac{3S + 4S^2}{3 + 4(2S + S^2)}; \quad \text{for } k_{11}, k_{22} \quad (9.74)$$

$$p = \frac{4S^2}{3 + 4(2S + S^2)}; \quad \text{for } k_{12}, k_{21} \quad (9.75)$$

$$p = \frac{2S + 4S^2}{3 + 4(2S + S^2)}; \quad \text{for } k_{ij} \begin{cases} i = 1, 2; & j = 3, 4 \\ i = 3, 4; & j = 1, 2, 3, 4 \end{cases} \quad (9.76)$$

The above three equations reveal that, with both ends nonlinear, we have a different S and p relationship for moments due to rotations, but have an identical S and p relationship for moments due to deflections and shears due to rotations and/or deflections. This is because the curvilinear model's moment transformed from the i th end to the j th end is itself a nonlinear moment; the relationship is more complicated than for a bilinear model. While the bilinear model is simpler in computation, the curvilinear model can better solve a highly nonlinear problem.

9.6. RAMBERG–OSGOOD HYSTERESIS MODEL

9.6.1. Parameter Evaluations of the Ramberg–Osgood Stress–Strain Curve

W. Ramberg and W.R. Osgood proposed an analytical expression of the stress–strain relationship [20]. Commonly referred to as the Ramberg–Osgood hysteresis model, the stress–strain relationship is

$$\varepsilon = \frac{\sigma}{E} + K \left(\frac{\sigma}{E} \right)^r \quad (9.77)$$

where σ/E and $K(\sigma/E)^r$ represent linear and nonlinear parts, respectively, in which ε is strain, E is Young's modulus, and K and r are constants. Let σ_y be the yielding stress and be \bar{b} be $K(\sigma_y/E)^{r-1}$. Then Eq. (9.77) becomes

$$\varepsilon = \frac{\sigma}{E} + K \left(\frac{\sigma_y}{E} \right)^{r-1} \left(\frac{\sigma}{\sigma_y} \right)^{r-1} \frac{\sigma}{E} = \frac{\sigma}{E} + \bar{b} \left(\frac{\sigma}{\sigma_y} \right)^{r-1} \frac{\sigma}{E} = \frac{\sigma}{E} \left[1 + \bar{b} \left| \frac{\sigma}{\sigma_y} \right|^{r-1} \right] \quad (9.78)$$

in which \bar{b} and r are positive constants chosen to fit the stress–strain curve of the structural material. The notation of absolute value of σ and σ_y is used in Eq. (9.78) because they always have the same sign. How to choose the parameters in \bar{b} and r is explained as follows.

Let the stress–strain curve of gradually yielding metals be as shown in Fig. 9.26, in which stress–strain has a linear relationship up to the yielding stress, σ_y . Using σ_y in elastic design for this type of material, such as alloy steel with yielding stress in the range of 80–110 ksi, would be unreasonably conservative. We normally use 0.2% of set strain, ε_0 , to determine the secant yielding stress, σ_1 , by drawing a line intersecting the stress–strain at point 1. This line is parallel to the elastic curve with a slope E while the line connecting the origin and point 1 has a slope $m_1 E$. Substituting σ_1 and ε_1 into Eq. (9.78) yields

$$\varepsilon_1 = \sigma_1 \frac{1}{m_1 E} = \sigma_1 \frac{1}{E} \left(1 + \bar{b} \left| \frac{\sigma_1}{\sigma_y} \right|^{r-1} \right) \quad (9.79)$$

from which

$$\bar{b} = \frac{1 - m_1}{m_1} \left| \frac{\sigma_y}{\sigma_1} \right|^{r-1} \quad (9.80)$$

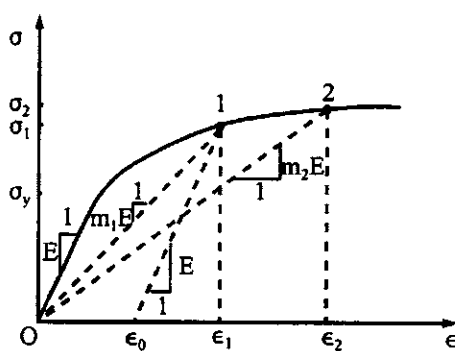


FIG. 9.26 Stress–strain curve of gradually yielding metals.

m_1 can be determined based on the strain shown in Fig. 9.26 where

$$\varepsilon_0 = 0.002 = \frac{\sigma_1}{m_1 E} - \frac{\sigma_1}{E} \quad (9.81)$$

in which the average value of σ_1/E may be taken as 0.00486. After substitution, we have

$$m_1 = 0.71 \quad (9.82)$$

To determine r , we use the second secant yielding stress, σ_2 , and the second secant modulus, $m_2 E$, for which \bar{b} can be similarly obtained as

$$\bar{b} = \frac{1 - m_2}{m_2} \left| \frac{\sigma_y}{\sigma_2} \right|^{r-1} \quad (9.83)$$

Equating Eqs. (9.80) and (9.83) leads to

$$r = 1 + \frac{\ell n[m_2(1 - m_1)/m_1(1 - m_2)]}{\ell n(\sigma_1/\sigma_2)} \quad (9.84)$$

where m_2 should be chosen between 0.7 and 1.0 and can be used as

$$m_2 = 0.85 \quad (9.85)$$

Since

$$K(\sigma_y/E)^{r-1} = \bar{b} \quad (9.86)$$

substituting Eq. (9.80) into the above gives

$$K = \frac{1 - m_1}{m_1} \left| \frac{E}{\sigma_1} \right|^{r-1} \quad (9.87)$$

Employing Eqs. (9.84) and (9.87) in Eq. (9.77), we have the stress-strain expression of a given metal.

9.6.2. Ramberg–Osgood Moment–Curvature Curves

Let stress σ be expressed as My/I where y is the distance between the neutral axis of a member's cross-section and the stress location. Then Eq. (9.78) can be expressed as

$$\varepsilon = \frac{My}{EI} \left[1 + \bar{b} \left| \frac{My/I}{M_y y/I} \right|^{r-1} \right] = \frac{My}{EI} \left[1 + \bar{b} \left| \frac{M}{M_y} \right|^{r-1} \right] = \frac{My}{EI} \left[1 + \bar{b} \left| \frac{M}{dM_p} \right|^{r-1} \right] = \frac{My}{EI} \left[1 + \bar{a} \left| \frac{M}{M_p} \right|^{r-1} \right] \quad (9.88)$$

in which $\bar{d} = S/Z$, the ratio of elastic section modulus S to plastic section modulus Z , and $\bar{a} = \bar{b}/(\bar{d})^{r-1}$. Since curvature is equal to the first derivative of the strain with respect to distance y , using Eq. (9.88) gives

$$\phi = \frac{d\varepsilon}{dy} = \frac{M}{EI} \left[1 + \bar{a} \left| \frac{M}{M_p} \right|^{r-1} \right] \quad (9.89)$$

which represents the Ramberg–Osgood moment–curvature relationship. ϕ/ϕ_p is graphically represented in Fig. 9.27 for various values of r . The graph also includes two limiting cases, the elastic ($\bar{a} = 0$, $r = 1$) and the elasto-plastic ($\bar{a} > 0$, $r = \infty$) relationships. Note that, theoretically, $\sigma = My/I$ can only be applied to the first term, $\varepsilon = \sigma/E$, of Eq. (9.77). Using Eq. (9.77) to find a moment will result in a highly nonlinear moment–stress equation.

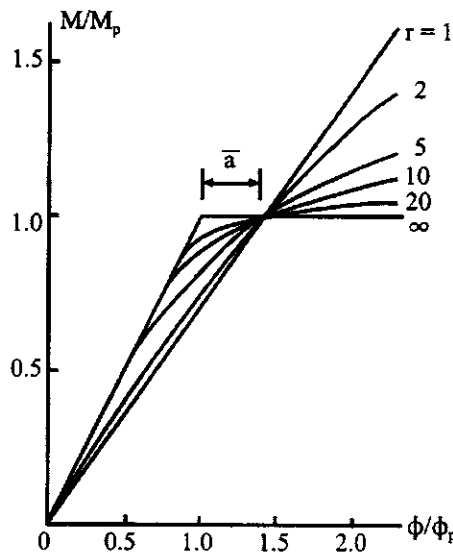


FIG. 9.27 M/M_p vs ϕ/ϕ_p for Ramberg–Osgood.

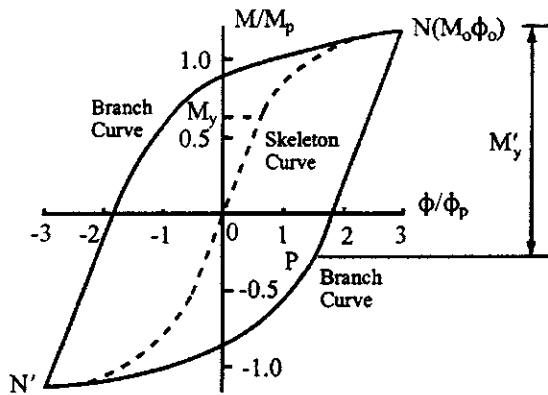


FIG. 9.28 Ramberg–Osgood moment reversal.

A cyclic moment–curvature relationship of the Ramberg–Osgood model is sketched in Fig. 9.28. As shown in the figure, immediately after the load is applied, the moment–curvature follows the *skeleton curve* from origin, 0, to load release point, N (or from 0 to N'). The load is then applied in the opposite direction, and moment–curvature follows the *branch curve* from N to N' . In the process of load reversal, the moment–curvature relationship is linear for a range of moments designated as M'_y . Because of the Bauschinger effect, the magnitude of M'_y is equal to $2M_y$.

Let point N be treated as the origin of the branch curve; then the curvature associated with the branch curve may be expressed as

$$\phi = \phi_0 + \Delta\phi \quad (9.90)$$

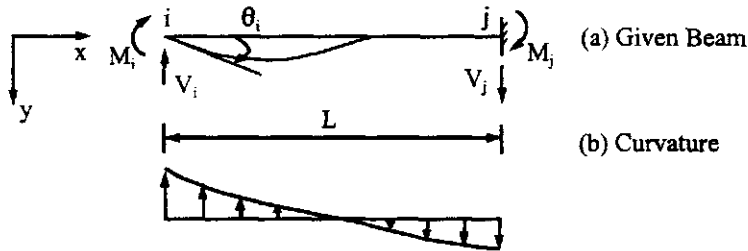


FIG. 9.29 Forces applied at *i*-end.

Employing Eq. (9.89) in the above yields

$$\phi = \phi_0 + \frac{M - M_0}{EI} \left(1 + \bar{a} \left| \frac{M - M_0}{2M_p} \right|^{r-1} \right) \quad (9.91)$$

where ϕ_0 and M_0 are the curvature and moment at point *N*. Eqs. (9.89) and (9.91) are used to derive bending stiffness coefficients in the next section.

9.6.3. Stiffness Matrix Formulation for Skeleton Curve

Let us consider a beam shown in Fig. 9.29 with a positive *x-y* coordinate, for which the curvature associated with a given moment may be sketched in the accompanying figure. The slope at the *i*-end may be expressed as

$$\theta_i = \int_0^L \phi \, dx = - \int_0^L \frac{M_x}{EI} \left(1 + \bar{a} \left| \frac{M_x}{M_p} \right|^{r-1} \right) dx \quad (9.92)$$

in which ϕ is curvature and $M_x = -V_i x - M_i$.

Integration of Eq. (9.92) yields

$$\begin{aligned} \theta_i &= \frac{-1}{EI} \int_0^L (-V_i x - M_i) \left(1 + \bar{a} \left| \frac{-V_i x - M_i}{M_p} \right|^{r-1} \right) dx \\ &= \frac{-1}{EI} \int_0^L \left[(-V_i x - M_i) + \frac{\bar{a}}{M_p^{r-1}} (-V_i x - M_i)^r \right] dx \\ &= \frac{-1}{EI} \left\{ \frac{-V_i L^2}{2} - M_i L + \frac{\bar{a}}{(r+1)(-V_i)} \left[\left| \frac{-V_i L - M_i}{M_p} \right|^{r-1} (-V_i L - M_i)^2 - \left| \frac{M_i}{M_p} \right|^{r-1} M_i^2 \right] \right\} \end{aligned} \quad (9.93)$$

The deflection at the i -end may be similarly obtained,

$$\begin{aligned}
 Y_i &= - \int_0^L \phi x \, dx = \frac{-1}{EI} \int_0^L x(-V_i x - M_i) \left(1 + \bar{a} \left| \frac{-V_i x - M_i}{M_p} \right|^{r-1} \right) dx \\
 &= \frac{-1}{EI} \left\{ \frac{-V_i L^3}{3} - \frac{M_i L^2}{2} + \frac{\bar{a}}{(r+1)(r+2)(V_i)^2} \left[(r+1)(-V_i L - M_i)^3 \left| \frac{-V_i L - M_i}{M_p} \right|^{r-1} \right. \right. \\
 &\quad \left. \left. + (r+2)(-V_i L - M_i)^2(M_i) \left| \frac{-V_i L - M_i}{M_p} \right|^{r-1} - (M_i)^3 \left| \frac{M_i}{M_p} \right|^{r-1} \right] \right\} \tag{9.94}
 \end{aligned}$$

Since an incremental procedure is used for analyzing the inelastic structure, the force-deformation relationship at the i -end can be obtained from Eqs. (9.93) and (9.94) in the following derivative forms. The derivation for force-rotational deformation may be obtained as

$$\begin{aligned}
 \frac{d\theta_i}{dM_i} &= -\frac{1}{EI} \left[-L - \frac{\bar{a}(-V_i L - M_i)^r(r+1)}{(r+1)(-V_i)M_p^{r-1}} - \frac{\bar{a}(r+1)M_i^r}{(r+1)(-V_i)M_p^{r-1}} \right] \\
 &= -\frac{1}{EI} \left\{ -L + \frac{\bar{a}}{V_i} \left[\left| \frac{M_i}{M_p} \right|^{r-1} (M_i) + \left| \frac{-V_i L - M_i}{M_p} \right|^{r-1} (-V_i L - M_i) \right] \right\} \tag{9.95}
 \end{aligned}$$

Using the equilibrium condition of $V_i = -(M_i + M_j)/L$ in the above, we have

$$\begin{aligned}
 \frac{d\theta_i}{dM_i} &= \frac{-1}{EI} \left\{ -L - \frac{L\bar{a}}{M_i + M_j} \left[\left| \frac{M_i}{M_p} \right|^{r-1} (M_i) + \left| \frac{M_i + M_j - M_i}{M_p} \right|^{r-1} (M_i + M_j - M_i) \right] \right\} \\
 &= \frac{-L}{EI} \left[-1 - \frac{\bar{a}}{\left(1 + \frac{M_j}{M_i} \right)} \left| \frac{M_i}{M_p} \right|^{r-1} - \frac{\bar{a}}{\left(1 + \frac{M_i}{M_j} \right)} \left| \frac{M_j}{M_p} \right|^{r-1} \right] \\
 &= f_{22} \tag{9.96}
 \end{aligned}$$

$$\begin{aligned}
 \frac{d\theta_i}{dV_i} &= \frac{-1}{EI} \left\{ \frac{-L^2}{2} - \frac{\bar{a}}{(r+1)} \left[-\frac{(-V_i L - M_i)^{r+1}}{V_i^2 M_p^{r-1}} - \frac{(r+1)(-V_i L - M_i)^r L}{M_p^{r-1} V_i} + \frac{\left(\left| \frac{M_i}{M_p} \right|^{r-1} M_i^2 \right)}{V_i^2} \right] \right\} \\
 &= \frac{L^2}{EI} \left\{ \frac{1}{2} + \frac{\bar{a}}{(r+1) \left(1 + \frac{M_j}{M_i} \right)^2} \left| \frac{M_i}{M_p} \right|^{r-1} + \frac{\bar{a}}{(r+1) \left(1 + \frac{M_i}{M_j} \right)^2} \left| \frac{M_j}{M_p} \right|^{r-1} \left[r + (r+1) \left(\frac{M_i}{M_j} \right) \right] \right\} \\
 &= f_{21} \tag{9.97}
 \end{aligned}$$

A similar derivation is performed for force-transverse displacement; the results are

$$\begin{aligned} \frac{dY_i}{dV_i} &= \frac{-L^3}{EI} \left\{ -\frac{1}{3} - \frac{2\bar{a}}{(r+1)(r+2)\left(1+\frac{M_j}{M_i}\right)^3} \left| \frac{M_i}{M_p} \right|^{r-1} \right. \\ &\quad \left. - \frac{\bar{a}}{(r+1)(r+2)\left(1+\frac{M_i}{M_j}\right)^3} \left| \frac{M_j}{M_p} \right|^{r-1} \left[r(r+1) + 2r(r+2)\left(\frac{M_i}{M_j}\right) + (r+1)(r+2)\left(\frac{M_i}{M_j}\right)^2 \right] \right\} \\ &= f_{11} \end{aligned} \quad (9.98)$$

$$\begin{aligned} \frac{dY_i}{dM_i} &= \frac{L^2}{EI} \left\{ \frac{1}{2} + \frac{\bar{a}}{(r+1)\left(1+\frac{M_j}{M_i}\right)^2} \left| \frac{M_i}{M_p} \right|^{r-1} + \frac{\bar{a}}{(r+1)\left(1+\frac{M_i}{M_j}\right)^2} \left| \frac{M_j}{M_p} \right|^{r-1} \left[r + (r+1)\left(\frac{M_i}{M_j}\right) \right] \right\} \\ &= f_{12} \end{aligned} \quad (9.99)$$

Note that Eq. (9.97) is identical to Eq. (9.99). Eqs. (9.96)–(9.99) are actually an incremental form of flexibility coefficients and can be symbolically expressed as

$$\begin{Bmatrix} dY_i \\ d\theta_i \end{Bmatrix} = \begin{bmatrix} f_{11} & f_{12} \\ f_{21} & f_{22} \end{bmatrix} \begin{Bmatrix} dV_i \\ dM_i \end{Bmatrix} \quad (9.100)$$

or

$$d\Delta_i = f dF_i \quad (9.101)$$

Let the incremental forces at end-*j* be expressed as

$$dF_j = [dV_j \ dM_j]^T \quad (9.102)$$

The forces at the *j*-end can be found from the forces at the *i*-end by using equilibrium matrix *E* as

$$dF_j = E dF_i \quad (9.103)$$

for which the sign convention is based on the typical member given in Fig. 9.29. Thus,

$$E = \begin{bmatrix} 1 & 0 \\ -L & -1 \end{bmatrix} \quad (9.104)$$

From Eq. (9.101), the forces at the i -end can be expressed in terms of displacements as

$$dF_i = f^{-1} d\Delta_i \quad (9.105)$$

where the inverse of flexibility matrix is based on Eq. (9.100); flexibility coefficients are derived in Eqs. (9.96)–(9.99). Eq. (9.105) expresses the force–deformation relationship for which stiffness coefficients can be obtained as

$$S_{ii} = f^{-1} = \frac{1}{f_{11}f_{22} - f_{12}^2} \begin{bmatrix} f_{22} & -f_{12} \\ -f_{12} & f_{11} \end{bmatrix} \quad (9.106)$$

Note that S_{ii} represents stiffness coefficients due to unit displacements at the i -end. Substituting Eq. (9.105) into Eq. (9.103) yields

$$dF_j = Ef^{-1} d\Delta_i \quad (9.107)$$

which expresses forces at the j -end due to unit displacements at i -end. Thus the stiffness coefficients can be obtained as

$$S_{ji} = Ef^{-1} = \frac{1}{f_{11}f_{22} - f_{12}^2} \begin{bmatrix} f_{22} & -f_{12} \\ -f_{22}L + f_{12} & f_{12}L - f_{11} \end{bmatrix} \quad (9.108)$$

To determine stiffness coefficients, S_{ji} , reciprocal relations may be used so that the work done by dF_i and $d\Delta_i$ (when the j -end is fixed) is equal to that done by dF_j and $d\Delta_j$ (when the i -end is fixed). Thus,

$$\frac{1}{2} dF_j^T d\Delta_j = \frac{1}{2} dF_i^T d\Delta_i = \frac{1}{2} d\Delta_i^T dF_i \quad (9.109)$$

Substituting Eqs. (9.107) and (9.108) into the above yields

$$d\Delta_i^T S_{ji}^T d\Delta_j = d\Delta_i^T dF_i \quad (9.110)$$

from which

$$dF_i = S_{ji}^T d\Delta_j \quad (9.111a)$$

Comparing Eqs. (9.108) with (9.111a) results in

$$S_{ji}^T = f^{-1} E^T \quad (9.111b)$$

Substituting the above into Eq. (9.111a), which is then employed in Eq. (9.103), we have

$$dF_j = Ef^{-1}E^T d\Delta_j \quad (9.112)$$

which gives the following stiffness matrix:

$$S_{jj} = Ef^{-1}E^T = \frac{1}{f_{11}f_{22} - f_{12}^2} \begin{bmatrix} f_{22} & -Lf_{22} + f_{12} \\ -Lf_{22} + f_{12} & f_{22}L^2 - 2f_{12}L + f_{22} \end{bmatrix} \quad (9.113)$$

Using Eqs. (9.106), (9.108), (9.113), and $S_{ij} = S_{ji}^T$ yields the following symbolic stiffness matrix:

$$\begin{bmatrix} S_{ii} & S_{ij} \\ S_{ji} & S_{jj} \end{bmatrix} = \begin{bmatrix} f^{-1} & f^{-1}E^T \\ Ef^{-1} & Ef^{-1}E^T \end{bmatrix} = \frac{1}{f_{11}f_{22} - f_{12}^2} \begin{bmatrix} f_{22} & -f_{12} & f_{22} & f_{12} - f_{22}L \\ f_{11} & f_{12} & f_{12}L - f_{11} & f_{22}L - f_{12} \\ f_{22} & f_{22} & f_{22}L^2 - 2f_{12}L + f_{11} \end{bmatrix}_{\text{symm}} \quad (9.114)$$

where

$$f_{11} = \frac{L^3}{6EI} (2 + 2W_i + W_j Q_j) \quad (9.115)$$

$$f_{12} = \frac{L^2}{6EI} (3 + U_i + U_j S_j) \quad (9.116)$$

$$f_{21} = \frac{L^2}{6EI} (3 + U_i + U_j S_j) \quad (9.117)$$

$$f_{22} = \frac{L}{6EI} (6 + R_i + R_j) \quad (9.118)$$

and

$$R_i = \frac{6\bar{a}}{(1 + M_j/M_i)} \left| \frac{M_i}{M_p} \right|^{r-1} \quad (9.119a)$$

$$R_j = \frac{6\bar{a}}{(1 + M_i/M_j)} \left| \frac{M_j}{M_p} \right|^{r-1} \quad (9.119b)$$

$$U_i = \frac{6\bar{a}}{(r+1)(1 + M_j/M_i)^2} \left| \frac{M_i}{M_p} \right|^{r-1} \quad (9.119c)$$

$$U_j = \frac{6\bar{a}}{(r+1)(1 + M_i/M_j)^2} \left| \frac{M_j}{M_p} \right|^{r-1} \quad (9.119d)$$

$$W_i = \frac{6\bar{a}}{(r+1)(r+2)(1 + M_j/M_i)^3} \left| \frac{M_i}{M_p} \right|^{r-1} \quad (9.119e)$$

$$W_j = \frac{6\bar{a}}{(r+1)(r+2)(1 + M_i/M_j)^3} \left| \frac{M_j}{M_p} \right|^{r-1} \quad (9.119f)$$

$$S_i = r + (r+1)(M_j/M_i) \quad (9.119g)$$

$$S_j = r + (r+1)(M_i/M_j) \quad (9.119h)$$

$$G_i = r + (r+2)(M_j/M_i) \quad (9.119i)$$

$$G_j = r + (r+2)(M_i/M_j) \quad (9.119j)$$

$$Q_i = r(r+1) + 2r(r+2)(M_j/M_i) + (r+1)(r+2)(M_j/M_i)^2 \quad (9.119k)$$

$$Q_j = r(r+1) + 2r(r+2)(M_i/M_j) + (r+1)(r+2)(M_i/M_j)^2 \quad (9.119l)$$

Substituting Eqs. (9.115)–(9.118) into Eq. (9.114) with proper rearrangement of coefficients' location yields the detailed stiffness matrix as follows:

$$\begin{bmatrix} \frac{dM_i}{dV_i} \\ \frac{dM_j}{dV_j} \\ \frac{dV_i}{dV_j} \\ \frac{dV_j}{dV_i} \end{bmatrix} = \frac{6EI}{LZ} \begin{bmatrix} 2 + 2W_i + W_jQ_j & 1 + W_iG_i + W_jG_j & -\frac{1}{L}(3 + U_i + U_jS_j) & -\frac{1}{L}(3 + U_i + U_jS_j) \\ 2 + 2W_j + W_iQ_i & -\frac{1}{L}(3 + U_j + U_iS_i) & -\frac{1}{L}(3 + U_j + U_iS_i) & \\ \text{symm} & \frac{1}{L^2}(6 + R_i + R_j) & \frac{1}{L^2}(6 + R_i + R_j) & \\ & \frac{1}{L^2}(6 + R_i + R_j) & & \end{bmatrix} \begin{bmatrix} d\theta_i \\ d\theta_j \\ dY_i \\ dY_j \end{bmatrix} \quad (9.120)$$

in which

$$Z = (2 + 2W_i + W_jQ_j)(6 + R_i + R_j) - (3 + U_i + U_jS_j)^2 \quad (9.121)$$

9.6.4. Stiffness Matrix Formulation for Branch Curve

The unloading case can be classified into two groups: (A) moment reversal at the i -end, and (B) moment reversal at the j -end. Moment reversals and their associated curvatures for (A) and (B) are sketched in Figs. 9.30 and 9.31, respectively.

(A) *Moment reversal at the i -end*—consider the moment at the i -end when subjected to a moment reversal, dM_i , as shown in Fig. 9.30a; the moment and shear at the i -end are

$$M_i = M_{ii} + dM_i \quad (9.122a)$$

$$V_i = V_{ii} + dV_i \quad (9.122b)$$

From Fig. 9.30c,

$$M_0 = -M_{ii} - V_{ii} x \quad (9.122c)$$

$$M_x = -M_i - V_i x \quad (9.122d)$$

Substituting Eqs. (9.122a and b) into the above yields

$$M_x = -M_i - V_i x = M_0 - dM_i - (dV_i)x \quad (9.122e)$$

Figure 9.30b shows the curvature changing from solid line to dashed line. Because of moment reversal, the curvature between 0 and x' ($\phi_{0x'}$) is reduced while the curvature between x' and L ($\phi_{x'L}$) is increased, where x' can be expressed as $-M_{ii}/V_{ii}$ or $-M_i/V_i$. ϕ_{0x} and $\phi_{x'L}$ correspond,

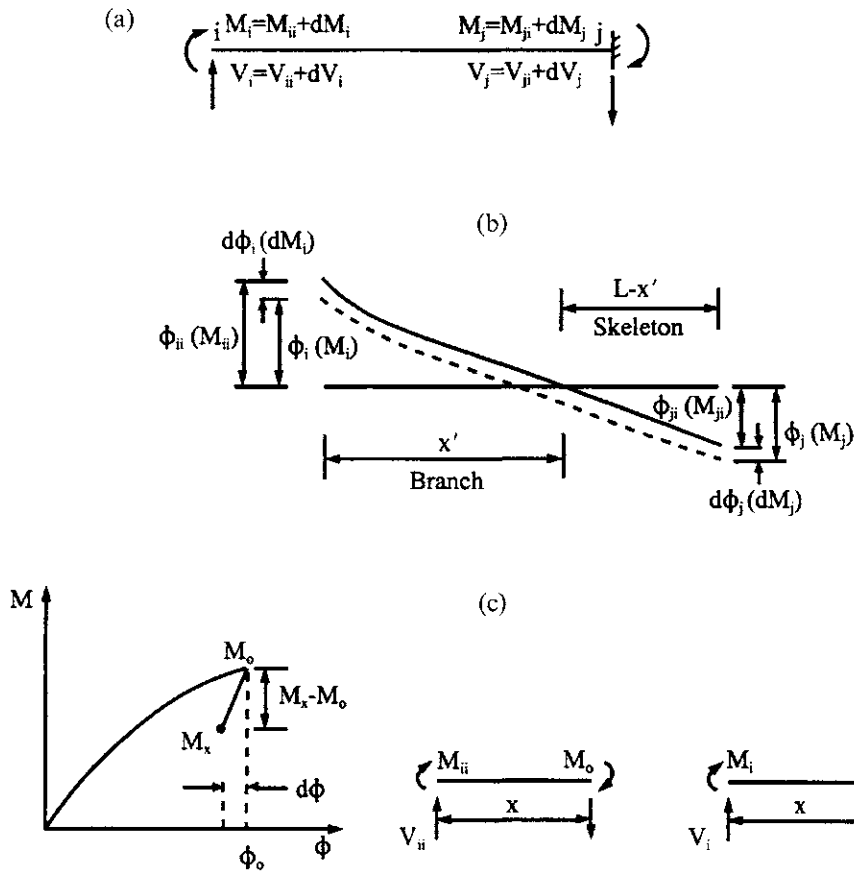


FIG. 9.30 Moment reversal at *i*-end. (a) Given beam. (b) Curvature. (c) Equilibrium state.

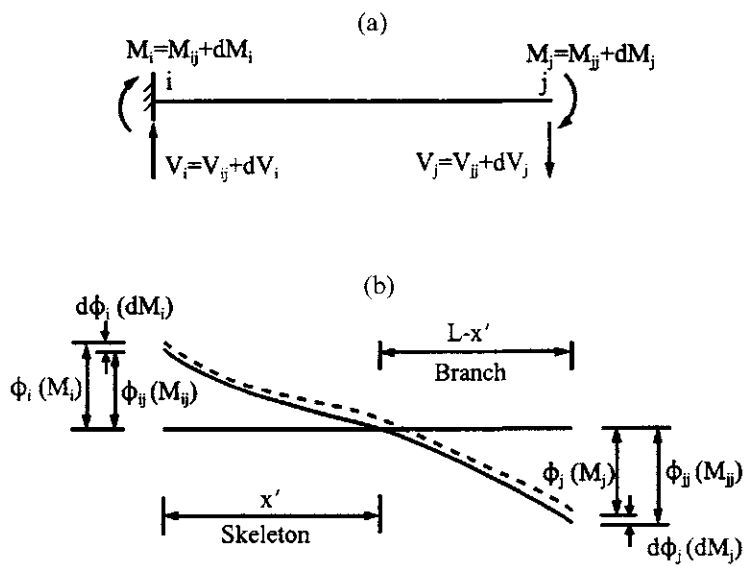


FIG. 9.31 Moment reversal at *j*-end. (a) Given beam. (b) Curvature.

respectively, to branch curve and skeleton curve. The slope may be calculated as

$$\theta_i = - \int_0^{x'} \phi_{0x'} dx - \int_{x'}^L \phi_{x'L} dx \quad (9.123)$$

From Eqs. (9.89) and (9.91),

$$\theta_i = - \int_0^{x'} \left[\phi_0 + \frac{M_x - M_0}{EI} \left(1 + \bar{a} \left| \frac{M_x - M_0}{2M_p} \right|^{r-1} \right) \right] dx - \int_{x'}^L \frac{M_x}{EI} \left(1 + \bar{a} \left| \frac{M_x}{M_p} \right|^{r-1} \right) dx \quad (9.124)$$

in which

$$\begin{aligned} \int_0^{x'} \phi_0 dx &= \int_0^{x'} \frac{M_0}{EI} \left(1 + \bar{a} \left| \frac{M_0}{M_p} \right|^{r-1} \right) dx = \frac{1}{EI} \int_0^{x'} (-V_{ii}x - M_{ii}) dx + \frac{\bar{a}}{EIM_p^{r-1}} \int_0^{x'} (-V_{ii}x - M_{ii})^r dx \\ &= \frac{1}{EI} \left[-V_{ii} \frac{(x')^2}{2} - M_{ii}x' - \frac{\bar{a}(M_{ii})^2}{(r+1)(-V_{ii})} \left| \frac{M_{ii}}{M_p} \right|^{r-1} \right] \end{aligned} \quad (9.125)$$

$$\int_0^{x'} \frac{(M_x - M_0)}{EI} dx = \frac{1}{EI} \int_0^{x'} (-V_i x - M_i + V_{ii}x + M_{ii}) dx = \frac{1}{EI} \left[-V_i \frac{(x')^2}{2} - M_i x' + V_{ii} \frac{(x')^2}{2} + M_{ii}x' \right] \quad (9.126)$$

$$\begin{aligned} \int_0^{x'} \frac{\bar{a}}{EI(2M_p)^{r-1}} (M_x - M_0)^r dx &= \frac{\bar{a}}{EI(2M_p)^{r-1}} \int_0^{x'} (-V_i x - M_i + V_{ii}x + M_{ii})^r dx \\ &= \frac{1}{EI(r+1)(V_i - V_{ii})} \left| \frac{M_i - M_{ii}}{2M_p} \right|^{r-1} (M_i - M_{ii})^2 \end{aligned} \quad (9.127)$$

$$\begin{aligned} \int_{x'}^L \frac{M_x}{EI} \left(1 + \bar{a} \left| \frac{M_x}{M_p} \right|^{r-1} \right) dx &= \frac{1}{EI} \left[-V_i \frac{L^2}{2} - M_i L + \frac{V_i(x')^2}{2} + M_i x' + \frac{\bar{a}}{(r+1)(-V_i)} \left| \frac{-V_i L - M_i}{M_p} \right|^{r-1} (-V_i L - M_i)^2 \right] \end{aligned} \quad (9.128)$$

Substituting Eqs. (9.125)–(9.128) into Eq. (9.124) yields

$$\begin{aligned}\theta_i &= -\frac{1}{EI} \left\{ -V_{ii} \frac{(x')^2}{2} - M_{ii}x' - \frac{\bar{a}}{(r+1)(-V_{ii})} \left| \frac{M_{ii}}{M_p} \right|^{r-1} (M_{ii})^2 - V_i \frac{(x')^2}{2} - M_i x' + V_{ii} \frac{(x')^2}{2} + M_{ii} x' \right. \\ &\quad \left. + \frac{\bar{a}}{(r+1)(V_i - V_{ii})} \left| \frac{M_i - M_{ii}}{2M_p} \right|^{r-1} (M_i - M_{ii})^2 - V_i \frac{L^2}{2} - M_i L + \frac{V_i(x')^2}{2} + M_i x' \right. \\ &\quad \left. + \frac{\bar{a}}{(r+1)(-V_i)} \left| \frac{-V_i L - M_i}{M_p} \right|^{r-1} (-V_i L - M_i)^2 \right\} \\ &= -\frac{1}{EI} \left[\frac{-\bar{a}}{(r+1)(-V_{ii})} \left| \frac{M_{ii}}{M_p} \right|^{r-1} (M_{ii})^2 - V_i \frac{L^2}{2} - M_i L \right. \\ &\quad \left. + \frac{\bar{a}}{(r+1)(-V_i)} \left| \frac{-V_i L - M_i}{M_p} \right|^{r-1} (-V_i L - M_i)^2 \right. \\ &\quad \left. + \frac{\bar{a}}{(r+1)(V_i - V_{ii})} \left| \frac{M_i - M_{ii}}{2M_p} \right|^{r-1} (M_i - M_{ii})^2 \right] \quad (9.129)\end{aligned}$$

Similarly

$$\begin{aligned}Y_i &= - \int_0^{x'} \phi_{0x'} x \, dx - \int_{x'}^L \phi_{x'L} x \, dx \\ &= - \int_0^{x'} x \left[\phi_0 + \frac{M_x - M_0}{EI} \left(1 + \bar{a} \left| \frac{M_x - M_0}{2M_p} \right|^{r-1} \right) \right] dx - \int_{x'}^L \frac{x M_x}{EI} \left(1 + \bar{a} \left| \frac{M_x}{M_p} \right|^{r-1} \right) dx \\ &\quad (9.130)\end{aligned}$$

in which

$$\int_0^{x'} x \phi_0 \, dx = \frac{1}{EI} \left[-V_{ii} \frac{(x')^3}{3} - M_{ii} \frac{(x')^2}{2} + \frac{\bar{a}(M_{ii})^3}{(r+2)V_{ii}^2} \left| \frac{M_{ii}}{M_p} \right|^{r-1} - \frac{\bar{a}(M_{ii})^3}{(r+1)V_{ii}^2} \left| \frac{M_{ii}}{M_p} \right|^{r-1} \right] \quad (9.131)$$

$$\int_0^{x'} \frac{x(M_x - M_0)}{EI} \, dx = \frac{1}{EI} \left[\frac{-V_i(x')^3}{3} - M_i \frac{(x')^2}{2} + V_{ii} \frac{(x')^3}{3} + M_{ii} \frac{(x')^2}{2} \right] \quad (9.132)$$

$$\begin{aligned}\int_0^{x'} \frac{\bar{a}x(M_x - M_0)^r}{EI(2M_p)^{r-1}} \, dx &= \frac{\bar{a}}{EI} \left[\frac{(M_i - M_{ii})^3}{(r+2)(-V_i + V_{ii})^2} \left| \frac{M_i - M_{ii}}{2M_p} \right|^{r-1} \right. \\ &\quad \left. - \frac{(M_i - M_{ii})^3}{(r+1)(-V_i + V_{ii})^2} \left| \frac{M_i - M_{ii}}{2M_p} \right|^{r-1} \right] \quad (9.133)\end{aligned}$$

$$\begin{aligned}\int_{x'}^L x \frac{M_x}{EI} \left(1 + \bar{a} \left| \frac{M_x}{M_p} \right|^{r-1} \right) \, dx &= \frac{1}{EI} \left[\frac{-V_i L^3}{3} - \frac{M_i L^2}{2} + \frac{\bar{a}}{(r+2)V_i^2} \left| \frac{-V_i L - M_i}{M_p} \right|^{r-1} (-V_i L - M_i)^3 \right. \\ &\quad \left. + \frac{\bar{a} M_i}{(r+1)V_i^2} \left| \frac{-V_i L - M_i}{M_p} \right|^{r-1} (-V_i L - M_i)^2 + \frac{V_i(x')^3}{3} + \frac{M_i(x')^2}{2} \right] \quad (9.134)\end{aligned}$$

Substituting Eqs. (9.131)–(9.134) into Eq. (9.130) yields

$$Y_i = \frac{-1}{EI} \left\{ \frac{-V_i L^3}{3} - M_i \frac{L^2}{2} - \frac{\bar{a}(M_{ii})^3}{(r+1)(r+2)V_{ii}^2} \left| \frac{M_{ii}}{M_p} \right|^{r-1} - \frac{\bar{a}(M_i - M_{ii})^3}{(r+1)(r+2)(-V_i + V_{ii})^2} \left| \frac{M_i - M_{ii}}{2M_p} \right|^{r-1} \right. \\ \left. + \frac{\bar{a}(-V_i L - M_i)^2}{(r+1)(r+2)V_i^2} \left| \frac{-V_i L - M_i}{M_p} \right|^{r-1} [(r+1)(-V_i L - M_i) + (r+2)M_i] \right\} \quad (9.135)$$

Similar to the derivation of Eqs. (9.96)–(9.99), we can find the derivatives of Eqs. (9.129) and (9.135) with respect to M_i and V_i and then substitute the following equilibrium equations into the derivative equations:

$$M_j = -V_i L - M_i \quad (9.136a)$$

$$M_{ji} = -V_{ii} L - M_{ii} \quad (9.136b)$$

$$M_{iid} = M_i - M_{ii} \quad (9.136c)$$

$$M_{jid} = M_j - M_{ji} \quad (9.136d)$$

$$M'_p = 2M_p \quad (9.136e)$$

$$V_i - V_{ii} = -(M_{iid} + M_{jid})/L \quad (9.136f)$$

Thus from Eq. (9.129),

$$\frac{d\theta_i}{dM_i} = \frac{1}{EI} \left[L + \frac{\bar{a}}{(-V_i)} \left| \frac{-V_i L - M_i}{M_p} \right|^{r-1} (-V_i L - M_i) - \frac{\bar{a}}{(V_i - V_{ii})} \left| \frac{M_i - M_{ii}}{2M_p} \right|^{r-1} (M_i - M_{ii}) \right] \\ = \frac{L}{EI} \left[1 + \frac{\bar{a}}{\left(1 + \frac{M_i}{M_j}\right)} \left| \frac{M_j}{M_p} \right|^{r-1} + \frac{\bar{a}}{\left(1 + \frac{M_{jid}}{M_{iid}}\right)} \left| \frac{M_{iid}}{M'_p} \right|^{r-1} \right] \quad (9.137)$$

Similar to the procedures shown above,

$$\frac{d\theta_i}{dV_i} = -\frac{L^2}{EI} \left\{ \frac{-1}{2} - \frac{\bar{a}}{(r+1)\left(1 + \frac{M_i}{M_j}\right)^2} \left| \frac{M_j}{M_p} \right|^{r-1} \left[r + (r+1)\left(\frac{M_i}{M_j}\right) \right] - \frac{\bar{a}}{(r+1)\left(1 + \frac{M_{jid}}{M_{iid}}\right)^2} \left| \frac{M_{iid}}{M'_p} \right|^{r-1} \right\} \quad (9.138)$$

$$\frac{dY_i}{dV_i} = \frac{L^3}{EI} \left\{ \frac{1}{3} + \frac{2\bar{a}}{(r+1)(r+2)\left(1 + \frac{M_{jid}}{M_{iid}}\right)^3} \left| \frac{M_{iid}}{M'_p} \right|^{r-1} \right. \\ \left. + \frac{\bar{a}}{(r+1)(r+2)\left(1 + \frac{M_i}{M_j}\right)^3} \left| \frac{M_j}{M_p} \right|^{r-1} \left[r(r+1) + 2r(r+2)\left(\frac{M_i}{M_j}\right) + (r+1)(r+2)\left(\frac{M_i}{M_j}\right)^2 \right] \right\} \quad (9.139)$$

$$\frac{dY_i}{dM_i} = \frac{L^2}{EI} \left\{ \frac{1}{2} + \frac{\bar{a}}{(r+1) \left(1 + \frac{M_{j\text{id}}}{M_{i\text{id}}} \right)^2} \left| \frac{M_{i\text{id}}}{M'_p} \right|^{r-1} + \frac{\bar{a}}{(r+1) \left(1 + \frac{M_i}{M_j} \right)^2} \left| \frac{M_j}{M_p} \right|^{r-1} \left[r + (r+1) \left(\frac{M_i}{M_j} \right) \right] \right\} \quad (9.140)$$

Eqs. (9.137)–(9.140) are similar to Eqs. (9.96)–(9.99) of the skeleton curve except for the two terms, M_j/M_i and $|M_i/M_p|^{r-1}$, which should be modified as

$$\frac{M_j}{M_i} \text{ replaced by } \frac{M_{j\text{id}}}{M_{i\text{id}}} \quad (9.141)$$

$$\left| \frac{M_i}{M_p} \right|^{r-1} \text{ replaced by } \left| \frac{M_{i\text{id}}}{M'_p} \right|^{r-1} \quad (9.142)$$

the terms M_i/M_j and M_j/M_p remain the same. Thus the stiffness coefficients of the branch curve are the same as those given in Eq. (9.120) in which the parameters of the coefficients of R_i , U_i , W_i , S_i , G_i , Q_i in Eq. (9.119a, c, e, g, i, and k) should be modified to replace M_j/M_i by $M_{j\text{id}}/M_{i\text{id}}$ and $|M_i/M_p|^{r-1}$ by $|M_{i\text{id}}/M'_p|^{r-1}$.

(B) *Moment reversal at the j-end*—following Fig. 9.31 and Eqs. (9.123)–(9.136), we can also find four derivative equations of $d\theta_i/dM_b$, $d\theta_i/dV_b$, dY_i/dM_i , and dY_i/dV_i . After substitution of the following equilibrium equations,

$$M_j = -V_i L - M_i \quad (9.143a)$$

$$M_{jj} = -V_{ij} L - M_{ij} \quad (9.143b)$$

$$M_{ij\text{id}} = M_i - M_{ij} \quad (9.143c)$$

$$M_{jj\text{id}} = M_j - M_{jj} \quad (9.143d)$$

$$M'_p = 2M_p \quad (9.143e)$$

the final results are

$$\frac{d\theta_i}{dM_i} = \frac{L}{EI} \left[1 + \frac{\bar{a}}{\left(1 + \frac{M_j}{M_i} \right)} \left| \frac{M_i}{M_p} \right|^{r-1} + \frac{\bar{a}}{\left(1 + \frac{M_{ij\text{id}}}{M_{jj\text{id}}} \right)} \left| \frac{M_{ij\text{id}}}{M'_p} \right|^{r-1} \right] \quad (9.144)$$

$$\frac{d\theta_i}{dV_i} = -\frac{L^2}{EI} \left\{ \frac{-1}{2} - \frac{\bar{a}}{(r+1) \left(1 + \frac{M_j}{M_i} \right)^2} \left| \frac{M_i}{M_p} \right|^{r-1} - \frac{\bar{a}}{(r+1) \left(1 + \frac{M_{ij\text{id}}}{M_{jj\text{id}}} \right)^2} \left| \frac{M_{ij\text{id}}}{M'_p} \right|^{r-1} \left[r + (r+1) \left(\frac{M_{ij\text{id}}}{M_{jj\text{id}}} \right) \right] \right\} \quad (9.145)$$

$$\frac{dY_i}{dV_i} = \frac{L^3}{EI} \left\{ \frac{1}{3} + \frac{2\bar{a}}{(r+1)(r+2) \left(1 + \frac{M_j}{M_i}\right)^3} \left| \frac{M_i}{M_p} \right|^{r-1} + \frac{\bar{a}}{(r+1)(r+2) \left(1 + \frac{M_{j\text{d}}}{M_{i\text{d}}} \right)^3} \left| \frac{M_{j\text{d}}}{M'_p} \right|^{r-1} \right. \\ \left. \left[r(r+1) + 2r(r+2) \left(\frac{M_{j\text{d}}}{M_{i\text{d}}} \right) + (r+1)(r+2) \left(\frac{M_{j\text{d}}}{M_{i\text{d}}} \right)^2 \right] \right\} \quad (9.146)$$

$$\frac{dY_i}{dM_i} = \frac{d\theta_i}{dV_i} \quad (9.147)$$

Comparing Eqs. (9.144)–(9.147) with Eqs. (9.96)–(9.99) leads to the following conclusion: replacing M_i/M_j by $M_{i\text{d}}/M_{j\text{d}}$, and $|M_j/M_p|^{r-1}$ by $|M_{j\text{d}}/M'_p|^{r-1}$ in Eq. (9.120) yields the desired stiffness coefficients for moment reversal at the j -end as shown in Eq. (9.114) or Eq. (9.120). Consequently, the parameters of R_j , U_j , W_j , S_j , G_j , and Q_j of Eqs. (9.119b, d, f, h, j, and l) should be modified by replacement of M_i/M_j with $M_{i\text{d}}/M_{j\text{d}}$ and $|M_j/M_p|^{r-1}$ with $|M_{j\text{d}}/M'_p|^{r-1}$.

EXAMPLE 9.6.1 Use the Ramberg–Osgood hysteresis model with $\bar{a}=1$ and $r=20$ to find the dynamic response of the framework given in Fig. 9.11 at (A) $t=0.1$ sec and (B) $t=1.2$ sec. Assume that the initial conditions at $t=0.1$ are zero and those at $t=1.2$ are based on the following results at $t=1.1$ sec: $x_s=12.596$ in, $\dot{x}_s=-1.5678$ in/sec, $\ddot{x}_s=-117.25$ in/sec², $x_{\theta 1}=x_{\theta 2}=8.68911 \times 10^{-2}$ rad; $M_1=M_6=0.38002$ k in, $M_3=M_4=-M_2=-M_5=0.298610$ k in, $\Delta x_{\theta 1}=\Delta x_{\theta 2}=2.6907 \times 10^{-3}$ rad; $\Delta x_s=0.376$ in, and the unbalanced force $\Delta U=-5.95916012 \times 10^{-3}$ k.

Solution: Using Eq. (9.120) in Eq. (a) of Example 9.4.1, the element stiffness matrix can be expressed as

$$[K_e] = \frac{6EI}{LZ} \begin{bmatrix} 2 + 2W_i + W_jQ_j & 1 + W_iG_i + W_jG_j & -\frac{1}{L}(3 + U_i + U_jS_j) & -\frac{1}{L}(3 + U_i + U_jS_j) \\ & 2 + 2W_j + W_iQ_i & -\frac{1}{L}(3 + U_j + U_iS_i) & -\frac{1}{L}(3 + U_j + U_iS_i) \\ & & \frac{1}{L^2}(6 + R_i + R_j) & \frac{1}{L^2}(6 + R_i + R_j) \\ & \text{symm} & & \frac{1}{L^2}(6 + R_i + R_j) \end{bmatrix} \quad (a)$$

in which

$$Z = (2 + 2W_i + W_jQ_j)(6 + R_i + R_j) - (3 + U_i + U_jS_j)^2 \quad (b)$$

(A) At $t=0$, the member's end moments M_i and M_j are zero; Eq. (9.119a–l) consequently becomes

$$R_i = R_j = U_i = U_j = W_i = W_j = 0 \quad (c)$$

$$S_i = S_j = G_i = G_j = r = 20 \quad (d)$$

$$Q_i = Q_j = r(r+1) = 420 \quad (e)$$

Substituting Eqs. (c)–(e) into Eqs. (a) and (b) leads to

$$Z = (2)(6) - (3)^2 = 3 \quad (f)$$

and

$$[K_e] = \frac{6EI}{3L} \begin{bmatrix} 2 & 1 & -3/L & -3/L \\ & 2 & -3/L & -3/L \\ & & 6/L^2 & 6/L^2 \\ \text{symm} & & & 6/L^2 \end{bmatrix} \quad (g)$$

which is identical to the static stiffness matrix.

From Example 9.4.1, $EI=1000$ k in 2 , $H=120$ in, and $\ell=240$ in, structural stiffness matrix $[K]$ is the same as the one given in Eq. (c) of that example. Thus the dynamic responses at $t=0.1$ sec are equal to those shown in Table 9.1.

(B) Based on initial conditions given at $t=1.1$ sec, the element stiffness matrix for element 1 can be obtained by using Eqs. (9.119)–(9.121). To illustrate, Eq. (9.119a and b) are calculated as

$$\begin{aligned} R_i &= \frac{6\bar{a}}{(1+M_j/M_i)} \left| \frac{M_i}{M_p} \right|^{r-1} = \frac{6(1)}{\left(1 + \frac{-0.298610}{-0.38002} \right)} \left| \frac{0.38002}{0.2} \right|^{(20-1)} \\ &= 665,391.6562 \end{aligned}$$

$$\begin{aligned} R_j &= \frac{6\bar{a}}{(1+M_i/M_j)} \left| \frac{M_j}{M_p} \right|^{r-1} = \frac{6(1)}{\left(1 + \frac{-0.38002}{-0.298610} \right)} \left| \frac{0.298610}{0.2} \right|^{(20-1)} \\ &= 5358.4012 \end{aligned}$$

The numerical values of other parameters are

$$\begin{aligned} U_i &= 17,743.1799; & U_j &= 112.27608; & W_i &= 451.6294 \\ W_j &= 2.2456; & S_i &= 36.5013; & S_j &= 46.7252 \\ G_i &= 37.2870; & G_j &= 47.9979; & Q_i &= 1,396.7395 \\ Q_j &= 2,288.1633; \text{ and } & Z &= 3,525,137,945.0 \end{aligned}$$

Substituting the above numerical values into Eq. (a) leads to

$$[K_e] = \begin{bmatrix} 0.857215 & 2.40398 & -0.0271766 & -0.0271766 \\ & 89.4739 & -0.765649 & -0.765649 \\ \text{symm} & & 0.660688 \times 10^{-2} & 0.660688 \times 10^{-2} \\ & & & 0.660688 \times 10^{-2} \end{bmatrix} 10^{-4} \quad (h)$$

Element stiffness matrices for elements 2 and 3 can be similarly calculated. Based on the d.o.f. given in Fig. 9.11, the structural stiffness matrix is assembled as

$$[K] = \begin{bmatrix} 0.01325714 & 0.205897 \times 10^{-3} & -0.765649 \times 10^{-4} \\ \text{symm} & 0.01325714 & -0.765649 \times 10^{-4} \\ & & 1.321376 \times 10^{-6} \end{bmatrix} \quad (i)$$

from which the condensed stiffness, K , corresponding to the transverse displacement, x_s , is

$$K = K_{22} - K_{21}K_{11}^{-1}K_{12} = 4.505199 \times 10^{-7} \text{ k/in} \quad (j)$$

Using the linear acceleration integration technique, the following parameters are calculated with

the initial conditions given in the problem:

$$A = -\frac{6}{\Delta t} \dot{x}_{s(n-1)} - 3\ddot{x}_{s(n-1)} = \frac{-6}{0.1}(-1.5678) - 3(-117.25) = 445.818 \quad (\text{k})$$

$$B = 10.5659 \quad (\text{l})$$

$$\Delta F(t) \Big|_{t=1.1}^{t=1.2} = -5.57536 \times 10^{-3} \quad (\text{m})$$

$$\bar{K} = 0.1200 \quad (\text{n})$$

$$\Delta \bar{F}(t) = (\Delta F(t) + \Delta U) - MA = -0.1007 \quad (\text{o})$$

$$\Delta x_s = \Delta \bar{F}(t)/\bar{K} = -0.8391 < 0 \quad (\text{p})$$

$$\begin{Bmatrix} \Delta x_{\theta 1} \\ \Delta x_{\theta 2} \end{Bmatrix} = -K_{11}^{-1} K_{12} \Delta x_s = \begin{Bmatrix} 5.6870 \times 10^{-3} \\ 5.6870 \times 10^{-3} \end{Bmatrix} \Delta x_s = \begin{Bmatrix} -4.7727 \times 10^{-3} \\ -4.7727 \times 10^{-3} \end{Bmatrix} \text{ rad} \quad (\text{q})$$

Since Δx_s , $\Delta x_{\theta 1}$, and $\Delta x_{\theta 2}$ changed direction due to their present values being less than zero, the signs of the element's incremental forces should also change; the element's moment-curvature relationship is now associated with the branch curve. Therefore, the member end's moment at reversal point should be determined by recalculating element stiffness for the branch curve at unloading point. Treat the point in an approximate sense by assuming that the loading reversal is at $t = 1.1$ sec; then the stiffness matrix for element 1 can be calculated by letting

$$M_{iid} = M_i - M_{ii} = M_i - M_i = 0 \quad (\text{r})$$

$$M_{jid} = M_j - M_{ji} = M_j - M_j = 0 \quad (\text{s})$$

$$M_{ijd} = M_i - M_{ij} = M_i - M_i = 0 \quad (\text{t})$$

$$M_{jjd} = M_j - M_{jj} = M_j - M_j = 0 \quad (\text{u})$$

$$M'_p = 2M_p = (2)0.2 = 0.4 \quad (\text{v})$$

The above calculations Eqs. (r)–(u) imply that unloading is assumed to begin at 1.1 sec. Therefore, replacing M_i , M_j , M_p in R_i , U_i , W_i , S_i , G_i and Q_i with M_{iid} , M_{jid} , and M'_p and replacing M_i , M_j , M_p in R_j , U_j , W_j , S_j , G_j , and Q_j with M_{ijd} , M_{jjd} , and M'_p lead to

$$R_i = R_j = U_i = U_j = W_i = W_j = 0 \quad (\text{w})$$

$$S_i = S_j = G_i = G_j = r = 20 \quad (\text{x})$$

$$Q_i = Q_j = r(r+1) = 20(22) = 420 \quad (\text{y})$$

Eqs. (w), (x) and (y) are identical to Eqs. (c), (d), and (e), respectively, signifying that the stiffness is elastic and that the moment-curvature is now on the branch curve.

Thus the condensed form of the elastic structural stiffness matrix is

$$K = K_{22} - K_{21} K_{11}^{-1} K_{12} = 0.0079365 \text{ k/in} \quad (\text{z})$$

Numerical values of A , B , $\Delta F(t)$ and $\Delta(t)$ are the same as Eqs. (k), (l), (m), and (n), but the stiffness matrix should be modified to include current values in Eq. (z) as

$$\bar{K} = \frac{6}{(\Delta t)^2} M + K = 0.1279365 \quad (\text{aa})$$

Other response results are then routinely calculated for which the lateral displacement is

$$\Delta x_s = \Delta \bar{F}(t)/\bar{K} = -0.78711 \text{ in} \quad (\text{bb})$$

$$x_s = x_{s(n-1)} + \Delta x_s = 12.596 + (-0.78711) = 11.80889 \text{ in} \quad (\text{cc})$$

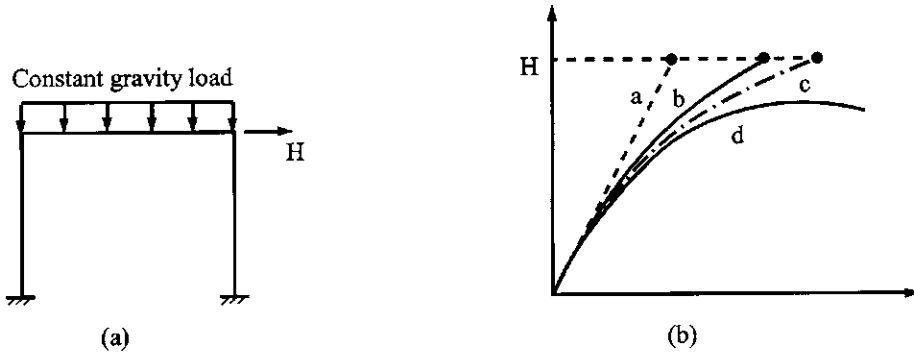


FIG. 9.32 Influence of nonlinearity. (a) Frame structure. (b) Lateral load vs. displacement.

PART B ADVANCED TOPICS

9.7. GEOMETRIC NONLINEARITY

In the previous sections we have introduced nonlinearities due to material properties. It has been assumed that the deformation in a structure is small. Thus the kinematic matrix based on structural configurations or equilibrium matrix based on internal forces and external loads remains unchanged during various loading stages. This holds true even when the second-order effect ($P-\Delta$) is included, whether the effect is implicitly considered in dynamic stiffness (see Chapter 5) or explicitly formulated as geometric stiffness matrix (see Chapter 6).

If structural deflection is large, then geometric nonlinearity should be considered. In this formulation, the geometric stiffness matrix ($P-\Delta$ effect) is not necessarily included. To illustrate the concept of geometric nonlinearity, consider the frame shown in Fig. 9.32 with constant gravity load and a slowly increasing lateral force. If geometric and material nonlinearity as well as the $P-\Delta$ effect are not considered, then lateral displacement vs lateral force relationship is linear, as shown by curve "a" in Fig. 9.32b. If geometric nonlinearity is considered without both the $P-\Delta$ effect and material nonlinearity, then lateral displacement is as shown in curve "b". If the geometric stiffness matrix is included, then the displacement curve is as shown in "c". If material nonlinearity is also included, then displacement will follow the path of curve "d".

Note that the geometric nonlinearity is due to large deflection for which the equilibrium equations between internal forces (deformations) and external nodal forces (displacements) should be changed at each loading stage. This change is based on the consideration that, when structural displacements are large, the directions of both external force (displacement) and internal force (deformation) are not the same as they were at the previous loading stage.

Let us consider member i in Fig. 9.33a at position AB with length L and inclined angle α . This member now moves to position $A'B'$ with an incremental joint displacement vector of

$$\{\Delta x\}_i = [\Delta x_A \quad \Delta x_B \quad \Delta \theta_A \quad \Delta \theta_B \quad \Delta y_A \quad \Delta y_B]_i^T \quad (9.148)$$

Joint displacements are in the direction of global coordinates X and Y as shown in Fig. 9.33a. Local displacements are given in Fig. 9.33b of which the incremental vector is

$$\{\Delta D\}_i = [\Delta u_A \quad \Delta u_B \quad \Delta \theta_A \quad \Delta \theta_B \quad \Delta Y_A \quad \Delta Y_B]_i^T \quad (9.149)$$

where Δu_A and ΔY_A are the member's axial and lateral displacements measured parallel and perpendicular, respectively, to the member axis AB at the current time step (see Fig. 9.33b); and $\Delta \theta_A$ and $\Delta \theta_B$ are the end rotational increments. From Fig. 9.33a and b, the transformation

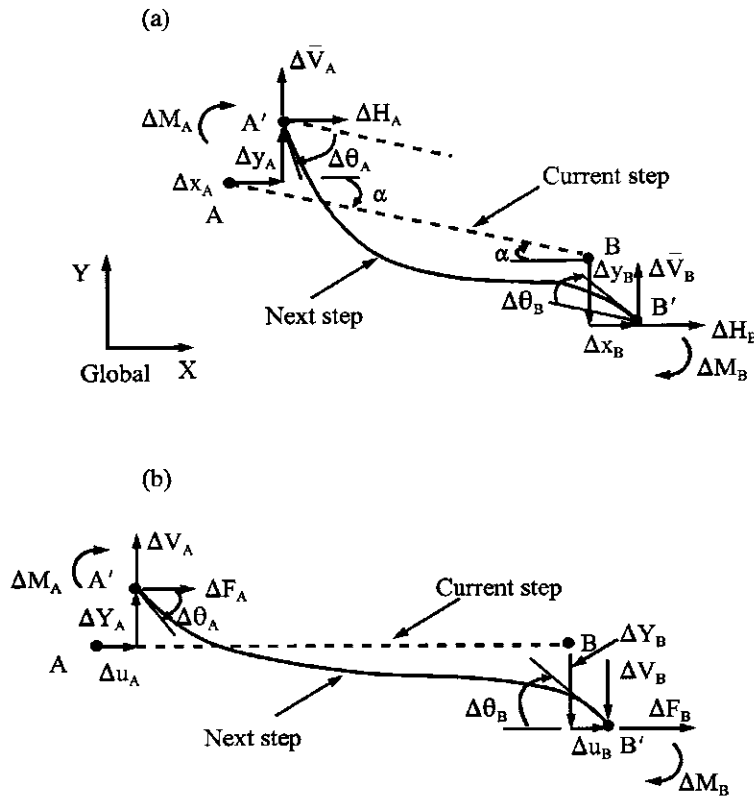


FIG. 9.33 Large deformations of a member. (a) Joint displacement for forces. (b) Member displacement and forces.

from joint displacements in local coordinates to global coordinates can be expressed as

$$\begin{Bmatrix} \Delta u_A \\ \Delta u_B \\ \Delta\theta_A \\ \Delta\theta_B \\ \Delta Y_A \\ \Delta Y_B \end{Bmatrix}_i = \begin{bmatrix} \cos \alpha & 0 & 0 & 0 & -\sin \alpha & 0 \\ 0 & \cos \alpha & 0 & 0 & 0 & -\sin \alpha \\ 0 & 0 & 1 & 0 & 0 & 0 \\ 0 & 0 & 0 & 1 & 0 & 0 \\ \sin \alpha & 0 & 0 & 0 & \cos \alpha & 0 \\ 0 & -\sin \alpha & 0 & 0 & 0 & -\cos \alpha \end{bmatrix}_i \begin{Bmatrix} \Delta x_A \\ \Delta x_B \\ \Delta\theta_A \\ \Delta\theta_B \\ \Delta y_A \\ \Delta y_B \end{Bmatrix}_i \quad (9.150a)$$

or

$$\{\Delta D\}_i = [B]_i \{\Delta x\}_i \quad (9.150b)$$

in which $[B]_i$ is the compatibility matrix of the member. In Eq. (9.150) the angle, α , can be calculated based on the coordinates of the member's joints.

Let the location of joint A in the global X-Y coordinates (see Fig. 9.23a) be (A_x, A_y) while joint B is (B_x, B_y) ; then the inclined angle can be expressed as

$$\alpha = -\tan^{-1}\left(\frac{B_y - A_y}{B_x - A_x}\right) \quad (9.151)$$

Let the force-deformation relationship of member i in its local coordinates be expressed as

$$\{\Delta F\}_i = [K_e^i]\{\Delta D\}_i = [\Delta F_A \quad \Delta F_B \quad \Delta M_A \quad \Delta M_B \quad \Delta V_A \quad \Delta V_B]^T \quad (9.152)$$

and let the force vector of member i in its global coordinates be

$$\{\Delta P\}_i = [\Delta H_A \quad \Delta H_B \quad \Delta M_A \quad \Delta M_B \quad \Delta \bar{V}_A \quad \Delta \bar{V}_B]^T \quad (9.153)$$

Based on the virtual load concept derived in Eq. (4.54), the transformation from local forces to global joint force can be expressed as

$$\{\Delta P\}_i = [B]_i^T \{\Delta F\}_i = [A]_i \{\Delta F\}_i \quad (9.154)$$

where $[A]_i$ represents the equilibrium matrix of member i . Substituting Eq. (9.150b) and (9.152) into (9.154) yields

$$\{\Delta P\}_i = [B]_i^T [K_e^i] \{\Delta D\}_i = [B]_i^T [K_e^i] [B]_i \{\Delta x\}_i = [K^i] \{\Delta x\}_i \quad (9.155)$$

where $[K^i]$ represents the stiffness matrix of member i in global coordinates, as was similarly presented for elastic case (see Section 4 of Chapter 5). Thus the stiffness matrix for a structural system can be obtained simply by adding the contributions of all member stiffnesses using the direct element formulation shown in section 5.4.3 as

$$[K] = \Sigma [K^i] \quad (9.156)$$

Note that when the member's axial deformation is not considered, i.e. $\Delta u_A = \Delta u_B = 0$ (see Fig. 9.33b), the compatibility matrix in Eq. (9.150a) becomes

$$\begin{Bmatrix} \Delta \theta_A \\ \Delta \theta_B \\ \Delta Y_A \\ \Delta Y_B \end{Bmatrix} = \begin{bmatrix} 0 & 0 & 1 & 0 & 0 & 0 \\ 0 & 0 & 0 & 1 & 0 & 0 \\ \sin \alpha & 0 & 0 & 0 & \cos \alpha & 0 \\ 0 & -\sin \alpha & 0 & 0 & 0 & -\cos \alpha \end{bmatrix} \begin{Bmatrix} \Delta x_A \\ \Delta x_B \\ \Delta \theta_A \\ \Delta \theta_B \\ \Delta y_A \\ \Delta y_B \end{Bmatrix} \quad (9.157)$$

EXAMPLE 9.7.1 Assume the truss shown in Fig. 9.34 is subjected to a vertical load of $0.2 P_{cr}$; P_{cr} represents the elastic buckling load of the structure, and a force of 20 k is applied horizontally at joint 3. Find the horizontal displacements of the structure: (A) due to horizontal force only without consideration of geometric stiffness and large deflection; (B) with consideration of horizontal force and geometric stiffness but without large deflection; and (C) with consideration of horizontal force and geometric stiffness and large deflection. Material properties are $A = 17$ in² and $E = 29000$ ksi.

Solution: Based on the diagrams of external action and internal resistance given in Fig. 9.34 and (Eq. 9.150a), the compatibility matrix can be established for the constituent members as shown in Eqs. (a) and (b).

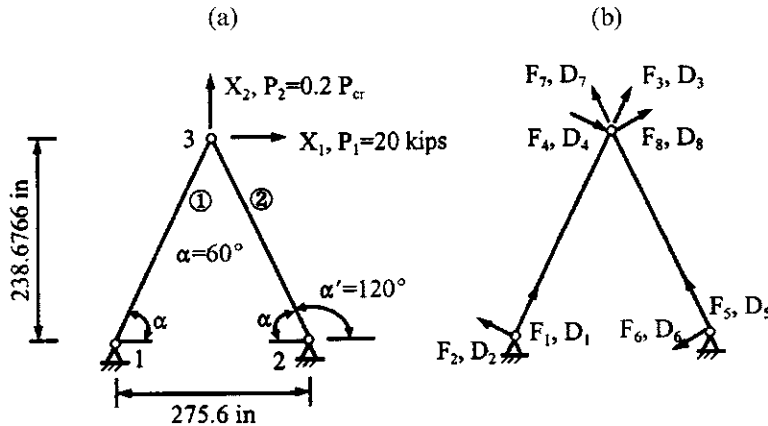


FIG. 9.34 Example 9.7.1. (a) External action $\{P\}$, $\{X\}$. (b) Internal resistance $\{F\}$, $\{D\}$.

For member 1

$$\alpha = -\tan^{-1}\left(\frac{238.6766 - 0}{137.8 - 0}\right) = -60^\circ \text{ (clockwise is positive)}$$

$$\theta_A = \theta_B = 0; \alpha = -60^\circ; \cos \alpha = 0.5; \sin \alpha = -\frac{\sqrt{3}}{2}$$

$$\begin{bmatrix} \Delta u_A \\ \Delta Y_A \\ \Delta u_B \\ \Delta Y_B \end{bmatrix}_1 = \begin{bmatrix} \Delta D_1 \\ \Delta D_2 \\ \Delta D_3 \\ \Delta D_4 \end{bmatrix}_1 = \begin{bmatrix} \cos \alpha & 0 & -\sin \alpha & 0 \\ \sin \alpha & 0 & \cos \alpha & 0 \\ 0 & \cos \alpha & 0 & -\sin \alpha \\ 0 & -\sin \alpha & 0 & -\cos \alpha \end{bmatrix} \begin{bmatrix} \Delta x_1 \\ \Delta x_2 \end{bmatrix} = \begin{bmatrix} 0 & 0 \\ 0 & 0 \\ \cos \alpha & -\sin \alpha \\ -\sin \alpha & -\cos \alpha \end{bmatrix}$$

$$\begin{bmatrix} \Delta x_1 \\ \Delta x_2 \end{bmatrix} = [B]_1 \{ \Delta x \}$$
(a)

For member 2

$$\alpha' = -\tan^{-1}\left(\frac{238.6766 - 0}{137.8 - 275.6}\right) = -120^\circ; \theta_A = \theta_B = 0; \cos \alpha' = -0.5; \sin \alpha' = -\frac{\sqrt{3}}{2}$$

$$\begin{bmatrix} \Delta u_A \\ \Delta Y_A \\ \Delta u_B \\ \Delta Y_B \end{bmatrix}_2 = \begin{bmatrix} \Delta D_5 \\ \Delta D_6 \\ \Delta D_7 \\ \Delta D_8 \end{bmatrix}_2 = \begin{bmatrix} \cos \alpha' & 0 & -\sin \alpha' & 0 \\ \sin \alpha' & 0 & \cos \alpha' & 0 \\ 0 & \cos \alpha' & 0 & -\sin \alpha' \\ 0 & -\sin \alpha' & 0 & -\cos \alpha' \end{bmatrix} \begin{bmatrix} \Delta x_1 \\ \Delta x_2 \end{bmatrix}$$
(b)

The element stiffness matrix of member 1 is

$$\begin{bmatrix} F_1 \\ F_2 \\ F_3 \\ F_4 \end{bmatrix} = \frac{AE}{L} \begin{bmatrix} 1 & 0 & -1 & 0 \\ 0 & 0 & 0 & 0 \\ -1 & 0 & 1 & 0 \\ 0 & 0 & 0 & 0 \end{bmatrix} \begin{bmatrix} D_1 \\ D_2 \\ D_3 \\ D_4 \end{bmatrix} = [K_e^1] \{ D \}_1$$
(c)

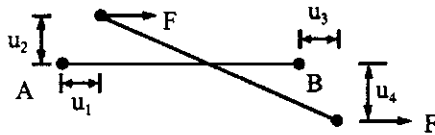


FIG. 9.35 Element's geometric stiffness.

Since these two members are identical, $[K_e^2] = [K_e^1]$.

Using the direct element stiffness formulation given in Eq. (9.156) yields

$$[K] = \sum_{i=1}^2 [K^i] = [B]_1^T [K_e^1] [B]_1 + [B]_2^T [K_e^2] [B]_2 = \begin{bmatrix} 0.25 \frac{AE}{L} & \frac{\sqrt{3}}{4} \frac{AE}{L} \\ \frac{\sqrt{3}}{4} \frac{AE}{L} & \frac{3}{4} \frac{AE}{L} \end{bmatrix} \\ + \begin{bmatrix} 0.25 \frac{AE}{L} & -\frac{\sqrt{3}}{4} \frac{AE}{L} \\ -\frac{\sqrt{3}}{4} \frac{AE}{L} & \frac{3}{4} \frac{AE}{L} \end{bmatrix} = \begin{bmatrix} 0.5 & 0 \\ 0 & 1.5 \end{bmatrix} \frac{AE}{L} \quad (d)$$

As to geometric stiffness formulation, the typical element's coefficients based on the sign convention shown in Fig. 9.35 are

$$[K_{eg}] = \frac{F}{L} \begin{bmatrix} 0 & 0 & 0 & 0 \\ 0 & 1 & 0 & 1 \\ 0 & 0 & 0 & 0 \\ 0 & 1 & 0 & 1 \end{bmatrix} \quad (e)$$

Note that the sign convention in Fig. 9.35 is similar to that in Fig. 6.25 of the geometric string stiffness. In the former, F is positive for tension and negative for compression; the system's stiffness is expressed as $[K] + [K_g]$ where the sign of F adjusts the sign of $[K_g]$. In the latter, P has already been treated as compression in Eq. (6.141); thus the system's stiffness matrix is $[K] - [K_g]$.

Similar to the formulation of Eq. (d), the system's geometric stiffness matrix is

$$[K_g] = \sum_{i=1}^2 [K_g^i] = [B]_1^T [K_{eg}^1] [B]_1 + [B]_2^T [K_{eg}^2] [B]_2 = \frac{F}{L} \begin{bmatrix} 1.5 & 0 \\ 0 & 0.5 \end{bmatrix} \quad (f)$$

of which numerical values depend on the amount of axial force acting on the members. Solution procedures are shown below for Case B.

(A) *Due to horizontal force only without consideration of geometric stiffness and large deflection*—for horizontal force of 20 k at joint 3, the displacement vector can be obtained from elastic analysis as

$$\{\Delta x\} = [K]^{-1} \{\Delta P\} = \begin{bmatrix} 2 & 0 \\ 0 & 0.66667 \end{bmatrix} \frac{L}{AE} \begin{Bmatrix} 20 \\ 0 \end{Bmatrix} = \begin{Bmatrix} 0.02236 \\ 0 \end{Bmatrix} \text{ in} \quad (g)$$

(B) *With consideration of horizontal force and geometric stiffness but without large deflection*—in this case, first find the members' forces due to vertical load, then find buckling load, P_{cr} , and finally apply $0.2P_{cr}$ to the structure along with horizontal load to obtain displacement. Structural displacements due to vertical load are

$$\{x\} = [K]^{-1} \{P\} = \frac{L}{AE} \begin{bmatrix} 2 & 0 \\ 0 & 0.66667 \end{bmatrix} \begin{Bmatrix} 0 \\ -P_{cr} \end{Bmatrix} = -\begin{Bmatrix} 0 \\ 0.66667 \end{Bmatrix} \left(\frac{P_{cr}L}{AE} \right) \quad (h)$$

The members' forces are

$$\{F\} = [[K_e^1][B]_1 [K_e^2][B]_2]\{x\} = -[-0.57735 \quad 0 \quad 0.57735 \quad 0 \quad -0.57735 \quad 0 \quad 0.57735 \quad 0]^T P_{cr} \quad (i)$$

which shows that members 1 and 2 are in compression. Thus F/L in Eq. (e) is $-0.57735 P_{cr}/L$ and Eq. (f) becomes

$$[K_g] = \frac{-0.57735 P_{cr}}{L} \begin{bmatrix} 1.5 & 0 \\ 0 & 0.5 \end{bmatrix} \quad (j)$$

Buckling load can be determined as

$$\det([K] + [K_g]) = \left(0.5 \frac{AE}{L} - 0.86603 \frac{P_{cr}}{L}\right) \left(1.5 \frac{AE}{L} - 0.28867 \frac{P_{cr}}{L}\right) = 0 \quad (k)$$

from which buckling loads of the first mode are

$$P_{cr} = 0.57735 AE = 284,633.55 \text{ k} \quad (l)$$

Displacements and internal forces due to the $0.2P_{cr}$ are obtained from Eq. (h) and (i) as

$$\{x\} = [0 \quad -21.2157]^T \text{ in} \quad (m)$$

and

$$\{F\} = [32,866.66 \quad 0 \quad -32,866.66 \quad 0 \quad 32,866.66 \quad 0 \quad -32,866.66 \quad 0]^T \quad (n)$$

Substituting $0.2P_{cr}$ of Eq. (l) into Eq. (j), which is then combined with Eq. (d), yields the displacement due to the horizontal force as

$$\begin{aligned} \{x\} &= ([K] + [K_g])^{-1} \{P\} = \begin{bmatrix} 894.41219 - 178.88242 & 0 \\ 0 & 2683.23657 - 59.62747 \end{bmatrix}^{-1} \begin{Bmatrix} 20 \\ 0 \end{Bmatrix} \\ &= \begin{Bmatrix} 0.02795 \\ 0 \end{Bmatrix} \text{ in} \end{aligned} \quad (o)$$

Note that the above solution is due to horizontal force with the $P-\Delta$ effect; displacements due to both $0.2P_{cr}$ and horizontal force should be the summation of Eqs. (m) and (o).

(C) *With consideration of horizontal force, geometric stiffness and large deflection—displacements obtained in Eq. (m) of (B) are shown in Fig. 9.36 where the change in structural geometry is also sketched for large deflection formulation. Using Eq. (9.151) gives*

$$\left. \begin{aligned} \theta_1 &= -\tan^{-1}\left(\frac{217.4609}{137.8}\right) = -57.6385^\circ = -1.0059816 \text{ rad} = \alpha \\ \theta_2 &= \tan^{-1}\left(\frac{137.8}{217.4609}\right) = 32.3615^\circ \\ \alpha' &= -\tan^{-1}\left(\frac{217.4609}{-137.8}\right) = -122.3615^\circ = (\pi - \theta_1) \end{aligned} \right\} \quad (p)$$

The compatibility matrix of members 1 and 2 may be expressed as

$$\begin{aligned} [[B]_1^T \quad [B]_2^T] &= \begin{bmatrix} 0 & 0 & \cos \theta_1 & -\sin \theta_1 & 0 & 0 & \cos(\pi - \theta_1) & -\sin(\pi - \theta_1) \\ 0 & 0 & -\sin \theta_1 & -\cos \theta_1 & 0 & 0 & -\sin(\pi - \theta_1) & -\cos(\pi - \theta_1) \end{bmatrix} \\ &= \begin{bmatrix} 0 & 0 & 0.535259 & 0.8446877 & 0 & 0 & -0.535259 & 0.8446877 \\ 0 & 0 & 0.8446877 & -0.535259 & 0 & 0 & 0.8446877 & 0.535259 \end{bmatrix} \end{aligned} \quad (q)$$

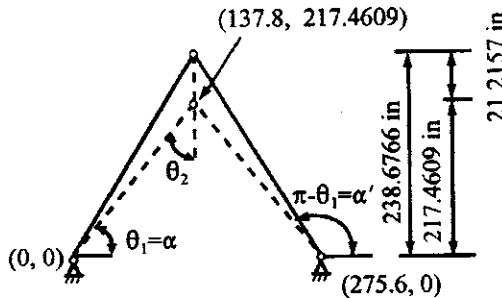


FIG. 9.36 Large deflection formulation.

Thus the new system matrices are obtained from Eqs. (d) and (f), with current member length $L' = 257.445$ in, as

$$\begin{aligned} [K] &= \begin{bmatrix} 0.2865 & 0 \\ 0 & 0.7135 \end{bmatrix} \frac{(2)(17)(29000)}{257.445} \\ &= \begin{bmatrix} 1097.2790 & 0 \\ 0 & 2732.6652 \end{bmatrix} \end{aligned} \quad (\text{r})$$

$$\begin{aligned} [K_g] &= \begin{bmatrix} 0.7135 & 0 \\ 0 & 0.2865 \end{bmatrix} \frac{(2)(0.57735)(-0.2 P_{cr})}{257.445} \\ &= \begin{bmatrix} -182.1717 & 0 \\ 0 & -73.1519 \end{bmatrix} \end{aligned} \quad (\text{s})$$

In Eqs. (r) and (s), $[K_e]$ and $[K_{eg}]$ have the same form as in Case (B) except the length is different and the compatibility matrix, $[B]$, is from Eq. (q).

Incremental displacements due to horizontal force and large deflection are

$$\begin{aligned} \{\Delta x\} &= ([K] + [K_g])^{-1} \{\Delta P\} = \begin{bmatrix} 915.1073 & 0 \\ 0 & 2659.5133 \end{bmatrix}^{-1} \begin{bmatrix} 20 \\ 0 \end{bmatrix} \\ &= \begin{Bmatrix} 0.02186 \\ 0 \end{Bmatrix} \text{ in} \end{aligned} \quad (\text{t})$$

which means that, with consideration of large deflection, the displacements shown in Fig. 9.36 should be increased by the amount given in Eq. (t).

The above example is intended to illustrate analytical procedures for and effects of large deflection. For simplicity, a statically loaded truss is used. Comparative studies of various influential parameters on dynamic response of a frame are presented in the next example.

EXAMPLE 9.7.2 Use the rigid frame given in Example 9.4.1 (see Fig. 9.11) to show various $P-\Delta$ effects and the influences of material as well as geometric nonlinearities on the frame's response. Structural properties and dynamic force can be found in the example just cited. This study involves the following seven cases:

- (A) Formulating $[K]$ and $[K_g]$ based on the general nonlinear analysis procedures given in Section 9.7.
- (B) Finding the buckling load of the frame by using the geometric string stiffness matrix presented in Section 6.6.3 (same model as shown in Fig. 9.35).
- (C) Linear analysis (L.A.) without $P-\Delta$ effect or geometric and material nonlinearities.

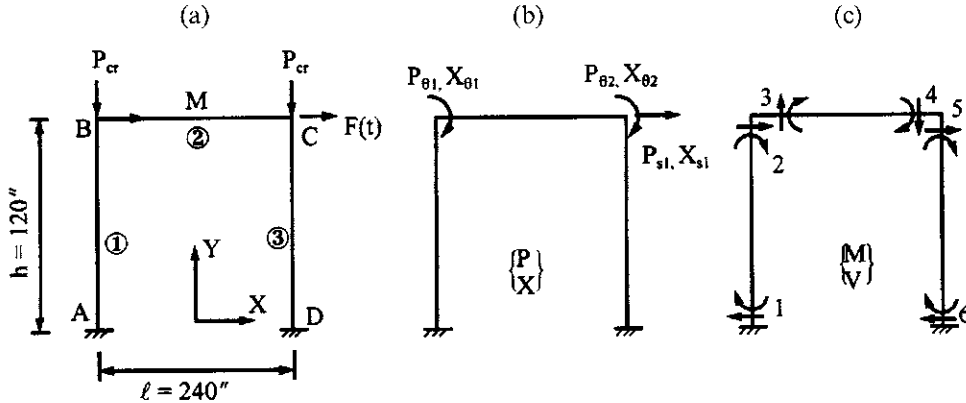


FIG. 9.37 One-story rigid frame for Example 9.7.2. (a) Given structure. (b) External action $\{P\}$, $\{X\}$. (c) Internal resistance $\{F\}$, $\{D\}$.

- (D) Nonlinear analysis (N.A.) having material nonlinearity of bilinear model with $p = 0.05$ but no $P-\Delta$ effect or large deflection.
- (E) Nonlinear analysis with $p = 0.05$ given in (D) combined with 4% of buckling load (N.A.; $0.04 P_{cr}$) but not including large deflection.
- (F) Same as (E) except for 20% of buckling load (N.A.; $0.2 P_{cr}$).
- (G) Nonlinear analysis with $p = 0.05$, 4% of critical load, and large deflection (N.A.; $0.04 P_{cr}$; Lg. D.).

Plot displacement vs time and moment at node 1 (M_1) vs time of these seven cases. Note that Case (D) is identical to the study of $p = 0.05$ in Example 9.4.1. The response behaviors of that example are shown in Figs. 9.12–9.14.

Solution: (A) *Formulation of $[K]$ and $[K_g]$* —for convenience, the rigid frame in Example 9.4.1 is shown again in Fig. 9.37.

The angles α for members 1, 2, and 3 are

$$\alpha_1 = -\tan^{-1}\left(\frac{B_y - A_y}{B_x - A_x}\right) = -\tan^{-1}\left(\frac{120 - 0}{-120 + 120}\right) = -\tan^{-1}(+\infty) = -90^\circ = -\pi/2 \quad (\text{a})$$

$$\alpha_2 = -\tan^{-1}\left(\frac{C_y - B_y}{C_x - B_x}\right) = -\tan^{-1}\left(\frac{120 - 120}{120 + 120}\right) = -\tan^{-1}(0) = 0^\circ = 0 \quad (\text{b})$$

$$\alpha_3 = -\tan^{-1}\left(\frac{D_y - C_y}{D_x - C_x}\right) = -\tan^{-1}\left(\frac{0 - 120}{120 - 120}\right) = -\tan^{-1}(-\infty) = 90^\circ = \pi/2 \quad (\text{c})$$

From Eq. (9.157), compatibility matrices, $[B]$, for members 1, 2, and 3 are respectively shown in Eqs. (d), (f), and (h).

$$\begin{bmatrix} 0 \\ \Delta\theta_2 \\ 0 \\ \Delta Y_2 \end{bmatrix} = \begin{bmatrix} 0 & 0 & 1 & 0 & 0 & 0 \\ 0 & 0 & 0 & 1 & 0 & 0 \\ \sin \alpha_1 & 0 & 0 & 0 & \cos \alpha_1 & 0 \\ 0 & -\sin \alpha_1 & 0 & 0 & 0 & -\cos \alpha_1 \end{bmatrix} \begin{bmatrix} 0 \\ \Delta x_s \\ 0 \\ \Delta x_{\theta 1} \\ 0 \\ 0 \end{bmatrix} \quad (\text{d})$$

or

$$\begin{Bmatrix} \Delta\theta_2 \\ \Delta Y_2 \end{Bmatrix} = \begin{bmatrix} 0 & 1 \\ -\sin \alpha_1 & 0 \end{bmatrix} \begin{Bmatrix} \Delta x_s \\ \Delta x_{\theta 1} \end{Bmatrix} = [B]_1 \begin{Bmatrix} \Delta x_s \\ \Delta x_{\theta 1} \end{Bmatrix} \quad (e)$$

$$\begin{Bmatrix} \Delta\theta_3 \\ \Delta\theta_4 \\ 0 \\ 0 \end{Bmatrix} = \begin{bmatrix} 0 & 0 & 1 & 0 & 0 & 0 \\ 0 & 0 & 0 & 1 & 0 & 0 \\ \sin \alpha_2 & 0 & 0 & 0 & \cos \alpha_2 & 0 \\ 0 & -\sin \alpha_2 & 0 & 0 & 0 & -\cos \alpha_2 \end{bmatrix} \begin{Bmatrix} \Delta x_s \\ \Delta x_s \\ \Delta x_{\theta 1} \\ \Delta x_{\theta 2} \\ 0 \\ 0 \end{Bmatrix} \quad (f)$$

or

$$\begin{Bmatrix} \Delta\theta_3 \\ \Delta\theta_4 \end{Bmatrix} = \begin{bmatrix} 1 & 0 \\ 0 & 1 \end{bmatrix} \begin{Bmatrix} \Delta x_{\theta 1} \\ \Delta x_{\theta 2} \end{Bmatrix} = [B]_2 \begin{Bmatrix} \Delta x_{\theta 1} \\ \Delta x_{\theta 2} \end{Bmatrix} \quad (g)$$

$$\begin{Bmatrix} \Delta\theta_5 \\ 0 \\ \Delta Y_5 \\ 0 \end{Bmatrix} = \begin{bmatrix} 0 & 0 & 1 & 0 & 0 & 0 \\ 0 & 0 & 0 & 1 & 0 & 0 \\ \sin \alpha_3 & 0 & 0 & 0 & \cos \alpha_3 & 0 \\ 0 & -\sin \alpha_3 & 0 & 0 & 0 & -\cos \alpha_3 \end{bmatrix} \begin{Bmatrix} \Delta x_s \\ \Delta x_{\theta 2} \\ 0 \\ 0 \\ 0 \\ 0 \end{Bmatrix} \quad (h)$$

or

$$\begin{Bmatrix} \Delta\theta_5 \\ \Delta Y_5 \end{Bmatrix} = \begin{bmatrix} 0 & 1 \\ \sin \alpha_3 & 0 \end{bmatrix} \begin{Bmatrix} \Delta x_s \\ \Delta x_{\theta 2} \end{Bmatrix} = [B]_3 \begin{Bmatrix} \Delta x_s \\ \Delta x_{\theta 2} \end{Bmatrix} \quad (i)$$

The structural stiffness matrix can be assembled as

$$\begin{aligned} [K] &= [B]_1^T \begin{bmatrix} k_{12}^1 & k_{24}^1 \\ k_{42}^1 & k_{44}^1 \end{bmatrix} [B]_1 + [B]_2^T \begin{bmatrix} k_{11}^2 & k_{12}^2 \\ k_{21}^2 & k_{22}^2 \end{bmatrix} [B]_2 + [B]_3^T \begin{bmatrix} k_{11}^3 & k_{13}^3 \\ k_{31}^3 & k_{33}^3 \end{bmatrix} [B]_3 \\ &= \begin{bmatrix} k_{11}^2 + k_{22}^1 & k_{12}^2 & -k_{24}^1 \sin \alpha_1 \\ k_{22}^2 + k_{11}^3 & k_{13}^3 \sin \alpha_3 & \\ \text{symm} & k_{44}^1 \sin^2 \alpha_1 + k_{33}^3 \sin^2 \alpha_3 & \end{bmatrix} \end{aligned} \quad (j)$$

which is identical to Eq. (b) in Example 9.4.1.

Similarly, the geometric string stiffness matrix is assembled as

$$[K_g] = \frac{-P_{cr}}{h} \begin{bmatrix} 0 & 0 & 0 \\ 0 & 0 & 0 \\ 0 & 0 & 2 \end{bmatrix} \quad (k)$$

which is obtained by assuming that the axial load on members 1 and 3 is due to externally applied load, P_{cr} , only.

(B) *Fundamental buckling load*—using the determinant of the summation of Eqs. (j) and (k) as

$$|[K] + [K_g]| = 0 \quad (l)$$

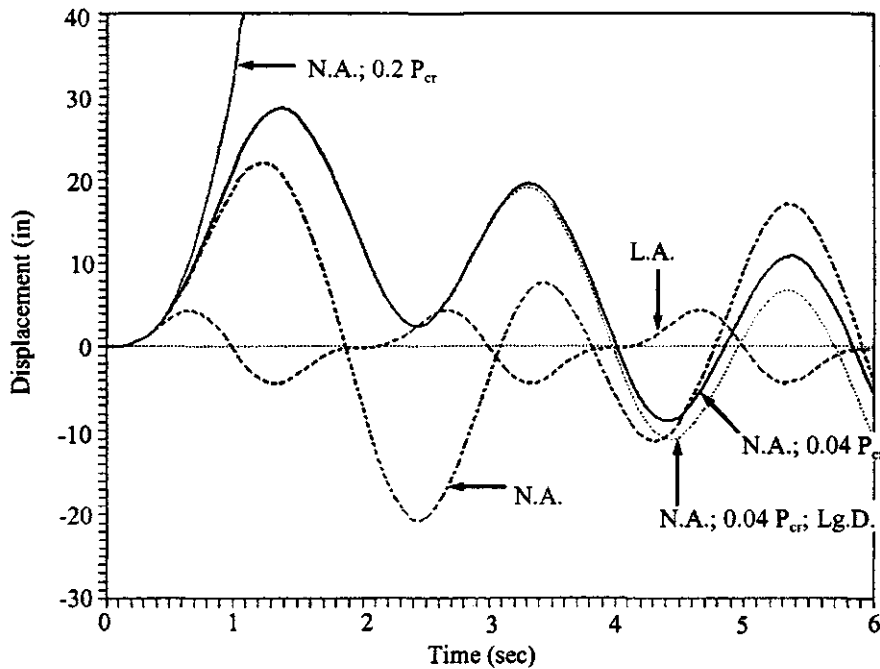


FIG. 9.38 Lateral displacement vs. time in Example 9.7.2.

and employing the given member properties gives

$$P_{cr} = \frac{48EI}{7h^2} = \frac{48}{7} \frac{1000}{[(10)(12)]^2} = 0.476 \text{ k} \quad (\text{m})$$

(C) *Linear analysis (L.A.)*—the motion equation is

$$M\Delta\ddot{x}_s + K\Delta x_s = \Delta F(t) \quad (\text{n})$$

in which $[K]$ is condensed as shown in Eqs. (d), (e), and (f) of Example 9.4.1. Numerical integration is then applied for structural response. The emphasis here and in later cases is on formulating the structural stiffness matrix.

(D) *Nonlinear analysis (N.A.)*—the motion equation is similar to Eq. (n). In this case $[K]$ must be modified in accordance with the plastic deformations of individual members and then condensed to become K

(E) *Nonlinear analysis with 4% of P_{cr} (N.A., $0.04 P_{cr}$)*—the motion equation is similar to Eq. (n); K is condensed from $([K] + [K_g])$ in which $[K_g]$ has $0.04 P_{cr} = 0.01904 \text{ k}$. Note that the axial forces on members 1 and 3 are solely due to the external loads; the change of internal axial forces is not considered for various deformation states. Member 2 is not involved in $[K_g]$.

(F) *Nonlinear analysis with 20% of P_{cr} (N.A., $0.2 P_{cr}$)*—the analysis is identical to (E) except that $0.2 P_{cr}=0.0952 \text{ k}$ is used in $[K_g]$.

(G) *Nonlinear analysis with 4% of P_{cr} and large deflection (N.A., $0.04 P_{cr}$, Lg. D.)*—the motion equation, Eq. (n), still applies to this analysis. However, $[K]$ and $[K_g]$ must be modified to include geometric changes in the structural nodes according to the state of inelastic deformation at each time increment.

Using numerical integration yields lateral displacement, x_s , vs time, and moment, M_1 , vs time shown in Figs. 9.38 and 9.39, respectively. Observation of these figures may be summarized as: linear analysis yields smaller displacement but larger internal moments than does nonlinear

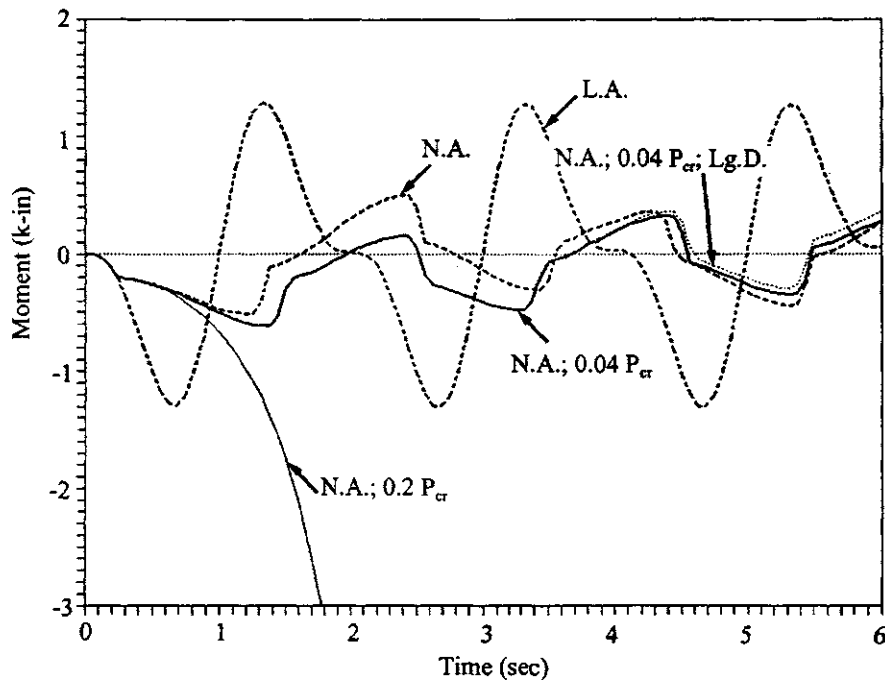


FIG. 9.39 Moment M_1 vs. time in Example 9.7.2.

analysis; large deflection gradually increases the permanent set of displacement and moments; the $P-\Delta$ effect can significantly increase structural response (with 20% of P_{cr} , the structure collapsed before 1 sec of excitation).

9.8. INTERACTION EFFECT ON BEAM COLUMNS

We have so far discussed several hysteresis models, based on pure bending only, for which normal stress and strain are shown in Fig. 9.40a. If a member is subjected to a combined bending moment and axial load, then normal stress and strain of the cross-section will be as shown in Fig. 9.40b. Thus the moment-curvature relationship is influenced by the magnitude and direction of applied axial load. This phenomenon is called the *interaction effect*. A typical moment-curvature-axial load relationship is shown in Fig. 9.41 in which we may observe that moment capacity decreases as compressive axial load increases. Since structural columns are mainly subjected to bending and compression, the compressive force has significant influence on the column's moment resistance capacity. The reduced moment-curvature relationship should be used in the hysteresis models for nonlinear analysis. For example, the reduced plastic moment capacity, M'_p , for a wide-flange member with axial load P can be calculated by the following equation [1]

$$M'_p = 1.2 \left(1 - \frac{P_u}{P_y} \right) M_p \leq M_p \quad (9.158)$$

where P_y is axial yield load without bending and P_u is the required axial strength. When a member in a three-dimensional system has biaxial bending and torsion, moment capacity should be further reduced due to torsional effect [7]. If axial load is time-dependent, then the moment-curvature-axial load relationship becomes highly complicated because of independent loading reversal of moments and axial force [5,6,8]. Research in this area has not reached maturity.

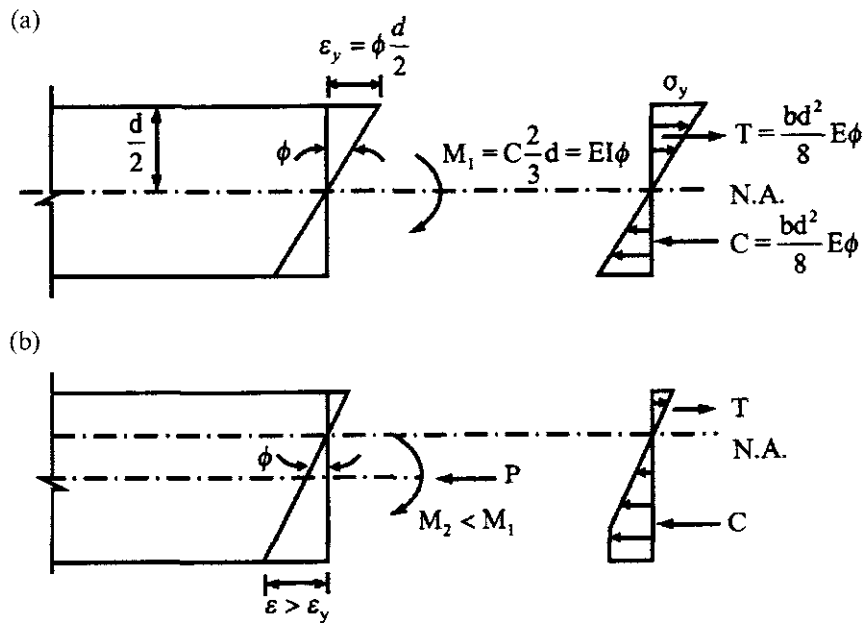


FIG. 9.40 Moment–axial load interaction effect. (a) Pure bending moment. (b) Coupling of bending moment and axial load.

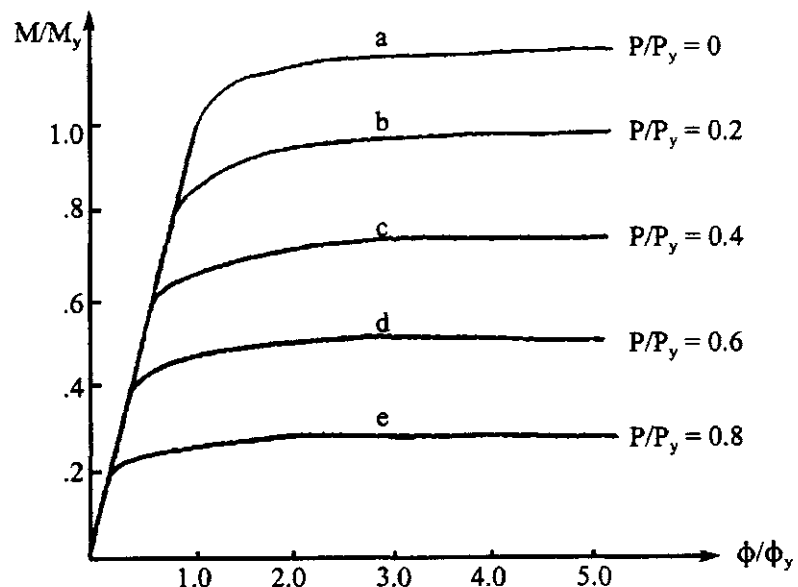


FIG. 9.41 Moment-curvature-axial load relationship.

9.9. ELASTO-PLASTIC ANALYSIS OF CONSISTENT MASS SYSTEMS

9.9.1. Stiffness Matrix Formulation

As shown by the elasto-plastic branch of II in Fig. 9.4, the moment-curvature relationship changes linearly from zero to ultimate moment capacity, called *plastic moment* (due to bending only) or *reduced plastic moment* (due to interaction of axial force and moment). A section of the member has a plastic hinge that behaves like a real hinge with a constant ultimate moment. When the member's section rotates in reverse, the moment-rotation relationship becomes elastically linear, and the plastic hinge is removed. This elastic behavior remains unchanged until the moment reaches ultimate moment capacity. Consequently, a plastic hinge is assumed and a cyclic process is applied.

Plastic hinge formation in a member of a consistent mass model should be similar to the behavior described above. Therefore, this formulation represents three possibilities, i.e. a hinge at the *i*-end, *j*-end, or both ends. Presented here is an elasto-plastic analysis of structural systems composed of Timoshenko beams. This general formulation can be simplified to include the Bernoulli-Euler theory of bending deformation only. By following Section 6.7.1, we can derive displacement functions and their associated functions of rotation and slope; results are summarized in Table 9.3 for the three cases of hinge formation. Note that, for simplicity, displacement functions for the hinge at the *j*-end are derived by using the origin of *x* at *j*.

Substituting displacement functions and their associated functions in Table 9.3 into Eqs. (6.155), (6.160), and (6.172), respectively, yields stiffness coefficient $[K_e]$ and mass coefficient matrices $[M_e^t]$, $[M_e^r]$ as well as geometric coefficient matrix $[K_{eg}]$. Results are listed as below.

(A) *Hinge at i-end*

$$[K_e] = \frac{12EI}{(4 + \phi)} \begin{bmatrix} 0 & 0 & 0 & 0 \\ \text{symm} & 1/L & -1/L^2 & -1/L^2 \\ & & 1/L^3 & 1/L^3 \\ & & & 1/L^3 \end{bmatrix} \quad (9.159)$$

$$[M_e^t] = \frac{mL}{(4 + \phi)^2} \begin{bmatrix} 0 & 0 & 0 & 0 \\ \text{symm} & 32L^2/105 & -7\phi L/30 + 22L/35 & -4\phi L/15 - 48L/35 \\ & & \phi^2/3 - 9\phi/5 + 132/35 & -\phi^2/6 - 13\phi/10 - 78/35 \\ & & & \phi^2/3 - 4\phi/5 + 272/35 \end{bmatrix} \quad (9.160)$$

$$[M_e^r] = \frac{\rho I}{(4 + \phi)^2} \begin{bmatrix} 0 & 0 & 0 & 0 \\ \text{symm} & (\phi^2 + 16/5)L & \phi - 16/5 & \phi - 16/5 \\ & & 96/5L & 96/5L \\ & & & 96/5L \end{bmatrix} \quad (9.161)$$

$$[K_{eg}] = \frac{P}{(4 + \phi)^2} \begin{bmatrix} 0 & 0 & 0 & 0 \\ \text{symm} & 16L/5 & -16/5 & -16/5 \\ & & (\phi^2 + 8\phi + 19.2)/L & (\phi^2 + 8\phi + 19.2)/L \\ & & & (\phi^2 + 8\phi + 19.2)/L \end{bmatrix} \quad (9.162)$$

TABLE 9.3 Displacement Functions and Associated Functions

Boundary Conditions $x=0$	Displacement Functions y		Rotation Function $y^a = -zy^{\dagger}$	Slope Function y'
	Displacement Functions y	Rotation Function $y^a = 0$		
age at i	$y = 0, y^{b'} = 0$	$y_1 = 0$	$y_2 = \frac{z}{4+\phi}[2 - 6r^2 - \phi]$	$y'_1 = 0$
$y = 0, y^{b''} = 0$	$y = 0, y^{b'} = q_2$	$y_2 = \frac{-L}{4+\phi}[\phi r^* - 2r^3 + 6r - (4+\phi)r]$	$y_2 = \frac{z}{4+\phi}(6r^2 - 2)$	$y'_2 = \frac{1}{4+\phi}(6r^2 - 2)$
$y = -q_3, y^{b''} = 0$	$y = 0, y^{b'} = 0$	$y_3 = \frac{1}{4+\phi}[\phi r^* - 2r^3 + 6r - (4+\phi)]$	$y_3 = \frac{-z}{4+\phi}(6 - 6r^2)$	$y'_3 = \frac{1}{4+\phi}(6 + \phi - 6r^2)$
$y = 0, y^{b''} = 0$	$y = q_4, y^{b'} = 0$	$y_4 = \frac{1}{4+\phi}[\phi(r-1)^* - 2(2+r^3) + 6r + \phi + 4]$	$y_4 = \frac{-z}{4+\phi}(6 - 6r^3)$	$y'_4 = \frac{1}{(4+\phi)L}(6 + \phi - 6r^2)$
age at j	$y = 0, y^{b''} = 0$	$y_1 = \frac{-L}{4+\phi}(\phi r^* + 6r - r(4+\phi) - 2r^3)$	$y_1 = \frac{z}{4+\phi}(2 - \phi - 6r^2)$	$y'_1 = \frac{1}{4+\phi}(6r^2 - 2)$
$y = 0, y^{b''} = 0$	$y = 0, y^{b'} = 0$	$y_2 = 0$	$y_2 = 0$	$y'_2 = 0$
$y = 0, y^{b''} = 0$	$y = -q_3, y^{b'} = 0$	$y_3 = \frac{1}{4+\phi}[\phi(r-1)^* - 2(2+r^3) + 6r + (4+\phi)]$	$y_2 = \frac{z}{(4+\phi)L}(6r^2 - 6)$	$y'_3 = \frac{1}{(4+\phi)L}(6 + \phi - 6r^2)$
$y = q_4, y^{b''} = 0$	$y = 0, y^{b'} = 0$	$y_4 = \frac{1}{4+\phi}[\phi r^* - 2r^3 + 6r - (4+\phi)]$	$y_4 = \frac{z}{(4+\phi)L}(6r^2 - 6)$	$y'_4 = \frac{1}{(4+\phi)L}(6 + \phi - 6r^2)$
age at j	$y = 0, y^{b''} = 0$	$y_1 = y_2 = 0$	$y_1 = y_2 = 0$	$y'_1 = y'_2 = 0$
$y = -q_3, y^{b''} = 0$	$y = 0, y^{b'} = 0$	$y_3 = r - 1$	$y_3 = -z/L$	$y'_3 = 1/L$
$y = 0, y^{b''} = 0$	$y = q_4, y^{b'} = 0$	$y_4 = r$	$y_4 = -z/L$	$y'_4 = 1/L$

The term with * in the displacement function, y , is dropped in the rotation function, y^a .

When the bending deformation only is considered, the above equations become

$$[K_e] = 3EI \begin{bmatrix} 0 & 0 & 0 & 0 \\ \text{symm} & 1/L & -1/L^2 & -1/L^2 \\ & & 1/L^3 & 1/L^3 \\ & & & 1/L^3 \end{bmatrix} \quad (9.163)$$

$$[M_e^t] = \frac{mL}{420} \begin{bmatrix} 0 & 0 & 0 & 0 \\ \text{symm} & 8L^2 & 33L/2 & 36L \\ & & 99 & -117/2 \\ & & & 204 \end{bmatrix} \quad (9.164)$$

$$[M_e^r] = \frac{\rho I}{5} \begin{bmatrix} 0 & 0 & 0 & 0 \\ \text{symm} & L & -1 & -1 \\ & & 6/L & 6/L \\ & & & 6/L \end{bmatrix} \quad (9.165)$$

$$[K_{eg}] = \frac{P}{5} \begin{bmatrix} 0 & 0 & 0 & 0 \\ \text{symm} & L & -1 & -1 \\ & & 6/L & 6/L \\ & & & 6/L \end{bmatrix} \quad (9.166)$$

(B) *Hinge at j-end*

$$[K_e] = \frac{12EI}{4+\phi} \begin{bmatrix} 1/L & 0 & -1/L^2 & -1/L^2 \\ \text{symm} & 0 & 0 & 0 \\ & & 1/L^3 & 1/L^3 \\ & & & 1/L^3 \end{bmatrix} \quad (9.167)$$

$$[M_e^t] = \frac{mL}{(4+\phi)^2} \begin{bmatrix} \frac{32L^2}{105} & 0 & \frac{-4\phi L}{15} - \frac{48L}{35} & \frac{7\phi L}{30} + \frac{22L}{35} \\ 0 & 0 & 0 & 0 \\ \text{symm} & \frac{\phi^2}{3} - \frac{4\phi}{5} + \frac{272}{35} & -\frac{\phi^2}{6} - \frac{13}{10}\phi - \frac{78}{35} & \frac{\phi^2}{3} - \frac{9}{5}\phi + \frac{132}{35} \end{bmatrix} \quad (9.168)$$

$$[M_e^r] = \frac{\rho I}{(4+\phi)^2} \begin{bmatrix} \left(\phi^2 + \frac{16}{5}\right)L & 0 & \phi - \frac{16}{5} & \phi - \frac{16}{5} \\ 0 & 0 & 0 & 0 \\ \text{symm} & \frac{96}{5L} & \frac{96}{5L} & \frac{96}{5L} \end{bmatrix} \quad (9.169)$$

$$[K_{eg}] = \frac{P}{(4+\phi)^2} \begin{bmatrix} \frac{16L}{5} & 0 & -\frac{16}{5} & -\frac{16}{5} \\ 0 & 0 & 0 & 0 \\ & \frac{(\phi+8\phi+19.2)}{L} & \frac{(\phi^2+8\phi+19.2)}{L} & \\ \text{symm} & & \frac{(\phi^2+8\phi+19.2)}{L} & \end{bmatrix} \quad (9.170)$$

For bending deformation only, Eqs. (9.167)–(9.170) become

$$[K_e] = 3EI \begin{bmatrix} 1/L & 0 & -1/L^2 & -1/L^2 \\ 0 & 0 & 0 & 0 \\ \text{symm} & & 1/L^3 & 1/L^3 \\ & & 1/L^3 & \end{bmatrix} \quad (9.171)$$

$$[M_e^t] = \frac{mL}{420} \begin{bmatrix} 8L^2 & 0 & -36L & 33L/2 \\ 0 & 0 & 0 & 0 \\ \text{symm} & & 204 & -117/2 \\ & & & 99 \end{bmatrix} \quad (9.172)$$

$$[M_e^r] = \frac{\rho I}{5} \begin{bmatrix} L & 0 & -1 & -1 \\ 0 & 0 & 0 & 0 \\ \text{symm} & & 6/L & 6/L \\ & & 6/L & \end{bmatrix} \quad (9.173)$$

$$[K_{eg}] = \frac{P}{5} \begin{bmatrix} L & 0 & -1 & -1 \\ 0 & 0 & 0 & 0 \\ \text{symm} & & 6/L & 6/L \\ & & 6/L & \end{bmatrix} \quad (9.174)$$

(C) *Hinges at both ends*—for this case, shear deformation does not affect the derivation of stiffness and mass coefficients. Thus the following Eqs. (9.175)–(9.178) apply to cases of (1) bending and shear deformations, and (2) bending deformation only:

$$[K_e] = 0 \quad (9.175)$$

$$[M_e^t] = \frac{mL}{3} \begin{bmatrix} 0 & 0 & 0 & 0 \\ 0 & 0 & 0 & 0 \\ \text{symm} & & 1 & -1/2 \\ & & & 1 \end{bmatrix} \quad (9.176)$$

$$[M_e^r] = \frac{\rho I}{L} \begin{bmatrix} 0 & 0 & 0 & 0 \\ 0 & 0 & 0 & 0 \\ \text{symm} & & 1 & 1 \\ & & & 1 \end{bmatrix} \quad (9.177)$$

$$[K_{eg}] = \frac{P}{L} \begin{bmatrix} 0 & 0 & 0 & 0 \\ & 0 & 0 & 0 \\ & & 1 & 1 \\ \text{symm} & & & 1 \end{bmatrix} \quad (9.178)$$

9.9.2. Moments, Shears and Plastic Hinge Rotations

As introduced in the preceding section, when an internal moment reaches ultimate moment capacity, a plastic hinge forms at that node and rotates in accordance with the moment-curvature behavior shown in branch II of Fig. 9.4. A hinge rotation can theoretically increase infinitely until it decreases. The amount of increase, however, is actually limited by material ductility capacity. When a hinge rotation decreases during response analysis, this indicates that the member has started to move in reverse. Consequently, the plastic hinge is removed and the member end becomes elastic. Internal moments and shears due to member deformation can be calculated on the basis of the force-deformation relationship established in Eq. (m) of Example 6.3.2,

$$\begin{Bmatrix} M \\ V \end{Bmatrix} = ([S] - [S_g]) \begin{bmatrix} A_\theta & 0 \\ 0 & A_s \end{bmatrix}^T \begin{Bmatrix} x_\theta \\ x_s \end{Bmatrix} \quad (9.179)$$

in which $[S]$ is the stiffness coefficient matrix, which is arranged using the notations in Eq. (6.159):

$$[S] = \begin{bmatrix} \begin{bmatrix} \backslash & SM\theta & \backslash \\ & & \backslash \end{bmatrix} & \begin{bmatrix} \backslash & SMY & \backslash \\ & & \backslash \end{bmatrix} \\ \text{symm} & \begin{bmatrix} \backslash & SVY & \backslash \\ & & \backslash \end{bmatrix} \end{bmatrix} \quad (9.180)$$

where the submatrices are diagonal band matrices with dimensions of $2(NM) \times 2(NM)$ and NM equals the number of members. $[S_g]$ is also composed of element matrices as given in Eq. (6.177) as

$$[S_g] = \begin{bmatrix} \begin{bmatrix} \backslash & GM\theta & \backslash \\ & & \backslash \end{bmatrix} & \begin{bmatrix} \backslash & GMY & \backslash \\ & & \backslash \end{bmatrix} \\ \text{symm} & \begin{bmatrix} \backslash & GVY & \backslash \\ & & \backslash \end{bmatrix} \end{bmatrix} \quad (9.181)$$

Since the coefficients of stiffness and geometric matrices can be modified according to plastic hinge conditions, Eq. (9.179) is a general equation for both elastic and elasto-plastic analyses.

When the structure is elastic, internal joint rotations must be compatible with external joint rotations. This compatibility condition requires the following:

$$\{\theta\} - [A_\theta]^T \{x_\theta\} = 0 \quad (9.182)$$

When the structure is beyond its elastic limit, Eq. (9.182) cannot be satisfied because some plastic hinges may have developed. Plastic hinge rotations, $\{H\}$, can be calculated by evaluating the difference between external joint rotations and internal rotations at member end

$$\{H\} = \{\theta\} - [A_\theta]^T \{x_\theta\} \quad (9.183)$$

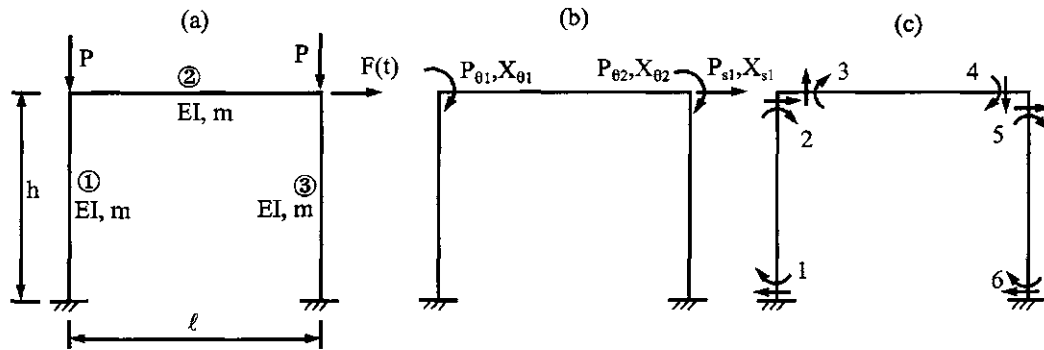


FIG. 9.42 Example 9.9.1. (a) Given structure. (b) External actions. (c) Internal resistance.

for which we first calculate moments from Eq. 9.179 as

$$\{M\} = [SM\theta - GM\theta][A_\theta]^T\{x_\theta\} + [SMY - GMY][A_s]^T\{x_s\} \quad (9.184)$$

Then obtain the rotations from the following force-deformation relationship:

$$\{\theta\} = [SM\theta - GM\theta]^{-1}(\{M\} - [SMY - GMY][A_s]^T\{x_s\}) \quad (9.185)$$

EXAMPLE 9.9.1 Using the consistent mass model with bending deformation, transverse inertia, and the incremental linear acceleration method, find the joint displacements, velocities, accelerations, and internal moments of the framework shown in Fig. 9.42a. Assume that $F(t) = 0.025 \sin \pi t$ k (111.205 sin πt N), $P = 1k(4.448222 \times 10^3$ N), $h = 10$ ft (3.048 m), $\ell = 20$ ft (6.096 m), $EI = 1000$ k in 2 (2.86967168 kN m 2), $m = 5.555 \times 10^{-6}$ k sec 2 /in 2 (3.905 kg sec 2 /m 2), $\bar{\rho} = 0.1$, $\bar{\rho} = 1.5$ rad/sec, and $\Delta t = 0.1$ sec.

Solution: Let the diagrams of external action and internal resistance be as shown in Fig. 9.42b and c, respectively, from which the equilibrium matrices can be formulated as follows:

$$[A_\theta] = \begin{bmatrix} 0 & 1 & 1 & 0 & 0 & 0 \\ 0 & 0 & 0 & 1 & 1 & 0 \end{bmatrix} \quad (a)$$

$$[A_s] = \begin{bmatrix} 0 & 1 & 0 & 0 & 1 & 0 \end{bmatrix} \quad (b)$$

The stiffness coefficients of the system are

$$[S] = \begin{bmatrix} [SM\theta] & [SMY] \\ [SMY] & [SVY] \end{bmatrix} = \begin{bmatrix} [SM\theta]_1 & 0 & 0 & [SMY]_1 & 0 & 0 \\ 0 & [SM\theta]_2 & 0 & 0 & [SMY]_2 & 0 \\ 0 & 0 & [SM\theta]_3 & 0 & 0 & [SMY]_3 \\ \text{symm} & & & [SVY]_1 & 0 & 0 \\ & & & 0 & [SVY]_2 & 0 \\ & & & 0 & 0 & [SVY]_3 \end{bmatrix} \quad (c)$$

in which subscripts refer to the member number. As given in Eqs. (6.158) and (6.159),

$$[SM\theta]_1 = [SM\theta]_3 = \frac{EI}{h} \begin{bmatrix} 4 & 2 \\ 2 & 4 \end{bmatrix} = \begin{bmatrix} 33.3333 & 16.6667 \\ 16.6667 & 33.3333 \end{bmatrix}$$

$$[SM\theta]_2 = \frac{EI}{\ell} \begin{bmatrix} 4 & 2 \\ 2 & 4 \end{bmatrix} = \begin{bmatrix} 16.6667 & 8.3333 \\ 8.3333 & 16.6667 \end{bmatrix}$$

$$[SMY]_1 = [SMY]_3 = \frac{EI}{\ell h^2} \begin{bmatrix} -6 & -6 \\ -6 & -6 \end{bmatrix} = \begin{bmatrix} -0.4167 & -0.4167 \\ -0.4167 & -0.4167 \end{bmatrix}$$

$$[SMY]_2 = \frac{EI}{\ell h^2} \begin{bmatrix} -6 & -6 \\ -6 & -6 \end{bmatrix} = \begin{bmatrix} -0.1042 & -0.1042 \\ -0.1042 & -0.1042 \end{bmatrix}$$

$$[SVY]_1 = [SVY]_3 = \frac{EI}{h^3} \begin{bmatrix} 12 & 12 \\ 12 & 12 \end{bmatrix} = \begin{bmatrix} 0.00694 & 0.00694 \\ 0.00694 & 0.00694 \end{bmatrix}$$

$$[SVY]_2 = \frac{EI}{\ell^3} \begin{bmatrix} 12 & 12 \\ 12 & 12 \end{bmatrix} = \begin{bmatrix} 0.00087 & 0.00087 \\ 0.00087 & 0.00087 \end{bmatrix}$$

The mass coefficients can also be expressed as

$$[M_e^t] = \begin{bmatrix} [MM\theta^t] & [MMY^t] \\ [MMY^t] & [MVY^t] \end{bmatrix} = \begin{bmatrix} [MM\theta^t]_1 & 0 & 0 & [MMY^t]_1 & 0 & 0 \\ [MM\theta^t]_2 & 0 & 0 & [MMY^t]_2 & 0 & 0 \\ [MM\theta^t]_3 & 0 & 0 & [MMY^t]_3 & 0 & 0 \\ [MVY^t]_1 & 0 & 0 & [MVY^t]_1 & 0 & 0 \\ [MVY^t]_2 & 0 & 0 & [MVY^t]_2 & 0 & 0 \\ [MVY^t]_3 & 0 & 0 & [MVY^t]_3 & 0 & 0 \end{bmatrix}_{\text{symm}} \quad (d)$$

According to Eqs. (6.168) and (6.170)

$$[MM\theta^t]_1 = [MM\theta^t]_3 = mh^3 \begin{bmatrix} 1/105 & -1/140 \\ -1/140 & 1/105 \end{bmatrix} = \begin{bmatrix} 0.09142 & -0.06856 \\ -0.06856 & 0.09142 \end{bmatrix}$$

$$[MM\theta^t]_2 = m\ell^3 \begin{bmatrix} 1/105 & -1/140 \\ -1/140 & 1/105 \end{bmatrix} = \begin{bmatrix} 0.73135 & -0.54852 \\ -0.54852 & 0.73135 \end{bmatrix}$$

$$[MMY^t]_1 = [MMY^t]_3 = mh^2 \begin{bmatrix} -11/210 & 13/420 \\ 13/420 & -11/210 \end{bmatrix} = \begin{bmatrix} -0.004190 & 0.002476 \\ 0.002476 & -0.004190 \end{bmatrix}$$

$$[MMY^t]_2 = m\ell^2 \begin{bmatrix} -11/210 & 13/420 \\ 13/420 & -11/210 \end{bmatrix} = \begin{bmatrix} -0.016760 & 0.009904 \\ 0.009904 & -0.016760 \end{bmatrix}$$

$$[MVY^t]_1 = [MVY^t]_3 = mh \begin{bmatrix} 13/35 & -9/70 \\ -9/70 & 13/35 \end{bmatrix} = \begin{bmatrix} 0.000248 & -0.000086 \\ -0.000086 & 0.000248 \end{bmatrix}$$

$$[MVY^t]_2 = m\ell \begin{bmatrix} 13/35 & -9/70 \\ -9/70 & 13/35 \end{bmatrix} = \begin{bmatrix} 0.00495 & -0.000171 \\ -0.000171 & 0.00495 \end{bmatrix}$$

Similarly, the coefficients in the geometric matrix are

$$[S_g] = \begin{bmatrix} [GM\theta] & [GMY] \\ [GMY] & [GVY] \end{bmatrix} = \begin{bmatrix} [GM\theta]_1 & 0 & 0 & [GMY]_1 & 0 & 0 \\ & [0]_2 & 0 & 0 & [0]_2 & 0 \\ & & [GM\theta]_3 & 0 & 0 & [GMY]_3 \\ & & & [GVY]_1 & 0 & 0 \\ & & & & [0]_2 & 0 \\ & & & & & [GVY]_3 \end{bmatrix}_{\text{symm}} \quad (e)$$

of which the coefficients are shown in Eq. (6.138) or Eqs. (6.173)–(6.177) (let $\phi = 0$)

$$[GM\theta]_1 = [GM\theta]_3 = Ph \begin{bmatrix} 2/15 & -1/30 \\ -1/30 & 2/15 \end{bmatrix} = \begin{bmatrix} 16 & -4 \\ -4 & 16 \end{bmatrix}$$

$$[GMY]_1 = [GMY]_3 = P \begin{bmatrix} -1/10 & -1/10 \\ -1/10 & -1/10 \end{bmatrix} = \begin{bmatrix} -0.1 & -0.1 \\ -0.1 & -0.1 \end{bmatrix}$$

$$[GVY]_1 = [GVY]_3 = \frac{P}{h} \begin{bmatrix} 6/5 & 6/5 \\ 6/5 & 6/5 \end{bmatrix} = \begin{bmatrix} 0.01 & 0.01 \\ 0.01 & 0.01 \end{bmatrix}$$

Consequently, the structural stiffness, geometric and mass matrices become

$$[K] = \begin{bmatrix} A_\theta & 0 \\ 0 & A_s \end{bmatrix} [S] \begin{bmatrix} A_\theta & 0 \\ 0 & A_s \end{bmatrix}^T = \begin{bmatrix} 50 & 8.3333 & -0.4167 \\ & 50 & -0.4167 \\ & & 0.01389 \end{bmatrix}_{\text{symm}} \quad (f)$$

$$[K_g] = \begin{bmatrix} A_\theta & 0 \\ 0 & A_s \end{bmatrix} [S_g] \begin{bmatrix} A_\theta & 0 \\ 0 & A_s \end{bmatrix}^T = \begin{bmatrix} 16 & 0 & -0.10 \\ & 16 & -0.10 \\ & & 0.02 \end{bmatrix}_{\text{symm}} \quad (g)$$

$$[M] = \begin{bmatrix} A_\theta & 0 \\ 0 & A_s \end{bmatrix} [M_e^t] \begin{bmatrix} A_\theta & 0 \\ 0 & A_s \end{bmatrix}^T + \begin{bmatrix} 0 & 0 & 0 \\ & 0 & 0 \\ & & ml \end{bmatrix} = \begin{bmatrix} 0.822774 & -0.548517 & -0.00419 \\ & 0.822774 & -0.00419 \\ & & 0.001829 \end{bmatrix}_{\text{symm}} \quad (h)$$

From Section 3.2.2

$$\alpha = \bar{\rho}\bar{p} = 0.1(1.5) = 0.15; \quad \beta = \bar{\rho}/\bar{p} = 0.1/1.5 = 0.06667$$

the damping matrix is

$$[C] = \alpha[M] + \beta[K - K_g] = \begin{bmatrix} 2.390076 & 0.473277 & -0.021734 \\ & 2.390076 & -0.021734 \\ & \text{symm} & -0.000134 \end{bmatrix} \quad (\text{i})$$

By employing incremental techniques of the linear acceleration method, we can perform the following calculations. At $t=0$

$$\{A\} = \frac{-6}{\Delta t} \{\dot{x}_{n-1}\} - 3\{\ddot{x}_{n-1}\} = 0; \quad \{B\} = -3\{\dot{x}_{n-1}\} - \frac{\Delta t}{2} \{\ddot{x}_{n-1}\} = 0$$

$$\{\Delta F(t)\} = 0; \quad \{\Delta \bar{F}\} = \{\Delta F(t) - [M]\{A\} - \frac{3}{\Delta t}\{B\}\} = 0$$

$$[\tilde{K}] = \frac{6}{(\Delta t)^2} [M] + [K - K_g] + \frac{3}{\Delta t} [C] = \begin{bmatrix} 559.366 & -306.580 & -3.4826 \\ & 559.366 & -3.4826 \\ & \text{symm} & 1.0873 \end{bmatrix}$$

$$[\tilde{K}]^{-1} = \begin{bmatrix} 0.0024006 & 0.0012967 & 0.011842 \\ & 0.0024005 & 0.011842 \\ & \text{symm} & 0.995610 \end{bmatrix} \quad (\text{j})$$

$$\{\Delta x\} = [\tilde{K}]^{-1} \{\Delta \bar{F}\} = 0; \quad \{x_n\} = \{x_{n-1}\} + \{\Delta x\} = 0$$

$$\{\dot{x}_n\} = \{\dot{x}_{n-1}\} + \frac{3}{\Delta t} \{\Delta t\} + \{B\} = 0; \quad \{\ddot{x}_n\} = \{\ddot{x}_{n-1}\} + \frac{6}{(\Delta t)^2} \{\Delta x\} + \{A\} = 0$$

At $t=0.1$ sec, in a manner similar to the preceding calculations, $\{x\}$, $\{\dot{x}\}$, and $\{\ddot{x}\}$ can be found as follows:

$$\{A\} = 0; \quad \{B\} = 0$$

$$\{\Delta F(t)\} = \begin{Bmatrix} 0 \\ 0 \\ 0.025 \sin(0.1\pi) \end{Bmatrix} = \begin{Bmatrix} 0 \\ 0 \\ 0.007724 \end{Bmatrix}$$

$$\{\Delta \bar{F}\} = \{\Delta F(t)\} - [M]\{A\} - \frac{3}{\Delta t}\{B\} = \begin{Bmatrix} 0 \\ 0 \\ 0.007724 \end{Bmatrix}$$

$$\begin{aligned} \{\Delta x\} &= [\bar{K}]^{-1}\{\Delta \bar{F}\} = [0.000091488 \quad 0.000091488 \quad 0.0076915]^T \\ \{x_n\} &= \{x_{n-1}\} + \{\Delta x\} = [0.000091488 \quad 0.000091488 \quad 0.0076915]^T \\ \{\dot{x}_n\} &= \{\dot{x}_{n-1}\} + \frac{3}{\Delta t}\{\Delta x_n\} + \{B\} \\ &= \{0\} + \frac{3}{0.1}[0.000091488 \quad 0.000091488 \quad 0.0076915]^T + \{0\} \\ &= [0.0027446 \quad 0.0027446 \quad 0.23075]^T \end{aligned}$$

$$\begin{aligned} \{\ddot{x}_n\} &= \{\ddot{x}_{n-1}\} + \frac{6}{(\Delta t)^2}\{\Delta x\} + \{A\} \\ &= \{0\} + \frac{6}{(0.1)^2}[0.000091488 \quad 0.000091488 \quad 0.0076915]^T + \{0\} \\ &= [0.054893 \quad 0.054893 \quad 4.61490]^T \end{aligned} \tag{k}$$

Internal moments and shears of structural members are attributed to three factors: (1) member deformation of rotations and deflections; (2) damping force resulting from velocity, and 3) inertia force associated with acceleration. The procedure of finding internal forces for the consistent mass model was illustrated in Example 6.3.2 with distributed time-dependent force but without damping. This example has damping, $P-\Delta$ effect, and a concentrated dynamic force applied at a structural node for which internal forces are calculated below.

(A) Internal moments and shears due to member deformations at $t=0.1$ sec are

$$\begin{aligned} \{M\} &= [SM\theta][A_\theta]^T\{x_\theta\} + [SMY][A_s]^T\{x_s\} \\ &\quad - [GM\theta][A_\theta]^T\{x_\theta\} - [GMY][A_s]^T\{x_s\} \\ &= \begin{Bmatrix} 0.0015248 \\ 0.0030496 \\ 0.0022872 \\ 0.0022872 \\ 0.0030496 \\ 0.0015248 \end{Bmatrix} + \begin{Bmatrix} -0.0032043 \\ -0.0032043 \\ 0 \\ 0 \\ -0.0032043 \\ -0.0032043 \end{Bmatrix} - \begin{Bmatrix} -0.00036595 \\ 0.0014638 \\ 0 \\ 0 \\ 0.0014638 \\ -0.00036595 \end{Bmatrix} - \begin{Bmatrix} -0.00076915 \\ -0.00076915 \\ 0 \\ 0 \\ -0.00076915 \\ -0.00076915 \end{Bmatrix} \end{aligned} \tag{l}$$

$$= [-0.0005444 \quad -0.0008493 \quad 0.0022872 \quad 0.0022872 \quad -0.0008493 \quad -0.0005444]^T \text{ k in}$$

$$\begin{aligned}
 \{V\} &= [SMY][A_\theta]^T\{x_\theta\} + [SVY][A_s]^T\{x_s\} \\
 &\quad - [GMY][A_\theta]^T\{x_\theta\} - [GVY][A_s]^T\{x_s\} \\
 &= \begin{Bmatrix} -3.81139 \\ -3.81139 \\ -1.90661 \\ -1.90661 \\ -3.81139 \\ -3.81139 \end{Bmatrix} 10^{-5} + \begin{Bmatrix} 5.3379 \\ 5.3379 \\ 0 \\ 0 \\ 5.3379 \\ 5.3379 \end{Bmatrix} 10^{-5} - \begin{Bmatrix} -9.1488 \\ -9.1488 \\ 0 \\ 0 \\ -9.1488 \\ -9.1488 \end{Bmatrix} 10^{-6} - \begin{Bmatrix} 7.6915 \\ 7.6915 \\ 0 \\ 0 \\ 7.6915 \\ 7.6915 \end{Bmatrix} 10^{-5} \quad (\text{m}) \\
 &= 10^{-5} [-5.25011 \quad -5.25011 \quad -1.90661 \quad -1.90661 \quad -5.25011 \quad -5.25011]^T
 \end{aligned}$$

(B) Internal moments and shears due to inertia force at $t = 0.1$ sec

$$\begin{aligned}
 \{M\} &= [MM\theta^t][A_\theta]^T\{\ddot{x}_\theta\} + [MMY^t][A_s]^T\{\ddot{x}_s\} \\
 &= \begin{Bmatrix} -0.06856 & 0 \\ 0.09142 & 0 \\ 0.73135 & -0.54852 \\ -0.54852 & 0.73135 \\ 0 & 0.09142 \\ 0 & -0.06856 \end{Bmatrix} \begin{Bmatrix} 0.054893 \\ 0.054893 \end{Bmatrix} + \begin{Bmatrix} 0.002476 \\ -0.004190 \\ 0 \\ 0 \\ -0.004190 \\ 0.002476 \end{Bmatrix} (4.61490) = \begin{Bmatrix} 7.66302832 \times 10^{-3} \\ -0.01431811 \\ 0.010036087 \\ 0.010036087 \\ -0.01431811 \\ 7.66302832 \times 10^{-3} \end{Bmatrix} \quad (\text{n})
 \end{aligned}$$

$$\begin{aligned}
 \{V\} &= [MMY^t][A_\theta]^T\{\ddot{x}_\theta\} + [MVY^t][A_s]^T\{\ddot{x}_s\} \\
 &= \begin{Bmatrix} 0.002476 & 0 \\ -0.004190 & 0 \\ -0.016760 & 0.009904 \\ 0.009904 & -0.016760 \\ 0 & -0.004190 \\ 0 & 0.002476 \end{Bmatrix} \begin{Bmatrix} 0.054893 \\ 0.054893 \end{Bmatrix} + \begin{Bmatrix} -0.000086 \\ 0.000248 \\ 0 \\ 0 \\ 0.000248 \\ -0.000086 \end{Bmatrix} (4.61490) = \begin{Bmatrix} -2.6096633 \\ 9.1449353 \\ -3.7634641 \\ -3.7634641 \\ 9.1449353 \\ -2.6096633 \end{Bmatrix} 10^{-4} \quad (\text{o})
 \end{aligned}$$

(C) Internal moments and shears due to damping force at $t=0.1$ sec are

$$\begin{aligned}
 \{M\} &= [CM\theta][A_\theta]^T\{\dot{x}_\theta\} + [CMY][A_s]^T\{\dot{x}_s\} \\
 &= \left(\beta \begin{bmatrix} [SM\theta]_1 - [GM\theta]_1 & 0 & 0 \\ \text{symm} & [SM\theta]_2 - [GM\theta]_2 & 0 \\ & & [SM\theta]_3 - [GM\theta]_3 \end{bmatrix} \right. \\
 &\quad \left. + \alpha \begin{bmatrix} [MM\theta^t]_1 & 0 & 0 \\ \text{symm} & [MM\theta^t]_2 & 0 \\ & & [MM\theta^t]_3 \end{bmatrix} \right) [A_\theta]^T\{\dot{x}_\theta\} \\
 &\quad + \left(\beta \begin{bmatrix} [SMY]_1 - [GMY]_1 & 0 & 0 \\ \text{symm} & [SMY]_2 - [GMY]_2 & 0 \\ & & [SMY]_3 - [GMY]_3 \end{bmatrix} \right. \\
 &\quad \left. + \alpha \begin{bmatrix} [MMY^t]_1 & 0 & 0 \\ \text{symm} & [MMY^t]_2 & 0 \\ & & [MMY^t]_3 \end{bmatrix} \right) [A_s]^T\{\dot{x}_s\} \quad (p) \\
 &= \begin{bmatrix} 1.3675648 & 0 & 0 \\ 1.1693241 & 0 & 0 \\ 1.2208715 & 0.4733064 & 0.0027446 \\ 0.4733064 & 1.2208715 & 0.0027446 \\ 0 & 1.1693241 & 0 \\ 0 & 1.3675648 & 0 \end{bmatrix} \begin{Bmatrix} 0.0027446 \\ 0.0027446 \end{Bmatrix} + \begin{Bmatrix} -0.02073632 \\ -0.02173622 \\ 0 \\ 0 \\ -0.02173622 \\ -0.02073632 \end{Bmatrix} (0.23075) \\
 &= \begin{Bmatrix} -1.03148749 \\ -1.80630584 \\ 4.649840664 \\ 4.649840664 \\ -1.80630584 \\ -1.03148749 \end{Bmatrix} 10^{-3}
 \end{aligned}$$

$$\begin{aligned}
\{V\} &= [CMY][A_\theta]^T\{\dot{x}_\theta\} + [CVY][A_s]^T\{\dot{x}_s\} \\
&= \left(\beta \begin{bmatrix} [SMY]_1 - [GMY]_1 & 0 & 0 \\ \text{symm} & [SMY]_2 - [GMY]_2 & 0 \\ & & [SMY]_3 - [GMY]_3 \end{bmatrix} \right. \\
&\quad \left. + \alpha \begin{bmatrix} [MMY^t]_1 & 0 & 0 \\ \text{symm} & [MMY^t]_2 & 0 \\ & & [MMY^t]_3 \end{bmatrix} \right) [A_\theta]^T\{\dot{x}_\theta\} \\
&\quad + \left(\beta \begin{bmatrix} [SVY]_1 - [GVY]_1 & 0 & 0 \\ \text{symm} & [SVY]_2 - [GVY]_2 & 0 \\ & & [SVY]_3 - [GVY]_3 \end{bmatrix} \right. \\
&\quad \left. + \alpha \begin{bmatrix} [MVY^t]_1 & 0 & 0 \\ \text{symm} & [MVY^t]_2 & 0 \\ & & [MVY^t]_3 \end{bmatrix} \right) [A_s]^T\{\dot{x}_s\} \\
&= \begin{bmatrix} -0.0207363 & 0 & 0 \\ -0.0217362 & 0 & 0 \\ -9.461014 \times 10^{-3} & -5.461414 \times 10^{-3} & 0 \\ -5.461414 \times 10^{-3} & -9.461014 \times 10^{-3} & 0 \\ 0 & -0.0217362 & 0 \\ 0 & -0.0207363 & 0 \end{bmatrix} \begin{Bmatrix} 0.0027446 \\ 0.0027446 \end{Bmatrix} + \begin{Bmatrix} -2.169102 \times 10^{-4} \\ -1.668102 \times 10^{-4} \\ 0 \\ 0 \\ -1.668102 \times 10^{-4} \\ -2.169102 \times 10^{-4} \end{Bmatrix} (0.23075) \\
&= \begin{Bmatrix} -10.6964877 \\ -9.81486281 \\ -4.095609589 \\ -4.095609589 \\ -9.81486281 \\ -10.6964877 \end{Bmatrix} 10^{-5} \tag{q}
\end{aligned}$$

Total moments are the summation of Eqs. (l), (n), and (p) as

$$\{M\} = 10^{-3}[6.08714 \quad -16.97372 \quad 16.97372 \quad 16.97372 \quad -16.97372 \quad 6.09714]^T k \text{ in } \tag{r}$$

Similarly, the addition of Eqs. (m), (o), and (q) yields the following total shears

$$\{V\} = 10^{-4}[-4.20432 \quad 7.63844 \quad -4.36369 \quad -4.36369 \quad 7.63844 \quad -4.20432]^T k \tag{s}$$

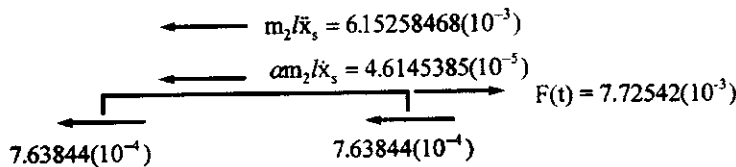


FIG. 9.43 Equilibrium check for shears.

The equilibrium check for moments can be easily observed from Eq. (r) as $\Sigma M_2 = 0$ and $\Sigma M_3 = 0$; the equilibrium check for shears can be obtained by using the free-body diagram in Fig. 9.43 as

$$\begin{aligned}\Sigma F_x &= 7.63844(10^{-4})(2) + 6.15258468(10^{-3}) + 4.6145385(10^{-5}) - 7.72542(10^{-3}) \\ &= 9.90065(10^{-7}) \approx 0\end{aligned}$$

Dynamic responses at $t = 0.2$ sec can be similarly calculated. At the end of each time-step, the moments must be compared with ultimate moment capacity. If any moment is equal to or greater than the ultimate moment, then the convergence technique presented in Section 9.4 should be employed for possible overshooting. The coefficients in $[S]$ should then be modified according to the location of plastic hinges as discussed in Section 9.9.1.

9.10. HYSTERESIS MODELS OF STEEL BRACING, RC BEAMS, COLUMNS AND SHEAR WALLS

Four hysteresis models for nonlinear analysis are included in Appendices J–M. Since these models are quite sophisticated, computer programs are provided so that readers can find detailed calculation procedures. Appendix J is for steel bracing (pinned-end truss member) based on Goel's work [17]. Appendix K, based on the Takeda model, is for slender RC members in bending such as beams and columns [23]. Appendix L, the Cheng–Mertz model for RC shear walls with consideration of coupling bending, shear, and axial deformations, is for both low- and high-rise shear walls [11]. Appendix M is the Cheng–Lou model for axial deformation of columns and walls [14]. These models can be used along with those presented in Chapter 8 on system analysis. For example, a braced steel frame needs a hysteresis model for beams, columns and bracing. Any model discussed in this chapter can be used for beams and columns, but a bracing member needs the model in Appendix J because a two-force member is vulnerable to yielding and buckling under cyclic loading. The latest version of INRESB-3D-II includes the aforementioned models for both PC and supercomputer [7,12,13]. The program has been used for case studies to verify different instances of building damage and collapse induced by strong ground motion [15].

9.11. OVERVIEW

This chapter presents the foundation of stiffness formulations for four well-known hysteresis models, namely, elasto-plastic, bilinear, curvilinear, and Ramberg–Osgood. These models have a wide range of engineering applications for both reinforced concrete and steel structures.

Relationships among these models are discussed, particularly the analogy between bilinear and curvilinear. Mathematical aspects are extended from small to large deflection with and without $P-\Delta$ effect. Eight numerical examples are provided to illustrate detailed calculations

of system response and member forces as well as equilibrium and compatibility checks. Various effects of material nonlinearity, $P\Delta$ effect, and geometric nonlinearity on structural response are shown.

The aforementioned work is mainly focused on the lumped mass model. In conjunction with the consistent mass model introduced in Chapter 6, this chapter extends the elasto-plastic model to the consistent mass model for both Bernoulli-Euler and Timoshenko theories. Readers should carefully study Example 9.9.1, which shows extensively how to consider inertia force, member deformation, damping, and $P\Delta$ effect to find member forces as well as external forces and to perform equilibrium checks.

BIBLIOGRAPHY

1. AISC Manual of Steel Construction. Load and Resistance Factor Design. 1st ed. AISC, 1986.
2. WF Chen, T Atsuta. Theory of Beam-Columns. Vol II. New York: McGraw-Hill, 1976, pp 283 and 290.
3. FY Cheng, ME Botkin. Second-order elasto-plastic analysis of tall buildings with damped dynamic excitations. Proceedings of Finite Element Method in Civil Engineering, McGill University, Montreal, 1972, pp 549–564.
4. FY Cheng. Dynamic response of nonlinear space frames by finite element methods. Proceedings of International Association for Shell Structures, Tokyo and Kyoto, paper 9–5, 1972, pp 817–826.
5. FY Cheng, KB Oster. Ultimate instability of earthquake structures. ASCE J Struct Engng 102(ST5):961–972, 1976.
6. FY Cheng, KB Oster. Effect of coupling earthquake motions on inelastic structural models. FY Cheng, ed. Proceedings of International Symposium on Earthquake Structural Engineering, Vol I, US Dept. of Commerce, National Technical Information Service, Virginia, NTIS No. PB29053, 1976, pp 107–126.
7. FY Cheng, P Kitipitayangkul. INRESB-3D: a computer program for inelastic analysis of RC and steel buildings subjected to 3-D ground motion. NSF Report. National Technical Information Service, US Department of Commerce, Virginia, NTIS no. PB80-165944, 1979 (101 pp).
8. FY Cheng, P Kitipitayangkul. Inelastic behavior of building systems of 3-D earthquake motion. Proceedings of 7th World Conference on Earthquake Engineering, Vol 7, Istanbul, 1980, pp 445–507.
9. FY Cheng. Inelastic analysis of 3-D mixed steel and RC seismic building systems. J Comput and Struct 13:189–196, 1981.
10. FY Cheng. Review of stiffness formulation for linear and second-order analysis. Honorary Professor Lecture Series, Harbin University of Architecture and Engineering, China, 1981.
11. FY Cheng, GE Mertz, MS Sheu and JF Ger. Computed versus observed inelastic seismic response of low-rise RC shear walls. ASCE J Struct Engng 119(11):3255–3275, 1993.
12. FY Cheng, JF Ger, D Li, JS Yang. INRESB-3D-SUPII program listing for supercomputer: general purpose program for inelastic analysis of RC and steel building systems for 3D static and dynamic loads and seismic excitations. NSF Report. National Technical Information Service, US Department of Commerce, Virginia, NTIS no. PB97-123616, 1996 (114 pp).
13. FY Cheng, JF Ger, D Li, JS Yang. INRESB-3D-SUPII program listing for PC: inelastic analysis of RC and steel building systems for 3D static and dynamic loads and seismic excitations. NSF Report. National Technical Information Service, US Department of Commerce, Virginia, NTIS no. PB97-123632, 1996 (109 pp).
14. FY Cheng, KY Lou. Hysteresis model of axially loaded shear walls. Structural Series 97-21. Department of Civil Engineering, University of Missouri-Rolla, MO, 1997.
15. JF Ger, FY Cheng, LW Lu. Collapse behavior of Pino-Suarez Building during 1985 Mexico Earthquake. ASCE J Struct Engng, 119(3):852–870, 1993.
16. MF Giberson. Two nonlinear beams with definitions of ductility. ASCE J Struct Div, 95(ST2):137–157, 1969.
17. AK Jain, SC Goel, RD Hanson. Hysteretic cycles of axially loaded steel members. ASCE J Struct Div 106:1775–1795, 1980.
18. WD Iwan. On a class of models for the yielding behavior of continuous and composite systems. ASME J Appl Mech 34(3):612–617, 1967.
19. MJ Kaldjian. Moment-curvature of beams as Ramberg-Osgood functions. ASCE J Struct Div 93(ST5):53–65, 1967.

20. W Ramberg, WR Osgood. Description of stress-strain curves by three parameters. Technical Note 902. National Advisory Committee for Aeronautics, 1943.
21. WE Saul, JF Fleming and SL Lee. Dynamic analysis of bilinear inelastic multiple-story shear buildings. Proceedings of 3rd World Conference on Earthquake Engineering, New Zealand, Vol II, 1965, pp 533–51.
22. CK Sun, GV Berg and RD Hanson. Gravity effect on single-degree inelastic system. ASCE J Engng Mech EM1:183–200, 1973.
23. T. Takeda, MA Sozen, NN Nielsen. Reinforced concrete response to simulated earthquakes. ASCE J Struct Div 96:2557–2573, 1970.

10

Static and Dynamic Lateral-Force Procedures and Related Effects in Building Codes of UBC-94, UBC-97 and IBC-2000

PART A FUNDAMENTALS

10.1. INTRODUCTION

Several seismic building codes such as Uniform Building Code-UBC (1994 and 1997), Standard Building Code-SBC (1994) and BOCA (1996) have been adopted in various regions in the U.S. Among these codes, the UBC is widely disseminated and recognized in the international engineering community. The UBC was first enacted by the International Conference of Building Officials in 1927. Since then, the code has been revised every three years (except during World War II). International Building Code of the year 2000, IBC-2000, was proposed as a final draft in 1998. It incorporates the above codes promulgated by representatives of BOCA, SBCCI, and ICBO. Thus IBC-2000 represents national uniformity in building codes and supersedes other codes such as UBC-97. Note that UBC-97 and IBC-2000 are closely related to NEHRP of 1991, which is partly based on ATC-3-06 of 1978. To illuminate later code provisions, a knowledge of UBC-94 is essential. Note also that UBC-94 remains valid in engineering practice even after the revisions published in UBC-97.

UBC-94 and UBC-97 stipulate two basic lateral-force procedures for minimum seismic design: static lateral-force and dynamic-lateral force, which are introduced in this chapter. The codes also stipulate time-history analysis as discussed earlier, particularly the numerical techniques in Chapter 7 and material and geometric nonlinearity in Chapter 9. For both UBCs, the average annual risk is 10% probability of being exceeded in any 50-year period. This means that if minimum design lateral-force requirements in the codes are met, then normal building structures may be expected to resist an upper-level earthquake with a recurrence interval of 475 years without collapse and without endangering life. However, structural and nonstructural damages are anticipated which may not be acceptable for essential facilities, such as hospitals and communication

centers. A higher-level design force is required to ensure their ability to function during and after an earthquake. With the same design philosophy as UBC, IBC-2000 has only a 2% probability of being exceeded in any 50-year period.

Organization of sections, figures, tables and the like in IBC-2000 differs from both UBCs. Therefore summary comparisons of code specifications and step-by-step numerical procedures are given in parallel layout (see Sections 10.6 and 10.7 for static lateral-force procedures, and 10.10 and 10.11 for dynamic-lateral procedures). This layout permits the reader to more easily grasp the specific requirements of various sections of these three codes.

10.2. BACKGROUND OF LATERAL FORCE PROCEDURES IN BUILDING CODES

10.2.1. Effective Earthquake Force and Effective Mass

Recall in Sections 2.5.2, 2.5.3, 3.2.1, and 4.9.2 that the structural response vector, $\{x\}$, can be expressed in terms of (1) a modal matrix $[\Phi]$ or normal modes $[X]$, and (2) a generalized response vector $\{x'\}$ [see Eqs. (2.46), 2.66), (3.7), and 3.8)] or $\{q\}$ [see Eqs. (4.115) and (4.139b)]. Here only $[X]$ and $\{q\}$ are used. For the sake of code comparison, $\{q\}$ is written as $\{q(t)\}$ with time variable t which was omitted previously. Thus the response vector is now expressed as

$$\{x(t)\} = [X]\{q(t)\} = \sum_{i=1}^n \{X\}_i q_i(t); \quad n = \text{no. of modes considered} \quad (10.1)$$

where the generalized response vector can be obtained from Eq. (2.63) [also see Eq. (1.123a) for Duhamel integrals] as

$$\begin{aligned} q_i(t) &= \frac{\{X\}_i^T [M] \{I_n\}}{\bar{M}_i P_i} \int_0^t \ddot{x}_g(\Delta) e^{\rho_i p_i(t-\Delta)} \sin p_i(t-\Delta) d\Delta \\ &= \frac{\{X\}_i^T [M] \{I_n\}}{\bar{M}_i} p_i v_i(t) = \frac{\sum_{r=1}^{ns} M_r X_{ri}}{\bar{M}_i} p_i v_i(t) \\ &= \gamma_i p_i v_i(t) \end{aligned} \quad (10.2)$$

where ns is the total floor number; $\{I_n\}$ is the influence coefficient matrix for incorporating appropriate ground excitations and may be expressed as $\{1\}$ for a multiple story building subjected to horizontal ground motion (see Fig. 7.44); $v_i(t)$ represents integration results and can be expressed in terms of response spectral value of velocity S_v , acceleration S_a , or displacement S_d [see Eqs. (7.114)–(7.116); and γ_i is the participation factor for the i th mode [see Eq. (7.205)]. If all modes are considered, then the participation factors are in a column matrix or diagonal matrix as

$$\{\gamma\} = \frac{[X]^T [M] \{1\}}{[X]^T [M] [X]} \quad (10.3)$$

Substituting Eq. (10.2) into Eq. (10.1) and replacing $v_i(t)$ by velocity spectral value S_v yields

$$\{x\} = [X] [\gamma] [S_v] [p]^{-1} \quad (10.4)$$

where $[S_v]$ and $[p]$ are diagonal matrices. Note that no time variable t is associated with $\{x\}$ above because the response spectral values are the absolute maximum values resulting from integration [see Eq. (1.123a) and (7.202)].

Let the *effective acceleration* of the i th mode be defined by the product of the natural frequency of the i th mode and the displacement amplitude in the generalized coordinates of that mode as follows:

$$\ddot{q}_i(t) = p_i^2 q_i(t) \quad (10.5)$$

Then the acceleration associated with a structure's d.o.f. for the i th mode can be expressed as

$$\{\ddot{x}(t)\}_i = \{X\}_i \ddot{q}_i(t) = \{X\}_i \gamma_i p_i v_i(t) \quad (10.6)$$

Thus the *effective earthquake force* at the i th mode for all floors is

$$\{P_E(t)\}_i = [M]\{\ddot{x}(t)\}_i = [M]\{X\}_i \gamma_i p_i v_i(t) \quad (10.7)$$

The effective earthquake force for all modes can be obtained by combining Eqs. (10.5)–(10.7) with the following result:

$$\{P_E(t)\} = \sum_{i=1}^n \{P_E(t)\}_i = [M] \sum_{i=1}^n \{X\}_i \frac{p_i^2 \gamma_i}{p_i} v_i(t) \quad (10.8)$$

From Eq. (10.7)

$$P_{Ei}(t) = \sum_{r=1}^{ns} M_r X_{ri} \gamma_i A_i(t) \quad (10.9)$$

which may be interpreted as the *effective mass* of the i th mode, M_{Ei} , times acceleration $A_i(t)$. Thus,

$$M_{Ei} = \sum_{r=1}^{ns} M_r X_{ri} \gamma_i = \bar{M}_i \gamma_i^2 = \frac{(\{X\}_i^T [M] \{1\})^2}{\bar{M}_i} \quad (10.10)$$

The moment at the base of the i th mode is due to the effective earthquake force at each floor times individual story height as

$$\begin{aligned} M_{Ti}(t) &= \sum_{r=1}^{ns} P_{Eir}(t) h_r = \sum_{r=1}^{ns} M_{ri} X_{ri} \gamma_i h_r A_i(t) \\ &= \frac{M_{Ei} \sum_{r=1}^{ns} M_r X_{ri} \gamma_i h_r}{M_{Ei}} A_i(t) = M_{Ei} \frac{\left(\sum_{r=1}^{ns} M_r X_{ri} h_r \right) \gamma_i}{\left(\sum_{r=1}^{ns} M_r X_{ri} \right) \gamma_i} A_i(t) \\ &= M_{Ei} \frac{\{X\}_i^T [M] \{h\}}{\{X\}_i^T [M] \{1\}} A_i(t) \\ &= M_{Ei} h_i^* A_i(t) \end{aligned} \quad (10.11)$$

in which

$$h_i^* = \frac{\{X\}_i^T [M] \{h\}}{\{X\}_i^T [M] \{1\}} \quad (10.12)$$

Equation (10.11) is interpreted as shown in Fig. 10.1. Note that the effective mass of all modes is equal to the total mass of the building.

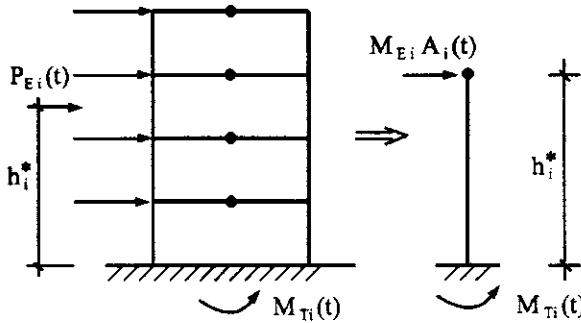


FIG. 10.1 Effective earthquake force and effective mass.

10.2.2. Base Shear and Overturning Moment

The base shear of the i th mode can be obtained by summing all the effective earthquake forces distributed at all floors along the building height as

$$\begin{aligned} V_i(t) &= \sum_{r=1}^{ns} P_{Eir} = \{1\}^T \{P_E(t)\}_i = M_{Ei} p_i v_i(t) \\ &= \frac{(\{X\}_i^T [M] \{1\})^2}{\{X\}_i^T [M] \{X\}_i} p_i v_i(t) = \frac{\left(\sum_{j=1}^{ns} M_j X_{ji} \right)^2}{\sum_{j=1}^{ns} M_j X_{ji}^2} p_i v_i(t) = \frac{\left(\sum_{j=1}^{ns} w_j X_{ji} \right)^2}{\sum_{j=1}^{ns} w_j X_{ji}^2} \frac{p_i v_i(t)}{g} \\ &= \frac{W_{Ei}}{g} p_i v_i(t) \end{aligned} \quad (10.13)$$

where

$$W_{Ei} = \frac{\left(\sum_{j=1}^{ns} w_j X_{ji} \right)^2}{\sum_{j=1}^{ns} w_j X_{ji}^2} \quad (10.14)$$

in which w_j represents lumped-mass weight at the j th floor; X_{ji} is the normal mode displacement of the j th floor at the i th mode; and W_{Ei} is the effective weight at the i th mode. From Eqs. (10.7) and (10.13), the effective earthquake force at the i th mode for all floors can be rewritten as

$$\begin{aligned} \{P_E(t)\}_i &= \frac{(\{X\}_i^T [M])^T V_i(t)}{\{1\}^T (\{X\}_i^T [M])^T} = \frac{[M] \{X\}_i V_i(t)}{(\{X\}_i^T [M] \{1\})^T} \\ &= \frac{[M] \{X\}_i V_i(t)}{\sum_{j=1}^{ns} M_j X_{ji}} \end{aligned} \quad (10.15)$$

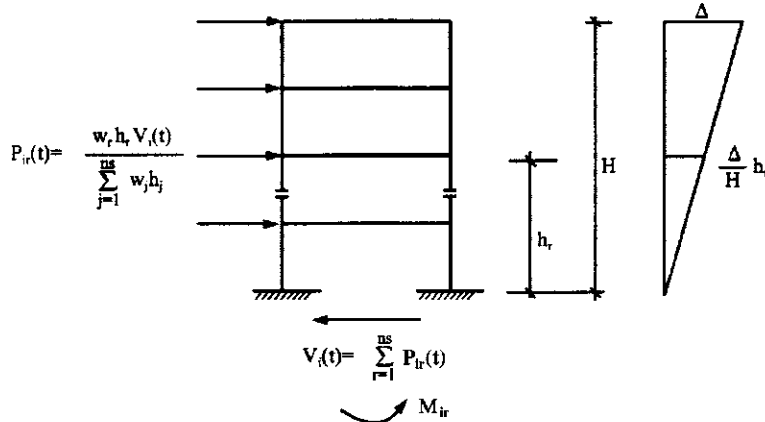


FIG. 10.2 Floor force, base shear, and overturning moment for linear first-mode-shape.

from which the effective earthquake force at the r th floor of the i th mode is

$$P_{ir}(t) = \frac{M_r X_{ri}}{\sum_{j=1}^{ns} M_j X_{ji}} V_i(t) \quad (10.16)$$

Considering the first mode only and assuming its mode shape is a straight line as shown in Fig. 10.2, Eq. (10.15) becomes

$$P_{ir}(t) = \frac{w_r \frac{\Delta}{H} h_r}{\sum_{j=1}^{ns} w_j \frac{\Delta}{H} h_j} V_i(t) = \frac{w_r h_r}{\sum_{j=1}^{ns} w_j h_j} V_i(t) \quad (10.17)$$

where H is building height, and h_r is height of the r th floor measured from the base. Base shear is the summation of earthquake forces distributed at all floors as

$$V_i(t) = \sum_{r=1}^{ns} P_{ir}(t) \quad (10.18)$$

The *overturning moment* at the base due to effective earthquake force at the r th floor of the i th mode is obtained from Eq. (10.16) as

$$M_{ir} = P_{ir} h_r = \frac{w_r h_r}{\sum_{j=1}^{ns} w_j h_j} h_r V_i(t) \quad (10.19)$$

Equations (10.16)–(10.18) are shown in Fig. 10.2.

UBC-94 static lateral-force procedures are closely related to the equations derived in this section. These procedures are further discussed in Section 10.3. Sections 10.4 and 10.5 describe new requirements in UBC-97 and IBC-2000, respectively. Section 10.6 compares static lateral-force procedures in UBC-94, UBC-97, and IBC-2000 and shows their similarities and differences. In Section 10.7 a structure is used to illustrate all the numerical procedures in these three codes. Similarly, dynamic lateral-force procedures for the three codes are discussed in Sec-

tion 10.9, required procedures are compared in Section 10.10, and numerical examples are provided in Section 10.11. For the reader's convenience, the UBC-94, UBC-97 and IBC-2000 section, table, or equation number is cited in parentheses for respective code requirements.

10.3. UBC-94 AND DESIGN PARAMETERS

10.3.1. Criteria for Appropriate Lateral Force Procedure

As noted, UBC-94 stipulates two procedures to determine seismic forces for structural analysis: (1) static lateral-force procedure; and (2) dynamic lateral-force procedure including time-history analysis. Requirements for selecting the appropriate procedure depend on structural irregularities, classified as *vertical structural irregularities* (UBC-94, Table 16-L) and *plan structural irregularities* (UBC-94, Table 16-M). Vertical structural irregularities come from an abrupt change in a structure's geometry, significantly uneven distribution of floor mass, or stiffness of adjacent stories. Sample configurations are shown in Fig. 10.3. Plan structural irregularities come from torsional irregularity, irregular geometry of re-entrant corner, diaphragm discontinuity, or out-of-plane effects. Criteria to satisfy such irregularities are shown in Fig. 10.4. Note that Fig. 10.4 refers to *rigid and flexible diaphragms*. In accordance with UBC-94, Section 1628.5, a diaphragm is considered flexible when its maximum lateral deformation exceeds twice the average story drift of the associated story. This can be determined by calculating the diaphragm's midpoint displacement under lateral load, including the story drift of adjoining vertical resisting elements. Flexible ones comprise diagonally sheathed wood, sheathed plywood, and steel deck diaphragms. When the criterion is not satisfied, the diaphragm is considered rigid. Rigid ones comprise reinforced concrete, precast concrete, and composite steel deck diaphragms.

The criteria for a flexible diaphragm appear in Fig. 10.5, where δ_{\max} represents the diaphragm's maximum lateral displacement; δ_1 and δ_2 are story drift at the vertical resisting elements of the diaphragm's end supports; and δ_m is midpoint displacement under uniform seismic force, which can be obtained by modeling the diaphragm as a simple beam shown in the figure.

10.3.2. Base Shear of Static Lateral-Force Procedure and Related Parameters

In the UBC-94 static lateral-force procedure, the total structural base shear is specified by

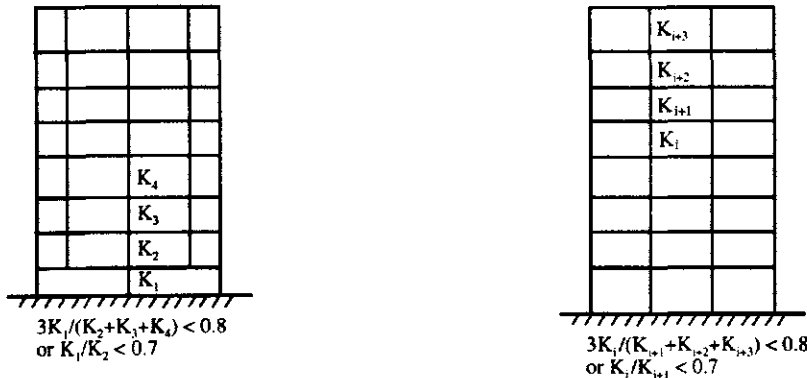
$$V = ZICW/R_w \quad (10.20)$$

where Z is the *seismic zone factor*, I is the *importance factor*, C is a numerical coefficient dependent on soil conditions at the site and on the fundamental period of the structure, W is the seismic dead load of the structure, and R_w is the *response modification factor*. Individual parameters are briefly depicted as follows.

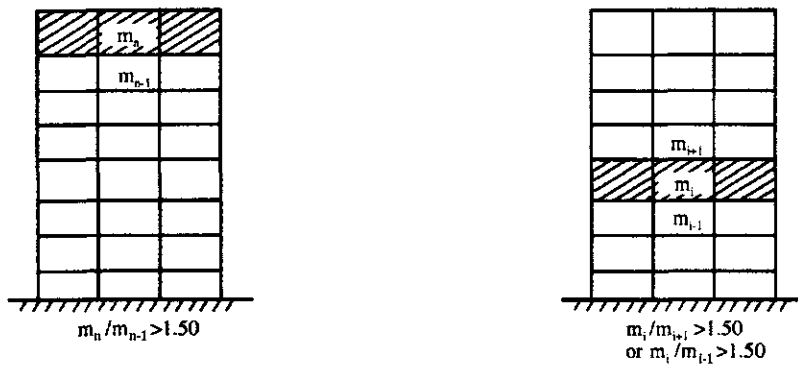
(A) *Seismic zone factor Z*—the U.S.A. is divided into five different seismic zones as shown in UBC-94, Figure 16.22, which is duplicated in Fig. 10.6. Zone factors are given in UBC-94, Table 16-I and listed in Table 10.1. The zone factor is an estimate of site-dependent *effective peak ground acceleration* expressed in terms of g , which reflects ground motion values at a recurrence interval of 475 years corresponding to a 10% probability of being exceeded in any 50-year period. Relationships among Z , effective peak ground acceleration (EGA), peak ground acceleration (PGA), maximum magnitude, and MM intensity are given in Table 7.1. The zone factor is used to scale the normalized design spectra in UBC-94, Figure 16.3, which are duplicated here as Fig. 7.31 in Chapter 7.

(B) *Importance factor I*—this factor is given in UBC-94, Table 16-K, and summarized in Table 10.2, where the factors pertain to four *occupancy categories*. Category 1, *essential facilities* such as hospitals, fire and police stations, and government communication centers, has a factor of 1.25. Thus the design of such buildings increases by 25% of the prescribed base shear of standard occupancy structures classified as category 4. The seismic design level is upgraded to ensure that essential facilities stay operational after an upper-level earthquake.

(a)



(b)



(c)

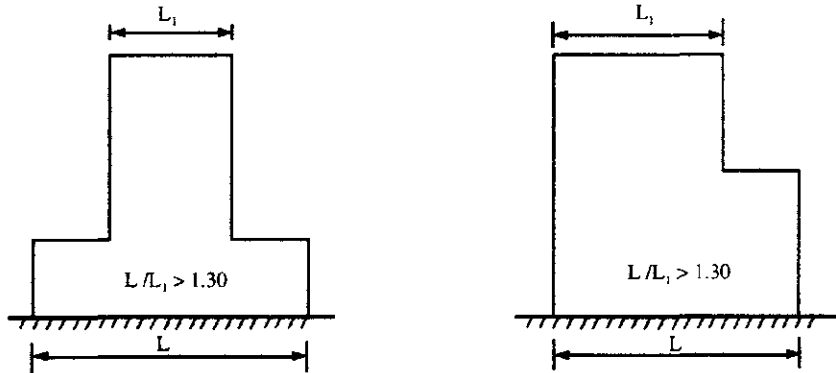


FIG. 10.3 Vertical structural irregularities. (a) Stiffness irregularity—soft story. (b) Mass irregularity. (c) Geometric irregularity.

(C) *Response modification factor R_w* — R_w is the ratio of seismic base shear for a linearly elastic structural system to prescribed design base shear for an inelastic structural system. Since designing a structure to remain elastic during a major earthquake is not economical, elastic base shear is reduced by this factor. The reduced base shear thus allows the designed structure to incur limited damage without jeopardizing gravity-load carrying capacity and yet provides energy-absorbing capacity. Inelastic deformation after yielding induces more damping and longer

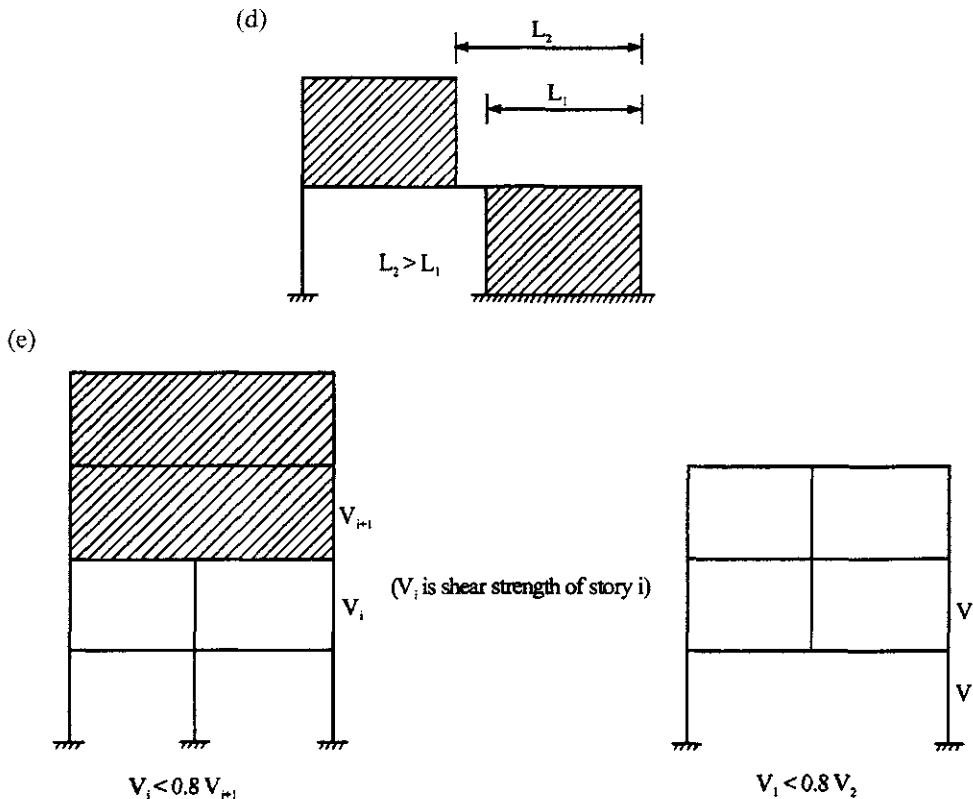


FIG. 10.3 Vertical structural irregularities. (d) In-plane discontinuity. (e) Weak story.

natural period, which in turn reduce seismic excitation developed in the structure. R_w also considers *design load factors*, *structural redundancy*, and seismic-resisting performance of materials and structural systems.

Figure 10.7 depicts R_w and illustrates some of the parameters just mentioned. In the figure V_e = maximum elastic base shear; V_y = base shear corresponding to structural collapse level or yield strength; V_s = base shear corresponding to the first hinge formation in the structural system; V_a = allowable base shear at service load level adopted by UBC-94; and δ_a , δ_s , δ_y , and δ_{\max} are the story drifts associated with the respective base shears. Thus the response modification factor can be expressed as

$$R_w = \frac{V_e}{V_a} = \frac{V_e}{V_y} \frac{V_y}{V_s} \frac{V_s}{V_a} = R_d \Omega_0 R_a \quad (10.21)$$

where R_d = *ductility reduction factor*, denoted by V_e/V_y and is well established for single-d.o.f. damped systems; $\Omega_0 = V_y/V_s$ is *seismic force amplification (or overstrength factor)* due to structural redundancy (internal force redistribution after first plastic hinge formation); and $R_a = V_s/V_a$ signifies the *allowable stress factor* to account for differences in the format of material codes. UBC-94 recommends a range of R_w values for various basic structural systems in UBC-4, Table 16-N and 16-P. This range is summarized in Table 10.3.

In general, bearing wall systems, such as shear walls or braced frames, support both gravity loads and lateral forces. These systems lack redundancy; R_w is therefore low. Building frame systems have separate structural units to independently support gravity loads by frames and lateral forces by bearing walls or braced systems; R_w is therefore relatively higher. Moment-resisting frames support both gravity loads and lateral forces. Such systems are specially detailed to provide

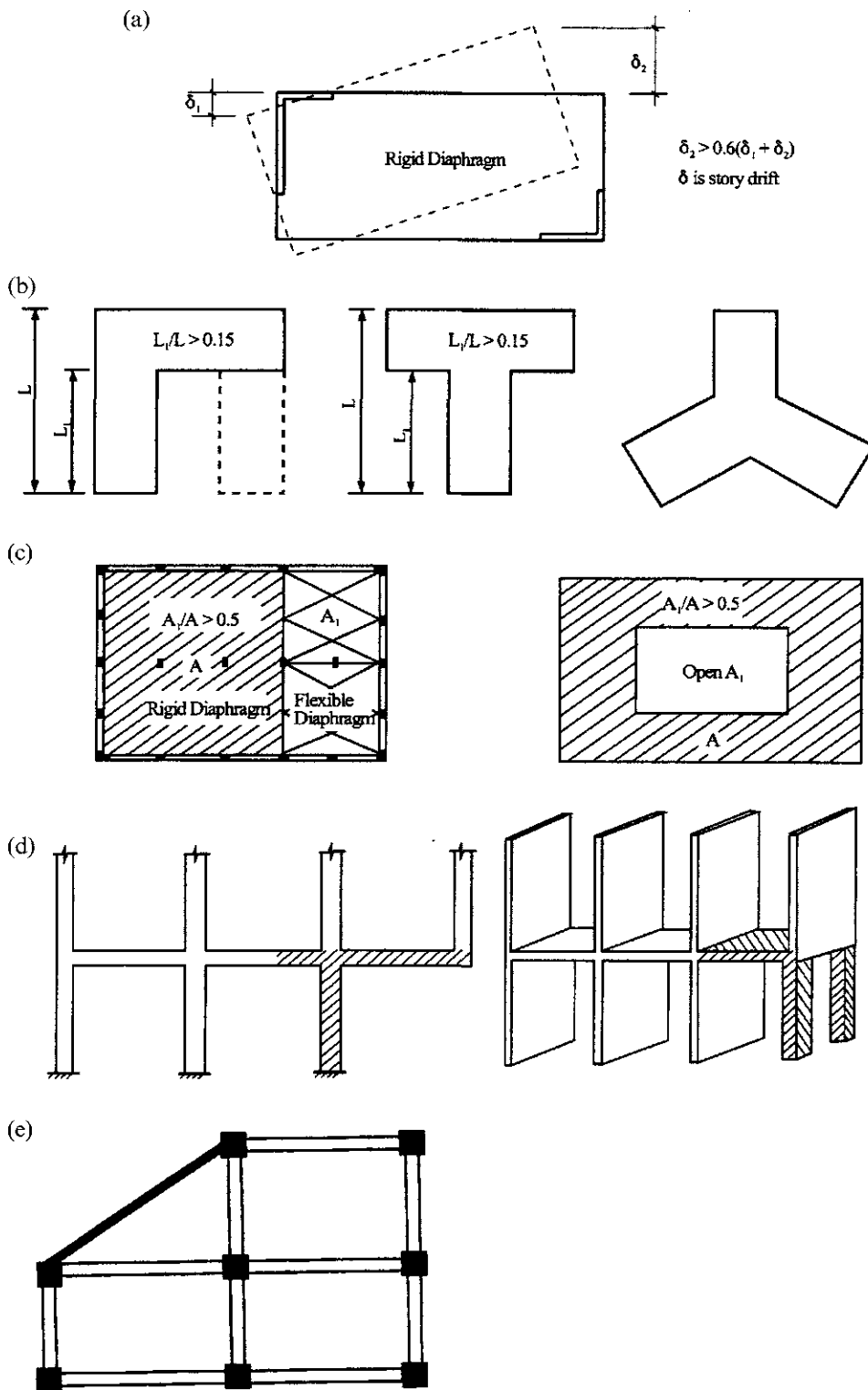


FIG. 10.4 Plan structural irregularities. (a) Torsional irregularity. (b) Irregular geometry of re-entrant corners. (c) Diaphragm discontinuity. (d) Out-of-plane offsets. (e) Nonparallel system

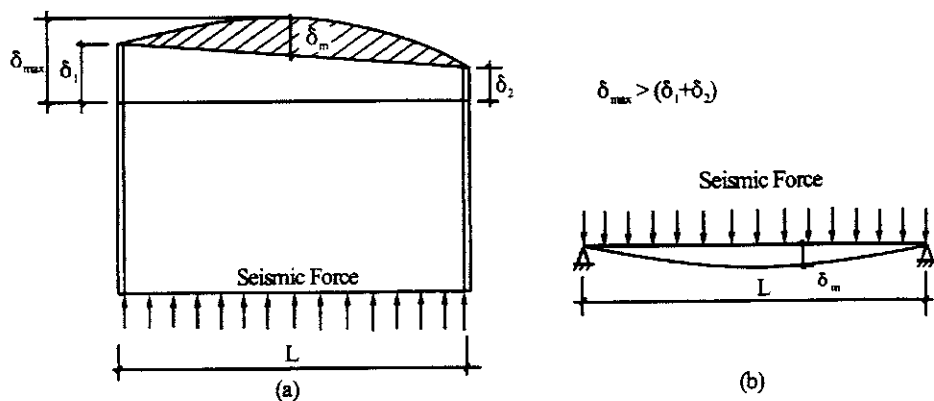


FIG. 10.5 Criteria and modeling of flexible diaphragm.

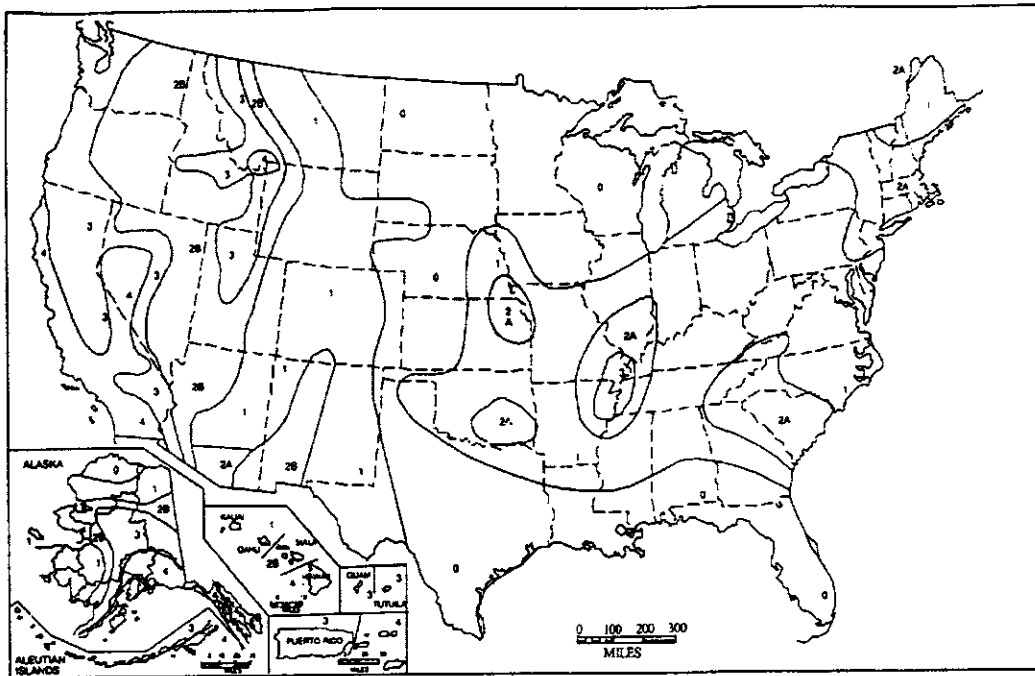


FIG. 10.6 Seismic zone map of U.S.A.

adequate ductility for the applied loads; R_w can therefore be as high as 12. Dual systems comprise nonbearing walls or braced systems to support lateral forces and moment-resisting frames to support gravity loads. The moment-resisting frames are also designed as backup systems for lateral forces. R_w values for dual systems can therefore be as high as 12. Four basic structural systems are illustrated in Fig. 10.8.

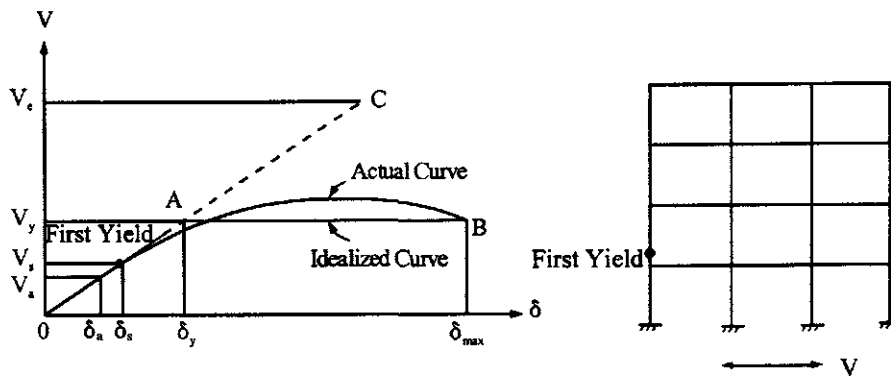
(D) *Seismic dead load W*—as specified in UBC-94, Section 1628.1, load W includes permanent equipment plus 25% of the floor live load (for warehouse or storage occupancy) plus the weight of snow when the design snow load is greater than $30 \text{ lb}/\text{ft}^2$ ($1.44 \text{ kN}/\text{m}^2$). The design

TABLE 10.1 Seismic Zone Factor Z

Zone	1	2A	2B	3	4
Z	0.075	0.15	0.20	0.30	0.40

TABLE 10.2 Occupancy Category and Importance Factor

Occupancy category	Importance factor I
1. Essential facilities	1.25
2. Hazardous facilities	1.25
3. Special occupancy structures	1.00
4. Standard occupancy structures	1.00

**FIG. 10.7** General story response of a structure.**TABLE 10.3** Range of R_w Values for Various Basic Structural Systems

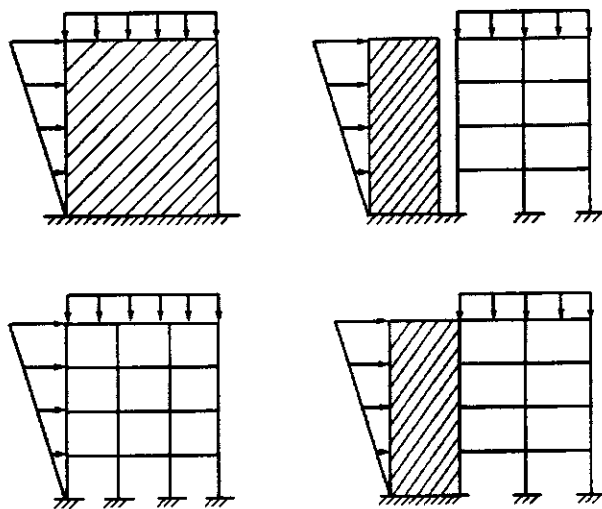
Basic structural systems	Range of R_w
Bearing wall systems	4–8
Building frame systems	7–10
Moment-resisting frame systems	5–12
Dual systems	6–12
Nonbuilding structures	3–5

snow load may be reduced by up to 75% on the basis of siting, configuration, and load duration warrant when approved by building officials. The partition load should also be included in W .

(E) *Seismic coefficient C and site coefficient S*—coefficient C , specified in UBC-94, Formula 28-2, is used to modify zone factor Z to produce maximum response acceleration CZ . This coefficient is dependent on the soil characteristics of the site and the fundamental period of the structure. The seismic coefficient, C , and design base shear, V , are formulated as

$$C = 1.25S/T^{2/3} \quad (10.22a)$$

$$V = \frac{ZIC}{R_w} W \quad (10.22b)$$

**FIG. 10.8** Basic structural systems.**TABLE 10.4** Site Coefficients

Type	Description	<i>S</i>
<i>S</i> ₁	Profile with either rock-like material or stiff/dense soil condition	1.0
<i>S</i> ₂	Profile with dense or stiff soil conditions	1.2
<i>S</i> ₃	Profile with soft to medium stiff clay	1.5
<i>S</i> ₄	Profile with very soft clay deposits	2.0

where *S* is a site coefficient and *T* is the fundamental period of the building. Values of site coefficient *S*, specified in UBC-94, Table 16-J, are listed in Table 10.4 with a brief description. The value of *C* need not exceed 2.75; the minimum value of the ratio *C/R_v* is governed by

$$C/R_v \geq 0.075 \quad (10.23)$$

(F) *Fundamental period T*—the fundamental period may be determined using an empirical formula (UBC-94, Method A) or analysis based on mechanics (UBC-94, Method B) as follows. *Method A*—UBC-94, Formula 28-3 is an empirical equation:

$$T = C_t(h_n)^{3/4} \quad (10.24)$$

where

$$C_t = \begin{cases} 0.035(0.0853) & \text{for steel moment-resisting frames;} \\ 0.030(0.0731) & \text{for reinforced concrete moment-resisting frames} \\ & \text{and eccentrically braced frames;} \\ 0.020(0.0488) & \text{for all other buildings.} \end{cases} \quad (10.25)$$

h_n = height in feet (or meters, m) above the base to story level *n* of the building. Values of *C_t* in parentheses are in SI units.

Without a preliminary structural design, an analysis based on mechanics cannot be used to calculate the vibration period of a building, but the vibration period can be estimated in order to calculate an initial base shear for preliminary design. This estimate is based on simple formulas

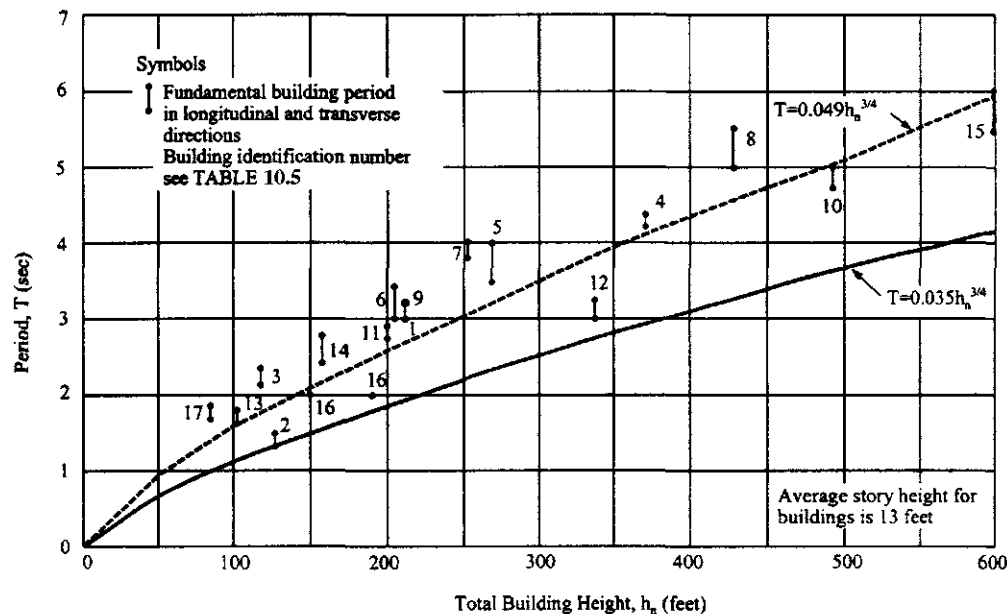


FIG. 10.9 Fundamental period of steel frames (ATC 3-06, 1978).

involving a general description of building type (such as steel moment-resisting frame or concrete moment-resisting frame) and overall dimensions (such as height). For preliminary member sizing, it is advisable to make the base shear conservative. Thus the estimated value of T should be smaller than the true period of the building.

A sample equation, $T = 0.035h_n^{3/4}$, for steel frames is shown in Fig. 10.9. This equation is compared with fundamental vibration periods computed from accelerograph records of the upper stories of several buildings during the 1971 San Fernando, California earthquake. The conservatism is evident from the comparison. The building identification number is presented in Table 10.5.

Method B—UBC-94, Formula 28-5 is based on mechanics analysis of Rayleigh's equation:

$$T = 2\pi \sqrt{\frac{\sum_{i=1}^n w_i \delta_i^2}{g \sum_{i=1}^n f_i \delta_i}} \quad (10.26)$$

in which n is the same as ns used previously to denote total number of stories; f_i represents any lateral force distributed approximately in accordance with Eqs. (10.28) and (10.29) or any other rational distribution; and w_i is the seismic dead load at level i . Elastic deflection, δ_i , is calculated using the applied lateral forces f_i .

The value of T from Method B should not be over 30% of period T from Method A in seismic zone 4 and 40% in zones 1, 2, and 3 (UBC-94, Section 1628.2.2). This is because the calculated period increases with an increase in flexibility of the structure; the δ term in the Rayleigh formula has the second power in the numerator but only the first power in the denominator. Thus the calculated deflections δ , without consideration of nonstructural elements in the structural stiffness, are exaggerated and the calculated period is lengthened. In turn, coefficient C and, consequently, design force are decreased. Nonstructural elements always affect the behavior of the structure, even though the designer may not rely on them to contribute any strength or stiffness to the structure. The limitation on the value of T is imposed as a safeguard.

TABLE 10.5 Fundamental Period Study of Steel Frame Buildings Based on 1991 San Fernando Earthquake [3]

ID No.	Name and address	ID no.	Name and address
1	K B Valley Center, 15910 Ventura	10	Union Bank Building, 445 South Figueroa
2	Jet Propulsion Lab, Administration Building, Bldg 180	11	Kajima International, 250 East First Street
3	6464 Sunset Boulevard	12	Bunker Hill Tower, 800 West First Street
4	1900 Avenue of the Stars, Century City	13	3407 West 6th Street
5	1901 Avenue of the Stars, Century City	14	Occidental Building, 1150 South Hill Street
6	1880 Century Park East Office Tower, Century City	15	Crocker Citizens Bank Building, 611 West 6th Street
7	1888 Century Park East Office Tower, Century City	16	Sears Headquarters.
8	Mutual Benefit Life Plaza, 5900 Wilshire Boulevard	17	900 South Fremont, Alhambra
9	Department of Water and Power, 111 N. Hope Street		5260 Century Boulevard

10.3.3. Vertical Distribution of Lateral Force

Once the base shear has been determined, base shear V is distributed over the height of the structure as a force at each level with consideration of a straight-line mode shape (see Fig. 10.2). An extra force F_t is considered at the top of the building to account for greater participation of higher modes in the response of longer-period structures. These requirements are specified in UBC-94, Formulas 28-6 through 28-8 (UBC-94, Section 1628.4) and summarized as follows:

$$V = F_t + \sum_{i=1}^n F_i; \quad n = \text{total number of stories} \quad (10.27)$$

in which

$$F_t = \begin{cases} 0.07TV & \leq 0.25V; \quad \text{if } T > 0.7 \text{ sec} \\ 0; & \text{if } T \leq 0.7 \text{ sec} \end{cases} \quad (10.28)$$

The remaining portion of the total base shear, $(V - F_t)$, is distributed over the height, including the roof top, by the following formula:

$$F_x = (V - F_t) \frac{\frac{w_x h_x}{n}}{\sum_{i=1}^n w_i h_i} \quad (10.29)$$

where w_x is the weight at a particular level and h_x is the height of a particular level above the base. At each floor the force F_x is located at mass center.

10.3.4. Story Shear and Overturning Moment

Story shear at level x , V_x , is the sum of all the lateral forces at and above that level.

$$V_x = F_t + \sum_{i=x}^n F_i \quad (10.30)$$

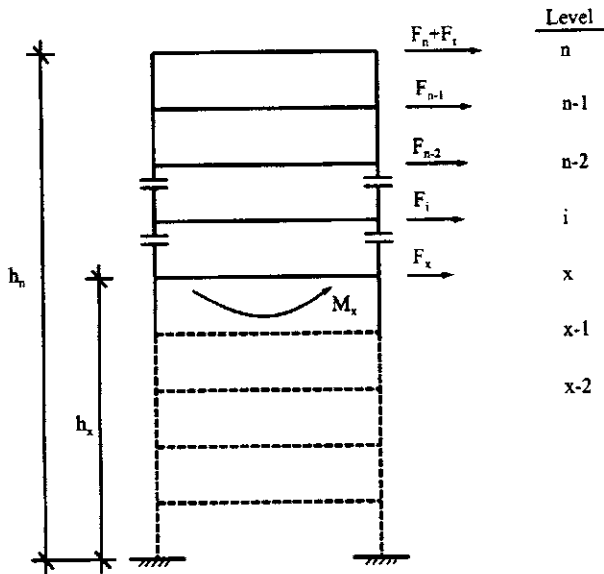


FIG. 10.10 Overturning moment.

The *overturning moment* at a particular level, M_x , is the sum of the moments of the story forces at and above that level as shown in Fig. 10.10 with the following expression:

$$M_x = F_t(h_n - h_x) + \sum_{i=x}^n F_i(h_i - h_x) \quad (10.31)$$

10.3.5. Torsion and P-Δ Effect

10.3.5.1. Torsion

When the rigidity center and the mass center do not coincide at a given story, where diaphragms are not flexible, the design story shear, V_x , at that story causes torsion. This is primary torsion defined as V_x multiplied by the eccentricity between mass center and rigidity center. V_x is the sum of forces F_t and F_x above that story. Due to uncertainty in mass and stiffness distribution, we must consider *accidental torsion* in order to increase the shears of structural elements. Accidental torsion can be obtained as follows. Assume the mass center is placed in each direction a distance equal to 5% of the building dimension at that level perpendicular to the direction of the force under consideration (UBC-94, Section 1628.5). This assumed mass center creates a new eccentricity relative to the rigidity center; thus accidental torsion is obtained from the multiplication of V_x by the new eccentricity. The mass center is placed in each direction so that we may obtain larger combined shear which results from primary torsion and accidental torsion for each individual structural element.

10.3.5.2. P-Δ Effect

UBC-94, Section 1628.9 stipulates that the $P-\Delta$ effect must be included to determine member forces and story drift when the ratio of secondary moment to primary moment exceeds 0.1. (A story drift is the difference in floor deflections between adjacent stories.) This ratio can be calculated for any story as follows: (1) find the sum of the total dead load, floor live load and snow load above the story as P_x ; (2) multiply P_x by structural drift in that story as secondary moment, $P_x\Delta_x$; and (3) divide $P_x\Delta_x$ by the primary moment, which is the product of seismic shear, V_x ,

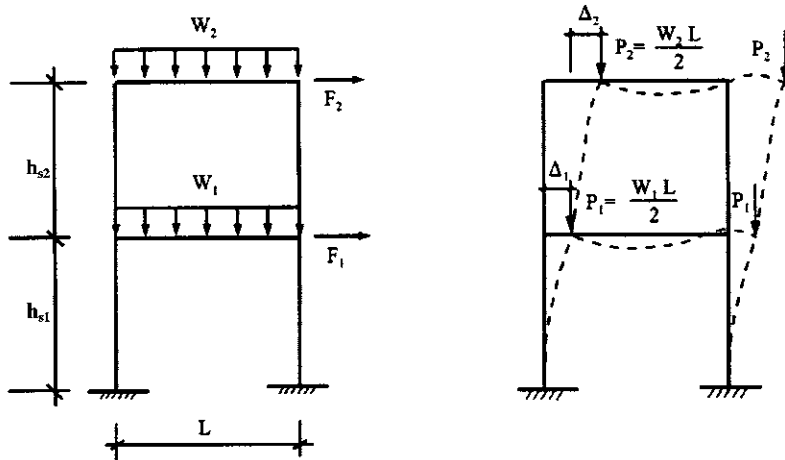


FIG. 10.11 *P*- Δ effect.

in that story times the height of that story. The ratio assessment becomes

$$\frac{P_x \Delta_x}{V_x h_{sx}} = 0 \quad (10.32)$$

where Δ_x is story drift at story level x (displacement of level x relative to displacement below level $x - 1$ due to design lateral force); and h_{sx} is the height of story level x . When θ is less than 0.1 for every story, then the P - Δ effect may be ignored. If $\theta > 0.1$ for any story, then the P - Δ effect on story drifts, shears, member forces, etc. for the whole building must be included by a rational analysis. In seismic zones 3 and 4, P - Δ effect need not be considered if

$$\frac{\Delta_x}{h_{sx}} \leq \frac{0.02}{R_w} \quad (10.33)$$

An example of the P - Δ effect is given in Fig. 10.11. Primary moment and secondary moment at the support as denoted by M_p and M_s , respectively, are

$$M_p = F_1 h_{s1} + F_2 (h_{s1} + h_{s2}); \quad M_s = 2P_2 (\Delta_1 + \Delta_2) + 2P_1 \Delta_1$$

When

$$M_s/M_p > 0.1$$

then the P - Δ effect should be considered in structural analysis from which the member forces are then used for final design. If the structure is in seismic zone 4 and $\Delta_1/h_{s1} < 0.02/R_w$ at the bottom floor, then Eq. (10.32) need not be checked for that floor.

As noted, the P - Δ effect for a whole building must be analyzed when $\theta > 0.10$ at any floor of the building. Among various analytical approaches, two are recommended as follows:

(A) Approximate analysis [5]

1. Calculate the P - Δ amplification factor for each story (where $\theta > 0.10$) as

$$\alpha_d = \frac{\theta}{1 - \theta} \quad (10.34)$$

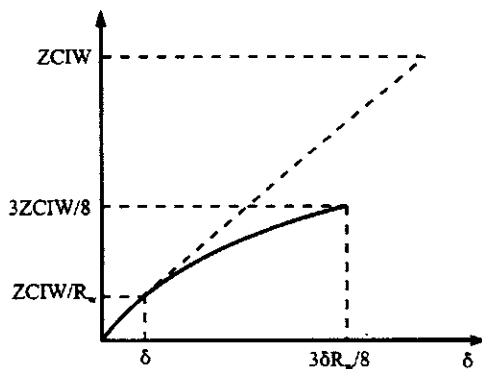


FIG. 10.12 Effect of $3R_w/8$ on design force and displacement.

2. Multiply story shear, V_x , in each story by the multiplier $(1 + \alpha_d)$ for that story and recalculate story shears, overturning moments, and other seismic force effects corresponding to these augmented story shears. The multiplier may be expressed as

$$(1 - \alpha_d) = \frac{1}{(1 - \theta)} = 1 + \theta + \theta^2 + \theta^3 + \dots \quad (10.35)$$

(B) Published computer programs which take the $P-\Delta$ effect into account.

10.3.6. Story Drift Limitations

Story drift limitations are that calculated story drift must be less than allowable story drift. Calculated story drift, Δ_x , includes deflections due to translation and torsional effects. Allowable drifts (UBC-94, Section 1628.8.2) are

$$\Delta_a = \begin{cases} \text{smaller of } \frac{0.04}{R_w} h_{sx} \text{ and } 0.005h_{sx}; & \text{when } T \leq 0.7 \text{ sec} \\ \text{smaller of } \frac{0.03}{R_w} h_{sx} \text{ and } 0.004h_{sx}; & \text{when } T > 0.7 \text{ sec} \end{cases} \quad (10.36)$$

which indicates that a more restrictive requirement should be imposed on flexible buildings ($T > 0.7$ sec) to control inelastic deformation and instability. Certain structures such as single-story steel-framed structures are an exception to this rule. Allowable drift limits may also be exceeded for taller structures, but only if it can be proved that greater drift could be tolerated by both structural elements and nonstructural elements without adversely affecting life safety. Lateral forces used to obtain calculated story drift may be derived from a value of C based on the period determined using Eq. (10.24) without the lower bound of 0.075 for C/R_w , or using Eq. (10.25) without the limitation of 30% in seismic zone 4 or 40% in zones 1, 2, and 3 (UBC-94, Section 1628.8.3). If allowable story drift cannot be satisfied then structural stiffness should be modified.

10.3.7. $3R_w/8$ factor

Base shear in Eq. (10.20) as recommended by UBC-94 is based on allowable stress levels (see Fig. 10.7). However, a structure is designed to be able to resist inelastic deformation for several cycles without collapse. The $3R_w/8$ factor is used to predict maximum inelastic force and maximum displacement relative to seismic design force as shown in Fig. 10.12. The factor is applied to critical element design for force determination in various UBC-94 sections such as 1627.9.1, 1628.7.2,

2211.5.1, and 2211.8.3.1, as well as for deformation requirements in sections 1631.2.4, 1631.2.4.2, 1631.2.11, and 2211.10.4. For instance, a column design for seismic zones 3 and 4 should satisfy the following loading combination in accordance with section 2211.5.1:

$$1.0P_{DL} + 0.7P_{LL} + 3(R_w/8)P_E \quad \text{for compression} \quad (10.37)$$

$$0.85P_{DL} \pm 3(R_w/8)P_E \quad \text{for tension} \quad (10.38)$$

where P_{DL} , P_{LL} , and P_E signify dead load, live load, and earthquake force, respectively. Deformation requirements can be illustrated by using a case where a nonstructural element, such as masonry wall, should have the following separation from adjacent structural elements of vertical column or horizontal beam in accordance with Section 1631.2.4.2:

$$\begin{aligned} \delta_{(\text{required})} &= \delta(3R_w/8) \\ &> 0.5 \text{ in} \end{aligned} \quad (10.39)$$

where δ is the calculated displacement of the structural element due to the required seismic force.

10.4. UBC-97 AND DESIGN PARAMETERS

10.4.1. Criteria for Appropriate Lateral-Force Procedure

UBC-97, like UBC-94, stipulates two procedures to determine seismic force in structural analysis: static lateral-force and dynamic lateral-force procedure (including time-history analysis). Static lateral-force procedure has a new feature, i.e., simplified method, which is explained below. Time-history analysis has two categories: elastic time-history analysis and nonlinear time-history analysis. Requirements for selecting between the two procedures depend on structural irregularities.

10.4.2. Base Shear of Static Lateral-Force Procedure and Related Parameters

In UBC-97 static lateral-force procedure (Section 1630.2), total structural base shear is determined according to seismic zones by using code formulas (30-4)–(30-7). The base shear in seismic zone 4 should be

$$V = \max \left\{ \frac{0.8N_v ZI}{R} W; \quad \min \left[\frac{2.5C_a I}{R} W; \quad \max \left(0.11C_a IW; \quad \frac{C_v I}{RT} W \right) \right] \right\} \quad (10.40)$$

and for other zones

$$V = \min \left[\frac{2.5C_a I}{R} W; \quad \max \left(0.11C_a IW; \quad \frac{C_v I}{RT} W \right) \right] \quad (10.41)$$

UBC-97 allows a simplified static lateral-force procedure for structures in occupancy category 4 or 5 with the following conditions (Section 1629.8.2): (1) buildings not more than three stories in height, excluding basements, that use light-frame construction; (2) other buildings not more than two stories in height, excluding basements. Base shear is determined as

$$V = \frac{3.0C_a}{R} W; \quad F_x = \frac{3.0C_a}{R} w_i \quad (10.42a, b)$$

This equation is based on code formulas (30-11) and (30-12) and meets the requirements in Section 1630.2.3.2. Note that Z , I , W , and w_i in Eqs. (10.40)–(10.42) are the same in UBC-94; C_a and C_v are seismic coefficients related to response parameters of acceleration and velocity, respectively; N_v is the near source factor; and R is a numerical coefficient for inherent overstrength and global capacity of lateral-force-resisting system. Parameters in UBC-97 differing from UBC-94 are briefly described as follows.

10.4.2.1. Seismic Coefficients C_a and C_v

In UBC-97, C_a and C_v determine base five seismic zones divide the U.S.A. (see

five seismic zones divide the U.S.A. (see Fig. 10.6), each with factor Z . UBC-97 classifies soil profile into six types: S_A , S_B , S_C , S_D , S_E and S_F (UBC-97, Section 1636). The use of soil profile types to determine base shear differs in UBC-94 and UBC-97. In the former, site coefficients, S , are given, according to the soil profiles, as shown in Table 10.4. In the latter, soil profile types are classified by determining average shear wave velocity for the top 100 ft of material on site. Profile types are used along with zone factors to determine seismic coefficients which are then employed for calculating base shear. Along with the seismic zone factors and soil profile types, C_a and C_v (UBC-97, Table 16-Q and Table 16-R) are listed in Table 10.6. Note that C_a and C_v are identical in each zone for soil profiles S_B corresponding to rock. Coefficients associated with S_B are decreased by 20% for S_A of hard rock and are increased by 230% for S_E of soft soil. This indicates that (1) ground vibration induced by an earthquake is greater on soft soil than on rock or hard rock; (2) C_a and C_v reflect the amplification of ground vibration due to different soil profiles. Hard rock and rock are mostly found in the eastern and western states, respectively. When the soil properties are not known, S_D can be used to determine the soil profile (UBC-97, Section 1629.3). By comparison, base shear in UBC-97 is close to that required by UBC-94 for rock and hard rock, but UBC-97 requires more base shear than UBC-94 for other soil profile types.

10.4.2.2. Near-Source Factors N_a , N_v

Table 10.6 shows that, in seismic zone 4, C_a and C_v are determined using N_a and N_v , which are near-source factors based on the proximity of a building or structure to known faults with magnitudes and slip rates. These factors, in UBC-97 Tables 16-S and 16-U, are summarized here in Table 10.7. To find N_a and N_v , we need three seismic source types of A, B, and C as given in Table 10.8 (UBC-97, Table 16-U). The rationale for source types is that ground motion is greater in the vicinity of a fault than some distance away, owing to rapid progression of fault rupture. This effect depends on moment magnitude, M , and slip rate, SR . Thus type A represents the most active fault with larger M and SR than the least active fault signified by type C.

TABLE 10.6 Seismic Coefficients C_a and C_v

Seismic Zone Factor Z										
Soil profile type	Z = 0.075 (zone 1)		Z = 0.15 (zone 2A)		Z = 0.2 (zone 2B)		Z = 0.3 (zone 3)		Z = 0.4 (zone 4)	
	C _a	C _v	C _a	C _v	C _a	C _v	C _a	C _v	C _a	C _v
S _A (hard rock)	0.06	0.06	0.12	0.12	0.16	0.16	0.24	0.24	0.32	0.32
S _B (rock)	0.08	0.08	0.15	0.15	0.20	0.20	0.30	0.30	0.40	0.40
S _C (soft rock, dense soil)	0.09	0.13	0.18	0.25	0.24	0.32	0.33	0.45	0.40	0.56
S _D (stiff soil)	0.12	0.18	0.22	0.32	0.28	0.40	0.36	0.54	0.44	0.64
S _E (soft soil)	0.19	0.26	0.30	0.50	0.34	0.64	0.36	0.84	0.36	0.96
S _F									N _a	N _v

TABLE 10.7 Near-source Factors N_a and N_v

Seismic source type	Closest distance to known seismic source					
	$\leq 2 \text{ km}$		5 km		$\geq 10 \text{ km}$	
	N_a	N_v	N_a	N_v	N_a	N_v
A	1.5	2.0	1.2	1.6	1.0	1.2
B	1.3	1.6	1.0	1.2	1.0	1.0
C	1.0	1.0	1.0	1.0	1.0	1.0

TABLE 10.8 Seismic Source Type

Seismic source type	Seismic source description	Seismic source definition	
		Maximum Magnitude	Slip Rate (mm/year)
A	Faults producing large magnitude events and having high rate of seismic activity	$M \geq 7.0$	$SR \geq 5$
B	All faults other than Types A and C	$M \geq 7.0$ $M < 7.0$	$SR < 5$ $SR > 2$
C	Faults producing large magnitude events and having relatively low rate of seismic activity	$M \geq 6.5$ $M < 6.5$	$SR < 2$ $SR < 2$

10.4.2.3. Numerical Coefficient R and Amplification Factor Ω_0

While the physical sense of this coefficient is similar to R_w in UBC-94, it does not have allowable stress factor R_a as shown in Eq. (10.21). This coefficient may be expressed as

$$R = R_d \Omega_0 \quad (10.43)$$

which represents inherent overstrength and global ductility capacity. A range of R and Ω_0 values for several basic structural systems is listed in Table 10.9 (UBC-97, Table 16-N, 16-P). Force amplification factors, Ω_0 , for various structural systems are given in UBC-97 but not in UBC-94.

10.4.3. R_w and R Relationship vs Load Combination

From Eq. (10.21), $R_w = R_d \Omega_0 R_a$, R_a is the allowable stress factor with a value of 1.4–1.5. This value can be found in the Manual of Steel Construction Allowable Stress Design published by the American Institute of Steel Construction (AISC). Average allowable stress is about 60% of nominal yielding stress for which specifications permit an increase of one-third. Considering a shape factor (i.e. S/Z =elastic section modulus/plastic section modulus) of 1.14 for a wide-flange section, we obtain

$$R_a = \frac{1}{0.6(4/3)} 1.14 = 1.4 \quad (10.44)$$

Thus the load combination has different modification factors in UBC-94 and UBC-97:

in UBC-94

$$1.0E \quad \text{for ASD}; \quad 1.5E \quad \text{for LRFD} \quad (10.45)$$

TABLE 10.9 Range of R and Ω_0 Values for Basic Structural Systems

Basic structural systems	Range of R	Range of Ω_0
Bearing wall systems	2.8–5.5	2.2–2.8
Building frame systems	5.0–7.0	2.2–2.8
Moment-resisting frame systems	3.5–8.5	2.8
Dual systems	4.2–8.5	2.8
Nonbuilding structures	2.2–3.6	2.0
Cantilevered column systems—inverted pendulum	2.2	2.0

TABLE 10.10 R_w vs R

R_w (UBC-94)	4	5	6	7	8	9	10	11	12
R (UBC-97)	2.8	3.5	4.2–4.5	5.0	5.5–5.6	6.4–6.5	7.0	7.5	8.5
$R_w/1.4$	2.86	3.57	4.29	5.0	5.71	6.43	7.14	7.86	8.57
$1.5R$	4.20	5.25	6.3–6.75	7.50	8.25–8.4	9.6–9.75	10.5	11.25	12.75

in UBC-97

$$\frac{E}{1.4} \quad \text{for ASD;} \quad 1.0E \quad \text{for LRFD} \quad (10.46)$$

The difference in modification factors can be further observed from the comparison given in Table 10.10.

10.4.4. Load Combination for Strength Design and Allowable Stress Design

Two design principles are used in structural engineering practice: (1) strength design (or load and resistance factor design-LRFD); and (2) allowable stress design (ASD). In the former, the design strength of elements cannot be less than the required ultimate strength. In the latter, the design stress of elements cannot exceed the permissible limit as allowable stress. Thus working loads (or service loads) are factored for various load combinations according to design principles.

10.4.4.1. Load Combination for LRFD and Evaluation of r_{max} and ρ

Let D = dead load, L = floor live load, L_r = roof live load, S = snow load, W = wind load, and E = earthquake load. From UBC-97, Section 1612.2.1, the load combination is summarized in Table 10.11, in which $f_1 = 1.0$ for floors of public assembly, for live loads in excess of 100 psf, and for garage live load; $f_1 = 0.5$ for other live loads; $f_2 = 0.7$ for roof configurations that do not shed snow off the structure; $f_2 = 0.2$ for other roof configurations. Note that dead load is decreased by 10% when seismic or wind loads are applied with omission of live load. Also note that seismic and wind loads are not applied simultaneously.

Earthquake load is

$$E = \rho E_h + E_v \quad (10.47)$$

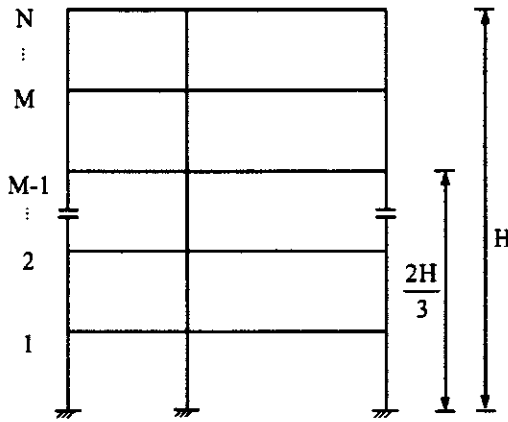
where

$$E_v = 0.5 C_a I D \quad (10.48)$$

E_h = earthquake load due to base shear, and

TABLE 10.11 Load Combination for Strength Design

Load Combination	D	L	Load Factors			E
			L_r	S	W	
D	1.4	—	—	—	—	—
$D + L + L_r$ (or S)	1.2	1.6	0.5	(0.5)	—	—
$D + L_r$ (or S) + L (or W)	1.2	f_1	1.6	(1.6)	(0.8)	—
$D + W + L + L_r$ (or S)	1.2	f_1	0.5	(0.5)	1.3	—
$D + E + (L + S)$	1.2	f_1	—	f_2	—	1.0
$D \pm E$ (or W)	0.9	—	—	—	(±1.3)	±1.0

**FIG. 10.13** Determination parameter M.

ρ = redundancy/reliability factor

$$= 2 - \frac{20}{r_{\max} \sqrt{A_B}}; \quad \left(SI : \rho = 2 - \frac{6.1}{r_{\max} \sqrt{A_B}} \right) \quad (10.49)$$

$1.0 \leq \rho \leq 1.5$; A_B = ground floor area of structure; and r_{\max} = maximum sum of shears in any adjacent columns divided by total design story shear for a given direction of loading = $\max_i (r_i)$, $i = 1, 2, \dots, M$, in which M is any story number at or below two-thirds the height level of the building as shown in Fig. 10.13. See special criteria for braced frames, moment resisting frames, shear walls, and dual systems. Note that ρ serves to encourage multiple lateral load path design: when one element fails, the load can be redistributed to the remaining elements so that collapse mechanism formation will be delayed. Thus ρ penalizes less redundant structures by increasing design lateral force up to 50%.

The determination of r_{\max} and ρ is illustrated in Fig. 10.14. Assume that the shear of the system is obtained as shown in Fig. 10.14a. Shear distribution to individual bays is given in the accompanying figures b–e. r_{\max} and ρ are calculated as follows.

In the N-S direction—Fig. 10.14b represents the two edge frames as a braced frame. Total shear is carried by the bracing member. Thus,

$$r_b = \frac{V/6}{V} = 0.167$$

Figure 10.14c represents the two middle frames as a moment-resisting frame; total shear is carried by all the columns as shown. For the columns common to two bays, 70% of the shear in the middle column should be combined with the shear of the column on the left side and with the shear of the column on the right side; whichever amount is larger should then be used. Thus

$$r_c = \frac{1}{V} \max \left\{ \begin{array}{l} V/12 + 0.7(V/6) \\ 0.7(V/6) + V/12 \end{array} \right\} = 0.2$$

Therefore in the N-S direction,

$$\begin{aligned} r_{\max} &= \max \left\{ \frac{r_b}{r_c} \right\} = \max \left\{ \frac{0.167}{0.2} \right\} = 0.2 \\ \rho &= 2 - 20 / (r_{\max} \sqrt{A_B}) \\ &= 2 - \frac{20}{0.2 \sqrt{90} (40)} = 2 - 1.67 = 0.33 < 1 \end{aligned}$$

The final result for the N-S direction is

$$\rho = 1$$

In the E-W direction—Figure 10.14d represents the two edge frames as a dual system with moment-resisting frame and braced frame. For the shears shown in the figure, the braced frame carries more shear and should be used to calculate r_{\max} as

$$r_d = \frac{1}{V} \left(\frac{3V}{20} \right) = 0.15$$

For a dual system, the value of ρ need not exceed 80% of the result from Eq. (10.49). Thus

$$\begin{aligned} \rho &= 0.8 \left[2 - 20 / (r_{\max} \sqrt{A_B}) \right] \\ &= 0.8 \left[2 - \frac{20}{0.15 \sqrt{90} (40)} \right] = -0.178 < 1 \end{aligned}$$

Therefore

$$\rho = 1$$

Figure 10.14e represents the middle frame as a moment-resisting frame. Column shears are as shown. Code stipulations on columns common to two bays with moment-resisting connections give three possible combinations as

$$r_e = \frac{1}{V} \max \left\{ \begin{array}{l} \frac{V}{12} + 0.7 \left(\frac{V}{6} \right) \\ 0.7 \left(\frac{V}{6} \right) + 0.7 \left(\frac{V}{6} \right) \\ 0.7 \left(\frac{V}{6} \right) + \frac{V}{12} \end{array} \right\} = 0.233$$

$$\rho = 2 - \frac{20}{r_{\max} \sqrt{A_B}} = 2 - \frac{20}{0.233 \sqrt{90} (40)} = 0.571 < 1$$

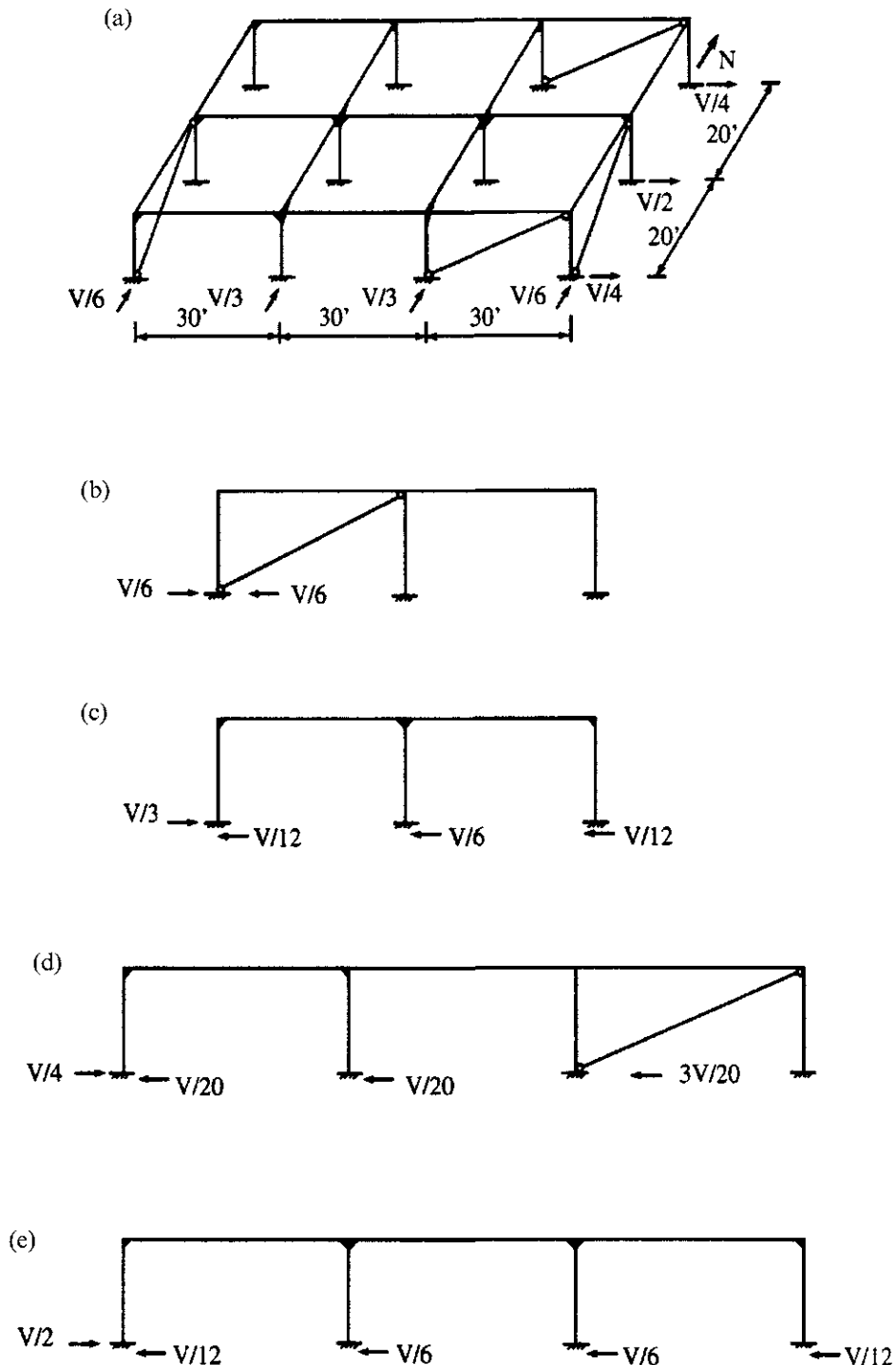


FIG. 10.14 Determination of r_{\max} and ρ . (a) Given shear distribution. (b) Edge frame in N-S direction. (c) Middle frame in N-S direction. (d) Edge frame in E-W direction. (e) Middle frame in E-W direction.

Therefore,

$$\rho = 1$$

The final result for the E-W direction is

$$\rho = 1$$

(B) *Load Combination for ASD*—two approaches of load combinations for allowable stress design are summarized in Table 10.12 as per UBC-97, Sections 1612.3.1 and 1612.3.2. Note that an increase of allowable stress is optional depending on the approach used, and that $E = \rho E_h$ (vertical ground motion E_v is not considered).

10.4.5. Story Shear, Overturning Moment and Restoring Moment

Story shear and overturning moment at level x , V_x and M_x , are the same as UBC-94. For restoring moment, dead load is multiplied by 0.85 in UBC-94 (Section 1631.1) and the moment is thus reduced, but there is no such reduction in UBC-97 (Section 1630.8). Both codes recognize that, in seismic zones 3 and 4, elements supporting discontinuous systems (see Fig. 10.4d) should be designed for maximum force on the system using load combinations. Thus UBC-94 Section 1628.7.2 requires

$$1.0 D + 0.8 L + 3(R_w/8) E \quad (10.50)$$

$$0.85 D \pm 3(R_w/8) E \quad (10.51)$$

and UBC-97 Sections 1630.8.2 and 1612.4 specify

$$1.2 D + f_1 L + 1.0 E_m \quad (10.52)$$

$$1.2 D + f_1 L + 1.0 \Omega_0 E_h \quad (10.53)$$

$$0.9 D \pm 1.0 E_m \quad (10.54)$$

for which all notations are defined in Section 10.4.4 except E_m , which is the estimated maximum

TABLE 10.12 Load Combination for ASD

Load combination	Load Factors											
	Section 1612.3.1 (no increase in allowable stress)			Section 1612.3.2 (1/3 increase in allowable stress)								
	D	L	L_r	S	W	E	D	L	L_r	S	W	E
D	1.0	—	—	—	—	—				N/A		
$D + L$												
$+L_r$ (or S)	1.0	1.0	1.0	(1.0)	—	—	1.0	1.0	1.0	(1.0)	—	—
$D + E$ (or W)	1.0	—	—	—	(1.0)	1/1.4				N/A		
$D \pm E$	0.9	—	—	—	—	1/1.4				N/A		
$D + [L + L_r]$												
(or S) + E (or W)	1.0	0.75	0.75	(0.75)	(1.0)	1/1.4				N/A		
$D + L + E$												
(or W)				N/A			1.0	1.0	—	—	(1.0)	1/1.4
$D + L + W + S$				N/A			1.0	1.0	—	1/2	1.0	—
$D + L + W + S$				N/A			1.0	1.0	—	1.0	1/2	—
$D + L + S + E$				N/A			1.0	1.0	—	1.0	—	1/1.4

earthquake force,

$$E_m = \Omega_0 E_h \quad (10.55)$$

10.4.6 Story Drift, $P-\Delta$ Effect and Torsion

10.4.6.1. Story Drift

Drift or horizontal displacement of a structure is classified as Δ_s and Δ_m . Δ_s is *design response displacement*, which is total drift or total story drift. This is computed using the design seismic forces shown in Eqs. (10.40) and (10.41) without restraints (UBC-97, Section 1630.10.3) imposed by (a) 0.11 C_aIW and (b) 30 or 40% limitation of the period obtained by Rayleigh's equation. Δ_M is the *maximum inelastic response displacement*, caused by design-basis ground motion and computed as follows:

$$\Delta_M = 0.7R\Delta_s \quad (10.56)$$

Alternatively, Δ_M may be computed by nonlinear time-history analysis (UBC-97, Section 1630.9.2).

Calculated story drift using Δ_M must be less than allowable story drift and should include deflection due to translation and torsional effect. Allowable drifts (UBC-97, Section 1630.10.2) are

$$\left. \begin{array}{ll} 0.025 h_{sx}; & \text{when } T \leq 0.7 \text{ sec} \\ 0.02 h_{sx}; & \text{when } T > 0.7 \text{ sec} \end{array} \right\} \quad (10.57)$$

which indicates that a more stringent requirement is imposed on flexible structures, as in UBC-94. When computing story drift, Δ_s , the mathematical model of a structure should include all elements of a lateral-force-resisting system and comply with the following: (1) for reinforced concrete and masonry elements, stiffness properties should consider the effects of cracked sections; (2) for steel moment frame systems, the contribution of panel zone deformations to overall story drift should be included (UBC-97, Section 1630.12). Note that no drift limit should be imposed on single-story steel-framed structures, as per UBC-94, Section 1628.8.2 and UBC-97, Section 1630.10.2 for certain classifications of occupancy.

10.4.6.2. $P-\Delta$ Effect

UBC-97 repeats UBC-94 (Section 1630.1.3); when the ratio of secondary moment to primary moment exceeds 0.1, the $P-\Delta$ effect must be considered in determining member forces and story drift. In seismic zones 3 and 4, the $P-\Delta$ effect need not be considered if

$$\frac{\Delta_x}{h_{sx}} \leq \frac{0.02}{R} \quad (10.58)$$

10.4.6.3. Torsion

The requirements for torsion in UBC-97 are the same as those in UBC-94.

10.4.7. Relationships among $3R_w/8$, Ω_0 and $0.7R\Delta_s$

In UBC-97, structures are designed to resist several cycles of inelastic deformation without collapse. Ω_0 is introduced to predict maximum inelastic force and maximum displacement relative to seismic design force, replacing $\frac{3}{8}R_w$ in UBC-94. Therefore column design for seismic zones 3 and

4, as per UBC-97 Section 2213.5.1, should be

$$1.0 P_{DL} + 0.7 P_{LL} + \Omega_0 P_E \quad \text{for compression} \quad (10.59)$$

$$0.85 P_{DL} + \Omega_0 P_E \quad \text{for tension} \quad (10.60)$$

which are analogous to Eqs. (10.37) and (10.38) based on UBC-94.

$0.7R\Delta_s$ replaces $3R_w/8$ in building separation as per UBC-97 Section 1633.2.4.2. Thus a nonstructural-element masonry wall should be separated from an adjacent structural element as follows:

$$\begin{aligned} \delta_{(\text{required})} &= 0.7 R \Delta_s \\ &> 0.5 \text{ in} \end{aligned} \quad (10.61)$$

which is analogous to Eq. (10.39) for UBC-94.

10.5. IBC-2000 AND DESIGN PARAMETERS

10.5.1. Criteria for Appropriate Lateral-Force Procedure

IBC-2000 classifies structures into two categories, seismically isolated and seismically non-isolated. For seismically non-isolated structures, two procedures apply to finding seismic forces: (1) equivalent lateral force; and (2) dynamic lateral force (not including time-history analysis). Likewise, two procedures apply to seismically isolated structures: (1) equivalent lateral force; and (2) dynamic lateral force (including time-history analysis). Vertical and plan structural irregularities in IBC-2000 are slightly different from both UBCs in that stiffness irregularity (see Fig. 10.3c) is categorized as (1) soft story or (2) extreme soft story, and torsional irregularity as (a) torsional irregularity, or (b) extreme torsional irregularity.

For non isolated structures, selecting the appropriate procedure depends on structural irregularities (see Section 10.3.1) and on *structural design categories A–F*. These categories are determined by *seismic use groups I, II, and III* and *design spectral response acceleration coefficients S_{DS} and S_{DI}* , at short and 1 sec periods, respectively. Table 10.13 shows the classification of seismic use groups (IBC-2000, Table 1604.5); Tables 10.14 and 10.15 delineate structural design categories [IBC-2000, Tables 1616.3(1) and (2)] for which S_{DS} and S_{DI} are found using code Equations 16-16–16-19 [see Eqs. (10.66)–(10.69)] to scale S_S and S_1 (maximum spectral response acceleration at short period and 1 sec period, respectively) from IBC-2000, Figures 1615(1) and (2) (see Figs. 10.15 and 10.16). When design response acceleration at 1 sec period, S_{DI} , exceeds $0.75g$, structures in groups I and II should be assigned to seismic design category E, and structures in group III should be assigned to seismic design category F.

IBC-2000 requires that structures assigned to seismic design category A use a simplified analysis defined as minimum lateral force (Section 1616.4.1), structures in categories B and C use equivalent lateral force or a more rigorous analysis, and structures in D, E, and F use the analysis procedure in Table 10.16 (IBC-2000, Section 1616.6 and Table 1616.6.3).

10.5.2. Base Shear of Equivalent Lateral-Force Procedure and Related Parameters

In IBC-2000 equivalent lateral-force procedure, the total base shear is specified according to design categories and can be summarized in (A)–(D) as follows.

(A) *For seismic design categories B–D*—(IBC-2000, Sections 1616.6.2 and 1616.6.3, Equations 16-34–16-37)

$$V = \min \left\{ \frac{S_{DI}}{\left(\frac{R}{I_E}\right)T} W; \quad \max \left[\frac{S_{DS}}{\left(\frac{R}{I_E}\right)} W; \quad 0.044 S_{DS} I_E W \right] \right\} \quad (10.62)$$

TABLE 10.13 Seismic Use Group and Occupancy Importance Factor

Seismic use group	Occupancy importance factor <i>I</i>	Nature of occupancy
Group I	1.0	All occupancies except those listed below
Group II	1.25	Eight occupancies listed in the code include: buildings and other structures where 300 or more people congregate in one area; elementary school, secondary school, day-care facilities with a capacity greater than 250; college or adult education facilities with a capacity greater than 500; health care facilities with a capacity of 50 or more resident patients; jail and detention facilities; any other occupancy with a capacity greater than 5000; power-generating stations and other public utility facilities not included in seismic use Group IV; water treatment facilities required for primary treatment and disinfection of potable water.
Group III	1.5	Nine occupancies listed in the code include: fire, rescue, and police stations; hospitals; designated emergency preparedness and operation centers as well as emergency shelters; power-generating stations or other utilities required as emergency back-up facilities for seismic use Group IV structures; structures containing highly toxic material; aviation control towers; designated communication centers; structures for critical national defense functions; water treatment facilities required to maintain water pressure for fire suppression.
Group IV	1.0	Three occupancies listed in the code include: agricultural facilities; certain temporary facilities; and minor storage facilities.

TABLE 10.14 Seismic Design Category Based on Short-Period Response Accelerations

Value of S_{DS}	Seismic use group		
	I	II	III
$S_{DS} < 0.167g$	A	A	A
$0.167g \leq S_{DS} < 0.33g$	B	B	C
$0.33g \leq S_{DS} < 0.50g$	C	C	D
$0.50g \leq S_{DS}$	D	D	D

TABLE 10.15 Seismic Design Category Based on 1 sec Period Response Accelerations

Value of S_{D1}	Seismic use group		
	I	II	III
$S_{D1} < 0.067g$	A	A	A
$0.067g \leq S_{D1} < 0.133g$	B	B	C
$0.133g \leq S_{D1} < 0.20g$	C	C	D
$0.20g \leq S_{D1}$	D	D	D

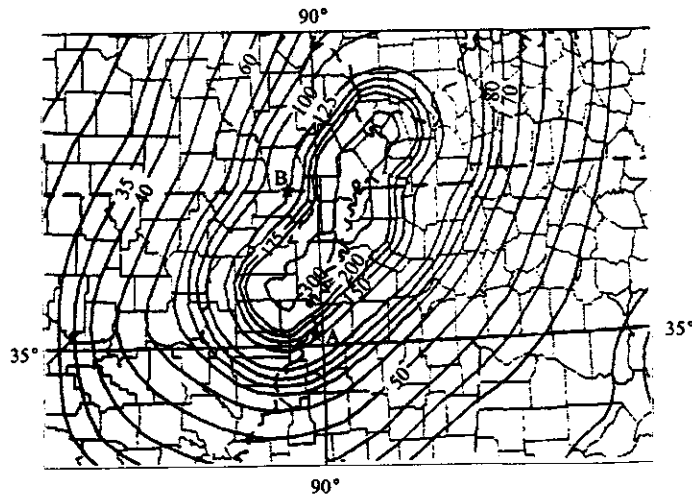


FIG. 10.15 Maximum considered earthquake ground motion for 0.2 sec spectral response acceleration (%g) site class B, S_S . *A: City of Memphis; *B: Location for Example 10.7.3.

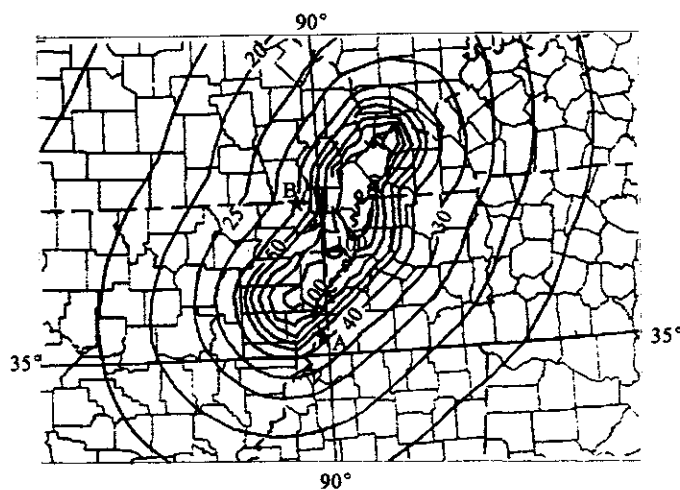


FIG. 10.16 Maximum considered earthquake ground motion for 1 sec spectral response acceleration (%g) site class B, S_1 . *A: City of Memphis; *B: Location for Example 10.7.3.

(B) For seismic design categories E and F and structures for which $S_1 \geq 0.6g$ —(IBC-2000, Section 1616.6.3, Equations 16-34–16-38)

$$V = \min \left\{ \frac{S_{D1}}{\left(\frac{R}{I_E}\right)T} W; \quad \max \left[\frac{S_{DS}}{\left(\frac{R}{I_E}\right)} W; \quad \frac{0.5S_1}{\left(\frac{R}{I_E}\right)} W; \quad 0.044S_{DS} I_E W \right] \right\} \quad (10.63)$$

where S_1 shall be determined from seismic maps (IBC-2000, Section 1615.1).

TABLE 10.16 Analysis Procedures for Seismic Design Categories D, E and F

Structure description	Minimum allowable analysis procedure for seismic design
1. Seismic use group I buildings of light-frame construction three stories or less in height and of other construction two stories or less in height with flexible diaphragms at every level.	Simplified procedure (see Section 10.5.2C)
2. Regular structures up to 240 ft in height.	Equivalent lateral force procedure (see Sections 10.5.2 and 10.6).
3. Structures that have only vertical irregularities of type 1a, 1b, 2, or 3 in Table 1616.5.2, or plan irregularities of type 1a, 1b of Table 1616.5.1, and have a height exceeding five stories or 65 ft, and all structures exceeding 240 ft in height.	Modal analysis procedure (see Section 10.9.3 and 10.10).
4. All other structures designated as having plan or vertical irregularities.	Equivalent lateral force procedure with dynamic characteristics included in the analytical model
5. Structures with all of the following characteristics:	Modal analysis procedure: site-specific response spectrum to be used with design base shear not less than that determined from Section 1617.4.1.
<ul style="list-style-type: none"> • located in an area with S_{D1} of 0.2 or greater; • located in an area assigned to site class E or F; and • with a natural period T of 0.7 sec or greater. 	

(C) For seismic design category A—simplified analysis can be used (IBC-2000, Equation 16-27)

$$V = 0.01W; \quad F_x = 0.01 w_x \quad (10.64)$$

(D) For seismic design categories B–F of Seismic Use Group I—simplified analysis can be used for light-frame construction not exceeding three stories in height, and any construction other than light frame not exceeding two stories in height with flexible diaphragms at every floor (building is fixed at the base) (Section 1617.5.1)

$$V = \frac{1.2S_{DS}}{R} W; \quad F_x = \frac{1.2 S_{DS}}{R} w_x \quad (10.65)$$

S_{DS} and S_{D1} are design spectral response acceleration coefficients at short and 1 sec periods, respectively; S_1 is the maximum considered earthquake spectral response acceleration at 1 sec period (Section 1615.1); I_E is the seismic importance factor given in Table 10.13; R is the response modification factor given in IBC-2000, Table 1617.6 (R values for basic structural systems are given in Table 10.10); and W is the seismic dead load. Parameters related to the variables in Eqs. (10.62)–(10.64) are further described in (E) and (F) as follows.

(E) Design spectral response acceleration coefficients S_{DS} and S_{D1} —site categorization in IBC-2000 is the same as UBC-97, where soil profiles S_A , S_B , S_C , S_D , S_E , and S_F are respectively identical to site classes A, B, C, D, E, and F defined in IBC-2000, Table 1615.1.1. Regionalization of the maximum considered earthquake ground motion for each site class is given in IBC-2000. From the regionalization maps, 0.2 sec and 1.0 sec spectral response acceleration (S_S and S_1)

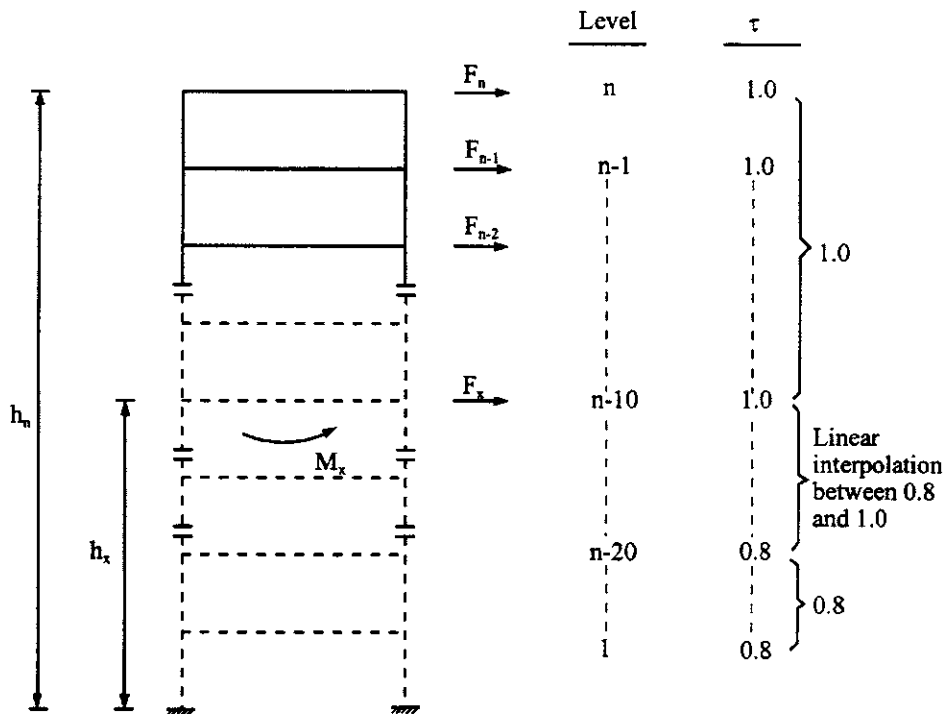


FIG. 10.17 Lateral forces and overturning moment.

can be obtained in terms of percentage of g . Figures 10.15 and 10.16 show a partial regionalization map near the New Madrid fault for site class B. These two figures illustrate typical contours of maximum earthquake spectral response accelerations at short period, S_s , and 1 sec period, S_1 . The adjusted maximum considered earthquake spectral response acceleration for short period, S_{MS} , and 1 sec period, S_{M1} , can then be obtained from the effects of site class (Section 1615.1.2) as

$$S_{MS} = F_a S_s \quad (10.66)$$

$$S_{M1} = F_v S_1 \quad (10.67)$$

where F_a and F_v are site coefficients defined in Tables 1615.1.2(1) and 2(2) (IBC-2000), listed here in Tables 10.17 and 10.18. In Tables 10.17 and 10.18 "a" signifies that site-specific geotechnical investigation and dynamic site response analysis should be performed to determine appropriate values.

In accordance with Section 1615.1.3 (IBC-2000), the design spectral response acceleration at short period, S_{DS} , and 1 sec period, S_1 , can be obtained as

$$S_{DS} = \frac{2}{3} S_{MS} \quad (10.68)$$

$$S_{D1} = \frac{2}{3} S_{M1} \quad (10.69)$$

which are used in Eqs. (10.62) and (10.63) to determine base shear.

(F) *Fundamental period T*—IBC-2000 specifies three approaches for computing fundamental period T in the direction under consideration:

1. Find the period from substantiated analysis with proper structural properties and deformational character of the resisting elements. The calculated period cannot exceed

TABLE 10.17 Values of Site Coefficient F_a as a Function of Site Class and Mapped Spectral Response Acceleration at Short Periods (S_s)

Site class	Mapped spectral response acceleration at short periods				
	$S_s \leq 0.25$	$S_s = 0.50$	$S_s = 0.75$	$S_s = 1.00$	$S_s \geq 1.25$
A	0.8	0.8	0.8	0.8	0.8
B	1.0	1.0	1.0	1.0	1.0
C	1.2	1.2	1.1	1.0	1.0
D	1.6	1.4	1.2	1.1	1.0
E	2.5	1.7	1.2	0.9	a
F	a	a	a	a	a

TABLE 10.18 Values of Site Coefficient F_v as a Function of Site Class and Mapped Spectral Response Acceleration at 1 sec Period (S_1)

Site Class	Mapped spectral response acceleration at 1 sec periods				
	$S_1 \leq 0.1$	$S_1 = 0.2$	$S_1 = 0.3$	$S_1 = 0.4$	$S_1 \geq 0.5$
A	0.8	0.8	0.8	0.8	0.8
B	1.0	1.0	1.0	1.0	1.0
C	1.7	1.6	1.5	1.4	1.3
D	2.4	2.0	1.8	1.6	1.5
E	3.5	3.2	2.8	2.4	a
F	a	a	a	a	a

the product of the coefficient for the upper limit on calculated period, C_u , and approximate fundamental period, T_a . Table 10.19 here gives C_u as does Table 1617.4.2 in IBC-2000.

- Find the approximate fundamental period T_a (IBC-2000, Equation 16-39) based on an empirical equation identical to Eq. (10.24) used in UBC-94 and UBC-97. IBC-2000 gives more detailed information for using this approach than UBC.
- Find the approximate fundamental period T_a (IBC-2000, Equation 16-40) for concrete and steel moment-resistant frame buildings not exceeding 12 stories and having a minimum story height of 10 ft from

$$T_a = 0.1 N \quad (10.70)$$

where N is the number of stories.

10.5.3. Vertical Distribution of Lateral Forces

After base shear, V , is determined, use Eqs. (10.71) and (10.72) (IBC-2000, Section 1617.4.3) to obtain vertical distribution of the shear over the height of a structure as lateral forces at each floor level

$$F_x = C_{vx} V \quad (10.71)$$

$$C_{vx} = \frac{w_x h_x^k}{\sum_{i=1}^n w_i h_i^k} \quad (10.72)$$

where w_x , w_i , h_x and h_i are defined in Eq. (10.29). Note how Eq. (10.72) differs from Eq. (10.29): (1) no extra force, $F(t)$, is considered at the top floor of the building; (2) the k factor takes into account a flexible structure's higher mode shapes.

TABLE 10.19 Coefficient for Upper Limit on Calculated Period

Design spectral response acceleration at 1 sec period, S_{DI}	Coefficient C_u
≥ 0.4	1.2
0.3	1.3
0.2	1.4
0.15	1.5
≤ 0.1	1.7

If the period of a structure is not more than 0.5 sec, then its shear distribution is based on a straight-line mode shape as shown in Fig. 10.2. If the period of a structure is more than 0.5 sec, then a nonlinear mode shape is used with distribution exponent k , which has the following range of variation:

$$k = \begin{cases} 1 & \text{if } T \leq 0.5 \text{ sec} \\ 2.5 & \text{if } T \geq 2.5 \text{ sec} \\ 2 \text{ or linear interpolation} & \text{between 1 and 2 if } 0.5 < T < 2.5 \text{ sec} \end{cases} \quad (10.73)$$

10.5.4. Horizontal Shear Distribution and Overturning Moment

Seismic design story shear at any floor level x is derived by summation of the lateral forces distributed above that level as

$$V_x = \sum_{i=1}^n F_i \quad (10.74)$$

The overturning moment at x level, M_x , is the sum of the moments caused by lateral forces above that level. At lower levels, M_x needs to be reduced through multiplying the overturning moment by a reduction factor τ as (IBC-2000, Section 1617.4.5):

$$M_x = \tau \sum_{i=x}^n F_i(h_i - h_x) \quad (10.75)$$

Lateral forces, overturning moment, and the variation range of overturning moment reduction factor are shown in Fig. 10.17.

10.5.5. Deflection and Story Drift

IBC-2000 (Section 1617.4.6.1) requires that design story drift, Δ , be computed as the difference between the deflections of the mass center at the top and at the bottom of the story under consideration. For structures assigned to seismic design category C, D, E or F having a plan with torsional irregularities (IBC-2000, Table 1616.5.1), design story drift Δ is computed as the largest difference between deflections along any edge of the structure at the top and bottom of the story under consideration.

At level x , deflection δ_x is determined according to code Equation 16-46 as

$$\delta_x = \frac{C_d \delta_{xe}}{I_E} \quad (10.76)$$

where δ_{xe} is deflection found by elastic analysis of the seismic force-resisting system. Hence δ_{xe} multiplied by deflection amplification factor, C_d , gives inelastic deflection within the code's

TABLE 10.20 Allowable Story Drift, Δ_a (in.)

Building	Seismic use Group		
	I	II	III
Buildings, other than masonry shear wall or masonry wall frame buildings, four stories or less in height with interior walls, partitions, ceilings, and exterior wall systems that have been designed to accommodate story drifts	0.025 h_{sx}	0.020 h_{sx}	0.015 h_{sx}
Masonry cantilever shear wall buildings	0.010 h_{sx}	0.010 h_{sx}	0.010 h_{sx}
Other masonry shear wall buildings	0.007 h_{sx}	0.007 h_{sx}	0.007 h_{sx}
Masonry wall frame buildings	0.013 h_{sx}	0.013 h_{sx}	0.010 h_{sx}
All other buildings	0.020 h_{sx}	0.015 h_{sx}	0.010 h_{sx}

Note: no drift limit should be considered for single-story buildings with interior walls, partitions, ceilings, and exterior wall systems that have been designed to accommodate the story drifts; and h_{sx} is the story height below level x .

ductility range. Designed story drift should not exceed allowable story drift Δ_a (i.e. $\Delta \leq \Delta_a$). Δ_a is given in Table 10.20 (IBC-2000, Table 1617.3) and is mainly based on construction material, characteristics of a structural system, and seismic use group. Note that design drift resulting from the simplified analysis procedure in Eq. (10.65) should be $\Delta \leq 0.01$ of story height (IBC-2000, Section 1617.5.3).

10.5.6. $P-\Delta$ Effect

The $P-\Delta$ effect on story shears and moments, the resulting member forces and moments, and story drifts thus induced need not be considered when the stability coefficient, θ , is equal to or less than 0.1 (Section 1617.4.6.2).

$$\theta = \frac{P_x \Delta}{V_x h_{sx} C_d} \quad (10.77)$$

where θ cannot exceed θ_{max} , which is calculated as follows:

$$\theta_{max} = \frac{0.5}{\beta C_d} \leq 0.25 \quad (10.78)$$

β is the ratio of shear demand to shear capacity for the story between level x and $x-1$. When this ratio is not calculated, a value of 1.0 is used. If θ is greater than θ_{max} , then a structure is potentially unstable and must be redesigned. To include the $P-\Delta$ effect in story drift, multiply design story drift by $a_d = 1/(1-\theta)$ [see Eq. (10.35)], where $0.1 < \theta \leq \theta_{max}$. Note that Eqs. (10.77) and (10.32) are actually the same. This is because the drift Δ in Eq. (10.77) is obtained from δ_x in Eq. (10.76) with multiplication factor C_d , which is the denominator in Eq. (10.77). Substituting Eq. (10.76) into Eq. (10.77) thus eliminates C_d . While the criterion for $\theta \leq 0.1$ is the same in UBC-94, UBC-97 and IBC-2000, the upper bound of stability coefficient, θ_{max} , is not part of either UBC. Using the structural optimization approach [8] shows the influence of effective peak acceleration and effective peak velocity on θ in various seismic zones specified in ATC-3. A rational analysis to include the $P-\Delta$ effect in building design is recommended, as discussed in Section 10.3.5.2.

10.6. SUMMARY COMPARISON OF UBC-94, UBC-97 AND IBC-2000 LATERAL FORCE PROCEDURES

UBC-94	IBC-97	Structural description (Section 1627.8.2)	Structural description (Section 1629.8.3)	Structural description (Section 1616.6.2 and 1616.6.3)
1. All structures, regular or irregular, in seismic zone 1 and occupancy category 4 in seismic zone 2.	1. All structures, regular or irregular, in seismic zone 1 and occupancy categories 4 and 5 in seismic zone 2.	1. Structures assigned to category B and C.	1. Structures assigned to category B and C.	1. Structures assigned to categories D, E, and F.
2. Regular structures under 240 ft in height with lateral-force resistance provided by system listed in Table 16-N except where Sec. 1627.8.3, item 4 applies.	2. Regular structures under 240 ft in height with lateral force resistance provided by system listed in Table 16-N, except where Sec. 1629.8.4, item 4 applies.	2. Structures assigned up to 240 ft in height.	2. Structures assigned up to 240 ft in height.	(a) Regular structures up to 240 ft in height.
3. Irregular structures not more than five stories or 65 ft in height.	3. Same as UBC-94.	3. All other structures designated as having plan or vertical irregularities.	3. All other structures designated as having plan or vertical irregularities.	(b) All other structures should use equivalent force procedure with dynamic characteristics included in the analytical model.
4. Structures having a flexible upper portion supported on a rigid lower portion where both portions of the structure considered separately can be classified as regular. Average story stiffness of the low portion is at least 10 times the average story stiffness of the upper portion, and period of the entire structure is not greater than 1.1 times the period of the upper portion considered as a separate structure fixed at the base.	4. Same as UBC-94.	See Tables 1615.5(1) and 1615.5(2) for classification of categories A-F.	See Tables 1615.5(1) and 1615.5(2) for classification of categories A-F.	
Base shear (Section 1628.2.1) bound limit (Section 1628.2.1)	Base shear (Section 1630.2.1)	Base shear (Section 1630.2.1)	Base shear (Section 1630.2.1)	Base shear (Section 1617.4.1)
$V = \frac{ZIC}{R_w} W$ $C = \frac{1.25S}{T^{2/3}}$	$V = \frac{C_v I}{R T} W$ Bound limit, Sec. 1632.2.1 V should not exceed	$V = C_s \psi$ $C_s = \frac{S_{D1}}{\left[\frac{R}{I_E} \right]}$	$\frac{2.5C_s I}{R} \psi$ Bound limit, Sec. 1617.4.1.1; C_s should not exceed	$C_s = \frac{S_{D1}}{\left[\frac{R}{I_E} \right]} T$ V should not be less than $0.11C_a I W$
$C \leq 2.75$				
Z = seismic zone factor, Table 16-I I = importance factor, Table 16-K S = site coefficient, Table 16-J				

		Base shear (Section 1628.2.1)		Base shear (Section 1630.2.1)		Base shear (Section 1617.4.1)	
=	total seismic dead load, Sec. 1628.1	In seismic zone 4, total base shear should not be less than	C_s should not be less than				
=	fundamental period of vibration (in sec) of structure in direction under consideration			$C_s = 0.044S_{\text{D}s}I_E$			
=	numerical coefficient, Tables 16-N and 16-P			In seismic design categories E and F, C_s should not be less than			
C_a , C_v	= seismic coefficient based on zone factor, Z , and soil profile, S_A , S_B ... S_F ; Tables 16-Q and 16-R, respectively.			$C_s = \frac{0.5S_1}{R/I_E}$			
S_o	Soil profile Table 16-J is derived from average shear wave velocity, v_s , Sec. 1636.2.1; average field standard penetration resistance, \bar{N} , and average standard penetration resistance for cohesionless soil layers, N_{CH} , Sec. 1636.2.2; and average undrained shear strength, S_{cu} , Sec. 1636.2.3.			C_s = seismic response coefficient ψ = effective seismic weight of structure, Sec. 1617.4.1			
N_v , N_a	= near source factor to determine C_v , and C_a (only in zone 4)			I_E = importance factor, Table 1604.5			
I	= same as UBC-94, Table 16-K			R = response modification factor, Table 1617.6			
R	= numerical coefficient representative of inherent overstrength and global ductility of lateral force-resisting system, Table 16-N or Table 16-P.			S_{Ds} = design spectral response acceleration at short period, Sec. 1615.1.3			
W	= same as UBC-94, Sec. 1630.1.1			S_1 = maximum considered earthquake spectral response acceleration at 1 sec period, Sec. 1615.1			
T	= same as UBC-94			S_{MS} = $\frac{2}{3}S_{MS}$			
				S_{D1} = $\frac{2}{3}S_{M1}$			
				S_{MS} = maximum considered earthquake spectral response acceleration for short period, Sec. 1615.1.2			
				S_{M1} = maximum considered earthquake spectral response acceleration for 1 sec period, Sec. 1615.1.2			
				$S_{MS} = F_a S_a$; $S_{M1} = F_v S_1$			
				F_a , F_v = site coefficient, Table 1615.1.2(1) and (2), respectively			
				S_s , S_1 = mapped spectral acceleration for short period, and 1 sec period, respectively (Sec. 1615.1).			

STATIC AND DYNAMIC LATERAL-FORCE PROCEDURES

643

<i>Period T (Section 1628.2.2)</i>	<i>Period T (Section 1630.2.2)</i>	<i>Period T (Section 1617.4.2)</i>
Method A $T_A = C_1(h_n)^{3/4}$	Method A Same as UBC-94	Method A T is established using structural properties and deformation characteristics with properly substantiated analysis.
C_1 = coefficient for different structures h_n = height of structure		
Method B	Method B Same as UBC-94	Method B Approximate fundamental period T_a , Sec. 1617.4.2.1
		$T_a = C_7(h_n)^{3/4}$
		Alternately for a steel and concrete frame building not exceeding 12 stories and having a minimum story height of 10 ft, the period can be determined as
		$T_a = 0.1N, \quad N = \text{no. of stories}$
		Relationship between T_A and T_B same as UBC-94.
		$T_B = 2\pi \sqrt{\frac{\left(\sum_{i=1}^n w_i \delta_i^2\right)}{g \sum_{i=1}^n f_i \delta_i}}$
		The relationship between T_A and T_B in seismic zone 4
		$T_B \leq 1.3T_A$
		and in seismic zones 1, 2, and 3
		$T_B \leq 1.4T_A$
		<i>Simplified method</i>
		<i>Simplified design base shear (Section 1630.2.3)</i>
		<i>Simplified analysis as minimum lateral force requirement (Sections 1616.4.1 and 1617.5)</i>
Not available	Base shear	Design lateral force at level x
	$V = \frac{3.0 C_a}{R} W$	$F_x = 0.01 w_x$ (for category A only--see criteria in Section 1616.4)
	Vertical distribution	$F_x = \frac{1.25 S_{DS}}{R} w_x$ (for category B, C, D, E, and F —see criteria in Section 1616.6.1)
	$F_x = \frac{3.0 C_a}{R} W_i$	w_x = gravity load at level x The seismic load, E , resulting from F_x can be directly used for load combinations.
		for structures conforming to Section 1629.8.2; when the simplified method is used, Sections 1630.1.2, 1630.1.3, 1630.5, 1630.9, 1630.10, and 1631 do not apply.

Vertical distribution of force (Section 16.28.4)

Vertical distribution of force (Section 1630.5)

Vertical distribution of force (Section 1617.4.3)

Same as UBC-94.

Lateral force at level x

$$V = F_i + \sum_{i=1}^n F_i$$

additional force at top of building

$$F_t = \begin{cases} 0, & 0.07TV \leq 0.25V, \quad T \leq 0.7 \text{ sec} \\ 0.07TV, & T > 0.7 \text{ sec} \end{cases}$$

force at each floor

$$F_x = \frac{(V - F_t)w_x h_x}{\sum_{i=1}^n w_i h_i}$$

$C_{vx} = \text{vertical distribution factor}$
 $V = \text{total design lateral force or shear at base of building}$
 $k = \text{distribution exponent related to building period as}$

$$k = \begin{cases} 1, & T \leq 0.5 \text{ sec} \\ 2, & T \geq 2.5 \text{ sec} \\ 2, & \text{or linear interpolation between 1 and} \\ 2, & 0.5 < T < 2.5 \text{ sec} \end{cases}$$

Horizontal distribution of shear and torsion (Sections 1630.6 and 1630.7)

Horizontal distribution of shear and torsion (Section 1617.4.4)

Same as UBC-94.

Same as UBC-94.

a rigid diaphragm structure, accidental torsion should be combined with primary torsion from which shear should be distributed to the various elements of the vertical lateral-force-resisting system proportional to their rigidities. When the diaphragm is flexible ($\delta_{\max} = 2 \delta_{\text{avg}}$), then accidental torsion should be amplified by

$$A_x = \left[\frac{\delta_{\max}}{1.2\delta_{\text{avg}}} \right]^2 \leq 3.0$$

<i>Overturning moment (Sections 1631.1 and 1628.7.1)</i>	<i>Overturning moment (Sections 1630.8.1)</i>	<i>Overturning moment (Sections 1617.4.5)</i>
Overturning moment at level x	Same as UBC-94 except dead load that causes restoring moment should not be multiplied by 0.85.	$M_x = \tau \sum_{i=x}^n F_i(h_i - h_x)$ <p>τ = overturning moment reduction factor determined as (see Fig. 10.17)</p> $\begin{cases} 1.0 & \text{for top 10 stories;} \\ 0.8 & \text{for 20th story from the top and below;} \\ & \text{value between 1.0 and 0.8 determined by a straight line interpolation for stories between the 20th and 10th stories below the top.} \end{cases}$
	For working stress design, dead load which causes restoring moment should be multiplied by 0.85 to reduce uplift.	
<i>Story drift determination (Section 1630.9.2)</i>	<i>Story drift determination (Section 1630.9.2)</i>	<i>Story drift determination (Section 1617.4.6.1)</i>
No specific recommendation; use rational elastic analysis for Δ	Maximum inelastic response displacement $\Delta_M = 0.7R\Delta_s$ Δ_s = elastic displacement or story drift.	Deflection of level x $\delta_x = \frac{C_d \delta_{xe}}{I_E}$ C_d = deflection amplification factor in Table 1617.6 δ_{xe} = deflection determined using elastic analysis.
<i>Story drift limitation (Section 1628.8.2)</i>	<i>Story drift limitation (Section 1630.10.2)</i>	<i>Story drift limitation (Section 1617.3)</i>
		$\begin{cases} \Delta \leq \frac{0.04h_i}{R_w} & T \leq 0.7 \text{ sec} \\ \Delta \leq 0.005h_i & T > 0.7 \text{ sec} \end{cases}$ Δ_a = allowable story drift which depends on building type and seismic use group, Table 1617.3, h_i = story height of i th floor.
		$\delta_v < \Delta_a$

h_i = story height of the i th floor.

<i>P</i> -Δ effect (Section 1628.9)	<i>P</i> -Δ effect (Section 1630.1.3)	<i>P</i> -Δ effect (Section 1617.4.6.2)
Seismic zones 3 and 4	In seismic zones 3 and 4	<i>P</i> -Δ effects need not be considered when
$\frac{\Delta}{h} \leq \frac{0.02}{R_w}$; <i>P</i> -Δ effect need not be considered	$\frac{\Delta}{h} \leq \frac{0.02}{R}$; <i>P</i> -Δ effect need not be considered	$\theta = \frac{P_x \Delta}{V_x h_{sx} C_d} \leq 0.1$; $\theta \leq \theta_{max} = \frac{0.5}{\beta C_d} \leq 0.25$
<i>P</i> -Δ effect need not be considered when ratio of secondary to primary moment does not exceed 0.1.	<i>P</i> -Δ effect need not be considered when ratio of secondary to primary moment does not exceed 0.1.	P_x = total unfactored vertical design load above level x . Δ = story drift occurring simultaneously with V_x acting between level x and $x-1$. h_{sx} = story height below level x . β = ratio of shear demand to shear capacity for story between level x and $x-1$; $\beta = 1$ when β is not calculated.
<i>LRFD</i> load combination (Chapter 22, Div. VII, D, A4)	<i>LRFD</i> load combination (Section 1612.2.1) (basic load combination)	<i>LRFD</i> load combination (Section 1605.2.1) (basic load combination)
1.4 <i>D</i>	1.4 <i>D</i>	1.4 <i>D</i>
$1.2D + 1.6L + 0.5(L_r \text{ or } S \text{ or } R)$	$1.2D + 1.6L + 0.5(L_r \text{ or } S \text{ or } R)$	$1.2D + 1.6(L_r \text{ or } S \text{ or } R) + (f_1 L \text{ or } 0.8W)$
$1.2D + 1.6(L_r \text{ or } S \text{ or } R) + (0.5L \text{ or } 0.8W)$	$1.2D + 1.6(L_r \text{ or } S \text{ or } R) + (f_1 L \text{ or } 0.8W)$	$1.2D + 1.6W + f_1 L + 0.5(L_r \text{ or } S \text{ or } R)$
$1.2D + 1.3W + 1.5L + 0.5(L_r \text{ or } S \text{ or } R)$	$1.2D + 1.3W + f_1 L + 0.5(L_r \text{ or } S \text{ or } R)$	$1.2D + 1.0E + f_1 L + f_2 S$
$1.2D + 1.0E + (f_1 L \text{ or } f_2 S)$	$1.2D + 1.0E + (f_1 L \text{ or } f_2 S)$	$0.9D + (1.0E \text{ or } 1.6W)$
$0.9D \pm (1.0E \text{ or } 1.3W)$		
re		where the earthquake load is (Section 1617.1.1)
	$E = \rho E_h + E_v$	$E = \rho Q_E + 0.2S_D D$
	$E_h = \text{earthquake load due to base shear}$	Other notations are defined as in UBC. When the effect of gravity counteracts seismic load
	$E_v = 0.5 C_a ID$	$E = \rho Q_E - 0.2S_D D$
	$\rho = \text{redundancy/reliability factor}$	$Q_E = \text{effect of horizontal seismic forces}$ $S_D = \text{design spectral response acceleration at short periods}$
	$= 2 - \frac{20}{r_{max} \sqrt{A_B}}$; $(SI : \rho = 2 - \frac{6.1}{r_{max} \sqrt{A_B}})$	
	$A_B = \text{ground floor area of the structure}$	
		$1 \leq \rho_i = 2 - \frac{20}{r_{max} \sqrt{A_i}}$
		$\leq 1.5 \quad (\text{for categories D, E, and F})$
		$\rho_i = 1 \quad (\text{for categories A, B, and C})$
	$r_{max} = \frac{\text{maximum sum of the shears in any adjacent columns}}{\text{total design story shear}}$	$r_{max} = \frac{\text{maximum sum of the shears in any adjacent columns}}{\text{total design story shear}}$
		$A_i = \text{floor area in square feet of diaphragm level immediately above that story.}$

<i>ASD (Section 1603.6) (basic load combination)</i>	<i>ASD (Section 1612.3.1) (basic load combination)</i>	<i>ASD (Section 1605.3.1) (basic load combination)</i>
$D + L + (L_r \text{ or } S)$	D	D
$D + L + (W \text{ or } E)$	$D + L + (L_r \text{ or } S)$	$D + L + (L_r \text{ or } S \text{ or } R)$
$D + L + W + \frac{S}{2}$	$D + \left(W \text{ or } \frac{E}{1.4} \right)$	$D + (W \text{ or } 0.7E) + L + (L \text{ or } S \text{ or } R)$
$D + L + S + \frac{W}{2}$	$0.9D \pm \frac{E}{1.4}$	$0.6D + W$
$D + L + S + E$	$D + 0.75 \left[L + (L_r \text{ or } S) + \left(W \text{ or } \frac{E}{1.4} \right) \right]$	$0.6 + 0.7E$

Note

1. Other notations listed above in UBC-94, UBC-97 and IBC-2000 are: D = dead load; W = wind load; R = rain load; S = snow load; L = live load; L_r = roof live load; E = earthquake load; f_1 and f_2 = coefficient to reduce magnitude of L and S , respectively (see Table 10.11).
2. In UBC-94 (Section 1603.5), allowable stress may be increased by one-third for E or W acting alone or combined with D .
3. In UBC-97 (Section 1612.3.1) and IBC-2000 (Section 1605.3.1), there is no increase in allowable stress. See Table 10.12 for alternate load combination and one-third increase of allowable stress in UBC-97.

10.7. NUMERICAL ILLUSTRATIONS OF LATERAL FORCE-PROCEDURE FOR UBC-94, UBC-97 AND IBC-2000

Lateral-force procedures presented in previous sections used here to analyze a sample problem. Calculations based on UBC-94, UBC-97, and IBC-2000. Numerical illustrations further compare these three codes (see discussion in Sections 10.3–10.6) and reveal similarities and differences among the requirements. Using preliminary design results of the three-story ordinary moment-resisting steel frame shown in Fig. 10.18, find internal forces of members, story drift, $P\Delta$ effect, load combination for ASD or LRFD. The frame height is 14 ft and the floor is composite steel sheeted as a rigid diaphragm. Columns and girders ASTM A36 steel; $E = 29,000$ ksi.

Girders	Columns
$W18 \times 71$	$W14 \times 32$
$A = 20.8 \text{ in}^2$	$A = 38.3 \text{ in}^2$
$I_x = 1170 \text{ in}^4$	$I_x = 1530 \text{ in}^4$
$I_y = 60.3 \text{ in}^4$	$I_y = 548 \text{ in}^4$

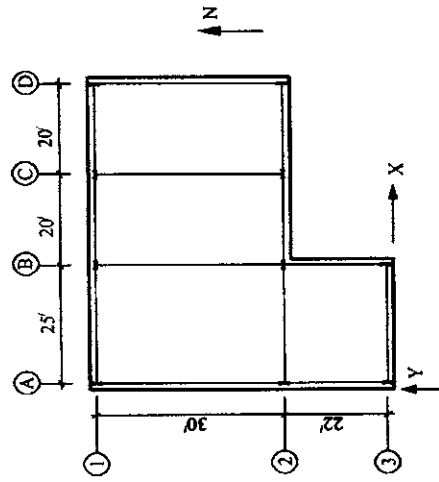


FIG. 10.18 Typical floor framing plan.

EXAMPLE 10.7.1 (based on UBC-94) Seismic zone for (UBC-94, Table 16-I)—the sample structure is in seismic zone 3; therefore $Z = 0.30$. Site coefficient for (UBC-94, Table 16-J)—the soil profile type at the site is S_2 ; therefore $S = 1.2$. Seismic importance factor for (UBC-94, Table 16-K or Table 10.2)—this structure is as a hazardous facility. It belongs to occupancy category 2, and the seismic importance factor is $I = 1.25$.

Assume all are dead load including weight of members and partitions. The load is uniformly distributed on each floor as: roof— $0.075 \text{ k}/\text{ft}^2$, total load = $0.075[(25)(52) + (30)(40)] = 187.5 \text{ k}/\text{floor}$; first and second floors— $0.080 \text{ k}/\text{ft}^2$, total load = $0.080[(25)52 + (30)(40)] = 200.0 \text{ k}/\text{floor}$. This structure is built on a thick layer (more than 200 ft) of mixed hard rock and dense soil. Site evaluation shows that the site belongs to soil profile S_2 for UBC-94, S_B for UBC-97, and class B for IBC-2000. The structure is for hazardous and water treatment facilities.

EXAMPLE 10.7.3 (based on IBC-2000) Site class (IBC, Table 1615.1.1)—soil profile type is S_B . The seismic importance factor (IBC, Table 1604.5 or Table 10.13)—since this building is for water treatment facilities, it belongs to seismic use group II, and the occupancy importance factor is $I = 1.25$.

Calculation steps:

1. Configuration requirements (UBC-94, Table 16-M; also see Fig. 10.4b)—for E-W direction $40/65 = 0.62 > 0.15$
N-S direction $22/52 = 0.42 > 0.15$
2. Thus this structure is plan irregular.
 R_w factor (UBC-94, Table 16-N or Table 10.5)—for the given moment-resisting frame system, $R_w = 6$.
3. Seismic design procedure—
 - 3.1. Selection of lateral-force procedure (UBC-94, Section 1627.8 or Section 10.3.1)—since this irregular structure is not more than five stories or 65 ft in height, static lateral-force procedure can be used. Lateral forces are evaluated in E-W and N-S directions, respectively. Orthogonal effects on irregular buildings can be considered by combining prescribed seismic forces to design the elements (UBC-94, Section 1631.1).
 - 3.2. Structural period [UBC-97, Section 1630.2.2 or Section 10.3.2(F)]—Method A is used here. For steel moment-resisting framing, $C_t = 0.035$
- 3.3. Coefficients C_v and C_a (UBC-97, Tables 16-Q, 16-R or Tables 10.6 and 10.7); for given $Z = 0.3$ and soil type S_B , seismic coefficient C_a is 0.3 and C_v is 0.3.
- 3.4. Design base shear (UBC-97, Section 1630.2 or Eq. 10.41);
for $C_v = 0.3$

$$T = 0.035[(3)(14)]^{3/4} = 0.58 \text{ sec}$$

$$V = \frac{C_v M W}{R T} = \frac{(0.3)(1.25)(200 + 200 + 187.5)}{4.5(0.58)} = 84.41 \text{ k}$$

$$C = \frac{1.25 S}{T^{2/3}} = (1.25) 1.2 / (0.58)^{2/3} = 2.16 < 2.75$$

Calculation steps:

Calculation steps:

1. Configuration requirements (UBC-97, Table 16-M; also see Fig. 10.4b)—same as calculated for UBC-94.
2. R factor (UBC-97, Table 16-N)—for the given moment-resisting system, $R = 4.5$.
3. Seismic design procedure—
 - 3.1. Selection of lateral-force procedure (UBC-97, Section 1629.8 or Section 10.3.1); selection process is the same as that of UBC-94.
 - 3.2. Structural period [UBC-97, Section 1630.2.2 or Section 10.3.2(F)]—Method A is used here. For steel moment-resisting framing, $C_t = 0.035$
- 3.3. Coefficients C_v and C_a (UBC-97, Tables 16-Q, 16-R or Tables 10.6 and 10.7); for given $Z = 0.3$ and soil type S_B , seismic coefficient C_a is 0.3 and C_v is 0.3.
- 3.4. Design base shear (UBC-97, Section 1630.2 or Eq. 10.41);
for $C_v = 0.3$

$$T = 0.035[(3)(14)]^{3/4} = 0.58 \text{ sec}$$

$$V = \frac{C_v M W}{R T} = \frac{(0.3)(1.25)(200 + 200 + 187.5)}{4.5(0.58)} = 84.41 \text{ k}$$

$$C = \frac{1.25 S}{T^{2/3}} = (1.25) 1.2 / (0.58)^{2/3} = 2.16 < 2.75$$

(C) Design spectral response acceleration parameters—for the response spectrum used here, design spectral response accelerations at short period and 1 sec [IBC, Section 1615.1.3 or Eq. (10.68) and (10.69)] are

$$S_{DS} = \frac{2}{3} S_{MS} = \frac{2}{3} (1.25g) = 0.833g$$

$$S_{DI} = \frac{2}{3} S_{MI} = \frac{2}{3} (0.40g) = 0.267g$$

3.4. Base shear [UBC-94, Section 1628.2.1 or Eq. (10.23)]

$$\frac{C}{R_w} = \frac{2.16}{6} = 0.36 > 0.075$$

Thus base shear is

$$V = \frac{ZIC}{R_w} W \\ = \frac{(0.30)(1.25)2.16}{6} (200 + 187.5) = 79.31 \text{ k}$$

3.5. Concentrated force at top floor [UBC-94, Section 1628.4 or Eq. (10.28)]

$$T < 0.7, \quad F_t = 0.$$

3.6. Vertical distribution of base shear to stories [UBC-94, Section 1628.4 or Eq. (10.29)]

$$F_x = \frac{(V - F_t)w_i h_i}{\sum_{i=1}^n w_i h_i} = (200)14 + (200)28 +$$

$$\sum_{i=1}^n w_i h_i = (200)14 + (200)28 +$$

$$(187.5)42 = 16,275 \text{ k ft}$$

$$F_1 = \frac{(84.4)(200)14}{16,275} = 14.52 \text{ k;}$$

$$V_1 = 84.41 \text{ k}$$

$$F_2 = \frac{(84.4)(200)28}{16,275} = 29.04 \text{ k;} \\ V_2 = 69.89 \text{ k}$$

$$F_3 = \frac{(84.4)(200)42}{16,275} = 40.85 \text{ k;} \\ V_3 = 40.85 \text{ k}$$

$$F_3 = \frac{(79.31)(187.5)42}{16,275} \\ = 38.38 \text{ k; } V_3 = 38.38 \text{ k}$$

for $C_a = 0.3$

$$\frac{2.5C_a I}{R} W$$

$$= \frac{(2.5)(0.3)(1.25)}{4.5} (200 + 200 + \\ 187.5) = 122.39 \text{ k} > V$$

$$0.11C_a I W = (0.11)(0.3)(1.25)$$

$$(200 + 200 + 187.5) = 24.23 \text{ k} < V$$

Design base shear is 84.41 k.

Concentrated force at top floor [UBC-97, Section 1630.5 or Eq. (10.28)]

$$T < 0.7, \quad F_t = 0.$$

3.6. Vertical distribution of base shear to stories [UBC-97, Section 1630.5 or Eq. (10.29)]

$$F_x = \frac{(V - F_t)w_i h_i}{\sum_{i=1}^n w_i h_i}$$

$$\sum_{i=1}^n w_i h_i = (200)14 + (200)28 +$$

$$(187.5)42 = 16,275 \text{ k ft}$$

$$F_1 = \frac{(84.4)(200)14}{16,275} = 14.52 \text{ k;}$$

$$V_1 = 84.41 \text{ k}$$

$$F_2 = \frac{(84.4)(200)28}{16,275} = 29.04 \text{ k;} \\ V_2 = 69.89 \text{ k}$$

$$F_3 = \frac{(84.4)(200)42}{16,275} = 40.85 \text{ k;} \\ V_3 = 40.85 \text{ k}$$

$$F_3 = \frac{(79.31)(187.5)42}{16,275} \\ = 38.38 \text{ k; } V_3 = 38.38 \text{ k}$$

(D) Selection of seismic design category—since $S_{DS} = 0.83g > 0.5g$, $S_{DS} > 0.2g$, and seismic use is group II, IBC Tables 1616.3(1) and (2), or Table 10.14 and 10.15 designate seismic design category D. In accordance with IBC, Table 1616.6.3 or Table 10.16 (item 4), the equivalent procedure can be used with dynamic characteristics included in the analytical model.

(E) Structural period T —assume unit load acting at the rigidity center of each floor; then find flexibility matrix $[delta]$. Since $[\delta]^{-1} = [K]$, frequencies are determined from

$$[K] - [M][p]^2 = 0$$

Fundamental frequencies in N-S and E-W directions are

$$p_{EW} = 11.38 \text{ rad/sec; } T_{EW} = 0.552 \text{ sec} \\ p_{NS} = 10.51 \text{ rad/sec; } T_{NS} = 0.598 \text{ sec}$$

Since $0.2 < S_{DS} < 0.3$, according to IBC, Section 1617.4.2,

$$T_{EW} = 0.552 < T_a C_u = 0.812 \text{ sec} \\ T_{NS} = 0.598 < T_a C_u = 0.812 \text{ sec}$$

in which $C_u = 1.4$ (IBC, Table 1617.4.2 or Table 10.19) and $T_a = C_u R^{3/4} = (0.035)(42)^{3/4} = 0.58$ sec. Thus T_{EW} and T_{NS} are used to calculate the earthquake base shear in E-W and N-S directions for this building.

3.4. Design base shear (IBC, Section 1617.4.1 or Section 10.5.2)

$$V = V_s W$$

Seismic response coefficient [IBC, Section 1617.4.1.1 or Eq. (10.62)]

$$C_s = \frac{S_{DS}}{\left(\frac{R}{I_E}\right)} = \frac{0.833}{\left(\frac{4}{1.25}\right)} = 0.260 \\ C_s = 0.044 S_{DS} I_E = 0.044(0.833)1.25 \\ = 0.046$$

Distribution of lateral force and shear is shown in Fig. 10.19a.

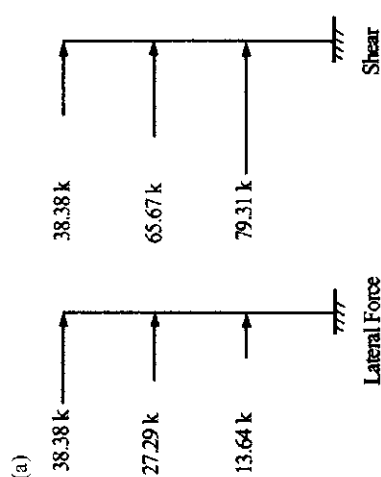


FIG. 10.19 (a) Lateral force and shear at each story.

3.7. Overturning moments [UBC-94, Sections 1628.7.1 and 1631.1 or Eq. (10.31)]—the building is designed to resist seismic overturning effect; 85% of dead load is considered for restoring moment. Thus

$$\begin{aligned} M_x &= \sum_{i=x}^n F_i(h_i - h_{x_i}) + F_i(h_n - h_{x_i}) \\ M_3 &= 0 \\ M_2 &= 38.38(42 - 28) = 537.32 \text{ k ft} \\ M_1 &= 38.38(42 - 14) + 27.29 \\ (28 - 14) &= 1456.7 \text{ k ft} \end{aligned}$$

The overturning moment at the base is

$$\begin{aligned} M_0 &= (38.38)42 + (27.29)28 \\ &+ (13.64)14 = 2567.04 \text{ k ft} \end{aligned}$$

Distribution of lateral force and shear is shown in Fig. 10.19b.

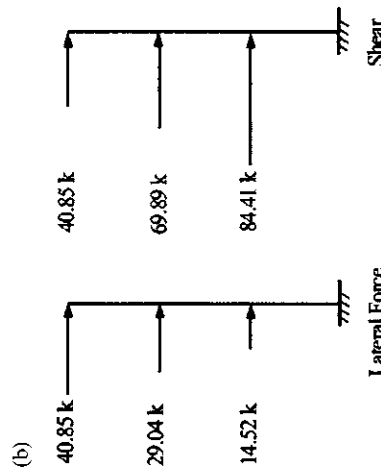


FIG. 10.19 (b) Lateral force and shear at each story.

3.7. Overturning moments [UBC-97, Sections 1630.8.1 and 1633.1 or Eq. (10.31)]—the building is designed to resist seismic overturning effect; 100% of dead load is considered for restoring moment. Thus

$$\begin{aligned} M_x &= \sum_{i=x}^n F_i(h_i - h_{x_i}) + F_i(h_n - h_{x_i}) \\ M_3 &= 0 \\ M_2 &= 40.85(42 - 28) = 571.9 \text{ k ft} \\ M_1 &= 40.85(42 - 14) + 29.04 \\ (28 - 14) &= 1550.36 \text{ k ft} \end{aligned}$$

The overturning moment at the base is

$$\begin{aligned} k &= 1 + \frac{2 - 1}{2.5 - 0.5}(0.552 - 0.5) \\ &= 1.026 \end{aligned}$$

for

$$\frac{S_{D1}}{\left(\frac{R}{I_E}\right)T_{EW}} = \frac{0.267}{\left(\frac{4}{1.25}\right)0.552} = 0.151 > 0.046$$

$$\frac{S_{D1}}{\left(\frac{R}{I_E}\right)T_{NS}} = \frac{0.267}{\left(\frac{4}{1.25}\right)0.598} = 0.140 > 0.046$$

Coefficients C_S along E-W and N-S directions shall be 0.151 and 0.140, respectively. Thus

$$V_{EW} = C_{SEW}W = (0.151)(200 + 200)$$

$$+ 187.5) = 88.71 \text{ k}$$

$$V_{NS} = C_{SNS}W = (0.140)(200 + 200)$$

$$+ 187.5) = 82.25 \text{ k}$$

Not applicable (NA). Vertical distribution of base shear (IBC, Section 1617.4.3 or Section 10.5.3) to stories

Periods in E-W and N-S directions are 0.552 sec and 0.598 sec, respectively, k is obtained by using linear interpolation:

$$F_A = \frac{w_x h_x^k}{\sum_{i=1}^n w_i h_i^k} V$$

for E-W direction

$$\begin{aligned} k &= 1 + \frac{2 - 1}{2.5 - 0.5}(0.552 - 0.5) \\ &= 1.026 \end{aligned}$$

restoring moment, allowing 85% reduction in dead load, is

$$M_r = 0.85(187.5 + 200 + 200)$$

$$(52 - 31.28) = 10,347.05 \text{ k ft}$$

where the number, $52-31.28 = 20.72$, is the shortest distance between mass center and south or north end (see Fig. 10.21). The factor of safety is

$$M_r/M_0 = 10347.05/2567.04 = 4.03$$

$M_r/M_0 = 12173/2732.1 = 4.5$

The overturning moment at the base is

$$M_0 = (40.85)42 + (29.04)28$$

$$+ (14.52)14 = 2732.1 \text{ k ft}$$

The restoring moment, with no reduction in dead load, is

$$M_r = (187.5 + 200 + 200)$$

$$(52 - 31.28) = 12,173 \text{ k ft}$$

where $52-31.28 = 20.72$, is the shortest distance between mass center and south or north end (see Fig. 10.21). The factor of safety is

$$M_r/M_0 = 12173/2732.1 = 4.5$$

$$\sum_{i=1}^n w_i h_i^k = (200)141.026 + (200)281.026 + (187.5)421.026 = 17,784.382$$

$$F_1 = \frac{w_x h_x^k}{\sum_{i=1}^n w_i h_i^k} V = \frac{(200)(14.026)}{17784.382} (88.71) = 14.95 \text{ k}$$

$$F_2 = \frac{w_x h_x^k}{\sum_{i=1}^n w_i h_i^k} V = \frac{(200)(281.026)}{17784.382} (88.71) = 30.46 \text{ k}$$

$$F_3 = \frac{w_x h_x^k}{\sum_{i=1}^n w_i h_i^k} V = \frac{(187.5)(421.026)}{17784.382} (88.71) = 43.29 \text{ k}$$

Similarly, for N-S direction

$$k = 1.049; \sum_{i=1}^n w_i h_i^k = 19,237.56$$

$$F_1 = 13.66 \text{ k}; F_2 = 28.20 \text{ k}; F_3 = 40.39 \text{ k}$$

The distribution of lateral force and shear is shown in Fig. 10.19c.

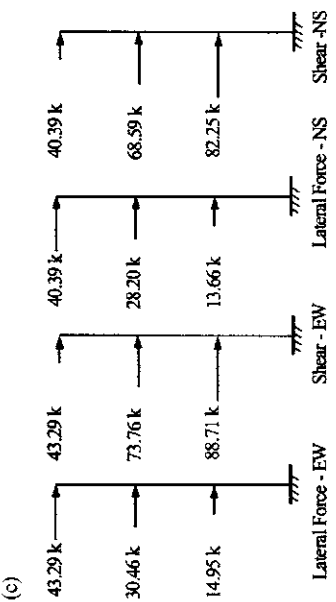


FIG. 10.19 (c) Lateral force and shear at each story in E-W and N-S directions.

STATIC AND DYNAMIC LATERAL-FORCE PROCEDURES

653

- 3.7. Overturning moments (IBC, Section 1617.4.5 or Section 105.4)—buildings should be designed to resist the overturning effect caused by seismic forces

$$M_x = \tau \sum_{i=x}^n F_i(h_i - h_x)$$

in which $\tau = 1$ because this building has less than 10 stories. For E-W direction

$$\begin{aligned} M_3 &= 0 \\ M_2 &= (1.0)(43.29)(42 - 28) = 606.06 \text{ k ft} \\ M_1 &= (1.0)[(43.29)(42 - 14) + (30.46) \\ &\quad (28 - 14)] = 1638.56 \text{ k ft} \\ M_0 &= (1.0)[(43.29)(42) + (30.46)(28) + \\ &\quad (14.95)(14)] = 2880.36 \text{ k ft} \end{aligned}$$

The restoring moment is (see Example 10.7.2)

$$\begin{aligned} M_r &= (187.5 + 200 + 200)(28.10) \\ &= 16508.75 \text{ k ft} \end{aligned}$$

Note that 28.10 is the shortest distance between mass center and east or west end. The factor of safety is

$$\frac{M_r}{M_0} = \frac{16508.75}{2880.36} = 5.73$$

Note also that if $M_0 > M_r$, then a proper design should be taken for columns to have hold-down forces. Similarly, for N-S direction

$$\begin{aligned} M_3 &= 0 \\ M_2 &= (1.0)(40.39)(42 - 28) = 565.46 \text{ k ft} \\ M_1 &= (1.0)[(40.39)(42 - 14) + (28.2) \\ &\quad (28 - 14)] = 1525.72 \text{ k ft} \\ M_0 &= (1.0)[(40.39)(42) + (28.2)(28) + \\ &\quad (13.66)(14)] = 2677.22 \text{ k ft} \end{aligned}$$

$$\frac{M_r}{M_0} = \frac{12173}{2677.2} = 4.55$$

in which $M_r = (187.5 + 200 + 200)(52 - 31.28) = 12173 \text{ k ft}$

-
- | | | | |
|--|---|---|---|
| 4. Calculation of torsion— | 4. Calculation of torsion— | 4. Calculation of torsion— | 4. Calculation of torsion
(IBC, Section 1617.4.4)— |
| 4.1. Centers of mass and rigidity; since weight per square foot of the floor is uniformly distributed, location of mass center coincides with floor geometric center which is then obtained as | 4.1. Centers of mass and rigidity; same as calculated for UBC-94. | 4.1. Centers of mass and rigidity; same as calculated for UBC-94. | 4.1. Centers of mass and rigidity; same as calculated for UBC-94. |
-

$$\begin{aligned} X_m &= \frac{(25)(22)12.5 + (30)(65)32.5}{(25)22 + (30)65} \\ &= 28.1 \text{ ft} \\ Y_m &= \frac{(25)(22)26 + (40)(30)37}{(25)22 + (30)65} \\ &= 31.28 \text{ ft} \end{aligned}$$

The center of rigidity can be obtained using various approximation techniques (see Section 10.8 in this chapter). The technique employed here is based on relative rigidity R_i , where $R_i = 1/\Delta_i$, and Δ_i is the deflection at the i th floor due to a unit load applied at that floor of the planar frame along lines 1, 2, 3, A, B, C and D, respectively. More detail is illustrated with method B in the next section. Relative rigidity calculations for the third floor are shown in Table 10.21. A summary of relative rigidities of the first and second floors is given in Table 10.22.

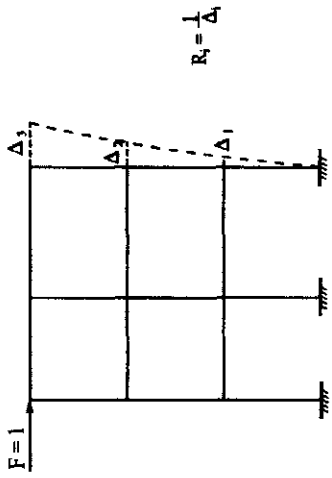


FIG. 10.20 Calculation of planar frame rigidity.

TABLE 10.21 Calculation of Relative Rigidities at the Third Floor

Line	$R_3 = 1/\Delta_3(\text{k/ft})$	X(ft)	Y(ft)	$RX(\text{k})$	$RY(\text{k})$
1	536	—	52	—	27,872
2	536	—	22	—	11,792
3	148	—	0	—	0
A	394	0	—	0	—
B	281	25	—	7025	—
C	135	45	—	6075	—
D	201	65	—	13,065	—

TABLE 10.22 Summary of Relative Rigidities at First and Second Floors

Line	1	2	3	A	B	C	D
R							
$1/\Delta_1$	2699	2699	725	2530.6	1574	698	1520
$1/\Delta_2$	926	926	254	738	503	235	400

Thus the rigidity centers at individual floors
are
at the third floor

$$\begin{aligned} X_R &= \frac{\sum RY}{\sum R_y} \\ &= \frac{0 + 7025 + 6075 + 13065}{(394 + 281 + 135 + 201)} \\ &= 25.88 \text{ ft} \\ Y_R &= \frac{\sum RX}{\sum R_x} = \frac{27872 + 11792 + 0}{(536 + 536 + 148)} \\ &= 32.51 \text{ ft} \end{aligned}$$

at the second floor

$$\begin{aligned} X_R &= \frac{\sum RX}{\sum R_x} \\ &= \frac{738(0) + 503(25) + 235(45) + 400(65)}{(738 + 503 + 235 + 400)} \\ &= 26.10 \text{ ft} \\ Y_R &= \frac{\sum RY}{\sum R_y} \\ &= \frac{926(52) + 926(22) + 254(0)}{(926 + 926 + 254)} = 32.54 \text{ ft} \end{aligned}$$

at the first floor

$$\begin{aligned} X_R &= \frac{\sum RX}{\sum R_x} \\ &= \frac{2530.6(0) + 1574(25) + 688(45) + 1520(65)}{(2530.6 + 1574 + 688 + 1520)} \\ &= 26.81 \text{ ft} \\ Y_R &= \frac{\sum RY}{\sum R_y} = \frac{2699(52) + 2699(22) + 725(0)}{(2699 + 2699 + 725)} \\ &= 32.61 \text{ ft} \end{aligned}$$

Note that the rigidity centers of individual floors are close to one vertical axis. The coincidence is expected for this building with columns having the same cross section. The difference shown here, however, results from the approximate approach of calculating the relative rigidity. Thus, using this approach, we may calculate a typical floor's rigidity center to represent the rest of the building.

Centers of mass and rigidity at the third floor are shown in Fig. 10.21.

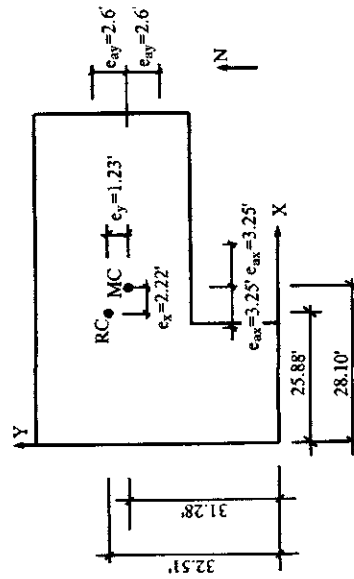


FIG. 10.21 Location of mass and rigidity centers at third floor.

4.2. Eccentricity e —for a given axis, let e_x and e_y be actual and e_a be accidental eccentricities [IBC-94, Section 1628.5 or Section 10.3.5 (A)]. Then

in E-W (X) direction

$$e_x = (28.10 - 25.88) = 2.22 \text{ ft};$$

$$e_{ax} = (0.05) 65 = 3.25 \text{ ft}$$

in N-S (Y) direction

$$e_y = (32.51 - 31.28) = 1.23 \text{ ft};$$

$$e_{ay} = (0.05) 52 = 2.6 \text{ ft}$$

The eccentricities are shown in Fig. 10.21.

4.3. Torsion—based on the eccentricities shown in Fig. 10.21, actual torsion (floor shear multiplied by e_x or e_y) will induce shears, acting on frame line 1, opposite the shear on that frame due to lateral forces. Accidental torsion can have a different direction from actual torsion depending on e_a relative to the mass center. Thus these two torsions are calculated separately, as given in (a) of Table 10.23.

4.2. Eccentricity e (IBC-97, Sec. 1630.6); same as calculated for UBC-94.

4.2. Eccentricity e (IBC, Section 1617.4.4.3 and 4.4); same as calculated for UBC-94.

4.3. Torsion—using the same procedures as UBC-94 yields the results shown in (b) of Table 10.23.

TABLE 10.23 Shear and Torsion

	Floor	Actual			Accidental		
		Shear $V(k)$	Actual torsion— EW, V_{e_y} (k ft)	Accidental torsion— EW, V_{e_y} (k ft)	Shear $V(k)$	Actual torsion— NS, V_{e_x} (k ft)	Accidental torsion— NS, V_{e_x} (k ft)
(a)	1	79.31	97.55	±206.21	176.07	±257.76	
	2	65.67	80.77	±170.74	145.78	±213.43	
	3	38.38	47.21	±99.79	85.20	±124.73	
(b)	1	84.41	103.82	±219.47	187.39	±274.33	
	2	69.89	85.96	±181.79	155.16	±227.14	
	3	40.85	50.25	±106.21	90.69	±132.76	
(c)	1	88.71	109.11	±230.65	182.55	±267.31	
	2	73.76	90.72	±191.78	68.59	±222.92	
	3	43.29	53.25	±112.55	40.39	±131.27	

where shear is $V = V_x$ or V_y in X or Y directions; actual torsion is $T = V_{e_y}$ or V_{e_x} and accidental torsion $T_a = V_{e_{ay}}$ or $V_{e_{ax}}$ at a given floor.

5. Equivalent lateral forces—
 5.1. Polar moment of inertia—torsion is distributed to vertical components using polar moment of inertia, J . Based on relative rigidities shown in Table 10.21 and X_R and Y_R in step 4.1 above, the polar moment of inertia of resisting elements can be obtained as follows. Multiply the relative rigidity (R) by the square of the distance between frame line and RC as

$$J = \Sigma R(\text{moment arm})^2. \text{ Thus}$$

$$\begin{aligned} J_3 &= 536(52 - 32.51)^2 + 536 \\ &\quad (22 - 32.51)^2 + 148(0 - 32.51)^2 \\ &\quad + 394(0 - 25.88)^2 + 281 \\ &\quad (25 - 25.88)^2 + 135(45 - 25.88)^2 \\ &\quad + 20(65 - 25.88)^2 = 1,040,299 \text{ ft} \\ J_2 &= 926(52 - 32.54)^2 + 926 \\ &\quad (22 - 32.54)^2 + 254(0 - 32.54)^2 \\ &\quad + 738(0 - 26.10)^2 + 903 \\ &\quad (25 - 26.10)^2 + 235(45 - 26.10)^2 \\ &\quad + 400(65 - 26.10)^2 = 1,915,057 \text{ k ft} \\ J_1 &= 2699(52 - 32.61)^2 + 2699 \\ &\quad (22 - 32.61)^2 + 725(0 - 32.61)^2 \\ &\quad + 253(0 - 26.81)^2 + 1574 \\ &\quad (25 - 26.81)^2 + 698(45 - 26.81)^2 \\ &\quad + 1520(65 - 26.81)^2 = 6,361,769 \text{ k ft} \end{aligned}$$

Note that if the rigidity center at the third floor is used for the other two floors to calculate J_1 and J_2 , the values are almost the same as above. For practical engineering analysis, we may simply use one floor's rigid center to represent other floors.

5. Equivalent lateral forces—
 5.1. Polar moment of inertia, same as calculated for UBC-94.

5. Equivalent lateral forces—
 5.1. Polar moment of inertia, same as calculated for UBC-94.

5. Equivalent lateral forces—
 5.1. Polar moment of inertia, same as calculated for UBC-94.

5.2. $EW (X)$ direction—the vertical component's shear resulting from the distribution of lateral force and torsion is represented by $V_y = V_{yQ} + V_{yT}$, where i and j denote i th floor and j th frame line, respectively; Q and T signify shear due to lateral force and torsion, respectively.

Thus for frame line 1 and first floor (see Fig. 10.22)

$$V_{11} = V_{11Q} + V_{11T} = \frac{R_{1X}}{\sum R_X} V_1 \\ + \left(\frac{R_{1Xr_{1Y}}}{J_1} T \pm \frac{R_{1Xr_{1Y}}}{J_1} T_a \right)$$

Thus for frame line 1 (see Fig. 10.22)

$$\sum R_Y = 2699 + 2699 + 725 = 6123 \text{ k/ft} \\ V_{11Q} = \frac{2699}{6123} (84.41) = 37.21 \text{ k}$$

where \pm accounts for the accidental eccentricity on either side of the mass center in order to obtain maximum combined torsional shear; $\sum R_X$ is total relative rigidity in X direction; R_{1X} is rigidity at the first floor in X direction; and r_{1Y} is the distance between planar frame line 1 and the center of rigidity.

for frame line 2

$$V_{12Q} = \frac{(2699)(84.41)}{6361.769} [103.82] \\ V_{12T} = \frac{2699}{6361.769} [103.82 - 52] [103.82 \\ \pm 219.47] = -0.86 \pm 1.81 = 0.95 \text{ k} \\ V_{11} = 37.21 + 0.95 = 38.16 \text{ k} \\ V_{12} = 39.1 + 1.529 = 40.63 \text{ k}$$

for frame line 2

$$V_{12Q} = \frac{2699}{6123} (88.71) = 39.1 \text{ k} \\ V_{12T} = \frac{(2699)(10.51)}{6361.769} [109.11 \pm 230.65] \\ = 0.486 \pm 1.027 = 1.529 \text{ k} \\ V_{12} = 39.1 + 1.529 = 40.63 \text{ k}$$

for frame line 3

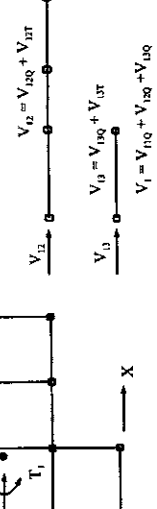


Fig. 10.22 Lateral-force distribution on planar frame of floor in E-W direction.

5.2. E-W (X) direction—vertical component's shear resulting from the distribution of lateral force and torsion is represented by $V_y = V_{yQ} + V_{yT}$. Use the same approach as in Example 10.7.1.

Thus at first floor for frame line 1

$$\Sigma R_X = 2699 + 2699 + 725 = 6123 \text{ k/ft}$$

as in Example 10.7.1; then

$$V_{11Q} = \frac{(2699)(88.71)}{6123} = 39.10 \text{ k}$$

$$V_{11T} = \frac{(2699)(-19.49)}{6361.769} (109.11 \pm 230.65)$$

$$= -0.90 \pm 1.90 = 1.00 \text{ k}$$

$$= -0.90 \pm 1.90 = -2.80 \text{ k}$$

for frame line 2

$$V_{12Q} = \frac{2699}{6123} (88.71) = 39.1 \text{ k}$$

$$V_{12T} = \frac{(2699)(10.51)}{6361.769} [109.11 \pm 230.65]$$

$$= 0.404 \pm 0.845 = 1.262 \text{ k}$$

$$V_{12} = 39.1 + 1.262 = 40.37 \text{ k}$$

for frame line 3

$$V_{13Q} = \frac{725}{6123} (84.41) = 9.99 \text{ k}$$

$$V_{13T} = \frac{(725)(32.51)}{6361.769} (103.82 \pm 219.47) \\ = 0.38 \pm 1.02 = 1.20 \text{ k}$$

$$V_{13} = 9.99 + 1.20 = 11.19 \text{ k}$$

Also for frame line 1,

$$\begin{aligned}\Sigma R_x &= 2699 + 2699 \\ &\quad + 725 = 6123 \text{ k/ft}\end{aligned}$$

$$V_{1Q} = \frac{2699}{6123} (79.31) = 34.96 \text{ k}$$

$$\begin{aligned}V_{1T} &= \frac{(2699)(-19.39)}{6361.769} [97.55 + \\ &\quad (\pm 206.21)] = -0.802 \\ &\quad \pm 1.696 = \begin{array}{r}0.89 \\ -2.50\end{array} \text{ k}\end{aligned}$$

Note UBC-94, Section 1603.3.3 requires that shear resulting from lateral force, when combined with torsional shear, not be decreased due to torsional effect. Based on a mechanics analysis, the actual torsion causes negative shear while the accidental torsion causes positive shear. Thus the combined result is

$$V_1 = 34.96 + 0.89 = 35.85 \text{ k}$$

for frame line 2

$$V_{12Q} = \frac{2699}{6123} (79.31) = 34.96 \text{ k}$$

$$\begin{aligned}V_{12T} &= \frac{(2699)(10.61)}{6361.769} [97.55 \\ &\quad + (\pm 206.21)] = \begin{array}{r}1.37 \\ -0.489\end{array} \text{ k} \\ V_{12} &= 34.96 + 1.37 = 36.33 \text{ k}\end{aligned}$$

for frame line 3

$$V_{13Q} = \frac{725}{6123} (79.31) = 9.39 \text{ k}$$

$$\begin{aligned}V_{13T} &= \frac{(725)(32.61)}{6361.769} [97.55 \\ &\quad + (\pm 206.21)] = 1.13 \text{ k} \\ V_{13} &= 9.39 + 1.13 = 10.52 \text{ k}\end{aligned}$$

5.3. The amplification factor for accidental torsion (UBC-94, Section 1628.6)—since the building has torsional irregularity (UBC-94, Table 16-M), amplification factor must be checked as follows:

$$A_x = \left[\frac{\delta_{\max}}{1.2 \delta_{\text{avg}}} \right]^2 \leq 3$$

where δ_{avg} is the average of displacements at the extreme points of the structure at level x ; δ_{\max} is maximum displacement at level x ; and A_x cannot be greater than 3. If

$$A_x > 1 \quad \text{then the accidental eccentricity must be amplified as}$$

$$e'_a = e_a A_x$$

Consequently, the shear force of each frame should be modified using the new eccentricity, e'_a . For the frames at the first floor, deflections are

$$\begin{aligned} \delta_{11} &= V_{11}/R_{1x} = 35.86/2699 = 0.013 \text{ ft} \\ \delta_{12} &= V_{12}/R_{2x} = 36.33/2699 = 0.014 \text{ ft} \\ \delta_{13} &= V_{13}/R_{3x} = 10.52/725 = 0.015 \text{ ft} \\ \delta_{\text{avg}} &= (\delta_{11} + \delta_{13})/2 = 0.014 \text{ ft} \\ \delta_{\max}/1.2\delta_{\text{avg}} &= \frac{0.015}{1.2(0.014)} = 0.89 < 1 \end{aligned}$$

Therefore no revision of accidental torsion is necessary. Similar computations are obtained for other floors in E-W direction as the three floors in the N-S direction. Results are summarized in (b) of Tables 10.24 and 10.25.

Table 10.24 Distribution of Lateral Forces (k) and Displacements (ft)—EW

Floor	Line 1			Line 2			Line 3		
	V	δ	ν	V	δ	ν	V	δ	ν
(a)									
1	V_{11}	35.85	δ_{11}	0.013	V_{12}	36.33	δ_{12}	0.014	V_{13}
2	V_{21}	29.72	δ_{21}	0.032	V_{22}	30.15	δ_{22}	0.033	V_{23}
3	V_{31}	17.39	δ_{31}	0.032	V_{32}	17.66	δ_{32}	0.033	V_{33}
(b)									
1	V_{11}	38.16	δ_{11}	0.014	V_{12}	38.66	δ_{12}	0.014	V_{13}
2	V_{21}	31.63	δ_{21}	0.034	V_{22}	32.09	δ_{22}	0.035	V_{23}
3	V_{31}	18.51	δ_{31}	0.035	V_{32}	18.80	δ_{32}	0.035	V_{33}
(c)									
1	V_{11}	40.10	δ_{11}	0.015	V_{12}	40.63	δ_{12}	0.015	V_{13}
2	V_{21}	33.38	δ_{21}	0.036	V_{22}	33.87	δ_{22}	0.037	V_{23}
3	V_{31}	19.61	δ_{31}	0.037	V_{32}	19.91	δ_{32}	0.037	V_{33}

Note: δ_{avg} is average displacement of frame lines 1 and 3. Since $\delta_{\max}/1.2\delta_{\text{avg}} < 1$, accidental torsion need not be amplified.

5.3. The amplification factor for accidental torsion (UBC-94, Section 1630.7)—since the building has torsional irregularity (UBC-97, Table 16-M), amplification is the same as in UBC-94. For the frames at the first floor, deflections are

$$\begin{aligned} \delta_{11} &= V_{11}/R_{1x} = 38.16/2699 = 0.014 \text{ ft} \\ \delta_{12} &= V_{12}/R_{2x} = 38.66/2699 = 0.014 \text{ ft} \\ \delta_{13} &= V_{13}/R_{3x} = 11.19/725 = 0.015 \text{ ft} \\ \delta_{\text{avg}} &= (\delta_{11} + \delta_{13})/2 = 0.015 \\ \delta_{\max}/1.2\delta_{\text{avg}} &= \frac{0.016}{1.2(0.015)} = 0.89 < 1 \end{aligned}$$

No revision of accidental torsion is necessary. Similar computations are obtained for other floors in E-W direction and all three floors in N-S direction. Results are summarized in (c) of Tables 10.24 and 10.25.

Table 10.24 Distribution of Lateral Forces (k) and Displacements (ft)—EW

Floor	Line 1			Line 2			Line 3		
	V	δ	ν	V	δ	ν	V	δ	ν
(a)									
1	V_{11}	35.85	δ_{11}	0.013	V_{12}	36.33	δ_{12}	0.014	V_{13}
2	V_{21}	29.72	δ_{21}	0.032	V_{22}	30.15	δ_{22}	0.033	V_{23}
3	V_{31}	17.39	δ_{31}	0.032	V_{32}	17.66	δ_{32}	0.033	V_{33}
(b)									
1	V_{11}	38.16	δ_{11}	0.014	V_{12}	38.66	δ_{12}	0.014	V_{13}
2	V_{21}	31.63	δ_{21}	0.034	V_{22}	32.09	δ_{22}	0.035	V_{23}
3	V_{31}	18.51	δ_{31}	0.035	V_{32}	18.80	δ_{32}	0.035	V_{33}
(c)									
1	V_{11}	40.10	δ_{11}	0.015	V_{12}	40.63	δ_{12}	0.015	V_{13}
2	V_{21}	33.38	δ_{21}	0.036	V_{22}	33.87	δ_{22}	0.037	V_{23}
3	V_{31}	19.61	δ_{31}	0.037	V_{32}	19.91	δ_{32}	0.037	V_{33}

No revision of accidental torsion is necessary. Similar computations are obtained for other floors in E-W direction and all three floors in N-S direction. Results are summarized in (c) of Tables 10.24 and 10.25.

No revision of accidental torsion is necessary. Similar computations are obtained for other floors in E-W direction and all three floors in N-S direction. Results are summarized in (c) of Tables 10.24 and 10.25.

5.4. N-S (Y) direction.5.4. N-S (Y) direction.5.4. N-S (Y) direction.**STATIC AND DYNAMIC LATERAL-FORCE PROCEDURES****663****TABLE 10.25** Distribution of Lateral Force (k) and Displacement (δ)—NS

Floor	V	Line A		Line B		Line C		Line D	
		δ	ν	δ	ν	δ	ν	δ	ν
(a)									
1	V_{1A}	32.61	δ_{1A}	0.013	V_{1B}	19.78	δ_{1B}	0.013	V_{1C}
2	V_{2A}	26.51	δ_{2A}	0.036	V_{2B}	17.63	δ_{2B}	0.035	V_{2C}
3	V_{3A}	15.34	δ_{3A}	0.039	V_{3B}	10.68	δ_{3B}	0.038	V_{3C}
(b)									
1	V_{1A}	34.71	δ_{1A}	0.014	V_{1B}	21.05	δ_{1B}	0.013	V_{1C}
2	V_{2A}	28.21	δ_{2A}	0.038	V_{2B}	18.75	δ_{2B}	0.037	V_{2C}
3	V_{3A}	16.33	δ_{3A}	0.041	V_{3B}	11.36	δ_{3B}	0.040	V_{3C}
(c)									
1	V_{1A}	33.82	δ_{1A}	0.013	V_{1B}	20.51	δ_{1B}	0.013	V_{1C}
2	V_{2A}	27.69	δ_{2A}	0.038	V_{2B}	18.41	δ_{2B}	0.037	V_{2C}
3	V_{3A}	16.15	δ_{3A}	0.041	V_{3B}	11.24	δ_{3B}	0.040	V_{3C}

Note: δ_{avg} is average displacement of frame lines A and D. Since $\delta_{max}/1.2\delta_{avg} < 1$, accidental torsion need not be amplified.

$$\frac{\delta_{max}}{1.2\delta_{avg}}$$

6. Drift check—
 6.1. Drift limitation (UBC-94, Section 1628.8.2
 or Section 10.3.6);
 For $T < 0.7$,
- $$\Delta_a = \min \left(0.04 h_{sv} / R_{us}, 0.005 h_{sv} \right)$$
- $$= \min \left(0.04 h_{sv}/6, 0.005 h_{sv} \right)$$
- $$= \min \left(0.0067 h_{sv}, 0.005 h_{sv} \right)$$
- from which the minimum value is
- $$\Delta_a = 0.005[1.4(1.2)] = 0.84 \text{ in}$$
- 6.2. Calculated drift—based on the known lateral forces shown in (a) of Tables 10.24 and 10.25, displacement and drift are calculated by using elastic frame analysis. Items in (b) of Tables 10.26 and 10.27 summarize the results.
6. Drift check—
 6.1. Drift limitation (UBC-97, Section 1630.10.2 or Section 10.4.5); for $T < 0.7$,
- $$\Delta_a = 0.025 h_{sv} = (0.025)14$$
- $$= 0.35 \text{ ft} = 4.9 \text{ in}$$
- 6.2. Calculated drift—based on the known lateral forces shown in (b) of Tables 10.24 and 10.25, displacement and drift are calculated and summarized in (c) of Tables 10.26 and 10.27 for E-W and N-S, respectively.

TABLE 10.26 Lateral Displacement and Drift (in)—EW

Floor	Line 1		Line 2		Line 3	
	Displacement	Drift	Displacement	Drift	Displacement	Drift
(a)						
1	0.201	0.201	0.204	0.204	0.218	0.218
2	0.449	0.248	0.456	0.252	0.489	0.271
3	0.605	0.156	0.614	0.158	0.660	0.171
(b)						
1	0.214	0.214	0.217	0.217	0.232	0.232
2	0.478	0.264	0.485	0.268	0.520	0.288
3	0.644	0.166	0.654	0.169	0.701	0.181
(c)						
1	0.225	0.225	0.228	0.228	0.244	0.244
2	0.504	0.279	0.511	0.283	0.548	0.304
3	0.680	0.176	0.689	0.178	0.740	0.192

TABLE 10.27 Lateral Displacement and Drift (in)—NS

Floor	Line A		Line B		Line C		Line D	
	Displacement	Drift	Displacement	Drift	Displacement	Drift	Displacement	Drift
(a)	1	0.217	0.217	0.203	0.218	0.218	0.266	0.266
	2	0.521	0.304	0.481	0.278	0.515	0.650	0.384
	3	0.739	0.218	0.670	0.189	0.714	0.920	0.270
(b)	1	0.231	0.231	0.216	0.216	0.232	0.283	0.283
	2	0.554	0.323	0.512	0.296	0.548	0.692	0.409
	3	0.776	0.222	0.712	0.200	0.760	0.980	0.288
(c)	1	0.226	0.226	0.211	0.211	0.226	0.277	0.277
	2	0.543	0.317	0.501	0.290	0.537	0.677	0.400
	3	0.761	0.218	0.699	0.198	0.745	0.961	0.284

- 6.3. Check drifts—in E-W direction, maximum drift is 0.271 in, which is less than the allowable value of 0.84 in. The structure in this direction thus satisfies the drift requirement. In N-S direction, maximum drift is 0.384 in, which also satisfies the drift requirement.
- 6.3. Check drifts—in E-W direction, maximum drift is $0.7 R \Delta_x = 0.7 (4.5) (0.288) = 0.907$ in, which is less than the allowable value at 4.9 in. The structure in this direction thus satisfies the drift requirement. In N-S direction, maximum drift is $0.7 R \Delta_x = 0.7 (4.5) (0.409) = 1.29$ in, which also satisfies the drift requirement.
- 6.3. Check drifts—since maximum elastic drift is 0.4 in. According to IBC, Section 1617.4.6.1 [see Eq. (10.76)]
- $$\delta_x = \frac{C_d \delta_{ve}}{I_E} = \frac{3.5}{1.25} (0.4) = 1.12 \text{ in} < 2.52 \text{ in}$$
- drift requirement satisfied

<p>7. $P-\Delta$ effect (UBC-94, Section 1628.9 or Section 10.3.5—in E-W direction In N-S direction</p> $\delta_{\max} = 0.271 < \frac{0.02}{R_w} h_{sx}$ $= \frac{0.02}{6} [(14)12] = 0.56 \text{ in}$ <p>$\delta_{\max} = 0.384 < 0.56 \text{ in}$</p> <p>$P-\Delta$ effect need not be considered.</p>	<p>7. $P-\Delta$ effect [UBC-97, Section 1630.1.3 or Section 10.4.5.5(B)] In E-W direction</p> $\delta_{\max} = 0.288 < \frac{0.02}{R} h_{sx}$ $= \frac{0.02}{4.5} [(14)12] = 0.75 \text{ in}$ <p>$\delta_{\max} = 0.409 < 0.75 \text{ in}$</p> <p>$P-\Delta$ effect need not be considered.</p>	<p>7. $P-\Delta$ effect (IBC, Section 1617.4.6.2 or Section 10.5.6). The stability coefficient is</p> $\theta = \frac{P_x \Delta}{V_y h_{sx} C_d}$ <p>When $\theta < 0.1$, $P-\Delta$ effect need not be considered. In E-W direction:</p> <p>for the first floor, maximum $\Delta = C_d(0.244)/I_E = 0.683$ in</p> $\theta = \frac{(187.5 + 200 + 200)(0.683)}{(14)(12)(88.71)(3.5)} = 0.008 < 0.1$ <p>for the second floor, maximum $\Delta = C_d(0.304)/I_E = 0.85$ in</p> $\theta = \frac{(187.5 + 200)(0.85)}{(14)(12)(73.73)(3.5)} = 0.008 < 0.1$ <p>for the third floor, maximum $\Delta = C_d(0.192)/I_E = 0.54$ in</p> $\theta = \frac{(187.5)(0.54)}{(14)(12)(43.29)(3.5)} = 0.004 < 0.1$ <p>In N-S direction:</p> <p>for the first floor, maximum $\Delta = C_d(0.277)/I_E = 0.78$ in</p> $\theta = \frac{(187.5 + 200 + 200)(0.78)}{(14)(12)(82.25)(3.5)} = 0.009 < 0.1$ <p>for the second floor, maximum $\Delta = C_d(0.4)/I_E = 1.12$ in</p> $\theta = \frac{(187.5 + 200)(1.12)}{(14)(12)(68.59)(3.5)} = 0.011 < 0.1$ <p>for the third floor, maximum $\Delta = C_d(0.284)/I_E = 0.8$ in</p> $\theta = \frac{(187.5)(0.8)}{(14)(12)(40.39)(3.5)} = 0.006 < 0.1$ <p>Thus the $P-\Delta$ effect need not be considered.</p>
---	--	--

8. Load combination—
8.1. Moments and axial force due to dead load—dead load should be distributed in each frame at every floor. As shown in Fig 10.23 for E-W direction, half the floors dead load is assumed to be shared by two frames.
8. Load combination—
8.1. Moments and axial force due to dead load, same as calculated for UBC-94.

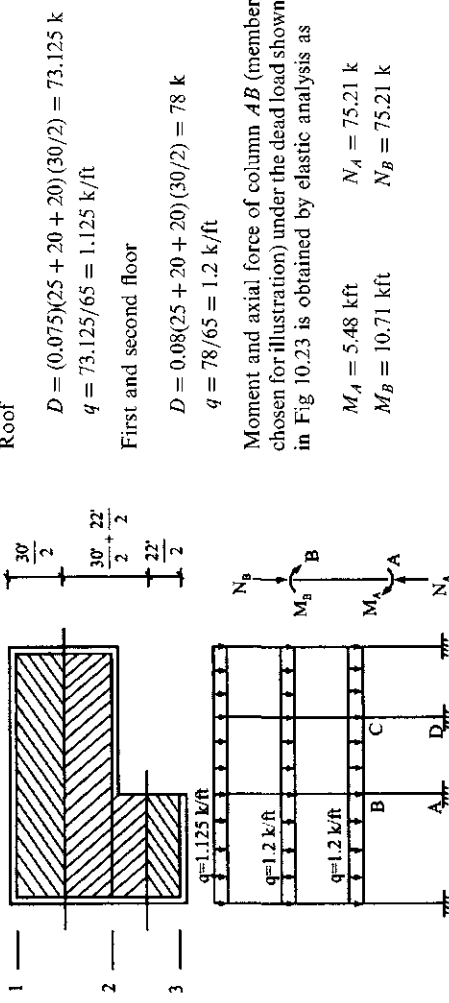


FIG. 10.23 Floor dead load on frame line 1 and forces on AB.

8.2. Moment and axial force of column *AB* under earthquake lateral forces—lateral forces shown in Fig. 10.24a are based on the shears in (a) of Table 10.24 (i.e. $6.13 = 35.85 - 29.72; 12.33 = 29.72 - 17.39$). Using elastic analysis of the frame yields internal forces on member *AB* as

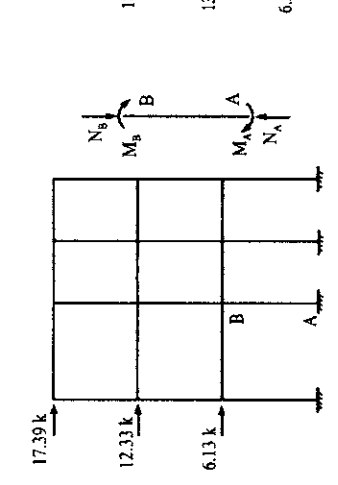


FIG. 10.24 (a) Earthquake lateral forces on frame line 1 and internal forces on *AB*.

$$\begin{aligned} M_A &= -111.62 \text{ k ft} \\ N_A &= -6.07 \text{ k} \\ M_B &= -65.29 \text{ k ft} \\ N_B &= -6.07 \text{ k} \end{aligned}$$

Because earthquake forces act at both ends, we select the maximum value for combined load.

$$\begin{aligned} M_E &= -44.46 \text{ k ft} & V_{AB} &= 13.45 \text{ k} \\ M_F &= -28.73 \text{ k ft} & V_{CD} &= 13.88 \text{ k} \\ M_G &= -46.23 \text{ k ft} & V_{EF} &= 5.23 \text{ k} \\ M_H &= -32.27 \text{ k ft} & V_{GH} &= 5.61 \text{ k} \end{aligned}$$

8.2. Moment and axial force of column *AB* under earthquake lateral forces—lateral forces shown in (a) of Table 10.24 are based on the shears in (b) of Table 10.24 (i.e. $6.53 = 38.16 - 31.63; 13.12 = 31.63 - 18.51$). Using elastic analysis of the frame yields internal forces on member *AB*. Design shears of all columns at first floor under the lateral force are calculated from moments using equilibrium condition of individual columns.

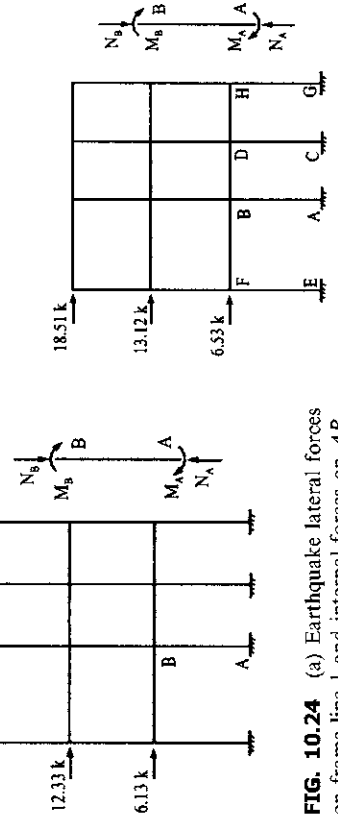


FIG. 10.24 (b) Earthquake lateral forces on frame line 1 and internal forces on *AB*, *CD*, *EF*, and *GH*.

$$\begin{aligned} M_A &= -118.78 \text{ k ft} & N_A &= -6.46 \text{ k} \\ M_B &= -69.48 \text{ k ft} & N_B &= -6.46 \text{ k} \\ M_C &= -120.79 \text{ k ft} & & \end{aligned}$$

$$\begin{aligned} M_D &= -73.50 \text{ k ft} & & \\ M_E &= -44.46 \text{ k ft} & V_{AB} &= 13.45 \text{ k} \\ M_F &= -28.73 \text{ k ft} & V_{CD} &= 13.88 \text{ k} \\ M_G &= -46.23 \text{ k ft} & V_{EF} &= 5.23 \text{ k} \\ M_H &= -32.27 \text{ k ft} & V_{GH} &= 5.61 \text{ k} \end{aligned}$$

8.2. Moments and axial force of column *AB* under earthquake lateral forces—lateral forces shown in Fig. 10.24c are based on the shears in (c) of Table 10.24. Using elastic analysis of the frame yields internal forces on member *AB*. Design shears of all columns at first floor under the lateral force are calculated from moments using equilibrium condition of individual columns.

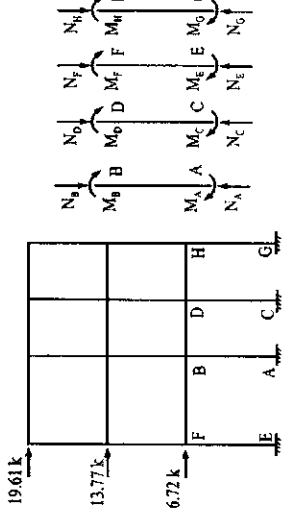


FIG. 10.24 (c) Earthquake lateral forces on frame line 1 and internal forces on *AB*, *CD*, *EF*, and *GH*.

$$\begin{aligned} M_A &= -124.87 \text{ k ft} & N_A &= -6.83 \text{ k} \\ M_B &= -72.95 \text{ k ft} & N_B &= -6.83 \text{ k} \\ M_C &= -126.98 \text{ k ft} & & \\ M_D &= -77.18 \text{ k ft} & & \\ M_E &= -46.75 \text{ k ft} & V_{AB} &= 14.13 \text{ k} \\ M_F &= -30.17 \text{ k ft} & V_{CD} &= 14.58 \text{ k} \\ M_G &= -48.61 \text{ k ft} & V_{EF} &= 5.49 \text{ k} \\ M_H &= -33.90 \text{ k ft} & V_{GH} &= 5.89 \text{ k} \end{aligned}$$

- 8.3. Load combination for ASD (UBC-94, Section 1603.6 or Section 10.6, this chapter)—since no live load is included in this example, the most critical load combinations for column *AB* are

$$\begin{aligned} & D & (a) & D & (a) \\ & D + E & (b) & D + 0.7E & (b) \\ & & & 0.6D + 0.7E & (c) \\ \text{Combination (a) yields} \\ M &= M_B = 10.71 \text{ k ft} & (c) \\ N &= N_A = N_B = 75.21 \text{ k} & (d) \end{aligned}$$

Combination (b) yields

$$\begin{aligned} M &= 5.48 + 111.62 = 117.1 \text{ k ft} \\ N &= 75.21 + 6.07 = 81.28 \text{ k} \end{aligned}$$

Design forces for column *AB* are

$$\begin{aligned} M &= 117.1 \text{ k ft} \\ N &= 81.28 \text{ k} \end{aligned}$$

- 8.3. Load combination for ASD (UBC-97, Section 1612.3.1 or Section 10.6)—since no live load is included in this example, the most critical load combinations for column *AB* are

$$\begin{aligned} & D & (a) & D & (a) \\ & 0.9D \pm \frac{E}{1.4} & (b) & D + 0.7E & (b) \\ & D + \frac{E}{1.4} & (c) & 0.6D + 0.7E & (c) \\ & D + 0.75 \left[\frac{E}{1.4} \right] & (d) \end{aligned}$$

where $E = \rho E_h + E_v$; E_h is earthquake load due to base shear; E_v is load effect due to vertical earthquake component; in allowable stress design, $E_v = 0$.

$$\rho = 20 - \frac{20}{r_{\max} \sqrt{A_i}}; \quad 1.0 \leq \rho \leq 1.5$$

$$r_{\max} =$$

maximum sum of the shears in any adjacent columns

$$= \frac{\text{total design story shear}}{\text{maximum sum of the shears in any adjacent columns}} = \frac{\max \left\{ \begin{array}{l} V_{EF} + 0.7V_{AB} \\ 0.7V_{AB} + 0.7V_{CD} \\ 0.7V_{CD} + V_{GH} \end{array} \right\}}{\max \left\{ \begin{array}{l} 14.65 \\ 19.13 \\ 15.33 \end{array} \right\}} = \frac{0.227}{84.41} = 0.227$$

A_1 = first floor area of structure to include area covered by all overhangs and projections
 $= (30)(25) + 20 + 20 + (22)(25)$
 $= 2500 \text{ ft}^2$

$$\begin{aligned} \rho &= 2 - \frac{20}{r_{\max(CD)} \sqrt{A_1}} = 0.24 < 1 \\ \rho &= 1 \end{aligned}$$

$$\rho = 2 - \frac{20}{r_{\max(GH)} \sqrt{A_1}} = 0.24 < 1; \text{ thus } \rho = 1$$

- 8.3. Load combination for ASD (IBC, Section 1605.3.1 or Section 10.6)—since no live load is included in this example, the most critical load combinations for column *AB* are

$$\begin{aligned} & D & (a) & D & (a) \\ & D + 0.7E & (b) & 0.6D + 0.7E & (b) \\ & & & 0.6D + 0.7E & (c) \\ & & & \text{where earthquake load is determined} \\ & & & \text{according to IBC, Sections 1617.1.1 and} \\ & & & 1617.1.2 as} \end{aligned}$$

$$\begin{aligned} E &= \rho Q_E \pm 0.2S_{Ed}D \\ \rho_i &= 2 - \frac{20}{r_{\max} \sqrt{A_i}} \end{aligned}$$

A_1 = floor area in square feet of diaphragm level immediately above ground story
 $= (30)(65) + (22)(25) = 2500 \text{ ft}^2$

$$\begin{aligned} r_{\max} &= \frac{\text{total design story shear}}{\text{total design story shear}} \\ &= \frac{\max \left\{ \begin{array}{l} V_{EF} + 0.7V_{AB} \\ 0.7V_{AB} + 0.7V_{CD} \\ 0.7V_{CD} + V_{GH} \end{array} \right\}}{\max \left\{ \begin{array}{l} 15.38 \\ 20.10 \\ 16.10 \end{array} \right\}} = \frac{0.227}{88.71} = 0.227 \end{aligned}$$

$$\begin{aligned} \rho &= 2 - \frac{20}{r_{\max(CD)} \sqrt{A_1}} = 0.24 < 1 \\ \rho &= 1 \end{aligned}$$

Combination (a) yields

$$M = M_A = 10.71 \text{ k ft}$$

$$N = N_A = N_B = 75.21 \text{ k}$$

Combination (b) yields

$$M = (0.9) 5.48 + \frac{(1) 118.78}{1.4} = \frac{89.77}{-79.91} \text{ k ft}$$

$$N = (0.9) 75.21 + \frac{(1) 6.46}{1.4} = \frac{72.30}{63.08} \text{ k}$$

Combination (c) yields

$$M = 5.48 + \frac{(1) 118.78}{1.4} = 90.32 \text{ k ft}$$

$$N = 75.21 + \frac{(1) 6.46}{1.4} = 79.82 \text{ k}$$

Combination (d) yields

$$M = 5.48 + 0.75 \frac{118.78}{1.4} = 69.11 \text{ k ft}$$

$$N = 75.21 + 0.75 \frac{6.46}{1.4} = 78.67 \text{ k}$$

Design force for column *AB* is

$$M = 90.32 \text{ k ft}$$

$$N = 79.82 \text{ k}$$

From step 3 (c) of the calculation,
 $S_{Ds} = 0.833g$. Combination (a) yields (see
solution due to *D* in Problem 10.7.1)

$$M = 10.71 \text{ k ft}$$

$$N = 75.21 \text{ k}$$

Combination (b) yields

$$\begin{aligned} M &= 5.48 + 0.7[(1) 124.87 \\ &\quad + 0.2(0.833)(5.48)] \\ &= 93.53 \text{ k ft} \end{aligned}$$

$$\begin{aligned} N &= 75.21 + 0.7[(1)(6.83) + 0.2(0.833) \\ &\quad (75.21)] = 88.76 \text{ k} \end{aligned}$$

Combination (c) yields

$$\begin{aligned} M &= 5.48(0.6) \\ &\quad + [(1)(124.87) + (0.2)(0.833)(5.48)]0.7 \\ &= 91.34 \text{ k ft} \\ N &= 75.21(0.6) \\ &\quad + [(1)(6.83) + (0.2)(0.833)(75.21)]0.7 \\ &= 64.49 \text{ k} \end{aligned}$$

Design loads are

$$M = 95.53 \text{ k ft}$$

$$N = 88.76 \text{ k}$$

<p>8.4. Load combination for LRFD (UBC-94, Chapter 22, Div. III, 249, A5 or Section 10.6). The most critical load combinations for column <i>AB</i> are</p> <table style="margin-left: 20px; border-collapse: collapse;"> <tr><td>1.4<i>D</i></td><td>(a)</td><td>1.4<i>D</i></td><td>(a)</td></tr> <tr><td>1.2<i>D</i> + 1.5<i>E</i></td><td>(b)</td><td>1.2<i>D</i> + 1.0<i>E</i></td><td>(b)</td></tr> <tr><td>0.9<i>D</i> - 1.5<i>E</i></td><td>(c)</td><td>0.9<i>D</i> ± 1.0<i>E</i></td><td>(c)</td></tr> </table>	1.4 <i>D</i>	(a)	1.4 <i>D</i>	(a)	1.2 <i>D</i> + 1.5 <i>E</i>	(b)	1.2 <i>D</i> + 1.0 <i>E</i>	(b)	0.9 <i>D</i> - 1.5 <i>E</i>	(c)	0.9 <i>D</i> ± 1.0 <i>E</i>	(c)	<p>8.4. Load combination for LRFD (UBC-97, Section 1612.2.1 or Section 10.6); the most critical load combinations for column <i>AB</i> are</p> <table style="margin-left: 20px; border-collapse: collapse;"> <tr><td>1.4<i>D</i></td><td>(a)</td><td>1.4<i>D</i></td><td>(a)</td></tr> <tr><td>1.2<i>D</i> + 1.0<i>E</i></td><td>(b)</td><td>1.2<i>D</i> + 1.0<i>E</i></td><td>(b)</td></tr> <tr><td>0.9<i>D</i> + 1.0<i>E</i></td><td>(c)</td><td>0.9<i>D</i> + 1.0<i>E</i></td><td>(c)</td></tr> </table>	1.4 <i>D</i>	(a)	1.4 <i>D</i>	(a)	1.2 <i>D</i> + 1.0 <i>E</i>	(b)	1.2 <i>D</i> + 1.0 <i>E</i>	(b)	0.9 <i>D</i> + 1.0 <i>E</i>	(c)	0.9 <i>D</i> + 1.0 <i>E</i>	(c)	<p>8.4. Load combination for LRFD (IBC, Section 1605.2.1, or Section 10.6); the most critical load combinations for column <i>AB</i> are</p> <table style="margin-left: 20px; border-collapse: collapse;"> <tr><td>1.4<i>D</i></td><td>(a)</td><td>1.4<i>D</i></td><td>(a)</td></tr> <tr><td>1.2<i>D</i> + 1.0<i>E</i></td><td>(b)</td><td>1.2<i>D</i> + 1.0<i>E</i></td><td>(b)</td></tr> <tr><td>0.9<i>D</i> + 1.0<i>E</i></td><td>(c)</td><td>0.9<i>D</i> + 1.0<i>E</i></td><td>(c)</td></tr> </table>	1.4 <i>D</i>	(a)	1.4 <i>D</i>	(a)	1.2 <i>D</i> + 1.0 <i>E</i>	(b)	1.2 <i>D</i> + 1.0 <i>E</i>	(b)	0.9 <i>D</i> + 1.0 <i>E</i>	(c)	0.9 <i>D</i> + 1.0 <i>E</i>	(c)
1.4 <i>D</i>	(a)	1.4 <i>D</i>	(a)																																			
1.2 <i>D</i> + 1.5 <i>E</i>	(b)	1.2 <i>D</i> + 1.0 <i>E</i>	(b)																																			
0.9 <i>D</i> - 1.5 <i>E</i>	(c)	0.9 <i>D</i> ± 1.0 <i>E</i>	(c)																																			
1.4 <i>D</i>	(a)	1.4 <i>D</i>	(a)																																			
1.2 <i>D</i> + 1.0 <i>E</i>	(b)	1.2 <i>D</i> + 1.0 <i>E</i>	(b)																																			
0.9 <i>D</i> + 1.0 <i>E</i>	(c)	0.9 <i>D</i> + 1.0 <i>E</i>	(c)																																			
1.4 <i>D</i>	(a)	1.4 <i>D</i>	(a)																																			
1.2 <i>D</i> + 1.0 <i>E</i>	(b)	1.2 <i>D</i> + 1.0 <i>E</i>	(b)																																			
0.9 <i>D</i> + 1.0 <i>E</i>	(c)	0.9 <i>D</i> + 1.0 <i>E</i>	(c)																																			
<p>Combination (a) yields</p> $\begin{aligned} M &= 1.4M_B = 1.4(10.71) \\ &= 14.994 \text{ k ft} \\ N &= 1.4N_B = 1.4(75.21) \\ &= 105.29 \text{ k} \end{aligned}$	<p>Combination (b) yields</p> $\begin{aligned} M &= 1.4M_B = 1.4(10.71) \\ &= 14.994 \text{ k ft} \\ N &= 1.4N_B = 1.4(75.21) \\ &= 105.29 \text{ k} \end{aligned}$	<p>Combination (c) yields</p> $\begin{aligned} M &= 1.4M_B = 1.4(10.71) \\ &= 14.994 \text{ k ft} \\ N &= 1.4N_B = 1.4(75.21) \\ &= 105.29 \text{ k} \end{aligned}$																																				
<p>Combination (b) yields</p> $\begin{aligned} M &= 1.2(5.48) + 1.5(111.62) \\ &= 174.0 \text{ k ft} \\ N &= 1.2(75.21) + 1.5(6.07) = 99.36 \text{ k} \end{aligned}$	<p>Combination (b) yields</p> $\begin{aligned} M &= 1.2(5.48) + 1.5(111.62) \\ &= 174.0 \text{ k ft} \\ N &= 1.2(75.21) + 1.5(6.07) = 99.36 \text{ k} \end{aligned}$	<p>Combination (b) yields</p> $\begin{aligned} M &= 1.2(5.48) + 1.5(111.62) \\ &= 174.0 \text{ k ft} \\ N &= 1.2(75.21) + 1.5(6.07) = 99.36 \text{ k} \end{aligned}$																																				
<p>Combination (c) yields</p> $\begin{aligned} M &= 0.9(5.48) - 1.5(111.62) \\ &= -162.5 \text{ k ft} \\ N &= 0.9(75.21) - 1.5(6.07) = 58.58 \text{ k} \end{aligned}$	<p>Combination (c) yields</p> $\begin{aligned} M &= 0.9(5.48) - 1.5(111.62) \\ &= -162.5 \text{ k ft} \\ N &= 0.9(75.21) - 1.5(6.07) = 58.58 \text{ k} \end{aligned}$	<p>Combination (c) yields</p> $\begin{aligned} M &= 0.9(5.48) - 1.5(111.62) \\ &= -162.5 \text{ k ft} \\ N &= 0.9(75.21) - 1.5(6.07) = 58.58 \text{ k} \end{aligned}$																																				
<p>Design forces for column <i>AB</i> are</p> $\begin{aligned} M &= 174.0 \text{ k ft} \\ N &= 105.29 \text{ k} \end{aligned}$	<p>Design forces for column <i>AB</i> are</p> $\begin{aligned} M &= 174.0 \text{ k ft} \\ N &= 105.29 \text{ k} \end{aligned}$	<p>Design forces for column <i>AB</i> are</p> $\begin{aligned} M &= 174.0 \text{ k ft} \\ N &= 105.29 \text{ k} \end{aligned}$																																				
<p>8.4. Load combination for LRFD (UBC-97, Section 1630.1.1). Combination (a) yields</p> $\begin{aligned} M &= \rho E_h + E_v; \quad E_v = 0.5 C_a ID \\ (a) &M = 1.4M_B = 1.4(10.71) = 14,994 \text{ k ft} \\ N &= 1.4N_B = 1.4(75.21) = 105.29 \text{ k} \end{aligned}$	<p>Combination (a) yields</p> $\begin{aligned} M &= \rho E_h + E_v; \quad E_v = 0.5 C_a ID \\ (a) &M = 1.4M_B = 1.4(10.71) = 14,994 \text{ k ft} \\ N &= 1.4N_B = 1.4(75.21) = 105.29 \text{ k} \end{aligned}$	<p>Combination (a) yields</p> $\begin{aligned} M &= \rho E_h + E_v; \quad E_v = 0.5 C_a ID \\ (a) &M = 1.4M_B = 1.4(10.71) = 14,994 \text{ k ft} \\ N &= 1.4N_B = 1.4(75.21) = 105.29 \text{ k} \end{aligned}$																																				
<p>Combination (a) yields</p> $\begin{aligned} M &= 1.4M_B = 1.4(10.71) \\ &= 14,994 \text{ k ft} \\ N &= 1.4N_B = 1.4(75.21) \\ &= 105.29 \text{ k} \end{aligned}$	<p>Combination (b) yields</p> $\begin{aligned} M &= 1.2(5.48) + (1)(1)(124.87) \\ &\quad + (0.2)(0.833)(5.48) = 132.36 \text{ k ft} \\ N &= 1.2(75.21) + (1)(1)(16.83) \\ &\quad + (0.2)(0.833)(75.21) = 109.61 \text{ k} \end{aligned}$	<p>Combination (b) yields</p> $\begin{aligned} M &= 1.2(5.48) + (1)(1)(124.87) \\ &\quad + (0.2)(0.833)(5.48) = 132.36 \text{ k ft} \\ N &= 1.2(75.21) + (1)(1)(16.83) \\ &\quad + (0.2)(0.833)(75.21) = 109.61 \text{ k} \end{aligned}$																																				
<p>Combination (c) yields</p> $\begin{aligned} M &= 0.9(5.48) + (1)(1)(118.78) \\ &\quad + (0.5)(0.3)(1.25)(5.48) = 126.38 \text{ k ft} \\ N &= 1.2(75.21) + (1)(1)(16.46) \\ &\quad + (0.5)(0.3)(1.25)(75.21) \\ &= 110.81 \text{ k} \end{aligned}$	<p>Combination (c) yields</p> $\begin{aligned} M &= 0.9(5.48) + (1)(1)(118.78) \\ &\quad + (0.5)(0.3)(1.25)(5.48) = 126.38 \text{ k ft} \\ N &= 1.2(75.21) + (1)(1)(16.46) \\ &\quad + (0.5)(0.3)(1.25)(75.21) \\ &= 110.81 \text{ k} \end{aligned}$	<p>Combination (c) yields</p> $\begin{aligned} M &= 0.9(5.48) + (1)(1)(118.78) \\ &\quad + (0.5)(0.3)(1.25)(5.48) = 126.38 \text{ k ft} \\ N &= 1.2(75.21) + (1)(1)(16.46) \\ &\quad + (0.5)(0.3)(1.25)(75.21) \\ &= 110.81 \text{ k} \end{aligned}$																																				
<p>Design forces for column <i>AB</i> are</p> $\begin{aligned} M &= 126.38 \text{ k ft} \\ N &= 110.81 \text{ k} \end{aligned}$	<p>Design forces for column <i>AB</i> are</p> $\begin{aligned} M &= 126.38 \text{ k ft} \\ N &= 110.81 \text{ k} \end{math>$	<p>Design forces for column <i>AB</i> are</p> $\begin{aligned} M &= 126.38 \text{ k ft} \\ N &= 110.81 \text{ k} \end{math>$																																				

10.8. TECHNIQUES FOR CALCULATING THE RIGIDITY CENTER

Two techniques are presented for determining the rigidity center (RC) of a floor: method A finds RC using stiffness of individual members (i.e. columns, walls, etc.) supporting a rigid floor as a shear building model; method B finds the relative rigidity of individual bays from which the RC is calculated (the structure is general with or without rigid floors). Both methods are approximate and both are acceptable in engineering practice.

10.8.1. Method A—Using Individual Member Stiffness for Rigid-floor Shear Buildings

Consider the rigid floor slab shown in Fig. 10.25 of a shear building whose supporting members such as columns may deform due to sidesway without end rotations. Let r_x and r_y be distances in the X and Y directions, respectively, from RC to a supporting member (i.e. r_{AX} and r_{AY} for column A as shown); let K_X and K_Y be the stiffness of the member when bent in the X and Y directions, respectively; let X_R and Y_R be the distance from RC to the origin of X and Y coordinates, respectively; let J be the total polar moment of inertia of all supporting members on this floor; let I_X and I_Y be the sectional moment of inertia of individual members about the X and Y axes, respectively; and let T be the torsional moment. For member A shown in the figure, the approximate equations to determine RC and torsional shear distribution may now be expressed as

$$V_{xe} = \frac{T r_{AY} K_X}{J} \quad (10.79a)$$

$$V_{ye} = \frac{T r_{AX} K_Y}{J} \quad (10.79b)$$

where torsional stiffness or polar moment of inertia is

$$J = \Sigma(K_X r_Y^2 + K_Y r_X^2) \quad (10.80)$$

$$X_R = \frac{\Sigma K_Y r_X}{\Sigma K_Y} \quad (10.81a)$$

$$Y_R = \frac{\Sigma K_X r_Y}{\Sigma K_Y} \quad (10.81b)$$

in which

$$K_X = \frac{12EI_Y}{L^3} \quad (10.82a)$$

$$K_Y = \frac{12EI_X}{L^3} \quad (10.82b)$$

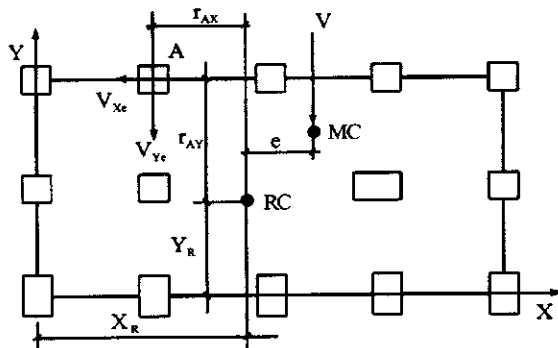


FIG. 10.25 Rigidity center and torsional shear distribution.

where V_{Xe} and V_{Ye} are shears in the X and Y directions, respectively, due to torsional moment T ; and L is the clear distance of a column between upper and lower floors. Eqs. 10.79a and 10.79b are applied separately for actual torsion and accidental torsion; the combination of shears is then determined according to building code specifications.

10.8.2. Method B—Using Relative Rigidity of Individual Bays for General Buildings

This technique is to apply a unit load at an individual floor i of a bay in one direction (say the X -direction) and to calculate the lateral displacement at that floor, Δ_{ix} . The rigidity corresponding to the displacement is $R_{ix} = 1/\Delta_{ix}$. If a building has N bays in X - and Y -directions, let bay j have distances X_j and Y_j from a reference point in the X - and Y -directions, respectively; then RC measured from the reference point is

$$X_R = \frac{R_{1Y}r_{1X} + R_{2Y}r_{2X} + \dots + R_{NY}r_{NX}}{R_{1Y} + R_{2Y} + \dots + R_{NY}} = \frac{\sum R_Y r_X}{\sum R_Y} \quad (10.83)$$

$$Y_R = \frac{R_{1X}r_{1Y} + R_{2X}r_{2Y} + \dots + R_{NX}r_{NY}}{R_{1X} + R_{2X} + \dots + R_{NX}} = \frac{\sum R_X r_Y}{\sum R_X} \quad (10.84)$$

The polar moment of inertia may be expressed as

$$J = \sum Rr^2 = R_{1Y}r_{1Y}^2 + R_{2Y}r_{2Y}^2 + \dots + R_{NY}r_{NY}^2 + R_{1X}r_{1X}^2 + R_{2X}r_{2X}^2 + \dots + R_{NX}r_{NX}^2 \quad (10.85)$$

A simple floor plan is shown in Fig. 10.26 for which the distribution of shear and torsion to bays A and B is calculated as follows:

(A) rigidity center and polar moment of inertia

$$X_R = \frac{R_A(0) + R_B(L)}{R_A + R_B} \quad (10.86a)$$

$$J = R_A r_{AX}^2 + R_B r_{BX}^2 + R_1 r_{1Y}^2 + R_2 r_{2Y}^2 + R_3 r_{3Y}^2 \quad (10.86b)$$

Note that R_1 and R_3 include walls W_S and W_N , respectively; R_A comprises the rigidity of W_W . Note also that wall W_W should not be considered in calculating R_1 , R_2 , and R_3 nor should W_N and W_S be considered in R_A and R_B . This is because the wall's out-of-plane stiffness is neglected.

(B) Torsion, T , and accidental torsion, T_a

$$T = V e_X \quad (10.87a)$$

$$T_a = V e_{ax} \quad (10.87b)$$

$$e_{ax} = 0.05L \quad (10.87c)$$

(C) Distribution of shear V

$$V_{AQ} = \frac{V R_A}{R_A + R_B} \quad (10.88a)$$

$$V_{BQ} = \frac{V R_B}{R_A + R_B} \quad (10.88b)$$

(D) Distribution of torsion, T , and accidental torsion, T_a

$$V_{AT} = -\frac{R_A r_{AX}}{J} T - \frac{R_A r_{AX}}{J} T_a \quad (10.89a)$$

$$V_{BT} = \frac{R_B r_{BX}}{J} T + \frac{R_B r_{BX}}{J} T_a \quad (10.89b)$$

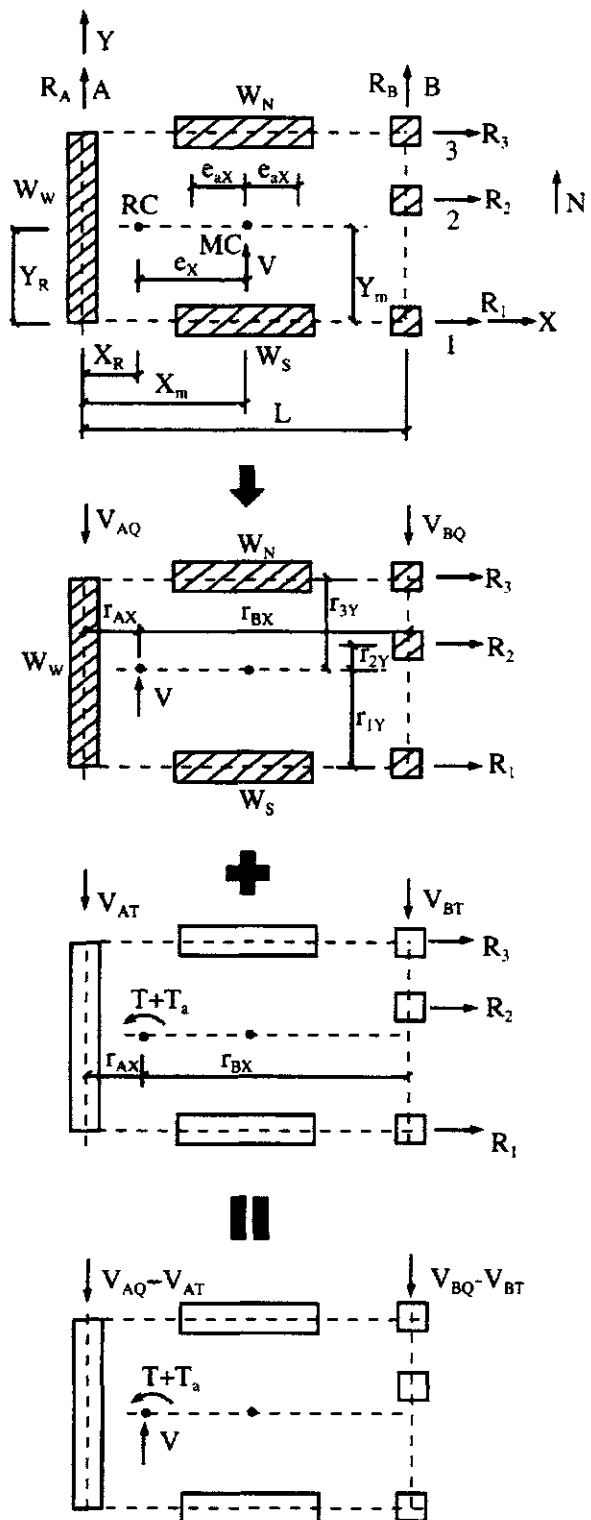


FIG. 10.26 Distribution of shear and torsion.

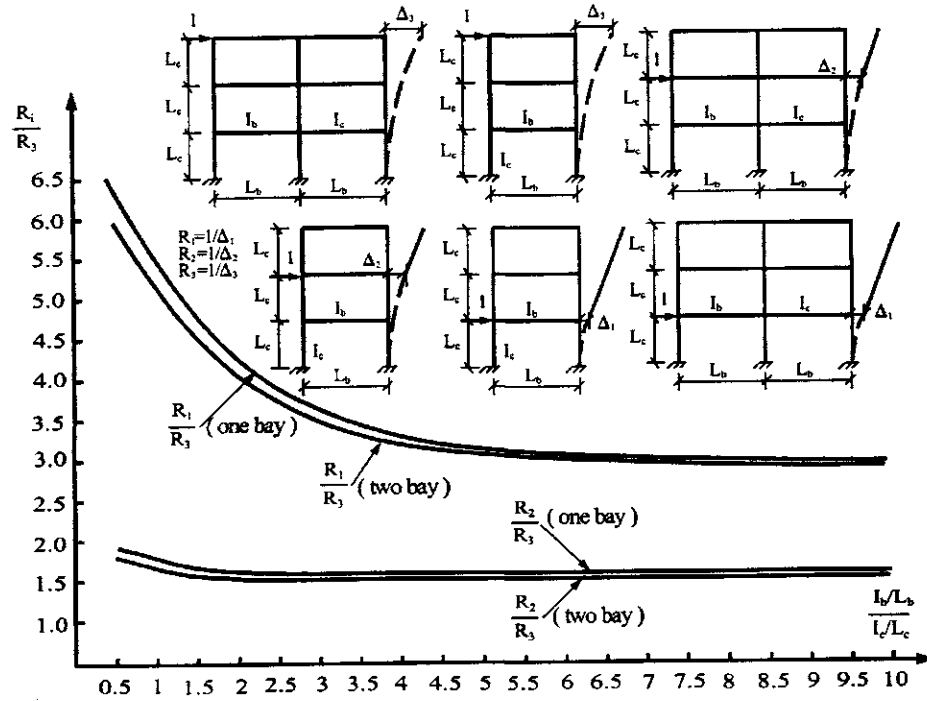


FIG. 10.27 R_i/R_3 for unit load applied at various floors.

(E) Final distribution

$$V_A = V_{AQ} - V_{AT}; \quad V_B = V_{BQ} + V_{BT} \quad (10.90)$$

Detailed calculation of the above equations is demonstrated in Example 10.7.1.

If the stiffness of beams is much greater than that of columns as in a shear building, only one-step analysis is needed to find all floor rigidities: apply a unit load on the top floor to find displacement, Δ , first and then rigidity (i.e. $R = 1/\Delta$) at that floor. Because the beam stiffness dominates the floor rigidity, the ratio of the i th floor rigidity, R_i , to top floor rigidity, R_{top} , is approximately constant; this ratio varies almost linearly from the first floor to the top. Thus X_R or Y_R has a common factor in numerator and denominator, so the factor is cancelled [see Eqs. (10.83) and (10.84)]. The influence of relative stiffness of columns and girders on rigidity ratio is illustrated in Fig. 10.27 for two rigid frames: a one-bay three-story frame and a two-bay three-story frame. When the value of $(I_b/L_b)/(I_c/L_c)$ is between 4 and 10, R_1/R_3 and R_2/R_3 are about 1.5 and 3, respectively. By applying a unit load at the top floor, an approximate determination of R_i is made in one-step analysis with negligible errors.

PART B ADVANCED TOPICS

10.9. DYNAMIC ANALYSIS PROCEDURES OF UBC-94, UBC-97 AND IBC-2000

10.9.1. UBC-94 Dynamic Analysis Procedure

Recall that previous sections discussed the static lateral-force analysis procedure. Not all building structures can be designed with this method because it may not adequately estimate the response of some structures. Dynamic analysis is thus required for the following structures (UBC-94, Section 1627.8.3).

- (A) All structures, regular or irregular, more than 240 ft in height except those in seismic zone 1, and of occupancy category 4 (UBC-94, Table 16-K) in seismic zone 2.
- (B) Structures with stiffness, mass, or geometric vertical irregularities as defined in UBC-94, Table 16-L or 16-M (see Figs. 10.3 and 10.4).
- (C) Structures exceeding five stories or 65 ft in height in seismic zones 3 and 4, not having the same structural system throughout their height except as permitted by Section 1628.3.2 in the code.
- (D) Regular or irregular structures located on soil profile type S₄ with period greater than 0.7 sec.

Dynamic analysis of building structures can be performed by response spectrum analysis (UBC-94, Section 1629.4.1) or time-history analysis (UBC-94, Section 1629.4.2). Both methods were extensively presented in previous chapters for lumped and distributed mass systems.

Some UBC requirements for dynamic and static lateral-force procedure are similar. Only the major design criteria of the dynamic analysis procedure are summarized here. Numerical examples are then to illustrate details such as checking certain criteria in static lateral-force level required for dynamic analysis procedure. Major criteria are explained as follows.

Since higher modes do not play a significant role in structural response, UBC provides an approximate method to simplify the determination of response parameters. Among them, one important parameter is the sufficient number of modes to be used so that 90% of structural mass contributes to system response (UBC-94, Section 1629.5.1).

Dynamic analysis of building structures, as discussed in previous chapters, indicates that maximum displacements and forces at each d.o.f. do not occur at the same time (Section 2.5.7) or in the same direction (Section 7.2.4 and 7.6). The square root of the sum of the squares (SRSS), a simple method with satisfactory accuracy, can be used for modal, force, and displacement combination. The adequacy of the SRSS method depends on the ratio of modal periods and the modal damping factors. The method is acceptable when the ratio of the period of any higher mode to its next lower mode is 0.75 or less and the damping factor does not exceed 5%. This is recommended in SEAOC Section c106.4.1.2 [26,27].

For regular buildings the base shear obtained by dynamic analysis should be increased to 90% of that obtained by static lateral-force procedure for which the period is based on Method B [see Eq. (10.26)]. Base shear should not be less than 80% of that result when the period is based on Method A [see Eq. (10.24)] (UBC-94, Section 1629.5.3). Either way, the dynamic base shear should not be more than the values obtained above.

When UBC-94 Figure 16.3 (see Figs. 7.31 and 10.28) is used to obtain spectral acceleration, soil type and seismic zone must first be designated. Soil type identifies which curve (see Fig. 10.28) to select. Seismic zone determines effective peak ground acceleration (EGA). The EGA is equal to zone factor times gravity g, as noted in Section 10.3.2.

Base shear, lateral shear at each floor level, structural displacement, and story drift are scaled by response modification factor R_w to obtain the corresponding design values.

Modal analysis should account for torsional effect, including accidental torsion. When 3-D models are used for analysis, the effects of accidental torsion should be taken into account by appropriate adjustments of mass location, or by equivalent static procedure.

10.9.2. UBC-97 Dynamic Analysis Procedure

Dynamic analysis procedures specified by UBC-97 are similar to those for dynamic lateral force in UBC-94. Identical requirements are not detailed here but new criteria in UBC-97 are discussed.

Structures requiring dynamic analysis are specified by UBC-97, Section 1629.8.4, and differ from UBC-94 as follows:

- (A) All structures in seismic zone 2 for occupancy categories 4 and 5 (only category 4 in UBC-94) are excluded.
- (B) All structures on soil profile type S_F (S₄ in UBC-94), having a period greater than 0.7 sec, require dynamic analysis.

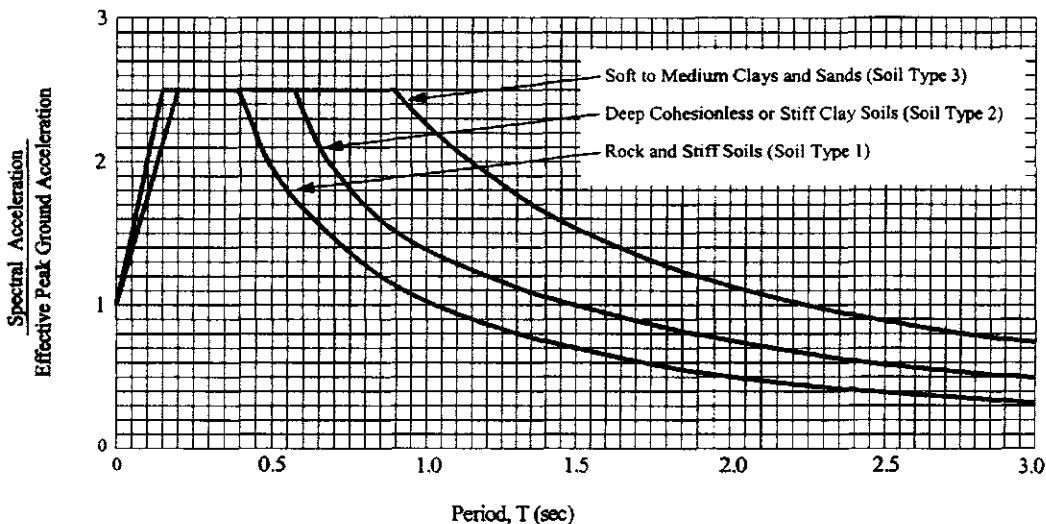


FIG. 10.28 UBC-94 normalized response spectra.

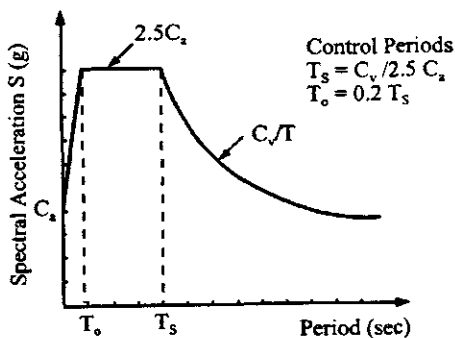


FIG. 10.29 UBC-97 design response spectra.

Dynamic analysis procedures comprise response spectrum analysis (UBC-97, Sections 1631.4.1 and 1631.5) and time-history analysis (UBC-97, Sections 1631.4.2 and 1631.6). UBC-97 design response spectra are defined in Figure 16-3 of the code and shown here in Fig. 10.29. The spectrum curve can be expressed as

$$\frac{S}{g} = \begin{cases} (1 + 1.5T/T_0)C_a & 0 \leq T < T_0 \\ 2.5C_a & T_0 \leq T < T_s \\ C_v/T & T_s \leq T \end{cases} \quad (10.91)$$

where S is spectral acceleration, g is acceleration due to gravity, and control periods $T_s = C_v/(2.5C_a)$, $T_0 = 0.2T_s$. The procedure to determine S is: (1) find C_a and C_v from code Tables 16-Q and 16-R (see Table 10.6) based on the seismic zone factor and soil profile type; (2) calculate T_s and T_0 ; and (3) use structural T to locate S from the figure. This analysis should account for torsional effects (UBC-97, Section 1631.5.6) similar to UBC-94 discussed in Section 10.9.1 of this chapter.

UBC-97 defines elastic response parameters (ERP) as forces and deformations obtained from elastic dynamic analysis using an unreduced ground motion representation. Elastic response parameters must be reduced for purposes of design (UBC-97, Section 1631.5.4). For regular

structures, ERP may be reduced such that corresponding design base shear is not less than 90% (for elastic design response spectrum as defined by UBC-97, Figure 16-3) or 80% (for site-specific elastic design response spectrum) of base shear obtained by static force procedure (UBC-97, Section 1630.2). For irregular structures, ERP may be reduced such that corresponding design base shear is not less than 100% of base shear obtained by static force procedure. Note that any reduction of ERP is limited in that the corresponding design base shear cannot be less than the elastic response base shear divided by the value R . Thus the ERP reduction factor cannot be greater than R . Finding the number of significant modes and the combination of structural response for each mode is the same as UBC-94.

Time-history analysis involves time-dependent seismic input requiring the use of appropriate ground motions for elastic as well as nonlinear structures as specified in UBC-97, Section 1631.6. A time-dependent response is obtained through numerical integration for which various numerical techniques are presented in Chapter 7. Capacities and characteristics of nonlinear elements should be consistent with test data for which various hysteresis models are discussed in Chapter 9. Pairs of horizontal ground motion components should be selected and scaled from not less than three recorded events with consideration of magnitude, fault distance and source mechanism. When three appropriate records are not available, simulated ground-motion pairs may be used to make up the total number required. For each pair, the SRSS method with 5% damping is used to construct a site-specific spectrum, which should be scaled such that it does not fall below 1.4 times the design spectra (see UBC-97, Figure 16-3 or Fig. 10.29) for periods 0.2 T –1.5 T sec. Each pair of time histories should be applied simultaneously to a structural model considering torsional effects. If three time-history analyses are performed, then the maximum response of the parameter of interest should be used for design. If seven or more time-history analyses are performed, then the average value of the parameter of interest may be used for design.

Response parameters from elastic time-history analysis (UBC-97, Section 1631.6.2) are denoted as elastic response parameters (ERP). ERP may be scaled by the reduction factor employed for response spectrum analysis as discussed earlier in this section. The maximum inelastic response displacement is not to be reduced (UBC-97, Section 1631.6.3). Story drift limitation, specified in Section 10.4.4 for static lateral-force procedure, must be met. A design review of the lateral-force-resisting system should be performed by a team of independent engineers when this method is used to justify structural design.

10.9.3. IBC-2000 Dynamic Analysis Procedure

For dynamic analysis of non-isolated building structures in IBC-2000, a modal analysis procedure is provided in detail; time-history analysis is permitted but only general guidelines are given. While modal analysis procedure is applicable to all kinds of building structures, the structures in seismic design categories D, E, and F (see IBC-2000, Tables 1616.3 (1), (2) and Table 1616.6.3; or Tables 10.13–10.16) must be designed by using the procedure. General guidelines for using modal analysis can be abstracted from Table 10.16 as follows:

- (A) All structures, regular or irregular, over 240 ft in height.
- (B) Structures with all of the following characteristics:
 - 1. located in an area where $S_{D1} \geq 0.2$ [S_{D1} is specified in Section 10.5.2(A) based on IBC-2000, Section 1615.1.3];
 - 2. located in an area assigned to site class E or F as specified in Table 10.15 based on IBC-2000, Section 1615.1.1; and
 - 3. having natural period $T \geq 0.7$ sec, as determined by the approximate method specified in Section 10.5.1(B) based on IBC-2000, Section 1617.4.2.

For structures described in (B), a site-specific response spectrum must be used but design base shear cannot be less than that determined by equivalent lateral-force procedure as expressed in Eqs. (10.62) and (10.63) (IBC-2000, Section 1617.4.1).

Some IBC requirements for dynamic lateral-force procedure are similar to those for static lateral-force procedure. Only the design criteria related to spectrum analysis are summarized below. Step-by-step dynamic analysis must be interwoven with certain criteria required in equivalent lateral-force procedure. Details are numerically illustrated by Example 10.11.3.

- (A) Similar to UBC, IBC-2000 requires a sufficient number of modes to be used so that 90% of structural mass contributes to system response (IBC-2000, Section 1618.2).
- (B) Also similar to UBC, SRSS and CQC can both be used for modal, force, and displacement combination (IBC-2000, Section 1618.7). For the SRSS method, SEAOC recommendations in Section c106.4.1.2 should be maintained (Section 10.9.2).
- (C) When design base shear V calculated by equivalent lateral-force procedure (IBC-2000, Section 1617.4.1) is larger than modal base shear V_t , the design story shears, moments, drifts and floor deflections are multiplied by modification factor C_m (IBC-2000, Section 1618.7) defined as

$$C_m = V/V_t \quad (10.92)$$

- (D) Modeling of buildings in IBC-2000 (Section 1618.1) is similar to UBC-97. Both are more comprehensive than UBC-94. A mathematical model should be constructed to represent spatial distribution of mass and stiffness throughout the structure. For regular structures with independent orthogonal seismic-force resisting systems, independent two-dimensional models may be constructed to represent each system. For irregular structures without independent orthogonal systems, a three-dimensional model must be constructed. At minimum, three dynamic d.o.f. consisting of translation in two orthogonal plan directions and torsional rotation about the vertical axis must be included at each level of the building. Additional dynamic d.o.f. are required to represent diaphragm flexibility where the diaphragm is not rigid relative to the rigidity of the vertical elements of the lateral force resisting system. This model must include the effect of cracked sections on stiffness properties of concrete and masonry elements, and the contribution of panel zone deformations to overall story drift for steel moment frame systems.
- (E) The distribution of horizontal shear is the same as for the equivalent lateral force method except that explicit amplification due to torsion is not required because torsional d.o.f. are included in the modal analysis model (IBC-2000, Section 1618.8).
- (F) The $P-\Delta$ effect on story drifts and shears is determined in the same way as equivalent lateral force procedure (IBC-2000, Section 1618.9).
- (G) Soil-structure interaction effects, although not required, can be considered on the basis of ASCE 7-98, Section 9.5.5 [2].

Computing procedures for modal analysis outlined above are detailed in the following working steps.

(A) Constructing design response spectrum – Unless a site-specific spectrum is required, a general design response spectrum must be developed as follows:

1. find maximum considered earthquake spectral response accelerations at short period S_s , at 1 sec period S_1 from IBC-2000, Figure 1615 (see Figs. 10.15 and 10.16);
2. find site coefficients F_a and F_v from IBC-2000, Tables 1615.1.2 (1) and (2) (see Tables 10.17 and 10.18);
3. calculate adjusted maximum considered earthquake spectral response accelerations for short period as $S_{MS} = F_a S_s$, and for 1 sec period as $S_{M1} = F_v S_1$ [IBC-2000, Section 1615.1.2; or Eqs. (10.66) and (10.67)];
4. determine design spectral response accelerations [IBC-2000, Section 1615.1.3; or Eqs. (10.68) and (10.69)] as

at short period,

$$S_{DS} = \frac{2}{3} S_{MS}$$

at 1 sec period,

$$S_{D1} = \frac{2}{3} S_{M1}$$

5. formulate general design response spectrum as in Eq. (10.93a) where $T_s = S_{D1}/S_{DS}$ and $T_0 = 0.2T_s$.

$$S_a = \begin{cases} \frac{0.6S_{DS}}{T_0} T + 0.4 S_{DS} & T \leq T_0 \\ S_{DS} & T_0 \leq T \leq T_s \\ \frac{S_{D1}}{T} & T \geq T_s \end{cases} \quad (10.93a)$$

$$S = \begin{cases} C_a \left(1 + 1.5 \frac{T}{T_0} \right) = \frac{0.6S_{DS}}{T_0} T + 0.4 S_{DS} & T \leq T_0 = 0.2T_s \\ 2.5C_a = S_{DS} & T_0 \leq T \leq T_s \\ \frac{C_v}{T} = \frac{S_{D1}}{T} & T \geq T_s \end{cases} \quad (10.93b)$$

Note that Eq. (10.93a) is analogous to Eq. (10.91), design response spectra in UBC-97. The analogy is shown in Eq. (10.93b). Let $C_a = 0.4S_{DS}$ and $C_v = S_{D1}$; then $T_s = C_v/(2.5C_a) = S_{D1}/[2.5(0.4 S_{DS})] = S_{D1}/S_{DS}$ and $C_v/T = S_{D1}/T$. Eqs. (10.93a) and (10.93b) are shown in Figs. 10.30a and b, respectively. The background of and relationship between C_a and S_{DS} as well as S_{D1}/T and C_v/T are discussed in Section 10.9.4(C).

(B) Modal base shear V_m for the m th mode is calculated in accordance with IBC-2000, Section 1618.4 as

$$V_m = C_{sm} \bar{W}_m \quad (10.94)$$

in which

$$C_{sm} = \frac{S_{am}}{R/I_E} \quad (10.95)$$

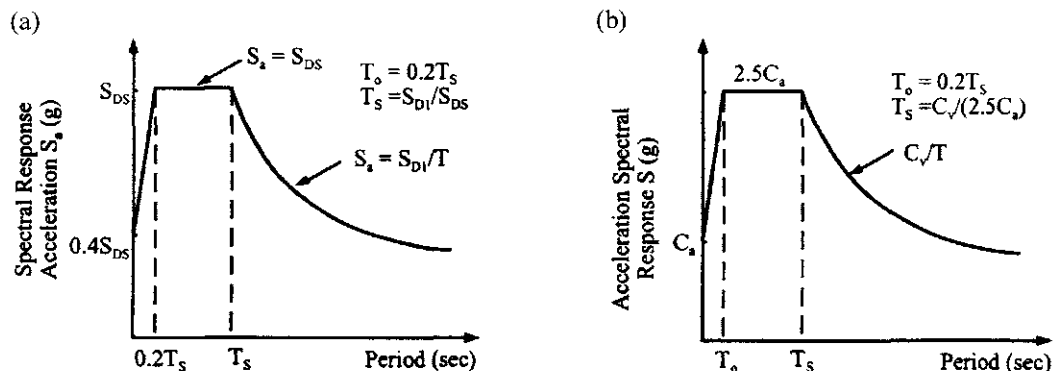


FIG. 10.30 Analogy between design response spectra in IBC-2000 and UBC-97. (a) IBC-2000 design response spectra. (b) UBC-97 design response spectra.

$$\bar{W}_m = \frac{\left(\sum_{i=1}^n w_i \phi_{im} \right)^2}{\sum_{i=1}^n w_i \phi_{im}^2} \quad (10.96)$$

Modal seismic response coefficient, C_{sm} , should be determined by the following criteria:

(1) for second or higher modes that have periods less than 0.3 second for buildings on site classes D, E, and F

$$C_{sm} = \frac{0.4S_{DS}}{R/I_E} (1.0 + 5.0T_m) \quad (10.97a)$$

(2) for modes with $T_m > 4.0$ sec

$$C_{sm} = \frac{4S_{D1}}{\frac{R}{I_E} T_m^2} \quad (10.97b)$$

(C) Modal forces are obtained as (IBC-2000, Section 1618.5)

$$F_{xm} = C_{v,xm} V_m \quad (10.98)$$

in which

$$C_{v,xm} = \frac{w_x \phi_{xm}}{\sum_{i=1}^n w_i \phi_{im}} \quad (10.99)$$

(D) Modal deflections are calculated in accordance with IBC-2000, Section 1618.5 as

$$\delta_{xm} = \frac{C_d \delta_{xem}}{I_E} \quad (10.100)$$

in which δ_{xem} is the deflection of level x in the m th mode at mass center determined by elastic analysis as

$$\delta_{xem} = \frac{g}{4\pi^2} \frac{T_m^2 F_{xm}}{w_x} \quad (10.101)$$

where F_{xm} is the portion of the seismic base shear in the m th mode, induced at level x ; w_x is the portion of the total gravity load of the building at level x . Modal drift in a story, Δ_m , should be computed as the difference between deflections δ_{xm} at the top and bottom of the story.

(E) Effective mass and number of modes are specified in IBC-2000, Section 1618.2 which requires a sufficient number of modes be used to obtain a combined modal mass participation of at least 90% of the actual building mass in each of two orthogonal directions.

(F) Determine design modal base shear, V_i , by SRSS or CQC method.

(G) Calculate base shear V by equivalent lateral-force method using a fundamental period of the building as $T = 1.2C_u T_a$ [Section 10.5.2(B)].

(H) Check V_i ; if $V > V_i$, then scaling is required. In this case, the design story shears, moments, drifts and floor deflections (a combination of corresponding modal values using SRSS or CQC method) are multiplied by modification factor C_m [Eq. (10.92)]. Design base shear V_1 need not exceed V . But V_1 should not be less than V when the design spectral response acceleration, S_{D1} is 0.2 or greater [Eq. (10.69)] with period, T , being 0.7 sec or greater (Section 10.5.2) for site class E or F.

(I) Horizontal shear distribution and $P-\Delta$ effect are calculated as for equivalent lateral-force procedure except that amplification of torsion is not required for that portion of torsion that is already included in modal analysis.

(J) Find the load combination for structural member design in accordance with load and resistance factor design, LRFD (IBC-2000, Section 1605.2.1) and allowable stress design, ASD (IBC-2000, Section 1605.3.1).

10.9.4. Regionalized Seismic Zone Maps and Design Response Spectra in UBC-97 and IBC-2000

This section focuses on: (A) general criteria for seismic zone maps; (B) importance of *effective peak acceleration* and *effective peak velocity* as parameters for these maps, and (C) relationship between seismic zone maps and design response spectra. Note that seismic zone maps are the same in UBC-94 and UBC-97, but design response spectra differ in these two codes. Note also that seismic zone maps in IBC-2000 are regionalized, making them entirely different from those in UBCs, while design response spectra in IBC-2000 are similar to those in UBC-97. Differences and similarities are discussed below.

10.9.4.1. General Criteria for Seismic Zone Maps

These criteria are summarized as follows:

1. Distance from anticipated earthquake sources. Field observation indicates that higher frequencies in ground motion attenuate more rapidly with distance than do lower frequencies; flexible structures may be more seriously affected than stiff structures at a distance of 60 miles or more from a major earthquake.
2. Nationwide standards for probability of exceeding design ground-shaking. The so-called *design ground-shaking* at a location is the ground motion that designers for a building project should have in mind to provide protection for life. This standard should be approximately the same throughout the U.S.A. A representation of design ground-shaking can be a smoothed elastic response spectra (see Fig. 7.26). In general, design ground-shaking should encompass a family of motion having the same overall intensity and frequency content, but differing in time sequence of motion. The elastic response spectrum, however, is not an ideal representation because it does not by itself give the duration of ground-shaking.
3. Regionalization maps of seismic zones. These maps should not attempt to *microzone*, i.e. delineate the location of actual faults or the variation of ground-shaking over short distances within 10 miles or less. Any such microzoning should be done under local jurisdictions.

10.9.4.2. Importance of EPA and EPV as Parameters for Seismic Zone Maps

Design ground-shaking should have an intensity which can be characterized by two parameters: *effective peak acceleration* (EPA) and *effective peak velocity* (EPV). The relationship between EPA and S_a (smoothed spectrum of peak ground acceleration) and between EPV and S_v (smoothed spectrum of peak ground velocity) with a proportional value of 2.5 is shown in Fig. 10.31. This figure shows that EPA is proportional to S_a for periods between 0.1 and 0.5 sec, while EPV is proportional to S_v at a period of about 1 sec. EPA is related to but not necessarily proportional to peak ground acceleration (S_a) as is EPV to peak ground velocity (S_v). In fact, with ground motion at very high frequencies, EPA may be significantly less than peak acceleration (see Fig. 10.31 for period <0.1). On the other hand, EPV is generally greater than peak velocity at long distances from a major earthquake. Ground motions, then, increase in duration and become more periodic with distance, which tends to increase EPV. Post-earthquake studies reveal that two motions of different duration but similar response spectrum cause different degrees of damage. This damage is usually less with motion of shorter duration. Thus EPV is an important parameter in developing a seismic zone map.

In ATC-3 a seismic zone map has two parts: one, based on EPA, is a "Map for Coefficient A_a "; the other, based on EPV, is a "Map for coefficient A_v ". Using both maps together, an index is obtained to evaluate the required design seismic force. Note that $A_a = \text{EPA}/g$, and $A_v = \text{EPV}/30$; a proportion value of 30 between EPV and A_v is used to establish three criteria: (1) a spectrum with $A_a = 0.4$ (i.e. $\text{EPA} = 0.4g$), necessitating $\text{EPV} = 12 \text{ in/sec}$; (2) a dimensionless

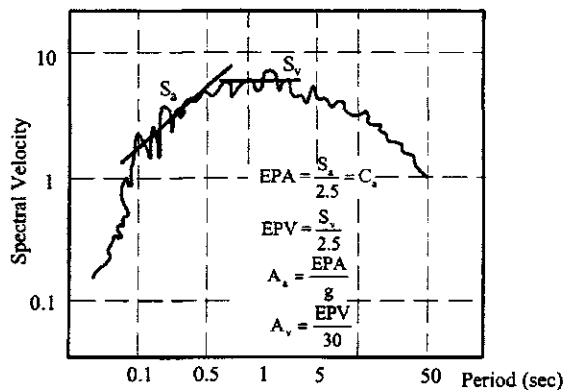


FIG. 10.31 Schematic representation of relationships among EPA, EPV, and response spectrum with 5% damping.

parameter A_v , called the *velocity-related acceleration coefficient*, which should never be greater than A_a ; (3) a factor of 2 to decrease EPV, requiring a distance of about 80 miles. Thus $A_v = 12/30 = 0.4$ is also a value of A_a . If $A_a = 0.2$, then $EPV = 6 \text{ in/sec}$, which is the next contour for $A_v = 0.4$, at a distance of 80 miles from the contour of $A_v = 0.4$. No contour of EPV should fall inside the corresponding contour of EPA. For example, the location of the contour for $EPV = 3 \text{ in/sec}$ in south-central Illinois was determined by the contour for $EPA = 0.1g$ rather than by distance from the contour for $EPV = 6 \text{ in/sec}$.

UBC-97 uses only one map, similar to the coefficient A_a map; parameter A_v is used in the code pertaining to the tabulated value of C_v . IBC-2000, however, uses two maps associated with S_s and S_1 (see Figs. 10.15 and 10.16), which are related to A_a and A_v , respectively.

10.9.4.3. Relationship between Seismic Zone Maps and Design Response Spectra

Seismic zone maps in UBC-97 and IBC-2000 result from continued efforts to improve seismic-resistant structural design. Early work by Algermissen and Perkins [1] covers peak ground accelerations on rock with a 10% probability of being exceeded in 50 years. ATC-3 modified that work with several features, such as transforming peak acceleration to EPA, smoothing EPA contours, and lowering the highest seismicity to $EPA = 0.4g$ (i.e. in zone 4, the original Algermissen-Perkins had contours of $0.6g$). With these modifications, the probability that the recommended EPA at a given location will not be exceeded during any 50-year period is estimated at 80–90%. UBC-97 modifies the ATC-3 map with seismic zone contours having a 10% probability of being exceeded in 50 years. Note that the probability of not being exceeded can be translated into other quantities such as *mean recurrence interval* or *return period*. Average annual risk for a 90% probability of not being exceeded in a 50-year interval is equivalent to a mean recurrence interval of 475 years or an average annual risk of 0.002 events per year.

Design response spectra in UBC-97 Figure 16-3 (Fig. 10.28) are based on ATC-3 in that $C_a = EPA$; C_v related to EPV is determined from tabulated values (Table 10.6), not directly from a map as in ATC-3. C_v is taken at 1 sec because it is about the average value at that period (see Fig. 10.31). Thus C_v/T yields response acceleration.

In IBC-2000, design spectral accelerations, S_{DS} and S_{D1} , are control parameters of design response spectra (Fig. 10.30a). S_{DS} and S_{D1} are based on mapped spectral accelerations, S_s , and S_1 , respectively, for which S_s is at 0.2 sec and S_1 is at 1 sec periods. The value of 0.2 sec is about the average period for EPA, and the value of 1.0 sec is about the average period for EPV (Fig. 10.31). Both S_s and S_1 , are determined by the code's maps (see Fig. 10.15 and 10.16). While S_{D1} is defined as design spectral response acceleration at 1 sec period, $S_a = S_{D1}/T$ for $T > T_s$ also represents design spectral acceleration. Thus $1/T$ should be interpreted as a scaling variable. Recall that IBC-2000 is more restrictive than both UBCs in that it has only a 2% probability of exceedance within a 50-year period (IBC-2000, Section 1615.2.1).

10. SUMMARY COMPARISON OF UBC-94, UBC-97 AND IBC-2000 DYNAMIC ANALYSIS PROCEDURES

Code	UBC-97	IBC-2000
C-94	<p><i>Near source effects</i></p> <p>In seismic zone 4 they are considered by specifying near source factors N_a and N_v to determine seismic coefficients C_a and C_v, respectively (Section 1629.4.2, Tables 16-Q-16-T, or Tables 10-6-10-8).</p> <p>Near source factors are determined by seismic source type (Table 16-U; or Table 10-7) and the closest distance of the structure to known seismic source. When the distance is more than 15 km, both near source factors are equal to 1.0 and near source effects need not be considered.</p>	<p><i>Near source effects</i></p> <p>They are considered using regionalized seismic maps accelerations [Figure 1615 (1)-(6)].</p>
	<p><i>Mathematical model of structures</i></p> <p>The effects of cracked sections on reinforced concrete and masonry elements as well as the contribution of panel zone deformations to overall story drift in steel moment frame systems must be considered for both static and dynamic procedures (Sections 1630.1.2 and 1631.3).</p> <p>The model includes not only all elements of lateral-force-resisting system, but also the stiffness and strength of elements significant in the distribution of forces. Also the model represents spatial distribution of the mass and stiffness of the structure. A three-dimensional model is used for structures with highly irregular plan configurations.</p>	<p><i>Mathematical model of structures</i></p> <p>The effects of cracked sections and panel zone deformations are considered (Section 1618.1).</p> <p>The model represents the spatial distribution of mass and stiffness throughout the structure. For regular structures with independent orthogonal seismic force-resisting systems, independent 2-D models may be constructed to represent each system. For irregular structures, at least three dynamic d.o.f. consisting of translation in two orthogonal plan directions and torsional about the vertical axis are included. Where the diaphragms are not rigid compared to vertical elements of lateral-force-resisting system, structural flexibility is considered for the modeling.</p>

<i>Structural irregularities</i>	<i>Structural irregularities</i>	<i>Structural irregularities</i>
Specifications (Tables 16-L and 16-M; or Fig. 10.3 and 10.4) are listed below.	Same as UBC-94 (UBC-97, Tables 16-L and 16-M).	In addition to UBC requirements, extreme torsional irregularity and extreme soft-story types are included. Limitations on seismic design category application due to structural irregularities are specified (Tables 1616.5.1 and 1616.5.2).

Vertical irregularities are:

1. Stiffness irregularity—soft story;
2. Weight (mass) irregularity;
3. Vertical geometric irregularity;
4. In-plane discontinuity in vertical lateral-force-resisting element;
5. Discontinuity in capacity—weak story.

Plan irregularities are:

1. Torsional irregularity;
2. Reentrant corners;
3. Diaphragm discontinuity;
4. Out-of-plane offsets;
5. Nonparallel systems.

Vertical irregularities are:

1. Stiffness irregularity—soft story;
2. Stiffness irregularity—extreme soft story;
3. Weight (mass) irregularity;
4. Vertical geometric irregularity;
5. In-plane discontinuity in vertical lateral-force-resisting elements;
6. Discontinuity in capacity—weak story.

Plan irregularities are:

1. Torsional irregularity;
2. Extreme torsional irregularity;
3. Reentrant corners;
4. Diaphragm discontinuity;
5. Out-of-plane offsets;
6. Nonparallel systems.

*Response spectrum analysis**Response spectrum analysis**Response spectrum analysis*

Normalized response spectrum (Figure 16-3; or Fig. 16-3a) is formulated as

$$\frac{S}{S_{\max}} = \begin{cases} 1.0 + 1.5T/T_g & T < T_0 \\ 2.5 & T_0 \leq T \leq T_g \\ 2.5T_g/T & T \geq T_g \end{cases}$$

and T_g depend on soil type and can be obtained from code's figure.

$$T_g = \frac{C_v}{2.5C_a}, \quad T_0 = 0.2T_s$$

where C_a and C_v are seismic coefficients related to soil

profile type, seismic zone factor and near source factors

(Tables 16-Q and 16-R, respectively; or Table 10.6).

$$\frac{S}{g} = \begin{cases} C_a + 1.5C_a T/T_0 & T < T_0 \\ 2.5C_a & T_0 \leq T < T_s \\ C_v T & T \geq T_s \end{cases}$$

$$T \geq T_s$$

$$T_0 = 0.2T_s, \quad T_s = S_{D1}/S_{Ds}$$

$$S_{Ds} = \frac{2}{3}F_a S_s$$

$$S_{D1} = \frac{2}{3}F_a S_I$$

T = fundamental period (in sec) of the building.

S_s and S_I are determined by the maps in Figure 1615 (1)-(10); F_a and F_v are related to site class and S_s as given in Tables 1615.1.2(1)-(2) (or Tables 10.17 and 10.18).

*Response spectrum analysis**Response spectrum analysis**Response spectrum analysis*

Number of modes required (Section 1629.5.1): significant modes must be included such that at least 90% of the participating mass is included for each principal horizontal direction.

Method for combining modes (Section 1629.5.2):

Responses are combined by recognized methods. When 'models' are used for analysis, modal interaction effects are considered when combining modal maxima.

Design response spectrum (Figure 16-3; or Fig. 10.29) is formulated as

$$\frac{S_a}{g} = \begin{cases} 0.6 \frac{S_{Ds}}{T_0} T + 0.4S_{Ds} & T < T_0 \\ S_{Ds} & T_0 \leq T < T_s \\ \frac{S_{D1}}{T} & T \geq T_s \end{cases}$$

Combination of modes—same as UBC-94 (UBC-97, Section 1631.5.3)

Combination of modes—same as UBC-94 (UBC-97, Section 1618.7).

Number of modes—same as UBC-94 (UBC-97, Section 1631.5.2).

Combination of modes is obtained by SRSS or CQC technique (Section 1618.7).

<i>Scaling dynamic analysis results</i>	<i>Scaling dynamic analysis results</i>	<i>Scaling dynamic analysis results</i>
Base shear V' obtained from the spectrum analysis is first reduced by factor R_w (Section 1629.5.3)	Forces and deformations, obtained by elastic time-history analysis and spectrum analysis with an unreduced-ground-motion model, are defined as elastic response parameters (ERP). ERP must be reduced such that (Section 1631.5.4)	Design story shear, moments, and drifts are multiplied by modification factor C_m defined as (Section 1618.7)
$V_D = V'/R_w$		$C_m = \frac{V}{V_t}$
If V_D is less than V_s (obtained by static procedure), then the design base shear (V'_D) is scaled upward as follows:		V_t is modal base shear and V is base shear calculated by equivalent lateral force procedure.
$V = \gamma_D V_D$ $\geq \begin{cases} 80\% V_s & \text{period by Method A for regular structures} \\ 90\% V_s & \text{period by Method B for irregular structures} \\ 100\% V_s & \text{irregular structures} \end{cases}$	$V' \leq \frac{V'}{R_f}$ $\geq \begin{cases} 90\% V_s & \text{period spectrum for regular structures} \\ 80\% V_s & \text{site-specified spectrum for regular structures} \\ 100\% V_s & \text{regardless of spectrum type for irregular structures} \end{cases}$	
Total reduction is R_w/γ_D . Seismic loads, forces, and deformations are reduced proportionally (Section 1629.5.3).	where V' is design base shear; V is base shear calculated by elastic response spectrum analysis; V_s is design base shear calculated by equivalent static procedure; and R_f is reduction factor $\leq R$.	
<i>Time-history analysis</i>	<i>Time-history analysis</i>	<i>Time-history analysis</i>
Recommended but no specifications (Secs. 1629.4.2 and 1629.6).	Requirements for ground-motion time histories, elastic time-history analysis and nonlinear time-history analysis are specified (Sections 1631.4.2 and 1631.6).	Specifications given for non-isolated structures (Section 1618.10) and seismically isolated structures (Section 1623.3.5.3).
	Pairs of appropriate horizontal ground-motion time history may count toward the total number where records are not available. These values are scaled upward if the corresponding average value of SRSS spectra falls below 1.4 times the design spectrum for periods from $0.2T$ to $1.5 T$ sec.	Specifications for non-isolated structures are similar to UBC-97 with design review by an independent team required for nonlinear time-history analysis.
		Results from elastic time-history analysis are denoted as elastic response parameters. Strength design is the basis for designing all elements. When nonlinear time-history analysis is used, a design review by an independent engineering team is performed.

11. NUMERICAL ILLUSTRATIONS OF DYNAMIC ANALYSIS PROCEDURE FOR UBC-94, UBC-97, AND IBC-2000

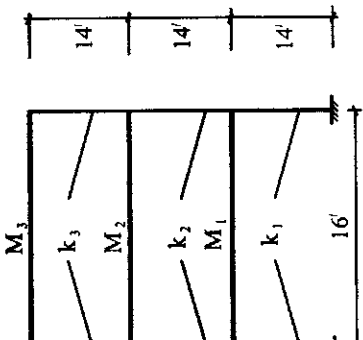


Fig. 10.32 Three-story building.

A three-story moment-resisting steel frame building is located in seismic zone 4 (Oakland, CA). For consistency in considering geologic conditions, soil profile is S₂ for UBC-94, S_c for UBC-97, and site class B for IBC-2000. Seismic importance factor γ is 1. An "A" type seismic source is 10 km from the structure. Dimensions of the structure are shown in Fig. 32, which is used in Example 2.6.2 in Chapter 2. Use the response spectrum analysis procedure for all three codes to determine:

1. Design base shear from dynamic lateral-force procedure.
2. Design base shear from static lateral-force procedure.
3. Design shear distribution at each floor.
4. Displacements and story drift of the building.
5. Load combination for ASD and LRFD.

In Example 2.6.2, the structure's mass and stiffness are

$$M_1 = M_2 = M_3 = M = 0.8431 \text{ k sec}^2/\text{ft}, \quad k_1 = 867.53 \text{ k}/\text{ft}, \quad k_2 = 639.21 \text{ k}/\text{ft}, \quad k_3 = 434.4 \text{ k}/\text{ft}$$

Normal modes and natural periods are

$$\begin{aligned} \{X\}_1 &= [1 & 2.1406 & 3.1387]^T, & \{X\}_2 &= [1 & 0.9985 & -0.9998]^T, \\ \{X\}_3 &= [1 & -0.7880 & 0.2152]^T, & T_1 &= 0.491 \text{ sec}, \quad T_2 = 0.195 \text{ sec}, \quad T_3 = 0.128 \text{ sec}. \end{aligned}$$

STATIC AND DYNAMIC LATERAL-FORCE PROCEDURES

689

EXAMPLE 10.11.1 (UBC-94)

1. Base shear from dynamic lateral-force analysis procedure
- 1.1. Spectral acceleration—based on this zone, soil type, and structural period, we obtain spectral acceleration from UBC-94, Figure 16.3 (or Fig. 10.28) as

$$S_{a1} = (2.5) \cdot 0.4g = g, \quad S_{a2} = (2.5) \cdot 0.4g = g,$$

$$S_{a3} = (2.3) \cdot 0.4g = 0.92g$$

$$[S_a] = \begin{bmatrix} g & 0 & 0 \\ 0 & g & 0 \\ 0 & 0 & 0.92g \end{bmatrix}$$

$$= \begin{bmatrix} 32.2 & 0 & 0 \\ 0 & 32.2 & 0 \\ 0 & 0 & 29.624 \end{bmatrix}$$

(a)

1.2. Modal displacements are calculated as

$$[x] = [X][v][S_a][\rho^2]^{-1}$$

$$= \begin{bmatrix} 1 & 1 & 1 \\ 2.1406 & 0.9964 & -0.7819 \\ 3.1387 & -0.9991 & 0.2211 \end{bmatrix}$$

EXAMPLE 10.11.2 (UBC-97)

1. Base shear from dynamic analysis procedure
- 1.1. Spectral acceleration—from UBC-97, Tables 16-S and 16-T (or Tables 10.7 and 10.8), near source factors are

$$N_a = 1, \quad N_v = 1.2$$

From UBC-97, Tables 16-Q and 16-R (or Table 10.6), seismic coefficients are

$$C_a = 0.4, \quad C_v = 0.56(1.2) = 0.672$$

The response spectrum is given by UBC-97, Figure 16-3 (or Fig. 10.29) with parameters as

$$2.5C_a = 2.5(0.4) = 1.0$$

$$T_s = \frac{C_v}{2.5C_a} = \frac{0.672}{1.0} = 0.672 \text{ sec}$$

$$T_0 = 0.22T_s = 0.2(0.672) = 0.1344 \text{ sec}$$

The spectrum with the above parameters is shown in Figure 10.33 from which or Eq. (10.91)

$$S_{a1} = g, \quad S_{a2} = g, \quad S_{a3}$$

$$= \left(0.4 + 0.6 \frac{0.12g}{0.1344} \right) g = 0.975g$$

$$[S_a] = \begin{bmatrix} g & 0 & 0 \\ 0 & g & 0 \\ 0 & 0 & 0.975g \end{bmatrix}$$

$$= \begin{bmatrix} 32.2 & 0 & 0 \\ 0 & 32.2 & 0 \\ 0 & 0 & 31.381 \end{bmatrix}$$

(a)

EXAMPLE 10.11.3 (IBC-2000)

1. Base shear from modal analysis procedure
- 1.1. Spectral acceleration—from UBC-97, Tables 16-S and 16-T (or Tables 10.7 and 10.8), near source factors are
- 1.1.1. Site class B. The structure belongs to seismic use group I with occupancy importance factor $I_E = 1$ (IBC, Table 1604.5). From IBC, Figure 1615, the mapped maximum considered earthquake spectral response accelerations at short period, S_s , and at 1 sec period, S_1 , can be determined for site-class B at Oakland, CA:

$$S_s = 150\% = 1.5$$

$$S_1 = 60\% = 0.6$$

(a)
From IBC, Table 1615.1.2(1) and (2) (or Tables 10.17 and 10.18 in Section 10.5.2), site coefficients F_a and F_v are

$$F_a = 1.0; \quad \text{for } S_s$$

$$F_v = 1.0; \quad \text{for } S_1$$

(b)
The adjusted maximum considered earthquake spectral response accelerations for short period, S_{MS} , and 1 sec period, S_{M1} , are

$$S_{MS} = F_a S_s = 1.0 (1.5) = 1.5$$

$$S_{M1} = F_v S_1 = 1.0 (0.6) = 0.6$$

(c)
Design spectral response accelerations at short period, S_{DS} , and 1 sec period, S_{D1} , are

$$S_{DS} = \frac{2}{3} S_{MS} = \frac{2}{3} (1.5) = 1.0$$

$$S_{D1} = \frac{2}{3} S_{M1} = \frac{2}{3} (0.6) = 0.4$$

EXAMPLE 10.11.1 (UBC-94)

$$\begin{bmatrix} \frac{1}{12.8^2} & & \\ & \frac{1}{32.11^2} & \\ & & \frac{1}{48.79^2} \end{bmatrix}$$

$$= \begin{bmatrix} 0.0890 & 0.0104 & 0.0032 \\ 0.1712 & 0.0104 & -0.0025 \\ 0.2510 & -0.0104 & 0.0007 \end{bmatrix} \quad (b)$$

in which the diagonal matrix $[\gamma]$ is obtained by

$$\begin{aligned} [\gamma] &= \frac{[X]^T [M] [1]}{[X]^T [M] [X]} \\ &= \begin{bmatrix} \frac{1}{13.0121} & & \\ & \frac{1}{2.5264} & \\ & & \frac{1}{1.4030} \end{bmatrix} \quad (b) \end{aligned}$$

where $[1]$ is calculated the same as UBC-94.

EXAMPLE 10.11.2 (UBC-97)

1.2. Modal displacements are

$$[x] = \begin{bmatrix} 1 & 1 & 1 \\ 2.1406 & 0.9985 & -0.7860 \\ 3.1387 & -0.9998 & 0.2152 \end{bmatrix}$$

$$\left. \begin{array}{l} T_s = \frac{S_{D1}}{S_{DS}} = \frac{0.4}{1.0} = 0.4 \text{ sec} \\ T_0 = 0.2T_s = 0.08 \text{ sec} \\ S_a = \begin{cases} \frac{0.6S_{DS}}{T_0} T + 0.4S_{DS} & T \leq T_0 \\ S_{DS} & T_0 \leq T \leq T_s \\ \frac{S_{D1}}{T} & T \geq T_s \end{cases} \end{array} \right\} \quad (e)$$

The design response spectrum S_a is shown here in Fig. 10.34.

EXAMPLE 10.11.3 (IBC-2000)

Design response spectrum S_a is developed by determining T_a and T_s [IBC, Section 1615.1.4 or Eq. (10.93a) and Fig. 10.30a)] as

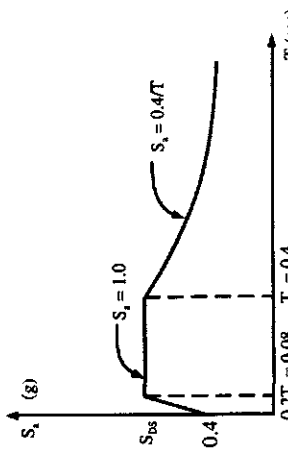


FIG. 10.33 Design response spectrum.

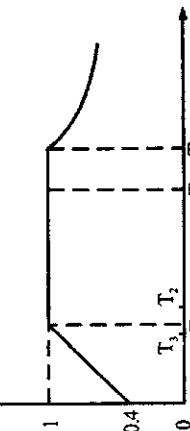


FIG. 10.34 Response spectrum.

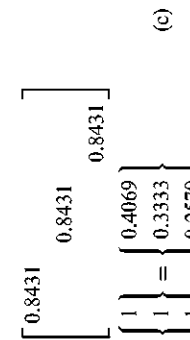


FIG. 10.35 Response spectrum.

STATIC AND DYNAMIC LATERAL-FORCE PROCEDURES

691

- 1.3. Lateral forces associated with these modes at each floor are

$$\begin{aligned} [F] &= [\mathbf{K}] [\mathbf{x}] \\ &= \begin{bmatrix} 1506.74 & -639.21 & 0 \\ -639.21 & 1073.61 & -434.4 \\ 0 & -434.4 & 434.4 \end{bmatrix} \\ &\quad \begin{bmatrix} 0.0800 & 0.0104 & 0.0032 \\ 0.1712 & 0.0104 & -0.0025 \\ 0.2510 & -0.0104 & 0.0007 \end{bmatrix} \\ &= \begin{bmatrix} 11.1064 & 9.0223 & 6.4196 \\ 23.6308 & 9.0355 & -5.3761 \\ 34.6651 & -9.0355 & 1.4770 \end{bmatrix} \end{aligned} \quad (\text{d})$$

- 1.3. Lateral forces associated with these modes at each floor are

$$\begin{aligned} [F] &= [\mathbf{K}] [\mathbf{x}] \\ &= \begin{bmatrix} 1506.14 & -639.21 & 0 \\ -639.21 & 1073.61 & -434.4 \\ 0 & -434.4 & 434.4 \end{bmatrix} \\ &\quad \begin{bmatrix} 0.0800 & 0.0104 & 0.0034 \\ 0.1712 & 0.0104 & -0.0027 \\ 0.2510 & -0.0104 & 0.0007 \end{bmatrix} \\ &= \begin{bmatrix} 11.1064 & 9.0223 & 6.8488 \\ 23.6308 & 9.0355 & -5.3761 \\ 34.6651 & -9.0355 & 1.4770 \end{bmatrix} \end{aligned} \quad (\text{c})$$

- Values of design response spectrum associated with modes are

$$\begin{aligned} S_{a1} &= S_a = \frac{0.4}{0.491} = 0.8147 \quad (T = 0.491) \\ S_{a2} &= S_a = 1.0 \quad (T = 0.195) \\ S_{a3} &= S_a = 1.0 \quad (T = 0.128) \end{aligned}$$

or in matrix form

$$[\mathbf{S}_a] = \begin{bmatrix} 0.8147 & 0 & 0 \\ 0 & 1.0 & 0 \\ 0 & 0 & 1.0 \end{bmatrix} \quad (\text{f})$$

Modal displacements and lateral forces calculated in steps 1.2 and 1.3 for UBC are not needed for IBC procedures.

- 1.4. The base shear is

$$\begin{aligned} [V] &= ([F]^T \{1\})^T \\ &= \begin{bmatrix} 69.4023 & 9.0223 & 2.9496 \end{bmatrix}^T \\ &\quad \begin{pmatrix} 1 \\ 1 \\ 1 \end{pmatrix}^T \\ &= [69.4023 \quad 9.0223 \quad 2.7761]^T \end{aligned} \quad (\text{e})$$

- 1.4. The base shear is

$$\begin{aligned} [V] &= ([F]^T \{1\})^T \\ &= \begin{bmatrix} 69.4023 & 9.0223 & 2.9496 \end{bmatrix}^T \\ &\quad \begin{pmatrix} 1 \\ 1 \\ 1 \end{pmatrix}^T \end{aligned} \quad (\text{d})$$

- 1.4. The modal base shear is [Eqs. (10.94)-(10.96)]

$$V_m = C_{sm} \bar{W}_m; \quad m = 1, 2, \text{ and } 3 \quad (\text{g})$$

where

$$C_{sm} = \frac{S_{am}}{R/I}, \quad \bar{W}_m = \frac{\left(\sum_{i=1}^n w_i \phi_{im} \right)^2}{\sum_{i=1}^n w_i \phi_{im}^2}$$

For this moment frame, $R = 8$, $\Omega_0 = 3$, $C_d = 5.5$ (IBC, Table 1617.6), modal seismic response coefficients C_{sm} (IBC, Equation 16-53) are

$$\begin{aligned} C_{s1} &= \frac{S_{a1}}{R/I_E} = \frac{0.8147}{8/1.0} = 0.102 \\ C_{s2} &= \frac{S_{a2}}{R/I_E} = \frac{1.0}{8/1.0} = 0.125 \\ C_{s3} &= \frac{S_{a3}}{R/I_E} = \frac{1.0}{8/1.0} = 0.125 \end{aligned} \quad (\text{h})$$

and effective modal gravity loads \bar{W}_1 are

$$\begin{aligned}\bar{W}_1 &= \frac{(w_1\phi_{11} + w_2\phi_{21} + w_3\phi_{31})^2}{w_1\phi_{11}^2 + w_2\phi_{21}^2 + w_3\phi_{31}^2} \\ &= \frac{(1+2.1406 + 3.1387)^2(Mg)^2}{(1^2 + 2.1406^2 + 3.1387^2)Mg} \\ &= 2.5548 (0.8431) (32.2) \\ &= 69.357 \text{ k}\end{aligned}\quad (\text{i})$$

where $w_1 = w_2 = w_3 = Mg$

$$\begin{aligned}\bar{W}_2 &= \frac{(w_1\phi_{12} + w_2\phi_{22} + w_3\phi_{32})^2}{w_1\phi_{12}^2 + w_2\phi_{22}^2 + w_3\phi_{32}^2} \\ &= \frac{(1+0.9985 - 0.9998)^2(Mg)^2}{(1^2 + 0.9985^2 + (-0.9998)^2)Mg} \\ &= 0.3328 (0.8431) (32.2) \\ &= 9.0336 \text{ k}\end{aligned}\quad (\text{j})$$

$$\begin{aligned}\bar{W}_3 &= \frac{(w_1\phi_{13} + w_2\phi_{23} + w_3\phi_{33})^2}{w_1\phi_{13}^2 + w_2\phi_{23}^2 + w_3\phi_{33}^2} \\ &= \frac{(1 - 0.7860 + 0.2152)^2(Mg)^2}{(1^2 + (-0.7860)^2 + 0.2152^2)Mg} \\ &= 0.1107 (0.8431) (32.2) \\ &= 3.005 \text{ k}\end{aligned}\quad (\text{k})$$

Modal base shears are

$$\begin{aligned}V_1 &= C_{S1} \bar{W}_1 = 0.102 (69.357) \\ &= 7.074 \text{ k} \\ V_2 &= C_{S2} \bar{W}_2 = 0.125 (9.036) \\ &= 1.1295 \text{ k} \\ V_3 &= C_{S3} \bar{W}_3 = 0.125 (3.005) = 0.3756 \text{ k}\end{aligned}\quad (\text{l})$$

1.5. The effective mass for each mode is

$$W_i = g \frac{V_i}{S_{ai}}; \quad (i = 1, 2, 3) \quad (f)$$

$$[W_i] = \left[\frac{69.4023}{1} \frac{9.0223}{1} \frac{2.7761}{0.92} \right]$$

$$= [69.4023 \quad 9.0223 \quad 3.0175]$$

$$\Sigma W_i = 69.4023 + 9.0223 + 3.0175$$

$$= 81.44 \text{ k} \quad (g)$$

which equals total structural weight, $W = (3)(0.8431)32.2 = 81.44 \text{ k}$. Thus the percentage of structural mass participating in each mode is

$$\frac{[W_i]}{W} (100)\% = [85.2\% \quad 11.1\% \quad 3.7\%] \quad (h)$$

1.5. The effective mass for each mode is

$$W_i = g \frac{V_i R}{S_{ai}}; \quad (i = 1, 2, 3) \quad (m)$$

$$[W_i] = \left[\frac{69.4023}{1} \frac{9.0223}{1} \frac{2.9496}{0.975} \right]$$

$$= [69.4023 \quad 9.0223 \quad 3.0252]$$

$$\Sigma W_i = 69.4023 + 9.0223 + 3.0252$$

$$= 81.44 \text{ k} \quad (e)$$

The percentage of structural mass participating in each mode is calculated the same as UBC-94 except slight difference associated with third mode.

$$\frac{[W_i]}{W} (100)\% = [85.3\% \quad 11.1\% \quad 3.7\%] \quad (n)$$

1.6. Design base shear—from Eq. (h), the first and second mode are used (UBC-94, Section 1629.5.1). Thus design base shear is

$$V_D = \frac{\sqrt{V_1^2 + V_2^2}}{R_w} = \frac{1}{12} \quad (i)$$

$$\sqrt{69.4023^2 + 9.0223^2} = 5.8322 \text{ k} \quad (i)$$

$$V_D = \frac{\sqrt{V_1^2 + V_2^2}}{R} = \frac{1}{8.5} \quad (j)$$

$$\sqrt{(69.4023)^2 + (9.0223)^2} = 8.2337 \text{ k} \quad (f)$$

1.6. Design base shear by response spectrum procedure: the first and second mode are used (UBC-97, Section 1613.5.2), thus the lower bound of design base shear is

$$V_1 = \sqrt{V_1^2 + V_2^2} = \sqrt{(7.0744)^2 + (1.1295)^2} = 7.164 \text{ k} \quad (o)$$

The SRSS method is used to combine each of the modal values here and in the following solution (IBC Section 1618.7).

2. Design base shear from static lateral-force analysis:

Method A

$$T_A = C_1(h_n)^{3/4} = 0.035(42)^{3/4} = 0.577 \text{ sec}$$

where $C_1 = 0.035$, $h_n = 42 \text{ ft}$

$$C_A = \frac{1.25S}{T_A^{2/3}} = \frac{1.25(1.2)}{0.577^{2/3}} = 2.164$$

where $S = 1.2$

$$\frac{C}{R_w} = \frac{2.164}{12} = 0.180 > 0.075$$

Thus

$$V_A = \frac{ZIC}{R_w} = \frac{(0.4)(1)(2.164)}{12} \quad (\text{j})$$

$$(81.44) = 5.875 \text{ k} \quad (\text{k})$$

Method B

$$T_B = 1.3 T_A = (1.3)(0.577) = 0.75$$

$$C_B = \frac{1.25(1.2)}{0.75^{3/4}} = 1.861$$

$$V_B = \frac{(0.4)(1)(1.861)}{12} (81.44) = 5.052 \text{ k} \quad (\text{k})$$

Since

$$V_D > \max [0.9V_B \quad 0.8V_A] \quad (\text{l})$$

$$= \max \{4.547 \quad 4.7\} = 4.7 \text{ k} \quad (\text{l})$$

the design base shear is

$$V = V_D = 5.8322 \text{ k}$$

No scaling is required.

2. Design base shear from static lateral-force analysis: from Eq. (10.40) (UBC-97, Formulas 30.4-30.7)

$$V_s = C_s W$$

$$T = C_1(h_n)^{3/4} = 0.035(42)^{3/4} = 0.577 \text{ sec}$$

$$V' = \frac{C_a Iw}{RT} = \frac{0.672(1)(81.44)}{8.5(0.577)} = 11.16 \text{ k}$$

The design base shear cannot exceed

$$\frac{2.5 C_a Iw}{R} = \frac{2.5(0.4)(1)(81.44)}{8.5} = 9.58 \text{ k}$$

Thus

$$V_s = 9.58 \text{ k} \quad (\text{g})$$

V_s must satisfy

$$\frac{0.11 C_a Iw}{R} = \frac{0.11(0.4)(1)(81.44)}{8.5} = 3.583 \text{ k} < V_s \text{ (OK)} \quad (\text{h})$$

$$\frac{0.8ZN_c Iw}{R} = \frac{0.8(0.4)(1.2)(1)(81.44)}{8.5} = 3.679 \text{ k} < V_s \text{ (OK)} \quad (\text{i})$$

Since $0.9 V_s = 0.9(9.58) = 8.62 \text{ k} > V_D$, the design base shear (UBC-97, Section 1613.5.4) is

$$V = 0.9V_s = 8.62 \text{ k} \quad (\text{j})$$

Since elastic response parameters cannot be reduced such that the corresponding design base shear is less than the elastic response base shear divided by R , thus the numerical coefficient, R , should be reduced as

$$V = \frac{V_s}{R} = \frac{9.58}{8.62} = 1.10 \quad (\text{k})$$

By comparing base shears V_s and V_t , the design story shears and floor deflections will then be multiplied by a modification factor (IBC, Section 1618.7) for which V_s is based on $T < 1.2 C_u T_a$. Thus

$$\frac{V_s}{R} = \frac{0.44}{8.0(0.4969)/1.0} = 0.102 \quad (\text{p})$$

Note the requirement (IBC, Section 1617.4.2) that $T < C_u T_a = 1.2 (0.577) = 0.692$. Thus

$C_s = \min[0.102, \max(0.044, 0.125)]$
 $= 0.102$
 $V_s = 0.102 (3)(0.8431)(32.2) = 8.307 \text{ k}$

(p)

By comparing base shears V_s and V_t , the design story shears and floor deflections will then be multiplied by a modification factor (IBC, Section 1618.7) for which V_s is based on $T < 1.2 C_u T_a$. Thus

$$\frac{V_s}{R} = \frac{0.44}{8.0(0.4969)/1.0} = 0.102 \quad (\text{q})$$

$R_f = \frac{8.5(8.2337)}{8.62} = 8.12 < R \quad (\text{k})$

R_f is then used to determine elastic response parameters as shown in Eqs. (f) and (m).

Note that V_D in Eq. (f) is used only for checking lateral-force results to find whether or not R should be reduced. V_D cannot be used for lateral force distribution because such distribution relies on the base shear of an individual mode, not on a single shear V_D .

STATIC AND DYNAMIC LATERAL-FORCE PROCEDURES

695

3. Design shear distribution: first mode—from Eq. (g), shear corresponding to the first mode is

$$V_1 = 69.4023 \text{ k} \quad (\text{m})$$

The lateral force at each mode is calculated by

$$F_{1i} = \frac{w_i X_i}{\sum w_i X_i} V_1 = \frac{X_i}{\sum X_i} V_1$$

where $w_1 = w_2 = w_3$. Force and shear at each floor V_{1i} are

Level	X_i	F_{1i}	V_{1i}
Roof	3.1387	34.6907	—
Third floor	2.1406	23.6591	34.6907
Second floor	1	11.0525	58.3498
First floor	—	—	69.4023
Total	—	—	69.4023

Second mode—similarly from Eq. (g), we have

$$\begin{aligned} V_2 &= 9.0223 \text{ k} \\ F_{2i} &= \frac{X_i}{\sum X_i} V_2 \end{aligned}$$

in which w_i is not included due to equal floor weight. Force and shear at each floor V_{2i} are

Level	X_i	F_{2i}	V_{2i}
Roof	-0.9998	-9.0322	—
Third floor	0.9985	9.0205	-9.0322
Second floor	1	9.0340	-0.0117
First floor	—	—	9.0223
Total	—	—	9.0223

3. Modal forces in design shear distribution: modal forces [IBC, Section 1618.5; or Eqs. (10.98) and (10.99)] are calculated by

$$F_{xm} = C_{v,xm} V_m, \quad \text{where } C_{v,xm} = \frac{w_x \phi_{xm}}{\sum_{i=1}^n w_i \phi_{xm}}$$

Thus for the first mode

$$\begin{aligned} \sum_{i=1}^3 w_i \phi_{1i} &= w_1 \phi_{11} + w_2 \phi_{21} + w_3 \phi_{31} \\ &= (\phi_{11} + \phi_{21} + \phi_{31}) M_g \\ &= (1.0 + 2.1406 + 3.1387) M_g \end{aligned}$$

$$\begin{aligned} F_{11} &= C_{v11} V_1 = \frac{w_1 \phi_{11}}{\sum_i w_i \phi_{im}} V_1 \\ &= 6.2793 M_g \\ &= \frac{Mg(1)}{6.2793 Mg} (7.0744) = 1.1266 \text{ k} \end{aligned}$$

$$\begin{aligned} F_{21} &= C_{v21} V_1 = \frac{w_2 \phi_{21}}{\sum_i w_i \phi_{im}} V_1 \\ &= \frac{Mg(2.1406)}{6.2793 Mg} (7.0744) = 2.4116 \text{ k} \end{aligned}$$

$$\begin{aligned} F_{31} &= C_{v31} V_1 = \frac{w_3 \phi_{31}}{\sum_i w_i \phi_{im}} V_1 \\ &= \frac{Mg(3.1387)}{6.2793 Mg} (7.0744) = 3.5361 \text{ k} \end{aligned}$$

and for the second mode

$$\begin{aligned} \sum_{i=1}^3 w_i \phi_{12} &= w_1 \phi_{12} + w_2 \phi_{22} + w_3 \phi_{32} \\ &= (\phi_{12} + \phi_{22} + \phi_{32}) M_g \\ &= (1.0 + 0.9985 - 0.9998) M_g \\ &= 0.9987 M_g \end{aligned}$$

$$\frac{T_3}{T_2} = \frac{0.128}{0.195} = 0.656 < 0.75$$

$$\frac{T_2}{T_1} = \frac{0.195}{0.491} = 0.397 < 0.75$$

Note that the ratio of any higher-mode period to any lower-mode period is less than 0.75 and damping factor does not exceed 5%. Thus SRSS is used to determine the combined lateral force and story shear at each floor as:

el	F_{it}	F_{2j}	F_i	V_{ti}	V_{2j}	V_i
df	34.6907	-9.0322	35.8472	34.6907	-9.0322	35.8472
rd	23.6591	9.0205	25.3204	58.3498	-0.0117	58.3498
or	11.0525	9.0340	14.2748	69.4023	9.0223	69.9863
ond						
or						
st	69.4023	9.0223	69.9863			
or						

$$\begin{aligned}
 F_{12} &= C_{v12} V_2 = \sum_i w_i \phi_{12} V_2 \\
 &= \frac{Mg(1)}{0.9987 Mg} (1.1295) = 1.130 \text{ k} \\
 F_{22} &= C_{v22} V_2 = \sum_i w_i \phi_{22} V_2 \\
 &= \frac{Mg(0.9985)}{0.9987 Mg} (1.1295) = 1.1293 \text{ k} \\
 F_{32} &= C_{v32} V_1 = \sum_i w_i \phi_{32} V_2 \\
 &= \frac{Mg(-0.9998)}{0.9987 Mg} (1.1295) = -1.1307 \text{ k}
 \end{aligned}$$

Modal forces are

$$\begin{aligned}
 F_1 &= \sqrt{F_{11}^2 + F_{12}^2} \\
 &= \sqrt{(1.1266)^2 + (1.1310)^2} = 1.396 \text{ k} \\
 F_2 &= \sqrt{F_{21}^2 + F_{22}^2} \\
 &= \sqrt{(2.4116)^2 + (1.1293)^2} = 2.663 \text{ k} \\
 F_3 &= \sqrt{F_{31}^2 + F_{32}^2} \\
 &= \sqrt{(3.5361)^2 + (-1.1307)^2} = 3.712 \text{ k}
 \end{aligned}$$

Design story shears are

$$\begin{aligned}
 V_3 &= C_m F_3 = 1.160(3.712) = 4.306 \text{ k} \\
 V_2 &= C_m(F_2 + F_3) = 1.160(2.663 \\
 &\quad + 3.712) = 7.395 \text{ k} \\
 V_1 &= C_m(F_1 + F_2 + F_3) = 1.160(1.596 \\
 &\quad + 2.663 + 3.712) = 9.246 \text{ k}
 \end{aligned}$$

4. Displacement and story drift at each floor:
First mode
- $$S_{d1} = \frac{S_{ad}}{\rho_1^2} = \frac{32.2}{12.8^2} = 0.1966 \text{ ft} \quad (\text{q})$$
- From Eq. (b), modal displacement may be written as
- $$x_i = \gamma_i X_i S_{d1} \quad (\text{r})$$
- where $\gamma_1 = 0.4069$; (from Eq. (c)). Displacement and drift are:
- | Level | x_{ii} | δ_{ii} |
|--------------|----------|---------------|
| Roof | 0.2510 | — |
| Third floor | 0.1712 | 0.0798 |
| Second floor | 0.0890 | 0.0912 |
| First floor | — | 0.0800 |
- Second mode—similarly, we obtain
- $$S_{d2} = \frac{S_{ad}}{\rho_2^2} = \frac{32.2}{32.11^2} = 0.0313 \text{ ft} \quad (\text{t})$$
- where $\gamma_2 = 0.3333$; (from Eq. (c))
- Displacement and drift are

4. Displacement and story drift at each floor:
displacement and story drift are calculated using the same as Eqs. (q)–(w) under UBC-94. The displacements and drifts denoted as elastic response parameters in Eq. (w) of Example 10.11.1 are based on the first and second modal base shears. These two shears are combined to produce design base shear as shown in Eq. (f) of this example. Combined base shear, however, is less than the shear required by the lateral-force procedure calculated in Eqs. (g)–(j) above; the reduction factor is consequently derived as R_f in Eq. (k).

Elastic design displacements and drifts (UBC-97, Section 1631.5.4) thus should be modified by using R_f ($R_f < R$) as

$$\begin{Bmatrix} x_{s1} \\ x_{s2} \\ x_{s3} \end{Bmatrix} = \frac{1}{R_f} \begin{Bmatrix} x_1 \\ x_2 \\ x_3 \end{Bmatrix} = \frac{1}{8.12} \begin{Bmatrix} 0.0807 \\ 0.1715 \\ 0.2512 \end{Bmatrix}$$

$$\begin{Bmatrix} 0.00994 \\ 0.02112 \\ 0.03094 \end{Bmatrix} \text{ ft} \quad (\text{l})$$

$$x_{2i} = \gamma_2 X_i S_{d2} \quad (\text{u})$$

where $\gamma_2 = 0.3333$; (from Eq. (c))

Displacement and drift are

$$\begin{Bmatrix} \delta_{s1} \\ \delta_{s2} \\ \delta_{s3} \end{Bmatrix} = \frac{1}{R_f} \begin{Bmatrix} \delta_1 \\ \delta_2 \\ \delta_3 \end{Bmatrix} = \frac{1}{8.12} \begin{Bmatrix} 0.0807 \\ 0.0912 \\ 0.0825 \end{Bmatrix}$$

$$\begin{Bmatrix} 0.00994 \\ 0.01123 \\ 0.01016 \end{Bmatrix} \text{ ft} \quad (\text{m})$$

For the first mode

$$\begin{aligned} \delta_{x1} &= \frac{C_d g T_m^2 F_{x1}}{I_E 4\pi^2 w_x}, \quad \delta_{xem} = -\frac{g}{4\pi^2} T_m^2 F_{xm} \\ &= \frac{5.532.2 (0.4909)^2 F_{x1}}{1.0 4\pi^2 w_x} \\ &= 4.4850 \frac{(0.4909)^2 F_{x1}}{w_x} = 1.081 \frac{F_{x1}}{w_x} \\ \delta_{11} &= 1.08 \frac{F_{11}}{w_1} = 1.081 \frac{1.1266}{0.8431(32.2)} \\ &= 0.0449 \text{ ft} \\ \delta_{21} &= 1.08 \frac{F_{21}}{w_2} = 1.081 \frac{2.4116}{0.8431(32.2)} \\ &= 0.0960 \text{ ft} \\ \delta_{31} &= 1.08 \frac{F_{31}}{w_3} = 1.081 \frac{3.5361}{0.8431(32.2)} \\ &= 0.1336 \text{ ft} \end{aligned}$$

SRSS yields the combined displacement and drift at each floor as

x_{2i}	x_i	δ_{1i}	δ_{2i}	δ_i
510	-0.0104	0.2512	0.0798	-0.0205
712	0.0104	0.1715	0.0912	0
800	0.0104	0.0807	0.080	0.0104

(w)

Maximum inelastic displacements and drifts (UBC-97, Section 1630.9.2) are

$$\begin{aligned} \begin{Bmatrix} x_{n1} \\ x_{n2} \\ x_{n3} \end{Bmatrix} &= 0.7 R \begin{Bmatrix} x_{s1} \\ x_{s2} \\ x_{s3} \end{Bmatrix} \\ &= 0.7(8.5) \begin{Bmatrix} 0.00994 \\ 0.02112 \\ 0.03094 \end{Bmatrix} = \begin{Bmatrix} 0.0591 \\ 0.1257 \\ 0.1841 \end{Bmatrix} \text{ ft} \end{aligned}$$

(n)

Since no scaling is required, design elastic displacement and drift are

$$\begin{aligned} \begin{Bmatrix} x_{s1} \\ x_{s2} \\ x_{s3} \end{Bmatrix} &= \frac{1}{R_w} \begin{Bmatrix} x_1 \\ x_2 \\ x_3 \end{Bmatrix} = \frac{1}{12} \begin{Bmatrix} 0.0807 \\ 0.1715 \\ 0.2512 \end{Bmatrix} \\ &= \begin{Bmatrix} 0.00673 \\ 0.01429 \\ 0.02093 \end{Bmatrix} \text{ ft} \end{aligned}$$

(x)

$$\begin{aligned} \begin{Bmatrix} \delta_{s1} \\ \delta_{s2} \\ \delta_{s3} \end{Bmatrix} &= 0.7 R \begin{Bmatrix} \delta_{s1} \\ \delta_{s2} \\ \delta_{s3} \end{Bmatrix} \\ &= 0.7(8.5) \begin{Bmatrix} 0.00994 \\ 0.01123 \\ 0.01016 \end{Bmatrix} = \begin{Bmatrix} 0.0591 \\ 0.0668 \\ 0.0605 \end{Bmatrix} \text{ ft} \end{aligned}$$

(o)

$$\begin{aligned} \begin{Bmatrix} \delta_{s1} \\ \delta_{s2} \\ \delta_{s3} \end{Bmatrix} &= \frac{1}{R_w} \begin{Bmatrix} \delta_1 \\ \delta_2 \\ \delta_3 \end{Bmatrix} = \frac{1}{12} \begin{Bmatrix} 0.0807 \\ 0.0912 \\ 0.0825 \end{Bmatrix} \\ &= \begin{Bmatrix} 0.00673 \\ 0.00760 \\ 0.00688 \end{Bmatrix} \text{ ft} \end{aligned}$$

(y)

Allowable drift based on UBC-94, Section 1628.8.2 is

$$\Delta_a = \min (0.04h_{sx}/R_w, 0.005 h_{sx})$$

(for $T < 0.7$ sec)

$$= \min (0.04h_{sx}/12, 0.005 h_{sx})$$

$$= \min (0.00333 h_{sx}, 0.005 h_{sx})$$

$$= 0.00333 h_{sx} = 0.00333 \times 1.1337 = 0.0037 \text{ in}$$

and for the second mode

$$\delta_{s2} = 4.4860 \frac{(0.1958)^2 F_{x2}}{w_x} = 0.172 \frac{F_{x1}}{w_x}$$

$$\delta_{12} = 0.172 \frac{1.1310}{0.8431(32.2)}$$

$$= (7.166) 10^{-3} \text{ ft}$$

$$\delta_{22} = 0.172 \frac{1.1293}{0.8431(32.2)}$$

$$= (7.154) 10^{-3} \text{ ft}$$

$$\delta_{33} = 0.172 \frac{(-1.1307)}{0.8431(32.2)}$$

$$= -(7.164) 10^{-3} \text{ ft}$$

Modal deflections are

$$\delta_1 = \sqrt{\delta_{11}^2 + \delta_{12}^2}$$

$$= \sqrt{(44.9)^2 + (7.166)^2} \times 10^{-3}$$

$$\delta_2 = \sqrt{\delta_{21}^2 + \delta_{22}^2}$$

$$= \sqrt{(0.0960)^2 + (7.154 \times 10^{-3})^2}$$

$$= 0.0963 \text{ ft}$$

$$\delta_3 = \sqrt{\delta_{31}^2 + \delta_{32}^2}$$

$$= \sqrt{(0.1336)^2 + (-7.164) \times 10^{-3}}^2$$

$$= 0.1337 \text{ ft}$$

Design floor deflections are

$$\delta_1 = 1.160(0.0454) = 0.0527 \text{ ft} = 0.63 \text{ in}$$

$$\delta_2 = 1.160(0.0963) = 0.117 \text{ ft} = 1.34 \text{ in}$$

$$\delta_3 = 1.160(0.1337) = 0.1551 \text{ ft} = 1.86 \text{ in}$$

Thus $\delta_{max} = 0.0076 < 0.00333$ (14) = 0.0467.
Story drift is OK.

Maximum inelastic displacement and drift are

$$\begin{aligned}\left\{\begin{array}{l}\delta_{n1} \\ \delta_{n2} \\ \delta_{n3}\end{array}\right\} &= \frac{3}{8} R_w \left\{\begin{array}{l}x_{s1} \\ x_{s2} \\ x_{s3}\end{array}\right\} = \frac{3}{8} \left\{\begin{array}{l}x_1 \\ x_2 \\ x_3\end{array}\right\} \\ &= \frac{3}{8} \left\{\begin{array}{l}0.0807 \\ 0.1715 \\ 0.2512\end{array}\right\} = \left\{\begin{array}{l}0.0643 \\ 0.0942 \\ 0.14\end{array}\right\} \text{ ft} \\ &= \left\{\begin{array}{l}\delta_1 \\ \delta_2 \\ \delta_3\end{array}\right\} = \frac{3}{8} \left\{\begin{array}{l}0.0807 \\ 0.0912 \\ 0.0825\end{array}\right\} \\ &= \left\{\begin{array}{l}0.0303 \\ 0.0342 \\ 0.0309\end{array}\right\} \text{ ft} \quad (\text{aa})\end{aligned}$$

which shall be applied for deformation requirements such as UBC-94, Sections 1631.2.4, 1631.2.4.2, 1631.2.11, and 2211.10.4.
Check $P-\Delta$ effect:

In checking $P-\Delta$ effect, $w = 0.8431$ (32.2) = 27.15 k. Calculation for the first, second and third story are

^① x	^② Story no. h_{sx} (ft)	^③ Vertical load P_x (k)	^④ Story shear V_x (k)	^⑤ Story drift Δ_x (ft)	$\theta = \frac{P_x \Delta_x}{V_x h_{sx}}$
3	14	27.15	35.8472	0.0825	0.45%
2	14	54.30	54.3498	0.0912	0.61%
1	14	81.45	69.9863	0.0807	0.67%

Since $\theta < 10\%$, the $P-\Delta$ effect need not be considered.

from which maximum drift is
 $\Delta_m = \max((1.34 - 0.63), (1.86 - 1.34))$
 $= 0.71 \text{ in}$

Allowable drift (IBC Table 1617.3) is

$$\begin{aligned}\Delta_a &= 0.020 h_{sx} = 0.020(14)(12) \\ &= 3.36 \text{ in} > \Delta_m \text{ OK}\end{aligned}$$

Check the $P-\Delta$ effect: $C_d = 5.5$, $w = 0.8431$
 $k \text{ sec}^2/\text{ft} \times 32.2 \text{ ft/sec}^2 = 27.15 \text{ k}$.

^① x	^② Story no. h_{sx} (ft)	^③ Vertical load P_x (k)	^④ Story shear V_x (k)	^⑤ Story drift Δ_x (in)	$\theta = \frac{P_x \Delta_x}{V_x h_{sx} C_d}$
3	14	w = 27.15	4.306	1.86-	0.35%
2	14	2w = 54.30	7.395	1.34- = 0.52	5.92
1	14	3w = 81.45	9.246	0.63- = 0.71	5.25

Since $\theta < 10\%$, the $P-\Delta$ effect need not be considered.

Since $\theta < 10\%$ the $P-\Delta$ effect need not be considered.

FIG. 10.35a Internal forces of a first-floor column.

$$\frac{1}{R_w} \begin{Bmatrix} F_1 \\ F_2 \\ F_3 \end{Bmatrix} = \frac{1}{12} \begin{Bmatrix} 35.847 \\ 25.320 \\ 14.274 \end{Bmatrix} = \begin{Bmatrix} 2.987 \\ 2.110 \\ 1.189 \end{Bmatrix} \text{ k}$$

(bb)

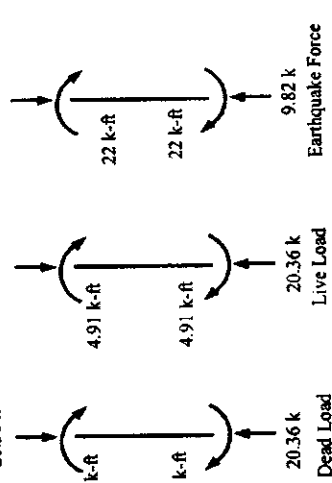


FIG. 10.35b Internal forces of a first-floor column.

FIG. 10.35c Internal forces of a first-floor column.

Load combinations: internal forces of a first-floor column due to dead and live loads as well as earthquake forces are given in Fig. 10.35b. Earthquake forces shown in the figure are obtained using lateral forces in Eq. (p) of Example 10.11.1 with reduction factor R_f in Eq. (k) of this example as

$$\frac{1}{R_f} \begin{Bmatrix} F_3 \\ F_2 \\ F_1 \end{Bmatrix} = \frac{1}{8.12} \begin{Bmatrix} 35.8472 \\ 25.3204 \\ 14.2748 \end{Bmatrix} = \begin{Bmatrix} 4.4147 \\ 3.1183 \\ 1.7580 \end{Bmatrix} \text{ k}$$

(q)

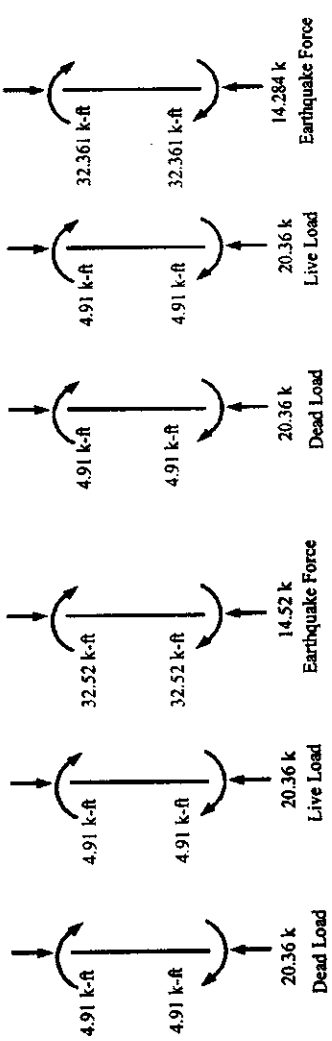


FIG. 10.35c Internal forces of a first-floor column.

Load combinations: internal forces of first-floor column due to dead and live loads as well as earthquake forces, are given in Fig. 10.35c. Earthquake forces shown in the figure are obtained using modal forces in Eq. (r) applied to the structure as

$$C_m \begin{Bmatrix} F_1 \\ F_2 \\ F_3 \end{Bmatrix} = 1.16 \begin{Bmatrix} 1.596 \\ 2.663 \\ 3.712 \end{Bmatrix} = \begin{Bmatrix} 1.851 \\ 3.089 \\ 4.306 \end{Bmatrix} \text{ k}$$

(v)

Load combinations: internal forces of a first-floor column due to dead and live loads as well as earthquake forces are given in Fig. 10.35b. Earthquake forces shown in the figure are obtained using lateral forces in Eq. (p) of Example 10.11.1 with reduction factor R_f in Eq. (k) of this example as

$$C_m \begin{Bmatrix} F_1 \\ F_2 \\ F_3 \end{Bmatrix} = 1.16 \begin{Bmatrix} 1.596 \\ 2.663 \\ 3.712 \end{Bmatrix} = \begin{Bmatrix} 1.851 \\ 3.089 \\ 4.306 \end{Bmatrix} \text{ k}$$

(v)

5.1. Allowable stress design—allowable stress design (Section 1603.6) for this problem requires

$$D + L, \quad D + L + E.$$

Thus

$$\begin{aligned} M &= \max \left\{ \frac{M_D + M_L}{M_D + M_L + M_E} \right\} \\ &= \max \left\{ \frac{4.9112 + 4.9112}{4.9112 + 4.9112 + 22.00} \right\} \\ &= \max \left\{ \frac{9.8224}{31.8224} \right\} = 31.82 \text{ k ft} \end{aligned}$$

(cc)

$$\begin{aligned} N &= \max \left\{ \frac{20.36 + 20.36}{20.36 + 20.36 + 9.82} \right\} \\ &= \max \left\{ \frac{40.72}{50.54} \right\} \text{ k} \end{aligned}$$

(dd)

5.1. Allowable stress design—required load combinations (UBC-97, Section 1612.3 or Table 10.12) for this problem are

$$D, D + L, \quad D + E/1.4, \quad D + 0.75(L + E/1.4), \quad 0.9D \pm E/1.4.$$

Thus load combinations for design moments yield

$$\begin{aligned} M &= \max \left\{ \begin{array}{l} M_D \\ M_D + M_L \\ M_D + M_E \\ M_D + M_L + M_E \end{array} \right\} \\ &= \max \left\{ \begin{array}{l} 4.9112 \\ 4.9112 + 4.9112 \\ 4.9112 + 4.9112 + 22.00 \\ 4.9112 + 4.9112 + 22.00 \end{array} \right\} \\ &= \max \left\{ \begin{array}{l} 9.8224 \\ 9.8224 + 4.9112 \\ 9.8224 + 4.9112 + 22.00 \\ 9.8224 + 4.9112 + 22.00 \end{array} \right\} = 27.64 \end{aligned}$$

(ee)

$$\begin{aligned} M &= \max \left\{ \begin{array}{l} 0.9M_D + \frac{M_E}{1.4} = 0.9(4.9112) + \frac{32.52}{1.4} = 27.64 \\ M_D + 0.75 \left(M_L + \frac{M_E}{1.4} \right) = 4.9112 + 0.75 \left(4.9112 + \frac{32.52}{1.4} \right) = 26.02 \\ 0.9M_D - \frac{M_E}{1.4} = 0.9(4.9112) - \frac{32.52}{1.4} = 18.81 \\ 28.14 \text{ k ft} \end{array} \right\} \\ &= \max \left\{ \begin{array}{l} 4.9112 + 32.361(0.7) + 4.9112 \\ 4.9112(0.6) + 0.7(32.361) \\ 4.9112 \\ 9.8224 \\ 25.5994 \end{array} \right\} \end{aligned}$$

(ff)

$$= 32.4751 \text{ k ft}$$

(ww)

The design axial force is

$$\begin{aligned}
 N &= \max \left\{ \begin{array}{l} N_D + N_L \\ N_D + \frac{N_E}{1.4} \\ N_D + 0.75 \left(N_L + \frac{N_E}{1.4} \right) \\ 0.9N_D + \frac{N_E}{1.4} \\ 0.9N_D - \frac{N_E}{1.4} \end{array} \right\} \\
 &\quad \left. \begin{array}{l} N_D \\ N_D + N_L \\ N_D + 0.7N_E + N_L \\ 0.6N_D + 0.7N_E \\ 20.36 \end{array} \right\} \\
 &= \max \left\{ 20.36 + 20.36 \right. \\
 &\quad \left. \begin{array}{l} 20.36 + 14.284(0.7) + 20.36 \\ 20.36(0.6) + 0.7(14.284) \\ 40.72 \\ 50.719 \\ 22.215 \end{array} \right\} \\
 &= \max \left\{ 20.36 + 0.75 \left(20.36 + \frac{14.54}{1.4} \right) \right. \\
 &\quad \left. \begin{array}{l} 0.9(20.36) + \frac{14.54}{1.4} \\ 0.9(20.36) - \frac{14.54}{1.4} \end{array} \right\} \\
 &= \max \left\{ \begin{array}{l} 40.72 \\ 30.73 \\ 43.42 \\ 28.71 \\ 7.94 \end{array} \right\} = 43.42 \text{ k}
 \end{aligned}$$

The design axis force is

- 5.2. Load and resistance factor design—for the given loading condition, the following load combinations (Section 2249.A4.1) are required:

$$\begin{aligned} & (1) 1.4D \\ & (2) 1.2D + 1.6L \\ & (3) 1.2D + 0.5L \\ & (4) 1.2D + 0.5L + 1.5E \\ & (5) 0.9D - 1.5E \end{aligned}$$

where live load is assumed to be less than 100 psf; thus factor for L is 0.5 for combinations (3) and (4). Design moment and axial force of the first-floor column are

$$M = \max \left\{ \begin{array}{l} 1.4M_D \\ 1.2M_D + 1.6M_L \\ 1.2M_D + 0.5M_L \\ 0.9M_D - 1.5M_E \\ 1.4(4.9112) \\ 1.2(4.9112) + 1.6(4.9112) \\ 1.2(4.9112) + 0.5(4.9112) \\ 1.2(4.9112) + 0.5(4.9112) + 1.0(32.52) \\ 0.9(4.9112) + 1.0(32.52) \\ 0.9(4.9112) - 1.0(32.52) \\ 6.8757 \\ 13.7514 \\ 8.3490 \\ 41.349 \\ -26.2249 \end{array} \right\} = 41.349 \text{ k ft}$$

- 5.2. Load and resistance factor design—required load combinations (UBC-97, Section 1612.2.1) for this problem are

$$\begin{aligned} & 1.4D, 1.2D + 1.6L, 1.2D + f_1L, \\ & 1.2D + f_1L + 1.0E, 0.9D \pm 1.0E \end{aligned}$$

where $f_1 = 0.5$ for live load less than 100 psf.

The design moment is

$$M = \max \left\{ \begin{array}{l} 1.4M_D \\ 1.2M_D + 1.6M_L \\ 1.2M_D + 0.5M_L \\ 0.9M_D + 1.0M_E \\ 0.9M_D - 1.0M_E \\ 1.4(4.9112) \\ 1.2(4.9112) + 1.6(4.9112) \\ 1.2(4.9112) + 0.5(4.9112) \\ 1.2(4.9112) + 0.5(4.9112) + 1.0(32.52) \\ 0.9(4.9112) + 1.0(32.52) \\ 0.9(4.9112) - 1.0(32.52) \\ 6.8757 \\ 13.7514 \\ 8.3490 \\ 40.8690 \\ 38.9101 \\ -30.0699 \end{array} \right\}$$

(ee)

- 5.2. Load and resistance factor design—required load combinations (IBC, Section 1605.2.1) are

$$\begin{aligned} & 1.4D, 1.2D + 1.6L, 1.2D + 0.5L, \\ & 1.2D + 0.5L + 1.0E, 0.9D + 1.0E \end{aligned}$$

The design bending moment is

$$M = \max \left\{ \begin{array}{l} 1.4(4.9112) \\ 1.2(4.9112) + 1.6(4.9112) \\ 1.2(4.9112) + 0.5(4.9112) + 1.0(32.361) \\ 0.9(4.9112) + 1.0(32.361) \\ 6.88 \\ 1.4(4.9112) \\ 1.2(4.9112) + 0.5(4.9112) + 1.0(32.361) \\ 0.9(4.9112) + 1.0(32.361) \\ 13.75 \\ 40.71 \end{array} \right\} = 40.71 \text{ k ft}$$

(y)

$$\begin{aligned}
 N &= \max \left\{ \begin{array}{l} 1.4N_D \\ 1.2N_D + 0.5N_L \\ 1.2N_D + 0.5N_L + 1.5N_E \\ 0.9N_D - 1.5N_E \end{array} \right\} \\
 &= \max \left\{ \begin{array}{l} 1.4(20.36) \\ 1.2(20.36) + 1.6(20.36) \\ 1.2(20.36) + 0.5(20.36) \\ 1.2(20.36) + 0.5(20.36) + 1.5(9.82) \end{array} \right\} \\
 &= \max \left\{ \begin{array}{l} 28.504 \\ 57.008 \\ 34.612 \end{array} \right\} = 57.008 \text{ k} \quad (\text{ff})
 \end{aligned}$$

The design axial force is

$$\begin{aligned}
 N &= \max \left\{ \begin{array}{l} 1.4N_D \\ 1.2N_D + 1.6N_L \\ 1.2N_D + 0.5N_L \\ 1.2N_D + 0.5N_L + 1.0N_E \\ 0.9N_D - 1.0N_E \end{array} \right\} \\
 &= \max \left\{ \begin{array}{l} 1.4(20.36) \\ 1.2(20.36) + 0.5N_E \\ 0.9N_D + 1.0N_E \\ 0.9N_D - 1.0N_E \end{array} \right\} \\
 &= \max \left\{ \begin{array}{l} 34.612 \\ 28.50 \\ 57.01 \end{array} \right\} = 57.01 \text{ k} \quad (\text{z}) \\
 &= \max \left\{ \begin{array}{l} 1.2(20.36) + 1.6(20.36) \\ 1.2(20.36) + 0.5(20.36) \\ 1.2(20.36) + 0.5(20.36) + 1.0(14.52) \end{array} \right\} \\
 &= \max \left\{ \begin{array}{l} 48.90 \\ 32.61 \end{array} \right\} = 48.90 \text{ k} \quad (\text{u})
 \end{aligned}$$

$$\begin{aligned}
 N &= \max \left\{ \begin{array}{l} 1.4(20.36) \\ 1.2(20.36) + 1.6(20.36) \\ 1.2(20.36) + 0.5(20.36) + 1.0(14.284) \end{array} \right\} \\
 &= \max \left\{ \begin{array}{l} 34.612 \\ 28.50 \\ 0.9(20.36) + 1.0(14.284) \end{array} \right\} = 34.612 \text{ k} \quad (\text{z})
 \end{aligned}$$

$$\begin{aligned}
 N &= \max \left\{ \begin{array}{l} 1.4(20.36) \\ 1.2(20.36) + 1.6(20.36) \\ 1.2(20.36) + 0.5(20.36) + 1.0(14.284) \end{array} \right\} \\
 &= \max \left\{ \begin{array}{l} 34.612 \\ 28.50 \\ 0.9(20.36) + 1.0(14.284) \end{array} \right\} = 34.612 \text{ k} \quad (\text{z})
 \end{aligned}$$

10.12. OVERVIEW

This chapter synthesizes the dynamic analysis principles established in Chapters 1, 2, 3 and Part A of Chapter 7 in connection with analysis procedures from building codes UBC-94, UBC-97, and IBC-2000. Similarities and differences among these three codes are discussed. Numerical examples for all three are presented step by step to illustrate static equivalent lateral-force procedure and dynamic analysis procedure.

Major differences among UBC-94, UBC-97, and IBC-2000 are summarized as follows:

- (A) In UBC-94 response modification, R_w , involves factors of ductility reduction, seismic force amplification, and allowable stress. In UBC-97 and IBC-2000, the allowable stress factor is not included in R but is considered in load combinations. Certain recommendations in ATC-3-06 and 1994 NEHRP are included in UBC-97 and IBC-2000, but not much in UBC-94.
- (B) UBC-97 and IBC-2000 adopt new response spectra. Fault location and characteristics of strong ground motion associated with a fault are roughly estimated in tabulated form for UBC-97, but comprehensively considered in regionalization maps in IBC-2000. UBC-94 lacks these features.
- (C) UBC-97 seismic zone maps are the same as UBC-94 with accelerations in five zones. IBC-2000 seismic zone maps contain greater detail than those in UBCs, featuring acceleration and velocity-related acceleration as well as highly defined regions. Regionalized seismic zones are more comprehensive and display more contours between zones.
- (D) In both UBC-97 and IBC-2000 the redundancy factor ρ accounts for multiple loading paths during inelastic response to delay collapse mechanism formation. Consequently, ρ requires a greater level of design force for a structure with less redundancy.
- (E) New soil factors and more comprehensive structural classifications are given in UBC-97 and IBC-2000.
- (F) IBC-2000 considers higher modes with distribution exponent, k , related to a range of building periods; UBC-94 and UBC-97 use a force, F_t , applied to the top of any building with a period greater than 0.7 sec.

It should again be noted that the organization of sections, figures, tables and the like in IBC-2000 differs from both UBCs. Therefore, comparisons and step-by-step numerical procedures are given in parallel layout with the hope that the reader can easily grasp the specific requirements of various sections of these three codes.

BIBLIOGRAPHY

1. ST Algermissen, DM Perkins. A probabilistic estimate of maximum acceleration in rock in the contiguous United States. Open File Report 76-416. US Geological Survey, 1976.
2. American Society of Civil Engineers. Minimum Design Loads for Buildings and Other Structures. New York: ASCE 7-98, 2000.
3. Applied Technology Council. Tentative provisions for the development of seismic regulations for buildings, ATC 3-06. Palo Alto, CA: 1978.
4. Building Officials and Code Administrators International Inc. BOCA. 13th ed. Country Club Hills, IL: BOCA, 1996.
5. Building Seismic Safety Council. NEHRP Recommended Provisions for the Development of Seismic Regulations for New Buildings. Parts 1 and 2. Washington, DC: Building Seismic Safety Council, 1991.
6. CC Chang, JR Ger, FY Cheng. Reliability-based optimum design for UBC and nondeterministic seismic spectra. ASCE J Struct Engng 120(1):139-160, 1994.
7. FY Cheng, CC Chang. Safety-based optimum design of nondeterministic structures subjected to various types of seismic loads. NSF Report. National Technical Information Service, U.S. Department of Commerce, Virginia, NTIS no. PB90-133489/AS, 1988 (326 pp).
8. FY Cheng, DS Juang. Assessment of various code provisions based on optimum design of steel structures. International J Earthq Engng Struct Dyn 16:45-61, 1988.

9. FY Cheng, topical ed. Comparison of building codes on stability under seismic loading in North America, Japan, New Zealand, Australia, China, Eastern Europe and Western Europe. In: Stability of Metal Structures: a World View. Structural Stability Research Council, 1991.
10. FY Cheng, JS Yang. Hysteresis rules and design parameter assessment of RC low-rise shear walls and buildings with openings. NSF Report. National Technical Information Service, U.S. Department of Commerce, Virginia, NTIS no. PB97-121362, 1996 (344 pp).
11. FY Cheng, S Suthiwong. Active control for seismic-resistant structures on embedded foundation in layered half-space. NSF Report. National Technical Information Service, U.S. Department of Commerce, Virginia, NTIS no. PB97-121354, 1996 (261 pp).
12. FY Cheng, D Li. Multiobjective optimization of structures with and without control. AIAA J Guid, Control and Dyn 19(2):392–397, 1996.
13. FY Cheng, D Li. Multiobjective optimization design with pareto genetic Algorithm. ASCE J Struct Engng 123(9):1252–1261, 1997.
14. FY Cheng, AH-S, Ang. Cost-effectiveness optimization for aseismic design criteria of RC buildings. DM Frangopol, ed. Proceedings of Case Studies in Optimal Design and Maintenance Planning of Civil Infrastructure Systems. ASCE, 1998, pp 13–25.
15. FY Cheng, HP Jiang. Optimal control of a hybrid system for seismic excitations with state observer technique. J Smart Mater Struct 7(5):654–663, 1998.
16. FY Cheng, HP Jiang. Hybrid control of seismic structures with optimal placement of control devices, ASCE J Aerospace Engng 11(2):52–58, 1998.
17. International Code Council. 2000 International Building Code, IBC-2000. Birmingham, AL: International Code Council; first draft, 1997; final draft, 1998.
18. International Conference of Building Officials. Uniform Building Code, UBC-94. Whittier, CA, 1994.
19. International Conference of Building Officials. Uniform Building Code, UBC-97. Whittier, CA, 1997.
20. RK McGuire. Seismic structural response risk analysis incorporating peak response progressions on earthquake magnitude and distance, Report R74-51. Cambridge, MA: Department of Civil Engineering, Massachusetts Institute of Technology, 1975.
21. RK McGuire. Methodology for incorporating parameter uncertainties into seismic hazard analysis for low-risk design intensities. FY Cheng, ed. International Symposium on Earthquake Structural Engineering, Vol II, 1976, pp 1007-1021.
22. NM Newmark, WJ Hall. Earthquake Spectra and Design. Oakland, CA: Earthquake Engineering Research Institute, 1982.
23. OW Nuttli. On the specification of a design earthquake. FY Cheng, ed. International Symposium on Earthquake Structural Engineering, Vol I, 1976, pp 1–19.
24. R Ridell, P Hidalgo, E Cruz. Response modification factors for earthquake-resistant design of short-period buildings. Earthq Spectra 5(3):571–590, 1989.
25. Southern Building Code Congress International. Standard Building Code-SBC, 1994. Birmingham, AL, 1994.
26. Structural Engineering Association of California. Recommended Lateral Force Requirements. Sacramento, CA, 1990.
27. Structural Engineering Association of California. Recommended Lateral Force Requirements. Sacramento, CA, 1996.
28. CM Uang. Establishing R (or R_w) and C_d factors for building seismic provisions. ASCE J Struct Engng 117(1):19–28, 1991.
29. A Williams. Seismic design of buildings and bridges. Austin, TX: Engineering Press, 1995.
30. Structural Engineering Association of California, Recommended Lateral Force Requirements. Sacramento, CA, 1999.

Chapter 1 Problems

FREE UNDAMPED VIBRATION

- 1.1. Find the natural frequency of the mass system shown in Fig. P.1.1.

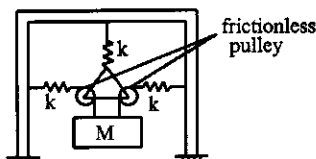


FIG. P.1.1

- 1.2. Find the period of free flexural vibrations for the pair of intersecting beams of a plane grid shown in the Fig. P.1.2. The beams are rigidly attached at their points of junction. Supporting conditions are as shown. For each beam, let $I=1000 \text{ in}^4$, $E=30,000 \text{ ksi}$, and one-half of the total mass of the structure (a weight of 50 lb/ft for each beam) be lumped at the point of junction.

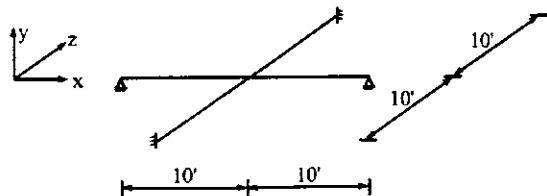


FIG. P.1.2

- 1.3. Find the natural frequency and period of the following beam (see Fig. P.1.3). Let $E = 29,000$ ksi, $I = 1728 \text{ in}^4$, and $W = 12 \text{ k}$.

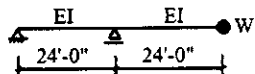


FIG. P.1.3

- 1.4. Derive the differential equation of motion of the system (see Fig. P.1.4) and find the natural frequency. Assume that the deflection is small and that $\sin \theta$ may be approximated as θ .

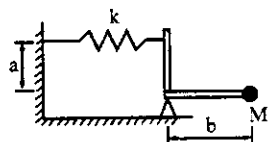


FIG. P.1.4

- 1.5. For the spring-mass system of $K = 100 \text{ lb/in}$ and $W = 200 \text{ lb}$ given in Fig. P.1.5: (a) find the motion equations of displacement x and velocity \dot{x} with the initial conditions of $x_0 = 1 \text{ in}$ and $\dot{x}_0 = 0$ at $t = 0$; (b) find the velocity and its corresponding time when the mass approaches the neutral position or equilibrium position; (c) use x , \dot{x} , and t from (b) as initial conditions and then find the motion equations of displacement and velocity.

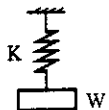


FIG. P.1.5

- 1.6. Rework Example 1.2.1 by changing the moment of inertia for the girder, I_g , to $I_g = I, 4I, 8I$, and ∞ . Find the angular frequency, natural frequency, period and then solve for the response of displacement and velocity based on the initial conditions given in the example.
 1.7. Find the angular frequency, natural frequency, and natural period of the frame in Fig. P.1.7. Vary the moment of inertia of the girder by $I_g = I, 4I, 8I$, and ∞ . Observe the differences between the solutions obtained in Problem 1.6 due to the change of the hinged support. Let $w = 25.0 \text{ lb/ft}$, $I = 166.67 \text{ in}^4$, and $E = 30,000$ ksi.

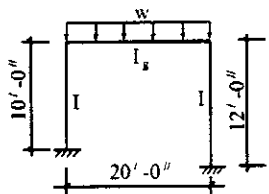


FIG. P.1.7

- 1.8. Derive Eqs. (b) and (c) in Example 1.5.1.

- 1.9. The simply supported beam in Fig. P.1.9 is subjected to initial conditions of $\dot{x}_0 = 0$, and $x_0 = 1\frac{1}{2}$ in at $t = 0$ applied at the center of the span. Find the bending stress at the center. For the given beam $I = 1340 \text{ in}^4$, $E = 30,000 \text{ ksi}$, $S = 114 \text{ in}^3$, and $W = 2.055 \text{ k/ft}$. Assume half the total weight is lumped at the beam center; the other half, lumped at the supports, should not be considered in the analysis.

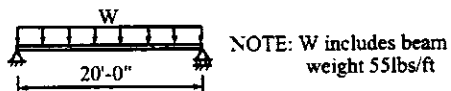


FIG. P.1.9

- 1.10. Find the angular frequency, natural frequency, and natural period of longitudinal and torsional (rocking) motions of the frame shown in Problem 1.7. Let $I_g = \infty$, $E = 30,000 \text{ ksi}$, $w = 25.0 \text{ lb/ft}$, and the cross-sectional area, A , and moment of inertia, I , of the columns be 6 in^2 and 166.67 in^4 , respectively. (a) Assume that both columns have the same height of 12 ft. (b) Column lengths are not the same; they are given in Problem 1.7.

FREE DAMPED VIBRATION

- 1.11. The cantilever in Fig. P.1.11 is subjected to initial conditions of $x_0 = 0$, and $\dot{x}_0 = 8 \text{ ft/sec}$. Find the response of x and \dot{x} at $t = 0.5$ and 1 sec for (a) no damping and (b) 10% of critical damping; $EI = 864 \times 10^5 \text{ k in}^2$ and $W = 4 \text{ k}$.

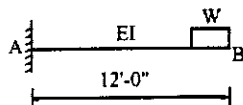


FIG. P.1.11

- 1.12. The amplitude of a single mass system decreases 12% in 40 cycles. Calculate the logarithmic decrement and the damping factor.
 1.13. A control tab on an airplane elevator is pivoted about an axis in the elevator and activated by a linkage system of which the torsional stiffness is K ; the torsional coefficient of viscous damping is C , as shown in part (a) of Fig. P.1.13. Since it is not possible to calculate K and C of the linkage system, two tests are conducted. The first one is shown in part (b) of the figure in which a spring of stiffness k is attached at a distance 'a' from the hinge. (a) Derive the equation of motion for the modified system. (b) If the amplitude of free vibration for the modified system is reduced to 1/10 after 10 cycles, find the logarithmic decrement. (c) Find the viscous damping factor.

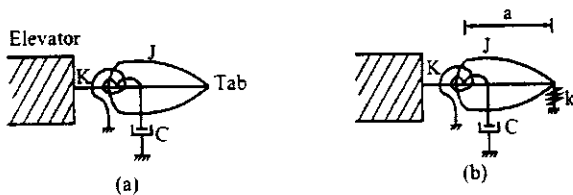


FIG. P.1.13

- 1.14. Establish the motion equation for the system shown in Fig. P.1.14 and then find the equation of p and ρ . (Hint: let $x = x_1 - x_2$.)

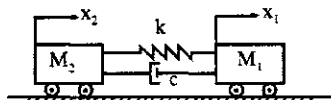


FIG. P.1.14

- 1.15. Find the expression of motion for the following system (see Fig. P.1.15). Let $M = 2 \text{ lb sec}^2/\text{in}$, $K = 2000 \text{ lb/in}$, $K_1 = 2000 \text{ lb/in}$, and $c = 20 \text{ lb sec/in}$.

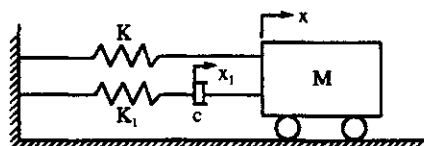


FIG. P.1.15

FORCED UNDAMPED VIBRATION

- 1.16. For a single spring-mass system subjected to the forcing function shown in Fig. P.1.16, find the amplification factor corresponding to three sets of natural frequency: 15, 30, and 40 cycles/sec.

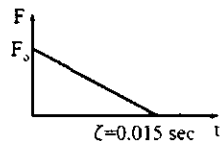


FIG. P.1.16

- 1.17. For a spring-mass model of mass, M , and stiffness, K , subjected to a force of $F \sin \omega t$, find the steady-state response (without considering initial conditions).
 1.18. A rectangular frame, shown in Fig. P.1.18, with period equal to 0.7 sec is subjected to ground acceleration of $\ddot{x}_g = 10 \sin \pi t \text{ in/sec}^2$. Find (a) the equation of the relative displacement of the girder, and (b) the maximum absolute acceleration of the girder if the acceleration lasts for 1 sec. (Hint: $M\ddot{x} + K(x - x_g) = 0$; let the relative displacement be $z = x - x_g$, $z_0 = \dot{z}_0 = 0$ at $t = 0$, and $M = 1 \text{ in sec}^2/\text{in}$.)

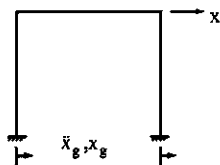


FIG. P.1.18

- 1.19. For the single mass-spring system subjected to a foundation acceleration shown in Fig. P.1.19, find the maximum absolute acceleration of the mass.

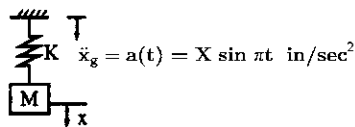


FIG. P.1.19

- 1.20. Find the dynamic load factor (amplifier factor) A_m of the forcing functions given in Fig. P.1.20.

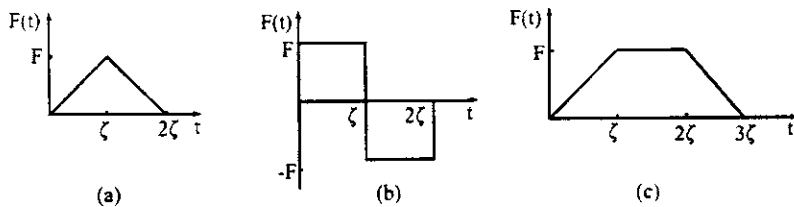


FIG. P.1.20

- 1.21. As a piece of heavy machinery is being readied for positioning on its supporting beam ($I = 248.6 \text{ in}^4$, $S = 49.1 \text{ in}^3$), it is suddenly dropped by the crane on the beam. Let the force of the machine on the beam be its weight of 12 k. Because the distance dropped is small, no increase in force due to acceleration from gravity should be considered. What is the maximum stress it causes? Neglect the beam mass. See Fig. P.1.21.

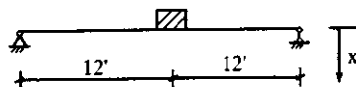


FIG. P.1.21

- 1.22. It is desired to design a spring bumper able to stop a 60,000 lb freight car moving at 4 ft/sec with a maximum negative acceleration not more than twice the acceleration of gravity (see Fig. P.1.22). Calculate: (a) the required spring constant; (b) the required travel distance of the spring; and (c) the maximum force applied through the spring to the block.



FIG. P.1.22

- 1.23. Find the displacement responses at $t = \zeta$, 2ζ and 3ζ for a single-d.o.f system having a mass, M , and a spring constant, K . The applied force is shown in Fig. P.1.23.

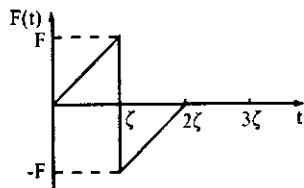


FIG. P.1.23

FORCED DAMPED VIBRATION

- 1.24. Solve Example 1.4.1 with consideration of damping as $\rho=0.1$ and 0.05 . (Hint: use $X=x_{st}/[(1-(\omega/p)^2 + (2\rho\omega/p)^2)^{1/2}]$.)
- 1.25. For Example 1.4.1, let $\omega=120$ rad/sec and $\rho=0.1$. Find the amplitude of the dynamic displacement and then the bending stress due to the static and dynamic displacement.
- 1.26. Find the motion equation and the steady-state motion of the system (see Fig. P.1.26).

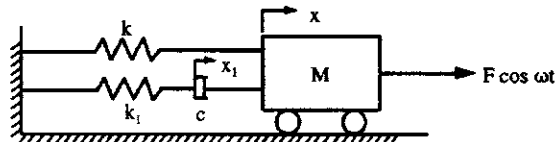


FIG. P.1.26

- 1.27. The base of a vibration-measuring instrument is shown to receive a harmonic motion, $x_1=X_1 \cos \omega t$. Find the displacement, x , for the mass, M . (See Fig. P.1.27).

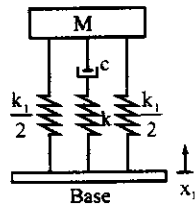


FIG. P.1.27

- 1.28. A 3860 lb machine rests on a spring and dashpot mounting which gives $k=12,250$ lb/in and $\rho=0.1$. A piston weighing 77.2 lb moves up and down with a speed of 467 cpm and a stroke of 10 in. The motion may be considered harmonic. Find (a) the amplitude of force transmitted to the foundation, and (b) the phase angle of the transmitted force. (See Fig. P.1.28).

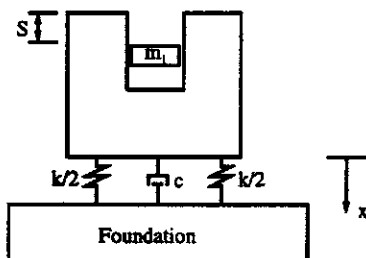


FIG. P.1.28

- 1.29. From a vibration test, the amplification factor is 1.5. Find the damping ratio based on the resonance method.
- 1.30. From a vibration test, the peak amplitude is 0.2 in and the frequencies corresponding to $0.2/\sqrt{2}$ are $p_1 = 100$ rad/sec and $p_2 = 121$ rad/sec. Find the damping ratio based on the band-width method.
- 1.31. The mass M of a system is subjected to a force as shown in Fig. P.1.31, starting from rest at $t = 0$. Find the motion.

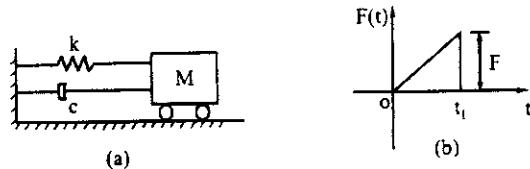


FIG. P.1.31

PRINCIPLES OF DYNAMIC ANALYSIS

- 1.32. Calculate the frequency of the small vibration of the pendulum (see Fig. P.1.32).

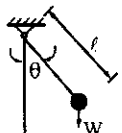


FIG. P.1.32

- 1.33. Calculate the frequency of the small vibration of the pendulum (see Fig. P.1.33).

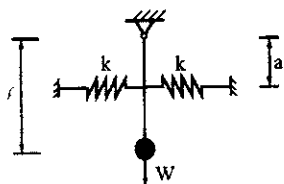


FIG. P.1.33

- 1.34. Calculate the frequency of the small vibration of the system shown in Fig. P.1.34.

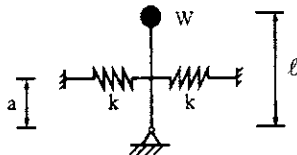


FIG. P.1.34

- 1.35. Considering small swings about the vertical static-equilibrium position, write the differential equation of motion for the system in Fig. P.1.35. If $M_2\ell_2 = 2M_1\ell_1$, what value of k_1 and k_2 will make the natural frequency zero?

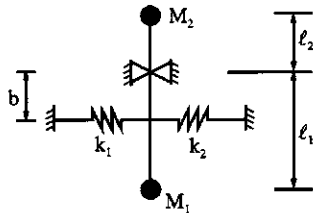


FIG. P.1.35

- 1.36. Add the two motion equations of $x_1 = 35 \cos(pt + 45^\circ)$ and $x_2 = 40 \sin(pt + 30^\circ)$ and then express the resultant motion in two solution forms of (a) sine function and (b) cosine function.

Chapter 2 Problems

SECTIONS 2.1 AND 2.2

- 2.1. Model the structures in Fig. P.2.1 a spring-mass system. Assume that the girders are infinitively rigid for cases (a) and (b), but flexible for case (c). For simplicity, let k represent a spring stiffness for each d.o.f. of these three cases. Write out the governing differential equations (motion equations) of the spring-mass models.

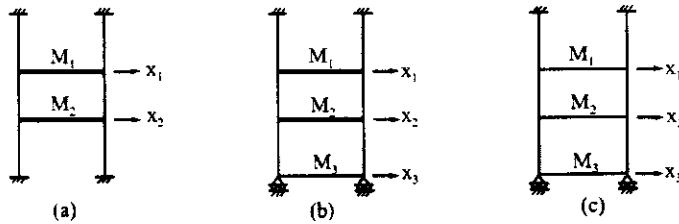


FIG. P.2.1

- 2.2. Set the mass matrix $[M]$ and the stiffness matrix $[K]$ for the equation $[M]\{\ddot{x}\} + [K]\{x\} = 0$ of the system shown in Fig. P.2.2.

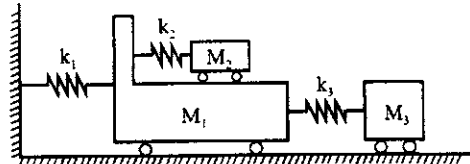


FIG. P.2.2

- 2.3. Establish $[M]$, $[K]$, and $\{F\}_t$ for the flexural vibration of the structure in Fig. P.2.3 in which k_a represents a spring constant of axial deformation.

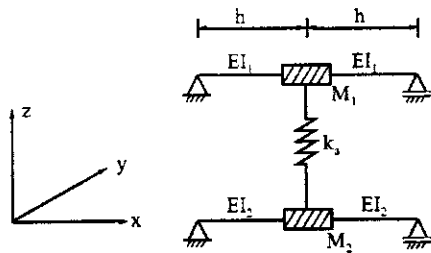


FIG. P.2.3

- 2.4. A symmetrically built machine of mass M and inertia J about a lateral gravity axis is mounted as shown in Fig. P.2.4. Considering only small vibrations in the plane of symmetry, find the differential equation of motion.

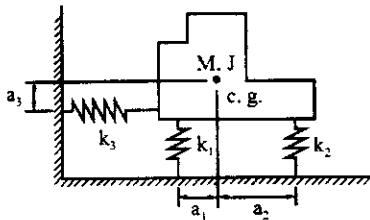


FIG. P.2.4

- 2.5. Establish a motion equation, $[M]\{\ddot{x}\} + [K]\{x\} = 0$, for the unsymmetric structure in Fig. P.2.5, in which M and I represent transverse and rotational masses, respectively, k_1 and k_2 the flexural spring constants, k_3 and k_4 the longitudinal spring constants, and c.g. the center of gravity of the mass.

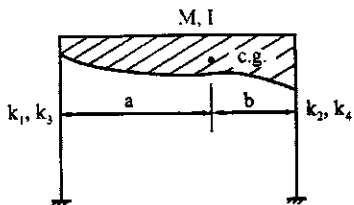


FIG. P.2.5

- 2.6. Find the motion equation for the displacement response of Example 2.2.1 with initial conditions of $x_1 = 0$, $\dot{x}_1 = 1$ ft/sec, $x_2 = 0$, and $\dot{x}_2 = 0$ at $t = 0$.

- 2.7. Set the dynamic matrix equation of the structure shown in Fig. P.2.7. Let $L_1 = 16$ ft, $L_2 = 12$ ft, $I = 144 \text{ in}^4$, $E = 30,000$ ksi, $W_1 = 2.4$ k, $W_2 = 3$ k and $I_g = \infty$. Find natural frequencies, natural periods, natural modes, and normal modes.

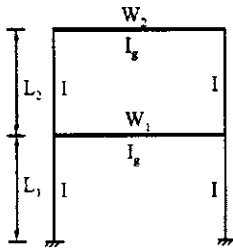


FIG. P.2.7

- 2.8. Using the structure given in Problem 2.7, find the motion equations of displacement for the following cases: (1) the initial conditions are $x_1 = 0$, $x_2 = 0.6$ in, $\dot{x}_1 = \dot{x}_2 = 0$; (2) the initial displacements are the same as the first mode, i.e. $x_1 = 1$ in and $x_2 = 1.2071$ in, and the initial velocities are zero; and (3) the initial conditions are $x_1 = 0$, $x_2 = 0$, $\dot{x}_1 = 0$, and $\dot{x}_2 = 12$ in/sec.
- 2.9. Find the displacements of Problem 2.8 at $t = 1, 2, 3$, and 4 sec.

SECTIONS 2.3–2.5

- 2.10. For a structure whose first modal matrix $\{\phi\}_1^T = [0.302 \quad 0.649 \quad 1]$ and whose second modal matrix $\{\phi\}_2^T = [0.80 \quad 0.90 \quad -1.0]$, prove whether or not the solutions of the normal modes are correct and which mode is correct. Assume the diagonal mass matrix has elements $m_{11} = 2$, $m_{22} = 1.50$, and $m_{33} = 1$.
- 2.11. Assume that a two-d.o.f. vibrating system has a diagonal mass matrix of $m_{11} = m_{22} = 2$ k sec²/in, and that the first natural frequency is $p_1 = 1.854$ rad/sec and the first normal mode $\{X\}^T = [0.618 \quad 1.000]$. Find the second frequency and its normal mode. Let one of the stiffness coefficients k_{22} be 18 k/in; the other coefficients are not given.
- 2.12. Rework Problem 2.8 using modal matrix formulation.
- 2.13. Rework Problem 2.9 using modal matrix formulation.
- 2.14. Find the displacements and accelerations at $t = 0.1, 0.2, 0.3$, and 0.4 sec of a two-d.o.f. vibrating system, and then make statics checks. Let the coefficients of the diagonal mass matrix be $m_{11} = m_{22} = 4.9692$ k sec²/ft, the stiffness coefficients be $k_{11} = 195.319$ k/ft, $k_{12} = k_{21} = -210.193$ k/ft, and $k_{22} = 296.937$ k/ft, and the applied forces be $F_1(t) = 20 [1-(t/0.4)]$ k and $F_2(t) = 30 [1-(t/0.4)]$ k. Show the influence of the two modes on the displacement response.
- 2.15. For the structural properties and the forcing function given in Problem 2.14, find the displacements based on (a) superposition and (b) root-mean-square technique. Use the response spectra given in Fig. 1.17.
- 2.16. Assume that the structure given in Problem 2.14 is subjected to earthquake ground motion. Find the displacement response by employing (a) superposition and (b) root-mean-square technique. Use the response spectra given in Fig. 1.30.
- 2.17. Find the displacements of the super-structure and the reaction of the foundation at $t = \pi/4$ sec of the structure subjected to a foundation movement of $x_f = 0.1 \sin 2t$ ft. Let $M = 60$ k sec²/ft, $EI = 50,000$ k/ft², $M_f = 80$ k sec²/ft, and $k_f = 1200$ k/ft. (See Fig. P.2.17).

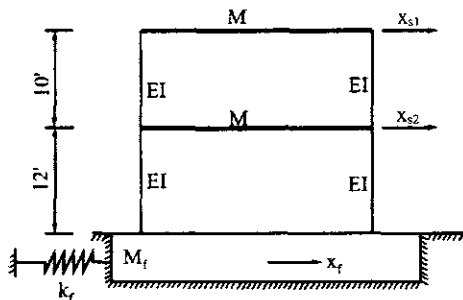


Fig. P.2.17

- 2.18. Let the structural properties of Fig. P.2.1a be given as moment of inertia of all columns $I = 1728 \text{ in}^4$, mass of the girders $M = 15 \text{ k sec}^2/\text{in}$, column length $L = 12 \text{ ft}$, and modulus of elasticity $E = 29,000 \text{ ksi}$. Find the natural frequencies and normal modes using the iteration method.
- 2.19. Rework Problem 2.18 using Choleski's decomposition method.
- 2.20. Rework Problem 2.18 using the generalized Jacobi method.
- 2.21. Rework Problem 2.18 using the Sturm sequences method.
- 2.22. Prove that applying the iteration method to $[K] \{X\} = p^2[M] \{X\}$ yields the highest mode first.
- 2.23. Find the natural frequency, period, and mode shape of Fig. P.2.23. Let $E = 29,000 \text{ ksi}$, $I = 1728 \text{ in}^4$, and $W = 12 \text{ k}$.

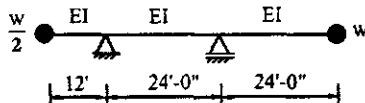


FIG. P.2.23

SECTIONS 2.7 AND 2.8

- 2.24. For the structure shown in Fig. 2.15, the mass and stiffness matrices are given in Eq. (2.172). Let $M_1 = M_2 = 60 \text{ k sec}^2/\text{ft}$, $\rho_1 = \rho_2 = 40 \text{ k sec}^2\text{-ft}$, $k_1 = k_2 = 1200 \text{ k/ft}$, $k_\theta = 800 \text{ k ft}$, and $\ell = 10 \text{ ft}$. Find the eigensolutions.
- 2.25. Find the motion equations which are then expressed in dynamic matrix form for Fig. P.2.25.

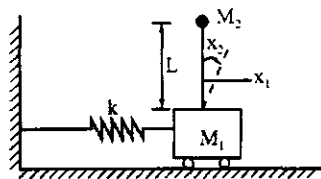


FIG. P.2.25

- 2.26. For the structure shown in Fig. 2.18a, let $M_1 = M_2 = M_3 = 12.318 \text{ kN sec}^2/\text{m}$, $k_1 = 9.329 \text{ MN/m}$, $k_2 = 6.340 \text{ MN/m}$. Find the natural frequencies and normal modes.

- 2.27. Find the displacements and accelerations at $t = 1/4$ s of Problem 2.26. Let initial conditions be $\{x_0\}^T = [1 \ 0 \ 1]$ m, and $\{\dot{x}_0\}^T = [1.5 \ 1.0 \ 1.0]$ m/s. Make statics checks.
- 2.28. Find the displacements and acceleration at $t = 1/4$ s of Problem 2.26. Let the applied force be $P_3(t) = 20 t/0.4$ kN, $P_1(t) = P_2(t) = 0$, and $\{x_0\} = \{\dot{x}_0\} = \{0\}$.
- 2.29. (a) The structure shown in Fig. P.2.29 is supported by a mat foundation and subjected to a horizontal ground acceleration \ddot{x}_g . The system can be modeled as shown in the accompanying figure (a) in which k_1 and k_2 represent flexural stiffnesses, k_θ torsional stiffness, and x_2 and x_3 assigned d.o.f. Establish $[M]\{\ddot{x}\} + [K]\{x\} = \{F\}_1$. (b) Let the structure have sidesway at M_2 and a rotational motion at the bottom for which the model is shown in part (b) of the figure. Establish $[M]\{\ddot{x}\} + [K]\{x\} = \{F\}_1$ (see details in Section 2.7.1).

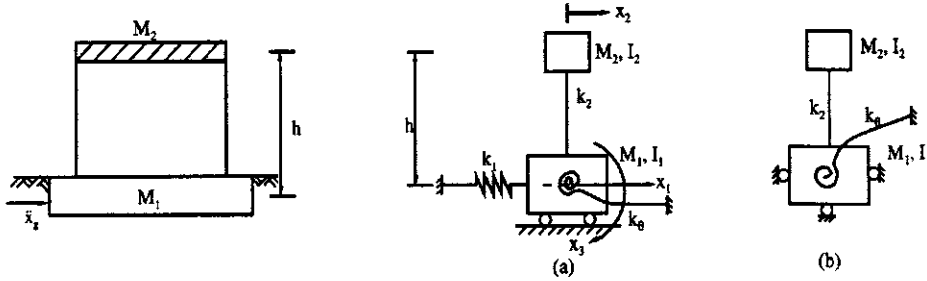


FIG. P.2.29

- 2.30. For Example 2.6.2, let $p_0 = 37$ rad/sec be extracted; find frequency p_v and $p = p_0 + p_v$. Show that the normal mode $\{X_v\}$ corresponding to p_v is the same as the normal mode $\{X\}$ associated with the eigenvalue p_v .
- 2.31. Use the Jacobi method to find the zero and repeating eigensolutions of Fig. 2.18e. Let $k_1 = k_2 = k_3 = 10$, $M_1 = M_2 = M_3 = 2$, and the convergence tolerance criterion s be 4.
- 2.32. Use the Choleski's technique to decompose $\tilde{K} = [L][S]$ and then apply the Strum sequence method to find the eigensolution of Example 2.6.4.

Chapter 3 Problems

SECTIONS 3.2

- 3.1. Derive Eqs. (3.13a) and (3.13b) by using normal modes.
- 3.2. Find the free vibration response of Eqs. (3.14) and (3.15) with initial displacement x_0 and initial velocity \dot{x}_0 .
- 3.3. Find the horizontal, vertical, and rotational motion equations at the center of gravity of the machine given in Fig. P.3.3. Let $k_1 = 100 \text{ lbs/in}$, $k_2 = 80 \text{ lbs/in}$, $k_3 = 20 \text{ lb/in}$, $c_1 = 10 \text{ lb sec/in}$, $c_2 = 2 \text{ lb sec/in}$, $M = 4 \text{ lbs sec}^2/\text{in}$, $J = 5,000 \text{ lb in sec}^2$, $d_1 = 40 \text{ in}$, $d_2 = 60 \text{ in}$, $d_3 = 20 \text{ in}$, and $d_4 = 10 \text{ in}$.

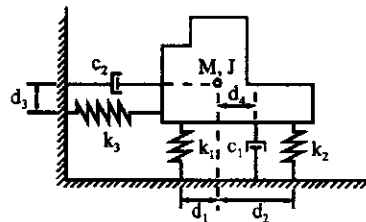


FIG. P.3.3

SECTIONS 3.3 AND 3.4

- 3.4. For a two-d.o.f. structure, the frequencies are $p_1 = 0.61803$, and $p_2 = 1.61802$. Let $\alpha = 0.05$ and $\beta = 0.05$; find the damping factors ρ_1 and ρ_2 .

- 3.5. For a two-d.o.f. system, let $\rho_1 = \rho_2 = 0.1118$, $M_1 = M_2 = 1.38197$, $p_1 = 0.61803$, and $p_2 = 1.61802$. Find the damping coefficients $[C]$ by using the method of all modes required.
- 3.6. Rework Example 3.4.1 for detailed calculations.
- 3.7. Rework Example 3.4.2 for detailed calculations.
- 3.8. For the structure given in Example 3.4.1, the damping factors are $\rho_{11} = \rho_{21} = \rho_{31} = 0.0107$, $\rho_{12} = \rho_{22} = \rho_{32} = 0.1$, and $\rho_{13} = \rho_{23} = \rho_{33} = 0.5001$. Find the damping matrix $[C]$ and its orthogonality matrix $[\bar{C}]$.
- 3.9. For the structure given in Example 3.4.1, let $C_1 = 0.05 C_{cr}$, $C_2 = 0.1 C_{cr}$, and $C_3 = 0.12 C_{cr}$. Find the damping matrix $[C]$.

SECTION 3.5

- 3.10. Normalize $x_1 = 2 + 2i$ and $x_2 = 3 - 2i$.
- 3.11. For a two-d.o.f. vibrating system, let $k_1 = k_2 = k = 3$ and $M_1 = M_2 = M = 6$. Using the state-vector formulation and determinant approach, find the eigenvalues and eigenvectors.
- 3.12. For Problem 3.11, let $k_1 = k_2 = k = 1$, $M_1 = M_2 = M = 1$, and damping coefficients $C_{11} = 0.4$, $C_{12} = C_{21} = 0.1$, and $C_{22} = 0.3$. Using the state-vector formulation and the determinant approach, find the eigenvalues and eigenvectors.

SECTION 3.6

- 3.13. Derive Eqs. (3.75) and (3.76) in detail.
- 3.14. Derive Eq. (3.82) in detail.
- 3.15. Rework Problem 3.11 using the state-vector formulation and the iteration method.

SECTION 3.7

- 3.16. Find the solution to the following integrals:

$$I = \int_0^t e^{-\alpha(t-\Delta)} \sin[p(t-\Delta) + c](a - b\Delta) d\Delta$$

- 3.17. Find the displacement response of $x_1(t)$ and $x_2(t)$ of Example 3.7.1 for the damping coefficients of $C_{11} = 0.3$, $C_{12} = C_{21} = -0.1$, and $C_{22} = 0.2$. Let the displacements be expressed in terms of first mode, second mode, and both modes at a time interval of $\Delta t = 0.02$ for $t \leq 0.2$ sec.

Chapter 4 Problems

SECTION 4.2

- 4.1. (a) Find the first and the second frequencies, p_1 and p_2 , of a cantilever beam with member properties L , EI , and m ; then determine the ratio of p_2/p_1 . (b) Find the equivalent mass at the end of the beam for the same giving fundamental frequency.
- 4.2. Derive the dynamic stiffness coefficients of a prismatic member with (A) both ends hinged and (B) i -end hinged and j -end restrained.
- 4.3. Carry out the L'Hospital operations between Eqs. (b) and (c) of Example 4.4.1.
- 4.4. Carry out the numerical procedures in Eq. (i) of Example 4.4.2.

SECTIONS 4.5–4.8

- 4.5. Use the dynamic stiffness method to find the first three frequencies of a simply supported beam of which $E = 29,000$ ksi, $I = 1340$ in 4 , $w = 55$ lb/ft, and $L = 24$ ft.
- 4.6. Formulate the structural system matrix for the frame shown in Fig. P.4.6a using the diagrams of external action and internal resistance given in the accompanying figure. Plot the determinant function and find the first three natural frequencies. Assume: $EI_1 = EI_2 = EI_3 = EI_5 = EI_6 = 82,640$ kN m 2 (200,000 k ft 2), $EI_4 = 66,112$ kN m 2 (160,000 k ft 2), $L_1 = L_2 = L_5 = L_6 = 3.048$ m (10 ft), $L_3 = L_4 = 2.438$ m (8 ft), $w_1 = w_3 = 9.584$ kg/m (6.44 lb/ft), $w_2 = w_5 = w_6 = 5.750$ kg/m, (3.864 lb/ft), and $w_4 = 7.667$ kg/m (5.152 lb/ft).

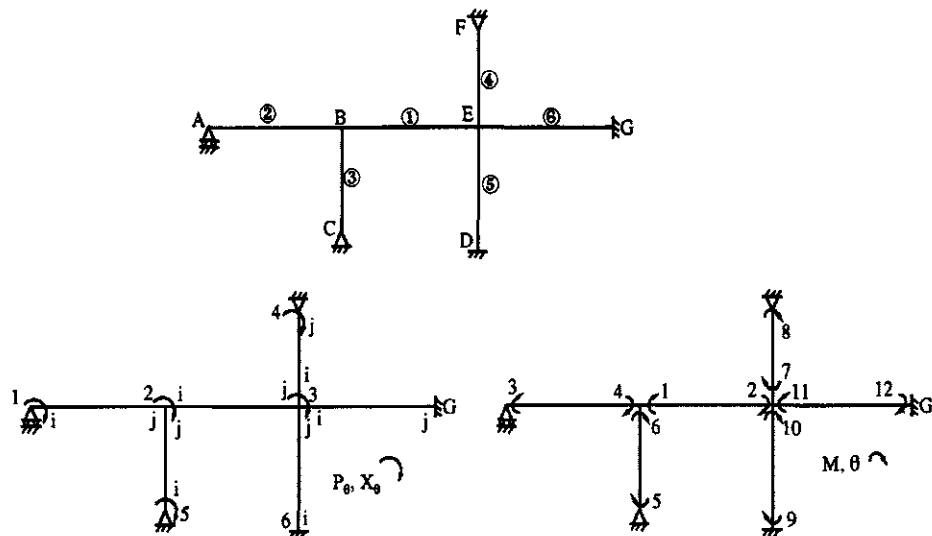


FIG. P.4.6 (a) Given structure. (b) External action. (c) Internal resistance.

- 4.7. For Example 4.7.1, find the eigenvalue and eigenvector of the second mode.
- 4.8. Use the eigenvector obtained in Example 4.7.1 as boundary conditions of members 1, 2, and 3. Divide each member into ten equal segments and plot mode shapes.
- 4.9. Find the moments and shears of the beam (see Fig. P.4.9) using (A) the conventional method based on differential equation, and (B) the dynamic stiffness matrix method. Uniform load is $w \cos \omega t$ and member properties are EI , m , and L .

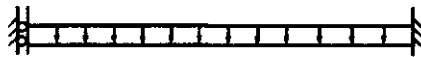


FIG. P.4.9

- 4.10. For Example 4.8.1 with loading condition number 1, find the steady-state response at $\phi_1 = 2.8$.
- 4.11. Find the deformations of members AB and BC , shown in Fig. P.4.11, due to steady-state vibration at the forcing frequency corresponding to $\phi_1 = \pi$; ϕ_1 is the stiffness parameter of member AB .

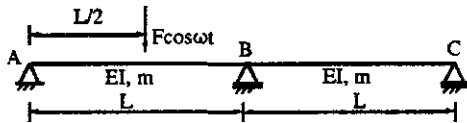


FIG. P.4.11

- 4.12. Find the internal deformations, moments, and shears of the steady-state vibration of the frame shown in Fig. P.4.12. Let $EI_1 = EI_2 = EI_3 = 1000$ ksi, $m_1 = m_2 = m_3 = 5.555 \times 10^{-6}$ k sec²/in², and $F(t) = 25 \sin \pi t$ lb.

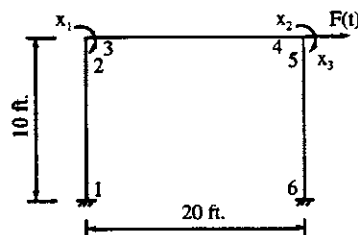


FIG. P.4.12

SECTION 4.9

- 4.13. Using the Lagrangian function $L = T - V$, derive the differential equation of motion of the pendulum shown in Fig. A-4. [see Ref. 7 of this chapter for Legrangian function.]
- 4.14. Prove that the orthogonality condition shown in Eqs. (4.131) and (4.132) is also true for the general case of elastic support.
- 4.15. For the beam in Fig. P.4.15, use the first three modes to (A) find the equations for moment and shear, (B) find the shears at the member ends at $t = 0.05$ sec., and (C) make an equilibrium check of $\sum F_y = 0$. Let $F(t) = Ff(t)$, $F = 3$ k, $f(t) = 1 - t/\zeta$, $\zeta = 0.1$ sec. $EI = 6.1 \times 10^6$ k in 2 , and $m = 0.2$ lb sec 2 /in 2 .

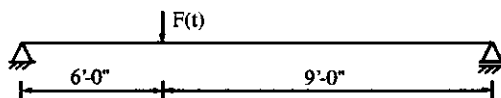


FIG. P.4.15

- 4.16. Find the displacement equation, $y(x,t)$, which may be used to determine the moments and shears in Fig. P.4.16. Let the forcing function be $f(t)$ and member properties be EI , m , and L . (Note: use the Fourier Series method in Ref. 7 of this chapter.)

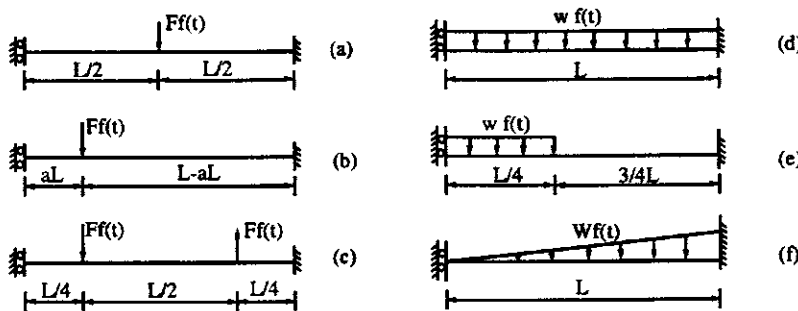


FIG. P.4.16

- 4.17. For loading case (a) given in Problem 4.16, consider the first three modes and find the absolute maximum [i.e. determine the time, t , from Eq. (1.83) for the maximum dynamic load factor of each mode, $DLF_{n,\max}$] displacement, moment, and shear under the loading point. Let $F(t) = 4(1 - t/0.1)$ k, $EI = 7 \times 10^9$ psi, $m = 0.2$ lb sec 2 /m 2 , and $L = 15$ ft. Use the formulas obtained in the previous problem.

- 4.18. In Example 4.9.1, consider 5% damping for the first four modes: (A) find the moments and shears at $t = 0.0379$ sec; and (B) make an equilibrium check of $\Sigma F_y = 0$.
- 4.19. Find the shears at the ends of member AB at $t = 0.05$ sec, and then make an equilibrium check with consideration of the first five modes (see Fig. P.4.19). Let $F(t) = 3(1 - t/0.1)$ k, $EI = 6 \times 10^6$ ksi, $m = 0.2$ lb sec 2 /in 2 , and $L = 150.3434$ in.

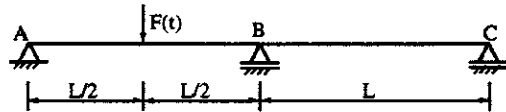


FIG. P.4.19

- 4.20. Show that, for the following two motion equations,

$$\begin{aligned}[M]\{\ddot{x}(t)\} + [K]\{x(t)\} &= \{F(t)\} \\ [M]\{\ddot{x}(t)\} + [C]\{\dot{x}(t)\} + [K]\{x(t)\} &= F(t)\end{aligned}$$

when $\{F(t)\} = \{P\}e^{i\omega t}$ and $\{F(t)\} = \{P\} \cos \omega t$, the undamped dynamic response can be treated the same (or equivalent) for these two functions, but the damped response should be treated differently for $e^{i\omega t}$ and $\cos \omega t$.

Chapter 5 Problems

SECTIONS 5.2 AND 5.3

- 5.1. Formulate the structural longitudinal stiffness matrix of the beam shown in Fig. P.5.1. Let member properties be $A_1 = A_2 = 232.26 \text{ cm}^2$, $L_1 = L_2 = 6.10 \text{ m}$, $E = 206.84 \text{ GN/m}^2$, $\gamma = 76.973 \text{ kN/m}^3$, and $I = (0.10144)10^{-3} \text{ m}^4$.



FIG. P.5.1

- 5.2. Find the natural frequencies and period of Problem 5.1.
5.3. Find the natural frequencies of the beam shown in Fig. P.5.3. Let $A = 232.26 \text{ cm}^2$, $L = 6.1 \text{ m}$, $\gamma = 76.973 \text{ kN/m}^3$, $E = 206.84 \text{ GN/m}^2$, $k' = EA/2L$.



Fig. P.5.3

- 5.4. Find the displacement at A and reaction at B of the beam given in Fig. P.5.4 where $A = 232.26 \text{ cm}^2$, $L = 12.2 \text{ m}$, $E = 206.84 \text{ GN/m}^2$, $\gamma = 76.973 \text{ kN/m}^3$, $\omega = 330.822 \text{ rad/sec}$, $q = m\omega^2/2$, $k' = EA/2L$, and $F(t) = 177.93 \sin \omega t \text{ kN}$. Consider steady state vibration.

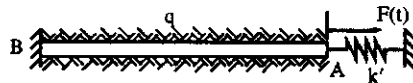


FIG. P.5.4

SECTIONS 5.4–5.7

- 5.5. Formulate the structural stiffness matrix using (A) fundamental structural mechanics based on equilibrium matrix, (B) physical interpretation, and (C) the direct stiffness method. (See Fig. P.5.5).

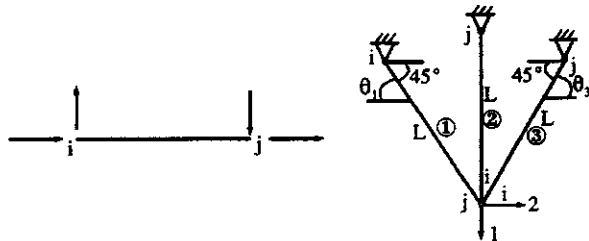


FIG. P.5.5

- 5.6. Find the frequencies of the truss given in Problem 5.5 for three groups of slenderness ratios: $L/R = 20, 60$ and 100 . Consider (A) coupling longitudinal and flexural frequencies, and (B) longitudinal frequencies only. Assume that all the members have the same cross section of square shape, $A = 10 \times 10^{-4} \text{ m}^2$, $E = 206.8 \times 10^6 \text{ kN/m}^2$, and $\gamma = 76.973 \text{ kN/m}^3$.
- 5.7. A shaft shown in Fig. P.5.7 of diameter d and length L supports a disk of thickness h and diameter D . Find the angular frequency without considering the mass of the shaft. The weight per unit volume of the disk is γ .

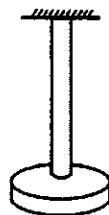


FIG. P.5.7

- 5.8. Find the frequency of a two-disk system given in Fig. P.5.8 as a propeller shaft carrying a propeller at one end and an engine at the other. Let I_1 and I_2 be the polar mass moments of inertia of the two disks and K_t be the torsional constant of the shaft. Neglect the mass of the shaft.

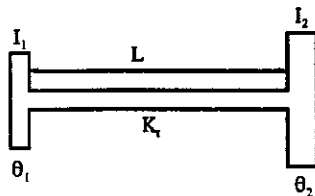


FIG. P.5.8

- 5.9. Formulate the structural stiffness matrix of the grid system shown in Fig. P.5.9 with consideration of (A) coupling dynamic torsional and flexural stiffness, (B) dynamic flexural stiffness and static torsional stiffness, and (C) dynamic flexural stiffness only.

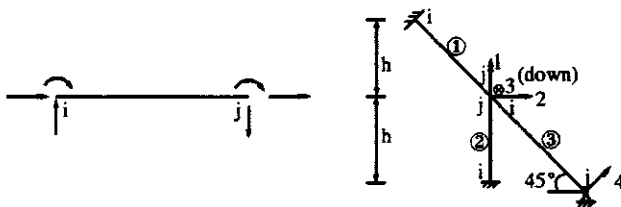


FIG. P.5.9

- 5.10. Find the first three frequencies for Problem 5.9. Let $I_x = 14.9843 \mu\text{m}^4$, $I_y = 1.66493 \mu\text{m}^4$, $I_p = J = I_x + I_y$, $\gamma = 76.9206 \text{ kN/m}^3$, $A = 7.742 \times 10^{-6} \text{ m}^2$, $h = 3.048 \text{ m}$, $E = 206.843 \text{ GPa}$, and $G = 82.737 \text{ GPa}$.
- 5.11. The uniform grillage shown in Fig. P.5.11 is made of steel pipe of which the outside diameter is 27.305 cm and the inside diameter 25.451 cm. $E = 206.843 (10^6) \text{ kN/m}^2$, $m = 0.241 \text{ kN sec}^2/\text{m}^2$, and $G = 3 E/8$. Vary the length, L , without changing other member parameters; then find the circular frequencies by considering (A) coupling bending and torsion, and (B) bending only. Compare the results for L/R varying as 10, 20, 30, 40, and 60.

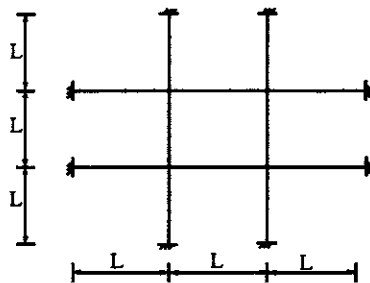


FIG. P.5.11

SECTIONS 5.8–5.11

- 5.12. Derive the dynamic stiffness coefficients for flexural vibration of a prismatic member subjected to axial compression P .
- 5.13. Derive the dynamic flexibility coefficients for flexural vibration of a prismatic member subjected to axial compression P .

- 5.14 Derive fixed-end forces of the beam shown in Fig. P.5.14 by application of the Timoshenko theory.



FIG. P.5.14

- 5.15. Derive fixed-end forces of the beam shown in Fig. P.5.15 with compression P and elastic media q .

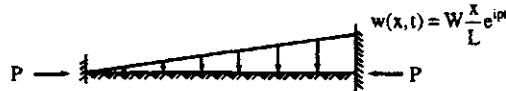


FIG. P.5.15

- 5.16. Find the response of deflection and moment at A and moment and shear at B shown in Fig. P.5.16 using Bernoulli–Euler theory. Let $A = 1.871 \text{ in}^2$, $E = 30,000 \text{ ksi}$, $I = 200 \text{ in}^4$, $L = 150 \text{ in}$, and $m = 0.2 \text{ lb sec}^2/\text{in}^2$, $F(t) = 3000(1 - t/0.1) \text{ lb/in}$. Consider the first three modes, four modes, and five modes. Make statics checks.



FIG. P.5.16

- 5.17. Analyze the beam given in Problem 5.16 with Timoshenko theory. Let $G = 1.12 \times 10^7 \text{ lb/in}^2$, $\kappa = 0.833$, other data are the same as given in that problem. Consider the first three modes.

ADDITIONAL PROBLEMS

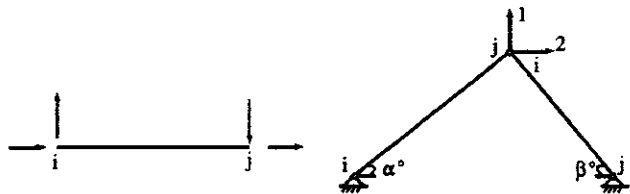
- 5.18. Find the first three circular frequencies of the truss shown in Fig. 5.6 with the following member properties:

Members 1 and 3— $EI = 752.205 \text{ MN m}^2$, $L = 6.096 \text{ m}$, $EA = 366.978 \text{ MN}$, $m = 13.857 \text{ Pa sec}^2$.

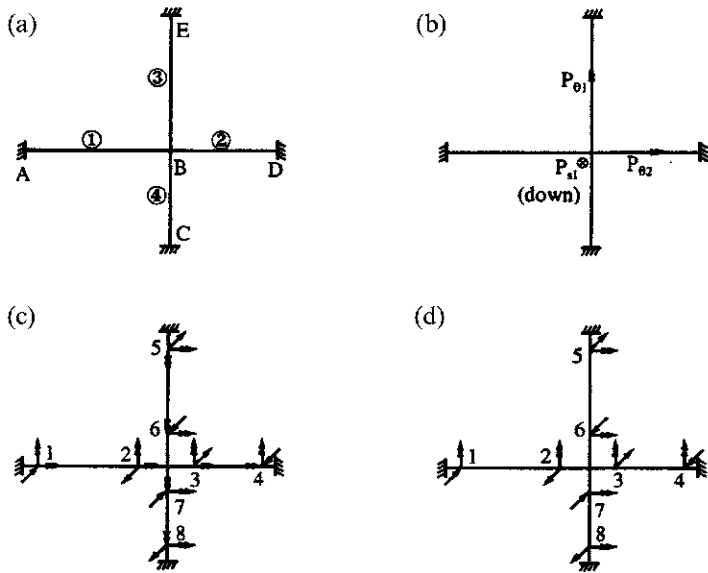
Member 2— $EI = 413.729 \text{ MN m}^2$, $L = 4.572 \text{ m}$, $EA = 300.254 \text{ MN}$, $m = 11.338 \text{ Pa sec}^2$.

Member 4— $EI = 196.213 \text{ MN m}^2$, $L = 7.620 \text{ m}$, $EA = 233.531 \text{ MN}$, $m = 8.818 \text{ Pa sec}^2$.

- 5.19. Find the first five frequencies of the truss shown in Fig. P.5.19 with various slenderness ratios of 20, 60, and 100 of each member for the following cases. (A) $\alpha = \beta = 45^\circ$ for three groups of analysis considering (1) longitudinal dynamic stiffness, (2) longitudinal and flexural dynamic stiffness, and (3) static longitudinal stiffness and dynamic flexural stiffness. (B) Same as (A) except $\alpha = 30^\circ$ and $\beta = 60^\circ$. Let the member properties be the same for all the analyses: $A = 0.023226 \text{ m}^2$, $E = 206.84 \times 10^6 \text{ kN/m}^2$, $\gamma = 76.973 \text{ kN/m}^3$, $m = 0.182426 \text{ kN sec}^2/\text{m}^2$, and $I = 0.10144 (10^{-3}) \text{ m}^4$. Let the length of members be the same, and change the length according to the value of L/R .

**Fig. P.5.19**

- 5.20. Find the first three frequencies and mode shapes of the plane grid system shown in Fig. P.5.20 considering: (A) coupling effect of flexural and torsional vibration by using dynamic bending and torsional stiffness; and (B) flexural vibration only. Assume that the cross sections of all the members are identical as $I_x = 36 \text{ in}^4 (1.49843 \times 10^{-5} \text{ m}^4)$, $I_y = 4 \text{ in}^4 (1.6649257 \times 10^{-6} \text{ m}^4)$, $I_p = I_x + I_y$, $\gamma = 490 \text{ lb/ft}^3 (7849 \text{ kg/m}^3)$, and $A = 12 \text{ in}^2 (7.742 \times 10^{-3} \text{ m}^2)$; let $L_1 = 25 \text{ ft} (7.620 \text{ m})$, $L_2 = 10 \text{ ft} (3.048 \text{ m})$, $L_3 = 15 \text{ ft} (4.572 \text{ m})$, $L_4 = 20 \text{ ft} (6.096 \text{ m})$, $E = 30,000 \text{ ksi} (206.895 \times 10^6 \text{ kN/m}^2)$, and $G = 12,000 \text{ ksi} (82.740 \text{ kN/m}^2)$.

**FIG. P.5.20** (a) Plane grid. (b) External action. (c) Internal resistance for bending and torsion. (d) Internal resistance for bending only.

Chapter 6 Problems

SECTIONS 6.2 AND 6.3

- 6.1. Find the natural frequencies of the double pendulum shown in Fig. P.6.1 using Lagrange's equation for small amplitudes of motion.

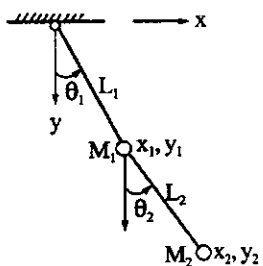


FIG. P.6.1

- 6.2. Using Lagrange's equation, find the motion equation of the damped-spring-mass system shown in Fig. P.6.2

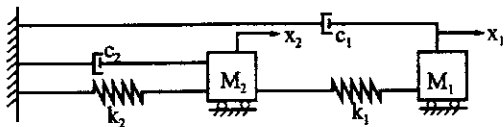


FIG. P.6.2

- 6.3. Using the consistent mass method, find the natural frequencies and normal modes of the truss shown in Fig. P.6.3 by considering (A) inertia force in both longitudinal and transverse direction [use MVY^t in Eq. (6.63)]; (B) inertia force in longitudinal direction only. Member properties are $A_1 = 2 \text{ in}^2$, $A_2 = 2 \text{ in}^2$, $A_3 = 3 \text{ in}^2$, $E = 29,000 \text{ ksi}$, and $\gamma = 490 \text{ lb}/\text{ft}^3$. Assume a superimposed mass, $M_1 = M_2 = (1.0402) \text{ lb sec}^2/\text{in}$, acting in x_1 and x_2 directions, respectively, for both cases.

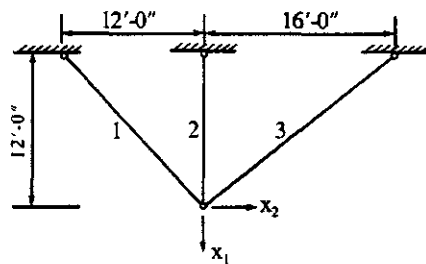


FIG. P.6.3

- 6.4. Formulate the structural stiffness matrix and mass matrix of the rigid frame shown in Fig. P.6.4 using (A) the lumped mass method and (B) the consistent mass method. Assume all the members have the same EI . Use the global d.o.f. given in the figure.

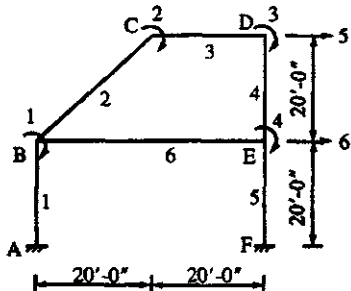


Fig. P.6.4

- 6.5. Rework Problem 6.4. Let members BE and CD be infinitely rigid; other structural properties are not changed. Note that the rotational d.o.f. should not be considered in this problem.
 6.6. Find the natural frequencies and normal modes of the virendeel truss shown in Fig. P.6.6. Let $I = 1728 \text{ in}^4$ and $E = 29,000 \text{ ksi}$. Use the global d.o.f. diagram shown in the accompanying figure and the lumped mass method for the superimposed weight $W = 1.5 \text{ k/ft}$.

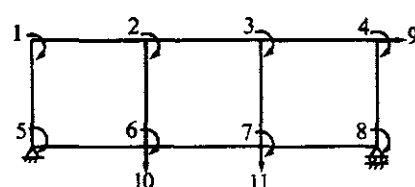
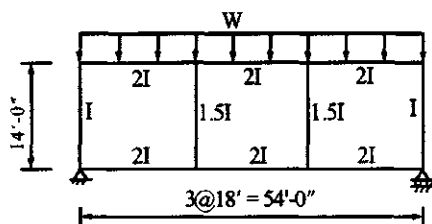


Fig. P.6.6

- 6.7. Find the natural frequencies and normal modes of the tower shown in Fig. P.6.7. Let $I = 1728 \text{ in}^4$ and $E = 29,000 \text{ ksi}$. The superimposed weight, W , is 1.2 k/ft . Use the lumped mass method.

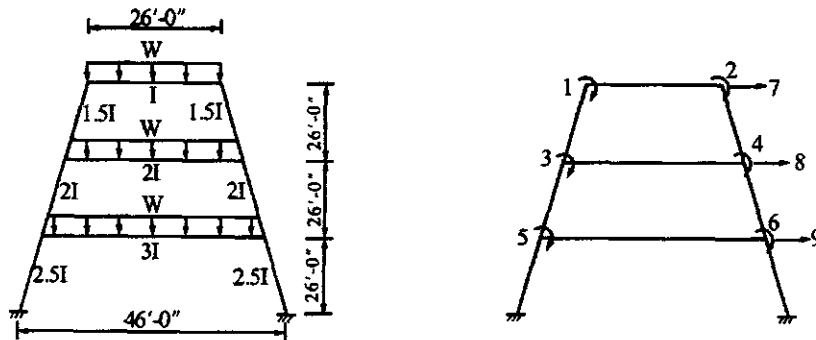


FIG. P.6.7

- 6.8. Formulate the structural stiffness matrix and mass matrix of the structure shown in Fig. P.6.8. Members AB and BC are beam elements without axial deformation; members AE , BE , and CE are truss elements. Use the global d.o.f. given in the accompanying figure. Structural properties are: $I_1 = I_2 = 5832 \text{ in}^4$, $E_1 = E_2 = 29,000 \text{ ksi}$, $A_1 = A_2 = 216 \text{ in}^2$, $A_3 = 24 \text{ in}^2$, $E_3 = E_1/4$, $A_4 = A_5 = 2 \text{ in}^2$, and $E_4 = E_5 = 3E_1/4$. The given weight, W_1 and W_2 , includes structural mass and superimposed mass. Use the lumped mass technique.

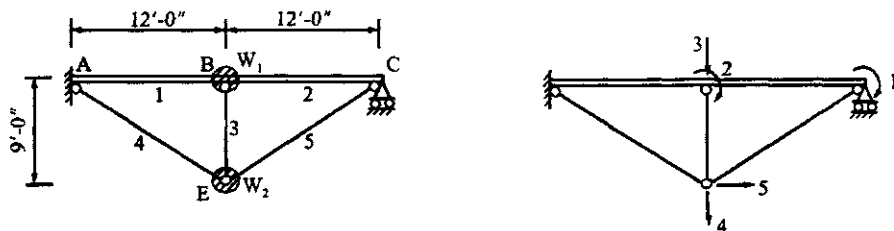


FIG. P.6.8

- 6.9. Using the consistent mass method and modal matrix technique, find the displacements and internal forces of the beam shown in Fig. P.6.9. Check the equilibrium conditions by considering the internal forces due to deformation, inertia force, and external load including fixed-end forces. The beam is divided into two segments as shown in the accompanying figure. Let $E = 30,000 \text{ ksi}$, $I = 13,824 \text{ in}^4$, $m = 0.0304 \text{ k sec}^2/\text{ft}^2$ and $F(x,t) = 1.44(1 - t/\zeta) \text{ k/ft}$, $\zeta = 0.038 \text{ sec}$.



FIG. P.6.9.

- 6.10. Rework Problem 6.9 using the lumped mass model. The lumped mass is $0.27026 \text{ k sec}^2/\text{ft}$ at node B.

- 6.11. Find the nodal displacements and internal forces of the beam shown in Fig. P.6.11 based on steady-state vibration analysis. Use both the consistent mass method and the dynamic stiffness method and compare the results from these two methods. Let $A = 0.1858 \text{ m}^2$ (288 in^2), $I = 5.7539(10^{-3}) \text{ m}^4$ ($13,824 \text{ in}^4$), $\gamma = 7849.045 \text{ kg/m}^3$ (490 lb/ft^3), $W = 222.41 (10^4) \text{ N}$ (500 k), $\omega = 150 \text{ rad/sec}$, and $E = 20,684.47 \text{ kN/cm}^2$ ($30,000 \text{ k}$).



FIG. P.6.11

- 6.12. Using the lumped mass method and modal matrix technique, find the displacements and internal forces at $t = 0.0419 \text{ sec}$ at which time maximum displacement occurs ($\cos \omega t = 1$). Let $L = 12 \text{ ft}$, $I = 13,824 \text{ in}^4$, $E = 30,000 \text{ ksi}$, $\gamma = 490 \text{ lb/ft}^3$, $A = 288 \text{ in}^2$, $W = 500 \text{ k/ft}$, and $\omega = 150 \text{ rad/sec}$. Assume that the lumped mass has two components: mass associated with rotational inertia, $M_1 = 0.54053 \text{ k sec}^2$; mass associated with transverse inertia, $M_2 = 0.27025 \text{ k sec}^2/\text{ft}$. Check the equilibrium conditions of internal forces due to deformation, inertia force, and applied load including fixed-end forces (see Fig. P.6.12).

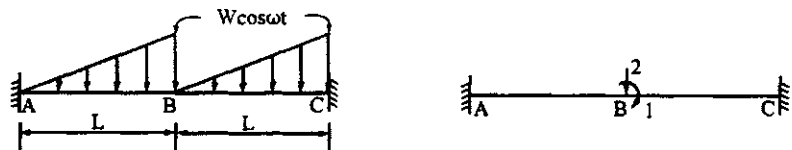


FIG. P.6.12

- 6.13. (A) Using Eq. (2.45) and the consistent mass method, find the displacement and accelerations, at $t = 0.1 \text{ sec}$, of the structure shown in Fig. P.6.13. Use the given global d.o.f. diagram and consider structural mass only for the modal matrix formulation. Let all three members be identical for which $m = 6.88 (10^{-5}) \text{ lb sec}^2/\text{in}^2$, $I = 6.886 (10^{-5}) \text{ in}^4$, $E = 30 \times 10^6 \text{ psi}$, and $L = 9.5 \text{ in}$. Note that the structural properties are the same as given for Fig. 6.13. The external load is $F(x,t) = W f(t)$, where $W = 1.667 \text{ lb/in}$, $f(t) = 1 - t/\zeta$, $\zeta = 0.3 \text{ sec}$. (B) Find eigenvalues and eigenvectors with consideration of structural mass and of superimposed mass due to the applied load.

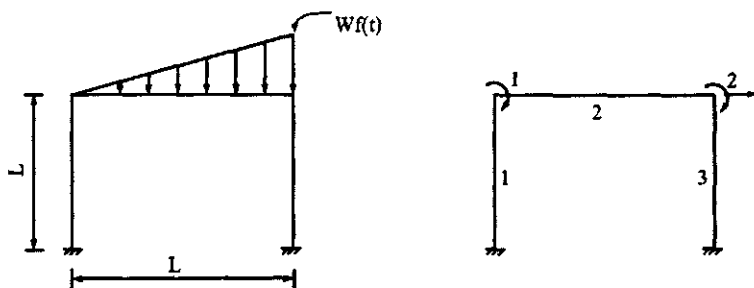


FIG. P.6.13

SECTION 6.5

- 6.14. Formulate the structural stiffness matrix $[K]$ of the plane stress problem shown in Fig. P.6.14 using the generalized coordinate approach and the given global d.o.f. diagram. Let $E = 30(10^6)$ psi, $\mu = 1/4$, and $t = 0.1$ in. Assume a uniform load $p = 100$ lb/in is applied along the edge BD ; find the displacements of the structure and stresses of element 1. Lump half of the static load acting along d.o.f. 1 and 3, respectively.

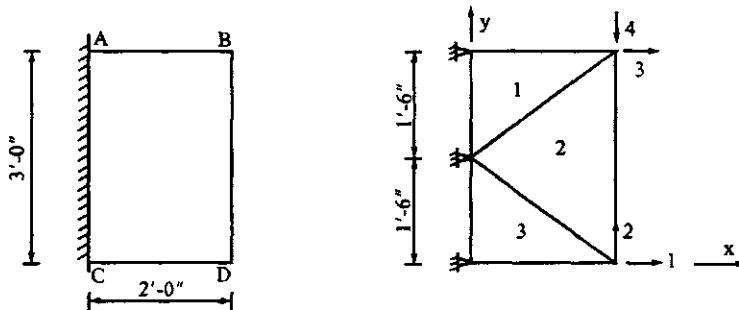


FIG. P.6.14

- 6.15. Use the generalized coordinates and formulate $[K]$ of the structure shown in Fig. P.6.15. Elements 1 and 2 are triangular plane stress plates; elements 3, 4, and 5 are truss members. Let $\mu = 1/4$, $t = 0.2$ in, $E = 30 \times 10^6$ psi, and $A_3 = A_4 = A_5 = 2$ in 2 . Find the mass matrix by assuming one-third of the triangle's mass and one-half of the bar's mass lumped at the node; the mass density is ρ .

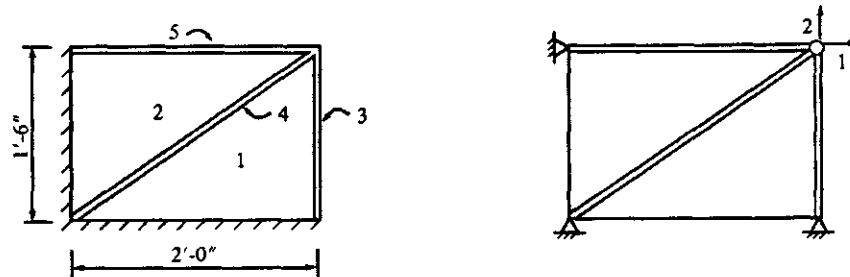


FIG. P.6.15

- 6.16. Use the generalized coordinates and formulate $[K]$ and $[M]$ for longitudinal vibration of the nonuniform bars shown in Fig. P.6.16. Let $E = 30,000$ ksi and $\gamma = 490$ lb/ft 3 .

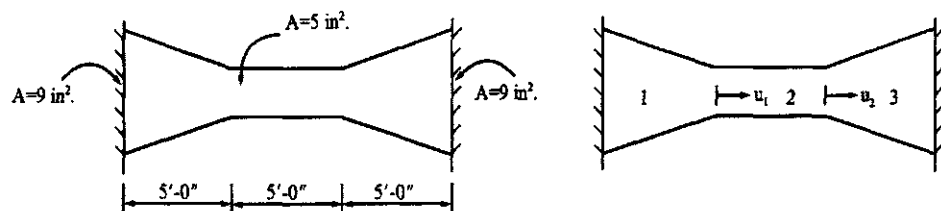


FIG. P.6.16

- 6.17. Use the isoparametric quadrilateral element to find the stiffness matrix of the structure shown (see Fig. P.6.17). Let $E = 30(10^6)$ psi, $\mu = 0.25$, and $t = 0.1$ in. (A) Find the principal stress in these two elements by lumping the static load at d.o.f. 1 and 3; (B) find the mass matrix of element 1; and (C) find the load matrix due to body force $b(x,y) = w$ for element 1.

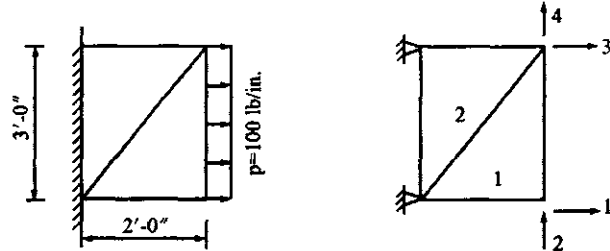


FIG. P.6.17

- 6.18. Find the stiffness coefficient k_{14} , mass coefficient M_{14} , and the generalized force P_{41} of the quadrilateral element shown in Fig. P.6.18. Let the plate thickness be t , Poisson's ratio μ , and body force w .

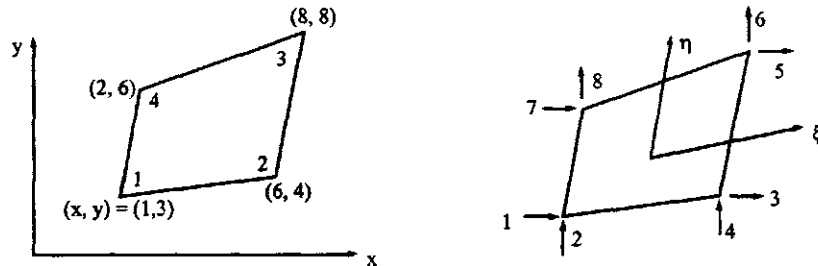


FIG. P.6.18

SECTIONS 6.6 AND 6.7

- 6.19. Find the structural stiffness matrix, $[K]$, geometric matrix, $[K_g]$, and lumped mass matrix, $[M]$, of the truss shown in Fig. P.6.19. Let $A_1 = 1.44 \text{ in}^2$, $A_2 = 2 \text{ in}^2$, $A_3 = 1.8 \text{ in}^2$, $A_4 = 2 \text{ in}^2$, $E = 30,000 \text{ ksi}$, and $\gamma = 490 \text{ lb/ft}^3$. Use the given global d.o.f. diagram and form the geometric matrix in terms of P based on the internal forces from the first-order analysis.

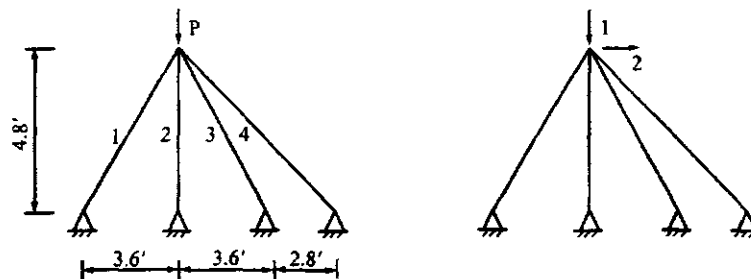


FIG. P.6.19

- 6.20. Using the string stiffness matrix, formulate $[K_g]$ of the beam shown in Fig. P.6.20. Establish the motion equation of the system.

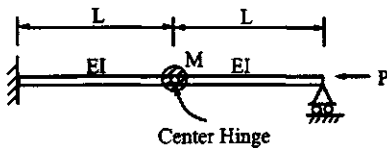


FIG. P.6.20

- 6.21. Using the string stiffness matrix, formulate $[K_g]$ of the structure shown in Fig. P.6.21 of which the member properties are $I_{AB}=I_{BC}=I_{DE}=I_{EF}=4020 \text{ in}^4$, $I_{CD}=6740 \text{ in}^4$, $I_{BE}=9030 \text{ in}^4$, $E=29,000 \text{ ksi}$, and $P=2248 \text{ k}$. The mass on CD and BE is due to the load 1.2 k/ft. Establish the motion equation of the structure.

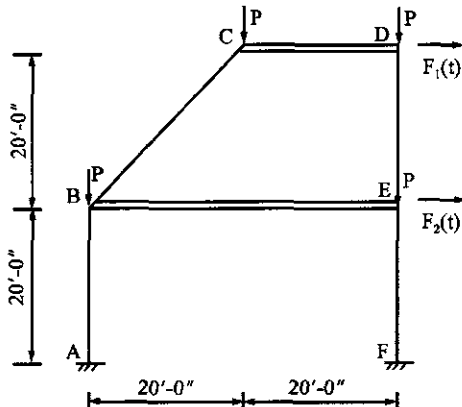


FIG. P.6.21

SUPPLEMENTARY PROBLEMS

- 6.22. Derive the Lagrange's interpolation formula in Eq. (6.99) with detailed interpretation.
 6.23. Find the internal stresses of the following beam subjected to a uniform load using (A) conventional matrix formulation and (B) finite element technique. Show that the finite element solution must include the fixed-end moment (also called initial stress) for the correct solution. Otherwise, lump the uniform load at the nodal points (see Fig. P.6.23).

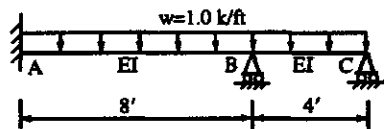


FIG. P.6.23

- 6.24. Derive m_{ij} in Eq. (6.13) using Lagrange's equation.
 6.25. Considering the $P-\Delta$ effect, derive the Lagrange's equation in Eq. (6.135).
 6.26. Considering the $P-\Delta$ effect, derive the motion equation in Eq. (6.136).

Chapter 7 Problems

SECTION 7.2

- 7.1. An earthquake occurred, felt by most people living in the vicinity. Many were frightened. Some heavy furniture moved; some dishes and windows broke. Only a few instances of fallen plaster in structures were reported afterwards, and no other damage was observed. What is the intensity of this earthquake using the Modified Mercalli scale?
- 7.2. A station located in a city has a seismometer which traced an earthquake. It showed that the maximum amplitude on the seismograph was 10 mm, and the time between the arrival of P- and S-waves was 8 sec. Determine the Richter magnitude of the earthquake and estimate the distance between the epicenter and station.

SECTION 7.3

- 7.3. Assume that over an interval of time h , acceleration of the system is a constant, i.e. $\ddot{x} = \ddot{x}_n$ as shown in Fig. P.7.3. Derive the numerical integration formulas for \ddot{x}_{n+1} , \dot{x}_{n+1} , and x_{n+1} .

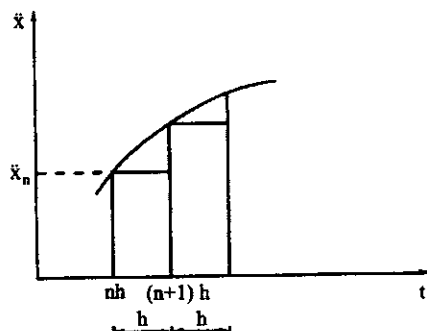


FIG. P.7.3

- 7.4. Assume that the velocity and displacement expressions of a system are

$$\dot{x}_{n+1} = a_1 \dot{x}_n + a_2 \ddot{x}_n + R_1; \quad X_{n+1} = b_1 x_n + b_2 \dot{x}_n + b_3 \ddot{x}_n + R_2$$

where R_1 and R_2 are the error terms. Use expressions of the general numerical integration method to find the integration formulas for \ddot{x}_{n+1} , \dot{x}_{n+1} , and x_{n+1} . Compare the results with those in Problem 7.3.

- 7.5. Using the Newmark method with $\alpha=1/6$ and $\delta=1/2$, find the structural response at $t=0.01$ sec in Example 7.3.3.

SECTION 7.4

- 7.6. A structure modeled as a single d.o.f. system has a natural period $T=0.5$ sec. Use the Newmark elastic design spectra to determine maximum acceleration S_a , maximum relative displacement S_d , and maximum velocity S_v for the earthquake with a peak ground acceleration equal to $0.2g$. Assume 5% of the critical damping.
- 7.7. Draw the Newmark inelastic design spectra for damping ratio of 5%. Also calculate S_a , S_v , and S_d from the inelastic spectra for a single d.o.f. system with $T=0.5$ sec. Assume the design ductility is 4.
- 7.8. Use UBC normalized design spectra to find the maximum acceleration S_a of a structure with period $T=1.0$ sec. The structure is located in an area with medium clay soil, and is designed to resist an earthquake with effective peak ground acceleration of $0.2g$.

SECTION 7.5

- 7.9. A seismometer shows that earthquake acceleration records at a certain time instant t are $\ddot{u}_{E-W}(t)=6$ ft/sec² and $\ddot{u}_{N-S}(t)=3$ ft/sec². The earthquake has wave velocity of 10,000 ft/sec. Find the ground rotational velocity at time t .

SECTION 7.6

- 7.10. Using SRSS modal combination method, find the structural response for the three-story building shown in Fig. P.7.10. Structural mass matrix and normal modes are

$$[M] = \begin{bmatrix} 0.07399 & 0 & 0 \\ 0 & 0.07301 & 0 \\ 0 & 0 & 0.07138 \end{bmatrix} \text{ks}^2/\text{in}; \quad [X] = \begin{bmatrix} 0.2571 & 0.94263 & 1 \\ 0.67747 & 1 & -0.7314 \\ 1 & -0.94372 & 0.24080 \end{bmatrix}$$

Velocity response spectral values corresponding to the three modes are $S_v(p_1)=2$ ft/sec; $S_v(p_2)=1.15$ ft/sec; and $S_v(p_3)=0.6$ ft/sec. Three fundamental frequencies are $p_1=7.3068$; $p_2=23.6255$; and $p_3=44.4920$ in rad/sec.

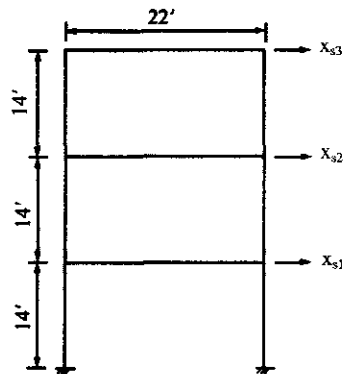


FIG. P.7.10

SECTION 7.7

- 7.11. Find the worst-case response of d.o.f. D_1 in the one-story shear building in Example 7.6.2, and find the corresponding critical seismic input angle for D_1 by the CQC method. Use Eqs. (7.226) and (7.227) to determine the worst-case response and critical seismic input angle.

ADDITIONAL PROBLEMS

- 7.12. A cantilever beam shown in Fig. P.7.11 is subjected to a concentrated load for which the relationship of stress and strain is given in the accompanying figure. Determine the ductility based on the moment curvature.

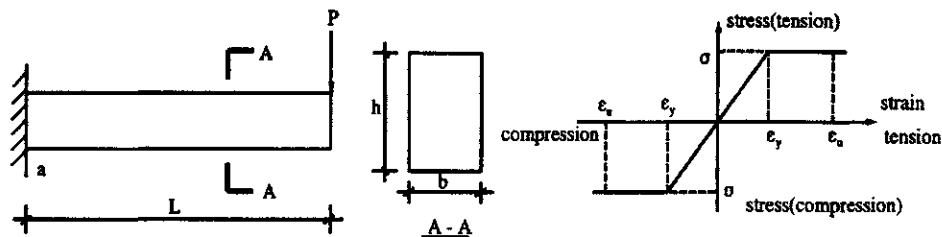


FIG. P.7.12

- 7.13. The following data are part of earthquake records:

t	$\dot{u}_{E\ W}$	$\dot{u}_{N\ S}$	\dot{u}_v	$\ddot{u}_{E\ W}$	$\ddot{u}_{N\ S}$	\ddot{u}_v
0.02	-2.103	-0.914	-0.848	6.631	6.113	7.069
0.04	-2.001	-0.801	-0.619	3.507	5.105	15.72

in which the units of velocity and acceleration are cm/sec and cm/sec², respectively. The wave velocity of the earthquake is 1000 cm/sec. Determine rotational deformations, velocities and accelerations at 0.04 sec.

- 7.14. Based on the data in Problem 7.10, find the structural response using the CQC modal combination method. Assume the damping ratio is 0.07.
- 7.15. Prove $\alpha_{ij} = \alpha_{ji}$ in Eq. (7.209).

Chapter 8 Problems

- 8.1. Find $[C_j]$ of joint a for the structure shown in Fig. P.8.1 using Method 1 and Method 2. GCS, JCS and structural dimensions are as shown.

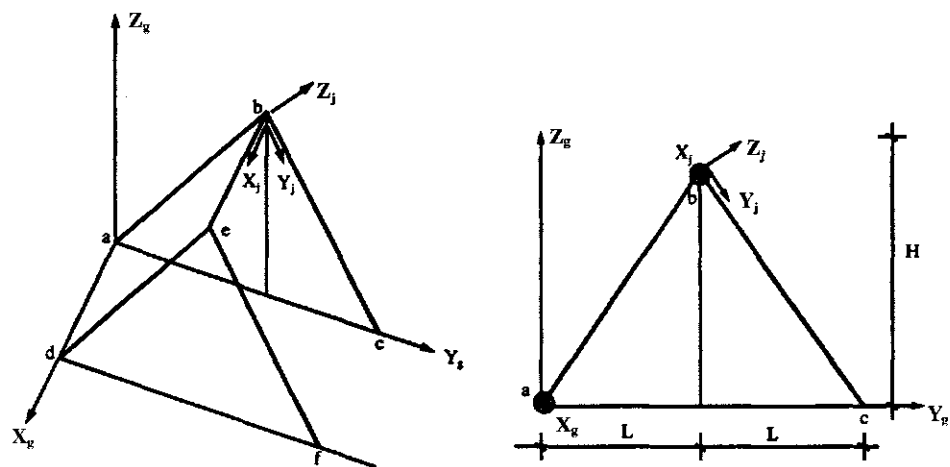


FIG. P.8.1

- 8.2. Find $[C_j]$ of joints a and b of the structure shown in Fig. P.8.2 by using Method 1 and Method 2 based on the given information of the GCS and JCS.

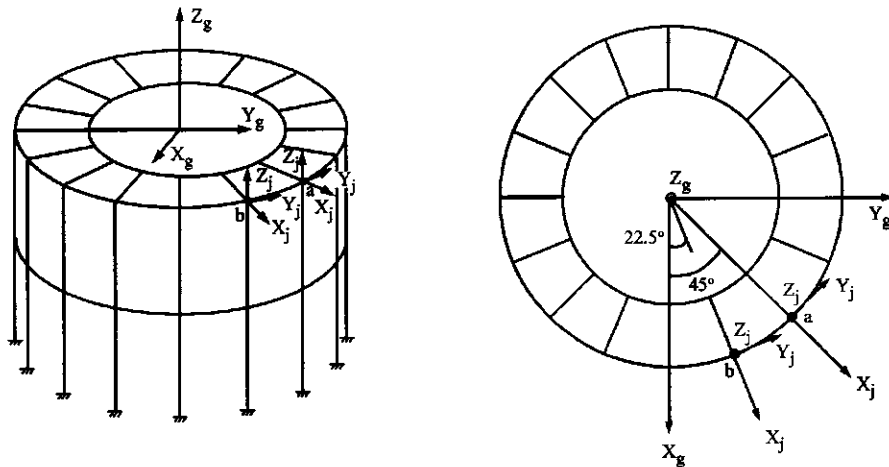


FIG. P.8.2

- 8.3. Find the transformation matrices $[C_j]$ and $[T_{ms}]$ of joints 8 and 12 for the structure shown in Fig. P.8.3. The JCS of master joint (15) at the first floor is parallel to the GCS. On the top floor, axes of JCS of the master joint (16) are defined as follows: X_j axis is parallel to X_g ; Y_j axis is parallel to the roof and has a 15° angle to the Y_g-X_g plane. Coordinates (GCS) of points 8, 12, 15 and 16 are $P_8(0,20,18)$, $P_{12}(0,20,32)$, $P_{15}(-15,8,18)$, and $P_{16}(-15,10,34)$.

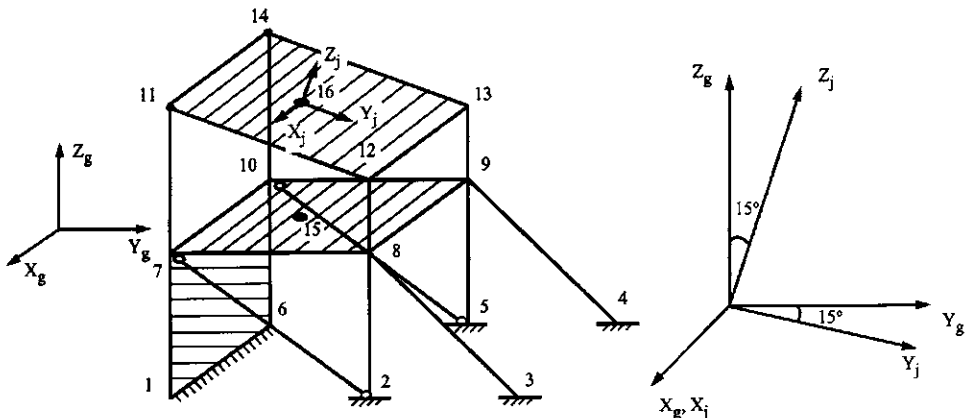


FIG. P.8.3

- 8.4. Rework Problem 8.6.1 assuming that JCS of joint 6 (see Fig. 8.9) is not parallel to the GCS, but that the X_j axis is parallel to the axis of bracing shown in Fig. P.8.4.

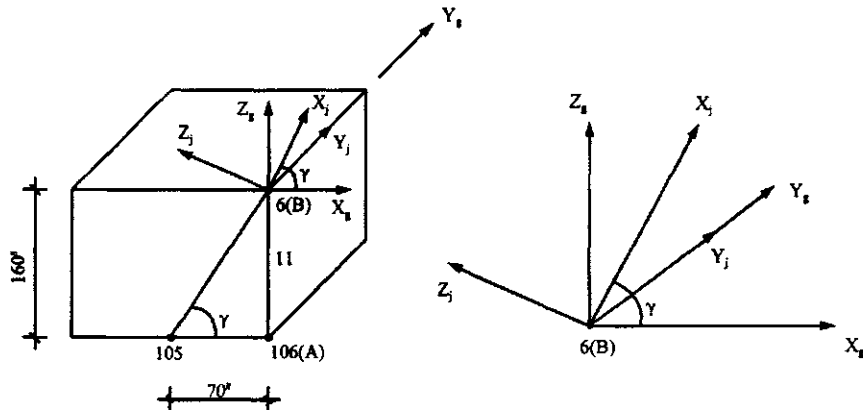


FIG. P.8.4

- 8.5. Find the individual matrices of $[A_1]^T$, $[A_2]^T$, $[A_3]^T$, $[A_4]^T$ and $[A_5]^T$ directly on the basis of physical interpretation. These matrices are used to find $[K^t] = [A] [K_e] [A]^T$ in Eq. (8.84) where $[A]^T = [[A_5] [A_4] [A_3] [A_2] [A_1]]^T$.
- 8.6. In Fig. P.8.6 a shear wall is connected to joints 9, 2, 102, and 109. The wall's dimension and material properties are the same as those of the wall in Example 8.7.1. Let $L = 1,000$ mm, $h = 500$ mm, and mass center (MC) of nodes 11 and 111 be the centroid of its individual slab. Determine the wall's stiffness in GCS using Method 1.

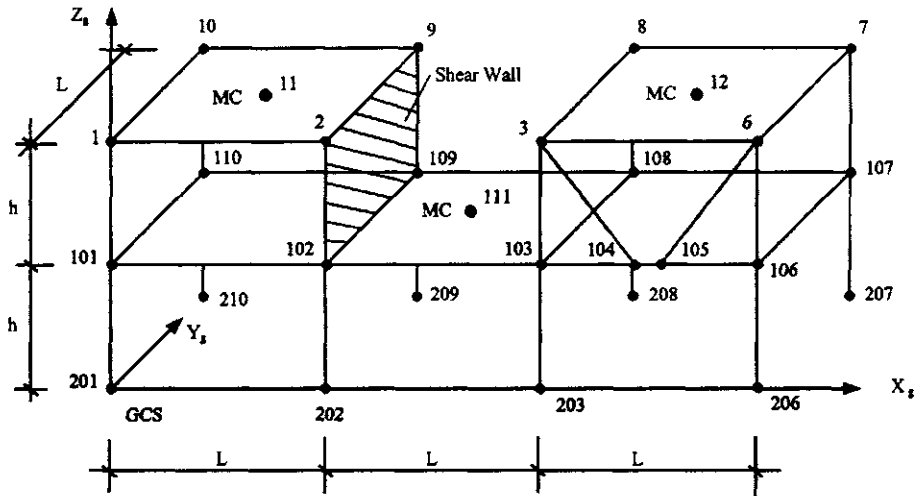


FIG. P.8.6

- 8.7. Rework Problem 8.6 using Method 2.
 8.8. Find the stiffness matrix in the GCS of the beam connecting at nodes 101 and 110 of Fig. P.8.6 using Method 1. The beam's cross section and material properties are given in Example 8.6.1.
 8.9. Rework Problem 8.8 using Method 2.
 8.10. Rework Example 8.6.1 using Method 2.
 8.11. Rework Example 8.8.1 using Method 2.

- 8.12. Determine the stiffness matrix in GCS of bracing member *ab* shown in Fig. P.8.12 using Method 1. Let the slave and master joints be at the same joint identified as *A* and *a*, respectively, on the lower floor. Let the master and slave joints on the upper floor be at different joints designated as *B* and *b*, respectively. Member cross section and material properties are the same as those given in Example 8.8.1.

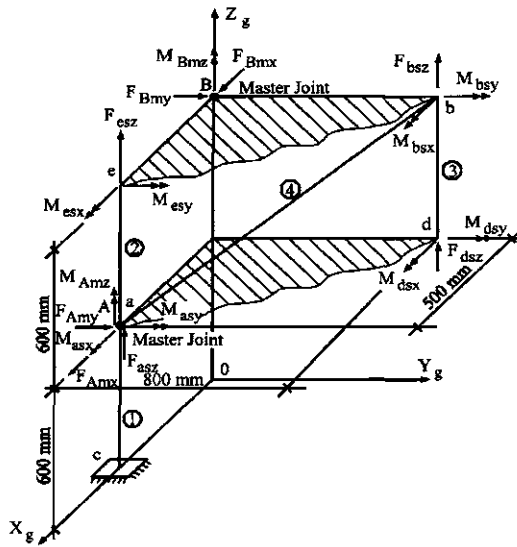


FIG. P.8.12

- 8.13. Rework Problem 8.12 using Method 2.
 8.14. For the structure shown in Fig. P.8.14a, find the system stiffness in GCS using Method 1. The columns (members 1,2,3) are identical, having $A = 12,710 \text{ mm}^2$, $E = 210,000 \text{ MPa}$, $I_z = I_y = 60,000 \text{ mm}^4$, $J_x = 40,000 \text{ mm}^4$, and $G = 150,000 \text{ MPa}$. The bracing (member 4) has the same cross-sectional area and modulus of elasticity as those of the columns. Use the global d.o.f. given in Fig. P.8.14b for which d.o.f. 1–12 are assigned first (i.e. starting from 1) for convenience of matrix condensation; d.o.f. 13–18 remain for analysis as a six-d.o.f. system.

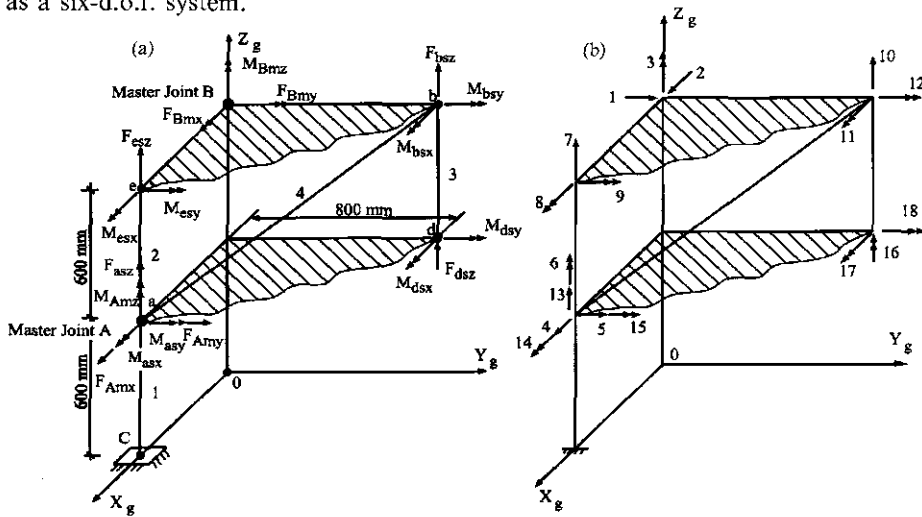


FIG. P.8.14

- 8.15. Rework Problem 8.14 using Method 2.
 8.16. Find the global d.o.f. of the two-story building shown in Fig. P.8.16 using the FFA method. Formulate the global stiffness matrix of beam-column 1 and beam b_1 of the first floor and beam-column 1 of the second floor.

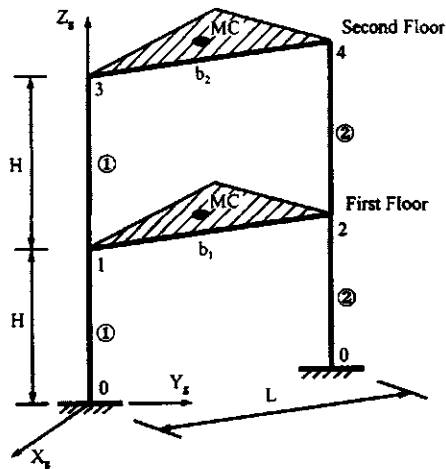


FIG. P.8.16

- 8.17. Find the structural stiffness matrix of the building structure shown in Fig. P.8.17a. Members have the same box-shape cross section with the following properties: $A = 20 \text{ in}^2$, $I_y = 500 \text{ in}^4$, $I_z = 500 \text{ in}^4$, $J_x = 10 \text{ in}^4$, $E = 30,000 \text{ ksi}$, and $G = 13,000 \text{ ksi}$. Global d.o.f. are given in Fig. P.8.17b where MC is the middle of the floor.

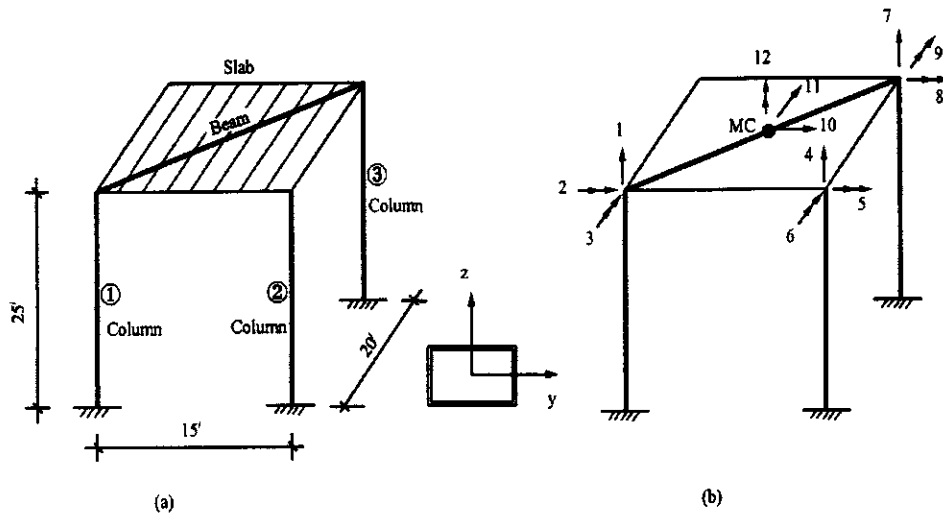


FIG. P.8.17

- 8.18. Assume that the structure given in Problem 8.17 is subjected to the loading shown in Fig. P.8.18 where the fixed-end forces of beam AB are given. Find the loading matrix.

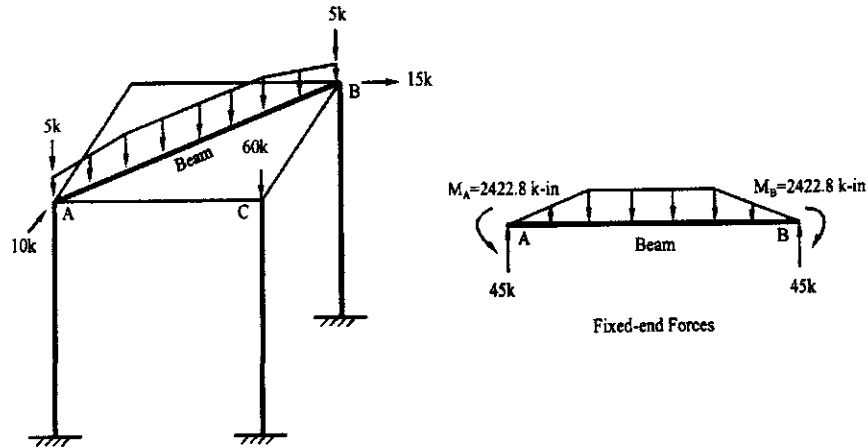


FIG. P.8.18

- 8.19. Using the forces of 5 k, 5 k, and 60 k applied at nodes A , B , and C , respectively, as well as the fixed-end shears at A and B shown in Fig. P.8.18, find the geometric matrix $[K_g]$. (Note: after combining the beam's fixed-end shears with the applied forces given, $P_1 = 50$ k, $P_2 = 60$ k, and $P_3 = 50$ k.)
 8.20. Using the solution of $[K]$, $\{R\}$, and $[K_G]$ from Problems 8.17, 8.18, and 8.19, find the structural displacements.
 8.21. The structure in Problem 8.17 has five lumped masses as shown in Fig. P.8.21. Mass m_4 is at node 4, which is assumed to be the mass center of the floor. Masses 1, 2, 3, and 5 are due to machinery weight at the given points. The masses are $m_1 = m_3 = 0.018$ k sec²/in, $m_2 = m_4 = 0.015$ k sec²/in, $m_5 = 0.1$ k sec²/in. Using Eq. (8.179), find the natural frequencies and normal modes.

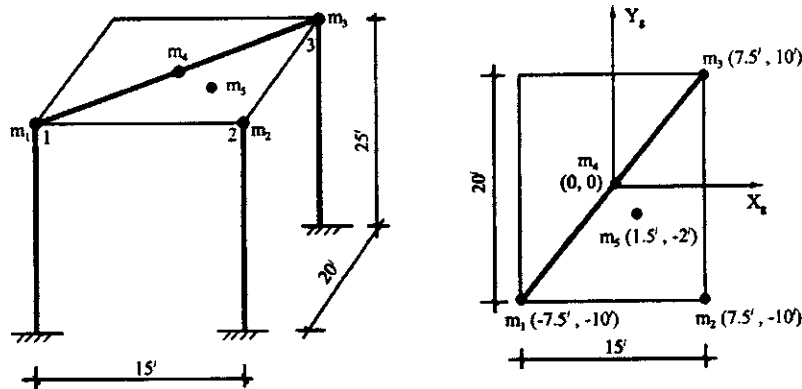


FIG. P.8.21

8.22. The 10-story shear building shown in Fig. P.8.22 has three d.o.f. at the mass center (MC) of each floor. All the columns have a rectangular cross section of 6×6 in. Let $E = 4.32(10)^6$ ksf and $G = 1.66(10)^6$ ksf. The mass per square foot on each floor is $10 \text{ k sec}^2 \text{ ft}$. MC is at $X_c = 10.833 \text{ ft}$ and $Y_c = 14.167 \text{ ft}$ as shown in the figure. Consequently, the mass matrix for each story is obtained as

$$[M] = \begin{bmatrix} 259,374.98 & 0 & 0 \\ 0 & 2250 & 0 \\ 0 & 0 & 2250 \end{bmatrix} \quad \text{symm}$$

(A) Find the ground main and intermediate principal components shown in Fig. 8.22 for 18 May, 1940 El Centro earthquake. (B) Obtain the response spectral values by applying main and intermediate components in structural reference axes X_1 and X_2 , respectively. (C) Apply the main and intermediate components in X_1 and X_2 , respectively; then find seismic critical input angle θ_{cr} . (D) Apply the main and intermediate components in x and y axes, respectively; then find the response using critical input angle θ_{cr} obtained in (D) (one response analysis for each θ_{cr}), and compare the result with that when the components are applied in the X_1 and X_2 axes (i.e. $\theta_{cr} = 0$).

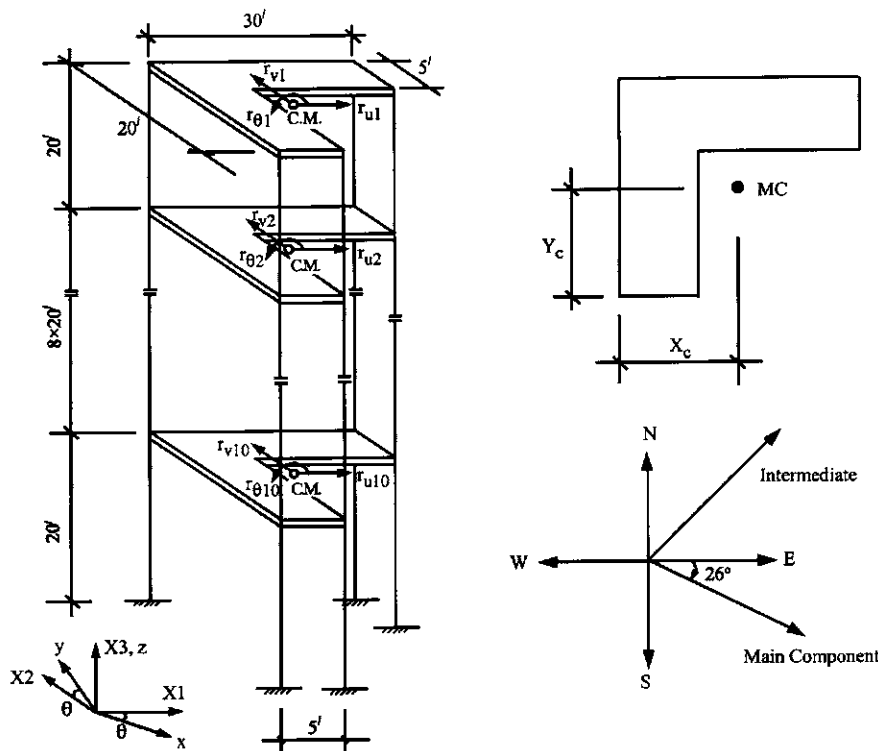


FIG. P.8.22

Chapter 9 Problems

SECTIONS 9.2–9.4

- 9.1. Using the incremental linear acceleration method with unbalanced force technique, find the dynamic response of the following shear building from $t = 0$ –0.95 sec with $\Delta t = 0.05$ sec. The elasto-plastic hysteresis model is assumed for all members. Assume $EI_1 = 3 \text{ kN m}^2$, $EI_2 = 5 \text{ kN m}^2$, $\ell = 6 \text{ m}$, $h_1 = 3 \text{ m}$, $h_2 = 5 \text{ m}$, $F(t) = 90 \sin(\pi t) \text{ N}$, $M = 35 \text{ N sec}^2/\text{m}$, and ultimate moment capacity $M_p = 23 \text{ N m}$. (See Fig. P.9.1.)

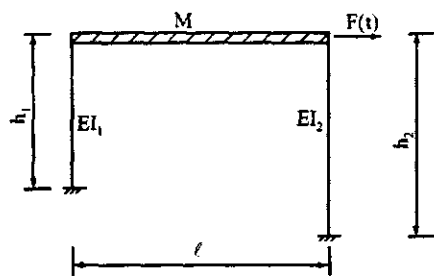
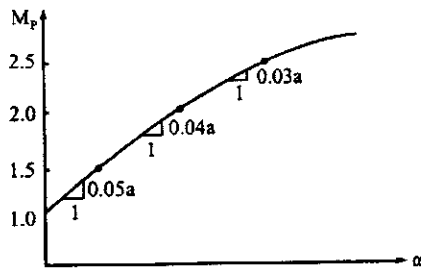


FIG. P.9.1

- 9.2. Rework Problem 9.1 by using bilinear hysteresis model for all members with $p = 0.05$.

SECTION 9.5

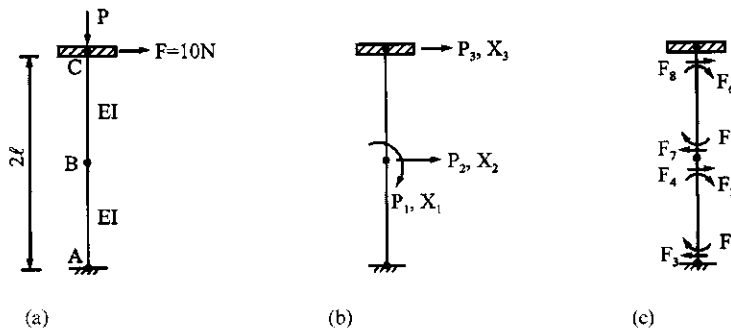
- 9.3. If a bilinear curve is used in the curvilinear model (Fig. 9.23), compare stiffness coefficients of the curvilinear model with those of the bilinear model for inelastic systems; if there is any difference, explain why.
- 9.4. Find the stiffness matrix of the curvilinear beam shown in Fig. 9.22. The moment-plastic angle relationship of the beam is shown in Fig. P.9.4. Assume $S_i = 0.05$, $S_j = 0.03$, $EI = 5 \text{ kN m}^2$, $L = 4 \text{ m}$, and $a = 4EI/L = 5 \text{ kN m}$.

**FIG. P.9.4****SECTION 9.6**

- 9.5. Find the stiffness matrix of a Ramberg-Osgood beam with $\bar{a} = 1$, $r = 20$, and $M_p = 23 \text{ N m}$. Assume $M_i = 15 \text{ N m}$ in the skeleton curve and $M_j = 22 \text{ N m}$ at the reversal point, ready to unload to the branch curve.

SECTION 9.7

- 9.6. The following structure (Fig. P.9.6) is subjected to a vertical load, P , and a horizontal force, F , at C . Find the buckling load, P_{cr} , of the structure. Find the horizontal displacement of the structure at joint C corresponding to $F = 10 \text{ N}$: (A) without consideration of geometric stiffness and large deflection; (B) with consideration of geometric stiffness (with $P = P_{cr}/2$), but without large deflection; and (C) with consideration of geometric stiffness (with $P = P_{cr}/2$) and large deflection. Assume that $\ell = 3 \text{ m}$, $EI = 3 \text{ kN m}^2$, and that member geometric stiffness formulation is based on stringer model (see Fig. 9.35). Material nonlinearity is not considered. Note: for case (C), large deflection formulation is based on previous deflection when $F = 5 \text{ N}$.

**FIG. P.9.6** (a) Structure. (b) External actions. (c) Internal resistance.

- 9.7. Change the general expression of Ramberg–Osgood's stress–strain relationship to the following parabolic relationship:

$$\varepsilon = \frac{\sigma}{E} + k \left(\frac{\sigma}{E} \right)^2$$

Derive the moment–stress equation of a rectangular beam with width b and depth h .

SECTION 9.8

- 9.8. Using the reduced plastic moment equation [Eq. (9.158)], calculate the reduced plastic moment of the frame shown in Fig. P.9.8. Then use the incremental linear acceleration method with unbalanced force technique to find the dynamic response of the structure from $t=0$ –1.4 sec. Assume an elasto-plastic hysteresis model for all members, and that $EI=2.86967168 \text{ kN m}^2$, $M=35.023622 \text{ N sec}^2/\text{m}$, $h=3.048 \text{ m}$, $\ell=6.096 \text{ m}$, $F(t)=88.96 \sin(\pi t) \text{ N}$, $\Delta t=0.1 \text{ sec}$, $M_p=22.59584 \text{ N m}$, and $P/P_y=0.4$.

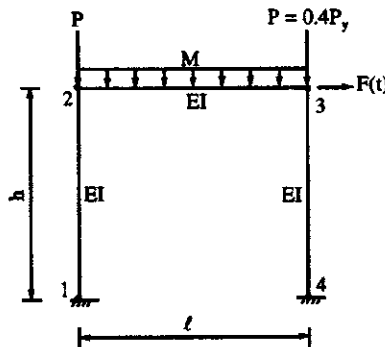


FIG. P.9.8

SECTION 9.9

- 9.9. Using the consistent mass method, find displacements, accelerations, and internal forces at $t=0.05 \text{ sec}$ of the structure shown in Fig. P. 9.1 by the incremental linear acceleration method.

Chapter 10 Problems

- 10.1. Determine the design-forces, based on UBC-94, UBC-97 and IBC-2000, for a three-story symmetric steel office building shown in Fig. P.10.1. The building, located in St Louis, MO, has an ordinary moment-resisting frame. Soil type is determined as S₃ (UBC-94), S_c (UBC-97), and site class B (IBC-2000). The dead load at each story is 609.4 k, 590.9 k, and 217.2 k at levels 1, 2, 3, respectively. Use the importance factor $I=1.0$.
- 10.2. For the building in Problem 10.1, find accidental torsion and torsional shear distribution. Assume that moments of inertia for each column are $I_x=249.3 \text{ in}^4$ and $I_y=66.8 \text{ in}^4$. Let $E=29000 \text{ ksi}$. Use the formulas presented in Eqs. (10.79)–(10.82) of Method A and analyze the individual bent as a planar frame.
- 10.3. Based on lateral force distribution obtained from Problem 10.1 and illustrated in Fig. P.10.3, displacements at each floor level are shown as follows by using analysis of the rigid frame. $\delta_1=3422.392/EI_x$; $\delta_2=5637.492/EI_x$; $\delta_3=6682.332/EI_x$. Find period T based on the rational analysis of Rayleigh's equation [see Eq. (10.26)] for UBC-94, UBC-97, and IBC-2000.
- 10.4. Determine the design forces, based on UBC-94, UBC-97 and IBC-2000, for a nine-story ductile moment-resisting steel frame office building located in Los Angeles, CA, with consideration of soil profile type 2 (UBC-94), S_B (UBC-97), and site class B (IBC-2000). Building height is 135 ft; the plan area is 100 by 170 ft as shown in Fig. P.10.4. Total dead load is 120 lb/ft² at each floor. Plot the story force distribution of the building. Use the importance factor $I=1.0$.
- 10.5. The moment diagram of a structural frame is shown in Fig. P.10.5. Using force distribution from Problem P.10.1, determine the shear effects due to torsion and lateral force at each floor. Shear due to accidental torsion was presented in Problem 10.2.

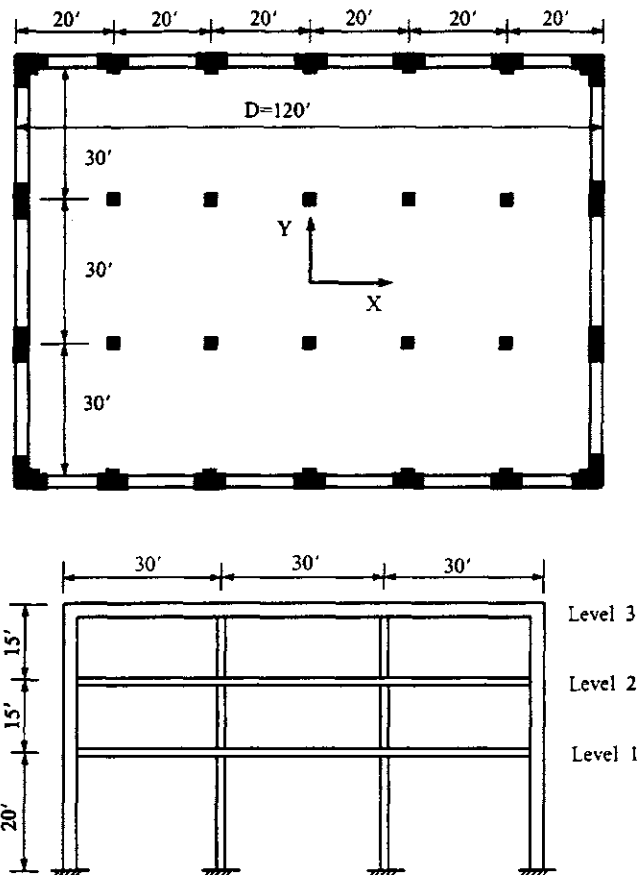


FIG. P.10.1 (a) Plan view. (b) Side view.

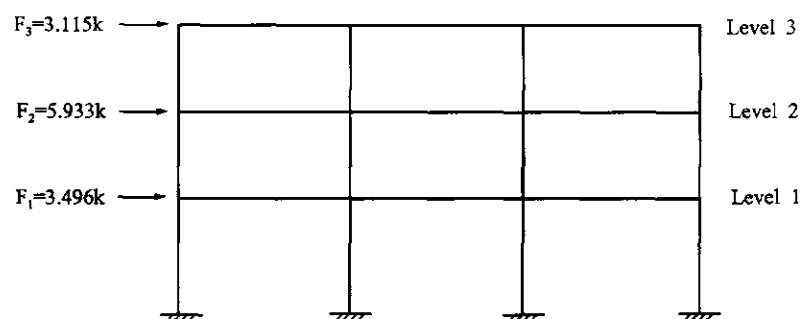


FIG. P.10.3

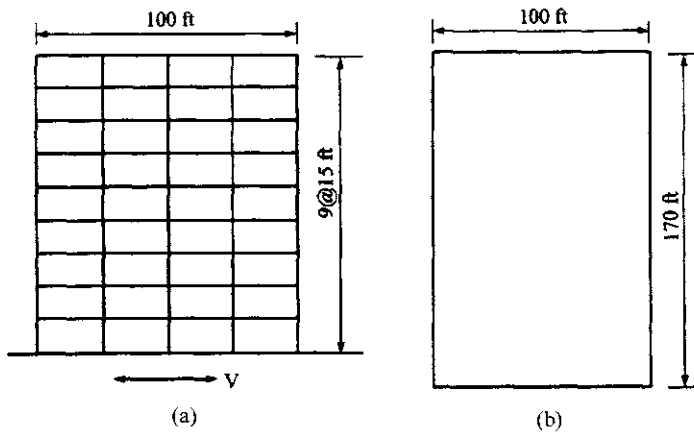


FIG. P.10.4 (a) Elevation. (b) Floor plan.

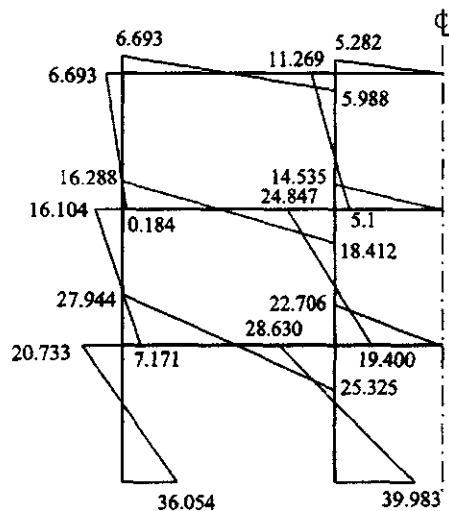


FIG. P.10.5

- 10.6. For the shear combination of accidental torsional moment and lateral force obtained from Problem 10.5, displacements at each level are $\delta_1 = 3635.041/EI_x$; $\delta_2 = 5987.401/EI_x$; $\delta_3 = 7096.814/EI_x$, for which $EI_x = 50206.25 \text{ k}/\text{ft}^2$. Check allowable drift and $P-\Delta$ effect for UBC-94, UBC-97 and IBC-2000.
- 10.7. A rigid floor plan in Fig. P.10.7 is subjected to a lateral force applied at the mass center of the floor. Column properties in the X direction are EI_x , EI_x , $2EI_x$, $2EI_x$ and $3EI_x$ for columns 1, 2, 3, 4 and 5. Column properties in the Y direction are EI_y for all columns. Find the shear force of the column 3 due to plane irregularities. All columns have a length of L , and $EI_y = 0.5 EI_x$.

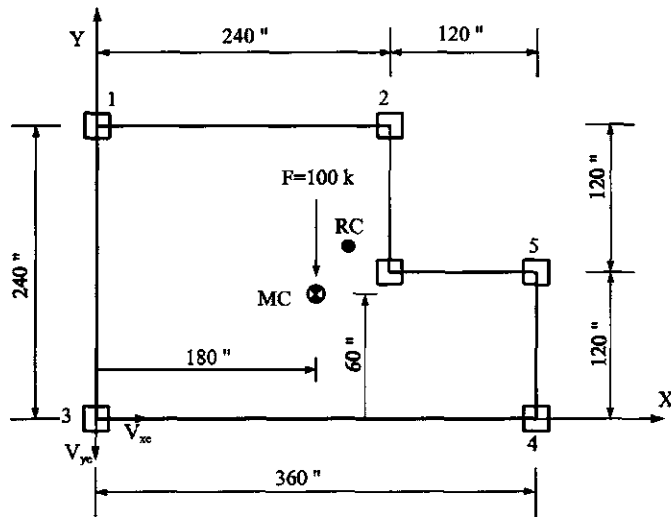


FIG. P.10.7

- 10.8. For the four-story shear building shown in Fig. P.10.8 with the masses, material properties, natural frequencies (periods), and response spectral values given below, find \bar{M}/M (for each mode) as well as displacements, member forces, and inertia forces. $E = 3.6(10)^3$ ksi; $I = 9677.7$ in 4 . (a) Natural frequency and period: $p_1 = 8.6933$ rad/sec; $p_2 = 25.78$ rad/sec; $p_3 = 40.599$ rad/sec; $p_4 = 50.469$ rad/sec; $T_1 = 0.723$ sec; $T_2 = 0.244$ sec; $T_3 = 0.154$ sec; $T_4 = 0.124$ sec. (b) Eigenvectors:

$$[X] = \begin{bmatrix} 0.462 & 1 & 1 & -0.536 \\ 0.723 & 0.748 & -0.617 & 1 \\ 0.909 & -0.189 & -0.832 & -0.973 \\ 1 & -0.953 & 0.843 & 0.470 \end{bmatrix}$$

(c) Response spectrum values: $S_d(p_1) = 1.19$ in; $S_d(p_2) = 0.155$ in; $S_d(p_3) = 0.0622$ in; $S_d(p_4) = 0.039$ in; $S_a(p_1) = 1.19p_1^2$; $S_a(p_2) = 0.15p_2^2$; $S_a(p_3) = 0.062p_3^2$; $S_a(p_4) = 0.039p_4^2$.

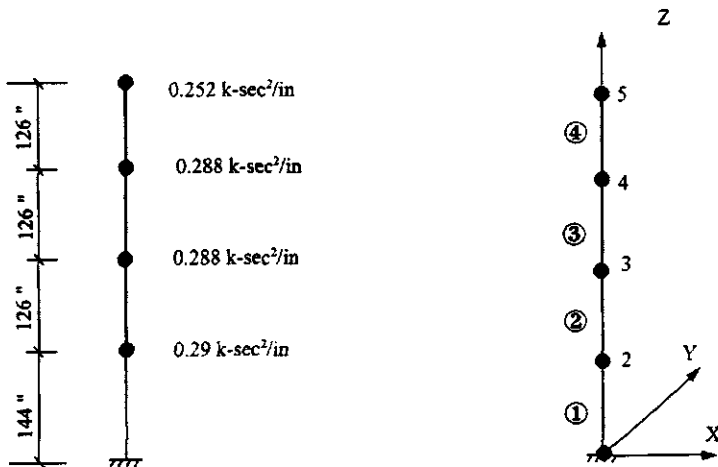


FIG. P.10.8

- 10.9. A two-story building with plane irregularities is shown in Fig. P.10.9. The column cross-section is 15×15 in. The story height is 12 ft. Diaphragms are rigid in their planes. Using Method B in this chapter's Section 10.8, determine the eccentricities between mass and rigidity centers. The floor supports a uniform load. Let $E = 29,000$ ksi.

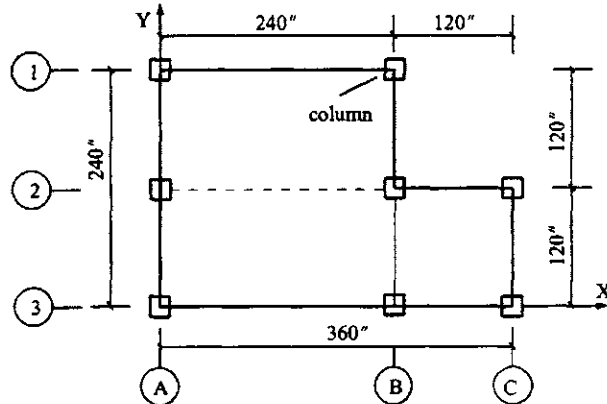


FIG. P.10.9

- 10.10. A two-story moment-resisting steel frame building is shown in Fig. P.10.10a. This structure, located in seismic zone 4 at Oakland, CA, is a storage facility for explosive chemicals. Use dynamic lateral-force analysis procedure (UBC-94 and UBC-97) and the given average spectra recorded at the site (see Fig. P.10.10b) to determine:

1. Significant modes for inclusion according to UBC.
2. Base shear and required scaling factor.
3. Distribution of lateral force at each floor.
4. Design displacement and drift.

Structural properties are $k_1 = k_2 = k = 2260$ k/ft, and $W_1 = W_2 = W = 450$ k. For UBC-94, the soil profile is type S₃. For UBC-97, the soil profile is S_c and the seismic source is 20 km from this building.

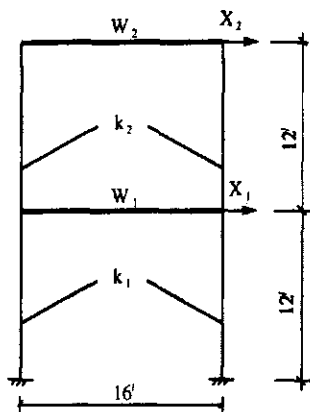


FIG. P.10.10a

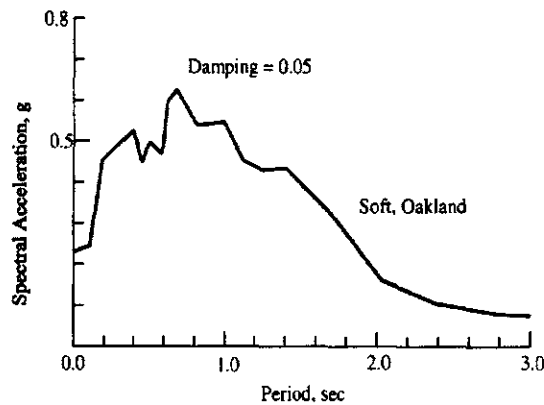


FIG. P.10.10b

10.11. A three-story moment-resisting steel frame building is located in Oakland, CA. This structure (see Fig. P.10.11a) has an importance factor of $I = 1.0$. Evaluation of the building site shows dense soil depth to be about 250 ft with soil shear-wave velocity $V_s = 1500$ ft/sec. The closest known seismic fault is 20 km away. Dimensions are shown in the figure. Structural properties are: (1) mass coefficients $m_1 = m_2 = m_3 = 1132.2141$ (lb sec²/ft); (2) natural frequencies $p_1 = 7.30916$, $p_2 = 23.58844$, $p_3 = 40.04150$ (rad/sec); (3) normal mode shapes $\{X\}_1 = [0.2555, 0.6752, 1.0]^T$, $\{X\}_2 = [0.9413, 1.0, -0.9421]^T$, $\{X\}_3 = [-0.4655, 1.0, -0.6895]^T$. For the site-specific response spectra shown in Fig. P.10.11b, use UBC-94, UBC-97 and IBC 2000 to determine:

1. Significant modes to be used.
2. Base shear by dynamic lateral force procedure.
3. Base shear by static lateral force procedure.
4. Design story shear distribution using site-specific response spectrum.
5. Design displacement and story drift ratios.

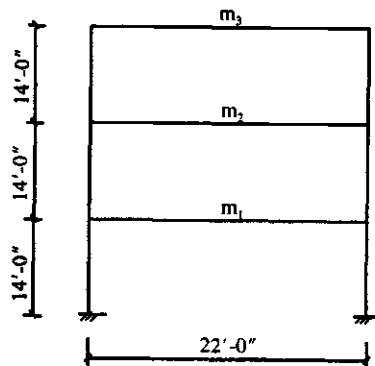


FIG. P.10.11a

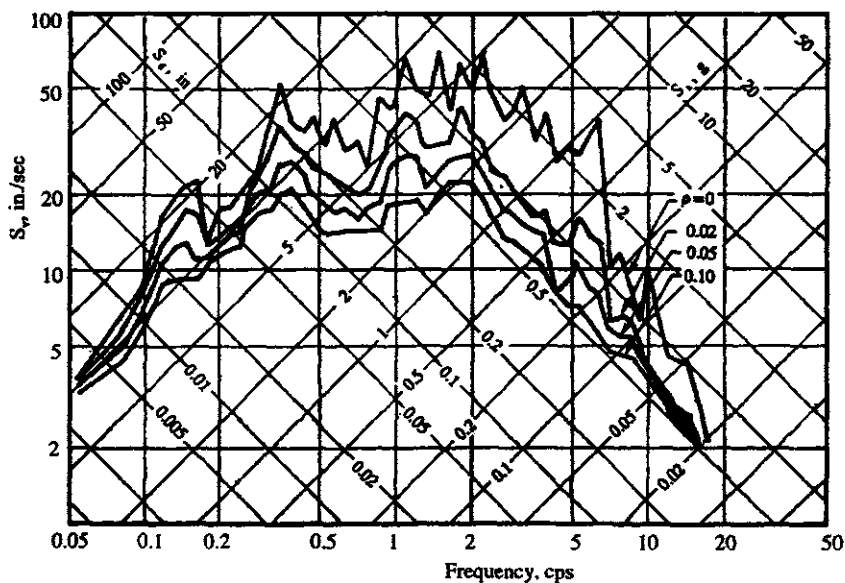


FIG. P.10.11b

Chapter 1 Solutions

1.1

$$f = \frac{1}{2\pi} \sqrt{\frac{2k}{3M}}$$

- 1.2. $T = 0.0141$ sec.
1.3. $f = 1.6$ cps; $T = 0.624$ sec.
1.4.

$$f = \frac{a}{2\pi b} \sqrt{\frac{K}{M}}$$

- 1.5. (a) $x = \cos 13.9t$; $\dot{x} = -13.9 \sin 13.9t$; (b) $\dot{x} = -13.9$ in./sec; $t = 0.113$ sec; (c) $x = \cos 13.9t$; $\dot{x} = -13.9 \sin 13.9t$
1.6. ($I_g = I$), $p = 129.20$ rad/sec; ($I_g = 4I$), $p = 154.94$ rad/sec; ($I_g = 8I$), $p = 163.33$; ($I_g = \infty$),
 $p = 175.4$ rad/sec
1.7. ($I_g = I$), $p = 157.10$ rad/sec; ($I_g = 4I$), $p = 186.29$ rad/sec; ($I_g = 8I$), $p = 195.04$ rad/sec;
($I_g = \infty$), $p = 206.15$ rad/sec.
1.9. 110.20 ksi (due to initial conditions); 10.82 ksi (due to beam weight).
1.10. (a) Uncoupling case (single-d.o.f. system); p (longitudinal) = 1392 rad/sec; p (torsional) = 2524 rad/sec, (b) Coupling case (two-d.o.f. system); $p_1 = 1451$ rad/sec;
 $p_2 = 2530$ rad/sec.
1.11. (a) At $t = 0.5$ sec, $x = 1.023$ in; $\dot{x} = -21.14$ in/sec. At $t = 1$ sec, $x = -0.45$ in; $\dot{x} = 86.73$ in/sec. (b) At $t = 0.5$ sec, $x = 0.01084$ in; $\dot{x} = -0.09175$ in/sec. At $t = 1$ sec, $x = 1.68110^{-6}$ in; $\dot{x} = -0.01016$ in/sec.

1.12. $\beta = 0.00322$; $\rho = 0.051\%$.

1.13. (a) $J\ddot{\theta} + c\dot{\theta} + (K + Ka^2)\theta = 0$; (b) $\beta = 0.2303$; (c) $\rho = 0.0366$.

1.14.

$$M_1 M_2 \ddot{x} + (M_1 + M_2)c\dot{x} + (M_1 + M_2)Kx = 0; p = \sqrt{\frac{(M_1 + M_2)K}{M_1 M_2}}; \rho = \frac{cp}{2K} = \frac{c}{2} \sqrt{\frac{M_1 + M_2}{M_1 M_2 K}}$$

1.15.

$$\ddot{x} + \frac{K_1}{c} \ddot{x} + \frac{K_1 + K}{M} \dot{x} + \frac{K_1 K}{Mc} x = 0; x = A e^{r_1 t} + B e^{r_2 t} + C e^{r_3 t}; r^3 + \frac{K_1}{c} r^2 + \frac{K_1 + K}{M} r + \frac{K_1 K}{Mc} = 0$$

1.16. 0.6685; 1.1294; 1.304.

1.17.

$$x_p = \frac{F}{K - M\omega^2} \sin \omega t$$

1.18. (a) $z = A \cos pt + B \sin pt - \frac{10 \sin \pi t}{p^2 - \pi^2}$; $p = 8.976$;
 (b) $\ddot{x}_{\max} = 15.35$ in/sec².

1.19. (a)

$$z = -\frac{X\omega^3}{p^3[1 - (\omega/p)^2]} \sin pt + \frac{X\omega^2}{p^2[1 - (\omega/p)^2]} \sin \dot{\omega}t$$

(b)

$$x = -\left[\frac{\omega X}{p} + \frac{MX\omega^3}{p(K - M\omega^2)} \right] \sin pt + \frac{X\omega^2}{p^2[1 - (\omega/p)^2]} \sin \omega t + X \sin \omega t$$

1.20. (a)

$$A_m = \left(\frac{t}{\zeta} - \frac{\sin pt}{p\zeta} \right), \quad 0 \leq t \leq \zeta; \quad A_m = 2 - \frac{t}{\zeta} + \frac{1}{p\zeta}[2 \sin p(t - \zeta) - \sin pt], \quad \zeta \leq t \leq 2\zeta$$

$$A_m = \frac{1}{\zeta p}[2 \sin p(t - \zeta) - \sin pt - \sin p(t - 2\zeta)]; \quad t \geq 2\zeta$$

(b) $A_m = 1 - \cos pt$; $0 \leq t \leq \zeta$, $A_m = 2 \cos p(t - \zeta) - \cos pt - 1$; $\zeta \leq t \leq 2\zeta$.
 $A_m = 2(1 - \cos p\zeta) \cos p(t - \zeta)$; $t \geq 2\zeta$.

(c)

$$A_m = \left(\frac{t}{\zeta} - \frac{\sin pt}{p\zeta} \right); \quad 0 \leq t \leq \zeta, A_m = \left[1 + \frac{1}{p\zeta}(\sin p(t - \zeta) - \sin pt) \right]; \quad \zeta \leq t \leq 2\zeta$$

$$A_m = 3 - \frac{t}{\zeta} + \frac{1}{p\zeta}[\sin p(t - 2\zeta) + \sin p(t - \zeta) - \sin pt]; \quad 2\zeta \leq t \leq 3\zeta$$

$$A_m = \frac{1}{p\zeta}[-\sin pt + \sin p(t - \zeta) + \sin p(t - 2\zeta) - \sin p(t - 3\zeta)]; \quad t \geq 3\zeta$$

1.21. 35.19 ksi.

1.22. (a) 40.3 k/in; (b) 0.249 ft; (c) 121.0 k.

1.23.

$$\begin{aligned}x &= \frac{F}{K\zeta} \left(\zeta - \frac{\sin p\zeta}{p} \right) \\x &= \frac{F}{K} \left(2 \cos p\zeta - \frac{\sin 2p\zeta}{p\zeta} \right) \\x &= \frac{F}{K} \left(2 \cos p\zeta - \frac{\sin 2p\zeta}{p\zeta} \right) \cos p\zeta + \frac{F}{Kp\zeta} (1 - \cos 2p\zeta - 2p\zeta \sin p\zeta) \sin p\zeta\end{aligned}$$

- 1.24. No frequency causes bending stress greater than F_b . Maximum displacements are $x_{\rho=0.05}=0.132$ in; $x_{\rho=0.1}=0.07$ in.
 1.25. $x=0.066$ in; $\sigma=4.832$ ksi.
 1.26.

$$\ddot{x} + \frac{k_1}{c}\ddot{x} + \frac{k_1+k}{M}\dot{x} + \frac{k_1k}{cM}x = \frac{k_1}{Mc}F \cos \omega t - \frac{\omega}{M}F \sin \omega t$$

Hint: use $x=A \cos \omega t + B \sin \omega t$ to find the following solution:

$$x = \frac{\frac{F}{M} \left[\frac{k_1}{M} \left(\frac{k_1k}{c^2} + \omega^2 \right) - \left(\frac{k_1^2}{c^2} - \frac{k}{M} + \omega^2 \right) \omega^2 \cos \omega t + \frac{k_1^2 \omega F}{M^2 c} \sin \omega t \right]}{\left(\frac{k_1 k}{M c} - \frac{k_1 \omega^2}{c} \right)^2 + \left[\frac{(k_1+k)\omega}{M} - \omega^3 \right]^2}$$

1.27.

$$\begin{aligned}\ddot{x} + \frac{k}{c}\ddot{x} + \frac{1}{M}(k+k_1)\dot{x} + \frac{kk_1}{cM}x &= -\frac{X\omega}{M}(k+k_1) \sin \omega t + \frac{kX}{cM}(k_1+k) \cos \omega t \\x &= \frac{\frac{k_1^2 X \omega}{c M^2} (k+k_1) \sin \omega t + \frac{X}{M} (k_1+k) \left[\left(\frac{k_1}{M} - \omega^2 \right) \left(\frac{k^2}{c^2} + \omega^2 \right) + \frac{k}{M} \omega^2 \right] \cos \omega t}{\left[\frac{kk_1}{cM} - \frac{k_1}{c} \omega^2 \right]^2 + \left[\frac{1}{M} (k+k_1) \omega - \omega^3 \right]^2}\end{aligned}$$

1.28.

$$A_f = F \sqrt{\frac{1 + (2\rho\omega/p)^2}{[1 - (\omega/p)^2]^2 + (2\rho\omega/p)^2}} = 5.004 k; \quad \beta = \tan^{-1} \frac{-2\rho(\omega/p)^3}{1 - (\omega/p)^2 + (2\rho\omega/p)^2} = 0.558 \text{ rad}$$

where $F=m_1\omega^2$ (stroke)=4.78 k.

- 1.29. $\rho=0.333$.
 1.30. $\rho=0.095$.
 1.31.

$$\begin{aligned}x &= \frac{x_{st}}{t_1} \left[e^{-\rho p t} \left(\frac{2\rho}{p} \cos p*t + \frac{2\rho^2 - 1}{p*} \sin p*t \right) + t - \frac{2\rho}{p} \right]; \quad t < t_1 \\x &= e^{-\rho(t-t_1)} (A \sin p*(t-t_1) + \beta \cos p*(t-t_1)); \quad t > t_1 \\A &= \frac{x_{st}}{p*t_1} \{ e^{-\rho p t_1} [(1+2\rho^2) \cos p*t_1 - 2p*\sin p*t_1] + \rho p t_1 - 2\rho^2 + 1 \} \\B &= \frac{x_{st}}{t_1} \left[e^{-\rho p t_1} \left(\frac{2\rho^2 - 1}{p*} \sin p*t_1 + \frac{2\rho}{p} \cos p*t_1 \right) - \frac{2\rho}{p} + t_1 \right]\end{aligned}$$

1.32. $p=\sqrt{g/\ell}$.

1.33.

$$p = \sqrt{\left(1 + \frac{2ka^2}{W\ell}\right)g/\ell}$$

1.34.

$$p = \sqrt{\left(\frac{2ka^2}{W\ell} - 1\right)g/\ell}$$

1.35.

$$p = \sqrt{\frac{(k_1 + k_2)b^2 + M_1 g \ell_1 - M_2 g \ell_2}{M_1 \ell_1^2 + M_2 \ell_2^2}}, \quad \text{if } M_2 \ell_2 = 2M_1 \ell_1,$$

$$\text{then } k_1 + k_2 = \frac{M_1 \ell_1 g}{b^2} \text{ for } p = 0$$

1.36. (a) $x = 45.829 \sin(pt + 1.353)$; (b) $x = 45.829 \cos(pt - 0.2176)$.

Chapter 2 Solutions

2.1. (a)

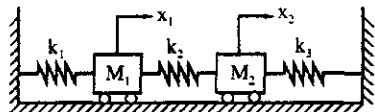


FIG. SOL. 2.1a

$$\begin{bmatrix} M_1 & 0 \\ 0 & M_2 \end{bmatrix} \begin{Bmatrix} \ddot{x}_1 \\ \ddot{x}_2 \end{Bmatrix} + \begin{bmatrix} k_1 + k_2 & -k_2 \\ -k_2 & k_1 + k_2 \end{bmatrix} \begin{Bmatrix} x_1 \\ x_2 \end{Bmatrix} = 0$$

(b)

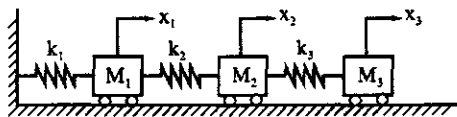
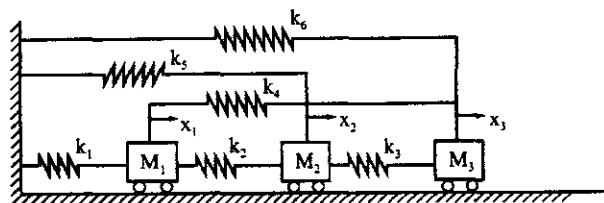


FIG. SOL. 2.1b

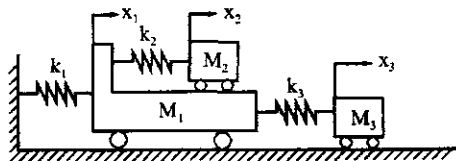
$$\begin{bmatrix} M_1 & 0 & 0 \\ 0 & M_2 & 0 \\ \text{symm} & & M_3 \end{bmatrix} \begin{Bmatrix} \ddot{x}_1 \\ \ddot{x}_2 \\ \ddot{x}_3 \end{Bmatrix} + \begin{bmatrix} k_1 + k_2 & -k_2 & 0 \\ \text{symm} & k_2 + k_3 & -k_3 \\ 0 & -k_3 & k_3 \end{bmatrix} \begin{Bmatrix} x_1 \\ x_2 \\ x_3 \end{Bmatrix} = 0$$

(c)

**FIG. SOL 2.1c**

$$\begin{bmatrix} M_1 & 0 & 0 \\ M_2 & 0 & 0 \\ \text{symm} & M_3 \end{bmatrix} \begin{Bmatrix} \ddot{x}_1 \\ \ddot{x}_2 \\ \ddot{x}_3 \end{Bmatrix} + \begin{bmatrix} k_1 + k_2 + k_4 & -k_2 & -k_4 \\ \text{symm} & k_2 + k_3 + k_5 & -k_3 \\ k_3 + k_4 + K_6 \end{bmatrix} \begin{Bmatrix} x_1 \\ x_2 \\ x_3 \end{Bmatrix} = 0$$

2.2.

**FIG. SOL. 2.2**

$$\begin{bmatrix} M_1 & 0 & 0 \\ M_2 & 0 & 0 \\ \text{symm} & M_3 \end{bmatrix} \begin{Bmatrix} \ddot{x}_1 \\ \ddot{x}_2 \\ \ddot{x}_3 \end{Bmatrix} + \begin{bmatrix} k_1 + k_2 + k_3 & -k_2 & -k_3 \\ \text{symm} & k_2 & 0 \\ k_3 \end{bmatrix} \begin{Bmatrix} x_1 \\ x_2 \\ x_3 \end{Bmatrix} = 0$$

2.3.

$$\begin{bmatrix} M_1 & 0 \\ 0 & M_2 \end{bmatrix} \begin{Bmatrix} \ddot{x}_1 \\ \ddot{x}_2 \end{Bmatrix} + \begin{bmatrix} \frac{6EI_1}{h^3} + k_a & -k_a \\ \text{symm} & \frac{6EI_2}{h^3} + k_a \end{bmatrix} \begin{Bmatrix} x_1 \\ x_2 \end{Bmatrix} = 0$$

2.4.

$$\begin{bmatrix} M & 0 & 0 \\ M & 0 & J \\ \text{symm} & J \end{bmatrix} \begin{Bmatrix} \ddot{x}_1 \\ \ddot{x}_2 \\ \dot{\theta} \end{Bmatrix} + \begin{bmatrix} k_3 & 0 & k_3 a_3 \\ \text{symm} & k_1 + k_3 & k_2 a_2 - k_1 a_1 \\ k_1 a_1^2 + k_2 a_2^2 + k_3 a_3^2 \end{bmatrix} \begin{Bmatrix} x_1 \\ x_2 \\ \theta \end{Bmatrix} = 0$$

2.5.

$$\begin{bmatrix} M & 0 & 0 \\ M & 0 & I \\ \text{symm} & I \end{bmatrix} \begin{Bmatrix} \ddot{x}_1 \\ \ddot{x}_2 \\ \ddot{x}_3 \end{Bmatrix} + \begin{bmatrix} k_1 + k_2 & 0 & 0 \\ \text{symm} & k_3 + k_4 & ak_3 - bk_4 \\ a^2 k_3 + b^2 k_4 \end{bmatrix} \begin{Bmatrix} x_1 \\ x_2 \\ x_3 \end{Bmatrix} = 0$$

2.6.

$$x_1 = \frac{0.276}{p_1} \sin p_1 t + \frac{0.724}{p_2} \sin p_2 t$$

$$x_2 = \frac{0.447}{p_1} \sin p_1 t - \frac{0.447}{p_2} \sin p_2 t$$

- 2.7. $p_1 = 30.279$ rad/sec; $p_2 = 107.256$ rad/sec; $f_1 = 4.819$ cycle/sec; $f_2 = 17.070$ cycle/sec;
 $T_1 = 0.207$ sec/cycle; $T_2 = 0.0586$ sec/cycle.

First natural mode

$$X_1^{(1)} = 0.795 X_2^{(1)}$$

Second natural mode

$$X_2^{(2)} = -0.636 X_1^{(2)}$$

First normal mode

$$\{X\}_1 = \begin{Bmatrix} 0.795 \\ 1.000 \end{Bmatrix}$$

Second normal mode

$$\{X\}_2 = \begin{Bmatrix} 1 \\ -0.636 \end{Bmatrix}$$

2.8. Case 1:

$$x_1 = 0.317 \cos p_1 t - 0.317 \cos p_2 t$$

$$x_2 = 0.399 \cos p_1 t + 0.202 \cos p_2 t$$

$$p_1 = 30.2788 \text{ rad/sec}; p_2 = 107.256 \text{ rad/sec}$$

Case 2:

$$x_1 = 0.973 \cos p_1 t + 0.027 \cos p_2 t$$

$$x_2 = 1.244 \cos p_1 t - 0.017 \cos p_2 t$$

Case 3:

$$x_1 = 0.209 \sin p_1 t - 0.059 \sin p_2 t$$

$$x_2 = 0.263 \sin p_1 t + 0.038 \sin p_2 t$$

2.9.

Case	x (in)	Time			
		1 sec	2 sec	3 sec	4 sec
1	x_1	-0.1534	-0.4062	-0.3825	0.0102
	x_2	0.3503	-0.130	-0.3356	-0.1046
2	x_1	0.4333	-0.6123	-0.9312	-0.1640
	x_2	0.4989	-0.8026	-1.1838	-0.1962
3	x_1	-0.2149	-0.2050	-0.0015	0.1483
	x_2	-0.2225	-0.1711	0.1070	0.2968

- 2.10. Both solutions are incorrect because

$$\{\Phi\}_1^T [M] \{\Phi\}_2 \neq 0$$

$$\{\Phi\}_1^T [M] \{\Phi\}_1 \neq [I]$$

$$\{\Phi\}_2^T [M] \{\Phi\}_2 \neq [I]$$

- 2.11. $p_2 = 4.854$ rad/sec

$$\{X\}_2^T = [1 \quad -0.618]$$

- 2.12. Same as given in Problem 2.8.

- 2.13. Same as given in Problem 2.9.

- 2.14. x_1 and x_2 are influenced by individual modes:

	t (sec)	0.1	0.2	0.3	0.4
x_1 (in)	First mode, $(\phi)_{11} x'_1$	0.29652	1.06044	2.08452	3.14544
	Second mode $(\phi)_{12} x'_2$	-0.07068	-0.19668	-0.23076	-0.1050
x_2 (in)	First mode, $(\phi)_{21} x'_1$	0.23328	0.83448	1.6404	2.47536
	Second mode $(\phi)_{22} x'_2$	0.08988	0.24984	0.29316	0.13333

- 2.15. (a) Superposition:

Displacement (ft)	First mode	First and second mode
x_1	0.4326	0.4128
x_2	0.3405	0.3656

- (b) Root-mean-square:

$$x_1 = 0.4330 \text{ ft}$$

$$x_2 = 0.3414 \text{ ft}$$

- 2.16. (a) Superposition:

Displacement (in)	First mode	First and second mode
x_1	13.5049	12.8621
x_2	10.6297	11.4477

- (b) Root-mean-square:

$$x_1 = 13.5202 \text{ in}$$

$$x_2 = 10.6611 \text{ in}$$

- 2.17. $x_{s1} = 0.0512$ ft; $x_{s2} = 0.0720$ ft; $P_f = 107.43$ k.

- 2.22. Hint: use $[M]^{-1}[K]\{X\} = p^2\{X\}$; assume $|p_1^2| > |p_2^2| \dots > |p_n^2|$. The

final result is

$$\frac{([M]^{-1}[K])^r}{p_1^{2r}} = [G_1] + \frac{p_2^{2r}}{P_1^{2r}}[G_2] + \dots + \frac{p_n^{2r}}{P_2^{2r}}[G_n]$$

Therefore p_1^2 is the largest that is the highest frequency.

- 2.23. $p_1 = 10.018$ rad/sec; $p_2 = 34.517$ rad/sec; $f_1 = 1.594$ cycles/sec; $f_2 = 5.493$ cycles/sec;
 $T_1 = 0.627$ sec; $T_2 = 0.182$ sec; $\{X\}_1^T = [0.136 \quad 1]$; $\{X\}_2^T = [1 \quad -0.068]$.
- 2.29. (a)

$$\begin{bmatrix} M_1 & 0 & 0 \\ 0 & M_2 & 0 \\ 0 & 0 & I_1 + I_2 \end{bmatrix} \begin{Bmatrix} \ddot{x}_1 \\ \ddot{x}_2 \\ \ddot{x}_3 \end{Bmatrix} + \begin{bmatrix} k_2 + k_2 & -k_2 & hk_2 \\ -k_2 & k_2 & -hk_2 \\ M_2g + hk_2 & -M_2g - hk_2 & k\theta \end{bmatrix} \begin{Bmatrix} x_1 \\ x_2 \\ x_3 \end{Bmatrix} = \begin{Bmatrix} M_1 \ddot{x}_g \\ 0 \\ 0 \end{Bmatrix}$$

(b)

$$\begin{bmatrix} I_1 + I_2 & \\ 0 & M_2 \end{bmatrix} \begin{Bmatrix} \ddot{x}_1 \\ \ddot{x}_2 \end{Bmatrix} + \begin{bmatrix} k_\theta & -k_2 h \\ -k_2 h & k_2 \end{bmatrix} \begin{Bmatrix} x_1 \\ x_2 \end{Bmatrix} = \begin{Bmatrix} 0 \\ 0 \end{Bmatrix}$$

- 2.30. $p_v = 31.804$ rad/sec; $\{X\}^T = [1 \quad -0.782 \quad -0.220]$; $p = 48.79$ rad/sec; $\{X\}^T = [1 \quad -0.782 \quad -0.220]$.
- 2.31. $p_1 = 0$; $\{X\}_1^T = 0.4082 [1 \quad 1 \quad 1]$; $p_2 = 15$ rad/sec; $\{X\}_2^T = 0.5 [1 \quad -1 \quad 0]$; $p_3 = 15$ rad/sec; $\{X\}_3^T = 0.5774 [-0.5 \quad -0.5 \quad 1]$.
- 2.32. Same as given in Example 2.6.4.

Chapter 3 Solutions

3.2.

$$\{x\} = [X] \left\{ \begin{bmatrix} e^{-\rho p t} (\cos p t + \rho \sin p t) \\ e^{-\rho p t} (\sin p t) \end{bmatrix} [\bar{M}]^{-1} [X]^T [M] \{x_0\} \right. \\ \left. + [p]^{-1} \begin{bmatrix} e^{-\rho p t} (\sin p t) \\ e^{-\rho p t} (-\cos p t) \end{bmatrix} [\bar{M}]^{-1} [X]^T [M] \{\dot{x}_0\} \right\}$$

3.3.

$$[M]\{\ddot{x}\} + [C]\{\dot{x}\} + [K]\} = \{0\}; \quad \{x\} = [x \quad y \quad \theta]^T$$

$$[M] = \begin{bmatrix} M & & \\ & M & \\ & & J \end{bmatrix}; \quad [K] = \begin{bmatrix} k_3 & 0 & k_3 d_3 \\ & k_1 + k_2 & k_1 d_1 - k_2 d_2 \\ \text{symm} & & k_1 d_1^2 + k_2 d_2^2 + k_3 d_3^2 \end{bmatrix}$$

$$[C] = \begin{bmatrix} c_2 & 0 & 0 \\ & c_1 & -c_1 d_4 \\ \text{symm} & & c_1 d_4^2 \end{bmatrix}$$

3.4. $\rho_1 = \rho_2 = 0.0559$.

3.5.

$$[C] = \begin{bmatrix} 0.41457 & -0.13820 \\ -0.13820 & 0.27638 \end{bmatrix}$$

3.8.

$$[C] = \begin{bmatrix} 0.76601 & -0.72288 & 0.24304 \\ & 1.00905 & -0.47984 \\ \text{symm} & & 0.28617 \end{bmatrix}$$

3.9.

$$[C] = \begin{bmatrix} 0.2913 & -0.11945 & -0.01404 \\ & 0.27726 & -0.13349 \\ \text{symm} & & 0.15781 \end{bmatrix}$$

3.10.

$$x_1/x_2 = 0.15385 + 0.76923i$$

$$x_2/x_2 = 1$$

$$\text{or } x_1/x_2 = \sqrt{8/13}e^{i(1.3734)}$$

$$x_2/x_2 = 1$$

3.11.

$$p_1 = |p_{1,2}| = \left| \frac{1}{\lambda_{1,2}} \right| = 0.618\sqrt{k/M}$$

$$p_2 = |p_{3,4}| = \left| \frac{1}{\lambda_{3,4}} \right| = 1.618\sqrt{k/M}$$

$$\{z\} = \begin{bmatrix} 0.270i & -0.270i & -0.707i & 0.707i \\ 0.437i & -0.437i & 1.144i & -1.144i \\ 0.618 & 0.618 & 1.0 & 1.0 \\ 1.0 & 1.0 & -0.618 & -0.618 \end{bmatrix} \{X\} = \begin{bmatrix} 0.618 & 1 \\ 1.0 & -0.618 \end{bmatrix}$$

3.12.

$$|\lambda[I] - [D]| = \lambda^4 + 1.2\lambda^3 + 3.11\lambda^2 + 0.7\lambda + 1. = 0$$

$$p_1 = \left| \frac{1}{\lambda_{1,2}} \right| = 0.619 \text{ rad/sec}$$

$$p_2 = \left| \frac{1}{\lambda_{3,4}} \right| = 1.615 \text{ rad/sec}$$

$$\{z\}_{1,2} = \begin{bmatrix} -0.1134 \mp 0.3738i \\ -0.2093 \mp 0.5826i \\ 0.6301 \pm 0.317i \\ 1.0 \end{bmatrix}$$

$$\{z\}_{3,4} = \begin{bmatrix} -0.1406 \mp 1.6090i \\ -0.0530 \pm 1.0275i \\ 1.0 \\ -0.6309 \mp 0.0881i \end{bmatrix}$$

$$\{x\} = \begin{bmatrix} 0.6301 & 1.0 \\ 1.0 & -0.6039 \end{bmatrix}$$

3.16.

$$I = \frac{1}{\alpha^2 + p^2} \left\{ \sin c [\alpha(a - bt) + b(\alpha^2 - p^2)] + \cos c [p(a - bt) + 2\alpha pb] - e^{-\alpha t} \left[SD \left(a\alpha + \frac{b(\alpha^2 - p^2)}{\alpha^2 + p^2} \right) + CD \left(ap + \frac{2\alpha pb}{\alpha^2 + p^2} \right) \right] \right\}$$

where $SD = \sin(pt + c)$, and $CD = \cos(pt + c)$.

Chapter 4 Solutions

4.1.

$$p_1 = \frac{3.51604}{L^2} \sqrt{\frac{EI}{m}}$$

$$p_2 = \frac{22.03448}{L^2} \sqrt{\frac{EI}{m}}$$

$$p_2/p_1 = 6.26685$$

$$M = 0.2426 \text{ m}\cdot\text{L}$$

4.2. Let $s = \sin \phi$; $s' = \sinh \phi$; $c = \cos \phi$; $c' = \cosh \phi$; and $\phi = L \sqrt[4]{(p^2 m/EI)}$. (A) For both ends hinged

$$\begin{bmatrix} SVY'_1 & SVY'_2 \\ SVY'_2 & SVY'_1 \end{bmatrix} = \begin{bmatrix} cs' - c's & s' - s \\ s' - s & cs' - c's \end{bmatrix} \frac{\phi^3 EI}{2s'sL^3}$$

(B) For i -end hinged and j -end restrained

$$\begin{Bmatrix} V_i \\ V_j \\ M_j \end{Bmatrix} = \begin{bmatrix} SVY''_1 & SVY''_2 & SV\theta''_1 \\ SVY'''_1 & SV\theta''_2 & SM\theta''_2 \\ \text{symm} & & \end{bmatrix} \begin{Bmatrix} Y_i \\ Y_j \\ \theta_j \end{Bmatrix}$$

$$\begin{aligned} SVY_1'' &= \frac{s^2 - s'^2 c}{(c'c - 1)(s'c - c's)} \frac{\phi^3 EI}{L^3} \\ SVY_2'' &= \frac{s^2 c' - s'^2 c}{(c'c - 1)(s'c - c's)} \frac{\phi^3 EI}{L^3} \\ SV\theta_1'' &= \frac{s' + s}{s'c - c's} \frac{\phi^2 EI}{L^2} \\ SVY_1''' &= \frac{-2c'c}{s'c - c's} \frac{\phi^3 EI}{L^3} \\ SV\theta_2'' &= \frac{c's + s'c}{s'c - c's} \frac{\phi^2 EI}{L^2} \\ SM\theta_2'' &= \frac{-2s's}{s'c - c's} \frac{\phi EI}{L} \end{aligned}$$

4.4.

$$\int_0^L xm\ddot{y}(x, t) dx = g(t) \frac{EI}{L} (-4.0646 + 2.4298 - 34.17697 + 32.5411) = -3.2707 \frac{EI}{L} g(t)$$

4.5.

$$\begin{aligned} p_n &= c_n \sqrt{\frac{EI}{m L^4}} \\ c_1 &= 1.57(2\pi) \\ c_2 &= 6.28(2\pi) \\ c_3 &= 14.1(2\pi) \end{aligned}$$

 $EI = \text{lb in}^2$; $m = \text{lb sec/in}^2$; and $L = \text{in}$.

4.6. The solutions are expressed in terms of member 1:

$$\begin{aligned} p_1 &= 13.486 \sqrt{\frac{EI_1}{m_1 L_1^4}} \\ p_2 &= 18.179 \sqrt{\frac{EI_1}{m_1 L_1^4}} \\ p_3 &= 23.532 \sqrt{\frac{EI_1}{m_1 L_1^4}} \end{aligned}$$

4.7. $\phi_2 = 3.24398$; $p_2 = 47.4898$ rad/sec. $[X_{\theta 1} \quad X_{\theta 2} \quad X_{\theta 3}]^T = [-0.4536 \quad 1 \quad -0.3156]^T$.4.8. $p = 31$ rad/sec;

$$\lambda = \sqrt{\frac{p^2 m_1}{EI}} = 0.1747$$

Let $\lambda x = x_1 = 0.1747x$, x is from joint A to joint B for member 1; the displacement is expressed as

$$Y_1(x) = -0.5450 \sin x_1 - 4.3727 \cos x_1 - 4.9342 \sinh x_1 + 4.3727 \cosh x_1$$

Find the displacements of $Y_1(x)$ by substituting the x 's at the 10 segments' nodes of the member from joints A to B . The results are:

Segments (ft)	1.5	3.0	4.5	6.0	7.5	9.0	10.5	12.0	13.5	15.0
$Y_1(x)$	-1.149	-1.777	-1.971	-1.824	-1.439	-0.925	-0.402	0.01	0.189	0.0

Using the same procedure yields the mode shapes of members 2 and 3.
 4.9. (A)

$$\text{At } x = 0; \quad V_1 = 0; \quad M_1 = \frac{wL^2}{\phi^2} (s - s') / (cs' + sc')$$

$$\text{At } x = L; \quad V_2 = -\frac{wL^2}{\phi} (2ss') / (cs' + sc'); \quad M_2 = \frac{wL^2}{\phi^2} (sc' - s'c) / (s'c + c's)$$

where $\phi = \sqrt[4]{[(\omega^2 m)/EI]L}$; $s' = \sinh \phi$; $s = \sin \phi$, $c' = \cosh \phi$; and $c = \cos \phi$.
 4.10.

$$\begin{Bmatrix} M_1 \\ M_2 \\ M_3 \\ M_4 \end{Bmatrix} = \begin{Bmatrix} 19.316 \\ 25.773 \\ -25.773 \\ 0 \end{Bmatrix}_{\phi_1=2.8} \text{ ft k}$$

$$\begin{Bmatrix} V_1 \\ V_2 \\ V_3 \\ V_4 \end{Bmatrix} = \begin{Bmatrix} -6.3296 \\ -1.889 \\ 17.7987 \\ -13.1202 \end{Bmatrix}_{\phi_1=2.8} \text{ k}$$

4.11. When $\phi_1 = \pi$, member 1

$$Y(x) = -1463.361 \frac{FL^3}{EI} \sin \frac{\pi}{L} x; \quad x \text{ is from } A \text{ to } B$$

member 2

$$Y(x) = 1463.361 \frac{FL^3}{EI} \sin \frac{\pi}{L} x; \quad x \text{ is from } B \text{ to } C$$

4.12.

$$[X_1 \quad X_2 \quad X_3]^T = [-0.018197 \quad -0.018197 \quad -2.697368]^T$$

$$[M_1 \quad M_2 \quad M_3 \quad M_4 \quad M_5 \quad M_6] = [0.8757 \quad 0.4207 \quad -0.4207 \quad -0.4207 \quad 0.4207 \quad 0.8757]$$

$$[V_1 \quad V_2 \quad V_3 \quad V_4 \quad V_5 \quad V_6] = [-0.01616 \quad -0.005245 \quad 0.002511 \quad 0.002511 \quad -0.005245 \quad -0.01616]$$

4.13. $\ddot{q}_1 + (g/q_2) \sin q_1 = 0$.

4.14. For the general case of elastic support, k_s and k_θ are linear and rotational springs, respectively; then $d/dx(EIY'') = \mp k_s Y$, $EIX'' = \pm k_\theta Y'$ from the first term of the right-hand side of Eqs. (4.128),

$$[Y_m(EIY_k'')' - Y_m'(EIY_k'')]_0^L = k_s Y_k(L)Y_m(L) + k_\theta Y_m'(L)Y_k'(L) + k_s Y_k(0)Y_m(0) + k_\theta Y_k'(0)Y_m'(0)$$

which leads to the conclusion resulting from Eqs. (4.131) and (4.132).

4.15.

$$V(x, t) = 0.05628\lambda_1^3 EIA_1(t) \cos \lambda_1 x + 0.0021897\lambda_2^3 EIA_2(t) \cos \lambda_2 x \\ - 0.00043\lambda_3^3 EIA_3(t) \cos \lambda_3 x$$

$$A_k(t) = 1 - \cos p_k t + \frac{\sin p_k t}{p_k \zeta} - \frac{t}{\zeta}$$

$$[p_1 \quad p_2 \quad p_3] = [53 \quad 212 \quad 477]$$

$$y(x, t) = 0.056280 A_1(t) \sin \lambda_1 x + 0.0021897 A_2(t) \sin \lambda_2 x - 0.00043 A_3(t) \sin \lambda_3 x$$

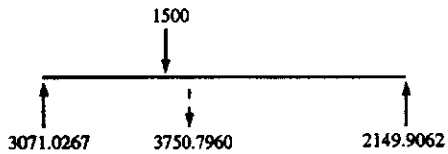


FIG. SOL. 4.15

$$\Sigma F_y = 5250.7960 - 5220.9329 = 29.8631 \text{ lb}$$

4.16. The solutions are based on Fourier series technique:

(a)

$$y(x, t) = \frac{F}{m} \sum \left[\cos(4n-1) \frac{\pi}{8} - \frac{\cos(4n-1)\pi/4}{\cosh(4n-1)\pi/4} \cosh(4n-1) \frac{\pi}{8} \right] (DLF)_n \phi_n(x) / (p_n^2 B_n)$$

$$\phi_n(x) = \cos(4n-1) \frac{\pi x}{4L} - \frac{\cos(4n-1)\pi/4}{\cosh(4n-1)\pi/4} \cosh(4n-1) \frac{\pi x}{4L}; \quad p_n = \left(\frac{4n-1}{4} \right)^2 \pi^2 \sqrt{\frac{EI}{mL^4}}$$

$$B_n = \frac{L}{2} + \frac{L}{(4n-1)\pi} \left[1 - 2 \tanh(4n-1) \frac{\pi}{4} \right] + \frac{L}{2 \cosh^2(4n-1)} \frac{\pi}{4} \left[\frac{\sin(4n-1)\pi}{(4n-1)\pi} + \frac{1}{2} \right]$$

$$DLF_n \text{ (amplification factor)} = 1 - \cos p_n t + \frac{\sin p_n t}{p_n \zeta} - \frac{t}{\zeta}; \quad \text{for } f(t) = 1 - \frac{t}{\zeta}$$

(b)

$$y(x, t) = \frac{F}{m} \sum_{n=1}^{\infty} \left[\cos(4n-1) \frac{a\pi}{4} - \frac{\cos(4n-1)a\pi/4}{\cosh(4n-1)a\pi/4} \cosh(4n-1)a\pi/4 \right] (DLF)_n \phi_n(x) / (p_n^2 B_n)$$

(c)

$$y(x, t) = \frac{F}{m} \sum_{n=1}^{\infty} \left[\cos(4n-1)\pi/16 - \cos(4n-1)3\pi/16 - \frac{\cos(4n-1)\pi/4}{\cosh(4n-1)\pi/4} \right. \\ \left. + [\cosh(4n-1)\pi/16 + \cosh(4n-1)3\pi/16] \frac{(DLF)_n \phi_n(x)}{p_n B_n} \right]$$

(d)

$$y(x, t) = \frac{4Lw}{m\pi} \sum_{n=1}^{\infty} \left[\sin(4n-1) \frac{\pi}{4} - \frac{\cos(4n-1)\pi/4}{\cosh(4n-1)\pi/4} \sinh(4n-1)\pi/4 \right] \frac{(DLF)_n \phi_n(x)}{p_n^2 B_n (4n-1)}$$

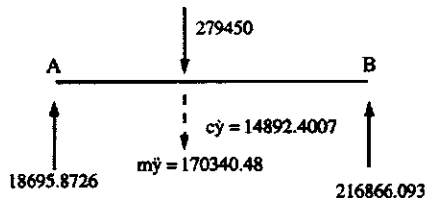


FIG. SOL. 4.18

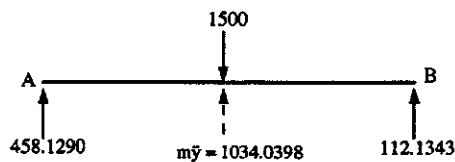


FIG. SOL. 4.19

(e)

$$y(x, t) = \frac{4Lw}{m\pi} \sum_{n=1}^{\infty} \left[\sin(4n-1)\frac{\pi}{16} - \frac{\cos(4n-1)\pi/4}{\cosh(4n-1)\pi/4} \sinh(4n-1)\pi/16 \right] \frac{(DLF)_n \phi_n(x)}{P_n^2 B_n (4n-1)}$$

4.17. $y(7.5 \text{ ft}) = 0.0978 \text{ (first mode)} + 0.0125 \text{ (second mode)} + 3.212410^{-4} \text{ (third mode)} = 0.1106 \text{ in}$

$$\begin{aligned} M(7.5 \text{ ft}) &= 2.31 \text{ (first mode)} + 6.318 \text{ (second mode)} + 0.4535 \text{ (third mode)} \\ &= 8.9015 \text{ ft k} \end{aligned}$$

$$\begin{aligned} V(7.5 \text{ ft}) &= -2788.70 \text{ (first mode)} + 874.13 \text{ (second mode)} - 609.79 \text{ (third mode)} \\ &= -2524.36 \text{ lbs} \end{aligned}$$

4.18. (A) $M_2 = -M_3 = -2998.3523 \text{ ft k}$

(B) (see Fig. Sol. 4.18)

$$\begin{aligned} \Sigma F_y &= 279,450 + 171,124.77 + 14,892.4007 - 185,695.8726 - 216,866.093 \\ &= 465,467.1707 - 402,581.9656 = 62,885.205 \end{aligned}$$

Note: $62,885.205 / 465,467.1707 = 0.135$ (this error is due to neglecting the modes higher than the fourth)

4.19. The first five modes yield the following equilibrium check (see Fig. Sol. 4.19):

$$\Sigma F_y = 1604.3031 - 1500 = 104.3031 \text{ lb}$$

Considering the first four modes, we have

$$\Sigma F_y = 1500 - 895.1914 - 478.2249 - 549.1967 = -422.6130$$

Note: the third mode does not affect the response results.

4.20. $\{P\} \cos \omega t$ and $\{P\} e^{i\omega t}$ can be treated as equivalent to undamped vibration and $\{x\} = (-\omega^2[M] + [K])^{-1}\{P\}$. These two functions are not equivalent to damped vibration; for $\{P\} e^{i\omega t}$, $\{x\} = [\tilde{K}(\omega)]^{-1}\{P\}$ in which $\tilde{K}(\omega) = -\omega^2[M] + i\omega[C] + [K]$ is frequency domain.

Chapter 5 Solutions

5.1.

$$[K] = \begin{bmatrix} SNU_{11} + SNU_{12} & SNU_{22} \\ SNU_{22} & SNU_{12} \end{bmatrix}$$

5.2.

$$\{p\} = [660.7256 \quad 1982.1768 \quad 3303.6281 \quad 4625.0793 \quad 5946.5306]^T$$

5.3.

$$\{p\} = [1545.0594 \quad 4051.3851 \quad 6660.3155 \quad 9288.2305 \quad 11922.7282]^T$$

5.4. $X_A = 3.23977 \times 10^{-4}$ m; $N_B = -134.39578$ kN

5.5.

$$[K] = \begin{bmatrix} c^2(SVY'_{11} + SVY'_{13}) + SNU_{12} & sc(SNU_{11} - SNU_{13} - SVY'_{11} + SVY'_{13}) \\ +s^2(SNU_{11} + SNU_{13}) & \text{symm} \end{bmatrix}$$

$$s^2(SVY'_{11} + SVY'_{13}) + SVY'_{12} \\ +c^2(SNU_{11} + SNU_{13})$$

$$s = \sin \theta_1 = \sin \theta_3; \quad c = \cos \theta_1 = \cos \theta_3; \quad \theta_1 = \theta_3$$

- 5.6. When flexural frequency is not considered, then

$$[K] = \begin{bmatrix} s^2(SNU_{11} + SNU_{13}) + SNU_{12} & 0 \\ 0 & c^2(SNU_{11} + SNU_{13}) \end{bmatrix}$$

Let p' represent coupling longitudinal and flexural frequencies of (A) and p represent longitudinal frequencies of (B); the numerical results are tabulated as

Mode	$L/R = 20$		$L/R = 60$		$L/R = 100$	
	p	p'	p	p'	p	p'
1	44151.2	13676.1	14717.1	1539.10	8830.2	554.5
2	132453.0	40765.5	44151.2	6123.9	26490.7	2214.4
3	220754.0	57816.3	73585.1	13084.9	44151.1	4962.4
4	309058.0	124092.0	103019.0	15169.4	61811.6	9276.9

- 5.7. The stiffness of the shaft $K_t = (\pi d^4 G)/32L$. The polar mass moment of inertia of the disk $I = (\gamma h \pi D^4)/32g$

$$p = \sqrt{K_t/I}$$

- 5.8. $p = \sqrt{K_t(I_1 + I_2)/I_1 I_2}$
 5.9. (A)

$$[K] = \begin{bmatrix} K_{11} & K_{12} & K_{13} & K_{14} \\ & K_{22} & K_{23} & K_{24} \\ & & K_{33} & K_{34} \\ \text{symm} & & & K_{44} \end{bmatrix}$$

$$K_{11} = c^2(SM\theta_{11} + SM\theta_{13}) + s^2(ST\gamma_{11} + ST\gamma_{13}) + ST\gamma_{12}$$

$$K_{12} = sc(SM\theta_{11} + SMY_{13}) - sc(ST\gamma_{11} + ST\gamma_{13})$$

$$K_{13} = c(SMY_{11} - SMY_{13})$$

$$K_{14} = cSM_{23}$$

$$K_{22} = s^2(SM\theta_{11} + SM\theta_{13}) + c^2(ST\gamma_{11} + ST\gamma_{13}) + SM\theta_{12}$$

$$K_{23} = s(SMY_{11} - SMY_{13}) + SMY_{12}$$

$$K_{24} = sSM\theta_{23}; \quad K_{33} = SVY_{11} + SVY_{12} + SVY_{13}; \quad K_{34} = -SMY_{23};$$

$$K_{44} = SM\theta_{13}$$

$$s = \sin \alpha; \quad c = \cos \alpha$$

(B) Use

$$ST\gamma_{11} = \frac{GJ_1}{L_1}, \quad ST\gamma_{12} = \frac{GJ_2}{L_2}, \quad ST\gamma_{13} = \frac{GJ_3}{L_3}$$

in (A); then [K] is composed of dynamic flexural stiffness and static torsional stiffness.
 (C) Let $ST\gamma_{11} = ST\gamma_{12} = ST\gamma_{13} = 0$ in (A); then [K] becomes dynamic flexural stiffness matrix.

- 5.10. Let p be the frequency due to bending only, p' be the frequency due to coupling dynamic torsional and flexural stiffness, and p'' due to dynamic flexural and static torsional stiffness; the solutions are tabulated as:

Mode	Frequency		
	p	p'	p''
1	54.43	58.11	58.11
2	150.24	159.74	159.77
3	290.56	293.94	293.99

- 5.11. Let p be the frequency due to bending only; p' be the frequency due to coupling bending and torsion; the solutions are tabulated as:

Mode	$L/R = 10$			$L/R = 20$			$L/R = 30$		
	p	p'	p'/p	p	p'	p'/p	p	p'	p'/p
1	1877.96	1844.76	0.98	571.47	565.67	0.99	269.67	267.73	0.99
2	3481.55	3203.54	0.92	870.39	870.92	1.00	386.84	391.64	1.01
3	4570.44	4371.91	0.96	1182.03	1201.63	1.02	534.68	545.51	1.02
4	5083.78	4742.41	0.93	1270.95	1284.27	1.01	564.87	573.37	1.02
5	6951.60	5146.66	0.78	2227.11	2300.56	1.03	1061.88	1064.98	1.00
$L/R = 40$			$L/R = 50$			$L/R = 60$			
Mode	p	p'	p'/p	p	p'	p'/p	p	p'	p'/p
	156.16	155.29	0.99	101.68	101.21	0.99	71.41	71.14	0.99
1	217.60	221.12	1.02	139.26	141.76	1.02	96.71	98.54	1.02
2	304.00	310.33	1.02	195.97	200.04	1.02	136.80	139.62	1.01
3	317.74	322.97	1.02	203.35	206.82	1.02	141.22	143.68	1.02
4	617.72	618.22	1.00	403.21	403.29	1.00	283.66	283.65	1.00

- 5.12. The stiffness coefficients are the same as given in Eq. (5.84) with $\lambda^4 = mp^2/EI$ because $q=0$.

- 5.14. For $b^2r^2s^2 \leq 1$

$$M_{0i} = \frac{WL^2b}{D_2} \left[\frac{-b(\alpha^2 + s^2)(\beta^2 - s^2)(\alpha^2 + \beta^2)(c' - c)}{\alpha\beta} + \frac{(\alpha^2 + s^2)(\alpha^2 + \beta^2)(1 - c)n'}{\alpha(1 - b^2r^2s^2)} \right. \\ \left. - \frac{(\beta^2 - s^2)(\alpha^2 + \beta^2)(1 - c')n}{\beta(1 - b^2r^2s^2)} \right]$$

$$M_{0j} = \frac{WL^2b}{D_2} \left[\frac{b(\alpha^2 + s^2)(\beta^2 - s^2)(r^2 - s^2)(1 - cc')}{\alpha\beta} \right. \\ \left. + \frac{b(\alpha^2 + s^2)(\beta^2 - s^2)(2 - b^2r^2s^2 + b^2s^4)nn'}{1 - b^2r^2s^2} \right. \\ \left. + \frac{(\alpha^2 + s^2)(\alpha^2 + \beta^2)(1 - c)n'}{\alpha(1 - b^2r^2s^2)} - \frac{(\beta^2 - s^2)(\alpha^2 + \beta^2)(1 - c')n}{\beta(1 - b^2r^2s^2)} \right]$$

$$V_{0i} = \frac{WL}{s^2 D_2} \left[\frac{-bs^2(\alpha^2 + s^2)(\alpha^2 + \beta^2)n}{\alpha^2\beta} - \frac{bs^2(\beta^2 - s^2)(\alpha^2 + \beta^2)n'}{\alpha\beta^2} + \frac{(2 - b^2s^2r^2 + b^2s^4)s^2nn'}{(1 - b^2r^2s^2)^2} \right. \\ \left. + \frac{\alpha(\beta^2 - s^2)(c' - 1)(c + 1)}{\alpha(1 - b^2r^2s^2)} - \frac{2(\alpha^2 + s^2)(\beta^2 - s^2)(cc' - 1)}{\alpha\beta(1 - b^2r^2s^2)} + \frac{\beta(\alpha^2 + s^2)(c' + 1)(c - 1)}{\alpha(1 - b^2r^2s^2)} \right] \\ + \frac{WLr^2}{1 - b^2r^2s^2}$$

$$V_{0j} = \frac{WL}{s^2 D_2} \left[\frac{-bs^2(\alpha^2 + s^2)(\alpha^2 + \beta^2)nc'}{\alpha^2\beta} - \frac{bs^2(\beta^2 - s^2)(\alpha^2 + \beta^2)cn'}{\alpha\beta^2} \right. \\ \left. + \frac{s^2(2 - b^2s^2r^2 + b^2s^4)nn'}{(1 - b^2r^2s^2)^2} + \frac{\alpha(\beta^2 - s^2)(c' - 1)(c + 1)}{\beta(1 - b^2r^2s^2)} - \frac{\beta(\alpha^2 + s^2)(c' + 1)(c - 1)}{\beta(1 - b^2r^2s^2)} \right. \\ \left. - \frac{2(\alpha^2 + s^2)(\beta^2 - s^2)(cc' - 1)}{\alpha\beta(1 - b^2r^2s^2)} \right] + \frac{WLr^2}{1 - b^2r^2s^2}$$

in which

$$D_2 = \frac{b^2(\alpha^2 + s^2)(\beta^2 - s^2)D_1}{\alpha\beta}$$

5.16. Three modes:

$$M_A = 16,074,249.62 \text{ in lb}; \\ M_B = -29,154,267.98 \text{ in lb}; \\ V_B = -490,048.238 \text{ lb};$$

Four modes:

$$M_A = 15,938,417.05 \text{ in lb}; \\ M_B = -29,346,361.65 \text{ in lb};$$

$$V_B = -505,135.307 \text{ lb};$$

$$\begin{aligned} F &= \sum_{i=1}^4 \int_0^L Y_{sti} \ddot{A}_i Y_i(x) dx \\ &= -351,527.638 \text{ lb} \\ P &= F(x, t)L = 169,366.5 \text{ lb} \\ \Sigma F_y &= V_B - P - F = 15,758.831 \text{ lb} \end{aligned}$$

Five modes:

$$\begin{aligned} M_A &= 15,902,849.86 \text{ in lb} \\ M_B &= -29,296,060.03 \text{ in lb} \\ V_B &= -500,131.453 \text{ lb} \end{aligned}$$

$$\begin{aligned} F &= \sum_{i=1}^5 \int_0^L Y_{sti} \ddot{A}_i Y_i(x) dx \\ &= -343,480.576 \text{ lb} \\ P &= F(x, t)L = 169,366.5 \text{ lb} \\ \Sigma F_y &= V_B - P - F = 12,751.62 \text{ lb} \end{aligned}$$

5.17.

$$\begin{aligned} Y_A &= 15.7387 \text{ in} \\ M_A &= 15,771,439.5 \text{ in lb} \\ M_B &= -24,689,524.24 \text{ in lb} \\ V_B &= -374,006.56 \text{ lb} \end{aligned}$$

5.19.

$$[K] = \begin{bmatrix} c^2 SVY'_{11} + c'^2 SVY'_{12} + s^2 SNU_{11} + s' SNU_{12} & -sc SVY'_{11} + s'c' SVY'_{12} + sc SNU_{11} - s'c' SNU_{12} \\ \text{symm} & s^2 SVY'_{11} + s'^2 SVY'_{12} + c^2 SNU_{11} + c'^2 SNU_{12} \end{bmatrix}$$

where $s = \sin \alpha$; $c = \cos \alpha$; $s' = \sin \beta$; $c' = \cos \beta$. Let p be the frequencies based on SNU only, p' be the frequencies based on SVY' and SNU , and p'' be the frequencies based on SVY' and AE/L (to replace SNU); the solutions are tabulated as:

$\alpha = \beta$ $= 45^\circ$	Mode	$L/R = 20$				$L/R = 60$				$L/R = 100$			
		p	p'	p''	p''/p'	p	p'	p''	p''/p'	p	p'	p''	p''/p'
$\alpha = 30^\circ$ $\beta = 60^\circ$	1	6098.7	1865.0	1868.9	1.00	2032.9	212.3	1.00	1219.7	76.6	76.6	1.00	
	2	18296.1	5312.0	6853.4	1.29	6098.7	842.1	1.00	3659.2	305.3	305.3	1.00	
	3	30493.5	8186.6	13225.2	1.62	10164.5	1738.8	1.07	6098.7	681.0	683.5	1.00	
	4	42690.9	15793.6	22088.8	1.40	14230.3	2123.2	1.52	8538.2	1108.7	1205.5	1.09	
	5	54888.2	19103.6	35597.2	1.86	18296.1	3434.8	1.41	10977.7	1299.2	1861.7	1.43	
$\alpha = 30^\circ$ $\beta = 60^\circ$	1	6098.7	1888.7	1888.7	1.00	2032.9	212.5	1.00	1219.7	76.6	76.6	1.00	
	2	10563.2	5606.7	5606.8	1.00	3521.1	636.7	1.00	2112.6	229.7	229.7	1.00	
	3	18296.0	7201.3	7201.6	1.00	6098.7	846.1	1.00	3659.2	305.8	305.9	1.00	
	4	30493.2	14659.0	14665.1	1.00	10164.4	1877.8	1.01	6098.6	685.8	686.2	1.00	
	5	31689.5	20523.3	20560.2	1.00	10563.2	1991.0	1.27	6337.9	912.2	916.0	1.00	

5.20.

Case A			Case B		
ϕ_1	p' (rad/sec)	Normal modes $X_{\theta 1}, X_{\theta 2}, X_{sl}$	ϕ_1	p (rad/sec)	Normal modes $X_{\theta 1}, X_{\theta 2}, X_{sl}$
3.422349	45.574	-0.117	3.378601	44.4165	-0.127
		0.032			0.036
		1.000			1.000
4.893443	93.196	0.097	4.874966	92.4718	0.106
		0.150			0.187
		1.000			1.000
5.665379	124.890	-0.011	5.609432	122.4356	-0.007
		-0.350			-0.360
		1.000			1.000

Chapter 6 Solution

6.1.

$$p^2 - \left(1 + \frac{M_2}{M_1}\right) \frac{g}{L_1 L_2} [(L_1 + L_2)p^2 - g] = 0$$

6.2.

$$\begin{aligned} U &= \frac{1}{2}k_2x_2^2 + \frac{1}{2}k_1(x_2 - x_1)^2 \\ T &= \frac{1}{2} \begin{Bmatrix} \dot{x}_1 \\ \dot{x}_2 \end{Bmatrix}^T \begin{bmatrix} M_1 & 0 \\ 0 & M_2 \end{bmatrix} \begin{Bmatrix} \dot{x}_1 \\ \dot{x}_2 \end{Bmatrix} \\ D &= \frac{1}{2} \begin{Bmatrix} \dot{x}_1 \\ \dot{x}_2 \end{Bmatrix}^T \begin{bmatrix} c_1 & 0 \\ 0 & c_2 \end{bmatrix} \begin{Bmatrix} \dot{x}_1 \\ \dot{x}_2 \end{Bmatrix} \end{aligned}$$

- 6.3. (A) $p_1 = 512.9$ rad/sec; $p_2 = 694.6$ rad/sec; $\{X\}_1 = [0.1069 \quad 1]^T$; $\{X\}_2 = [1. \quad -0.1057]^T$. (B)
 $p_1 = 557.0$ rad/sec; $p_2 = 743.0$ rad/sec; $\{X\}_1 = [0.0703 \quad 1.0]^T$; $\{X\}_2 = [1.0 \quad -0.0447]^T$.
- 6.6. $M_1 = 2.5155 \text{ k sec}^2/\text{ft}$; $M_2 = M_3 = 0.8385 \text{ k sec}^2/\text{ft}$; $p_1 = 40.625$ rad/sec; $p_2 = 45.042$ rad/sec; $p_3 = 97.616$ rad/sec.

$$X = \begin{bmatrix} 0 & 1 & 0.0199 \\ 1 & -0.0298 & 1.0 \\ 1 & 0.0298 & -1.0 \end{bmatrix}$$

6.7. $M_1 = 0.9689 \text{ k sec}^2/\text{ft}$; $M_2 = 1.2052 \text{ k sec}^2/\text{ft}$; $M_3 = 1.4415 \text{ k sec}^2/\text{ft}$; $p_1 = 10.148 \text{ rad/sec}$; $p_2 = 24.0709 \text{ rad/sec}$; $p_3 = 42.4281 \text{ rad/sec}$.

$$[X] = \begin{bmatrix} 1.00 & -1.00 & 0.4851 \\ 0.8045 & 0.4698 & -1.000 \\ 0.4143 & 0.8595 & 0.8364 \end{bmatrix}$$

6.8. The motion equation in matrix form is

$$\begin{bmatrix} 0 & | & & & \\ 0 & | & & & \\ - & - & - & - & - \\ | & M_3 & & & \\ | & & M_4 & & \\ | & & & M_5 & \end{bmatrix} \begin{Bmatrix} \ddot{x}_1 \\ \ddot{x}_2 \\ \ddot{x}_3 \\ \ddot{x}_4 \\ \ddot{x}_5 \end{Bmatrix} + \begin{bmatrix} \frac{4EI}{L} & \frac{2EI}{L} & | & \frac{6EI}{L^2} & 0 & 0 \\ \frac{2EI}{L} & \frac{8EI}{L} & | & 0 & 0 & 0 \\ \dots & \dots & \dots & \dots & \dots & \dots \\ \frac{6EI}{L^2} & 0 & | & \frac{24EI}{L^3} + \frac{A_3E_3}{L_3} & -\frac{A_3E_3}{L_3} & 0 \\ 0 & 0 & | & -\frac{A_3E_3}{L_3} & \frac{A_3E_3}{L_3} + \frac{162A_4E_4}{225L_4} & 0 \\ 0 & 0 & | & 0 & 0 & \frac{288A_4E_4}{225L_4} \end{bmatrix} \begin{Bmatrix} x_1 \\ x_2 \\ x_3 \\ x_4 \\ x_5 \end{Bmatrix} = \begin{Bmatrix} 0 \\ 0 \\ 0 \\ 0 \\ 0 \end{Bmatrix}$$

or

$$\begin{bmatrix} \frac{W_3}{g} & 0 & 0 \\ \frac{W_4}{g} & 0 & 0 \\ \text{symm} & \frac{W_5}{g} & \end{bmatrix} \begin{Bmatrix} \ddot{x}_3 \\ \ddot{x}_4 \\ \ddot{x}_5 \end{Bmatrix} + \begin{bmatrix} 28654.77 & -19333.33 & 0 \\ \text{symm} & 21421.33 & 0 \\ 0 & 0 & 3712.00 \end{bmatrix} \begin{Bmatrix} x_3 \\ x_4 \\ x_5 \end{Bmatrix} = 0$$

in which $[K]$ is obtained by matrix condensation as

$$\begin{aligned} [K] &= [K_{22}] - [K_{21}][K_{11}]^{-1}[K_{12}] \\ &= \begin{bmatrix} 28654.7689 & 19333.3333 & 0 \\ -19333.3333 & 21421.3333 & 0 \\ 0 & 0 & 3712.00 \end{bmatrix} \end{aligned}$$

Mass matrix for structural mass is

$$\begin{aligned} W_3 &= \gamma A_1 L_1 \left(\frac{1}{2}\right) + \gamma A_2 L_2 \left(\frac{1}{2}\right) + \gamma A_3 L_3 \left(\frac{1}{2}\right) \\ W_4 &= W_5 = \gamma A_4 L_4 \left(\frac{1}{2}\right) + \gamma A_5 L_5 \left(\frac{1}{2}\right) + \gamma A_3 L_3 \left(\frac{1}{2}\right) \end{aligned}$$

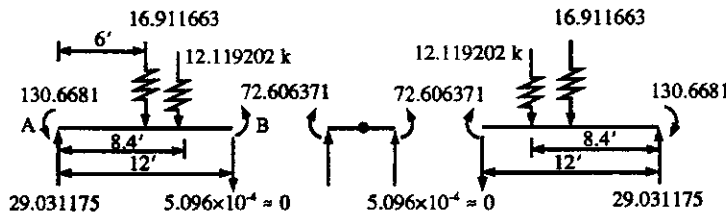


FIG. SOL. 6.9

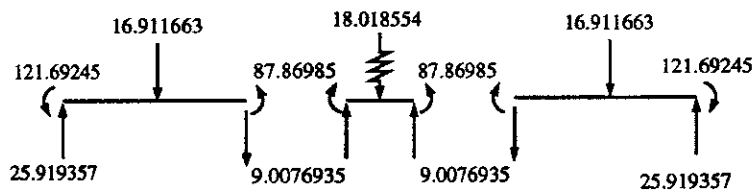


FIG. SOL 6.10

Thus

$$M_3 = \frac{(W'_1 + W_3)}{g}, \quad M_4 = M_5 = \frac{(W'_2 + W)}{g}$$

in which W'_1 and W'_2 are superimposed weight.

- 6.9. The maximum response is during the pulse at $\Delta=0.0081$ sec. The responses are $[x_1 \ x_2]=[0 \ 8.7295(10^{-4})\text{ft}]$ and $[M_1 \ M_2 \ M_3 \ M_4 \ V_1 \ V_2 \ V_3 \ V_4]=[-130.6681 \ -72.6064 \ 72.6064 \ 130.6681 \ 29.0312 \ 0 \ 0 \ -29.0312]$. Equilibrium checks at $t=0.0081$ sec. (Note: external load, $F=1.44 [1-(0.008/0.38)] 12=16.911663$.)
- Equilibrium at left segment (AB): $\Sigma M=0$, $\Sigma F_y=0$, equilibrium at node: $\Sigma M=0$, $\Sigma F_y=0$. (see Fig. Sol. 6.9).
- 6.10. The maximum response is during the pulse at $\Delta=0.0081$ sec and the responses are $[x_1 \ x_2]=[0 \ 8.7318(10^{-4})\text{ft}]$ and $[M_1 \ M_2 \ M_3 \ M_4]=[-121.692 \ -87.870 \ 87.870 \ 121.692]$. Equilibrium checks are: equilibrium at left segment, $\Sigma M=0$; $\Sigma F_y=0$; equilibrium at node: $\Sigma M=0$; $\Sigma F_y=0$. (see Fig. Sol. 6.10).
- 6.11. Results from the consistent mass method are $[x_1 \ x_2]=[0 \ 0.014752 \text{ ft}]$ and $[M_1 \ M_2 \ M_3 \ M_4 \ V_1 \ V_2 \ V_3 \ V_4]=[-1815.27 \ -1694.03 \ 1694.03 \ 1815.27 \ 310.63 \ 250.01 \ -250.01 \ -310.63] \text{ (k, ft)}$. Results from the dynamic stiffness method are $[x_1 \ x_2]=[0 \ 0.01477 \text{ ft}]$ and $[M_1 \ M_2 \ M_3 \ M_4 \ V_1 \ V_2 \ V_3 \ V_4]=[-1818.07 \ -1695.45 \ 1695.45 \ 1818.07 \ 311.23 \ 250.03 \ -250.03 \ -311.23] \text{ k, ft}$.
- 6.12.

$$[x_1 \ x_2]=[4.2464916 \times 10^{-3} \ -0.0479739]$$

$$[\ddot{x}_1 \ \ddot{x}_2]=[-17303.815 \ 18021.593]$$

$$[M_1 \ M_2 \ M_3 \ M_4]=[5395.18 \ 13433.5 \ -4080.24 \ -118.55]$$

$$[M_1 \ddot{x}_1 \ M_2 \ddot{x}_2]=[-9353.23 \ 4918.98]$$

6.13. (A) $p_1 = 194.5$; $p_2 = 891.4$; $p_3 = 1988.6$ rad/sec

$$[X_1 \ X_2 \ X_3] = \begin{bmatrix} 0.0582 & 1.0 & -1.000 \\ 0.0582 & -1.0 & -1.000 \\ 1.00 & 0 & -0.546 \end{bmatrix}$$

at $t = 0.1$ sec; $[x_1 \ x_2 \ x_3] = [0.7161 \text{ rad} \ -2.1934 \text{ rad} \ 0.1166 \text{ in}] 10^{-3}$.

(B) $p_1 = 4.434$; $p_2 = 20.755$; $p_3 = 83.869$ rad/sec

$$[X_1 \ X_2 \ X_3] = \begin{bmatrix} 0.0630 & -0.8633 & 1 \\ 0.0637 & 1 & 0.7778 \\ 1 & -0.0226 & -0.0166 \end{bmatrix}$$

6.14.

$$[K] = \begin{bmatrix} 22.0 & -5.0 & 2.0 & -1.00 \\ & 17.417 & 1.0 & -8.4169 \\ & & 22.0 & 5.00 \\ \text{symm} & & & 17.417 \end{bmatrix} \times 10^5 \text{ (lb/in)}$$

$\{x\} = [7.70 \ 1.192 \ 7.70 \ -1.192] 10^{-4} \text{ in}; [\sigma_{xx} \ \sigma_{yy} \ \sigma_{xy}] = [256.6 \ 1027 \ 59.58] \text{ psi}$

6.15.

$$\begin{aligned} [M] &= \begin{bmatrix} M & 0 \\ 0 & M \end{bmatrix}; \quad M = \frac{1}{3}\rho(A_1t + A_2t) + \frac{1}{2}\rho(L_3A_3 + A_5L_5 + A_4L_4); \quad [K] = \sum_{i=1}^5 [k_e^i] \\ &= \begin{bmatrix} 7.78 & 0.96 \\ 0.96 & 9.22 \end{bmatrix} 10^6 \text{ psi} \end{aligned}$$

6.16.

$$\begin{aligned} [K] &= \begin{bmatrix} 6000 & -2500 \\ -2500 & 6000 \end{bmatrix} \text{ k/in} \\ [M] &= \begin{bmatrix} M & 0 \\ 0 & M \end{bmatrix}; \quad M = 3.3464 \text{ lb sec}^2/\text{ft} \end{aligned}$$

6.17. System Stiffness matrix

$$\begin{aligned} [K] &= \begin{bmatrix} 28.0 & -10.0 & -4.0 & 4.0 \\ & 19.6667 & 6.0 & -10.6667 \\ & & 28.0 & 0 \\ \text{symm} & & & 19.6667 \end{bmatrix} 10^5 \text{ lb/in} \\ \left. \begin{array}{l} \sigma_{\max} = 1031.184 \text{ lb/in}^2 \\ \sigma_{\min} = 63.706 \text{ lb/in}^2 \\ \alpha = 2.5972^\circ \end{array} \right\} \text{ element 1} \end{aligned}$$

$$[M] = \begin{bmatrix} 11.205 & 0 & 4.546 & 0 & 4.2 & 0 \\ & 11.205 & 0 & 4.546 & 0 & 4.2 \\ & & 11.205 & 0 & 4.2 & 0 \\ \text{symm} & & & 11.205 & 0 & 4.2 \\ & & & & 7.2 & 0 \\ & & & & & 7.2 \end{bmatrix} \text{ element 1}$$

$$\{P\} = [17.239 \quad 17.239 \quad 17.239 \quad 17.239 \quad 14.4 \quad 14.4]^T \text{ element 1}$$

6.18.

$$k_{14} = \frac{-Eh}{4(1-\mu)}; \quad M_{14} = 0; \quad P_{14} = -wh$$

6.19.

$$[K] = \begin{bmatrix} 2,130,666.7 & 372,000 \\ 372,000 & 886,000 \end{bmatrix} \text{ lb/in}$$

$$[K_g] = \begin{bmatrix} 0.003197 & 0.000325 \\ 0.000325 & 0.014657 \end{bmatrix} P_{cr}$$

$$[M] = \begin{bmatrix} 2.3798 & 0 \\ 0 & 2.3798 \end{bmatrix} \text{ lb sec}^2/\text{ft}$$

6.20.

$$M\ddot{x} + \frac{3EI}{L^3}x - P\left(\frac{2}{L}\right) = 0$$

$$K = \frac{3EI}{L^3}; \quad K_g = \frac{2}{L}$$

6.21.

$$[K] = \begin{bmatrix} 2918.014 & -3368.157 \\ -3368.157 & 5706.583 \end{bmatrix}$$

$$[K_g] = \begin{bmatrix} 296.865 & -296.865 \\ -296.865 & 746.465 \end{bmatrix}$$

- 6.23. (A) Conventional matrix method: at A, $\sigma_x = -0.6667y/I$ (due to $SA^T x$) + $(-5.3333y)/I$ (due to fixed-end moment). (B) Finite element method: at A, $\sigma_x = -0.6667y/I$ (due to $\sigma = -Ey d^2v/dx^2$) + $(-5.3333y)/I$ (due to uniform load considered as initial stress). Conclusion: finite element method must include uniform load in calculating final stress; otherwise lump the uniform load with small segments.

Chapter 7 Solutions

7.1. MM intensity of VI.

7.2. Magnitude is 4.5 and distance is 250 km.

7.3.

$$x_{n+1} = x_n + h\dot{x}_n + h^2\ddot{x}_n/2; \quad \dot{x}_{n+1} = h\ddot{x}_n + \dot{x}_n$$

$$\ddot{x}_{n+1} = \{F_{n+1} - Kx_n - (hK + C)\dot{x}_n - (Ch + Kh^2/2)\ddot{x}_n\}/M$$

7.4. When $x = t^3$, $R = x^3(\xi)h^3/6$;

$$x_{n+1} = x_n + h\dot{x}_n + \ddot{x}_n h^2/2 + x^3(\xi)h^3/6$$

7.5. $\dot{x}(0.01) = 0.5100$ in/sec; $\ddot{x}(0.01) = 21.311$ in/sec².

7.6. $S_d = 1.3$ in; $S_v = 16$ in/sec; $S_a = 0.56g$.

7.7. $S_d = 1.4$ in; $S_v = 4.75$ in/sec; $S_a = 0.14$ in/sec².

7.8. $(Sa)_i = 1.8138$; $S_a = (Sa)_i (0.2g) = 0.363g$

7.9. $\phi_z(t) = 0.00015$ rad/sec.

7.10. $\{x\}^T = [0.09138 \ 0.23697 \ 0.34914]^T$ ft.

7.11. $x^1 = 0.0478$ rad = D_1

7.12.

$$\mu = \frac{\phi_u}{\phi_y} = \frac{\varepsilon_u}{\varepsilon_y}$$

7.13.

$$\ddot{\phi}_x = \frac{1}{2 \times 1000} (-50.4 - 432.55) = -0.241 \text{ rad/sec}^2$$

7.13.

$$\ddot{\phi}_y = \frac{1}{2 \times 1000} (432.55 + 156.2) = 0.294 \text{ rad/sec}^2$$

$$\ddot{\phi}_z = \frac{1}{2 \times 1000} (-156.2 + 50.4) = -0.053 \text{ rad/sec}^2$$

7.14.

$$\{x\}^2 = \begin{Bmatrix} 8.3925 \times 10^{-3} \\ 0.0563 \\ 0.1220 \end{Bmatrix}; \quad \{x\} = \begin{Bmatrix} 0.0916 \\ 0.2373 \\ 0.3493 \end{Bmatrix} \text{ ft}$$

7.15.

$$\alpha_{ji} = \frac{8\rho^2(1+q)q^{3/2}}{(1-q^2)^2 + 4\rho^2q(1+q)^2} = \alpha_{ij}$$

Chapter 8 Solutions

8.1.

$$[C_j] = \begin{bmatrix} 1 & 0 & 0 \\ 0 & \frac{L}{\sqrt{H^2+L^2}} & \frac{-H}{\sqrt{H^2+L^2}} \\ 0 & \frac{H}{\sqrt{H^2+L^2}} & \frac{L}{\sqrt{H^2+L^2}} \end{bmatrix}$$

8.2.

$$[C_j]_a = \begin{bmatrix} 0.707 & 0.707 & 0 \\ -0.707 & 0.707 & 0 \\ 0 & 0 & 1 \end{bmatrix}; \quad [C_j]_b = \begin{bmatrix} 0.924 & 0.383 & 0 \\ -0.383 & 0.924 & 0 \\ 0 & 0 & 1 \end{bmatrix}$$

8.3.

$$[C_j]_8 = \begin{bmatrix} 1 & 0 & 0 \\ 0 & 1 & 0 \\ 0 & 0 & 1 \end{bmatrix}; \quad [C_j]_{12} = \begin{bmatrix} 1 & 0 & 0 \\ 0 & \cos(15) & -\sin(15) \\ 0 & \sin(15) & \cos(15) \end{bmatrix}$$

$$[T_{ms}]_8 = \begin{bmatrix} 1 & 0 & 0 & 0 & 0 & 0 \\ 0 & 1 & 0 & 0 & 0 & 0 \\ 0 & 0 & 1 & 0 & 0 & 0 \\ 0 & 0 & 0 & 1 & 0 & 0 \\ 0 & 0 & 0 & 0 & 1 & 0 \\ -12 & 15 & 0 & 0 & 0 & 1 \end{bmatrix}; \quad [T_{ms}]_{12} = \begin{bmatrix} 1 & 0 & 0 & 0 & 0 \\ 0 & 1 & 0 & 0 & 0 \\ 0 & 0 & 1 & 0 & 0 \\ 0 & 0 & 0 & 1 & 0 \\ 0 & 0 & 0 & 0 & 1 \\ -10.18 & 15 & 0 & 0 & 0 \end{bmatrix}$$

8.4.

$$[K^{(1)}] = [A][k_e][A]^T$$

$$= \begin{bmatrix} 0.78 & 0 & 0 & 0 & 6.2 & 6.2 & -0.311 & 0 & 0.71 & 0 & 62 & -2.486 \\ 0.62 & 0 & -4.963 & 0 & 14.89 & 0 & -0.62 & 0 & -1.990 & 0 & -0.417 \\ 4.894 & 0 & 0 & 0 & -4.482 & 0 & -1.962 & 0 & 0 & 0 & -358.6 \\ 529.4 & 0 & -1191 & 0 & 4.963 & 0 & 106.14 & 0 & 0 & 0 & 154.57 \\ 661.4 & 496 & -2.486 & 0 & 5.679 & 0 & 330.7 & -198.9 \\ 4169 & -2.486 & -14.89 & 5.680 & -568.2 & 496 & -338.69 \\ 4.119 & 0 & 1.769 & 0 & -2.486 & 329.5 \\ 4.963 & 0 & 1.990 & 0 & 0 & 392.49 \\ 0.852 & 0 & 5.679 & 0 & 141.534 \\ \text{symm} & & & 178.21 & 0 & -22.072 \\ & & & & 6.614 & -198.9 \\ & & & & 5.791(10)^4 \end{bmatrix} \quad (10)^3$$

- 8.5. $[A_1]^T$, $[A_2]^T$, $[A_3]^T$, $[A_4]^T$, and $[A_5]^T$ are obtained directly and are respectively identical to Eqs. (8.61), (8.69), (8.74), (8.7), and (8.80).
 8.6. From Example 8.7.1 and Eq. (8.62) we have

$$[S_I] = \frac{10^9}{500} \begin{bmatrix} 2.648(10)^5 & 0 & 0 \\ & 1.104 & 0 \\ \text{symm} & & 3.18 \end{bmatrix}$$

Thus the stiffness matrix of the element (say no. 37) is

$$[K^{37}] = ([A_5][A_4][A_3][A_2][A_1])[S_I]([A_5][A_4][A_3][A_2][A_1])^T = \begin{bmatrix} K_{11} & | & K_{12} \\ \hline \cdots & | & \cdots \\ K_{21} & | & K_{22} \end{bmatrix}$$

in which

$$[K_{12}] = \begin{bmatrix} 0 & 0 & 0 & 0 & 0 & 0 & 0 & 0 & 0 & 0 \\ 0 & -5.52 & 0 & 0 & 0 & 0 & -22.08 & 5.52 & 0 & 0 & 1.1(10)^4 \\ -11.984 & 0 & 0 & 0 & 0 & 0 & -5.52 & -19.816 & 0 & 0 & 2.76(10)^3 \\ 0 & 0 & 0 & 0 & 0 & 0 & 0 & 0 & 0 & 0 & 0 \\ 0 & 0 & 0 & 0 & 0 & 0 & 0 & 0 & 0 & 0 & 0 \\ 0 & 0 & 0 & -1.1(10)^4 & 2.76(10)^3 & 0 & 0 & 0 & 0 & 5.52(10)^6 & 10^5 \\ 0 & 0 & 0 & 0 & 0 & 0 & 0 & 0 & 0 & 0 & 0 \\ 0 & 0 & 0 & 0 & 0 & 0 & 0 & 0 & 0 & 0 & 0 \\ -11.984 & 0 & 0 & 0 & 0 & 0 & 0 & 0 & 0 & 0 & -2.8(10)^3 \\ \text{symm} & & & & & & 0 & 0 & 0 & 0 & 0 \\ & & & & & & 0 & 0 & 0 & 0 & 0 \\ & & & & & & 0 & 0 & 0 & 0 & 0 \end{bmatrix}$$

$$[K_{22}] = \begin{bmatrix} 0 & 0 & 0 & 0 & 0 & 0 & 0 & 0 & 0 & 0 \\ 0 & 0 & 0 & 0 & 0 & 0 & 0 & 0 & 0 & 0 \\ 22.576 & 0 & 0 & 0 & 0 & 0 & 5.520 & 9.224 & 0 & 0 & -2.8(10)^3 \\ 0 & 0 & 0 & 0 & 0 & 0 & 0 & 0 & 0 & 0 & 0 \\ 0 & 0 & 0 & 0 & 0 & 0 & 0 & 0 & 0 & 0 & 0 \\ 0 & 0 & 0 & 0 & 0 & 0 & 0 & 0 & 0 & 0 & 0 \\ 0 & 0 & 0 & 0 & 0 & 0 & 0 & 0 & 0 & 0 & 0 \\ 22.08 & 22.576 & 0 & 0 & 0 & 0 & -5.52 & 0 & 0 & -1.1(10)^4 & 2.76(10)^3 \\ \text{symm} & & & & & & 0 & 0 & 0 & 0 & 0 \\ & & & & & & 0 & 0 & 0 & 0 & 0 \\ & & & & & & 0 & 0 & 0 & 0 & 5.52(10)^6 \end{bmatrix} 10^5$$

and

$$[K_{21}] = [K_{12}]^T$$

8.8.

$$[K^{24}] = \begin{bmatrix} 0 & 0 & 0 & 0 & 0 & 0 & 0 & 0 & 0 & 0 \\ 0 & 0 & 0 & 0 & 0 & 0 & 0 & 0 & 0 & 0 \\ 17.332 & 1386.563 & 0 & 0 & 0 & 0 & -17.332 & 1386.563 & 0 & 0 \\ 147900 & 0 & 0 & 0 & 0 & 0 & -1386.563 & 73950 & 0 & 0 \\ 24.375 & 0 & 0 & 0 & 0 & 0 & 0 & 0 & -24.375 & 0 \\ 0 & 0 & 0 & 0 & 0 & 0 & 0 & 0 & 0 & 0 \\ 0 & 0 & 0 & 0 & 0 & 0 & 0 & 0 & 0 & 0 \\ 0 & 0 & 0 & 0 & 0 & 0 & 0 & 0 & 0 & 0 \\ \text{symm} & & & & & & 17.332 & -1386.563 & 0 & 0 \\ & & & & & & 147900 & 0 & 0 & 0 \\ & & & & & & 24.375 & 0 & 0 & 0 \end{bmatrix}$$

8.12.

$$\begin{aligned}
 & \left\{ \begin{array}{l} F_{Amx} \\ F_{Amy} \\ F_{asz} \\ M_{bsx} \\ M_{bsy} \\ M_{bmz} \\ F_{Bmx} \\ F_{Bmy} \\ F_{bsz} \\ M_{bsx} \\ M_{bsy} \\ M_{bmz} \end{array} \right\} = 10^5 \\
 & \left[\begin{array}{ccccccccc} 4.769 & -7.64 & -5.73 & 0 & 0 & -4.769 & 7.640 & 5.730 & 0 & 0 \\ 12.24 & 9.178 & 0 & 0 & 0 & 7.639 & -12.24 & -9.178 & 0 & 0 \\ 6.383 & 0 & 0 & 0 & 0 & 5.730 & -9.178 & -6.833 & 0 & 0 \\ 0 & 0 & 0 & 0 & 0 & 0 & 0 & 0 & 0 & 0 \\ 0 & 0 & 0 & 0 & 0 & 0 & 0 & 0 & 0 & 0 \\ 0 & 0 & 0 & 0 & 0 & 0 & 0 & 0 & 0 & 0 \\ 4.769 & -7.640 & -5.730 & 0 & 0 & -3816 & 0 & 0 & 0 & 0 \\ 12.24 & 9.178 & 0 & 0 & 0 & 0 & 0 & 0 & 0 & 0 \\ 6.883 & 0 & 0 & 0 & 0 & 0 & 0 & 0 & 0 & 0 \\ 0 & 0 & 0 & 0 & 0 & 0 & 0 & 0 & 0 & 0 \\ 3.052(10)^6 & & & & & & & & & \end{array} \right] \\
 & \text{symm}
 \end{aligned}$$

8.14. The structural system matrix is

$$K = \sum_{i=1}^4 K^i = \begin{bmatrix} [K_{11}]_{6 \times 6} & | & [K_{12}]_{6 \times 12} \\ \hline [K_{21}]_{12 \times 6} & | & [K_{22}]_{12 \times 12} \end{bmatrix}$$

in which

$$[K_{21}] = [K_{12}]^T$$

and the displacement vector has the order of 1-18 as shown in the figure. Submatrices are

$$[K_{11}] = \begin{bmatrix} 4.783 & -7.640 & -3822 & -4.783 & 7.639 & 3822 \\ & 1225 & 6116 & 7.640 & -12.25 & -6116 \\ & & 3058(10)^3 & 3822 & -6116 & -4680 \\ & & & 4.790 & -7.640 & -5.6 \\ & & \text{symm} & & 12.26 & -3.5 \\ & & & & & 6530 \end{bmatrix} (10)^5$$

$$[K_{12}] = [K_{21}]^T$$

$$= \begin{bmatrix} 0 & 0 & -2.1 & -5.730 & 0 & -2.1 & 5.730 & 0 & -2.1 & 0 & 0 & -2.1 \\ 0 & 2.1 & 0 & 9.178 & 2.1 & 0 & -9.178 & 2.1 & 0 & 0 & 2.1 & 0 \\ 0 & 1.05(10)^3 & 0 & 4.584(10)^3 & 0 & 1.68(10)^3 & -4.584(10)^3 & 1.05(10)^3 & 0 & 0 & 0 & 1.68(10)^3 \\ 0 & 0 & 2.1 & 5.730 & 0 & 2.1 & -5.730 & 0 & 0 & 0 & 0 & 2.1 \\ 0 & -2.1 & 0 & -9.178 & -2.1 & 0 & 9.178 & 2.1 & 0 & 0 & -2.1 & 0 \\ 0 & 0 & 0 & -4.584(10)^3 & 1.05(10)^3 & -1.68(10)^3 & 0 & 0 & 0 & 0 & 1.05(10)^3 & -1.68(10)^3 \end{bmatrix} (10)^5$$

- 8.16. At the first floor, d.o.f. at node 1 are 4, 5, 6; at node 2 they are 7, 8, 9; at master joint they are 1, 2, 3. At the second floor, d.o.f. at node 1 are 13, 14, 15; at node 2 they are 16, 17, 18; at the master joint they are 10, 11, 12. The stiffness matrix of the first floor is

$$[K]_{\text{1st Flr}} = \begin{bmatrix} k_{7,7}^{c1} + k_{7,7}^{c2} & k_{7,8}^{c1} + k_{7,8}^{c2} & k_{7,12}^{c1} + k_{7,12}^{c2} & k_{7,9}^{c1} & k_{7,10}^{c1} & k_{7,11}^{c1} & k_{7,9}^{c2} & k_{7,10}^{c2} & k_{7,11}^{c2} \\ k_{8,8}^{c1} + k_{8,8}^{c2} & k_{8,12}^{c1} + k_{8,12}^{c2} & k_{8,9}^{c1} & k_{8,10}^{c1} & k_{8,11}^{c1} & k_{8,9}^{c2} & k_{8,10}^{c2} & k_{8,11}^{c2} & \\ k_{12,12}^{c1} + k_{12,12}^{c2} & k_{9,12}^{c1} & k_{10,12}^{c1} & k_{11,12}^{c2} & k_{9,12}^{c2} & k_{10,12}^{c2} & k_{11,12}^{c2} & & \\ k_{9,9}^{c1} + k_{3,3}^{b1} & k_{9,10}^{c1} + k_{3,4}^{b1} & k_{9,11}^{c1} + k_{3,5}^{b1} & k_{9,9}^{b1} & k_{9,10}^{b1} & k_{9,11}^{b1} & k_{3,10}^{b1} & k_{3,11}^{b1} & \\ k_{10,10}^{c1} + k_{4,4}^{b1} & k_{10,11}^{c1} + k_{4,5}^{b1} & k_{4,9}^{b1} & k_{4,10}^{b1} & k_{4,11}^{b1} & k_{4,9}^{b1} & k_{4,10}^{b1} & k_{4,11}^{b1} & \\ k_{11,11}^{c1} + k_{5,5}^{b1} & k_{5,9}^{b1} & k_{5,10}^{b1} & k_{5,11}^{b1} & k_{9,9}^{c2} + k_{9,9}^{b1} & k_{9,10}^{c2} + k_{9,10}^{b1} & k_{9,11}^{c2} + k_{9,11}^{b1} & & \\ & & & & k_{10,10}^{c2} + k_{10,10}^{b1} & k_{10,11}^{c2} + k_{10,11}^{b1} & & & \\ & \text{symm} & & & & & k_{10,11}^{c2} + k_{11,11}^{b1} & & \end{bmatrix}$$

- 8.17. The structural stiffness is

$$[K] = \begin{bmatrix} K_{11} & | & K_{12} \\ \cdots & - & \cdots \\ K_{21} & | & K_{22} \end{bmatrix} = \begin{bmatrix} 2006.7 & 800 & -600 & 0 & 0 & 0 & -20/3 & 800 & -600 & 0 & 0 & 0 \\ 328,156 & -95,792 & 0 & 0 & 0 & -800 & 63,844 & -48,208 & 0 & 1000 & -90,000 & \\ 272,277 & 0 & 0 & 0 & 600 & -48,208 & 107,268/3 & -1000 & 0 & -120,000 & \\ 2000 & 0 & 0 & 0 & 0 & 0 & 0 & 0 & 0 & 0 & 0 & 0 \\ 200,000 & 0 & 0 & 0 & 0 & 0 & 0 & 0 & 1000 & 90,000 & & \\ & 200,000 & 0 & 0 & 0 & 0 & 0 & -1000 & 0 & -120,000 & & \\ & & 2006.7 & -800 & 600 & 0 & 0 & 0 & & & & \\ & & 328,156 & -95,792 & 0 & 1000 & 90,000 & & & & & \\ & \text{symm} & & & 272,277 & -1000 & 0 & 120,000 & & & & \\ & & & & 20 & 0 & 800 & & & & & \\ & & & & 20 & 600 & & & & & & \\ & & & & & & 451,300 & & & & & \end{bmatrix}$$

- in which $[K_{11}]$ has a dimension of 9 by 9 associated with the first nine d.o.f. (1–9); $[K_{12}]$ has a dimension of 9 by 3; and $[K_{22}]$ has a dimension of 3 by 3 associated with d.o.f. 10–12.
- 8.18. The loading matrix associated with d.o.f. 1–12 is $\{R\} = [-50 \quad 1938.24 \quad -1453.68 \quad -60 \quad 0 \quad 0 \quad -50 \quad -1938.24 \quad 1453.68 \quad 15 \quad 10 \quad -2700]^T$ where the units are in and k.

- 8.19. The geometric matrix is

$$[K_g]_{12 \times 12} = \begin{bmatrix} K_{g11} & | & K_{g12} \\ \cdots & - & \cdots \\ K_{g21} & | & K_{g22} \end{bmatrix} = \begin{bmatrix} [0]_{9 \times 9} & | \\ \cdots & - \\ \text{symm} & | \\ & \begin{bmatrix} 0.533 & 0 & 24 \\ 0.533 & 0 & 18 \\ 0 & 0 & 0 \end{bmatrix}_{3 \times 3} \end{bmatrix}$$

where the units are in and k.

8.20.

$$\{\Delta\} = [[K] - [K_G]]^{-1}\{R\} = \begin{bmatrix} -0.02061 & -0.00464 & -0.01228 & -0.03 & 0.00923 \\ -0.00355 & -0.02939 & 0.00798 & 0.031477 & 2.71075 & 0.72042 & -0.02851 \end{bmatrix}^T$$

8.21. $f_1 = 0.535$; $f_2 = 0.730$; $f_3 = 0.888$

$$\{X\} = \begin{bmatrix} 1.00000 & 0.56996 & 0.89753 \\ -0.69197 & 1.00000 & 1.00000 \\ -0.00130 & -0.00957 & 0.01611 \end{bmatrix}$$

- 8.22. The response spectral quantities of the first five modes due to excitations applied in X_1 and X_2 , respectively, are shown in Table Sol.8.22.1. Modal cross-correlation coefficients are listed in Table Sol.8.22.2. The response due to application of ground main and intermediate components using corresponding CQC and SRSS modal combination techniques is given in Tables Sol.8.22.3 and Sol.8.22.4, respectively. In these two tables, column (a) results from applying ground main and intermediate components in x and y axes, respectively. A response is obtained for each critical angle θ_{cr} , which is found using the method presented in Section 7.7 with ground main and intermediate components applied in X_1 and X_2 , respectively. Column (b) results from ground main and intermediate components applied in X_1 and X_2 , respectively. Column (c) shows the ratios between (b) and (c), which indicates that the maximum difference is about 34%. For each d.o.f., the critical angle calculated by the conventional SRSS approach is different from that based on the CQC approach. This is because the conventional SRSS approach does not consider

TABLE SOL. 8.22.1 Response Spectral Values

Mode	p (Hz)	$R_x(p)$ (ft)	$R_y(p)$ (ft)
1	0.0395	1.392	1.260
2	0.0409	1.392	1.259
3	0.0686	1.387	1.246
4	0.1175	1.377	1.215
5	0.1219	1.376	1.212

TABLE SOL. 8.22.2 Modal Cross-correlation Coefficients

Mode	1	2	3	4	5
1	1	0.9359	0.0564	0.0127	0.0118
2	0.9359	1	0.0647	0.0138	0.0127
3	0.0564	0.0647	1	0.0599	0.0526
4	0.0127	0.0138	0.0599	1	0.9361
5	0.0118	0.0127	0.0526	0.9361	1

TABLE SOL. 8.22.3 Response Comparison (CQC Approach)

d.o.f.	Response based on critical input angle (a)		Response based on $\theta=0$ (b)	Ratio (c)
	θ_{cr}	Displacement (ft)	Displacement (ft)	(b)/(a)
$r_{\theta 1}$	172.26	0.0626	0.0621	0.99
r_{u1}	137.55	2.4259	1.8126	0.75
r_{v1}	49.61	2.4609	1.6263	0.66
$r_{\theta 2}$	172.30	0.0591	0.0586	0.99
r_{u2}	137.54	2.3103	1.7257	0.75
r_{v2}	49.57	2.3423	1.5485	0.66
$r_{\theta 5}$	171.96	0.0486	0.0481	0.99
r_{u5}	137.44	1.8761	1.3993	0.75
r_{v5}	49.51	1.9045	1.2605	0.66
$r_{\theta 10}$	172.28	0.0136	0.0134	0.99
r_{u10}	135.54	0.8635	0.6218	0.72
r_{v10}	46.48	0.8698	0.6047	0.70

TABLE SOL. 8.22.4 Response Comparison (SRSS Approach)

d.o.f.	Response based on critical input angle (a)		Response based on $\theta=0$ (b)	Ratio (c)
	θ_{cr}	Displacement (ft)	Displacement (ft)	(b)/(a)
$r_{\theta 1}$	172.17	0.0637	0.0631	0.99
r_{u1}	172.26	2.0329	2.0238	0.99
r_{v1}	82.22	2.1101	1.4076	0.66
$r_{\theta 2}$	172.28	0.0602	0.0597	0.99
r_{u2}	172.21	1.9253	1.9165	0.99
r_{v2}	82.24	1.9978	1.3329	0.67
$r_{\theta 5}$	172.07	0.0490	0.0485	0.99
r_{u5}	172.17	1.5620	1.5548	0.96
r_{v5}	82.08	1.6218	1.0821	0.67
$r_{\theta 10}$	170.51	0.0179	0.0176	0.99
r_{u10}	171.27	0.5782	0.5749	0.99
r_{v10}	80.75	0.6014	0.4031	0.67

the cross modal terms in the modal combination. As shown in Table Sol.8.22.2, the first and second modes are strongly coupled. This implies that the first and second natural frequencies are not well-separated.

Chapter 9 Solutions

9.1. Dynamic responses in F(t) direction are

Step	Time	Load	Displacement	Velocity	Acceleration
0	0.00000×10^0	0.00000×10^0	0.00000×10^0	0.00000×10^0	0.00000×10^0
1	5.00000×10^{-2}	14.079	1.64061×10^{-4}	9.84368×10^{-3}	0.39375
2	1.00000×10^{-1}	27.812	1.28766×10^{-3}	3.78850×10^{-2}	0.72791
3	0.15000	40.860	4.18460×10^{-3}	7.98483×10^{-2}	0.95062
4	0.20000	52.901	9.39613×10^{-3}	0.12923	1.0246
5	0.25000	63.640	1.71000×10^{-2}	0.17815	0.93234
6	0.30000	72.812	2.71361×10^{-2}	0.22255	0.84342
7	0.35000	80.191	3.93601×10^{-2}	0.26726	0.94495
8	0.40000	85.595	5.39685×10^{-2}	0.31837	1.0994
9	0.45000	88.892	7.13002×10^{-2}	0.37569	1.1936
10	0.50000	90.000	9.15898×10^{-2}	0.43616	1.2252
11	0.55000	88.892	0.11492	0.49663	1.1936
12	0.60000	85.595	0.14120	0.55395	1.0994
13	0.65000	80.191	0.17021	0.60506	0.94495
14	0.70000	72.812	0.20155	0.64704	0.73412
15	0.75000	63.640	0.23471	0.67719	0.47207
16	0.80000	52.901	0.26904	0.69312	0.16525
17	0.85000	40.860	0.30376	0.69279	-0.17878
18	0.90000	27.812	0.33802	0.67453	-0.55159
19	0.95000	14.079	0.37089	0.63714	-0.94396

9.2. Dynamic responses in the $F(t)$ direction are

Step	Time	Load	Displacement	Velocity	Acceleration
0	0.00000×10^0	0.00000×10^0	0.00000×10^0	0.00000×10^0	0.00000×10^0
1	5.0000×10^{-2}	14.079	1.64061×10^{-4}	9.84368×10^{-3}	0.39375
2	1.0000×10^{-1}	27.812	1.28766×10^{-3}	3.78850×10^{-2}	0.72791
3	0.15000	40.860	4.18460×10^{-3}	7.98483×10^{-2}	0.95062
4	0.20000	52.901	9.39613×10^{-3}	0.12923	1.0246
5	0.25000	63.640	1.71000×10^{-2}	0.17815	0.93234
6	0.30000	72.812	2.71326×10^{-2}	0.22234	0.83502
7	0.35000	80.191	3.93247×10^{-2}	0.26598	0.91049
8	0.40000	85.595	5.38103×10^{-2}	0.31442	1.0274
9	0.45000	88.892	7.08366×10^{-2}	0.36704	1.0775
10	0.50000	90.000	9.05275×10^{-2}	0.42043	1.0581
11	0.55000	88.892	0.11283	0.47110	0.96867
12	0.60000	85.595	0.13753	0.51558	0.81049
13	0.65000	80.191	0.16423	0.55052	0.58691
14	0.70000	72.812	0.19237	0.57277	0.30318
15	0.75000	63.640	0.22125	0.57951	-3.36759×10^{-2}
16	0.80000	52.901	0.25003	0.56829	-0.41504
17	0.85000	40.860	0.27775	0.53714	-0.83088
18	0.90000	27.812	0.30338	0.48462	-1.2701
19	0.95000	14.079	0.32584	0.40985	-1.7206

- 9.3. (A) Elastic case: both models are equal. (B) One end hinged: both models are equal if S_i or $S_j = p/q$. (C) Both ends hinged: models are not equal. However, the stiffness matrix based on bilinear model can be transformed to curvilinear model by multiplying different p values as

$$[K_e] = \begin{bmatrix} p_1a & p_2b & p_3c & p_3c \\ p_2a & p_1a & p_3c & p_3c \\ & p_4d & p_4d & p_4d \\ & & p_4d & \end{bmatrix}$$

where

$$p_1 = \frac{3S + 4(S)^2}{3 + 8S + 4(S)^2}$$

$$p_2 = \frac{4(S)^2}{3 + 8S + 4(S)^2}$$

$$p_3 = \frac{2S + 4(S)^2}{1 + 8S + 4(S)^2}$$

$$p_4 = \frac{2S + 4(S)^2}{1 + 8S + 4(S)^2}$$

$$S = S_i = S_j$$

The curvilinear model lumps inelastic deformation at the ends while the bilinear model has its inelastic stiffness distributed along the member length.

9.4. The member stiffness matrix is

$$[K_e] = \begin{bmatrix} 0.234516 & 0.0045099 & -0.059756 & -0.059756 \\ & & -0.059756 & -0.059756 \\ \text{symm} & & -0.0242408 & 0.0242408 \\ & & & 0.0242408 \end{bmatrix}$$

9.6. Buckling load, N_{cr} , is 1000 N. (a) 0.06 m. (b) 0.12 m. (c) 0.120006 m.

9.7.

$$M = \frac{Eb}{K} \left\{ \frac{yh}{(\sigma/E) + K(\sigma/E)^2} \left[\frac{2Kh}{y} \left(\frac{\sigma}{E} \right)^2 + 1 \right]^{\frac{3}{2}} - \frac{1}{8} h^2 \right\}$$

which is not same as $\sigma(bh^3/12)y$ based on a linear stress-strain relationship.

9.8. Horizontal responses in the $F(t)$ direction are:

Step	Time	Load	Displacement	Velocity	Acceleration
0	0.00000×10^0	0.00000×10^0	0.00000×10^0	0.00000×10^0	0.00000×10^0
1	0.10000	27.490	1.22703×10^{-3}	3.68110×10^{-2}	0.73622
2	0.20000	52.290	9.23943×10^{-3}	0.12994	1.1263
3	0.30000	71.970	2.75881×10^{-2}	0.23426	0.96015
4	0.40000	84.606	5.57233×10^{-2}	0.32752	0.90506
5	0.50000	88.960	9.32082×10^{-2}	0.42425	1.0294
6	0.60000	84.606	0.14057	0.52097	0.90506
7	0.70000	71.970	0.19659	0.59343	0.54428
8	0.80000	52.290	0.25772	0.61977	-1.76458×10^{-2}
9	0.90000	27.498	0.31843	0.58260	-0.72572
10	1.0000	-3.55271E-14	0.37175	0.47078	-1.5106
11	1.1000	-27.490	0.40997	0.28047	-2.2955
12	1.2000	-52.290	0.42536	1.55122×10^{-2}	-3.0036
13	1.3000	-71.970	0.41095	-0.31295	-3.5655
14	1.4000	-84.606	0.36366	-0.61460	-2.4676

Chapter 10 Solutions

- 10.1. For UBC-94: $F_1 = 24.475$ k; $F_2 = 41.531$ k; $F_3 = 21.808$ k. For IBC-2000: $F_1 = 82.29$ k, $F_2 = 139.96$ k, $F_3 = 73.33$ k
- 10.2. Accidental torsion: T_r or $M_t = 526.885$ k ft; 380.016 k ft; 130.830 k ft for first, second, and third level, respectively. Torsional shear distribution at first level based on UBC-94

$$J_r = \Sigma(K_x\bar{y}^2 + K_y\bar{x}^2) = [14(3.3075) + 14(0.3376) + 8(1.4472) + 8(0.6432) + 8(0.1608)] \\ EI_x = 65.26EI_x$$

For columns 1, 2, 3, 4, 5, 6, 7, 22, 23, 24, 25, 26, 27 and 28

$$V_{xe} = \frac{M_{t1}\bar{y}K_x}{J_r} = \frac{526.848(45)(0.0015)EI_x}{65.26EI_x} = 0.545 \text{ k}$$

For columns 8, 9, 10, 11, 12, 13, 14, 15, 16, 17, 18, 19, 20 and 21

$$V_{xe} = \frac{526.848(60)(0.0015)EI_x}{65.26EI_x} = 0.182 \text{ k}$$

For columns 1, 8, 15, 22, 7, 14, 21 and 28

$$V_{xe} = \frac{526.848(18)(0.000402)EI_x}{65.26EI_x} = 0.195 \text{ k}$$

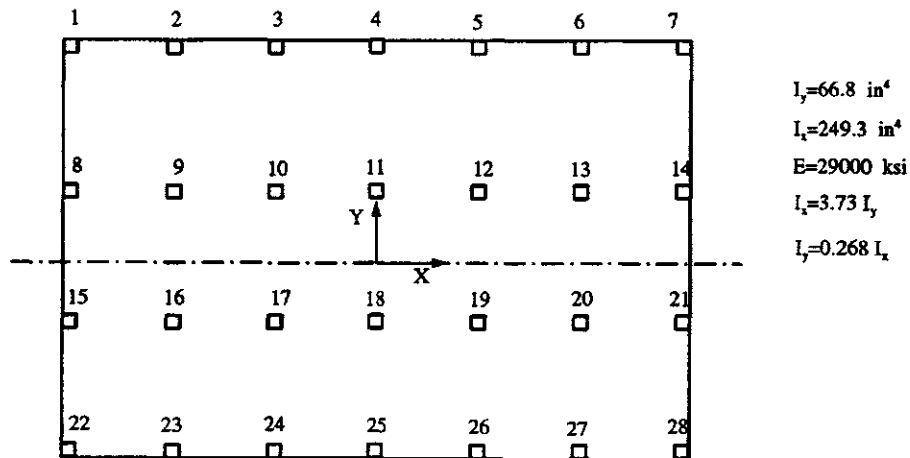


FIG. SOL. 10.2

10.3.

$$T_B = 2\pi \sqrt{\frac{\sum w_i \delta_i^2}{g \sum f_i \delta_i}} = 2\pi \sqrt{\frac{14.343}{42.4818}} = 1.3697 \text{ sec}$$

$T_A = 0.658 \text{ sec}$ (UBC-94, Section 1628.2.2)

$$\frac{T_B}{T_A} = \frac{1.3697}{0.658} = 2.08 > 1.4$$

for seismic zone 2. According to UBC-94, $T_B = 1.4 T_A = 0.921$.

10.4.

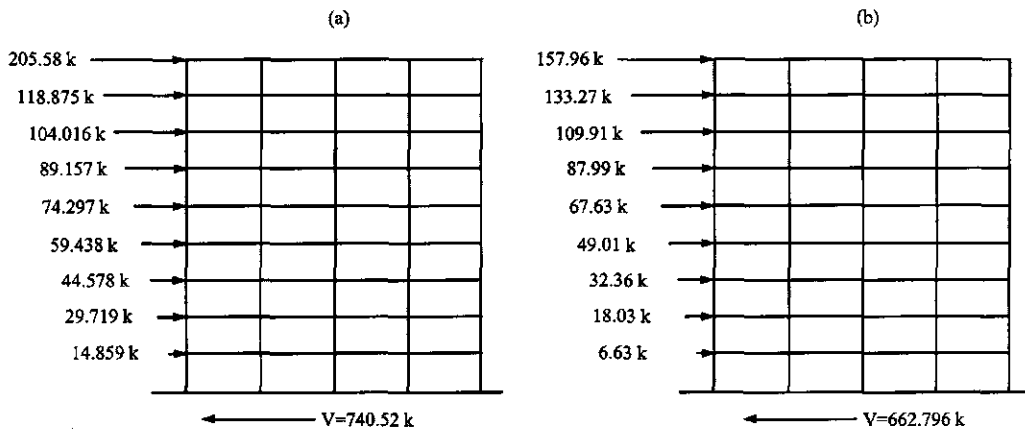


FIG. SOL. 10.4 (a) UBC-94, (b) IBC-2000.

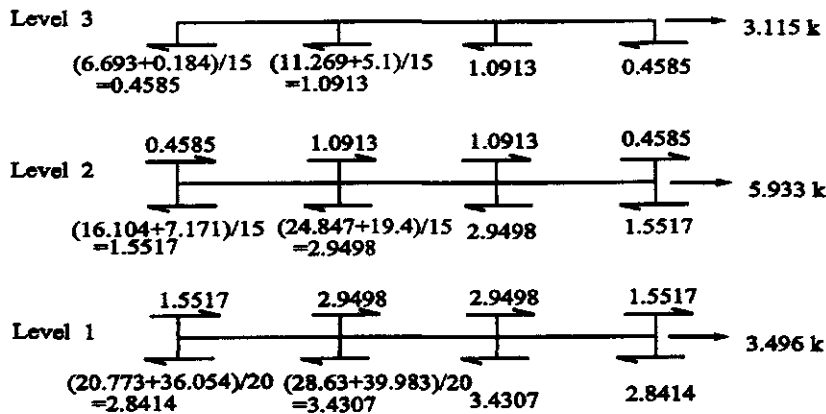


FIG. SOL. 10.5

10.5. First level:

Column no.	V_x	V'_y (torsion)	V''_y (horizontal shear)	$V_y = V'_y + V''_y$
1	0.545	0.195	2.8414	2.8954
7	0.545	0.195	2.8414	2.8945
8	0.182	0.195	3.4307	3.4847
14	0.182	0.195	3.4307	3.4847
15	0.182	0.195	3.4307	3.4847
21	0.182	0.195	3.4307	3.4847
22	0.545	0.195	2.8414	2.8954
28	0.545	0.195	2.8414	2.8954

10.6. For UBC-94 story drift is:

$$\begin{aligned} \text{for level 1, } \Delta_{01} &= 0.072 < 0.75 \text{ (OK)} \\ \text{for level 2, } \Delta_{12} &= 0.047 < (0.005)(15) = 0.075 \text{ (OK)} \\ \text{for level 3, } \Delta_{23} &= 0.022 < 0.075 \text{ (OK)} \end{aligned}$$

 $P-\Delta$ effect:

$$\theta_1 = 0.057 < 0.1; \quad \theta_2 = 0.061 < 0.1; \quad \theta_3 = 0.014 < 0.1 \text{ (OK)}$$

10.7. $M_r = F_e = 100 \text{ k}$ (46.67 k in.) For column 3.

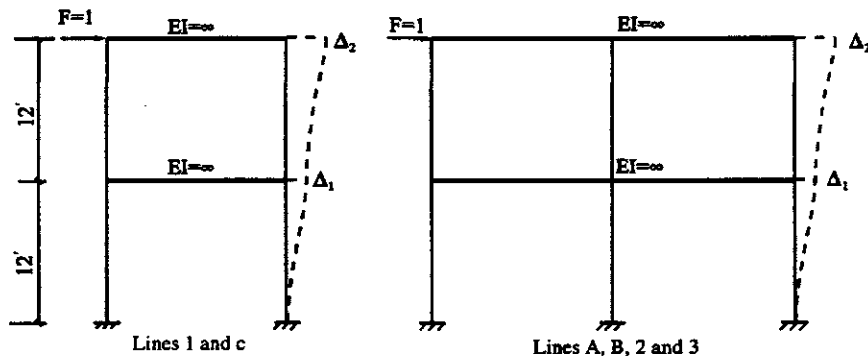
$$V_{xe} = \frac{M_r \bar{y} k_x}{J_r} = \frac{(4667)(120)(12EI_y)}{2647448.53EI_x} = 1.269 \text{ k}$$

$$V_{ye} = \frac{M_r \bar{x} k_y}{J_r} = \frac{(4667)(226.67)(24EI_x)}{2647448.53EI_x} = 9.590 \text{ k}$$

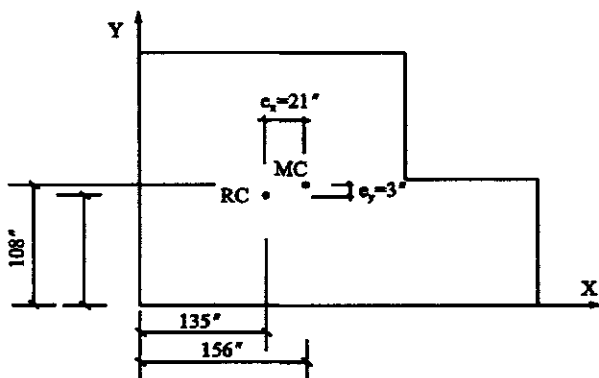
10.8. Without $P-\Delta$ effect,

Mode	\bar{M}/M	Displacements (SRSS)	Member forces (SRSS)	Inertia forces
1	0.9331	0.672 in	94.054 k	17.6 k
2	0.575×10^{-1}	1.049 in	79.206 k	23.92 k
3	0.829×10^{-2}	1.318 in	57.068 k	28.89 k
4	0.111×10^{-2}	1.451 in	28.734 k	28.73 k

10.9.



Calculation of planar frame rigidity

**FIG. SOL. 10.9** (a) Calculation of planar frame rigidity. (b) Location of mass and rigidity centres.

10.10.

1. First mode only (UBC-94); first mode only (UBC-97).
2. $\gamma = 2.235$, $V = 92.813$ k (UBC-94); $V = 105.88$ k (UBC-97).
3. $F_1 = 35.452$ k; $F_2 = 57.1$ k (UBC-94); $F_1 = 40.443$ k; $F_2 = 65.437$ k (UBC-97).
- 4.

$$\begin{Bmatrix} x_{s1} \\ x_{s2} \end{Bmatrix} = \begin{Bmatrix} 0.0411 \\ 0.0166 \end{Bmatrix} \text{ ft (UBC-94)}$$

$$\begin{Bmatrix} x_{s1} \\ s_{s2} \end{Bmatrix} = \begin{Bmatrix} 0.0469 \\ 0.0759 \end{Bmatrix} \text{ ft (UBC-97)}$$

10.11. UBC-94

1. First two modes.
2. $V_u = 46.04$ k.
3. $V = 79.49$ k.
4. $F(\text{roof}) = 41.81$ k; $F(\text{flr2}) = 31.59$ k; $F(\text{flr1}) = 19.83$ k.
- 5.

$$\{x_u\} = \begin{Bmatrix} 2.90 \\ 1.96 \\ 0.75 \end{Bmatrix} \text{ in}; \quad \{\Delta_u\} = \begin{Bmatrix} 0.97 \\ 1.22 \\ 0.75 \end{Bmatrix} \text{ in}$$

UBC-97:

1. First two modes.
2. $V_D = 65$ k.
3. $V_s = 149.86$ k.
4. $F(\text{roof}) = 66.16$ k; $F(\text{flr2}) = 49.9$ k; $F(\text{flr1}) = 31.39$ k.
- 5.

$$\begin{aligned} \{x_s\} &= \begin{Bmatrix} 1.67 \\ 1.13 \\ 0.43 \end{Bmatrix} \text{ in} \\ \{x_M\} &= \begin{Bmatrix} 9.94 \\ 6.72 \\ 2.56 \end{Bmatrix} \text{ in} \\ \{\Delta_s\} &= \begin{Bmatrix} 0.56 \\ 0.70 \\ 0.43 \end{Bmatrix} \text{ in} \\ \{\Delta_M\} &= \begin{Bmatrix} 3.22 \\ 4.16 \\ 2.56 \end{Bmatrix} \text{ in} \end{aligned}$$

IBC-2000:

1. First two modes
2. $V_t = 69.05$ k.
3. $V_s = 102.63$ k.
4. $F(\text{roof}) = 56.8$ k; $F(\text{flr2}) = 42.91$ k; $F(\text{flr1}) = 26.95$ k.
- 5.

$$\begin{aligned} \{\delta\} &= \begin{Bmatrix} 4.71 \\ 3.18 \\ 1.22 \end{Bmatrix} \text{ in} \\ \{\Delta\} &= \begin{Bmatrix} 1.59 \\ 1.97 \\ 0.22 \end{Bmatrix} \text{ in} \end{aligned}$$

Appendix A—Lagrange's Equation

Consider a vibrating structural system shown in Fig. A-1; the symbolic displacements may be defined as A_i where $i = 1, 2, \dots, m$, and m is the possible longitudinal, transverse, and rotational motion. Let the generalized coordinates be q_i , $i = 1, 2, \dots, n$, as given in Fig. A-2. Thus the position of a mass k can be defined as

$$A_k = A_k(q_1, q_2, \dots, q_m, t) \quad (\text{A-1})$$

From Eq. (A-1)

$$\frac{dA_i}{dt} = \dot{A}_i = \frac{\partial A_i}{\partial q_1} \dot{q}_1 + \frac{\partial A_i}{\partial q_2} \dot{q}_2 + \dots + \frac{\partial A_i}{\partial q_m} \dot{q}_m \quad (\text{A-2})$$

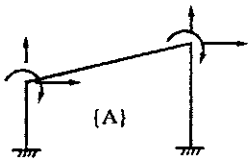


FIG. A-1

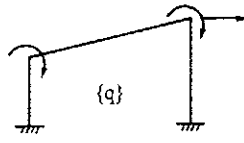


FIG. A-2

The derivation of Eq. (A-2) with respect to time \dot{q}_k yields

$$\frac{\partial \dot{A}_i}{\partial \dot{q}_k} = \frac{\partial A_i}{\partial q_k} \quad (\text{A-3})$$

From Eq. (A-1)

$$\frac{\partial A_i}{\partial q_k} = \frac{\partial A_i}{\partial q'_s} (q'_s, t) \quad (\text{A-4})$$

Then

$$\frac{d}{dt} \left(\frac{\partial A_i}{\partial q_k} \right) = \frac{\partial^2 A_i}{\partial q_1 \partial q_k} \frac{\partial q_1}{\partial t} + \frac{\partial^2 A_i}{\partial q_2 \partial q_k} \frac{\partial q_2}{\partial t} + \cdots + \frac{\partial^2 A_i}{\partial q_m \partial q_k} \frac{\partial q_m}{\partial t} \quad (\text{A-5})$$

From Eq. (A-2)

$$\frac{\partial \dot{A}_i}{\partial q_k} = \frac{\partial^2 A_i}{\partial q_1 \partial q_k} \dot{q}_1 + \frac{\partial^2 A_i}{\partial q_2 \partial q_k} \dot{q}_2 + \cdots + \frac{\partial^2 A_i}{\partial q_m \partial q_k} \dot{q}_m \quad (\text{A-6})$$

Comparing Eq. (A-5) with Eq. (A-6) yields

$$\frac{d}{dt} \left(\frac{\partial A_i}{\partial q_k} \right) = \frac{\partial \dot{A}_i}{\partial q_k} \quad (\text{A-7})$$

Virtual work δ_w and virtual displacement δA_k can be expressed as

$$\delta_w = \sum_{k=1}^p F_k \delta A_k \quad (\text{A-8})$$

where $p \geq m$ and

$$\delta A_k = \frac{\partial A_k}{\partial q_1} \delta q_1 + \frac{\partial A_k}{\partial q_2} \delta q_2 + \cdots + \frac{\partial A_k}{\partial q_m} \delta q_m \quad (\text{A-9})$$

in which F_k is the one of p forces acting at and along the respective coordinates. The virtual work can be also expressed in terms of generalized coordinates and generalized forces as

$$\delta_w = \sum_{i=1}^m Q_i \delta q_i = \sum_{k=1}^p F_k \delta A_k = \sum_{i=1}^m \sum_{k=1}^p F_k \frac{\partial A_k}{\partial q_i} \delta q_i \quad (\text{A-10})$$

Therefore the generalized forces associated with the generalized coordinates may be written on the basis of Eqs. (A-8)–(A-10) as

$$Q_i = \sum_{k=1}^p F_k \frac{\partial A_k}{\partial q_i} \quad (\text{A-11})$$

If the external forces of the masses F_k are equal to their respective inertial forces

$$F_k = M_k \ddot{A}_k \quad (\text{A-12})$$

then Eq. (A-11) may now be expressed as

$$Q_i = \sum_{k=1}^p M_k \ddot{A}_k \frac{\partial A_k}{\partial q_i} \quad (\text{A-13})$$

Since kinetic energy T has the following form:

$$T = \frac{1}{2} \sum_{k=1}^p M_k \dot{A}_k^2 \quad (\text{A-14})$$

then

$$\frac{\partial T}{\partial q_i} = \sum_{k=1}^p M_k \dot{A}_k \frac{\partial \dot{A}_k}{\partial q_i} \quad (\text{A-15})$$

$$\frac{\partial T}{\partial \dot{q}_i} = \sum_{k=1}^p M_k \dot{A}_k \frac{\partial \dot{A}_k}{\partial \dot{q}_i} = \sum_{k=1}^p M_k \dot{A}_k \frac{\partial A_k}{\partial q_i} \quad (\text{A-16})$$

From Eq. (A-16),

$$\frac{d}{dt} \frac{\partial T}{\partial \dot{q}_i} - \frac{\partial T}{\partial q_i} = \sum_{k=1}^p M_k \left(\ddot{A}_k \frac{\partial A_k}{\partial q_i} + \dot{A}_k \frac{\partial \dot{A}_k}{\partial q_i} \right) \quad (\text{A-17})$$

Comparing Eq. (A-17) with Eqs. (A-13) and (A-15) gives

$$\frac{d}{dt} \frac{\partial T}{\partial \dot{q}_i} - \frac{\partial T}{\partial q_i} = Q_i \quad (\text{A-18})$$

Let the generalized forces be

$$Q_i = Q_{v,i} + Q_{D,i} + Q_{w,i} \quad (\text{A-19})$$

in which $Q_{v,i}$ = spring forces, $Q_{D,i}$ = damping forces, and $Q_{w,i}$ = applied forces. Let the spring force due to change of the potential energy V be

$$Q_{v,i} = -\frac{\partial V}{\partial q_i} \quad (\text{A-20})$$

the damping force due to dissipated energy D be

$$Q_{D,i} = -\frac{\partial D}{\partial q_i} \quad (\text{A-21})$$

and the applied forces, acting along the generalized coordinates, due to change of work W , be

$$Q_{w,i} = \frac{\partial W}{\partial q_i} \quad (\text{A-22})$$

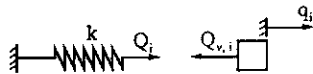
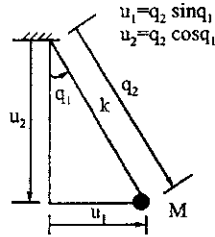
Then Lagrange's equation may be written by using Eqs. (A-18)–(A-22) as

$$\frac{d}{dt} \left(\frac{\partial T}{\partial \dot{q}_i} \right) - \frac{\partial T}{\partial q_i} + \frac{\partial V}{\partial q_i} + \frac{\partial D}{\partial q_i} = \frac{\partial W}{\partial q_i} \quad (\text{A-23})$$

More details about Lagrange's equation can be found in Chapter 4 of Tuma and Cheng (1983).

Equation (A-21) is derived using the virtual work principle. Since potential energy V can be uniquely defined by the generalized coordinates of the structure,

$$V = V(q_1, q_2, q_3, \dots, q_n, t) \quad (\text{A-24})$$

**FIG. A-3****FIG. A-4**

A variation of V , δV , associated with an arbitrary set of virtual displacements, δq , is

$$\delta V = \sum_{i=1}^n \frac{\partial V}{\partial q_i} \delta q_i \quad (\text{A-25})$$

Based on the principle of virtual work, this change in strain energy may be expressed in terms of the virtual work done by the generalized forces acting through these same virtual displacements.

$$\delta V = \sum_{i=1}^n Q_i \delta q_i \quad (\text{A-26})$$

Because the generalized coordinates q_1, \dots, q_n are all independent, the corresponding virtual displacements can be arbitrarily defined. Then the two expressions in Eqs. (A-25) and (A-26) may be compared term by term, which yields

$$Q_i = \frac{\partial V}{\partial q_i} \quad (\text{A-27})$$

Eq. (A-27) has a positive sign since the force is considered to be applied to the elastic element as the spring of the spring-mass system shown in Fig. A-3. When generalized force is applied to the mass, it has the opposite sign as in Eq. (A-28):

$$Q_{v,i} = -\frac{\partial V}{\partial q_i} \quad (\text{A-28})$$

Equation (A-21) can again be derived using the principle of virtual work. Let F_j be the applied damping forces along virtual displacements δu_j in the u constrained coordinate system. The virtual work done by these forces in the u -system is

$$\delta W_D = \sum_j F_j \delta u_j \quad (\text{A-29})$$

We now apply a coordinate transformation

$$u_j = u_j(q_1, q_2, \dots, q_n) \quad (\text{A-30})$$

which is illustrated in the system shown in Fig. A-4. This example shows the transformation from the constrained coordinates, u , to the generalized coordinates, q . Thus

$$\delta u_j = \sum_{i=1}^n \frac{\partial u_j}{\partial q_i} \delta q_i \quad (\text{A-31})$$

Consequently

$$\left. \begin{aligned} \delta u_1 &= q_2 \cos q_1 \delta q_1 + \sin q_1 \delta q_2 \\ \delta u_2 &= -q_2 \sin q_1 \delta q_1 + \cos q_1 \delta q_2 \end{aligned} \right\} \quad (\text{A-32})$$

Substituting Eq. (A-31) into Eq. (A-29) yields

$$\delta W_D = \sum_j F_j \sum_i \frac{\partial u_j}{\partial q_i} \delta q_i \quad (\text{A-33})$$

Interchanging the order of summation, we obtain

$$\delta W_D = \sum_i \delta q_i \sum_j F_j \frac{\partial u_j}{\partial q_i} \quad (\text{A-34})$$

Virtual work δW_D can also be expressed as the sum of the work done by the generalized damping force Q_i along their corresponding virtual displacements δq_i ,

$$\delta W_D = \sum_i Q_i \delta q_i \quad (\text{A-35})$$

Comparing Eqs. (A-34) with Eq. (A-35) gives

$$Q_i = \sum_j F_j \frac{\partial u_j}{\partial q_i}; \quad i = 1, 2, \dots, n \quad (\text{A-36})$$

The damping force in Eq. (A-36) must be taken as negative since a positive damping force always takes a direction opposite to the generalized displacement of the mass. Therefore

$$Q_{D,i} = - \sum_j \frac{F_i \partial u_j}{\partial q_i} = - \frac{\partial D}{\partial q_i} \quad (\text{A-37})$$

where $D = \sum_j F_i u_j$.

Equation (A-22) can also be derived using the principle of virtual work. Let G_j be the applied forces along virtual displacements δS_j in the S constrained coordinate system. Virtual work becomes

$$\delta W_w = \sum_j G_j \delta S_j \quad (\text{A-38})$$

Apply a coordinate transformation as in Eq. (A-30) into generalized coordinates

$$S_j = S_j(q_1, q_2, \dots, q_n) \quad (\text{A-39})$$

Then

$$\delta S_j = \sum_{i=1}^n \frac{\partial S_j}{\partial q_i} \delta q_i \quad (\text{A-40})$$

Substituting Eq. (A-40) into Eq. (A-38) yields

$$\delta W_w = \sum_i \delta q_i \sum_j G_j \frac{\partial S_j}{\partial q_i} \quad (\text{A-41})$$

Virtual work δW_w can also be expressed as the sum of the work done by the generalized external forces $Q_{w,i}$ along their corresponding virtual displacements δq_i

$$\delta W_w = \sum_i Q_{w,i} \delta q_i \quad (\text{A-42})$$

Comparing Eq. (A-41) with Eq. (A-42) gives

$$Q_{w,i} = \sum_j G_j \frac{\partial S_j}{\partial q_i} = \frac{\partial W}{\partial q_i} \quad (\text{A-43})$$

where $W = \sum_j G_j S_j$.

Appendix B—Derivation of Ground Rotational Records

Derivation of the rotational component ϕ_x due to displacement components u_z and u_y is shown here. Rotation of an elastic soil volume is assumed to be the mean value of infinitesimal line elements emanating from point P as shown in Fig. B-1. Since we are concerned only with rotations of line elements, let position p^* of the soil particle in the deformed medium coincide with its position P in the undeformed medium. In the figure, \overline{PQ} represents the line element at the undeformed stage and $\overline{P^*Q^*}$ represents the line element after deformation. Differentials of dis-

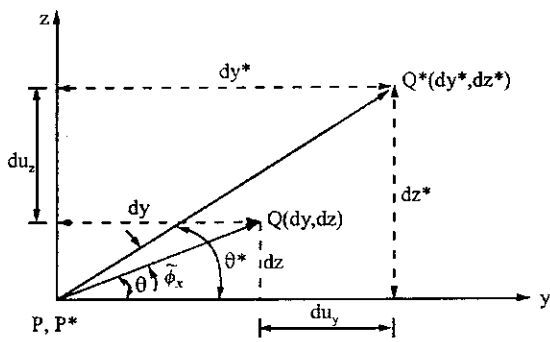


FIG. B-1 Elastic line element.

placement components u_y and u_z can be expressed as

$$du_y = \left(\frac{\partial u_y}{\partial y} dy + \frac{\partial u_y}{\partial z} dz \right) \quad (B-1)$$

$$du_z = \left(\frac{\partial u_z}{\partial y} dy + \frac{\partial u_z}{\partial z} dz \right) \quad (B-2)$$

Because $dy^* = dy + du_y$, $dz^* = dz + du_z$ (see Fig. B-1), dy^* and dz^* can be expressed as

$$\begin{aligned} dy^* &= dy + \left(\frac{\partial u_y}{\partial y} dy + \frac{\partial u_y}{\partial z} dz \right) \\ &= \left(1 + \frac{\partial u_y}{\partial y} \right) dy + \left(\frac{\partial u_y}{\partial z} \right) dz \end{aligned} \quad (B-3)$$

$$\begin{aligned} dz^* &= dz + \left(\frac{\partial u_z}{\partial y} dy + \frac{\partial u_z}{\partial z} dz \right) \\ &= \left(\frac{\partial u_z}{\partial z} \right) dy + \left(1 + \frac{\partial u_z}{\partial z} \right) dz \end{aligned} \quad (B-4)$$

Now define the following notation:

$$e_y = \frac{\partial u_y}{\partial y}; \quad e_z = \frac{\partial u_z}{\partial z}; \quad \text{and } e_{yz} = \left(\frac{\partial u_z}{\partial y} + \frac{\partial u_y}{\partial z} \right) \quad (B-5)$$

and let

$$\omega_x = \frac{1}{2} \left(\frac{\partial u_z}{\partial y} - \frac{\partial u_y}{\partial z} \right) \quad (B-6)$$

Then Eqs. (B-3) and (B-4) become

$$dy^* = (1 + e_y) dy + \left(\frac{1}{2} e_{yz} - \omega_x \right) dz \quad (B-7)$$

$$dz^* = \left(\frac{1}{2} e_{yz} + \omega_x \right) dy + (1 + e_z) dz \quad (B-8)$$

From Fig. B-1,

$$\begin{aligned} \tan \theta^* &= \frac{dz^*}{dy^*} = \frac{\left(\frac{1}{2} e_{yz} + \omega_x \right) dy + (1 + e_z) dz}{(1 + e_y) dy + \left(\frac{1}{2} e_{yz} - \omega_x \right) dz} \\ &= \frac{\left(\frac{1}{2} e_{yz} + \omega_x \right) + (1 + e_z) \tan \theta}{(1 + e_y) + \left(\frac{1}{2} e_{yz} - \omega_x \right) \tan \theta} \end{aligned} \quad (B-9)$$

The angle of rotation of line element \overline{PQ} about the x axis is

$$\tilde{\phi}_x = \theta^* - \theta \quad (B-10)$$

Because

$$\tan \tilde{\phi}_x = \frac{\tan \theta^* - \tan \theta}{1 + \tan \theta^* \tan \theta} \quad (\text{B-11})$$

From Eqs. (B-9) and (B-11)

$$\begin{aligned} \tan \tilde{\phi}_x &= \frac{\left(\frac{1}{2}e_{yz} + \omega_x \right) + (1 + e_z) \tan \theta}{\left((1 + e_y) + \left(\frac{1}{2}e_{yz} - \omega_x \right) \tan \theta \right)} - \tan \theta \\ &= \frac{\left(\frac{1}{2}e_{yz} + \omega_x \right) \tan \theta + (1 + e_z) \tan^2 \theta}{1 + \frac{\left(\frac{1}{2}e_{yz} + \omega_x \right) \tan \theta + (1 + e_z) \tan^2 \theta}{\left((1 + e_y) + \left(\frac{1}{2}e_{yz} - \omega_x \right) \tan \theta \right)}} \\ &= \frac{\left(\frac{1}{2}e_{yz} + \omega_x \right) + (1 + e_z) \tan \theta - (1 + e_y) \tan \theta - \left(\frac{1}{2}e_{yz} - \omega_x \right) \tan^2 \theta}{\left((1 + e_y) + \left(\frac{1}{2}e_{yz} - \omega_x \right) \tan \theta \right)} \\ &= \frac{\left((1 + e_y) + \left(\frac{1}{2}e_{yz} - \omega_x \right) \tan \theta + \left(\frac{1}{2}e_{yz} + \omega_x \right) \tan \theta + (1 + e_z) \tan^2 \theta \right)}{\left((1 + e_y) + \left(\frac{1}{2}e_{yz} - \omega_x \right) \tan \theta \right)} \quad (\text{B-12}) \\ &= \frac{\frac{1}{2}e_{yz} + \omega_x + (e_z - e_y) \tan \theta - \left(\frac{1}{2}e_{yz} - \omega_x \right) \tan^2 \theta}{(1 + e_y) + e_{yz} \tan \theta + (1 + e_z) \tan^2 \theta} \\ &= \frac{\frac{1}{2}e_{yz} \cos^2 \theta + \omega_x + (e_z - e_y) \sin \theta \cos \theta - \frac{1}{2}e_{yz} \sin^2 \theta}{\cos^2 \theta + e_y \cos^2 \theta + e_{yz} \sin \theta \cos \theta + \sin^2 \theta + e_z \sin^2 \theta} \\ &= \frac{\omega_x + \frac{1}{2}(e_z - e_y) \sin 2\theta + \frac{1}{2}e_{yz} \cos 2\theta}{1 + e_y \cos^2 \theta + e_z \sin^2 \theta + \frac{1}{2}e_{yz} \sin 2\theta} \end{aligned}$$

If deformation is small, then e_y , e_z , and e_{yz} are small in comparison with the unit value in the denominator and thus can be negligible. Therefore, the denominator of Eq. (B-12) is approximately equal to 1. Thus Eq. (B-12) becomes

$$\tan \tilde{\phi}_x = \omega_x + \frac{1}{2}(e_z - e_y) \sin 2\theta + \frac{1}{2}e_{yz} \cos(2\theta) \quad (\text{B-13})$$

Because $\tilde{\phi}_x$ is a small angle,

$$\tan \tilde{\phi}_x \simeq \tilde{\phi}_x \quad (\text{B-14})$$

We may approximate Eq. (B-13) as follows:

$$\begin{aligned}
 \phi_x &= \frac{1}{2\pi} \int_0^{2\pi} \tilde{\phi}_x d\theta \\
 &= \frac{1}{2\pi} \int_0^{2\pi} \left(\omega_x + \frac{1}{2} (e_z - e_y) \sin 2\theta + \frac{1}{2} e_{yz} \cos(2\theta) \right) d\theta \\
 &= \omega_x - \frac{1}{8\pi} (e_z - e_y) \cos 2\theta \Big|_0^{2\pi} + \frac{1}{8\pi} e_{yz} \sin 2\theta \Big|_0^{2\pi} \\
 &= \omega_x \\
 &= \frac{1}{2} \left(\frac{\partial u_z}{\partial y} - \frac{\partial u_y}{\partial z} \right)
 \end{aligned} \tag{B-15}$$

Similar derivations can be obtained for ϕ_y and ϕ_z .

Appendix C—Vector Analysis Fundamentals

A vector is a quantity having both magnitude and direction, such as displacement, velocity, force and acceleration. In a right-hand rectangular coordinate system, any vector \vec{A} can be expressed as

$$\vec{A} = \vec{A}_x i + \vec{A}_y j + \vec{A}_z k \quad (\text{C-1})$$

where A_x, A_y, A_z are known as scalar components of \vec{A} ; \vec{i}, \vec{j} , and \vec{k} are unit vectors along X_g, Y_g , and Z_g directions, respectively, as shown in Fig. C-1. ‘Unit vector’ means that a vector has unit magnitude which can be expressed as the vector divided by its length (non-zero).

The length of vector \vec{A} is

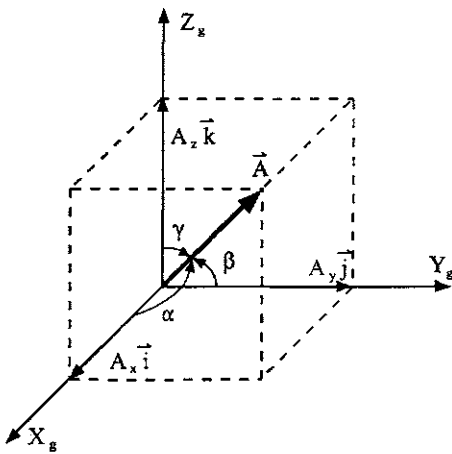
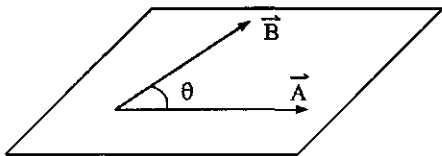
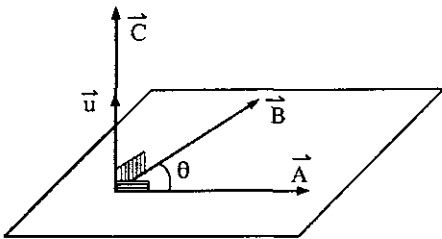
$$|\vec{A}| = \sqrt{A_x^2 + A_y^2 + A_z^2} \quad (\text{C-2a})$$

and the direction cosines of \vec{A} are

$$\cos \alpha = \frac{A_x}{|\vec{A}|}, \quad \cos \beta = \frac{A_y}{|\vec{A}|}, \quad \cos \gamma = \frac{A_z}{|\vec{A}|} \quad (\text{C-2b})$$

in which α, β , and γ are angles of vector \vec{A} to the X_g, Y_g , and Z_g axes, respectively. Thus Eq. (C-1) can be expressed as

$$\vec{A} = (\cos \alpha \vec{i} + \cos \beta \vec{j} + \cos \gamma \vec{k}) |\vec{A}| \quad (\text{C-3})$$

**FIG. C-1** Vector notations.**FIG. C-2** Vector dot product.**FIG. C-3** Vector cross product.

Two technical terms, *dot* and *cross product*, are used in fundamental vector analysis. Dot, or *scalar product*, of two vectors \vec{A} and \vec{B} is defined as the product of the magnitudes of \vec{A} and \vec{B} and the cosine of angle θ between them as shown in Fig. C-2

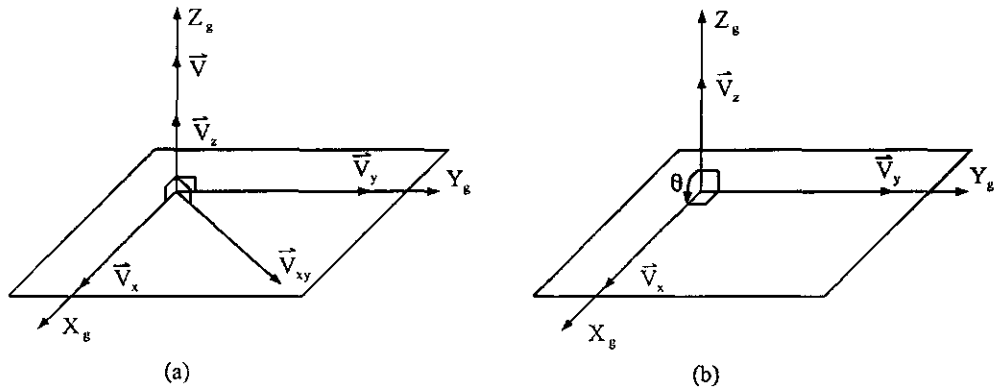
$$\vec{A} \cdot \vec{B} = |\vec{A}| |\vec{B}| \cos \theta \quad 0 \leq \theta \leq \pi \quad (\text{C-4})$$

$\vec{A} \cdot \vec{B}$ is a scalar and not a vector. If $\vec{A} \cdot \vec{B} = 0$, and \vec{A} or \vec{B} is not a null vector, then \vec{A} and \vec{B} are perpendicular. Since the scalar product is commutative, $\vec{A} \cdot \vec{B} = \vec{B} \cdot \vec{A}$. It is unnecessary to determine the direction of angle θ .

The cross product of \vec{A} and \vec{B} is vector $\vec{C} = \vec{A} \times \vec{B}$. The magnitude of $\vec{A} \times \vec{B}$ is the product of the magnitudes of \vec{A} and \vec{B} and the sine of angle θ between them, as shown in Fig. C-3. The direction of vector $\vec{C} = \vec{A} \times \vec{B}$ is perpendicular to plane \vec{A} and \vec{B} .

$$\vec{A} \times \vec{B} = |\vec{A}| |\vec{B}| \sin \theta \vec{u} \quad (\text{C-5})$$

\vec{u} is a unit vector indicating the direction of $\vec{A} \times \vec{B}$. If \vec{A} is parallel to \vec{B} , then $\sin \theta = 0$, $\vec{A} \times \vec{B} = 0$.

**FIG. C-4** Vectors in GCS.

Assume that \vec{V}_x , \vec{V}_y , and \vec{V}_z are unit vectors along the X_g , Y_g and Z_g axes, respectively, in the right-hand rectangular coordinate system of GCS, as shown in Fig. C-4. If vector \vec{V}_x is given and \vec{V}_{xy} can be an arbitrary vector in the X_g-Y_g plane, then \vec{V} can be determined by using the cross product as

$$\vec{V} = \vec{V}_x \times \vec{V}_{xy} \quad (\text{C-6})$$

where \vec{V} is along the Z_g direction. The length of \vec{V} is $|\vec{V}_x \times \vec{V}_{xy}|$ and unit vector \vec{V}_z is

$$\vec{V}_z = \frac{\vec{V}_x \times \vec{V}_{xy}}{|\vec{V}_x \times \vec{V}_{xy}|} \quad (\text{C-7})$$

Unit vector \vec{V}_y is also determined using the cross product as

$$\vec{V}_y = \frac{\vec{V}_z \times \vec{V}_x}{|\vec{V}_z \times \vec{V}_x|} \quad (\text{C-8})$$

in which

$$|\vec{V}_z \times \vec{V}_x| = |\vec{V}_z| |\vec{V}_x| \sin \theta$$

Since θ is an angle of 90° between the X_g and Z_g axes

$$|\vec{V}_z \times \vec{V}_x| = |\vec{V}_z| |\vec{V}_x| = 1$$

and

$$\vec{V}_y = \vec{V}_z \times \vec{V}_x \quad (\text{C-9})$$

Equations (C-6) and (C-7) are shown in Fig. C-4a and Eq. (C-9) is shown in Fig. C-4b.

Appendix D—Transformation Matrix Between JCS and GCS

The transformation matrix between JCS and GCS can be obtained using one of the following two methods. The first uses direction cosines to define the transformation; the second requires transforming each of three joint coordinates one at a time. The results of these two approaches are the same. The methods are first derived; identical results are then proved.

METHOD 1

The relationship between GCS and JCS is shown in Fig. D-1, where X_g , Y_g , and Z_g represent axes of GCS; X_j , Y_j , and Z_j are axes of JCS. \vec{V}_{xj} , \vec{V}_{yj} , and \vec{V}_{zj} are unit vectors along X_j , Y_j , and Z_j axes in JCS; the direction cosine angles of the unit vector \vec{V}_{xj} are α_1 , β_1 , and γ_1 in GCS. From Eq. (C-3)

$$\vec{V}_{xj} = (\cos \alpha_1 \vec{i} + \cos \beta_1 \vec{j} + \cos \gamma_1 \vec{k}) | \vec{V}_x | \quad (D-1)$$

Since \vec{V}_{xj} is a unit vector, $| \vec{V}_{xj} | = 1$,

$$\vec{V}_{xj} = (\cos \alpha_1 \vec{i} + \cos \beta_1 \vec{j} + \cos \gamma_1 \vec{k}) (1) = C_{11} \vec{i} + C_{12} \vec{j} + C_{13} \vec{k} \quad (D-2)$$

where

$$C_{11} = \cos \alpha_1; \quad C_{12} = \cos \beta_1; \quad C_{13} = \cos \gamma_1$$

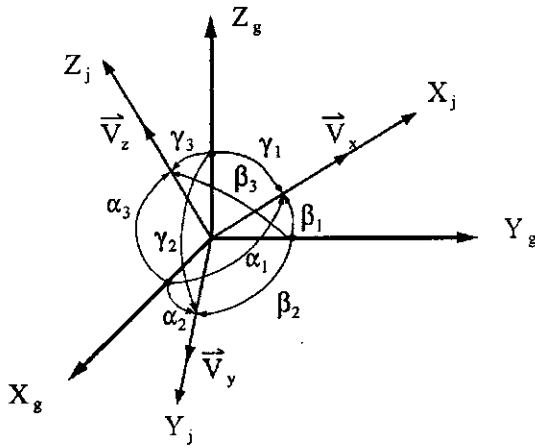


FIG. D-1 JCS vs GCS.

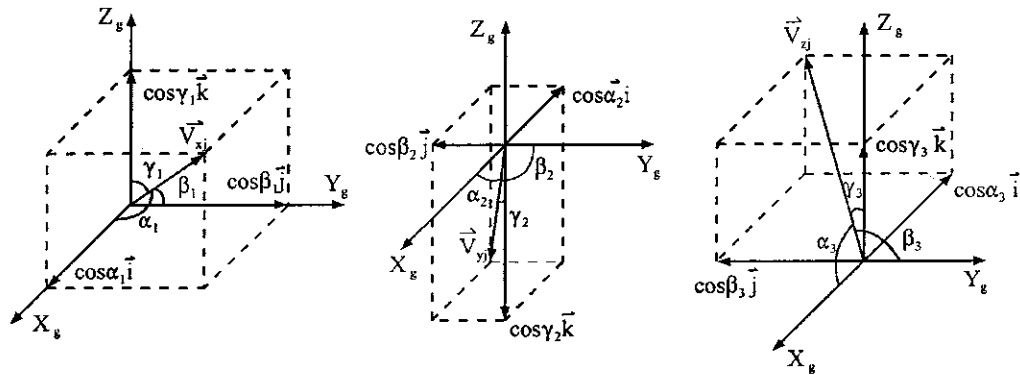


FIG. D-2 Vector of JCS related to GCS.

The direction cosine angles of unit vector \vec{V}_{yj} are α_2 , β_2 , and γ_2 in GCS and can be expressed in the following form:

$$\vec{V}_{yj} = (\cos \alpha_2 \vec{i} + \cos \beta_2 \vec{j} + \cos \gamma_2 \vec{k}) = C_{21} \vec{i} + C_{22} \vec{j} + C_{23} \vec{k} \quad (D-3)$$

A similar expression of the direction cosine angles of unit vector \vec{V}_{zj} is

$$\vec{V}_{zj} = (\cos \alpha_3 \vec{i} + \cos \beta_3 \vec{j} + \cos \gamma_3 \vec{k}) = C_{31} \vec{i} + C_{32} \vec{j} + C_{33} \vec{k} \quad (D-4)$$

Eqs. (D-2)–(D-4) form Eq. (8.1) as

$$\begin{Bmatrix} \vec{V}_{xj} \\ \vec{V}_{yj} \\ \vec{V}_{zj} \end{Bmatrix} = \begin{bmatrix} C_{11} & C_{12} & C_{13} \\ C_{21} & C_{22} & C_{23} \\ C_{31} & C_{32} & C_{33} \end{bmatrix} \begin{Bmatrix} \vec{i} \\ \vec{j} \\ \vec{k} \end{Bmatrix} = [C_j] \begin{Bmatrix} \vec{i} \\ \vec{j} \\ \vec{k} \end{Bmatrix} \quad (8.1)$$

Equations (D-2)–(D-4) are illustrated in Fig. D-2.

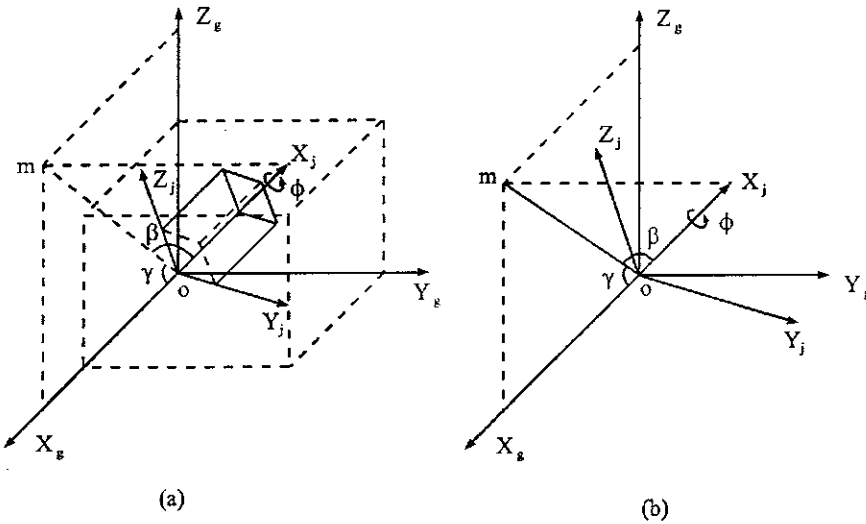


FIG. D-3 General orientation of JCS and GCS.

METHOD 2

Method 2 provides another approach to the transformation matrix between GCS and JCS. Let Fig. D-3 show the two coordinate systems where line \overline{om} is on the X_g - Z_g plane with angle γ to the X_g axis, line \overline{om} and the X_j axis are on a plane with an angle β , and the positive rotational angle about the X_j -axis is signified by ϕ . These three angles are used to transform global coordinates into joint coordinates. Three steps employed for the transformation are depicted as follows.

Step 1

Let the X_g - Y_g - Z_g axes rotate about the Y_g axis with angle γ as indicated in Fig. D-4a. Then a new set of X_γ - Y_γ - Z_γ axes is obtained for which X_γ and Z_γ axes are on the original X_g - Z_g plane and the Y_γ axis coincides with the original Y_g axis.

For arbitrary point p^* , its location in space can be represented by X_g , Y_g , and Z_g in GCS, and by X_γ , Y_γ , and Z_γ in X_γ - Y_γ - Z_γ system (see Fig. D-4b). Since the Y_γ axis is parallel to the Y_g axis, we obtain $Y_\gamma = Y_g$. The projection of p^* in the X_γ - Z_γ plane is expressed as p . Figure D-4c shows p 's coordinate relationship between GCS and the X_γ - Y_γ - Z_γ system, from which we have $\overline{yw} = \overline{ox} = X_g$. Since \overline{ox} is parallel to \overline{yw} and \overline{sw} is parallel to \overline{ol} , angle $\angle xol$ is the same as angle $\angle uwv$ and equal to γ . Thus and $\overline{xn} = \overline{yu} = \overline{ot} = \overline{sr}$ and $\overline{wu} = \overline{on} = \overline{ml}$. Coordinates X_γ and Z_γ can be expressed in terms of X_g and Z_g

$$\begin{aligned}\bar{X}_\gamma &= \overline{ol} = \overline{om} + \overline{ml} = \overline{om} + \overline{on} = X_g \cos \gamma + Z_g \sin \gamma \\ \bar{Z}_\gamma &= \overline{os} = \overline{or} - \overline{sr} = \overline{or} - \overline{ot} = -X_g \sin \gamma + Z_g \cos \gamma\end{aligned}$$

from which the first step transformation is formed:

$$\begin{Bmatrix} X_\gamma \\ Y_\gamma \\ Z_\gamma \end{Bmatrix} = \begin{bmatrix} \cos \gamma & 0 & \sin \gamma \\ 0 & 1 & 0 \\ -\sin \gamma & 0 & \cos \gamma \end{bmatrix} \begin{Bmatrix} X_g \\ Y_g \\ Z_g \end{Bmatrix} = [C_1] \begin{Bmatrix} X_g \\ Y_g \\ Z_g \end{Bmatrix} \quad (\text{D-5})$$

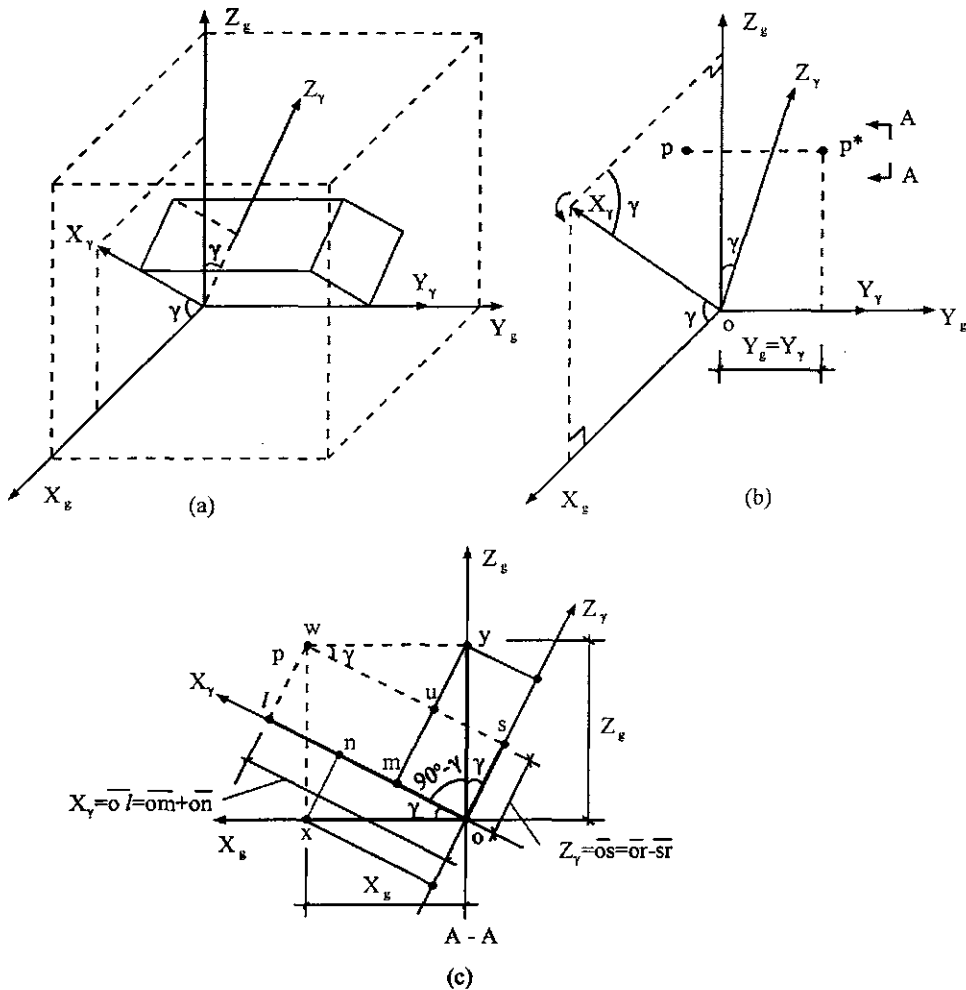


FIG. D-4 Rotation of $X_g-Y_g-Z_g$ Axes about Y_g to form $X_y-Y_y-Z_y$ axes.

Step 2

Let the $X_y-Y_y-Z_y$ axes (see Fig. D-4) rotate about the Z_y axis through angle β . Then a new set of $Y_\beta-Z_\beta$ axes is constructed as shown in Fig. D-5. In this new system, the X_β axis coincides with the X_j axis, the Z_β axis is the same as the Z_y axis, the Y_β axis has an angle of β to the Y_g axis, and $Y_\beta-Z_\beta$ plane is in the Y_j-Z_j plane. Assume that coordinates of point p^* in the $X_\beta-Y_\beta-Z_\beta$ system are X_β , Y_β , and Z_β ; the relationship of coordinates between the $X_y-Y_y-Z_y$ system and $X_\beta-Y_\beta-Z_\beta$ system is shown in Fig. D-5b. The projection p^* on $X_\beta-Y_\beta$ plane is denoted by p' shown in Fig. D-5c.

Following the procedure used to establish a similar triangle relationship in Fig. D-4c, coordinates X_β and Y_β in Fig. D-5c can be expressed as

$$X_\beta = \overline{ol} = \overline{om} + \overline{on} = X_y \cos \beta + Y_y \sin \beta$$

$$Y_\beta = \overline{os} = \overline{or} - \overline{ol} = -X_y \sin \beta + Y_y \cos \beta$$

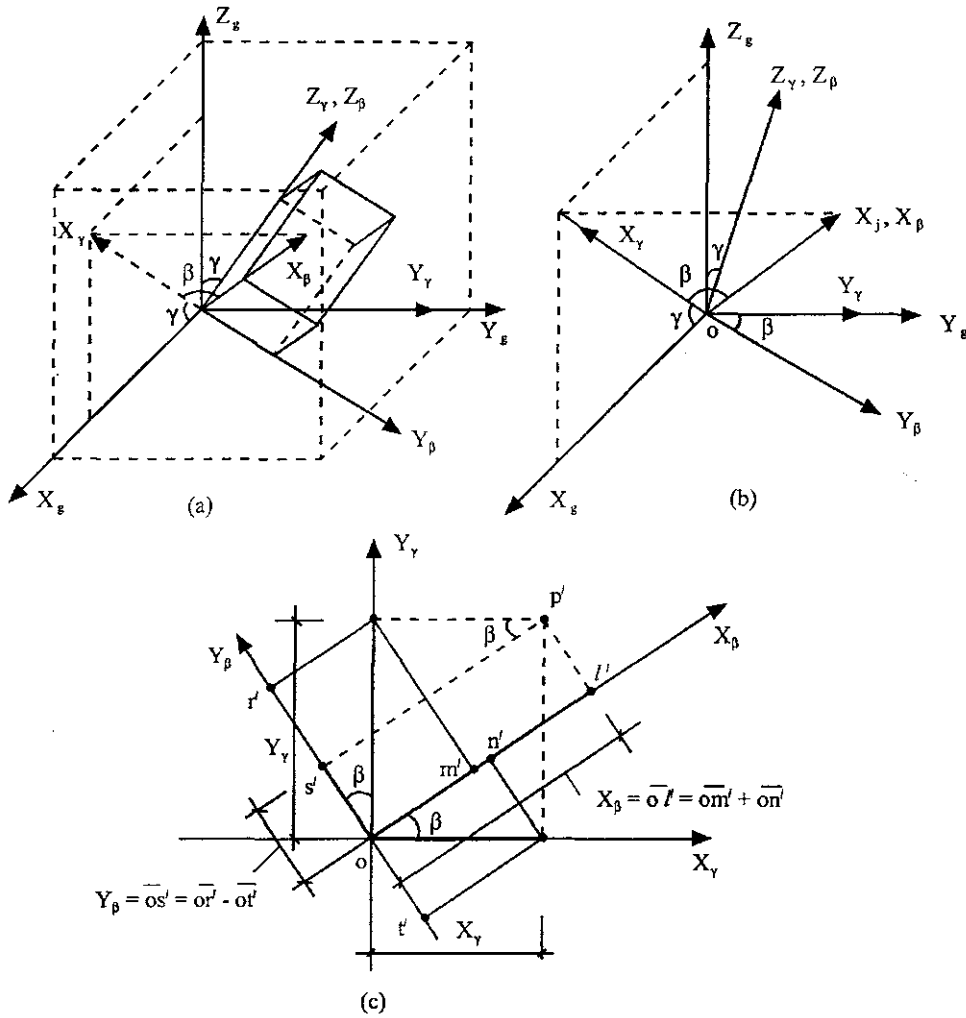


FIG. D-5 Rotation of X_γ - Y_γ - Z_γ axes about the Z_γ axis to form X_β - Y_β - Z_β axes.

Since the Z_γ axis is parallel to the Z_β axis,

$$Z_\beta = Z_\gamma$$

The second step transformation yields

$$\begin{Bmatrix} X_\beta \\ Y_\beta \\ Z_\beta \end{Bmatrix} = \begin{bmatrix} \cos \beta & \sin \beta & 0 \\ -\sin \beta & \cos \beta & 0 \\ 0 & 0 & 1 \end{bmatrix} \begin{Bmatrix} X_\gamma \\ Y_\gamma \\ Z_\gamma \end{Bmatrix} = [C_2] \begin{Bmatrix} X_\gamma \\ Y_\gamma \\ Z_\gamma \end{Bmatrix} \quad (\text{D-6})$$

Step 3

Finally rotate the X_β - Y_β - Z_β axes relative to the X_β axis through angle ϕ . Now the new X_ϕ - Y_ϕ - Z_ϕ axes coincide with the JCS as shown in Fig. D-6.

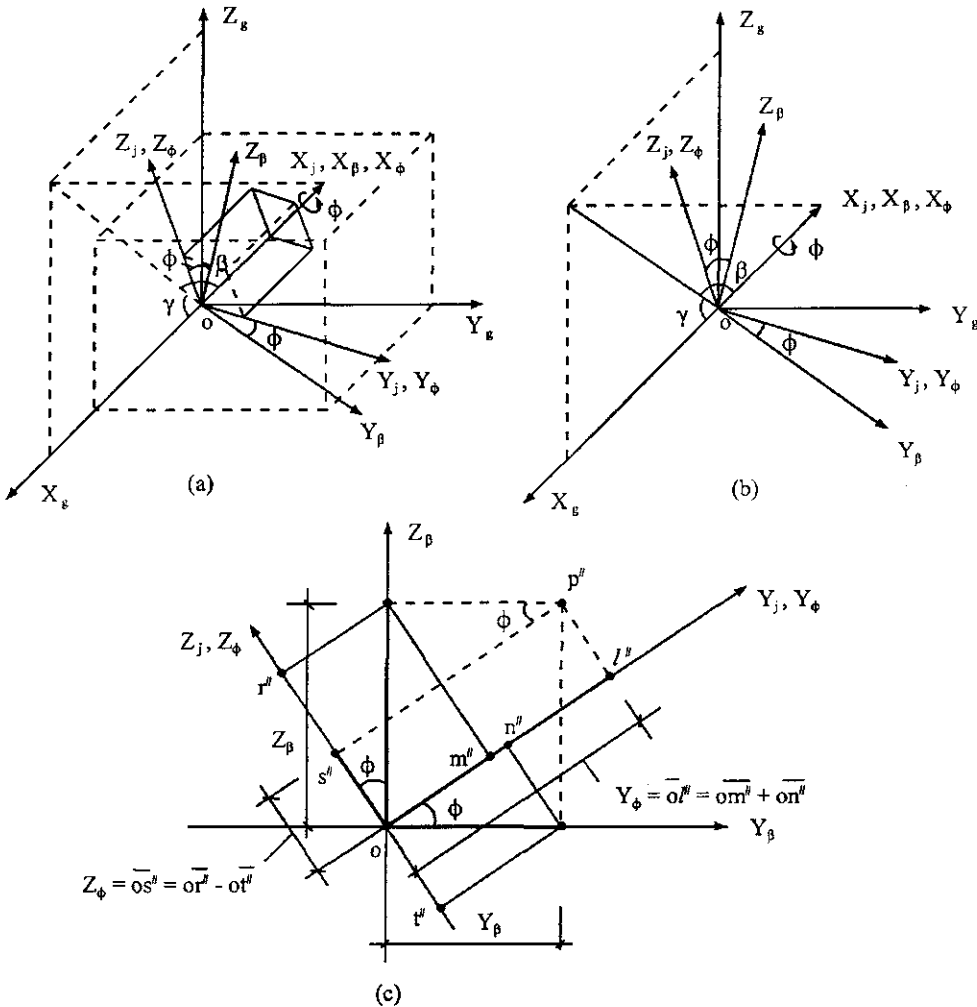


FIG. D-6 Rotation of X_β - Y_β - Z_β axes about the X_β axis to form X_j - Y_j - Z_j axes.

Assume that coordinates of point P'' in the X_ϕ - Y_ϕ - Z_ϕ system are X_ϕ , Y_ϕ , and Z_ϕ . The relationship of coordinates between the X_ϕ - Y_ϕ - Z_ϕ and X_β - Y_β - Z_β systems is shown in Fig. D-6c, where p'' is the projection of p^* in the Y_β - Z_β plane. The coordinate relationship is

$$\begin{aligned} Y_j &= Y_\phi = \overline{ol''} = \overline{om''} + \overline{on''} = Y_\beta \cos \phi + Z_\beta \sin \phi \\ Z_j &= Z_\phi = \overline{os''} = \overline{or''} - \overline{ot''} = -Y_\beta \sin \phi + Z_\beta \cos \phi \\ X_j &= X_\phi = X_\beta \end{aligned}$$

The third step transformation gives

$$\begin{Bmatrix} X_j \\ Y_j \\ Z_j \end{Bmatrix} = \begin{Bmatrix} X_\phi \\ Y_\phi \\ Z_\phi \end{Bmatrix} = \begin{bmatrix} 1 & 0 & 0 \\ 0 & \cos \phi & \sin \phi \\ 0 & -\sin \phi & \cos \phi \end{bmatrix} \begin{Bmatrix} X_\beta \\ Y_\beta \\ Z_\beta \end{Bmatrix} = [C_3] \begin{Bmatrix} X_\beta \\ Y_\beta \\ Z_\beta \end{Bmatrix} \quad (D-7)$$

It is assumed that \vec{V}_{xj} , \vec{V}_{yj} and \vec{V}_{zj} are unit vectors along the X_j , Y_j and Z_j axes, respectively. Based on Eqs. (D-5)–(D-7), the three transformations can be written in matrix form to express JCS in GCS as

$$\{V_j\} = \begin{Bmatrix} \vec{V}_{xj} \\ \vec{V}_{yj} \\ \vec{V}_{zj} \end{Bmatrix} = [C_3][C_2][C_1] \begin{Bmatrix} \vec{i} \\ \vec{j} \\ \vec{k} \end{Bmatrix} \begin{bmatrix} C_{11} & C_{12} & C_{13} \\ C_{21} & C_{22} & C_{23} \\ C_{31} & C_{32} & C_{33} \end{bmatrix} \begin{Bmatrix} \vec{i} \\ \vec{j} \\ \vec{k} \end{Bmatrix} = [C_j] \begin{Bmatrix} \vec{i} \\ \vec{j} \\ \vec{k} \end{Bmatrix} \quad (8.1)$$

in which

$$[C_j] = \begin{bmatrix} \cos \beta \cos \gamma & \sin \beta & \cos \beta \sin \gamma \\ -\cos \phi \sin \beta \cos \gamma - \sin \phi \sin \gamma & \cos \phi \cos \beta & -\sin \gamma \sin \phi \sin \beta + \sin \phi \cos \gamma \\ \cos \gamma \sin \phi \sin \beta - \sin \gamma \cos \phi & -\sin \phi \cos \beta & \sin \phi \sin \beta \sin \gamma + \cos \phi \cos \gamma \end{bmatrix} \quad (8.1a)$$

PROOF OF IDENTICAL RESULTS FOR METHODS 1 AND 2

While these methods have two different equations, they yield the same numerical results for a given problem. This phenomenon can be verified as follows. From Fig. D-7.

\overline{oa} is the projection of unit vector, \vec{V}_{xj} , on the X_g-Z_g plane with an angle of β ;
 \overline{oc} is the projection of \overline{oa} with an angle of γ ;
 \overline{ob} is the projection of \overline{oa} with an angle of $90^\circ - \gamma$; and
 \overline{od} is the projection of \vec{V}_{xj} on the Y_g axis with an angle of $90^\circ - \beta$;
 α_1 , β_1 , and γ_1 are angles between \vec{V}_{xj} and X_g , Y_g , and Z_g , respectively.

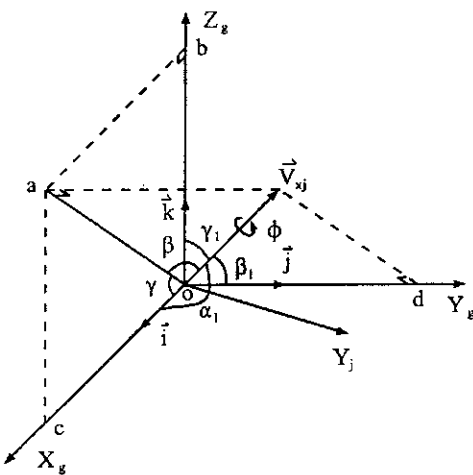


FIG. D-7 Transformation of \vec{V}_{xj} .

These projections, say \overline{od} , can be calculated as follows:

$$\overline{od} = |\vec{V}_{xj}| \cos(90^\circ - \beta) = \sin \beta |\vec{V}_{xj}| \quad (\text{D-8})$$

Since

$$\cos \beta_1 = \frac{\overline{od}}{|\vec{V}_{xj}|}; \quad |\vec{V}_{xj}| = 1$$

then

$$\overline{od} = \cos \beta_1 \quad (\text{D-9})$$

Using the same procedure leads to

$$\overline{oa} = |\vec{V}_{xj}| \cos \beta = \cos \beta \quad (\text{D-10})$$

$$\overline{oc} = \overline{oa} \cos \gamma = \cos \beta \cos \gamma \quad (\text{D-11})$$

Since

$$\cos \alpha_1 = \frac{\overline{oc}}{|\vec{V}_{xj}|}$$

then

$$\overline{oc} = \cos \alpha_1 = \cos \beta \cos \gamma \quad (\text{D-12})$$

Similarly

$$\overline{ob} = \overline{oa} \cos(90^\circ - \gamma) = \cos \beta \sin \gamma = \cos \gamma_1 \quad (\text{D-13})$$

This result becomes the first row of the matrix in Eq. (8.1) or (8.1a) as

$$\begin{aligned} \vec{V}_{xj} &= \overline{oc} \vec{i} + \overline{od} \vec{j} + \overline{ob} \vec{k} = \cos \beta \cos \gamma \vec{i} + \sin \beta \vec{j} + \cos \gamma \sin \beta \vec{k} \\ &= \cos \alpha_1 \vec{i} + \cos \beta_1 \vec{j} + \cos \gamma_1 \vec{k} \\ &= C_{11} \vec{i} + C_{12} \vec{j} + C_{13} \vec{k} \end{aligned} \quad (\text{D-14})$$

Vector \vec{V}_{xj} is a unit vector along the Y_j axis as shown in Fig. D-8a in which α_2 , β_2 , and γ_2 are angles between \vec{V}_{xj} and X_g , Y_g , and Z_g , respectively.

From Fig. D-8,

\overline{od}' is the projection of \vec{V}_{xj} with an angle of ϕ ;

\overline{oi}' is the projection of \overline{od}' on the Y_g axis with an angle of β ;

\overline{ob}' is the projection of \overline{od}' on the X_g-Z_g plane with an angle of $90^\circ - \beta$; and

\overline{ob}' has an angle of γ with X_g .

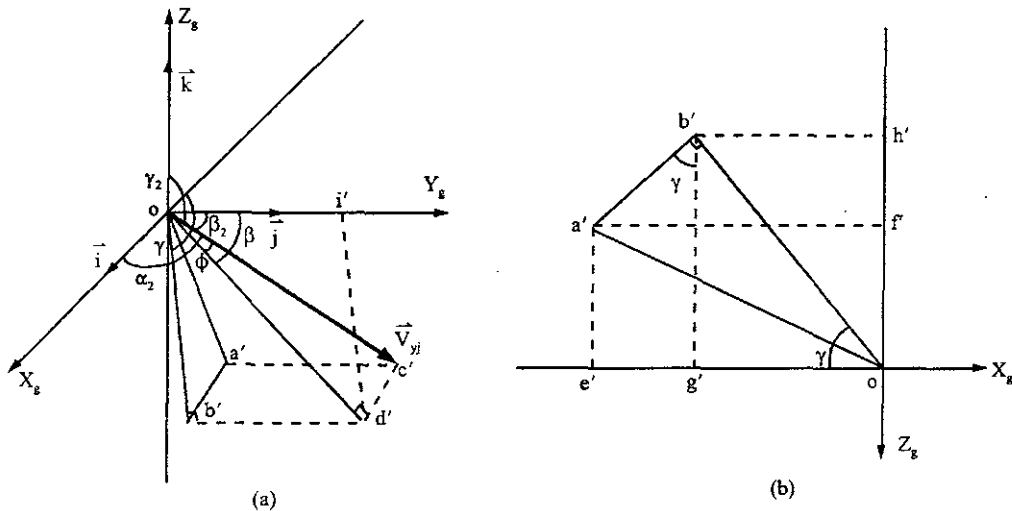


FIG. D-8 Transformation of \vec{V}_{yj} .

These projections may be expressed as

$$\begin{aligned}
 \overline{od'} &= \overline{oc'} \cos \phi = |\vec{V}_{yj}| \cos \phi = \cos \phi \quad (\text{Note } |\vec{V}_{yj}| = 1) \\
 \overline{ol'} &= \overline{od'} \cos \beta = \cos \phi \cos \beta \\
 \cos \beta_2 &= \frac{\overline{ol'}}{|\vec{V}_{yj}|} = \cos \phi \cos \beta \tag{D-15} \\
 \overline{cd'} &= \overline{ab'} = |\vec{V}_{yj}| \sin \phi = \sin \phi \\
 \overline{ob'} &= \overline{od'} \cos(90^\circ - \beta) = \cos \phi \sin \beta
 \end{aligned}$$

From the detailed diagram of \$od'b'\$ shown in Fig. D-8b, we obtain

$$\overline{oe'} = \overline{og'} + \overline{e'g'} = \overline{ab'} \sin \gamma + \overline{ob'} \cos \gamma = \sin \phi \sin \gamma + \cos \phi \sin \beta \cos \gamma$$

Thus

$$\cos \alpha_2 = \frac{-\overline{oe'}}{|\vec{V}_{yj}|} = -\overline{oe'} = -\cos \phi \sin \beta \cos \gamma - \sin \phi \sin \gamma \tag{D-16}$$

Similarly

$$\begin{aligned}
 \overline{of'} &= \overline{oh'} - \overline{f'h'} = \overline{ob'} \sin \gamma - \overline{ab'} \cos \gamma = \cos \phi \sin \beta \sin \gamma - \sin \phi \cos \gamma \\
 \cos \gamma_2 &= \frac{-\overline{of'}}{|\vec{V}_{yj}|} = -\overline{of'} = -\cos \phi \sin \beta \sin \gamma + \sin \phi \cos \gamma \tag{D-17}
 \end{aligned}$$

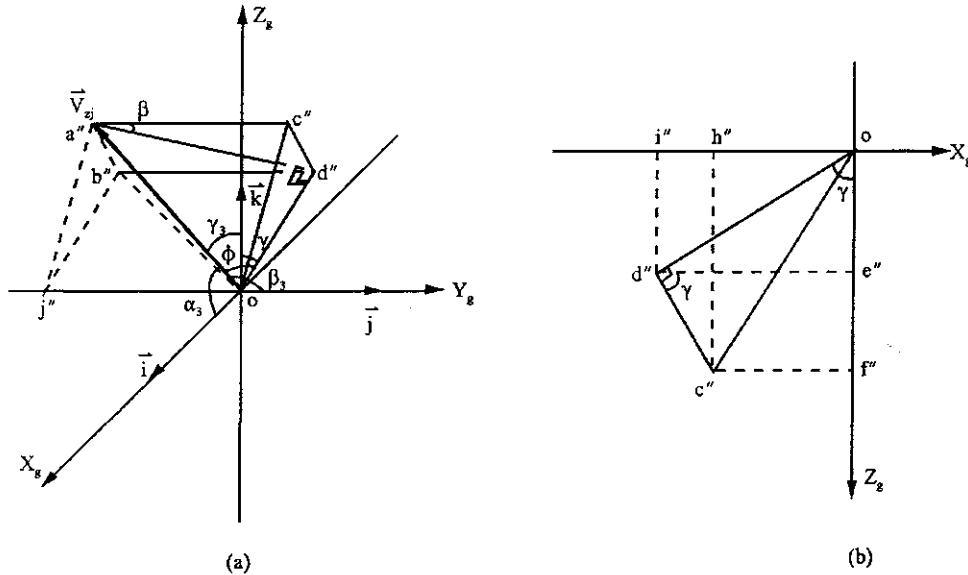


FIG. D-9 Transformation of \vec{V}_{zj} .

Eqs. (D-15)–(D-17) form the second row of the matrix in Eq. (8.1) or (8.1a) as

$$\begin{aligned}
 \vec{V}_{zj} &= -\overline{oe'} \vec{i} + \overline{oi'} \vec{j} - \overline{of'} \vec{k} \\
 &= (-\cos \phi \sin \beta \cos \gamma - \sin \phi \sin \gamma) \vec{i} + \cos \phi \cos \beta \vec{j} + (-\cos \phi \sin \beta \sin \gamma + \sin \phi \cos \gamma) \vec{k} \\
 &= \cos \alpha_3 \vec{i} + \cos \beta_3 \vec{j} + \cos \gamma_3 \vec{k} \\
 &= C_{21} \vec{i} + C_{22} \vec{j} + C_{23} \vec{k}
 \end{aligned} \tag{D-18}$$

Vector \vec{V}_{zj} is a unit vector along the Z_j axis. α_3 , β_3 and γ_3 are the angles between \vec{V}_{zj} and X_g , Y_g and Z_g , respectively, as shown in Fig. D-9.

From Fig. D-9,

- $\overline{od''}$ is the projection of \vec{V}_{zj} with an angle of ϕ ;
- $\overline{a''d''}$ has an angle of β to $\overline{b''d''}$; and
- $\overline{od''}$ has an angle of γ relative to Z_g .

The projections are calculated as follows

$$\begin{aligned}
 \overline{od''} &= \overline{oa''} \cos \phi = \cos \phi; \quad \text{Note: } \overline{oa''} = |\vec{V}_{zj}| = 1 \\
 \overline{a''b''} &= \overline{c''d''}; \quad \overline{a''d''} = \overline{oa''} \sin \phi = \sin \phi \\
 \overline{c''d''} &= \overline{a''d''} \sin \beta = \sin \phi \sin \beta \\
 \overline{oj''} &= \overline{b''d''} = \overline{a''b''} \cos \beta = \sin \phi \cos \beta
 \end{aligned} \tag{D-19a}$$

$$\cos \beta_3 = -\frac{\overline{oj''}}{|\vec{V}_{zj}|} = \cos \beta_3 = -\sin \phi \cos \beta \tag{D-19b}$$

$$\overline{of''} = \overline{oe''} + \overline{e''f''} = \overline{od''} \cos \gamma + \overline{c''d''} \sin \gamma = \cos \phi \cos \gamma + \sin \phi \sin \beta \sin \gamma \quad (\text{D-20a})$$

$$\cos \gamma_3 = \frac{\overline{of''}}{|\vec{V}_{zj}|} = \cos \phi \cos \gamma + \sin \phi \sin \beta \sin \gamma \quad (\text{D-20b})$$

$$\overline{oh''} = \overline{oi''} - \overline{i''h''} = \overline{od''} \sin \gamma - \overline{c''d''} \cos \gamma = \cos \phi \sin \gamma - \sin \phi \sin \beta \cos \gamma \quad (\text{D-21a})$$

$$\cos \alpha_3 = -\frac{\overline{oh''}}{|\vec{V}_{zj}|} = \sin \phi \sin \beta \cos \gamma - \cos \phi \sin \gamma \quad (\text{D-21b})$$

Summarizing Eqs. (D-19)–(D-21) yields the third row of the matrix in Eq. (8.1) or (8.1a) as

$$\begin{aligned} \vec{V}_{zj} &= -\overline{oh''} \vec{i} - \overline{oj''} \vec{j} + \overline{of''} \vec{k} \\ &= (\sin \phi \sin \beta \cos \gamma - \cos \phi \sin \gamma) \vec{i} - \sin \phi \cos \beta \vec{j} + (\sin \phi \sin \beta \sin \gamma + \cos \phi \cos \gamma) \vec{k} \\ &= \cos \alpha_3 \vec{i} + \cos \beta_3 \vec{j} + \cos \gamma_3 \vec{k} \\ &= C_{31} \vec{i} + C_{32} \vec{j} + C_{33} \vec{k} \end{aligned} \quad (\text{D-22})$$

Based on Eqs. (D-14), (D-18), and (D-22), the transformation matrix expressed with direction cosines of \vec{V}_{xj} , \vec{V}_{yj} and \vec{V}_{zj} is the same as that in Eq. (8.1) or Eq. (8.1a).

$$\begin{bmatrix} C_{11} & C_{12} & C_{13} \\ C_{21} & C_{22} & C_{23} \\ C_{31} & C_{32} & C_{33} \end{bmatrix} = \begin{bmatrix} \cos \beta \cos \gamma & \sin \beta & \cos \beta \sin \gamma \\ -\cos \phi \sin \beta \cos \gamma - \sin \phi \sin \gamma & \cos \phi \cos \beta & -\sin \gamma \cos \phi \sin \beta + \sin \phi \cos \gamma \\ \cos \gamma \sin \phi \sin \beta - \sin \gamma \cos \phi & -\sin \phi \cos \beta & \sin \phi \sin \beta \sin \gamma + \cos \phi \cos \gamma \end{bmatrix} \quad (\text{8.1})$$

or

$$= \begin{bmatrix} \cos \beta \cos \gamma & \sin \beta & \cos \beta \sin \gamma \\ -\cos \phi \sin \beta \cos \gamma - \sin \phi \sin \gamma & \cos \phi \cos \beta & -\sin \gamma \cos \phi \sin \beta + \sin \phi \cos \gamma \\ \cos \gamma \sin \phi \sin \beta - \sin \gamma \cos \phi & -\sin \phi \cos \beta & \sin \phi \sin \beta \sin \gamma + \cos \phi \cos \gamma \end{bmatrix} \quad (\text{8.1a})$$

Appendix E—Transformation Matrix Between ECS and GCS for Beam Column

For a beam-column element, the transformation matrix can be determined by using its vector \vec{V}_x along the element's longitudinal direction and by using angle α to rotate the element around vector \vec{V}_x . Location of vector \vec{V}_x in GCS, shown in Fig. D-5, results from the combination of steps 1 and 2 of Method 2 in Appendix D. During these two steps, vector \vec{V}_x has rotated at an angle of γ from the X_g axis and an angle of β from the $X_\gamma-Y_\gamma$ plane. Consequently, \vec{V}_x coincides with the X_β axis and the coordinate system for vector \vec{V}_x is $X_\beta-Y_\beta-Z_\beta$, shown in Fig. E-1. The unit vector along the X_β axis is defined as \vec{v} and can be expressed as direction cosines in GCS. Based on Eq. (8.8), direction cosines c_x , c_y , and c_z are as follows:

$$c_x = \frac{X_{ge} - X_{gs}}{D_{se}} \quad c_y = \frac{Y_{ge} - Y_{gs}}{D_{se}} \quad c_z = \frac{Z_{ge} - Z_{gs}}{D_{se}} \quad (E-1)$$

Since \vec{i} , \vec{j} and \vec{k} are unit vectors, \vec{V}_x is written as $\vec{V}_x = c_x \vec{i} + c_y \vec{j} + c_z \vec{k}$. Unit vectors along the Y_β and Z_β axes need to be determined in order to calculate the third step for the rotation of α . Assume that unit vectors along the Y_β and Z_β axes are \vec{y}_β and \vec{z}_β , respectively. Due to Y_g in the $X_\beta-Y_\beta$ plane vector, \vec{j} is chosen to determine \vec{z}_β as shown in Eq. (8.9) from which

$$\vec{z}_\beta = \frac{\vec{v} \times \vec{j}}{|\vec{v} \times \vec{j}|} = -\frac{c_z}{m} \vec{i} + \frac{c_x}{m} \vec{k} \quad (E-2)$$

where $m = \sqrt{c_x^2 + c_z^2}$. From Eq. (8.10),

$$\vec{y}_\beta = \vec{z}_\beta \times \vec{V}_x = -\frac{c_x c_y}{m} \vec{i} + m \vec{j} - \frac{c_y c_z}{m} \vec{k} \quad (E-3)$$

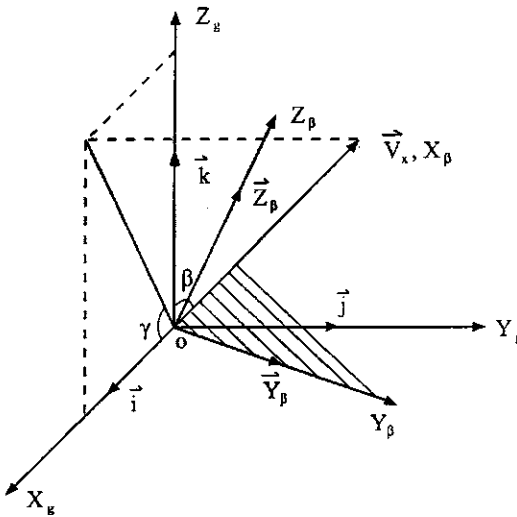


FIG. E-1 \vec{V}_x vs X_β - Y_β - Z_β coordinate system.

Details of Eqs. (E-2) and (E-3) are given in Example E-1. Thus the relationship between the GCS and X_β - Y_β - Z_β is expressed as

$$\begin{Bmatrix} \vec{X}_\beta \\ \vec{Y}_\beta \\ \vec{Z}_\beta \end{Bmatrix} = \begin{bmatrix} c_x & c_y & c_z \\ -\frac{c_x c_y}{m} & m & -\frac{c_y c_z}{m} \\ -\frac{c_z}{m} & 0 & \frac{c_x}{m} \end{bmatrix} \begin{Bmatrix} \vec{i} \\ \vec{j} \\ \vec{k} \end{Bmatrix} = [C_2][C_1] \begin{Bmatrix} \vec{i} \\ \vec{j} \\ \vec{k} \end{Bmatrix} \quad (E-4)$$

where $\vec{X}_\beta = \vec{V}_x$. From Eqs. (D-5) and (D-6), the transformation matrix between X_β - Y_β - Z_β and the GCS can be expressed as $[C_2][C_1]$ given in Eq. (E-4).

Let vector \vec{V}_x rotate at an angle of α around the X_β axis to obtain ECS (see Fig. E-2). Based on Eq. (D-7), the relationship between ECS and X_β - Y_β - Z_β can be expressed as

$$\begin{Bmatrix} \vec{V}_x \\ \vec{V}_y \\ \vec{V}_z \end{Bmatrix} = \begin{bmatrix} 1 & 0 & 0 \\ 0 & \cos \alpha & \sin \alpha \\ 0 & -\sin \alpha & \cos \alpha \end{bmatrix} \begin{Bmatrix} \vec{X}_\beta \\ \vec{Y}_\beta \\ \vec{Z}_\beta \end{Bmatrix} = [C_3] \begin{Bmatrix} \vec{X}_\beta \\ \vec{Y}_\beta \\ \vec{Z}_\beta \end{Bmatrix} \quad (E-5)$$

From Eqs. (E-4) and (E-5) the transformation between the GCS and ECS is

$$\begin{Bmatrix} \vec{V}_x \\ \vec{V}_y \\ \vec{V}_z \end{Bmatrix} = [C_3][C_2][C_1] \begin{Bmatrix} \vec{i} \\ \vec{j} \\ \vec{k} \end{Bmatrix} = [C_e] \begin{Bmatrix} \vec{i} \\ \vec{j} \\ \vec{k} \end{Bmatrix} \quad (E-6)$$

in which

$$[C_e] = \begin{bmatrix} c_x & c_y & c_z \\ -\frac{1}{m}(c_x c_y \cos \alpha + c_z \sin \alpha) & m \cos \alpha & \frac{1}{m}(c_x \sin \alpha - c_y c_z \cos \alpha) \\ \frac{1}{m}(c_x c_y \sin \alpha - c_z \cos \alpha) & -m \sin \alpha & \frac{1}{m}(c_y c_z \sin \alpha + c_x \cos \alpha) \end{bmatrix} \quad (E-7)$$

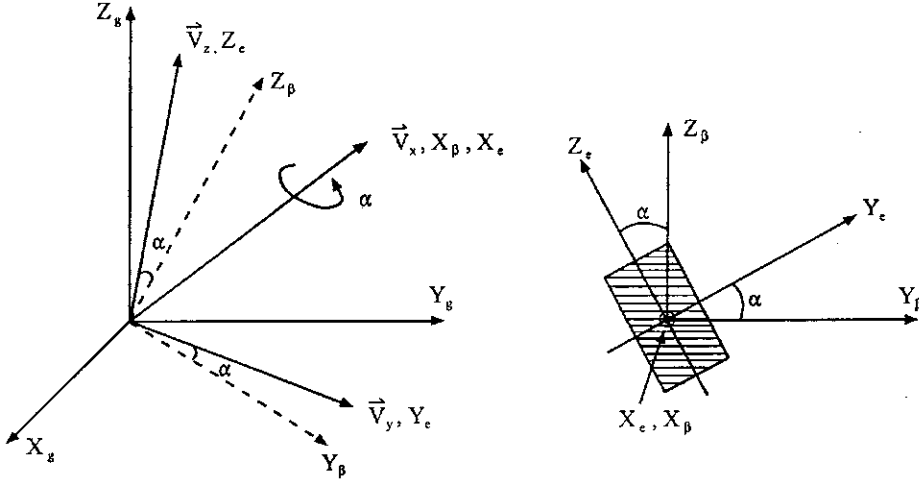


FIG. E-2 Rotating angle α about \vec{V}_x , X_β , and X_e .

EXAMPLE E-1 Derive Eqs. (E-2) and (E-3) in full detail.

Solution: $\vec{V}_x = c_x \vec{i} + c_y \vec{j} + c_z \vec{k}$ is a vector along a member's axis for which

$$|\vec{V}_x| = \sqrt{c_x^2 + c_y^2 + c_z^2} = \left[\left(\frac{X_{ge} - X_{gs}}{D_{se}} \right)^2 + \left(\frac{Y_{ge} - Y_{gs}}{D_{se}} \right)^2 + \left(\frac{Z_{ge} - Z_{gs}}{D_{se}} \right)^2 \right]^{\frac{1}{2}} = \frac{D_{se}}{D_{se}} = 1$$

Thus \vec{V}_x is a unit vector. To show Eqs. (E-2) and (E-3), let us examine the following vector product:

$$\begin{aligned} \vec{A} \times \vec{B} &= (A_1 \vec{i} + A_2 \vec{j} + A_3 \vec{k}) \times (B_1 \vec{i} + B_2 \vec{j} + B_3 \vec{k}) \\ &= (A_2 B_3 - A_3 B_2) \vec{i} + (A_3 B_1 - A_1 B_3) \vec{j} + (A_1 B_2 - A_2 B_1) \vec{k} \\ &= \begin{vmatrix} \vec{i} & \vec{j} & \vec{k} \\ A_1 & A_2 & A_3 \\ B_1 & B_2 & B_3 \end{vmatrix} \end{aligned} \quad (a)$$

Because unit vector \vec{j} is in the $X_\beta - Y_\beta$ plane (see Fig. E-1), it is used to determine \vec{Z}_β by applying Eq. (8.9). Then $\vec{V}_{xy} = \vec{j}$, and $|\vec{V}_{xy}| = 1$. Thus

$$\vec{V}_x \times \vec{V}_{xy} = \begin{vmatrix} \vec{i} & \vec{j} & \vec{k} \\ c_x & c_y & c_z \\ 0 & 1 & 0 \end{vmatrix} = -c_z \vec{i} + c_x \vec{k} \quad (b)$$

$$|\vec{V}_x \times \vec{V}_{xy}| = \sqrt{c_z^2 + c_x^2} = m \quad (c)$$

$$\vec{Z}_\beta = \frac{\vec{V}_x \times \vec{V}_{xy}}{|\vec{V}_x \times \vec{V}_{xy}|} = -\frac{c_z}{m} \vec{i} + \frac{c_x}{m} \vec{k} \quad (d)$$

$$|\vec{Z}_\beta| = \sqrt{\left(\frac{c_z}{m}\right)^2 + \left(\frac{c_x}{m}\right)^2} = \frac{1}{m} \sqrt{c_z^2 + c_x^2} = 1 \quad (e)$$

Eq. (d) is Eq. (E-2) and \vec{Z}_β is a unit vector. The relationship of \vec{V}_x (X_β), \vec{V}_{xy} (\vec{j}), and \vec{Z}_β is shown in Fig. E-3.

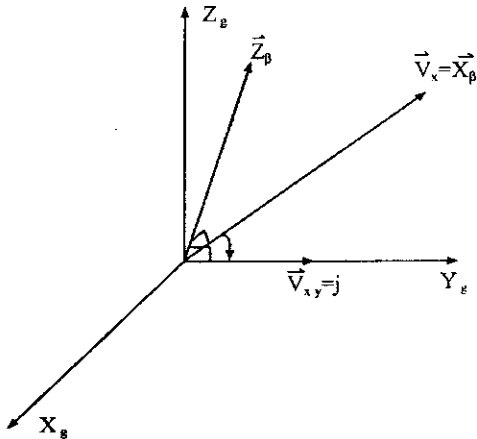


FIG. E-3 \vec{V}_x (\vec{X}_β), \vec{V}_{xy} (\vec{j}), and \vec{Z}_β .

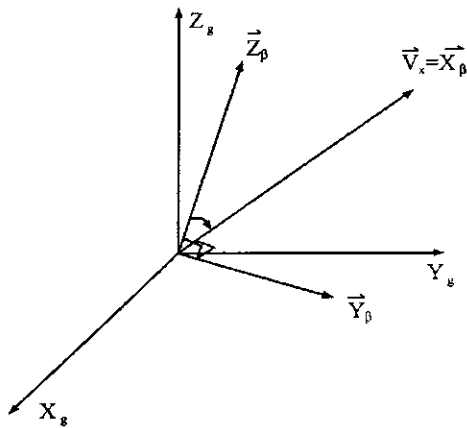


FIG. E-4 \vec{V}_x (\vec{X}_β), \vec{V}_{xy} (\vec{j}), and \vec{Z}_β .

Equation (E-3) can be similarly derived as

$$\begin{aligned}\vec{Y}_\beta &= \vec{Z}_\beta \times \vec{V}_x = \begin{vmatrix} \vec{i} & \vec{j} & \vec{k} \\ -c_z & 0 & c_x \\ m & c_y & c_z \end{vmatrix} = -\frac{c_x c_y}{m} \vec{i} + \frac{c_x^2 + c_z^2}{m} \vec{j} - \frac{c_y c_z}{m} \vec{k} \\ &= -\frac{c_x c_y}{m} \vec{i} + m \vec{j} - \frac{c_y c_z}{m} \vec{k}\end{aligned}\quad (f)$$

for which the unit vector can be shown as

$$\begin{aligned}|\vec{Y}_\beta| &= \sqrt{\left(\frac{c_x c_y}{m}\right)^2 + m^2 + \left(\frac{c_y c_z}{m}\right)^2} = \frac{1}{m} \sqrt{c_x^2 c_y^2 + (c_x^2 + c_z^2)^2 + c_y^2 c_z^2} \\ &= \frac{1}{m} \sqrt{(c_x^2 + c_z^2)(c_x^2 + c_y^2 + c_z^2)} = \frac{1}{m} m |\vec{V}_x| = 1\end{aligned}\quad (g)$$

The relationship of \vec{V}_x (\vec{X}_β), \vec{Y}_β , and \vec{Z}_β is shown in Fig. E-4.

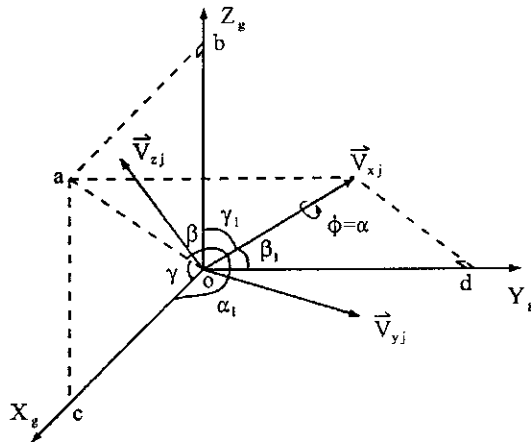


FIG. E-5 Composite of Figs. 8.4 and B-3.

IDENTITY BETWEEN EQS. (8.1a) AND (E-7)

Note that the elements of the transformation matrix in Eq. (8.1a) are different from those in Eq. (E-7). This is due to different definitions of angles used in these two equations. Yet the equations are actually the same and their identity can be proved as follows. (While this instance is only for the transformation matrix between the GCS and JCS, the same principle applies to the transformation matrix between the GCS and ECS.)

Figs. 8.4 and E-1 are used to derive Eqs. (8.1a) and (E-7), respectively. The angles employed in these two figures to define unit vector \$\vec{V}_{xj}\$ are summarized in Fig. E-5. In Fig. D-3, the location of vector \$\vec{V}_{xj}\$ is expressed by angles \$\gamma\$ and \$\beta\$ while in Fig. 8.4a, the location of \$\vec{V}_{xj}\$ is determined by \$\alpha_1\$, \$\beta_1\$, and \$\gamma_1\$. From Fig. E-5, the projection of \$\vec{V}_{xj}\$ in the \$X_g\$-\$Z_g\$ plane is

$$\overline{oa} = |\vec{V}_{xj}| \cos \beta \quad (E-8)$$

Since \$\vec{V}_{xj}\$ is a unit vector, \$|\vec{V}_{xj}| = 1\$, then \$\overline{oa} = \cos \beta\$. Similarly

$$\overline{oc} = \overline{oa} \cos \gamma = \cos \beta \cos \gamma \quad (E-9)$$

$$\overline{od} = |\vec{V}_{xj}| \cos(90^\circ - \beta) = \sin \beta \quad (E-10)$$

$$\overline{ob} = \overline{oa} \cos(90^\circ - \gamma) = \cos \beta \sin \gamma \quad (E-11)$$

Eqs. (E-9)–(E-11) comprise the first row of Eq. (8.1a)

$$C_{11} = \cos \beta \cos \gamma, \quad C_{12} = \sin \beta, \quad C_{13} = \cos \beta \sin \gamma \quad (E-12)$$

Based on the direction cosines of vector \$\vec{V}_{xj}\$

$$\cos \alpha_1 = \frac{\overline{oc}}{|\vec{V}_{xj}|} = \overline{oc} = \cos \beta \cos \gamma = c_x \quad (E-13)$$

$$\cos \beta_1 = \frac{\overline{od}}{|\vec{V}_{xj}|} = \overline{od} = \sin \beta = c_y \quad (E-14)$$

$$\cos \gamma_1 = \frac{\overline{ob}}{|\vec{V}_{xj}|} = \overline{ob} = \cos \beta \sin \gamma = c_z \quad (E-15)$$

By definition

$$\begin{aligned} m &= \sqrt{c_x^2 + c_z^2} = \sqrt{(\cos \beta \cos \gamma)^2 + (\cos \beta \sin \gamma)^2} = \cos \beta \sqrt{\cos^2 \gamma + \sin^2 \gamma} \\ &= \cos \beta \end{aligned} \quad (\text{E-16})$$

Thus

$$c_x = \cos \beta \cos \gamma = m \cos \gamma; \quad \cos \gamma = \frac{c_x}{m} \quad (\text{E-17})$$

and

$$c_z = \cos \beta \sin \gamma = m \sin \gamma; \quad \sin \gamma = \frac{c_z}{m} \quad (\text{E-18})$$

Substituting Eqs. (E-13)–(E-18) into Eq. (8.1a), and defining $\phi = \alpha$, their identical nature emerges as

$$\begin{aligned} &\begin{bmatrix} \cos \beta \cos \gamma & \sin \beta & \cos \beta \sin \gamma \\ -\cos \phi \sin \beta \cos \gamma - \sin \phi \sin \gamma & \cos \phi \cos \beta & -\sin \gamma \cos \phi \sin \beta + \sin \phi \cos \gamma \\ \cos \gamma \sin \phi \sin \beta - \sin \gamma \cos \phi & -\sin \phi \cos \beta & \sin \phi \sin \beta \sin \gamma + \cos \phi \cos \gamma \end{bmatrix} \\ &= \begin{bmatrix} c_x & c_y & c_z \\ \frac{-1}{m}(c_x c_y \cos \alpha + c_z \sin \alpha) & m \cos \alpha & \frac{1}{m}(c_x \sin \alpha - c_y c_z \cos \alpha) \\ \frac{1}{m}(c_x c_y \sin \alpha - c_z \cos \alpha) & -m \sin \alpha & \frac{1}{m}(c_y c_z \sin \alpha + c_x \cos \alpha) \end{bmatrix} \end{aligned}$$

EXAMPLE E-2 A W-shape member, W24 × 62, is used as a beam-column for which start-joint *A* and end-joint *B* are given in Fig. E-6 in GCS. Determine transformation matrix $[C_e]$.

Solution: Based on the data, start-joint *A* and end-joint *B* are (0,0,0) and (18 ft, 24 ft, 20 ft), respectively. Thus the distance D_{se} is calculated from Eq. (8.7) as

$$D_{se} = \sqrt{(X_{ge} - X_{gs})^2 + (Y_{ge} - Y_{gs})^2 + (Z_{ge} - Z_{gs})^2} = \sqrt{18^2 + 24^2 + 20^2} = 36.056 \text{ ft} \quad (\text{a})$$

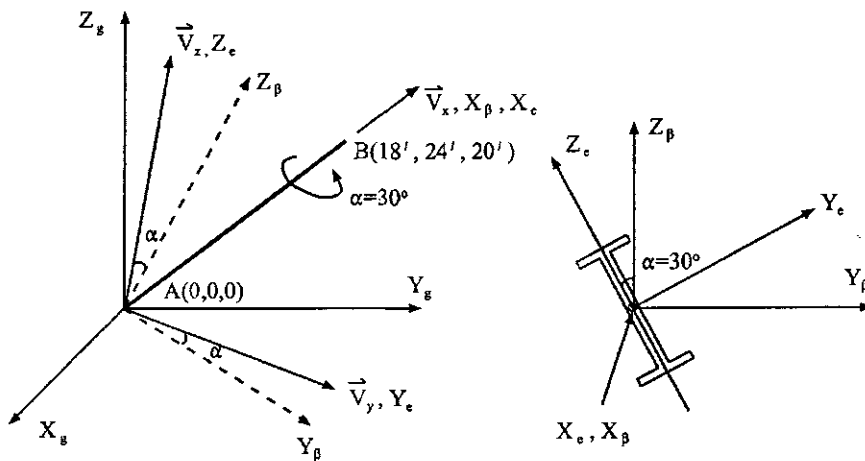


FIG. E-6 Example E-2.

Using Eqs. (8.13)–(8.15) yields the following direction cosines:

$$c_x = \frac{X_{ge} - X_{gs}}{D_{se}} = \frac{18}{36.056} = 0.499 \quad (\text{b})$$

$$c_y = \frac{Y_{ge} - Y_{gs}}{D_{se}} = \frac{24}{36.056} = 0.666 \quad (\text{c})$$

$$c_z = \frac{Z_{ge} - Z_{gs}}{D_{se}} = \frac{20}{36.056} = 0.555 \quad (\text{d})$$

Thus

$$m = \sqrt{c_x^2 + c_z^2} = \sqrt{0.499^2 + 0.555^2} = 0.746$$

From the given data, $\alpha = 30^\circ$, we have

$$\cos \alpha = 0.866; \quad \sin \alpha = 0.5 \quad (\text{e})$$

Substituting Eqs. (b)–(e) into Eq. (8.12) yields the following transformation matrix elements:

$$-\frac{1}{m}(c_x c_y \cos \alpha + c_z \sin \alpha) = -0.758 \quad (\text{f})$$

$$m \cos \alpha = 0.646 \quad (\text{g})$$

$$\frac{1}{m}(c_x \sin \alpha - c_y c_z \cos \alpha) = -0.095 \quad (\text{h})$$

$$\frac{1}{m}(c_x c_y \sin \alpha - c_z \cos \alpha) = -0.422 \quad (\text{i})$$

$$-m \sin \alpha = -0.373 \quad (\text{j})$$

$$\frac{1}{m}(c_y c_z \sin \alpha + c_x \cos \alpha) = 0.827 \quad (\text{k})$$

The transformation matrix then becomes

$$[C_e] = \begin{bmatrix} 0.499 & 0.666 & 0.555 \\ -0.758 & 0.646 & -0.095 \\ -0.422 & -0.373 & 0.827 \end{bmatrix} \quad (\text{l})$$

Appendix F—Transformation Matrix [A'] and Stiffness Matrix [K_{eg}] of Beam Column with Rigid Zone

Transformation matrix [A'] for a general beam–column is

$$\begin{aligned}
 & \left\{ \begin{array}{l} F_{Ax} \\ F_{Ay} \\ F_{Az} \\ M_{Ax} \\ M_{Ay} \\ M_{Az} \\ F_{Bmx} \\ F_{Bmy} \\ F_{Bmz} \\ M_{Bmx} \\ M_{Bmy} \\ M_{Bmz} \end{array} \right\} = [A'] \left\{ \begin{array}{l} F_{xa} \\ F_{ya} \\ F_{za} \\ M_{xa} \\ M_{ya} \\ M_{za} \\ F_{xb} \\ F_{yb} \\ F_{zb} \\ M_{xb} \\ M_{yb} \\ M_{zb} \end{array} \right\} = [\bar{T}_m] [\bar{C}_j] [\bar{C}_e] [T_{je}] \left\{ \begin{array}{l} F_{xa} \\ F_{ya} \\ F_{za} \\ M_{xa} \\ M_{ya} \\ M_{za} \\ F_{xb} \\ F_{yb} \\ F_{zb} \\ M_{xb} \\ M_{yb} \\ M_{zb} \end{array} \right\} \\
 & = \begin{bmatrix} A_{11} & A_{12} & A_{13} & 0 & 0 & 0 & 0 & 0 & 0 & 0 & 0 & 0 \\ A_{21} & A_{22} & A_{23} & 0 & 0 & 0 & 0 & 0 & 0 & 0 & 0 & 0 \\ A_{31} & A_{32} & A_{33} & 0 & 0 & 0 & 0 & 0 & 0 & 0 & 0 & 0 \\ 0 & A_{42} & A_{43} & A_{11} & A_{12} & A_{13} & 0 & 0 & 0 & 0 & 0 & 0 \\ 0 & A_{52} & A_{53} & A_{21} & A_{22} & A_{23} & 0 & 0 & 0 & 0 & 0 & 0 \\ A_{61} & A_{62} & A_{63} & A_{31} & A_{32} & A_{33} & 0 & 0 & 0 & 0 & 0 & 0 \\ 0 & 0 & 0 & 0 & 0 & 0 & B_{11} & B_{12} & B_{13} & 0 & 0 & 0 \\ 0 & 0 & 0 & 0 & 0 & 0 & B_{21} & B_{22} & B_{23} & 0 & 0 & 0 \\ 0 & 0 & 0 & 0 & 0 & 0 & B_{31} & B_{32} & B_{33} & 0 & 0 & 0 \\ 0 & 0 & 0 & 0 & 0 & 0 & 0 & B_{42} & B_{43} & B_{11} & B_{12} & B_{13} \\ 0 & 0 & 0 & 0 & 0 & 0 & 0 & B_{52} & B_{53} & B_{21} & B_{22} & B_{23} \\ 0 & 0 & 0 & 0 & 0 & 0 & B_{61} & B_{62} & B_{63} & B_{31} & B_{32} & B_{33} \end{bmatrix} \left\{ \begin{array}{l} F_{xa} \\ F_{ya} \\ F_{za} \\ M_{xa} \\ M_{ya} \\ M_{za} \\ F_{xb} \\ F_{yb} \\ F_{zb} \\ M_{xb} \\ M_{yb} \\ M_{zb} \end{array} \right\} \quad (\text{F-1})
 \end{aligned}$$

The above transformation matrix is based on Eq. (8.108). Rigid zone transformation matrix $[T_{je}]$ is defined by Eq. (8.100). The coordinate transformation matrices $[C_e]$ and $[C_j]$ are given at Eqs. (8.110) and (8.111), respectively. The constraint transformation matrix $[T_{ms}]$ is defined by Eq. (8.6). In Eq. (F-1), the parameters are defined as follows:

$$\begin{aligned}
 A_{11} &= i_{1A} l_1 + i_{2A} l_2 + i_{3A} l_3; & A_{12} &= i_{1A} m_1 + i_{2A} m_2 + i_{3A} m_3; & A_{13} &= i_{1A} n_1 + i_{2A} n_2 + i_{3A} n_3 \\
 A_{21} &= j_{1A} l_1 + j_{2A} l_2 + j_{3A} l_3; & A_{22} &= j_{1A} m_1 + j_{2A} m_2 + j_{3A} m_3; & A_{23} &= j_{1A} n_1 + j_{2A} n_2 + j_{3A} n_3 \\
 A_{31} &= k_{1A} l_1 + k_{2A} l_2 + k_{3A} l_3; & A_{32} &= k_{1A} m_1 + k_{2A} m_2 + k_{3A} m_3; & A_{33} &= k_{1A} n_1 + k_{2A} n_2 + k_{3A} n_3 \\
 A_{42} &= A_{13} L_{ys}; & A_{43} &= -A_{12} L_{zs} \\
 A_{52} &= A_{23} L_{ys}; & A_{53} &= -A_{22} L_{zs} \\
 A_{61} &= -Y_{msA} i_{1A} l_1 - Y_{msA} i_{2A} l_2 - Y_{msA} i_{3A} l_3 + X_{msA} j_{1A} l_1 + X_{msA} j_{2A} l_2 + X_{msA} j_{3A} l_3 \\
 A_{62} &= -Y_{msA} i_{1A} m_1 - Y_{msA} i_{2A} m_2 - Y_{msA} i_{3A} m_3 + X_{msA} j_{1A} m_1 + X_{msA} j_{2A} m_2 + X_{msA} j_{3A} m_3 + L_{ys} A_{33} \\
 A_{63} &= -Y_{msA} i_{1A} n_1 - Y_{msA} i_{2A} n_2 - Y_{msA} i_{3A} n_3 + X_{msA} j_{1A} n_1 + X_{msA} j_{2A} n_2 + X_{msA} j_{3A} n_3 - L_{zs} A_{32} \\
 B_{11} &= i_{1B} l_1 + i_{2B} l_2 + i_{3B} l_3; & B_{12} &= i_{1B} m_1 + i_{2B} m_2 + i_{3B} m_3; & B_{13} &= i_{1B} n_1 + i_{2B} n_2 + i_{3B} n_3 \\
 B_{21} &= j_{1B} l_1 + j_{2B} l_2 + j_{3B} l_3; & B_{22} &= j_{1B} m_1 + j_{2B} m_2 + j_{3B} m_3; & B_{23} &= j_{1B} n_1 + j_{2B} n_2 + j_{3B} n_3 \\
 B_{31} &= k_{1B} l_1 + k_{2B} l_2 + k_{3B} l_3; & B_{32} &= k_{1B} m_1 + k_{2B} m_2 + k_{3B} m_3; & B_{33} &= k_{1B} n_1 + k_{2B} n_2 + k_{3B} n_3 \\
 B_{42} &= -B_{13} L_{ye}; & B_{43} &= B_{12} L_{ze} \\
 B_{52} &= -B_{23} L_{ye}; & B_{53} &= B_{22} L_{ze} \\
 B_{61} &= -Y_{msB} i_{1B} l_1 - Y_{msB} i_{2B} l_2 - Y_{msB} i_{3B} l_3 + X_{msB} j_{1B} l_1 + X_{msB} j_{2B} l_2 + X_{msB} j_{3B} l_3 \\
 B_{62} &= -Y_{msB} i_{1B} m_1 - Y_{msB} i_{2B} m_2 - Y_{msB} i_{3B} m_3 + X_{msB} j_{1B} m_1 + X_{msB} j_{2B} m_2 + X_{msB} j_{3B} m_3 - L_{ye} B_{33} \\
 B_{63} &= -Y_{msB} i_{1B} n_1 - Y_{msB} i_{2B} n_2 - Y_{msB} i_{3B} n_3 + X_{msB} j_{1B} n_1 + X_{msB} j_{2B} n_2 + X_{msB} j_{3B} n_3 + L_{ze} B_{32}
 \end{aligned}$$

The element stiffness matrix for GCS can be expressed as

$$\begin{aligned}
 & \left\{ \begin{array}{l} F_{Amx} \\ F_{Amy} \\ F_{Amz} \\ M_{Amx} \\ M_{Amy} \\ M_{Amz} \\ F_{Bmx} \\ F_{Bmy} \\ F_{Bmz} \\ M_{Bmx} \\ M_{Bmy} \\ M_{Bmz} \end{array} \right\} = [K^i] \left\{ \begin{array}{l} \delta_{Amx} \\ \delta_{Amy} \\ \delta_{Amz} \\ \theta_{Amx} \\ \theta_{Amy} \\ \theta_{Amz} \\ \delta_{Bmx} \\ \delta_{Bmy} \\ \delta_{Bmz} \\ \theta_{Bmx} \\ \theta_{Bmy} \\ \theta_{Bmz} \end{array} \right\} = [A'] [K_e] [A']^T \left\{ \begin{array}{l} \delta_{Amx} \\ \delta_{Amy} \\ \delta_{Amz} \\ \theta_{Amx} \\ \theta_{Amy} \\ \theta_{Amz} \\ \delta_{Bmx} \\ \delta_{Bmy} \\ \delta_{Bmz} \\ \theta_{Bmx} \\ \theta_{Bmy} \\ \theta_{Bmz} \end{array} \right\} \\
 & = \left[\begin{array}{cccccccccccc} K_{1,1} & K_{1,2} & K_{1,3} & K_{1,4} & K_{1,5} & K_{1,6} & K_{1,7} & K_{1,8} & K_{1,9} & K_{1,10} & K_{1,11} & K_{1,12} & \delta_{Amx} \\ & K_{2,2} & K_{2,3} & K_{2,4} & K_{2,5} & K_{2,6} & K_{2,7} & K_{2,8} & K_{2,9} & K_{2,10} & K_{2,11} & K_{2,12} & \delta_{Amy} \\ & & & K_{3,3} & K_{3,4} & K_{3,5} & K_{3,6} & K_{3,7} & K_{3,8} & K_{3,9} & K_{3,10} & K_{3,11} & K_{3,12} & \delta_{Amz} \\ & & & & K_{4,4} & K_{4,5} & K_{4,6} & K_{4,7} & K_{4,8} & K_{4,9} & K_{4,10} & K_{4,11} & K_{4,12} & \theta_{Amx} \\ & & & & & K_{5,5} & K_{5,6} & K_{5,7} & K_{5,8} & K_{5,9} & K_{5,10} & K_{5,11} & K_{5,12} & \theta_{Amy} \\ & & & & & & K_{6,6} & K_{6,7} & K_{6,8} & K_{6,9} & K_{6,10} & K_{6,11} & K_{6,12} & \theta_{Amz} \\ & & \text{symm} & & & & & K_{7,7} & K_{7,8} & K_{7,9} & K_{7,10} & K_{7,11} & K_{7,12} & \delta_{Bmx} \\ & & & & & & & & K_{8,8} & K_{8,9} & K_{8,10} & K_{8,11} & K_{8,12} & \delta_{Bmy} \\ & & & & & & & & & K_{9,9} & K_{9,10} & K_{9,11} & K_{9,12} & \delta_{Bmz} \\ & & & & & & & & & & K_{10,10} & K_{10,11} & K_{10,12} & \theta_{Bmx} \\ & & & & & & & & & & & K_{11,11} & K_{11,12} & \theta_{Bmy} \\ & & & & & & & & & & & & K_{12,12} & \theta_{Bmz} \end{array} \right]
 \end{aligned}$$

where $[K_e]$ is given in Eq. (8.31). Stiffness coefficients are

$$\begin{aligned}
K_{1,1} &= A_{11}^2 H + A_{12}^2 S_{22} + A_{13}^2 S_{33} \\
K_{1,2} &= A_{11} H A_{21} + A_{12} S_{22} A_{22} + A_{13} S_{33} A_{23} \\
K_{1,3} &= A_{11} H A_{31} + A_{12} S_{22} A_{32} + A_{13} S_{33} A_{33} \\
K_{1,4} &= A_{12} S_{22} A_{42} + A_{13} S_{33} A_{43} - A_{13} S_{35} A_{12} + A_{12} S_{26} A_{13} \\
K_{1,5} &= A_{12} S_{22} A_{52} + A_{13} S_{33} A_{53} - A_{13} S_{35} A_{22} + A_{12} S_{26} A_{23} \\
K_{1,6} &= A_{11} H A_{61} + A_{12} S_{22} A_{62} + A_{13} S_{33} A_{63} - A_{13} S_{35} A_{32} + A_{12} S_{26} A_{33} \\
K_{1,7} &= -A_{11} H B_{11} - A_{12} S_{22} B_{12} - A_{13} S_{33} B_{13} \\
K_{1,8} &= -A_{11} H B_{21} - A_{12} S_{22} B_{22} - A_{13} S_{33} B_{23} \\
K_{1,9} &= -A_{11} H B_{31} - A_{12} S_{22} B_{32} - A_{13} S_{33} B_{33} \\
K_{1,10} &= -A_{12} S_{22} B_{42} - A_{13} S_{33} B_{43} - A_{13} S_{35} B_{12} + A_{12} S_{26} B_{13} \\
K_{1,11} &= -A_{12} S_{22} B_{52} - A_{13} S_{33} B_{53} - A_{13} S_{35} B_{22} + A_{12} S_{26} B_{23} \\
K_{1,12} &= -A_{11} H B_{61} - A_{12} S_{22} B_{62} - A_{13} S_{33} B_{63} - A_{13} S_{35} B_{32} + A_{12} S_{26} B_{33} \\
K_{2,2} &= A_{21}^2 H + A_{22}^2 S_{22} + A_{23}^2 S_{33} \\
K_{2,3} &= A_{21} H A_{31} + A_{22} S_{22} A_{32} + A_{23} S_{33} A_{33} \\
K_{2,4} &= A_{22} S_{22} A_{42} + A_{23} S_{33} A_{43} - A_{23} S_{35} A_{12} + A_{22} S_{26} A_{13} \\
K_{2,5} &= A_{22} S_{22} A_{52} + A_{23} S_{33} A_{53} - A_{23} S_{35} A_{22} + A_{22} S_{26} A_{23} \\
K_{2,6} &= A_{21} H A_{61} + A_{22} S_{22} A_{62} + A_{23} S_{33} A_{63} - A_{23} S_{35} A_{32} + A_{22} S_{26} A_{33} \\
K_{2,7} &= -A_{21} H B_{11} - A_{22} S_{22} B_{12} - A_{23} S_{33} B_{13} \\
K_{2,8} &= -A_{21} H B_{21} - A_{22} S_{22} B_{22} - A_{23} S_{33} B_{23} \\
K_{2,9} &= -A_{21} H B_{31} - A_{22} S_{22} B_{32} - A_{23} S_{33} B_{33} \\
K_{2,10} &= -A_{22} S_{22} B_{42} - A_{23} S_{33} B_{43} - A_{23} S_{35} B_{12} + A_{22} S_{26} B_{13} \\
K_{2,11} &= -A_{22} S_{22} B_{52} - A_{23} S_{33} B_{53} - A_{23} S_{35} B_{22} + A_{22} S_{26} B_{23} \\
K_{2,12} &= -A_{21} H B_{61} - A_{22} S_{22} B_{62} - A_{23} S_{33} B_{63} - A_{23} S_{35} B_{32} + A_{22} S_{26} B_{33} \\
K_{3,3} &= A_{31}^2 H + A_{32}^2 S_{22} + A_{33}^2 S_{33} \\
K_{3,4} &= A_{32} S_{22} A_{42} + A_{33} S_{33} A_{43} - A_{33} S_{35} A_{12} + A_{32} S_{26} A_{13} \\
K_{3,5} &= A_{32} S_{22} A_{52} + A_{33} S_{33} A_{53} - A_{33} S_{35} A_{22} + A_{32} S_{26} A_{23} \\
K_{3,6} &= A_{31} H A_{61} + A_{32} S_{22} A_{62} + A_{33} S_{33} A_{63} - A_{33} S_{35} A_{32} + A_{32} S_{26} A_{33} \\
K_{3,7} &= -A_{31} H B_{11} - A_{32} S_{22} B_{12} - A_{33} S_{33} B_{13} \\
K_{3,8} &= -A_{31} H B_{21} - A_{32} S_{22} B_{22} - A_{33} S_{33} B_{23} \\
K_{3,9} &= -A_{31} H B_{31} - A_{32} S_{22} B_{32} - A_{33} S_{33} B_{33} \\
K_{3,10} &= -A_{32} S_{22} B_{42} - A_{33} S_{33} B_{43} - A_{33} S_{35} B_{12} + A_{32} S_{26} B_{13} \\
K_{3,11} &= -A_{32} S_{22} B_{52} - A_{33} S_{33} B_{53} - A_{33} S_{35} B_{22} + A_{32} S_{26} B_{23} \\
K_{3,12} &= -A_{31} H B_{61} - A_{32} S_{22} B_{62} - A_{33} S_{33} B_{63} - A_{33} S_{35} B_{32} + A_{32} S_{26} B_{33} \\
K_{4,4} &= A_{42}^2 S_{22} + 2 A_{42} A_{13} S_{26} + A_{43}^2 S_{33} - 2 A_{43} A_{12} S_{35} + A_{11}^2 Q + A_{12}^2 B + A_{13}^2 A \\
K_{4,5} &= A_{52} A_{42} S_{22} + A_{52} A_{13} S_{26} + A_{53} A_{43} S_{33} - A_{53} A_{12} S_{35} + A_{11} Q A_{21} - A_{22} A_{43} S_{35} + A_{22} A_{12} B + A_{23} \\
&\quad A_{42} S_{26} + A_{23} A_{13} A \\
K_{4,6} &= A_{62} A_{42} S_{22} + A_{62} A_{13} S_{26} + A_{63} A_{43} S_{33} - A_{63} A_{12} S_{35} + A_{11} Q A_{31} - A_{32} A_{43} S_{35} + A_{32} A_{12} B + A_{33} \\
&\quad A_{42} S_{26} + A_{33} A_{13} A \\
K_{4,7} &= -B_{12} A_{42} S_{22} - B_{12} A_{13} S_{26} - B_{13} A_{43} S_{33} + B_{13} A_{12} S_{35} \\
K_{4,8} &= -B_{22} A_{42} S_{22} - B_{22} A_{13} S_{26} - B_{23} A_{43} S_{33} + B_{23} A_{12} S_{35} \\
K_{4,9} &= -B_{32} A_{42} S_{22} - B_{32} A_{13} S_{26} - B_{33} A_{43} S_{33} + B_{33} A_{12} S_{35} \\
K_{4,10} &= -B_{42} A_{42} S_{22} - B_{42} A_{13} S_{26} - B_{43} A_{43} S_{33} + B_{43} A_{12} S_{35} - A_{11} Q B_{11} - B_{12} A_{43} S_{35} + B_{12} A_{12} \\
&\quad D + B_{13} A_{42} S_{26} + B_{13} A_{13} C \\
K_{4,11} &= -B_{52} A_{42} S_{22} - B_{52} A_{13} S_{26} - B_{53} A_{43} S_{33} + B_{53} A_{12} S_{35} - A_{11} Q B_{21} - B_{22} A_{43} S_{35} + B_{22} A_{12} \\
&\quad D + B_{23} A_{42} S_{26} + B_{23} A_{13} C \\
K_{4,12} &= -B_{62} A_{42} S_{22} - B_{62} A_{13} S_{26} - B_{63} A_{43} S_{33} + B_{63} A_{12} S_{35} - A_{11} Q B_{31} - B_{32} A_{43} S_{35} + B_{32} A_{12} \\
&\quad D + B_{33} A_{42} S_{26} + B_{33} A_{13} C \\
K_{5,5} &= A_{52}^2 S_{22} + 2 A_{52} A_{23} S_{26} + A_{53}^2 S_{33} - 2 A_{53} A_{22} S_{35} + A_{21}^2 Q + A_{22}^2 B + A_{23}^2 A \\
K_{5,6} &= A_{62} A_{52} S_{22} + A_{62} A_{23} S_{26} + A_{63} A_{53} S_{33} - A_{63} A_{22} S_{35} + A_{21} Q A_{31} - A_{32} A_{53} S_{35} + A_{32} A_{22} B + A_{33} \\
&\quad A_{52} S_{26} + A_{33} A_{23} A \\
K_{5,7} &= -B_{12} A_{52} S_{22} - B_{12} A_{23} S_{26} - B_{13} A_{53} S_{33} + B_{13} A_{22} S_{35} \\
K_{5,8} &= -B_{22} A_{52} S_{22} - B_{22} A_{23} S_{26} - B_{23} A_{53} S_{33} + B_{23} A_{22} S_{35} \\
K_{5,9} &= -B_{32} A_{52} S_{22} - B_{32} A_{23} S_{26} - B_{33} A_{53} S_{33} + B_{33} A_{22} S_{35} \\
K_{5,10} &= -B_{42} A_{52} S_{22} - B_{42} A_{23} S_{26} - B_{43} A_{53} S_{33} + B_{43} A_{22} S_{35} - A_{21} Q B_{11} - B_{12} A_{53} S_{35} + B_{12} A_{22} \\
&\quad D + B_{13} A_{52} S_{26} + B_{13} A_{23} C
\end{aligned}$$

$$\begin{aligned}
K_{5,11} &= -B_{52} A_{52} S_{22} - B_{52} A_{23} S_{26} - B_{53} A_{53} S_{33} + B_{53} A_{22} S_{35} - A_{21} Q B_{21} - B_{22} A_{53} S_{35} + B_{22} A_{22} \\
&\quad D + B_{23} A_{52} S_{26} + B_{23} A_{23} C \\
K_{5,12} &= -B_{62} A_{52} S_{22} - B_{62} A_{23} S_{26} - B_{63} A_{53} S_{33} + B_{63} A_{22} S_{35} - A_{21} Q B_{31} - B_{32} A_{53} S_{35} + B_{32} A_{22} \\
&\quad D + B_{33} A_{52} S_{26} + B_{33} A_{23} C \\
K_{6,6} &= A_{61}^2 H + A_{62}^2 S_{22} + 2 A_{62} A_{33} S_{26} + A_{63}^2 S_{33} - 2 A_{63} A_{32} S_{35} + A_{31}^2 Q + A_{32}^2 B + A_{33}^2 A \\
K_{6,7} &= -A_{61} H B_{11} - B_{12} A_{62} S_{22} - B_{12} A_{33} S_{26} - B_{13} A_{63} S_{33} + B_{13} A_{32} S_{35} \\
K_{6,8} &= -A_{61} H B_{21} - B_{22} A_{62} S_{22} - B_{22} A_{33} S_{26} - B_{23} A_{63} S_{33} + B_{23} A_{32} S_{35} \\
K_{6,9} &= -A_{61} H B_{31} - B_{32} A_{62} S_{22} - B_{32} A_{33} S_{26} - B_{33} A_{63} S_{33} + B_{33} A_{32} S_{35} \\
K_{6,10} &= -B_{42} A_{62} S_{22} - B_{42} A_{33} S_{26} - B_{43} A_{63} S_{33} + B_{43} A_{32} S_{35} - A_{31} Q B_{11} - B_{12} A_{63} S_{35} + B_{12} A_{32} \\
&\quad D + B_{13} A_{62} S_{26} + B_{13} A_{33} C \\
K_{6,11} &= -B_{52} A_{62} S_{22} - B_{52} A_{33} S_{26} - B_{53} A_{63} S_{33} + B_{53} A_{32} S_{35} - A_{31} Q B_{21} - B_{22} A_{63} S_{35} + B_{22} A_{32} \\
&\quad D + B_{23} A_{62} S_{26} + B_{23} A_{33} C \\
K_{6,12} &= -A_{61} H B_{61} - B_{62} A_{62} S_{22} - B_{62} A_{33} S_{26} - B_{63} A_{63} S_{33} + B_{63} A_{32} S_{35} - A_{31} Q B_{31} - B_{32} A_{63} \\
&\quad S_{35} + B_{32} A_{32} D + B_{33} A_{62} S_{26} + B_{33} A_{33} C \\
K_{7,7} &= B_{11}^2 H + B_{12}^2 S_{22} + B_{13}^2 S_{33} \\
K_{7,8} &= B_{11} H B_{21} + B_{12} S_{22} B_{22} + B_{13} S_{33} B_{23} \\
K_{7,9} &= B_{11} H B_{31} + B_{12} S_{22} B_{32} + B_{13} S_{33} B_{33} \\
K_{7,10} &= B_{12} S_{22} B_{42} + B_{13} S_{33} B_{43} + B_{13} S_{35} B_{12} - B_{12} S_{26} B_{13} \\
K_{7,11} &= B_{12} S_{22} B_{52} + B_{13} S_{33} B_{53} + B_{13} S_{35} B_{22} - B_{12} S_{26} A_{23} \\
K_{7,12} &= B_{11} H B_{61} + B_{12} S_{22} B_{62} + B_{13} S_{33} B_{63} + B_{13} S_{35} B_{32} - B_{12} S_{26} A_{33} \\
K_{8,8} &= B_{21}^2 H + B_{22}^2 S_{22} + B_{23}^2 S_{33} \\
K_{8,9} &= B_{21} H B_{31} + B_{22} S_{22} B_{32} + B_{23} S_{33} B_{33} \\
K_{8,10} &= B_{22} S_{22} B_{42} + B_{23} S_{33} B_{43} + B_{23} S_{35} B_{12} - B_{22} S_{26} B_{13} \\
K_{8,11} &= B_{22} S_{22} B_{52} + B_{23} S_{33} B_{53} + B_{23} S_{35} B_{22} - B_{22} S_{26} B_{23} \\
K_{8,12} &= B_{21} H B_{61} + B_{22} S_{22} B_{62} + B_{23} S_{33} B_{63} + B_{23} S_{35} B_{32} - B_{22} S_{26} B_{33} \\
K_{9,9} &= B_{31}^2 H + B_{32}^2 S_{22} + B_{33}^2 S_{33} \\
K_{9,10} &= B_{32} S_{22} B_{42} + B_{33} S_{33} B_{43} + B_{33} S_{35} B_{12} - B_{32} S_{26} B_{13} \\
K_{9,11} &= B_{32} S_{22} B_{52} + B_{33} S_{33} B_{53} + B_{33} S_{35} B_{22} - B_{32} S_{26} B_{23} \\
K_{9,12} &= B_{31} H B_{61} + B_{32} S_{22} B_{62} + B_{33} S_{33} B_{63} + B_{33} S_{35} B_{32} - B_{32} S_{26} B_{33} \\
K_{10,10} &= B_{42}^2 S_{22} - 2 B_{42} B_{13} S_{26} + B_{43}^2 S_{33} + 2 B_{43} B_{12} S_{35} + B_{11}^2 Q + B_{12}^2 B + B_{13}^2 A \\
K_{10,11} &= B_{52} B_{42} S_{22} - B_{52} B_{13} S_{26} + B_{53} B_{43} S_{33} + B_{53} B_{12} S_{35} + B_{11} Q B_{21} + B_{22} B_{43} S_{35} + B_{22} B_{12} B - B_{23} \\
&\quad B_{42} S_{26} + B_{23} B_{13} A \\
K_{10,12} &= B_{62} B_{42} S_{22} - B_{62} B_{13} S_{26} + B_{63} B_{43} S_{33} + B_{63} B_{12} S_{35} + B_{11} Q B_{31} + B_{32} B_{43} S_{35} + B_{32} B_{12} B - B_{33} \\
&\quad B_{42} S_{26} + B_{33} B_{13} A \\
K_{11,11} &= B_{52}^2 S_{22} - 2 B_{52} B_{23} S_{26} + B_{53}^2 S_{33} + 2 B_{53} B_{22} S_{35} + B_{21}^2 Q + B_{22}^2 B + B_{23}^2 A \\
K_{11,12} &= B_{62} B_{52} S_{22} - B_{62} B_{23} S_{26} + B_{63} B_{53} S_{33} + B_{63} B_{22} S_{35} + B_{21} Q B_{31} + B_{32} B_{53} S_{35} + B_{32} B_{22} B - B_{33} \\
&\quad B_{52} S_{26} + B_{33} B_{23} A \\
K_{12,12} &= B_{61}^2 H + B_{62}^2 S_{22} - 2 B_{62} B_{33} S_{26} + B_{63}^2 S_{33} + 2 B_{63} B_{32} S_{35} + B_{31}^2 Q + B_{32}^2 B + B_{33}^2 A
\end{aligned}$$

Appendix G—Computer Program for Newmark Method

The computer program for Newmark's integration method with $\alpha = 1/6$ and $\delta = 1/2$ (linear acceleration method) is listed here, followed by explanatory details.

```
C ****
C *          (TIME HISTORY COMPUTATION) *
C *          LINEAR ACCELERATION METHOD *
C *          FOR SEISMIC RESPONSE OF STRUCTURES (USING INTEGRATION METHOD) *
C *
C ****
C
C VARIABLES:
C NDCA = TIME HISTORY RECORD DATA CAPACITY
C NW = WORK ARRAY CAPACITY GREATER OR EQUAL TO 2* NM
C NM = NUMBER OF D.O.F.
C ND = TOTAL NO.OF TIME HISTORY DATA FOR EACH GROUND COMPONENT

C G = GRAVITY
C DT = TIME INCREMENT
C ANGLE = ANGLE FROM GROUND N-S COMP. TO STRUCT, REFERENCE AXIS OF X1
C
C     PARAMETER (NDCA=2400, NW=20)
C     CHARACTER*1 CHAR(3), DIRECT
C     DIMENSION SNA(NDCA), EWA(NDCA), VER(NDCA), CC(NW,NW), WN(NW,NW)
C     DIMENSION DF(NW,NW), SC(NW,NW), SK(NW,NW), DP2(NW,NW)
C     DIMENSION UDX(NW), UVX(NW), UAX(NW), UDY(NW), UVY(NW), UAY(NW)
C     DIMENSION UDZ(NW), UV2(NW), UAZ(NW), PX(NW,NW), AMX(NW,NW)
C     DIMENSION RX(NW,NW), RY(NW,NW), RZ(NW,NW), AMY(NW,NW), AMZ(NW,NW)
C     DIMENSION FY(NW,NW), FZ(NW,NW), FFX(NW,NW), FFY(NW,NW), FFZ(NW,NW)
C     DIMENSION DIS(NW), PX(NW), PY(NW), PZ(NW), WNNN(NW), STI(NW,NW)
C     DIMENSION AM(NW,NW), AMIV(NW,NW), GER(NW,NW), CG(NW,NW)
C     DATA NM, ND, G, DT, ANGLE/1, 7, 1., 0.005, 0./
C
```

```

C
C =====
C DEFINE EXTERNAL FILE UNITS FOR INPUT DATA AND OUTPUT
C =====
OPEN(UNIT=5,FILE=STRING(8))
OPEN(UNIT=6,FILE=STRING(9))
C
C      WRITE(6,*)'      LINEAR ACCELERATION METHOD'
C      WRITE(6,*)'      ====='
C      WRITE(6,*)'
READ(5,*)NM,ND,G,DT,ANGLE
WRITE(6,100)NM, ND, G, DT, ANGLE
100 FORMAT(1x,'NUMBER OF D.O.F.      =',I5,
& /1X,'TOTAL NO. OF TIME HISTORY DATA FOR EACH COMPONENT =',I5,
& /1X,'GRAVITY, G      =',F15.6,
& /1X,'TIME INCREMENT      =',F15.6,
& /1X,'ANGLE      =',F15.6/)
CHAR(1)='X'
CHAR(2)='Y'
CHAR(3)='Z'
C      WRITE(6,*)'INPUT MASS:'
DO 33 I=1, NM
33 READ(5,*)(AM(I,J),J=1, NM)
C      WRITE(6,*)'INPUT STIFFNESS:'
DO 34 I=1, NM
34 READ(5,*)(STI(I,J), J=1, NM)
C      WRITE(6,*)' DAMPING RATION:'
DO 35 I=1, NM
35 READ(5,*)(DF(I,J), J=1, NM)
C
      WRITE(6,*)'THE MASS MATRIX:'
CALL PRIN(AM, NM, NM, NW, NW)
      WRITE(6,*)'THE STIFFNESS MATRIX:'
CALL PRIN(STI, NM, NM, NW, NW)
      WRITE(6,*)'THE DAMPING MATRIX:'
CALL PRIN(DF, NM, NM, NW, NW)
C
C----- READ EARTHQUAKE INPUT ACCELERATION DATA ( UNIT=G)
C EWA = EASE-WEST DIRECTION
C SNA = SOUTH-NORTH DIRECTION
C VER = VERTICAL DIRECTION
C
      WRITE(6,*)'INPUT EAST-WEST EARTHQUAKE ACCELERATION DATA'
READ(5,*)(EWA(I), I=1, ND)
WRITE(6,45)(EWA(I), I=1, ND)
READ(5,*) DUMMY
IF (DUMMY.NE.0.) WRITE(6,31)
31 FORMAT (1X, 'INPUT DATA INCORRECT!')
45 FORMAT (1X, 8F9.6)
      WRITE(6,*)'INPUT NORTH-SOUTH EARTHQUAKE ACCELERATION DATA'
READ(5,*)(SNA(I), I=1, ND)
WRITE(6,45)(SNA(I), I=1, ND)
READ(5,*) DUMMY2
IF (DUMMY2.NE.0.) WRITE (6,31)
      WRITE(6,*)'INPUT VERTICAL EARTHQUAKE ACCELERATION DATA'
READ(5,*)(VER(I), I=1, ND)
WRITE(6,45)(VER(I), I=1, ND)
READ(5,*) DUMMY3
IF (DUMMY3.NE.0.) WRITE (6,31)
DO 30 I=1, ND
SNA(I) = SNA(I)*G
VER(I) = VER(I)*G
30 EWA(I) = EWA(I)*G
C
C      INPUT INFLUENCE COEFFICIENT FACTOR
READ(5,*)(RX(I,1), I=1, NM)

```

```

READ(5,*) (RY(I,1), I=1, NM)
READ(5,*) (RZ(I,1), I=1, NM)
WRITE(6,*) 'INFLUENCE COEFFICIENT FACTORS RX:'
CALL PRIN(RX, NM, 1, NW, NW)
WRITE(6,*) 'INFLUENCE COEFFICIENT FACTORS RY:'
CALL PRIN(RY, NM, 1, NW, NW)
WRITE(6,*) 'INFLUENCE COEFFICIENT FACTORS RZ:'
CALL PRIN(RZ, NM, 1, NW, NW)
CALL MULTIP (AM, RX, AMX, NM, NM, 1, NW, NW)
CALL MULTIP (AM, RY, AMY, NM, NM, 1, NW, NW)
CALL MULTIP (AM, RZ, AMZ, NM, NM, 1, NW, NW)
SS=SIN(ANGLE)
CS=COS(ANGLE)

C SET INITIAL DISP., VELO., & ACC. FOR EACH DOF TO ZEROS.
DO 37 I=1, NM
  UDX(I) = 0.
  UVX(I) = 0.
  UAX(I) = 0.
  UDY(I) = 0.
  UVY(I) = 0.
  UAY(I) = 0.
  UDZ(I) = 0.
  UVZ(I) = 0.
  UAZ(I) = 0.

37 CONTINUE
C INPUT INITIAL DISP., VELO., & ACC. FOR A DOF DUE TO GROUND COMP. IN X DIRECTION.
C I.E., T=0.0 SEC.
84  READ(5,*) DIRECT, IDOF, DISP, VELO, ACCEL
    IF (IDOF .LE. 0) GO TO 65
    IF (DIRECT .EQ. 'X') THEN
      UDX(IDOF) = DISP
      UVX(IDOF) = VELO
      UAX(IDOF) = ACCEL
    ELSE IF (DIRECT .EQ. 'Y') THEN
      UDY(IDOF) = DISP
      UVY(IDOF) = VELO
      UAY(IDOF) = ACCEL
    ELSE IF (DIRECT .EQ. 'Z') THEN
      UDZ(IDOF) = DISP
      UVZ(IDOF) = VELO
      UAZ(IDOF) = ACCEL
    ENDIF

C
  GO TO 84
C
65  WRITE(6,*)'STRUCTURAL TIME HISTORY RESPONSE:'

C
  WRITE(6,81)
81 FORMAT(1X, 'DOF      TIME      DISPLACEMENT',
      &           '      VELOCITY ACCELERATION')
  T=0.0
  DO 385 I=1, NM
    WRITE(6,36) I, CHAR(1), T, UDX(I),UVX(I),UAX(I)
    WRITE(6,36)I, CHAR(2), T, UDY(I), UVY(I), UAY(I)
    WRITE(6,36)I, CHAR(3), T, UDZ(I), UVZ(I), UAZ(I)

385 CONTINUE
C
  T=DT
  DO 40 II=2, ND
    AX=SNA(II)*CS+EWA(II)*SS
    AY=-SS*SNA(II)+EWA(II)*CS
    AZ=VER(II)
    DO 38 I=1, NM
      FX(I,1)= AMX(I, 1)*AX
      FY(I,1)= AMY(I, 1)*AY
38   FZ(I,1)= AMZ(I, 1)*AZ
C

```

```

CALL ACC(AM, STI, DF, FX, UDX, UVX, UAX, DT, NM)
CALL ACC(AM, STI, DF, FY, UDY, UVY, UAY, DT, NM)
CALL ACC(AM, STI, DF, FZ, UDZ, UVZ, UAZ, DT, NM)
DO 380 I=1, NM
WRITE(6,36) I, CHAR(1), T, UDX(I),UVX(I),UAX(I)
WRITE(6,36)I, CHAR(2), T, UDY(I), UVY(I), UAY(I)
WRITE(6,36)I, CHAR(3), T, UDZ(I), UVZ(I), UAZ(I)
36 FORMAT (1X, 'DOF', I2, A, 2X, 'TIME=', F7.3,3F15.7)
380 CONTINUE
T=T+DT
40 CONTINUE
C
CLOSE(5)
CLOSE(6)
WRITE(*,*)'PROGRAM NORMAL STOP -----'
STOP
END
C
C
SUBROUTINE ACC(SM, SK, SC, F, UD, UV, UA, DT, NM)
PARAMETER (NDCA=2400,NW=20)
DIMENSION SM(NW, NW), SMA(NW, NW), F(NW, NW), UD(NW), UV(NW), UA(NW)
DIMENSION A(NW,NW), B(NW, NW), SC(NW, NW), SK(NW, NW), BAK(NW, NW)
DIMENSION C(NW,NW), BAKIV(NW,NW), SCB(NW,NW), BAF(NW,NW), DD(NW,NW)
DIMENSION VV(NW,NW), AA(NW,NW), CC(NW,NW), UNIT(NW,NW), GER(NW,NW)
DO 107 I=1, NM
A(I,1)=(-6.*UD(I)/(DT*DT))-(6.*UV(I)/DT)-(2.*UA(I))
B(I,1)=-2.*UV(I)-(DT*UA(I)/2.)-(3.*UD(I)/DT)
C WRITE(6,*) 'A AND B:', A(I, 1), B(I, 1)
107 CONTINUE
DO 108 I=1, NM
DO 108 J=1, NM
BAK(I,J)=(6./(DT**2))*SM(I,J)+(3.*SC(I,J)/DT)+SK(I,J)
C WRITE(6,*) ' KBAR :, BAK(I,J)'
108 CONTINUE
CALL MATIRV(BAK, NM, NW, NW, BAKIV, CC)
CALL MULTIP(SC, B, SCB, NM, NM, 1, NW, NW)
CALL MULTIP(SM, A, SMA, NM, NM, 1, NW, NW)
DO 109 I=1, NM
BAF(I,1)=F(I,1)-SMA(I,1)-SCB(I,1)
C WRITE(6,*) 'BAF :, BAF(I, 1)'
109 CONTINUE
CALL MULTIP(BAKIV, BAF, DD, NM, NM, 1, NW, NW)
DO 210 I=1, NM
VV(I, 1)=(3.*DD(I,1)/DT)+B(I,1)
AA(I, 1)=(6.*DD(I,1)/(DT*DT))+A(I,1)
210 CONTINUE
DO 211 I=1, NM
UD(I)=DD(I, 1)
UV(I)=VV(I,1)
UA(I)=AA(I,1)
211 CONTINUE
RETURN
END
C
C
SUBROUTINE PRIN(A, NS, MS, NSS, MSS)
DIMENSION A(NSS, MSS)
DO 1 I=1,NS
WRITE(6,2) (A(I,J), J=1, MS)
2 FORMAT (1X, 10F12.4)
1 CONTINUE
WRITE(6,777)
777 FORMAT(5X, '-----')
RETURN
END
C

```

```

C *SUBROUTINE ADD A+B
C
      SUBROUTINE ADD(C1, C2, C3, NF, NLC, M, N)
      DIMENSION C1(M,N), C2(M,N), C3(M,N)
      DO 10 I=1, NF
      DO 10 J=1, NLC
10   C3(I,J)=C1(I,J)+C2(I,J)
      RETURN
      END

      SUBROUTINE MINUS (C1, C2, C3, NF, NLC, M, N)
      DIMENSION C1(M, N), C2(M, N), C3(M, N)
      DO 10, I=1, NF
      DO 10 J=1, NLC
10   C3(I,J)=C1(I, J)-C2(I, J)
      RETURN
      END

C
C *SUBROUTINE MULTIP A*B
C
      SUBROUTINE MULTIP(C1, C2, C3, L, M, N, MM, NN)
      DIMENSION C1(MM,NN), C2(MM,NN), C3(MM,NN)
      DO 10 I=1, L
      DO 10 J=1, N
      C3(I,J)=0.
      DO 10 K=1, M
10   C3(I,J)=C3(I,J)+ C1(I,K)*C2(K,J)
      RETURN
      END

C
C *A TRANSPOSE
C
      SUBROUTINE TRANP (C1, C3, M, N, MM, NN)
      DIMENSION C1(MM, NN), C3(MM, NN)
      DO 1000 I=1, M
      DO 1000 J=1, N
      C3(J,I)=C1(I,J)
1000 CONTINUE
      RETURN
      END

C
C *SUBROUTINE INVERS 1/A
C
      SUBROUTINE MATIRV(A,N,NN,MM,B,CC)
      DIMENSION A(NN,MM), B(NN,NN), CC(NN,MM), INDEX(10,10)
      DO 1111 I=1, 10
      DO 1111 J=1, 10
      INDEX(I, J)=0.
1111 CONTINUE
      L=N+1
      M=2*N
      DO 1 I=1, N
      DO 1, J=L, M
      A(I, J)=0
      IF(I+N-J) 1,2,1
2   A(I, J)=1
1 CONTINUE
      DO 103 I=1, N
      DO 103 J=1, N
103 INDEX(I,J)=0
      DO 4 IN=1,N
      AMAX=-1.0
      DO 106 I=1, N
      DO 100 J=1, N
      IF (INDEX(I, J))100, 105, 100
105 TEMP=ABS(A(I,J))
      IF(TEMP-AMAX) 100, 100, 101

```

```

101 IROW=I
    ICOL=J
    AMAX=TEMP
100 CONTINUE
106 CONTINUE
    DO 80 I=1, N
80 INDEX(I, ICOL)=1
    DO 81 J=1, N
81 INDEX(IROW, J)=1
    DIV=A(IROW, ICOL)
    IF(DIV)104, 17, 104
104 DO 3 J=1,M
3 A(IROW, J)=A(IROW, J)/DIV
    DO 4 K=1, N
        DELT=A(K, ICOL)
        IF (DELT) 5, 4, 5
5 IF(K-IROW)6, 4, 6
6 DO 7 J=1, M
7 A (K, J)=A(K, J)-A(IROW, J)*DELT
4 CONTINUE
    DO 30 I=1, N
    DO 31 J=1, N
        IF(A(I,J)) 32, 31, 32
31 CONTINUE
32 IICOL=J
    DO 33 JJ=1, M
33 CC(IICOL, JJ)=A(I,JJ)
30 CONTINUE
    DO 10 I=1, N
    DO 10 J=L, M
        K=J-N
10 B(I, K)=CC(I,J)
    GO TO 11
11 CC(1,1)=0
11 RETURN
    END

```

Input Data:

```

2 7 1.0 0.005 0. |NM, ND, G, DT, ANGLE
0.5823 0. |MASS
0. 1.5 |MASS
4166.7 2000. |STIFFNESS
2000. 7000. |STIFFNESS
9.8515 0. |DAMPING
0. 9.0 |DAMPING
77.28 64.4 51.52 38.64 25.76 12.88 0.0 |E-W RECORDS
0. |DUMMY
77.28 64.4 51.52 38.64 25.76 12.88 0.0 |N-S RECORDS
0. |DUMMY
38.64 32.2 25.76 19.32 12.88 6.44 0.0 |VERTICAL RECORDS
0. |DUMMY
1.0 0 |RX
0.0 0 |RY
0.0 1.0 |RZ
'X' 1 0.0 0.0 77.28 |STRUCTURE INITIAL RESPONSES
'Z' 2 0.0 0.0 38.64 |STRUCTURE INITIAL RESPONSES
'X' -1 0.0 0.0 0.0 |STRUCTURE INITIAL RESPONSES

```

Output Data:

```

LINEAR ACCELERATION METHOD
=====

```

```

NUMBER OF D.O.F.      = 2
TOTAL NO.OF TIME HISTORY DATA FOR EACH COMPONENT = 7
GRAVITY, G          =     1.000000

```

COMPUTER PROGRAM FOR NEWARK METHOD**861**

TIME INCREMENT = 0.005000
ANGLE = 0.000000

THE MASS MATRIX:
0.5823 0.0000
0.0000 1.5000

THE STIFFNESS MATRIX:
4166.7002 2000.0000
2000.0000 7000.0000

THE DAMPING MATRIX:
9.8515 0.0000
0.0000 9.0000

INPUT EAST-WEST EARTHQUAKE ACCELERATION DATA
77.27999964.40000251.52000038.63999925.76000012.880000 0.000000
INPUT NORTH-SOUTH EARTHQUAKE ACCELERATION DATA
77.27999964.40000251.52000038.63999925.76000012.880000 0.000000
INPUT VERTICAL EARTHQUAKE ACCELERATION DATA
38.63999932.20000125.76000019.32000012.880000 6.440000 0.000000
INFLUENCE COEFFICIENT FACTORS RX:
1.0000
0.0000

INFLUENCE COEFFICIENT FACTORS RY:
0.0000
0.0000

INFLUENCE COEFFICIENT FACTORS RZ:
0.0000
1.0000

STRUCTURAL TIME HISTORY RESPONSE:

DOF	TIME	DISPLACEMENT	VELOCITY	ACCELERATION
DOF 1X	TIME= 0.000	0.0000000	0.0000000	77.2799988
DOF 1Y	TIME= 0.000	0.0000000	0.0000000	0.0000000
DOF 1Z	TIME= 0.000	0.0000000	0.0000000	0.0000000
DOF 2X	TIME= 0.000	0.0000000	0.0000000	0.0000000
DOF 2Y	TIME= 0.000	0.0000000	0.0000000	0.0000000
DOF 2Z	TIME= 0.000	0.0000000	0.0000000	38.6399994
DOF 1X	TIME= 0.005	0.0008637	0.3250407	52.7362823
DOF 1Y	TIME= 0.005	0.0000000	0.0000000	0.0000000
DOF 1Z	TIME= 0.005	-0.0000059	-0.0035508	-1.4203136
DOF 2X	TIME= 0.005	-0.0000046	-0.0027832	-1.1132989
DOF 2Y	TIME= 0.005	0.0000000	0.0000000	0.0000000
DOF 2Z	TIME= 0.005	0.0004433	0.1694063	29.1225185
DOF 1X	TIME= 0.010	0.0030177	0.5104787	21.4389038
DOF 1Y	TIME= 0.010	0.0000000	0.0000000	0.0000000
DOF 1Z	TIME= 0.010	-0.0000554	-0.0190631	-4.7846150
DOF 2X	TIME= 0.010	-0.0000434	-0.0148961	-3.7318230
DOF 2Y	TIME= 0.010	0.0000000	0.0000000	0.0000000
DOF 2Z	TIME= 0.010	0.0016024	0.2838446	16.6527939
DOF 1X	TIME= 0.015	0.0057043	0.5374137	-10.6649513
DOF 1Y	TIME= 0.015	0.0000000	0.0000000	0.0000000
DOF 1Z	TIME= 0.015	-0.0002256	-0.0520264	-8.4006863
DOF 2X	TIME= 0.015	-0.0001762	-0.0405757	-6.5400329
DOF 2Y	TIME= 0.015	0.0000000	0.0000000	0.0000000
DOF 2Z	TIME= 0.015	0.0031722	0.3325316	2.8220065
DOF 1X	TIME= 0.020	0.0081444	0.4158823	-37.9476624
DOF 1Y	TIME= 0.020	0.0000000	0.0000000	0.0000000
DOF 1Z	TIME= 0.020	-0.0005998	-0.0994290	-10.5603561
DOF 2X	TIME= 0.020	-0.0004678	-0.0774543	-8.2114267
DOF 2Y	TIME= 0.020	0.0000000	0.0000000	0.0000000
DOF 2Z	TIME= 0.020	0.0048140	0.3129292	-10.6629248
DOF 1X	TIME= 0.025	0.0096738	0.1807213	-56.1166725

DOF 1Y TIME= 0.025	0.0000000	0.0000000	0.0000000
DOF 1Z TIME= 0.025	-0.0012264	-0.1507277	-9.9591446
DOF 2X TIME= 0.025	-0.0009557	-0.1173189	-7.7344007
DOF 2Y TIME= 0.025	0.0000000	0.0000000	0.0000000
DOF 2Z TIME= 0.025	0.0061971	0.2306998	-22.2287960
DOF 1X TIME= 0.030	0.0098477	-0.1168297	-62.9038315
DOF 1Y TIME= 0.030	0.0000000	0.0000000	0.0000000
DOF 1Z TIME= 0.030	-0.0020881	-0.1906388	-6.0052867
DOF 2X TIME= 0.030	-0.0016262	-0.1482844	-4.6517782
DOF 2Y TIME= 0.030	0.0000000	0.0000000	0.0000000
DOF 2Z TIME= 0.030	0.0070377	0.0985044	-30.6492558

Appendix H—Computer Program for Wilson- θ Method

The computer program for the Wilson- θ method is listed here, followed by explanatory details.

```
C ****
C *          (TIME HISTORY COMPUTATION) *
C *          WILSON THETA METHOD *
C *          FOR SEISMIC RESPONSE OF STRUCTURES (USING INTEGRATION METHOD) *
C *
C ****
C
C VARIABLES:
C NDCA = TIME HISTORY RECORD DATA CAPACITY
C NW  = WORK ARRAY CAPACITY GREATER OR EQUAL 2* NM
C NM  = NUMBER OF D.O.F.
C ND  = TOTAL NO.OF TIME HISTORY DATA FOR EACH GROUND COMPONENT

C G    = GRAVITY
C DT   = TIME INCREMENT
C ANGLE = ANGLE FROM GROUND N-S COMP. TO STRUCT, REFERENCE AXIS OF X1
C
PARAMETER (NDCA=2400, NW=20)
CHARACTER*1 CHAR(3), DIRECT
DIMENSION SNA(NDCA), EWA(NDCA), VER(NDCA), CC(NW,NW), WN(NW,NW)
DIMENSION DF(NW,NW), SC(NW,NW), SK(NW,NW), DF2(NW,NW)
DIMENSION UDX(NW), UVX(NW), UAX(NW), UDY(NW), UVY(NW), UAY(NW)
DIMENSION UDZ(NW), UVZ(NW), UAZ(NW), FX(NW,NW), AMX(NW,NW)
DIMENSION RX(NW,NW), RY(NW,NW), RZ(NW,NW), AMY(NW,NW), AMZ(NW,NW)
DIMENSION FY(NW,NW), FZ(NW,NW), FFX(NW,NW), FFY(NW,NW), FFZ(NW,NW)
DIMENSION DIS(NW), PX(NW), PY(NW), PZ(NW), WWNN(NW), STI(NW,NW)
DIMENSION AM(NW,NW), AMIV(NW,NW), GER(NW,NW), CG(NW,NW)
DIMENSION PPX(NW,NW), PPY(NW,NW), PPZ(NW,NW)
C     DATA NM, ND, G, DT, ANGLE/1, 7, 1., 0.005, 0./
```

```

C
C
C
C =====
C DEFINE EXTERNAL FILE UNITS FOR INPUT DATA AND OUTPUT
C =====
      OPEN(UNIT=5,FILE=STRING(8))
      OPEN(UNIT=6,FILE=STRING(9))

C
C
      WRITE(6,*)
      WRITE(6,*)
      WRITE(6,*)
      READ(5,*)NM, ND, G, DT, ANGLE
      WRITE(6,100)NM, ND, G, DT, ANGLE
100 FORMAT(1X,'NUMBER OF D.O.F.      =',I5,
      & /1X,'TOTAL NO.OF TIME HISTORY DATA FOR EACH COMPONENT =',I5,
      & /1X,'GRAVITY, G =',F15.6,
      & /1X,'TIME INCREMENT =',F15.6,
      & /1X,'ANGLE =',F15.6/)
      CHAR(1)='X'
      CHAR(2)='Y'
      CHAR(3)='Z'
C   WRITE(6,*)
      DO 33 I=1, NM
      33 READ(5,*) (AM(I,J), J=1, NM)
C   WRITE(6,*)
      DO 34 I=1, NM
      34 READ(5,*) (STI(I,J), J=1, NM)
C   WRITE(6,*)
      DO 35 I=1, NM
      35 READ(5,*) (DF(I,J), J=1, NM)
C
      WRITE(6,*)
      CALL PRIN(AM, NM, NM, NW, NW)
      WRITE(6,*)
      CALL PRIN(STI, NM, NM, NW, NW)
      WRITE(6,*)
      CALL PRIN(DF, NM, NM, NW, NW)

C
C-----READ EARTHQUAKE INPUT ACCELERATION DATA (UNIT=G)
C   EWA = EASE-WEST DIRECTION
C   SNA = SOUTH-NORTH DIRECTION
C   VER = VERTICAL DIRECTION
C
      WRITE(6,*)
      READ(5,*) (EWA(I), I=1, ND)
      WRITE(6,45) (EWA(I), I=1, ND)
      READ(5,*) DUMMY
      IF (DUMMY.NE.0.) WRITE(6,31)
31 FORMAT (1X, 'INPUT DATA INCORRECT!')
45 FORMAT (1X, 8F9.6)
      WRITE(6,*)
      READ(5,*) (SNA(I), I=1, ND)
      WRITE(6,45) (SNA(I), I=1, ND)
      READ(5,*) DUMMY2
      IF (DUMMY .NE. 0.) WRITE (6,31)
      WRITE(6,*)
      READ(5,*) (VER(I), I=1, ND)
      WRITE(6,45) (VER(I), I=1, ND)
      READ(5,*) DUMMY3
      IF (DUMMY3 .NE. 0.) WRITE (6,31)
      DO 30 I=1, ND
      SNA(I) = SNA(I)*G
      VER(I) = VER(I)*G
30 EWA(I) = EWA(I)*G

```

```

C
C---- INPUT INFLUENCE COEFFICIENT FACTOR
READ(5,*) (RX(I,1), I=1, NM)
READ(5,*) (RY(I,1), I=1, NM)
READ(5,*) (RZ(I,1), I=1, NM)
WRITE(6,*) 'INFLUENCE COEFFICIENT FACTORS RX:'
CALL PRIN(RX, NM, 1, NW, NW)
WRITE(6,*) 'INFLUENCE COEFFICIENT FACTORS RY:'
CALL PRIN(RY, NM, 1, NW, NW)
WRITE(6,*) 'INFLUENCE COEFFICIENT FACTORS RZ:'
CALL PRIN(RZ, NM, 1, NW, NW)
CALL MULTIP (AM, RX, AMX, NM, NM, 1, NW, NW)
CALL MULTIP (AM, RY, AMY, NM, NM, 1, NW, NW)
CALL MULTIP (AM, RZ, AMZ, NM, NM, 1, NW, NW)
SS=SIN(ANGLE)
CS=COS(ANGLE)
C SET INITIAL DISP., VELO., & ACC. FOR EACH DOF TO ZEROS.
DO 37 I=1, NM
  UDX(I) = 0.
  UVX(I) = 0.
  UAX(I) = 0.
  UDY(I) = 0.
  UVY(I) = 0.
  UAY(I) = 0.
  UDZ(I) = 0.
  UVZ(I) = 0.
  UAZ(I) = 0.
37 CONTINUE
C INPUT INITIAL DISP., VELO., & ACC. FOR A DOF DUE TO GROUND COMP. IN X DIRECTION.
C I.E., T=0.0 SEC.
84 READ(5,*) DIRECT, IDOF, DISP, VELO, ACCEL
  IF (IDOF .LE. 0) GO TO 65
  IF (DIRECT .EQ. 'X') THEN
    UDX(IDOF) = DISP
    UVX(IDOF) = VELO
    UAX(IDOF) = ACCEL
  ELSE IF (DIRECT .EQ. 'Y') THEN
    UDY(IDOF) = DISP
    UVY(IDOF) = VELO
    UAY(IDOF) = ACCEL
  ELSE IF (DIRECT .EQ. 'Z') THEN
    UDZ(IDOF) = DISP
    UVZ(IDOF) = VELO
    UAZ(IDOF) = ACCEL
  ENDIF
C
  GO TO 84
C
65 WRITE(6,*) 'STRUCTURAL TIME HISTORY RESPONSE:'
C
  WRITE(6,81)
81 FORMAT(1X, 'DOF      TIME      DISPLACEMENT',
      &           ' VELOCITY ACCELERATION')
T=0.0
DO 385 I=1, NM
  WRITE(6,36) I, CHAR(1), T, UDX(I), UVX(I), UAX(I)
  WRITE(6,36) I, CHAR(2), T, UDY(I), UVY(I), UAY(I)
  WRITE(6,36) I, CHAR(3), T, UDZ(I), UVZ(I), UAZ(I)
385 CONTINUE
C
C CALCULATE INITIAL FORCES AT EACH DOF DUE TO EACH GROUND COMPONENT AT T=0.0 SEC.
  AX0=SNA(1)*CS+EWA(1)*SS
  AYO=-SS*SNA(1)+EWA(1)*CS
  AZ0=VER(1)
  DO 48 I=1, NM
    PPX(I,1)= AMX(I, 1)*AX0
    PPY(I,1)= AMY(I, 1)*AYO

```

```

48 PPZ(I,1)=AMZ(I, 1)*AZ0
C
      T=DT
      DO 40 II=2,ND
        AX=SNA(II)*CS+EWA(II)*SS
        AY=-SS*SNA(II)+EWA(II)*CS
        AZ=VER(II)
        DO 38 I=1, NM
          FX(I,1)=AMX(I, 1)*AX
          FY(I,1)=AMY(I, 1)*AY
38   FZ(I,1)=AMZ(I, 1)*AZ
C
      DO 438 I=1,NM
        FX(I,1)=FX(I,1)-PPX(I,1)
        FY(I,1)=FY(I,1)-PPY(I,1)
        FZ(I,1)=FZ(I,1)-PPZ(I,1)
438 CONTINUE
      DO 448 I=1,NM
        PPX(I,1)=AMX(I,1)*AX
        PPY(I,1)=AMY(I,1)*AY
        PPZ(I,1)=AMZ(I,1)*AZ
448 CONTINUE
C
      CALL ACC(AM, STI, DF, FX, UDX, UVX, UAX, DT, NM)
      CALL ACC(AM, STI, DF, FY, UDY, UVY, UAY, DT, NM)
      CALL ACC(AM, STI, DF, FZ, UDZ, UVZ, UAZ, DT, NM)
      DO 380 I=1, NM
        WRITE(6,36) I, CHAR(1), T, UDX(I),UVX(I),UAX(I)
        WRITE(6,36) I, CHAR(2), T, UDY(I),UVY(I),UAY(I)
        WRITE(6,36) I, CHAR(3), T, UDZ(I),UVZ(I),UAZ(I)
36   FORMAT (1X, 'DOF', I2, A, 2X, 'TIME=', F7.3,3F15.7)
380 CONTINUE
      T=T+DT
      40 CONTINUE
C
      CLOSE(5)
      CLOSE(6)
      WRITE(*,*) 'PROGRAM NORMAL STOP -----*'
      STOP
      END
C
      SUBROUTINE ACC(SM,SK,SC,F,UD,UV,UA,DT,NM)
      PARAMETER (NDCA=2400, NW=20)
      DIMENSION SM(NW,NW),SMA(NW,NW),F(NW,NW),UD(NW),UV(NW),UA(NW)
      DIMENSION Q(NW,NW),R(NW,NW),SC(NW,NW),SK(NW,NW),BAK(NW,NW)
      DIMENSION C(NW,NW),BAKIV(NW,NW),SCB(NW,NW),BAF(NW,NW),DD(NW,NW)
      DIMENSION VV(NW,NW),AA(NW,NW),CC(NW,NW),UNIT(NW,NW),GER(NW,NW)
C
      THETA=1.4
      DTT=DT*THETA
      DO 107 I=1,NM
        Q(I,1)=(6*UV(I)/DTT) + 3*UA(I)
        R(I,1)=3*UV(I) + DTT*UA(I)/2
C      WRITE(6,*) ' UV AND UA:', UV(I),UA(I)
C      WRITE(6,*) ' Q AND R:', Q(I,1),R(I,1)
107 CONTINUE
      DO 108 I=1,NM
        F(I,1)=F(I,1)*THETA
108 CONTINUE
      CALL MULTIP(SC,R,SCB,NM,NM,1,NW,NW)
      CALL MULTIP(SM,Q,SMA,NM,NM,1,NW,NW)
      DO 109 I=1,NM
        BAF(I,1)=F(I,1)+SMA(I,1)+SCB(I,1)
C      WRITE(6,*) 'BAF,F,SMA,SCNB:', BAF(I,1),F(I,1),SMA(I,1),SCB(I,1)
109 CONTINUE
      DO 110 I=1,NM
      DO 110 J=1,NM

```

```

      BAK(I,J)=(6./(DTT**2))*SM(I,J)+(3.*SC(I,J)/DTT)+SK(I,J)
C  WRITE(6,*)' KBAR: ', BAK(I,J)
110 CONTINUE
      CALL MATIRV(BAK,NM,NW,NW,BAKIV,CC)
      CALL MULTIP(BAKIV,BAF,DD,NM,NM,1,NW,NW)
      DO 111 I=1,NM
      AA(I,1)=(6.*DD(I,1)/(DTT*DTT)) - (6*UV(I)/DTT) - 3*UA(I)
C  WRITE(6,*)'AA: ', AA(I,1)
111 CONTINUE
      DO 112 I=1,NM
      AA(I,1)=AA(I,1)/THETA
      VV(I,1)=UA(I)*DT + 0.5*DT*AA(I,1)
      DD(I,1)=UV(I)*DT + (0.5*UA(I)*DT*DT) + (DT*DT*AA(I,1))/6
112 CONTINUE
      DO 211 I=1,NM
      UD(I)=UD(I)+DD(I,1)
      UV(I)=UV(I)+VV(I,1)
      UA(I)=UA(I)+AA(I,1)
211 CONTINUE
      RETURN
      END

C
      SUBROUTINE PRIN(A, NS, MS, NSS, MSS)
      DIMENSION A(NSS, MSS)
      DO 1 I=1,NS
      WRITE(6,2) (A(I,J), J=1, MS)
2 FORMAT (1X, 10F12.4)
1 CONTINUE
      WRITE(6,777)
777 FORMAT(5X, '-----')
      RETURN
      END

C
C *SUBROUTINE ADD A+B
C
      SUBROUTINE ADD(C1, C2, C3, NF, NLC, M, N)
      DIMENSION C1(M,N), C2(M,N), C3(M,N)
      DO 10 I=1, NF
      DO 10 J=1, NLC
10 C3(I,J)=C1(I,J)+C2(I,J)
      RETURN
      END

      SUBROUTINE MINUS (C1, C2, C3, NF, NLC, M, N)
      DIMENSION C1(M, N), C2(M, N), C3(M, N)
      DO 10, I=1, NF
      DO 10 J=1, NLC
10 C3(I,J)=C1(I, J)-C2(I, J)
      RETURN
      END

C
C *SUBROUTINE MULTIP A*B
C
      SUBROUTINE MULTIP(C1, C2, C3, L, M, N, MM, NN)
      DIMENSION C1(MM,NN), C2(MM,NN), C3(MM,NN)
      DO 10 I=1, L
      DO 10 J=1, N
      C3(I,J)=0.
      DO 10 K=1, M
10 C3(I,J)=C3(I,J)+ C1(I,K)*C2(K,J)
      RETURN
      END

C
C * A TRANPOSE
C

```

```

SUBROUTINE TRANP (C1, C3, M, N, MM, NN)
DIMENSION C1(MM, NN), C3(MM, NN)
DO 1000 I=1, M
DO 1000 J=1, N
C3(J,I)=C1(I,J)
1000 CONTINUE
      RETURN
      END
C
C *SUBROUTINE INVERS 1/A
C
      SUBROUTINE MATIRV(A,N,NN,MM,B,CC)
DIMENSION A(NN,MM), B(NN,NN), CC(NN,MM), INDEX(10,10)
DO 1111 I=1, 10
DO 1111 J=1, 10
INDEX(I, J)=0.
1111 CONTINUE
L=N+1
M=2*N
DO 1 I=1, N
DO 1 J=L, M
A(I, J)=0
IF (I+N-J) 1,2,1
2 A(I, J)=1
1 CONTINUE
DO 103 I=1, N
DO 103 J=1, N
103 INDEX(I, J)=0
DO 4 IN=1,N
AMAX=-1.0
DO 106 I=1, N
DO 100 J=1, N
IF (INDEX(I, J)>100, 105, 100
105 TEMP=ABS(A(I,J))
IF (TEMP>AMAX) 100, 100, 101
101 IROW=I
ICOL=J
AMAX=TEMP
100 CONTINUE
106 CONTINUE
DO 80 I=1, N
80 INDEX(I, ICOL)=1
DO 81 J=1, N
81 INDEX(IROW, J)=1
DIV=A(IROW, ICOL)
IF (DIV)>104, 17, 104
104 DO 3 J=1,M
3 A(IROW, J)=A(IROW, J)/DIV
DO 4 K=1, N
DELT=A(K, ICOL)
IF (DELT) 5, 4, 5
5 IF(K-IROW)6, 4, 6
6 DO 7 J=1, M
7 A(K, J)=A(K, J)-A(IROW, J)*DELT
4 CONTINUE
DO 30 I=1, N
DO 31 J=1, N
IF(A(I,J)) 32, 31, 32
31 CONTINUE
32 IICOL=J
DO 33 JJ=1, M
33 CC(IICOL, JJ)=A(I,JJ)
30 CONTINUE
DO 10 I=1, N
DO 10 J=L, M
K=J-N
10 B(I, K)=CC(I,J)

```

```

GO TO 11
17 CC(1,1)=0
11 RETURN
END

```

Input Data:

```

2 7 1.0 0.005 0. |NM, ND, G, DT, ANGLE
0.5823 0. |MASS
0. 1.5 |MASS
4166.7 2000. |STIFFNESS
2000. 7000. |STIFFNESS
9.8515 0. |DAMPING
0. 9.0 |DAMPING
77.28 64.4 51.52 38.64 25.76 12.88 0.0 |E-W RECORDS
0. |DUMMY
77.28 64.4 51.52 38.64 25.76 12.88 0.0 |N-S RECORDS
0. |DUMMY
38.64 32.2 25.76 19.32 12.88 6.44 0.0 |VERTICAL RECORDS
0. |DUMMY
1.0 0 |RX
0.0 0 |RY
0.0 1.0 |RZ
'X' 1 0.0 0.0 77.28 |STRUCTURE INITIAL RESPONSES
'Z' 2 0.0 0.0 38.64 |STRUCTURE INITIAL RESPONSES
'X' -1 0.0 0.0 0.0 |STRUCTURE INITIAL RESPONSES

```

Output Data:

```

WILSON THETA METHOD
=====

NUMBER OF D.O.F.      =      2
TOTAL NO.OF TIME HISTORY DATA FOR EACH COMPONENT = 7
GRAVITY, G           =      1.000000
TIME INCREMENT       =      0.005000
ANGLE                =      0.000000

THE MASS MATRIX:
 0.5823  0.0000
 0.0000  1.5000
-----
THE STIFFNESS MATRIX:
 4166.7002  2000.0000
 2000.0000  7000.0000
-----
THE DAMPING MATRIX:
 9.8515  0.0000
 0.0000  9.0000
-----
INPUT EAST-WEST EARTHQUAKE ACCELERATION DATA
77.27999964.40000251.52000038.63999925.76000012.880000 0.000000
INPUT NORTH-SOUTH EARTHQUAKE ACCELERATION DATA
77.27999964.40000251.52000038.63999925.76000012.880000 0.000000
INPUT VERTICAL EARTHQUAKE ACCELERATION DATA
38.63999932.20000125.76000019.32000012.880000 6.440000 0.000000
INFLUENCE COEFFICIENT FACTORS RX:
 1.0000
 0.0000
-----
INFLUENCE COEFFICIENT FACTORS RY:
 0.0000
 0.0000
-----
```

INFLUENCE COEFFICIENT FACTORS RZ:

0.0000
1.0000

STRUCTURAL TIME HISTORY RESPONSE:

DOF	TIME	DISPLACEMENT	VELOCITY	ACCELERATION
-----	------	--------------	----------	--------------

DOF 1X	TIME= 0.000	0.0000000	0.0000000	77.2799988
DOF 1Y	TIME= 0.000	0.0000000	0.0000000	0.0000000
DOF 1Z	TIME= 0.000	0.0000000	0.0000000	0.0000000
DOF 2X	TIME= 0.000	0.0000000	0.0000000	0.0000000
DOF 2Y	TIME= 0.000	0.0000000	0.0000000	0.0000000
DOF 2Z	TIME= 0.000	0.0000000	0.0000000	38.6399994
DOF 1X	TIME= 0.005	0.0008577	0.3214106	51.2842560
DOF 1Y	TIME= 0.005	0.0000000	.0000000	0.0000000
DOF 1Z	TIME= 0.005	-0.0000076	-0.0045591	-1.8236529
DOF 2X	TIME= 0.005	-0.0000060	-0.0035882	-1.4352933
DOF 2Y	TIME= 0.005	0.0000000	0.0000000	0.0000000
DOF 2Z	TIME= 0.005	0.0004408	0.1678605	28.5042038
DOF 1X	TIME= 0.010	0.0029756	0.4997246	20.0413189
DOF 1Y	TIME= 0.010	0.0000000	0.0000000	0.0000000
DOF 1Z	TIME= 0.010	-0.0000670	-0.0219415	-5.1292934
DOF 2X	TIME= 0.010	-0.0000527	-0.0172682	-4.0366907
DOF 2Y	TIME= 0.010	0.0000000	0.0000000	0.0000000
DOF 2Z	TIME= 0.010	0.0015835	0.2786786	15.8230181
DOF 1X	TIME= 0.015	0.0055967	0.5230830	-10.6979256
DOF 1Y	TIME= 0.015	0.0000000	0.0000000	0.0000000
DOF 1Z	TIME= 0.015	-0.0002538	-0.0554036	-8.2555351
DOF 2X	TIME= 0.015	-0.0001998	-0.0436142	-6.5017066
DOF 2Y	TIME= 0.015	0.0000000	0.0000000	0.0000000
DOF 2Z	TIME= 0.015	0.0031180	0.3237807	2.2178221
DOF 1X	TIME= 0.020	0.0079733	0.4065635	-35.9098969
DOF 1Y	TIME= 0.020	0.0000000	0.0000000	0.0000000
DOF 1Z	TIME= 0.020	-0.0006401	-0.1002992	-9.7027006
DOF 2X	TIME= 0.020	-0.0005039	-0.0790010	-7.6530361
DOF 2Y	TIME= 0.020	0.0000000	0.0000000	0.0000000
DOF 2Z	TIME= 0.020	0.0047109	0.3026144	-10.6843233
DOF 1X	TIME= 0.025	0.0094898	0.1865241	-52.1058655
DOF 1Y	TIME= 0.025	0.0000000	0.0000000	0.0000000
DOF 1Z	TIME= 0.025	-0.0012577	-0.1457433	-8.4749556
DOF 2X	TIME= 0.025	-0.0009906	-0.1149016	-6.7071700
DOF 2Y	TIME= 0.025	0.0000000	0.0000000	0.0000000
DOF 2Z	TIME= 0.025	0.0060455	0.2222215	-21.4728394
DOF 1X	TIME= 0.030	0.0097474	-0.0881784	-57.7751350
DOF 1Y	TIME= 0.030	0.0000000	0.0000000	0.0000000
DOF 1Z	TIME= 0.030	-0.0020749	-0.1776462	-4.2861900
DOF 2X	TIME= 0.030	-0.0016354	-0.1402606	-3.4364567
DOF 2Y	TIME= 0.030	0.0000000	0.0000000	0.0000000
DOF 2Z	TIME= 0.030	0.0068563	0.0957290	-29.1241684

Appendix I—Computer Program for CQC Method

The computer program for CQC modal analysis is listed here, followed by explanatory details.

```
C ****
C ----- C.Q.C. METHOD -----
C FOR STRUCTURAL RESPONSE (USING MODE SUPERPOSITION METHOD)
C =====
C INPUT: NORMAL MODE MATRIX, MASS MATRIX,
C        MODAL DAMPING MATRIX, NATURAL FREQUENCIES,
C        INFLUENCE COEFFICIENT VECTOR, SPECTRA DATA
C =====
C N: SYSTEM D.O.F.
C M: NO. OF NORMAL MODES (NOT LARGER THAN N)
C NN: NO. OF GROUND MOTION CONDITION.
C MM: NO. OF MODES WHICH WILL BE ROOT-MEAN-SQUARE
C X(N,M): NORMAL MODE MATRIX
C AM(N,N): SYSTEM MASS MATRIX
C R(N,NN): INFLUENCE COEFFICIENT VECTOR MATRIX
C FI: TIMES OF MASS
C SD(M,NN) SPECTRA DATA MATRIX
C FK: MASS INCREMENT UPPER LIMIT: KK*AM
C ****
C      IMPLICIT REAL*8(A-H,O-Z)
      DIMENSION X(30,30),XT(30,30),AM(30,30),XMAX(30)
      DIMENSION R(30,30),XTAM(30,30),XTAMX(30,30),XTAMR(30,30)
      DIMENSION FTMF(30),FTMR(30,3),F(30,30),SD(30,30),XX(30,30,3)
      DIMENSION W(30),SX(30,30),CMC(30,30),RD(30,30),PP(30,30)
      DATA N,M,NN,MM,FK,ITDOF/3,3,2,3,1.00000000000,3/
      WRITE (6,*) 'THE CONVENTIONAL CQC METHOD'
      WRITE (6,*) '=====
      WRITE (6,*) 'INPUT DAMPING RATIO:'
      READ(5,*)DAM
      WRITE(6,222) DAM
222 FORMAT(1X,'THE DAMPING RATIO=', F10.4)
      WRITE (6,*) 'INPUT MASS MATRIX:'
```

```

      DO 999 I=1,N
      READ(5,*)(AM(I,J),J=1,N)
999 CONTINUE
      WRITE (6,*) 'INPUT NORMAL MODE MATRIX'
      DO 1000 I=1,N
      READ(5,*)(X(I,J),J=1,M)
1000 CONTINUE
      WRITE(6,*)" THE MASS MATRIX:' 
      CALL PRIN(AM,N,N,30,30)
      WRITE(6,*)" THE NORMAL MODE MATRIX:' 
      CALL PRIN(X,N,M,30,30)
      WRITE(6,*)" INPUT SPECTRA DATA MATRIX'
      DO 200 I=1,N
      READ(5,*)(SD(I,J),J=1,NN)
1007 FORMAT(3F20.6)
200 CONTINUE
      WRITE(6,*)" THE RESPONSE SPECTRA TABLES:' 
      CALL PRIN(SD,N,NN,30,30)
      WRITE (6,*) 'INPUT NATURAL FREQUENCIES'
      READ(5,*)(W(L),L=1,M)
      WRITE(6,457)(W(L),L=1,MM)
457 FORMAT(1X,'THE NATURAL FREQUENCIES:'/1X,10F12.5)
      WRITE(6,8885)
8885 FORMAT(1X,'THE INFLUENCE COEFF. VECTOR IN REFERENCE DIRECTIONS:')
      WRITE(6,*) 'INPUT INFLUENCE COEFF. VECTOR'
      DO 998 I=1,N
      READ(5,*)(RD(I,J),J=1,NN)
1225 FORMAT(3F10.6)
998 CONTINUE
      CALL PRIN(RD,N,NN,30,30)
      WRITE(6,4532)
4532 FORMAT(1X,'THE TOTAL RESPONSES:'/)
      ANGG=-1
1212 ANGG=ANGG+1
      IF(ANGG.GT. 360) GO TO 1213
C  WRITE(6,765)ANGG
C 765 FORMAT(1X,'THE MAIN TRANSLATION PRIN. COMP. INPUT DIRECTION',
C * '(RAD.)=',F20.9)
      ANG=ANGG*3.1415926/180.
      DO 329 I=1,ITDOF
      R(I,1)=RD(I,1)*COS(ANG)+RD(I,2)*SIN(ANG)
      R(I,2)=RD(I,1)*(-SIN(ANG))+RD(I,2)*COS(ANG)
      R(I,3)=RD(I,3)
329 CONTINUE
C4435 WRITE(6,4444)ANGG
C4444 FORMAT(1X,'INFLU. COEFF. VECTOR FOR ANGLE=',F20.9,' INPUT')
C  CALL PRIN(R,N,NN,30,30)
      CALL TRANP(X,XT,N,MM,30,30)
      CALL MULTIP(XT,AM,XTAM,MM,N,N,30,30)
      CALL MULTIP(XTAM,X,XTAMX,MM,N,MM,30,30)
      CALL MULTIP(XTAM,R,XTAMR,MM,N,NN,30,30)
      DO 1980 I=1,MM
      FTMF(I)=XTAMX(I,I)
1980 CONTINUE
      DO 10 I=1,N
      DO 10 J=1,MM
      F(I,J)=X(I,J)
10 CONTINUE
      DO 109 I=1,MM
      DO 109 J=1,NN
      FTMR(I,J)=XTAMR(I,J)
109 CONTINUE
      DO 1500 K=1,NN
C  WRITE(6,202) K
C 202 FORMAT(1X,'GROUND MOTION IN ',13, ' TH DIRECTION,THE STRUCTURE',
C * 'RESPONSES SHOW BELOW.', ,
C * '/1X,'NOTE:NO. OF COLUMN=NO. OF MODES'/

```

```

DO 3000 J=1,MM
DO 3000 L=1,N
XX(L,J,K) =F(L,J)*FTMR(J,K)*SD(J,K)/FTMF(J)
3000 CONTINUE
1500 CONTINUE
    DO 3001 J=1,MM
    DO 3001 L=1,N
    PP(L,J)=0.
    DO 3001 K=1,NN
    PP(L,J)=PP(L,J)+XX(L,J,K)
3001 CONTINUE
C
C ----- CALCULATE CROSS MODAL COEFFICIENT -----
436 DO 438 J=1,MM
    DO 438 JJ=1,MM
    RR=W(JJ)/W(J)
    AA=8.*DAM*DAM*(1.+RR)*RR*SQRT(RR)
    BB=(1.-RR*RR)**2
    CC=4.*DAM*DAM*RR*(1.+RR)*(1.+RR)
    CMC(J,JJ)=AA/(BB+CC)
438 CONTINUE
C WRITE(6,7777)
C7777 FORMAT(1X,'MODAL CROSS-CORRELATION COEFFICIENTS:')
C CALL PRIN(CMC,MM,MM,30,30)
C
C----- CALCULATE 3-DIMENSIONAL STRUCTURE RESPONSES -----
C
    DO 426 L=1,N
    SUM=0.
    DO 428 J=1,MM
    DO 428 JJ=1,MM
428 SUM=SUM+PP(L,J)*CMC(J,JJ)*PP(L,JJ)
    SUM=ABS(SUM)
    XMAX(L)=SQRT(SUM)
426 CONTINUE
    WRITE(6,442)ANGG,(XMAX(L),L=1,N)
442 FORMAT(1X,'ANGLE= ',F10.3,5F15.6)
    GO TO 1212
1213 STOP
    END

SUBROUTINE PRIN(A, NS, MS, NSS, MSS)
DIMENSION A(NSS, MSS)
DO 1 I=1,NS
    WRITE(6,2) (A(I,J), J=1, MS)
2 FORMAT (1X, 10F12.4)
1 CONTINUE
    WRITE(6,777)
777 FORMAT(5X, '-----')
    RETURN
    END

C
C * A TRANSPOSE
C
SUBROUTINE TRANP (C1, C3, M, N, MM, NN)
DIMENSION C1(MM, NN), C3(MM, NN)
DO 1000 I=1, M
    DO 1000 J=1, N
    C3(J,I)=C1(I,J)
1000 CONTINUE
    RETURN
    END

C
C *SUBROUTINE MULTIP A*B
C

```

```

SUBROUTINE MULTIP(C1, C2, C3, L, M, N, MM, NN)
DIMENSION C1(MM,NN), C2(MM,NN), C3(MM,NN)
DO 10 I=1, L
   DO 10 J=1, N
      C3(I,J)=0.
   DO 10 K=1, M
10 C3(I,J)=C3(I,J)+ C1(I,K)*C2(K,J)
      RETURN
   END

```

Input Data:

```

0.07 |DAMPING
259375 0 0 0 2250 0 0 0 2250 |MASS
-0.0222 0 0.5730 1.0 -0.6842 1.0 0.6842 1.0 0.6842 |MODE MATRIX
1.5411 1.3688 1.5323 1.3844 1.2652 1.3925 | SPECTRA DATA
0.264 0.2738 0.4594 | NATURAL FREQUENCIES
0 0 1 0 0 1 | INFLUNCE COEFF. VECTOR

```

Output Data:

THE CONVENTIONAL CQC METHOD
=====

THE DAMPING RATIO= 0.0700

THE MASS MATRIX:

```

259375.0000 0.0000 0.0000
0.0000 2250.0000 0.0000
0.0000 0.0000 2250.0000
-----
```

THE NORMAL MODE MATRIX:

```

-0.0222 0.0000 0.5730
1.0000 -0.6842 1.0000
0.6842 1.0000 0.6842
-----
```

THE RESPONSE SPECTRA TABLES:

```

1.5411 1.3688
1.5323 1.3844
1.2652 1.3925
-----
```

THE NATURAL FREQUENCIES:

```

0.26400 0.27380 0.45940
-----
```

THE INFLUENCE COEFF. VECTOR IN REFERENCE DIRECTIONS:

```

0.0000 0.0000
1.0000 0.0000
0.0000 1.0000
-----
```

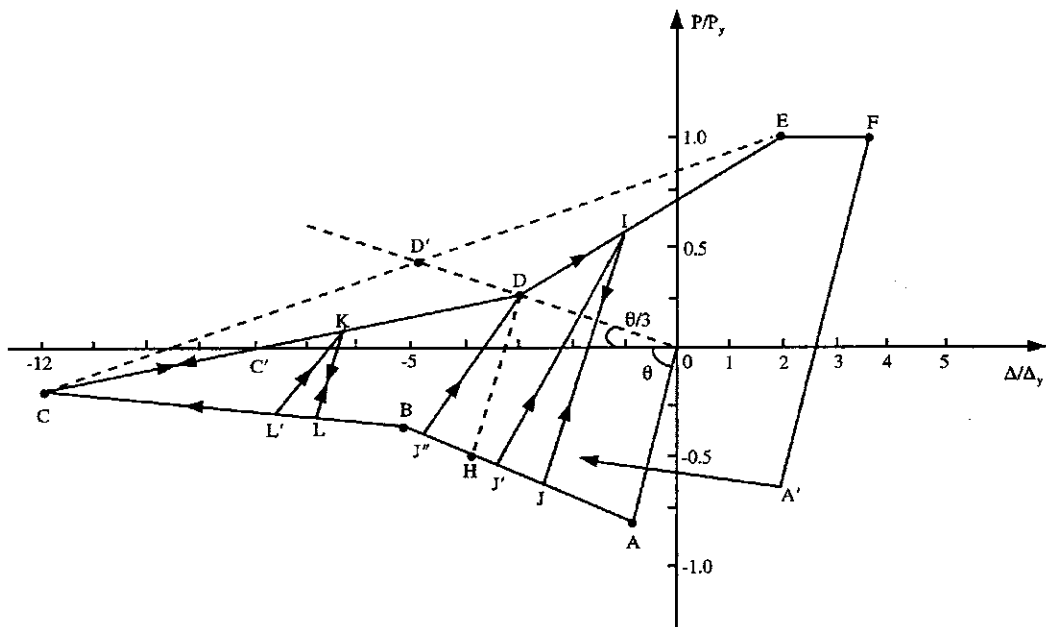
THE TOTAL RESPONSES:

```

ANGLE= 0.000 0.047056 1.483318 1.331185
ANGLE= 1.000 0.046904 1.460894 1.356712
ANGLE= 2.000 0.046738 1.438069 1.381880
.
.
.
ANGLE= 359.000 0.047193 1.505332 1.305312
ANGLE= 360.000 0.047056 1.483318 1.331185

```

Appendix J—Jain-Goel-Hanson Steel-Bracing Hysteresis Model and Computer Program



```

C =====
C THIS IS A TYPICAL MAIN PROGRAM FOR CALL JAIN-GOEL-HANSON
C HYSTERESIS MODEL SUBROUTINE NAMED "MAT08". THE PARAMETERS
C TRANSFERRED INTO SUBROUTINE MAT08 ARE SHOWN AS FOLLOWS.
C SINCE MAT08 IS A GENERAL PURPOSE SUBROUTINE, SOME PARAMETERS
C HAVE BEEN RESERVED AND NOT USED. THEREFORE THEY ARE ASSIGNED
C WITH A NUMBER "1" IN THIS DEMONSTRATION AS A MAIN PROGRAM.
C=====
C VARIABLES:
C MAT = USER DEFINED MATERIAL ID NUMBER
C IELNO = USER DEFINED ELEMENT ID NUMBER
C LENGTH= BRACE ELEMENT LENGTH, STORED IN SE(5)
C SLK = EFFECTIVE LENGTH FACTOR OF ELEMENT STORED IN SE(2)
C P = CURRENT AXIAL LOAD
C PL = PREVIOUS STEP AXIAL LOAD
C D = CURRENT AXIAL DISPLACEMENT
C DL = PREVIOUS STEP AXIAL DISPLACEMENT
C V = DUMMY VARIABLE
C VL = DUMMY VARIABLE
C DUCT = RESERVED DUCTILITY ARRAY (NOT USED)
C EXCR = RESERVED EXCURSION ARRAY (NOT USED)
C LELEM = 39
C LMAT = 9
C SMAT = MATERIAL ARRAY, SMAT(LMAT)

```

```

C SE = ELEMENT ARRAY, SE(LELEM)
C IOPT = 1 INITIALIZE MATERIAL
C      2 GET BRACING MEMBER INITIAL STIFFNESS
C      3 GET BRACING MEMBER STIFFNESS
C ERR = DUMMY LOGICAL VARIABLE
C FIRST = LOGICAL VARIABLE. If FIRST=.TRUE., THE MATERIAL
C      PROPERTIES OF BRACING MEMBER ARE PRINTED.
C PRINT = DUMMY LOGICAL VARIABLE
C BUG = LOGICAL VARIABLE. If BUG=.TRUE., THE HYSTERESIS
C      ENVELOPE CONTROL POINTS ARE PRINTED.
C DAMAGE= RESERVED VARIABLE FOR DAMAGE INDEX (NOT USED)
C EESE = RESERVED VARIABLE FOR ELASTIC STRAIN ENERGY(NOT USED)
C EPSE = RESERVED VARIABLE FOR PLASTIC STRAIN ENERGY(NOT USED)
C =====
C      LOGICAL ERR, FIRST, PRINT, BUG
C      DIMENSION SE(100), SMAT(9), DUCT(3), EXCR(6)
C      CHARACTER*80 TYPE
C
C =====
C DEFINE EXTERNAL FILE UNITS FOR INPUT DATA AND OUTPUT
C =====
C      OPEN(UNIT=5,FILE=STRING(8))
C      OPEN(UNIT=6,FILE=STRING(9))
C
C =====
C
C      IOPT=1
C      ERR=.FALSE.
C      FIRST=.TRUE.
C      PRINT = .FALSE.
C      BUG=.FALSE.
C      READ(5,*)IELNO, MAT, ELENGH, SLK
C      SE(5)=ELENGH
C      SE(2)=SLK
C
C INPUT MATERIAL PROPERTIES
C      CALL MAT08
& (IOPT ,IELNO ,ERR ,FIRST ,PRINT ,BUG ,
& MAT ,SE ,P,PL,D,DL,V,VL,LELEM,LMAT,
& SMAT,DUMMY,DUMMY,DUCT,EXCR,DUMMY)
C
C INITIALIZE ELEMENT STIFFNESS
C      IOPT=2
C      BUG=.TRUE.
C      CALL MAT08
& (IOPT ,IELNO ,ERR ,FIRST ,PRINT ,BUG ,
& MAT ,SE ,P,PL,D,DL,V,VL,LELEM,LMAT,
& SMAT,DUMMY,DUMMY,DUCT,EXCR,DUMMY)
C      STIF=SE(1)
C      BUG=.FALSE.
C
C      WRITE(6,*)' STIFFNESS LOAD DISP. RULE'
C READ AXIAL DISPLACEMENT
C      DMAX=-0.5
C      F=0.
C      FL=0.
C      D=0.
C      DL=0.
C
C      800  READ(5,* , END=5000)DMIN, DMAX, NUMB
C          DD=(DMAX-DMIN)/NUMB
C      700  DL=D
C          D=D+DD
C          FL=F
C          F=F+STIF*DD
C          P=F
C          PL=FL

```

```

IOPT=3
CALL MAT08
& (IOPT ,IELNO ,ERR ,FIRST ,PRINT ,BUG ,
& MAT ,SE ,P,PL,D,DL,V,VL,LELEM,LMAT,
& SMAT,DUMMY,DUMMY,DUCT,EXCR,DUMMY)
F=P
STIF=SE(1)
WRITE(6,98)SE(1), F, D, SE(4)
98 FORMAT(3F15.5, 3X, F4.1)
IF (DMAX .GT. 0) THEN
  IF (D .LE. DMAX) THEN
    GO TO 700
  ELSE IF (D .GT. DMAX) THEN
    D=DMAX
    GO TO 800
  ENDIF
ELSE IF (DMAX .LE. 0) THEN
  IF (D .GE. DMAX) THEN
    GO TO 700
  ELSE IF (D .LT. DMAX) THEN
    D=DMAX
    GO TO 800
  ENDIF
ENDIF
C
5000 CLOSE(5)
CLOSE(6)
STOP
END
C
C =====
C     DEBUG UNIT(6),TRACE,SUBCHK,INIT,SUBTRACE
C     END DEBUG
C =====
SUBROUTINE MAT08
& (IOPT ,IELNO ,ERR ,FIRST ,PRINT ,BUG ,
& MAT ,SE ,P,PL,D,DL,V,VL,LELEM,LMAT,
& SMAT,ESE,EPSE,DUCT,EXCR,DAMAGE)
C
IMPLICIT REAL(A-H,O-Z)
LOGICAL ERR,FIRST,PRINT,BUG
LOGICAL BTTEST
DIMENSION SE(100),SMAT(9),DUCT(3),EXCR(6)
CHARACTER*80 TYPE
C
C ---- RESERVE STORAGE FOR ELEMENT
LELEM=39
IF (IOPT.EQ.0) RETURN
C
C -----
C VARIABLES:
C -----
C ----- GLOBAL VARIABLES
C IOPT = 1, INITIALIZE MATERIAL
C      = 2, GET STIFFNESS
C RINPUT = INPUT DATA
C SMAT = INTERNAL STORAGE
C SE = OUTPUT STIFFNESS
C -----
GO TO (100,200,300,400,500),IOPT
C
100 CONTINUE
C
C ----- INTERPRET INPUT DATA
C E = SMAT( 1) ELASTIC MODULUS OF MEMBER
C A = SMAT( 2) CROSS SECTION AREA OF MEMBER
C R = SMAT( 3) RADIUS OF GYRATION

```

```

C YS = SMAT( 4) YIELD STRESS OF MEMBER
C PY = SMAT( 5) YIELD AXIAL LOAD OF MEMBER
C CC = SMAT( 6) SQRT(2*PI*PI*E/FY). PI=3.14159
C DMAX = SMAT( 7) : ULTIMATE DISPLACEMENT = DUCMAX*DELY
C BDAM = SMAT( 8) : BATA PARAMETER
C SHAPE = SMAT( 9) : CROSS SECTION SHAPE
C      1: FOR BOX OR ANGLE SECTION
C      2: FOR I SHAPE SECTION
C      3: FOR BOX SECTION CONSIDERING
C          LOCAL BUCKLING. THIS IS ONLY FOR MEMBER
C          WITH KL/R LESS THAN 40 CASE
C =====
C
C     READ (5,*) TYPE ,(SMAT(I),I=1,4), SHAPE,DUCMAX, BDAM
C
C     LMAT = 9
C     PI=3.1415926
C     SMAT(5)=SMAT(2)*SMAT(4)
C     SMAT(6)=SQRT(2.*PI*PI*SMAT(1)/SMAT(4) )
C     SMAT(7)=DUCMAX
C     SMAT(8)=BDAM
C     SMAT(9)=SHAPE
C
C     IF (FIRST .OR. BUG) WRITE (6,191)
C     WRITE (6,192) MAT,(SMAT(K),K=1,4),SHAPE,DUCMAX, BDAM
C
C191 FORMAT (///' JAIN-GOEL-HANSON HYSTERESIS MODEL PARAMETERS'/
C & ' ======'//'
C & ' MAT.',3X,' E',6X,' A',6X,' R',6X,' YS',
C & 6X,' SHAPE',6X, 'MAX DUC', 6X,' BETA')
C192 FORMAT (1X,I5,7G12.6/)
C
C     RETURN
C
C===== INITIALIZE STIFFNESS TERMS =====
C200 CONTINUE
C ---- JAIN-GOEL-HANSON HYSTERESIS MODEL DATA STORAGE FOR MEMBER ----
C SE( 1)= STIFMEMBER AXIAL STIFFNESS
C SE( 2)= K EFFECT SLENDER COEFFICIENT (TRANSFERED FROM ELE08)
C SE( 3)= NOCY NO. OF CYCLE
C SE( 4)= NRULE RULE NUMBER
C SE( 5)= EL MEMBER LENGTH (TRANSFERED FROM ELE08)
C SE( 6)= IRV 0:REVRSC=.FALSE. 1:REVRSC=.TRUE.
C SE( 7)= IDUC 0: HC=-12 1: HC .LT. -12
C SE( 8)= PBOT
C SE( 9)= DBOT
C SE(10)= PTOP
C SE(11)= DTOP
C SE(12)= KEQ UNLOADING EQUIVALENT STIFFNESS
C SE(13)= DUCT(1)
C SE(14)= DUCT(2)
C SE(15)= DUCT(3)
C SE(16)= EXCR(1)
C SE(17)= EXCR(2)
C SE(18)= EXCR(3)
C SE(19)= EXCR(4)
C SE(20)= EXCR(5)
C SE(21)= EXCR(6)
C SE(22)= DELY YIELDING DISPLACEMENT
C SE(23)= EESE(1)
C SE(24)= EESE(2)
C SE(25)= EESE(2)
C SE(26)= EPSE
C SE(27)= PSEOLD
C SE(28)= CSE
C SE(29)= DMAX ULTIMATE DISPLACEMENT
C SE(30)= D_MAX MAXIMUM ELEMENT DISPLACEMENT FOR DAMAGE INDEX

```

```

C SE(31)= P_MAX ELEMENT LOAD CORRESPONDING TO D_MAX
C SE(32)= HA CURRENT CONTROL POINT HA
C SE(33)= VA CURRENT CONTROL POINT VA
C SE(34)= HC CURRENT CONTROL POINT HC
C SE(35)= VC CURRENT CONTROL POINT VC

C SE(36)= RSN CURRENT RESIDUAL STRAIN VALUE
C SE(37)= DEMAX CURRENT MAXIMUM AXIAL DISPLACEMENT FOR DUCTILITIES
C SE(38)= REGIN CURRENT REGINE ZONE NUMBER
C SE(39)= PREGIN PREVIOUS REGIN ZONE NUMBER
C =====
SE(1)=1
SE(3)=1
SE(4)=1
DO 210 I=6,28
210 SE(I)=0
  SE(37)=0
  SE(38)=1
  SE(39)=1
C
CALL HYST08(0.,0.,0.,0.,V,VL,SE(5),SE(2),
& SMAT(1),SMAT(2),SMAT(3),SMAT(4),SMAT(5),SMAT(9),
& SMAT(6),SE(3),SE(4),SE(1),SE(6),SE(7),
& SE(32),SE(33),SE(34),SE(35),SE(36),SE(37),SE(38),SE(39),
& SE(8),SE(9),SE(10),SE(11),BUG,
& SE(12),SE(13),SE(16),SE(22),SE(23),SE(26),SE(27),SE(28) )
SE(28)=SE(22)*SMAT(5)/2
SE(29)=SE(22)*SMAT(7)
SE(30)=0
SE(31)=0
C
  RETURN
C ===== GET STIFFNESS TERMS =====
300 CONTINUE
C
C----- CALL HYST08 TO CALC NEW STIFFNESS STIF
CALL HYST08(P,PL,D,DL,V,VL,SE(5),SE(2),
& SMAT(1),SMAT(2),SMAT(3),SMAT(4),SMAT(5),SMAT(9),
& SMAT(6),SE(3),SE(4),SE(1),SE(6),SE(7),
& SE(32),SE(33),SE(34),SE(35),SE(36),SE(37),SE(38),SE(39),
& SE(8),SE(9),SE(10),SE(11),BUG,
& SE(12),SE(13),SE(16),SE(22),SE(23),SE(26),SE(27),SE(28) )
C
C --- STORE MAXIMUM DISPLACEMENT AND CORRESPONDING LOAD
IF(ABS(D) .GT. ABS(SE(30))) THEN
  SE(30)=D
  SE(31)=P
ENDIF
C
C === GET ENERGIES, DUCTILITY AND EXCURSION FOR BOTH IOPT=3 AND 4 ===
400 CONTINUE
C
C --- TRANSFER ENERGIES FOR BOTH IOPT=3 AND 4.
EESE=SE(23)
EPSE=SE(26)
C
C --- TRANSFER DUCTILITIES AND EXCURSION RATIOS FOR BOTH IOPT=3 AND 4.
DO 410 I=1,3
  DUCT(I)=SE(12+I)
  EXCR(I+3)=SE(15+I+3)
410 EXCR(I)=SE(15+I)
C
  RETURN
C ===== DAMAGE INDEX =====
500 CONTINUE
EESE=SE(23)
EPSE=SE(26)

```

```

DMAX=SE(29)
D=SE(30)
P=SE(31)
PY=SMAT(5)
BDAM=SMAT(8)
DAMGE=ABS(D)/DMAZ + BDAM / (PY*DMAZ) * EPSE
C
RETURN
END

C
C***** HYST08 *****
C      DEBUG UNIT(6),TRACE,SUBCHK,INIT,SUBTRACE
C      END DEBUG
C
C JAIN-GOEL-HANSON TRUSS HYSTERESIS MODEL FOR ANGLE AND BOX SECTION
C
SUBROUTINE HYST08(P,PLA,DE,DELA,V,VLA,EL,SLK,
& EM,AREA,RADG,YS,PY, SHAPE,
& CC,CYCLE,RULE,STIF,IRV,IDUC,
& HA,VA,HC,VC,RSN,DEMAX,REGIN,PREGIN,
& PBOT,DBOT,PTOP,DTOP,PRINT,
& EKI,DUC,EXCR,DELY,ESE,PSE,PSEOLD,CSE)
COMMON/IDSTEP/ISEP
DIMENSION DUC(3), EXCR(6), ESE(3)
LOGICAL REVRSC,PRINT
REAL*4 IRV, IDUC
IF( IRV .EQ. 0.) REVRSC=.FALSE.
IF( IRV .EQ. 1.) REVRSC=.TRUE.
PI=3.1415926
ES=AREA*EM/EL
DELY=PY/ES
DEL=DE/DELY
PL=P/PY
ESR=SLK*EL/RADG
SLOP7=STIF/ES
DA=ABS(DE)
C
DP=P-PLA
DDE=DE-DELA
DDEL=DDE/DELY
C ===== CALCULATE EXCURSION RATE AT EVERY ZERO CROSSING =====
C
IF( P*PLA .LE. 0 ) THEN
C   CALL DNE(0, DUC,EXCR,DELY, DA,ESE(1),PSE,PSEOLD,CSE)
ENDIF
C
C=====
C DUC ---- ELEMENT DUCTILITY RATE
C EXCR ---- ELEMENT EXCURSION RATE
C DELY ---- ELEMENT YIELDING DISPLACEMENT
C ESE ---- ELEMENT ELASTIC STRAIN ENERGY
C PSE ---- ELEMENT PLASTIC STRAIN ENERGY
C PSEOLD ---- ELEMENT PLASTIC STRAIN ENERGY AT LAST ZERO CROSSING
C CSE ---- ELEMENT CONSTANT STRAIN ENERGY
C
C DP ---- ELEMENT AXIAL LOAD INCREMENT (KIPS)
C ESR ---- EFFECTIVE SLENDER RATIO (KL/R)
C YS ---- YIELDING STRESS
C AREA ---- CROSS SECTION AREA (A)
C EM ---- ELASTIC MODULUS (E)
C DP ---- ELEMENT AXIAL LOAD INCREMENT (KIPS)
C P ---- CURRENT AXIAL LOAD (KIPS)
C PL ---- P - PY RATIO (P/PY)
C PLA ---- LAST AXIAL LOAD
C DDEL ---- DISPLACEMENT INCREMENT (IN)

```

```

C DE ---- CURRENT AXIAL DISPLACEMENT (IN)
C DEMAX ---- MAXIMUM AXIAL DISPLACEMENT (IN)
C DA ---- CURRENT ABSOLUTE AXIAL DISPLACEMENT (IN)
C DELA ---- LAST AXIAL DISPLACEMENT
C DDE ---- ELEMENT DISPLACEMENT INCREMENT
C DEL ---- DEL=DE/DELY
C DELY ---- YIELDING DISPLACEMENT
C V ---- CURRENT VELOCITY
C VLA ---- LAST VELOCITY
C ES ---- ELEMENT ELASTIC STIFFNESS
C EKI ---- UNLOADING EQUIVALENT STIFFNESS FOR CALCULATING ESE
C PY ---- TENSION YIELDING LOAD
C EL ---- ELEMENT LENGTH (IN)
C CC ---- C SUB. C CONSTANT
C PMAX ---- BUCKING LOAD (KIPS)
C DELMAX ---- BUCKING DISPLACEMENT (IN)
C HA,HB,,,HC1,HD1,,,HF ---- P/PY - DE/DELY PLOT'S DE/DELY COORDINATE
C VA,VB,,,VC1,VD1,,,VF ---- P/PY - DE/DELY PLOT'S P/PY COORDINATE
C RSN ---- RESIDUAL STRAIN
C RULE ---- RULE NUMBER
C CYCLE ---- NO. OF CYCLE
C STIF ---- ELEMENT STIFFNESS
C REVRSC ---- LOGICAL INDEX FOR REVERSING CURVE OCCURRED
C IDUC ---- 1: HC LESS THAN 12, 0:HC=12
C REGIN ---- REGIN 1: DE GREATER OR EQUAL TO HA
C      2: DE = (HH, HA)
C      3: DE = (HB, HH)
C      4: DE = (HC, HB)
C PREGIN ---- PREVIOUS STEP REGIN ID NUMBER
C SHAPE ---- 1: FOR BOX OR ANGLE SECTION
C      2: FOR I SHAPE SECTION
C      3: FOR BOX SECTION CONSIDERING LOCAL BUCKLING
C      NOTE: THIS IS ONLY FOR KL/R LESS THAN 40
C=====
C
C INITIAL BUCKLING LOAD
C
C IF( ESR .LT. CC .AND. CYCLE .EQ. 1 ) THEN
C   PMAX=(1.-(ESR**2/(2.*CC**2)))*YS*AREA
C ELSE IF( ESR .GE. CC .AND. CYCLE .EQ. 1 ) THEN
C   PMAX=-PI*PI*AREA*EM/(ESR**2)
C ENDIF
C
C RESIDUAL ELOGATION FACTOR RFAC
C
C   /** FOR BOX AND ANGLE SECTION **/
C IF(SHAPE .EQ. 1) THEN
C   RFAC=1.75
C ELSE IF(SHAPE .EQ. 3) THEN
C   RFAC=0
C   /** FOR I SHAPE SECTION **/
C ELSE IF(SHAPE .EQ. 2) THEN
C   RFAC=1.4
C ENDIF
C
C GENERATE CONTROL POINTS COORDINATE
C
C (1) POINT A
C
C IF( SHAPE .NE. 3 ) THEN
C   IF( CYCLE .EQ. 1 ) THEN
C     VA=PMAX/PY
C     HA=PMAX/(ES*DELY)
C   ELSE IF( CYCLE .EQ. 2 ) THEN
C     IF( ESR .LE. 40 ) THEN
C       PMAX=-(23.4/ESR)*PY
C     ELSE IF( ESR .GT. 40 ) THEN

```

```

PMAX=-(30./ESR)*PY
ENDIF
ELSE IF( CYCLE .GT. 2) THEN
  IF( ESR .LE. 40 ) THEN
    PMAX=-(18.5/ESR)*PY
  ELSE IF( ESR .GT. 40 ) THEN
    PMAX=-(25./ESR)*PY
  ENDIF
ENDIF
ELSE IF( SHAPE .EQ. 3 ) THEN
  IF( CYCLE .EQ. 1) THEN
    VA=PMAX/PY
    HA=PMAX/(ES*DELY)
  ELSE IF( CYCLE .EQ. 2) THEN
    PMAX=PMAX
  ELSE IF( CYCLE .EQ. 3) THEN
    PMAX=-(23.4/ESR)*PY
  ELSE IF( CYCLE .GT. 3) THEN
    PMAX=-(18.5/ESR)*PY
  ENDIF
ENDIF
C
C (2) POINT B
C
HB=-5.
IF( ESR .LE. 40 ) THEN
  VB=-17./ESR
ELSE IF( ESR .GT. 40 ) THEN
  C      /** FOR BOX AND ANGLE SECTION **/
  IF( SHAPE .EQ. 1 .OR. SHAPE .EQ. 3 ) THEN
    VB=-18./ESR
  C      /** FOR I SHAPE SECTION **/
  ELSE IF( SHAPE .EQ. 2 ) THEN
    VB=-11.3/ESR
  ENDIF
ENDIF
C
C (3) POINT C
C
IF( IDUC .EQ. 0.) THEN
  HC=-12.
  IF( ESR .LE. 40 ) THEN
    VC=-15./ESR
  ELSE IF( ESR .GT. 40 ) THEN
  C      /** FOR BOX AND ANGLE SECTION **/
  IF( SHAPE .EQ. 1 .OR. SHAPE .EQ. 3 ) THEN
    VC=-12./ESR
  C      /** FOR I SHAPE SECTION **/
  ELSE IF( SHAPE .EQ. 2 ) THEN
    VC=-8.5/ESR
  ENDIF
ENDIF
ENDIF
C
C (4) POINT E
C
HE=1.+(RSN*EL/DELY)
VE=1.
C
C (5) POINT D1
C
SLOPE=(VE-VC)/(HE-HC)
HD1=(SLOPE*HC-VC)/(SLOPE+0.267949)
VD1=-0.267949*HD1
C
C (6) POINT D
C

```

```

IF( ESR .LE. 40 ) THEN
  HD=HD1*31./ESR
  VD=VD1*31./ESR
ELSE IF( ESR .GT. 40 ) THEN
C      /** FOR BOX AND ANGLE SECTION */
  IF( SHAPE .EQ. 1 .OR. SHAPE .EQ. 3 ) THEN
    HD=HD1*60./ESR
    VD=VD1*60./ESR
C      /** FOR I SHAPE SECTION */
  ELSE IF( SHAPE .EQ. 2 ) THEN
    HD=HD1*20./ESR
    VD=VD1*20./ESR
  ENDIF
  ENDIF
C
C DEFINE ENVELOPE SLOPE
C
SLOP1=1.
SLOP2=(VB-VA)/(HB-HA)
SLOP3=(VC-VB)/(HC-HB)
SLOP4=(VD-VC)/(HD-HC)
SLOP5=(VE-VD)/(HE-HD)
SLOP6=0.0001
C
C DEFINE ENVELOPE INTERMIDIATE POINTS
C
C (1) POINT H
C
VH=(VB+SLOP2*(-VD+HD-HB))/(1.-SLOP2)
HH=VH-VD+HD
C
C (2) POINT C1
C
VC1=0.
HC1=HC-(VC/SLOP4)
C
C (3) POINT (PREF,DREF) : CALCULATE IN RULE NO. 4
C
C (4) POINT (HREF,VREF) : CALCULATE IN RULE NO. 5
C
C--- DEFINE CURRENT REGIN ZONE NUMBER
PREGIN=REGIN
IF( DEL .GE. HA) REGIN=1
IF( DEL .GE. HH .AND. DEL .LT. HA ) REGIN=2
IF( DEL .GE. HB .AND. DEL .LT. HH ) REGIN=3
IF( DEL .GE. HC .AND. DEL .LT. HB ) REGIN=4
C
IF (PRINT) THEN
  WRITE(6,567)CYCLE,RULE,HA,VA,HB,VB,HC,VC,HC1,VC1,
  & HD,VD,HD1,VD1,HH,VH,HE,VE
567 FORMAT(5X,'JAIN-GOEL-HANSON HYSTERESIS ENVELOPE CONTROL POINTS....'/
  & 5X,'=====--=-',F10.4,/
  & 5X,'CYCLE -----=-',F10.4,/
  & 5X,'RULE -----=-',F10.4,/
  & 5X,'(HA, VA) -----=-',1X,'( ',F10.4,' ',F10.4,' ')',/
  & 5X,'(HB, VB) -----=-',1X,'( ',F10.4,' ',F10.4,' ')',/
  & 5X,'(HC, VC) -----=-',1X,'( ',F10.4,' ',F10.4,' ')',/
  & 5X,'(HC1, VC1) -----=-',1X,'( ',F10.4,' ',F10.4,' ')',/
  & 5X,'(HD, VD) -----=-',1X,'( ',F10.4,' ',F10.4,' ')',/
  & 5X,'(HD1, VD1) -----=-',1X,'( ',F10.4,' ',F10.4,' ')',/
  & 5X,'(HH, VH) -----=-',1X,'( ',F10.4,' ',F10.4,' ')',/
  & 5X,'(HE, VE) -----=-',1X,'( ',F10.4,' ',F10.4,' ')',/
ENDIF
C
C JAIN-GOEL-HANSON'S HYSTORESIS LOOP RULES

```

```

C
C (1) RULE 1
C
IF( RULE .EQ. 1.) THEN
  IF( P. GE. PMAX .AND. P .LT. PY ) THEN
    STIF=SLOP1*ES
    EKI=SLOP1*ES
    IF( DEMAX .LT. 0 .AND. DE .LE. DEMAX ) THEN
      RSN=((0.55*ABS(DE)/ESR)+0.0002*ABS(DE)**2)*RFAC
    ENDIF
  ELSE IF( P. GE. PY ) THEN
    STIF=SLOP6
    RULE=6
    RSN=0
    EKI=SLOP1*ES
  ELSE IF( P. LT. PMAX) THEN
    C      HA=DEL
    C      VA=PL
    C      SLOP2=(VB-VA)/(HB-HA)
    C      STIF=SLOP2*ES
    C
    D1=DE-HA*DELY
    SLOP2=(VB-VA)/(HB-HA)
    STIF=SLOP2*ES
    P=PMAX+(STIF*D1)
    PL=P/PY
    C
    RULE=2
    IF( DEMAX .LT. 0 .AND. DE .LE. DEMAX ) THEN
      RSN=((0.55*ABS(DE)/ESR)+0.0002*ABS(DE)**2)*RFAC
    ENDIF
    EKI=SLOP1*ES
  ENDIF
  CALL STRENG(ESE,PSE,PSEOLD,P,PLA,DE,DELA,STIF,EKI)
  CALL DNE(1,DUC,EXCR,DELY, DA, ESE(1), PSE, PSEOLD, CSE )
  RETURN
ENDIF
C
C (2) RULE 2
C
IF( RULE .EQ. 2.) THEN
  IF( DEL .GE. HH) THEN
    IF( DDE .LE. 0. ) THEN
      IF(PREGIN .NE. REGIN ) REVRSC= .FALSE.
      STIF=SLOP2*ES
    IF( DEMAX .LT. 0 .AND. DE .LE. DEMAX ) THEN
      RSN=((0.55*ABS(DE)/ESR)+0.0002*ABS(DE)**2)*RFAC
    ELSE IF( DEMAX .GT. 0 ) THEN
      RSN=((0.55*ABS(DE)/ESR)+0.0002*ABS(DE)**2)*RFAC
    ENDIF
    =====
    IF(.NOT. REVRSC )THEN
      EKI=SLOP1*ES
    ELSE IF( REVRSC )THEN
      EKI=ES*((PTOP-PL)/(DTOP-DEL))
    ENDIF
    =====
    ELSE IF( DDE .GT. 0. )THEN
      IF(.NOT. REVRSC )THEN
        RULE=7
        STIF=SLOP1*ES
      C
      PLA=PL-SLOP2*DDEL
      DLA=DEL-DDEL
      DBOT=DLA
      PBOT=PLA
      PL=PLA+SLOP1*DDEL
    ENDIF
  ENDIF
ENDIF

```

```

P=PL*PY
C
      PTOP=VE+(SLOP5*(PBOT-VE-SLOP1*DBOT
*           +SLOP1*HE)/(SLOP5-SLOP1))
      DTOP=(PBOT-VE+SLOP5*HE-SLOP1*DBOT)
*           /(SLOP5-SLOP1)
      EKI=ES*SLOP1
      ELSE IF( REVRSC ) THEN
          RULE=12
          DBOT=DEL
          PBOT=P/PY
          SLOP7=(PTOP-PBOT)/(DTOP-DBOT)
          STIF=SLOP7*ES
          EKI=ES*SLOP7
      ENDIF
      ENDIF
      ELSE IF(DEL .LT. HH .AND. DEL .GE. HB ) THEN
          IF( DDE .LE. O. ) THEN
              IF(PREGIN .NE. REGIN ) REVRSC=.FALSE.
              STIF=SLOP2*ES
              IF( DEMAX .LT. O .AND. DE .LE. DEMAX ) THEN
                  RSN=((0.55*ABS(DE)/ESR)+0.0002*ABS(DE)**2)*RFAC
              ELSE IF( DEMAX .GT. O ) THEN
                  RSN=((0.55*ABS(DE)/ESR)+0.0002*ABS(DE)**2)*RFAC
              ENDIF
C
              =====
              IF(.NOT. REVRSC )THEN
                  EKI=SLOP1*ES
              ELSE IF( REVRSC )THEN
                  EKI=ES*((PTOP-PL)/(DTOP-DEL))
              ENDIF
C
              =====
              ELSE IF( DDE .GT. O.)THEN
                  IF( .NOT. REVRSC ) THEN
                      RULE=8
                      STIF=SLOP1*ES
C
                      PLA=PL-SLOP2*DDEL
                      DLA=DEL-DDEL
                      DBOT=DLA
                      PBOT=PLA
                      PL=PLA+SLOP1*DDEL
                      P=PL*PY
C
                      PTOP=VD+(SLOP4*(PBOT-VD-SLOP1*DBOT
*                         +SLOP1*HD)/(SLOP4-SLOP1))
                      DTOP=(PBOT-VD+SLOP4*HD-SLOP1*DBOT)
*                         /(SLOP4-SLOP1)
                      EKI=ES*SLOP1
                      ELSE IF( REVRSC ) THEN
                          RULE=11
                          DBOT=DEL
                          PBOT=P/PY
                          PTOP=VD
                          DTOP=HD
                          SLOP7=(PTOP-PBOT)/(DTOP-DBOT)
                          STIF=SLOP7*ES
                          EKI=ES*SLOP7
                      ENDIF
                      ENDIF
                      ELSE IF( DEL .LT. HB) THEN
                          IF(PREGIN .NE. REGIN ) REVRSC=.FALSE.
                          RULE=3
                          EKI=ES*SLOP1
                      ENDIF
                      IF( REVRSC ) IRV=1.
                      IF( .NOT. REVRSC) IRV=0.

```

```

C CALL STRENG(ESE,PSE,PSEOLD,P,PLA,DE,DELA,STIF,EKI)
  IF( ABS(DEMAX) .LT. ABS(DE) ) THEN
    CALL DNE(1,DUC,EXCR,DELY, DA, ESE(1), PSE, PSEOLD, CSE )
    DEMAX=DE
  ENDIF
  RETURN
  ENDIF
C
C (3) RULE 3
C
  IF( RULE .EQ. 3.) THEN
    IF( DEL .GT. HC ) THEN
      IF( DDE .LE. 0. ) THEN
        IF(PREGIN .NE. REGIN ) REVRSC= .FALSE.
        STIF=SLOP3*ES
      IF( DEMAX .LT. 0 .AND. DE .LE. DEMAX ) THEN
        RSN=((0.55*ABS(DE)/ESR)+0.0002*ABS(DE)**2)*RFAC
      ELSE IF( DEMAX .GT. 0 ) THEN
        RSN=((0.55*ABS(DE)/ESR)+0.0002*ABS(DE)**2)*RFAC
      ENDIF
    C =====
      IF(.NOT. REVRSC )THEN
        EKI=SLOP1*ES
      ELSE IF( REVRSC )THEN
        EKI=ES*((PTOP-PL)/(DTOP-DEL))
      ENDIF
    C =====
      ELSE IF( DDE .GT. 0. )THEN
        IF( DEL .GT. -12. ) THEN
          IF( .NOT. REVRSC )THEN
            RULE=9
            STIF=SLOP1*ES
          C
            PLA=PL-SLOP2*DDEL
            DLA=DEL-DDEL
            DBOT=DLA
            PBOT=PLA
            PL=PLA+SLOP1*DDEL
            P=PL*PY
          C
            PTOP=VD+(SLOP4*(PBOT-VD-SLOP1*DBOT
*           +SLOP1*HD)/(SLOP4-SLOP1))
            DTOP=(PBOT-VD+SLOP4*HD-SLOP1*DBOT)
*           /(SLOP4-SLOP1)
            EKI=ES*SLOP1
          ELSE IF( REVRSC ) THEN
            RULE=10
            DBOT=DEL
            PBOT=P/PY
            SLOP7=(PTOP-PBOT)/(DTOP-DBOT)
            STIF=SLOP7*ES
            EKI=ES*SLOP7
          ENDIF
        ELSE IF ( DEL .LE. -12. ) THEN
          REVRSC= .FALSE.
          RULE=4
          STIF=SLOP4*ES
          EKI=ES*SLOP4
        ENDIF
      ENDIF
    ELSE IF( DEL .LE. HC ) THEN
      IF( DDE .LT. 0 ) THEN
        RULE=3
        HC=DEL
        VC=PL
        IDUC=1.
        STIF=-SLOP6*ES
      ENDIF
    ENDIF
  ENDIF

```

```

EKI=ES*((VD-VC)/(HD-HC))
  IF( DEMAX .LT. 0 .AND. DE .LE. DEMAX ) THEN
    RSN=((0.55*ABS(DE)/ESR)+0.0002*ABS(DE)**2)*RFAC
  ELSE IF( DEMAX .GT. 0 ) THEN
    RSN=((0.55*ABS(DE)/ESR)+0.0002*ABS(DE)**2)*RFAC
  ENDIF
  ELSE IF( DDE .GT. 0 ) THEN
    RULE=4
    STIF=SLOP4*ES
    EKI=ES*SLOP4
  ENDIF
  ENDIF
  IF( REVRSC ) IRV=1.
  IF ( .NOT. REVRSC) IRV=0.
C CALL STRENG(ESE,PSE,PSEOLD,P,PLA,DE,DELA,STIF,EKI)
  IF( ABS(DEMAX) .LT. ABS(DE) ) THEN
C     CALL DNE(1,DUC,EXCR,DELY, DA, ESE(1), PSE, PSEOLD, CSE )
    DEMAX=DE
  ENDIF
  RETURN
  ENDIF
C
C (4) RULE 7
C
  IF( RULE .EQ. 7.) THEN
    IF( DEL .GT. DBOT .AND. DEL .LT. DTOP .AND. P .GT. PMAX) THEN
      STIF=SLOP1*ES
      EKI=ES*SLOP1
    ELSE IF(DEL .LT. DBOT .OR. P .LE. PMAX) THEN
      IF( P .LE. PMAX ) THEN
        REVRSC=.FALSE.
        PTOP=0
        DTOP=0
        PBOT=PL
        DBOT=DEL
        S1=PLA/PY
        S2=PMAX/PY
        HA=(DELA/DELY) + ((S2-S1)/(SLOP1))
        VA=S2
        SLOP2=(VB-VA)/(HB-HA)
      ENDIF
      STIF=SLOP2*ES
      RULE=2
    C
      PL=VA+ SLOP2*(DBOT-HA)
      P=PL*PY
    C
      EKI=ES*((PTOP-PL)/(DTOP-DEL))
    ELSE IF(DEL .GT. DTOP .AND. PL .LT. VE) THEN
      STIF=SLOP5*ES
      RULE=5
      EKI=ES*SLOP1
    ELSE IF(DEL .GT. DTOP .AND. PL .GE. VE) THEN
      STIF=SLOP6*ES
      RULE=6
      EKI=ES*SLOP1
    ENDIF
    IF( REVRSC ) IRV=1.
    IF ( .NOT. REVRSC) IRV=0.
C     CALL STRENG(ESE,PSE,PSEOLD,P,PLA,DE,DELA,STIF,EKI)
    RETURN
  ENDIF
C
C (5) RULE 8
C
  IF( RULE .EQ. 8.) THEN
    IF( DEL .GT. DBOT .AND. DEL .LT. DTOP ) THEN

```

```

        STIF=SLOP1*ES
        EKI=ES*SLOP1
        ELSE IF(DEL .LT. DBOT ) THEN
          STIF=SLOP2*ES
          RULE=2
C
        PL=PBOT-(DBOT-DEL)*SLOP2
        P=PL*PY
C
        EKI=ES*((PTOP-PL)/(DTOP-DEL))
        ELSE IF(DEL .GT. DTOP ) THEN
          STIF=SLOP4*ES
          RULE=4
          EKI=ES*SLOP1
        ENDIF
        IF( REVRSC ) IRV=1.
        IF ( .NOT. REVRSC) IRV=0.
C  CALL STRENG(ESE,PSE,PSEOLD,P,PLA,DE,DELA,STIF,EKI)
        RETURN
        ENDIF
C
C (6) RULE 9
C
        IF( RULE .EQ. 9.) THEN
          IF( DEL .GT. DBOT .AND. DEL .LT. DTOP ) THEN
            STIF=SLOP1*ES
            EKI=ES*SLOP1
          ELSE IF(DEL .LT. DBOT ) THEN
            STIF=SLOP3*ES
            RULE=3
C
            PL=PBOT-(DBOT-DEL)*SLOP3
            P=PL*PY
C
            EKI=ES*((PTOP-PL)/(DTOP-DEL))
            ELSE IF(DEL .GT. DTOP ) THEN
              STIF=SLOP4*ES
              RULE=4
              EKI=ES*SLOP1
            ENDIF
            IF( REVRSC ) IRV=1.
            IF ( .NOT. REVRSC) IRV=0.
C  CALL STRENG(ESE,PSE,PSEOLD,P,PLA,DE,DELA,STIF,EKI)
            RETURN
            ENDIF
C
C (7) RULE 4
C
        IF( RULE .EQ. 4.) THEN
          IF (DEL .GE. HC1 .AND. DEL .LT. HD ) THEN
            IF(DDE .GE. O. ) THEN
              STIF=SLOP4*ES
              EKI=ES*SLOP1
            ELSE IF( DDE .LT. O. ) THEN
              PREF=VD+(SLOP4*(VB-VD-SLOP1*HB
*               +SLOP1*HD)/(SLOP4-SLOP1))
              DREF=(VB-VD+SLOP4*HD-SLOP1*HB)/(SLOP4-SLOP1)
              IF( DEL .LT. DREF) THEN
                PTOP=P/PY
                DTOP=DEL
                DBOT=(SLOP3*HB-VB+PTOP-SLOP1*DEL)/(SLOP3-SLOP1)
                PBOT=VB+SLOP3*(DBOT-HB)
                STIF=SLOP1*ES
                RULE=9
                REVRSC=.TRUE.
                EKI=ES*SLOP1
              ELSE IF( DEL .GE. DREF) THEN

```

```

PTOP=P/PY
DTOP=DEL
DBOT=(SLOP2*HA-VA+PTOP-SLOP1*DEL)/(SLOP2-SLOP1)
PBOT=VA+SLOP2*(DBOT-HA)
STIF=SLOP1*ES
RULE=8
REVRSC=.TRUE.
EKI=ES*SLOP1
ENDIF
ENDIF
ELSE IF( DEL .GT. HD .AND. DDE .GT. 0. ) THEN
STIF=SLOP5*ES
RULE=5
EKI=ES*SLOP1
ELSE IF( DEL .LT. HC1 .AND. DEL .GE. HC ) THEN
REVRSC=.FALSE.
RULE=4
STIF=SLOP4*ES
EKI=ES*SLOP4
ELSE IF( DEL .LT. HC ) THEN
REVRSC=.FALSE.
RULE=3
HC=DEL
VC=PL
IDUC=1.
STIF=-SLOP6*ES
EKI=ES*((VD-VC)/(HD-HC))
ENDIF
IF( REVRSC ) IRV=1.
IF( .NOT. REVRSC ) IRV=0.
C CALL STRENG(ESE,PSE,PSEOLD,P,PLA,DE,DELA,STIF,EKI)
IF( ABS(DEMAX) .LT. ABS(DE) ) THEN
C CALL DNE(1,DUC,EXCR,DELY, DA, ESE(1), PSE, PSEOLD, CSE )
DEMAX=DE
ENDIF
RETURN
ENDIF
C
C (8) RULE 5
C
IF( RULE .EQ. 5. ) THEN
IF( DEL .LT. HE ) THEN
IF(DDE .GE. 0. ) THEN
STIF=SLOP5*ES
EKI=ES*SLOP1
ELSE IF( DDE .LT. 0. ) THEN
BREF=VA-SLOP1*HA
HREF=(VD-SLOP5*HD-BREF)/(SLOP1-SLOP5)
IF( DEL .GE. HREF ) CYCLE=CYCLE+1
PTOP=P/PY
DTOP=DEL
DBOT=(SLOP2*HA-VA+PTOP-SLOP1*DEL)/(SLOP2-SLOP1)
PBOT=VA+SLOP2*(DBOT-HA)
STIF=SLOP1*ES
RULE=7
REVRSC=.TRUE.
EKI=ES*SLOP1
ENDIF
ELSE IF( DEL .GE. HE .AND. DDE .GT. 0. ) THEN
STIF=SLOP6
RULE=6
EKI=ES*SLOP1
ENDIF
IF( REVRSC ) IRV=1.
IF( .NOT. REVRSC ) IRV=0.
C CALL STRENG(ESE,PSE,PSEOLD,P,PLA,DE,DELA,STIF,EKI)
IF( ABS(DEMAX) .LT. ABS(DE) ) THEN

```

```

C      CALL DNE(1,DUC,EXCR,DELY, DA, ESE(1), PSE, PSEOLD, CSE )
      DMAX=DE
      ENDIF
      RETURN
      ENDIF
C
C (9) RULE 6
C
      IF( RULE .EQ. 6.) THEN
          IF(DDE .GE. 0.) THEN
              STIF=SLOP6
              EKI=ES*SLOP1
          ELSE IF(DDE .LT. 0.) THEN
              STIF=SLOP1*ES
              RULE=1
              CYCLE=CYCLE+1.
              REVRSC=.FALSE.
              EKI=ES*SLOP1
          ENDIF
          IF( REVRSC ) IRV=1.
          IF ( .NOT. REVRSC) IRV=0.
C      CALL STRENG(ESE,PSE,PSEOLD,P,PLA,DE,DELA,STIF,EKI)
          IF( ABS(DEMAX) .LT. ABS(DE) ) THEN
              CALL DNE(1,DUC,EXCR,DELY, DA, ESE(1), PSE, PSEOLD, CSE )
              DMAX=DE
          ENDIF
          RETURN
          ENDIF
C
C (10) RULE 10
C
      IF( RULE .EQ. 10.) THEN
          IF( DEL .GT. DBOT .AND. DEL .LT. DTOP ) THEN
              STIF=SLOP7*ES
              EKI=ES*SLOP7
          ELSE IF(DEL .LT. DBOT ) THEN
              STIF=SLOP3*ES
              RULE=3
              REVRSC=.FALSE.
              PTOP=0
              DTOP=0
              PBOT=0
              DBOT=0
              EKI=ES*((PTOP-PL)/(DTOP-DEL))
          ELSE IF(DEL .GT. DTOP ) THEN
              STIF=SLOP4*ES
              RULE=4
              EKI=ES*SLOP1
          ENDIF
          IF( REVRSC ) IRV=1.
          IF ( .NOT. REVRSC) IRV=0.
C      CALL STRENG(ESE,PSE,PSEOLD,P,PLA,DE,DELA,STIF,EKI)
          RETURN
          ENDIF
C
C (11) RULE 11
C
      IF( RULE .EQ. 11.) THEN
          IF( DEL .GT. DBOT .AND. DEL .LT. DTOP ) THEN
              STIF=SLOP7*ES
              EKI=ES*SLOP7
          ELSE IF(DEL .LT. DBOT ) THEN
              STIF=SLOP2*ES
              RULE=2
              REVRSC=.FALSE.
              PTOP=0
              DTOP=0

```

```

PBOT=0
DBOT=0
EKI=ES*((VD-PL)/(HD-DEL))
ELSE IF(DEL .GT. DTOP ) THEN
  STIF=SLOP5*ES
  RULE=5
  EKI=ES*SLOP1
ENDIF
IF( REVRSC ) IRV=1.
IF ( .NOT. REVRSC) IRV=0.
C CALL STRENG(ESE,PSE,PSEOLD,P,PLA,DE,DELA,STIF,EKI)
RETURN
ENDIF
C
C (12) RULE 12
C
IF( RULE .EQ. 12.) THEN
  IF( DEL .GT. DBOT .AND. DEL .LT. DTOP ) THEN
    STIF=SLOP7*ES
    EKI=ES*SLOP7
  ELSE IF(DEL .LT. DBOT ) THEN
    STIF=SLOP2*ES
    RULE=2
    REVRSC=.FALSE.
    PTOP=0
    DTOP=0
    PBOT=0
    DBOT=0
    EKI=ES*((PTOP-PL)/(DTOP-DEL))
  ELSE IF(DEL .GT. DTOP ) THEN
    STIF=SLOP5*ES
    RULE=5
    EKI=ES*SLOP1
  ENDIF
ENDIF
IF( REVRSC ) IRV=1.
IF ( .NOT. REVRSC) IRV=0.
C CALL STRENG(ESE,PSE,PSEOLD,P,PLA,DE,DELA,STIF,EKI)
RETURN
END

```

Input Data:

```

1 1 101.82 1.0 |IELNO MAT ELENGH SLK
'BRACE' 29000. 7.0 1.39 36. 1. 0. 0. |TYPE SMAT
0. -0.5 50 |DMIN DMAX NUMB
-0.5 0.5 100 |DMIN DMAX NUMB
0.5 -0.8 100 |DMIN DMAX NUMB
-0.8 0.8 200 |DMIN DMAX NUMB
0.8 -1.0 200 |DMIN DMAX NUMB
-1.0 1.0 200 |DMIN DMAX NUMB
1.0 -2.0 300 |DMIN DMAX NUMB
-2.0 0.5 300 |DMIN DMAX NUMB
0.5 -2.0 300 |DMIN DMAX NUMB

```

Output Data:

```

JAIN-GOEL-HANSON HYSTERESIS MODEL PARAMETERS
=====

```

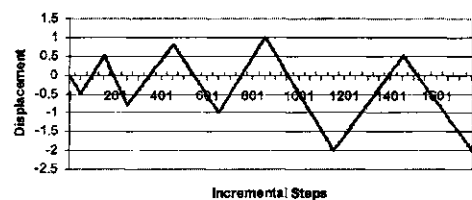
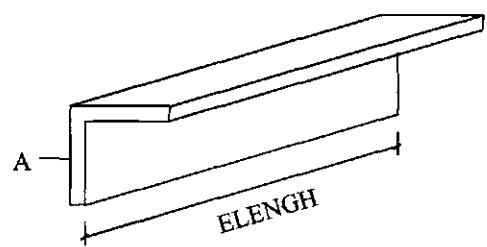
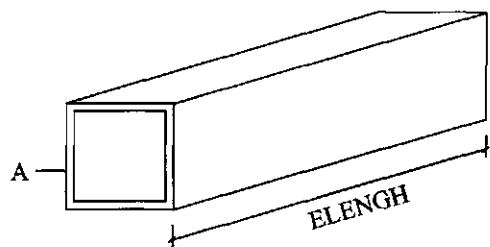
MAT.	E	A	R	YS	SHAPE	MAX DUC	BETA
1	29000.0	7.00000	1.39000	36.0000	1.00000	0.00000	0.00000

```
JAIN-GOEL-HANSON HYSTERESIS ENVELOPE CONTROL POINTS...
=====
```

```
CYCLE ----- = 1.0000
RULE ----- = 1.0000
```

(HA, VA) -----= (-0.8313, -0.8313)
(HB, VB) -----= (-5.0000, -0.2457)
(HC, VC) -----= (-12.0000, -0.1638)
(HC1, VC1) -----= (-9.7531, 0.0000)
(HD, VD) -----= (-2.0862, 0.5590)
(HD1, VD1) -----= (-2.5470, 0.6825)
(HH, VH) -----= (-3.1507, -0.5055)
(HE, VE) -----= (1.0000, 1.0000)

STIFFNESS LOAD DISP. RULE
1993.71436 -19.93714 -0.01000 1.0
1993.71436 -39.87429 -0.02000 1.0
1993.71436 -59.81143 -0.03000 1.0
. .
-15.01257 -41.30552 -2.00000 3.0
-15.01257 -41.18042 -2.00833 3.0



Diagrams Represent Input Data for Appendix J

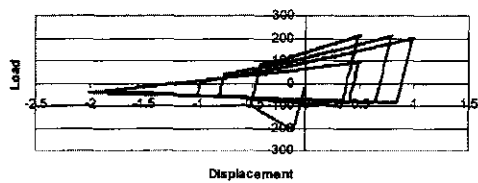
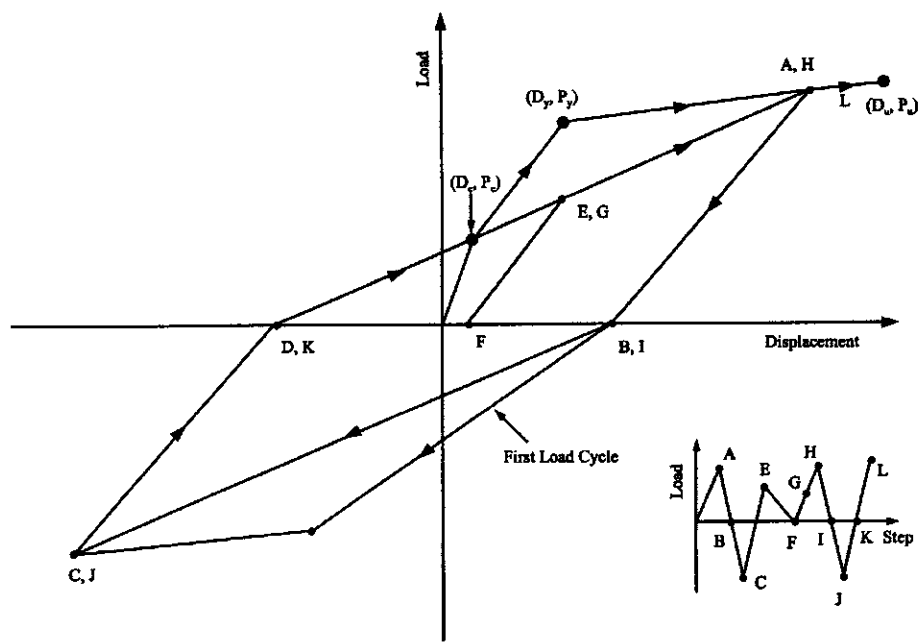


Diagram Represents Output Solution for Appendix J

Appendix K—Takeda Model for RC Columns and Beams and Computer Program



```

C=====
C THIS IS A TYPICAL MAIN PROGRAM FOR CALLING TAKEDA
C HYSTERESIS MODEL SUBROUTINE NAMED "MAT06". THE PARAMETERS
C TRANSFERRED INTO SUBROUTINE MAT06 ARE SHOWN AS FOLLOWS.
C SINCE MAT06 IS A GENERAL PURPOSE SUBROUTINE, SOME PARAMETERS
C HAVE BEEN RESERVED AND NOT USED. THEREFORE THEY ARE ASSIGNED
C WITH A NUMBER "1" IN THIS DEMONSTRATION AS A MAIN PROGRAM.
C=====
C VARIABLES:
C MAT = USER DEFINED MATERIAL ID NUMBER
C IELNO = USER DEFINED ELEMENT ID NUMBER
C P = CURRENT LOAD
C PL = PREVIOUS STEP LOAD
C D = CURRENT DISPLACEMENT
C DL = PREVIOUS STEP DISPLACEMENT
C V = DUMMY VARIABLE
C VL = DUMMY VARIABLE
C DUCT = RESERVED DUCTILITY ARRAY (NOT USED)
C EXCR = RESERVED EXCURSION ARRAY (NOT USED)
C DAMAGE= RESERVED VARIABLE FOR DAMAGE INDEX (NOT USED)
C EESE = RESERVED VARIABLE FOR ELASTIC STRAIN ENERGY(NOT USED)
C EPSE = RESERVED VARIABLE FOR PLASTIC STRAIN ENERGY(NOT USED)
C LELEM = 49
C LMAT = 13
C SMAT = MATERIAL ARRAY, SMAT(LMAT)

```

```

C SE = ELEMENT ARRAY, SE(LELEM)
C IOPT = 1 INITIALIZE MATERIAL
C      2 GET INITIAL STIFFNESS
C      3 GET MEMBER STIFFNESS
C ERR = DUMMY LOGICAL VARIABLE
C FIRST = LOGICAL VARIABLE. If FIRST=.TRUE., THE MATERIAL
C      PROPERTIES OF THE MEMBER ARE PRINTED.
C PRINT = DUMMY LOGICAL VARIABLE
C BUG = LOGICAL VARIABLE. If BUG=.TRUE., THE HYSTERSIS
C      ENVELOPE CONTROL POINTS ARE PRINTED.
C=====
LOGICAL ERR, FIRST, PRINT, BUG
DIMENSION SE(100), SMAT(9), DUCT(3), EXCR(6)
CHARACTER*80 TYPE
C
C=====
C DEFINE EXTERNAL FILE UNITS FOR INPUT DATA AND OUTPUT
C=====
OPEN(UNIT=5,FILE=STRING(8))
OPEN(UNIT=6,FILE=STRING(9))
C
C=====
C
IOPT=1
ERR=.FALSE.
FIRST=.TRUE.
PRINT = .FALSE.
BUG=.FALSE.
READ(5,*)IELNO, MAT
C
C INPUT MATERIAL PROPERTIES
C CALL MAT06
C & (IOPT ,IELNO ,ERR ,FIRST ,PRINT ,BUG,
C & MAT ,SE ,P,PL,D,DL,V,VL,LELEM,LMAT,
C & SMAT,EESE,EPSE,DUCT,EXCR,DAMAGE)
CALL MAT06
& (IOPT ,IELNO ,ERR ,FIRST ,PRINT ,BUG,
& MAT ,SE ,P,PL,D,DL,V,VL,LELEM,LMAT,
& SMAT,DUMMY,DUMMY,DUCT,EXCR,DUMMY)
C
C INITIALIZE ELEMENT STIFFNESS
IOPT=2
BUG=.TRUE.
C
CALL MAT06
& (IOPT ,IELNO ,ERR ,FIRST ,PRINT ,BUG,
& MAT ,SE ,P,PL,D,DL,V,VL,LELEM,LMAT,
& SMAT,DUMMY,DUMMY,DUCT,EXCR,DUMMY)
C
STIF=SE(1)
BUG=.FALSE.
C
WRITE(6,*)' STIFFNESS LOAD DISP. RULE'
C READ DISPLACEMENT
F=0.
FL=0.
D=0.
DL=0.
C
800  READ(5,* , END=5000)DMIN, DMAX, NUMB
      DD=(DMAX-DMIN)/NUMB
700  DL=D
      D=D+DD
      FL=F
      F=F+STIF*DD
      P=F
      PL=FL

```

```

IOPT=3
CALL MAT06
& (IOPT ,IELNO ,ERR ,FIRST ,PRINT ,BUG ,
& MAT ,SE ,P,PL,D,DL,V,VL,LELEM,LMAT,
& SMAT,DUMMY,DUMMY,DUCT,EXCR,DUMMY)
C
F=P
STIF=SE(1)
WRITE(6,98)SE(1), F, D, SE(2)
98 FORMAT(3F15.5, 3X, F4.1)
IF (DMAX .GT. 0) THEN
IF (D .LE. DMAX) THEN
GO TO 700
ELSE IF (D .GT. DMAX) THEN
D=DMAX
GO TO 800
ENDIF
ELSE IF (DMAX .LE. 0) THEN
IF (D .GE. DMAX) THEN
GO TO 700
ELSE IF (D .LT. DMAX) THEN
D=DMAX
GO TO 800
ENDIF
ENDIF
C
5000 CLOSE(5)
CLOSE(6)
STOP
END

C=====
C      DEBUG UNIT(6),TRACE,SUBCHK,INIT,SUBTRACE
C      END DEBUG
C=====

SUBROUTINE MAT06
& (IOPT ,IELNO ,ERR ,FIRST ,PRINT ,BUG ,
& MAT ,SE ,P,PL,D,DL,V,VL,LELEM,LMAT,
& SMAT,ESE,EPS,ESE,EPSE,DUCT,EXCR,DAMAGE)
C
IMPLICIT REAL(A-H,O-Z)
LOGICAL ERR,FIRST,PRINT,BUG
LOGICAL BTTEST
DIMENSION SE(100),SMAT(13),DUCT(3),EXCR(6)
CHARACTER*80 TYP
C
LELEM=49
IF (IOPT.EQ.0) RETURN
C
C-----.
C VARIABLES:
C-----.
C----- GLOBAL VARIABLES
C IOPT = 1, INITIALIZE MATERIAL
C = 2, GET STIFFNESS
C RINPUT = INPUT DATA
C SMAT = INTERNAL STORAGE
C SE = OUTPUT STIFFNESS
C-----.
C ---- TAKEDA DATA ----.
C SMAT( 1)= EI,    ELASTIC STIFFNESS
C SMAT( 2)= PC,    CRACKING LOAD
C SMAT( 3)= DC,    CRACKING DISPLACEMENT
C SMAT( 4)= PY,    YEILD LOAD
C SMAT( 5)= DY,    YEILD DISPLACEMENT
C SMAT( 6)= PU,    ULTIMATE LOAD
C SMAT( 7)= DU,    ULTIMATE DISPLACEMENT

```

```

C SMAT( 8)= OC,      INITIAL STIFFNESS
C SMAT( 9)= CY,      CRACKED STIFFNESS
C SMAT(10)= YU,      ULTIMATE STIFFNESS
C SMAT(11)= CY',     RELOADING STIFFNESS
C SMAT(12)= CSE      CONSTANT STRAIN ENERGY AT YEILD
C SMAT(13)= BDAM     BETA FOR DAMAGE INDEX
C
C----- INPUT DATA FOR TAKEDA HYSTERESIS MODEL -----
C   THE FOLLOWING DATA IS INPUT ONCE FOR EACH MODEL
C
C PC,DC = CRACKING LOAD AND DISPLACEMENT
C PY,DY = YEILD LOAD AND DISPLACEMENT
C PU,DU = ULTIMATE LOAD AND DISPLACEMENT
C
C-----
GO TO (100,200,300,400,500),IOPT
C
100 CONTINUE
READ (5,*) TYP , (SMAT(I),I=2,7)
BDAM=0
C
LMAT = 13
SMAT( 8)= SMAT(2) / SMAT(3)
SMAT( 9)=(SMAT(4)-SMAT(2))/(SMAT(5)-SMAT(3))
SMAT(10)=(SMAT(6)-SMAT(4))/(SMAT(7)-SMAT(5))
SMAT(11)=(SMAT(2)+SMAT(4))/(SMAT(3)+SMAT(5))
SMAT( 1)=SMAT(1)
SMAT(12)=SMAT(2)*SMAT(3)/2 + .5*(SMAT(2)+SMAT(4))*(SMAT(5)-SMAT(3))
SMAT(13)=BDAM
C
IF (FIRST .OR. BUG) WRITE (6,5)
WRITE (6,6) MAT,BDAM, SMAT(2),SMAT(4),SMAT(6),
& SMAT(3),SMAT(5),SMAT(7)
5 FORMAT('///' TAKEDA HYSTERESIS MODEL- FOR UNIT LENGTH MEMBER'
& ' ======'//'
& ' MAT. BETA ',
& 7X,'CRACK',10X,'YEILD', 7X,'ULTIMATE')
6 FORMAT (/1X,I5,G15.6, 18X,3G15.6,/39X,3G15.6/)
C   WRITE (6,6) MAT,SMAT(1),SMAT(12),SMAT(2),SMAT(4),SMAT(6),
C & SMAT(3),SMAT(5),SMAT(7)
C 5 FORMAT('///' TAKEDA HYSTERESIS MODEL- FOR UNIT LENGTH MEMBER'
C & ' ======'//'
C & ' MAT. ELASTIC ET MOMT. GRADIENT ',
C & 7X,'CRACK',10X,'YEILD',10X,'ULTIMATE',// )
C 6 FORMAT (1X,I5,G15.6,1X,G15.6,2X,3G15.6,/39X,3G15.6/)
C
RETURN
===== GET STIFFNESS TERMS =====
200 CONTINUE
C ---- TAKEDA MODEL DATA STORAGE FOR MEMBER ----
C SE( 1)= S
C SE( 2)= HRN
C SE( 3)= A
C SE( 4)= B
C SE( 5)= IDRC
C SE( 6)= RF
C SE( 7)= RNRL
C SE( 8)= UM1
C SE( 9)= UM2
C SE(10)= UM3
C SE(11)= UM4
C SE(12)= S1
C SE(13)= X0
C SE(14)= XOUML
C SE(15)= XOY
C SE(16)= UOD
C SE(17)= UO

```

```

C SE(18)= X1UM
C SE(19)= U1
C SE(20)= U1D
C SE(21)= X2UU0
C SE(22)= U2
C SE(23)= X3U1
C SE(24)= U3
C SE(25)= QY
C SE(26)= MAXFLG
C SE(27)= ACHNG
C SE(28)= S_EQ_UNLOAD
C SE(29)= EESE
C SE(30)= EES0
C SE(31)= EES0
C SE(32)= EPSE
C SE(33)= PSE_OLD
C SE(34)= UPOS(1)
C SE(35)= UPOS(2)
C SE(36)= UPOS(3)
C SE(37)= UNEG(1)
C SE(38)= UNEG(2)
C SE(39)= UNEG(3)
C SE(40)= EXCR(1)
C SE(41)= EXCR(2)
C SE(42)= EXCR(3)
C SE(43)= EXCR(4)
C SE(44)= EXCR(5)
C SE(45)= EXCR(6)
C SE(46)= P_MAX
C SE(47)= D_MAX
C SE(48)= SMAT(8)
C SE(49)= SMAT(1)
C
  EI=SMAT(1)
  GRAD=SMAT(12)
  DO 210 I=1,47
210 SE(I)=0
C SE(26)=1
  CALL HYST06(P,D,PL,DL,V ,VL,
  & SE( 1),SE( 2),SE( 3),SE( 4),SE( 5),SE( 6),
  & SMAT( 2),SMAT( 3),SMAT( 4),SMAT( 5),SMAT( 6),SMAT( 7),SMAT( 8),
  & SMAT( 9),SMAT(10),SMAT(11),SMAT(12),
  & SE( 7),SE( 8),SE( 9),SE(10),SE(11),SE(12),SE(13),SE(14),SE(15),
  & SE(16),SE(17),SE(18),SE(19),SE(20),SE(21),SE(22),SE(23),SE(24),
  & SE(25),SE(26),SE(27),BUG,
  & SE(28),SE(29),SE(32),SE(33),SE(34),SE(37),SE(40))
C
  SE(48)=SMAT(8)
  SE(49)=EI
C
  RETURN
C
C===== GET STIFFNESS TERMS =====
300 CONTINUE
C SE( 1)= STIFF
C SE(27)= A
C SE(28)= S_EQ_UNLOAD
  ICYC=0
  IF (BUG) THEN
    WRITE (6,*) '----- IN MAT06 -----'
    WRITE (6,*) ' P,D=',P,D,' V=',V
    WRITE (6,*) ' PL,DL=',PL,DL,' VL=',VL
  ENDIF
310 STIFF=SE(1)
  P=PL+(D-DL)*STIFF
  A=SE(27)
  IF (A.EQ.0 .AND. SE(7).EQ.0) A=SMAT(2)

```

```

ICYC=ICYC+1
IF (BUG) THEN
  WRITE (6,*) 'STIFF=',STIFF,' A=',A
  WRITE (6,*) ' P=',P,' ICYC=',ICYC
ENDIF
C
C----- IS P WITHIN LIMITS ?
IF (ICYC.GT.5) THEN
  WRITE (6,*) 'MORE THAN 5 CYCLES IN MAT06'
  WRITE (6,*) 'MORE THAN 5 CYCLES IN MAT06, IELNO:',IELNO
C-- ELSE IF ((PL.LE.P .AND. P.LT.A) .OR. (PL.GE.P .AND. P.GT.A) .OR.
ELSE IF ((PL.LE.P .AND. P.LE.A) .OR. (PL.GE.P .AND. P.GE.A) .OR.
  & (DL.EQ.D)) THEN
  IF (BUG) WRITE (6,*) 'C----- IS P WITHIN LIMITS ? '
  CALL STRENG(SE(29),SE(32),SE(33),P,PL,D,DL,SE(1),SE(28))
  CALL HYST06( P,D ,PL,DL,V ,VL,
  & SE( 1),SE( 2),SE( 3),SE( 4),SE( 5),SE( 6),
  & SMAT( 2),SMAT( 3),SMAT( 4),SMAT( 5),SMAT( 6),
  & SMAT( 7),SMAT( 8),SMAT( 9),SMAT(10),SMAT(11),SMAT(12),
  & SE( 7),SE( 8),SE( 9),SE(10),SE(11),SE(12),SE(13),
  & SE(14),SE(15),SE(16),SE(17),SE(18),SE(19),SE(20),
  & SE(21),SE(22),SE(23),SE(24),SE(25),SE(26),SE(27),BUG,
  & SE(28),SE(29),SE(32),SE(33),SE(34),SE(37),SE(40))
  V=VL
C----- IS P GREATER THAN LIMITS ?
ELSE IF (((PL.LE.A .AND. A.LT.P) .OR. (PL.GE.A .AND. A.GE.P)).AND.
  & (STIFF.NE.0.00)) THEN
  D1=DL+(A-PL)/STIFF
  P1=A
  CALL STRENG(SE(29),SE(32),SE(33),P1,PL,D1,DL,SE(1),SE(28))
  IF (BUG) THEN
    WRITE (6,*) 'C----- IS P GREATER THAN LIMITS ? '
    WRITE (6,*) 'PL,DL=',PL,DL
  C   WRITE (6,*) 'PI,DI=',PI,DI
  ENDIF
  CALL HYST06(P1,D1,PL,DL,1.,1.,
  & SE( 1),SE( 2),SE( 3),SE( 4),SE( 5),SE( 6),
  & SMAT( 2),SMAT( 3),SMAT( 4),SMAT( 5),SMAT( 6),
  & SMAT( 7),SMAT( 8),SMAT( 9),SMAT(10),SMAT(11),SMAT(12),
  & SE( 7),SE( 8),SE( 9),SE(10),SE(11),SE(12),SE(13),
  & SE(14),SE(15),SE(16),SE(17),SE(18),SE(19),SE(20),
  & SE(21),SE(22),SE(23),SE(24),SE(25),SE(26),SE(27),BUG,
  & SE(28),SE(29),SE(32),SE(33),SE(34),SE(37),SE(40))
  DL=D1
  PL=P1
  C   DL=D1
  C   PL=P1
  C   PI=PL+(P-PL)*.001
  C   DI=DL+(D-DL)*.001
  C   IF (BUG) THEN
  C     WRITE (6,*) 'C----- IS P GREATER THAN LIMITS ? '
  C     WRITE (6,*) 'PL,DL=',PL,DL
  C     WRITE (6,*) 'PI,DI=',PI,DI
  C   ENDIF
  CALL HYST06(PI,DI,PL,DL,1.,1.,
  & SE( 1),SE( 2),SE( 3),SE( 4),SE( 5),SE( 6),
  & SMAT( 2),SMAT( 3),SMAT( 4),SMAT( 5),SMAT( 6),
  & SMAT( 7),SMAT( 8),SMAT( 9),SMAT(10),SMAT(11),SMAT(12),
  & SE( 7),SE( 8),SE( 9),SE(10),SE(11),SE(12),SE(13),
  & SE(14),SE(15),SE(16),SE(17),SE(18),SE(19),SE(20),
  & SE(21),SE(22),SE(23),SE(24),SE(25),SE(26),SE(27),BUG,
  & SE(28),SE(29),SE(32),SE(33),SE(34),SE(37),SE(40))
  GO TO 310
C----- IS P LESS THAN LIMITS ?
ELSE IF ((P.LT.PL .AND. PL.LE.A) .OR. (P.GT.PL .AND. PL.GE.A))THEN
  IF (ABS(P-PL).GT. 0.0005*ABS(P+PL)) THEN

```

```

PI=PL+(P-PL)*.001
DI=DL+(D-DL)*.001
ELSE
  PI=P
  DI=D
ENDIF
C    PI=PL+(P-PL)*.001
C    DI=DL+(D-DL)*.001
IF (BUG) THEN
  WRITE (6,*) 'C----- IS P LESS THAN LIMITS ? '
  WRITE (6,*) 'PI,DI=',PI,DI
ENDIF
CALL HYST06(PI,DI,PL,DL,1.,1.,
& SE( 1),SE( 2),SE( 3),SE( 4),SE( 5),SE( 6),
& SMAT( 2),SMAT( 3),SMAT( 4),SMAT( 5),SMAT( 6),
& SMAT( 7),SMAT( 8),SMAT( 9),SMAT(10),SMAT(11),SMAT(12),
& SE( 7),SE( 8),SE( 9),SE(10),SE(11),SE(12),SE(13),
& SE(14),SE(15),SE(16),SE(17),SE(18),SE(19),SE(20),
& SE(21),SE(22),SE(23),SE(24),SE(25),SE(26),SE(27),BUG,
& SE(28),SE(29),SE(32),SE(33),SE(34),SE(37),SE(40))
GO TO 310
ENDIF
C
IF (BUG) WRITE (6,*) 'STIFF=',STIFF,' A,B=',SE(3),SE(4),SE(27)
C
C----- MAXIMUM DISPLACEMENT
IF (ABS(D).GT.ABS(SE(47))) THEN
  SE(46)= P
  SE(47)= D
ENDIF
C
C----- TRANSFER ENERGIES FOR BOTH IOPT=3 AND 4.
400 EESE=SE(29)
EPSE=SE(32)
C
C----- TRANSFER DUCTILITIES AND EXCRUSION RATIOS FOR BOTH IOPT=3 AND 4.
DO 410 I=1,3
DUCT(I)=MAX(SE(33+I),SE(36+I))
EXCR(I)=SE(39+I)
410 EXCR(I+3)=SE(42+I)
RETURN
C
C===== DAMAGE INDEX =====
500 EESE=SE(29)
EPSE=SE(32)
PY= SMAT( 4)
PU= SMAT( 6)
DU= SMAT( 7)
P = SE(46)
D = SE(47)
BDAM=SMAT(13)
DAMAGE=ABS(D)/DU + BDAM/(PY*DU) * EPSE
C
RETURN
END

C@PROCESS SDUMP OPT(0) GOSTMT XREF MAP
C=====
C== TAKEDA HYSTERESIS MODEL ..... HYST06 .....
C=====
C      DEBUG UNIT(6),TRACE,SUBCHK,INIT,SUBTRACE
C      AT 8000
C      TRACE ON
C      END DEBUG
C=====
C

```

```

C TAKEDA HYSTERESIS MODEL - REFERANCE, S. OTANI, UILU-ENG-74-2029
C           TAKEDA & SOZEN, J. ASCE ST. DIV. - DEC. 1970
C
C PI  CURRENT LOAD
C DI  CURRENT DISPL
C PS  PREVIOUS LOAD
C DS  PREVIOUS DISPL
C VI  CURRENT VELOCITY
C VL  PREVIOUS VELOCITY
C S   CURRENT STIFFNESS
C HRLN CURRENT RULE NUMBER
C A   UPPER LOAD LIMIT BEFORE RULE CHANGE
C B   LOWER LOAD LIMIT BEFORE RULE CHANGE
C IDRO ??PREVIOUS DIRECTION
C RF
C PC,DC CRACKING LOAD AND DISPLACEMENT
C PY,DY YEILD LOAD AND DISPLACEMENT
C PU,DU ULTIMATE LOAD AND DISPLACEMENT
C OC  ELASTIC STIFFNESS PD/DC
C CY  POST CRACKING STIFFNESS (PY-PC)/(DY-DC)
C YU  POST YEILD STIFFNESS (PU-PY)/(DU-DY)
C CPY CRACKING', YEILD STIFFNESS (PY+PC)/(DY+DC)
C CSE
C RNRL NEXT RULE NUMBER
C UM1 PEAK DISPLACEMENT IN THE POSITIVE DIRECTION
C UM2 PEAK LOAD IN THE POSITIVE DIRECTION
C UM3 PEAK DISPLACEMENT IN THE NEGATIVE DIRECTION
C UM4 PEAK LOAD IN THE NEGATIVE DIRECTION
C S1  UNLOADING STIFFNESS
C XO
C X0UM
C X0Y
C UOD
C UO
C XIUM
C U1
C UID
C X2UO
C U2
C X3U1
C U3
C QY
C MAXFLG FLAG, IF MAXFLG=0 STIFFNESS=0 BEYOND FAILURE POINT (DU,PU)
C ACHNG LOAD WHERE RULE CHNGS IF LOADING CONTINUES IN CURR DIRECTION
C PRINT PRINT DATA FOR TRACING
C SE  ELASTIC UNLOADING CURVE
C ESE ELASTIC STRAIN ENERGY
C PSE PLASTIC STRAIN ENERGY
C PSEOLD PLASTIC STRAIN ENERGY AT LAST ZERO CROSSING
C UPOS POSITIVE DUCTILITY INFO.
C UNEG NEGATIVE DUCTILITY INFO.
C EXCR EXCRUSION RATIO INFO.
C
C JT  #FOR CURRENT DIRECTION FOR LOADING AND UNLOADING
C      # FOR NEW DIRECTION FOR REVERSAL
C      # = 2 FOR POSITIVE LOAD , # = 1 FOR NEGATIVE LOAD
C IREVSL SIGN OF LOAD IN NEW DIRECTION
C ISGN SIGN OF THE CURRENT LOAD FOR LOADING AND UNLOADING
C      SIGN OF THE NEW LOAD FOR REVERSAL
C
C
C SUBROUTINE HYST06(PI,DI,PS,DS,VI,VS ,S,HRLN,A,B,IDRO,RF ,
& PC,DC,PY,PU,DU,OC,CY,YU,CPY,CSE,RNRL,UM1,UM2,UM3,UM4,
& S1,XO ,X0UM,X0Y,UOD,UO,XIUM,U1,UID ,X2UO,U2,X3U1,U3,QY,MAXFLG,
& ACHNG,PRINT,SE,ESE,PSE,PSEOLD,UPOS,UNEG,EXCR)
C
REAL UM(2,2),IDRO,MAXFLG,UPOS(3),UNEG(3),EXCR(6),ESE(3)

```

```

LOGICAL PRINT,BTEST

C8000 IF (PRINT) WRITE (6,8010) PI,DI,PS,DS,VI,VS,S,HRLN,A,B,RF,
C & PC,DC,PY,DU,OC,CY,YU,CPY,RNRL,UM1,UM2,UM3,UM4,
C & S1,XO ,XOUM,XOY,UOD,U0,X1UM,U1,U1D ,X2U0,U2,X3U1,U3,QY,
C & ACHNG, IDRO,MAXFLG,CSE,
C & SE,ESE(1),PSE,PSEOLD,UPOS,UNEG,EXCR
C8010 FORMAT(
C & ' TAKEDA-PI=',G12.5,' DI=',G12.5,' PS=',G12.5,' DS=',G12.5/
C & ' TK- VI=',G12.5,' VS=',G12.5,' S=',G12.5,' HRLN=',G12.5/
C & ' TK- A=',G12.5,' B=',G12.5,' RF=',G12.5,' PC=',G12.5/
C & ' TK- DC=',G12.5,' PY=',G12.5,' DY=',G12.5,' PU=',G12.5/
C & ' TK- DU=',G12.5,' OC=',G12.5,' CY=',G12.5,' YU=',G12.5/
C & ' TK- CPY=',G12.5,' RNRL=',G12.5,' UM1=',G12.5,' UM2=',G12.5/
C & ' TK- UM3=',G12.5,' UM4=',G12.5,' S1=',G12.5,' XO=',G12.5/
C & ' TK- XOUNM=',G12.5,' XOY=',G12.5,' UOD=',G12.5,' U0=',G12.5/
C & ' TK- X1UM=',G12.5,' U1=',G12.5,' UID=',G12.5,' X2U0=',G12.5/
C & ' TK- U2=',G12.5,' X3U1=',G12.5,' U3=',G12.5,' QY=',G12.5/
C & ' TK- ACHNG=',G12.5,' IDRO=',G12.5,' MAXF=',G12.5,' CSE=',G12.5/
C & ' TK- SE=',G12.3,' ESE=',G12.5,' PSE=',G12.5,' PSEOLD=',G12.5/
C & ' TK- UP1=',G12.3,' UP2=',G12.5,' UP3=',G12.5/
C & ' TK- UN1=',G12.3,' UN2=',G12.5,' UN3=',G12.5/
C & ' TK- EX1=',G12.3,' EX2=',G12.5,' EX3=',G12.5/
C & ' TK- EX4=',G12.3,' EX5=',G12.5,' EX6=',G12.5)
C..... RTN IF CURRENT STATE = PREVIOUS STATE
  IF ((PI.EQ.PS .OR. DI.EQ.DS) .AND. RNRL.NE.0 ) RETURN
C
C..... GET DIRECTION AND RTN IF CURRENT STATE IS WITHIN LIMITS...
  CALL IDRECT (IDR, IDRV, IDRVO, PI, PS, VI, VS)
  IF (A.GT.B .AND. PI.LE.A .AND. PI.GT.B .AND. IDR.EQ.IDRO) RETURN
  IF (A.LT.B .AND. PI.GT.A .AND. PI.LT.B .AND. IDR.EQ.IDRO) RETURN
C
C..... CALC EXCURSION RATIO AT EVERY ZERO CROSSING...
C IF (PI*PS.LE.0)CALL DNE(0,UPOS,EXCR,DY,DI,ESE(1),PSE,PSEOLD,CSE)
C
C..... INITILIZE DATA FOR FIRST CALL TO SUBROUTINE
1 IF (RNRL.EQ.0) THEN
  RNRL=1
  UM1=-DC
  UM2=-PC
  UM3= DC
  UM4= PC
ENDIF
C
C..... INITILIZE DATA
  NRL=RNRL
  UM(1,1)=UM1
  UM(1,2)=UM2
  UM(2,1)=UM3
  UM(2,2)=UM4
C
  IF (PI.GT.0) THEN
  901 ISGN =1
    JI=2
  ELSE IF (PI.LT.0) THEN
  902 ISGN =-1
    JI=1
  ELSE IF (DI.LT.DS) THEN
  903 ISGN =-1
    JI=1
  ELSE IF (DI.GT.DS) THEN
  904 ISGN =1
    JI=2
  ELSE
  905 ISGN =1
    JI=1
ENDIF

```

```

C
  IF (DI.LE.DS) THEN
    IREVSL=-1
  ELSE
    IREVSL= 1
  ENDIF
C
  IF (IDR.LT.0) THEN
    C   IF (ISGN.GT.0) CALL DNE(1,UPOS,EXCR, DY,DI,ESE(2),PSE,PSEOLD,CSE)
    C   IF (ISGN.LT.0) CALL DNE(1,UNEG,EXCR,-DY,DI,ESE(3),PSE,PSEOLD,CSE)
  ENDIF
C
  GO TO ( 100, 200, 300, 400, 500, 600, 700, 800, 900,1000,
  1   1100,1200,1300,1400,1500,1600),NRL
C ===== TAKEDA RULE 1.0 ===== ELASTIC STAGE
100 IF (IDR) 130,130,110
110 IF (ABS(PI).GE.PC) GO TO 200
  B=PI
  A=PC*ISGN
  S=OC
  SE=S
  NRL=1
  HRLN=1.11
  GO TO 2000
130 B=0.
  A=PC*IREVSL
  IF (PI.NE.0) A=PC*SIGN(1.0,PI)
  S=OC
  SE=S
  NRL=1
  HRLN=1.2
  GO TO 2000
C ===== TAKEDA RULE 2.0 ===== LOADING ON PRIMARY CURVE UP TO YEILD
200 IF (IDR) 230,230,210
210 IF (ABS(PI).GE.PY) GO TO 300
  B=PI
  A=PY*ISGN
  S=CY
  S1=(PI+(PC*ISGN))/(DI+DC*ISGN)
  SE=S1
  NRL=2
  HRLN=2.11
  GO TO 2000
230 B=0.
  A=PI
  S1=(PI+(PC*ISGN))/(DI+DC*ISGN)
  S=S1
  SE=S1
  NRL=5
  HRLN=2.2
  GO TO 2000
C ===== TAKEDA RULE 3.0 ===== LOADING ON PRIMARY CURVE AFTER YEILD
300 BOTT=MAX(ABS(DI),ABS(UM1),ABS(UM3) )
  S1=CPY* SQRT(DY/BOTT)
  SE=S1
  IF (IDR) 330,330,310
310 IF (ABS(PI).GE.PU) GO TO 320
  A=PU*ISGN
  B=PI
  S=YU
  NRL=3
  HRLN=3.11
  GO TO 2000
320 A=PU*ISGN
  B=PI
  S=0.00001
C IF (MAXFLG.NE.0) S=YU

```

```

NRL=3
HRLN=3.12
GO TO 2000
330 B=0.
A=PI
BOTT=MAX(ABS(DI),ABS(UM1),ABS(UM3) )
S1=CPY* SQRT(DY/BOTT)
S=S1
NRL=4
HRLN=3.2
GO TO 2000
C ===== TAKEDA RULE 4.0 ===== UNLOADING FROM POINT UM ON THE PRIMARY
C           CURVE AFTER YEILDING
400 IF (IDR) 430,440,410
410 IF (ABS(PI).GE.ABS(UM(JI,2))) GO TO 420
  A=UM(JI,2)
  B=PI
  S=S1
  NRL=4
  HRLN=4.11
  GO TO 2000
420 A=PU*ISGN
  B=PI
  S=YU
  NRL=3
  HRLN=4.12
  GO TO 2000
430 A=PI
  B=0.
  S=S1
  NRL=4
  HRLN=4.2
  GO TO 2000
440 IF (DI.LE.DS) IDRVO=1
  IF (DI.GT.DS) IDRVO=2
  IF (ABS(UM(IDRVO,1)).GT.DC) GO TO 450
  A=PC*IREVSL
  B=0.
  S=S1
  NRL=15
  HRLN=4.31
  GO TO 2000
450 X0=DI
  X0UM=(0.-UM(IDRVO,2))/(X0-UM(IDRVO,1))
  X0Y =(0.-PY*ISGN)/(X0-DY*ISGN)
  IF (PY.GT.ABS(UM(IDRVO,2)) .AND. X0Y.GT.X0UM) GO TO 460
  A=UM(IDRVO,2)
  B=0.
  S2=X0UM
  S=S2
  NRL=6
  HRLN=4.32
  GO TO 2000
460 UM(JI,1)=DY*ISGN
  UM(JI,2)=PY*ISGN
  A=UM(JI,2)
  B=0.
  S2=X0Y
  S=S2
  NRL=6
  HRLN=4.33
  GO TO 2000
C ===== TAKEDA RULE 5.0 ===== UNLOADING FROM POINT UM ON THE PRIMARY
C           CURVE BEFORE YEILDING
500 IF (IDR) 530,540,510
510 IF (ABS(PI).GE.ABS(UM(JI,2))) GO TO 200
  A=UM(JI,2)

```

```

B=PI
S=S1
NRL=5
HRLN=5.11
GO TO 2000
530 A=PI
B=0.
S=S1
NRL=5
HRLN=5.2
GO TO 2000
540 IF (DI.LE.DS) IDR=2
IF (DI.GT.DS) IDR=1
IF (ABS(UM(IDR,1)).GT.DC) GO TO 450
A=PC*IREVSL
B=0.
S=S1
NRL=14
HRLN=5.31
GO TO 2000
C ===== TAKEDA RULE 6.0 ===== LOADING TOWARDS POINT UM ON THE PRIMAR
C CURVE.
600 IF (IDR) 630,630,610
610 IF (ABS(PI).GE.ABS(UM(JI,2))) GO TO 210
A=UM(JI,2)
B=PI
XOUM=(PI-UM(JI,2))/(DI-UM(JI,1))
S=XOUM
NRL=6
HRLN=6.11
GO TO 2000
630 UOD=DI
UO=PI
A=PI
B=0.
S=S1
NRL=7
HRLN=6.20
GO TO 2000
C ===== TAKEDA RULE 7.0 ===== UNLOADING FROM POINT UM AFTER RULE 6
700 IF (IDR) 730,740,710
710 IF (ABS(PI).GE.ABS(UO)) GO TO 720
A=UO
B=PI
S=S1
NRL=7
HRLN=7.11
GO TO 2000
720 A=UM(JI,2)
B=PI
XOUM=(0.-UM(JI,2))/(XO-UM(JI,1))
S=XOUM
NRL=6
HRLN=7.12
GO TO 2000
730 A=PI
B=0.
S=S1
NRL=7
HRLN=7.2
GO TO 2000
740 A=UM(JI,2)
B=0.
XIUM=(PI-UM(JI,2))/(DI-UM(JI,1))
S=XIUM
NRL=8
HRLN=7.3

```

```

GO TO 2000
C ===== TAKEDA RULE 8.0 ===== LOADING TOWARDS POINT UM ON THE PRIMAR
C           CURVE
800 IF (IDR) 830,830,810
810 IF (ABS(PI).GE.ABS(UM(JI,2))) GO TO 210
  A=UM(JI,2)
  B=PI
  X1UM=(PI-UM(JI,2))/(DI-UM(JI,1))
  S=X1UM
  NRL=8
  HRLN=8.11
  GO TO 2000
830 U1=PI
  U1D=DI
  A=PI
  B=0.
  S=S1
  NRL=9
  HRLN=8.2
  GO TO 2000
C ===== TAKEDA RULE 9.0 ===== UNLOADING FROM POINT U1 AFTER RULE 8
900 IF (IDR) 930,940,910
  910 IF (ABS(PI).GE.ABS(U1 )) GO TO 810
  A=U1
  B=PI
  S=S1
  NRL=9
  HRLN=9.11
  GO TO 2000
930 A=PI
  B=0.
  S=S1
  NRL=9
  HRLN=9.2
  GO TO 2000
940 A=U0
  B=0.
  X2U0=(PI-U0)/(DI-UOD)
  S=X2U0
  NRL=10
  HRLN=9.3
  GO TO 2000
C ===== TAKEDA RULE 10.0 ===== LOADING TOWARDS POINT U0
1000 IF (IDR) 1030,1030,1010
1010 IF (ABS(PI).GE.ABS(U0 )) GO TO 610
  A=U0
  B=PI
  X2U0=(PI-U0)/(DI-UOD)
  S=X2U0
  NRL=10
  HRLN=10.11
  GO TO 2000
1030 U2=PI
  A=PI
  B=0.
  S=S1
  NRL=11
  HRLN=10.2
  GO TO 2000
C ===== TAKEDA RULE 11.0 ===== UNLOADING FROM POINT U2 AFTER RULE 10
1100 IF (IDR) 1130,1140,1110
1110 IF (ABS(PI).GE.ABS(U2 )) GO TO 1010
  A=U2
  B=PI
  S=S1
  NRL=11
  HRLN=11.11

```

908**APPENDIX K**

```
GO TO 2000
1130 A=PI
  B=0.
  S=S1
  NRL=11
    HRLN=11.2
  GO TO 2000
1140 A=U1
  B=0.
  X3U1=(PI-U1)/(DI-U1D)
  S=X3U1
  NRL=12
    HRLN=11.3
  GO TO 2000
C ===== TAKEDA RULE 12.0 ===== LOADING TOWARDS POINT U1
1200 IF (IDR) 1230,1230,1210
1210 IF (ABS(PI).GE.ABS(U1 )) GO TO 810
  A=U1
  B=PI
  X3U1=(PI-U1)/(DI-U1D)
  S=X3U1
  NRL=12
    HRLN=12.11
  GO TO 2000
1230 U3=PI
  A=PI
  B=0.
  S=S1
  NRL=13
    HRLN=12.2
  GO TO 2000
C ===== TAKEDA RULE 13.0 ===== UNLOADING FROM POINT U3 AFTER RULE 12
1300 IF (IDR) 1330, 940,1310
1310 IF (ABS(PI).GE.ABS(U3 )) GO TO 1210
  A=U3
  B=PI
  S=S1
  NRL=13
    HRLN=13.11
  GO TO 2000
1330 A=PI
  B=0.
  S=S1
  NRL=13
    HRLN=13.2
  GO TO 2000
C ===== TAKEDA RULE 14.0 ===== LOADING IN THE UNCRACKED DIRECTION AFTE
C           CRACKING IN THE OTHER DIRECTION.
1400 IF (IDR) 1430,1440,1410
1410 IF (ABS(PI).GE. PC ) GO TO 210
  A=PC*ISGN
  B=0.
  S=S1
  NRL=14
    HRLN=14.11
  GO TO 2000
1430 A=PI
  B=0.
  S=S1
  NRL=14
    HRLN=14.2
  GO TO 2000
1440 A=UM(JI,2)
  B=0.
  S=S1
  NRL=5
    HRLN=14.3
```

```

GO TO 2000
C ===== TAKEDA RULE 15.0 ===== LOADING IN THE UNCRACKED DIRECTION AFTE
C           YEILDING IN THE OTHER DIRECTION.
1500 IF (IDR) 1530,1540,1510
1510 IF (ABS(PI).GE. PC ) GO TO 1520
  A=PC*ISGN
  B=PI
  S=S1
  NRL=15
    HRLN=15.11
  GO TO 2000
1520 PQ=PC*ISGN
  DQ=(PQ-PI)/S1+DI
  QY=(PY*ISGN-PQ)/(DY*ISGN-DQ)
  A=PY*ISGN
  B=PQ
  S=QY
  NRL=16
    HRLN=15.12
  GO TO 2000
1530 A=PI
  B=0.
  S=S1
  NRL=15
    HRLN=15.2
  GO TO 2000
1540 IF (ABS(PI) .GE. ABS(UM(JI,2))) GO TO 1550
  A=UM(JI,2)
  B=0.
  S=S1
  NRL=4
    HRLN=15.31
  GO TO 2000
1550 A=PU*TREVSL
  B=0.
  S=YU
  NRL=3
    HRLN=15.32
  GO TO 2000
C ===== TAKEDA RULE 16.0 ===== LOADING TOWARDS THE YEILD POINT AFTER
C           RULE 15.
1600 IF (IDR) 1630,1630,1610
1610 IF (ABS(PI).GE. PY ) GO TO 300
  A=PY*ISGN
  B=PI
  S=QY
  NRL=16
    HRLN=16.11
  GO TO 2000
1630 UM(JI,1)=DY
  UM(JI,2)=PY
  UO=PI
  UOD=DI
  A=PI
  B=0.
  S=S1
  S2=QY
  X0=DI-PI/S2
  NRL= 7
    HRLN=16.2
  GO TO 2000
C
C ======> CALCULATE MAXIMUM PREVIOUS DEFORMATION
2000  UM1=MIN(UM(1,1),DI)
      UM2=MIN(UM(1,2),PI)
      UM3=MAX(UM(2,1),DI)
      UM4=MAX(UM(2,2),PI)

```

```

RNRL=NRL
IDRO=IDR
RF=0.
IF (IDR.GE.0) ACHNG=A
IF (IDR.LT.0) ACHNG=B
RETURN
END
C@PROCESS SDUMP OPT(0) GOSTMT XREF MAP
C*****
C      DEBUG UNIT(6),TRACE,SUBCHK,INIT,SUBTRACE
C      END DEBUG
C
C      SUBROUTINE IDRECT (IDR,IDRV,IDRVO,PI,PS,VI,VS)
C
LOGICAL A,NA,B,NB,C,NC,D,ND,E
LOGICAL BTTEST
C
C      WRITE (6,*) 'IDR,IDRV,IDRVO,PI,PS,VI,VS'
C      WRITE (6,*) IDR,IDRV,IDRVO,PI,PS,VI,VS
C
A = ABS(PI).GE.ABS(PS)
B = PI*PS .GE.0
C B = PI*PS .GT.0
C = PI.EQ.0
D = VS*VI.GE.0
NA= .NOT. A
NB= .NOT. B
NC= .NOT. C
ND= .NOT. D
C
IF ( A .AND. B .AND. NC .AND. D ) IDR=1
IF ( NB .AND. NC .AND. ND ) IDR=-1
IF ( NA .AND. B .AND. NC .AND. ND ) IDR=1
IF ( C .AND. D ) IDR=0
IF ( NB .AND. NC .AND. D ) IDR=0
IF ( A .AND. B .AND. NC .AND. ND ) IDR=-1
IF ( C .AND. ND ) IDR=-1
IF ( NA .AND. B .AND. NC .AND. D ) IDR=-1
E = PI .GE. PS
IDRV=1
IDRVO=2
IF (E) IDRV=2
IF (E) IDRVO=1
RETURN
END

```

Input Data:

```

1 1 |TELNO MAT
'RECTANGULAR BEAM' 242. 0.001 1500. 0.015 1550. 0.086 |TYP, SMAT
0. 0.01 50 |DMIN DMAX NUMB
0.01 -0.03 100 |DMIN DMAX NUMB
-0.03 0.01 100 |DMIN DMAX NUMB
0.01 -0.01 50 |DMIN DMAX NUMB
-0.01 0.02 100 |DMIN DMAX NUMB
0.02 -0.02 200 |DMIN DMAX NUMB
-0.02 0.04 300 |DMIN DMAX NUMB

```

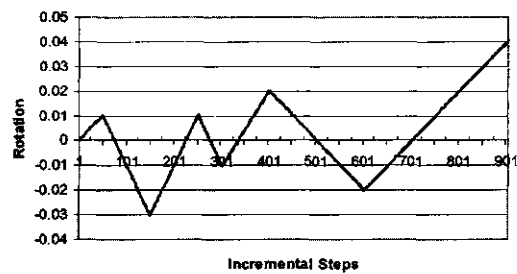
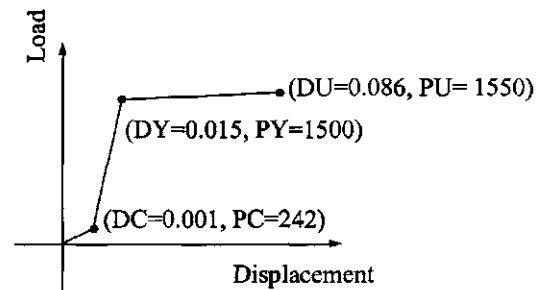
Output Data:

TAKEDA HYSTERESIS MODEL- FOR UNIT LENGTH MEMBER

MAT.	BETA	CRACK	YEILD	ULTIMATE
1	0.00000	242.000	1500.00	1550.00
		0.100000E-02	0.150000E-01	0.860000E-01

TAKEDA MODEL FOR RC COLUMNS AND BEAMS**911**

STIFFNESS	LOAD	DISP.	RULE
241999.98438	48.39999	0.00020	1.1
241999.98438	96.79999	0.00040	1.1
241999.98438	145.19998	0.00060	1.1
.			
.			
.			
704.22534	1539.52002	0.04000	3.1
704.22534	1539.66089	0.04020	3.1



Diagrams Represent Input Data for Appendix K

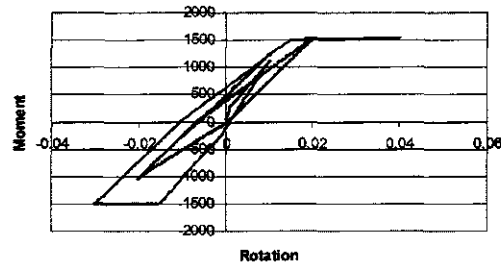
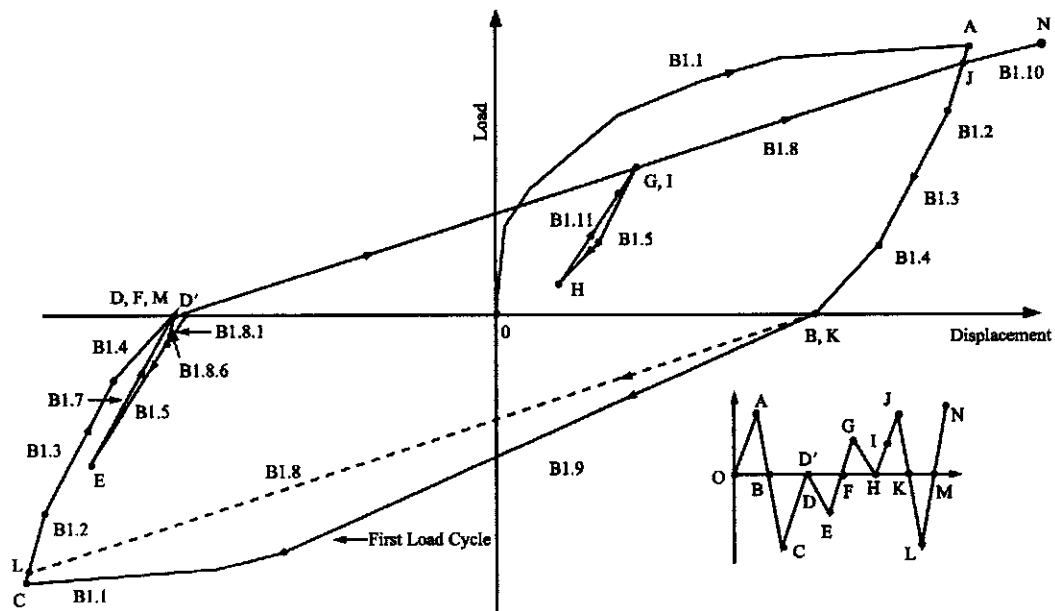


Diagram Represents Output Solution for Appendix K

Appendix L—Cheng-Mertz Model for Bending Coupling with Shear and Axial Deformations of Low-Rise Shear Walls and Computer Program

BENDING: Low-Rise Shear Wall Cheng-Mertz Hysteresis Model



```

C=====
C THIS IS A TYPICAL MAIN PROGRAM FOR CALLING CHENG-MERTZ BENDING
C HYSTERESIS MODEL SUBROUTINE NAMED "MAT03". THE PARAMETERS
C TRANSFERRED INTO SUBROUTINE MAT03 ARE SHOWN AS FOLLOWS.
C SINCE MAT03 IS A GENERAL PURPOSE SUBROUTINE, SOME PARAMETERS
C HAVE BEEN RESERVED AND NOT USED. THEREFORE THEY ARE ASSIGNED
C WITH A NUMBER "1" IN THIS DEMONSTRATION AS A MAIN PROGRAM.
C=====
C VARIABLES:
C MAT = USER DEFINED MATERIAL ID NUMBER
C IELNO = USER DEFINED ELEMENT ID NUMBER
C P = CURRENT LOAD
C PL = PREVIOUS STEP LOAD
C D = CURRENT DISPLACEMENT
C DL = PREVIOUS STEP DISPLACEMENT
C V = DUMMY VARIABLE
C VL = DUMMY VARIABLE
C DUCT = RESERVED DUCTILITY ARRAY (NOT USED)

```

```

C EXCR = RESERVED EXCURSION ARRAY (NOT USED)
C DAMAGE= RESERVED VARIABLE FOR DAMAGE INDEX (NOT USED)
C ESE = RESERVED VARIABLE FOR ELASTIC STRAIN ENERGY(NOT USED)
C EPSE = RESERVED VARIABLE FOR PLASTIC STRAIN ENERGY(NOT USED)
C LELEM = 34+3*NI+2, WHERE NI=NUMBER OF SMALL AMPLITUDE LOOPS
C LMAT = 5+2*NSEG, WHERE NSEG=NUMBER OF BACKBONE SEGMENTS
C SMAT = MATERIAL ARRAY, SMAT(LMAT)
C SE = ELEMENT ARRAY, SE(LELEM)
C IOPT = 1 INITIALIZE MATERIAL
C      2 GET INITIAL STIFFNESS
C      3 GET MEMBER STIFFNESS
C ERR = DUMMY LOGICAL VARIABLE
C FIRST = LOGICAL VARIABLE. If FIRST=.TRUE., THE MATERIAL
C      PROPERTIES OF BENDING HYSTERESIS MODEL ARE PRINTED.
C PRINT = DUMMY LOGICAL VARIABLE
C BUG = LOGICAL VARIABLE. If BUG=.TRUE., THE HYSTERESIS
C      ENVELOPE CONTROL POINTS ARE PRINTED.
C BDAM = RESERVED PARAMETER FOR ANG's DAMAGE INDEX
C=====
LOGICAL ERR, FIRST, PRINT, BUG
DIMENSION SE(100), SMAT(9), DUCT(3), EXCR(6)
CHARACTER*80 TYPE
C=====
C DEFINE EXTERNAL FILE UNITS FOR INPUT DATA AND OUTPUT
C=====
OPEN(UNIT=5,FILE=STRING(8))
OPEN(UNIT=6,FILE=STRING(9))
C
C=====
C
IOPT=1
ERR=.FALSE.
FIRST=.TRUE.
PRINT = .FALSE.
BUG=.FALSE.
READ(5,*)IELNO, MAT
C
C INPUT MATERIAL PROPERTIES
C CALL MAT03
C & (IOPT ,IELNO ,ERR ,FIRST ,PRINT ,BUG ,
C & MAT ,SE ,P,PL,D,DL,V,VL,LELEM,LMAT,
C & SMAT,ESE,EPSE,DUCT,EXCR,DAMAGE)
CALL MAT03
& (IOPT ,IELNO ,ERR ,FIRST ,PRINT ,BUG ,
& MAT ,SE ,P,PL,D,DL,V,VL,LELEM,LMAT,
& SMAT,DUMMY,DUMMY,DUCT,EXCR,DUMMY)
C
C INITIALIZE ELEMENT STIFFNESS
IOPT=2
BUG=.FALSE.
C
CALL MAT03
& (IOPT ,IELNO ,ERR ,FIRST ,PRINT ,BUG ,
& MAT ,SE ,P,PL,D,DL,V,VL,LELEM,LMAT,
& SMAT,DUMMY,DUMMY,DUCT,EXCR,DUMMY)
C
STIF=SE(1)
BUG=.FALSE.
C
WRITE(6,*)' STIFFNESS LOAD DISP. RULE'
C READ DISPLACEMENT
F=0.
FL=0.
D=0.
DL=0.
C
800 READ(5,*, END=5000)DMIN, DMAX, NUMB

```

```

DD=(DMAX-DMIN)/NUMB
700 DL=D
D=D+DD
  FL=F
  F=F+STIF*DD
  P=F
  PL=FL
  IOPT=3
  CALL MAT03
& (IOPT ,IELNO ,ERR ,FIRST ,PRINT ,BUG ,
& MAT ,SE ,P,PL,D,DL,V,VL,LELEM,LMAT,
& SMAT,DUMMY,DUMMY,DUCT,EXCR,DUMMY)
C
  F=P
  STIF=SE(1)
  WRITE(6,98)SE(1), F, D, SE(2)
98 FORMAT(3F15.5, 3X, F4.1)
  IF (DMAX .GT. 0) THEN
    IF (D .LE. DMAX) THEN
      GO TO 700
    ELSE IF (D .GT. DMAX) THEN
      D=DMAX
      GO TO 800
    ENDIF
  ELSE IF (DMAX .LE. 0) THEN
    IF (D .GE. DMAX) THEN
      GO TO 700
    ELSE IF (D .LT. DMAX) THEN
      D=DMAX
      GO TO 800
    ENDIF
  ENDIF
C
5000 CLOSE(5)
CLOSE(6)
STOP
END
C
C=====
C     DEBUG UNIT(6),SUBCHK,INIT,SUBTRACE
C     END DEBUG
C=====
SUBROUTINE MAT03
& (IOPT ,IELNO ,ERR ,FIRST ,PRINT ,BUG ,
& MAT ,SE ,P,PL,D,DL,V,VL,LELEM,LMAT,
& SMAT,EESE,EPSE,DUCT,EXCR,DAMAGE)
C
  IMPLICIT REAL(A-H,O-Z)
  LOGICAL ERR,FIRST,PRINT,BUG
  LOGICAL BTTEST
  DIMENSION SE(100),SMAT(30),DUCT(3),EXCR(6)
C
  DIMENSION COPY(100)
  CHARACTER*4 SSE(100)
C
  CHARACTER*80 TYPE
C
  EQUIVALENCE (SSE(1),COPY(1))
C
  IF (IOPT.NE.1) LELEM=34+3*SMAT(2)+2
  IF (IOPT.EQ.0) RETURN
C
C-----
C VARIABLES:
C-----
C----- GLOBAL VARIABLES
C IOPT = 1, INITIALIZE MATERIAL

```

```

C      = 2, GET STIFFNESS
C SMAT = INTERNAL STORAGE
C SE = OUTPUT STIFFNESS
C-----
C ---- BEND1 DATA -----
C SMAT(1)= NSEGS, NUMBER OF BACKBONE SEGMENTS
C SMAT(2)= NI , NUMBER OF SMALL AMPLITUDE LOOPS
C SMAT(3)= CSE, CONSTANT STRAIN ENERGY...
C SMAT(4)= DY, YEILD POINT FOR DUCTILITIES
C SMAT(5) = BDAM BETA FOR DAMAGE INDEX
C SMAT(5+I) = PP, BACKBONE MOMENT FOR POINT I
C SMAT(5+I+NSEGS)= DP, BACKBONE ROTATION FOR POINT I
C
C      GO TO (100,200,300,400,500), IOPT
C
C
100 CONTINUE
C----- INPUT DATA FOR BEND1 HYSTERESIS MODEL ----- C
C
C NSEG = NUMBER OF BACKBONE SEGEMENTS
C NI = NUMBER OF SMALL LOOP POINTS
C BDAM = PARAMETER FOR ANG's DAMAGE INDEX
C EI = ELASTIC STIFFNESS
C G = MOMENT GRADINET
C PP = BACKBONE LOAD
C DP = BACKBONE DISPLACEMENT
C
C----- C
READ (5,*) TYPE ,NSEG,NI,DY, BDAM
READ(5,*) ( SMAT(5+I ),I=1,NSEG)
READ(5,*) ( SMAT(5+I+NSEG),I=1,NSEG)
C
LELEM = 34+3*NI +2
LMAT = 5+2*NSEG
SMAT(1)=NSEG
SMAT(2)=NI
CCC SMAT(3)=SMAT(6)/SMAT(6+NSEG)
SMAT(4)=DY
SMAT(5)=BDAM
C----- CALC CONSTANT STRAIN ENERGY....
DL=0
PL=0
DO 10 I=1,NSEG
P=SMAT(5+I)
D=SMAT(5+I+NSEG)
IF (D.LE.DY) THEN
CSE=CSE + 0.5*(P+PL)*(D-DL)
PL=P
DL=D
ELSE IF (D.EQ.DL) THEN
GO TO 20
ELSE
PY=PL+ (DY-DL)*(P-PL)/(D-DL)
CSE=CSE + 0.5*(PY+PL)*(DY-DL)
GO TO 20
ENDIF
10 CONTINUE
20 SMAT(3)=CSE
C
IF (FIRST .OR. BUG) WRITE (6,55)
WRITE (6,57) MAT,NI,DY, BDAM,(SMAT(5+K),SMAT(5+K+NSEG),K=1,NSEG)
WRITE (6,*) ''
C
55 FORMAT(/' BEND1 HYSTERESIS MODEL DATA - UNIT LENGTH MEMBER'
& /' =====',
& /' BACKBONE CURVE POINTS - MATL NI ',5X,'DY',9X,
& ' BETA ',3X,' MOMENT',8X,'ROTATION')

```

```

      5? FORMAT ( (28X,2I4,2X,G15.6,3G15.6)/(68X,2G15.6))
C
      RETURN
C===== GET STIFFNESS TERMS =====
200 CONTINUE
C ---- BEND1 MODEL DATA STORAGE FOR MEMBER ----
C SE( 1)= K
C SE( 2)= RULE
C SE( 3)= DIR
C SE( 4)= A
C SE( 5)= PMG
C SE( 6)= PMH
C SE( 7)= DMG
C SE( 8)= DMH
C SE( 9)= BACKB
C SE(10)= ALPHA1
C SE(11)= ALPHA2
C SE(12)= IR
C SE(13)= SR1
C SE(14)= SR2
C SE(15)= SR3
C SE(16)= SRM
C SE(17)= E_EQ_UNLOAD
C SE(18)= UPOS(1)
C SE(19)= UPOS(2)
C SE(20)= UPOS(3)
C SE(21)= UNEG(1)
C SE(22)= UNEG(2)
C SE(23)= UNEG(3)
C SE(24)= EXCR(1)
C SE(25)= EXCR(2)
C SE(26)= EXCR(3)
C SE(27)= EXCR(4)
C SE(28)= EXCR(5)
C SE(29)= EXCR(6)
C SE(30)= EESE(1)
C SE(31)= EESE(2)
C SE(32)= EESE(3)
C SE(33)= EPSE
C SE(34)= PSE_OLD
C SE(34+1 )=PR( 1)
C SE(34+ NI)=PR(NI)
C SE(34+1+ NI)=DR( 1)
C SE(34+ 2*NI)=DR(NI)
C SE(34+1+2*NI)=FR( 1)
C SE(34+ 3*NI)=FR(NI)
C SE(35+ 3*NI)=P_MAX
C SE(36+ 3*NI)=D_MAX
C
      NSEG=SMAT(1)
      NI =SMAT(2)
      J1= NSEG+6
      J3= NI+35
      J4=2*NI+35
      J5=3*NI+35-1 +2
      SI=SMAT(6)/SMAT(6+NSEG)
      C* EI= SMAT(4)
      DO 210 I=1,J5
210  SE(I)=0
C
      DO 189 I=J4, J4+NI-1
      COPY(I)=SE(I)
189  CONTINUE
C
      CALL HYSTO3(P,D,PL,DL,V ,NSEG,NI,
      & SMAT( 6),SMAT(J1),SMAT( 6),SMAT(J1),SI,SMAT(3),
      & SE( 1),SE( 2),SE( 3),SE( 4),SE( 5),SE( 6),SE( 7),SE( 8),SE( 9),

```

```

& SE(10),SE(11),SE(12),SE(13),SE(14),SE(15),SE(16),SE(35),SE(J3),
& SSE(J4),BUG,
& SE(17),SMAT(4),SE(30),SE(33),SE(34),SE(18),SE(21),SE(24))
C
DO 89 I=J4, J4+NI-1
SE(I)=COPY(I)
89 CONTINUE
C
RETURN
C
===== GET STIFFNESS TERMS =====
300 CONTINUE
C SE(4)=A
NSEG=SMAT(1)
NI=SMAT(2)
J1=NSEG+6
J3=NI+35
J4=2*NI+35
SI=SMAT(6)/SMAT(6+NSEG)
C* EI= SMAT(4)
C SET VELOCITY FLAG TO 1 TO REMOVE INFL OF HIGH FREQ VELOC
C DVEL=V*VL
DVEL = 1
ICYC=0
IF (BUG) THEN
WRITE (6,*) '----- IN MAT03 -----'
WRITE (6,*) 'P,D',P,D
WRITE (6,*) 'PL,DL',PL,DL
ENDIF
310 STIFF=SE(1)
P=PL+(D-DL)*STIFF
A=SE(4)
IF (A.EQ.0 .AND. SE(2).EQ.0) THEN
A=SIGN(SMAT(6),P)
IF (P.LT.PL .AND. PL.GT.0 .AND. P.GT.0) A=0
IF (P.GT.PL .AND. PL.LT.0 .AND. P.LT.0) A=0
ENDIF
ICYC=ICYC+1
IF (BUG) THEN
WRITE (6,*) 'STIFF=',STIFF,' A=',A
WRITE (6,*) ' P=',P,' ICYC=',ICYC
ENDIF
C
C---- IS P WITHIN LIMITS ?
IF (ICYC.GT.10) THEN
WRITE (6,*) 'MORE THAN 10 CYCLES IN MAT03, IELNO:',IELNO
ELSE IF ((PL.LE.P .AND. P.LT.A) .OR. (PL.GE.P .AND. P.GT.A) .OR.
& (DL.EQ.D)) THEN
IF (BUG) WRITE (6,*) 'C---- IS P WITHIN LIMITS ? '
C     CALL STRENG (SE(30),SE(33),SE(34),P,PL,D,DL,SE(1),SE(17) )
C
DO 199 I=J4, J4+NI-1
COPY(I)=SE(I)
199 CONTINUE
C
CALL HYST03(P,D,PL,DL,DVEL ,NSEG,NI,
& SMAT(6),SMAT(J1),SMAT(6),SMAT(J1),SI,SMAT(3),
& SE(1),SE(2),SE(3),SE(4),SE(5),SE(6),
& SE(7),SE(8),SE(9),
& SE(10),SE(11),SE(12),SE(13),SE(14),SE(15),
& SE(16),SE(35),SE(J3),
& SSE(J4),BUG,
& SE(17),SMAT(4),SE(30),SE(33),SE(34),SE(18),SE(21),SE(24))
C
DO 99 I=J4, J4+NI-1
SE(I)=COPY(I)
99 CONTINUE

```

```

C
      DVEL=1
C----- IS P GREATER THAN LIMITS ?
      ELSE IF ((PL.LE.A .AND. A.LE.P) .OR. (PL.GE.A .AND. A.GE.P)).AND.
      & (STIFF.NE.0.00) THEN
          D1=DL+(A-PL)/STIFF
          P1=A
C          CALL STRENG (SE(30),SE(33),SE(34),P1,PL,D1,DL,SE(1),SE(17) )
          DL=D1
          PL=P1
C          PI=PL+(P-PL)*.001
C          DI=DL+(D-DL)*.001
          IF (ABS(P-PL).GT. 0.0005*ABS(P+PL)) THEN
              PI=PL+(P-PL)*.001
              DI=DL+(D-DL)*.001
          ELSE
              PI=P
              DI=D
          ENDIF
          IF (BUG) THEN
              WRITE (6,*) 'C----- IS P GREATER THAN LIMITS ? '
              WRITE (6,*) 'PL,DL=',PL,DL
              WRITE (6,*) 'PI,DI=',PI,DI
          ENDIF
C
          DO 179 I=J4, J4+NI-1
              COPY(I)=SE(I)
179 CONTINUE
C
          CALL HYSTO3(PI,DI,PL,DL,1.00 ,NSEG,NI,
          & SMAT( 6),SMAT(J1),SMAT( 6),SMAT(J1),SI,SMAT(3),
          & SE( 1),SE( 2),SE( 3),SE( 4),SE( 5),SE( 6),
          & SE( 7),SE( 8),SE( 9),
          & SE(10),SE(11),SE(12),SE(13),SE(14),SE(15),
          & SE(16),SE(35),SE(J3),
          & SSE(J4),BUG,
          & SE(17),SMAT(4),SE(30) ,SE(33),SE(34),SE(18),SE(21),SE(24))
C
          DO 79 I=J4, J4+NI-1
              SE(I)=COPY(I)
79 CONTINUE
C
          GO TO 310
C----- IS P LESS THAN LIMITS ?
      ELSE IF ((P.LT.PL .AND. PL.LE.A) .OR. (P.GT.PL .AND. PL.GE.A))THEN
C          PI=PL+(P-PL)*.001
C          DI=DL+(D-DL)*.001
          IF (ABS(P-PL).GT. 0.0005*ABS(P+PL)) THEN
              PI=PL+(P-PL)*.001
              DI=DL+(D-DL)*.001
          ELSE
              PI=P
              DI=D
          ENDIF
          IF (BUG) THEN
              WRITE (6,*) 'C----- IS P LESS THAN LIMITS ? '
              WRITE (6,*) 'PI,DI=',PI,DI
          ENDIF
C
          DO 169 I=J4, J4+NI-1
              COPY(I)=SE(I)
169 CONTINUE
C
          CALL HYSTO3(PI,DI,PL,DL,1.00 ,NSEG,NI,
          & SMAT( 6),SMAT(J1),SMAT( 6),SMAT(J1),SI,SMAT(3),
          & SE( 1),SE( 2),SE( 3),SE( 4),SE( 5),SE( 6),
          & SE( 7),SE( 8),SE( 9),

```

```

& SE(10),SE(11),SE(12),SE(13),SE(14),SE(15),
& SE(16),SE(35),SE(J3),
& SSE(J4),BUG,
& SE(17),SMAT(4),SE(30),SE(33),SE(34),SE(18),SE(21),SE(24))
C
DO 69 I=J4, J4+NI-1
    SE(I)=COPY(I)
69 CONTINUE
C
GO TO 310
ENDIF
C
C-----SAVE MAXIMUM DISPL AND IT'S LOAD
IF (ABS(D).GT.ABS(SE(36+3*NI))) THEN
    SE(35+ 3*NI)=P
    SE(36+ 3*NI)=D
ENDIF
C
IF (BUG) WRITE (6,*) 'STIFF=',SE(1),' A=',SE(4)
C
C----- TRANSFER ENERGIES FOR BOTH IOPT=3 AND 4.
400 EESE=SE(30)
EPSE=SE(33)
C
C----- TRANSFER DUCTILITIES AND EXCRUSION RATIOS FOR BOTH IOPT=3 AND 4.
DO 410 I=1,3
    DUCT(I)=MAX(SE(17+I),SE(20+I))
    EXCR(I+3)=SE(23+I+3)
410 EXCR(I)=SE(23+I)
C
RETURN
C
C===== DAMAGE INDEX =====
500 EESE =SE(30)
EPSE =SE(33)
NSEGS=SMAT(1)
NI =SMAT(2)
DMAX =SMAT(5+2*NSEGS)
DY =SMAT(4)
BDAM =SMAT(5)
P =SE(35+ 3*NI)
D =SE(36+ 3*NI)

D1 =SMAT(6+NSEGS)
IF (DY.LE.D1) THEN
    PY=SMAT(6)*DY/D1
ELSE
    DO 510 I=2,NSEGS
        P1=SMAT(4+I)
        P2=SMAT(5+I)
        D1=SMAT(4+I+NSEGS)
        D2=SMAT(5+I+NSEGS)
        IF (DY.GE.D1 .AND. DY.LE.D2) THEN
            PY=P1+(DY-D1)*(P2-P1)/(D2-D1)
            GO TO 520
        ENDIF
    510 CONTINUE
ENDIF
520 DAMAGE=ABS(D)/DMAX + BDAM / (PY*DMAX) * EPSE
C
RETURN
END

C
C=====
C     DEBUG UNIT(6),TRACE,SUBCHK,INIT,SUBTRACE
C     END DEBUG

```

```

=====
C== BENDING HYSTERESIS MODEL ..... HYST03 .....
=====
C
C INPUT VARIABLES
C P = CURRENT LOAD
C D = CURRENT DISPLACEMENT
C PL = LAST LOAD
C VEL = PRODUCT OF LAST AND CURRENT VELOCITY
C NB = NUMBER OF BACKBONE CURVE POINTS
C NI = MAXIMUM NUMBER OF SECONDARY LOOPS
C PC = CRACKING LOAD
C DC = CRACKING DISPLACEMENT
C PB(j) = BACKBONE CURVE LOADING POINT j, j=1,NB
C DB(j) = BACKBONE CURVE DISPLACEMENT POINT j,1,NB
C SI = INITIAL STIFFNESS, PC/DC
C
C OUTPUT VARIABLES
C .....AN INITIAL VALUE OF ZERO , OR FALSE
C IS REQUIRED FOR ALL OUTPUT VARIABLES...
C K = STIFFNESS
C RULE = RULE NUMBER, STORED IN THE FORMAT RN.DIR UPON EXIT OF
C      THIS SU_BROU_TINE
C A = LOAD LIMIT BEFORE NEXT RULE CHANGE, IN THE CURRENT DIR
C PMG = MAXIMUM PAST LOAD IN THE POSITIVE DIRECTION
C PMH = MAXIMUM PAST LOAD IN THE NEGATIVE DIRECTION
C DMG = MAXIMUM PAST DISPLACEMENT IN THE POSITIVE DIRECTION
C DMH = MAXIMUM PAST DISPLACEMENT IN THE NEGATIVE DIRECTION
C PR(I) = SECONDARY LOOP LOADING POINT, I
C DR(I) = SECONDARY LOOP DISPLACEMENT POINT, I
C FR(I) = SECONDARY LOOP FLAG
C IR = NUMBER OF SECONDARY LOOPS ACTIVE
C ALPHA1 = POSITIVE LOAD DEGRADING STIFFNESS FACTOR
C ALPHA2 = NEGATIVE LOAD DEGRADING STIFFNESS FACTOR
C BACKB = BACKBONE LOADING FLAG
C
C INTERNAL VARIABLES
C J = BACKBONE CURVE POINT # IN THE CURRENT DIRECTION
C JO = TEMPORARY VARIABLE
C I,IT = SECONDARY LOOP NUMBER
C      DIR = CURRENT DIRECTION
C      DIR=1, POSITIVE LOADING
C      DIR=2, POSITIVE UNLOADING
C      DIR=3, NEGATIVE LOADING
C      DIR=4, NEGATIVE UNLOADING
C DDIR = LAST DIRECTION
C IRULE = INTEGER VALUE OF RULE #
C LRULE = INTEGER VALUE OF LAST RULE #
C REVRSL = LOAD REVERSAL FLAG
C PRINT = PRINT FLAG, USED FOR DEBU_GGING
C AP = ABSOLUTE VALUE OF THE LOAD, P.
C PM = MAXIMUM PAST LOAD IN THE CURRENT DIRECTION
C DM = MAXIMUM PAST DISPLACEMENT IN THE CURRENT DIRECTION
C DMAX = MAXIMUM PAST DISPLACEMENT IN BOTH DIRECTIONS
C Q1 = ONE QUARTER OF PM, USED BY UNLOADING CURVES
C Q3 = THREE QUARTERS OF PM, USED BY UNLOADING CURVES
C DQ1 = DISPLACEMENT AT Q1 ON UNLOADING BRANCH
C DQ3 = DISPLACEMENT AT Q3 ON UNLOADING BRANCH
C D01 = INTERMEDIATE DISPLACEMENT INTERCEPT OF UNLOADING BRANCH
C D02 = INTERMEDIATE DISPLACEMENT INTERCEPT OF UNLOADING BRANCH
C DO = DISPLACEMENT INTERCEPT OF UNLOADING BRANCH
C DP = DIFFERENCE IN LOAD, USED FOR CALCULATING K
C DD = DIFFERENCE IN DISPLACEMENT, USED FOR CALCULATING K
C PX = LOAD INTERCEPT OF LOADING AND BACKBONE CURVE
C DX = DISPLACEMENT INTERCEPT OF LOADING AND BACKBONE CURVE
C PC3 = PC/3
C DC3 = DISPLACEMENT AT PC3

```

```

C P2,D2 = INTERSECTION OF LOADING AND UNLOADING CURVES
C PI,DI = SMALL LOOP UNLOADING POINTS
C X = MAXIMUM DISPLACEMENT
C K8 = STIFFNESS FROM RULE 8
C FLAG1 = UPPER SECONDARY LOOP FLAG
C FLAG2 = LOWER SECONDARY LOOP FLAG
C ALPHAAB = DEGRADING FACTOR FOR FIRST CYCLE
C ALPHAB = DEGRADING FACTOR FOR SUBSEQUENT CYCLES
C S = TEMPORARY STIFFNESS
C S1 = UNLOADING STIFFNESS FROM FS1
C S2 = UNLOADING STIFFNESS FROM FS2
C S3 = UNLOADING STIFFNESS FROM FS3
C SU = STIFFNESS BETWEEN CURRENT AND RELOADING POINT
C SO2 = STIFFNESS BETWEEN PA AND DO
C SO3 = STIFFNESS BETWEEN PB AND DO
C
C INTERNAL FUNCTIONS
C FD2 = DISPLACEMENT INTERCEPT OF LOADING AND UNLOADING CURVE
C FS1 = UNLOADING STIFFNESS WHEN P>.75 PMAX
C FS2 = UNLOADING STIFFNESS WHEN .75 PMAX > P > .25 PMAX
C FS3 = UNLOADING STIFFNESS WHEN .25 PMAX > P
C FSL = LOADING STIFFNESS WHEN .P < PC/3 WITHOUT REVERSAL...
C
C SU_BROU_TINES CALLED
C DIRECT = DETERMINES THE VALUES OF DIR AND DIRL
C INTSCT = DETERMINES THE INTERSECTION OF TWO LINES IN POINT-SLOPE
C FORM
C KMIN = DETERMINES THE STIFFNESS BASED ON DP,DD AND K_DEFAULT
C
SUBROUTINE HYST03(P,D,PL,DL,VEL,NB,NI,PC,DC,PB,DB,SI,CSE,
& K,RULE,DIR,A,PMG,PMH,DMG,DMH,BACKB,ALPHA1,ALPHA2,
& IR,SR1,SR2,SR3,SRM,PR,DR,FR,PRINT,
& SE,DY,ESE,PSE,PSEOLD,UPOS,UNEG,EXCR)
C
IMPLICIT REAL(A-H,K,O-Z)
IMPLICIT INTEGER(I,J,L-N)
INTEGER DIR,DIRL
CHARACTER*4 FR(1)
LOGICAL BACKB,REVRSL,PRINT,BTEST
DIMENSION PB(1),DB(1),PR(1),DR(1),UPOS(3),UNEG(3),EXCR(6),ESE(3)
DATA ALPHAAB/1.129/,ALPHAB/1.029/
C
FS1(X)= SI *(DC/X)**.294
FS2(X)= SI *(0.8344*(DC/X-1) +1)
FS3(X)= SI *(0.9092*(DC/X-1) +1)
FSL(X)= SI *(DC/X)**.285
FD2(X)= DM-.05*PM/(FS1(X))
C
C
1000 IF (PRINT) WRITE (6,1010) P,D,PL,DL,NB,NI,PC,DC,SI,K,
& RULE,A,PMG,PMH,DMG,DMH,BACKB,IR,DIR,
& SE,DY,ESE(1),PSE,PSEOLD,UPOS,CSE,UNEG,EXCR,VEL
1010 FORMAT(
& ' B1- P=','G13.5,' D=','G13.5,' PL=','G13.5,' DL=','G13.5/
& ' B1- NB=','G13.5,' NI=','G13.5,' PC=','G13.5,' DC=','G13.5/
& ' B1- SI=','G13.5,' K=','G13.5,' RULE=','G13.5,' A=','G13.5/
& ' B1- PMG=','G13.5,' PMH=','G13.5,' DMG=','G13.5,' DMH=','G13.5/
& ' B1- BACKB=','G13.5,' IR=','G13.5,' DIR=','G13.5,' SE=','G13.5/
& ' B1- DY=','G13.5,' ESE=','G13.5,' PSE=','G13.5,' PSOE=','G13.5/
& ' B1- UP1=','G13.5,' UP2=','G13.5,' UP3=','G13.5,' CSE=','G13.5/
& ' B1- UN1=','G13.5,' UN2=','G13.5,' UN3=','G13.5/
& ' B1- EX1=','G13.5,' EX2=','G13.5,' EX3=','G13.5/
& ' B1- EX4=','G13.5,' EX5=','G13.5,' EX6=','G13.5/' VEL=','G13.5)
IF (IR.GT.0.AND.PRINT) WRITE (6,1020) (I,PR(I),DR(I),FR(I),I=1,IR)
1020 FORMAT(
& (' B1- I=','G13.5,' PR=','G13.5,' DR=','G13.5,' FR=','A )
C

```

```

AP=ABS(P)
C..... DETERMINE IF ELASTIC
IF (RULE.EQ.0 .AND. AP.LT.PC ) THEN
  K=SI
  SE=K
  RETURN
ENDIF
C
C..... DETERMINE IF WALL IS INACTIVE , IF SO RETURN
IF (RULE.LT.0.0) RETURN
C
C..... DETERMINE CURRENT DIRECTION
LRULE=INT(RULE)
DIR =RDIR
CALL DIRECT(DIR,DIRL,P,PL,VEL)
RDIR =DIR
IF (PRINT) WRITE (6,1030) DIR,DIRL
1030 FORMAT
  & (' B1- DIR=',I8 , ' DIRL=',I8)
C
C..... DETERMINE MAXIMUM AND MINIMUM VALUES
PMG=MAX(P,PMG, PC)
DMG=MAX(D,DMG, DC)
PMH=MIN(P,PMH,-PC)
DMH=MIN(D,DMH,-DC)
DMAX=MAX(DMG,-DMH)
PMAX=MAX(PMG,-PMH)

C
C..... SET MAXIMUM AND MINIMUM VALUES...
IF (DIR.EQ.1 .OR. DIR.EQ.2 ) THEN
  PM=PMG
  DM=DMG
ELSE IF (DIR.EQ.3 .OR. DIR.EQ.4) THEN
  PM=PMH
  DM=DMH
ENDIF
C
C..... CALCULATE EQUIVALENT UNLOADING STIFFNESS FOR ENERGY...
IF (BACKB .OR. RULE.EQ.1.0) THEN
  S1=FS1(DMAX)
  S2=FS2(DMAX)
  S3=FS3(DMAX)
  DO =DM - PM*(DMH-DMG)/(PMH-PMG)
  Q1=PM/4
  Q3=3*Q1
  DQ3=DM - 0.25*PM/S1
  S02=KMIN((DQ3-DO),Q3,SI)
  DQ1=DQ3-0.50*PM/MAX(S2,S02)
  S03=KMIN((DQ1-DO),Q1,SI)
  SE= 0.5 * PM**2 /
&           (PM+Q3)*0.5*(DM-DQ3)
&           +(Q3+Q1)*0.5*(DQ3-DQ1)
&           +( Q1)*0.5*( Q1)/MAX(S3,S03) )
ENDIF
C
C..... CHECK TO SEE IF LAST RULE IS STILL IN EFFECT
IF (DIR.EQ.DIRL .AND.
& ((DIR.EQ.1 .AND. P.LT.A) .OR. (DIR.EQ.2 .AND. P.GT.A) .OR.
& (DIR.EQ.3 .AND. P.GT.A) .OR. (DIR.EQ.4 .AND. P.LT.A))) THEN
  RETURN
ENDIF
C
C..... CALC EXCURSION RATIO AT EVERY ZERO CROSSING...
C    IF (P*PL.LE.0) CALL DNE(0,UPOS,EXCR, DY,DLI,ESE,PSE,PSEOLD,CSE)
C
C..... ERASE SMALL LOOP FLAGS
IF (IR.GT.0) THEN

```

```

IT=IR
DO 10 I=1,IT
  IF ((FR(I).EQ.'L' .AND. ( P.LE.PR(I) .OR. D.LE.DR(I) )) .OR.
&   (FR(I).EQ.'7' .AND. ( P.GE.PR(I) .OR. D.GE.DR(I) ))) THEN
    IR=I-1
    GO TO 15
  ENDIF
10 CONTINUE
  ENDIF
15 I=IR+1
C
  IF (DIR.EQ.1 .OR. DIR.EQ.3 ) THEN
C..... LOADING RULES ..... RULES 1,6-11
C
C..... LOADING ON BACKBONE RULE 1
  1  IF (BACKB .OR. RULE.EQ.0.0) THEN
    K=0.
    DO 18 J=2,NB
      DD=DB(J)-ABS(D)
      DP=PB(J)-AP
      IF (AP.LT.PB(J) .AND. (DD*DP).GT.0.) THEN
        S=DP/DD
        IF (S.GT.K) THEN
          K=S
          A=SIGN(PB(J),P)
        ENDIF
      ENDIF
18 CONTINUE
  RULE=1
  BACKB=.TRUE.
  IR=0
  IF (DIR.EQ.1) THEN
    ALPHA1=ALPHAA
  ELSE
    ALPHA2=ALPHAA
  ENDIF
C
C..... LOADING AFTER UNLOADING
  ELSE
C..... RELOADING INSIDE SMALL LOOPS           RULE 11
  20 I=I-1
  IF (I.GT.0 ) THEN
    IF (.NOT.(( FR(I).EQ.'7' .AND. DIR.EQ.1 ) .OR.
&          ( FR(I).EQ.'L' .AND. DIR.EQ.3 ))) GO TO 20
    K=KMIN((D-DR(I)),(P-PR(I)),SI)
    A=PR(I)
    RULE=11+I/1000.

C
C..... INITIAL RELOADING BELOW PC/3
C..... WITH REVERSAL           RULE 8
  ELSE IF (AP.LT.(PC/3) )THEN
    BACKB=.FALSE.
    IF ((DIR.EQ.1 .AND. DIRL.EQ.4) .OR.
&      (DIR.EQ.3 .AND. DIRL.EQ.2)) THEN
      P2=.95*PM
      D2=FD2(DMAX)
      K=KMIN((D-D2),(P-P2),SI)
      K8=K
      A= P2
      RULE=8
    C
    PC3=SIGN(PC/3,PM)
    D01=DM-PM*(1./FS1(DMAX)+2./FS2(DMAX)+1./FS3(DMAX))/4.
    D02=DM - PM*(DMH-DMG)/(PMH-PMG)
    IF (DIR.EQ.1) D0=MAX(D01,D02)
    IF (DIR.EQ.3) D0=MIN(D01,D02)
    DC3=D0+PC3/FSL(DMAX)
  ENDIF

```

```

S=KMIN((D-DC3),(P-PC3),SI)
IF (S.GT.K) THEN
  K=S
  A= PC3
  RULE=8.1
ENDIF
C
C..... WITH REVERSAL, FAR SIDE LOADING RULE 9
IF ((DIR.EQ.1 .AND. D.LT.0) .OR.
&      (DIR.EQ.3 .AND. D.GT.0)) THEN
  K=K8
  DO 40 J=2,NB
    IF ( PB(J) .LT. ABS(PM) ) GO TO 40
    DD= -SIGN(DB(J),D)-D
    DP= -SIGN(PB(J),D)-P
    IF ( (DD*DP).LE.0.) GO TO 40
    S=DP/DD
    IF (S.GT.K .AND. S.LE.SI) THEN
      K=S
      A=SIGN(PB(J),PM)
      RULE=9
      BACKB=.TRUE.
    ENDIF
  40  CONTINUE
ENDIF
C
C..... WITHOUT REVERSAL RULE 6
ELSE
  K=FSL(DMAX)
  A= SIGN((PC/3),PM)
  RULE=6
ENDIF
C
C..... MIDRANGE RELOADING CURVE RULE 7
ELSE IF (AP.LT.ABS(.95*PM) ) THEN
  BACKB=.FALSE.
  P2=.95*PM
  D2=FD2(DMAX)
  K=KMIN((D-D2),(P-P2),SI)
  A=P2
  RULE=7
C
C..... LOADING TOWARDS THE BACKBONE CURVE RULE 10
ELSE
  BACKB=.TRUE.
  IF (AP.GE.ABS(PM) .OR. (ABS(DM)).LE.DC) GO TO 1
  IR=0
  IF (DIR.EQ.1) THEN
    IF (ALPHA1.NE.ALPHAA .AND. ALPHA1.NE.ALPHAB)
&        ALPHA1=ALPHAA
    DD=ALPHA1*DM-D
  ELSE
    IF (ALPHA2.NE.ALPHAA .AND. ALPHA2.NE.ALPHAB)
&        ALPHA2=ALPHAA
    DD=ALPHA2*DM-D
  ENDIF
  DP=PM-P
  IF ((DP*DD).GT.0) THEN
    K=MIN( (DP/DD),SI)
  ELSE
    K=SI
  ENDIF
  DO 50 J=2,NB
    IF ( PB(J).LE.ABS(PM) ) GO TO 50
    JO=J-1
    DD=DB(J)-DB(JO)
    DP=PB(J)-PB(JO)

```

```

        IF ((DP*DD).LE.0.) GO TO 50
        CALL INTSCT(DX,PX,D,P,K,SIGN(DB(J),P),
&           SIGN(PB(J),P),(DP/DD) )
        PX=PX
        DX=DX
        IF (ABS(DX).GE.DB(J0) .AND. ABS(DX).LE.DB(J).AND.
&           ABS(PX).GT.ABS(PM) .AND. PM*PX.GT.0) THEN
          IF (AP.GT.ABS(PX)) GO TO 1
          A= PX
          RULE=10
          IF (DIR.EQ.1) THEN
            ALPHA1=ALPHAB
          ELSE
            ALPHA2=ALPHAB
          ENDIF
          GO TO 100
          ENDIF
50      CONTINUE
        GO TO 1
      ENDIF
    ENDIF
    C
    C
    ELSE
C... UNLOADING RULES ..... RULES 2-5
    C
    C..... INITILIZE VALUES
      BACKB=.FALSE.
      S1=FS1(DMAX)
      S2=FS2(DMAX)
      S3=FS3(DMAX)
      D0 =DM - PM*(DMH-DMG)/(PMH-PMG)
      Q1=PM/4
      Q3=3*Q1
      DQ3=DM -0.25*PM/S1
      S02=KMIN((DQ3-D0),Q3,S1)
      DQ1=DQ3-0.50*PM/MAX(S2,S02)
      S03=KMIN((DQ1-D0),Q1,S1)
      SU=0.
    C
    C..... UNLOADING INSIDE SMALL POSITIVE LOOPS RULE 5
      I=IR+1
70      I=I-1
      IF (I.GT.0) THEN
        IF (.NOT.((DIR.EQ.2 .AND. FR(I).EQ.'L') .OR.
&           (DIR.EQ.4 .AND. FR(I).EQ.'7')) ) GO TO 70
        IF ((DIR.EQ.2 .AND.( (P.GT.Q3 .AND. PR(I).GT.Q3) .OR.
&           (Q3.GE.P .AND. P.GT.Q1 .AND. PR(I).GT.Q1) .OR.
&           (Q1.GE.P .AND. PR(I).GT.0 )) ) .OR.
&           (DIR.EQ.4 .AND.( (P.LT.Q3 .AND. PR(I).LT.Q3) .OR.
&           (Q3.LE.P .AND. P.LT.Q1 .AND. PR(I).LT.Q1) .OR.
&           (Q1.LE.P .AND. PR(I).LT.0 )) ) ) THEN
          K=(PR(I)-P)/(DR(I)-D)
          IF (K.LE.0 .OR. K.GT.SI) GO TO 70
          A=PR(I)
          RULE=5+I/1000.
          GO TO 100
        ELSE
          SU=KMIN((DR(I)-D),(PR(I)-P),SI)
        ENDIF
      ENDIF
    C
    C..... CALC DUCTILITY AND EXCURSION RATIO..
      IF (RULE.EQ.1 .OR. RULE.GT.5) THEN
        IF (DIR.EQ.2) THEN
          DLI= MAX( D , DL )

```

```

C      CALL DNE(1,UPOS,EXCR, DY,DLI,ESE(2),PSE,PSEOLD,CSE)
C      ELSE IF (DIR.EQ.4) THEN
C          DLI= MIN( D , DL )
C          CALL DNE(1,UNEG,EXCR,-DY,DLI,ESE(3),PSE,PSEOLD,CSE)
C      ENDIF
C      ENDIF
C
C..... UNLOADING ON THE TOP SEGMENT RULE 2
IF(AP.GT.ABS(Q3)) THEN
    K=MAX(S1,SU)
    A=Q3
    RULE=2
C..... UNLOADING ON THE MIDDLE SEGMENT RULE 3
ELSE IF(AP.GT.ABS(Q1)) THEN
    K=MAX(S2,S02,SU)
    A=Q1
    RULE=3
C..... UNLOADING ON THE BOTTOM SEGMENT RULE 4
ELSE
    K=MAX(S3,S03,SU)
    A=0.
    RULE=4
ENDIF
ENDIF
C..... SAVE REVERSAL POINTS FOR SMALL LOOPS.....
100 IRULE=INT(RULE)
REVRSL=IRULE.EQ.1.OR.IRULE.EQ.10.OR.LRULE.EQ.1.OR.LRULE.EQ.10
IF ((DIRL.EQ.1 .AND. DIR.EQ.2 .AND. .NOT. REVRSL)
& .OR. (DIRL.EQ.4 .AND. DIR.EQ.3) ) THEN
    IF (IR.LT.NI) THEN
        IR=IR+1
        PR(IR)=P
        DR(IR)=D
        FR(IR)='7'
    ENDIF
ELSE IF ((DIRL.EQ.3 .AND. DIR.EQ.4 .AND. .NOT. REVRSL)
& .OR. (DIRL.EQ.2 .AND. DIR.EQ.1) ) THEN
    IF (IR.LT.NI) THEN
        IR=IR+1
        PR(IR)=P
        DR(IR)=D
        FR(IR)='L'
    ENDIF
ENDIF
IF (PRINT) WRITE (6,1040) S1,S2,S3
1040 FORMAT(
& ' B1- S1=',G13.5,' S2=',G13.5,' S3=',G13.5,' =',G13.5)

IF ((1.05*SI).GT.K .AND. K.GT.0 ) RETURN
C
K=0
RULE==RULE
RETURN
C
END
C=====
C - DIRECTION OF LOADING .....
C DEBUG UNIT(6),SUBCHK,SUBTRACE
C END DEBUG
C P = CURRENT LOAD
C PL = LAST LOAD
C D = CURRENT DISPLACEMENT
C DIR = CURRENT DIRECTION
C     DIR=1, POSITIVE LOADING
C     DIR=2, POSITIVE UNLOADING
C     DIR=3, NEGATIVE LOADING

```

```

C      DIR=4, NEGATIVE UNLOADING
C DIRL = LAST DIRECTION
C VEL = PRODUCT OF LAST AND CURRENT VELOCITIES

SUBROUTINE DIRECT(DIR,DIRL,P,PL,VEL)
IMPLICIT REAL(A-H,O-Z)
IMPLICIT INTEGER(I-N)
INTEGER DIR,DIRL
LOGICAL BTTEST

IF (P.GT.0) THEN
  IF (P.GT.PL .AND. PL.GT.0) THEN
    DIRL=1
  ELSE IF (P.GT.PL .AND. PL.LT.0) THEN
    DIRL=4
  ELSE IF (P.LT.PL) THEN
    DIRL=2
  ELSE
    DIRL=DIR
  ENDIF
ELSE IF (P.LT.0) THEN
  IF (P.LT.PL .AND. PL.LT.0) THEN
    DIRL=3
  ELSE IF (P.LT.PL .AND. PL.GT.0) THEN
    DIRL=2
  ELSE IF (P.GT.PL) THEN
    DIRL=4
  ELSE
    DIRL=DIR
  ENDIF
ELSE
  IF (PL.LT.0) THEN
    DIRL=4
  ELSE IF (PL.GT.0) THEN
    DIRL=2
  ELSE
    DIRL=DIR
  ENDIF
ENDIF

IF (DIRL.EQ.1 .OR.DIRL.EQ.0) THEN
  IF (VEL.GT.0) THEN
    DIR=1
  ELSE
    DIR=2
  ENDIF

ELSE IF (DIRL.EQ.2) THEN
  IF (VEL.GT.0) THEN
    IF (P.GT.0) THEN
      DIR=2
    ELSE
      DIR=3
    ENDIF
  ELSE
    DIR=1
  ENDIF

ELSE IF (DIRL.EQ.3) THEN
  IF (VEL.GT.0) THEN
    DIR=3
  ELSE
    DIR=4
  ENDIF

ELSE IF (DIRL.EQ.4) THEN
  IF (VEL.GT.0) THEN

```

```

      IF (P.LT.0) THEN
        DIR=4
      ELSE
        DIR=1
      ENDIF
      ELSE
        DIR=3
      ENDIF
      ELSE
        WRITE (6,5)
      5 FORMAT(5X,'ER','ROR IN SUBROUTINE DIRECT, DIRL.NE. 1,2,3,OR 4')
        WRITE (6,10) DIR,DIRL,P,PL,VEL
      ENDIF
      IF (DIR.EQ.0) DIR=1

C WRITE (6,10) DIR,DIRL,P,PL,VEL
      10 FORMAT (5X,'*** IN DIRECT ',1X,
      & ' DIR=',I4,' Dirl=',I4,' P=',F8.3,' PL=',F8.3,' VEL=',F10.3)

      RETURN
    END
C=====
C
C - INTERSECTION OF TWO LINES IN POINT SLOPE FORM .....
C DEBUG UNIT(6),SUBCHK,SUBTRACE
C END DEBUG
C X = X COORDINATE OF INTERSECTION
C Y = Y COORDINATE OF INTERSECTION
C X1 = X COORDINATE OF LINE 1
C Y1 = Y COORDINATE OF LINE 1
C S1 = SLOPE OF LINE 1
C X2 = X COORDINATE OF LINE 2
C Y2 = Y COORDINATE OF LINE 2
C S2 = SLOPE OF LINE 2

SUBROUTINE INTSCT(X,Y,X1,Y1,S1,X2,Y2,S2)
IMPLICIT REAL(A-H,O-Z)
IMPLICIT INTEGER(L-N)
LOGICAL BTEST
IF (S1.NE.S2) THEN
  B1= Y1 - S1*X1
  B2= Y2 - S2*X2
  X=(B1-B2)/(S2-S1)
  Y=(B1*S2-B2*S1)/(S2-S1)
ELSE
  WRITE (6,10) X1,Y1,S1,X2,Y2,S2
  10 FORMAT ('***** ER','ROR IN INTSCT.....',1X,
  & ' S1=S2, NO SOLN, THUS SET X=Y=0.',/
  & ' X1=',1P,G15.5,' Y1=',G15.5,' S1=',G15.5/
  & ' X2=',1P,G15.5,' Y2=',G15.5,' S2=',G15.5/)
  X=0
  Y=0
C CALL ERRTRA
ENDIF
CC  WRITE (6,5) X1,Y1,S1,B1,X2,Y2,S2,B2,X,Y
CC 5  FORMAT (' IN INTSCT.....',/
CC & ' X1=',1P,G15.5,' Y1=',G15.5,' S1=',G15.5,' B1=',G15.5/
CC & ' X2=',1P,G15.5,' Y2=',G15.5,' S2=',G15.5,' B2=',G15.5/
CC & ' X=',1P,G15.5,' Y=',G15.5/)
RETURN
END
C=====
C
C - KMIN - CALCULATES STIFFNESS BASED ON DX AND DY .....
C DEBUG UNIT(6),SUBCHK,SUBTRACE
C END DEBUG
C KMIN =

```

```

C DD = CHANGE IN DISPLACEMENT
C DP = CHANGE IN LOAD
C SI = MAXIMUM AND DEFULT STIFFNESS
REAL FUNCTION KMIN(DD,DP,SI)
LOGICAL BTTEST
IF ((DD*DP).GT. 0.00) THEN
  KMIN=MIN((DP/DD),SI)
ELSE
  KMIN=SI
ENDIF
RETURN
END

```

Input Data:

```

1 1 |IELNO MAT
'BENDING' 8 10 0.160 0.2 |TYPE NSEG NI DY BDAM
  6.120 8.080 9.950 12.010 13.670 15.490 15.910 30. |SMAT
  0.065 0.120 0.181 0.485 0.731 1.069 1.155 10. |SMAT
0. 1.0 50 |DMIN DMAX NUMB
1.0 -1.0 100 |DMIN DMAX NUMB
-1.0 1.10 100 |DMIN DMAX NUMB
1.10 -0.5 50 |DMIN DMAX NUMB
-0.5 1.2 100 |DMIN DMAX NUMB
1.2 1.10 10 |DMIN DMAX NUMB

```

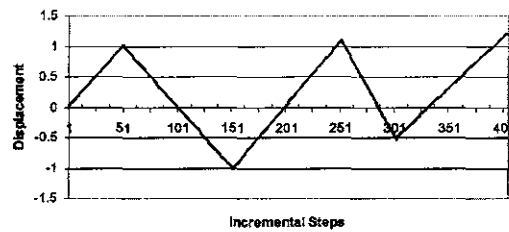
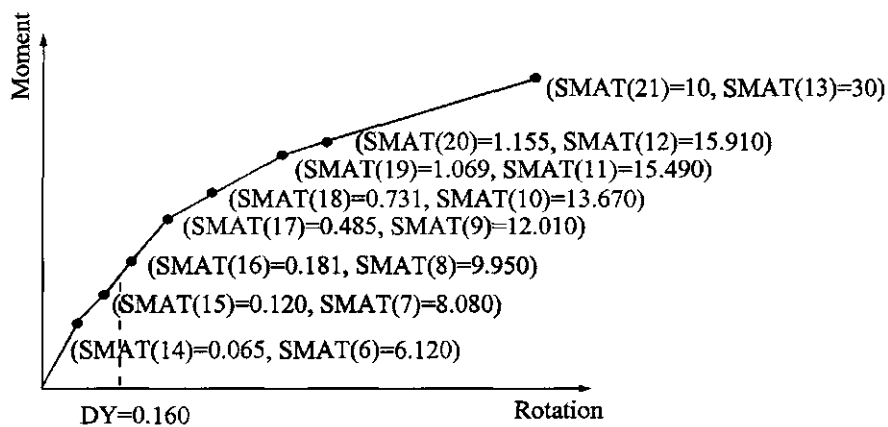
Output Data:

```

BEND1 HYSTERESIS MODEL DATA - UNIT LENGTH MEMBER
=====
BACKBONE CURVE POINTS - MATL NI   DY     BETA    MOMENT   ROTATION
                   1 10 0.160000  0.200000  6.12000  0.650000E-01
                                         8.08000  0.120000
                                         9.95000  0.181000
                                         12.0100  0.485000
                                         13.6700  0.731000
                                         15.4900  1.06900
                                         15.9100  1.15500
                                         30.0000  10.0000

STIFFNESS   LOAD     DISP.    RULE
63.99350   1.39350  0.02000  4.0
53.14461   2.45639  0.04000  11.0
53.14461   3.51928  0.06000  11.0
.
.
.
4.85335   15.51975  1.21700  10.0
39.78865   15.12186  1.19000  2.0

```



Diagrams Represent Input Data for Appendix L (Bending)

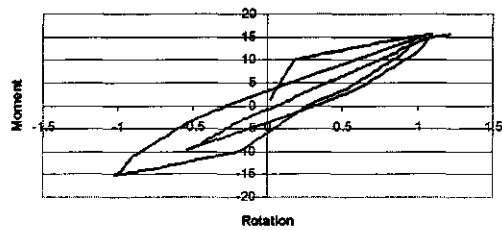
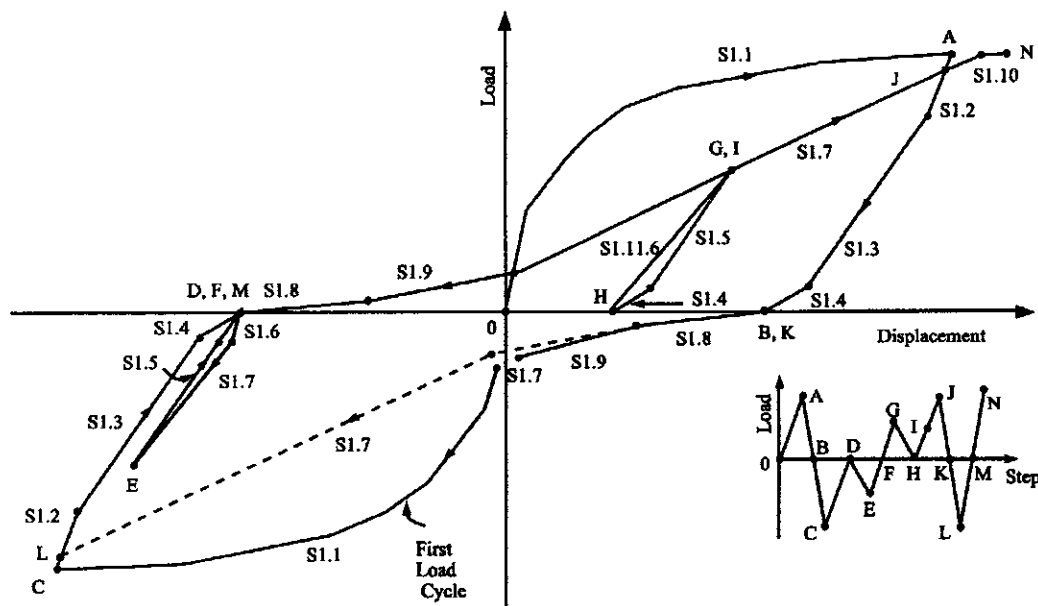


Diagram Represents Output Solution for Appendix L (Bending)

SHEAR: Low-Rise Shear Wall Cheng-Mertz Hysteresis Model



```

C=====
C THIS IS A TYPICAL MAIN PROGRAM FOR CALLING CHENG-MERTZ SHEAR
C HYSTERESIS MODEL SUBROUTINE NAMED "MAT04". THE PARAMETERS
C TRANSFERRED INTO SUBROUTINE MAT04 ARE SHOWN AS FOLLOWS.
C SINCE MAT04 IS A GENERAL PURPOSE SUBROUTINE, SOME PARAMETERS
C HAVE BEEN RESERVED AND NOT USED. THEREFORE THEY ARE ASSIGNED
C WITH A NUMBER "1" IN THIS DEMONSTRATION AS A MAIN PROGRAM.
C=====
C VARIABLES:
C MAT = USER DEFINED MATERIAL ID NUMBER
CIELNO = USER DEFINED ELEMENT ID NUMBER
C P = CURRENT LOAD
C PL = PREVIOUS STEP LOAD
C D = CURRENT DISPLACEMENT
C DL = PREVIOUS STEP DISPLACEMENT
C V = DUMMY VARIABLE
C VL = DUMMY VARIABLE
C DUCT = RESERVED DUCTILITY ARRAY (NOT USED)
C EXCR = RESERVED EXCURSION ARRAY (NOT USED)
C DAMAGE= RESERVED VARIABLE FOR DAMAGE INDEX (NOT USED)
C ESE = RESERVED VARIABLE FOR ELASTIC STRAIN ENERGY(NOT USED)
C EPSE = RESERVED VARIABLE FOR PLASTIC STRAIN ENERGY(NOT USED)
C LELEM = 32+3*NI+2 , WHERE NI=NUMBER OF SMALL AMPLITUDE LOOPS
C LMAT = 5+2*NSEG, WHERE NSEG=NUMBER OF BACKBONE SEGMENTS
C SMAT = MATERIAL ARRAY, SMAT(LMAT)

```

```

C SE = ELEMENT ARRAY, SE(LELEM)
C IOPT = 1 INITIALIZE MATERIAL
C      2 GET INITIAL STIFFNESS
C      3 GET MEMBER STIFFNESS
C ERR = DUMMY LOGICAL VARIABLE
C FIRST = LOGICAL VARIABLE. IF FIRST=.TRUE., THE MATERIAL
C      PROPERTIES OF SHEAR HYSTERESIS MODEL ARE PRINTED.
C PRINT = DUMMY LOGICAL VARIABLE
C BUG = LOGICAL VARIABLE. IF BUG=.TRUE., THE HYSTERESIS
C      ENVELOPE CONTROL POINTS ARE PRINTED.
C BDAM = RESERVED PARAMETER FOR ANG's DAMAGE INDEX
C=====
LOGICAL ERR, FIRST, PRINT, BUG
DIMENSION SE(100), SMAT(9), DUCT(3), EXCR(6)
CHARACTER*80 TYPE
C=====
C DEFINE EXTERNAL FILE UNITS FOR INPUT DATA AND OUTPUT
C=====
OPEN(UNIT=5,FILE=STRING(8))
OPEN(UNIT=6,FILE=STRING(9))
C
C=====
C
IOPT=1
ERR=.FALSE.
FIRST=.TRUE.
PRINT = .FALSE.
BUG=.FALSE.
READ(5,*)IELNO, MAT
C
C INPUT MATERIAL PROPERTIES
C CALL MAT04
C & (IOPT ,IELNO ,ERR ,FIRST ,PRINT ,BUG ,
C & MAT ,SE ,P,PL,D,DL,V,VL,LELEM,LMAT,
C & SMAT,EESE,EPSE,DUCT,EXCR,DAMAGE)
CALL MAT04
& (IOPT ,IELNO ,ERR ,FIRST ,PRINT ,BUG ,
& MAT ,SE ,P,PL,D,DL,V,VL,LELEM,LMAT,
& SMAT,DUMMY,DUMMY,DUCT,EXCR,DUMMY)
C
C INITIALIZE ELEMENT STIFFNESS
IOPT=2
BUG=.FALSE.
C
CALL MAT04
& (IOPT ,IELNO ,ERR ,FIRST ,PRINT ,BUG ,
& MAT ,SE ,P,PL,D,DL,V,VL,LELEM,LMAT,
& SMAT,DUMMY,DUMMY,DUCT,EXCR,DUMMY)
C
STIF=SE(1)
BUG=.FALSE.
C
WRITE(6,*)' STIFFNESS LOAD DISP. RULE'
C READ DISPLACEMENT
F=0.
FL=0.
D=0.
DL=0.
C
800  READ(5,*, END=5000)DMIN, DMAX, NUMB
      DD=(DMAX-DMIN)/NUMB
700  DL=D
      D=D+DD
      FL=F
      F=F+STIF*DD
      P=F
      PL=FL

```

```

      IOPT=3
      CALL MAT04
      & (IOPT ,IELNO ,ERR ,FIRST ,PRINT ,BUG ,
      & MAT ,SE ,P,PL,D,DL,V,VL,LELEM,LMAT,
      & SMAT,DUMMY,DUMMY,DUCT,EXCR,DUMMY)
C
      F=P
      STIF=SE(1)
      WRITE(6,98)SE(1), F, D, SE(2)
98 FORMAT(3F15.5, 3X, F4.1)
      IF (DMAX .GT. 0) THEN
        IF (D .LE. DMAX) THEN
          GO TO 700
        ELSE IF (D .GT. DMAX) THEN
          D=DMAX
          GO TO 800
        ENDIF
      ELSE IF (DMAX .LE. 0) THEN
        IF (D .GE. DMAX) THEN
          GO TO 700
        ELSE IF (D .LT. DMAX) THEN
          D=DMAX
          GO TO 800
        ENDIF
      ENDIF
C
5000 CLOSE(5)
      CLOSE(6)
      STOP
      END
C=====
C     DEBUG UNIT(6),TRACE,SUBCHK,INIT,SUBTRACE
C     END DEBUG
C=====
SUBROUTINE MAT04
      & (IOPT ,IELNO ,ERR ,FIRST ,PRINT ,BUG ,
      & MAT ,SE ,P,PL,D,DL,V,VL,LELEM,LMAT,
      & SMAT,EESE,EPSE,DUCT,EXCR,DAMAGE)
C
      IMPLICIT REAL(A-H,O-Z)
      LOGICAL ERR,FIRST,PRINT,BUG
      LOGICAL BTTEST
      DIMENSION SE(100),SMAT(20),DUCT(3),EXCR(6)
C
      DIMENSION COPY(100)
      CHARACTER*4 SSE(100)
C
      CHARACTER*80 TYPE
C
      EQUIVALENCE (SSE(1),COPY(1))
C
      IF (IOPT.NE.1) LELEM=32+3*SMAT(2) +2
      IF (IOPT.EQ.0) RETURN
C
C-----
C VARIABLES:
C-----
C----- GLOBAL VARIABLES
C IOPT = 1, INITIALIZE MATERIAL
C      = 2, GET STIFFNESS
C RINPUT = INPUT DATA
C SMAT = INTERNAL STORAGE
C SE = OUTPUT STIFFNESS
C-----
C      ---- SHEAR1 DATA ----
C      SMAT(1)= NSEGS, NUMBER OF BACKBONE SEGMENTS
C      SMAT(2)= NI, NUMBER OF SMALL AMPLITUDE LOOPS

```

```

C      SMAT(3)= CSE, CONSTAIN STRAIN ENERGY...
C      SMAT(4)= DY, YEILD DISPLACEMENT
C      SMAT(4+I)= PP, BACKBONE SHEAR FOR POINT I
C      SMAT(4+I+NSEG)= DP, BACKBONE DISPLACEMENT FOR POINT I
C      SMAT(5+2*NSEG)= BDAM BETA FOR DAMAGE INDEX
C
C      GO TO (100,200,300,400,500),IOPT
C
100 CONTINUE
C
C----- INPUT DATA FOR SHEAR1 HYSTERESIS MODEL -----C
C
C NSEG = NUMBER OF BACKBONE SEGEMENTS          C
C NI = NUMBER OF SMALL LOOP POINTS            C
C PP = BACKBONE LOAD                         C
C DP = BACKBONE DISPLACEMENT                  C
C-----C
READ (5,*) TYPE ,NSEG,NI,DY,BDAM
READ (5,*) ( SMAT(4+I ),I=1,NSEG)
READ (5,*) ( SMAT(4+I+NSEG),I=1,NSEG)
LELEM = 32+3*NI +2
LMAT = 5+2*NSEG
SMAT(1)=NSEG
SMAT(2)=NI
SMAT(4)=DY
SMAT(5+2*NSEG)=BDAM
C----- CALC CONSTANT STRAIN ENERGY....
DL=0
PL=0
DO 10 I=1,NSEG
P=SMAT(4+I)
D=SMAT(4+I+NSEG)
IF (D.LE.DY) THEN
  CSE=CSE + 0.5*(P+PL)*(D-DL)
  PL=P
  DL=D
ELSE IF (D.EQ.DL) THEN
  GO TO 20
ELSE
  PY=PL+ (DY-DL)*(P-PL)/(D-DL)
  CSE=CSE + 0.5*(PY+PL)*(DY-DL)
  GO TO 20
ENDIF
10 CONTINUE
20 SMAT(3)=CSE
C
C
IF (FIRST .OR. BUG) WRITE (6,65)
WRITE (6,67) MAT,NI,DY,BDAM,(SMAT(4+K),SMAT(4+K+NSEG),K=1,NSEG)
WRITE (6,*) ' '
65 FORMAT(///' SHEAR1 HYSTERESIS MODEL DATA - UNIT LENGTH MEMBER'
& /' =====',
& //' BACKBONE CURVE POINTS - MAT. NI DY ',
& & 5X,'BETA',6X, 3X,' STRESS',8X,' STRAIN')
67 FORMAT ( (28X,2I4,2X,4G15.6)/(68X,2G15.6))
C
RETURN
C===== GET STIFFNESS TERMS =====
200 CONTINUE
C --- SHEAR1 MODEL DATA STORAGE FOR MEMBER ---
C SE( 1)= K
C SE( 2)= RULE
C SE( 3)= DIR
C SE( 4)= A
C SE( 5)= PMG
C SE( 6)= PMH
C SE( 7)= DMG

```

```

C SE( 8)= DMH
C SE( 9)= BACKB
C SE(10)= SR1
C SE(11)= SR2
C SE(12)= SR3
C SE(13)= SRM
C SE(14)= IR
C SE(15)= S_EQ_UNLOAD
C SE(16)= UPOS(1)
C SE(17)= UPOS(2)
C SE(18)= UPOS(3)
C SE(19)= UNEG(1)
C SE(20)= UNEG(2)
C SE(21)= UNEG(3)
C SE(22)= EXCR(1)
C SE(23)= EXCR(2)
C SE(24)= EXCR(3)
C SE(25)= EXCR(4)
C SE(26)= EXCR(5)
C SE(27)= EXCR(6)
C SE(28)= ESE
C SE(29)= ESE
C SE(30)= ESE
C SE(31)= PSE
C SE(32)= PSE_OLD
C SE(32+1 )=PR( 1)
C SE(32+ NI)=PR(NI)
C SE(32+1+ NI)=DR( 1)
C SE(32+ 2*NI)=DR(NI)
C SE(32+1+2*NI)=FR( 1)
C SE(32+ 3*NI)=FR(NI)
C SE(33+ 3*NI)=P_MAX
C SE(34+ 3*NI)=D_MAX
C
NSEG=SMAT(1)
NI =SMAT(2)
SI = SMAT(5)/SMAT(5+NSEG)
J1=NSEG+5
J3=NI+33
J4=2*NI+33
J5=3*NI+33-1 +2
DO 210 I=1,J5
210 SE(I)=0
C
DO 189 I=J4, J4+NI-1
    COPY(I)=SE(I)
189 CONTINUE
C
CALL HYSTO4( P, D,PL,DL, V ,NSEG,NI,BUG,
&   SMAT( 5),SMAT(J1),SMAT( 5),SMAT(J1),SI,SMAT(3),SMAT(4),
&   SE( 1) ,SE( 2) ,SE( 3) ,SE( 4) ,SE( 5) ,SE( 6) ,
&   SE( 7) ,SE( 8) ,SE( 9) ,SE(10) ,SE(11) ,SE(12) ,
&   SE(13) ,SE(14) ,SE(15) ,SE(16) ,SE(19) ,SE(22) ,
&   SE(28) ,SE(31) ,SE(32) ,SE(33) ,SE(J3) ,SSE(J4) )
C
DO 89 I=J4, J4+NI-1
    SE(I)=COPY(I)
89 CONTINUE
C
RETURN
C
===== GET STIFFNESS TERMS =====
300 CONTINUE
C      SE( 4)= A
NSEG=SMAT(1)
NI =SMAT(2)
SI = SMAT(5)/SMAT(5+NSEG)

```

```

J1=NSEG+5
J3=NI+33
J4=2*NI+33
DVEL=V*VL
C SET VELOCITY FLAG TO 1 TO REMOVE INFL OF HIGH FREQ VELOC
DVEL = 1
ICYC=0
IF (BUG) THEN
  WRITE (6,*)
  WRITE (6,*)
  WRITE (6,*)
ENDIF
310 STIFF=SE(1)
P=PL+(D-DL)*STIFF
A=SE(4)
IF (A.EQ.0 .AND. SE(2).EQ.0) THEN
  A=SIGN(SMAT(5),P)
  IF (P.LT.PL .AND. PL.GT.0 .AND. P.GT.0) A=0
  IF (P.GT.PL .AND. PL.LT.0 .AND. P.LT.0) A=0
ENDIF
ICYC=ICYC+1
IF (BUG) THEN
  WRITE (6,*)
  WRITE (6,*)
ENDIF
C
C----- IS P WITHIN LIMITS ?
IF (ICYC.GT.10) THEN
  WRITE (6,*)
ELSE IF ((PL.LE.P .AND. P.LT.A) .OR. (PL.GE.P .AND. P.GT.A) .OR.
& (DL.EQ.D)) THEN
  IF (BUG) WRITE (6,*)
C      CALL STRENG (SE(28),SE(31),SE(32),P,PL,D,DL,SE(1),SE(15) )
C
DO 199 I=J4, J4+NI-1
  COPY(I)=SE(I)
199 CONTINUE
C
CALL HYSTO4( P, D,PL,DL,DVEL,NSEG,NI,BUG,
& SMAT( 5),SMAT(J1),SMAT( 5),SMAT(J1),SI,SMAT(3),SMAT(4),
& SE( 1) ,SE( 2) ,SE( 3) ,SE( 4) ,SE( 5) ,SE( 6) ,
& SE( 7) ,SE( 8) ,SE( 9) ,SE(10) ,SE(11) ,SE(12) ,
& SE(13) ,SE(14) ,SE(15) ,SE(16) ,SE(19) ,SE(22) ,
& SE(28) ,SE(31) ,SE(32) ,SE(33) ,SE(J3) ,SSE(J4) )
C
DO 99 I=J4, J4+NI-1
  SE(I)=COPY(I)
99 CONTINUE
C
C----- IS P GREATER THAN LIMITS ?
ELSE IF ((PL.LE.A .AND. A.LE.P) .OR. (PL.GE.A .AND. A.GE.P)).AND.
& (STIFF.NE.0.00) THEN
  D1=DL+(A-PL)/STIFF
  P1=A
C      CALL STRENG (SE(28),SE(31),SE(32),P1,PL,D1,DL,SE(1),SE(15) )
  DL=D1
  PL=P1
C  PI=PL+(P-PL)*.001
C  DI=DL+(D-DL)*.001
  IF (ABS(P-PL).GT. 0.0005*ABS(P+PL)) THEN
    PI=PL+(P-PL)*.001
    DI=DL+(D-DL)*.001
  ELSE
    PI=P
    DI=D
  ENDIF
  IF (BUG) THEN

```

```

      WRITE (6,*) 'C---- IS P GREATER THAN LIMITS ? '
      WRITE (6,*) 'PL,DL=',PL,DL
      WRITE (6,*) 'PI,DI=',PI,DI
      ENDIF
C
      DO 179 I=J4, J4+NI-1
         COPY(I)=SE(I)
      179 CONTINUE
C
      CALL HYSTO4(PI,DI,PL,DL,1.00,NSEG,NI,BUG,
      &   SMAT( 5),SMAT(J1),SMAT( 5),SMAT(J1),SI,SMAT(3),SMAT(4),
      &   SE( 1),SE( 2),SE( 3),SE( 4),SE( 5),SE( 6),
      &   SE( 7),SE( 8),SE( 9),SE(10),SE(11),SE(12),
      &   SE(13),SE(14),SE(15),SE(16),SE(19),SE(22),
      &   SE(28),SE(31),SE(32),SE(33),SE(J3),SSE(J4) )
C
      DO 79 I=J4, J4+NI-1
         SE(I)=COPY(I)
      79 CONTINUE
C
      GO TO 310
C---- IS P LESS THAN LIMITS ?
      ELSE IF ((P.LT.PL .AND. PL.LE.A) .OR. (P.GT.PL .AND. PL.GE.A))THEN
C     PI=PL+(P-PL)*.001
C     DI=DL+(D-DL)*.001
      IF (ABS(P-PL).GT. 0.0005*ABS(P+PL)) THEN
         PI=PL+(P-PL)*.001
         DI=DL+(D-DL)*.001
      ELSE
         PI=P
         DI=D
      ENDIF
      IF (BUG) THEN
         WRITE (6,*) 'C---- IS P LESS THAN LIMITS ? '
         WRITE (6,*) 'PI,DI=',PI,DI
      ENDIF
C
      DO 169 I=J4, J4+NI-1
         COPY(I)=SE(I)
      169 CONTINUE
C
      CALL HYSTO4(PI,DI,PL,DL,1.00,NSEG,NI,BUG,
      &   SMAT( 5),SMAT(J1),SMAT( 5),SMAT(J1),SI,SMAT(3),SMAT(4),
      &   SE( 1),SE( 2),SE( 3),SE( 4),SE( 5),SE( 6),
      &   SE( 7),SE( 8),SE( 9),SE(10),SE(11),SE(12),
      &   SE(13),SE(14),SE(15),SE(16),SE(19),SE(22),
      &   SE(28),SE(31),SE(32),SE(33),SE(J3),SSE(J4) )
C
      DO 69 I=J4, J4+NI-1
         SE(I)=COPY(I)
      69 CONTINUE
C
      GO TO 310
      ENDIF
C
      IF (BUG) WRITE (6,*) 'STIFF=',STIFF,' A=',SE(4)
C
C----- SAVE MAXIMUM DISPL AND LOAD
      IF (ABS(D).GT.ABS(SE(34+3*NI))) THEN
         SE(33+ 3*NI)=P
         SE(34+ 3*NI)=D
      ENDIF
C
C----- TRANSFER ENERGIES FOR BOTH IOPT=3 AND 4.
      400 EESE=SE(28)
      EPSE=SE(31)
C

```

```

C----- TRANSFER DUCTILITIES AND EXCRUSION RATIOS FOR BOTH IOPT=3 AND 4.
DO 410 I=1,3
  DUCT(I)=MAX(SE(15+I),SE(18+I))
  EXCR(I)=SE(21+I)
410 EXCR(I+3)=SE(21+I+3)
  RETURN
C
C===== DAMAGE INDEX =====
500 EESE =SE(28)
  EPSE =SE(31)
  NSEGS=SMAT(1)
  NI =SMAT(2)
  DMAX =SMAT(4+2*NSEGS)
  DY =SMAT(4)
  BDAM =SMAT(5+2*NSEG)
  P=SE(33+ 3*NI)
  D=SE(34+ 3*NI)
  IF (DY.LE.SMAT(5+NSEGS)) THEN
    PY=SMAT(5)*DY/SMAT(5+NSEGS)
  ELSE
    DO 510 I=2,NSEGS
      P1=SMAT(3+I)
      P2=SMAT(4+I)
      D1=SMAT(3+I+NSEGS)
      D2=SMAT(4+I+NSEGS)
      IF (DY.GE.D1 .AND. DY.LE.D2) THEN
        PY=P1+(DY-D1)*(P2-P1)/(D2-D1)
        GO TO 520
      ENDIF
    510 CONTINUE
    ENDIF
  520 DAMAGE=ABS(D)/DMAX + BDAM / (PY*DMAX) * EPSE
C
  RETURN
C1111 FORMAT (1P,
C & ' S1A- P=',G13.5,' D=',G13.5,' K=',G18.9,' RULE=',G13.5,
C & ' DIR=',F6.3,' A=',G13.5,' IR=',I3)
C1112 FORMAT (1P,
C & ' S1B- P=',G13.5,' D=',G13.5,' K=',G18.9,' RULE=',G13.5,
C & ' DIR=',F6.3,' A=',G13.5,' IR=',I3)
C1113 FORMAT (1P,
C & ' S1C- P=',G13.5,' D=',G13.5,' K=',G18.9,' RULE=',G13.5,
C & ' DIR=',F6.3,' A=',G13.5,' IR=',I3)
  END
CC=====
C== SHEAR HYSTERESIS MODEL.... HYST04 .....
C=====
C     DEBUG UNIT(6),TRACE,SUBCHK,INIT,SUBTRACE
C     END DEBUG
C=====
C
C INPUT VARIABLES
C P = CURRENT LOAD
C D = CURRENT DISPLACEMENT
C PL = LAST LOAD
C VEL = PRODUCT OF LAST AND CURRENT VELOCITY
C NS = NUMBER OF BACKBONE CURVE POINTS
C NI = MAXIMUM NUMBER OF SECONDARY LOOPS
C PC = CRACKING LOAD
C DC = CRACKING DISPLACEMENT
C SI = INITIAL STIFFNESS PC/DC
C PS = BACKBONE CURVE LOADING POINTS
C DS = BACKBONE CURVE DISPLACEMENT POINTS
C
C OUTPUT VARIABLES
C AN INITIAL VALUE OF ZERO IS REQUIRED FOR ALL OUTPUT VARIABLES...
C K = STIFFNESS

```

```

C RULE = RULE NUMBER, STORED IN THE FOR_MAT RN.DIR UPON EXIT OF
C      THIS SU_BROU_TINE
C A = LOAD LIMIT BEFORE NEXT RULE CHANGE
C PMG = MAXIMUM PAST LOAD IN THE POSITIVE DIRECTION
C PMH = MAXIMUM PAST LOAD IN THE NEGATIVE DIRECTION
C DMG = MAXIMUM PAST DISPLACEMENT IN THE POSITIVE DIRECTION
C DMH = MAXIMUM PAST DISPLACEMENT IN THE NEGATIVE DIRECTION
C PR = SECONDARY LOOP LOADING POINT
C DR = SECONDARY LOOP DISPLACEMENT POINT
C FR = SECONDARY LOOP FLAG
C IR = SECONDARY LOOP NUMBER
C BACKB = BACKBONE LOADING FLAG
C SR1 = RELOADING STIFFNESS FROM RULE 8 - USED BY RULE 11
C SR2 = RELOADING STIFFNESS FROM RULE 9 - USED BY RULE 11
C SR3 = RELOADING STIFFNESS FROM RULE 7 - USED BY RULE 11
C SRF = RELOADING STIFFNESS FROM RULES 8 & 9 - USED BY RULE 11
C

C INTERNAL VARIABLES
C J = BACKBONE CURVE POINT # IN THE CURRENT DIRECTION
C DIR = CURRENT DIRECTION
C      DIR=1, POSITIVE LOADING
C      DIR=2, POSITIVE UNLOADING
C      DIR=3, NEGATIVE LOADING
C      DIR=4, NEGATIVE UNLOADING
C DIRL = LAST DIRECTION
C IRULE = INTERGER VALUE OF RULE
C LRULE = INTEGER VALUE OF LAST RULE #
C CRACKD = CRACKED WALL FLAG
C REVRLS = LOAD REVERSAL FLAG
C PRINT = PRINT FLAG, USED FOR DEBU_GGING
C PC2 = PC/2, USED BY LOADING CURVES
C DC2 = DISPLACEMENT CORRESPONDING TO PC2 ON THE LOADING BRANCH
C S = INTERMEDIATE STIFFNESS
C SR = RELOADING STIFFNESS
C SRP = MINIMUM RELOADING STIFFNESS
C DO = DISPLACEMENT INTERSEPT OF PEAK DISPLACEMENTS
C DOP = DISPLACEMENT INTERSEPT OF THE UNLOADING BRANCH
C AP = ABSOLUTE VALUE OF CURRENT LOAD P.
C PM = MAXIMUM PAST LOAD IN THE CURRENT DIRECTION
C DM = MAXIMUM PAST DISPLACEMENT IN THE CURRENT DIRECTION
C DMAX = MAXIMUM PAST DISPLACEMENT IN EITHER DIRECTION
C PMAX = MAXIMUM PAST LOAD IN EITHER DIRECTION
C PA = PM-PC, USED BY UNLOADING CURVES
C PB = PC/2, USED BY UNLOADING CURVES
C DA = DISPLACEMENT AT PA, USED BY UNLOADING CURVES
C DB = DISPLACEMENT AT PB, USED BY UNLOADING CURVES
C DF = DIFFERANCE IN LOAD, USED FOR CALCULATING K
C DD = DIFFERANCE IN DISPLACEMENT, USED FOR CALCULATING K
C PX = LOAD INTERCEPT OF LOADING AND BACKBONE CURVE
C DX = DISPLACEMENT INTERCEPT OF LOADING AND BACKBONE CURVE
C P2,D2 = POINT ON THE LOADING CURVE BETWEEN RULES 7 AND 10
C X = MAXIMUM DISPLACEMENT
C      = DISPLACEMENT INTERCEPT FOR RULE 11
C X1 = 75% PC DISPLACEMENT FOR RULE 11
C X2 = 25% PC DISPLACEMENT FOR RULE 11
C I,IT = TEMPORARY LABEL FOR SMALL LOOP LOADING AND UNLOADING PTS
C JO = J-1
C ALPHA = DEGRADING STIFFNESS FACTOR
C ALPHAP = DEGRADING STIFFNESS FACTOR USED BY RULE 10
C S1 = STIFFNESS FROM FUNCTION FS1
C S2 = STIFFNESS FROM FUNCTION FS2
C S3 = STIFFNESS FROM FUNCTION FS3
C SU = STIFFNESS BETWEEN CURRENT AND RELOADING POINT
C SO2 = STIFFNESS BETWEEN PA AND DO
C SO3 = STIFFNESS BETWEEN PB AND DO
C

C INTERNAL FUNCTIONS

```

```

C FD2 = DISPLACEMENT INTERCEPT OF LOADING AND UNLOADING CURVE
C FS1 = UNLOADING STIFFNESS WHEN P>(PM-PC)=PA
C FS2 = UNLOADING STIFFNESS WHEN PA>P>(PC/2)=PB
C FS3 = UNLOADING STIFFNESS WHEN P>PB
C FSR = LOADING BELOW PC/2, WITH PINCHING
C
C SU_BROU_TINES CALLED
C DIRECT = DETERMINES THE VALUES OF DIR AND DIRL
C INTSCT = DETERMINES THE INTERSECTION OF TWO LINES IN POINT-SLOPE
C FORM
C KMIN = DETERMINES THE STIFFNESS BASED ON DP,DD AND K_DEFAULT
C
C
SUBROUTINE HYST04(P,D,PL,DL,VEL,NS,NI,PRINT,
& PC ,DC ,PS ,DS ,SI ,CSE ,DY ,
& K ,RULE ,RDIR ,A ,PMG ,PMH ,
& DMG ,DMH ,BACKB ,SR1 ,SR2 ,SR3 ,
& SRM ,IR ,SE ,UPOS ,UNEG ,EXCR ,
& ESE ,PSE ,PSEOLD,PR ,DR ,FR )
C
IMPLICIT REAL(A-H,K,O-Z)
IMPLICIT INTEGER(I,J,L-N)
INTEGER DIR,DIRL
LOGICAL BACKB,CRACKD,REVRSL,PRINT,BTEST
CHARACTER*4 FR(NI)
DIMENSION PS(NS),DS(NS),PR(NI),DR(NI)
DIMENSION UPOS(3),UNEG(3),EXCR(6),ESE(3)
DATA ALPHA/1.04/
C
C SYMMETRIC COEFFICIENTS
CC   FS1(X)= SI *MIN((1.03 *(DC/X)**.388 ),1.)
CC   FS2(X)= SI *MIN((1.036 *(DC/X)**.458 ),1.)
CC   FS3(X)= SI *MIN((0.789 *(DC/X)**.692 ),1.)
C UNSYMMETRIC COEFFICIENTS
FS1(X)= SI *MIN((1.4675*(DC/X)**.343 ),1.)
FS2(X)= SI *MIN((0.7761*(DC/X)**.3195),1.)
FS3(X)= SI *MIN((0.0707+(DC/X)*1.369 ),1.)
FSR(X)= SI *MIN(( (ABS(DC/X))**1.02),1.)
FD2(X)= SIGN(DMAX,PM)-.05*SIGN(PMAX,PM)/(FS1(X))
C
1000 IF (PRINT) WRITE (6,1010) P,D,PL,DL,NS,NI,PC,DC,SI,K,RULE,A,
& PMG,PMH,DMG,DMH,SR1,SR2,SR3,SRM,BACKB,IR,PSEOLD,VEL,
& SE,DY,ESE(1),PSE,UPOS,CSE,UNEG,EXCR
1010 FORMAT (
' S1- P='' ,G13.5,' D='' ,G13.5,' PL='' ,G13.5,' DL='' ,G13.5/
' S1- NS='' ,G13.5,' NI='' ,G13.5,' PC='' ,G13.5,' DC='' ,G13.5/
' S1- SI='' ,G13.5,' K='' ,G13.5,' RULE='' ,G13.5,' A='' ,G13.5/
' S1- PMG='' ,G13.5,' PMH='' ,G13.5,' DMG='' ,G13.5,' DMH='' ,G13.5/
' S1- SR1='' ,G13.5,' SR2='' ,G13.5,' SR3='' ,G13.5,' SRM='' ,G13.5/
' S1-BACKB='' ,G13.5,' IR='' ,G13.5,' PSEO='' ,G13.5,' VEL='' ,G13.5/
' S1- SE='' ,G13.5,' DY='' ,G13.5,' ESE='' ,G13.5,' PSE='' ,G13.5/
' S1- UP1='' ,G13.5,' UP2='' ,G13.5,' UP3='' ,G13.5,' CSE='' ,G13.5/
' S1- UN1='' ,G13.5,' UN2='' ,G13.5,' UN3='' ,G13.5/
' S1- EX1='' ,G13.5,' EX2='' ,G13.5,' EX3='' ,G13.5/
' S1- EX4='' ,G13.5,' EX5='' ,G13.5,' EX6='' ,G13.5)
IF (IR.GT.0.AND.PRINT) WRITE (6,1020) (I,PR(I),DR(I),FR(I),I=1,IR)
1020 FORMAT
& (' I='' ,G13.5,' PR='' ,G13.5,' DR='' ,G13.5,' FR='' ,A )
C
AP=ABS(P)
C
C..... DETERMINE IF ELASTIC
IF (RULE.EQ.0 .AND. AP .LT.PC ) THEN
  K=SI
  SE=K
  GO TO 9999
ENDIF

```

```

C
C..... DETERMINE IF WALL IS INACTIVE, IF SO RE_TURN
  IF (RULE.LT.0.0) GO TO 9999
C
C..... DETERMINE CURRENT DIRECTION
  LRULE=INT(RULE)
  DIR =RDIR
  CALL DIRECT(DIR,DIRL,P,PL,VEL)
  RDIR =DIR
  IF (PRINT) WRITE (6,1030) DIR,DIRL
1030 FORMAT(' DIR=',I8 , ' DIRL=',I8 )
C
C..... DETERMINE MAXIMUM AND MINIMUM VALUES
  PMG=MAX(PMG, PC,P)
  DMG=MAX(DMG, DC,D)
  PMH=MIN(PMH,-PC,P)
  DMH=MIN(DMH,-DC,D)
  DMAX=MAX(DMG,-DMH)
  PMAX=MAX(PMG,-PMH)
C
C..... SET MAXIMUM AND MINIMUM VALUES...
  IF (DIR.EQ.1 .OR. DIR.EQ.2 ) THEN
    PM=PMG
    DM=DMG
  ELSE IF (DIR.EQ.3 .OR. DIR.EQ.4) THEN
    PM=PMH
    DM=DMH
  ENDIF
C
C..... CALCULATE EQUIVALENT UNLOADING STIFFNESS FOR ENERGY...
  IF (BACKB .OR. RULE.EQ.0.0) THEN
    S1=FS1(DMAX)
    S2=FS2(DMAX)
    S3=FS3(DMAX)
    DO=DM-PM*(DMG-DMH)/(PMG-PMH)
    PA=PM-SIGN(PC,PM)
    DA=DM-SIGN(PC,PM)/S1
    PB=SIGN( (MIN(ABS(PA),(PC/2)) ),PM)
    S02=KMIN((DA-DO),PA,SI)
    DB=DA-(PA-PB)/MAX(S2,S02)
    S03=KMIN((DB-DO),PB,SI)
    SE= 0.5 * PM**2 / (
      & (PM+PA)*0.5*(DM-DA)
      & +(PA+PB)*0.5*(DA-DB)
      & +( PB)*0.5*( PB)/MAX(S3,S03) )
  ENDIF
C
C..... CHECK TO SEE IF LAST RULE IS STILL IN EFFECT
  IF (DIR.EQ.DIRL .AND.
  & ((DIR.EQ.1 .AND. P.LT.A) .OR. (DIR.EQ.2 .AND. P.GT.A) .OR.
  & (DIR.EQ.3 .AND. P.GT.A) .OR. (DIR.EQ.4 .AND. P.LT.A))) THEN
    RETURN
  ENDIF
C
C..... CALC EXCURSION RATIO AT EVERY ZERO CROSSING...
C IF (P*PL.LE.0) CALL DNE(0,UPOS,EXCR, DY,DLI,ESE,PSEOLD,CSE)
C
C..... ERASE SMALL LOOP FLAGS
  IF (IR.GT.0) THEN
    IT=IR
    DO 10 I=1,IT
    IF ((PR(I).EQ.'L' .AND. ( P.LE.PR(I) .OR. D.LE.DR(I) )) .OR.
    & (PR(I).EQ.'7' .AND. ( P.GE.PR(I) .OR. D.GE.DR(I) ))) THEN
      IR=I-1
      GO TO 15
    ENDIF
  10 CONTINUE

```

```

        ENDIF
15 I=IR+1
C
    IF (DIR.EQ.1 .OR. DIR.EQ.3 ) THEN
C..... LOADING RULES ..... RULES 1,5-11
    PC2=SIGN((PC/2),PM)
C
C..... LOADING ON BACKBONE RULE 1
30   IF (BACKB .OR. RULE.EQ.0.0) THEN
    K=0.
    DO 40 J=2,NS
    DD=DS(J)-ABS(D)
    DP=PS(J)-AP
    IF (AP.LT.PS(J) .AND. (DD*DP).GT.0.) THEN
    S=DP/DD
    IF (S.GT.K .AND. S.LE.SI) THEN
    K=S
    A=SIGN(PS(J),P)
    ENDIF
    ENDIF
40 CONTINUE
RULE=1
BACKB=.TRUE.
IR=0
C
C..... LOADING AFTER UNLOADING RULES 6-11
ELSE
    CRACKD=(ABS(DM).GT.DC)
    REVRSL=((DIR.EQ.1 .AND. DIRL.EQ.4) .OR. LRULE.EQ.8
& .OR. (DIR.EQ.3 .AND. DIRL.EQ.2) .OR. LRULE.EQ.9
& .OR. LRULE.EQ.5 .OR. LRULE.EQ.11)
    IF (CRACKD) THEN
    P2=.95*SIGN(PMAX,PM)
    D2=FD2(DMAX)
    ELSE
    P2=PM
    D2=DM
    ENDIF
    S=KMIN((D2-D),(P2-P),SI)
20 I=I-1
C
C..... RELOADING INSIDE SMALL LOOPS RULE 11
IF (I.GT.0 ) THEN
    IF (.NOT.(( FR(I).EQ.'7' .AND. DIR.EQ.1 ) .OR.
& ( FR(I).EQ.'L' .AND. DIR.EQ.3 ))) GO TO 20
    IF (SR1.LE.0 .OR. SR2.LE.0 .OR. SR3.LE.0 .OR.
& SRM.LE.0 ) THEN
    I=1
    GO TO 20
ENDIF
    IF (AP.LT.ABS(PC2) .AND. S.GT.SRM) THEN
    REVRSL=.FALSE.
    I=1
    GO TO 20
ENDIF
    IF (ABS(PR(I)).LE. PC/4) THEN
    K=KMIN((D-DR(I)),(P-PR(I)),SI)
    A=PR(I)
    RULE=11.1+I/1000.
    ELSE IF (ABS(PR(I)).LE.3*PC/4) THEN
    X2=D2-(P2-1.5*PC2)/SR3
    X1=X2-PC2/SR2
    X=D+(PC2/2-P) /SR2
    IF (AP.LT.PC/4 .AND. ((DIR.EQ.1 .AND. X.LT.X1).OR.
& (DIR.EQ.3 .AND. X.GT.X1))) THEN
    K=KMIN((X1-D),(PC2/2-P),SI)
    A=SIGN((PC/4),PM)

```

```

        RULE=11.2+I/1000.
    ELSE
        K=KMIN((DR(I)-D),(PR(I)-P),SI)
        A=PR(I)
        RULE=11.3+I/1000.
    ENDIF
ELSE
    X2=DR(I)-(PR(I)-1.5*PC2)/SRM
    X1=X2-PC2/SR2
    X=D+(PC2/2-P) /SR2
    IF (AP.LT.PC/4 .AND. ((DIR.EQ.1 .AND. X.LT.X1).OR.
    &      (DIR.EQ.3 .AND. X.GT.X1))) THEN
        K=KMIN((X1-D),(PC2/2-P),SI)
        A=SIGN((PC/4),PM)
        RULE=11.4+I/1000.
    ELSE
        X=D+(1.5*PC2-P) /SR3
        IF (AP.LT. 3*PC/4 .AND.
    &          ((DIR.EQ.1 .AND. X.LT.X2)
    &          .OR. (DIR.EQ.3 .AND. X.GT.X2))) THEN
            K=KMIN((X2-D),(1.5*PC2-P),SI)
            A=SIGN((3*PC/4),PM)
            RULE=11.5+I/1000.
        ELSE
            SR3=SRM
            K=KMIN((DR(I)-D),(PR(I)-P),SI)
            A=PR(I)
            RULE=11.6+I/1000.
        ENDIF
    ENDIF
ENDIF
C
C..... INITIAL RELOADING BELOW PC/2 W/O REVERSAL      RULE 6
ELSE IF (AP.LT.ABS(PC2) .AND. .NOT.REVRS ) THEN
    K=FS1(DMAX)
    A=PC2
    RULE=6
C
C..... RELOADING TO P2                      RULE 7
ELSE IF (AP.LT.ABS(P2) .AND.
&      (.NOT.REVRS .OR. AP.GE.PC*0.75)) THEN
    K=S
    A=P2
    RULE=7
C
C..... RELOADING BELOW PC WITH REVERSAL      RULES 8 & 9
ELSE IF (AP.LT.PC*0.75 ) THEN
    SR=FSR(DMAX)
    S1=FS1(DMAX)
    S2=FS2(DMAX)
    S3=FS3(DMAX)
    PA=SIGN(PMAX,PM)-SIGN(PC,PM)
    DA=SIGN(DMAX,PM)-SIGN(PC,PM)/S1
    PB=SIGN( (MIN(ABS(PA),(PC/2)) ),PM)
    DB=DA-(PA-PB)/S2
    DOP=DB-(PB)/S3
    DO=DM-PM*(DMG-DMH)/(PMG-PMH)
    IF (DIR.EQ.1) DOP=MAX(DOP,DO)
    IF (DIR.EQ.3) DOP=MIN(DOP,DO)
    DC2=DOP+PC2/S1
    SRM=KMIN((DC2-D2),(PC2-P2),S1)
    IF (S.GT.SRM) THEN
        REVRS=.FALSE.
        GO TO 20
    ENDIF
    SRP=KMIN((DC2-D),(PC2-P),S1)
    SRI=MAX(SRP,MIN(SR,S))

```

```

DC2P=D+(PC2-P)/SR1
SR3=KMIN((D2-DC2P),(P2-PC2),SI)
SR2=2.00/( 1./SR1 + 1./SR3 )
IF (AP.LT.(PC/4) ) THEN
  K=SR1
  A=SIGN((PC/4),PM)
  RULE=8
ELSE
  K=SR2
  A=SIGN(PC,PM)*0.75
  RULE=9
ENDIF
C
C..... LOADING TOWARDS THE BACKBONE CURVE RULE 10
ELSE
  BACKB=.TRUE.
  IF (.NOT. CRACKD) GO TO 30
  IR=0
  ALPHAP=1.0
  IF (ABS(DM).EQ.ABS(DMAX)) ALPHAP=ALPHA
  K=KMIN((ALPHAP*SIGN(DMAX,D2)-D2),(SIGN(PMAX,P2)-P2)
& ,SI)
  DO 50 J=2,NS
    IF ( PS(J).LE.ABS(PMAX) ) GO TO 50
    JO=J-1
    DD=DS(J)-DS(JO)
    DP=PS(J)-PS(JO)
    IF ((DP*DD).LE.0.) GO TO 50
    CALL INTSCT(DX,PX,D,P,K,SIGN(DS(J),P),
& SIGN(PS(J),P),(DP/DD) )
    IF (ABS(DX).GE.DS(JO) .AND. ABS(DX).LE.DS(J).AND.
& ABS(PX).GT.ABS(PMAX).AND. PM*PX.GT.0) THEN
      IF (AP.GE.ABS(PX)) GO TO 30
      K=KMIN((DX-D),(PX-P),SI)
      A= PX
      RULE=10
      GO TO 100
    ENDIF
  50  CONTINUE
    GO TO 30
  ENDIF
ENDIF
C
C
ELSE
C..... UNLOADING RULES .....
C
C..... INITILIZE VALUES          RULES 2-5
BACKB=.FALSE.
S1=FS1(DMAX)
S2=FS2(DMAX)
S3=FS3(DMAX)
DO=DM-PM*(DMG-DMH)/(PMG-PMH)
PA=PM-SIGN(PC,PM)
DA=DM-SIGN(PC,PM)/S1
PB=SIGN( MIN(ABS(PA),(PC/2)),PM)
S02=KMIN((DA-DO),PA,SI)
DB=DA-(PA-PB)/MAX(S2,S02)
S03=KMIN((DB-DO),PB,SI)
SU=0.

C
C..... UNLOADING INSIDE SMALL POSITIVE LOOPS          RULE 5
I=IR+1
70  I=I-1
  IF (I.GT.0) THEN
    IF (.NOT.((DIR.EQ.2 .AND. FR(I).EQ.'L') .OR.
& (DIR.EQ.4 .AND. FR(I).EQ.'7')) ) GO TO 70

```

```

C
IF ((DIR.EQ.2 .AND.( (P.GT.PA .AND. PR(I).GT.PA) .OR.
& (PA.GE.P .AND. P.GT.PB .AND. PR(I).GT.PB) .OR.
& (PB.GE.P .AND. PR(I).GT.0 ))) .OR.
& (DIR.EQ.4 .AND.( (P.LT.PA .AND. PR(I).LT.PA) .OR.
& (PA.LE.P .AND. P.LT.PB .AND. PR(I).LT.PB) .OR.
& (PB.LE.P .AND. PR(I).LT.0 )) ) THEN
K=(PR(I)-P)/(DR(I)-D)
IF (K.LE.0 .OR. K.GT.SI) GO TO 70
A=PR(I)
RULE=5+I/1000.
GO TO 100
ELSE
SU=KMIN((DR(I)-D),(PR(I)-P),SI)
ENDIF
C
ENDIF
C..... CALC DUCTILITY AND EXCURSION RATIO...
IF (RULE.EQ.1 .OR. RULE.GT.5) THEN
C   IF ((RULE.EQ.1 .OR. RULE.GT.5) .AND. AP.GE.0.95*PMAX) THEN
IF (DIR.EQ.2) THEN
DLI= MAX( D , DL )
CALL DNE(1,UPOS,EXCR, DY,DLI,ESE(2),PSE,PSEOLD,CSE)
ELSE IF (DIR.EQ.4) THEN
DLI= MIN( D , DL )
CALL DNE(1,UNEG,EXCR,-DY,DLI,ESE(3),PSE,PSEOLD,CSE)
ENDIF
ENDIF
C
C..... UNLOADING ON THE TOP SEGMENT          RULE 2
IF(AP.GT.ABS(PA)) THEN
K=MAX(S1,SU)
A=PA
RULE=2
C..... UNLOADING ON THE MIDDLE SEGMENT        RULE 3
ELSE IF(AP.GT.ABS(PB)) THEN
K=MAX(S2,S02,SU)
A=PB
RULE=3
C..... UNLOADING ON THE BOTTOM SEGMENT        RULE 4
ELSE
K=MAX(S3,S03,SU)
A=0.
RULE=4
ENDIF
C
ENDIF
C..... SAVE REVERSAL POINTS FOR SMALL LOOPS.....
100 IRULE=INT(RULE)
REVRSL=IRULE.EQ.1.OR.IRULE.EQ.10.OR.LRULE.EQ.1.OR.LRULE.EQ.10
IF ((DIRL.EQ.1 .AND. DIR.EQ.2 .AND. .NOT. REVRSL)
& .OR. (DIRL.EQ.4 .AND. DIR.EQ.3) ) THEN
IF (IR.LT.NI) THEN
IR=IR+1
PR(IR)=P
DR(IR)=D
FR(IR)='7'
ENDIF
ELSE IF ((DIRL.EQ.3 .AND. DIR.EQ.4 .AND. .NOT. REVRSL)
& .OR. (DIRL.EQ.2 .AND. DIR.EQ.1) ) THEN
IF (IR.LT.NI) THEN
IR=IR+1
PR(IR)=P
DR(IR)=D
FR(IR)='L'
ENDIF

```

```

        ENDIF
        ENDIF
        IF ((1.05*SI).GT.K .AND. K.GT.0 ) GO TO 9999
C
        K=0
        RULE==RULE
9999 CONTINUE
C WRITE (6,1111) P,D,K,RULE,DIR,A
C1111 FORMAT (1P,
C &' S1- P=',G13.5,' D=',G13.5,' K=',G18.9,' RULE=',G13.5,
C &' DIR=',I5,' A=',G13.5)
        RETURN
C
        END
C
C=====
C - DIRECTION OF LOADING .....
C DEBUG UNIT(6),SUBCHK,SUBTRACE
C END DEBUG
C P = CURRENT LOAD
C PL = LAST LOAD
C D = CURRENT DISPLACEMENT
C DIR = CURRENT DIRECTION
C     DIR=1, POSITIVE LOADING
C     DIR=2, POSITIVE UNLOADING
C     DIR=3, NEGATIVE LOADING
C     DIR=4, NEGATIVE UNLOADING
C DIRL = LAST DIRECTION
C VEL = PRODUCT OF LAST AND CURRENT VELOCITIES

SUBROUTINE DIRECT(DIR,DIRL,P,PL,VEL)
IMPLICIT REAL(A-H,O-Z)
IMPLICIT INTEGER(I-N)
INTEGER DIR,DIRL
LOGICAL BTTEST

IF (P.GT.0) THEN
    IF (P.GT.PL .AND. PL.GT.0) THEN
        DIRL=1
    ELSE IF (P.GT.PL .AND. PL.LT.0) THEN
        DIRL=4
    ELSE IF (P.LT.PL) THEN
        DIRL=2
    ELSE
        DIRL=DIR
    ENDIF
ELSE IF (P.LT.0) THEN
    IF (P.LT.PL .AND. PL.LT.0) THEN
        DIRL=3
    ELSE IF (P.LT.PL .AND. PL.GT.0) THEN
        DIRL=2
    ELSE IF (P.GT.PL) THEN
        DIRL=4
    ELSE
        DIRL=DIR
    ENDIF
ELSE
    IF (PL.LT.0) THEN
        DIRL=4
    ELSE IF (PL.GT.0) THEN
        DIRL=2
    ELSE
        DIRL=DIR
    ENDIF
ENDIF

IF (DIRL.EQ.1 .OR.DIRL.EQ.0) THEN

```

```

IF (VEL.GT.0) THEN
  DIR=1
ELSE
  DIR=2
ENDIF

ELSE IF (DIRL.EQ.2) THEN
  IF (VEL.GT.0) THEN
    IF (P.GT.0) THEN
      DIR=2
    ELSE
      DIR=3
    ENDIF
  ELSE
    DIR=1
  ENDIF

ELSE IF (DIRL.EQ.3) THEN
  IF (VEL.GT.0) THEN
    DIR=3
  ELSE
    DIR=4
  ENDIF

ELSE IF (DIRL.EQ.4) THEN
  IF (VEL.GT.0) THEN
    IF (P.LT.0) THEN
      DIR=4
    ELSE
      DIR=1
    ENDIF
  ELSE
    DIR=3
  ENDIF
ELSE
  WRITE (6,5)
5 FORMAT(5X,'ER','ROR IN SUBROUTINE DIRECT, DIRL.NE. 1,2,3,OR 4')
WRITE (6,10) DIR,DIRL,P,PL,VEL
ENDIF
IF (DIR.EQ.0) DIR=1

C WRITE (6,10) DIR,DIRL,P,PL,VEL
10 FORMAT (5X,'*** IN DIRECT ',1X,
  & ' DIR=',I4,' DIRL=',I4,' P=',F8.3,' PL=',F8.3,' VEL=',F10.3)

RETURN
END
=====
C
C - INTERSECTION OF TWO LINES IN POINT SLOPE FORM .....
C DEBUG UNIT(6),SUBCHK,SUBTRACE
C END DEBUG
C X = X COORDINATE OF INTERSECTION
C Y = Y COORDINATE OF INTERSECTION
C X1 = X COORDINATE OF LINE 1
C Y1 = Y COORDINATE OF LINE 1
C S1 = SLOPE OF LINE 1
C X2 = X COORDINATE OF LINE 2
C Y2 = Y COORDINATE OF LINE 2
C S2 = SLOPE OF LINE 2

SUBROUTINE INTSCT(X,Y,X1,Y1,S1,X2,Y2,S2)
IMPLICIT REAL(A-H,O-Z)
IMPLICIT INTEGER(L-N)
LOGICAL BTEST
IF (S1.NE.S2) THEN
  B1= Y1 - S1*X1

```

```

B2= Y2 - S2*X2
X=(B1-B2)/(S2-S1)
Y=(B1*S2-B2*S1)/(S2-S1)
ELSE
  WRITE (6,10) X1,Y1,S1,X2,Y2,S2
10   FORMAT ('***** ER','ROR IN INTSCT.....',1X,
  &   'S1=S2, NO SOLN, THUS SET X=Y=0.',/
  &   ' X1=',1P,G15.5,' Y1=',G15.5,' S1=',G15.5/
  &   ' X2=',1P,G15.5,' Y2=',G15.5,' S2=',G15.5/)
  X=0
  Y=0
C CALL ERRTRA
ENDIF
CC   WRITE (6,5) X1,Y1,S1,B1,X2,Y2,S2,B2,X,Y
CC 5 FORMAT (' IN INTSCT....',/
CC &   ' X1=',1P,G15.5,' Y1=',G15.5,' S1=',G15.5,' B1=',G15.5/
CC &   ' X2=',1P,G15.5,' Y2=',G15.5,' S2=',G15.5,' B2=',G15.5/
CC &   ' X=',1P,G15.5,' Y=',G15.5/)
  RETURN
END
C=====
C
C - KMIN - CALCULATES STIFFNESS BASED ON DX AND DY .....
C DEBUG UNIT(6),SUBCHK,SUBTRACE
C END DEBUG
C KMIN =
C DD = CHANGE IN DISPLACEMENT
C DP = CHANGE IN LOAD
C SI = MAXIMUM AND DEFAULT STIFFNESS
  REAL FUNCTION KMIN(DD,DP,SI)
LOGICAL BTTEST
  IF ((DD*DP).GT. 0.00) THEN
    KMIN=MIN((DP/DD),SI)
  ELSE
    KMIN=SI
  ENDIF
  RETURN
END

```

Input Data:

```

1 1 |IELNO MAT
'SHEAR' 8 10 0.160 0.2 |TYPE NSEG NI DY BDAM
  6.120 8.080 9.950 12.010 13.670 15.490 15.910 30. |SMAT
  0.065 0.120 0.181 0.485 0.731 1.069 1.155 10. |SMAT
0. 1.0 50 |DMIN DMAX NUMB
1.0 -1.0 100 |DMIN DMAX NUMB
-1.0 1.10 100 |DMIN DMAX NUMB
1.10 -0.5 50 |DMIN DMAX NUMB
-0.5 1.2 100 |DMIN DMAX NUMB
1.2 1.10 10 |DMIN DMAX NUMB

```

Output Data:

```

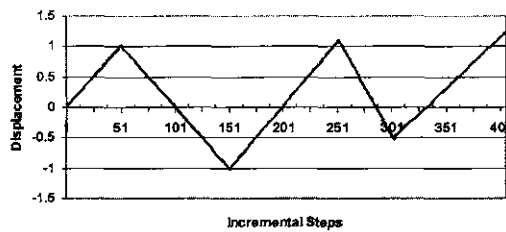
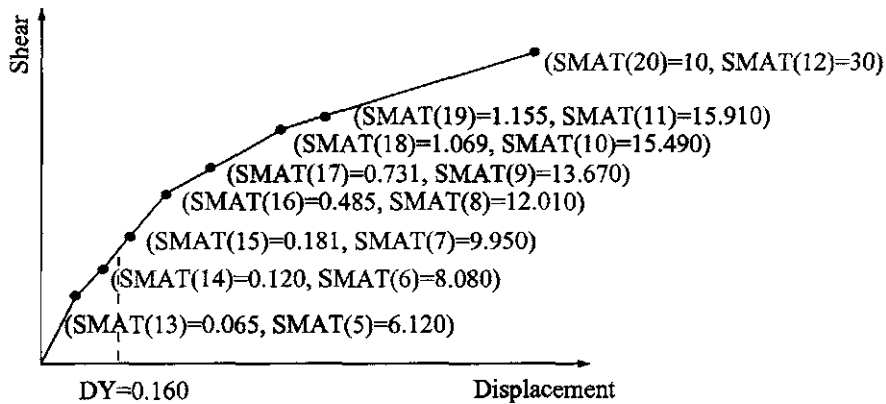
SHEAR1 HYSTERESIS MODEL DATA - UNIT LENGTH MEMBER
=====
BACKBONE CURVE POINTS - MAT. NI DY BETA STRESS STRAIN
      1 10 0.160000 0.200000 6.12000 0.650000E-01
                                         8.08000 0.120000
                                         9.95000 0.181000
                                         12.0100 0.485000
                                         13.6700 0.731000
                                         15.4900 1.06900
                                         15.9100 1.15500
                                         30.0000 10.0000
STIFFNESS LOAD      DISP.      RULE

```

950

6.77632 0.13553 0.02000 1.0
6.77632 0.27105 0.04000 1.0
6.77632 0.40658 0.06000 1.0
. . .
9.59639 11.04017 1.21700 10.0
50.58140 10.53436 1.19000 2.0

APPENDIX L



Diagrams Represent Input Data for Appendix L (Shear)

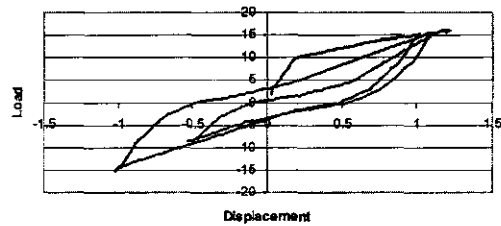
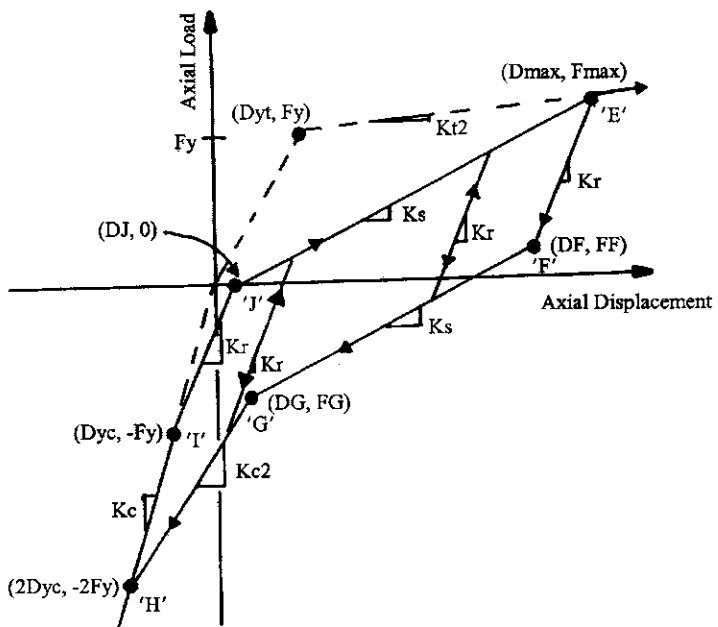


Diagram Represents Output Solution for Appendix L (Shear)

AXIAL: Low-Rise Shear Wall Cheng-Mertz Hysteresis Model



```

=====
C THIS IS A TYPICAL MAIN PROGRAM FOR CALLING CHENG-MERTZ AXLMOD
C HYSTERESIS MODEL SUBROUTINE NAMED "MAT02". THE PARAMETERS
C TRANSFERRED INTO SUBROUTINE MAT02 ARE SHOWN AS FOLLOWS.
C SINCE MAT02 IS A GENERAL PURPOSE SUBROUTINE, SOME PARAMETERS
C HAVE BEEN RESERVED AND NOT USED. THEREFORE THEY ARE ASSIGNED
C WITH A NUMBER "1" IN THIS DEMONSTRATION AS A MAIN PROGRAM.
=====
C VARIABLES:
C MAT = USER DEFINED MATERIAL ID NUMBER
C IELNO = USER DEFINED ELEMENT ID NUMBER
C P = CURRENT LOAD
C PL = PREVIOUS STEP LOAD
C D = CURRENT DISPLACEMENT
C DL = PREVIOUS STEP DISPLACEMENT
C V = DUMMY VARIABLE
C VL = DUMMY VARIABLE
C DUCT = RESERVED DUCTILITY ARRAY (NOT USED)
C EXCR = RESERVED EXCURSION ARRAY (NOT USED)
C DAMAGE= RESERVED VARIABLE FOR DAMAGE INDEX (NOT USED)
C EESE = RESERVED VARIABLE FOR ELASTIC STRAIN ENERGY(NOT USED)
C EPSE = RESERVED VARIABLE FOR PLASTIC STRAIN ENERGY(NOT USED)
C LELEM = 33
C LMAT = 11
C SMAT = MATERIAL ARRAY, SMAT(LMAT)
C SE = ELEMENT ARRAY, SE(LELEM)
C IOPT = 1 INITIALIZE MATERIAL

```

```

C      2 GET INITIAL STIFFNESS
C      3 GET MEMBER STIFFNESS
C ERR = DUMMY LOGICAL VARIABLE
C FIRST = LOGICAL VARIABLE. IF FIRST=.TRUE., THE MATERIAL
C      PROPERTIES OF AXIAL HYSTERESIS MODEL ARE PRINTED.
C PRINT = DUMMY LOGICAL VARIABLE
C BUG = LOGICAL VARIABLE. IF BUG=.TRUE., THE HYSTERESIS
C      ENVELOPE CONTROL POINTS ARE PRINTED.
C BDAM = RESERVED PARAMETER FOR ANG's DAMAGE INDEX
C=====
LOGICAL ERR, FIRST, PRINT, BUG
DIMENSION SE(100), SMAT(23), DUCT(3), EXCR(6)
CHARACTER*80 TYPE
C=====
C DEFINE EXTERNAL FILE UNITS FOR INPUT DATA AND OUTPUT
C=====
OPEN(UNIT=5,FILE=STRING(8))
OPEN(UNIT=6,FILE=STRING(9))
C
C=====
C
IOPT=1
ERR=.FALSE.
FIRST=.TRUE.
PRINT = .FALSE.
BUG=.FALSE.
READ(5,*)IELNO, MAT
C
C INPUT MATERIAL PROPERTIES
C CALL MAT02
C & (IOPT ,IELNO ,ERR ,FIRST ,PRINT ,BUG ,
C & MAT ,SE ,P,PL,D,DL,V,VL,LELEM,LMAT,
C & SMAT,EESE,EPSE,DUCT,EXCR,DAMAGE)
CALL MAT02
& (IOPT ,IELNO ,ERR ,FIRST ,PRINT ,BUG ,
& MAT ,SE ,P,PL,D,DL,V,VL,LELEM,LMAT,
& SMAT,DUMMY,DUMMY,DUCT,EXCR,DUMMY)
C
C INITIALIZE ELEMENT STIFFNESS
IOPT=2
BUG=.FALSE.
C
CALL MAT02
& (IOPT ,IELNO ,ERR ,FIRST ,PRINT ,BUG ,
& MAT ,SE ,P,PL,D,DL,V,VL,LELEM,LMAT,
& SMAT,DUMMY,DUMMY,DUCT,EXCR,DUMMY)
C
STIF=SE(1)
BUG=.FALSE.
C
WRITE(6,*)" STIFFNESS LOAD DISP. RULE"
C READ DISPLACEMENT
F=0.
FL=0.
D=0.
DL=0.
C
800  READ(5,*,END=5000)DMIN, DMAX, NUMB
      DD=(DMAX-DMIN)/NUMB
700  DL=D
      D=D+DD
      FL=F
      F=F+STIF*DD
      P=F
      PL=FL
      IOPT=3
      CALL MAT02

```

```

& (IOPT ,IELNO ,ERR ,FIRST ,PRINT ,BUG ,
& MAT ,SE ,P,PL,D,DL,V,VL,LELEM,LMAT,
& SMAT,DUMMY,DUMMY,DUCT,EXCR,DUMMY)
C
      F=P
      STIF=SE(1)
      WRITE(6,98)SE(1), F, D, SE(2)
98 FORMAT(3F15.5, 3X, F4.1)
      IF (DMAX .GT. 0) THEN
        IF (D .LE. DMAX) THEN
          GO TO 700
        ELSE IF (D .GT. DMAX) THEN
          D=DMAX
          GO TO 800
        ENDIF
      ELSE IF (DMAX .LE. 0) THEN
        IF (D .GE. DMAX) THEN
          GO TO 700
        ELSE IF (D .LT. DMAX) THEN
          D=DMAX
          GO TO 800
        ENDIF
      ENDIF
C
5000 CLOSE(5)
      CLOSE(6)
      STOP
      END
C=====
C   DEBUG UNIT(6),TRACE,SUBCHK,INIT,SUBTRACE
C   END DEBUG
C=====
SUBROUTINE MAT02
& (IOPT ,IELNO ,ERR ,FIRST ,PRINT ,BUG ,
& MAT ,SE ,P,PL,D,DL,V,VL,LELEM,LMAT,
& SMAT,EESE,EPSE,DUCT,EXCR,DAMAGE)
C
      IMPLICIT REAL(A-H,O-Z)
      LOGICAL ERR,FIRST,PRINT,BUG
      LOGICAL BTEST
      DIMENSION SE(100),SMAT(23),DUCT(3),EXCR(6)
      CHARACTER*80 TYPE

C
C----- --- LENGTH OF ELEMENT DATA REQUIRED...
      LELEM=33
      IF (IOPT.EQ.0) RETURN
C
C----- -----
C  VARIABLES:
C-----
C----- GLOBAL VARIABLES
C  IOPT = 1, INITIALIZE MATERIAL
C      = 2, GET STIFFNESS
C  RINPUT = INPUT DATA
C  SMAT = INTERNAL STORAGE
C  SE = OUTPUT STIFFNESS
C-----
C  ---- AXLMOD DATA ----
C  SMAT(1)= SC,    COMPRESSION STIFFNESS
C  SMAT(2)= ST1,   INITIAL TENSILE STIFFNESS
C  SMAT(3)= ST2,   POST YEILD TENSILE STIFFNESS
C  SMAT(4)= PY,    YEILD POINT
C  SMAT(5)= ALPHA, AXLMOD PARAMETER
C  SMAT(6)= BETA,  AXLMOD PARAMETER
C  SMAT(7)= DYT,   AXLMOD PARAMETER
C  SMAT(8)= DYC,   AXLMOD PARAMETER

```

```

C SMAT(9)= CSE,    CONSTANT STRAIN ENERGY
C SMAT(10)=DMAX,   ULTIMATE DISPLACEMENT
C SMAT(11)=BDAM,   BETA FOR DAMAGE INDEX
C
C----- INPUT DATA FOR AXLMOD HYSTERESIS MODEL ----- C
C THE FOLLOWING DATA IS INPUT ONCE FOR EACH MODEL       C
C
C SC = COMPRESSION STIFFNESS                          C
C ST1 = INITIAL TENSILE STIFFNESS                   C
C ST2 = POST YEILD TENSILE STIFFNESS                C
C PY = YEILD LOAD                                     C
C ALPHA = MODEL COIEFICIENTS                         C
C BETA = MODEL COIEFICIENTS                         C
C
C----- C
C
C GO TO (100,200,300,400,500),IOPT
C
100 CONTINUE
C
READ (5,*) TYPE , ( SMAT(I),I=1,6),DUCMAX,BDAM
LMAT = 11
SMAT(7)= SMAT(4)/SMAT(2)
SMAT(8)= -SMAT(4)/SMAT(1)
SMAT(9)= SMAT(4)**2/(2*SMAT(2))
SMAT(10)=DUCMAX*SMAT(7)
SMAT(11)=BDAM
C
IF (FIRST .OR. BUG) WRITE (6,192)
WRITE (6,191) MAT,(SMAT(K),K=1,6),DUCMAX,BDAM
C
191 FORMAT (1X,I5,8G15.6/)
192 FORMAT (///' AXLMOD HYSTERESIS MODEL- FOR UNIT LENGTH MEMBER'/
& ' ======'//'
& ' MAT.',6X,'SC',10X,'ST1',10X,'ST2',10X,'PY',
& 10X,'ALPHA',10X,'BETA',6X,'MAX DUCT.',7X,'BETA-DI')
C
GO TO 9999
C===== GET STIFFNESS TERMS =====
200 CONTINUE
C ---- AXLMOD MODEL DATA STORAGE FOR MEMBER ----
C SE( 1)= S
C SE( 2)= HRN
C SE( 3)= FMAX
C SE( 4)= DMAX
C SE( 5)= FX
C SE( 6)= DX
C SE( 7)= FP
C SE( 8)= DP
C SE( 9)= KR
C SE(10)= KS
C SE(11)= KT
C SE(12)= NRL
C SE(13)= A
C SE(14)= S_EQ_UNLOAD - EQUIVALENT UNLOADING STIFFNESS
C SE(15)= UPOS(1)
C SE(16)= UPOS(2)
C SE(17)= UPOS(3)
C SE(18)= UNEG(1)
C SE(19)= UNEG(2)
C SE(20)= UNEG(3)
C SE(21)= EXCR(1)
C SE(22)= EXCR(2)
C SE(23)= EXCR(3)
C SE(24)= EXCR(4)
C SE(25)= EXCR(5)

```

```

C SE(26)= EXCR(6)
C SE(27)= ESE(1)
C SE(28)= ESE(2)
C SE(29)= ESE(3)
C SE(30)= PSE
C SE(31)= PSE_OLD
C SE(32)= POS_DMAX
C SE(33)= POS_PMAX
C
DO 210 I=1,LELEM
210 SE(I)=0
CALL HYSTO2(P ,D ,PL,DL,V ,VL,SE(1),SE(2),
& SMAT(1),SMAT(2),SMAT(3),SMAT(4),SMAT(5),SMAT(6),SMAT(7),SMAT(8),
& SMAT(9),
& SE(3),SE(4),SE(5),SE(6),SE(7),SE(8),SE(9),SE(10),SE(11),SE(12),
& SE(13),BUG, SE(14),SE(27),SE(30),SE(31),SE(15),SE(18),SE(21),
& IDR)
IF (BUG) WRITE (6,*) 'STIFF=' ,STIFF,' A=' ,A
GO TO 9999
C
C===== GET STIFFNESS TERMS =====
300 CONTINUE
C SE( 1)= A
C SE(13)= A
ICYC=0
IF (BUG) THEN
  WRITE (6,*) '----- IN MAT02 ---- IELNO:',IELNO,
  & '-----'
  WRITE (6,*) 'A:',SE(13)
  WRITE (6,*) ' P,D= ',P,D , ' V= ',V
  WRITE (6,*) 'PL,DL= ',PL,DL , ' VL= ',VL
ENDIF
IDR=999
310 STIFF=SE(1)
P=PL+(D-DL)*STIFF
A=SE(13)
IF (A.EQ.0 .AND. SE(2).EQ.0) A=P
ICYC=ICYC+1
IF (BUG) THEN
  WRITE (6,*) 'STIFF=' ,STIFF,' A=' ,A,' IDR=' ,IDR
  WRITE (6,*) ' P= ',P , 'ICYC=' ,ICYC
ENDIF
C
C---- IS P WITHIN LIMITS ?
IF (ICYC.GT.5) THEN
  WRITE (6,*) 'MORE THAN 5 CYCLES IN MAT02, IELNO:',IELNO
ELSE IF ((PL.LE.P .AND. P.LT.A) .OR. (PL.GE.P .AND. P.GT.A) .OR.
& (DL.EQ.D)) THEN
  CALL STRENG (SE(27),SE(30),SE(31),P,PL,D,DL,SE(1),SE(14) )
  IF (BUG) WRITE (6,*) 'C---- IS P WITHIN LIMITS ? '
  CALL HYSTO2(P ,D ,PL,DL,V ,VL,SE(1),SE(2),
& SMAT(1),SMAT(2),SMAT(3),SMAT(4),SMAT(5),SMAT(6),
& SMAT(7),SMAT(8),SMAT(9),SE(3),SE(4),SE(5),SE(6),SE(7),SE(8),
& SE(9),SE(10),SE(11),SE(12),SE(13),BUG,
& SE(14),SE(27),SE(30),SE(31),SE(15),SE(18),SE(21),IDR )
  V=VL
C---- IS P GREATER THAN LIMITS ?
ELSE IF (((PL.LE.A .AND. A.LE.P) .OR. (PL.GE.A .AND. A.GE.P)).AND.
& (STIFF.NE.0.00)) THEN
  D1=DL+(A-PL)/STIFF
  P1=A
  CALL STRENG (SE(27),SE(30),SE(31),P1,PL,D1,DL,SE(1),SE(14))
  DL=D1
  PL=P1
  IF (ABS(P-PL).GT. 0.005*ABS(P+PL)) THEN
    PI=PL+(P-PL)*.01
    DI=DL+(D-DL)*.01

```

```

ELSE
  PI=P
  DI=D
ENDIF
IF (BUG) THEN
  WRITE (6,*) 'C---- IS P GREATER THAN LIMITS ? '
  WRITE (6,*) 'PI,DL=',PL,DL
  WRITE (6,*) 'PI,DI=',PI,DI
ENDIF
CALL HYSTO2(PI,DI,PL,DL,1.,1.,SE(1),SE(2),
& SMAT(1),SMAT(2),SMAT(3),SMAT(4),SMAT(5),SMAT(6),
& SMAT(7),SMAT(8),SMAT(9),SE(3),SE(4),SE(5),SE(6),SE(7),SE(8),
& SE(9),SE(10),SE(11),SE(12),SE(13),BUG,
& SE(14),SE(27),SE(30),SE(31),SE(15),SE(18),SE(21),IDR )
  V=VL
GO TO 310
C---- IS P LESS THAN LIMITS ?
ELSE IF ((P.LT.PL .AND. PL.LE.A) .OR. (P.GT.PL .AND. PL.GE.A))THEN
  IF (ABS(P-PL).GT. 0.005*ABS(P+PL)) THEN
    PI=PL+(P-PL)*.01
    DI=DL+(D-DL)*.01
  ELSE
    PI=P
    DI=D
  ENDIF
  IF (BUG) THEN
    WRITE (6,*) 'C---- IS P LESS THAN LIMITS ? '
    WRITE (6,*) 'PI,DI=',PI,DI
  ENDIF
  CALL HYSTO2(PI,DI,PL,DL,1.,1.,SE(1),SE(2),
& SMAT(1),SMAT(2),SMAT(3),SMAT(4),SMAT(5),SMAT(6),
& SMAT(7),SMAT(8),SMAT(9),SE(3),SE(4),SE(5),SE(6),SE(7),SE(8),
& SE(9),SE(10),SE(11),SE(12),SE(13),BUG,
& SE(14),SE(27),SE(30),SE(31),SE(15),SE(18),SE(21),IDR )
  V=VL
GO TO 310
ENDIF
C
C----- SAVE MAXIMUM PEAK POSITIVE DISPL
  IF (D.GT.SE(32)) THEN
    SE(32)=D
    SE(33)=P
  ENDIF
C
  IF (BUG) WRITE (6,*) 'STIFF=',STIFF,' A=',SE(13)
C
C----- TRANSFER ENERGIES FOR BOTH IOPT=3 AND 4.
400 EESE=SE(27)
  EPSE=SE(30)
C
C----- TRANSFER DUCTILITIES AND EXCRUSION RATIOS FOR BOTH IOPT=3 AND 4.
  DO 410 I=1,3
    DUCT(I)=MAX(SE(14+I),SE(17+I))
    EXCR(I)=SE(20+I)
  410 EXCR(I+3)=SE(20+I+3)
C
  RETURN
C
C===== DAMAGE INDEX ======
500 CONTINUE
  EESE=SE(27)
  EPSE=SE(30)
  BDAM=SMAT(11)
  D =SE(32)
  P =SE(33)
  DAMAGE=ABS(D)/SMAT(10) + BDAM / ( SMAT(4)*SMAT(10) ) * EPSE
C

```

```

9999 CONTINUE
C
  RETURN
END
C
C===== HYSTO2 =====
C DEBUG UNIT(6),TRACE,SUBCHK,INIT,SUBTRACE
C END DEBUG
C=====
C SU_BROUTINE AXLMOD - AXIAL HYSTERESIS MODEL
C      REFERENCE: ANALYSIS OF THE FULL SCALE SEVEN
C      STORY R/C TEST STRUCTURE.
C
C P = CURRENT LOAD, POSITIVE IS TENSION
C D = CURRENT DISPLACEMENT, POSITIVE IS ELONGATION
C S = STIFFNESS
C KC = VIRGIN COMPRESSION STIFFNESS, EC
C KT1 = PRE-YIELD VIRGIN TENSILE STIFFNESS, 0.9*KC
C KT2 = POST-YIELD VIRGIN TENSILE STIFFNESS, 0.001*KC
C PY = TENSILE YIELD POINT, PH0*FY
C FMAX = MAXIMUM TENSILE FORCE BEFORE UNLOADING
C DMAX = MAXIMUM TENSILE DISPLACEMENT BEFORE UNLOADING
C FX = FORCE AT STIFFNESS CHANGE POINT ON THE UNLOADING CURVE
C DX = DISPL. AT STIFFNESS CHANGE POINT ON THE UNLOADING CURVE
C PI,DI = INTERSECTION OF TWO LINES
C DYT = TENSILE YIELD DISPLACEMENT = PY/KT1
C DYC = COMPRESSION YIELD DISPLACEMENT = PY/KC
C FP = FORCE AT COMPRESSION STIFFNESS CHANGE POINT
C DP = COMPRESSION AT COMPRESSION STIFFNESS CHANGE POINT
C KR = UNLOADING STIFFNESS = KC/(DMAX/DYT)**(.20)
C KS = LOADING STIFFNESS, LINE BETWEEN (FX,DX) AND (FP,DP)
C KT = LOADING STIFFNESS, LINE BETWEEN (FP,DP) AND (-2PY,-2DY)
C
C
SUBROUTINE HYSTO2(P,D,PL,DL,V,VL,S,HRLN,KC,KT1,KT2,PY,ALPHA,BETA,
& DYT,DYC,CSE,FMAX,DMAX,FX,DX,FP,DP,KR,KS,KT,NRL,A,PRINT,
& SEQ,ESE,PSE,PSEOLD,UPOS,UNEG,EXCR,IDR)
C
REAL*4 KC,KT1,KT2,KR,KS,KT,NRL
DIMENSION UPOS(3),UNEG(3),EXCR(6),ESE(3)
INTEGER RULEI
LOGICAL LT,PRINT,PGTPL,PLTPL
C
8000 IF (PRINT) WRITE (6,8010) P,D,PL,DL,V,VL,S,HRLN,KC,KT1,KT2,PY,
& ALPHA,BETA,DYT,DYC,FMAX,DMAX,FX,DX,FP,DP,KR,KS,KT,NRL,A,
& SEQ,ESE(3),PSE,PSEOLD,CSE,UPOS,UNEG,EXCR
8010 FORMAT(
  & ' AXLMOD-P=''G13.5,' D=''G13.5,' PL=''G13.5,' DL=''G13.5,/'
  & ' AX- V=''G13.5.' VL=''G13.5.' S=''G13.5.' HRLN=''G13.5./'
  & ' AX- KC=''G13.5.' KT1=''G13.5.' KT2=''G13.5.' PY=''G13.5./'
  & ' AX- ALPHA=''G13.5.' BETA=''G13.5.' DYT=''G13.5.' DYC=''G13.5./'
  & ' AX- FMAX=''G13.5.' DMAX=''G13.5.' FX=''G13.5.' DX=''G13.5./'
  & ' AX- FP=''G13.5.' DP=''G13.5.' KR=''G13.5.' KS=''G13.5./'
  & ' AX- KT=''G13.5.' NRL=''G13.5.' A=''G13.5.' SEQ=''G13.5./'
  & ' AX- ESE=''G13.5.' PSE=''G13.5.' PSEO=''G13.5.' CSE=''G13.5./'
  & ' AX- UP1=''G13.5.' UP2=''G13.5.' UP3=''G13.5./'
  & ' AX- UN1=''G13.5.' UN2=''G13.5.' UN3=''G13.5./'
  & ' AX- EX1=''G13.5.' EX2=''G13.5.' EX3=''G13.5./'
  & ' AX- EX4=''G13.5.' EX5=''G13.5.' EX6=''G13.5.')

C..... SET INITIAL STIFFNESS AND RETURN
IF (NRL.EQ.0) THEN
IF (P.LE.0) THEN
  NRL=1
  HRLN=1.1
  S=KC
  SEQ=KC

```

```

      A=P
      ELSE
        NRL=2
        HRLN=2.1
        S=KT1
        SEQ=KC
        A=P
      ENDIF
      RETURN
    ENDIF

C..... RETURN IF NO STEP HAS BEEN TAKEN
  IF (P.EQ.PL .OR. D.EQ.DL ) RETURN

C..... SET LOADING FLAGS
  PGTPL=P.GT.PL
  PLTPL=P.LT.PL
C
C..... CALC EXCURSION RATIO AT EVERY ZERO CROSSING...
C IF (P*PL.LE.0 .AND. PL.GT.0)
C & CALL DNE(0,UPOS,EXCR,DYT,D,ESE,PSE,PSEOLD,CSE)
  IF (P*PL.LE.0 .AND. PL.LE.0) THEN
    EXCR(4)=0
    EXCR(5)=0
    EXCR(6)=0
  ENDIF
C
C..... CALC DUCTILITY IF LOAD GT PAST LOAD
C
C DUCTILITY FOR POSITIVE LOADS ONLY
C IF (P.GT.0 .AND. PGTPL)
C & CALL DNE(1,UPOS,EXCR,DYT,D ,ESE(2),PSE,PSEOLD,CSE)

999 CALL IDRECT(IDR,IDRV,IDRVO,P,PL,V,VL)
      IDR=IDR

      1 IF (NRL.EQ.0) NRL=1
C
      RULEI=NRL
C
      GO TO (100,200,300,400,500,600,700,800,900,
      & 1000,1100,1200,1300),RULEI
C
C RULE 1 - LOADING AND UNLOADING ON THE COMPRESSION BRANCH BEFORE YEILD
C
100 SEQ=KC
      IF (P.GT.0) GO TO 200
      S=KC
      NRL=1
      HRLN=1.1
      IF (PLTPL) A=MIN(10.*P,-2.*PY)
      IF (PGTPL) A=0.
      RETURN
C
C RULE 2 - TENSION LOADING BEFORE YEILD
C
200 IF (IDR) 230,230,210
210 IF (P.GE.PY) GO TO 600
      S=KT1
      NRL=2
      HRLN=2.1
      A=PY
      RETURN
230 IF (PL.LE.0) GO TO 210
      FMAX=AMAX1(P,FMAX)
      DMAX=AMAX1(D,DMAX)
      FX =FMAX-PY

```

```

DX =DMAX-PY/KC
S=KC
NRL=3
HRLN=2.2
A=FX
RETURN
C
C RULE 3 - UNLOADING ON TENSION BEFORE YEILD
C
300 IF (PGTPL) GO TO 500
IF (P.GT.0) GO TO 330
310 IF (KC.NE.KT1) THEN
CALL INTSCT(DI,PI,D,P,KC,DX,FX,KT1)
ELSE
PI=P
DI=D
ENDIF
IF (P.LE.PI) GO TO 320
S=KC
NRL=3
RLN=3.11
A=PI
RETURN
320 S=KT1
NRL=4
HRLN=3.12
A=PY
RETURN
330 IF (P.GE.FMAX) GO TO 200
S=KC
NRL=3
HRLN=3.2
A=FX
RETURN
C
C RULE 4 - LOADING TOWARDS Y' FROM FX.
C
400 IF (IDR) 500,500,410
410 IF (ABS(P).GE.PY) GO TO 100
S=KT1
NRL=4
HRLN=4.1
A=-PY
RETURN
C
C RULE 5 - LOADING AND UNLOADING BETWEEN BRANCHES O-Y AND FX-Y'
C
500 IF (KC.NE.KT1) THEN
CALL INTSCT(DITENS,PITENS,D,P,KC,DYT,PY,KT1)
CALL INTSCT(DICOMP,PICOMP,D,P,KC,DX ,FX,KT1)
ELSE
PITENS=P
DITENS=D
PICOMP=P
DICOMP=D
ENDIF
IF (P.LE.PICOMP) GO TO 330
IF (P.GE.PITENS) GO TO 210
S=KC
NRL=5
HRLN=5.1
IF (PGTPL ) A=PITENS
IF (PLTPL ) A=PICOMP
RETURN
C
C RULE 6 - LOADING AFTER TENSION YEILD
C

```

```

600 IF (IDR) 630,630,610
610 S=KT2
  NRL=6
  HRLN=6.1
  A=5*p
C..... CALC UNLOADING CURVE FOR ENERGY INFO
  FMAX=AMAX1(P,FMAX)
  DMAX=AMAX1(D,DMAX)
  KR=KC*(DMAX/DYT)**(-1. * ALPHA)
  FX =FMAX-PY
  DX =DMAX-PY/KR
  KS =(PY+FX)/(DX-DYC)
C----- FORCE KR GE KS , TO PREVENT UNSTABLE LOOPS...
  IF (KS.GT.KR) KR=(FMAX+PY)/(DMAX-DYC)
  SEQ=KR
  RETURN
630 FMAX=AMAX1(P,FMAX)
  DMAX=AMAX1(D,DMAX)
  KR=KC*(DMAX/DYT)**(-1. * ALPHA)
  FX =FMAX-PY
  DX =DMAX-PY/KR
  KS =(PY+FX)/(DX-DYC)
C----- FORCE KR GE KS , TO PREVENT UNSTABLE LOOPS...
  IF (KS.GT.KR) THEN
    KR=(FMAX+PY)/(DMAX-DYC)
    KS=KR
    DX=DMAX-PY/KR
  ENDIF
  DP =DYC + BETA*(DX-DYC)
  FP =FX - (DX-DP)*KS
  KT =(2*PY+FP)/(DP-2*DYC)
  DQ =DYC + PY/KR
  S=KR
  NRL=7
  HRLN=6.2
  A=FX
  RETURN
C
C RULE 7 - UNLOADING AFTER YEILD
C
700 SEQ=KR
  IF (IDR) 730,730,710
710 IF (P.GE.FMAX) GO TO 600
  S=KR
  NRL=7
  HRLN=7.1
  A=FMAX
  RETURN
730 IF (P.LE.FX) GO TO 800
  S=KR
  NRL=7
  HRLN=7.2
  A=FX
  RETURN
C
C RULE 8 - ON BRANCH BETWEEN DX & DP
C
800 IF (PGTPL) THEN
  IF (KR.EQ.KS) GO TO 1200
  GO TO 1300
ENDIF
IF (P.LE.FP) GO TO 900
  S=KS
  NRL=8
  HRLN=8.1
  A=FP
  RETURN

```

```

C
C RULE 9 - ON BRANCH FP-Y"
C
900 IF (PGTPL) GO TO 1300
  IF (P.LE.(-2*PY) ) GO TO 1000
  S=KT
  NRL=9
  HRLN=9.1
  A=-2*PY
  RETURN
C
C RULE 10 - ON THE COMPRESSION CURVE AFTER YELDING
C
1000 SEQ= 1. / ( 1./KC + (4./KR - 4./KC)*(PY/P)**2 )
C
  IF (IDR) 1030,1030,1010
1010 S=KC
  NRL=10
  HRLN=10.1
  A=10*p
  RETURN
1030 IF (ABS(P).LE.PY) GO TO 1100
  S=KC
  NRL=10
  HRLN=10.2
  A=-PY
  RETURN
C
C RULE 11 - UNLOADING BETWEEN Y' & Q
C
1100 SEQ=KR
  IF (ABS(P).GT.PY ) GO TO 1000
  IF ( P .GE. 0.) GO TO 1200
  S=KR
  NRL=11
  HRLN=11.1
  IF (PGTPL) A=0
  IF (PLTPL) A=-PY
  RETURN
C
C RULE 12 - LOADING FORM Q TO M
C
1200 IF (PLTPL) THEN
  IF (KS.EQ.KR .AND. P.GT.FP) GO TO 800
  GO TO 1300
ENDIF
  IF ( P .GE.FMAX) GO TO 600
  S=KS
  NRL=12
  HRLN=12.1
  A=FMAX
  RETURN
C
C RULE 13 - LOADING AND UNLOADING INSIDE Q-M-D-P-Y"-Y'
C
1300 IF (KR.NE.KS) THEN
  CALL INTSCT(DITENS,PITENS,D,P,KR,DMAX,FMAX,KS)
  CALL INTSCT(DICOMP,PICOMP,D,P,KR,DX ,FX,KS )
ELSE
  IF (PGTPL) GO TO 1200
  PITENS=P
  DITENS=D
  PICOMP=P
  DICOMP=D
ENDIF
C-----IS POINT WITHIN PY'-FP-PY" ?

```

```

IF (PICOMP.LE.FP) THEN
  IF (KC.NE.KT) THEN
    CALL INTSCT(DICOMP,PICOMP,D,P,KC,DP,FP,KT )
  ELSE
    IF (PLTPL) GO TO 900
    PICOMP=P
    DICOMP=D
  ENDIF
  IF (KR.EQ.KS .AND. PLTPL) GO TO 800
  S2=KT
ELSE
  S2=KR
ENDIF
IF (PGTPL) THEN
  IF (P.GT.PITENS) GO TO 1200
  A=PITENS
  HRLN=13.1
ENDIF
IF (PLTPL) THEN
  IF (P.LT.PICOMP) GO TO 800
  A=PICOMP
  HRLN=13.2
ENDIF
S=MAX(KR,S2)
NRL=13
RETURN
C
END
C
C=====
C - INTERSECTION OF TWO LINES IN POINT SLOPE FORM .....
C   DEBUG UNIT(6),SUBCHK, SUBTRACE
C   END DEBUG
C X = X COORDINATE OF INTERSECTION
C Y = Y COORDINATE OF INTERSECTION
C X1 = X COORDINATE OF LINE 1
C Y1 = Y COORDINATE OF LINE 1
C S1 = SLOPE OF LINE 1
C X2 = X COORDINATE OF LINE 2
C Y2 = Y COORDINATE OF LINE 2
C S2 = SLOPE OF LINE 2

SUBROUTINE INTSCT(X,Y,X1,Y1,S1,X2,Y2,S2)
IMPLICIT REAL(A-H,O-Z)
IMPLICIT INTEGER(L-N)
LOGICAL BTTEST
IF (S1.NE.S2) THEN
  B1= Y1 - S1*X1
  B2= Y2 - S2*X2
  X=(B1-B2)/(S2-S1)
  Y=(B1*S2-B2*S1)/(S2-S1)
ELSE
  WRITE (6,10) X1,Y1,S1,X2,Y2,S2
10 FORMAT ('/***** ER','ROR IN INTSCT....',1X,
  &      'S1=S2, NO SOLN, THUS SET X=Y=0.',/
  &      'X1=',1P,G15.5,' Y1=',G15.5,' S1=',G15.5/
  &      'X2=',1P,G15.5,' Y2=',G15.5,' S2=',G15.5/)
  X=0
  Y=0
C   CALL ERRTRA
ENDIF
CC   WRITE (6,5) X1,Y1,S1,B1,X2,Y2,S2,B2,X,Y
CC5  FORMAT ('/ IN INTSCT...',...
CC&  ' X1=',1P,G15.5,' Y1=',G15.5,' S1=',G15.5,' B1=',G15.5/
CC&  ' X2=',1P,G15.5,' Y2=',G15.5,' S2=',G15.5,' B2=',G15.5/
CC&  ' X=',1P,G15.5,' Y=',G15.5/)
```

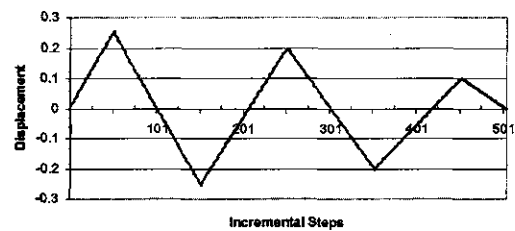
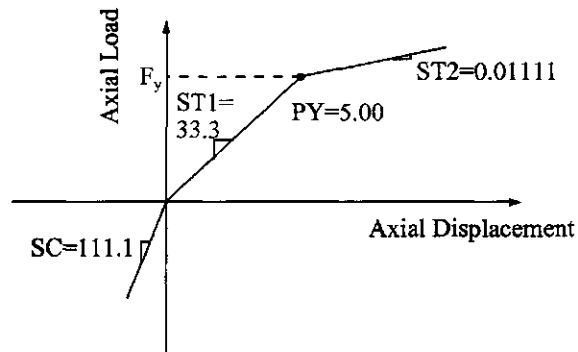
```

      RETURN
      END
=====
C
C@PROCESS SDUMP OPT(0) GOSTMT XREF MAP
*****
C DEBUG UNIT(6),TRACE,SUBCHK,INIT,SUBTRACE
C END DEBUG
C
      SUBROUTINE IDRECT (IDR,IDRV,IDRVO,PI,PS,VI,VS)
C
      LOGICAL A,NA,B,NB,C,NC,D,ND,E
      LOGICAL BTTEST
C
C WRITE (6,*) 'IDR,IDRV,IDRVO,PI,PS,VI,VS'
C WRITE (6,*) IDR,IDRV,IDRVO,PI,PS,VI,VS
C
      1 A = ABS(PI).GE.ABS(PS)
      B = PI*PS .GE.0
C     B = PI*PS .GT.0
      C= PI.EQ.0
      D = VS*VI.GE.0
      NA= .NOT. A
      NB= .NOT. B
      NC= .NOT. C
      ND= .NOT. D
C
      IF ( A .AND. B .AND. NC .AND. D ) IDR=1
      IF ( NB .AND. NC .AND. ND ) IDR=1
      IF (NA .AND. B .AND. NC .AND. ND ) IDR=1
      IF ( C .AND. D ) IDR=0
      IF ( NB .AND. NC .AND. D ) IDR=0
      IF ( A .AND. B .AND. NC .AND. ND ) IDR=-1
      IF ( C .AND. ND ) IDR=-1
      IF (NA .AND. B .AND. NC .AND. D ) IDR=-1
      E = PI .GE. PS
      IDRVO=1
      IDRVO=2
      IF (E) IDRV=1
      IF (E) IDRVO=1
      RETURN
      END

Input Data:
1 1 |IELNO MAT
'AXLMod' 111.1 33.3 0.01111 5.00 0.9 0.2 20 0.2 |TYPE SMAT DUCMAX BDAM
0. 0.25 50 |DMIN DMAX NUMB
0.25 -0.25 100 |DMIN DMAX NUMB
-0.25 0.2 100 |DMIN DMAX NUMB
0.2 -0.2 100 |DMIN DMAX NUMB
-0.2 0.1 100 |DMIN DMAX NUMB
0.1 0. 50 |DMIN DMAX NUMB

Output Data:
AXLMod HYSTERESIS MODEL- FOR UNIT LENGTH MEMBER
=====
MAT.    SC     ST1     ST2     PY     ALPHA     BETA     MAX     DUCT.     BETA-DI
1 111.100 33.3000 0.111100E-01 5.000000 0.900000 0.200000 20.0000 0.200000
STIFFNESS   LOAD     DISP.     RULE
33.30000  0.16650  0.00500  2.1
33.30000  0.33300  0.01000  2.1
33.30000  0.49950  0.01500  2.1
.
.
.
66.29627  -4.03274  0.00000  9.1
66.29627  -4.16533  -0.00200  9.1

```



Diagrams Represent Input Data for Appendix L (Axial)

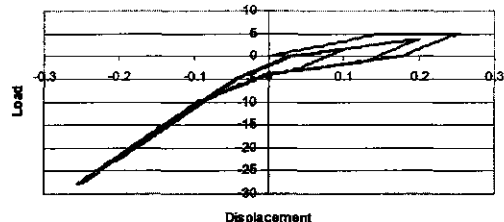
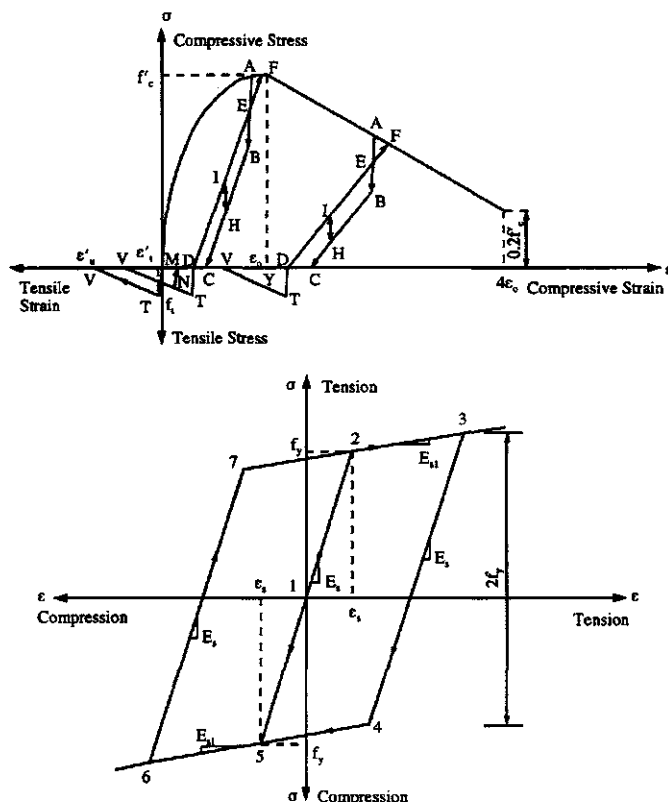


Diagram Represents Output Solution for Appendix L (Axial)

Appendix M—Cheng-Lou Axial Hysteresis Model for RC Columns and Walls and Computer Program



```

C
C -----
C THIS PROGRAM IS FOR SHEAR WALL UNDER AXIAL LOAD REVERSALS.
C -----
PROGRAM HYSAXIAL
IMPLICIT REAL*8 (A-H,O-Z)
C -----
C DISPL ----- AXIAL DISPLACEMENT OF SHEAR WALL (mm)
C PLOAD ----- AXIAL LOADING (N)
C STRAN ----- AXIAL STRAIN OF SHEAR WALL
C SIGNC ----- CONCRETE STRESS (MPa)
C SIGNS ----- STEEL STRESS (MPa)
C -----
DIMENSION DISPL(1200),PLOAD(1200),STRAN(1200),

```

```

* SIGNC(1200),SIGNS(1200)
C -----
C EXPLANATION OF INPUT DATA
C XWALL ----- THE LENGTH OF SHEAR WALL (mm)
C WWALL ----- THE WIDTH OF SHEAR WALL (mm)
C HWALL ----- THE HEIGHT OF SHEAR WALL (mm)
C FCCON ----- COMPRESSIVE STRESS OF CONCRETE (MPa)
C FTCON ----- TENSILE STRESS OF CONCRETE (MPa)
C EICON ----- INITIAL ELASTIC MODULUS OF CONCRETE (MPa)
C ASTEL ----- AREA OF TOTAL REINFORCEMENT (mm)
C FYSTL ----- TENSILE STRENGTH OF STEEL(MPa)
C YSTEL ----- YIELDING STRAIN OF STEEL
C RATIO ----- RATIO OF MODULUS AFTER STEEL YIELDING
C NOINC ----- NUMBER OF DISPLACEMENT STEPS
C -----
READ(1,*) XWALL,WWALL,HWALL,FCCON,FTCON,EICON,ASTEL,FYSTL,
* YSTEL,RATIO,NOINC
WRITE(2,4000)
WRITE(2,5000) XWALL,WWALL,HWALL,FCCON,FTCON,EICON,ASTEL,FYSTL,
* YSTEL,RATIO
DO 1 IOINC=1, NOINC
READ(1,*) DISPL(IOINC)
1 STRAN(IOINC)=DISPL(IOINC)/HWALL
ARCON=XWALL*WWALL
ESTEL=FYSTL/YSTEL
ETCON=FTCON/EICON
IF(STRAN(1).LE.0.D0) THEN
SIGNC(1)=FCCON*(2.D0*STRAN(1)/(-2.D-3)-2.5D5*STRAN(1)*STRAN(1))
ELSE
SIGNC(1)=EICON*STRAN(1)
ENDIF
SIGNS(1)=ESTEL*STRAN(1)
JSIGN=0
ISIGN=0
LSIG1=0
LSIG2=0
MSIG1=0
MSIG2=0
STRND=0.D0
YSTC1=0.D0
C -----
C INCREMENT OF DISPLACEMENT, CONCRETE STRESS
C -----
DO 1000 IOINC=2, NOINC
IF(JSIGN.EQ.1.AND.STRND.LE.-8.D-3) THEN
SIGNC(IOINC)=0.D0
GOTO 1000
ENDIF
IF(STRAN(IOINC-1)-STRAN(IOINC)) 100,100,300
C
C POSITIVE INCREMENT
C
100 IF(SIGNC(IOINC-1)) 110,110,130
C
C UNLOADING FROM COMPRESSION, BOTH NEGATIVE DISPLACEMENT
C AND STRESS
C
110 IF(STRNA.GT.STRXA.AND.STRXA.LT.0.D0) THEN
STRNA=STRXA
STRNB=STRXB
STRNC=STRXC
STRND=STRXD
STRNE=STRXE
ECMAX=ECMXX
ENDIF
IF(STRAN(IOINC).LE.0.D0) THEN

```

CHENG-LOU AXIAL HYSTERESIS MODEL FOR RC COLUMNS AND WALLS 969

```
ISIGN=1
ENDIF
LSIG1=0
LSIG2=1
IF(STRAN(IOINC).GE.STRND) GOTO 130
200 IF(LSIG2.EQ.1.AND.LSIG4.EQ.0) THEN
  IF(STRAN(IOINC).LE.STRNB) THEN
    SIGNC(IOINC)=SIGNC(IOINC-1)+EICON*(STRAN(IOINC)-STRAN(IOINC-1))
    JSIG1=1
    JSIG2=0
  ELSE
    IF(STRAN(IOINC).LE.STRNC) THEN
      SIGNC(IOINC)=ECMAX*(STRAN(IOINC)-STRNC)
      JSIG1=0
      JSIG2=1
    ELSE
      SIGNC(IOINC)=0.D0
      JSIG1=0
      JSIG2=1
    ENDIF
  ENDIF
  ENDIF
  IF(LSIG4.EQ.1) THEN
    IF(STRAN(IOINC).LE.STRMA) THEN
      LSIG4=0
      GOTO 200
    ELSE
      SIGMX=SIGNC(IOINC-1)+EICON*(STRAN(IOINC)-STRAN(IOINC-1))
      SIGMY=ECMAX*(STRAN(IOINC)-STRNC)
      SIGNC(IOINC)=DMIN1(SIGMX,SIGMY)
      IF(STRAN(IOINC).LE.STRND.AND.STRAN(IOINC).GE.STRNC) THEN
        SIGNC(IOINC)=0.D0
      ENDIF
      JSIG1=0
      JSIG2=1
    ENDIF
  ENDIF
  GOTO 1000
C
C LOADING, RELOADING, OR UNLOADING FROM COMPRESSION
C ZERO OR POSITIVE STRESS
C
130 IF(LSIG1.EQ.0.AND.LSIG2.EQ.0) THEN
  IF((STRAN(IOINC)-STRND).LE.ETCON) THEN
    SIGNC(IOINC)=EICON*(STRAN(IOINC)-STRND)
    USTC1=STRND
  ELSE
    IF((STRAN(IOINC)-STRND).LE.2.D-3) THEN
      SIGNC(IOINC)=FTCON*(1.D0-((STRAN(IOINC)-STRND)-ETCON)/1.9D-3)
      YSTC1=STRAN(IOINC)-STRND
      USTC1=YSTC1-SIGNC(IOINC)/EICON
    ELSE
      SIGNC(IOINC)=0.D0
      YSTC1=STRAN(IOINC)-STRND
      USTC1=YSTC1
    ENDIF
  ENDIF
  ENDIF
  IF(LSIG1.GE.1.OR.LSIG2.EQ.1) THEN
    IF(USTC1.EQ.STRND.OR.USTC1.EQ.0.D0) THEN
      LSIG1=0
      LSIG2=0
      GOTO 130
    ELSE
      IF((STRAN(IOINC)-STRND).LE.USTC1) THEN
        SIGNC(IOINC)=0.D0
      ELSE
        IF((STRAN(IOINC)-STRND).LE.STRND) THEN
          SIGNC(IOINC)=0.D0
        ELSE
          IF((STRAN(IOINC)-STRND).LE.STRNB) THEN
            SIGNC(IOINC)=EICON*(STRAN(IOINC)-STRAN(IOINC-1))
            JSIG1=1
            JSIG2=0
          ELSE
            SIGNC(IOINC)=ECMAX*(STRAN(IOINC)-STRNC)
            JSIG1=0
            JSIG2=1
          ENDIF
        ENDIF
      ENDIF
    ENDIF
  ENDIF
END
```

```

IF((STRAN(IOINC)-STRND).LE.YSTC1) THEN
SIGNC(IOINC)=EICON*(STRAN(IOINC)-STRND-USTC1)
ELSE
IF((STRAN(IOINC)-STRND).LE.2.D-3) THEN
SIGNC(IOINC)=FTCON*(1.D0-(STRAN(IOINC)-STRND-ETCON)/1.9D-3)
YSTC2=STRAN(IOINC)-STRND
USTC2=YSTC2-SIGNC(IOINC)/EICON
ELSE
SIGNC(IOINC)=0.DO
YSTC2=STRAN(IOINC)-STRND
USTC2=YSTC2
ENDIF
ENDIF
ENDIF
ENDIF
GOTO 1000
C
C NEGATIVE INCREMENT
C
300 IF(-SIGNC(IOINC-1)) 350,350,400
C
C LOADING, RELOADING, OR UNLOADING FROM COMPRESSION
C
350 LSIG1=1
LSIG2=0
IF(YSTC1.LT.YSTC2) THEN
YSTC1=YSTC2
USTC1=USTC2
ENDIF
IF(STRAN(IOINC).LT.STRND) GOTO 400
IF(USTC1.EQ.STRND) THEN
SIGNC(IOINC)=SIGNC(IOINC-1)+EICON*(STRAN(IOINC)-STRAN(IOINC-1))
ELSE
IF((STRAN(IOINC)-STRND).GE.2.D-3) THEN
SIGNC(IOINC)=0.DO
ELSE
IF((STRAN(IOINC)-STRND).LE.YSTC1.AND.(STRAN(IOINC)-STRND)
*.GE.USTC1) THEN
SIGNC(IOINC)=SIGNC(IOINC-1)+EICON*(STRAN(IOINC)-STRAN(IOINC-1))
ELSE
SIGNC(IOINC)=0.DO
ENDIF
ENDIF
ENDIF
GOTO 1000
C
C LOADING, RELOADING, OR UNLOADING FROM TENSION
C
400 IF(LSIG1.EQ.0.AND.LSIG2.EQ.0) THEN
LSIG4=0
IF(STRAN(IOINC).GE.-2.D-3) THEN
SIGNC(IOINC)=FCCON*(2.D0*STRAN(IOINC)/(-2.D-3)
*-2.5D5*STRAN(IOINC)*STRAN(IOINC))
STRNA=STRAN(IOINC)
STRNB=STRAN(IOINC)-SIGNC(IOINC)/2.D0/EICON
SIGMB=.5D0*SIGNC(IOINC)
STRNC=.478D0*STRAN(IOINC)+0.087D0*STRAN(IOINC)*
* STRAN(IOINC)/(-2.D-3)-.4D0*SIGNC(IOINC)/EICON
STRND=.145D0*(STRAN(IOINC))**2/(-2.D-3)+.13D0*STRAN(IOINC)
STRNE=STRAN(IOINC)-SIGNC(IOINC)/6.D0/EICON
SIGME=5.D0*SIGNC(IOINC)/6.D0
ECMAX=DABS(SIGME/(STRNE-STRND))
IF(ECMAX.GT.EICON) THEN
ECMAX=EICON
STRAND=STRAN(IOINC)-SIGNC(IOINC)/EICON
STRNB=SIGMB/EICON+STRND

```

CHENG-LOU AXIAL HYSTERESIS MODEL FOR RC COLUMNS AND WALLS 971

```
STRNE=SIGME/EICON+STRND
STRNC=STRND
ENDIF
ELSE
IF(STRAN(IOINC).GE.-8.D-3) THEN
SIGNC(IOINC)=FCCON*(19.D0-4.D0*STRAN(IOINC)/(-2.D-3))/15.D0
STRNA=STRAN(IOINC)
STRNB=DMIN1(STRAN(IOINC)-FCCON/3.D0/EICON,
* STRAN(IOINC)-2.D0*SIGNC(IOINC)/3.D0/EICON)
ECMAX=DMAX1((SIGNC(IOINC)-FCCON/6.D0)/(8.7D0*STRAN(IOINC)
* -.145D0*STRAN(IOINC)*STRAN(IOINC)/(-2.D-3)
* -FCCON/6.D0/EICON), 2.D0*SIGNC(IOINC)/(2.61D0
* *STRAN(IOINC)-.435D0*STRAN(IOINC)*STRAN(IOINC)
* /(-2.D-3)-SIGNC(IOINC)/6.D0/EICON))
STRNC=DMAX1(STRAN(IOINC)-FCCON/3.D0/EICON-(SIGNC(IOINC)
* -FCCON/3.D0)/ECMAX, STRAN(IOINC)-2.D0*SIGNC(IOINC)
* /3.D0/EICON-SIGNC(IOINC)/3.D0/ECMAX)
STRND=.145D0*(STRAN(IOINC))**2/(-2.D-3)+.13D0*STRAN(IOINC)
STRNE=DMIN1(STRAN(IOINC)-FCCON/6.D0/EICON, STRAN(IOINC)
* -SIGNC(IOINC)/3.D0/EICON)
ENDIF
EPSLO=2.D-3*ECMAX/FCCON+2.D0
VALUE=EPSLO*EPSLO+4.D0*ECMAX*STRND/FCCON
IF(VALUE.GE.0.D0) THEN
STRMA=-1.D-3*(EPSLO+DSQRT(EPSLO*EPSLO+4.D0*ECMAX*STRND/FCCON))
ELSE
STRMA=-2.D-3*(19.D0+15.D0*ECMAX*STRND/FCCON)
* /(4.D0-15.D0*2.D-3*ECMAX/FCCON)
ENDIF
IF(STRMA.LT.-2.D-3) THEN
STRMA=-2.D-3*(19.D0+15.D0*ECMAX*STRND/FCCON)
* /(4.D0-15.D0*2.D-3*ECMAX/FCCON)
ENDIF
IF(STRAN(IOINC).LT.-8.D-3) THEN
SIGNC(IOINC)=0.D0
STRND=STRAN(IOINC)
STRNC=STRND
JSIGN=1
ENDIF
ENDIF
ENDIF
IF(LSIG1.EQ.1.AND.LSIG2.EQ.0) THEN
IF(JSIGN) 500,500,600
500 LSIG1=0
GOTO 400
600 IF(STRAN(IOINC).GE.STRND) THEN
SIGNC(IOINC)=0.D0
ELSE
EPSLO=2.D-3*ECMAX/FCCON+2.D0
VALUE=EPSLO*EPSLO+4.D0*ECMAX*STRND/FCCON
IF(VALUE.GE.0.D0) THEN
STRMA=-1.D-3*(EPSLO+DSQRT(EPSLO*EPSLO+4.D0*ECMAX*STRND/FCCON))
ELSE
STRMA=-2.D-3*(19.D0+15.D0*ECMAX*STRND/FCCON)
* /(4.D0-15.D0*2.D-3*ECMAX/FCCON)
ENDIF
IF(STRMA.LT.-2.D-3) THEN
STRMA=-2.D-3*(19.D0+15.D0*ECMAX*STRND/FCCON)
* /(4.D0-15.D0*2.D-3*ECMAX/FCCON)
ENDIF
IF(STRAN(IOINC).LE.STRMA) THEN
LSIG1=0
GOTO 400
ELSE
LSIG4=1
SIGNC(IOINC)=SIGNC(IOINC-1)+ECMAX*(STRAN(IOINC)-STRAN(IOINC-1))
IF(STRMA.GE.-2.D-3) THEN
```

```

IF(STRAN(IOINC).LE.STRNE) THEN
EPSL1=2.D-3*ECMAX/FCCON+2.D0
STRXA=-1.D-3*(EPSL1+DSQRT(EPSL1*EPSL1+4.D0*(EICON*
* STRAN(IOINC)-SIGNC(IOINC))/FCCON))
SIGXA=FCCON*(2.D0*STRXA/(-2.D-3)-2.5D5*STRXA*STRXA)
STRXB=STRXA-SIGXA/2.D0/EICON
STRXC=.478D0*STRXA+0.087D0*STRXA*
* STRXA/(-2.D-3)-.4D0*SIGXA/EICON
STRXD=-.145D0*STRXA**2/(-2.D-3)+.13D0*STRXA
STRXE=STRXA-SIGXA/6.D0/EICON
ENDIF
ELSE
IF(STRAN(IOINC).LE.STRNE) THEN
STRXA=-2.D-3*(19.D0+15.D0*(EICON*STRAN(IOINC)-SIGNC(IOINC)-
*/FCCON)/(4.D0-15.D0*2.D-3*EICON/FCCON))
SIGXA=FCCON*(19.D0-4.D0*STRXA/(-2.D-3))/15.D0
STRXB=DMIN1(STRXA-FCCON/3.D0/EICON,STRXA-2.D0*SIGXA/3.D0/EICON)
ECMXX=DMAX1((SIGXA-FCCON/6.D0)/(.87D0*STRXA
* -.145D0*STRXA*STRXA/(-2.D-3)-FCCON/6.D0/EICON),
* 2.D0*SIGXA/(2.61D0*STRXA-.435D0*STRXA*STRXA
* /(-2.D-3)-SIGXA/6.D0/EICON))
STRXC=DMAX1(STRXA-FCCON/3.D0/EICON-(SIGXA-FCCON/3.D0)/ECMXX,
* STRXA-2.D0*SIGXA/3.D0/EICON-SIGXA/3.D0/ECMXX)
STRXD=.145D0*STRXA**2/(-2.D-3)+.13D0*STRXA
STRXE=DMIN1(STRXA-FCCON/6.D0/EICON,STRXA-SIGXA/3.D0/EICON)
ENDIF
ENDIF
ENDIF
ENDIF
ENDIF
ENDIF
ENDIF
IF(LSIG1.EQ.0.AND.LSIG2.GE.1) THEN
IF(JSIG1.EQ.1) THEN
IF(STRAN(IOINC).GE.STRNA) THEN
SIGNC(IOINC)=SIGNC(IOINC-1)+EICON*(STRAN(IOINC)-STRAN(IOINC-1))
ELSE
LSIG2=0
GOTO 400
ENDIF
ELSE
IF(JSIG2.EQ.1) THEN
IF(STRAN(IOINC).GE.STRMA) THEN
STRS1=SIGNC(IOINC-1)+EICON*(STRAN(IOINC)-STRAN(IOINC-1))
STRS2=ECMAX*(STRAN(IOINC)-STRND)
SIGNC(IOINC)=DMAX1(STRS1,STRS2)
IF(STRAN(IOINC).LE.STRNE) THEN
STRXA=-2.D-3*(19.D0+15.D0*(EICON*STRAN(IOINC)-SIGNC(IOINC)-
*/FCCON)/(4.D0-15.D0*2.D-3*EICON/FCCON))
SIGXA=FCCON*(19.D0-4.D0*STRXA/(-2.D-3))/15.D0
STRXB=DMIN1(STRXA-FCCON/3.D0/EICON,STRXA-2.D0*SIGXA/3.D0/EICON)
ECMXX=DMAX1((SIGXA-FCCON/6.D0)/(.87D0*STRXA
* -.145D0*STRXA*STRXA/(-2.D-3)-FCCON/6.D0/EICON),
* 2.D0*SIGXA/(2.61D0*STRXA-.435D0*STRXA*STRXA
* /(-2.D-3)-SIGXA/6.D0/EICON))
STRXC=DMAX1(STRXA-FCCON/3.D0/EICON-(SIGXA-FCCON/3.D0)/ECMXX,
* STRXA-2.D0*SIGXA/3.D0/EICON-SIGXA/3.D0/ECMXX)
STRXD=.145D0*STRXA**2/(-2.D-3)+.13D0*STRXA
STRXE=DMIN1(STRXA-FCCON/6.D0/EICON,STRXA-SIGXA/3.D0/EICON)
ENDIF
ELSE
LSIG2=0
GOTO 400
ENDIF
ENDIF
ENDIF
ENDIF
1000 CONTINUE
C -----

```

CHENG-LOU AXIAL HYSTERESIS MODEL FOR RC COLUMNS AND WALLS 973

```
C INCREMENT OF DISPLACEMENT, STEEL STRESS
C -----
DO 2000 IOINC=2, NOINC
  IF(STRAN(IOINC-1)-STRAN(IOINC)) 700,700,800
  700 IF(-STRAN(IOINC)) 710,710,720
C
C LOADING, RELOADING, OR UNLOADING FROM COMPRESSION
C POSITIVE DISPLACEMENT
C
  710 IF(MSIG1.EQ.0.AND.MSIG2.EQ.0) THEN
    IF(STRAN(IOINC).LE.YSTEL) THEN
      SIGNS(IOINC)=ESTEL*STRAN(IOINC)
      YSTN1=-YSTEL
      USTN1=-YSTN1
    ELSE
      SIGNS(IOINC)=FYSTL+RATIO*ESTEL*(STRAN(IOINC)-YSTEL)
      YSTN1=STRAN(IOINC)-2.D0*YSTEL
      USTN1=STRAN(IOINC)
    ENDIF
    YSTN2=USTN1
    USTN2=YSTN1
  ENDIF
  IF(MSIG1.GE.1.AND.MSIG2.EQ.0) THEN
    IF(STRAN(IOINC).LE.YSTN2) THEN
      SIGNS(IOINC)=SIGNS(IOINC-1)+ESTEL*(STRAN(IOINC)-STRAN(IOINC-1))
      YSTN1=USTN2
    ELSE
      SIGNS(IOINC)=FYSTL+RATIO*ESTEL*(STRAN(IOINC)-YSTEL)
      YSTN1=STRAN(IOINC)-2.D0*YSTEL
      USTN1=STRAN(IOINC)
    ENDIF
    ENDIF
    IF(MSIG1.EQ.0.AND.MSIG2.GE.1) THEN
      IF(STRAN(IOINC).LE.YSTN2) THEN
        SIGNS(IOINC)=SIGNS(IOINC-1)+ESTEL*(STRAN(IOINC)-STRAN(IOINC-1))
      ELSE
        SIGNS(IOINC)=FYSTL+RATIO*ESTEL*(STRAN(IOINC)-YSTEL)
        YSTN1=STRAN(IOINC)-2.D0*YSTEL
        USTN1=STRAN(IOINC)
      ENDIF
      ENDIF
    GOTO 2000
C
C UNLOADING FROM COMPRESSION, NEGATIVE DISPLACEMENT
C
  720 IF(YSTN2.EQ.YSTEL) THEN
    MSIG2=1
  ELSE
    MSIG2=2
  ENDIF
  MSIG1=0
  IF(MSIG4.EQ.0) THEN
    IF(MSIG2.EQ.1) THEN
      SIGNS(IOINC)=ESTEL*STRAN(IOINC)
    ELSE
      IF(STRAN(IOINC).LE.YSTN2) THEN
        SIGNS(IOINC)=SIGNS(IOINC-1)+ESTEL*(STRAN(IOINC)-STRAN(IOINC-1))
        YSTN1=USTN2
      ELSE
        SIGNS(IOINC)=FYSTL+RATIO*ESTEL*(STRAN(IOINC)-YSTEL)
        YSTN1=STRAN(IOINC)-2.D0*YSTEL
        USTN1=STRAN(IOINC)
      ENDIF
      ENDIF
    ELSE
      SIGNS(IOINC)=SIGNS(IOINC-1)+ESTEL*(STRAN(IOINC)-STRAN(IOINC-1))
    ENDIF
  ENDIF
```

```

GOTO 2000
C
C LOADING, RELOADING, OR UNLOADING FORM TENSION
C NEGATIVE DISPLACEMENT
C
800 IF(STRAN(IOINC).LE.0.D0) THEN
  IF(MSIG1.EQ.0.AND.MSIG2.EQ.0) THEN
    IF(STRAN(IOINC).GE.-YSTEL) THEN
      SIGNS(IOINC)=ESTEL*STRAN(IOINC)
      YSTN2=YSTEL
      USTN2=-YSTN2
    ELSE
      SIGNS(IOINC)=-FYSTL+RATIO*ESTEL*(STRAN(IOINC)+YSTEL)
      YSTN2=STRAN(IOINC)+2.D0*YSTEL
      USTN2=STRAN(IOINC)
    ENDIF
    YSTN1=USTN2
    USTN1=YSTN2
  ELSE
    IF(MSIG2.GE.1.AND.MSIG1.EQ.0) THEN
      IF(STRAN(IOINC).GE.YSTN1) THEN
        SIGNS(IOINC)=SIGNS(IOINC-1)+ESTEL*(STRAN(IOINC)-STRAN(IOINC-1))
        YSTN2=USTN1
      ELSE
        SIGNS(IOINC)=-FYSTL+RATIO*ESTEL*(STRAN(IOINC)+YSTEL)
        YSTN2=STRAN(IOINC)+2.D0*YSTEL
        USTN2=STRAN(IOINC)
      ENDIF
      ENDIF
      ENDIF
      ENDIF
    ELSE
      IF(MSIG2.EQ.0.AND.MSIG1.GE.1) THEN
        IF(STRAN(IOINC).GE.YSTN1) THEN
          SIGNS(IOINC)=SIGNS(IOINC-1)+ESTEL*(STRAN(IOINC)-STRAN(IOINC-1))
        ELSE
          SIGNS(IOINC)=-FYSTL+RATIO*ESTEL*(STRAN(IOINC)+YSTEL)
          YSTN2=STRAN(IOINC)+2.D0*YSTEL
          USTN2=STRAN(IOINC)
        ENDIF
        ENDIF
        ENDIF
        ENDIF
      ELSE
    C
    C UNLOADING FROM TENSION, POSITVE DISPLACEMENT
    C
    IF(YSTN1.GT.-YSTEL) THEN
      MSIG1=2
    ELSE
      MSIG1=1
    ENDIF
    MSIG2=0
    IF(MSIG3.EQ.0) THEN
      IF(MSIG1.LE.1) THEN
        SIGNS(IOINC)=ESTEL*STRAN(IOINC)
      ELSE
        IF(STRAN(IOINC).GE.YSTN1) THEN
          SIGNS(IOINC)=SIGNS(IOINC-1)+ESTEL*(STRAN(IOINC)-STRAN(IOINC-1))
          YSTN2=USTN1
        ELSE
          SIGNS(IOINC)=-FYSTL+RATIO*ESTEL*(STRAN(IOINC)+YSTEL)
          YSTN2=STRAN(IOINC)+2.D0*YSTEL
          USTN2=STRAN(IOINC)
        ENDIF
        ENDIF
        ENDIF
      ELSE
        SIGNS(IOINC)=SIGNS(IOINC-1)+ESTEL*(STRAN(IOINC)-STRAN(IOINC-1))
      ENDIF
      ENDIF
    ENDIF
  ENDIF

```

CHENG-LOU AXIAL HYSTERESIS MODEL FOR RC COLUMNS AND WALLS 975

```
2000 CONTINUE
C -----
C AXIAL LOADING DUE TO CONCRETE AND STEEL FORCES
C -----
DO 3000 IOINC=1,NOINC
3000 PLOAD(IOINC)=ARCON*SIGNC(IOINC)+ASTEL*SIGNS(IOINC)
4000 FORMAT(1H /
* 59H ****
* 59H *
* 59H * AN ALGORITHM FOR SHEAR WALL UNDER AXIAL LOAD REVERSALS */
* 59H *
* 59H ****
* 1H /
* 1H )
5000 FORMAT(1H /
* 43H THE LENGTH OF SHEAR WALL(mm): F15.3/
* 43H THE WIDTH OF SHEAR WALL(mm): F15.3/
* 43H THE HEIGHT OF SHEAR WALL(mm): F15.3/
* 43H COMPRESSIVE STRENGTH OF CONCRETE(MPa): F15.3/
* 43H TENSIL STRENGTH OF CONCRETE(MPa): F15.3/
* 43H INITIAL MODULUS OF CONCRETE(MPa): F15.3/
* 43H AREA OF TOTAL STEEL(mm): F15.3/
* 43H TENSILE STRENGTH OF STEEL(MPa): F15.3/
* 43H YIELDING STRAIN OF STEEL: F15.5/
* 43H RATIO OF MODULUS AFTER STEEL YIELDING: F15.5/
* 1H /
* 1H )
      WRITE(2,'('' STEP INCREMENT CONCRETE STRESS'',
* '' STEEL STRESS AXIAL LOADING'')')
      WRITE(2,'(1X)')
      DO 6000 IOINC=1,NOINC
      WRITE(2,'(1X,I5,1X,F10.4,3(1X,E15.8))') IOINC,DISPL(IOINC),
* SIGNC(IOINC),SIGNS(IOINC), PLOAD(IOINC)
6000 CONTINUE
      STOP
      END
```

Input Data:

```
1000. 100. 500. -25. 2.5 25000. 1000. 414. 0.002 0.005 534 |XWALL WWALL HWALL FCCON FTCON EICON
|ASTEL FYSTL STEL RATIO NOINC
.0500 |DISPL
1.0000|DISPL
3.7500|DISPL
. |DISPL
. |DISPL
. |DISPL
3.5550|DISPL
3.9975|DISPL
```

Output Data:

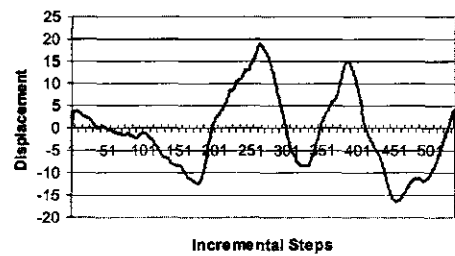
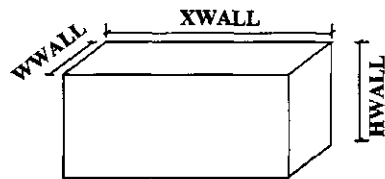
```
*****
*
* AN ALGORITHM FOR SHEAR WALL UNDER AXIAL LOAD REVERSALS *
*
*****
```

THE LENGTH OF SHEAR WALL(mm) : 1000.000
THE WIDTH OF SHEAR WALL(mm) : 100.000
THE HEIGHT OF SHEAR WALL(mm) : 500.000
COMPRESSIVE STRENGTH OF CONCRETE(MPa) : -25.000
TENSILE STRENGTH OF CONCRETE(MPa) : 2.500
INITIAL MODULUS OF CONCRETE(MPa) : 25000.000
AREA OF TOTAL STEEL(mm) : 1000.000
TENSILE STRENGTH OF STEEL(MPa) : 414.000
YIELDING STRAIN OF STEEL: .00200
RATIO OF MODULUS AFTER STEEL YIELDING: .00500

STEP INCREMENT CONCRETE STRESS STEEL STRESS AXIAL LOADING

1	.0500	.25000000E+01	.20700000E+02	.27070000E+06
2	1.0000	-.53396957E-16	.41400000E+03	.41400000E+06
3	3.7500	.00000000E+00	.41969250E+03	.41969250E+06
.				
.				
.				
533	3.5550	.00000000E+00	.41928885E+03	.41928885E+06
534	3.9975	.00000000E+00	.42020483E+03	.42020483E+06

CHENG-LOU AXIAL HYSTERESIS MODEL FOR RC COLUMNS AND WALLS 977



Diagrams Represent Input Data for Appendix M

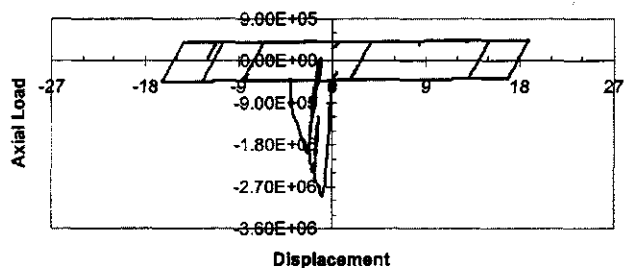


Diagram Represents Output Solution for Appendix M

Notation

ROMAN SYMBOLS

A	area of cross-section	$[A]_i$	equilibrium matrix for the i th member
A_B	ground floor area of a structure	$[A_n]$	equilibrium matrix for axial forces
A_f	amplitude of transmitting force	$[A_s]$	equilibrium matrix for shears
A_m	amplification factor, defined as X/x_{st}	$[A_t]$	equilibrium matrix for torsional moments
A_{mi}	amplification factor for the i th mode	$[A_\theta]$	equilibrium matrix for moments
A_1	first floor area of a structure	a_1	modified acceleration defined by Eq. (7.4)
A_x	amplification factor for accidental torsion	$[B]$	compatibility matrix of a system; strain–stress relation matrix
$[A]$	equilibrium matrix of a system; integration approximation matrix	$[B]_i$	compatibility matrix for the i th member
$[A']$	transformation matrix		

NOTATION

$[B_s]$	compatibility matrix for transverse displacements	E_c	concrete modulus of elasticity
$[B_\theta]$	compatibility matrix for rotations	E_{ds}	dissipated strain energy
C_n	generalized damping defined by Eq. (7.197)	E_n	earthquake load due to base shear
$[C]$	damping matrix	E_m	estimated maximum earthquake force
$[\bar{C}]$	$[X]^T [C] [X]$, defined by Eq. (3.23)	E_{nv}	dissipated energy due to nonviscous damping
C	coefficient of viscous damping; numerical coefficient for soil conditions; seismic coefficient	E_s	steel modulus of elasticity
$C_a; C_v$	seismic coefficients for effective peak acceleration and velocity-related acceleration, respectively	E_{tos}	total elastic strain energy
C_d	deflection amplification factor	E_v	load effect due to vertical earthquake component; dissipated energy due to viscous damping
C_s	seismic response coefficient	e	eccentricity
C_{sm}	modal seismic response coefficient	e_a	accidental eccentricity
C_u	coefficient for upper limit on calculated period	F	force
C_{cr}	critical damping	$F(t)$	forcing function
C_{eq}	equivalent viscous damping	$F_a; F_v$	site coefficients related to acceleration at short period and 1 sec period, respectively
$C_x; C_y; C_z$	wave velocities in x, y, z directions, respectively	F_f	force transmitted to foundation
$c_x; c_y; c_z$	direction cosine	F_e	the element force
D	work done due to damping forces; dissipated energy due to damping; dead load	F_g	global force
$[D]$	reduced stiffness matrix defined by $[K]^{-1}[M]$	F_j	joint force
$[D]_q$	reduced dynamic matrix for the q th mode	F_{js}	transverse force at slave joint
E	modulus of elasticity; earthquake load	F_{jm}	transverse force at master joint
		F_{jmx}	force at the master joint in the JCS x -direction
		F_{jsx}	force at slave joint in the JCS x -direction

F_t	portion of base shear applied at the top of structure	i	$\sqrt{-1}$, imaginary unit
F_k	participation factor of the k th mode	$\vec{i}; \vec{j}; \vec{k}$	unit vectors in GCS
F_r	force reduction factor	J	torsional inertia; Jacobian; wall's four corners, $J1, J2, J3$ and $J4$
$F_l(\Delta); F_m(\Delta)$	forces acting at the ℓ th and m th d.o.f., respectively	K	stiffness
$\{F\}$	force vector	K_a	axial stiffness of unit-height wall
f	natural frequency	K_b	bending stiffness of unit-height wall
f_d	damping force	K_{br}	axial stiffness coefficient
f_k	restoring force	$K_x; K_y$	stiffness of the member in the x and y directions, respectively
G	torsional stiffness; shear modulus	K_n	generalized stiffness
$[G_i]$	defined by $[\Phi] [g_i] [\Phi]^{-1}$	$[K]$	stiffness matrix
g	acceleration of gravity	$[K^c]$	beam-column stiffness matrix
$[g_i]$	diagonal matrix whose i th diagonal element is 1 and remaining elements are 0	$[K']$	bracing stiffness matrix
H	building height	$[K_e]; [K_e^i]$	element stiffness matrix
h	wall height (also defined as length)	$[K_{eg}]; [K_{eg}^i]$	element geometric stiffness matrix
$h_n; h_r; h_{sx}$	height above the base to level n , r , or x , respectively	$[K_g]$	geometric stiffness matrix
$\{H\}$	plastic hinge rotation matrix	$[K^i]$	stiffness matrix of the i th member
I	importance factor; moment of inertia	K_s	shear stiffness of unit-height wall
I_p	polar moment of inertia	L	span length; floor live load
$I_x; I_y$	cross-sectional moment of inertia about the x and y axes, respectively	L_r	roof live load
$\{I_n\}$	influence coefficient matrix	$L_{ys}; L_{ye}$	length of rigid zone in the X_e-Y_e plane
$\{I_n\}_i$	influence coefficient matrix corresponding to the i th structural reference axis	$L_{zs}; L_{ze}$	length of rigid zone in the Z_e-Y_e plane
		L_u	length vector at the u th mode

$M_a; M_b$	moments at top and bottom of bending spring, respectively; magnitude of an earthquake	$[MS]$	mass coefficient matrix
M_c	calculated moment	M	meter
M_D	moment due to dead load	N	axial force
M_E	moment due to earthquake	$N_a; N_v$	near source factor to determine C_a and C_v , respectively
M_{EI}	effective mass of i th mode defined by Eq. (10.10)	N_D	axial force due to dead load
M_f	foundation mass	N_L	axial force due to floor live load
$M_i; M_j$	moments at end- i and end- j , respectively	N_E	axial force due to earthquake
M_{js}	moments at slave joint	N_i	coefficients of shape function
M_{jm}	moments at master joint	$N(x)$	shape function
M_0	overturning moment	NJ	number of structural joints
M_r	restoring moment	NM	number of structural members
M_n	generalized mass defined by Eq. (7.196)	NP	total degrees of freedom
M_p	ultimate moment; primary moment	NFJ	number of fixed supports
M_s	super-structural mass; secondary moment	NHJ	number of hinged supports
$M_{T(i)}$	moment at the base of the i th mode	NMR	number of roller supports
M_{zs}	moments at start-joint	NM_k	largest number of modes at k th story
M_{ze}	moments at end-joint	NPS	d.o.f. in linear displacement; number of sideways
$MC; CM$	mass center	$\{N\}$	interpolation function of a shape function
$ML(t)$	lower yield bending moment at time t	$N_{i/x}$	$\partial N_i/\partial x$; similarly for $N_{i/y}, N_{i/\xi}, N_{i/\eta}$
$MU(t)$	upper yield bending moment at time t	P	external load
$[M]$	mass matrix	$P_a; P_b$	axial force at top and bottom of axial spring, respectively
$[\bar{M}]$	defined as $[X]^T [M] [X]$	P_{cr}	buckling load
$[M_e]$	mass matrix of a member	$P_{DL}; P_{LL}; P_E$	dead load, live load, and earthquake force, respectively

$p_{EW}; p_{NS}$	fundamental frequency in E-W and N-S directions, respectively	q	spring constant
P_E	inertia force	$q_i(t); q_k$	i th or k th generalized coordinate
P_n	generalized loading defined by Eq. (7.199)	R	radius of gyration; response modification; numerical coefficient
P_r	leading principal minor defined by Eq. (2.162)	R_1	distance from epicenter to structure
P_{equ}	equivalent force	R_2	distance from epicenter to instrument station
P_x	vertical design load above level x	R_a	allowable stress factor
$P_b(t)$	effective earthquake force at r th floor of i th mode	$RC; CR$	rigidity center
$\{P_E(t)\}_i$	effective earthquake force at the i th mode defined by Eq. (10.7)	R_d	ductility reduction factor
$\{P_s\}$	transverse external load matrix	R_f	reduction factor
$\{P_\theta\}$	external moment matrix	R_w	response modification factor
$\{P_f(t)\}$	time-dependent reactions at foundation	$R_i(p_j)$	displacement spectral quantity of the j th mode in the structural i th reference-axis direction
$\{P_s(t)\}$	time-dependent external loads	$R_t^i(p_j)$	composite torsional spectral quantity of the j th mode
p	angular frequency		rotational spectral quantity of the j th mode in the structural i th reference-axis direction
p_i	angular frequency corresponding to the i th mode	$r(A)$	spectral radius defined by Eq. (7.96)
p_0	frequency to be extracted	$r_i(t)$	relative displacement in the i th principal direction
p_v	frequency corresponding to the v th mode	S	section modulus; site coefficient; snow load
Q_e	equivalent elastic force	$S_A; S_B; S_C;$ $S_D; S_E; S_F$	soil profile type
Q_y	yielding force		
$\{Q\}$	generalized forces	$S_{DS}; S_{DI}$	design spectral response acceleration coefficients at short and 1 sec periods, respectively
$\{Q\}_n$	maximum base shear of structure due to the n th mode, defined by Eq. (7.211)	$S_S; S_1$	maximum considered earthquake spectral response acceleration at short and 1 sec periods, respectively
$\{Q_e\}$	generalized forces of a member		

$S_{MS}; S_{M1}$	adjusted maximum considered earthquake spectral response acceleration for short and 1 sec periods, respectively	$[T_{ms}]$	constraint matrix between the forces $\{F_{jm}\}$ and $\{F_{js}\}$ acting at master and slave joint, respectively
$S_d; S_v; S_a$	elastic pseudo-displacement, pseudo-velocity and pseudo-acceleration, respectively	T_r	transmissibility, A_r/F
S_{vi}	velocity response spectrum of the i th mode	$[T]^{(r)}$	orthogonal transformation matrix at the r th iteration defined by Eq. (2.141)
S_t^i	torsional spectrum in the i th earthquake principal direction	t_m	time at maximum response
$S_{dy}; S_{vy}; S_{ay}$	inelastic pseudo-displacement, pseudo-velocity and pseudo-acceleration, respectively	U	strain (potential) energy; longitudinal displacement
$SM0; SMY; SVY$	flexural dynamic stiffness coefficients	$u_x; u_y$	displacement functions of element in x and y directions, respectively
$S_c(R_d)$	composite translational spectrum	$\ddot{u}_x; \ddot{u}_y; \ddot{u}_z$	accelerations of main, intermediate and minor seismic principal components, respectively
$S_r(R_r)$	composite torsional spectrum	$\ddot{u}_{x1}; \ddot{u}_{x2}; \ddot{u}_{x3}$	accelerations of seismic components in structural reference axes, x_1, x_2, x_3 , respectively
$[S]$	stiffness coefficient matrix	$\ddot{u}_{E-W}; \ddot{u}_{N-S}; \ddot{u}_{vertical}$	acceleration records in E-W, N-S and vertical directions, respectively
$[S_g]$	geometric stiffness coefficient matrix	$\{u\}$	displacement matrix
$[SNU]$	dynamic axial stiffness coefficient matrix	$u_a; u_b$	axial deformation at top and bottom of axial spring, respectively
$[STy]$	dynamic torsional stiffness coefficient matrix	V	structural base shear
T	period; torsional moment; kinetic energy	$V_a; V_b$	shears at top and bottom of shear spring, respectively
T_a	approximate fundamental period	V_D	design base shear
$T_{EW}; T_{NS}$	period in E-W and N-S directions, respectively	V'	base shear calculated by elastic response spectrum analysis
$[T_{je}]$	rigid-zone transfer matrix		

V_s	base shear calculated by equivalent static procedure	$x_e; x_m; x_y$	equivalent elastic, maximum and yield displacements, respectively
$v_a; v_b$	lateral shear deformation at top and bottom of shear spring, respectively	$x_h; x_p$	homogeneous and particular solution, respectively
v_u	relative unit shear deformation	x_i	displacement of the i th mode
$\vec{V}_y; \vec{V}_z$	unit vectors in element's Y_e and Z_e axes, respectively	$x'_i; \ddot{x}'_i$	uncoupled displacement and acceleration of the i th mode, respectively
\vec{V}_{xt}	vector at wall top	x'_{sti}	pseudo-static displacement of i th mode
\vec{V}_{xb}	vector at wall bottom	x_{st}	static deflection, F/K
\vec{V}'_y	vector along with the average longitudinal axis of wall	\ddot{x}_g	earthquake record in terms of g (acceleration of gravity)
$V_i; V_j$	shears at end- i and end- j , respectively	$x_{\ell,m}, x_{m,\ell}$	displacement at $\ell(m)$ th dynamic d.o.f. due to force applied at the $m(\ell)$ th dynamic d.o.f.
V_p	primal wave	x'_{i0}, \dot{x}'_{i0}	uncoupled initial displacement and velocity of the i th mode at $t = t_0$ respectively
V_s	secondary wave	x_{total}^k	displacement of the k th d.o.f. due to translational and rotational seismic components
$V(x,t)$	time-dependent shear force	x_{n+1}	displacement at time $(n+1)h$ in which h is the time interval
$W; w$	weight; work done due to external forces; wind load	x_{ji}	normal mode displacement of j th floor at i th mode
W_{Ei}	effective weight at the i th mode defined by Eq. (10.14)	X_m	location of mass center
$W_x; w_x$	weight at level x	X_R	Location of rigidity center
$W_i; w_i$	weight factor	$x'; x''; x^{(m)}$	1st, 2nd and m th differentials of x
$w(x,t)$	time-dependent load	$x'_\xi; x'_\eta$	$\partial x/\partial\xi$ and $\partial x/\partial\eta$
$[X]$	eigenvector matrix	$\{x\}; \{\dot{x}\}; \{\ddot{x}\}$	displacement, velocity and acceleration vectors, respectively
$[X]_q$	eigenvector for the q th mode	$\{x'\}; \{\ddot{x}'\}$	uncoupled displacement and acceleration vectors, respectively
${}^r[X]$	eigenvector at the r th iteration		
$x; \dot{x}; \ddot{x}$	displacement, velocity and acceleration, respectively		
$x_0; \dot{x}_0$	initial displacement and velocity at $t=0$, respectively		
$x_{i0}; \dot{x}_{i0}$	initial displacement and velocity at $t=t_0$, respectively		

		GREEK SYMBOLS
$\{x\}_e; \{x\}_r$	displacement due to elastic and rigid-body motion, respectively	$\alpha_i; \alpha_j$ plastic angles at end- <i>i</i> and end- <i>j</i> , respectively
$\{x_f\}; \{\ddot{x}_f\}$	displacement and acceleration of foundation, respectively	α_{ij} cross-correlation coefficient between mode <i>i</i> and mode <i>j</i> , defined by Eq. (7.209)
$\{x_s\}; \{\ddot{x}_s\}$	displacement and acceleration of super-structure, respectively	$\alpha; \beta$ a fraction of the wall's height at top and bottom, respectively
$\{x\}_n$	<i>n</i> th normal mode vector	β logarithmic decrement, $\ln(X_n/X_{n+1})$; shear slope
$\{x'_0\}; \{\dot{x}'_0\}$	uncoupled initial displacement and velocity, respectively	γ_{ij} participation factor of the <i>j</i> th mode in the structural <i>i</i> th reference axis
$\{x\}_{e(in)}$ $\{x\}_{e(D)}$	elastic displacements due to initial condition and applied force, respectively	$\gamma(x)$ torsional displacement function
$\{\dot{x}\}_{avg}; \{\ddot{x}\}_{avg}$	average velocity and acceleration, respectively	δ deflection; variation symbol
$\{\Delta x\}$	incremental velocity	$[\delta]$ flexibility matrix
$\{\Delta \dot{x}_t\}; \{\Delta \dot{x}_\theta\}$	incremental velocity from t to $t + \zeta$ and from t to $t + \theta \Delta t$, respectively	δ_{ij} Kronecker delta
$Y_i; Y_j$	deflections at end- <i>i</i> and end- <i>j</i>	$\delta_w; \delta A_K$ virtual work and virtual displacement, respectively
Y_m	location of mass center	δ_{avg} average displacement at extreme points of structure at level <i>x</i>
Y_R	location of rigidity center	δ_{max} maximum displacement at level <i>x</i>
Y_r	yield reduction factor	δ_e element deformation
Y_{stk}	pseudo-static displacement at <i>k</i> th mode	δ'_e deformation of joint-center
$Y(x)$	shape function	$\{\delta_{jm}\}$ displacement of master joint
$y(x, t)$	time-dependent deflection	$\{\delta_{js}\}$ displacement of slave joint
$y'_\xi; y'_\eta$	$\partial y / \partial \xi$ and $\partial y / \partial \eta$	δ_{xe} deflection by elastic analysis
$\{z\}$	state vector, $\{\dot{x}\} / \{x\}$, defined by Eq. (3.35a)	δ_x deflection at level <i>x</i>
Z	seismic zone factor	δ_{xem} deflection of level <i>x</i> in the <i>m</i> th mode at mass center by elastic analysis

$\delta_x; \delta_y; \theta_z$	displacement at master joint	$\theta_{ya}; \theta_{yb}$	rotations in V_y direction
$\delta_{xj}; \delta_{yj}; \theta_{yj}$	displacement at j th node	$\theta_{za}; \theta_{zb}$	rotations in V_z direction
Δ	increment symbol; dummy variable in integral; story drift; global displacement	θ_u	relative unit rotation
$\{\Delta\}_i$	displacement at the i th story	θ'	critical seismic input angle
Δ_a	allowable drift	λ	angle from \ddot{u}_{E-W} component to \ddot{u}_x component
Δ_M	maximum inelastic response displacement or story drift	λ_q	eigenvalue
Δ_m	modal drift in a story	λ_i	eigenvalue of the q th mode
Δ_s	elastic response displacement or story drift		spectral distribution factor corresponding to ground principal translational component
Δ_x	story drift at story level x	μ	Poisson's ratio; ductility factor
$\Delta M(t)$	incremental bending moment prior to time t	ρ	viscous damping factor defined by Eq. (1.31); redundancy/reliability factor
$\{\Delta U\}$	unbalanced force		damping factor of the j th mode at the i th d.o.f.
$\{\Delta D\}_i$	incremental displacement of member i	ρ_{ij}	
$\{\Delta P\}_i$	incremental force of member i	$[\Phi]$	modal matrix
$\{\Delta x\}_i$	incremental joint displacement of member i	$\{\Phi\}_i$	modal displacement of the i th mode
Σ	summation operation	$\{\Phi\}_u; \{\Phi\}_v$	modal displacement of the u th and v th modes, respectively
Π	multiplication operation		
$\sigma; \{\sigma\}$	stress and stress matrix	$\phi_x; \phi_y; \phi_z$	components of rotational deformations
$\epsilon; \{\epsilon\}$	strain and strain matrix	$\ddot{\Phi}_i(t)$	ground rotational acceleration in the i th earthquake principal direction
ξ	natural coordinate		
ζ	forced period	ψ	torsional frequency parameter; bending slope
θ	parameter in Wilson's method	$\psi_i(t)$	total rotation of oscillator in the i th earthquake principal direction
$\theta_i; \theta_j$	rotations at end i and end j , respectively		
$\theta_a; \theta_b$	flexural rotations at top and bottom of bending spring, respectively	ω	angular frequency of excitations

$\Omega_i(t)$	relative rotation in the i th earthquake principal direction	EPV	effective peak velocity
Ω_0	seismic force amplification for overstrength factor	FFA	floor-by-floor assembly
τ	reduction factor	ft	feet
		GCS	global coordinate system

MATRIX SYMBOLS

{ }	column matrix	in	inch
[0]	zero matrix	JCS	joint coordinate system
[I]	unit matrix	k	1000 pounds
[·] ⁻¹	inverse of matrix	kg	kilogram
[·] ^T	transpose of matrix	kN	1000 Newtons
[··]	diagonal matrix	ksi	1000 lb/in ²
det [·];	determinant of matrix	lb	pound
		LHS	left-hand side

ABBREVIATIONS

BOCA	Basic Building Code	N	Newton, a unit of force; axial force
BT	backtracking	NEHRP	National Earthquake Hazard Reduction Program
cm	centimeter	OS	overshooting
CQC	complete-quadratic-combination	PGA	peak ground acceleration
cps	cycle per second	rad	radian
det	determinant	RHS	right-hand side
d.o.f.	degree of freedom	SBC	Standard Building Code
ECS	element coordinate system	sec; s	second
EPA	effective peak acceleration	SRSS	square root of the sum of the squares
EPGA	effective peak ground acceleration	UBC	Uniform Building Code

Index

- Abcissa, 187
ABSSUM (summation of individual absolute value of individual modes)
(see Modal combination method)
- Acceleration(s), 280, 281
effective, 609
pseudo, 367
spectral value, 394
- Acceleration method:
average, 329, 358
linear, 330–332, 358, 560
incremental, 542, 546, 596
- Amplification factor, deflection, 17, 20, 22, 64, 207, 210, 639
for accidental torsion, 662
force, 626
spectral, 367, 372
- Amplitude, 3, 51, 157
decay, 32,
maximum, 20
method, 43
peak, 30
resonant, 30
of transmitting force, 38
- Assembly, floor by floor, 490, 498
general system, 490
- ATC-3-06, 607, 682, 705
- Average annual risk, 607
- Axial displacement transformation
(see Force transformation)
- Base shear, 610, 641, 650, 693
maximum, 394
- Backtracking (*see* Yield limit)
- Bandwidth method, 43
- Bauschinger effect, 528, 534, 564
- Bernoulli-Euler equation, 163
compared to Timoshenko theory, 252
with elastic media, 237
with elastic media and P- Δ effect, 238
- Binomial expansion, 44
- Bisection procedure, 97
- Branch curve (*see* Stiffness formulation)
- Building Code:
IBC-2000, 607, 633, 641, 648, 675, 689
UBC-94, 123, 607, 612, 641, 648, 675, 689
UBC-97, 123, 607, 624, 641, 648, 676, 689

- Castigliano's first theorem, 266
 Center, geometric, 295–296
 mass, 621, 657
 rigidity, 621, 657, 672, 673
 Centroid, inertia force, 174, 280
 Chain rule for differentiation, 298
 Choleski's decomposition, 47, 81–83, 98
 Coding method, 490
 Coefficient, cross correlation, 394
 damping, evaluation:
 all modes required, 125
 two modes required, 121
 equivalent damping, 42, 43
 mass, 271, 275
 numerical, 626
 stability, 640
 stiffness, 166, 214, 230, 244, 267, 269, 288
 coupling flexural and longitudinal, 225
 coupling flexural and torsional, 234
 matrix, 54, 178, 220, 266, 435, 535
 with static stability (two cases), 240
 with torsional vibration, 229, 230, 233, 235–237
 viscous damping, 8, 13, 42
 Cofactor method, 298
 Collapse mechanism formation, delay of 628
 Compatibility condition, 304–305
 Composite response spectrum (*see* Spectrum)
 Composite spectral modal analysis (*see* Modal analysis)
 Composite torsional spectral quantity
 (*see* Spectra, composite torsional)
 Composite translational spectral value
 (*see* Spectra, composite translational)
 Conservation of energy method, 375
 Constraint matrix (*see* Matrix)
 Coordinate(s), generalized:
 in finite element formulation, 262, 286
 global, 218, 222, 262
 local (*see also* d.o.f. local and global), 221, 262, 264
 natural, in finite element formulation, 262, 286, 291
 system, global, 418
 element, 418
 joint, 418
 CQC (*see* Modal combination method)
 Curve-fitting technique, 122
 D'Alembert's method, 45
 Damping, 7, 283
 absolute, 120
 coefficient (*see* Coefficient, damping)
 coulomb, 117
 critical, 9
 [Damping]
 equivalent, 42, 43
 evaluation of, 42
 factor (*see also* Factor), 9
 calculated from damping coefficient, 125, 126
 matrix, nonproportional vs.
 proportional, 126–128
 nonproportional, 152, 156–157
 nonviscous, 42
 over, 10
 proportional, 120, 126–128, 156
 relative, 120
 structural, 117
 subcritical, 10
 supercritical, 10
 under, 10
 viscous, 7, 8, 43, 117
 Dashpot, 8, 37
 Deflection, dynamic, 263
 large, 527
 small, theory, 162, 527
 static, 1
 Deformation, axial, 581
 bending, 213, 240, 312
 boundary, 174
 capacity, 377
 displacement, relationship (*see* Matrices, compatibility)
 end, 166, 223
 force, 476
 magnitude of elastic curve (*see* Elastic curve, deformation magnitude)
 peak, 374
 virtual, 178
 Degrees of freedom (d.o.f.), for elastic structure, 175
 dummy, 455
 global, 220, 221, 426
 local, 221
 linear displacement, 175
 linear inertia force, 306
 multiple (*see* Multiple d.o.f. system)
 out-of-plane, 444
 rigid frame, 175
 rotational, 273, 306
 side-sway, 175, 176, 273
 single (*see* Single d.o.f. system)
 rotation, 176
 truss, 175
 two (*see* Two d.o.f. system)
 Determinant method, 50, 99, 101, 107
 function, 187, 190
 solution, 191, 193
 zero, 186, 191, 194, 226, 227, 257

- Design, allowable stress (ASD), 627, 648
 strength (LRFD), 627, 648
- Design:
 ground shaking, 682
 response displacement, 632
 response spectra, 677
 spectral response acceleration
 coefficient, 633
 at 1-second, 636
 at short-period, 636
 structural categories, 633
- Diaphragms, rigid and flexible, 612
- Differential equation, 5, 8, 17, 49, 230, 238
 for foundation movement, 185
 in matrix, 58
 nonhomogeneous, 181
 ordinary, 181
 of uniform load, 182
- Direct element formulation, 218, 220, 223, 233, 490
- Direct stiffness method, 179
- Displacement:
 axial, 264, 303
 deformation, relationship (*see* Matrices, compatibility)
 elastic, 109–111
 end, 243
 force, relationship (*see* Rayleigh's dynamic reciprocal principle)
 function, in finite element formulation, 286
 linear (*see* Degrees of freedom, linear)
 longitudinal, 214, 263
 maximum, 20, 23, 210
 pseudo, 367
 pseudo-static, 64, 207, 248, 250
 response, 65, 66, 112–113, 148, 152, 156
 spectral value, 393
 strain relationship, 288
 transverse, 263
 steady-state, 171
 virtual, 178
- Dot (scalar) product (*see* Product)
- Drift, 632, 645, 664, 697
 allowable story, 623, 640
 calculated story, 623
 design story, 639
- Ductility, 315, 377
 allowable, 377
 capacity, 377
 demand, 377
 load displacement, 380
 moment curvature, 381
 moment energy, 381
 moment rotation, 381
 structural system, 382
- Duhamel's integral, 24, 26, 34, 59, 282, 346, 349, 363
- Dynamic stiffness, (*see* Coefficient, dynamic stiffness):
 method, 194, 195
 vs. lumped mass method, 196, 197
- Earthquake, epicenter, 322
 focal depth, 322
 ground motion components
 rotational, 383, 389
 translational, 327, 383
 hypocenter, 322
 principal components:
 main, intermediate and minor, 327, 385
- Eccentricity, 658
- Effective earthquake force, 609, 611
 mass, 609
 peak acceleration, 682
 peak velocity, 682
- Eigenpair, 95, 98, 402
- Eigensolution, 146, 161, 240, 306, 318
 Choleski's decomposition, 47
 damped vs. undamped, 130–132
 determinant, 186
 extraction, 47, 80
 iteration, 47, 72–74, 101–103
 Jocobi method, 47, 87–89
 Sturm sequence, 47, 95–96
 for symmetric matrix, 47, 107
 for unsymmetric matrix, 47, 101–102
- Eigenvalue:
 comparison of lumped mass, dynamic stiffness and consistent mass, 283–285
 complex, 128, 130
 damped vs. undamped, 135–136
 multiple, 105
 zero and repeating, 105–114
- Eigenvector:
 complex, 128, 139
 iteration, 79
 polar form, 153
 upper triangle, 189
- El Centro earthquake, 35, 328
- Elastic curve, 281
 frame, 226, 265
 media, 238, 252, 258
 response parameter, 677
 structure, 216
 support, 252
- Elasticity, fundamental theory, 388
- Element coordinate system (ECS)
 (*see* Coordinate system)

- Element(s), finite, 261
 isoparametric, 262, 286, 291
 quadrilateral, 286, 295–300, 299–300
 rectangular, 286, 299–300
 subparametric, 292
 superparametric, 292
 triangular, 286, 299–300
- Energy, dissipated, 43
 kinetic, 203, 264
 potential, 264, 303–304
 strain, 179, 204, 266–267
- Energy method, 117, 203
- Energy theorem, 265
- Equilibrium:
 condition, 549, 550
 equation, 5, 176, 213, 221
 position, 1, 2
- Equivalent damping coefficient method, 42
- Equivalent lateral force procedure, 514
- Error, numerical (or computational), 358
 characteristics of, 358
 truncation, 340
- Essential facilities, 612
- Euler buckling load, 257
- Factor:
 allowable stress, 614, 626
 damping, 9, 121, 131, 137, 373
 design load, 614
 ductility, 373–374
 ductility reduction, 614
 dynamic load (*see* Amplification factor)
 force reduction, 373
 importance, 612
 magnification, 298
 near source, 624, 625, 684
 overstrength, 614
 participation, 65, 207, 249, 393
 response modification, 613
 seismic zone, 612
 spectral distribution, 412
 weight, 294, 299
 yield reduction, 373
- Fault rupture, 625
- Finite element (*see* Element, finite)
- Fixed-end moments (and shears):
 derivation of, 180–183
- Fixed-end forces, 186, 256, 276, 278
- Floor-by-floor assembly (*see* Assembly)
- Force(s):
 axial, 214, 238, 252, 258, 267, 303
 compressive, 240, 589
 its effect, and use of negative sign, 305
 damping, nonlinear, 43
- [Force(s)]
 deformation, relationship, 166, 183, 255, 476, 566, 581
 rotational, 566
 shear, 213, 240, 254, 258
 bending, 213, 240
- displacement, relationship, 267
- dynamic, 58, 61
- end, 167, 243
- equivalent, 18
- final, 282
- fixed-end (*see* Fixed-end forces)
- harmonic, 29
- impulsive, 19
- inertia, 186, 193, 216, 262, 280
- nodal, due to unit global displacement, 290
- rectangular, 19
- restoring, 42
- tensile, use of positive sign, 305
- transformation, 479, 480
- transverse inertia, 216, 221
- triangular, 21, 511
- unbalanced (nodal), 193, 220, 223, 550
 technique, 546, 550
- Foundation movement, 36, 185
- Fourier integral, 387
- Frames, moment-resisting, 617
- Frequency, angular, 5
 complex, 129, 132
 coupling, 227, 233–237
 damped, 11
 damping effect on, 119
 equation, 50, 134, 136, 165, 225
 flexural, 226, 235
 forcing, 17, 198, 199
 fundamental, 50, 72, 75, 79
 highest, 79
 longitudinal and flexural, 224–226
 natural, 5
 parameter, 187, 199, 252
 pseudo-coupling, 227, 228
 repeating, 56, 107–108, 111
 torsional, 234
- Function, determinant, 187–189
 displacement, 248, 250, 208–209, 304
 shape, 49, 163, 204, 264, 266, 271, 297
 bending and shear slope in, 308
- sine (*see* Sine function)
- time, 49, 163, 214
- trigonometric, 163
- Fundamental structural mechanics, 218, 221, 272
- Gauss elimination, 191, 194, 541
- Gaussian quadrature, 293, 295, 298
- Generalized forces and displacements, 175

- General system assembly (*see* Assembly)
 Geometric nonlinearity (*see* Nonlinearity)
 Global coordinate system (GCS) (*see* Coordinate system)
 Global d.o.f. (*see* d.o.f.)
 Grillage, 231 (*see also* Plane grid system)
- Hooke's law, 288
 Housner's average design spectra, 369
 Hysteresis model (*see* Model)
- Impulse, rectangular, 21
 triangular, 21
 (*see also* Force, rectangular and triangular)
 Inelastic analysis (*see* Nonlinear analysis, scope of)
 Inelastic response displacement, maximum, 632
 Inertia force (*see* Force, inertia)
 Inertia: rotatory, 213, 240–242, 258, 311, 315, 317
 torsional, 229
 transverse, 258, 311, 315–316
 Initial condition, 3, 33
 Initial yield moment (*see* Moment)
 Integrals (*see also* Duhamel's integral)
 impulse, 27
 Integration by parts, 34
 Interaction effect, 589
 Internal moments due to shears, 600–602
 Interpolation function (*see also* Function, shape), 291
 scheme, 297
 Inverse transform, 151
 Inversion, 270, 279, 298
 matrix (*see* Matrix)
 Irregularities:
 extreme torsional, 633
 plan structural, 612, 685
 torsional, 633
 vertical structural, 612, 676, 685
 Iteration method/procedure, 74, 76, 79, 82, 101–105
 for complex eigensolutions, 137–138, 156
- Jacobian, 292, 298
 Jacobi method, 47, 87–89, 95
 Joint coordinate system (JCS)
 (*see* Coordinate system)
 Joint, start, end, 429
 Joint plastification, 553
- Kinematics, 276
 Kronecker delta, 118, 120, 126
- Lagrange's equation, 203, 264, 304
 interpolation, 292, 297
- [Lagrange's equation]
 multiplier form, 402
 Laplace transform, 45, 150
 Lateral force:
 horizontal shear distribution, 639, 644
 procedure, 624
 vertical distribution, 620, 638, 644, 650, 695
 Lateral force, dynamic, 633
 equivalent, 633, 659
 L'Hospital's operations/rule, 173, 561
 Load, buckling, 240, 583, 584
 Load combination, ASD, 631, 647, 669, 701
 LRFD, 627, 646, 671, 703
 Local d.o.f. (*see* d.o.f.)
 Logarithmic decrement, 12, 13, 120
 Logarithmic plot, tripartite, 36, 363–365
- Map, microzonation, 682
 regionalization, 682
 seismic zone, 682, 683
 Mapping concept, 490
 Mass, consistent, 68, 70, 269, 318–319
 distributed, 68, 161
 effective, 608
 foundation, 67
 inertia effect, 427
 lumped, (*see also* Model, mass lumped):
 method vs. dynamic stiffness method, 197
 pseudo-dynamic, 250
 rotary (see Inertia, rotary)
 superstructure, 67
- Matrix (matrices)
 band, skyline of, 490
 coefficient, 189
 mass (*see* Coefficient)
 stiffness (*see* Coefficient)
 compatibility, 177–179, 276
 condensation, 490, 541
 constraint, 425
 damping, 120, (*see also* Damping matrix)
 nonsymmetric, 117
 symmetric, 117
 diagonal, 81, 505–506
 dynamic, equilibrium, 72, 99–100, 108
 dynamic load, 179
 dynamic, reduced, 72, 74, 76
 zero, 77
 dynamic system, 184–185, 193, 199
 eigensolution (*see* Eigensolution)
 equation, 215, 222
 equilibrium, 177, 178
 transpose of, 179
 flexibility, 81, 508
 generalized force, 268, 270, 272, 312, 317
 geometric, 303, 305–306, 312, 438

- [Matrix (matrices)]
 - half band, 490
 - identity, 78
 - inertial force (*see* Force, inertia, matrix)
 - inversion, 81, 279
 - kinematic (*see* Matrices, compatibility)
 - linear array, 490
 - load, 193, 201, 278
 - mass:
 - consistent (*see* Mass consistent)
 - lumped (*see* Model lumped)
 - modal, 56, 64, 149
 - analysis, 281
 - nonsingular, 77
 - reduced dynamic, 74, 76
 - partition, 68
 - singular, 187
 - stiffness:
 - consistent mass model, 266, 271
 - distributed mass model, 178
 - lumped mass model, 55, 435, 438
 - string stiffness (*see* String stiffness)
 - sweeping, 74, 105
 - system, equation, 180, 186
 - transformation, 87
 - triangular, 81, 98
 - unsymmetric, 99
- Maxwell's reciprocal theorem, 60
- Mean recurrence interval, 683
- Mean-value theorem, 336, 340
- Modal combination method:
- ABSSUM, 514
 - CQC 67, 394, 404–405, 514, 679
 - deflection, 681
 - drift, 681
 - SRSS, 67, 393, 394, 400–402, 514, 676, 678
- Modal analysis, 676, 678
- composite spectral, 412
- Mode, buckling, 240
- characteristic, 165
 - first, 75, 102, 144, 217
 - fundamental, 72, 101, 137
 - higher, 73, 101
 - dynamic stiffness vs.
 - lumped mass, 197
 - natural, 49, 50, 67
 - normal, 49, 50, 203
 - shape, in relation to torsional vs. flexural vibration, 237
- Model(s), bilinear, 528, 534, 560–561
- consistent mass (*see* Mass, consistent; Matrix, mass)
 - coordinate, 100
 - curvilinear, 528, 555, 560–561
 - distributed mass (*see* Mass, distributed)
 - [Model(s), bilinear]
 - elastic frame (*see* Elastic frame)
 - elasto-plastic, 375, 532–534, 560
 - hysteresis, 528
 - lumped mass, 48, 68, 71
 - mathematical, 100
 - physical, 99
 - Ramberg-Osgood (*see* Ramberg-Osgood)
 - rigid-body spring, 442
 - spring mass, 47
 - string stiffness (*see* P–Δ effect)
- Modified Mercalli Intensity Scale, 322
- Moment, bending, 243, 271, 462
- initial yield, 528
 - overturning, 611, 621, 639, 645, 651
 - primary, 622
 - restoring, 631
 - secondary, 622
 - second-order, 303
 - and shear equation, 250
 - ultimate, 532, 604
 - unbalanced, 226
- Moment-curvature relationship, 238
- axial load on, 589
- Motion (displacement), elastic, 109, 111
- equation 25, 49, 264
 - uncoupled, 58, 150, 206
 - harmonic, 6, 52, 199
 - foundation movement due to 185
 - periodic, 6, 52
 - rigid-body, 80, 105, 108–110
 - time-periodic, 11
- Müller-Breslau principle, 173
- Multiple-component seismic input, 397
- Multiple d.o.f. system, 55–60, 117, 390, 393
- NEHRP, 607, 705
- Newmark elastic design spectra, 371–372
- Newmark inelastic design spectra, 372–378
- Newmark integration method, 329, 337, 346–347, 356–358
 - in relation to average acceleration and linear acceleration method, 329–330
 - in relation to general numerical integration, 334
 - in relation to numerical stability and error, 350
 - in relation to trapezoidal rule, 329
- Newton's second law, 26
- Nonlinear:
 - analysis, scope of, 527
 - time-history analysis, 632
- Nonlinearity, geometric, 579–581
- Normalization (*see* Vector, normalized)

- Numerical elimination technique, 507
 Numerical error:
 amplitude decay, 358
 periodic elongation, 358
- Occupancy categories, 612
 Ordinates, spectral, 371
 Orthogonality, 55, 73, 101–102, 105–107, 137, 203–205, 392
 proof for eigenvectors, 130
 Out-of-plane d.o.f. (*see* d.o.f.)
 stiffness (*see* Stiffness)
 Overdamping (*see* Damping, supercritical)
 Overshooting (*see* Yield limit)
- P–Δ effect, 100, 238, 252, 303, 314, 438, 579, 585–586, 589, 621, 632, 640, 646, 666
 string stiffness model (*see also* String stiffness), 438
- Participation factors (*see* Factor)
 Peak ground acceleration, 326–327
 Period, elongation (*see also* Numerical error)
 damped, 10
 forcing, 20
 fundamental, equation, 123, 618, 637
 return, 683
 natural, 5, 20, 361
 undamped, 10
 Phase angle, 4, 37, 151, 156
 Physical interpretation, 179, 193, 218, 220, 223
 Pin-connected member, 216 (*see also* Coefficient, stiffness; Dynamic)
 Planar constraint, 426
 Plane grid system (*see also* Grillage), 230, 233, 234
 Plane strain, 285, 288, 298
 Plane stress, 285, 288, 298
 Plastic hinge formation, 532, 591
 rotation(s), 591
 Plastic moment, 591
 reduced, 591
 Points, infinite, 257
 inflectional, 187
 sampling, 294, 299
 zero, 257
 Poisson's ratio, 288
 Polar moment of inertia, 269, 659, 672, 673
 Polynomial equation, 19, 183
 Position:
 equilibrium, 2
 neutral, 4
 Principles, d'Alembert's, 45
 Hamilton's, 45
 virtual displacement, 45
 Pseudo acceleration, 36
 displacement, 36
- [Pseudo acceleration]
 dynamic procedure (based on response spectra), 514
 static displacement, 64
 velocity, 36
- Pulse, 20
 after, 20
 during, 20
- Quadratic equation, 88
- Radius of gyration, 99
 Ratio, amplitude, 12, 40
 damping, 38, 45, 368
 frequencies, 39, 252
 natural period to forcing period, 19
 Poisson's (*see* Poisson's ratio)
 slenderness, 227, 257
 effect on coupling vs.
 pseudo-coupling frequencies in higher modes, 235–236
- Ramberg-Osgood:
 hysteresis model, 528, 562, 576
 moment-curvature, 563
 stress-strain, 562
- Rayleigh's dynamic reciprocal principle, 171, 173
 equation, 619
- Reciprocal theorem, 60
 Reduced plastic moment (*see* Plastic moment)
 Redundancy/reliability factor, 628
 Region of convergence, 187
 of divergence, 187 (*see also* Inflectional points)
 Resonance, 16, 168
 Response analysis:
 displacement (*see* Displacement, response)
 due to forces, initial disturbance, seismic excitation, 58
 maximum (worst-case), 399–400
 modal matrix analysis, (*see* Displacement, response)
 steady-state 15, 198
 Richter Magnitude Scale, 322, 324
 Rigid-body spring model (*see* Model)
 Rigid zone, 464
 Rigid-zone transfer matrix, 465
 Root-mean-square (*see* SSRs)
 Runge-Kutta fourth-order method, 338–346
 in relation to numerical stability, 358, 360
- Scalar product (*see* Product)
 SEAOC, 676
 Secant:
 modulus, 563
 yielding stress, 562–563
 Second-order moment, 238

- Seismic:
 acceleration, 326
 coefficient, 617, 624, 625
 dead load, 616
 design categories, 634, 635
 force amplification, 614
 intensity, 323
 magnitude, 224
 use group, 633
- Seismic waves, types of, 322
- Separation, element, 624
- Separation of variables, 163
- Shear:
 deformation, 314
 maximum base, 394
 modulus, 241, 269
 stress, 269
 strain, 241, 269
- Side-sway, 180, 193
- Sine function, 7
- Site coefficient, 617
- Skeleton curve (*see* Stiffness formulation)
- Slip rate, 625
- Slope, bending, 240–241, 308
 shear, 240–241, 308
- Soil:
 profiles, 380
 stiffness, 71
- Spectral distribution factor (*see* Factor)
- Spectrum (spectra):
 acceleration, 36
 composite response, 410
 composite torsional, 411, 412
 spectral quantity (value), 412
 composite translational, 412
 spectral quantity (value), 412
 design, 367
 elastic, 375
 inelastic, 375
(see Housner's average design spectra)
(see Newmark elastic and
 inelastic design spectra)
 normalized, 369, 371
 ordinates (*see* Ordinates, spectral)
 principal component, 362
 intermediate, 369
 main, 369
 minor, 369
 pseudo, 36, 365–368
 response, 21, 36, 362–363, 366–367,
 368–369
 rock, 625
 hard, 625
 shock, 21, 35, 67
 site dependent, 378
- [Spectrum (spectra)]
 torsional response, 383, 389, 390
 UBC design, 378
 velocity response, 36, 64, 393
- Spring constant, 237
- SSRS (square-root-of-the-sum-of-the-squares
 method (or root-mean-square method))
(see Modal combination method)
- Stability criterion, 351
 coefficient, 640
- Stability, conditional, 357
 unconditional, 357
- Stability, numerical, 350
- State vector, 129, 133, 135, 149
- Static deflection, 1
- Steel, alloy, yielding stress, 562
 structural, stress-strain relationship, 528
- Step function method, 32
- Stiffness formulation matrix (*see also* Physical
 interpretation; fundamental structural
 mechanics)
 branch curve, 572–575, 578
 direct element, 583
 geometric, 583 (*see also* Matrix, geometric)
 out-of-plane, 455
 skeleton curve, 565–570, 575
 unsymmetric, 72
- String stiffness, geometric, 583
 matrix, 306, 587
 model (*see* P–Δ effect)
- Structure, flexible, 632
 isolated, 633
 nonisolated, 633
- Structural joint/node, model, 417
 node, 462
 optimization, 640
 redundancy, 614
- Sturm sequence method, 95–98
- Substitution, backward, forward, 82
- Superposition technique, 28
- Sweeping cycle, first, 90–92
 second, 93–94
- Systems, bearing-wall, building-frame,
 dual, 617
- Tall buildings, 499
- Taylor series, 335–341, 358
- Time-history response (using numerical
 integration), 514, 515, 523
 analysis, 515, 523, 678, 687
 nonlinear, 632
- Time-dependence, 131
- Timoshenko beam, 240, 244, 309, 313
 bending moment and shear, 243
 compared to Bernoulli-Euler theory, 252

- [Timoshenko beam]
equation, 240, 252
fixed-end forces, 246
member's geometric matrix, 305 (*see also* Matrix, geometric)
member's mass matrix, 272 (*see also* Mass consistent)
shear coefficient, 241
tapered and prismatic, 317
- Torsion, 621, 632, 654, 658
accidental, 621, 676
primary, 621
for uniform force, 200
- Torsional response spectra (*see* Spectra)
- Torsional member:
consistent mass method, 268–270
dynamic stiffness method, 229–230
- Transformation technique, 465
- Transformed section method, 444
- Transmissibility, 38, 40
- Triangular distributed wind forces, 511
- Truss(es), 216, 220
dynamic stiffness matrix for, 218–221
vierendeel, 276
- Two d.o.f. system, 49, 105, 126, 135
- Two-force member (*see also* Truss(es)), 265
- Unbalanced force technique, 539
- Uncoupled equation, 58, 63–64
- Underdamping (*see also* Damping, subcritical), 10, 130
- Vector, displacement, 55, 583
complex, normalization of, 132
force, 276, 581
generalized response, 58
incremental joint, 579
influence coefficient, 390
length, 56
real trial, 138–139
rotating, 131
- [Vector, displacement]
state (*see* State-vector)
sum, 7
- Vibration, bending (flexural), 161, 224, 234, 240, 270
coupling, 224, 234
rigid-frame, behavior, 192
forced, 14, 60, 63–64
forced damped, 29
forced undamped, 14
free, 2, 14, 51, 162, 193
free damped, 14
free undamped, 14
longitudinal, 213, 224–227
pseudo-coupling, 234–236
steady-state, 15, 65, 180, 185, 198, 240, 276
steady-state forced damped, 30
torsional (*see also* Torsional member), 229, 234
transient, 15, 30
uncoupled (uncoupling), 224, 225
with elastic media, 214, 215
- Virtual displacement (*see* Displacement, virtual)
- Virtual load concept, 581
- Virtual work, 276
- Wilson- θ method, 332–333, 346, 351, 356–358
in relation to amplitude decay, 358
in relation to general numerical integration, 334
in relation to linear acceleration method, 332–333
in relation to numerical stability and error, 350
in relation to period elongation, 358
- Worst-case response analysis (*see* Response analysis, maximum)
- Yield limit
backtracking (nonlinear state), 539–545
overshooting (linear state), 539–546
- Yield, state(s) of, 536, 538–539, 552
- Young's modulus, 562

